Integrated feasibility study for the permanent disposal of carbon dioxide in the geothermal aquifer at the Bockovac location

Report prepared for: CROATIAN HYDROCARBON AGENCY



Funded by the European Union
NextGenerationEU

10 June 2026





The “Integrated Feasibility Study of Permanent Carbon Dioxide Storage in the Geothermal Aquifer at the Bockovac location” was prepared as part of the “Carbon Capture and Storage” project (NPOO.C7.1.R1-I1.05.0001). The project was co-financed by the European Union under the NextGenerationEU instrument through the Recovery and Resilience Facility. The views and opinions expressed in the study are those of the author(s) only and do not necessarily reflect those of the European Union or the European Commission. Neither the European Union nor the European Commission can be held responsible for them.

Revision	Date Prepared	Issue Description
1.0	10 June 2026	Final Issue

Any interpretation, research, analysis, data, results, estimates, or recommendation furnished with the services or otherwise communicated by SLB to CHA at any time in connection with the services are opinions based on inferences from measurements, empirical relationships and/or assumptions, which inferences, empirical relationships and/or assumptions are not infallible, and with respect to which professionals in the industry may differ. Accordingly, SLB cannot and does not warrant the accuracy, correctness or completeness of any such interpretation, research, analysis, data, results, estimates or recommendation.CHA acknowledges that it is accepting the services "as is," that SLB makes no representation or warranty, express or implied, of any kind or description in respect thereto. Specifically, CHA acknowledges that SLB does not warrant that any interpretation, research, analysis, data, results, estimates, or recommendation is fit for a particular purpose, including but not limited to compliance with any government request or regulatory requirement. CHA further acknowledges that such services are delivered with the explicit understanding and agreement that any action taken based on the services received shall be at its own risk and responsibility and no claim shall be made against SLB as a consequence thereof.

Table of Contents

Executive Summary 1
Project introduction 7
Project objectives 7
Report structure 8
1 Introduction 11
1.1 Areal analysis of emitters location 11
1.1.1 Emitter mapping and clustering 11
1.1.2 Evaluating existing pipeline infrastructure 14
1.2 Transportation and capture method comparison 16
1.2.1 Transport solution comparison 17
1.2.1.1 Dedicated CO_2 Pipelines 17
1.2.1.2 Ship/Marine Transport 18
1.2.1.3 Road Tanker Transport 19
1.2.1.4 Rail Transport 20
1.2.1.5 Innovative & Emerging Transport Methods 21
1.2.1.6 Comparative Analysis&Method Selection Framework 22
1.2.1.7 Regulatory& Safety Considerations 23
1.2.1.8 Conclusions&Recommendations 24
1.2.2 CO_2 stream composition 25
1.2.3 CO_2 capture cost comparison 30
1.2.4 Key recommendations 34
1.3 Overview of existing legal frameworks for CCS projects 36
1.3.1 Introduction 36
1.3.1.1 Purpose of the analysis 36
1.3.1.2 Methodology and data sources 36
1.3.2 Legal framework for permanent CO_2 storage in the EU 37
1.3.2.1 Geological CO_2 storage 38
1.3.2.2 Permitting and authorisation regime 40
1.3.2.3 Environmental protection and nature conservation 41
1.3.2.4 EU ETS and carbon accounting 43
1.3.2.5 Infrastructure and network regulation 44
1.3.2.6 Safety and extraordinary events 45
1.3.3 Legal framework for permanent CO_2 storage in Croatia 46
1.3.3.1 Geological CO_2 Storage – Fundamental Croatian Legal Acts 47
1.3.3.2 Permitting and authorisation regime 51
1.3.3.3 Environmental protection and nature protection 54
1.3.3.4 Infrastructure and Network Regulation 58
1.3.3.5 Safety and Extraordinary Events 60
1.3.4 Comparative legal overview of the CCS value chain in the EU and Croatia 61
1.3.4.1 Energy, CCS and Geothermal Framework aspect 62

1.3.4.2 Environmental and nature protection aspect ... 65
1.3.4.3 Spatial planning, property and safety aspect ... 69
1.3.5 Key findings ... 70
2 Geological and reservoir engineering solution 73
2.1 Overview of the exploration area ... 73
2.1.1 Geological overview ... 73
2.1.2 Data available ... 77
2.2 Seismic interpretation ... 78
2.2.1 Location and data QC ... 79
2.2.2 Seismic Well Tie ... 82
2.2.3 Dataset and Seismic Characteristics ... 94
2.2.4 Machine learning assisted fault prediction ... 96
2.2.5 Seismic Attribute analysis and seismic restoration ... 98
2.2.6 Fault QC and validation ... 101
2.2.7 Horizon interpretation ... 104
2.2.8 Velocity Modeling and time depth conversion ... 112
2.2.9 Geophysical Conclusions and Recommendations ... 120
2.3 Petrophysical analysis ... 120
2.3.1 Available Well Data Review ... 120
2.3.2 Log Quality Control and Log Prediction ... 125
2.3.3 Petrophysical Analysis ... 129
2.4 Well correlation ... 141
2.5 Geological modeling ... 146
2.5.1 Upper formations Alfa (D') to Z' ... 148
2.5.2 Lower formations Z' to Tg ... 166
2.6 Geomechanical quicklook analysis ... 177
2.7 CCS site screening ... 186
2.7.1 Methodology ... 187
2.7.1.1 Eligibility Criteria ... 188
2.7.1.2 Legal and regulatory ... 190
2.7.1.3 Technical criteria ... 194
2.7.1.4 Volumetric estimation ... 196
2.7.2 Assessment ... 200
2.7.2.1 Assessment of upper formations ... 200
2.7.2.2 Assessment of lower formations ... 239
2.7.3 Theoretical Capacity and Site Ranking ... 249
2.8 CO_2 injection simulations ... 251
2.8.1 Reservoir simulation executive summary ... 251
2.8.2 Input data overview ... 253
2.8.3 Simulation model set up ... 256
2.8.3.1 Model assumptions ... 256
2.8.3.2 Initial and boundary conditions ... 258
2.8.3.3 Rock and fluid properties ... 260

2.8.4 Simulation scenarios 262
2.8.5 CO_2 injection Results and Analysis 266
2.8.5.1 Effective Capacity and Injected volumes per scenario 266
2.8.5.2 Pressure validation and distribution 285
2.8.5.3 CO_2 plume migration 305
2.8.6 Risk Assessment and Mitigation 321
2.8.7 Conclusions and Recommendations 322
2.9 Geothermal site selection 325
2.9.1 Geothermal site selection methodology 326
2.9.2 Rs5 Geothermal Reservoir Evaluation 330
2.9.3 Rs7 Geothermal Reservoir Evaluation 335
2.9.3.1 Target C – Geological Interpretation and Uncertainty Analysis 340
2.9.4 Pn Geothermal Reservoir Evaluation 344
2.9.5 Global Geothermal Chance of Success Analysis 349
2.9.6 Geothermal COS Risk Assessment and Recommendations 351
2.10 Fluid geochemistry review of selected geothermal sites 351
2.11 Geothermal doublet simulations 363
2.11.1 Reservoir Simulation Executive Summary 364
2.11.2 Simulation Model Set-up 365
2.11.2.1 Model Assumptions 366
2.11.2.2 Gridding 369
2.11.2.3 Initial and boundary conditions 371
2.11.2.4 Rock and Fluid Properties 376
2.11.3 Geothermal simulation results and analysis 377
2.11.3.1 Rasovac AOI 380
2.11.3.2 Bockovci AOI 381
2.11.4 Risk Assessment and Mitigation 383
2.11.5 Conclusions and Recommendations 384
3 Elaboration of the transport system 386
3.1 Study Basis 387
3.2 Approach and Methodology 388
3.3 Development Case Overview 390
3.4 Development Premise and Assumptions 390
3.5 Development Configuration 390
3.6 Source to Site 391
3.7 Well Modelling 392
3.8 Network (Transportation) configuration 395
3.9 Sensitivity on CO_2 Purity 397
3.10 System Overview (CCS Implementation) 399
3.10.1 Energy Required 399
3.11 Cost Estimates (CCS Systems) 400

4 CO_2 injection system 405
4.1 Design of a CO_2 borehole system 405
4.1.1 Conceptual well design and drilling time estimation 406
4.1.2 Well cost estimates 431
4.1.3 Data acquisition 432
5 Geothermal Energy Generation System 435
5.1 Design of geothermal boreholes 435
5.1.1 Conceptual well design and drilling time estimation 436
5.1.1.1 Rasovac Injector Well 440
5.1.1.2 Rasovac Producer Well 447
5.1.1.3 Recommendations for future stages of the study 455
5.1.2 Well cost estimates 456
5.1.3 Data acquisition 457
5.2 Design of electricity production from the geothermal system 465
5.2.1 Power generation potential 465
5.2.2 Analysis of energy losses through pipelines from friction and elevation changes 473
5.2.3 Residual heat for domestic and agricultural uses 475
5.2.4 Geothermal System Costs 476
5.2.5 Conclusions on power generation and project viability 485
6 Security, monitoring and tracking measures 487
6.1 Risk Assessment 488
6.1.1 Risk Evaluation Criteria 489
6.1.2 Risk Register 492
6.1.3 Risk Assessment 523
6.2 Near-Surface (Groundwater and Soil Gas) Monitoring Plan 525
6.2.1 Groundwater Baseline Sampling 525
6.2.2 Soil Gas Baseline Sampling 526
6.3 Surface Leak Detection and Monitoring Plan 526
6.4 Subsurface Leak Detection and Monitoring Plan 527
6.5 Plume Monitoring Methods 528
6.5.1 Direct Monitoring Methods 528
6.5.2 Indirect Monitoring Methods 528
6.6 Monitoring Technologies 529
6.6.1 Monitoring Technologies for Identified Monitoring Tasks 530
6.6.2 Monitoring Technologies Screening 535
6.6.3 Monitoring Technologies Selection 537
6.7 Monitoring Plan 543
6.8 Emergency Response Plan 543
6.9 Responsibilities 544
6.10 Monitoring Cost Assessment (High Level) 544

6.10.1 Baseline Monitoring Cost 552
7 Project Execution and Cost Estimates 555
7.1 CCS Project Cost Estimate Summary 555
7.2 Geothermal Project Cost Estimate Summary 556
8 Conclusions 557
References 559

List of Figures

1.1 Emitters exceeding 50kT/year of CO_2 13
1.2 Potential CO_2 transportation route along existing infrastructure 14
1.3 Pressure drop for various pipeline sizes - Supercritical state 15
1.4 Pressure drop for various pipeline sizes - gas phase 16
1.5 CCS Value Chain - CO_2 Composition Evolution 25
1.6 Effect of Impurities on CO_2 Phase Envelope 26
1.7 Impurity Risk Map 27
1.8 Reported cost ranges across CCS value chain 30
1.9 Capture - Technology Comparison : Cost, Energy and Recovery 32
1.10 Capture Cost by source-purity tier 33
1.11 Bockovac area of interest and Study area 47
1.12 Natura 2000 and UNESCO Man and Biosphere areas 57
1.13 Infrastructure and protected cultural heritage (Archaeological Sites Borik, Janjevci, Kraka, Ograd, Prinčevac and Selište) 59
2.1 Regional Map of the Study Area 73
2.2 Chrono and Lithostratigraphic chart for the area of study (Drava Depression) 75
2.3 Area of interest 76
2.4 Regional Structural Framework of the SW Panonian Basin 76
2.5 Data Coverage Overview 77
2.6 Location map with available dataset 80
2.7 CRS and SRD definition from raw data 81
2.8 Overlay of 3D and 2D vintages 82
2.9 Map of wells for SWT 84
2.10 Composite well-section before SWT 85
2.11 Composite well-section after SWT 86
2.12 Bockovci-1 SWT 87
2.13 Camagajevci-4 SWT 88
2.14 Krunoslavlje-2 SWT 89
2.15 Ladislavci-9 SWT 90
2.16 Ladislavci-18 SWT 91
2.17 Sjece-2 SWT 92
2.18 Stjepanik-1 SWT 93
2.19 Seismic composite line passing through key wells 95
2.20 Seismic frequency spectrum 96
2.21 Machine learning fault prediction results- XL5760 97
2.22 Machine learning fault prediction results- IL1940 97
2.23 Machine learning fault prediction results- Slice 850 ms 98
2.24 Variance attribute slices at 850, 1100, 1350, 1500, 1700, and 2000 ms 99
2.25 Amplitude contrast attribute slices at 850, 1100, 1350, 1500, 1700, and 2000 ms 100
2.26 Fault interpretation results - XL5720 102
2.27 Fault interpretation results:IL2170, IL2330, IL2500 103
2.28 Horizon interpretation result: composite seismic lines with interpreted horizons 106
2.29 Alfa horizon TWT structural maps with fault boundaries and well locations 107
2.30 C horizon TWT structural maps with fault boundaries and well locations 108
2.31 D horizon TWT structural maps with fault boundaries and well locations 109
2.32 Rs7 horizon TWT structural maps with fault boundaries and well locations 110

2.33 Tg horizon TWT structural maps with fault boundaries and well locations 111
2.34 Layer-cake velocity model without adjustment 113
2.35 Alfa depth residual map 114
2.36 D depth residual map 115
2.37 Rs7 depth residual map 116
2.38 Final velocity model Inline and Xline displayed in the 3D window 117
2.39 Converted seismic, faults and horizons - XL 5720 118
2.40 Converted seismic, faults and horizons - IL 2500 119
2.41 Log digitization for well Karas Suma -1 : example of RES_DEEP log 121
2.42 Core digitization for well Sjece-2 122
2.43 Cuttings digitization for well Bockovci-1 123
2.44 Well Selection Criteria 124
2.45 Depth Shifting for well Stjepanik-1 126
2.46 Log Prediction modeling 127
2.47 Compressional Slowness Log Prediction 128
2.48 Compressional Slowness prediction results for wells 129
2.49 Gamma Ray–Based Volume of Shale (VSH) calculation for Zone Alpha: example from well Ladislavci-9 130
2.50 Volume of Shale calculation from Resistivity method 130
2.51 Gamma Ray and Thorium–Based VSH calculation for Pn zonation: example of well Rasovac-1 131
2.52 VSH Quality Control through cross-validation with logs and cuttings data 132
2.53 Lithology and porosity evaluation: input data and interpretation results 133
2.54 Core Porosity-Permeability relationship for Zones B, C, D and E 134
2.55 Core Porosity-Permeability relationship for Zones Z, Rs5-7, Pn and Tg 135
2.56 Reservoir identification from mudcake development, resistivity contrast, and VSH profiles 137
2.57 Determination of Reservoir cut-offs using VSH and Effective Porosity (PHIE) 138
2.58 Cross-plot of Formation Temperature versus True Vertical Depth Subsea 140
2.59 Bockovci-1 143
2.60 Structural modeling workflow 146
2.61 Fault Modeling 149
2.62 Pillar Gridding 150
2.63 Make Horizons (Petrel) 151
2.64 Layering 152
2.65 Facies codes 153
2.66 Upscaling Facies 154
2.67 QC of upscaling process 155
2.68 Upscaling Effective Porosity 155
2.69 Frequency spectrum 157
2.70 Normalized RMS 158
2.71 Instantaneous frequency 159
2.72 Sand trend 160
2.73 Resampled Seismic Sand Trend into Grid 160
2.74 Facies Modeling process with trend 161
2.75 Section Mag-1 - DM-3 - DM-4 162
2.76 Section Bc-1 - Mag-1 - Sj-2 163
2.77 Section Bc-1 - Kš-1 - DM-1 163

2.78 Section Mag-1 - DM-1 - DM-4 164
2.79 Permeability 165
2.80 Reservoir - Non-reservoir 166
2.81 Faults in a Z'-Tg model 167
2.82 2 fault systems visualized for the entire section from Alfa top to Tg top 168
2.83 Faults from the lower model visualized on stereonet 168
2.84 'Z'' Series (Top of Seal) 169
2.85 'Rs5' Series (Top of Reservoir) 170
2.86 'Rs7' Series (Top of Reservoir) 170
2.87 'Pn' Series (Top of Reservoir) 171
2.88 'Tg' Series (Top of Formation) 171
2.89 Horizon modeling process input data 172
2.90 Zone settings while modeling horizon Rs5 172
2.91 Average porosity map for Rs5 zone 173
2.92 Average porosity maps for Rs7 zone 173
2.93 Average permeability map for Rs5 zone 174
2.94 Average permeability map for Rs7 zone 174
Average Vsh map for Rs5 zone 175
Average Vsh map for Rs7 zone 175
2.95 Facies classes from LITHP_FINAL log 176
2.96 Illustration on the wellbore stability analysis interpretation 179
2.97 Wellbore Stability window limits. 179
2.98 Bockovac-1 1D Mechanical Earth Model results. 180
2.99 Sjece-2 1D Mechanical Earth Model results. 181
2.100 Injection limit definition based on calculated fracture gradient for Bockovci-1 and Sjece-2. 182
2.101 Bockovci-1 single depth analysis of shear failure threshold variation with hole angle and azimuth. 184
2.102 Bockovci-1 single depth analysis of breakdown threshold variation with hole angle and azimuth. 185
2.103 Principle for Chance of Success Mapping 188
2.104 Eligibility Criteria 189
2.105 Inhabited areas 191
2.106 Sanitary protected area 191
2.107 Polygons reflecting the protected areas 192
2.108 Roads & railroads; 192
2.109 Surface Criteria Chance of Success Map 194
2.110 Distance to Wells 195
2.111 Efficiency factor after Goodman (2014) 196
2.112 Closed system 197
2.113 Open system 197
2.114 Efficiency factor explanation 198
2.115 Techno-Economic Resource (and Reserve) Pyramid for CO_2 199
2.116 Structural Map Alfa (D') 200
2.117 Composite Map: Gross Thickness of Alfa (“D”) with Structural Contours 201
2.118 Composite Map: Dip Angle of Alfa (D') with Structural contours 202
2.119 Cross-Sections showing Fault extent 203
2.120 Stratigraphy above Alfa (D') 203

2.121 Composite Map: "Alfa (D')" Series - Reservoir Net Thickness 204
2.122 Composite Map: "Alfa (D')" Series - Net Pay Thickness 205
2.123 Composite Map: "Alfa (D')" Series - Average PHIE 206
2.124 COS Subsurface Alfa (D') 207
2.125 Alfa (D') : Chance of Success (Subsurface x Surface) 208
2.126 3D View of "Alfa (D')" formation potential sites 209
2.127 Structural Map "B" Series 210
2.128 Composite Map: Gross thickness of B with Structural contours 211
2.129 Composite Map: Caprock Thickness of "B" Series with Structural contours 212
2.130 Well correlation section between Mag-1 and Cam-4 213
2.131 Composite Map: Gross Thickness "B" Series (Top of Reservoir zone) 214
2.132 Composite Map: Average PHIE "B" Series (Top of Reservoir zone) 215
2.133 Composite Map: Net Thickness "B" Series (Top of Reservoir zone) 216
2.134 Composite Map: Net Pay Thickness "B" Series (Top of Reservoir zone) 217
2.135 "B" Series Chance of Success - Subsurface 218
2.136 "B" Series - Chance of Success (Subsurface x Surface) 219
2.137 3D View of "B" series proposed sites 220
2.138 Structural Map - "C" Series (Top of Seal) 221
2.139 Composite Map: "C" Series Gross Thickness with Structural Contours 222
2.140 Composite Map: "C" Series - Dip Angle 223
2.141 Composite Map: "C" Series (Top of Seal) - Caprock Thickness 224
2.142 Composite Map: Gross Thickness of "C" Reservoir with Structural Contours 225
2.143 Composite Map: Net Thickness of "C" Reservoir with Structural Contours 226
2.144 Composite Map: Net Pay Thickness of "C" Reservoir with Structural Contours 227
2.145 Composite Map: Average PHIE of "C" Reservoir with Structural Contours 228
2.146 COS Subsurface "C" Series 229
2.147 Chance of Success (Surface x Subsurface) 230
2.148 3D View of "C" Series potential sites 231
2.149 Structural Map "D" Series 232
2.150 "D" Series - Sand - Shale alternation 233
2.151 Composite Map: "D" Series (Top of Seal) Cumulative Reservoir Average PHIE 234
2.152 Composite Map: "D" Series (Top of Seal) Cumulative Reservoir Net Thickness 235
2.153 Composite Map: "D" Series (Top of Seal) Cumulative Reservoir Net Pay Thickness 236
2.154 COS Subsurface - "D" Series 237
2.155 Chance of Success (Surface x Subsurface) 238
2.156 3D View of "D" Series proposed sites 239
Well logs zones Rs5 Rs7 Sjece 2 240
2.157 Rs5 series Dip Angle 242
2.158 Rs7 series Dip Angle 243
2.159 Rs5 P50 Potential CO_2 storage capacity (recoverable oil) map 244
2.160 Rs7 P50 Potential CO_2 storage capacity (recoverable oil) map 245
2.161 RS5 COS Total map 246
2.162 RS7 COS Total map 246
2.163 RS5 COS comparison Dip angle 247
2.164 RS7 COS comparison Dip angle 248
2.165 Static model for the area of interest (porosity distribution) 257
2.166 Bockovci-1 and Sječe-2 fracture gradient and injection limit 258

2.167 Pressure calibrated based on DST information available for wells (Sječe-2, Ladislavci-10 and Ladislavci-11) 259
2.168 Temperature calibrated on estimated log gradient and well data 259
2.169 Aquifers to model boundary conditions 260
2.170 Average CO_2 properties based on Zones index 261
2.171 Porosity - Permeability cross plot per zone 262
2.172 Pre-selected sites per zone overplayed by COS (chance of success maps) 263
2.173 Selected sites for optimization as per base case scenario results (2D view) 264
2.174 Selected sites for optimization as per base case scenario results (3D view) 264
2.175 Field level gas injection rate, gas cumulative and reservoir pressure for the base case 267
2.176 Scenario 1 perforated intervals for wells Kara1, Kara2, Mag1, Cam1 @Jan 2027 268
2.177 Scenario 1 perforated intervals for wells Kara1, Kara2, Mag1, Cam1 @Jan 2042 269
2.178 Scenario 1 perforated intervals for wells Kara1, Kara2, Mag1, Cam1 @Jan 2050 269
2.179 Scenario 1 well locations and plume saturation at the end of injection @2057 270
2.180 Scenario 1 simulation plots (gas injection rate, cumulative, reservoir pressure) 270
2.181 Scenario 1 injection and pressure profiles per well 271
2.182 Scenario 2 perforated intervals for wells Kara1, Kara2, Mag1, Cam1 @Jan 2027 272
2.183 Scenario 2 well locations and plume saturation at the end of injection @2057 272
2.184 Scenario 2 simulation plots (gas injection rate, cumulative, reservoir pressure) 273
2.185 Scenario 2 CO_2 injection and pressure profiles per well 273
2.186 Scenario 3 perforated intervals for wells KS1, KS2, KS3 @Jan 2027 274
2.187 Scenario 3 well locations and plume saturation at the end of injection @2057 275
2.188 Scenario 4 perforated intervals for wells KS1, KS2, KS3, KS4 @Jan 2027 276
2.189 Scenario 4 well locations and plume saturation at the end of injection @2057 277
2.190 Scenario 3 and 4 simulation plots (gas injection rate, cumulative, reservoir pressure) 277
2.191 Scenario 3 Injection and pressure profiles per well 278
2.192 Scenario 4 Injection and pressure profiles per well 279
2.193 Scenario 4 with deviated well locations in Karas Suma-1 - Bockovci-1 area 280
2.194 Deviated wells Scenario perforated intervals for wells K1, K2, K3, K4 @Jan 2027 281
2.195 Scenario with deviated well locations and CO_2 plume distribution at the end of injection @2057 282
2.196 Scenario 4 deviated wells simulation plots (gas injection rate, cumulative, reservoir pressure) 282
2.197 Deviated wells Scenario simulation plots (gas injection rate, cumulative, reservoir pressure) 283
2.198 Initial pressure profile vs fracture gradient in wells Kara1, Kara2, Mag1, Cam1 286
2.199 Pressure profile vs fracture gradient in wells Kara1, Kara2, Mag, Cam1 @Jan 2028 286
2.200 Pressure profile vs fracture gradient in wells Kara1, Kara2, Mag, Cam1 @Jan 2030 287
2.201 Pressure profile vs fracture gradient in wells Kara1, Kara2, Mag, Cam1 @Jan 2040 287
2.202 Pressure profile vs fracture gradient in wells Kara1, Kara2, Mag, Cam1 @Jan 2057 288
2.203 Pressure profile vs fracture gradient in wells Kara1, Kara2, Mag, Cam1 @Jan 2257 288
2.204 Pressure difference profile with initial reservoir pressure for the cross-section in Scenario 2 289
2.205 Pressure difference profile with initial reservoir pressure for the cross-section in Scenario 2 @Jan 2028 289
2.206 Pressure difference profile with initial reservoir pressure for the cross-section in Scenario 2 @Jan 2030 290

2.207 Pressure difference profile with initial reservoir pressure for the cross-section in Scenario 2 @Jan 2040 290
2.208 Pressure difference profile with initial reservoir pressure for the cross-section in Scenario 2 @Jan 2057 291
2.209 Pressure difference profile with initial reservoir pressure for the cross-section in Scenario 2 @Jan 2257 291
2.210 Initial pressure profile vs fracture gradient in wells KS1, KS2, KS3, KS4 292
2.211 Pressure profile vs fracture gradient in wells KS1, KS2, KS3, KS4 @Jan 2028 292
2.212 Pressure profile vs fracture gradient in wells KS1, KS2, KS3, KS4 @Jan 2030 293
2.213 Pressure profile vs fracture gradient in wells KS1, KS2, KS3, KS4 @Jan 2040 293
2.214 Pressure profile vs fracture gradient in wells KS1, KS2, KS3, KS4 @Jan 2057 294
2.215 Pressure profile vs fracture gradient in wells KS1, KS2, KS3, KS4 @Jan 2257 294
2.216 Pressure difference profile with initial reservoir pressure for the cross-section in Scenario 4 295
2.217 Pressure difference profile with initial reservoir pressure for the cross-section in Scenario 4 @Jan 2028 295
2.218 Pressure difference profile with initial reservoir pressure for the cross-section in Scenario 4 @Jan 2030 296
2.219 Pressure difference profile with initial reservoir pressure for the cross-section in Scenario 4 @Jan 2040 296
2.220 Pressure difference profile with initial reservoir pressure for the cross-section in Scenario 4 @Jan 2057 297
2.221 Pressure difference profile with initial reservoir pressure for the cross-section in Scenario 4 @Jan 2257 297
2.222 Initial pressure profile vs fracture gradient in deviated wells K1, K2, K3, K4 298
2.223 Pressure profile vs fracture gradient in deviated wells K1, K2, K3, K4 @Jan 2028 299
2.224 Pressure profile vs fracture gradient in deviated wells K1, K2, K3, K4 @Jan 2030 299
2.225 Pressure profile vs fracture gradient in deviated wells K1, K2, K3, K4 @Jan 2040 300
2.226 Pressure profile vs fracture gradient in deviated wells K1, K2, K3, K4 @Jan 2057 300
2.227 Pressure profile vs fracture gradient in wells KS1, KS2, KS3, KS4 @Jan 2257 301
2.228 Pressure difference profile with initial reservoir pressure for the cross-section in Scenario 4 with deviated wells 301
2.229 Pressure difference profile with initial reservoir pressure for the cross-section in Scenario 4 with deviated wells@Jan 2028 302
2.230 Pressure difference profile with initial reservoir pressure for the cross-section in Scenario 4 with deviated wells@Jan 2030 302
2.231 Pressure difference profile with initial reservoir pressure for the cross-section in Scenario 4 with deviated wells@Jan 2040 303
2.232 Pressure difference profile with initial reservoir pressure for the cross-section in Scenario 4 with deviated wells@Jan 2057 303
2.233 Pressure difference profile with initial reservoir pressure for the cross-section in Scenario 4 with deviated wells@Jan 2257 304
2.234 Plume saturation per zone at the end of monitoring period @2257 for Scenario 1 306
2.235 Plume saturation per zone at the end of monitoring period @2257 for Scenario 2 306
2.236 Plume saturation per zone at the end of monitoring period @2257 for Scenario 3 307
2.237 Plume saturation per zone at the end of monitoring period @2257 for Scenario 4 307
2.238 Plume saturation per zone at the end of monitoring period @2257 for Scenario 4 - deviated wells 308

2.239 Gas saturation for Scenario 1 after 1 year of injection @Jan 2028 308
2.240 Gas saturation for Scenario 1 after 3 years of injection @Jan 2030 309
2.241 Gas saturation for Scenario 1 after 13 years of injection @Jan 2040 309
2.242 Gas saturation for Scenario 1 after 30 years of injection @Jan 2057 310
2.243 Gas saturation for Scenario 1 after 200 years post injection @Jan 2257 310
2.244 Gas saturation for Scenario 2 after 1 year of injection @Jan 2028 311
2.245 Gas saturation for Scenario 2 after 3 year of injection @Jan 2030 311
2.246 Gas saturation for Scenario 2 after 13 year of injection @Jan 2040 312
2.247 Gas saturation for Scenario 2 after 30 year of injection @Jan 2057 312
2.248 Gas saturation for Scenario 2 after 200 years post injection @Jan 2257 313
2.249 Gas saturation for Scenario 3 after 1 year of injection @Jan 2028 313
2.250 Gas saturation for Scenario 3 after 3 year of injection @Jan 2030 314
2.251 Gas saturation for Scenario 3 after 13 year of injection @Jan 2040 314
2.252 Gas saturation for Scenario 3 after 30 year of injection @Jan 2057 315
2.253 Gas saturation for Scenario 3 after 200 years post injection @Jan 2257 315
2.254 Gas saturation for Scenario 4 after 1 year of injection @Jan 2028 316
2.255 Gas saturation for Scenario 4 after 3 year of injection @Jan 2030 316
2.256 Gas saturation for Scenario 4 after 13 year of injection @Jan 2040 317
2.257 Gas saturation for Scenario 4 after 30 year of injection @Jan 2057 317
2.258 Gas saturation for Scenario 4 after 200 years post injection @Jan 2257 318
2.259 Gas saturation for Scenario 4 deviated wells after 1 year of injection @Jan 2028 318
2.260 Gas saturation for Scenario 4 deviated wells after 3 year of injection @Jan 2030 319
2.261 Gas saturation for Scenario 4 deviated wells after 13 year of injection @Jan 2040 319
2.262 Gas saturation for Scenario 4 deviated wells after 30 year of injection @Jan 2057 320
2.263 Gas saturation for Scenario 4 deviated wells after 200 years post injection @Jan 2257 320
2.264 Geothermal energy application based on temperature 325
2.265 Workflow diagram for geothermal screening and chance of success (COS) methodology 327
2.266 Location of Natura 2000 protected ecological zones 328
2.267 location of regulatory sanitary protection zones 329
2.268 Location of inhabited areas in the area of interest 329
2.269 Location of pipelines, roads (primary & secondary) and railroads 330
2.270 Rs5 Temperature and Permeability model 1 332
2.271 Rs5 Temperature and Permeability model 2 333
2.272 Rs5 volume of shale (VSH) and effective porosity model 334
2.273 Rs5 Geothermal COS map 335
2.274 Rs7 temperature model and permeability model 1 337
2.275 Rs7 temperature model and permeability model 2 338
2.276 Rs7 volume of shale (VSH) and effective porosity model 339
2.277 Rs7 Geothermal COS map 340
2.278 Correlation Stjepanik-1 and Rasovac-1 wells showing VShale, Effective Porosity, Total permeability, lithology type and temperatures 341
2.279 Column stratigraphic, Rasovac-1 well tops and lithology type (from end of well report) . 341
2.280 Geological cross-section along the Rasovac-1 well showing the interpretation of Rs7 . 342
2.281 Pn Temperature and Permeability model 1 345
2.282 Pn Temperature and Permeability model 2 346
2.283 volume of shale (VSH) and effective porosity model 347
2.284 Pn Geothermal COS map 348

2.285 Map of identified geothermal targets for the Rs5, Rw7 and Pn layers 350
2.286 Chemical relationships among water samples from the CHA geothermal project area ... 358
2.287 3D view of effective porosity distribution of the static model. 367
2.288 3D view of horizontal permeability distribution of the static model 368
2.289 Extent of 3D geothermal model showing distribution of water saturation. 370
2.290 Close-up visualization of refined gridding in the geothermal AOIs. 370
2.291 Visualization of the model's vertical layering and water saturation distribution 371
2.292 Thermally active and flow active cell distribution. 372
2.293 Pressure distribution of the initial state run projected onto the Pn horizon 373
2.294 Temperature distribution of the initial state run projected onto the Pn horizon 373
2.295 Cross-sectional view of the initial-state pressure (in bar) 374
2.296 Cross-sectional view of the initial-state temperature 375
2.297 Calibrated pressure, temperature and permeability of the initial state model 375
2.298 Pn Pressure and Temperature Simulation Maps Over Time 378
2.299 Pressure and Temperature Profiles 379
2.300 Pressure and Temperature Difference Maps 380
2.301 Simulation Forecast Parameters; Rasovac AOI 381
2.302 Simulation Forecast Parameters; Bockovci AOI 382
3.1 Nexe cement plant and CO_2 injection site 386
3.2 Temperature profile in Croatia (From Weather Spark Website) 388
3.3 SFR Workflow 389
3.4 Development Configuration 391
3.5 Pipeline routing from Nexe plant to the injection site 391
3.6 Pipeline profile 392
3.7 KS1 Tubing Selection - Temperature Profile 393
3.8 KS1 Tubing Selection - Pessure Profile 394
3.9 Development configuration 395
3.10 Network Results-Beginning of Injection 396
3.11 Network Results-End of Injection 396
3.12 Phase envelope 398
3.13 Network results - Beginning of injection-Sensitivity on CO_2 Purity 398
3.14 Network results - End of injection-Sensitivity on CO_2 Purity 398
3.15 System overview for the base case 399
3.16 Power requirements. Fluid temperature 40deg C 400
3.17 Power requirements Fluid temperature 30deg C 400
3.18 AACE Cost Estimate Classification for Capital Projects 401
3.19 Development CAPEX Breakdown 403
3.20 OPEX Breakdown 404
4.1 Surface locations for 4 CO_2 injector wells 406
4.2 Target locations for new CO_2 injector wells 409
4.3 Trajectories for all 4 new CO_2 injector wells 411
4.4 KS1 Wall Plot 412
4.5 KS2 Wall Plot 413
4.6 KS3 Wall Plot 414
4.7 KS4 Wall Plot 415
4.8 Pore and Fracture pressures plot for KS4 416
4.9 Completion schematic for CCS well 418
4.10 KS4 well Schematic for casing 420

4.11 KS4 well Schematic with completions 421
4.12 Drilling fluid weight window for KS4 well 427
4.13 TvD KS4 CO_2 injector 429
5.1 Location of Wellhead and Targets 436
5.2 Pore and Fracture pressure plot 437
5.3 Spider Plot of Rasovac Injector and Producer wells 438
5.4 Ladder Plot of Rasovac Injector and Producer wells 439
5.5 Rasovac Injector Well Plot 440
5.6 Rasovac Injector Well Schematic 444
5.7 Drilling Fluid Weight Window with pore and fracture pressure 445
5.8 Rasovac Injector Well Days vs. Depth Plot 447
5.9 Rasovac Producer Well Plot 448
5.10 Rasovac Producer Well Schematic 452
5.11 Drilling Fluid Weight Window with pore and fracture pressure 453
5.12 Rasovac Producer Well Days vs Depth Chart (includes 20% NPT) 455
5.13 Fractured interval from slim-diameter core well. 458
5.14 Rig test of geothermal well. 460
5.15 Typical equipment set-up for a geothermal well test. 462
5.16 Geothermal production test with James tube equipment. 463
5.17 Long-term multi-well geothermal test. 464
5.18 Proposed baseline ORC configuration 466
5.19 Temperature vs. heat load diagram for heat exchange network design 468
5.20 Baseline ORC configuration: focus on turbine and air-cooled condenser (ACC) 468
5.21 Climate table (monthly weather indicators) for Osijek, Croatia 470
5.22 Monthly temperature variations for Osijek, Croatia 470
5.23 Rasovac geothermal wellheads locations 474
5.24 The Kópsvatn power plant in Iceland (source: Climeon) 476
5.25 Variations in MSP and manufacturing cost breakdown 479
6.1 Monitoring zones 488
6.2 Adopted risk matrix 490
6.3 Risk-Action-Issue Register 492
6.4 Summary of the Qualitative Risk Management process (3 steps) 493
6.5 Bockovci area - Potential Risk matrix 523
6.6 Bockovci area - Residual Risk matrix 524
6.7 MMV Technologies Scoring Steps 531
6.8 MMV Methodology Selection 535
Boston Square 536
Monitoring wells location 537
Cross-section with Injection and monitoring conceptual monitoring requirements 538
6.9 MMV Plan 543
6.10 Bockovci cost evaluation against major projects 552
7.1 Bockovac CCS project development timeline and milestones (2027-2033) 555

List of Tables

1.1 Registered CO_2 emitters with emissions > 50 kTon/year. 12
1.2 CO_2 Transport Methods at a Glance 17
Key Technical Parameters 17
Advantages vs. Disadvantages 17
Key Technical Parameters 18
Advantages vs. Disadvantages 19
Key Technical Parameters 20
Advantages vs. Disadvantages 20
Key Technical Parameters 21
Advantages vs. Disadvantages 21
Advantages vs. Disadvantages 22
Key Decision Criteria Comparison 23
1.3 Purification and Conditioning Requirements 28
1.4 CCS Projects Specification (Benchmark) 29
1.5 Typical CO2 Partial Pressures by Source 31
1.6 Common CO_2 Capture Technology Comparison 32
1.7 Selected Large Scale Cement CO_2 Capture Projects 33
1.8 Industry Approach to CO_2 stream Conditioning 35
1.9 Case in point - Porthos Emitters 35
2.1 SWT Data availability 83
2.2 Well Inventory: Year and Total Depth Summary 125
2.3 Overview of available well logs and data quality assessment for selected wells 125
2.4 Estimated efficiency factor for case when Net reservoir thickness and Efficiency porosity are known 198
2.5 Reservoir zone: Alfa (D') 206
2.6 Alfa D' - Sites 208
2.7 Reservoir zone "B" Series 217
2.8 "B" Series - Potential Sites 219
2.9 Reservoir zone "C" Series 228
2.10 "C" Series - Potential sites 230
2.11 Reservoir zone "D" Series 236
2.12 "D" Series - Potential Sites 238
2.13 Theoretical Capacity and Site Ranking (Upper formations) 249
2.14 Theoretical Capacity and Site Ranking for "Rs5" formation 250
2.15 Theoretical Capacity and Site Ranking for "Rs7" formation 250
2.16 Base simulation case injection volumes per zone 252
2.17 Optimized cases injection volumes 252
2.18 Key reference pressure point from DST reports 253
2.19 Pressure vs depth for wells Ladislavci-10 and Ladislavci-11 253
2.20 Well information from previous studies 254
2.21 Water salinity 256
2.22 Base case simulation scenario volumes per pre-selected site 267
2.23 Base case simulation scenario volumes per zone 267
2.24 Scenario 1 injection rate per year and cumulative injection per site 271
2.25 Scenario 2 injection rate per year and cumulative injection per site 273
2.26 Scenario 3 and 4 injection rate per year and cumulative injection per site 278

2.27 CO_2 storage distribution per zone for Scenario 3 @ year 2257 279
2.28 CO_2 storage distribution per zone for Scenario 4 @ year 2257 279
2.29 Scenario 4 with deviated wells injection rate per year and cumulative injection per site.... 283
2.30 Scenario 4 - deviated wells injection rate per year and cumulative injection per well..... 283
2.31 CO_2 storage distribution per zone for Scenario 4 with deviated wells @ year 2257 284
2.32 Water composition of samples collected from wells within the study area from formations within Rs7 354
2.33 Water composition of samples collected from wells within the study area from formations within Pn 357
2.34 Chromatographic dry gas analysis of samples collected from Rs7 360
2.35 Chromatographic dry gas analysis of samples collected from Pn 362
2.36 Results of the base case of geothermal simulation in 2 AOI: Rasovac and Bockovci..... 364
2.37 Key reference pressure and temperature points from DST reports for geothermal simulations..... 377
2.38 Thermal properties of the model 377
3.1 Injection site atributes 387
3.2 Input data for well modeling 393
3.3 KS1 Tubing selection - sensitivity on internal diameter 394
3.4 Optimal tubing size 395
Impure CO_2 fluid 397
3.5 Development CAPEX and OPEX 402
4.1 Reservoir target locations 408
4.2 Trajectories summary for all 4 CO_2 injector wells 410
4.3 Pore Pressure & Fracture Gradient for KS4 410
4.4 KS4 well geometry 419
4.5 Typical Load Scenarios Analyzed for CCS Wells 422
4.6 Minimum Design Factors for stress anaylsis 423
4.7 KS4 Casing Design Results 423
4.8 CO_2 stream composition for Bockovac project 424
4.9 KS4 CO_2 injector well drilling fluid volume estimation by section 426
4.10 KS4 well cement volume estimation by section 428
4.11 KS4 Well Bit Run and ROP estimations by Section 428
4.12 Time breakdown for all sections for well KS4 430
4.13 Cost breakdown for well KS4 432
5.1 Wellhead and Target Coordinates 435
5.2 Pore Pressure 436
5.3 Fracture Pressure 437
5.4 Rasovac Injector Well Target Coordinates 440
5.5 Rasovac Injector Well Trajectory Surveys 440
5.6 Rasovac Injector Well Formation Tops 442
5.7 Rasovac Injector Well Geometry 443
5.8 Rasovac Injector Well Casing Design Results 445
5.9 Rasovac Injector Well Downhole Drilling Fluid Volume Estimations by Section 445
5.10 Rasovac Injector Well Cement Volume Estimations by Section 446
5.11 Rasovac Injector Well Bit Run and ROP estimations by Section 446
5.12 Rasovac Injector Well Days vs Depth Chart (includes 20% NPT) 447
5.13 Rasovac Producer Well Target Coordinates 448
5.14 Rasovac Producer Well Trajectory Surveys 448

5.15 Rasovac Producer Well Formation Tops 450
5.16 Rasovac Producer Well Geometry 451
5.17 Rasovac Producer Well Casing Design Results 453
5.18 Rasovac Producer Well Downhole Drilling Fluid Volume Estimations by Section 453
5.19 Rasovac Producer Well Cement Volume Estimations by Section 454
5.20 Rasovac Producer Well Bit Run and ROP estimations by Section 454
5.21 Rasovac Producer Well Days vs Depth Chart (includes 20% NPT) 455
5.22 Rasovac Injector and Producer Wells Budgetary Cost Estimates 457
5.23 Characteristics of the geothermal resource avaialble 467
5.24 Summary of the thermodynamic outputs 472
5.25 Summary of the power forecast analysis for one nominal year of operation 473
5.26 Coordinates of the producer / injector Rasovac geothermal wellhead 474
5.27 Process simulation results for the preheater 480
5.28 Process simulation results for the vaporizer 480
5.29 Process simulation results for the ACC 481
5.30 Main equipment cost estimate for geothermal 482
5.31 Cost breakdown of utility scale ORC in Western United States 482
5.32 Reference cost of utility scale ORC unit in Western United States 483
6.1 Risk Matrix - HSE Frequency / Likelihood and Description 490
6.2 Risk Matrix - Severity and Evaluation Criteria 490
6.3 Risk Register for Bockovci area CO_2 sequestration 494
6.4 Issue log example 520
6.5 Actions, decisions and information log example 521
6.6 Revision control 522
6.7 Baseline (Pre-injection), Operational, and Post-operational Monitoring 525
6.8 Baseline Groundwater Sampling Results 526
6.9 Soil Gas Sampling Results 526
6.10 Monitoring for Groundwater Quality and Geochemical Modeling 527
6.11 The Monitoring Tasks Identified from Risk Analysis 530
6.12 Table with scoring for M1: Geophysical monitoring for conformance 531
6.13 Table with scoring for M2: Geophysical monitoring for induced seismicity 532
6.14 Table with scoring for M3: Downhole monitoring for containment and well integrity 532
6.15 Table with scoring for M4: Downhole logging for well integrity 533
6.16 Table with scoring for M5: Downhole monitoring for conformance 533
6.17 Table with scoring for M6: Land environmental monitoring 533
6.18 Table with scoring for M7: Downhole monitoring for borehole blockage 534
6.19 Table with scoring for M8: Detect wellbore instability 534
6.20 Table with scoring for M9: CO_2 fingerprint 534
6.21 Monitoring technologies summary with a final selection 539
6.22 MMV Roles and Responsibilities 544
6.23 Bockovci area - MMV Cost Assessment 546
6.24 Potential Monitoring wells cost (final after market budget exercise) 553
6.25 Potential Baseline analysis cost (estimate) 554
7.1 CAPEX Schedule 556
7.2 Geothermal CAPEX estimate (MEUR) 556

Executive Summary

Croatian Hydrocarbon Agency (CHA) is planning to implement GT-CCS Bockovac project that represents a pioneering effort to integrate carbon capture and storage (CCS) with geothermal energy production in the Drava Depression of eastern Croatia. Therefore, CHA and SLB contracted preparation of an integrated feasibility study for the permanent disposal of CO2 in an aquifer at the Bockovac site, with a specific focus on the implementation of a combined Geothermal–Carbon Capture and Storage (GT-CCS) concept (this Study).

The ultimate purpose of the study is to define a robust development concept that is:

- Economically viable – ensuring competitive project economics and scalable implementation
- Environmentally safe – guaranteeing long-term containment integrity and minimal environmental impact
- Technically and operationally feasible – supported by sound reservoir engineering, well design, and surface integration

The project is articulated in three phases:

- *Phase 1* focuses on transport and storage engineering, starting with an introductory analysis of the CO_2 emitters, transport options, and regulatory framework (1 Introduction) and following with detailed subsurface characterization for CCS and geothermal site selection (2 Geological and reservoir engineering solution) and the CO_2 transport and injection system design (3 Elaboration of the transport system).
- *Phase 2* covers the remainder of the surface facility engineering, notably the design of CO_2 injector wells (4 CO_2 injection system) as well as of a geothermal doublet and power plant (5 Geothermal Energy Generation System)
- *Phase 3* consists of the analysis of the safety aspects of the project and of the design of a monitoring plan (described together in 6 Security, monitoring and tracking measures)

Finally, the cost and schedule of the project are summarized in 7 Project Execution and Cost Estimates, and conclusions are summarized in 8 Conclusions.

Chapter 1: Introduction

The project's foundation rests on a spatial and technical analysis of Croatia's major CO_2 emitters (1.1-1.2), with the Bockovac Area of Interest near the Eastern cluster of industrial sources. The largest local emitter, a cement plan, generates over 600,000 tons of CO_2 annually and is situated merely 35 kilometers from the planned injection site. This proximity, together with the presence of existing natural gas pipelines, provides logistical advantage for CO_2 transport. A comparative review of CO_2 transport methods finds that pipelines are the preferred approach for large volumes; the proposed approach is to purpose-build CO_2 pipelines along the existing rights of way, although repurposing the existing pipelines could be considered. Benchmarking of CO_2 stream compositions (purity, water, oxygen, impurities) shows that the CO_2 stream aligns with international

Copyright © SLB. All Rights Reserved. Private & Confidential. Reproduction only by permission.

standards; special attention should be given to minimizing water and oxygen content to prevent corrosion and maximize transport safety. The findings demonstrate that the Bockovac Area and regional emitters have a feasible pathway for CCS integration.

Croatia's legal framework for CCS (1.3) is harmonized with European Union standards and provides a robust context for this undertaking. The permitting process in the Bockovac area is enabled by the region's extensive geological data and relatively few ecological or regulatory challenges. This places Bockovac in a favorable position for integrated CCS and geothermal development that supports the country's energy transition aims.

Chapter 2: Geological and reservoir engineering solution

The geological survey of the Bockovac area reveals a complex but promising subsurface, shaped by tectonic and sedimentation processes. Leveraging data from dozens of wells, seismic interpretation, and historical documentation, the study identified productive intervals exhibiting dual porosity systems and, in some instances, oil and gas accumulations. Based on seismic interpretation, petrophysical data analysis and well correlation, a detailed geological model was built, providing a consistent and reliable reservoir characterization for ongoing CCS and geothermal feasibility.

The seismic interpretation study (2.2) integrated seismic-to-well ties, attribute analysis, fault and horizon mapping, and time-to-depth conversion, focusing on key stratigraphic horizons: Alfa, B, C, D, Z', Rs7, and Tg. The interpretation delivered time-domain structural maps and an initial velocity model for time-to-depth conversion, identifying two main fault families contributing to structural complexity and compartmentalization.

Petrophysical analysis (2.3) focused on 16 selected wells with high-quality logs, which enabled the assessment of shale volume (Vsh), effective porosity, and permeability, as well as the identification of storage and containment units and the determination of formation temperatures, crucial for the geothermal potential. The well correlation study (2.4) documented the vertical and lateral stratigraphic relationships across the area of interest, using log markers and lithological descriptions to correlate key reservoir and seal intervals and mapping lateral facies variability. An initial geomechanical assessment (2.6) was also carried out, focusing on determining safe injection pressure limits for CCS.

The geological model of the area (2.5) was divided into two zones, the upper section (Alpha to Z horizon) and the more structurally complex lower zone (below Z), to improve grid integrity. Property modeling was performed for shale volume, porosity, permeability, temperature, and pressure, as well as lithology modeling. Volumetric estimations and reserves ranking used distinct strategies for the upper and lower zones, focusing on net thickness and area calculations.

The site selection for CCS operations (2.7) was rigorously benchmarked for technical and regulatory compliance. Storage capacities were estimated to be between 15 and 21 million metric tons of CO_2, with annual injectivity requirements shaping the evaluation. Reservoirs were selected at depths needed to maintain supercritical CO_2, with suitable containment performance, while sites

Copyright © SLB. All Rights Reserved. Private & Confidential. Reproduction only by permission.

near residential or protected zones were avoided to reduce health, safety, and environmental risks. Volumetric analysis and chance-of-success mapping helped pinpoint optimal locations, resulting in three top-ranked sites, respectively near Bockovci-1, Magadenovac-1 and Camagajevci-1 well, all exploiting multiple target formations to maximize storage capacity.

Detailed CO_2 injection simulations (2.8), built on the integrated reservoir model, focused on 3 candidate sites in the Karas Suma-Bockovci area. The optimal scenario uses four deviated injection wells to store approximately 19 million tons of CO_2 over thirty years in the Karas Suma site. Simulation results show stable reservoir pressure, effective plume confinement, and trapping mechanisms that promote long-term security. Recommendations are provided to further build confidence in storage performance, notably containment.

The geothermal site selection and feasibility study (2.9) focuses on the deep geological horizons (Rs5, Rs7, and Pn), with a stacked-reservoir approach to increase the chances of intersecting productive intervals. Two key development areas were identified: the Rasovac and the Bockovci AOI, with more favorable subsurface conditions and surface constraints respectively. The study details the uncertainties, including limited well test and chemistry data; fluid geochemistry analyses (2.10) indicated variability in water and gas compositions, with possible scaling and corrosion risks.

Long-term simulations (2.10) confirmed technical feasibility for geothermal doublets in both AOIs, enabling sustained production rates of 80 liters per second over 30 years. Minimum production temperatures remained above 148°C in Rasovac and 152°C in Bockovci, supported by favorable characteristics of the lower Pn formation.

Chapter 3: Elaboration of the transport system

Surface facility design connects the main emitter (cement plant) to the storage site through a pipeline network that follows existing infrastructure corridors. The project's surface facilities requirements are structured around three main pillars: safe and effective injection at the reservoir level, optimal wellhead conditions and well configuration, and secure transport of CO_2 from the emission source to the storage site. The development targets a base injection rate of 0.636 million tons per annum (MTPA) over a 30-year operational period, with each well assigned a specific injection rate based on reservoir characteristics.

The pipeline network is routed primarily along existing natural gas infrastructure, minimizing environmental impact and avoiding population centers and protected zones such as Natura 2000 areas. The flowline is 37 kilometers long, buried to a depth of 1.5 meters, and is designed to operate without insulation. A 304.8-mm (12-in) internal diameter (ID) offers greater flexibility for handling surges or increased volumes. The elevation profile reduces pressure losses and compression requirements.

Well modeling established the optimal tubing size at 76 mm ID (3 in), balancing the need for lower injection wellhead pressures and erosional velocity ratios against cost. Injectivity improves as CO_2 displaces water over time. The pressure drop across the perforations is significant, primarily due to

Copyright © SLB. All Rights Reserved. Private & Confidential. Reproduction only by permission.

fluid cooling in the reservoir, but the system remains safely outside hydrate formation conditions. Multiple operational scenarios were simulated, including variations in pipeline diameter, ambient temperature, and CO_2 purity.

Energy requirements for the system include compression of CO_2 to approximately 100 bar at the source, with heat exchangers cooling the fluid to 40°C before pipeline entry. Several scenarios were run, resulting in requirements between 1.9 and 2.8 MW for the expected outlet pressure at the emitter.

Compressor power and heat exchanger duty were calculated for various scenarios, ensuring that all rotating equipment is electrically driven and power is sourced from the grid. The system overview confirms that the design avoids hydrate formation and two-phase flow under all modeled conditions.

Chapter 4: CO_2 injection system

The CO_2 borehole system employs four deviated J-type CO_2 injector wells, KS1 to 4, drilled from a shared pad to access deep reservoir formations beneath the Karas Suma protected forest area, with surface infrastructure carefully placed outside the reserve to comply with environmental regulations. The design process included schematics, stress and hydraulic calculations, and preliminary cost analysis, centering on the KS4 well, which serves as a template for other injectors. Key engineering challenges highlighted are managing reservoir pressure during injection, addressing the long-term effects of CO_2 on well integrity, and selecting suitable materials such as CO_2-resistant cements and premium alloys for casing and completion equipment.

Well trajectories were chosen to minimize environmental impact, and the plan incorporates rigorous stress and load assessments to ensure structural durability throughout the well lifecycle. The proposed casing and cementing strategies are tailored to guarantee zonal isolation and prevent CO_2 migration, with water-based muds used for drilling. The estimated drilling time for KS4 is about 45 days, and extensive data acquisition is planned for the first well drilled on the site. A preliminary budget for KS4 stands at €10 million, spanning all major operational and material requirements. Recommendations for future work are provided, including further subsurface data collection, expansion of engineering analyses to dynamic scenarios and laboratory confirmation of materials.

Chapter 5: Geothermal Energy Generation System

The conceptual design for the Rasovac geothermal plant features two J-profile wells, one injector and one producer, positioned so that all key surface infrastructure avoids encroaching on protected areas. Pressure estimates from KS4 well plan inform the drilling plan, mud weight selection, and casing design to ensure borehole stability and controlled operations. The casing plan includes several strings, engineered for strength against high temperature and various stress scenarios, with appropriate material choices and derating for thermal loads. Drilling fluid programs are outlined for each section. The estimated drilling time for the Rasovac Injector is about 49 days,

Copyright © SLB. All Rights Reserved. Private & Confidential. Reproduction only by permission.

including mobilization and demobilization, with a similar schedule for the Producer well. Data acquisition plans are proposed to improve the characterization of the geothermal system. The plan accommodates non-productive time and contingencies.

Electricity production from geothermal resources at Rasovac is planned using an Organic Rankine Cycle (ORC) power plant. This system is modeled for summer, winter, and annual operating conditions, with its air-cooled condenser specifically optimized for hot summer periods. Forecasts suggest gross output fluctuates seasonally between 1.9 and 3.3 megawatts, with a net annual export of approximately 18 gigawatt-hours to the grid after accounting for internal consumption. Notably, modeling confirmed there is no hydraulic connection between the CO_2 and geothermal reservoirs, so CO_2 injection will not compromise power output.

Chapter 6: Security, monitoring and tracking measures

Chapter 6 of this study presents a thorough framework for managing risk, security, monitoring, and tracking measures at the Bockovac CO_2 storage and geothermal project. The approach integrates international best practices and Croatian regulatory standards, with a structured methodology for identifying, evaluating, mitigating, and continuously tracking risks throughout the project's lifecycle. Risks are appraised using multiple criteria—financial, scheduling, reputational, environmental, legal, cost, and rated for likelihood and severity. Critical risk categories include storage site containment and performance, well integrity, environmental protection, and legal and social concerns.

A detailed, site-specific monitoring and tracking plan is provided, covering subsurface and surface tracking of CO_2 operations. Controls span fault and seal analysis, geomechanical surveys, core integration, high-resolution seismic, robust well design, rigorous cementing and monitoring, laboratory testing, and real-time pressure surveillance. Environmental risks are addressed through baseline water sampling and comprehensive monitoring of both surface and subsurface conditions, supported by health monitoring and rapid response protocols. Project governance outlines clear responsibilities, with risk ownership shifting to the operator as the project advances. Adaptive management features prominently, with ongoing data acquisition, stakeholder engagement, and regulatory compliance supporting continual refinement of risk assessments.

Chapter 7: Project execution and cost estimates

The capital cost estimate for the realization of this project amounts to 225 million euros for the CCS component and 28.5 million euros for the geothermal component.

In particular, for the CCS facilities, 21 MEUR are estimated for the site exploration and appraisal; 153 MEUR or the project execution (construction) (of which 58 MEUR are estimated for transport, 39 MEUR for surface facilities, 41 for the injection wells and 15 for the injection site); 13 MEUR for project maturation (concept definition FEED and FID); and 39 MEUR for the monitoring plan implementation. Operative costs of 19.95 MEUR per year are estimated, inclusive of monitoring.

The estimated capital cost of the geothermal component amounts to 17.7 MEUR for the well doublet and 10.8 MEUR for the surface facilities (power plant).

Copyright © SLB. All Rights Reserved. Private & Confidential. Reproduction only by permission.

Chapter 8: Conclusions

In conclusion, the Bockovac CCS & Geothermal Project is a technically, environmentally, and strategically robust initiative. Its integrated approach combines geological opportunity with sound engineering and responsible risk management, establishing a model for sustainable decarbonization and renewable energy production in Croatia and the broader region.

Copyright © SLB. All Rights Reserved. Private & Confidential. Reproduction only by permission.

Project introduction

This Introduction outlines the overall **project objectives** and presents the **structure of the report**, providing context for the reader.

Project objectives

The objective of this project is to conduct an **integrated feasibility study** for the **permanent disposal of CO_2** in an aquifer at the **Bockovac site**, with a specific focus on the implementation of a combined Geothermal–Carbon Capture and Storage (**GT-CCS**) concept.

The study aims to assess the full range of technical and economic aspects associated with the future development of the site, including:

- The potential for CO_2 sequestration within a suitable reservoir to store emissions from selected sources
- Net-zero concepts for a geothermal power plant enabling renewable energy generation
- The integration of CO_2 injection and geothermal operations into a unified system to support a net-zero geothermal power project

The GT-CCS concept is based on the simultaneous achievement of two strategic objectives:

1. Generation of renewable geothermal energy through the production of geothermal fluids
2. Permanent and safe geological storage of CO_2, contributing to decarbonization targets

The ultimate purpose of the study is to define a robust development concept that is:

- **Economically viable** – ensuring competitive project economics and scalable implementation
- **Environmentally safe** – guaranteeing long-term containment integrity and minimal environmental impact
- **Technically and operationally feasible** – supported by sound reservoir engineering, well design, and surface integration

This work will provide the foundation for future exploration and development decisions, enabling the Bockovac site to be assessed as a potential flagship GT-CCS project combining clean energy production with carbon storage.

Copyright © SLB. All Rights Reserved. Private & Confidential. Reproduction only by permission.

Report structure

This report covers the full scope of work contractually agreed with the Croatian Hydrocarbon Agency (CHA) to meet the project objectives outlined above. However, the report structure does not necessarily mirror the organization of the contractual scope. The following paragraphs clarify the structure of this report to facilitate navigation and understanding.

1 Introduction corresponds entirely to Chapter 1 in the contractual scope. It consists of an introduction to the surface scope - areal analysis of the emitters in section 1.1, existing and recommended transport options in section 1.2 - as well as of an extensive overview of the Croatian and European regulatory framework for CO_2 storage in section 1.3.

2 Geological and reservoir engineering solution covers the full scope defined in Chapter 2 of the contractual specification. It addresses the subsurface characterization and engineering aspects related to both CO_2 storage and geothermal energy development. Specifically: chapters 2.1 to 2.6 cover the geoscientific work common to both applications, chapters 2.7 and 2.8 focus on CO_2 storage, and chapters 2.9 to 2.11 to geothermal energy:

- Section 2.1 provides an overview of the geological setting of the area of interest, along with the data available for this study. Seismic interpretation is presented in Section 2.2, while well data interpretation is detailed in Sections 2.3 (petrophysical analysis of well logs) and 2.4 (well marker correlation). Section 2.5 describes the integration of these interpretations into the geological models of the area. Two separate models were developed for the upper (Alfa to Z) and lower formations (Z' to Tg), reflecting their differing structural contexts and respective suitability for the project objectives. Finally, Section 2.6 presents a preliminary geomechanical assessment based on two key wells.
- Section 2.7 outlines the site screening and ranking for CO_2 storage, performed jointly by formation (vertical assessment) and structure (lateral assessment), as agreed with CHA. The methodology is detailed and results are presented in terms of theoretical storage capacity. Section 2.8 presents the dynamic simulation of CO_2 injection for the three highest-ranked sites, including plume extent and effective storage capacity, leading to the selection of a recommended site.
- Section 2.9 focuses on the identification of the most suitable site for geothermal energy production, building on the analyses in Sections 2.1 to 2.5, with emphasis on target formations and reservoir temperature modeling. Section 2.10 summarizes the review of fluid geochemistry data. Section 2.11 presents the simulation of geothermal injection and production scenarios for the selected sites, providing estimates of flow rates and temperature evolution over the project lifetime.

3 Elaboration of the transport system covers the corresponding chapter in the contractual scope, focusing on the framing of the CO_2 transport systems. It also includes the configuration (notably under section 3.8), estimation of the energy requirement (under section 3.10) and of the cost (under section 3.11) of CO_2 injection systems (originally in Chapter 4.1, 4.3 and 4.4 of the contractual scope), since the surface facilities were modeled and framed together with the transport system. The chapter is organized as follows:

Copyright © SLB. All Rights Reserved. Private & Confidential. Reproduction only by permission.

- Sections 3.1 to 3.5 detail the approach, methodology and underlying assumptions for the integrated modeling of CO_2 transport and surface facilities (corresponding to chapter 3.2 of the contractual scope)
- Section 3.6 describe the routing of the transport system, from the CO_2 emitter (source) to the injector wells (site) (corresponding to chapter 3.1 of the contractual scope)
- Section 3.7 focuses on the modeling of the flow in the injection wells, to optimize the completion system and understand the required conditions at the wellhead, which inform the dimensioning of the transport facilities in Section 3.8. Several scenarios are modeled to account for variability in the operational conditions at the inlet (emitter) and outlet (injector wells) of the pipeline. Section 3.9 in particular focuses on the impact of varying degrees of purity on the phase behavior of CO_2. This includes the characteristics of the compression systems (originally in Chapter 4.1 of the contractual scope)
- Section 3.10 summarizes the end-to-end configuration of the system and analyzes the energy required for transport and injection under varying operational scenarios (corresponding to chapters 3.3 and 4.3 of the contractual scope)
- Section 3.11 captures the cot estimation approach and methodology for the estimation of the CAPEX and OPEX of the CCS overall system (corresponding to chapters 3.5 and 4.4 of the contractual scope). Also included is the Class V (AACE) cost estimate of both the CAPEX and OPEX of the CCS system; the CAPEX Schedule of the CCS project is compiled in Chapter 7.

Systems for measuring, monitoring and locating critical points of risk in the transport systems (corresponding to chapter 3.4 of the contractual scope) are described in Chapter 6 of this study.

4 CO_2 injection system focuses on the design of the CO_2 injection wells (corresponding Chapter 4.2 of the contractual scope), including a description of the well cost estimates. The remainder of the Chapter 4 contractual scope is reported as follows:

- CO_2 surface facilities design (Chapter 4.1 of the contractual scope) is described in Chapter 3, together with transport systems, since they were designed and modeled together.
- Specifications for leak detection and safety are included in Chapter 6, together with the monitoring and tracking measures for the other components of the system.
- Analysis of the energy required for CO2 injection (Chapter 4.3 of the contractual scope) is described in section 3.10, together with the transport system.
- The analysis of the cost of CO_2 injection system (Chapter 4.4 of the contractual scope) are detailed in section 4.1.2 and compiled in Chapter 7, together with the cost and energy analysis of the entire system.

5 Geothermal Energy Generation System covers the contractual scope of Chapter 5, notably the design of geothermal wellbores (section 5.1) and geothermal power plant (section 5.2). Moreover, the cost of geothermal facilities (corresponding to Chapter 5.3 of the contractual scope) are detailed in sections 5.1.2 and 5.2.4, then compiled in Chapter 7 together with the cost and energy analysis of the entire system.

Copyright © SLB. All Rights Reserved. Private & Confidential. Reproduction only by permission.

6 Security, monitoring and tracking measures, as indicated by the title, covers the scope of Chapters 6 and 7 in the contractual specifications. The combination of these two items reflects the approach taken in the definition of monitoring and tracking measures (described in sections 6.2 to 6.7 and corresponding to Chapter 7.1 of the contractual scope) on the basis of the risk and safety analysis (described in section 6.1 and corresponding to Chapter 6 of the contractual scope). The monitoring and tracking measures include those designed for the CO_2 transport and injection system, originally part of Chapter 3 of the contractual scope. Other requirements from the contractual Chapter 6 are included here, such as the ERP (section 6.8). Finally, the responsibilities (section 6.9) and cost (section 6.10, corresponding to Chapter 7.2 of the contractual scope) related to monitoring and tracking conclude this chapter.

7 Project Execution and Cost Estimates compiles the cost estimates for the entire project, based on the respective contributions from the various elements of the system (originally part of the contractual scope of the respective chapters). The project execution schedule is also presented in the section.

Finally, the project results are summarized in **8 Conclusions**, with references to the recommendations for future actions provided in this study.

Copyright © SLB. All Rights Reserved. Private & Confidential. Reproduction only by permission.

1 Introduction

1.1 Areal analysis of emitters location

1.1.1 Emitter mapping and clustering

The National Register of Environmental Pollution (https://roo.azo.hr) tracks air emissions from all sources across Croatia. Based on the latest available data for 2024, the table below lists all registered CO_2 emitters with annual emissions exceeding 50 kilotons (kt/yr).

Copyright © SLB. All Rights Reserved. Private & Confidential. Reproduction only by permission.

Table 1.1 Registered CO_2 emitters with emissions > 50 kTon/year.

Nr.	Operator	Name of the organizational unit at the location	Cluster	City of organizational unit	kTone/ year CO_2
1	HEP-PROIZVODNJA d.o.o.	TE-TO Zagreb	Central	Zagreb	826.72
2	HEP-PROIZVODNJA d.o.o.	TE Plomin	Western	Labin	680.28
3	INA-Industrija nafte, d.d.	Rafinerija nafte Rijeka	Western	Kostrena	663.74
4	NEXE d.d. za proizvodnju građevinskih materijala	NEXE d.d.	Eastern	Našice	610.47
5	CEMEX HRVATSKA D.D.	TVORNICA CEMENTA "SVETI JURAJ"	Western	Kaštel Sućurac	544.27
6	HEP-PROIZVODNJA d.o.o.	TE-TO Sisak	Central	Sisak-Caprag	455.15
7	Holcim (Hrvatska) d.o.o.	Proizvodnja cementa Koromačno	Western	Labin	314.46
8	INA-Industrija nafte, d.d.	Objekti prerade plina Molve	Central	Đurđevac	215.84
9	Petrokemija d.d.tvornica gnojiva	Proizvodnja gnojiva	Central	Kutina	208.27
10	HEP-PROIZVODNJA d.o.o.	EL-TO Zagreb	Central	Zagreb	194.09
11	INA-Industrija nafte, d.d.	INA d.d. Istr. i proizv. NiP, Regija središnja Hrvatska, Objekti frakcionacije Ivanić Grad	Central		110.59
12	Vetropack Straža d.d.	Vetropack Straža d.d.	Central	Hum na Sutli	99.08
13	UNI VIRIDAS društvo s ograničenom odgovornošću za energetiku	Kogeneracijsko postrojenje Viridas Biomass	Eastern	Županja	99.02
14	Calucem d.o.o.,Calucem društvo s ograničenom odgovornošću za proizvodnju specijalnih cemenata	Proizvodnja aluminatnog cementa	Western	Pula (Pola)	97.19
15	DS Smith Belišće Croatia društvo s ograničenom odgovornošću za proizvodnju papira i kartonske ambalaže	Tvornica papira, ambalaže i energetika	Eastern	Belišće	97.17
16	SLAVONIJA OIE d.o.o. obnovljivi izvori energije i trgovina	Slavonija OIE	Eastern	Slavonski Brod	93.81
17	CEMEX HRVATSKA D.D.	TVORNICA CEMENTA "SVETI KAJO"	Western	Solin	92.47
18	DRVNI CENTAR GLINA d.o.o	DCG	Central	Glina	91.65
19	Elektrana Grubišno Polje društvo s ograničenom odgovornošću za proizvodnju, trgovinu i usluge	Elektrana Grubišno Polje	Central	Grubišno Polje	73.94
20	BE-TO KARLOVAC d.o.o. za proizvodnju i usluge	BE-TO Karlovac	Central	Karlovac	71.19
21	Rockwool Adriatic d.o.o.	ROCKWOOL Adriatic d.o.o.	Western	Podpićan	70.62
22	ENERGANA ŽUPANJA društvo s ograničenom odgovornošću za proizvodnju energije	Energana Županja d.o.o.	Eastern	Županja	69.15
23	BE-TO BRINJE d.o.o. za proizvodnju, trgovinu i usluge	BE-TO Brinje	Western	Brinje	66.82
24	HEP-PROIZVODNJA d.o.o.	TE-TO OSIJEK	Eastern	Osijek	65.22
25	KRONOSPAN CRO d.o.o	Proizvodnja iverice	Central		64.70
26	ENERGY 9 d.o.o. za proizvodnju i trgovinu	BE SLATINA	Eastern		62.65
27	INTERCAL d.o.o.	Tvornica vapna II	Central	Daruvar	55.41
28	ENERGANA BENKOVAC društvo s ograničenom odgovornošću za proizvodnju energije	Energana Benkovac d.o.o.	Western	Benkovac	53.70
29	ĐAKOVO HRAST d.o.o. proizvodnja namještaja	ĐAKOVO HRAST D.O.O.	Eastern	Đakovo	52.03

Table 1 CO_2 emitters from National Register of Environmental Pollution, 2024

Copyright © SLB. All Rights Reserved. Private & Confidential. Reproduction only by permission.

The geographical distribution of the CO_2 emitters along with the existing infrastructure for transportation (pipelines and railway) and the area of interest for CCS injection is displayed in Fig. 1.1.

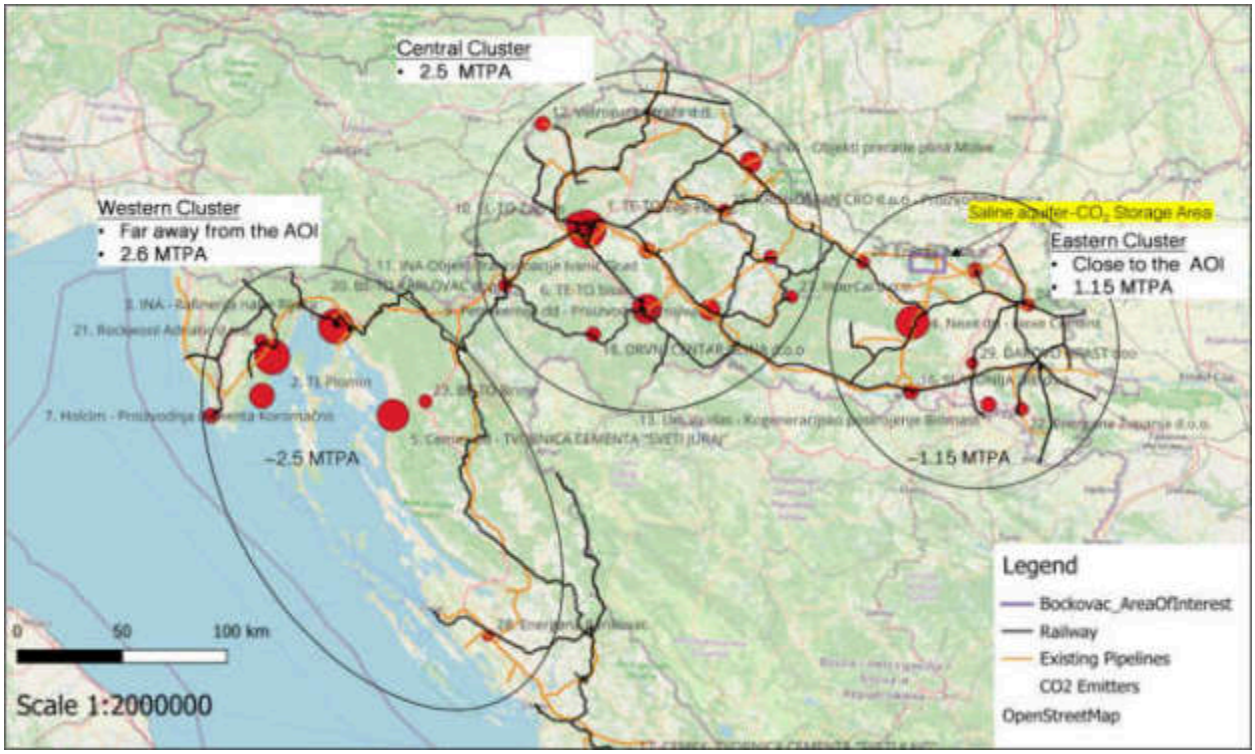


Fig. 1.1 Emitters exceeding 50kT/year of CO_2

Based on the geographical distribution of emitters, three distinct clusters have been identified: a Western cluster with total emissions of 2.6 Mt/yr, a Central cluster with 2.5 Mt/yr, and an Eastern cluster with 1.15 Mt/yr.

Given its proximity to the Bockovac CCS injection and storage site, the Eastern cluster is considered the most relevant.

The largest emitter in this cluster is the NEXE cement plant, which reported CO_2 emissions of 610 kt/yr in 2024. The plant is located approximately 35 km south of the proposed injection site, along an existing pipeline corridor.

Other nearby emitters include ENERGY 9 d.o.o., located approximately 30–35 km to the west, and DS Smith Belišće (20–25 km to the east) and TE-TO Osijek (55–60 km to the east). Although relatively close, these sources have comparatively lower emissions: ENERGY 9 d.o.o. (62.65 kt/yr), DS Smith Belišće (97.17 kt/yr), and TE-TO Osijek (65.22 kt/yr). Additionally, their positions on opposite sides of the injection site would require dedicated transport routes.

Further south several smaller emitters could potentially be aggregated along a CO_2 gathering corridor that includes the NEXE cement plant. These include SLAVONIJA OIE d.o.o. (93.81 kt/yr),

Copyright © SLB. All Rights Reserved. Private & Confidential. Reproduction only by permission.

ĐAKOVO HRAST d.o.o. (52.03 kt/yr), UNI VIRIDAS (99.02 kt/yr), and ENERGANA ŽUPANJA (69.15 kt/yr). In addition, a planned power plant in Slavonski Brod, with expected emissions of approximately 500 kt/yr, could also be integrated into this transport route.

1.1.2 Evaluating existing pipeline infrastructure

The main emitter for this CCUS project is the NEXE cement plant. The NEXE cement plant lays along the existing natural gas transportation pipeline system (Fig. 1.2 below).

If the exiting infrastructure can be repurposed to transport CO_2 from NEXE cement plant to the injection site will depend on the following factors:

- Availability of current pipeline infrastructure.
- The transport capacity of available pipeline infrastructure.
- Mechanical condition of existing pipeline infrastructure for safe transportation of CO_2.

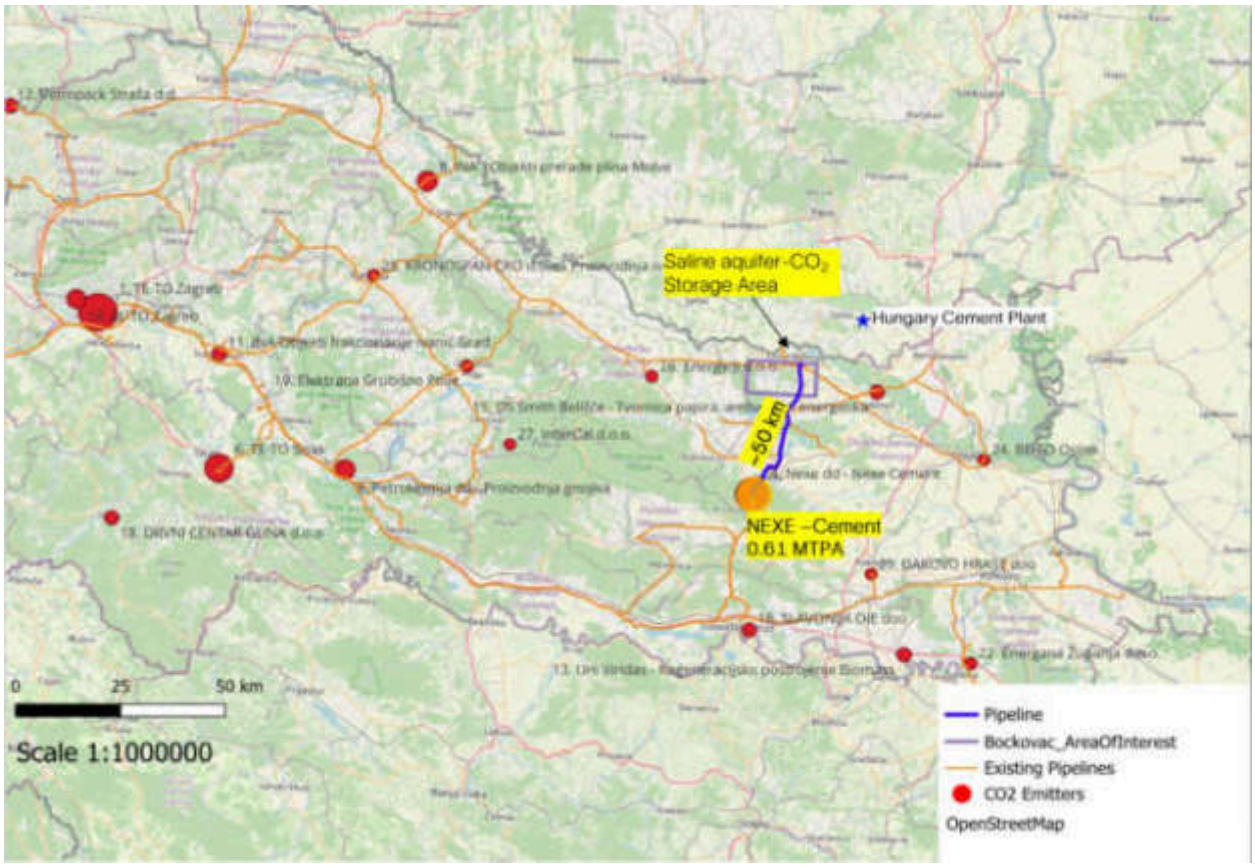


Fig. 1.2 Potential CO_2 transportation route along existing infrastructure

The current natural gas pipeline infrastructure from the NEXE cement plant towards the injection site is currently in use. Nevertheless, any new pipeline built for the purpose of CO_2 transportation is recommended to follow the existing infrastructure, through the usage of "rights of way".

Copyright © SLB. All Rights Reserved. Private & Confidential. Reproduction only by permission.

The transportation of CO_2 through the pipelines can be performed at high pressure with CO_2 in dense phase or at low pressure with CO_2 in gas phase. Transportation in dense phase/high pressure allows for higher amounts of CO_2 to be transported, while transportation in gas phase - the pipeline will be operated at lower pressure but on the other hand the CO_2 transportation capacity is reduced.

The next two figures (Fig. 1.3 and Fig. 1.4) show simulated pressure drop for CO_2 transportation from NEXE cement plant in dense phase and in gas phase for various sizes of pipelines to the injection site.

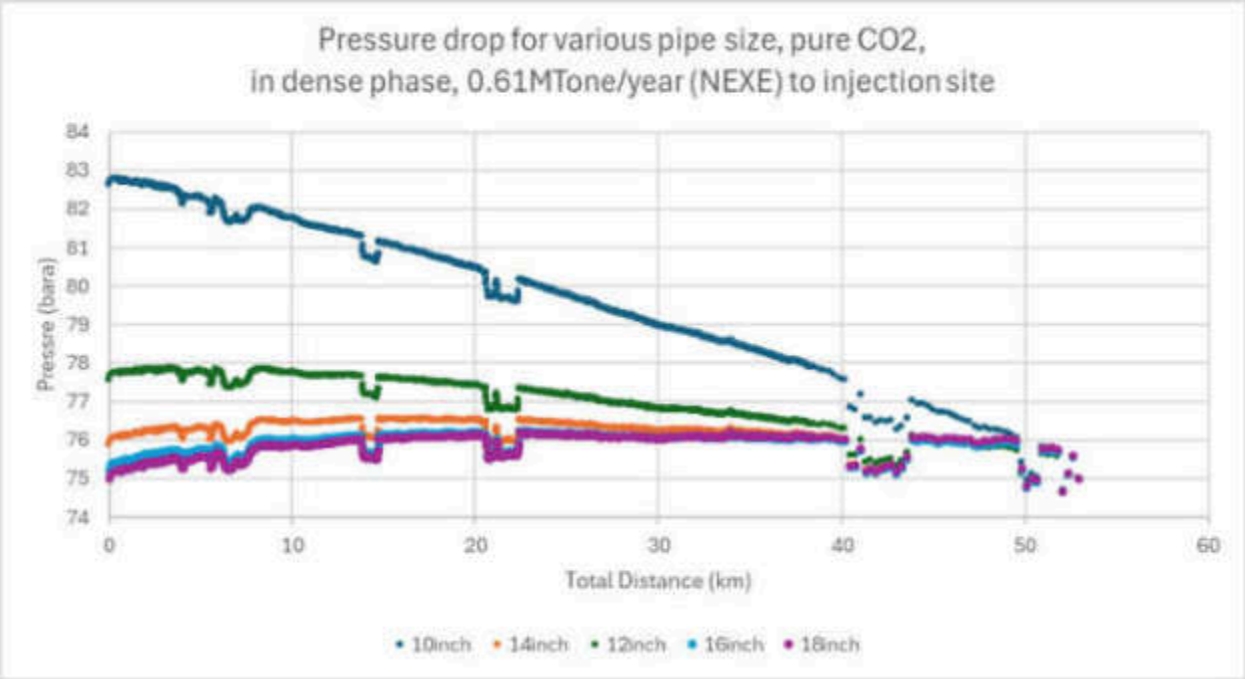


Fig. 1.3 Pressure drop for various pipeline sizes - Supercritical state
Pure CO_2, in dense phase, 0.61MT/y from NEXE to the injection site

Copyright © SLB. All Rights Reserved. Private & Confidential. Reproduction only by permission.

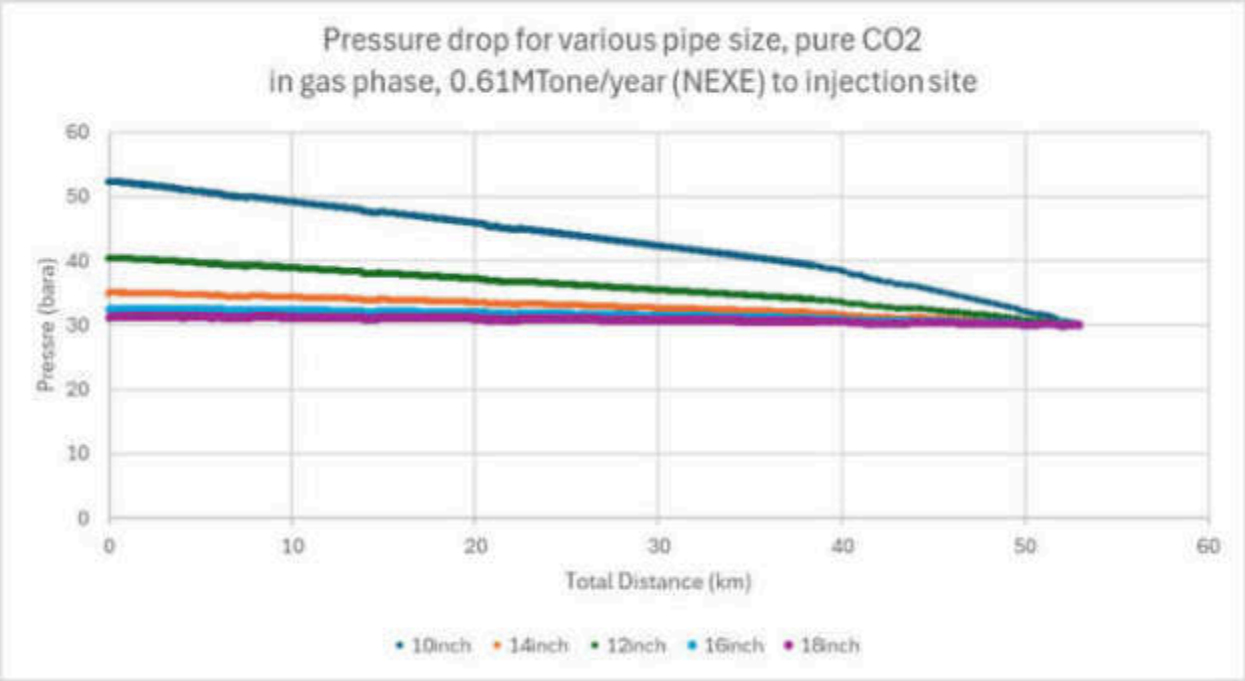


Fig. 1.4 Pressure drop for various pipeline sizes - gas phase
Pure CO_2, in gas phase, 0.61MT/y from NEXE to the injection site

1.2 Transportation and capture method comparison

The safe, efficient, and cost-effective transportation of carbon dioxide (CO_2) is a critical enabler for large-scale Carbon Capture, Utilization, and Storage (CCUS) projects. As governments and industry advance toward net-zero targets, a clear understanding of the available CO_2 transport options—including their technical capabilities, limitations, economics, and risk profiles—is essential for project developers, policymakers, and investors.

This report presents a comprehensive technical and commercial assessment of the five principal CO_2 transport modalities: pipelines, ship (marine) transport, road tankers, rail transport, and emerging innovative solutions. For each option, it provides real-world project examples, quantitative performance metrics, and a structured evaluation of advantages and limitations.

Key Findings

- Pipelines remain the dominant and most cost-efficient solution for large-scale, continuous CO_2 transport.
- Ship transport is rapidly gaining commercial momentum, particularly for offshore storage hubs, emerging markets, and early-stage CCUS developments, with several European projects having reached Final Investment Decision (FID).
- Road and rail transport continue to play an important role in small-scale, distributed, and industrial CO_2 supply chains, including food-grade applications.

Copyright © SLB. All Rights Reserved. Private & Confidential. Reproduction only by permission.

1.2.1 Transport solution comparison

Table 1.2 CO_2 Transport Methods at a Glance

Method	Typical Phase	Scale	Cost Range (USD/tCO_2)	Maturity	Key Use Case
Pipeline	Liquid / Dense	Large (>0.1 Mtpa)	$1–8/ tCO_2/100km	Commercial	Onshore/offshore CCS hubs
Ship	Liquid (cryogenic)	Medium–Large	$15–30/$tCO_2$	Early commercial	Offshore & cross-border CCS
Road Tanker	Liquid / Gas	Small (<1,000 t/d)	$50–150/$tCO_2$	Commercial	Industrial/food supply
Rail	Liquid / Gas	Small–Medium	$30–80/$tCO_2$	Commercial	Mid-distance, no pipeline
Innovative	Various	Varies	TBD	Emerging/R&D	Niche & future applications

1.2.1.1 Dedicated CO_2 Pipelines

Pipelines are the backbone of large-scale CO_2 transport infrastructure. CO_2 is compressed to supercritical or dense-phase conditions (typically >73.8 bar and >31.1°C) to achieve liquid-like density while maintaining gas-like viscosity. This maximizes throughput while minimising pumping energy. Steel pipelines (carbon or corrosion-resistant alloys) with internal diameter ranging from 8 to 42 inches are used, depending on flow volumes.

Key Technical Parameters

Parameter	Typical Value / Range
Operating Pressure	80–200 bar (dense/supercritical phase)
Operating Temperature	10–40°C (onshore); –10 to +30°C (offshore)
Pipeline Diameter	8–42 inches (200–1,050 mm)
Flow Rate Capacity	0.1 – 40+ Mtpa per pipeline
Transport Cost	$1–8 per tonne per 100 km
Pipeline Material	Carbon steel (X65/X70), internally coated or inhibited
CO_2 Purity Required	>95% CO_2; water content <50 ppmv (to prevent corrosion)
Recompression Stations	Every 100–200 km for onshore pipeline

Advantages vs. Disadvantages

✓ ADVANTAGES	✖ DISADVANTAGES
Lowest cost per tonne for high-volume, continuous flows	Very high capital expenditure ($1–4M per km onshore; $3–8M/km offshore)
Proven, commercially mature technology with decades of operating history	Requires large, sustained CO_2 volumes to justify investment
High throughput capacity (0.1–40+ Mtpa per line)	Routing constraints: terrain, land rights, populated areas
Low operational energy intensity once established	CO_2 purity specifications are strict — impurities cause corrosion
Can serve as open-access shared infrastructure for multiple emitters	Risk of sudden large-volume release in rupture events (asphyxiation hazard)
Subsea variants enable offshore storage site access	Regulatory frameworks for CO_2 pipelines are still evolving in many jurisdictions
Long asset life (30–50+ years) with low marginal operating cost	Long lead times (5–15 years from planning to commissioning)

Detailed Real-World Examples

Copyright © SLB. All Rights Reserved. Private & Confidential. Reproduction only by permission.

Denbury Green Pipeline — USA
Operator: Denbury Resources (acquired by ExxonMobil, 2023). The Denbury CO_2 pipeline network is the largest dedicated CO_2 pipeline system in the United States, spanning over 1,300 miles (2,100 km) across the Gulf Coast and Rocky Mountain regions. Originally developed to supply CO_2 for Enhanced Oil Recovery (EOR), the network is now being repurposed and extended to serve CCUS projects under ExxonMobil's low-carbon strategy. Flow capacity exceeds 40 Mtpa across the combined network.

Northern Lights / Longship Project — Norway
Operator: Equinor, Shell, TotalEnergies. The Longship project includes a CO_2 pipeline from the Sleipner receiving terminal to the Aurora storage site beneath the North Sea. The offshore pipeline is 110 km long, operates at dense-phase conditions, and targets an initial capacity of 1.5 Mtpa, scalable to 5 Mtpa. This is Europe's first full-chain open-access CCS infrastructure project.

Weyburn-Midale CO_2 Project — Canada
Operator: Cenovus Energy / Apache (now Occidental). CO_2 captured from the Great Plains Synfuels Plant in North Dakota is transported via a 320-km pipeline into Saskatchewan, Canada, for EOR and permanent geological storage. The pipeline transports approximately 3 Mtpa of CO_2 and has been operating since 2000, making it one of the longest-running commercial CO_2 pipeline systems in the world.

1.2.1.2 Ship/Marine Transport

Ship transport of CO_2 involves liquefying CO_2 at low temperatures (approximately −52°C at 6–7 bar, or −29°C at 15 bar) and loading it into insulated, pressure-rated cargo tanks aboard semi-refrigerated or fully refrigerated tankers. This method is directly analogous to LPG (liquefied petroleum gas) shipping and leverages mature maritime engineering.

The CO_2 is loaded at an onshore liquefaction terminal, shipped to an offshore injection platform or reception terminal, and injected into sub-seabed geological formations. Ship transport decouples the emitter location from the storage site, enabling flexible cross-border and intercontinental CO_2 logistics.

Key Technical Parameters

Parameter	Typical Value / Range
Cargo Tank Condition	Liquid CO_2, ~−52°C at 6–7 bar (mid-pressure)
Vessel Capacity	Current: 7,500 m^3; Planned: 20,000–40,000 m^3
Annual Throughput (fleet)	0.5–5 Mtpa per dedicated vessel fleet
Transport Cost	$15–30 per tonne (varies by distance)
Boil-off Rate	~0.1–0.2% per day (insulated tanks)
Loading/Discharge Time	12–36 hours per voyage (port-dependent)
Export Terminal Requirement	Liquefaction plant, jetty, storage buffer tanks

Copyright © SLB. All Rights Reserved. Private & Confidential. Reproduction only by permission.

Advantages vs. Disadvantages

✓ ADVANTAGES	✖ DISADVANTAGES
Flexible routing — no fixed pipeline infrastructure required	Higher cost per tonne than pipelines at large scale (>5 Mtpa)
Enables cross-border CO_2 trade and shared storage hubs	Requires liquefaction energy and infrastructure at export terminal
Scalable: fleet size can be adjusted to match volume growth	CO_2 boil-off losses during loading, transit, and unloading
Leverages mature LPG shipping industry expertise and assets	Weather/port constraints introduce scheduling and supply risk
Lower upfront capital per project than a dedicated pipeline	Limited vessel fleet size available currently (global supply constrained)
Ideal for early-phase CCUS before pipeline networks are built	GHG emissions from vessel propulsion (improving with LNG/ammonia propulsion)
Can serve emitters in islands or regions with no pipeline access	Intermediate storage buffer tanks add cost and footprint

Detailed Real-World Examples

Northern Lights — Ship Transport Segment (Norway)

The Northern Lights project (Equinor/Shell/TotalEnergies) initially relies on ship transport while the offshore pipeline is constructed. Captured CO_2 from Heidelberg Materials' cement plant in Brevik and Hafslund Oslo Celsio's waste-to-energy plant in Oslo is liquefied and loaded onto the 7,500 m^3 CO_2 tanker 'Solitaire' (operated by Nippon Yusen Kaisha) for the journey to the Øygarden terminal on the west coast of Norway, then injected into the Aurora storage formation 2,600 metres below the seabed.

CCUS Hub — Harbour Energy / Ervia (Ireland to UK)

The Viking CCS project led by Harbour Energy proposes ship transport of liquefied CO_2 from Irish emitters across the Irish Sea to the Endurance storage site in the UK Southern North Sea. This cross-border arrangement demonstrates ship transport's unique ability to serve emitters in countries without domestic geological storage capacity.

Mitsubishi / MOL — Japan Pilot (2021–2024)

Japan's NEDO-funded pilot project transported a 1,000-tonne cargo of liquefied CO_2 in a small carrier (the 'Takachiho Maru') from Hokkaido to Tomakomai for offshore storage. This was the world's first ship-based CO_2 transport to a dedicated offshore storage site, validating the full loading, transport, and injection chain at pilot scale.

1.2.1.3 Road Tanker Transport

Road tankers transport liquid CO_2 in insulated cryogenic semi-trailers, typically carrying 15–30 tonnes per load at approximately –20°C and 20 bar. This is the most established CO_2 distribution method for small-scale industrial and commercial consumers, including food and beverage carbonation, fire suppression systems, welding/metal fabrication, dry ice production, and pharmaceutical applications.

Copyright © SLB. All Rights Reserved. Private & Confidential. Reproduction only by permission.

Key Technical Parameters

Parameter	Typical Value / Range
Tank Capacity	15–30 tonnes per semi-trailer
Cargo Condition	Liquid CO_2 at ~–20°C, ~20 bar
Tank Type	Vacuum-insulated cryogenic vessel
Annual Throughput	<0.5 Mtpa per large operator fleet
Transport Cost	$50–150 per tonne (highly distance-sensitive)
Maximum Practical Range	~500–800 km (limited by economics and regulations)
Delivery Frequency	Daily to weekly, depending on customer demand

Advantages vs. Disadvantages

✓ ADVANTAGES	✖ DISADVANTAGES
Maximum flexibility — no fixed infrastructure required	Highest cost per tonne of all transport methods at scale
Commercially mature and widely available globally	Very low throughput — impractical for CCUS volumes above ~50,000 tpa
Low capital entry — uses existing vehicle and road infrastructure	Road congestion, traffic regulation, and Hours of Service limits
Excellent for small, dispersed, or remote customer locations	High carbon footprint from diesel trucking (partially offset by alternative fuels)
Rapid deployment for new customers or locations	Driver shortage and logistics complexity in high-growth markets
Door-to-door delivery capability with precise volume control	Road damage and community impact of heavy HGV movements
Highly regulated supply chain ensuring CO_2 quality and safety	Only economical within ~500 km of liquefaction source

Detailed Real-World Examples

Air Products & BOC / Linde — Global Industrial CO_2 Distribution

Industrial gas majors such as Air Products, BOC (Linde), Air Liquide, and Messer operate global fleets of road tankers numbering in the thousands. In the UK alone, BOC operates one of Europe's largest CO_2 tanker fleets, supplying food-grade liquid CO_2 to major breweries (Heineken, Carlsberg, AB InBev), soft drink manufacturers (Coca-Cola, PepsiCo), and supermarket chains. The supply chain relies on CO_2 sourced from ammonia plants and bioethanol fermentation, liquefied, and distributed by road within a 400–600 km radius.

CCUS Pilot Projects — Small-Scale Direct Air Capture

In early-phase CCUS projects and Direct Air Capture (DAC) deployments, road tankers serve as the primary CO_2 transport method before permanent infrastructure is in place. For example, Climeworks' Orca and Mammoth DAC plants in Iceland transported initial batches of captured CO_2 via tanker to nearby CarbFix mineral storage injection points before on-site piping was complete.

1.2.1.4 Rail Transport

Rail transport of CO_2 uses dedicated cryogenic tank wagons (railcars) coupled into unit trains. Each wagon carries 50–80 tonnes of liquid CO_2, providing far greater per-trip capacity than road tankers. Rail is particularly suitable for medium-distance transport (200–1,000 km) in regions with established freight rail networks but without CO_2 pipeline infrastructure. The method is widely used for industrial gas distribution in the USA, Eastern Europe, and Australia.

Copyright © SLB. All Rights Reserved. Private & Confidential. Reproduction only by permission.

Key Technical Parameters

Parameter	Typical Value / Range
Tank Wagon Capacity	50–80 tonnes liquid CO_2 per wagon
Train Consist (typical)	20–60 wagons per unit train
Throughput per Train	1,000–5,000 tonnes per trip
Cargo Condition	Liquid CO_2 at –20°C to –28°C, ~20 bar
Transport Cost	$30–80 per tonne (route-dependent)
Practical Range	200–2,000 km (economically competitive)
Terminal Requirements	Loading/unloading sidings, storage tanks, refrigeration

Advantages vs. Disadvantages

✓ ADVANTAGES	✖ DISADVANTAGES
Higher throughput per trip than road tankers (3–5× capacity per wagon)	Dependent on suitable rail freight network and gauge compatibility
Lower carbon intensity per tonne-km than road transport	Limited flexibility — fixed by rail network routing
Cost-effective for medium distances (200–1,000 km)	Requires dedicated terminal facilities (sidings, cryogenic storage)
Existing freight rail infrastructure in many regions	Transit times can be unpredictable (network congestion, priority rules)
Reduced road congestion and community impact vs. HGV fleets	Less accessible than road for remote or off-rail locations
Can be combined with last-mile road delivery for full distribution	Higher empty return-wagon costs vs. shared road fleets
Less sensitive to fuel price volatility than road transport	Not suitable for offshore storage applications

Detailed Real-World Examples

Praxair / Linde Rail Operations — United States

In the United States, industrial gas companies including Praxair (now Linde) and Air Products operate fleets of CO_2 tank wagons to distribute CO_2 from large production facilities in the Gulf Coast (sourced from ammonia plants and ethanol production) to industrial users across the Midwest and Southeast. Unit trains of 30–60 wagons deliver up to 3,000 tonnes per trip, making this the economically preferred option for distances of 400–1,200 km where pipelines are unavailable.

Eastern Europe — Cross-Border Rail CO_2 Distribution

In Eastern Europe, where CO_2 pipeline infrastructure is sparse, industrial gas companies such as Messer and Air Liquide rely heavily on rail for inter-country distribution. Poland, Czech Republic, Hungary, and Romania are interconnected via rail CO_2 tank wagon networks, with CO_2 sourced from ammonia and petrochemical facilities and transported to regional distribution hubs.

1.2.1.5 Innovative & Emerging Transport Methods

Beyond the four established transport methods, several emerging and innovative approaches are under development or early deployment for specific CCUS applications. These range from modular containerised systems to novel carrier fluids and conversion pathways.

Containerised / ISO Tank Transport

ISO 20-foot tank containers rated for cryogenic liquid CO_2 (up to 20 tonnes per container) can be

Copyright © SLB. All Rights Reserved. Private & Confidential. Reproduction only by permission.

transported intermodally — by road, rail, and ship — without transferring the CO_2 itself. This provides maximum logistical flexibility for distributed small emitters (e.g., DAC plants, biogas upgraders) supplying CO_2 to shared aggregation hubs. Companies such as Messer and Cryostar are developing standardised CO_2 ISO containers optimised for CCUS feeder applications.

CO_2 Conversion and Carrier Approaches
Research programmes in Japan (NEDO), the EU (Horizon Europe), and the US DOE are investigating conversion of CO_2 into more easily transportable carrier molecules such as methanol, formic acid, or synthetic natural gas (methanation) — which can be transported via existing gas/chemical infrastructure. While not pure CO_2 transport, these pathways allow CO_2 to be embedded in value-added products distributed through existing logistics chains.

Dense-Phase CO_2 in Flexible Hose Systems (Subsea)
For offshore CCUS applications, flexible riser and flowline technology is being adapted for dense-phase CO_2 injection service. Projects such as the Sleipner and Snøhvit (Equinor) fields use dedicated subsea CO_2 injection flowlines that are distinct from rigid pipelines, enabling tie-back of injection wells at varying water depths (up to 2,500 m). Flexible CO_2 service hoses for ship-to-platform transfer are also under qualification by companies including TechnipFMC and Trelleborg.

Drone / Autonomous Vessel CO_2 Micro-Transport (Conceptual)
At the very early research stage, autonomous underwater vehicles (AUVs) and surface vessels are being investigated for micro-scale CO_2 delivery to distributed sub-seabed injection points — particularly relevant for archipelago nations (Indonesia, Philippines) and small-island developing states without pipeline or large tanker port infrastructure. No commercial deployment exists as of 2026.

Advantages vs. Disadvantages

✓ ADVANTAGES	✖ DISADVANTAGES
Intermodal ISO tanks offer maximum supply chain flexibility	Generally higher cost per tonne than established methods
No new large-scale infrastructure required for early-phase projects	Most approaches still at pilot or R&D stage — unproven at commercial scale
Conversion pathways (e-methanol, SNG) leverage existing infrastructure	Conversion pathways involve energy penalty and CO_2 accounting complexity
Subsea flexible systems enable deepwater storage access	Regulatory standards for new vessel/container types still being established
Modular approaches can scale incrementally with CCUS project growth	Long development timelines before commercial readiness

1.2.1.6 Comparative Analysis&Method Selection Framework

Selecting the optimal CO_2 transport method requires balancing volume, distance, geography, project maturity, and available infrastructure. The table below provides a consolidated comparison across key decision criteria.

Copyright © SLB. All Rights Reserved. Private & Confidential. Reproduction only by permission.

Key Decision Criteria Comparison

Criterion	Pipeline	Ship	Road Tanker	Rail	Innovative
Cost at Scale	★★★★★	★★★☆☆	★☆☆☆☆	★★★☆☆	★★☆☆☆
Volume Capacity	★★★★★	★★★★☆	★☆☆☆☆	★★☆☆☆	★★☆☆☆
Flexibility	★☆☆☆☆	★★★★☆	★★★★★	★★★☆☆	★★★★☆
Capital Cost	★☆☆☆☆	★★★☆☆	★★★★★	★★★★☆	★★★☆☆
Technology Maturity	★★★★★	★★★☆☆	★★★★★	★★★★☆	★★☆☆☆
Environmental Impact	★★★★☆	★★★☆☆	★★☆☆☆	★★★☆☆	★★★☆☆
Offshore Suitability	★★★★☆	★★★★★	★☆☆☆☆	★☆☆☆☆	★★★☆☆
Cross-Border Capability	★★☆☆☆	★★★★★	★★★☆☆	★★★☆☆	★★★☆☆

★★★★★ = *Excellent* | ★★★☆☆ = *Good* | ★★☆☆☆ = *Fair* | ★☆☆☆☆ = *Poor*

Decision Flowchart Guidance

- If volume > 1 Mtpa and geography allows: evaluate dedicated pipeline as primary option.
- If offshore storage or cross-border logistics required: evaluate ship transport, potentially with pipeline as long-term follow-on.
- If volume < 100,000 tpa or locations are dispersed: road tanker is likely the only practical option.
- If medium distance (200–1,000 km) with rail access: evaluate rail as a cost-effective middle-ground solution.
- For early-phase, pilot, or DAC projects: ISO container intermodal or road tanker provides maximum flexibility.

1.2.1.7 Regulatory& Safety Considerations

CO_2 transport is subject to a growing body of national and international regulation. Key considerations include:

Pipeline Regulation

- USA: CO_2 pipelines are regulated by PHMSA under 49 CFR Part 195 (hazardous liquid pipelines). New rules proposed in 2022–2023 would tighten emergency response, valve spacing, and class location requirements following incidents such as the Satartia, Mississippi CO_2 pipeline rupture (2020).
- EU: The revised EU CCS Directive (2009/31/EC) and emerging Hydrogen/CO_2 network regulations govern cross-border CO_2 infrastructure.
- UK: The Energy Act 2023 establishes the CO_2 Transport & Storage regulatory framework, with the North Sea Transition Authority (NSTA) as permitting authority.

Ship Transport Regulation

- CO_2 tankers are regulated under the IMO International Gas Carrier Code (IGC Code) for cargo tank design, stability, and gas detection.

Copyright © SLB. All Rights Reserved. Private & Confidential. Reproduction only by permission.

- Ship-to-shore transfers and loading arms are subject to OCIMF and SIGTTO guidelines.
- Classification societies (DNV, Lloyd's Register, Bureau Veritas) are developing CO_2 carrier class notations specific to CCUS applications.

Road & Rail Transport Regulation

- Road: ADR (European Agreement on the Transport of Dangerous Goods by Road) governs liquid CO_2 transport in Europe. In the USA, DOT HMR 49 CFR applies.
- Rail: RID (Regulation for the International Carriage of Dangerous Goods by Rail) in Europe; AAR Tank Car Standards in the USA.

Safety Note — Satartia, Mississippi (2020)
A 24-inch CO_2 pipeline operated by Denbury Green Pipeline ruptured in February 2020, releasing approximately 7,700 tonnes of CO_2. The dense gas cloud displaced oxygen in a valley, causing 45 people to require medical attention and hundreds of residents to be evacuated. This incident prompted a significant reassessment of CO_2 pipeline emergency response planning, valve spacing requirements, and community risk communication — and underscores the importance of robust safety management for all CO_2 transport methods.

1.2.1.8 Conclusions&Recommendations

The global CCUS industry requires a portfolio of CO_2 transport solutions tailored to project scale, geography, timeline, and regulatory environment. No single method dominates across all use cases.

- Pipelines will remain the dominant method for large, sustained flows at the heart of CCUS infrastructure clusters — but require substantial capital, volume certainty, and long lead times.
- Ship transport is the method of the moment for European CCUS scale-up, enabling flexible access to offshore storage without requiring committed pipeline routes during the early commercialisation phase.
- Road tankers and rail provide essential feeder and distribution functions for small emitters, food-grade markets, and early-phase projects, but are economically unsuitable for gigatonne-scale storage.
- Innovative approaches — ISO container intermodal, flexible subsea systems, and conversion pathways — will play growing niche roles, particularly for DAC and distributed CCUS applications.

Strategic Recommendation
For new CCUS projects in 2024–2030, the recommended approach is to plan for ship transport as the initial phase (enabling early CO_2 monetisation and volume ramp-up), with a phased transition to pipeline infrastructure once sustained volumes above 1–2 Mtpa are demonstrated. This dual-track approach mirrors the successful model employed by the Northern Lights project and is increasingly endorsed by the IEA, IEF, and major energy companies.

Copyright © SLB. All Rights Reserved. Private & Confidential. Reproduction only by permission.

1.2.2 CO_2 stream composition

Captured CO_2 is never pure. The way it behaves in pipelines, compressors and storage wells is governed less by the headline "CO_2 %" and more by the type and concentration of the impurities it carries. This report draws together the three questions that most often drive a CCS design decision: what the CO_2 stream is made of, what it costs to capture, and how it should be conditioned and transported.

Composition controls integrity. Water, oxygen, light gases (H_2, N_2, Ar, CH_2...), and acid/toxic species (SO , NO , H_2S, CO) each create distinct corrosion, hydrate, embrittlement and safety risks. Free water with CO_2 forms carbonic acid that can corrode carbon steel at rates up to ~20 mm/yr.

CO_2 Composition Stream in Typical CCS Operations

A CCS chain moves CO_2 from an emitter through capture, conditioning, compression and transport to permanent storage. The composition of the stream is set at capture and "locked in" at the conditioning step, which is the specification gate the stream must pass before it enters shared infrastructure.

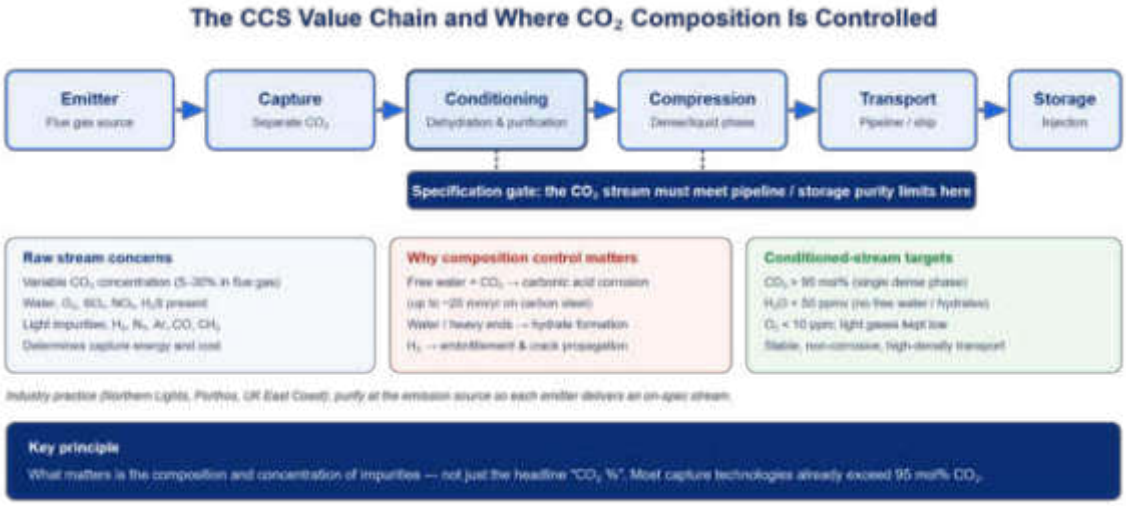


Fig. 1.5 CCS Value Chain - CO_2 Composition Evolution

Why composition — not just "CO_2 %" — matters

Most capture technologies already deliver more than 95 mol% CO_2, so the purity headline rarely distinguishes one stream from another. What distinguishes them, and what governs material selection and operating windows, is the identity and concentration of the remaining few percent. A stream that is 96% CO_2 with a little water behaves very differently from one that is 96% CO_2 with a percent of hydrogen or a few hundred ppm of H_2S.

Insight. Because the impurity slate — not the CO_2 percentage — drives risk, specifications are best written component-by-component (water, O_2, H_2, H_2S, SO , NO , CO...) rather than as a single minimum-purity number.

Copyright © SLB. All Rights Reserved. Private & Confidential. Reproduction only by permission.

Effect of light impurities on the phase envelope

Light impurities — H_2, Ar, N_2, CO, CH_2 and C_2H_2 — shift the CO_2 phase envelope: they raise the bubble-point curve and lower the critical temperature of the mixture. The practical consequences are:

- Minimal effect on gaseous-phase operation.
- A significant effect on maintaining a single liquid or dense phase — the preferred state for efficient transport.
- Compression challenges and reduced storage capacity because the mixture is less dense.

Hydrogen is the worst offender. Because of its low molecular weight, H_2 raises the bubble-point curve the most and reduces density significantly. In two-phase regions it preferentially partitions into the gas phase, raising the H_2 partial pressure in any bubbles, which in turn raises the risk of hydrogen-enhanced crack propagation in steel. Carbon monoxide (CO) is treated separately as a toxic impurity whose limits are driven by health and safety rather than by phase behaviour.

Fig. 1.6. shows schematic of how light impurities shift the CO_2 phase envelope (after Luna-Ortiz et al., 2022).

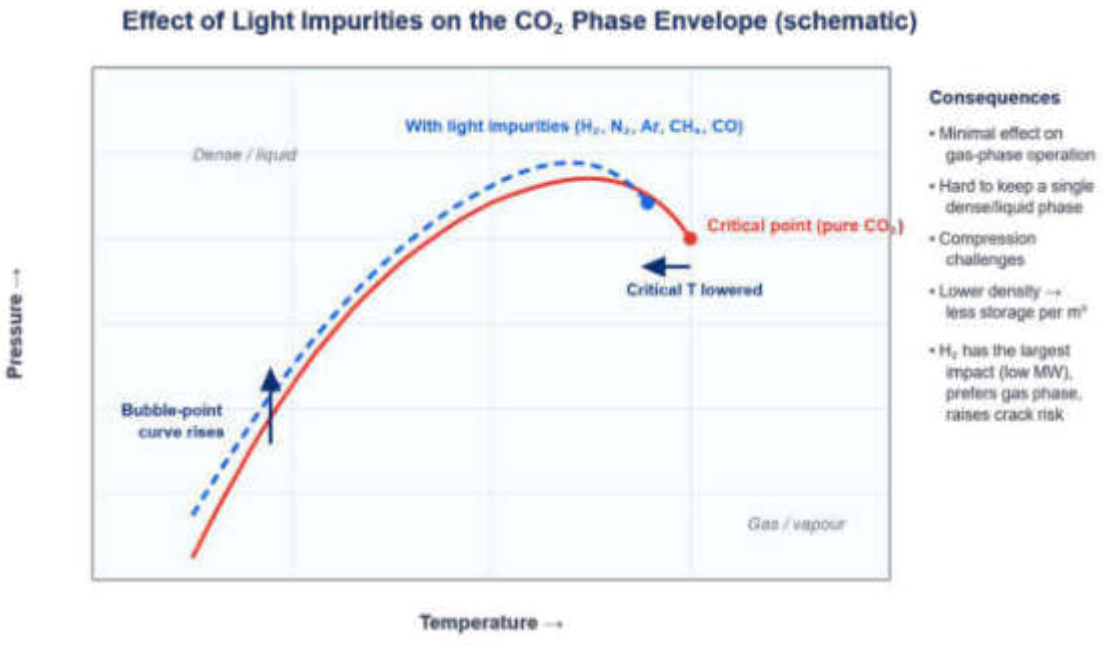


Fig. 1.6 Effect of Impurities on CO_2 Phase Envelope

Copyright © SLB. All Rights Reserved. Private & Confidential. Reproduction only by permission.

Water and oxygen — the corrosion drivers

Water is the single most important impurity to control. When water in the CO_2 exceeds its solubility it forms a separate aqueous phase, which leads to:

- Corrosion of carbon steel — up to ~20 mm/yr — from the carbonic acid formed when CO_2 dissolves in water.
- Accelerated corrosion and cracking when water is combined with other impurities such as SO_2, NO and H_2S.
- Hydrate formation and the operational problems that follow (blockages, instrumentation issues).

Design intent is no free water anywhere in the system. For the CO_2–H_2O binary the maximum water dew point is about –28°C at 14 barg; in practice a water content of 50 ppmv maximum is targeted to avoid corrosion and hydrate risk. Oxygen must be kept below ~10 ppm to avoid corrosion in the pipeline and wellbore — a problem that is worst when O_2 and water occur together.

Impurity risk map

The four families of impurities and their control limits are summarised below. The limits shown are representative of the ranges adopted across current European CCS projects.

Fig. 1.7. Tabulates typical CO_2 Impurity risk map: drivers and representative limits for a CO_2 transport stream.

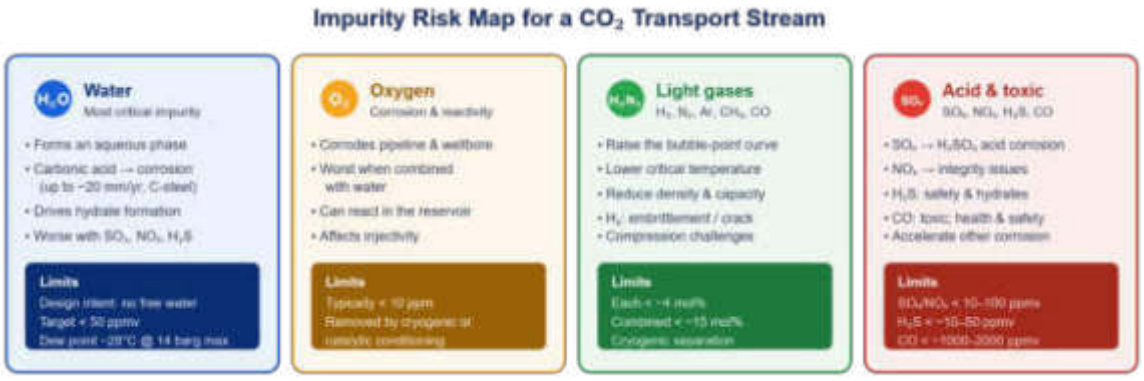


Fig. 1.7 Impurity Risk Map

Representative purity requirements for CCS

Table 1 lists indicative component limits for a generic CCS application alongside the CHA reference composition (the NEXE cement plant), the technical challenge each component poses, and the purification technology typically used to address it.

Copyright © SLB. All Rights Reserved. Private & Confidential. Reproduction only by permission.

Table 1.3 Purification and Conditioning Requirements

Component	Required level	CHA project (NEXE cement)	Technical challenge	Purification technology
CO_2	>95%	85–90%	Maintain miscibility & efficiency	(see note)
H_2O	<50 ppmv	<600 ppm	Prevent corrosion & hydrate formation; critical to control carbonic-acid formation	Molecular sieve / TSA / dehydration
H_2S	<10–50 ppmv	<10 ppm	Safety & hydrate prevention	Amine absorption / scavengers
N_2, Ar, H_2	<4% (each)	<15% (combined, with CH_4)	Avoid miscibility-pressure increase; H_2 embrittlement *	Cryogenic separation
O_2	<10 ppmv	<15% (combined, with CH_4)	Avoid pipeline / wellbore corrosion, worst when combined with water *	Cryogenic, catalytic reaction
CO	<2000 ppmv	<1000 ppm	Health & safety *	PSA / cryogenic
NO	<100 ppmv	<25 ppm	Corrosion & integrity	Chemical scrubbing (amines, alkaline washing)
SO	<50 ppmv	<25 ppm	Acid formation (H_2SO_4) & corrosion	Chemical scrubbing (amines, alkaline washing)
Hydrocarbons	<2%	combined <15 mol% (with N_2, Ar, H_2, O_2)	Hydrate formation & miscibility — raises pressure	Cryogenic, PSA

*Table 1.3 Purity requirements for CCS applications. * Other problems at geological storage: storage-capacity reduction, decreased injectivity and reduced solubility trapping. Note: what matters more is the composition and concentration of impurities, not just CO_2 %; most capture technologies achieve >95 mol%. After Zeina Abbas et al., Energy Procedia 37 (2013).*

Reference composition: the CHA / NEXE cement plant

The reference case for this study is the CHA composition based on the NEXE cement plant in Croatia. Three features define it:

1. **Wide-range CO_2 (85–90 mol%).** Lower than the >95% target, so the stream sits closer to the boundary where light impurities can disturb the phase behaviour.
2. **Very high water content (<600 ppm).** Well above the 50 ppm pipeline target; the stream carries a real risk of hydrate formation and must be dehydrated after capture.
3. **Combined light gases (H_2, N_2, Ar, CH_2, O_2) below ~15 mol%, with O_2 specifically below 10 ppm.**

Climate context. The Bockovac area sees winter lows of –5 to –1°C and summer averages of 17–30°C. Within the relevant operating window (illustrative points at –25°C / 11 bar and 16°C / 48 bar), a 600 ppm water content sits inside the hydrate-formation region, whereas drying to 50 ppm moves the hydrate boundary safely away from operating conditions.

Conclusion. The NEXE composition has a maximum water content of 600 ppm that carries hydrate risk; dehydration must take place after capture to meet the pipeline specification (<50 ppm) and so avoid corrosion and hydrate problems.

Copyright © SLB. All Rights Reserved. Private & Confidential. Reproduction only by permission.

Table A1 benchmarks the component limits of six CCS projects. It highlights how widely specifications vary, and underlines the CHA / NEXE reference characteristics: a wide CO_2 range (>85%), a very high water allowance (<600 ppm), and combined light gases (H_2, N_2, Ar, CH_4, O_2) below 15 mol%, with O_2 below 10 ppm in stricter specs.

Table 1.4 CCS Projects Specification (Benchmark)

Specification	Horisont Energi	Carbfix	INEOS	Northern Lights	Porthos	Croatia (NEXE)
CO_2	≥ 98 mol%	≥ 95%	—	≥ 99 mol%	≥ 95 mol%	> 85
H_2O	≤ 10 ppm (mol)	< 480 kg *	≤ 30 ppm	≤ 30 ppm	≤ 70 ppm	< 600 ppm
H_2	≤ 600 ppm (mol)	≤ 1%	≤ 50 ppm	≤ 50 ppm	≤ 0.75 mol%	**< 15% mol (combined H_2, N_2, Ar, CH_4, O_2)**
N_2	≤ 0.32 mol%	< 4%	—	—	≤ 2.4 mol%	
Ar	< 0.5 mol%	< 1 ppmv	—	—	≤ 0.4 mol%	
CH_4	< 0.91 mol%	—	—	—	≤ 1 mol%	
O_2	≤ 10 ppm (mol)	< 10 ppmw	≤ 10 ppm	≤ 10 ppm	≤ 40 ppm	
CO	< 300 ppm (mol)	< 4250 ppmv	≤ 100 ppm	≤ 100 ppm	≤ 750 ppm	< 1000 ppm
H_2S	≤ 9 ppm (mol)	≤ 20 ppmv	≤ 9 ppm	≤ 9 ppm	≤ 5 ppm (sulfur ≤ 20 ppm)	< 10 ppm
SO	≤ 10 ppm (mol)	< 1 ppmw	≤ 10 ppm	≤ 10 ppm	—	< 25 ppm
NO	≤ 10 ppm (mol)	< 1 ppmw	≤ 10 ppm	≤ 10 ppm	≤ 5 ppm	< 25 ppm
Ammonia	—	< 50 ppmv	—	≤ 10 ppm	≤ 3 ppm	< 10 ppm
Amine	—	< 1 ppmv	—	≤ 10 ppm	≤ 1 ppm	< 10 ppm
Formaldehyde	—	—	—	≤ 10 ppm	≤ 10 ppm	—
Hg	≤ 0.03 ppm (mol)	≤ 0.03 mg/L	≤ 20 ppm	≤ 0.03 ppm	—	< 0.001 ppm
Arsenic	—	≤ 0.1 mg/L	—	—	—	—
Lead	—	≤ 0.2 mg/L	—	—	—	—
Chromium	—	≤ 0.5 mg/L	—	—	—	—
Copper	—	≤ 0.5 mg/L	—	—	—	—
Nickel	—	≤ 0.5 mg/L	—	—	—	—
Zinc	—	≤ 0.5 mg/L	—	—	—	—
Dioxins, furans	—	≤ 1.5 mg/L	—	—	—	—
Glycol	—	≤ 40 kg/m^3	—	—	—	—
Sulfur	—	< 35 ppmw	—	—	—	—
C_2	≤ 2 mol	—	—	—	—	—
Total VOCs †	—	—	—	—	—	< 100 ppm
Solids / particles / dust	—	—	—	—	—	< 1 mg/Nm^3

Copyright © SLB. All Rights Reserved. Private & Confidential. Reproduction only by permission.

*Table 1.4. Comparison of CO_2 stream specifications across CCS projects. * Mass-based water allowance. † Total volatile organic compounds: formaldehyde (CH_2O), acetaldehyde (CH_3CHO), methanol (CH_3OH), ethanol (C_2H_5OH), BTEX, ethylene (C_2H_4), ethane (C_2H_6), aliphatic hydrocarbons (C_3+) and hydrogen cyanide (HCN). Blank cells (—) indicate no published limit.*

1.2.3 CO_2 capture cost comparison

Cost in a CCS project is concentrated in the capture step. Understanding what drives capture cost — and how the main capture technologies compare — is therefore central to project economics.

Cost across the value chain

Of the three CCS activities, capture is by far the largest, representing roughly 70–80% of total cost. Transport adds 10–15% and storage 10–25%. The figure below shows the reported cost ranges per tonne of CO_2 for each activity.

Fig. 1.8. Reported cost ranges across the CCS value chain (transport quoted per 100 km).



Fig. 1.8 Reported cost ranges across CCS value chain

What drives capture cost

Six factors govern how expensive it is to capture CO_2 from a given source:

1. **CO_2 partial pressure.** This indicates how easily CO_2 can be separated from a gas mixture. Higher partial pressures make capture easier and cheaper because less external energy is needed to reach the pressure of the final CO_2 stream; lower partial pressures are more energy-intensive and costly.

Copyright © SLB. All Rights Reserved. Private & Confidential. Reproduction only by permission.

2. **Flue CO_2 concentration.** Gas processing >60 mol%; coal power ~14–30 mol%; cement typically ~10–30 mol%; gas-fired power <5 mol%. The more dilute the stream, the higher the cost.
3. Technology type.
4. Plant size.
5. Energy requirement.
6. Capture rate.

Table 1.5 shows how CO_2 partial pressure — the key cost lever — varies across point sources. Cement and power streams sit at the low-pressure, harder-to-capture end; gas processing, fertiliser and ethanol streams are far easier because CO_2 is concentrated (and in some cases captured inherently as part of the process).

Table 1.5 Typical CO2 Partial Pressures by Source

Industry	Point source	CO_2 partial pressure (wet), kPa	Inherent CO_2 capture
Power	Natural gas combined cycle (NGCC)	3.8 – 4.6	No
Power	Coal-fired power plant	12.2 – 14.2	No
Power	Biomass / waste-fired power plant	10.1 – 12.2	No
Cement	Kiln flue gas	~18	No
Cement	Pre-calciner	20 – 30	No
Iron & steel	COREX smelting reduction	32 – 35	No
Iron & steel	Hot stove	24 – 28	No
Petrochem	Steam methane reforming (H_2)	300 – 480	No
Fertiliser	Coal gasification syngas	750 – 2500	Yes *
Fertiliser	Natural gas reforming syngas	300 – 1200	Yes *
Natural gas	Natural gas processing	Varies, up to 5000	Yes (acid-gas removal)
Bioethanol	Ethanol fermentation	>85	Yes **

** CO_2 from the syngas stream is captured for downstream urea production. ** Only dehydration and compression required. Gas-stream pressure is atmospheric unless noted. After Global CCS Institute (2021).*

Capture technology comparison

The four most common capture technologies — absorption, adsorption, membrane and cryogenic — trade off cost, energy, recovery and maturity in different ways. Figure 5 compares them across capture cost, energy use and CO_2 recovery; Table 3 gives the detailed comparison.

Fig. 1.9 Capture-technology comparison across cost, energy and recovery (after Font-Palma et al., 2021).

Copyright © SLB. All Rights Reserved. Private & Confidential. Reproduction only by permission.

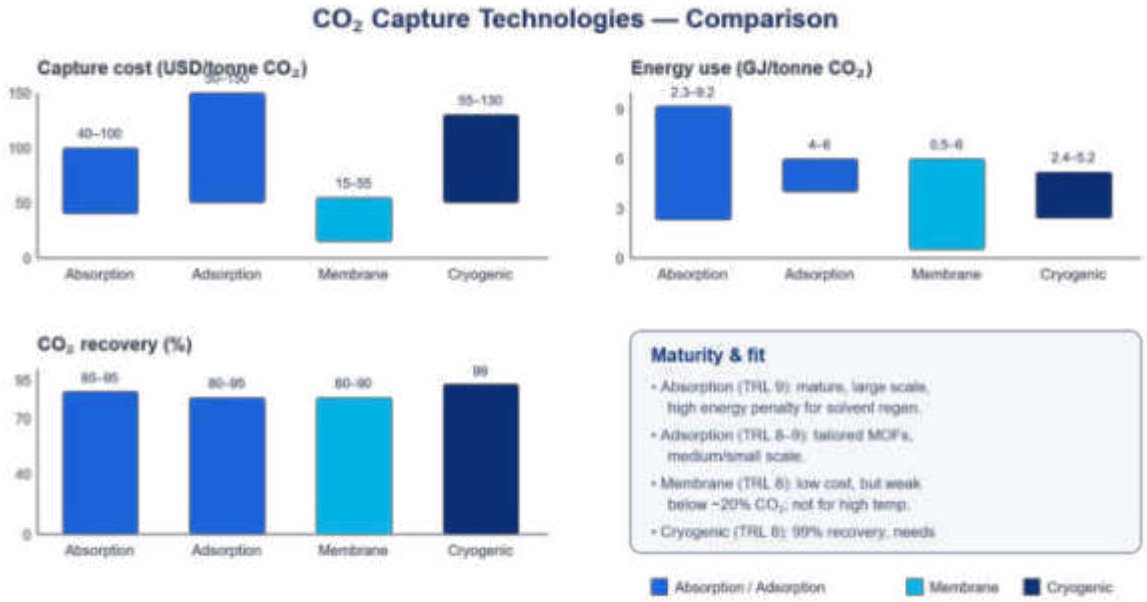


Fig. 1.9 Capture - Technology Comparison : Cost, Energy and Recovery

Table 1.6 Common CO_2 Capture Technology Comparison

Attribute	Absorption	Adsorption	Membrane	Cryogenic
Advantages	Cheap solvents; suited to high-temperature; large scale	Mature; low-cost sorbents; sorbents regenerated & reused	High purity & recovery; short start-up; low energy; low-cost separation	Recovers high-purity CO_2; operates at atmospheric pressure; very high purity
Disadvantages	High energy penalty for solvent regeneration; large capital cost	High energy for pressure/ temperature regeneration; sorbent degradation; medium/ small scale	Capital-intensive at large scale; weak below ~20% CO_2; not for high temperature	Uneconomical for dilute feeds; feed must be water-free to prevent ice; high cooling energy
Sorbent	Common MEA; high-performance proprietary solvents	Tailored nanomaterials & metal-organic frameworks (MOF)	n/a	n/a
CO_2 recovery	85 – 95%	80 – 95%	60 – 90%	99%
Energy (GJ/tCO_2)	2.3 – 9.2	4 – 6	0.5 – 6	2.4 – 5.2
Capture cost (USD/ tCO_2)	40 – 100	50 – 150	15 – 55	55 – 130
Technology readiness	TRL 9	TRL 8–9	TRL 8	TRL 8

Table 1.6 shows comparison of the most common CO_2 capture technologies. After Font-Palma C, Cann D, Udemu C., C. 2021; 7(3):58.

Reading the comparison. Absorption is the mature default (TRL 9) but carries a heavy regeneration energy penalty. Membranes are the cheapest option but lose effectiveness below ~20% CO_2, which limits them on dilute cement and gas-power streams. Cryogenic capture delivers the highest recovery (99%) and very high purity but needs a water-free feed and significant cooling energy — which is why several cement projects pair it with oxy-fuel.

Copyright © SLB. All Rights Reserved. Private & Confidential. Reproduction only by permission.

Capture cost by source purity

Pulling the cost drivers together, capture cost falls as the source CO_2 concentration rises. Global CO_2 emissions (~21 Gt) split into three purity tiers, and the bulk of the opportunity — about 16.6 Gt — sits in the medium-purity tier where most industrial sources, including cement, are found.

Fig. 1.10. Illustrates the Capture cost by source-purity tier, with associated global emissions.

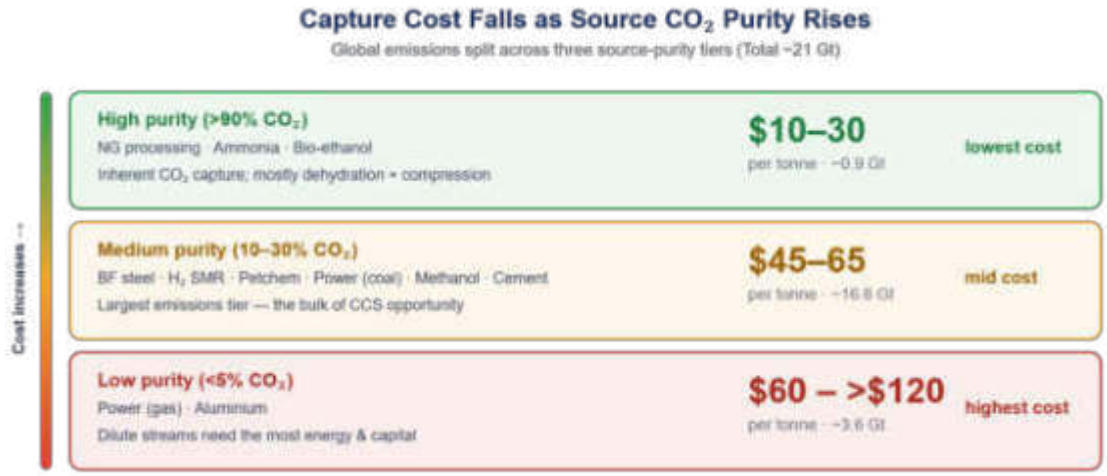


Fig. 1.10 Capture Cost by source-purity tier

Large-scale cement CO_2 capture projects

Cement is one of the hardest sectors to decarbonise, and a wave of large-scale capture projects is now in construction or planning. The reference NEXE plant sits among them. Brevik (Norway), using SLB Capturi absorption technology, is the first operational large-scale cement capture plant.

Table 1.7 Selected Large Scale Cement CO_2 Capture Projects

Project	Location	Capacity (t/yr)	TRL	Capture technology	Status	Cost ($/t)
Brevik	Norway	400,000	9	Absorption (SLB Capturi)	Operating since 2025	60–65
Olympus	Greece	1,000,000	7–8	Hybrid (oxy-fuel + cryogenic, Air Liquide)	Under construction; ready by 2029	70–90
NEXE	Croatia	610,000	7–8	Oxy-fuel	Planned 2029	90–117
LEILAC 2	Germany	100,000	6	Direct separation (LEILAC)	Under construction; maybe 2026	50–70

Table 1.7 shows selected large-scale cement CO_2 capture projects

Copyright © SLB. All Rights Reserved. Private & Confidential. Reproduction only by permission.

Insight. The cement projects illustrate the cost spread in Table 3 in practice: the mature absorption route (Brevik) and direct-separation route (LEILAC 2) report the lowest costs (50–65 $/t), while oxy-fuel and hybrid oxy-fuel/cryogenic routes (NEXE, Olympus) sit higher (70–117 $/t) but offer very high recovery and purity.

1.2.4 Key recommendations

The composition and cost analysis above leads to a consistent set of recommendations for designing and operating a CCS transport and storage network.

1. **Use pipeline transportation.** Pipeline is the recommended transport option for the volumes and continuity that a capture hub requires.
2. **Dry the stream below 50 ppm before pipeline entry.** The CHA composition (NEXE cement plant) has a high water content that must be reduced to <50 ppm to protect against corrosion and hydrate formation.
3. **Specify impurities, not just CO_2 %.** What matters more is the composition and concentration of impurities, not the headline CO_2 mol%. As per industry practice, set component specifications for the CO_2 stream delivered by each emitter.
4. **Purify at each emitter (at source).** Purifying CO_2 at each emitter is the preferred approach: it protects pipeline integrity and recognises that different emitters require different purification technologies. Porthos is a strong example of a system where purification is performed directly at the emission source.
5. **Budget capture as the dominant cost.** CO_2 capture represents 70–80% of total cost. It depends on many factors, but for cement and coal-fired plants it is typically around 45–60 $/tonne, while gas-fired power plants are more expensive at roughly 60–120 $/tonne.

Conditioning at the emitter vs. at the hub

CO_2 conditioning is performed before compression and transport. It is recommended at the emitter for four reasons:

- To protect the compressor from rapid wear caused by corrosion and chemical stress.
- To protect the pipeline from corrosion (deterioration and leakage, with significant HSE consequences).
- To maximise CO_2 credit payments, since credits are determined on the basis of the mass of CO_2 injected.
- To avoid solid drop-out and mechanical erosion from entrained solids, and to avoid hydrate formation.

Consequently, industry practice is to set specifications for the CO_2 composition delivered by the emitters; it is then up to each emitter to respect those limits and build the infrastructure needed to provide an on-spec stream. The table below shows the approach taken by several major projects.

Copyright © SLB. All Rights Reserved. Private & Confidential. Reproduction only by permission.

Table 1.8 Industry Approach to CO_2 stream Conditioning

Project	Approach
Northern Lights	Purification at source
UK East Coast	Purification at source
Porthos (NL)	Purification at source
US CO_2 pipeline	Dry CO_2 at entry

Table 1.8. Industry approaches to CO_2 stream conditioning.

Case in Point : the Porthos project

Porthos (Rotterdam) is a European Project of Common Interest that takes CO_2 from industrial emitters, transports it by onshore pipeline to a compression station, and then sends it offshore for storage in a depleted gas field. Final investment decision was taken at the end of 2023 with injection starting in 2026. It illustrates the at-source purification model recommended above.

- **Emitters:** Air Products, Air Liquide, ExxonMobil and Shell.
- **Onshore pipeline:** 42-inch, 30 km from Botlek to Maasvlakte; operating pressure 30 bar (gas phase); capacity 2.5 Mt/yr for 15 years.
- **Compression:** three compressors, discharge pressure 130 bar.
- **Offshore transport & storage:** 16-inch, 22 km offshore pipeline to a platform connecting four wells on a depleted gas field.

Each Porthos emitter applies its own pre- and post-treatment purification to meet the pipeline specification, as summarised in Table 6 — concrete evidence that different emitters use different technologies to reach a common spec.

Table 1.9 Case in point - Porthos Emitters

Partner	Capture technology	Description	Purification / compression	Industry
Air Liquide	Cryocap · TRL 9 · 99.9%	Cryogenic cooling to −50°C and P>20 bar, separating non-condensable gases from liquid CO_2; liquid CO_2 re-evaporated	Dehydration before cold box (PSA); compression before PSA at 20–25 bar	Hydrogen plant (SMR)
Air Products	Vacuum swing adsorption (VSA) · TRL 9 · 95–99%	Solid adsorbents attract CO_2 at near-atmospheric pressure through adsorption / regeneration cycles	Downstream VSA unit (1–2 bar) with dehydration, compression and contaminant removal	Hydrogen plant (SMR)
ExxonMobil	Carbonate fuel cell (CFC) · TRL 7 · >95%	Flue gas fed to the fuel-cell cathode; CO_2 reacts with air and fuel to produce concentrated CO_2 and energy; operating pressure 1–2 bar	Post-treatment: dehydration, O_2 removal and compression	Power plant / refinery furnace
Shell	ADIP ultra solvent · TRL 9 · >95%	Amine-based chemical absorption	Post-treatment: dehydration and purity-polishing compression	Refinery hydrogen units

Table 1.9 shows the capture technologies and purification approach of the Porthos project emitters. Each partner sits a trunkline a few km from (or <5 km from) the Porthos onshore pipeline.

Copyright © SLB. All Rights Reserved. Private & Confidential. Reproduction only by permission.

1.3 Overview of existing legal frameworks for CCS projects

1.3.1 Introduction

1.3.1.1 Purpose of the analysis

The purpose of this overview is to provide a comprehensive and structured assessment of the legal environment governing carbon capture and storage (CCS) in Croatia and its alignment with the corresponding European Union (EU) framework.

The analysis focuses on:

- The current state of CCS-related legislation in EU and Croatia,
- Reviewing ongoing legislative, strategic, institutional initiatives aimed and the national framework supporting future CCS deployment, and
- Identifying the extent to which existing laws enable, restrict, or condition the development of CO_2 capture, transport, injection, and permanent geological storage.

Beyond mapping the Croatian legal landscape, the analysis evaluates the entire CCS value chain, starting from obligations applicable to CO_2-emitting industrial installations and extending through capture, compression, transport networks, site characterisation, injection operations, monitoring, closure, and long-term stewardship. Each stage of this chain is compared with the EU's regulatory baseline, which includes not only binding legislation such as directives and regulations, but also relevant non-binding instruments that shape policy expectations. By systematically comparing Croatian provisions with EU requirements, the analysis identifies areas of alignment, partial transposition, and regulatory gaps that may require future harmonisation.

Ultimately, the purpose of this report is to provide a clear understanding of how well Croatia's existing legal framework supports the development of CCS, and how it aligns with the wider European Union baseline. By mapping the full CCS value chain against both EU and Croatian requirements, the analysis offers clarity on the regulatory environment in which a future project would operate highlighting the obligations, permitting pathways and compliance expectations that apply at each stage, from CO_2 generation and capture to permanent geological storage.

1.3.1.2 Methodology and data sources

The analysis was carried out through systematic desk research, drawing exclusively on relevant, authoritative, and publicly available online sources, including EU legislation databases, Croatian Official Gazette, regulatory agency publications, and policy documentation. The first step involved compiling a comprehensive list of EU-level and Croatian regulations, strategies, technical guidelines, and other documentation relevant to permanent CO_2 storage, covering the full CCS value chain from emitters to geological storage.

Once this regulatory inventory was established, a targeted comparative assessment was conducted to examine how EU requirements are reflected in Croatian law. This included a close

Copyright © SLB. All Rights Reserved. Private & Confidential. Reproduction only by permission.

review of the key EU instruments and their national counterparts, with attention to procedural obligations, technical standards, and the allocation of responsibilities across competent authorities. The comparison enabled the identification of regulatory equivalence, divergence, and omissions at the national level, forming the basis for the gap analysis presented as an Annex to this report.

All findings are grounded in publicly accessible and verifiable legal and policy sources, ensuring transparency, traceability, and consistency throughout the analytical process.

The Geographic Information System (GIS) analysis supporting this study was conducted using the two spatial extents provided by the client: the Bockovac Area of Interest and the wider Study Area, which were supplied as line-based shapefiles and polygonised prior to processing. Core infrastructural and environmental datasets were assembled from authoritative open-source platforms and national GIS services. Road networks, railways, waterways and waterbodies were obtained from OpenStreetMap, with road categories (primary, secondary, tertiary and related links) aligned to Croatian classifications of state, county and local roads. Cultural-heritage features, specifically archaeological sites, were manually digitised from the Ministry of Culture and Media's ISPU/Geoportal service, providing spatial representations suitable for analysis, while noting the inherent positional limitations of manual capture.

Due to the absence of publicly available vector data on oil and gas pipelines, these infrastructure elements were digitised in QGIS directly from county spatial plans accessed through the national MGIPU WMS services, recognising that WMS layers are view-only and cannot be downloaded or symbolically modified. In parallel, key environmental layers, including Natura 2000 sites, UNESCO Man and the Biosphere zones, and nationally protected areas, were incorporated via WFS services from Bioportal, enabling full retrieval of vector geometries and attribute data for spatial queries and overlay analysis. All mapping was performed using ESRI World Imagery as the basemap. This combined workflow ensured a coherent, multi-source geospatial dataset suitable for assessing spatial constraints, infrastructure interactions and environmental sensitivities across both project extents.

1.3.2 Legal framework for permanent CO_2 storage in the EU

This chapter provides an overview of the European Union legal framework governing permanent geological CO_2 storage. It focuses on the core regulatory instruments that directly shape the development, authorisation, operation and oversight of storage projects. The analysis is structured across six key areas:

- Geological CO_2 storage,
- Permitting and authorisation regime,
- Environmental protection and nature conservation,
- EU ETS and carbon accounting framework,
- Infrastructure and network regulation, and
- Safety and extraordinary events.

Copyright © SLB. All Rights Reserved. Private & Confidential. Reproduction only by permission.

Within each section, the most relevant and legally determinative EU instruments are highlighted and examined in detail. Additional legislative acts that may apply in specific circumstances or that are indirectly relevant such as horizontal environmental, industrial, financial or monitoring rules are referenced in the Annex to this report. Together, these instruments form a layered and interdependent legal framework that governs permanent CO_2 storage across the EU, combining climate policy objectives with environmental safeguards, market mechanisms and infrastructure regulation.

1.3.2.1 Geological CO_2 storage

The principal legal framework for the geological storage of CO_2 in the European Union is established by **Directive 2009/31/EC on the geological storage of carbon dioxide (the "CCS Directive")**, which provides a comprehensive regime aimed at ensuring that the capture, transport and underground storage of CO_2 are conducted in a manner that prevents significant negative impacts on human health and the environment and contributes to climate mitigation objectives. Under the CCS Directive, "geological storage of CO_2" is defined as the injection of CO_2 into deep geological formations with the purpose of permanent containment, and it applies to storage activities over their full life cycle, from site selection to long-term post-closure monitoring.

To facilitate consistent and technically informed implementation across Member States, the European Commission has updated in 2024 a suite of non-binding guidance documents that support the practical application of the Directive's requirements. These **guidance documents** include:

- CO_2 storage life cycle and risk management framework,
- Characterisation of the storage complex, CO_2 stream composition, monitoring and corrective measures,
- Criteria for transfer of responsibility to the competent authority, and
- Financial security and financial contribution.

They set out recommended methodologies for risk assessment over the storage life cycle, detailed characterisation of geological formations and CO_2 streams, monitoring strategies and corrective actions, and the financial provisions required to ensure obligations can be met. The guidance is intended to assist competent authorities and operators in interpreting and applying the CCS Directive's technical provisions and promotes harmonised practice across the EU.

In parallel, the EU's **Regulation (EU) 2024/3012 establishing a Union certification framework for permanent carbon removals, carbon farming and carbon storage in products** introduces an EU-wide certification regime for permanent carbon storage that recognises geological storage in line with the CCS Directive's definition of permanent containment. This regulation, while primarily focused on the certification of carbon removals, explicitly references geological storage under the CCS Directive and reinforces its role within the broader carbon management framework. The European Commission's **Industrial Carbon Management Strategy** (COM/2024/62) further situates geological storage within a cohesive EU strategy to develop a single market for CO_2

Copyright © SLB. All Rights Reserved. Private & Confidential. Reproduction only by permission.

capture, transport and storage services, reflecting the increased importance of CCS technologies for achieving climate neutrality and the need for regulatory clarity and market development.

Under the CCS Directive, an exploration permit must first be obtained from the competent authority of the host Member State to enable the assessment and characterisation of a potential storage site. This exploration phase allows operators to carry out the necessary studies and data acquisition required to determine whether a geological formation is suitable for CO_2 storage. Following this, a storage permit must be obtained from the competent authority of the host Member State before any CO_2 injection can take place. A storage permit is granted only after comprehensive site characterisation demonstrates that the selected geological formation is suitable for long-term containment, with no significant risk of leakage or adverse environmental impact. This characterisation requirement, set out in Annex I to the Directive and elaborated in Commission guidance, entails detailed geological, geophysical, hydrogeological and geochemical analyses, three-dimensional reservoir modelling and risk assessments, supported by sufficient data to substantiate predictions about the behaviour of the CO_2 plume and the integrity of the storage complex over time.

Once a permit is issued, the operator must implement an approved monitoring plan and submit regular reports to the competent authority. The monitoring regime is designed to track the distribution and behaviour of the injected CO_2, detect any irregularities or leaks at an early stage, and ensure compliance with performance criteria. It includes both routine monitoring at intervals appropriate to the site's characteristics and corrective measures to be taken immediately if monitoring indicates leakage or unexpected conditions. Monitoring plans and corrective procedures are subject to periodic review and adjustment with the approval of the competent authority.

The CCS Directive also sets out closure and post-closure obligations. After cessation of CO_2 injection, the storage site enters a post-closure phase during which monitoring continues, and the operator remains responsible for managing the site and addressing any occurrences of leakage or other significant irregularities. A storage site may be closed only once all closure conditions specified in the permit are met, including sealing of the site, removal of injection facilities and confirmation that the CO_2 will be permanently contained.

A distinctive feature of the CCS Directive is the regulated mechanism for the transfer of responsibility from the private operator to the Member State competent authority. Article 18 of the Directive allows transfer only after a minimum monitoring period, which must be determined by the competent authority and is not less than 20 years, and only once all available evidence indicates that the injected CO_2 will be safely and permanently stored. Transfer is also contingent upon fulfilment of financial security obligations and payment of a financial contribution to support future monitoring by the competent authority, typically covering at least 30 years of anticipated costs. After transfer, the competent authority assumes responsibility for long-term liability under the Directive, although in cases of negligence or failure to exercise due diligence prior to transfer, the competent authority may recover costs from the former operator.

In addition to the CCS Directive's own liability framework, the EU's **Environmental Liability Directive** (**ELD**, Directive 2004/35/EC) applies as a liability overlay to geological storage activities.

Copyright © SLB. All Rights Reserved. Private & Confidential. Reproduction only by permission.

The ELD establishes a harmonised regime requiring operators to prevent and remedy environmental damage caused by occupational activities, including storage site operations cited in its Annex III, and imposes strict liability for remediation of environmental harm irrespective of fault. The ELD thus complements the CCS Directive by ensuring that operators remain accountable for remediation of environmental damage associated with CO_2 storage activities, alongside the Directive's own corrective and transfer mechanisms.

Finally, under the waste classification context, the **Waste Framework Directive** (Directive 2008/98/EC) is relevant insofar as it clarifies the legal status of captured CO_2. While captured CO_2 destined for geological storage under the CCS Directive is generally not classified as waste, proper legal interpretation at the Member State level is important to avoid conflicts with waste law, particularly where capture or transport activities intersect with waste streams regulated under separate EU law.

In summary, geological CO_2 storage in the EU is legally defined under the CCS Directive as injection into suitable geological formations with the purpose of permanent containment, subject to rigorous site characterisation, permitting, monitoring and closure requirements. The Directive provides a structured pathway for eventual transfer of responsibility to competent authorities after a defined monitoring period and fulfilment of financial obligations. Complementary EU frameworks, including updated guidance documents, the ELD, the EU certification framework for carbon removals, and the Industrial Carbon Management Strategy, support consistent implementation and reinforce liability and environmental protection throughout the storage life cycle.

1.3.2.2 Permitting and authorisation regime

The development and operation of a permanent CO_2 disposal project in a geothermal aquifer necessitate a comprehensive permitting and authorisation regime rooted in several interrelated EU directives that govern environmental assessment, industrial emissions, extractive waste management, and nature protection. The cornerstone of project authorisation is the **Environmental Impact Assessment (EIA) Directive** (Directive 2011/92/EU), which requires that public and private projects likely to have significant effects on the environment undergo an assessment of their potential impacts before consent is granted. Geological CO_2 storage facilities, including associated injection infrastructure and surface installations, are generally considered projects requiring EIA due to their scale and potential environmental consequences. Under the EIA Directive, the competent authority must decide whether a project listed in Annex I of the Directive automatically requires an environmental impact assessment or, in the case of projects listed in Annex II of the Directive, must be screened for significance. The process encompasses preparation of an environmental impact statement by the developer and effective public participation prior to decision making. Member States must ensure opportunities for public and affected parties to express their views and access information, in line with the Aarhus Convention principles, and any decision to grant consent can be subject to judicial review, thereby introducing litigation risk where environmental concerns are inadequately addressed or procedural requirements are not fully met. Typical timelines for an EIA procedure vary by jurisdiction but often extend over several months, with statutory minimum periods for scoping, impact statement review, and public consultation.

Copyright © SLB. All Rights Reserved. Private & Confidential. Reproduction only by permission.

In parallel, the **Industrial Emissions Directive** (**IED**, Directive 2010/75/EU) applies to industrial installations engaged in activities such as power generation, refining, chemical processing, and capture operations that fall within its scope. While geological storage itself is governed by the CCS Directive, the capture facility and associated equipment - particularly if part of an integrated industrial complex - will typically require an IED permit. An IED permit consolidates environmental requirements for emissions to air, water and soil, energy efficiency, waste management and accident prevention, and is granted only after a thorough assessment of best available techniques (BAT) in the relevant sector. The IED permitting process includes public consultation on the draft permit conditions and provides for appeals against permit decisions, which can give rise to litigation on grounds of inadequate application of BAT conclusions or failure to protect environmental quality standards. The sequencing of IED and EIA-driven permitting depends on national practice but generally requires coordination to avoid duplication and to align monitoring and compliance obligations. The timeline for IED permitting is influenced by the complexity of the installation and the extent of required public consultation and interagency coordination but often ranges from six months to more than a year.

Where CO_2 storage development involves drilling and subsurface works that intersect with mining and quarrying operations or the disposal of waste rock and tailings, the **Extractive Waste Directive** (Directive 2006/21/EC) may also apply. This Directive governs the management of waste from extractive industries to prevent or reduce adverse effects on the environment and human health. It requires the preparation of waste management plans and the adoption of appropriate waste disposal facilities that comply with prescribed operational and closure requirements. While not all borehole drilling activities fall under the definition of extractive waste operations, the interface between geological storage site preparation and existing extractive activities must be assessed, and, if applicable, permits in line with the Extractive Waste Directive should be obtained. Public participation in authorisations under this Directive is generally required where such decisions are capable of having significant environmental effects, and failure to involve the public or to meet technical standards can become a basis for legal challenge.

In practice, the sequencing of permits for a CO_2 storage project requires careful coordination among these regimes. The EIA process often runs in parallel with IED, with early scoping to define the extent of environmental assessment and potential need for Natura 2000 appropriate assessment. Extractive waste authorisations, if required, are typically sought once site preparation details are sufficiently defined. Public consultation is an integral part of most authorisation processes, with statutory minimum periods for comment and review built into the EIA and IED frameworks. Litigation risk is elevated where authorities grant consent without adequately addressing significant environmental effects, fail to undertake appropriate assessments for protected habitats, or do not ensure meaningful public participation, and such challenges can materially extend project timelines. Overall, developers should anticipate that permitting and authorisation may extend over a period of one to several years, depending on project scale, complexity of environmental issues, and the extent of required assessments and consultations.

1.3.2.3 Environmental protection and nature conservation

Environmental protection requirements applicable to geological CO_2 storage projects derive from a combination of EU water, biodiversity, soil, forestry and climate legislation. With respect to water

Copyright © SLB. All Rights Reserved. Private & Confidential. Reproduction only by permission.

protection, the **Water Framework Directive** (**WFD**, Directive 2000/60/EC) establishes a comprehensive framework for the protection of inland surface waters, transitional waters, coastal waters and groundwater. It requires Member States to prevent deterioration of the status of all water bodies and to achieve good status, subject to limited exemptions under Article 4(7). CO_2 injection activities must therefore be assessed to ensure that they do not cause deterioration of groundwater chemical status or compromise environmental objectives. The **Groundwater Directive** (Directive 2006/118/EC) complements the WFD by setting specific measures to prevent and control groundwater pollution, including the prohibition of direct discharges of pollutants into groundwater unless expressly authorised under strict conditions. Any risk of leakage, migration or induced pathways affecting protected aquifers must be evaluated in light of these non-deterioration and pollution prevention obligations.

Conservation of biodiversity is ensured primarily through the **Habitats Directive** (Directive 92/43/EEC) and the **Birds Directive** (Directive 2009/147/EC), which establish the **Natura 2000** network of protected sites and require assessment and protection of habitats and species of European interest. Any project that is likely to have a significant effect on a Natura 2000 site, either individually or in combination with other plans or projects, must undergo an appropriate assessment under Article 6 of the Habitats Directive, and may be approved only if it will not adversely affect the integrity of the site. The Birds Directive provides similar protections for avian species and their habitats. These requirements interact with the EIA process but have a more stringent substantive test: even where an EIA yields non-significant impacts, a Natura 2000 appropriate assessment may still find the project unacceptable unless compensatory measures are provided. Public authorities must consult with environmental authorities and involve stakeholders, including non-governmental organisations, during the assessment. Intervention by nongovernmental organizations (NGOs) and citizen groups is common in such procedures, and adverse decisions on appropriate assessments are frequently subject to judicial review, thereby representing a substantive litigation risk that can delay or block project authorisation.

Emerging EU soil policy further strengthens environmental oversight. The **Soil Monitoring and Resilience Directive** (Directive (EU) 2025/2360) establishes a framework for systematic soil monitoring and sustainable soil management across the Union. While it does not create a project-level permitting regime comparable to water or nature legislation, it reinforces obligations on Member States to identify and address soil degradation risks. Surface facilities associated with CO_2 storage, including well pads, pipelines and compression stations, must therefore be designed and operated in a manner consistent with national measures adopted under this Directive.

Forest and ecosystem monitoring obligations are supported by Commission Regulation (EC) No 1737/2006, which lays down detailed rules for monitoring forests and environmental interactions under the former Forest Focus framework. Although primarily directed at Member State monitoring systems rather than individual projects, it reflects the broader EU objective of safeguarding forest ecosystems that could be affected by large-scale infrastructure development.

Climate and sustainability legislation also interacts with environmental protection considerations. The **European Climate Law** (Regulation (EU) 2021/1119) establishes the legally binding objective of climate neutrality by 2050 and underpins the policy rationale for carbon capture and storage. The **Directive (EU) 2018/2001 on the promotion of the use of energy from renewable**

Copyright © SLB. All Rights Reserved. Private & Confidential. Reproduction only by permission.

sources (RED II) promotes renewable energy deployment and sets sustainability criteria for certain energy pathways, contributing to the broader decarbonisation context in which CO_2 storage projects operate. From an investment perspective, the **EU Taxonomy Regulation** (Regulation (EU) 2020/852) establishes criteria for determining whether economic activities, including certain CCS-related activities, like the transport of CO_2 and underground permanent geological storage of CO_2, can be considered environmentally sustainable, subject to compliance with "do no significant harm" requirements, including those relating to water, biodiversity and ecosystems.

Finally, the **Net-Zero Industry Act** (**NZIA**, Regulation (EU) 2024/1735) seeks to accelerate the deployment of net-zero technologies, including CO_2 storage capacity, by facilitating permitting and setting EU-level storage targets. However, it does not derogate from core environmental protection legislation; projects must remain fully compliant with water, biodiversity and other environmental safeguards.

Taken together, this framework ensures that geological CO_2 storage projects are embedded within a stringent system of environmental protection. Water non-deterioration obligations, Natura 2000 appropriate assessment requirements, soil monitoring frameworks and broader climate and sustainability rules operate cumulatively. As a result, environmental compliance is not limited to CCS-specific legislation but requires integrated assessment across multiple EU legal instruments, each of which may provide potential grounds for administrative challenge or judicial review if procedural or substantive requirements are not adequately met.

1.3.2.4 EU ETS and carbon accounting

The regulatory recognition of permanent CO_2 storage within the European Union is governed by the Directive 2003/87/EC, which establishes the **EU Emissions Trading System (EU ETS).** Under this Directive, operators of covered installations must surrender allowances corresponding to their verified greenhouse gas emissions. Crucially for carbon capture and storage, CO_2 that is captured, transported and permanently stored in accordance with the CCS Directive is not considered emitted for the purposes of allowance surrender. This provision constitutes the primary economic incentive for geological storage, as verified stored CO_2 reduces an operator's compliance obligation.

The detailed rules for quantifying and reporting captured and stored CO_2 are set out in the **Monitoring and Reporting Regulation** (**MRR,** Regulation (EU) 2018/2066), which requires operators to implement an approved monitoring plan covering capture, transfer, transport and injection. The MRR ensures that reported volumes are complete, consistent and accurate, and that no double counting occurs along the CO_2 value chain. Any leakage from a storage site must be reported as emissions, triggering an obligation to surrender allowances. Independent verification of emissions data is required under the **Accreditation and Verification Regulation** (**AVR,** Regulation (EU) 2018/2067), which sets accreditation and competence standards for verifiers and reinforces the integrity of reported reductions.

Failure to ensure permanent containment, for example, through leakage, would have direct financial consequences under the ETS and could coincide with breaches of environmental law.

Copyright © SLB. All Rights Reserved. Private & Confidential. Reproduction only by permission.

Litigation risk in the ETS context typically concerns the robustness of monitoring, reporting and verification, particularly where stakeholders question whether stored volumes genuinely qualify as permanent and properly accounted removals. For a geothermal aquifer storage project, strict alignment between CCS compliance and EU ETS monitoring obligations is therefore essential to secure both environmental integrity and financial viability.

1.3.2.5 Infrastructure and network regulation

The development of CO_2 transport infrastructure within the European Union is governed by the **TEN-E Regulation** (Regulation (EU) 2022/869), which establishes guidelines for trans-European energy infrastructure. The recast Regulation expressly includes dedicated CO_2 transport networks, such as pipelines, compressor stations and related facilities, within its scope, recognising them as essential infrastructure to enable large-scale carbon capture and storage and to support the EU's climate neutrality objectives.

Under the Regulation, cross-border CO_2 infrastructure projects may be designated as Projects of Common Interest (PCIs) if they demonstrate significant cross-border impact and contribute to sustainability and decarbonisation goals. PCI status does not exempt projects from environmental compliance but provides procedural advantages and eligibility for funding under the Connecting Europe Facility. A key benefit is streamlined permitting: Member States must designate a single competent authority to coordinate the permit-granting process, and the overall procedure is subject to defined time limits, generally not exceeding three and a half years, subject to justified extensions. Public participation and cross-border consultation remain mandatory.

The Regulation promotes non-discriminatory access to CO_2 transport infrastructure, particularly where projects receive public support or function as shared networks. Although it does not establish a fully harmonised third-party access regime, it encourages transparent and fair access conditions to facilitate multi-user CO_2 networks. This is particularly relevant where several industrial emitters rely on common transport corridors to reach storage sites.

Cross-border transport is a central objective of the TEN-E framework. The Regulation supports infrastructure connecting capture sites and storage locations across Member States, thereby fostering an integrated European CO_2 transport market. Such projects require coordination between national authorities and compliance with applicable EU environmental law and relevant international obligations governing transboundary CO_2 movement.

Finally, PCI designation and public financial support must comply with EU state aid rules. Any public funding for CO_2 networks must be necessary, proportionate and compatible with internal market principles. State aid approval processes may run in parallel with PCI and permitting procedures and should be factored into project timelines.

In summary, the TEN-E Regulation positions CO_2 networks as recognised energy infrastructure at EU level, facilitates cross-border development and streamlined permitting for eligible projects, and supports access to EU funding, while maintaining full compliance with environmental and competition law requirements.

Copyright © SLB. All Rights Reserved. Private & Confidential. Reproduction only by permission.

1.3.2.6 Safety and extraordinary events

Where the project involves the storage, handling or processing of dangerous substances above specified thresholds - for example, large volumes of compressed or liquefied CO_2, chemicals associated with capture solvents, or other hazardous materials - the **Seveso III Directive** (Directive 2012/18/EU) on the control of major-accident hazards may apply. This Directive aims to prevent major accidents involving dangerous substances and to limit the consequences for human health and the environment. If the installation qualifies as a Seveso site, the operator must prepare a safety report demonstrating compliance with stringent prevention and mitigation measures, and in the case of upper-tier establishments must develop internal emergency plans and cooperate with external emergency planners. The Seveso regime operates alongside the IED and EIA regimes, with cross-referencing of risk assessment information, and it entails additional consultation and information obligations for the public, particularly regarding emergency response arrangements. Non-compliance with Seveso requirements can lead to enforcement action by authorities and provides a basis for legal challenges by affected parties concerned about safety and risk management.

The **Aarhus Convention** establishes three binding procedural rights: access to environmental information, public participation in decision-making and access to justice when those rights are infringed. For a CCS investor, Aarhus obligations translate into a high level of documentation transparency, early public disclosure of alternatives and baseline studies, meaningful participation opportunities across EIA, Natura 2000, water-management and spatial-planning procedures, and a requirement to demonstrate how public input influenced routing, siting, mitigation, monitoring and design choices. The administrative record must be complete and defensible, as courts may annul any permit that fails to demonstrate compliance with Aarhus procedural guarantees.

The **Espoo Convention** requires Parties to evaluate transboundary environmental impacts of major projects, notify and consult neighbouring countries when significant cross-border effects are possible, and ensure that the affected State's public can participate in the assessment. These obligations are particularly relevant for CCS and GT-CCS projects whose geological, hydrological or ecological impacts may extend across borders, including subsurface pressure changes, groundwater interactions or linear infrastructure crossing sensitive border-proximate environments. For CCS project developers, this means preparing screening documentation early enough for Member States' authorities to determine whether notification to neighbouring States is required. Should a transboundary EIA be initiated, the investor must provide EIA documents suitable for translation and international review, participate in bilateral consultations, support cross-border public-participation processes and supply clarifications to address the concerns of both States. The final EIA decision must transparently demonstrate how cross-border comments, hydrological concerns or ecological-network interactions influenced the outcome.

Together, the Aarhus and Espoo Conventions impose a unified system of transparency, participation and cross-border accountability that directly shapes the permitting pathway for CCS and GT-CCS projects. These obligations require investors to maintain exemplary standards of openness, documentation quality, alternatives analysis and stakeholder engagement. For a CCS project, compliance with Aarhus ensures robust national transparency and participation, while Espoo governs interactions with neighbouring States where relevant. Properly addressed, these

Copyright © SLB. All Rights Reserved. Private & Confidential. Reproduction only by permission.

conventions strengthen the legal durability, environmental credibility and societal acceptance of the project, and form a critical procedural foundation for securing all downstream permits.

1.3.3 Legal framework for permanent CO_2 storage in Croatia

The development of permanent geological CO_2 storage and combined geothermal-CCS systems in the Republic of Croatia is governed by a structured body of national legislation that regulates subsurface rights, environmental protection, spatial planning, construction, industrial safety, and major-accident prevention. This chapter provides a consolidated overview of that legal framework, explaining the statutory and regulatory instruments that determine how geological formations may be explored, characterised, allocated and authorised for long-term CO_2 injection and storage. It also clarifies how these domestic instruments interact with the wider EU legislative context, forming the permitting and compliance basis on which all CCS and GT-CCS project activities must proceed.

The analysis presented in this chapter is based on two spatial reference areas:

- The first is the Bockovac Area of Interest - the smaller, geologically focused footprint corresponding to the preliminary exploration area described in the Environmental Protection Elaborate for Investigative Geothermal Wells Bockovac (2024). This area of interest defines the immediate geological zone relevant for characterisation of the target formations and for interpreting subsurface-related legal obligations under Croatian hydrocarbons legislation and the Regulation on Permanent CO_2 Storage.
- The second reference area is the expanded Study Area, a broader spatial extent provided by the client for the purpose of assessing all potentially applicable Croatian regulatory regimes. This extended perimeter allows systematic screening of legal requirements linked to spatial-planning conformity, Natura 2000 constraints, water-protection zones, flood-risk areas, industrial-safety regimes, pipeline routing, and any other statutory conditions that may influence CCS feasibility, permitting or design.

Copyright © SLB. All Rights Reserved. Private & Confidential. Reproduction only by permission.

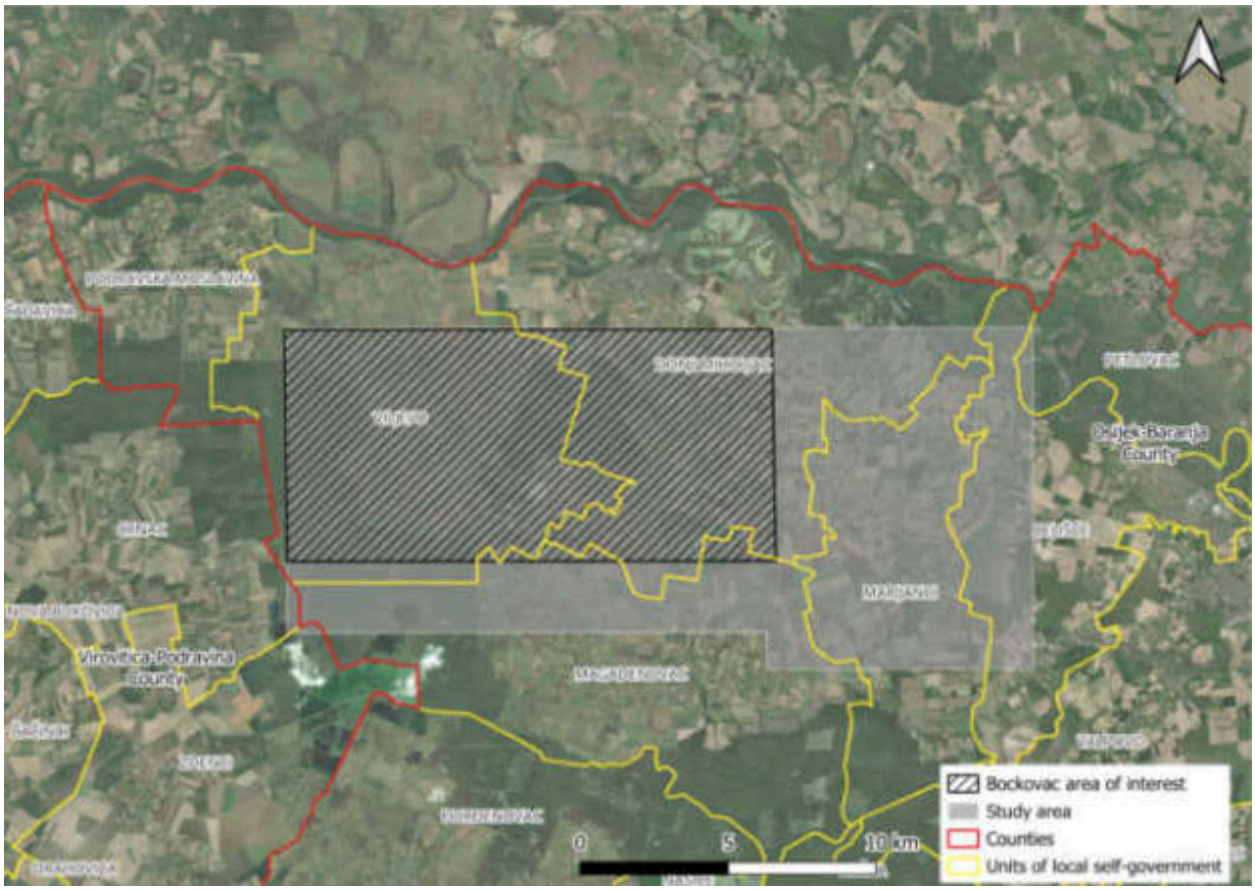


Fig. 1.11 Bockovac area of interest and Study area

Together, the Area of Interest and the expanded Study Area create a robust basis for determining the full set of legal instruments governing the project: from those that apply exclusively to the geological storage complex (e.g., the Act on the Exploration and Exploitation of Hydrocarbons and the Regulation on Permanent CO_2 Storage), to cross-cutting environmental, spatial, safety and construction laws that apply to CO_2 pipelines, compressor stations, geothermal installations and associated infrastructure. The sections that follow therefore set out Croatia's complete regulatory architecture for permanent CO_2 storage and integrated GT-CCS concepts, forming the legal foundation for all subsequent feasibility, permitting and project-development steps.

1.3.3.1 Geological CO_2 Storage – Fundamental Croatian Legal Acts

The legal possibility of conducting geological CO_2 storage, geothermal utilization and combined GT-CCS activities in the Republic of Croatia rests on a set of national acts and regulations that together determine how the subsurface may be explored, characterized, allocated and exploited. These legal instruments define not only the rights and obligations of investors, but also the procedural, spatial and financial conditions under which such complex subsurface projects can legally proceed. Their combined structure forms the backbone of Croatia's domestic regulatory framework for permanent CO_2 storage and geothermal resource exploitation, setting the foundation for planning, permitting, and long-term operation of CCS systems and integrated geothermal-CCS concepts.

Copyright © SLB. All Rights Reserved. Private & Confidential. Reproduction only by permission.

The **Act on the Exploration and Exploitation of Hydrocarbons** (OG 52/18, 52/19, 30/21) represents the central gateway into this framework because it is the statute that explicitly governs subsurface activities of national relevance, including the exploration and exploitation of geothermal waters, the management of underground gas storage and, crucially, the implementation of permanent CO_2 storage in geological structures. By defining which activities constitute exploration, which constitute exploitation and which require explicit State authorization, this Act determines the legal status of CCS and GT-CCS projects. It sets out how rights to the subsurface are awarded typically through public tendering or administrative procedures while specifying the obligations of operators in terms of geological investigations, data reporting, safeguarding of the subsurface, adherence to technical standards and responsible closure of wells and facilities. In practice, this Act establishes the primary permitting pathway for any investor intending to inject CO_2, use geothermal energy, or develop a dual-purpose geothermal CO_2 storage system, making it the legal foundation from which all downstream permitting stages flow.

Complementing the parent **Act is the Regulation on Permanent CO_2 Storage in Geological Structures** (OG 95/2018), which provides the technical, procedural and evidentiary requirements that must be met before a geological formation can be approved as suitable for permanent CO_2 containment. This Regulation plays a decisive role in project feasibility because it requires extensive geological, geophysical, hydrogeological and geochemical characterization to demonstrate that a formation possesses the necessary storage capacity, injectivity, containment integrity and long-term stability. Its provisions establish the mandatory scope of risk assessment, including evaluation of leakage pathways, induced seismicity, caprock integrity, and potential interactions with groundwater bodies or ecologically sensitive areas such as Natura 2000 sites. It also requires the development of a robust monitoring framework capable of detecting irregularities during both injection and post-closure phases. As such, this Regulation operationalizes the high-level obligations of the Act on Hydrocarbons and directly shapes the scientific, technical and financial inputs that a CCS or GT-CCS project must prepare throughout its permitting lifecycle.

Further clarification and refinement of this framework are provided by the **Regulation on Amendments and Supplements to the Regulation on Permanent CO_2 Storage** (OG 87/2022). The amended version modernises and adjusts the original 2018 Regulation, closing procedural gaps, updating definitions and aligning technical requirements with current expectations of national authorities. For investors, it is essential to recognise that the 2022 amendments represent the currently binding version of the regulatory text. All risk assessments, modelling efforts, monitoring strategies and technical studies must align with this consolidated regulatory standard, as competent authorities will assess compliance solely on the basis of the up-to-date requirements. Together, the 2018 Regulation and its 2022 amendment form the complete and current technical rulebook governing permanent CO_2 storage in Croatia.

A second regulatory pillar essential for CCS and GT-CCS development is the **Regulation on Reserves** (OG 95/2018, 87/2022), which governs the reservation, classification and formal recording of underground geological resources, including formations potentially suitable for CO_2 storage. This Regulation plays a strategic role at the earliest stages of project structuring because it determines whether a specific geological structure is officially recognised and whether its use is subject to pre-existing rights, reserved State interests or competing claims such as hydrocarbon exploration, geothermal production or groundwater protection. By defining how underground

Copyright © SLB. All Rights Reserved. Private & Confidential. Reproduction only by permission.

structures must be recorded and managed, the Regulation enables investors to verify whether a target aquifer or reservoir can be legally integrated into their development concept. It therefore safeguards exclusive access, reduces subsurface conflict risks, and provides a transparent basis for project area delineation.

Beyond subsurface rights and technical obligations, the Croatian legal framework for CCS also incorporates explicit financial obligations through the **Regulation on Compensation for the Exploration and Exploitation of Hydrocarbons** (OG 25/20). This Regulation prescribes mandatory, non-negotiable compensation fees payable to the Republic of Croatia for carrying out exploration and exploitation activities within the national subsurface domain, including activities related to permanent CO_2 storage and geothermal utilisation. For CCS investors, these fees represent critical cost components that directly influence early CAPEX/OPEX modelling and broader commercial structuring.

In addition to the general compensation regime, the Regulation sets out specific financial obligations for permanent geological CO_2 disposal, which form a decisive factor for project economics. First, a monetary fee is payable for the volumes of CO_2 injected into geological formations, with the exact per-unit tariff contractually determined between the investor and the Government of the Republic of Croatia on the basis of the issued storage permit; by design, the Regulation OG 25/20 establishes the obligation but does not fix the tariff in the ordinance, leaving the price level to the storage contract. This contract-based fee introduces a variable cost element proportional to annual injection volumes and is therefore central to long-term economic modelling, marginal abatement-cost calculations and tariff design for GT-CCS systems.

Furthermore, the Regulation establishes two fixed annual spatial fees tied to the size of the licensed area:

- For the approved research area designated for permanent CO_2 disposal, the monetary compensation amounts to HRK 500,000 per km² per year (≈ EUR 66,361 per km² per year), calculated from the date on which the permit and contract become effective and payable no later than the end of the fourth quarter of each calendar year.
- For an established exploitation field, the compensation increases to HRK 2,000,000 per km² per year (≈ EUR 265,444 per km² per year), likewise calculated annually from the date the exploitation field is formally established and payable by year-end. These area-based fees are fixed in the Regulation OG 25/20, unlike the volumetric tariff, and therefore operate as predictable, non-negotiable line items in financial models.

These spatial fees significantly impact the cost base of any CCS or GT-CCS project, as they scale directly with the geographic footprint of the licensed subsurface area. For commercial project planning, they encourage precise optimization of storage-complex delineation and careful evaluation of geological boundaries to minimize unnecessary spatial liability. Taken together, the contract-set volumetric fee for injected CO_2 and the fixed annual spatial fees for research and exploitation areas constitute a material, multi-layered financial framework governing permanent CO_2 storage in Croatia. Their magnitude and binding nature make them essential inputs in feasibility studies, financial modelling, tariff setting, service-pricing structures, and ultimately in assessing the bankability and long-term viability of CCS and GT-CCS projects.

Copyright © SLB. All Rights Reserved. Private & Confidential. Reproduction only by permission.

The regulatory picture is further shaped by the **Act on Spatial Planning** (OG 155/25), which governs how Croatia's territory is organized and how infrastructure including CO_2 pipelines, compressor stations, conditioning units and injection facilities is embedded within spatial planning documents. For CCS projects, spatial compatibility is not optional: no location or construction permit can be issued unless the proposed facilities and pipeline routes are aligned with the applicable spatial plans at national, county and municipal levels. This makes spatial planning a gatekeeper for buildability. In the context of the present study, relevant plans include those of:

- Spatial Plan Osijek-Baranja County,
- Spatial Plan Virovitica-Podravina County (a very small portion, only within the broader study area),
- Spatial Development Plan of the City of Donji Miholjac,
- Spatial Development Plan of the Municipality of Magadenovac,
- Spatial Development Plan of the Municipality of Viljevo,
- Spatial Development Plan of the Municipality of Marijanci,
- Spatial Development Plan of the City of Belišće,
- Spatial Development Plan of the Municipality of Crnac (a very small portion, only within the broader study area),
- Spatial Development Plan of the Municipality of Zdenci (a very small portion, only within the broader study area).

These plans define permissible land uses, constraints linked to Natura 2000 and other protected areas, corridor availability and routing restrictions, all of which strongly influence early-stage feasibility, pipeline design and site-selection logic.

Finally, the **Act on Construction** (OG 155/25) regulates the design, construction and commissioning of all buildings and infrastructure, including CO_2 pipelines, compressor stations and related facilities. It establishes the procedural sequence of obtaining a location permit, then a construction permit and ultimately a use permit, each requiring compliance with Croatian technical standards, validated project documentation, construction supervision obligations and safety requirements. For developers, this Act provides the procedural and engineering backbone that determines permitting timelines, documentation maturity thresholds and readiness for commissioning. It ensures that CCS infrastructure, once spatially permitted and environmentally approved, is built and operated in accordance with national construction standards and regulatory oversight.

Together, these acts and regulations create a coherent Croatian legal architecture that enables the implementation of CCS, geothermal energy projects and integrated GT-CCS systems. They define what activities are permissible, how subsurface rights are acquired, which technical and environmental standards must be met, how the territory must be planned, and how infrastructure must be designed, built, and commissioned. For investors and project developers, they represent the essential legal foundation upon which the feasibility, permitting strategy, financial modelling and long-term operational planning of CCS and GT-CCS projects in Croatia must be built.

Copyright © SLB. All Rights Reserved. Private & Confidential. Reproduction only by permission.

1.3.3.2 Permitting and authorisation regime

Spatial-Plan Conformity

Before any CCS or GT-CCS project can advance into environmental or construction permitting, it must first establish full alignment with Croatia's spatial-planning system under the **Act on Spatial Planning** (OG 155/25). Spatial-plan conformity is confirmed through county and municipal-level planning authorities, including those of Osijek-Baranja County, Virovitica-Podravina County and relevant local units such as Donji Miholjac, Magadenovac, Viljevo, Marijanci, Belišće, Crnac and Zdenci, depending on the project footprint. This stage ensures that the intended CO_2 pipeline corridors, compressor or conditioning stations, injection sites and geothermal installations are permissible within legally binding spatial documents. If incompatibilities arise, the developer must initiate plan amendments, a process that can take several months and require public consultation. Spatial compliance is therefore the earliest and most foundational regulatory checkpoint, as no location or construction permit may be issued unless the project is demonstrably aligned with the spatial-planning framework.

Environmental Impact Assessment

Following spatial compatibility, the project enters the environmental-assessment regime governed by the **Act on Environmental Protection** (OG 80/13, 153/13, 78/15, 12/18, 118/18) and operationalised through the **Regulation on Environmental Impact Assessment** (OG 61/14, 3/17). The competent environmental authority conducts a formal screening and scoping process to determine whether a full Environmental Impact Assessment is required something that, given the nature and scale of CCS infrastructure, is almost always the case. The EIA procedure includes detailed baseline surveys, environmental modelling, alternatives analysis, stakeholder consultation and interdisciplinary evaluation of expected impacts, covering not only environmental receptors such as water, soil, air and biodiversity, but also landscape, cultural and historical heritage, transport and infrastructure, population and human health, as well as hunting and land use considerations. The process concludes with an EIA decision (*cro. "rješenje o prihvatljivosti zahvata"*) that either approves the project subject to binding mitigation measures or requires design modifications. In addition to prescribing environmental protection measures, the decision also establishes a mandatory environmental monitoring programme, defining parameters, frequency and implementation responsibilities for tracking the actual impacts of the project during construction and operation. This decision becomes an anchor document influencing all subsequent permits, compelling the developer to integrate hydrological, ecological, noise, soil, agricultural-land, forest-use, air-quality and waste-management measures into project design and execution.

Natura 2000 and Appropriate Assessment

Where CCS or GT-CCS activities may affect Natura 2000 sites, species or habitats, the project must undergo screening and, if necessary, a full Appropriate Assessment under the **Act on Nature Protection** (OG 80/13, 15/18, 14/19, 127/19, 155/23). The process is informed by the **Regulation on the Ecological Network** (OG 80/19, 119/23), the **Regulation on Conservation Goals for Target Bird Species** (OG 25/20, 38/20), the **Habitat Inventory and Map Regulation**

Copyright © SLB. All Rights Reserved. Private & Confidential. Reproduction only by permission.

(OG 27/21, 101/22) and the **Regulation on Strictly Protected Species** (OG 144/13, 73/16). Competent nature-protection authorities assess potential impacts to protected habitats, groundwater-dependent ecosystems, migratory routes, breeding sites and priority species, imposing conditions such as micro-routing, timing restrictions or habitat-mitigation requirements. Because appropriate-assessment conclusions carry legal force equal to the EIA, CCS developers must ensure that project routing, construction methodology and subsurface behaviour (particularly pressure regimes affecting adjacent ecosystems) are fully aligned with the ecological constraints established during this process.

Environmental Permit for Industrial Installations

Where CCS installations meet defined thresholds typically CO_2 conditioning units, compressor stations or geothermal plants the developer must obtain an Environmental Permit issued under the **Regulation on Environmental Permits** (OG 8/2014). This permit serves as the binding operational licence for the facility, setting emission limits, monitoring obligations, technological standards and environmental-protection measures. It is typically issued after, and in full consistency with, the EIA decision. The competent environmental authority reviews the installation design, evaluates operational emissions, considers air-quality and noise-protection criteria under the Act on Air Protection, and ensures that waste-management obligations under the Waste Management Act and water-protection duties under the Water Act are integrated into operational conditions. The Environmental Permit therefore governs day-to-day compliance throughout the operational life of CCS assets.

Subsurface Rights for CO_2 Storage and Geothermal Use

Once environmental acceptability is established, the developer seeks subsurface rights under the **Act on the Exploration and Exploitation of Hydrocarbons** (OG 52/18, 52/19, 30/21) and, where applicable, the Act on Mining (OG 56/13, 14/14, 52/18, 115/18, 98/19, 83/23). These rights grant permission to explore, characterise and utilise the geological structure targeted for permanent CO_{2} storage or geothermal energy extraction.

Under the Act on the Exploration and Exploitation of Hydrocarbons, subsurface rights are not granted through classical concession mechanisms but through a licensing and contractual framework, typically involving the award of an exploration licence and the conclusion of an agreement with the Government of the Republic of Croatia defining the terms of exploration and potential exploitation.

The competent ministry issues the rights through administrative decisions and contractual arrangements that define the project area, work programme, reporting duties, financial securities and obligations for responsible subsurface management. Prior to issuing rights, authorities consult the **Regulation on Reserves** (OG 95/2018, 87/2022) to verify whether a geological structure is officially classified, reserved, or already allocated. This process protects against conflicts with hydrocarbon activities, groundwater extraction or geothermal licences and ensures that the CCS operator has legal certainty over subsurface access.

CO_2 Storage Permit

Copyright © SLB. All Rights Reserved. Private & Confidential. Reproduction only by permission.

The pivotal technical authorisation for a CCS project is the Storage Permit issued in accordance with the Act on the Exploration and Exploitation of Hydrocarbons (OG 52/18, 52/19, 30/21), and under the **Regulation on Permanent CO_2 Storage in Geological Structures** (OG 95/2018, 87/2022). This permit requires a rigorous demonstration of storage-complex characterisation, long-term containment potential, reservoir modelling, injectivity and pressure behaviour, caprock integrity, induced-seismicity risk, leakage pathways and possible interactions with groundwater bodies or protected ecosystems. The developer must submit a Monitoring Plan, Corrective-Measures Plan, Closure and Post-Closure Plan and financial security instruments. The competent authority evaluates whether the proposed formation can safely contain CO_2 for the long term and whether the developer satisfies all technical, environmental and operational requirements established by the hydrocarbons legislation and the environmental decisions. No injection may occur until the Storage Permit is granted.

Pipeline and Facility Construction Permits

With environmental and subsurface authorisations in place, the developer proceeds to construction under the **Act on Construction** (OG 155/25). Croatian law requires a sequential issuance of a location permit, construction permit and use permit, each confirming compliance with spatial-planning documents, EIA conditions, nature-protection measures, water-management requirements, fire-safety standards and engineering codes. Construction authorities review the technical design, safety studies, routing plans, geotechnical documentation, fire-prevention measures and land-use compatibility. For CO_2 pipeline corridors and compressor stations, this stage formalises design acceptance and grants legal permission to build and subsequently commission the infrastructure.

Major-Accident and Civil-Protection Compliance

Where installations store or handle hazardous substances above defined thresholds, the operator must satisfy Croatia's Seveso regime through the Regulation on the Prevention of Major Accidents Involving Hazardous Substances, requiring notification, major-accident policy or safety report, internal emergency plan and coordination with county authorities for external-emergency planning. This process is supported by obligations under the **Act on the Civil Protection System** (OG 82/15, 118/18, 31/20, 20/21, 114/22), which governs preparedness, alerting structures and cooperation with municipal and county civil-protection organisations. For compressor and conditioning sites, additional obligations arise from the **Act on Fire Protection** (OG 92/10, 114/22) and the **Regulation on the Preparation of Fire and Technological Explosion Risk Assessments** (OG 35/94, 110/05, 28/10), which mandate formal risk studies integrated into design documentation and enforceable during construction, operation and inspection.

Operational, Closure and Post-Closure Authorisation

Once facilities are constructed and tested, the use permit under the Act on Construction enables commissioning, after which the operator begins activities fully under the conditions of the Storage Permit, Environmental Permit and all nature-protection and water-management requirements. Operational compliance involves continuous environmental monitoring, subsurface performance monitoring, reporting obligations and timely implementation of corrective measures where

Copyright © SLB. All Rights Reserved. Private & Confidential. Reproduction only by permission.

required. During decommissioning, operators must execute the approved Closure Plan, abandon wells safely, remediate surfaces and continue monitoring during the post-closure period until the competent storage authority confirms that the CO_2 remains permanently contained and all long-term stability criteria under the CO_2 Storage Regulation and hydrocarbons legislation are met.

1.3.3.3 Environmental protection and nature protection

Environmental protection and nature conservation constitute one of the most consequential regulatory pillars for CCS-type projects in the Republic of Croatia, because they define the procedural obligations, substantive safeguards and institutional responsibilities that govern how any industrial activity interacts with the environment. For CCS and GT-CCS developers, this regulatory theme is not only a compliance requirement but the decisive procedural interface through which a project must pass in order to obtain environmental approval, secure public acceptance, demonstrate long-term safety and receive operational authorisation. The Croatian environmental framework governs the principles of environmental protection, instruments of environmental governance, public participation, access to information, access to justice, environmental impact assessment, environmental permits and special regimes for nature conservation, forming an integrated system that applies throughout the full life cycle of a CCS project from early feasibility assessments to long-term monitoring.

In parallel to these overarching procedural rules, project developers must also comply with Croatia's sectoral environmental laws including the Act on Air Protection, the Water Act and related groundwater-protection by-laws, the Act on Agricultural Land and soil-protection rules, as well as the Forest Act and Hunting Act which collectively ensure that CCS activities respect air-quality limits, groundwater integrity, agricultural and forestry values, and species-management obligations. Together, these instruments provide the operational environmental guardrails that apply regardless of project size or technology choice.

The centrepiece of this framework is the **Act on Environmental Protection** (OG 80/13, 153/13, 78/15, 12/18, 118/18), which establishes Croatia's fundamental environmental principles, including sustainable development, precaution, prevention, the polluter-pays principle and the obligation to integrate environmental considerations into sectoral legislation. The Act sets out instruments for environmental planning, environmental monitoring, access to environmental information, public participation in decision-making, and access to legal remedies, all of which shape the procedural foundation through which CCS-related works must be approved. For CCS and GT-CCS developers, this Act is the umbrella statute that determines how environmental oversight is exercised, what environmental documentation must be prepared, how the public must be consulted, and which authorities issue binding environmental decisions. Because it incorporates and operationalises Croatia's EIA and environmental permitting systems, the Act is inseparable from the project's regulatory path: no storage permit, no construction permit and no operational authorisation may be issued without procedures under this Act being fully completed.

Built upon this statutory foundation, the **Regulation on Environmental Impact Assessment** (OG 61/14, 3/17) provides the procedural framework and technical criteria for evaluating the environmental acceptability of projects with potentially significant environmental impacts. The

Copyright © SLB. All Rights Reserved. Private & Confidential. Reproduction only by permission.

Regulation specifies which types of projects are subject to mandatory EIA, including industrial installations, energy-related infrastructure, pipeline systems, facilities for the injection and permanent storage of CO_2 and geothermal production infrastructure. It defines the content of the EIA study, the scope of baseline surveys, the methods of impact assessment, and the procedural stages that lead to an EIA decision. For CCS and GT-CCS developers, this Regulation determines whether the project must undergo full EIA, which studies and surveys must be undertaken (e.g., hydrogeological assessments, biodiversity surveys, noise modelling, alternatives analysis), how stakeholder consultation must be structured and what level of evidence must be provided to secure a positive EIA decision. The **amended Regulation** (OG 3/2017) further refines methodology and procedural accuracy, meaning the operative EIA regime is the consolidated text and must be followed for any valid submission.

Alongside the EIA system, Croatian law establishes a dedicated environmental-permitting regime through the **Regulation on Environmental Permits** (OG 8/2014). This Regulation governs the issuance of environmental permits for industrial installations, including those associated with CCS infrastructure such as conditioning units, compressor stations and geothermal energy systems when they fall under relevant regulatory thresholds. The environmental permit functions as a binding, operational licence that sets emission limit values, monitoring obligations, operational constraints and environmental-protection measures for authorised facilities. For CCS developers, this permit represents an enforceable regulatory instrument that governs the daily functioning of the installation and must be secured before commissioning. It is typically granted following EIA procedures and remains valid throughout operation provided the operator meets its monitoring and reporting obligations.

Nature conservation is governed through a separate set of legal instruments, with the **Act on Nature Protection** (OG 80/13, 15/18, 14/19, 127/19, 155/23) providing the statutory framework for the conservation of habitats, species and landscape features, and establishing Croatia's Natura 2000 regime. This Act transposes the core obligations relating to habitat and species protection, placing strict requirements on projects that may affect Natura 2000 sites or protected species. For CCS and GT-CCS projects, it determines when a Natura 2000 screening must be undertaken, when a full appropriate assessment is required, and what conditions must be imposed to ensure conservation objectives are met. It also provides the basis for determining whether overriding public interest applies and what compensatory measures may be necessary, making it an essential parallel process to the EIA when Natura 2000 features are present within or near the project footprint.

Technical detail on Croatia's Natura 2000 network and governance is provided through the **Regulation on the Ecological Network and the Competences of Public Institutions for Managing Ecological Network Areas** (OG 80/19, 119/23). This Regulation defines the ecological network, lists and maps the Natura 2000 sites, establishes criteria for designation and confirms institutional responsibilities for site management. Importantly, it ensures that official Natura boundaries and conservation values are accessible through national GIS systems, enabling investors to determine whether pipeline routes, injection sites or geothermal installations intersect Natura 2000 areas. For CCS developers, this Regulation is essential for early routing and site-selection, as it identifies which conservation authorities must be consulted, and which ecological receptors require the greatest level of attention in assessment and mitigation planning.

Copyright © SLB. All Rights Reserved. Private & Confidential. Reproduction only by permission.

Further nature-protection specificity is introduced through the **Regulation on Conservation Goals and Measures for Target Bird Species in Ecological Network Areas** (OG 25/20, 38/20), which codifies conservation objectives and management measures for Special Protection Areas (SPAs). This Regulation determines the evidentiary and mitigation requirements when CCS infrastructure is located within, or may influence, areas designated for the protection of bird species. Timing restrictions, noise-avoidance measures, corridor-routing considerations and constraints on construction practices often derive from the conservation goals outlined in this Regulation and must be reflected within the project's appropriate assessment.

The **Regulation on the Inventory of Habitat Types and Habitat Map** (OG 27/21, 101/22) provides Croatia's official habitat classification system and habitat map, representing a technical reference point for field surveys and impact assessments. It defines habitat types of national interest and identifies threatened or rare habitats. For CCS and GT-CCS projects, this Regulation determines how field data must be collected, classified and mapped, ensuring that the environmental baseline accurately reflects site conditions and that impact assessments can correctly evaluate habitat sensitivity particularly for groundwater-dependent ecosystems, which may be relevant to geothermal or subsurface-pressure interactions.

Species-level protection is governed by the **Regulation on Strictly Protected Species** (OG 144/13, 73/16) and its amending Regulation, which establish lists of strictly protected species and regulate derogations, handling and disturbance thresholds. For CCS developers, these rules may require micro-routing, species relocation plans or seasonal construction windows where strictly protected species or their breeding/resting sites are present.

Within this broader nature-conservation context, special attention is warranted for the **UNESCO Man and the Biosphere (MAB) Mura-Drava-Danube Biosphere Reserve**, which contains hydrologically and ecologically sensitive floodplain systems. Although UNESCO designations do not impose the same legal constraints as Natura 2000, Croatian authorities routinely expect enhanced alternatives analysis, stronger mitigation hierarchies and early stakeholder engagement for projects intersecting MAB core or buffer areas.

Copyright © SLB. All Rights Reserved. Private & Confidential. Reproduction only by permission.

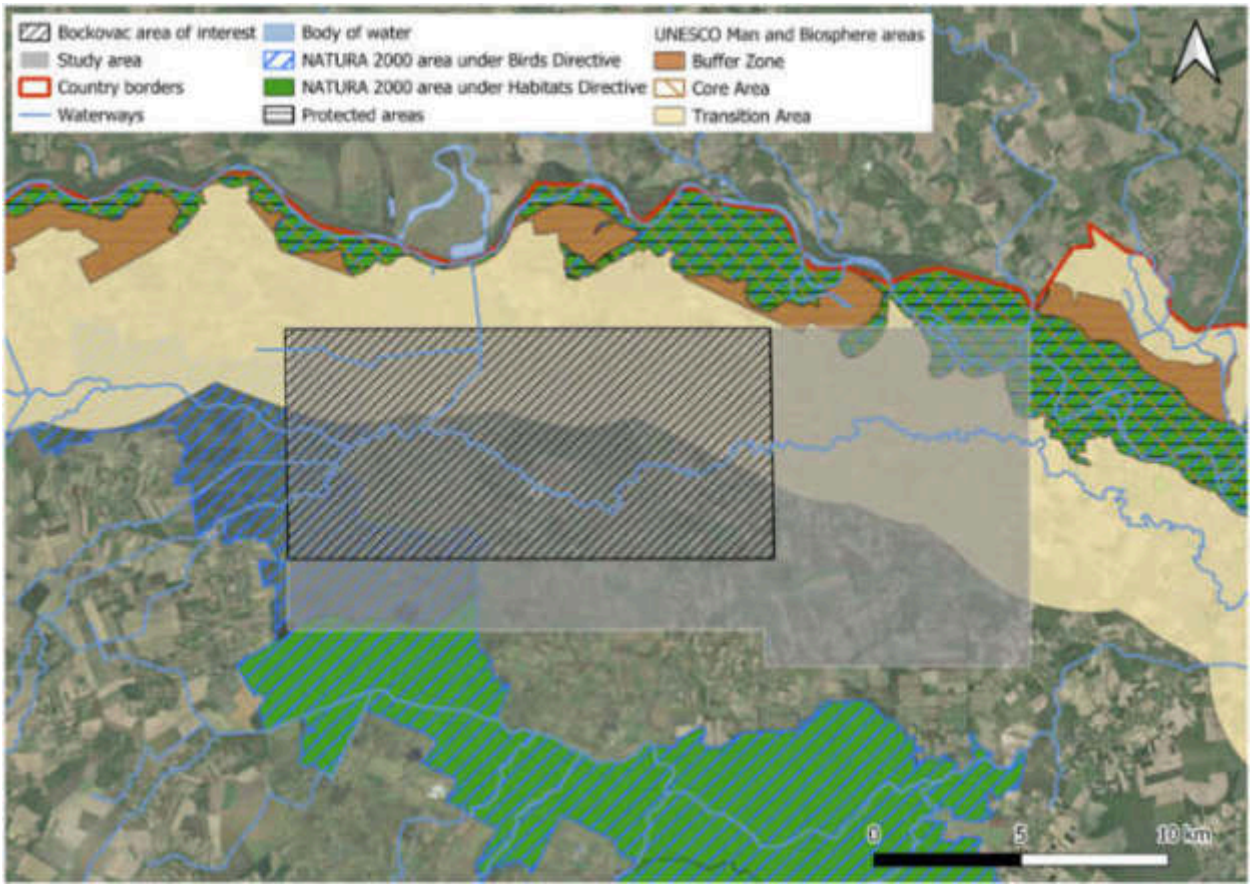


Fig. 1.12 Natura 2000 and UNESCO Man and Biosphere areas
Natura 2000 and UNESCO Man and Biosphere areas

The Bockovac Area of Interest lies partially within a designated Natura 2000 Birds Directive site and partly inside the Transition Zone of the UNESCO Mura-Drava-Danube Biosphere Reserve, as confirmed in the environmental baseline of the Bockovac Elaborate. Within these zones, restrictions are primarily ecological-impact related: in the Natura 2000 bird-protection area, activities must avoid disturbance of target bird species, maintain hydrological and habitat conditions, comply with seasonal constraints, and follow the conservation measures outlined for wetland and riparian bird assemblages, including preservation of reedbeds, open-water surfaces and surrounding foraging habitats.

In the UNESCO MAB Transition Area, while development is not prohibited, projects are expected to apply enhanced mitigation, maintain compatibility with landscape and ecological functions of the wider floodplain system, and prevent negative impacts on sensitive wetland and forest habitats that form part of the biosphere-reserve mosaic.

When comparing the Area of Interest with the broader Study Area, the Bockovac Area of Interest intersects fewer high-sensitivity Natura 2000 receptors and fewer UNESCO-related constraints and therefore represents the preferable area for permitting and technical implementation, reducing ecological-risk exposure and facilitating smoother regulatory approval.

Copyright © SLB. All Rights Reserved. Private & Confidential. Reproduction only by permission.

Beyond these principal instruments, a broader suite of environmental legislation applies to CCS and GT-CCS activities. The **Act on Air Protection** establishes obligations linked to air-quality standards and emissions from auxiliary equipment and industrial processes. The **Water Act** and its groundwater-protection by-laws regulate groundwater status, abstraction, discharge and protective zones critical for CO_2 storage in geological formations or geothermal-water extraction. The **Act on Agricultural Land** and soil-protection provisions govern disturbance of high-value agricultural soils and land remediation obligations. The **Forest Act and Hunting Act** regulate interventions in forested areas, game-management zones and wildlife corridors relevant for pipeline routing. Finally, the **Waste Management Act** governs the handling and disposal of drilling cuttings, construction waste and operational by-products, ensuring CCS-related works comply with national waste-management standards.

Together, these environmental and nature-protection instruments form an integrated and procedurally rigorous system that governs how CCS and GT-CCS projects must be assessed, conditioned and authorised in the Republic of Croatia. They ensure that geological CO_2 storage and geothermal-related developments proceed only on the basis of solid environmental evidence, transparent public participation, respect for ecological values and robust, enforceable operational safeguards throughout the project's full life cycle.

1.3.3.4 Infrastructure and Network Regulation

Infrastructure and network regulation in the Republic of Croatia forms the legal environment within which CCS-related transport systems particularly CO_2 pipelines and associated above-ground installations must be planned, authorised and operated. While Croatia does not maintain a dedicated CO_2-transport statute, the national energy and gas-market framework provides the structural analogies, institutional expectations and operational principles that guide how a future CO_2 network may be integrated into the national infrastructure system. These regulations define how energy-related networks are governed, which authorities supervise them, how licensing and oversight function, and under what broader energy-system rules linear infrastructure must be developed. For CCS investors, these acts frame the legal identity of a CO_2 transport corridor and outline which procedural interfaces and cross-sectoral obligations will apply.

The **Act on Energy** (OG 120/12, 14/14, 95/15, 102/15, 68/18) establishes Croatia's overarching framework for conducting energy activities and developing energy infrastructure. It defines the organisation of the energy sector, the roles and responsibilities of energy entities, the principles of energy-system planning, and the regulatory oversight exercised by competent authorities. Within the context of CCS, the Act is relevant because it provides the general legal envelope into which CO_2 transport infrastructure may be positioned when associated with energy-sector activities such as geothermal utilisation, industrial decarbonisation or integrated energy systems. It clarifies how energy infrastructure is licensed, how activities are classified, and how cross-sectoral obligations such as safety, market oversight, reporting and long-term system planning are carried out. Even though the Act does not explicitly regulate CO_2 networks, it offers a ready-made governance architecture that shapes expectations for regulatory compliance, institutional coordination and integration of CO_2 transport systems into Croatia's broader energy planning landscape.

Copyright © SLB. All Rights Reserved. Private & Confidential. Reproduction only by permission.

The **Act on the Gas Market** (OG 18/18, 23/20) provides a more technical parallel, as it governs pipeline-based energy transport systems, network operation, access rules and integrity standards for high-pressure linear infrastructure. While the Act focuses on natural gas, its regulatory approach particularly with regard to system operator responsibilities, third-party access, network maintenance, safety standards and operational reliability offers a valuable analogue for understanding how Croatia regulates pipeline systems of national importance. For CO_2 transport, where pipelines may share similar technical characteristics and safety considerations, the Act signals the type of institutional interfaces and regulatory expectations that may apply, including oversight by Croatia's national energy regulator, coordinated infrastructure planning and adherence to defined operational standards. For investors, this provides a practical preview of the procedural treatment that a CO_2 transport network is likely to encounter, even if the regulatory classification of CO_2 pipelines ultimately falls under a different legal category.

Although these two Acts do not regulate CCS infrastructure directly, together they establish the structural, procedural and operational reference points that a CO_2 transport system in Croatia must align with. They influence how investors conceptualise regulatory pathways, how permitting strategies are designed and how future network integration might be managed. Because infrastructure is inseparable from the viability of any CCS project, understanding these acts enables project developers to anticipate institutional expectations, design compliant transport systems and ensure that CO_2 pipelines and above-ground facilities fit coherently within Croatia's energy governance framework.

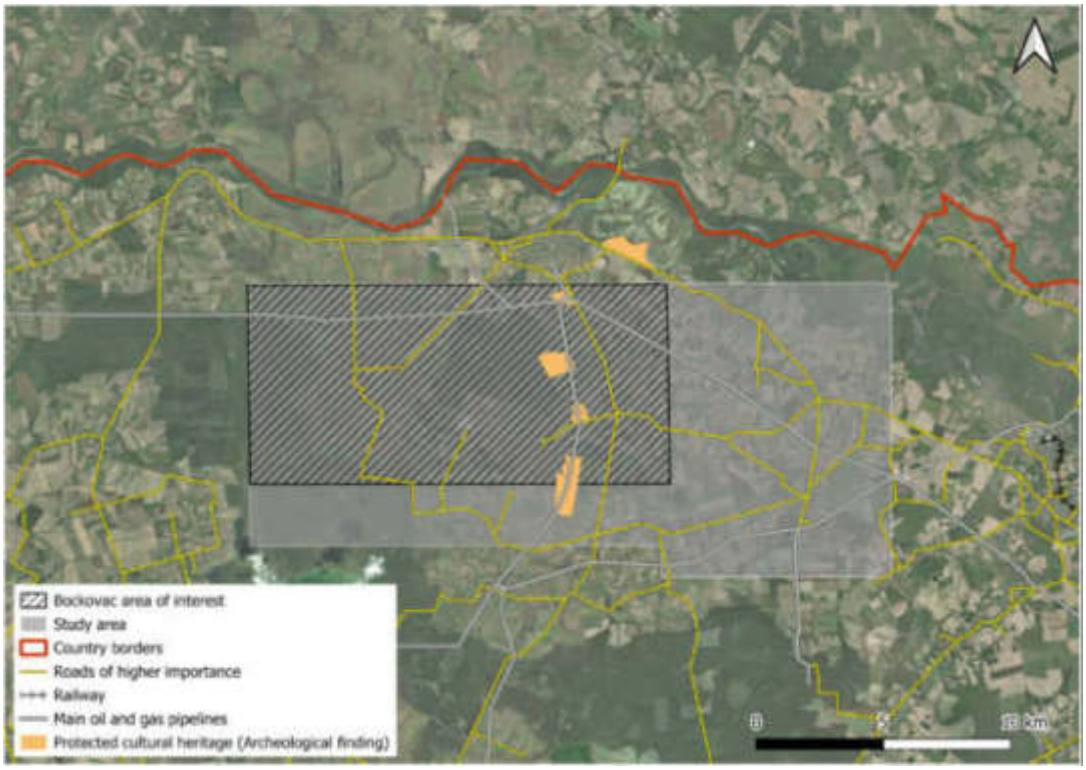


Fig. 1.13 Infrastructure and protected cultural heritage (Archaeological Sites Borik, Janjevci, Kraka, Ograd, Prinčevac and Selište)
Infrastructure and protected cultural heritage (Archaeological Sites Borik, Janjevci, Kraka, Ograd, Prinčevac and Selište)

Copyright © SLB. All Rights Reserved. Private & Confidential. Reproduction only by permission.

The Figure illustrates the relationship between the project's two spatial extents, the Bockovac Area of Interest and the wider Study Area, and the region's existing linear infrastructure, including higher-category roads, railway corridors and the main oil and gas transmission pipelines. It also identifies several protected cultural-heritage sites (Archaeological Sites Borik, Janjevci, Kraka, Ograd, Prinčevac and Selište), which fall under Croatia's cultural-heritage legislation and therefore require consideration during routing and permitting. Importantly, these archaeological sites are already intersected or closely paralleled by established transport and energy infrastructure, indicating long-standing compatibility between preservation requirements and linear-infrastructure development. In regulatory terms, this significantly reduces the likelihood of additional constraints for a future CO_2 pipeline, as Croatian spatial-planning and cultural-heritage authorities typically favour alignment with existing corridors where impacts have already been assessed, mitigated and operationalised. Accordingly, using or closely following these pre-existing routes is expected to minimise cultural-heritage risks, streamline permitting steps and offer a more predictable pathway for integrating CO_2 transport infrastructure into the national network system.

1.3.3.5 Safety and Extraordinary Events

Safety regulation in Croatia is a decisive layer for CCS projects because it governs how hazardous inventories are managed, which emergency-preparedness duties apply, and what evidence authorities require before commissioning compression, conditioning and pipeline assets. The **Regulation on the Prevention of Major Accidents Involving Hazardous Substances** (**Seveso III** - consolidated text) defines dangerous-substance lists, threshold quantities and the full procedural spine notification, safety policy or safety report, internal emergency plan, data for external plans, domino-effect and cross-border provisions determining whether a CO_2 conditioning/compression site falls under Seveso and, if so, the scope of design, CAPEX and documentation needed to comply (OPOT notice, registers, periodic reviews). If thresholds are met, this Regulation becomes the primary reference for permitting timelines and technical standards at the installation level.

The Act on the Civil Protection System (OG 82/15, 118/18, 31/20, 20/21, 114/22) provides the State-county-municipal framework for preparedness and response and ties Seveso establishments to external emergency planning with explicit roles, deadlines and coordination duties. For CCS promoters, this translates into scheduled data sharing with counties, alignment of internal and external plans, joint exercises where required and documented interfaces with first responders obligations that must be built into the project schedule and O&M procedures.

Fire-safety obligations derive from the **Act on Fire Protection** (OG 92/10, 114/22), which sets baseline design and operational requirements for industrial sites, covers technological explosions, and establishes enforcement and penalties (updated to euro amounts). In practice, compressor stations, valve stations and conditioning units must evidence compliance through approved designs, trained personnel, maintenance of fire systems and inspection readiness. The technical blueprint for these deliverables is the **Regulation on the Preparation of Fire and Technological Explosion Risk Assessments** (OG 35/94, 110/05, 28/10), which prescribes the content and method of the formal risk assessment hazardous-zone classification, inventories, sectorisation, hydrant networks, access routes and numerical analysis forming a mandatory input to design approval and a standing operational dossier.

Copyright © SLB. All Rights Reserved. Private & Confidential. Reproduction only by permission.

Taken together, these instruments keep CCS infrastructure within Croatia's major-accident, civil-protection and fire-safety expectations while remaining proportionate: if hazardous thresholds are triggered, Seveso dictates the depth and pace of safety submissions; regardless of thresholds, civil-protection and fire-safety regimes ensure credible emergency planning and enforceable site-level safeguards throughout the project life cycle.

Croatia's safety and emergency-management framework is complemented by two horizontal international instruments that shape the procedural environment for CCS projects: the **Aarhus Convention** and the **Espoo Convention**. Although these conventions do not impose technical design standards, they determine how environmental information is disclosed, how public and cross-border participation is carried out, and how decisions must be justified.

The Aarhus Convention is implemented through the Environmental Protection Act and Croatia's SEA/EIA system, which transpose EU directives on access to environmental information and public participation (Directives 2003/4/EC and 2003/35/EC) and govern participation rights throughout the assessment cycle. National implementation reporting confirms that these instruments operationalise Aarhus Articles 3-9 and ensure transparent disclosure, public consultation and access to justice in environmental matters. For CCS developers, this means that all significant environmental information must be made available to the public, that SEA/EIA procedures include formal participation steps, and that final decisions must withstand potential administrative and judicial review by affected stakeholders.

The Espoo Convention is embedded in the Environmental Protection Act and the Regulation on Environmental Impact Assessment, which integrate the full transboundary EIA procedure covering screening, notification, provision of documentation, cross-border consultations and transmission of the final decision. UNECE's implementation reviews confirm that Croatia applies these obligations systematically, while EU guidance highlights Espoo's relevance for major pipelines and industrial installations, directly applicable to CCS transport and storage infrastructure. A CCS project near the Hungarian border is therefore likely to trigger a transboundary assessment track: Croatia must notify Hungary, enable participation of Hungarian authorities and public, address comments in the final decision and formally communicate the outcome.

Together, Aarhus and Espoo establish the transparency, participation and cross-border procedural standards that govern environmental decision-making for CCS projects in Croatia. While they do not affect engineering design, they materially influence permitting timelines, documentation requirements and the defensibility of decisions actors that must be built into project planning from the outset.

1.3.4 Comparative legal overview of the CCS value chain in the EU and Croatia

This chapter provides an integrated comparison of the European Union's regulatory framework for carbon capture and storage with its Croatian counterparts, with the aim of identifying alignment, divergence and potential regulatory gaps across the full CCS value chain. In total, 67 EU-level regulations, directives, guidance documents and policy instruments relevant to permanent CO_2

Copyright © SLB. All Rights Reserved. Private & Confidential. Reproduction only by permission.

storage were analysed, alongside 47 Croatian legislative and regulatory acts applicable to CCS-related activities. Of the EU instruments reviewed, 27 were not transported into Croatian law, either because they are non-binding, such as European Commission guidance documents, strategies, plans and communications or because they take the form of Regulations, which are directly applicable in all Member States and therefore do not require national transposition.

This chapter highlights only the most important Croatian regulations for the CCS value chain and explains the key differences between EU-level requirements and their Croatian implementation. A complete, detailed gap analysis is provided as an Annex to this report, including a regulation-by-regulation comparison and assessment of how each Croatian act aligns with corresponding EU obligations. Each Croatian regulation examined in the Annex is assigned a relevance grade, where red indicates core, highly consequential legislation; yellow denotes legislation of medium relevance; and green marks supplementary or lower-impact acts. This structured overview supports a clear understanding of where Croatia's framework is aligned with EU standards and where divergences exist.

1.3.4.1 Energy, CCS and Geothermal Framework aspect

EU regulation	Relevance	Croatian regulation
Directive 2009/31/EC on the geological storage of carbon dioxide (CCS Directive)	HIGH	Act on Exploration and Exploitation of Hydrocarbons (OG 52/18, 52/19 and 30/21)
	HIGH	Ordinance on Permanent CO_2 Storage in Geological Structures (OG 95/2018)
	HIGH	Regulation on Amendments and Supplements to the Regulation on Permanent CO_2 Storage (OG 87/2022)
	HIGH	Regulation on Reserves (OG 95/2018, 87/2022)
	HIGH	Regulation on Compensation for the Exploration and Exploitation of Hydrocarbons (OG 25/20)
Directive 94/22/EC on the conditions for granting and using authorizations for the prospection, exploration and production of hydrocarbons	HIGH	Act on Exploration and Exploitation of Hydrocarbons (OG 52/18, 52/19 and 30/21)
Directive 2010/75/EU on industrial emissions (IED)	HIGH	Regulation on Environmental Permits (OG 8/2014)

Directive 2009/31/EC on the geological storage of carbon dioxide (CCS Directive) – Implementing Croatian regulation

Croatia has formally transposed the CCS Directive into its national framework, primarily through the Act on Exploration and Exploitation of Hydrocarbons (OG 52/18, 52/19, 30/21), which the Croatian Hydrocarbon Agency confirms as the legal act implementing Directive 2009/31/EC. Unlike the EU Directive, which establishes a dedicated, self-standing regime for geological CO_2 storage with explicit scope limitations such as the <100 kt exemption and a strict prohibition on water-column storage, Croatia embeds CO_2 disposal within a broader hydrocarbons and subsurface management statute, meaning CCS activities are processed through general hydrocarbon permitting pathways rather than CCS-specific procedures. This results in the absence of standalone provisions mirroring the Directive's explicit scope carve-outs or its detailed permitting logic (such as Article 8–10 requirements on site characterisation and permitting

Copyright © SLB. All Rights Reserved. Private & Confidential. Reproduction only by permission.

conditions). Similarly, where the Directive imposes bespoke financial security and long-term liability mechanisms tied to storage closure and post-closure responsibility (Articles 19–20), Croatian law relies on general hydrocarbon financial obligations, which do not provide an equivalent CCS-specific liability architecture.

Additional implementing instruments define the technical aspects of CO_2 storage, most notably the Ordinance on Permanent CO_2 Storage in Geological Structures (OG 95/2018). While this ordinance introduces technical criteria for site characterisation, monitoring, operation and closure, its requirements remain less prescriptive than those envisioned in the Directive and its updated 2024 Guidance Documents, which emphasise risk-based methodologies, leakage definitions, and geological uncertainties. The Croatian ordinance also does not explicitly differentiate between the geological certainty of depleted hydrocarbon reservoirs versus saline aquifers, an important distinction in the Directive's risk-assessment framework, and it does not fully articulate how potential conflicts between CO_2 storage and other subsurface uses should be resolved. Additionally, although the ordinance addresses monitoring-plan content, it does not reflect the Directive's detailed provisions on transfer of responsibility, nor does it establish a clear system for financial contributions linked to post-closure risk.

The Regulation on Amendments and Supplements to the Regulation on Permanent CO_2 Storage (OG 87/2022) makes technical refinements, particularly regarding fluid and reservoir behaviour, but does not introduce new standards; instead, it updates terminology while leaving the structural regulatory architecture unchanged. Likewise, the Regulation on Reserves (OG 95/2018, 87/2022) supports CCS implementation by defining how geological structures are classified and documented for "permanent CO_2 disposal," translating elements of the Directive's site-selection expectations into Croatian practice but at a higher, resource-mapping level rather than adopting the Directive's site-specific risk and suitability criteria. Finally, the Regulation on Compensation for the Exploration and Exploitation of Hydrocarbons (OG 25/20) governs fees and compensation for subsurface resource use; however, the Directive does not regulate economic compensation mechanisms, focusing instead on environmental liability and financial security, meaning this Croatian instrument introduces obligations that go beyond the Directive, but without substituting for the Directive's required CCS-specific financial safeguards.

Directive 94/22/EC on the conditions for granting and using authorizations for the prospection, exploration and production of hydrocarbons - Act on Exploration and Exploitation of Hydrocarbons (OG 52/18, 52/19 and 30/21)

Croatia transposes Directive 94/22/EC through the Act on Exploration and Exploitation of Hydrocarbons (OG 52/18, 52/19, 30/21), which incorporates the Directive's key requirements on transparent, objective and non-discriminatory licensing for hydrocarbon prospection and production. The national act aligns with the Directive's rules on open access, technical and financial capability criteria, and clearly defined licence duration and geographical scope. Unlike the EU Directive, which governs only hydrocarbon authorisations, Croatian law applies the same permitting framework to hydrocarbons, geothermal resources and even permanent CO_2 disposal, meaning it extends the Directive's licensing logic to activities not originally covered by EU law. This

Copyright © SLB. All Rights Reserved. Private & Confidential. Reproduction only by permission.

creates a system that satisfies the Directive's procedural obligations but does not introduce CCS-specific adaptations, instead treating CO_2 storage as part of the broader identified subsurface resource regime.

Directive 2010/75/EU on industrial emissions (IED) - Regulation on Environmental Permits (OG 8/2014)

Croatia's Regulation on Environmental Permits (OG 8/2014) broadly mirrors the Industrial Emissions Directive (2010/75/EU) by establishing an integrated permitting system and requiring the use of BAT principles, consistent with the Directive's structure. However, unlike the IED, which treats BAT conclusions as binding and requires that emission limit values be set strictly in line with BAT-AELs, with narrowly defined and rigorously justified exceptions under Article 15(4), the Croatian regulation applies BAT more as guidance, resulting in looser terminology, less prescriptive sequencing, and an absence of the IED's detailed compliance assessments, particularly the cost-benefit analysis required to justify derogations. As a result, while Croatia has structurally transposed the IED's integrated-permit model, it does not fully reflect the Directive's strict, enforceable approach to BAT obligations and Article 15(4) derogation criteria.

Copyright © SLB. All Rights Reserved. Private & Confidential. Reproduction only by permission.

1.3.4.2 Environmental and nature protection aspect

EU regulation	Relevance	Croatian regulation
Directive 2011/92/EU on Environmental Impact Assessment	HIGH	Act on Environmental Protection (OG 80/13, 153/13, 78/15, 12/18, 118/18) Regulation on Environmental Impact Assessment (OG 61/14, 3/17)
		Act on Spatial Planning (OG 155/25)
Directive 2001/42/EC on Strategic Environmental Assessment (SEA)	HIGH	Act on Spatial Planning (OG 155/25) Act on Environmental Protection (OG 80/13, 153/13, 78/15, 12/18, 118/18)
Directive 92/43/EEC on the conservation of natural habitats (Habitats Directive)	HIGH	Act on Nature Protection (OG 80/13, 15/18, 14/19, 127/19, 155/23) Regulation on the Ecological Network (OG 80/19, 119/23)
Directive 2009/147/EC on the conservation of wild birds (Birds Directive)	HIGH	Act on Nature Protection (OG 80/13, 15/18, 14/19, 127/19, 155/23)
Directive 2003/35/EC providing for public participation in respect of the drawing up of certain plans and programmes relating to the environment	HIGH	Regulation on Environmental Permits (OG 8/2014) Act on Environmental Protection (OG 80/13, 153/13, 78/15, 12/18, 118/18)
Regulation (EU) 2024/1735 – Net-Zero Industry Act (NZIA)	HIGH	Decision on implementing Regulation (EU) 2024/1735 establishing a framework of measures to strengthen the European ecosystem for the production of zero-emission technologies (OG 2/2025)
Directive 2006/118/EC on the protection of groundwater	HIGH	Act on Waters (OG 66/19, 84/21, 47/23)
Directive 91/271/EEC concerning urban waste-water treatment	HIGH	Act on Waters (OG 66/19, 84/21, 47/23)
Directive 2000/60/EC establishing a framework for Community action in the field of water policy	HIGH	Act on Waters (OG 66/19, 84/21, 47/23)
Directive 91/676/EEC concerning the protection of waters against pollution caused by nitrates from agricultural sources	HIGH	Act on Waters (OG 66/19, 84/21, 47/23)
Directive 2008/105/EC on environmental quality standards in the field of water policy, amending	HIGH	Act on Waters (OG 66/19, 84/21, 47/23)
Directive 2009/90/EC laying down technical specifications for chemical analysis and monitoring of water status	HIGH	Act on Waters (OG 66/19, 84/21, 47/23)
Directive 2003/87/EC establishing a scheme for greenhouse gas emission allowance trading within the Community	HIGH	Act on Climate Change and Protection of the Ozone Layer (OG 67/25)
Directive 2004/101/EC amending Directive 2003/87/EC establishing a scheme for greenhouse gas emission allowance trading within the Community, in respect of the Kyoto Protocol's project	HIGH	Act on Climate Change and Protection of the Ozone Layer (OG 67/25)
Directive 2009/29/EC amending Directive 2003/87/EC so as to improve and extend the greenhouse gas emission allowance trading scheme	HIGH	Act on Climate Change and Protection of the Ozone Layer (OG 67/25)
Directive (EU) 2018/410 amending Directive 2003/87/EC to enhance cost-effective emission reductions and low-carbon investments	HIGH	Act on Climate Change and Protection of the Ozone Layer (OG 67/25)
Directive (EU) 2023/959 amending Directive 2003/87/EC establishing a system for greenhouse gas emission allowance trading within the Union and Decision (EU) 2015/1814 concerning the establishment and operation of a market stability reserve	HIGH	Act on Climate Change and Protection of the Ozone Layer (OG 67/25)
Directive 2006/21/EC on the management of waste from extractive industries	HIGH	Regulation on Waste Management from the Mining Industry (OG 56/23)
Directive 2014/23/EU on the award of concession contracts	HIGH	Act on Concessions (OG 69/17, 107/20)

Copyright © SLB. All Rights Reserved. Private & Confidential. Reproduction only by permission.

Directive 2011/92/EU on Environmental Impact Assessment - Croatian EIA Framework
While the Directive 2011/92/EU provides a unified EU-level framework for EIA, Croatian legislation distributes these requirements across the Spatial Planning Act and the Act on Environmental Protection. The Spatial Planning Act integrates EIA requirements into development consent procedures and ensures alignment of projects with spatial plans, but it does not define the detailed EIA content, thresholds, or sector-specific obligations, these remain governed by the EIA Regulation. In contrast, the Act on Environmental not only transposes Directives 2011/92/EU and 2014/52/EU but establishes Croatia's broader EIA regime, including screening, public participation, and access-to-justice provisions. However, it also goes beyond the Directive by prescribing additional national procedures, authorities, and monitoring obligations. For CO_2 transport and storage infrastructure, this means that although the core EIA principles are aligned with EU law, project developers must navigate a more layered national system with additional local requirements that are not explicitly foreseen in the Directive, potentially influencing timelines, documentation depth, and coordination across spatial planning, permitting, and monitoring processes.

Directive 2001/42/EC on Strategic Environmental Assessment - Act on Spatial Planning (OG 155/25)
The SEA Directive is implemented through the Act on Spatial Planning, which references the Directive explicitly and conditions the adoption of spatial plans on compliance with SEA requirements. However, the SEA procedural detail, including scoping, study content and public participation, is not contained in the Spatial Planning Act, but instead resides in the Environmental Protection Act and the relevant SEA by-laws. This creates a dual-act structure where spatial planning governs the planning process while environmental legislation governs SEA execution. Although legally coherent, it places responsibility on the investor to ensure that planning documentation fully reflects SEA outputs, as the planning act itself does not restate or operationalise them.

Directive 2003/35/EC on Public Participation in Environmental Decision-Making - Regulation on Environmental Permits (OG 8/2014)
The Croatian Regulation on Environmental Permits implements Directive 2003/35/EC more explicitly and more procedurally than the Directive itself, detailing public-participation steps, information requirements, BAT/BREF integration and consultation processes. The EU-level obligations are therefore fully met and, in some respects, exceeded, as Croatian law includes binding annexes, forms and pollutant lists that are not found in the Directive. The gap is therefore one of structural expansion: Croatian requirements are more prescriptive and detailed than the Directive, meaning investors must meet stricter procedural documentation standards than those explicitly required by EU law.

Regulation (EU) 2024/1735 Net-Zero Industry Act (NZIA) - National Implementing Decision (OG 2/2025)
Croatia's implementing decision for the NZIA introduces the Regulation into the national legal order without material deviation. No structural or procedural gaps were identified. The obligations for

Copyright © SLB. All Rights Reserved. Private & Confidential. Reproduction only by permission.

strategic projects, permitting acceleration and infrastructure facilitation mirror the EU Regulation's objectives, meaning investors can rely on direct EU-law rights in Croatia without additional national barriers.

Directive 2006/118/EC on Groundwater Protection - Act on Waters (OG 66/19, 84/21, 47/23)
Croatia's Act on Waters incorporates the Directive's "*prevent or limit*" groundwater protection obligations and applies them directly to CCS-related activities, including drilling, injection, construction near aquifers and any abstraction/discharge needs. The gap relates primarily to interpretation risk, as Croatian water authorities apply groundwater-protection tests conservatively for subsurface projects. There is no legislative misalignment, but permitting practice often imposes higher evidentiary thresholds than the minimum defined in EU law, particularly for projects near drinking-water bodies or groundwater-dependent ecosystems.

Directive 91/271/EEC on Urban Waste-Water Treatment - Act on Waters (OG 66/19, 84/21, 47/23)
Croatia's water legislation incorporates UWWTD obligations for wastewater collection and treatment in agglomerations. There is no direct substantive connection to CCS; however, CCS construction or operational discharges must comply with UWWTD-aligned national discharge conditions. The gap is contextual rather than regulatory: the Directive's focus is municipal wastewater, while CCS is industrial. The indirect relevance means the Directive does not impose CCS-specific obligations, but compliance with national discharge rules derived from it remains mandatory.

Directive 2000/60/EC Water Framework Directive (WFD) - Act on Waters (OG 66/19, 84/21, 47/23)
Croatia's Act on Waters implements WFD principles, including non-deterioration, achievement of good status and enhanced protection for drinking-water bodies. For CCS projects, these obligations form part of the permit test applied by water authorities. The gap lies in the operationalisation of "*no deterioration*", where Croatian authorities typically require more detailed modelling and more conservative risk assessments than required under minimum EU standards, particularly concerning pressure interactions with groundwater bodies. While fully compliant with EU law, Croatia applies a precaution-weighted interpretation that may increase evidentiary requirements for CCS.

Directive 91/676/EEC (Nitrates Directive) - Act on Waters (OG 66/19, 84/21, 47/23)
Croatia's Act on Waters incorporates the Nitrates Directive through nitrate-vulnerable zone (NVZ) designations and mandatory action programmes aimed at reducing agricultural nitrate pollution. For CCS, the Directive's relevance is indirect: pipeline routing, landfall areas or surface facilities located within NVZs must comply with land-management and water-protection measures that were originally designed for agricultural pressures. The gap is therefore contextual rather than legislative, the Directive is fully transposed, but CCS developers must assess route impacts through agricultural NVZ constraints, which Croatian law does not tailor specifically to industrial linear infrastructure.

Copyright © SLB. All Rights Reserved. Private & Confidential. Reproduction only by permission.

Directive 2008/105/EC (Environmental Quality Standards for Priority Substances) - Act on Waters (OG 66/19, 84/21, 47/23)

EU standards for priority and priority-hazardous substances are incorporated through Croatia's water-quality classification system. These standards influence any discharge or groundwater interaction associated with CCS infrastructure. The gap is minimal: Croatia applies the EU EQS values, but national implementation may apply more conservative thresholds in practice depending on local water-body status. This can elevate the evidence required for CCS discharges, dewatering during construction, or monitoring in water-dependent habitats.

Directive 2009/90/EC (Technical Specifications for Water Monitoring) - Act on Waters (OG 66/19, 84/21, 47/23)

Croatia has transposed the Directive's analytical-quality and monitoring-performance criteria through its water-monitoring framework, ensuring consistency with WFD requirements. For CCS projects, the Directive becomes relevant whenever baseline or operational monitoring of groundwater or surface water is required, for instance at pipeline crossings, compressor stations, or storage-site monitoring wells. The gap lies not in transposition but in investor obligations: all monitoring data submitted in permitting must use Directive-compliant QA/QC, accredited methods and performance standards, otherwise results may be dismissed as legally insufficient.

Directive 2003/87/EC (ETS Directive) - Act on Climate Change and Protection of the Ozone Layer (OG 67/25)

The ETS Directive, as amended, explicitly recognises CO_2 transported to and permanently stored in compliant geological formations as "*not emitted*." Croatian climate legislation transposes ETS participation and reporting obligations but does not contain explicit provisions on CCS chain elements or "*non-emitted*" CO_2 recognition in the retrieved text. The gap is therefore a missing explicit reference: although ETS applies directly as EU law, national legislation does not restate the storage-related ETS provisions, requiring investors to rely directly on EU law without clear Croatian article-level guidance.

Directive 2004/101/EC (Linking Directive – CER/ERU under Kyoto) - Act on Climate Change (OG 67/25)

Croatia's climate act acknowledges the Directive via transposition reference but does not provide a detailed framework for national CER/ERU accounting or project-based mechanisms. The gap is one of incompleteness rather than inconsistency, the Directive's purpose has been overtaken by later ETS reforms, and the Croatian text reflects only the high-level legal basis without operational detail. There is no practical impact on CCS, but the transposition is formal rather than substantive.

Directive 2009/29/EC (ETS Amendment Extending ETS & Recognising CCS) - Act on Climate Change (OG 67/25)

Directive 2009/29/EC explicitly integrates CCS into the ETS by recognising captured and permanently stored CO_2 as "*not emitted*" and establishing rules for transport and injection. The Croatian act, in its retrieved form, does not reproduce these specific CCS-related ETS rules, instead referencing ETS obligations at a general level. This creates a functional gap: CCS investors do not find national, article-level confirmation of ETS treatment of stored CO_2, even though EU law applies directly. In practice, operators must rely on EU provisions rather than Croatian statutory text for certainty.

Copyright © SLB. All Rights Reserved. Private & Confidential. Reproduction only by permission.

Directive (EU) 2018/410 (ETS Reform) - Act on Climate Change (OG 67/25)
The Directive updates ETS allocation rules, the Market Stability Reserve, and low-carbon investment incentives. Croatia's act acknowledges ETS and MSR but does not reproduce detailed EU-level allocation or MSR rules. The gap is therefore procedural clarity: EU law remains directly binding, but Croatian legislation does not provide domestic interpretative or administrative detail. For CCS investors, the lack of national clarification means allowance-allocation expectations must be derived directly from EU texts, not Croatian ones.

Directive (EU) 2023/959 (ETS Revision and Market Stability Reserve) - Act on Climate Change (OG 67/25)
The Directive maintains ETS treatment of CCS without introducing additional CCS-specific obligations. Croatia's climate act continues to provide the general ETS framework but does not mention CCS transport or storage explicitly, nor does it incorporate detailed MSR rules. The gap is one of silence rather than misalignment: CCS treatment is correct under EU law but not explicitly confirmed in Croatian statutory language.

Directive 2006/21/EC (Extractive Waste Directive) - Regulation on Waste Management from the Mining Industry (OG 56/23)
Croatia's mining-waste rulebook transposes the Directive comprehensively and adds detailed annexes, templates and prescriptive content absent from the Directive. This results in a national framework that is more detailed and procedural than the EU baseline. For CCS, the relevance arises during drilling of wells where extractive waste is produced. The gap is additional national complexity, not a deficiency: investors must comply with expanded Croatian documentation and safety-system requirements beyond the Directive's minimum standards.

Directive 2014/23/EU (Concessions Directive) - Act on Concessions (OG 69/17, 107/20)
Croatia's Act on Concessions implements the Directive's principles and thresholds but adds mandatory forms, templates, a national concession register and Ministry of Finance oversight, creating significantly more granular domestic procedures than the Directive requires. EU law is principle-based; Croatian law is procedural and administratively dense. For CCS investors seeking concessions for subsurface rights or public land, the gap means higher administrative formality and potentially longer preparatory phases than envisioned in the Directive.

1.3.4.3 Spatial planning, property and safety aspect

EU regulation	Relevance	Croatian regulation
Directive 2014/23/EU on the award of concession contracts	HIGH	Act on Concessions (OG 69/17, 107/20)
Directive 2012/18/EU (Seveso III) on the control of major-accident hazards involving dangerous substances	HIGH	Act on Spatial Planning (OG 155/25) Act on Environmental Protection (OG 80/13, 153/13, 78/15, 12/18, 118/18) Civil Protection System Act (OG 82/15, 118/18, 31/20, 20/21, 114/22)

Directive 2014/23/EU on the award of concession contracts - Act on Concessions (OG 69/17, 107/20)
The Concessions Directive sets principle-based requirements on transparency, equal treatment,

Copyright © SLB. All Rights Reserved. Private & Confidential. Reproduction only by permission.

competition and threshold-driven procedures, leaving Member States broad discretion on administrative form. Croatia's Act on Concessions transposes those principles but goes considerably further in prescribing standardised forms, national concessions register, and finance-ministry oversight, together with detailed procedural templates and registry rules. There is no substantive misalignment with the Directive; the gap is one of administrative density: Croatian law introduces granular domestic formalities beyond EU minimums, which increases preparatory work and file-quality expectations for investors seeking concessions linked to subsurface use, corridor occupation or public assets. In practice, this elevates documentation effort and timeline discipline relative to the baseline EU requirements, even though the underlying award principles remain fully aligned.

Directive 2012/18/EU (Seveso III) on the control of major-accident hazards - Act on Spatial Planning (OG 155/25)

Croatia meets Seveso III's land-use duty through the Act on Spatial Planning (OG 155/25), ensuring accident-risk is integrated in zoning/siting; the establishment-level obligations are implemented separately. The Regulation on the Prevention of Major Accidents Involving Hazardous Substances (OG 44/14, 31/17, 45/17) expressly transposes Seveso III and sets dangerous-substance thresholds, OPOT notification (*cro. "Obavijest o prisutnosti opasnih tvari"*) and the content/approval of Major Accident Prevention Policy and the Safety Report, including supervision, updates and cross-border accident procedures. The Environmental Protection Act provides the legal basis for these Seveso procedures and competent-authority oversight (safety-report approval/inspection). Administrative by-laws establish the national Seveso register and the expert council that evaluates safety reports, while the Civil Protection System Act implements external emergency planning at county level (domino-effect and dangerous-substances definitions included). The Fire Protection Act and fire/explosion risk-assessment rules complement Seveso with national design-and-operation safety deliverables. Thus, the land-use risk integration sits in spatial planning, whereas operator-level Seveso compliance (notification, MAPP, Safety Report, internal plans, registers, external plans) is governed by environmental/civil-protection instruments requiring CCS promoters to run two coordinated tracks in permitting and design.

1.3.5 Key findings

This report provides targeted review of relevant EU legislation, as well as a comprehensive examination of Croatian legislation and a gap analysis to identify how Croatian law aligns with and operationalises EU requirements, with particular emphasis on the permitting environment, spatial and environmental constraints, and the practical implications of project siting. Across all analysed legislation, institutional requirements and GIS-based spatial datasets, the findings indicate that Croatia offers legal basis for permanent geological CO_2 storage and geothermal development, but the regulatory pathway can be complex, sequential, and highly sensitive to location.

At the national level, the Act on Exploration and Exploitation of Hydrocarbons, the Regulation on Permanent CO_2 Storage, the Regulation on Reserves, the Act on Environmental Protection and its accompanying EIA framework collectively establish the conditions under which geological formations may be licensed, evaluated, approved and monitored for long-term CO_2 containment.

Copyright © SLB. All Rights Reserved. Private & Confidential. Reproduction only by permission.

This framework is structurally sound, aligned with the EU CCS Directive, and operationalised through established administrative procedures. However, the practical feasibility of progressing through this framework depends heavily on the environmental, spatial-planning and land-use context of the selected area. The permitting system obliges the investors to demonstrate full alignment with spatial-plan designations, Natura 2000 conservation objectives, hydrological and geological stability, safety obligations and construction standards, making early strategic site selection the central driver of project success.

In that context, the spatial analysis undertaken for this report clearly demonstrates that the wider Study Area contains a much higher density of environmental constraints. It overlaps with extensive Natura 2000 sites designated under both the Birds and Habitats Directives, flood-risk zones, wetlands and sensitive hydrological systems, as well as transition areas of the UNESCO Mura-Drava-Dunav Biosphere Reserve. These areas trigger stringent and often time-intensive procedural obligations under Croatian and EU law, including Appropriate Assessment, habitat-specific mitigation requirements, restrictions on interventions in floodplains and groundwater-dependent ecosystems, and heightened scrutiny over potential ecological and hydrological effects. The Bockovac Environmental Elaborate (*Environmental Screening Study for the Construction of Investigative Geothermal Wells in the Preliminary Bockovac Exploration Area*) confirms how these environmental sensitivities shape feasibility even for relatively small investigative works, noting, for instance, the need to avoid impacts on specific habitat types, bird species and ecological networks within the region. For a CCS installation, which requires pipeline routing, surface infrastructure and long-term monitoring systems, these constraints would be significantly amplified.

By contrast, the Bockovac Area of Interest emerges as a materially safer and more permitting-efficient option. Although the Area of Interest also lies partly within a Natura 2000 Birds Directive area and the Transition Zone of the UNESCO biosphere reserve, the extent of protected habitats, ecological sensitivities and conflicting land-use restrictions is markedly lower. The Elaborate confirms that the Area of Interest can accommodate subsurface activities with manageable environmental impacts, provided best-practice mitigation measures are applied, and that the footprint of sensitive habitats is more limited, reducing the overall risk of an adverse environmental finding. Moreover, development within UNESCO Transition Zones is not prohibited; instead, it requires responsible management and mitigation, requirements which the Area of Interest demonstrably meets more easily than the wider region.

An additional, highly significant advantage is the presence of robust geological and geophysical datasets across the Area of Interest, including the seismic, hydrogeological and exploratory information gathered during decades of hydrocarbon research as well as the recent geothermal investigations described in The Bockovac Environmental Elaborate; moreover, the Integrated Feasibility Study carried out under the present contract will further consolidate the geological understanding of the Area of Interest and of its performance both for CO_2 storage and geothermal energy production. Under the Regulation on Permanent CO_2 Storage, the Storage Permit requires extensive demonstration of reservoir suitability, injectivity, containment integrity, sealing properties and long-term stability. Areas with pre-existing validated subsurface data not only reduce

Copyright © SLB. All Rights Reserved. Private & Confidential. Reproduction only by permission.

technical uncertainty but shorten the regulatory path to permit issuance. This reduces cost, compresses timelines and improves overall project bankability, critical factors for an integrated geothermal-CCS project.

Spatial-planning alignment is an equally decisive factor. The Area of Interest presents fewer conflicts with existing land-use plans, and where cultural-heritage sites exist, they are already situated near established infrastructure corridors. This implies that future CO_2 pipelines or geothermal-related surface installations could be routed in ways that avoid new impacts. Given Croatia's strict spatial-planning regime; under which no construction or location permits may be issued unless full consistency with binding spatial plans is demonstrated; this characteristic of the Area of Interest translates directly into reduced permitting risk.

Finally, the project's status as part of the European Union's Common Interest List (PCI) further elevates the importance of selecting a site that can realistically satisfy stringent regulatory expectations. PCI projects are expected to demonstrate environmental robustness, compliance with EU climate and biodiversity standards, and readiness for cross-border infrastructure integration. The Area of Interest, by virtue of its more favourable environmental and spatial-planning profile, is uniquely positioned to meet these expectations. Selecting the wider Study Area, by contrast, would expose the project to significantly higher uncertainty, extended permitting timeframes and potential setbacks during environmental or spatial-planning review.

In conclusion, based on the integrated review of Croatian legislation, environmental and spatial constraints, the gap analysis, and the findings of the Bockovac Environmental Elaborate, this report concludes that the Bockovac Area of Interest represents the most feasible, lowest-risk and most strategically aligned location for advancing a permanent CO_2 storage project in a geothermal aquifer in Croatia. The Area of Interest provides a clearer pathway through Croatia's demanding permitting system, presents fewer ecological and spatial conflicts, leverages existing subsurface knowledge and aligns with EU-level expectations for PCI-listed energy-transition infrastructure. Prioritising the Area of Interest therefore offers the strongest foundation for a viable, timely and regulatory-compliant integrated feasibility study and for the future development of Croatia's first permanent CO_2 storage site in a geothermal reservoir.

Copyright © SLB. All Rights Reserved. Private & Confidential. Reproduction only by permission.

2 Geological and reservoir engineering solution

2.1 Overview of the exploration area

2.1.1 Geological overview

Report: Geological Overview and Characterization of the Bockovac Area (Drava Depression, Croatia)

1. Introduction

Area of interest located near the Hungarian border close to Bockovac village in Osijek-Baranja County, Eastern Croatia. A rural setting within the flatter terrain of the county, with an elevation of about 95 meters above sea level.

2. Area of Interest Definition

The area of interest (AOI; Fig. 2.1, Fig. 2.2 and Fig. 2.3) is geographically defined by a specific polygon surrounding the Bockovac region. The AOI encompasses the eastern part of the Drava Depression, extending from the Ladislavci Field in the west to the Gat-1 and Marjanci-3 wells in the east, bordered by Hungary in the north and the Beničanci Field in the south.



Fig. 2.1 Regional Map of the Study Area
Location of the Drava Depression and of the area of interest (blue rectangle)

- The AOI includes the Ladislavci-Kućanci field (currently in production) as well as additional potential locations, such as Čamagajevci, Krunoslavlje, Marjanči, Sječe, and others. Some of these are not considered established fields.

Copyright © SLB. All Rights Reserved. Private & Confidential. Reproduction only by permission.

- Initial investigations were conducted primarily to evaluate CO_2 storage potential and geothermal energy usage in the area north of the Ladislavci-Kućanci field, including around Bockovac.
- The detailed study extended the previously defined polygon (shown as pink in datasets) to encompass a larger region in the current geological model.
- **Regional Geological Overview**
  The Drava basin in this region contains varied geological structures formed at different times. The area is classified as a graben or junction-type setting that was formed during the Miocene period and was later affected by tectonic inversion during the formation of the Pannonian Sea (Lake).
- **Early Depositional Environment**: Initially, shallow marine conditions prevailed with significant deposits of carbonates and breccias, later overlain by marine clays, marls, and sandstones.
- **Quaternary Deposits**: Recent sediments comprise gravels, sandstones, shaley and marly sandstones, and alluvial lake and marine deposits related to tectonic subsidence phases.
- **Lake Pannonian and Pliocene Epochs**: This period is marked by lacustrine sedimentation, and the formation of thick sand, gravel, silt, and clay layers, including thin coal seams (content varying up to 30%)—with the absence of coal in some wells indicating breaks in sedimentation.

3. Structural and Lithostratigraphic Summary (Fig. 2.2 and Fig. 2.4)

Geological formations within the AOI reflect the region's complex tectonic and sedimentary history [1] [2]:

- The area can be subdivided into two main parts based on geosynclinal development, each with distinct lithological characteristics.
- **Late Badenian and Sarmatian Ages**: Predominantly marine, with basal conglomerates, algal and reef limestones, thin reef post-rift boundaries, and marls.
- Overlying (Late Miocene) sediments are mainly clastics from the Lake Pannon period, such as interbedded sandstones and marls, with deltaic influences and carbonate cementing.
- **Pliocene and Quaternary (Vuka/ Moslavačka Gora Formation)**: Freshwater lacustrine deposits (Lake Slavonia) primarily consisting of sand, gravel, silt, clay, and coal (locally up to 50%).

4. Petrophysical and Reservoir Characteristics

Productive intervals are commonly associated with the Moslavačka Gora and Vukovarska formation (Valpovarska) formations, comprising breccias, conglomerates, dolomites, and limestones. These typically exhibit dual (fracture plus matrix) porosity systems. While primary porosity is low, effective porosity is locally enhanced due to fracturing. These formations are often oil-bearing, with traces of hydrocarbons found even in wells without significant production.

Other notable intervals include the Ivanić-Grad and Vinkovci formations, which contain fine-grained, quartz-mica sandstones (generally grey in color and gas-saturated). This interval shows gas traces in Sječe wells.

Copyright © SLB. All Rights Reserved. Private & Confidential. Reproduction only by permission.

5. Stratigraphic Correlation and Mapping

Stratigraphic attribution, especially at well locations, may differ depending on interpreter and available data. Different stratigraphic schemes exist, typically based on electric log markers. The correlation widely used by local and regional geologists is provided in Fig. 2.2 (right).

6. Conclusion

The Bockovac area exhibits significant stratigraphic, structural, and lithological diversity shaped by complex tectonic and sedimentation processes. The main fields and formations described in this report provide a basis for ongoing exploration, potential CO_2 storage, and geothermal energy utilization assessments.

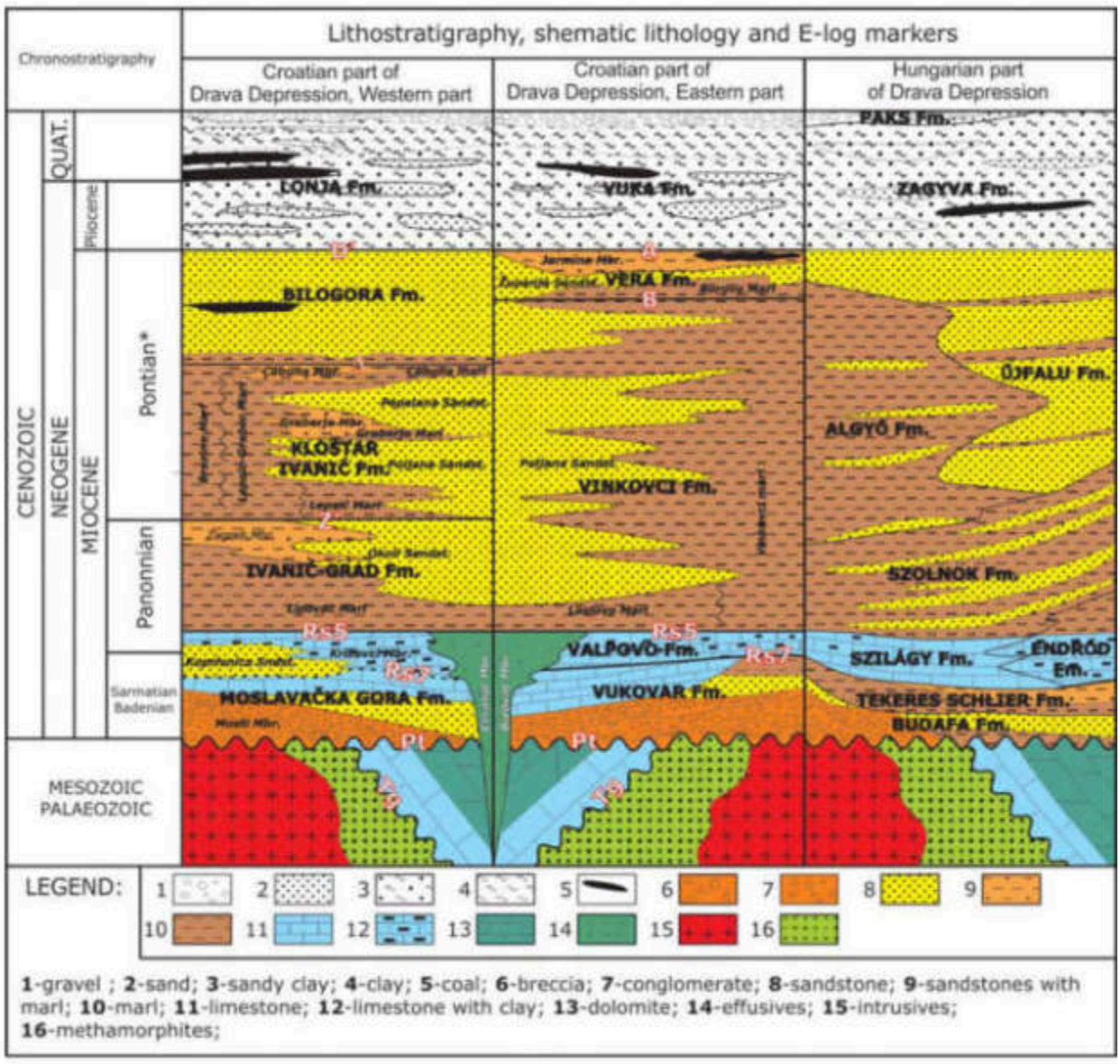


Fig. 2.2 Chrono and Lithostratigraphic chart for the area of study (Drava Depression)
Schematic representation of the correlation of units between Croatian and Hungarian parts of the Drava Depression

Copyright © SLB. All Rights Reserved. Private & Confidential. Reproduction only by permission.

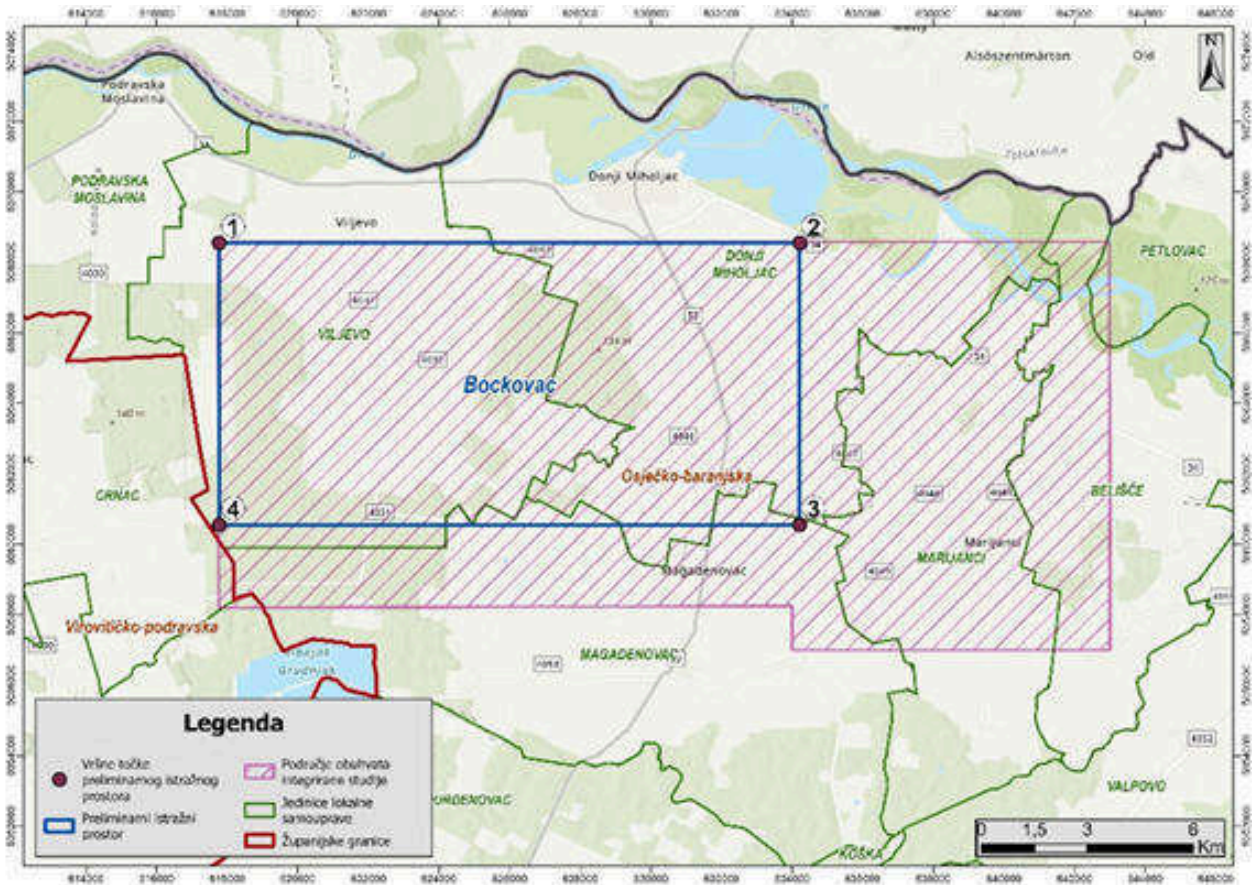


Fig. 2.3 Area of interest

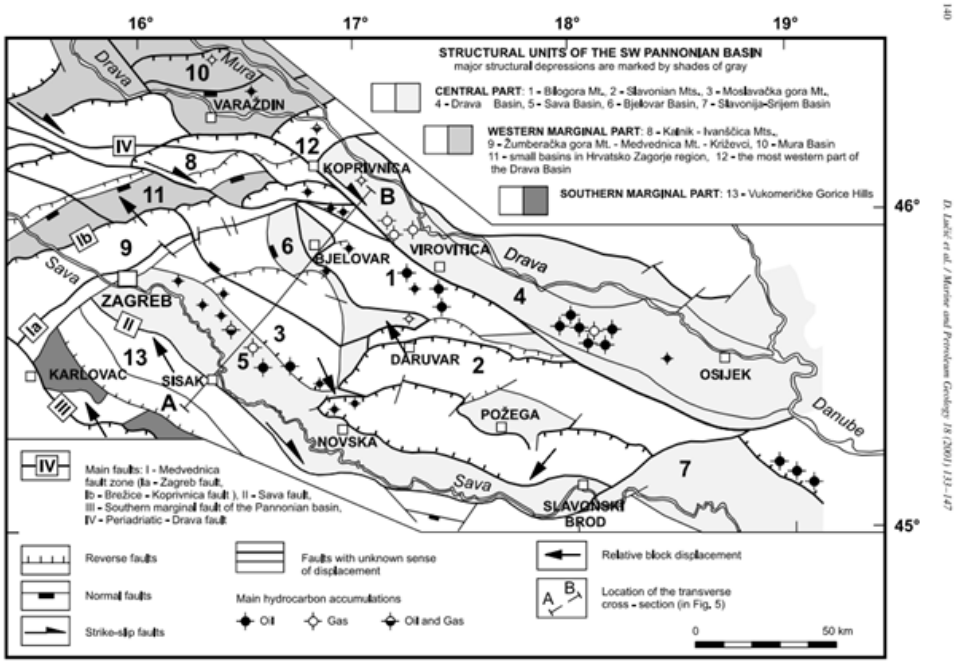


Fig. 4. Classification of structures, faults and major hydrocarbon accumulations.

Fig. 2.4 Regional Structural Framework of the SW Panonian Basin
Classification of structures, faults and major hydrocarbon accumulations

Copyright © SLB. All Rights Reserved. Private & Confidential. Reproduction only by permission.

2.1.2 Data available

The geological and reservoir characterization study was based on a dataset consisting of wells, well logs, seismic interpretation, deviation surveys, interpreted horizons, and historical well documentation (Fig. 2.5). Although the dataset provided sufficient regional coverage for structural and stratigraphic interpretation, significant variations in data quality, completeness, and format were encountered throughout the project.

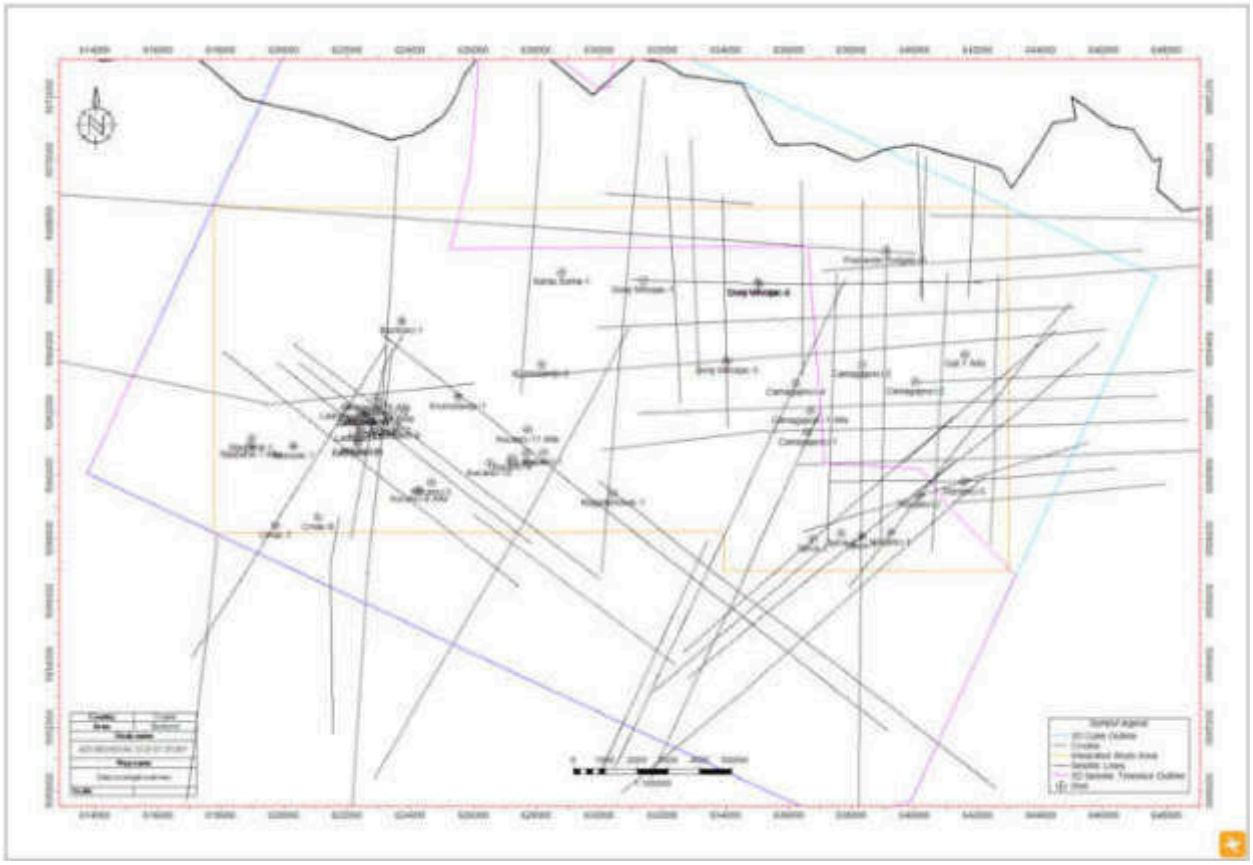


Fig. 2.5 Data Coverage Overview

Initially, a total of 46 wells were available within the study area. However, only 16 wells received processed petrophysical interpretations from the Petrophysics team. Among these, 12 wells contained interpreted effective porosity (PHIE) logs suitable for direct use in reservoir property modeling and petrophysical calibration.

The availability of wireline logs varied considerably between wells. Most wells included Spontaneous Potential (SP) and deep resistivity (RES_DEEP) logs, which formed the primary basis for stratigraphic correlation and identification of reservoir–seal transitions throughout the study area. These logs proved especially important for correlating the principal electric markers and tracking the continuity of the major reservoir intervals. In contrast, Gamma Ray (GR) logs were available only for a limited number of wells and therefore could not be used consistently as a regional correlation tool.

Copyright © SLB. All Rights Reserved. Private & Confidential. Reproduction only by permission.

Several wells also contained incomplete logging intervals. In at least two wells, the upper sections of the logs were missing, resulting in partial absence of petrophysical information within shallower stratigraphic intervals. In these cases, interpretation relied more heavily on nearby well control, seismic interpretation, and regional stratigraphic continuity.

Deviation survey information represented an additional limitation within the dataset. For many wells, deviation data were available only in scanned paper format and therefore required manual digitization prior to import into Petrel.

The structural framework was constrained using six interpreted seismic horizons that had already been depth converted prior to the modeling workflow. These surfaces formed the basis for grid construction.

Historical well reports were available in PDF format for a significant portion of the well inventory. These reports provided valuable geological descriptions, formation tops, lithological observations, DST results, and reservoir information. However, the completeness and reliability of the reports varied considerably. In some cases, only prognosed or forecast geological sections were available

Formation tops extracted from the reports were imported into Petrel and subsequently reviewed and correlated regionally. Due to inconsistencies between historical interpretations, nomenclature differences, and variable report quality, several tops required reinterpretation and adjustment during the correlation process in order to achieve regional consistency between wells.

The seismic dataset also presented spatial limitations. Available 3D seismic coverage does not extend into the northeastern corner of the study area, resulting in reduced structural and stratigraphic control within that sector. Consequently, geological interpretation in the northeastern area relied more heavily on well correlation and regional geological trends rather than direct seismic mapping.

2.2 Seismic interpretation

The seismic interpretation study was undertaken to establish the structural framework supporting the select phase of the CCS screening and geothermal feasibility assessments. Its primary objective was to deliver a robust subsurface understanding through detailed seismic interpretation, integrating seismic-to-well ties, attribute analysis, fault and horizon mapping, and time-to-depth conversion.

Interpretation focused on the key stratigraphic horizons—Alfa, B, C, D, Z', Rs7, and Tg. The shallow section is characterized by strong reflector continuity and stable frequency content, allowing high-confidence horizon picking. At greater depths, particularly around Rs7 and Tg, seismic image quality deteriorates due to reduced signal-to-noise ratios, resulting in increased interpretation uncertainty. These limitations were addressed through the application of calibrated seismic attributes and a conservative interpretation strategy.

Copyright © SLB. All Rights Reserved. Private & Confidential. Reproduction only by permission.

Machine-learning-based fault prediction provided effective guidance in mapping the shallow fault network. In deeper intervals, however, fault identification remains more challenging due to structural complexity and frequency attenuation, requiring predominantly manual interpretation.

The study delivered a comprehensive set of time-domain structural maps, supported by an initial velocity model to enable time-to-depth conversion and generate structural depth maps for all key horizons. It concludes with recommendations and an assessment of uncertainties relevant to CCS and geothermal development workflows.

The interpretation followed a structured workflow comprising:

- Data gathering and quality control
- Seismic-to-well tie and resolution analysis
- Seismic attribute evaluation
- Fault and horizon interpretation
- Velocity modeling and depth conversion

The results provide CHA with a consistent structural model foundation to guide ongoing CCS screening and geothermal feasibility assessments, highlighting areas of higher confidence, zones requiring additional scrutiny, and recommended next steps for de-risking the subsurface evaluation.

2.2.1 Location and data QC

Bockovac area is located in the north-east part of Croatia, close to the Hungarian border, geologically situated within the southern margin of the Pannonian Basin. Available dataset includes (Fig. 2.6):

- 3D seismic (PSTM processing) with extent of 406 km^2
- 120 2D lines (ranging from 1970 to 1990) with total length of 150 km
- 46 wells with a suite of logs in both LAS and raster format
- 12 checkshot files (5 in digital format, 7 in raster format)
- Cultural data in shapefile format

Copyright © SLB. All Rights Reserved. Private & Confidential. Reproduction only by permission.

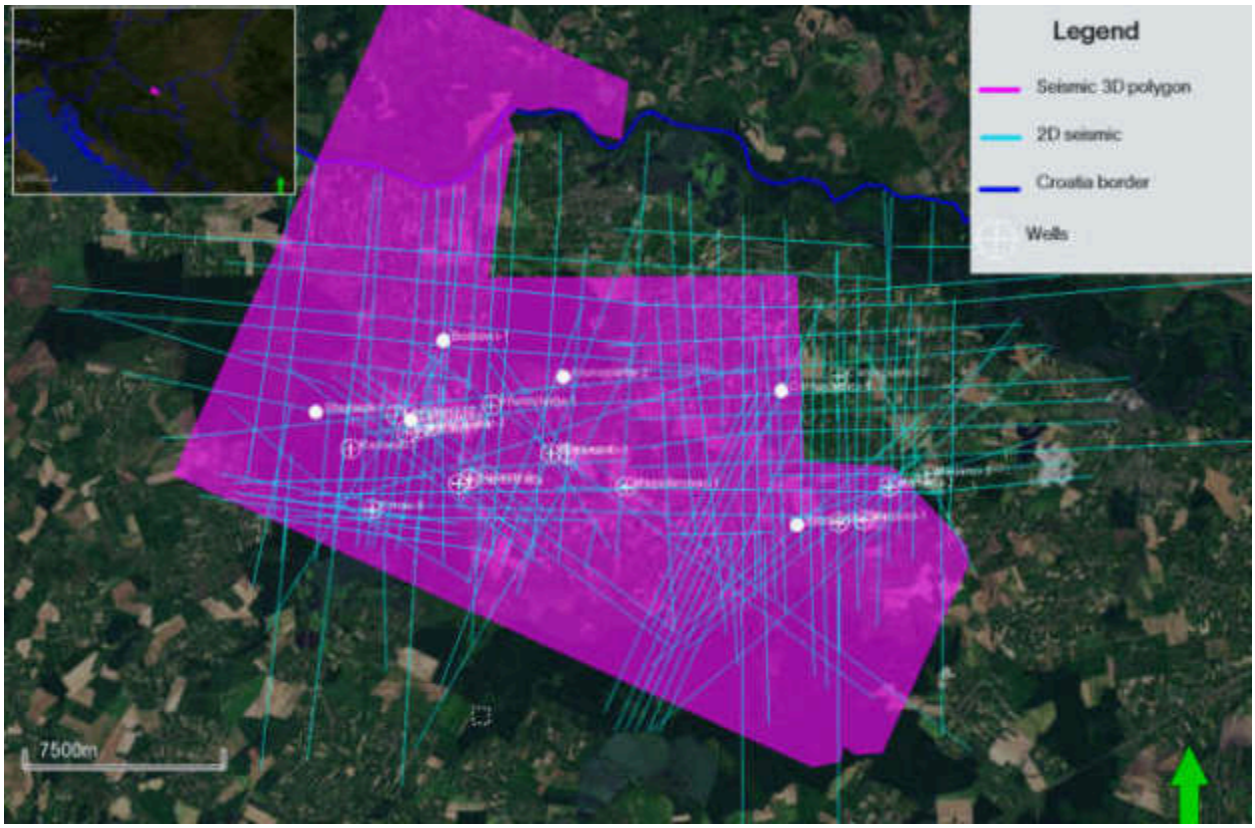


Fig. 2.6 Location map with available dataset

The first step in the study is preparation of the project data and proper loading to Petrel software, which includes definition of two key parameters:

- Coordinate Reference System (CRS)
- Seismic Reference Datum (SRD)

Since the available data were acquired over an extended period, the selection of the Coordinate Reference System (CRS) and Seismic Reference Datum (SRD) was based on the most recent and highest-quality dataset, namely the 3D seismic cube. According to the shapefile attributes and seismic header information, the CRS of the study area is **HTRS96_Croatia_TM** (EPSG:3765), with a transformation to WGS defined by EPSG:15967. As the 3D seismic processing report was not available at the time of the study, the SRD value was adopted from the 2D seismic line processing report, corresponding to 100 m. (Fig. 2.7)

Copyright © SLB. All Rights Reserved. Private & Confidential. Reproduction only by permission.

```
PROJCS["HTRS96
_Croatia_TM",GEOGCS["GCS_HTRS96",DATUM["D_Croatian_Terrestrial_Reference_System",SPHEROID["GRS_
1980",6378137.0,298.257222101]],PRIMEM["Greenwich",0.0],UNIT["Degree",0.0174532925199433295]],PROJECT
ION["Transverse_Mercator"],PARAMETER["False_Easting",500000.0],PARAMETER["False_Northing",0.0],PARAM
ETER["Central_Meridian",16.5],PARAMETER["Scale_Factor",0.9999],PARAMETER["Latitude_Of_Origin",0.0],U
NIT["Meter",1.0]]
```



GEOFIZIKA - Zagreb
Odjel za terensku seizmiku

STATIČKE KOREKCIJE

TEREN: DRAVSKA POTOLINA
PROFIL: BOK-KU-1-88-P

Aparatura:	DFS-IV
Izvor:	ALN
Prekrivanje:	CDP-2400%
Raspon izmedu T.P. =	40m
Offset:	240m
D.P.=	100m

Izvor podataka za račun statičkih korekcija:
Lokacija plitke refrakcije
Lokacija seizmičke mikrokarotaže

Fig. 2.7 CRS and SRD definition from raw data
CRS (top) from shapefile and SRD (bottom) from 2D line report

Quality control (QC) of the available seismic data was conducted prior to interpretation. Due to the generally poor quality of the 2D seismic data—characterized by low signal-to-noise ratio, the presence of artefacts, and reliance on legacy migration workflows—and inconsistencies with the overlaid 3D cube, the 3D seismic dataset was selected as the primary interpretation basis. The 2D seismic lines were used only in areas lacking 3D coverage. However, differences in data vintage and quality significantly limit the integration and merging of interpretations between the two datasets (Fig. 2.8)

Copyright © SLB. All Rights Reserved. Private & Confidential. Reproduction only by permission.

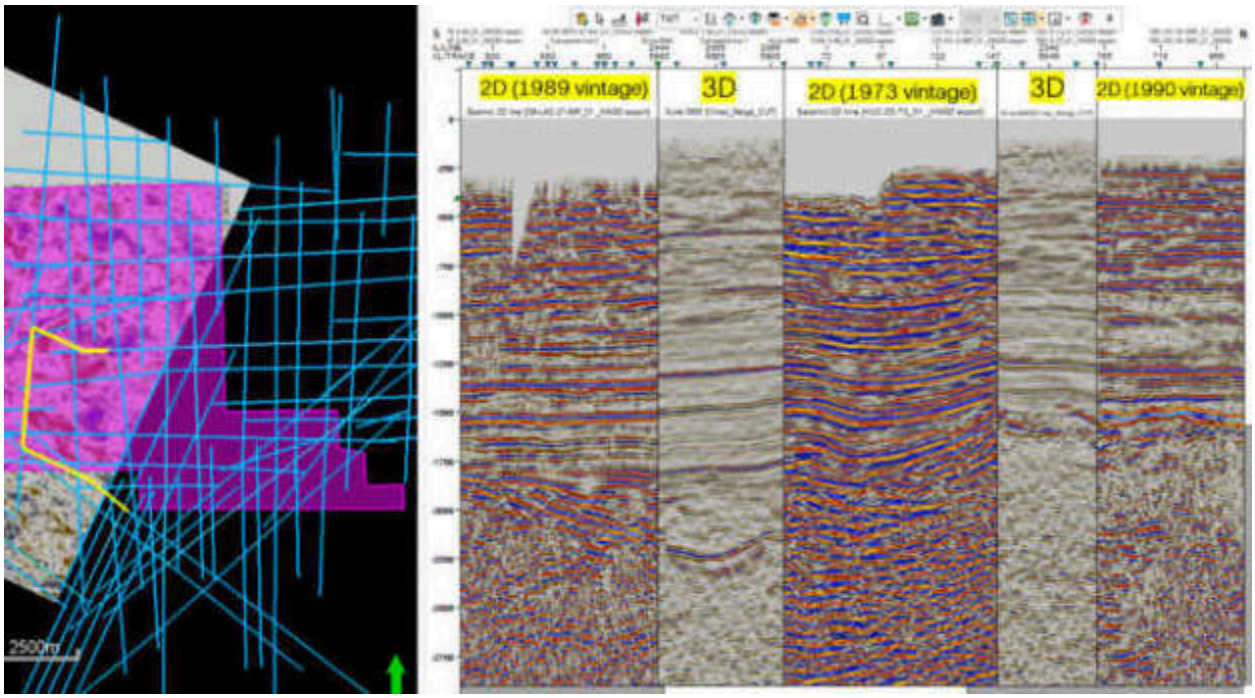


Fig. 2.8 Overlay of 3D and 2D vintages
Sample line showing variations of quality and processing results in various vintages

2.2.2 Seismic Well Tie

In order to begin seismic well tie (SWT) the following data is needed:

- Acoustic (DT) log
- Density (DEN) log (or it's replacement through Gardner equation)
- VSP/checkshot data

VSP files (7 out of 12) were digitized from raster tables, while DT and DEN were provided in LAS format. The following table shows full SWT data availability and extent of each parameter (Table 2.1)

Copyright © SLB. All Rights Reserved. Private & Confidential. Reproduction only by permission.

Table 2.1 SWT Data availability

Well Name	VSP_Length	DT_length	DEN_length
Bockovci-1	2498	835	855
Camagajevci-1 Alfa		1175	1170
Camagajevci-2	1380	237	255
Camagajevci-3		450	460.8
Camagajevci-4	1050	419	419
Crnac-7		1180	80.1
Crnac-8 Alfa		894.4	900
Donji Miholjac-1			
Donji Miholjac-2		85	90
Donji Miholjac-3	1545	250	250
Donji Miholjac-4	1200	400	405
Gat-1 Alfa	1006	1825	510
Karas Suma-1	2008		
Krunoslavlje-1		412	235
Krunoslavlje-2	2120	681.5	723.4
Kucanci-1			
Kucanci-11 Alfa		530	415.1
Kucanci-12		460	301
Kucanci-3		808	474.1
Kucanci-4		1170	160
Kucanci-8 Alfa		770.1	530
Kucanci-9		460	320
Ladislavci-1		752.1	746.1
Ladislavci-10		420.1	635
Ladislavci-11		415	415
Ladislavci-18		280	280
Ladislavci-18 Alfa			
Ladislavci-18 Beta	1319	1380	1395
Ladislavci-2		761.6	
Ladislavci-21		730	680
Ladislavci-4		550.4	550.2
Ladislavci-6		185	370
Ladislavci-8			535.3
Ladislavci-9	1380	2174	966.9
Magadenovac-1		650	650
Marjanci-1		49.7	708
Marjanci-2		1750	1275
Marjanci-3		1525.1	1525.1
Podravski Podgajci-1			345
Rasovac-1		2465	2825
Sjece-1		1275.1	1825
Sjece-2	3200	1895	260.1
Sjece-3			337.4
Stjepanik-1	2425	3385	2460
Stjepanik-1 Alfa			

VSP data is a critical input for SWT; in its absence, the robustness of the analysis is significantly constrained. Consequently, a subset of 12 wells with available VSP data was selected for the SWT workflow. Of these, two wells (Camagajevci-2 and Gat-1 Alfa) lie outside the 3D seismic coverage, and one well (Karas-Suma-1) lacks log data in LAS format. As a result, a total of nine wells were retained and used in the SWT analysis.(Fig. 2.9)

Copyright © SLB. All Rights Reserved. Private & Confidential. Reproduction only by permission.

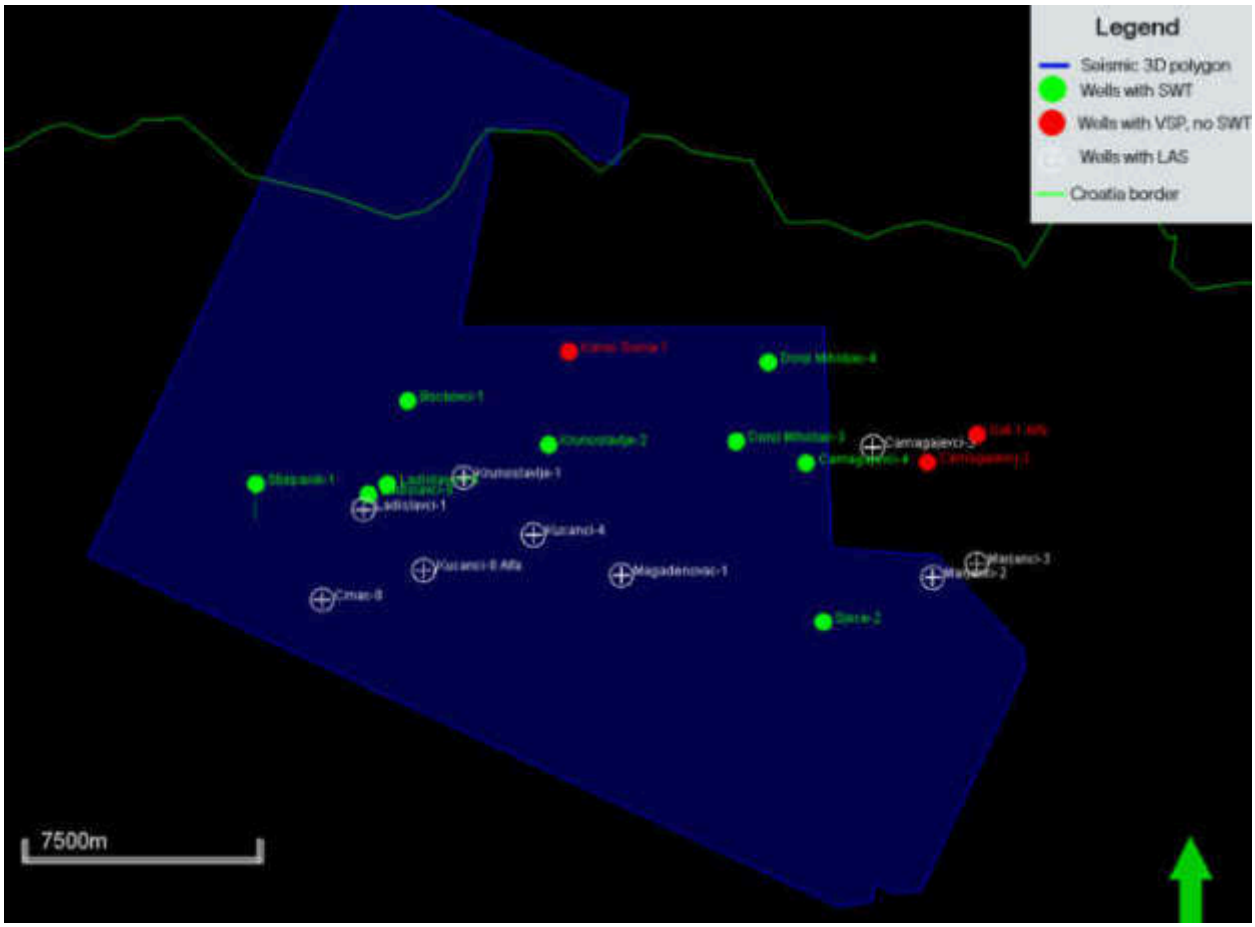


Fig. 2.9 Map of wells for SWT
Legend showing data availability for SWT

Seismic well ties (SWT) were performed following a minimum-adjustment approach to preserve the integrity of the original data, primarily relying on bulk shifts. However, due to limited data availability, localized stretch and squeeze operations were applied at selected wells, constrained within the limits of vertical seismic resolution. (Fig. 2.10, Fig. 2.11)

The following figures present each seismic-to-well tie calibration, within a tie panel, for reference.

Copyright © SLB. All Rights Reserved. Private & Confidential. Reproduction only by permission.

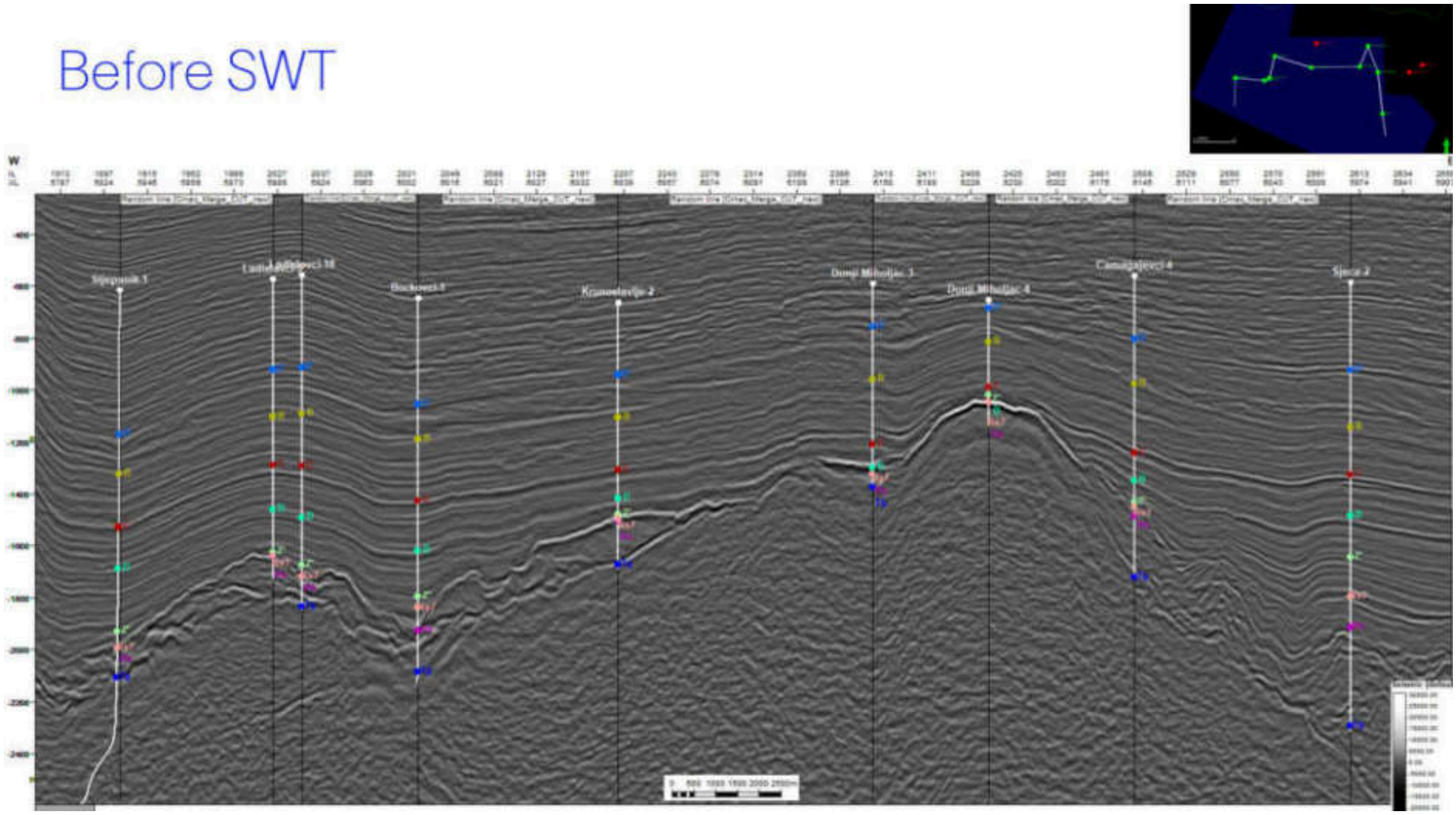


Fig. 2.10 Composite well-section before SWT

Copyright © SLB. All Rights Reserved. Private & Confidential. Reproduction only by permission.

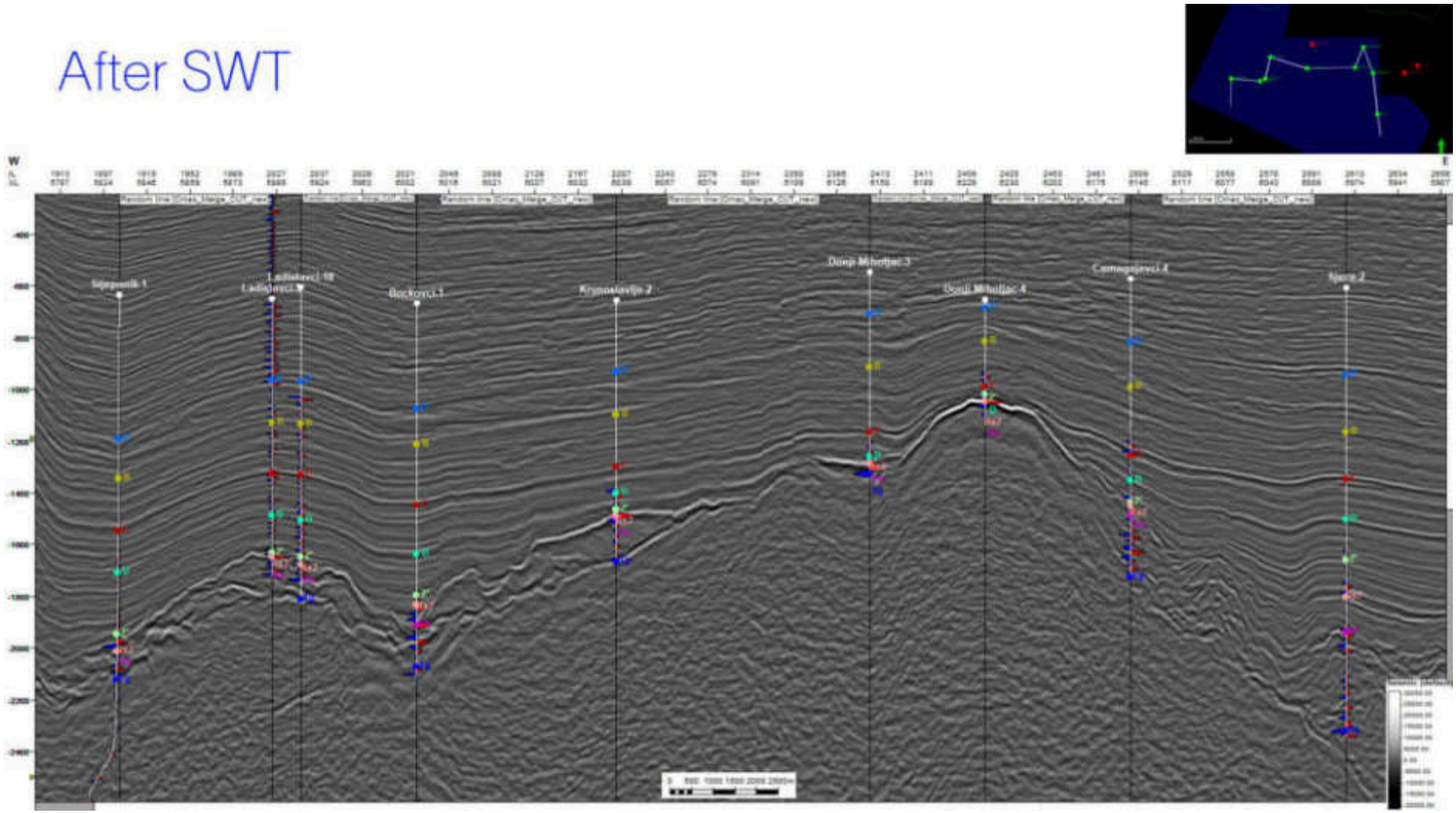


Fig. 2.11 Composite well-section after SWT

Copyright © SLB. All Rights Reserved. Private & Confidential. Reproduction only by permission.

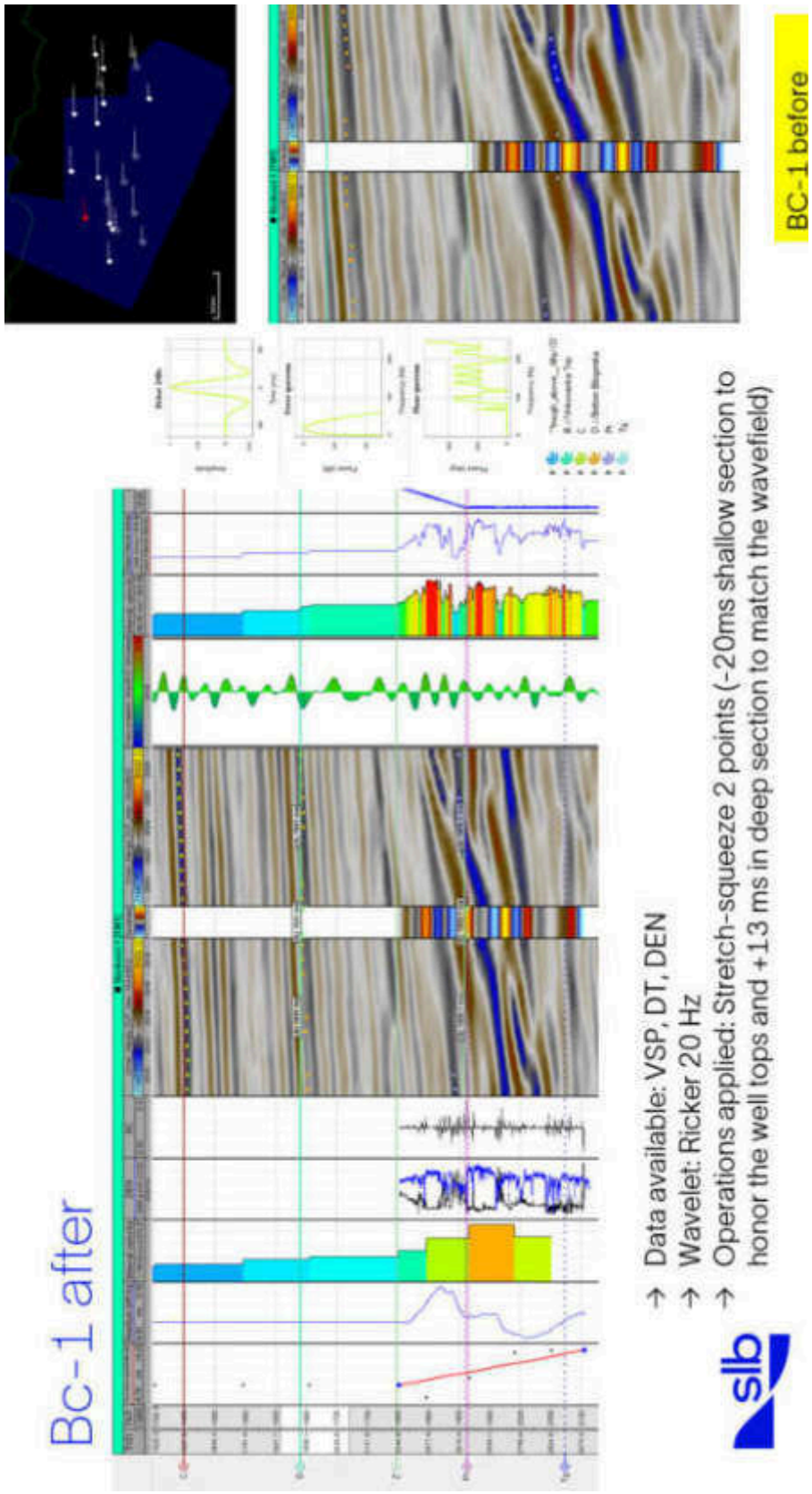


Fig. 2.12 Bockovci-1 SWT

Copyright © SLB. All Rights Reserved. Private & Confidential. Reproduction only by permission.

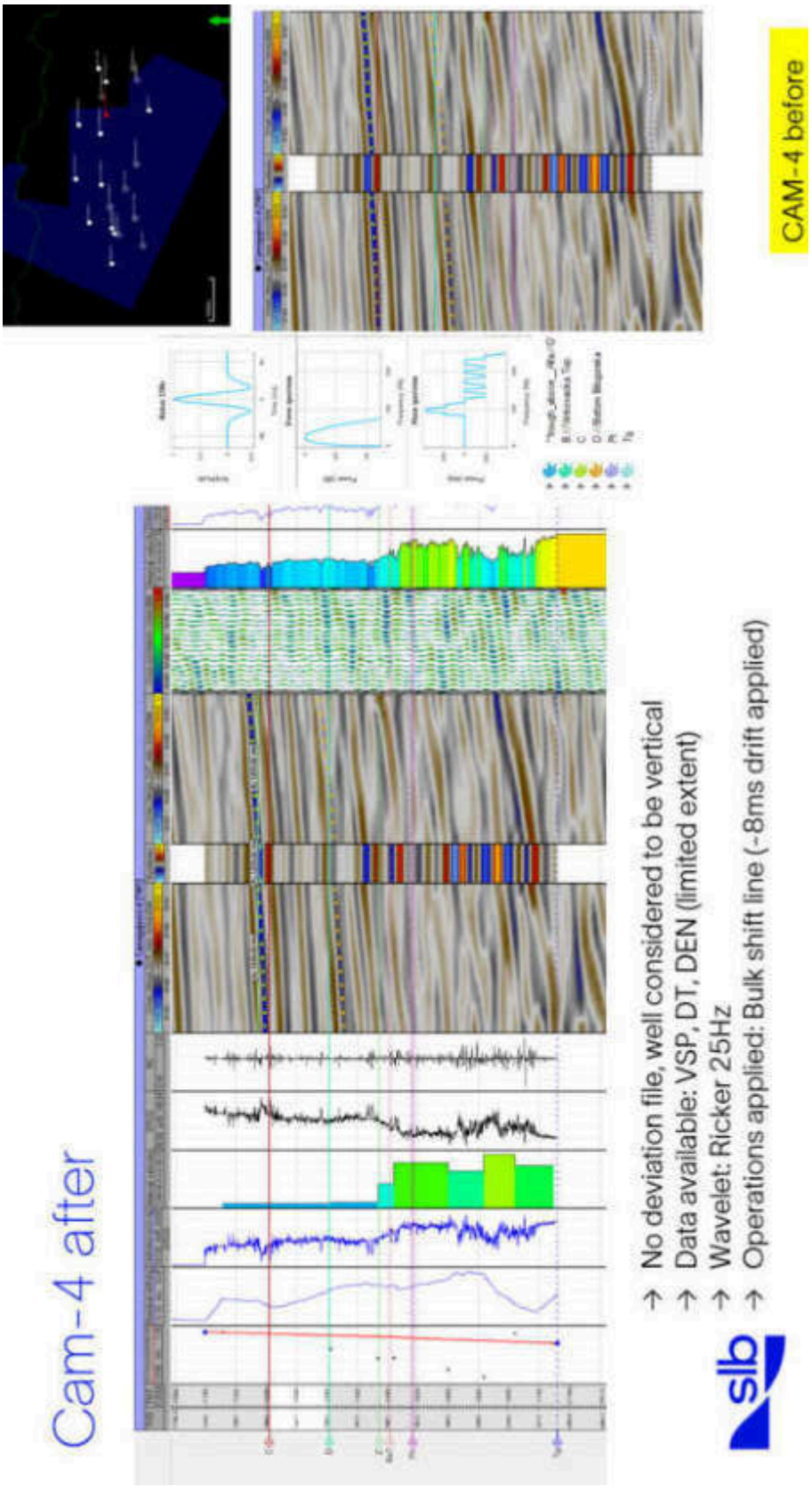


Fig. 2.13 Camagajevci-4 SWT

Copyright © SLB. All Rights Reserved. Private & Confidential. Reproduction only by permission.

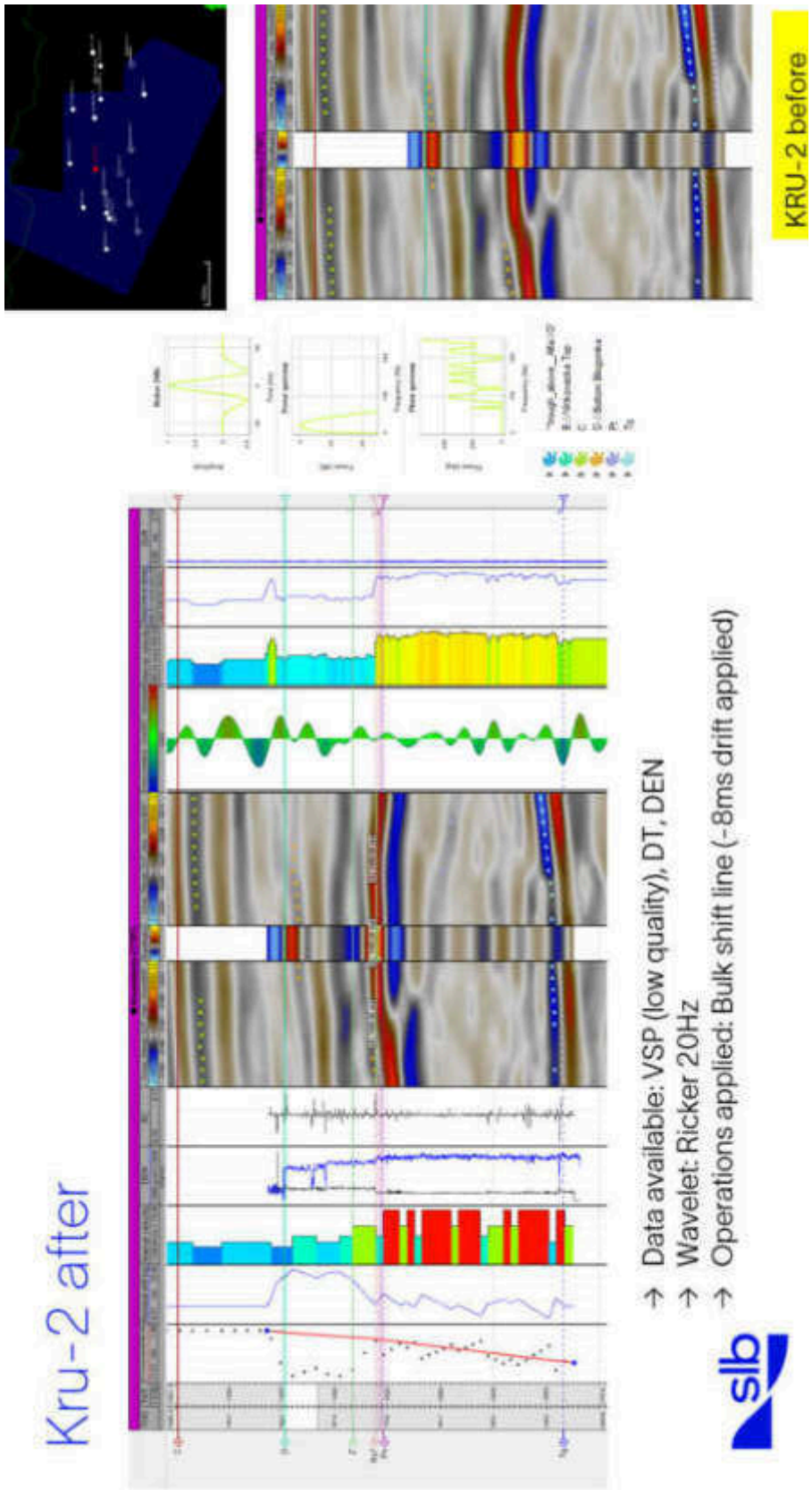


Fig. 2.14 Krunoslavlje-2 SWT

Copyright © SLB. All Rights Reserved. Private & Confidential. Reproduction only by permission.

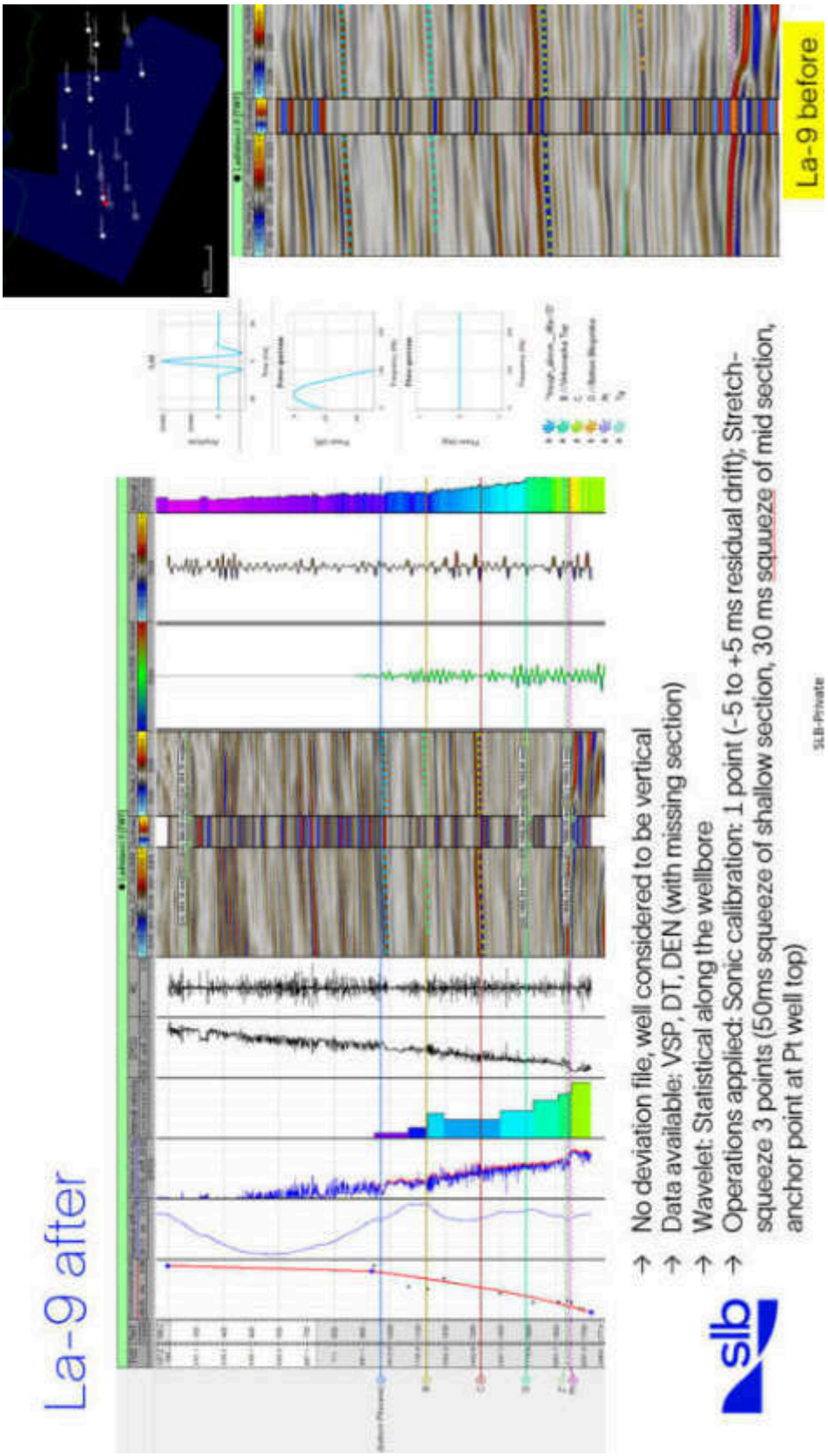


Fig. 2.15 Ladislavci-9 SWT

Copyright © SLB. All Rights Reserved. Private & Confidential. Reproduction only by permission.

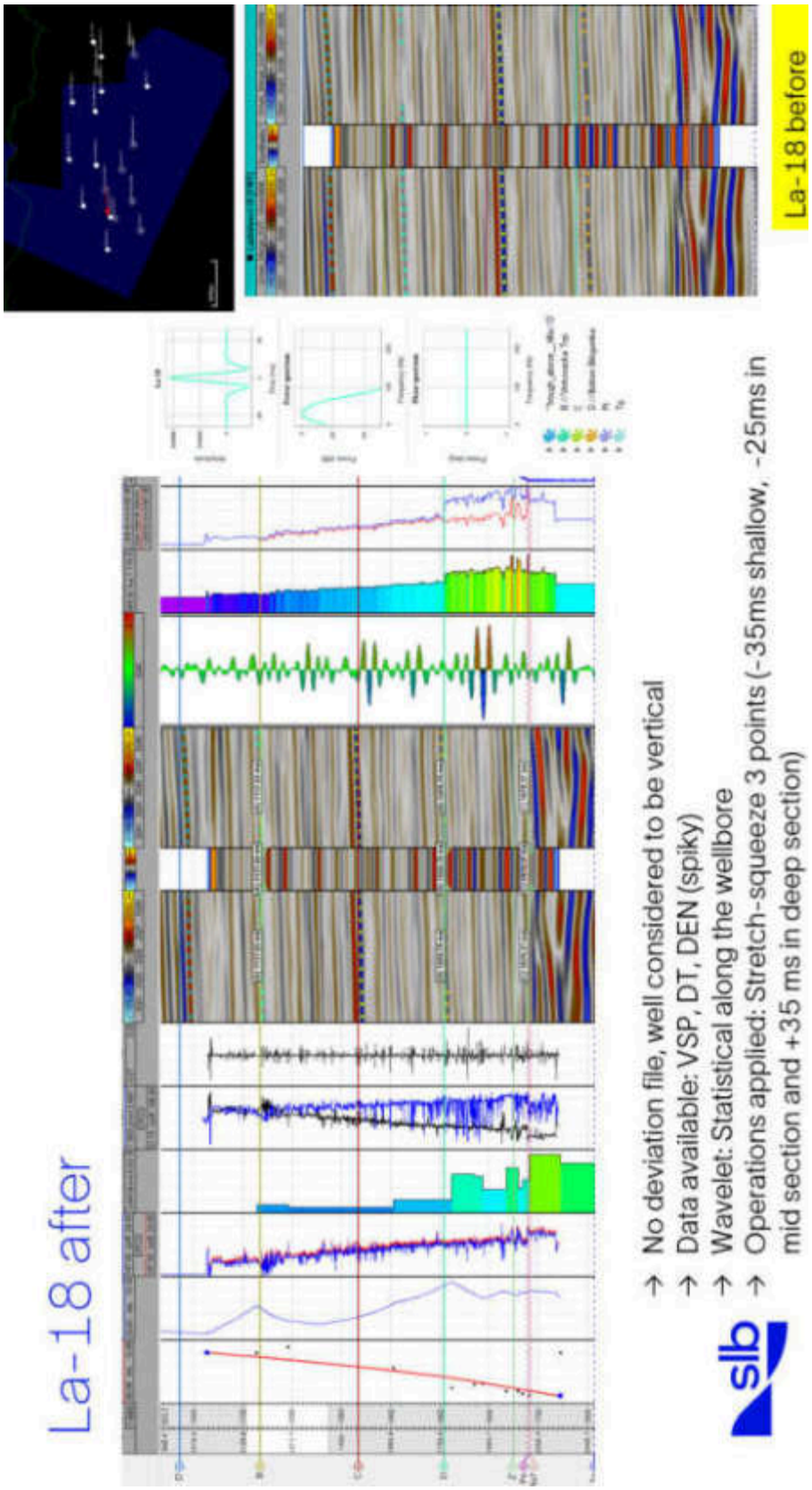


Fig. 2.16 Ladislavci-18 SWT

Copyright © SLB. All Rights Reserved. Private & Confidential. Reproduction only by permission.

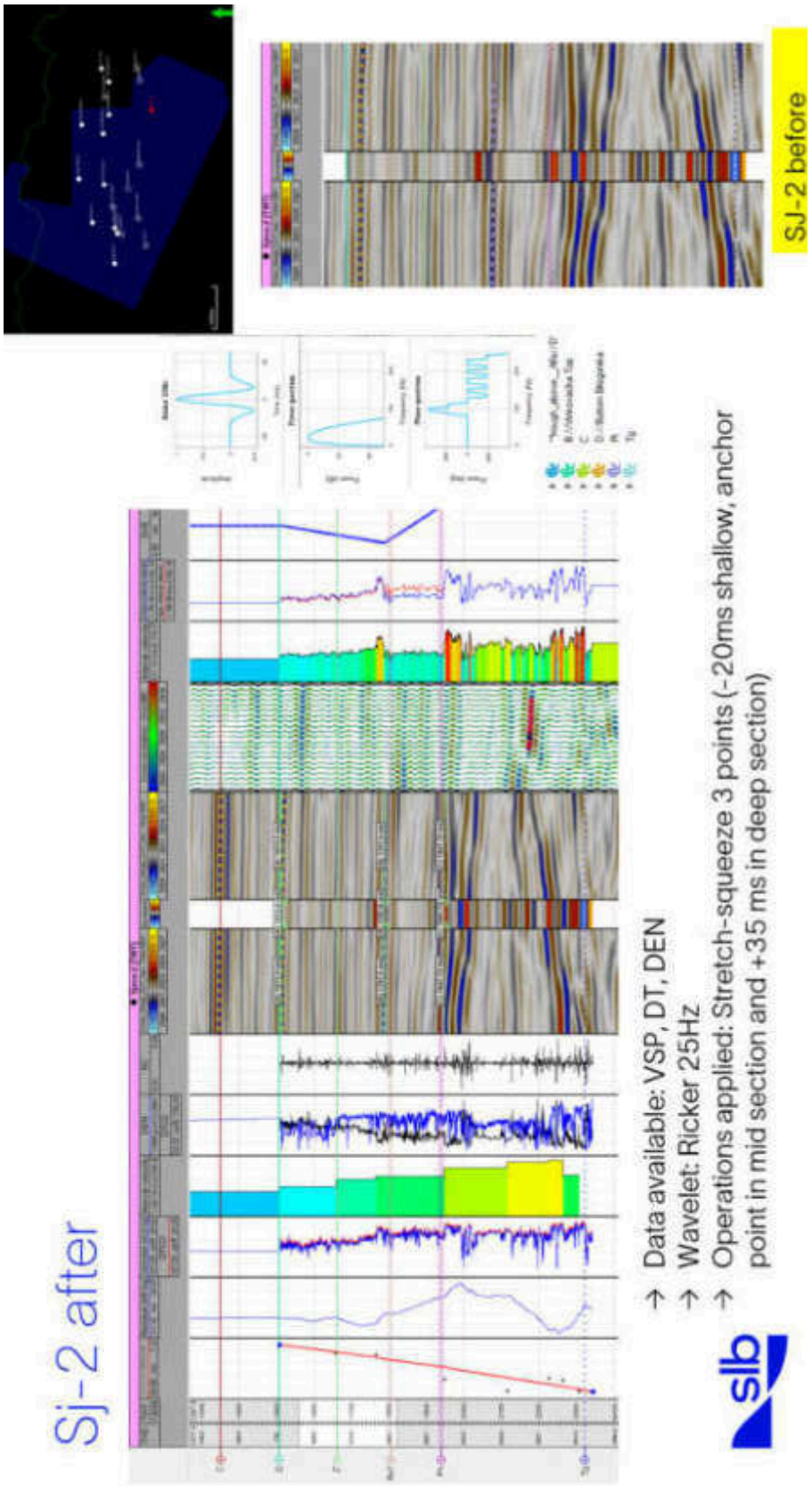


Fig. 2.17 Sjece-2 SWT

Copyright © SLB. All Rights Reserved. Private & Confidential. Reproduction only by permission.

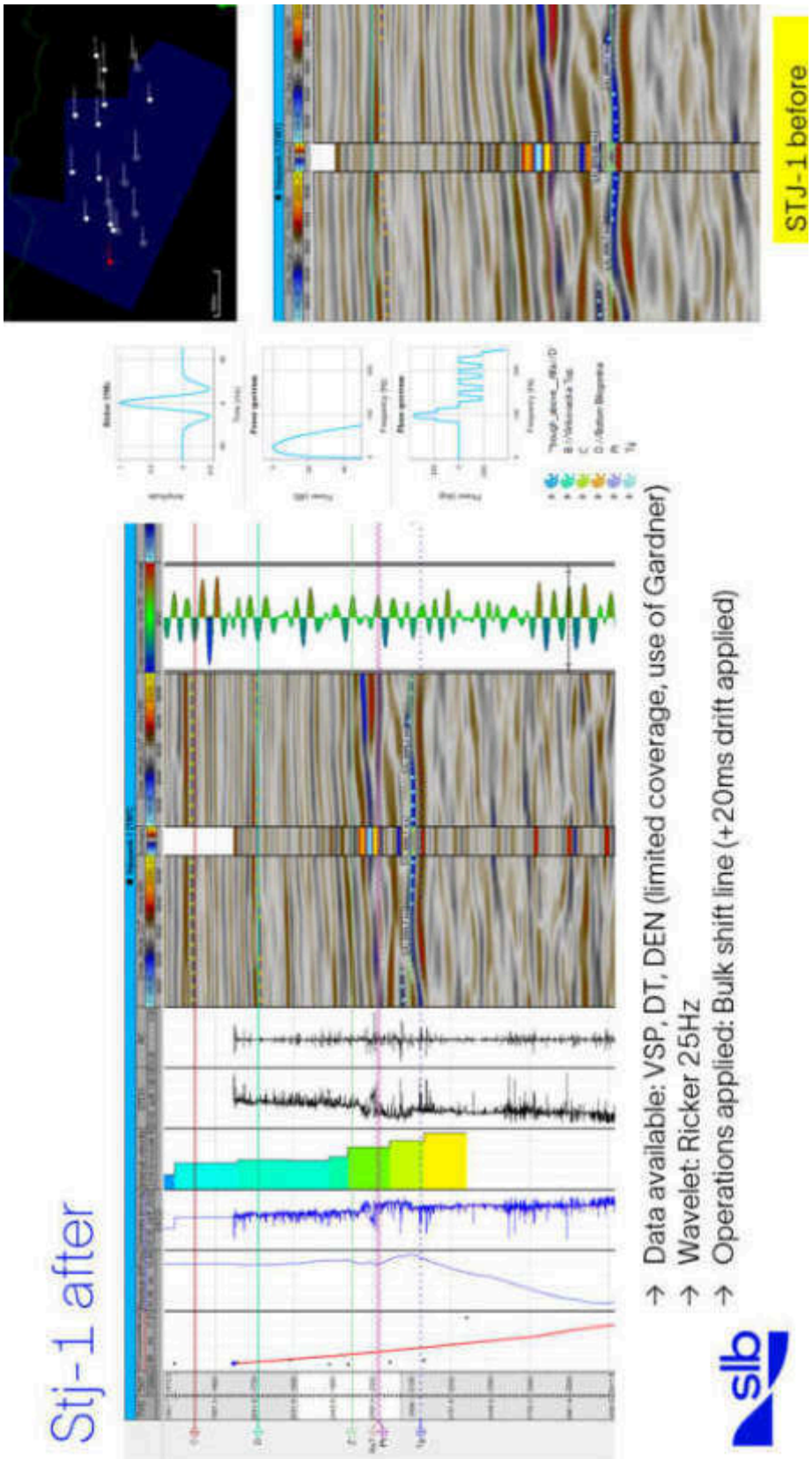


Fig. 2.18 Stjepanik-1 SWT

Copyright © SLB. All Rights Reserved. Private & Confidential. Reproduction only by permission.

2.2.3 Dataset and Seismic Characteristics

The seismic interpretation was performed on a 3D seismic cube comprising 1123 inlines and 805 crosslines, acquired with an inline/crossline spacing of 25 m. The seismic dataset exhibits a maximum usable frequency of 60 Hz, with a total record length of 5 seconds, allowing imaging from shallow stratigraphy down to the deeper Rs7–Tg interval.

Below 2.5 seconds TWT, the seismic bandwidth decreases significantly, reducing resolution. As a result, the minimum resolvable fault throw is estimated at 11 m based on the calculation of vertical resolution, limiting the detectability of smaller structural displacements in the deeper part of the section (Fig. 2.19)

Overall, imaging quality varies considerably with depth:

- Shallow sequence: Reflectors exhibit good continuity and a stable wavelet character, enabling reliable horizon tracking and structural interpretation.
- Deep sequence (Rs7–Tg interval): Reflection continuity deteriorates and the signal-to-noise ratio decreases, making both horizon picking and fault validation more challenging due to complex geology and limited seismic resolution (Fig. 2.20)

Copyright © SLB. All Rights Reserved. Private & Confidential. Reproduction only by permission.

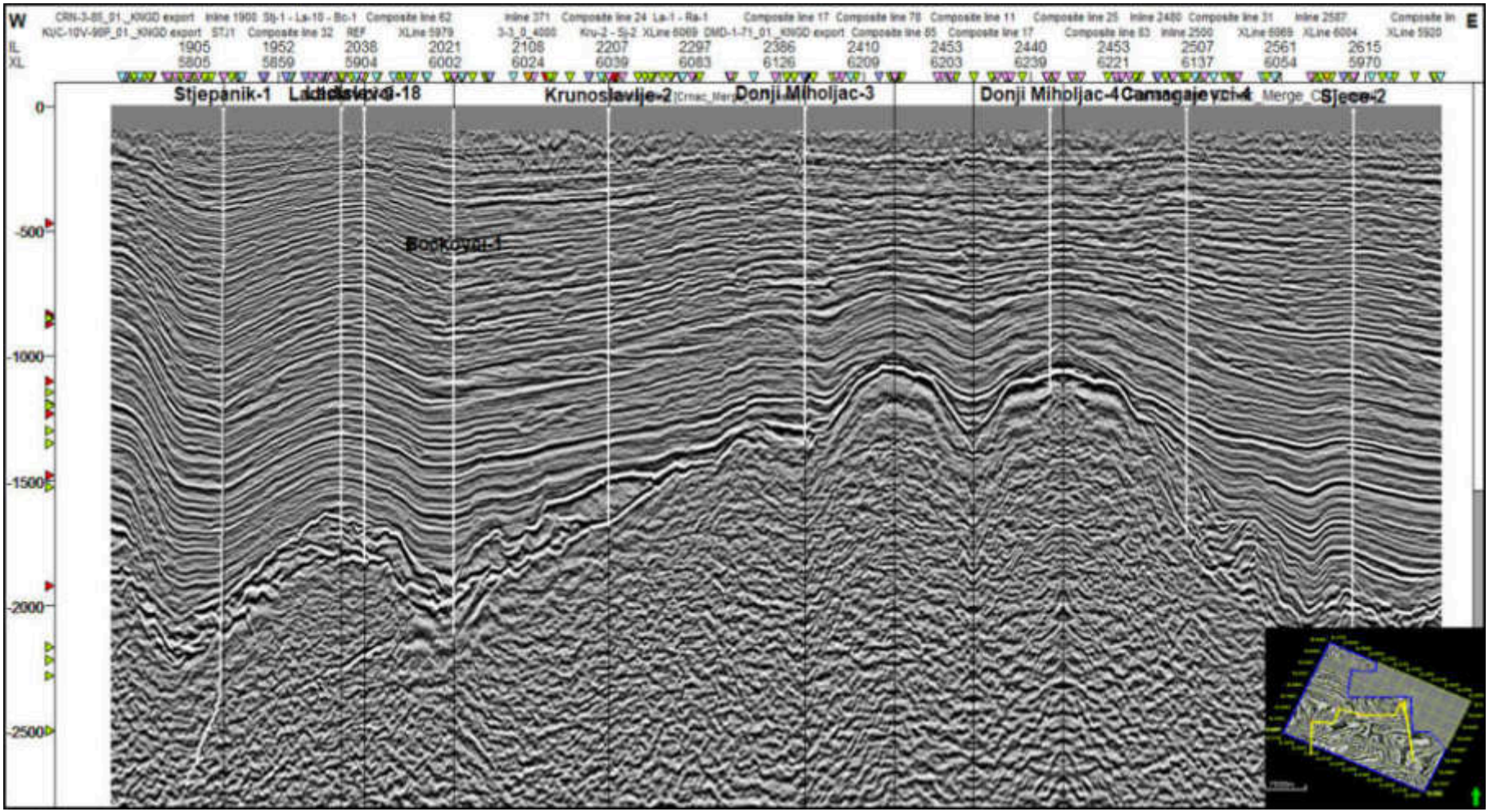


Fig. 2.19 Seismic composite line passing through key wells

Good seismic continuity in the shallow section indicating a more uniform and less disturbed geological setting. Reduced continuity in the deeper intervals around RS7 to Tg where the signal becomes more complex making the deeper interpretation more challenging.

Copyright © SLB. All Rights Reserved. Private & Confidential. Reproduction only by permission.

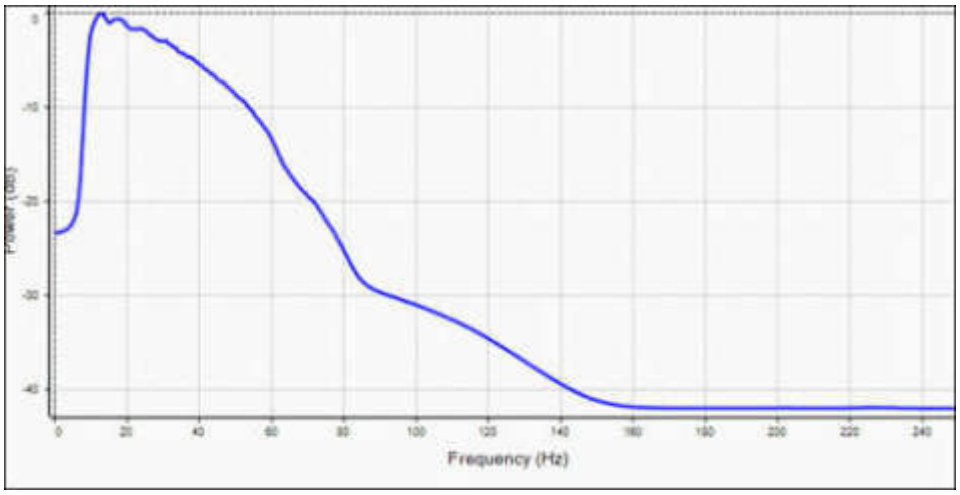


Fig. 2.20 Seismic frequency spectrum
Frequency content is limited to 60 Hz, seismic trace length is 5sec. Seismic resolution has a medium quality below 2.5s and any resolvable faults need to have a minimum throw of ~11m.

2.2.4 Machine learning assisted fault prediction

Machine learning (ML) was applied to support and enhance structural interpretation, with a focus on detecting and validating seismic discontinuities across the study area. A pre-trained deep convolutional neural network (CNN) was executed on the 3D seismic volume to generate an initial prediction of fault-related lineaments.

In the shallow interval, where seismic data quality is higher (better continuity and bandwidth), the ML output delineates a coherent and geologically plausible fault network. Predicted fault lineaments show strong spatial consistency and closely match interpreter-picked faults, as well as discontinuities evident in key seismic attributes (e.g., variance, spectral decomposition, and edge-detection attributes). This agreement increased confidence in the shallow structural interpretation and enabled rapid screening of structural trends prior to detailed manual refinement.

Model performance decreases with depth due to reduced signal-to-noise ratio (SNR), attenuation of higher frequencies, and increased wavelet complexity. Consequently, ML predictions in deeper intervals were treated as indicative only. All fault interpretations at depth were systematically validated through targeted attribute analysis and seismic section review before inclusion in the final structural framework.

Overall, the ML-assisted workflow provided clear value in the shallow section by accelerating fault identification and improving interpretation consistency. Manual interpretation remained essential in the deeper Rs7–Tg interval, where seismic quality limits the reliability of automated detection.

The results of machine learning assisted fault prediction are presented in Fig. 2.21, Fig. 2.22 and Fig. 2.23 below.

Copyright © SLB. All Rights Reserved. Private & Confidential. Reproduction only by permission.

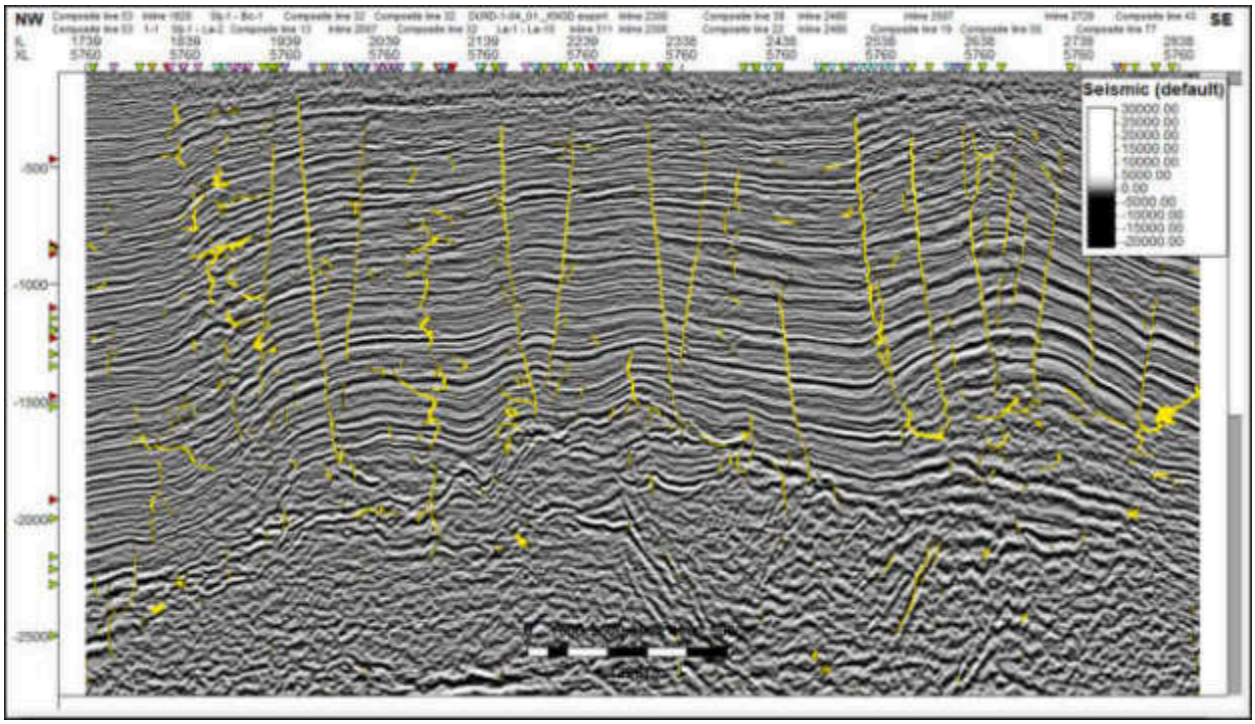


Fig. 2.21 Machine learning fault prediction results- XL5760
Fault prediction successfully highlighted the shallow fault network. However, faults in the deeper intervals were not reliably detected due to the lower signal-to-noise ratio.

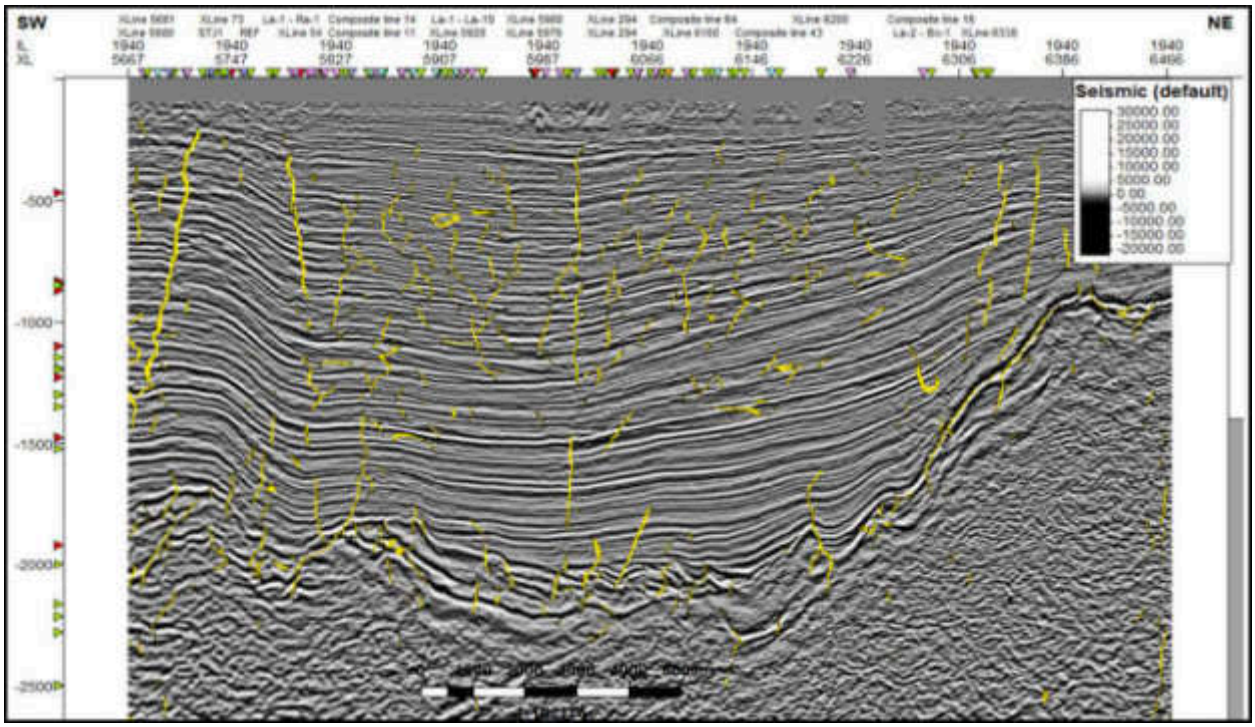


Fig. 2.22 Machine learning fault prediction results- IL1940
Pre-trained ML fault detection results

Copyright © SLB. All Rights Reserved. Private & Confidential. Reproduction only by permission.

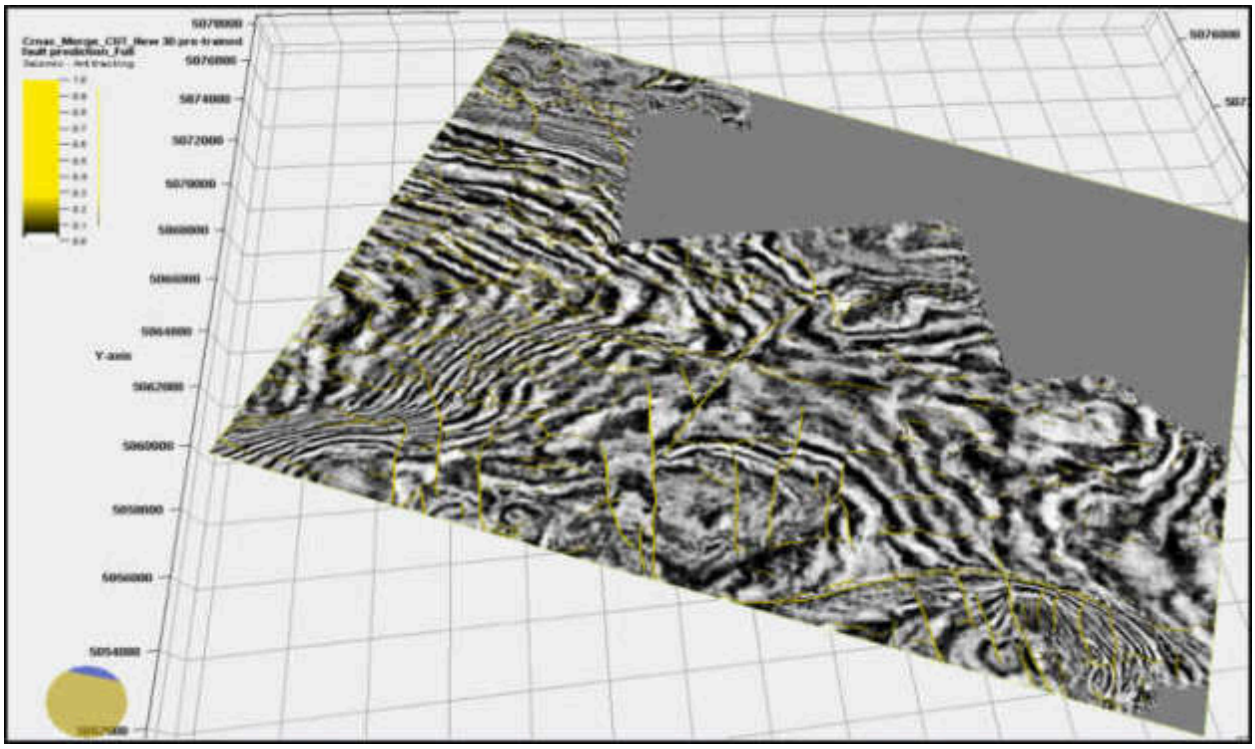


Fig. 2.23 Machine learning fault prediction results- Slice 850 ms
Pre-trained ML fault detection results

2.2.5 Seismic Attribute analysis and seismic restoration

A comprehensive suite of seismic attribute volumes was deployed to support fault identification, delineate structural discontinuities, and enhance reflector continuity, particularly within intervals affected by low signal-to-noise ratios. The integrated use of these attributes enabled a more robust structural framework and provided systematic cross-validation between manual interpretation and machine-learning–derived fault predictions.

Variance and edge-enhancement attributes were applied to highlight lateral amplitude discontinuities and improve fault edge definition. These attributes proved critical in confirming the geometry and spatial extent of faults initially identified through machine-learning workflows. Dip illumination further enhanced the imaging of steeply dipping features by increasing dip-related contrast, enabling the discrimination of subtle structural elements from background reflectivity.

Amplitude-based attributes, including envelope, RMS amplitude, and cosine phase, were used to support horizon interpretation in zones characterized by reduced seismic continuity. These attributes improved reflector stability by emphasizing consistent phase behaviour and amplitude gradients along key stratigraphic markers. Additional attributes, such as relative acoustic impedance and spectral decomposition, provided frequency-dependent insights into stratigraphic variability and structural complexity, facilitating the identification of fault terminations, compartmentalization patterns, and lateral facies variations.

Copyright © SLB. All Rights Reserved. Private & Confidential. Reproduction only by permission.

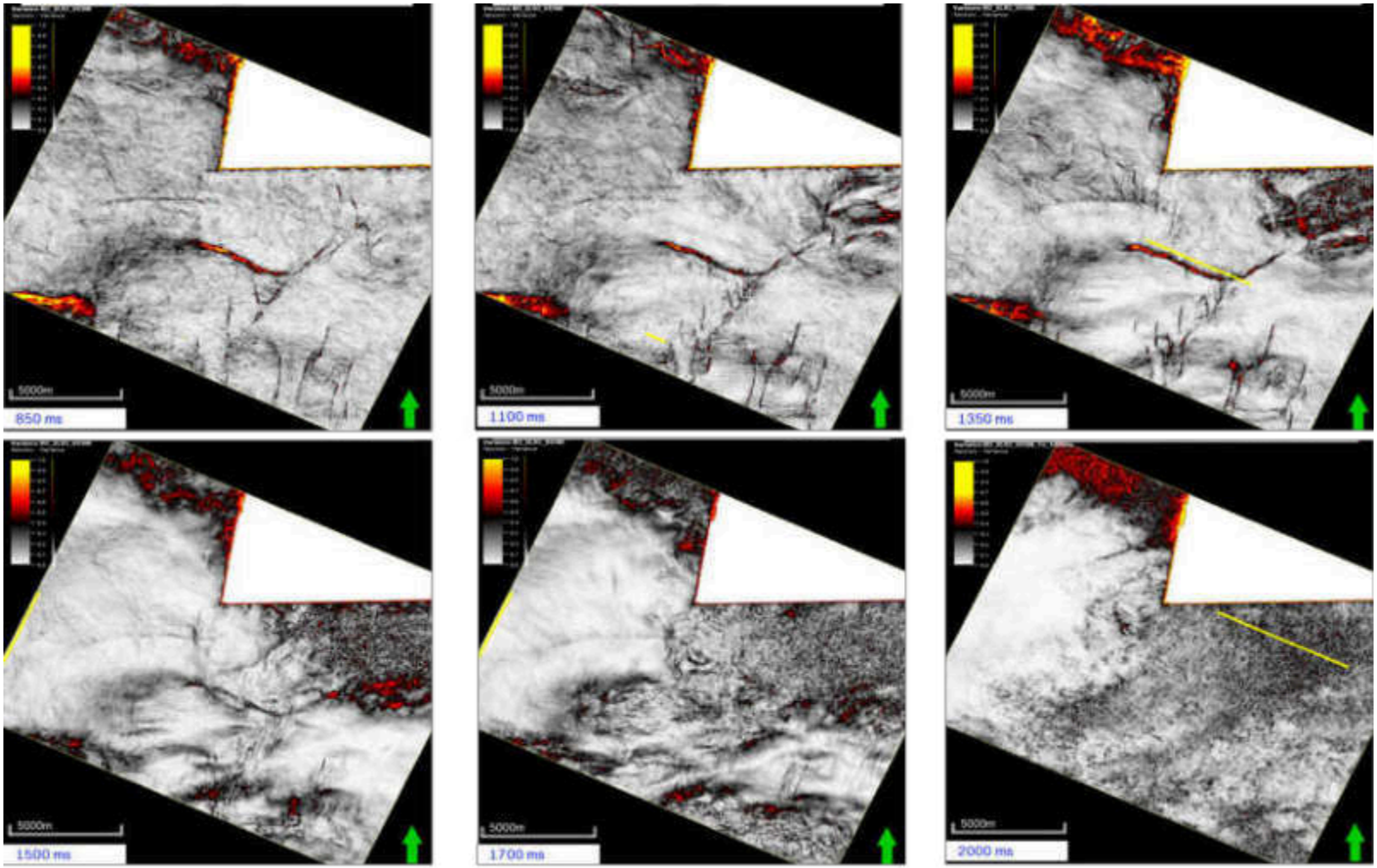


Fig. 2.24 Variance attribute slices at 850, 1100, 1350, 1500, 1700, and 2000 ms
Variance attributes was used to emphasize lateral amplitude discontinuities and delineate fault edges with greater clarity.

Copyright © SLB. All Rights Reserved. Private & Confidential. Reproduction only by permission.

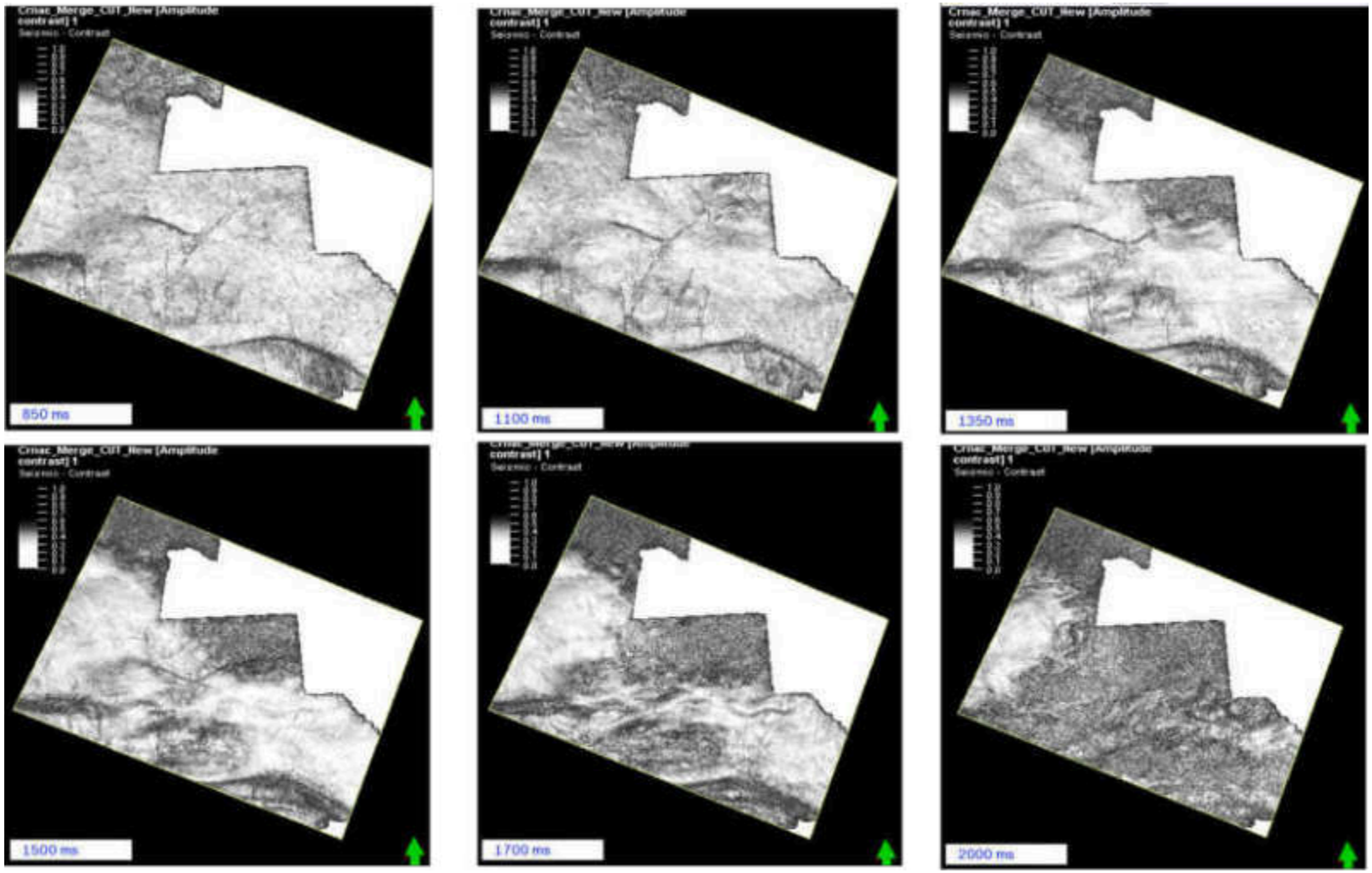


Fig. 2.25 Amplitude contrast attribute slices at 850, 1100, 1350, 1500, 1700, and 2000 ms
Amplitude contrast attribute was applied to support fault identification in areas where seismic continuity is reduced

Copyright © SLB. All Rights Reserved. Private & Confidential. Reproduction only by permission.

Attribute time slices were systematically evaluated at 850, 1100, 1350, 1500, 1700, and 2000 ms to ensure vertical consistency in structural interpretation. This multi-level analysis enabled cross-validation of major and secondary faults, improved the correlation of discontinuities across multiple orientations, and increased interpreter confidence in structurally complex intervals (Fig. 2.24 and Fig. 2.25 below).

2.2.6 Fault QC and validation

The fault interpretation derived from seismic attribute analysis was further quality-checked and refined. The results identify two distinct fault families, each associated with different stratigraphic levels and structural regimes.

The shallow fault system, located above the Rs7 horizon, is characterized by relatively continuous and well-defined discontinuities, supported by higher seismic bandwidth and strong reflector coherence. In contrast, the deeper fault population, extending below Rs7 toward the Tg horizon, exhibits reduced continuity and more complex geometries, reflecting the lower signal-to-noise ratio (SNR) in this interval.

A clear depth-dependent change in fault orientation is observed. In the shallow section, the dominant structural trend is NE–SW, whereas at greater depth the structural grain progressively rotates to a NW–SE orientation (Fig 3.23). This variation in azimuth suggests the influence of deeper-seated tectonic processes and evolving stress regimes across the stratigraphic column.

The deeper structural framework is further controlled by a detachment level interpreted at the Tg horizon (Fig.3.26). This feature provides a plausible explanation for the lateral offset and structural shift observed at the Tg base. The detachment acts as a structural boundary, from which secondary faults propagate upward through the intermediate section, locally reaching the Rs7 horizon. This geometry indicates a multi-phase deformation history and highlights the mechanical coupling between deep tectonic structures and overlying stratigraphy.

Due to reduced seismic resolution and lower SNR within the Rs7–Tg interval, the interpretation of deeper faults carries higher uncertainty. Accordingly, conservative acceptance criteria were applied, requiring multi-attribute consistency and manual validation prior to incorporation into the final structural model.

The results of the fault interpretation are presented below in Fig. 2.26, Fig. 2.27.

Copyright © SLB. All Rights Reserved. Private & Confidential. Reproduction only by permission.

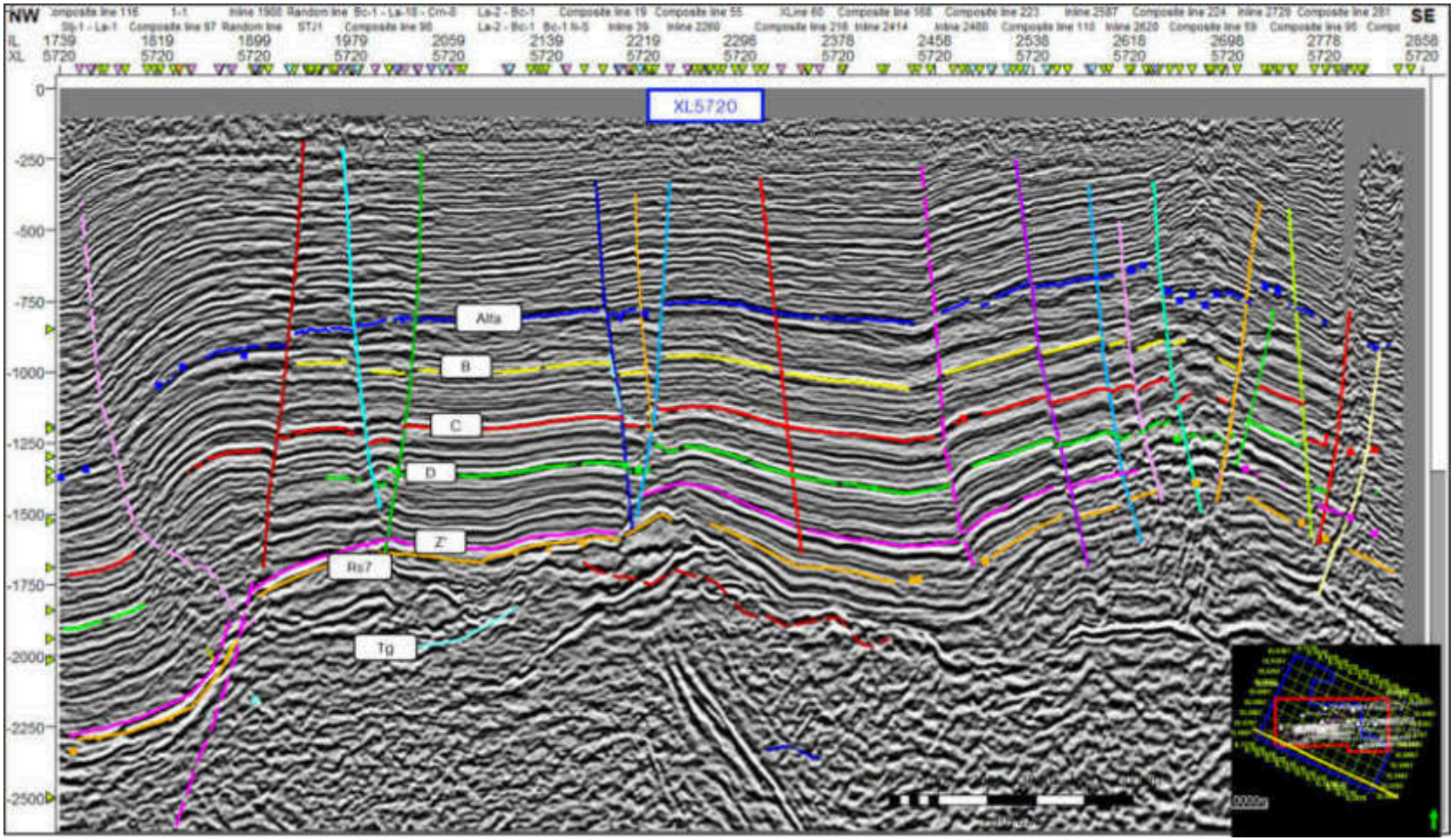


Fig. 2.26 Fault interpretation results - XL5720

2 fault families identified above and below Rs7 level, the main fault trend along the horizon varies with time: it is predominantly NE–SW in the shallow section, shifting to an NW-SE in the deeper levels

Copyright © SLB. All Rights Reserved. Private & Confidential. Reproduction only by permission.

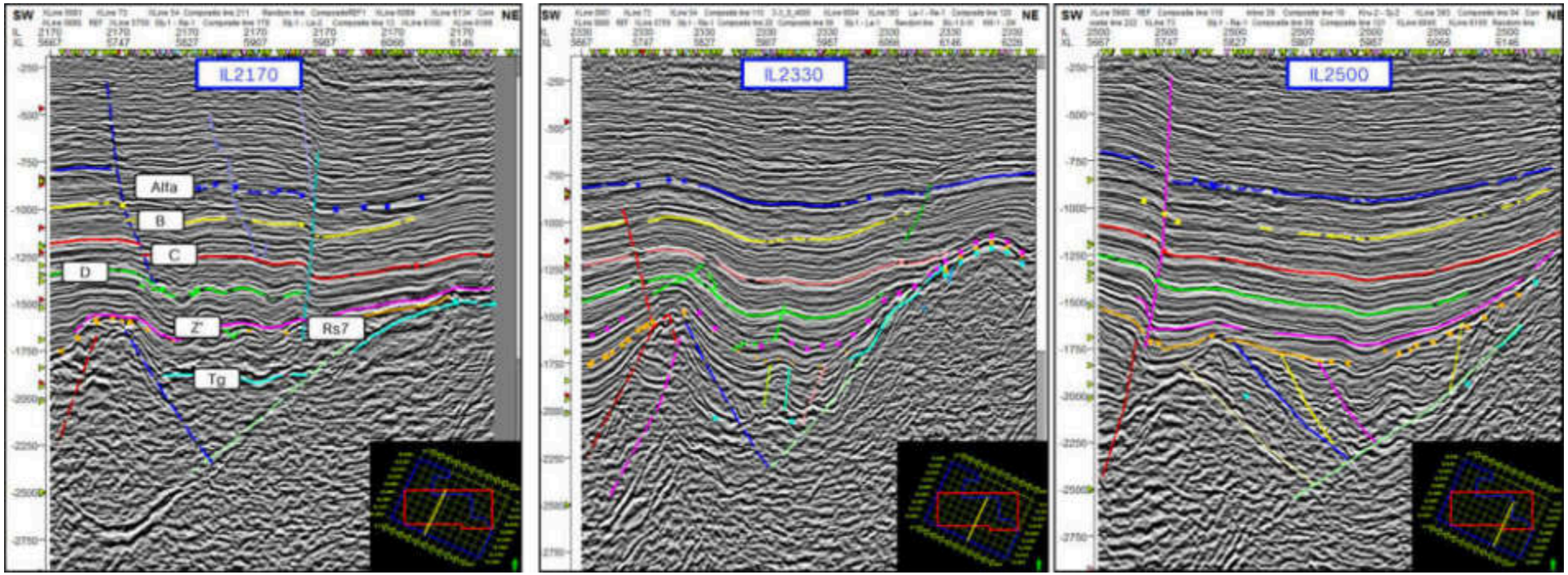


Fig. 2.27 Fault interpretation results:IL2170, IL2330, IL2500
The deeper fault family, located below Rs7 and extending toward the Tg horizon, exhibits more complex geometries and reduced continuity due to the lower signal-to-noise ratio inherent to this part of the dataset.

Copyright © SLB. All Rights Reserved. Private & Confidential. Reproduction only by permission.

2.2.7 Horizon interpretation

The interpretation of seismic horizons was performed across seven key reflectors: Alfa, B, C, D, Z′, Rs7, and Tg. Overall, horizon picking is well constrained in the shallow section of the seismic volume, where reflectors display strong lateral continuity, broader bandwidth, and a stable wavelet character. These favorable seismic attributes enable confident and consistent horizon interpretation across the survey area.

To ensure geological consistency, composite seismic lines (Fig. 2.28) across key wells were used to validate interpreted horizons against available well tops. This calibration maintained stratigraphic alignment and provided additional control in areas with variable lateral reflector quality.

A suite of seismic attributes—including RMS amplitude, envelope, cosine phase, relative acoustic impedance, and dip-related attributes—was applied to enhance reflector continuity, particularly where the native seismic response was unstable. These attributes were effective in strengthening horizon correlation within the shallow interval and in supporting the identification of subtle stratigraphic features.

In contrast, interpretation of the deeper section (Rs7 –Tg interval) proved significantly more challenging. Reduced signal-to-noise ratio, attenuation of high frequencies, and increased wavelet complexity at depth resulted in weaker reflector continuity. Consequently, the Rs7 and Tg horizons required careful manual picking, supported by multi-attribute validation and conservative interpretation criteria to avoid misidentifying noise as geological signal.

Following completion of fault and horizon interpretation, an intermediate structural framework was constructed in the time domain to support the generation of structural maps for all key horizons. These maps provide an integrated representation of fault architecture, structural trends, and large-scale geometries defining the subsurface configuration across the study area.

Structural Maps of Alfa horizon Fig. 2.29
The Alpha horizon was displayed with a 25 ms contour interval, enabling clear delineation of structural trends and fault compartmentalization. The structural map reveals a fault controlled extensional system dominated by a major NE–SW which separates a deeper northwestern domain from a relatively shallower southeastern domain, consistent with a regional NW-dipping geometry. This main fault is associated with several synthetic secondary faults, mainly oriented N–S to NNE–SSW, forming segmented tilted blocks, additional short transfer faults indicate local segmentation and relay zones, contributing to structural complexity and compartmentalization, particularly in the central area.

Structural Maps of C, D, Z′, and Rs7 Horizons
(Maps for horizons C Fig. 2.30, D Fig. 2.31, and Rs7 Fig. 2.32 are presented at then end of the chapter). The map of the horizons display structural patterns largely consistent with the Alpha horizon. Each map exhibits:

Copyright © SLB. All Rights Reserved. Private & Confidential. Reproduction only by permission.

- A predominant NE–SW fault orientation, characteristic of the shallow fault family
- A northeastward maximum dip direction,

This internal consistency across horizons supports the robustness of the shallow to mid-level interpretation and confirms the stratigraphic and structural coherence of the model.

Tg Base Structural Map (Fig. 2.33)
A marked shift in structural behavior is observed when examining the Tg Base structural map. At this depth, the fault orientation rotates significantly, showing a transition from the familiar NE–SW trend to a predominantly E–W structural direction. This change is associated with a major deep detachment fault, which appears to act as a structural boundary separating the deeper tectonic regime from the overlying stratigraphy.

Secondary faults originating from this detachment fault propagate upward and intersect the Rs7 horizon, linking the deeper structural system to the shallower sequence. This upward propagation provides supporting evidence for a multi-phase deformation history, with deeper structural events influencing overlying layers.

Interpretation Challenges
The interpretation of the Tg Base horizon and its associated fault system proved particularly challenging due to the low signal-to-noise ratio and reduced reflector continuity within the deepest portion of the seismic cube. To mitigate these limitations, conservative picking strategies were systematically applied. All major fault interpretations in this interval were further validated through iterative seismic attribute analysis and rigorous structural consistency checks, ensuring robustness despite data quality constraints.

The horizons B , C Fig. 2.30 , D Fig. 2.31, Z’ , and Rs7 Fig. 2.32 are presented below:

Copyright © SLB. All Rights Reserved. Private & Confidential. Reproduction only by permission.

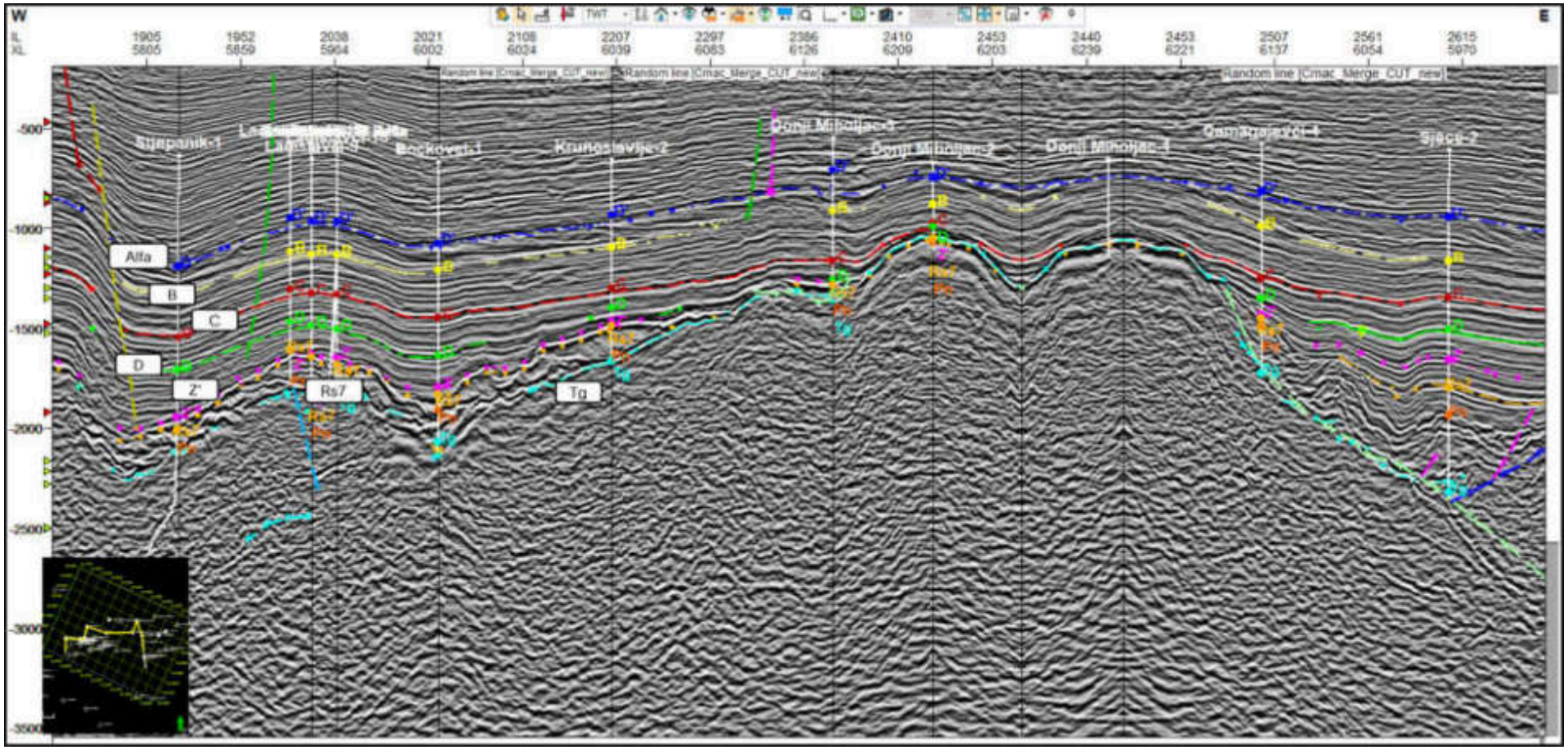


Fig. 2.28 Horizon interpretation result: composite seismic lines with interpreted horizons
Horizon picking was more reliable in the shallow section due to strong seismic continuity. In the deeper intervals the reduced signal-to-noise ratio significantly increased the difficulty of interpreting the Rs7 and Tg.

Copyright © SLB. All Rights Reserved. Private & Confidential. Reproduction only by permission.

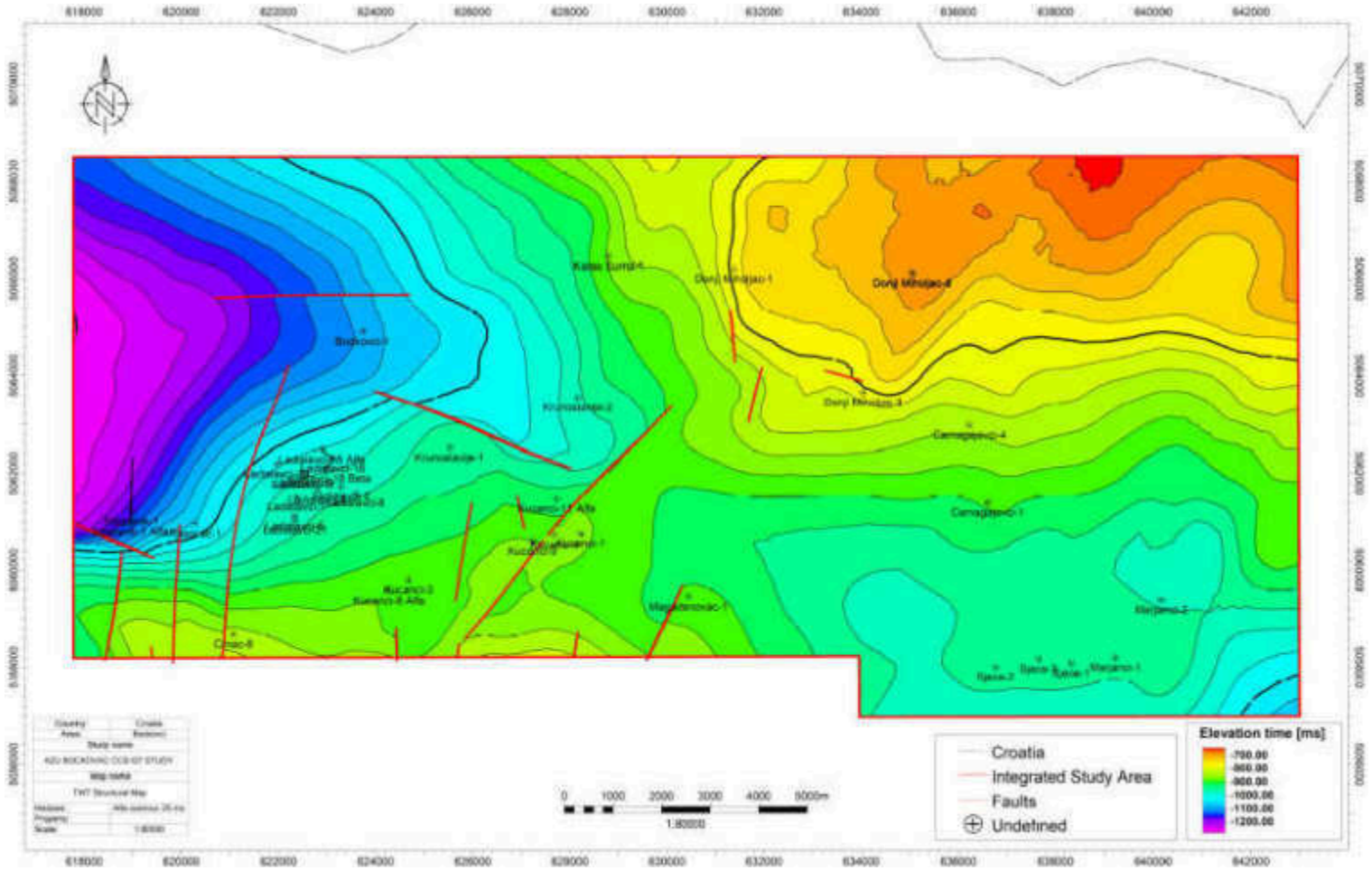


Fig. 2.29 Alfa horizon TWT structural maps with fault boundaries and well locations
25ms contour
significant fault zone observed in Krunoslavlje, Stjepanik, Ladislavci areas

Copyright © SLB. All Rights Reserved. Private & Confidential. Reproduction only by permission.

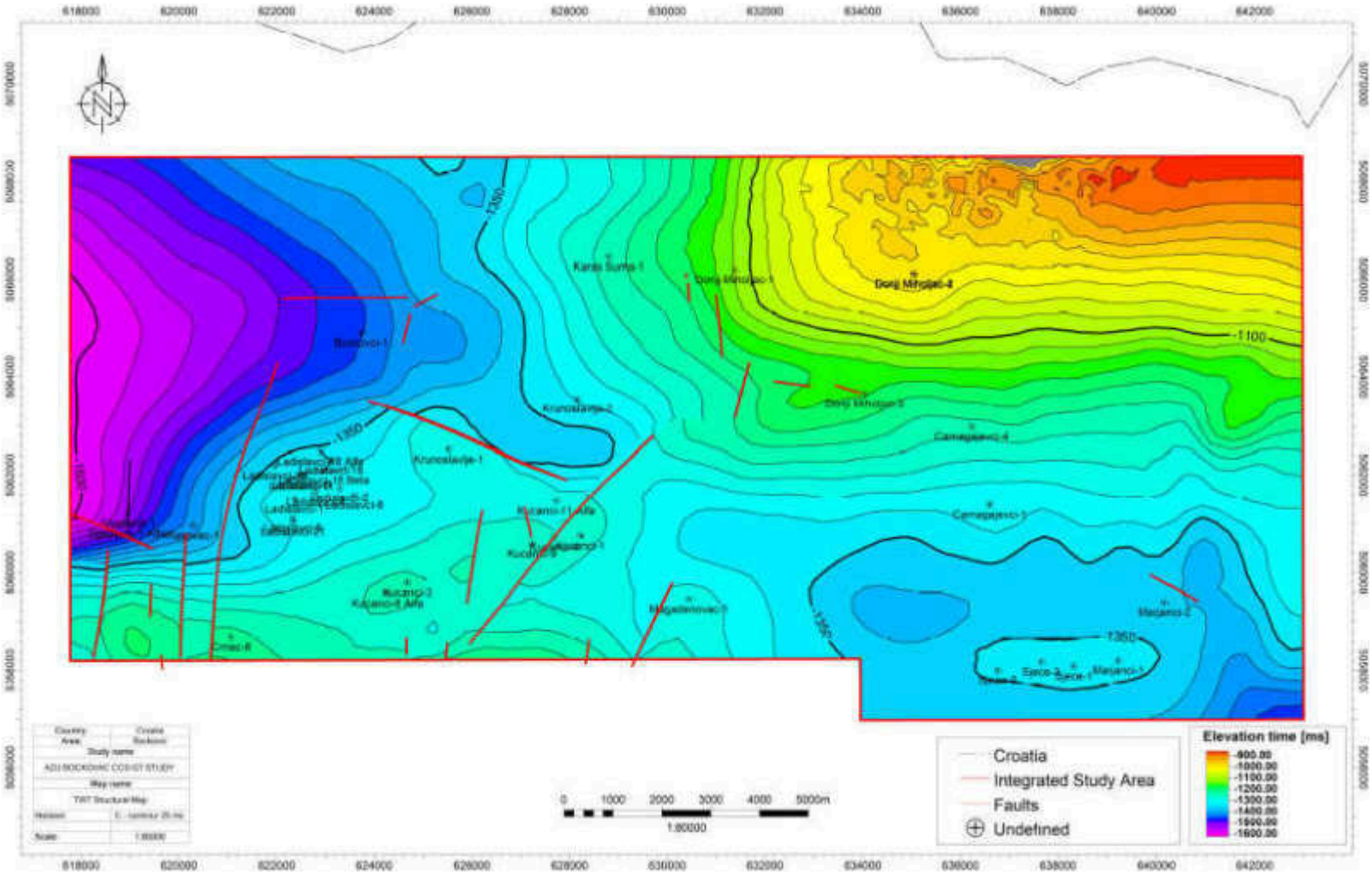


Fig. 2.30 C horizon TWT structural maps with fault boundaries and well locations
25m contour

Copyright © SLB. All Rights Reserved. Private & Confidential. Reproduction only by permission.

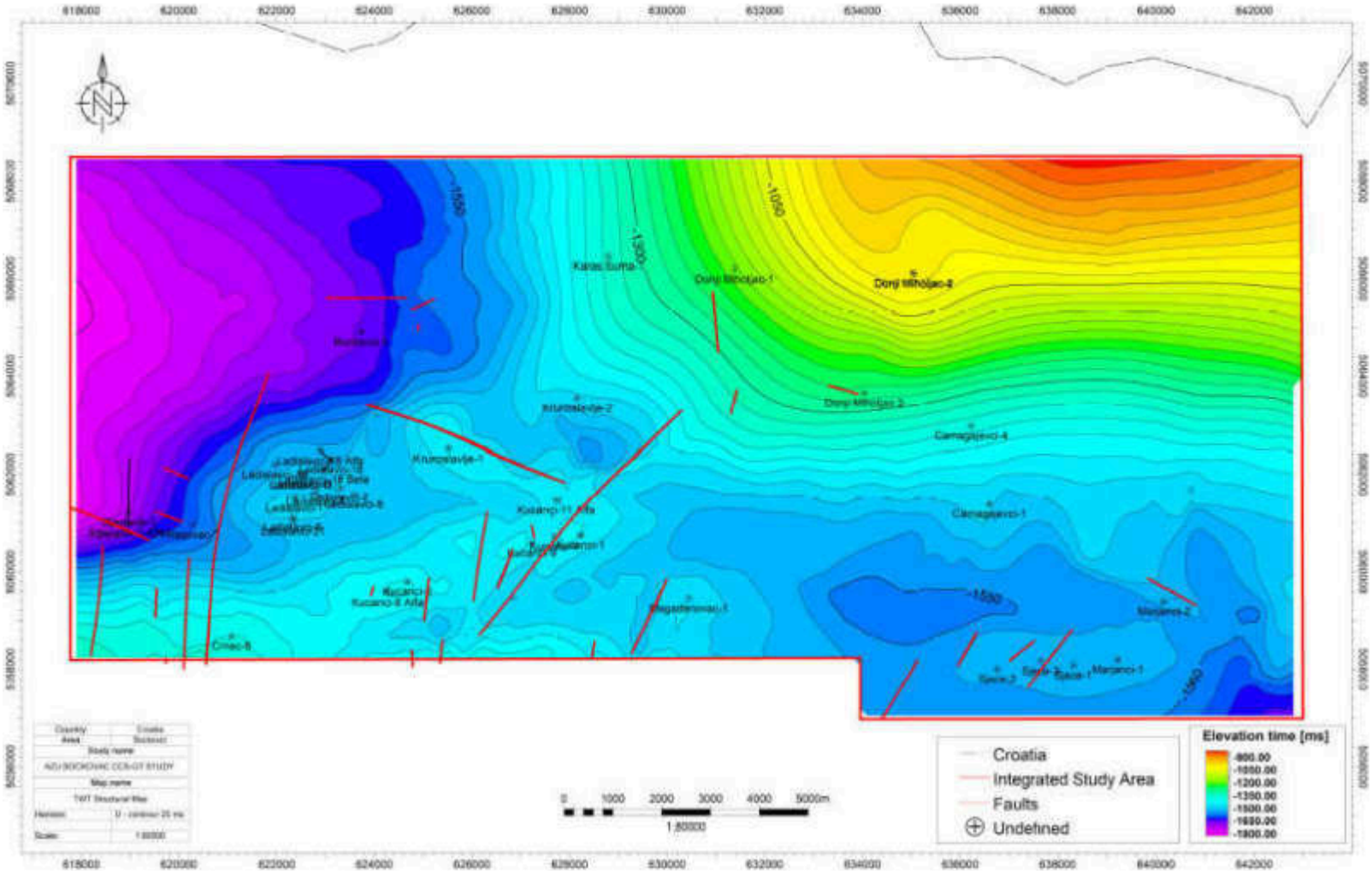


Fig. 2.31 D horizon TWT structural maps with fault boundaries and well locations
25m contour

Copyright © SLB. All Rights Reserved. Private & Confidential. Reproduction only by permission.

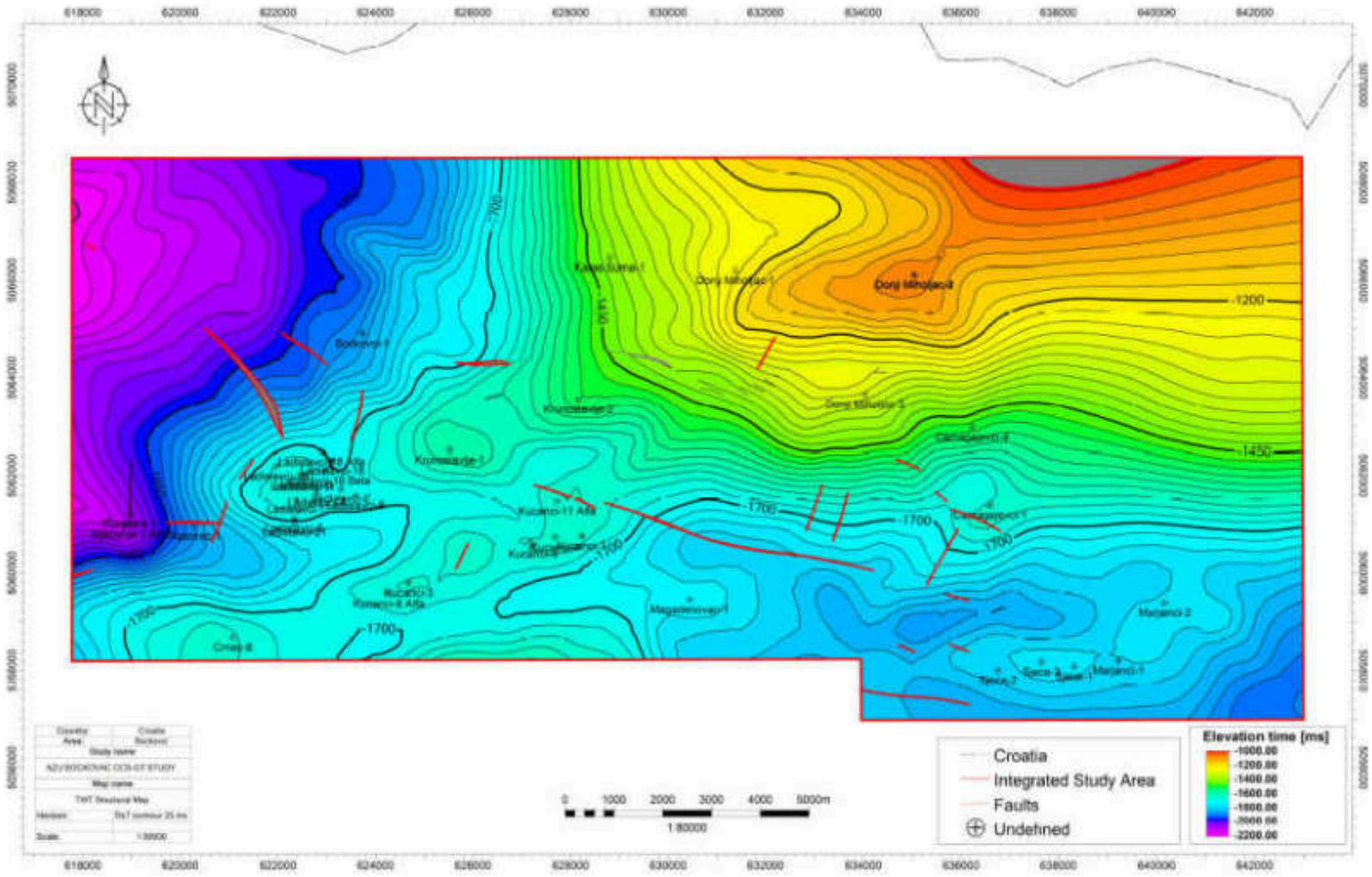


Fig. 2.32 Rs7 horizon TWT structural maps with fault boundaries and well locations
25m contour

Copyright © SLB. All Rights Reserved. Private & Confidential. Reproduction only by permission.

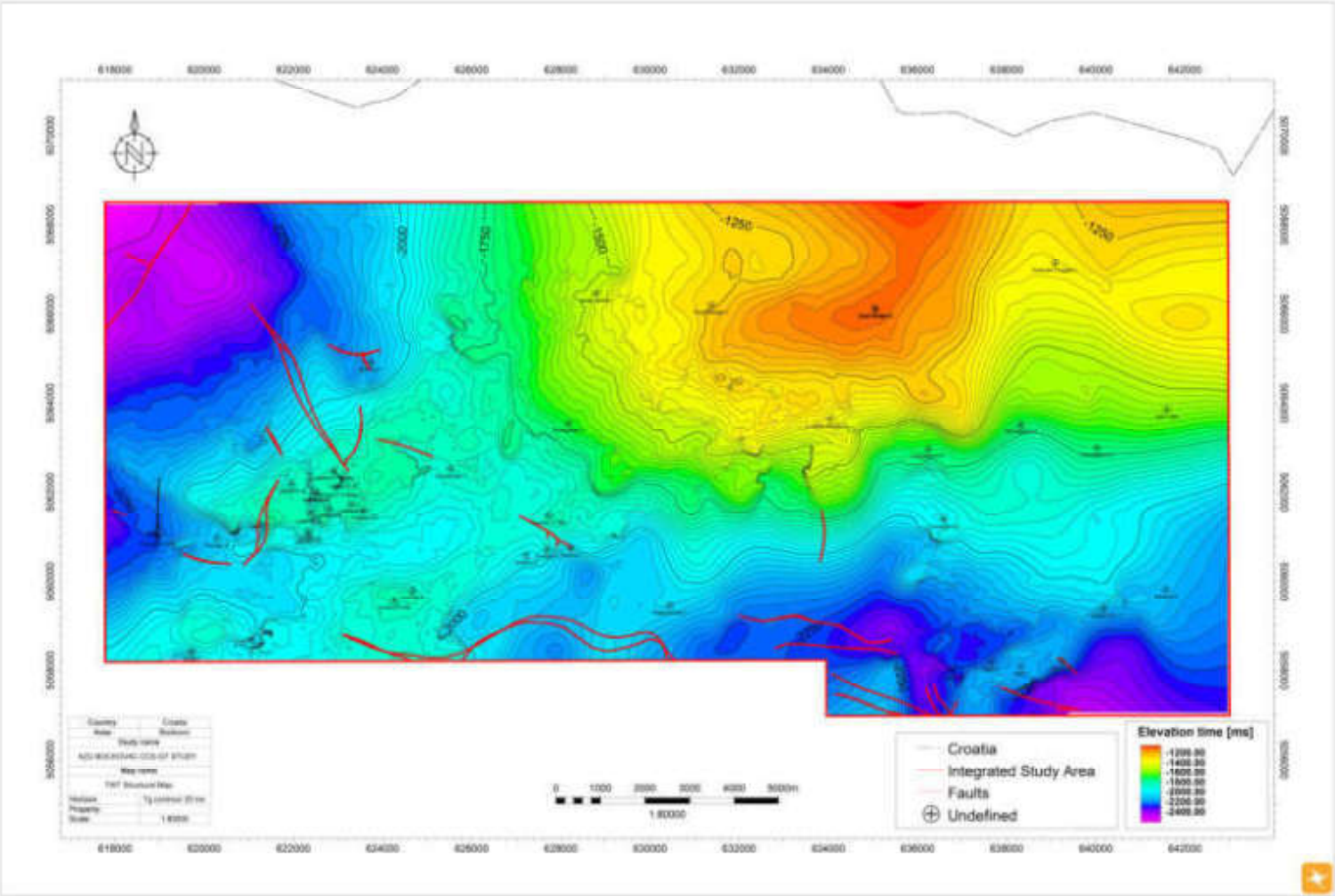


Fig. 2.33 Tg horizon TWT structural maps with fault boundaries and well locations
25m contour

Copyright © SLB. All Rights Reserved. Private & Confidential. Reproduction only by permission.

2.2.8 Velocity Modeling and time depth conversion

A layer-cake velocity model was constructed to support time–depth conversion of the interpreted seismic horizons and corresponding fault framework. The model spans SRD down to 4s level and was developed using a combination of constant interval velocity and velocity surfaces derived from well time–depth relationships, depending on the level of available control and seismic quality.

Methodology
The velocity model (Fig. 2.34) is composed of 4 principal intervals :

1. SRD to Alfa Horizon
   Due to limited well control in the shallow interval, a constant velocity of 2000 m/s was assigned. This choice was based on the only available well providing log measurements from surface to Alfa, making a uniform velocity the most consistent and stable option for this layer.
2. Alfa to D Horizon
   In this interval, calculated velocity surfaces were generated by tying the interpreted seismic horizons in time to well tops in time. Velocities were derived at these intersections using the well time–depth relationship (TDR), then interpolated laterally. Velocity increases gradually with depth, following the trends observed in the TDR samples.
3. D to Rs7 Horizon
   The velocity field was obtained through well-based time–depth calibration. Computed interval velocities were again extracted at seismic–well intersections, and the velocity gradient was allowed to increase progressively with depth, reflecting compaction and lithological trends observed in the available well data.
4. RS- 4 s level
   The deepest portion of the model was assigned a constant velocity of 5500 m/s. This decision reflects the lack of wells penetrating the Tg basement interval, combined with lower seismic quality at depth. The constant velocity ensures stability in the conversion while avoiding unrealistic velocity fluctuations in poorly constrained zones.

Copyright © SLB. All Rights Reserved. Private & Confidential. Reproduction only by permission.

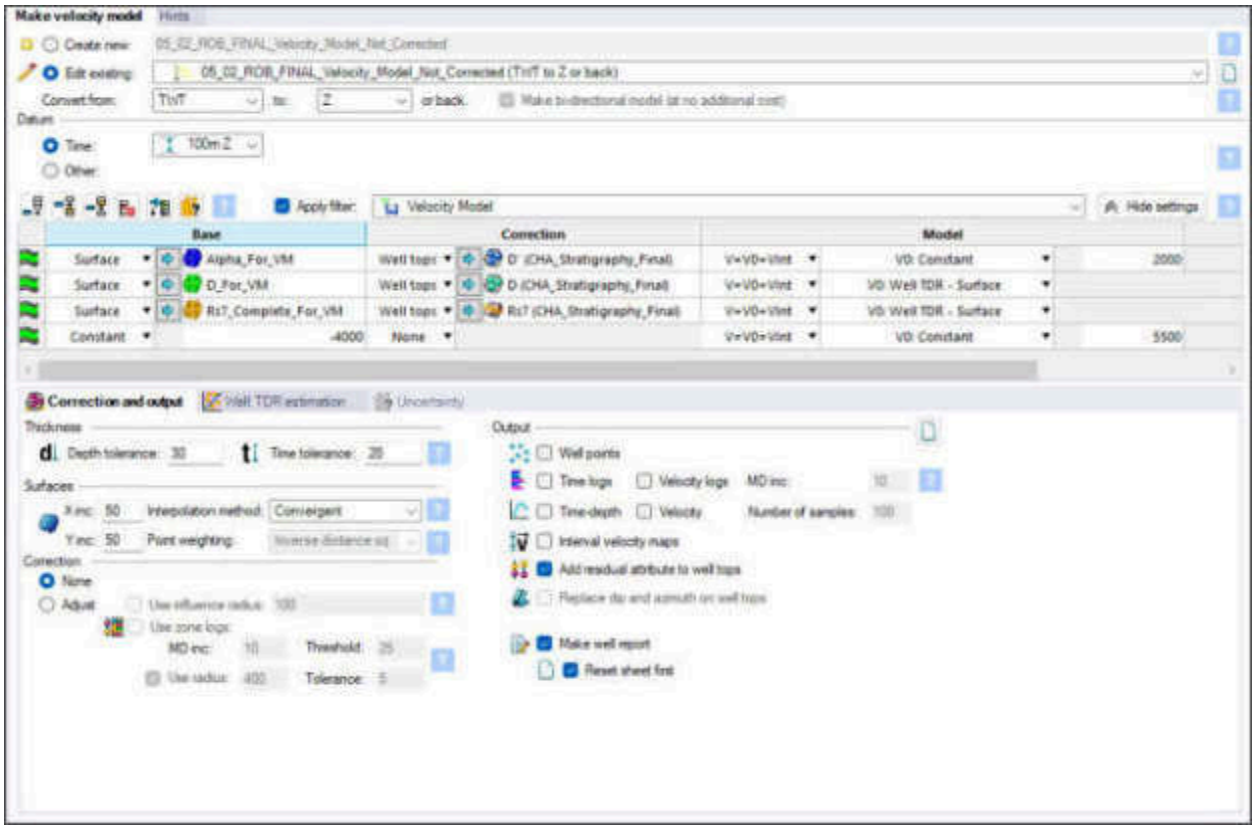


Fig. 2.34 Layer-cake velocity model without adjustment
The velocity model is composed of 4 principal intervals:
- SRD to Alfa Horizon
- Alfa to D Horizon
- D to Rs7 Horizon
- Rs- 4s level

Velocity model testing and residual evaluation

The first velocity model was used to perform an initial time–depth conversion of the interpreted horizons. Depth-converted surfaces were compared against the measured well tops to evaluate accuracy. The following residual ranges were observed:

- Alfa Horizon: –25 m to +25 m Fig. 2.35
- D Horizon: –42 m to +42 m Fig. 2.36
- Rs7 Horizon: –53 m to +40 m Fig. 2.37
- Deep interval (Rs7 to ~4000 ms): –55 m to +68 m

Copyright © SLB. All Rights Reserved. Private & Confidential. Reproduction only by permission.

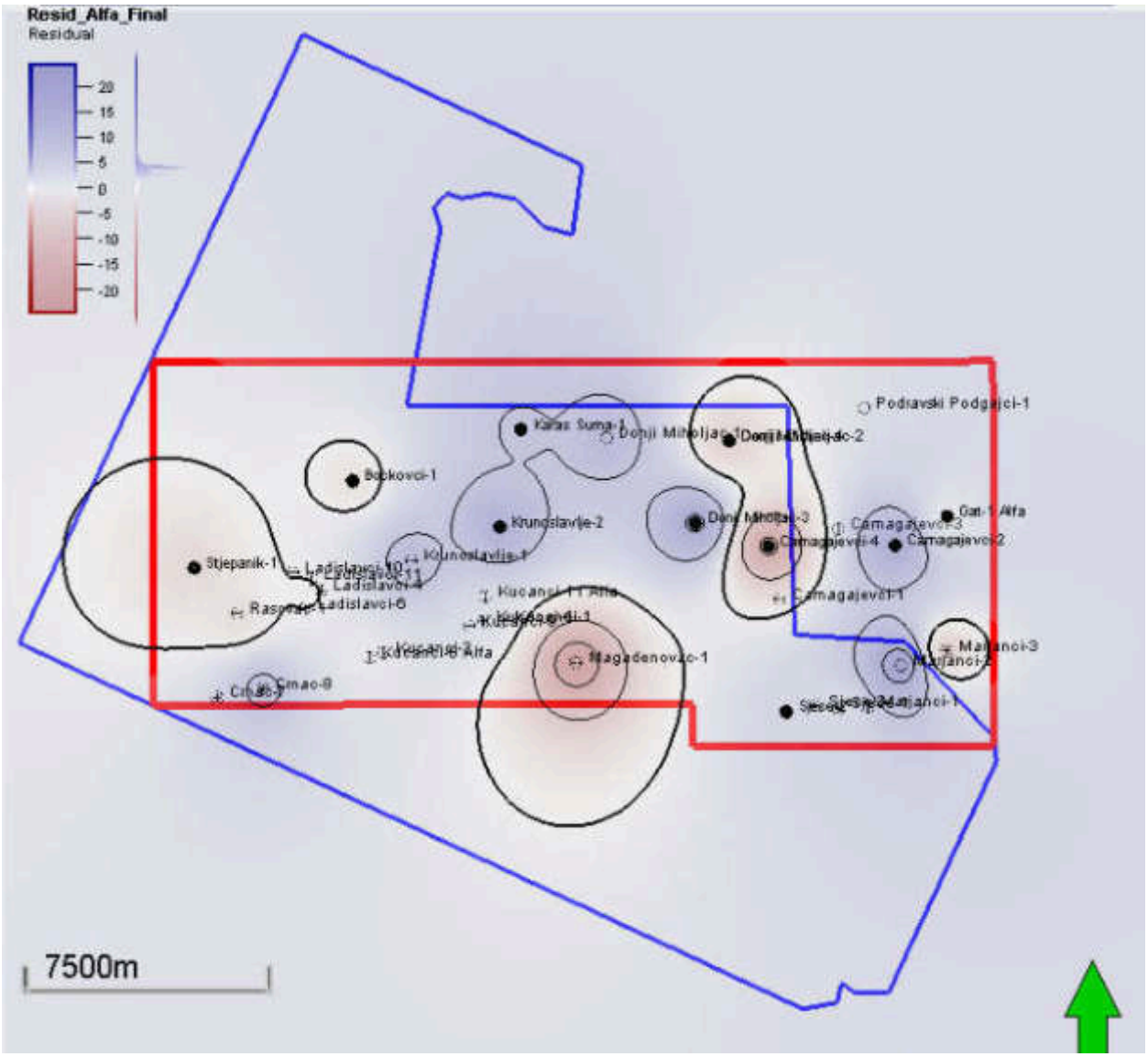


Fig. 2.35 Alfa depth residual map
Alfa depth residual map: –25 m to +25 m

Copyright © SLB. All Rights Reserved. Private & Confidential. Reproduction only by permission.

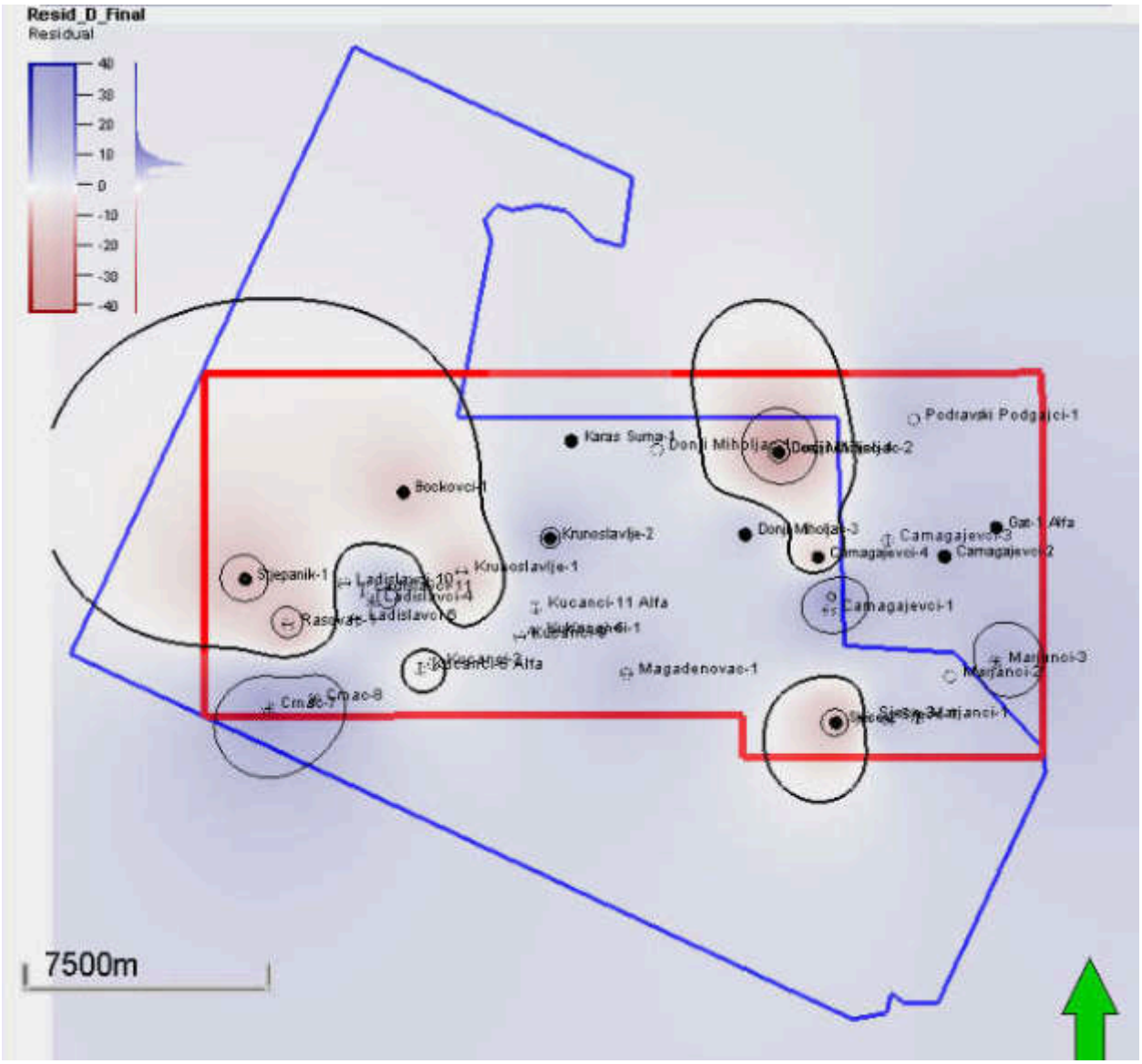


Fig. 2.36 D depth residual map
D depth residual map: –42 m to +42 m

Copyright © SLB. All Rights Reserved. Private & Confidential. Reproduction only by permission.

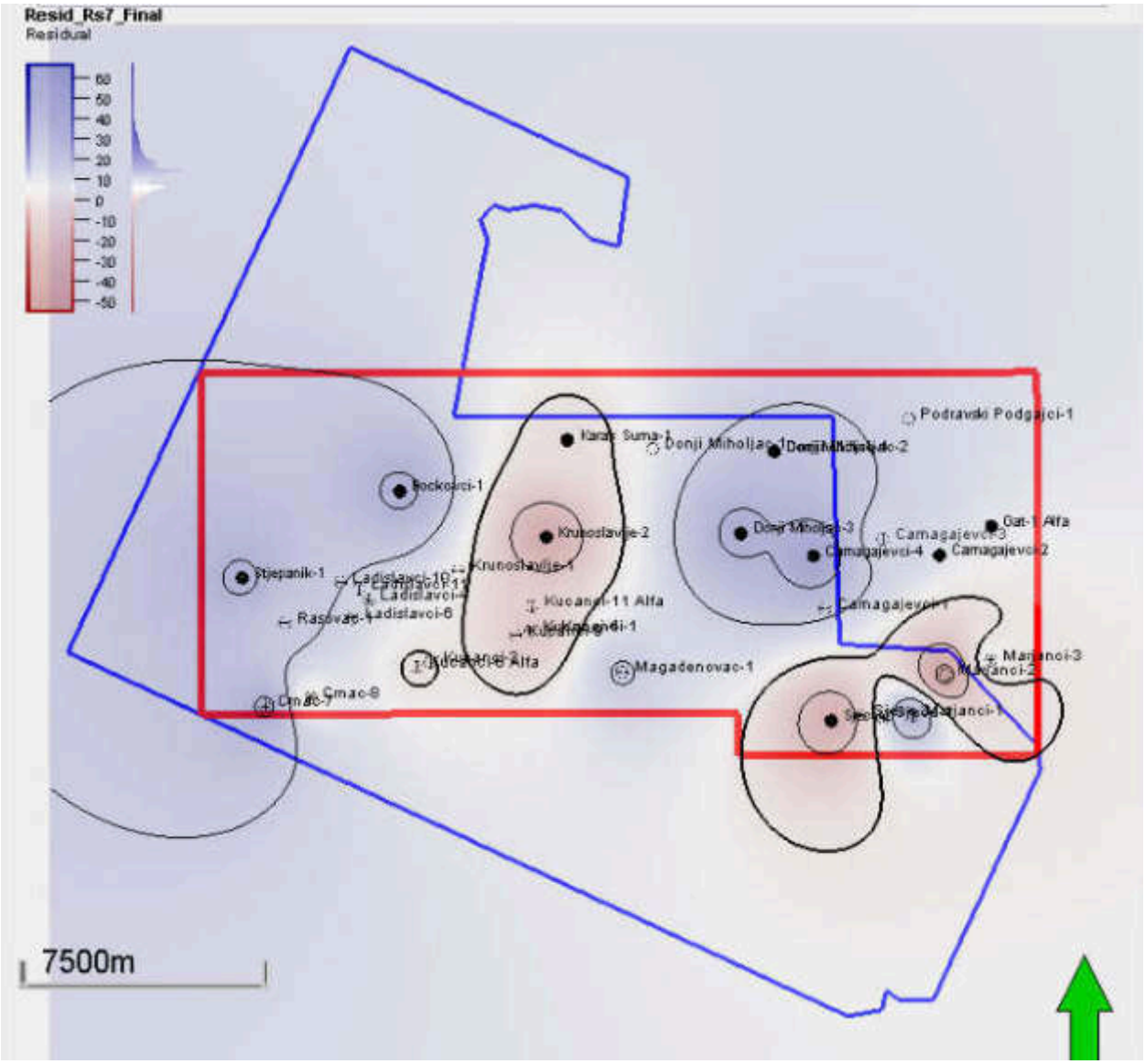


Fig. 2.37 Rs7 depth residual map
Rs7 depth residual map: –42 m to +42 m

These results were considered acceptable for a first-pass velocity model, given the data quality and depth of investigation. However, to further improve the correlation with well control, a second model version was generated by analyzing depth residuals at all control points and selecting the most reliable wells for targeted velocity adjustments.

Adjusted Model

The velocity model applied targeted velocity adjustments to reduce depth mismatches at key well tops. This refinement improved the lateral consistency of depth surfaces across all intervals, particularly at Rs7 and Tg, where the initial model showed broader residual ranges. The adjusted model provides a more reliable basis for structural analysis and was adopted for the final conversion (Fig. 2.38 below)

Copyright © SLB. All Rights Reserved. Private & Confidential. Reproduction only by permission.

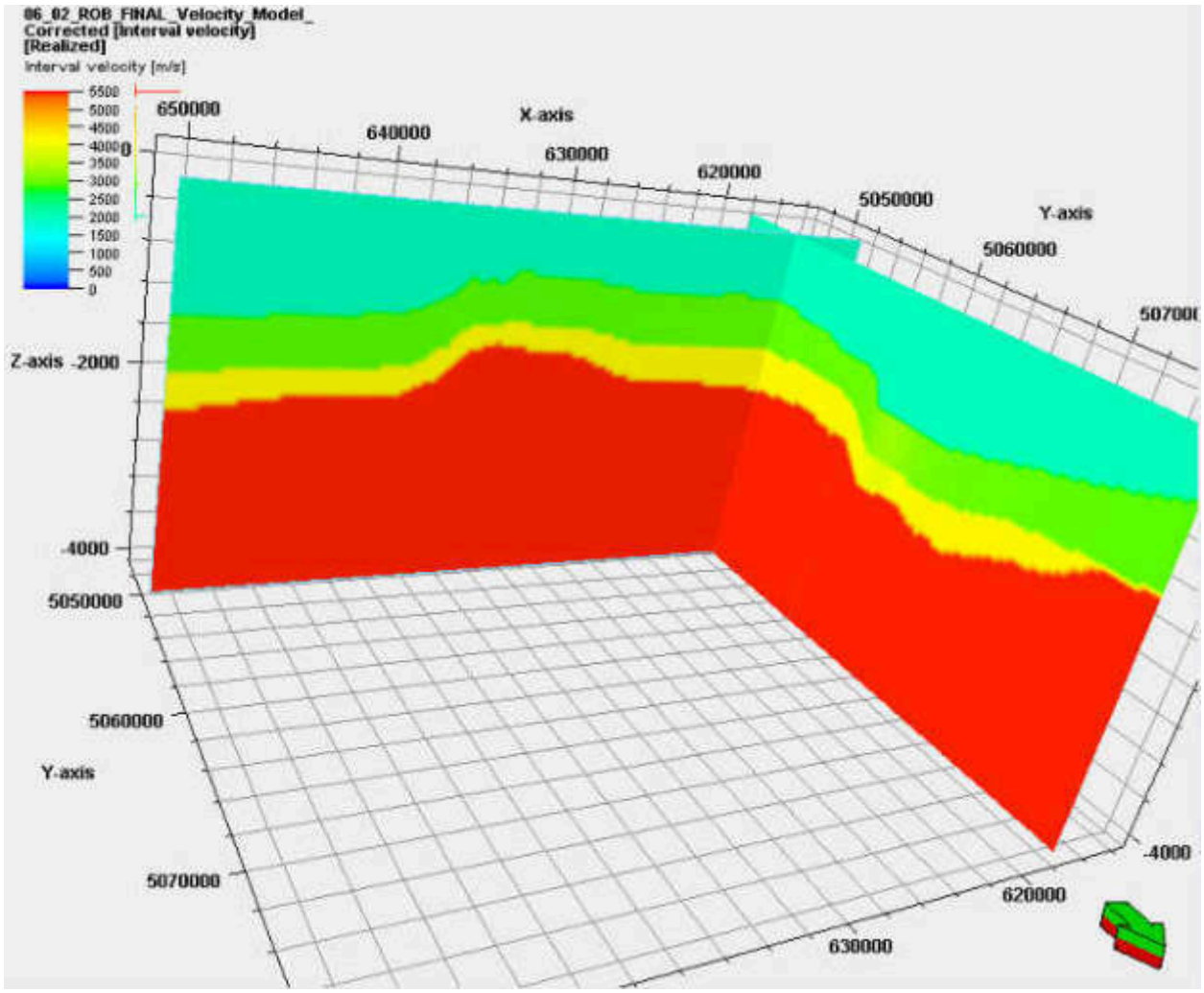


Fig. 2.38 Final velocity model Inline and Xline displayed in the 3D window

Final Time–Depth Conversion and Outputs (Fig. 2.39 and Fig. 2.40)

Using the adjusted model, full time–depth conversion was performed for:

- All interpreted seismic horizons (Alfa, B, C, D, Z', Rs7, Tg)
- The complete fault framework
- The corresponding interpreted seismic sections

The resulting depth-converted seismic section, displayed with both converted faults and horizons, represents the final product delivered to the modeling team for use in the next stage of structural and reservoir framework modeling.

Copyright © SLB. All Rights Reserved. Private & Confidential. Reproduction only by permission.

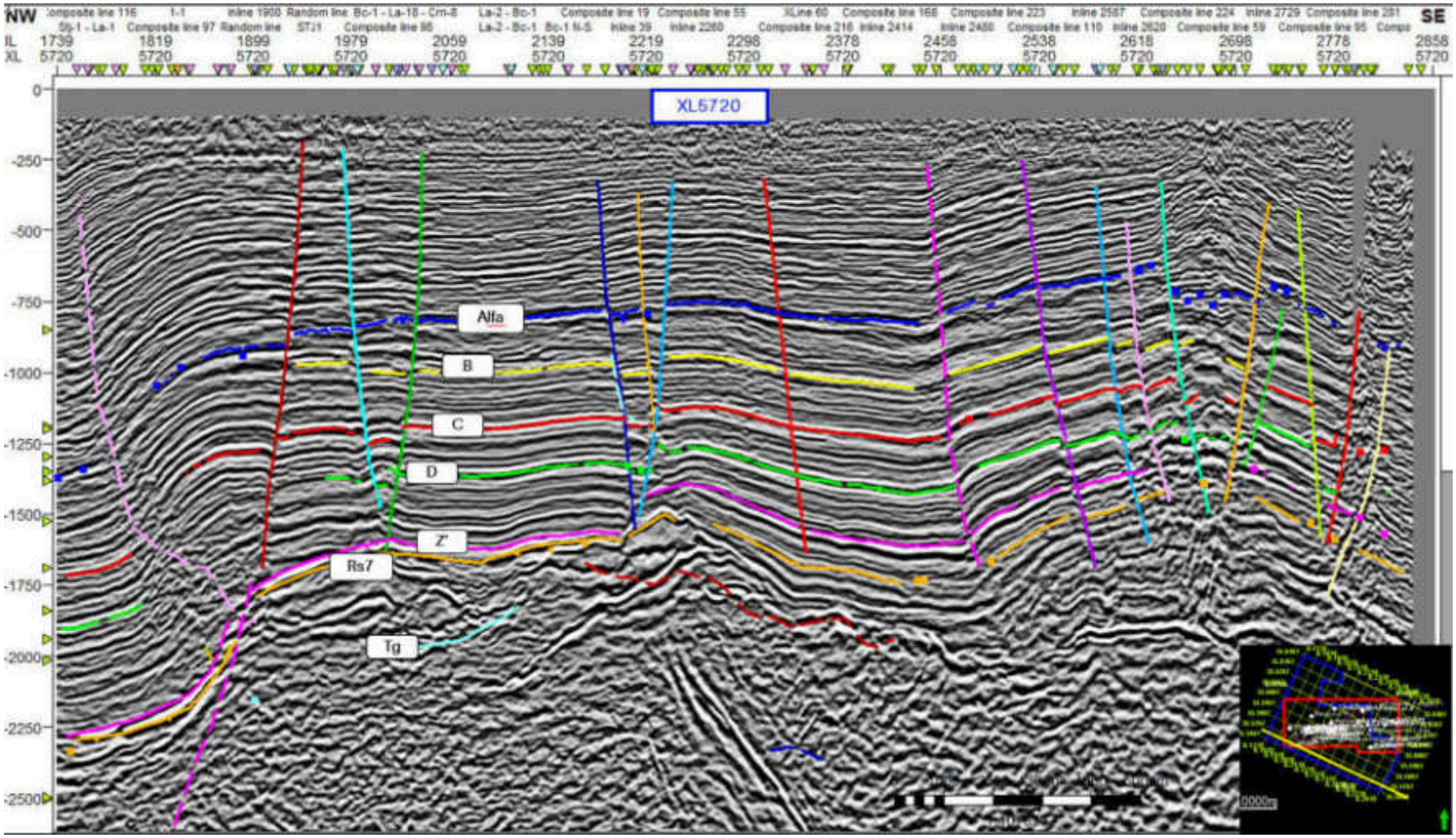


Fig. 2.39 Converted seismic, faults and horizons - XL 5720
XL 5720 - Converted seismic, faults and horizons using adjusted velocity model

Copyright © SLB. All Rights Reserved. Private & Confidential. Reproduction only by permission.

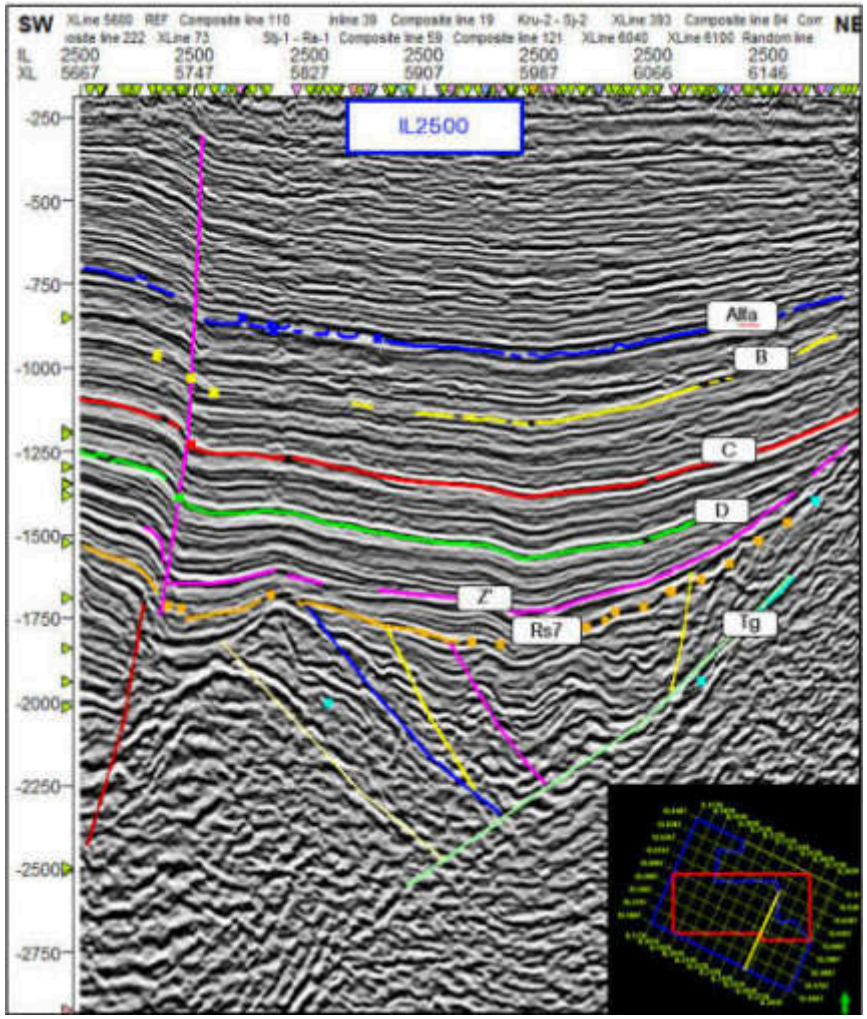


Fig. 2.40 Converted seismic, faults and horizons - IL 2500
IL 2500 - Converted seismic, faults and horizons using adjusted velocity model

Copyright © SLB. All Rights Reserved. Private & Confidential. Reproduction only by permission.

2.2.9 Geophysical Conclusions and Recommendations

This study delivers a coherent structural framework built on integrated seismic interpretation, machine-learning–assisted fault detection, and multi-attribute validation. Shallow intervals are well constrained, while deeper sections (Rs7–Tg) carry higher uncertainty due to lower SNR and complex tectonics. The combined use of variance, spectral decomposition, and dip-related attributes provides a robust and well-supported fault and horizon model.

The calibrated layer cake velocity model supports reliable first-pass time–depth conversion and depth mapping. To further de-risk the deeper structural elements, particularly basement penetrating faults of interest for geothermal evaluation, we recommend:

- Exploring the possibility of seismic reprocessing aimed at bandwidth extension and depth imaging,
- And iterative velocity updates incorporating new well control.

These steps will tighten depth confidence, improve fault continuity at depth, and strengthen the basis for subsequent structural modeling and decision-making.

2.3 Petrophysical analysis

2.3.1 Available Well Data Review

A comprehensive petrophysical database was established for the CHA Bockovac CCS & Geothermal study based on the data provided. The dataset included LAS well logs, rasterized log images (TIF/PDF), core analysis reports, mudlog cuttings, water analysis reports, and temperature measurements. In total, LAS data from more than 40 wells were received, with multiple LAS files often present for a single well. These files were ingested into a unified Techlog platform, where extensive data harmonization and quality control were performed.

The available log suite across the evaluated wells typically includes Measured Depth (MD), Gamma Ray (GR), Spontaneous Potential (SP), Resistivity (mainly deep resistivity RES_DEEP), Bulk Density, Neutron Porosity, and Compressional Slowness (DTCO). Log coverage is variable: SP and Apparent Deep Resistivity logs are available for all wells, GR is available for approximately 85–90% of wells, while Density and Neutron logs commonly exhibit partial coverage and variable quality. Sonic logs (DTCO) are present in most wells but are often absent or degraded in key stratigraphic intervals of interest. Core data are available in a limited number of wells, mainly in deeper formations, and are unevenly distributed by zone.

A major component of the data review involved resolving inconsistencies such as duplicated logs with depth offsets, inconsistent well naming, missing log units, and undefined measurement families. Where multiple LAS files existed for a well, a single reference dataset covering the longest interval was selected where possible. All logs were resampled to a consistent vertical resolution,

Copyright © SLB. All Rights Reserved. Private & Confidential. Reproduction only by permission.

and family and unit harmonization was carried out to ensure compatibility across workflows. These steps were critical to enable robust well-to-well comparisons and subsequent petrophysical interpretation.

Data Digitization

Deep resistivity (RES_DEEP) logs for the Karas Suma-1 well, available only in raster image format, were digitized to reconstruct continuous log curves suitable for quantitative analysis (Fig. 2.41). The digitization was performed in Techlog, ensuring preservation of the original scale (0.2–2000 ohm·m) and careful depth alignment with existing logs to maintain consistency across the dataset. These reconstructed RES_DEEP and SP curves were subsequently integrated into the LQC dataset and used as key inputs for petrophysical analysis.

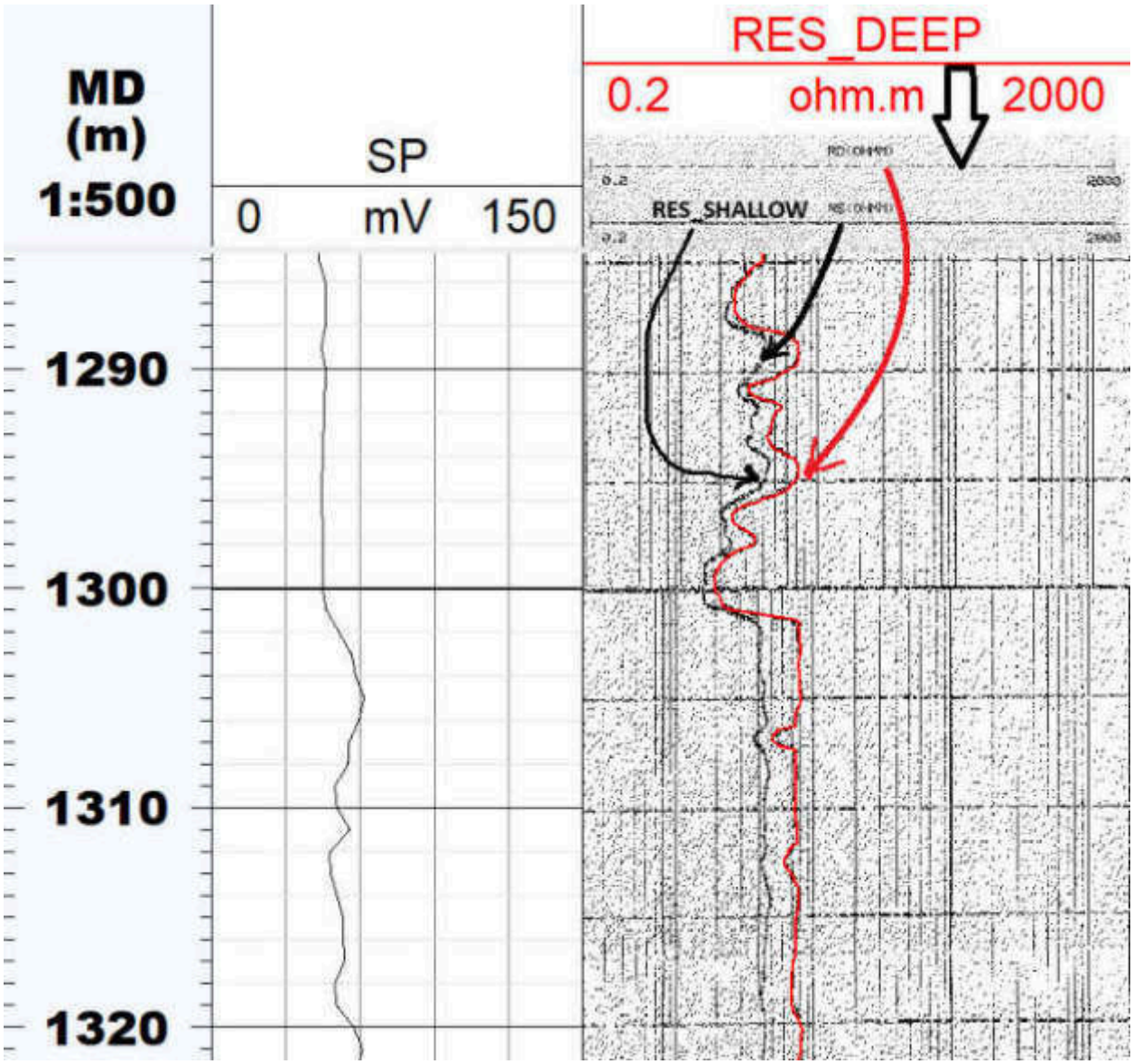
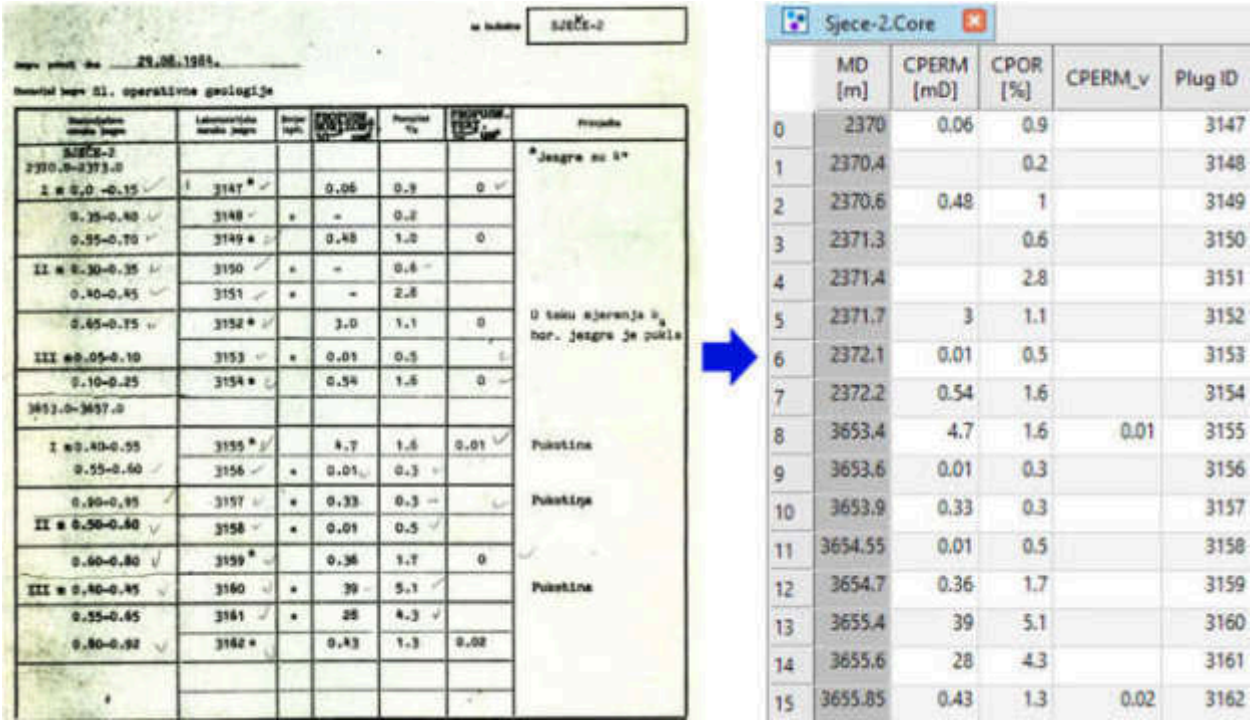


Fig. 2.41 Log digitization for well Karas Suma -1 : example of RES_DEEP log

Copyright © SLB. All Rights Reserved. Private & Confidential. Reproduction only by permission.

A core analysis dataset was compiled for 20 wells through digitization of legacy reports and subsequent depth alignment during evaluation. The final dataset comprises 469 porosity measurements and 269 permeability measurements, with 237 paired samples available for porosity–permeability (CPOR–CPERM) analysis.



Sjece-2.Core

	MD [m]	CPERM [mD]	CPOR [%]	CPERM_v	Plug ID
0	2370	0.06	0.9		3147
1	2370.4		0.2		3148
2	2370.6	0.49	1		3149
3	2371.3		0.6		3150
4	2371.4		2.8		3151
5	2371.7	3	1.1		3152
6	2372.1	0.01	0.5		3153
7	2372.2	0.54	1.6		3154
8	3653.4	4.7	1.6	0.01	3155
9	3653.6	0.01	0.3		3156
10	3653.9	0.33	0.3		3157
11	3654.55	0.01	0.5		3158
12	3654.7	0.36	1.7		3159
13	3655.4	39	5.1		3160
14	3655.6	28	4.3		3161
15	3655.85	0.43	1.3	0.02	3162

Fig. 2.42 Core digitization for well Sjece-2

LITHO_Cuttings datasets were compiled for 15 wells through the digitization of mudlog cutting descriptions, providing consistent lithological information along the wellbore. These datasets were primarily used to support well-to-well correlation by identifying key stratigraphic markers and lateral continuity. In addition, the interpreted lithology was integrated into the petrophysical workflow to constrain interval-based (zone-level) lithological classification. This approach enhanced the reliability of petrophysical interpretation, particularly in intervals with limited log or core data coverage.

Copyright © SLB. All Rights Reserved. Private & Confidential. Reproduction only by permission.

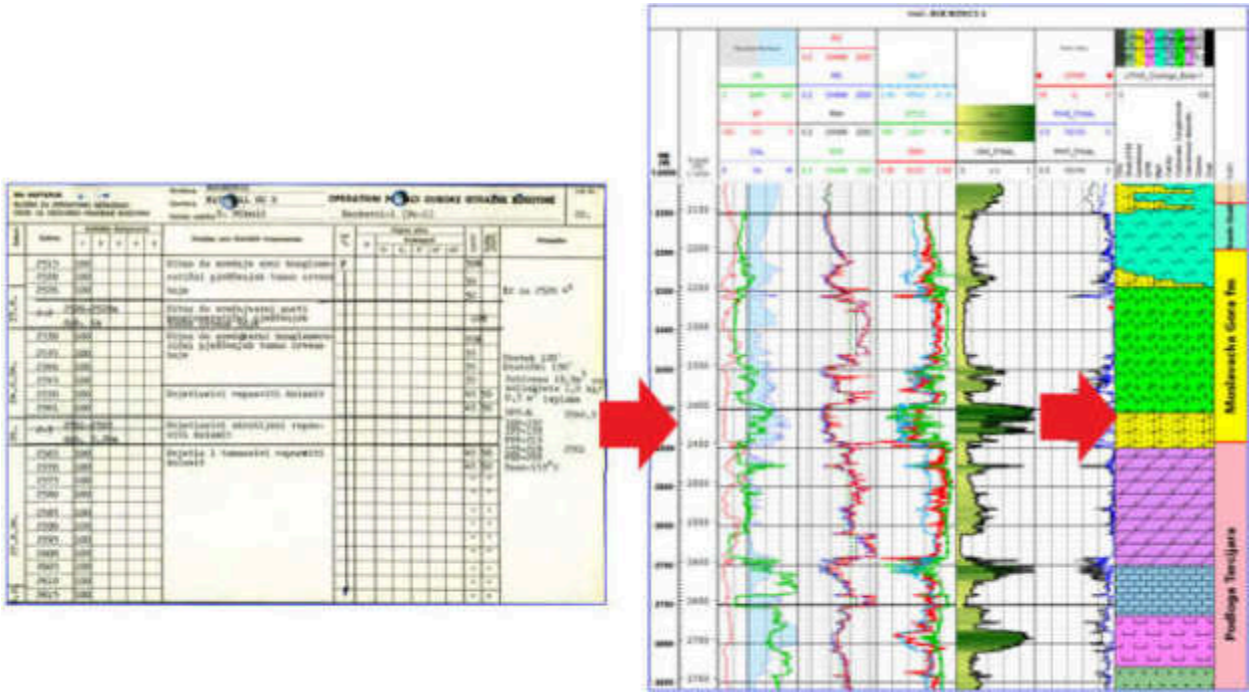


Fig. 2.43 Cuttings digitization for well Bockovci-1

Well Selection Criteria for Petrophysical Evaluation

A total of **15** wells were selected for advancing the petrophysical analysis; the well selection (Fig. 2.44) was based on depth, spatial distribution, and data availability to ensure coverage of target intervals and representative areal sampling. Priority was given to wells with adequate log suites (GR, resistivity, density, neutron, sonic) and available core data for calibration. Preference was also assigned to more recent wells to ensure higher data quality and acquisition standards.

Copyright © SLB. All Rights Reserved. Private & Confidential. Reproduction only by permission.

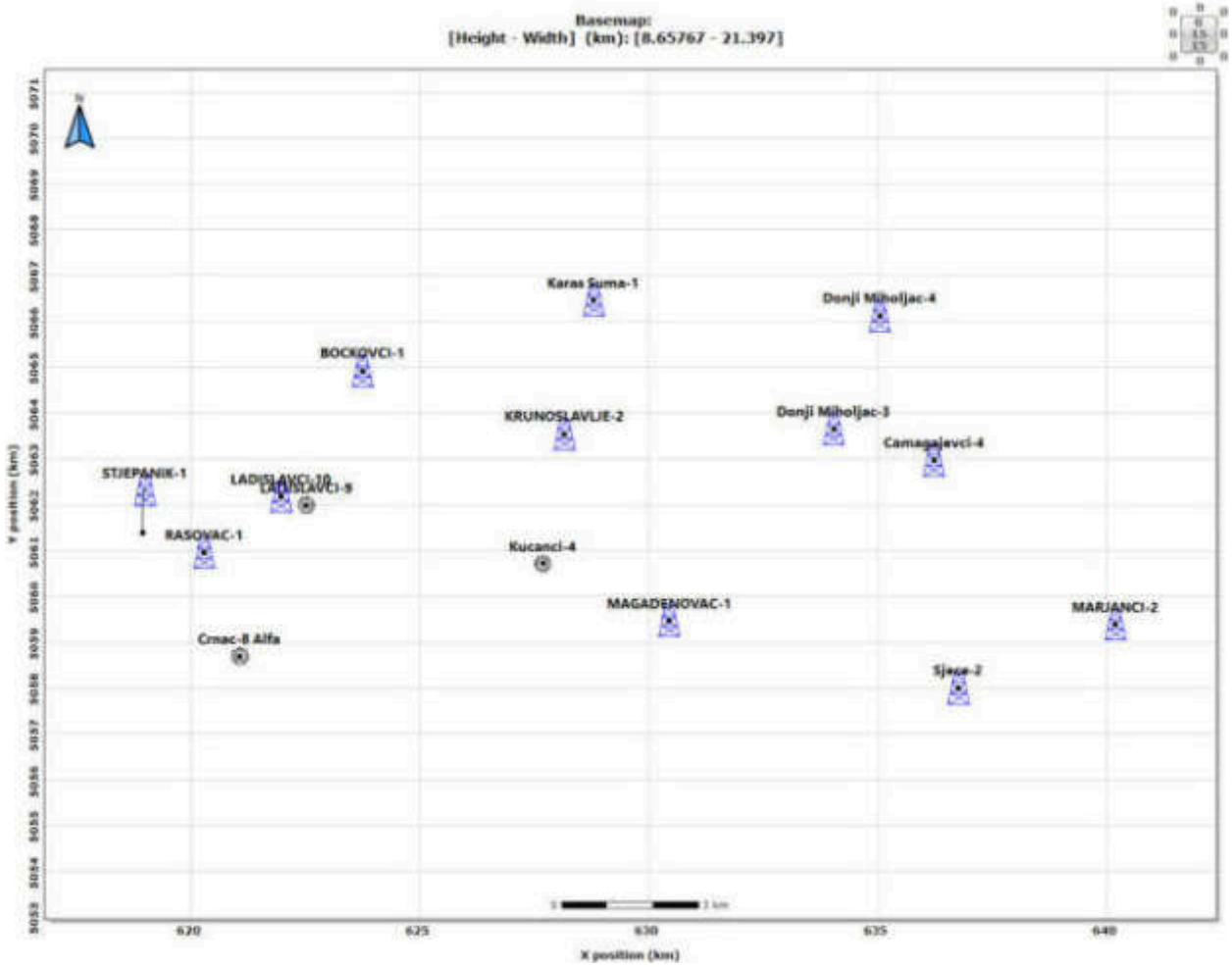


Fig. 2.44 Well Selection Criteria

The table below (Table 2.2) summarizes the selected wells used in the study, including drilling year and total depth (TD), providing essential context on data availability, acquisition practices, and overall data quality. In general, older wells tend to exhibit data limitations in terms of number of measurements available for interpretation, while newer wells benefit from improved logging technologies and more comprehensive data coverage.

The following table (Table 2.3) presents a consolidated overview of the available well logs used in the petrophysical evaluation for selected wells. It summarizes the main log types, their coverage across the studied wells, and an assessment of data quality based on initial screening. The evaluation highlights variations in log availability and reliability, reflecting differences in acquisition conditions and historical data completeness. This overview supports the identification of key data gaps and informs subsequent quality control and conditioning workflows. It also serves as a reference for selecting appropriate logs for petrophysical interpretation across different stratigraphic intervals. A few wells (Stjepanik-1, Sjece-2) were specifically selected to reach the maximum depth with the highest expected temperatures for geothermal assessment.

Copyright © SLB. All Rights Reserved. Private & Confidential. Reproduction only by permission.

Table 2.2 Well Inventory: Year and Total Depth Summary

Well	Spud Year	TD (m)
BOCKOVCI-1	1984	3102
Camagajevci-4	1986	2324
Crnac-8 Alfa	1980	2948
Donji Miholjac-3	1973	1546.5
Donji Miholjac-4	1994	1303
Karas Suma-1	1990	2330
KRUNOSLAVLJE-2	2013	2273
Kucanci-4	1974	2819.2
LADISLAVCI-9	1987	2327
LADISLAVCI-10	1986	2410
MAGADENOVAC-1	1973	2798
MARJANCI-2	1978	3497.5
RASOVAC-1	1997	2969
Sjece-2	1984	3657
STJEPANIK-1	1983	5034

Table 2.3 Overview of available well logs and data quality assessment for selected wells

Logs	Wells Coverage	Quality	Comments
Measured Depth	15		11 wells with 2 borehole sections 8.5 and 12.25 in
Caliper	14	Moderate to Poor	8 wells with poor borehole
Gamma Ray	12	Good	Priority for VSH computation. Absent in DM-3, KS-1 and Mag-1
Bulk Density	14	Moderate to Poor	Priority for Porosity computation. Ras-1 only 1 well with full DENS coverage
Compressional Slowness	14	Moderate	Second priority for Porosity computation. Better coverage for all wells than NEUT-DENS
Neutron Porosity	13	Good	Priority for Porosity computation. Not converted for Kuc-4 and Mag-1
Resistivity - Deep	15	Good	Full coverage. Proxy for VSH computation
Spontaneous Potential	14	Good to moderate	Proxy for VSH computation. Required Baseline shift
Discrete Temperature			Temperature calibration for Geothermal Formation Temperature Analysis

2.3.2 Log Quality Control and Log Prediction

Log Quality Control (LQC) was a critical step preceding all petrophysical computations. Borehole conditions were evaluated using caliper data, and intervals impacted by washouts, mudcake, or poor hole conditions were flagged. Logs exhibiting acquisition artefacts or poor environmental conditions were excluded from primary interpretation or retained only for qualitative QC purposes.

Although 15 wells were selected for detailed petrophysical analysis, LQC datasets were generated for a broader set of 28 wells to support additional studies, including seismic correlation and geophysical interpretation. Depth matching and depth shifting were performed prior to log splicing and integration, with approximately 35 logs of the 15 wells corrected for systematic depth offsets resulting from different acquisition runs or reference datums. A single, consistent dataset

Copyright © SLB. All Rights Reserved. Private & Confidential. Reproduction only by permission.

with a unified sampling rate was then established for each well through log splicing. The consolidated LQC datasets were subsequently shared with the geology and geophysics teams to support well-to-well correlation and seismic well ties.

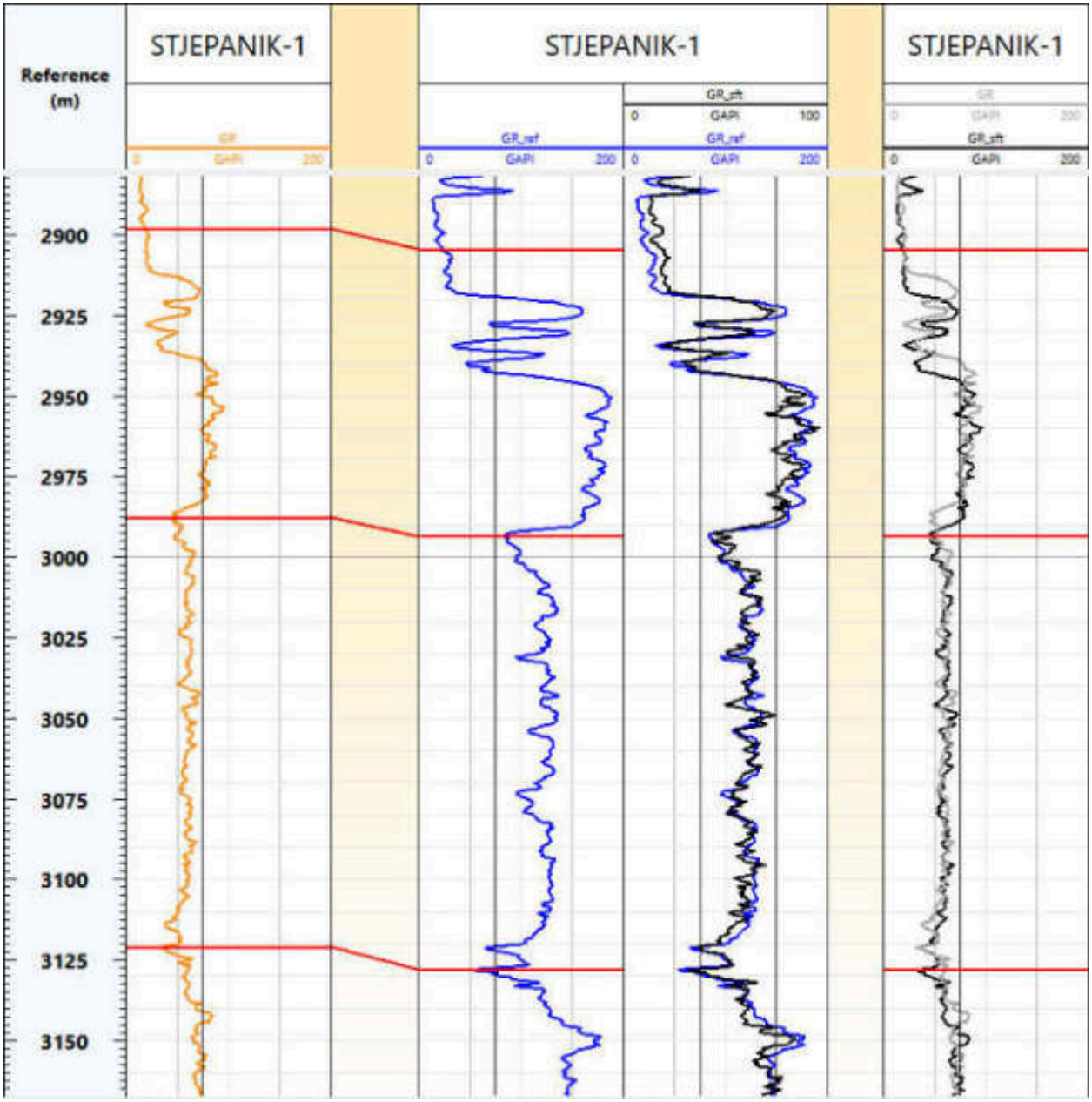


Fig. 2.45 Depth Shifting for well Stjepanik-1

A critical challenge identified during LQC was the absence or poor quality of compressional slowness (DTCO) logs in several wells and zones. DTCO is a key input for porosity estimation and rock mechanical properties—particularly where density and neutron logs are unreliable—log prediction workflows were implemented to reconstruct missing DTCO data.

Copyright © SLB. All Rights Reserved. Private & Confidential. Reproduction only by permission.

DTCO Log Prediction Using Machine Learning

During log quality control, it was identified that compressional slowness (DTCO) logs were missing or of insufficient quality in several upper and shallow intervals, where the available log suite was limited primarily to deep resistivity (RES_DEEP) and spontaneous potential (SP). Although Neutron, Density, and DTCO logs were present in many wells, their coverage was generally restricted to deeper sections. To ensure consistent porosity computation across all stratigraphic intervals of interest, DTCO prediction was therefore required in these shallow zones with limited log availability.

Two predictive approaches were evaluated: a deterministic Multi-Linear Regression (MLR) model and a machine-learning-based solution using the KMOD module with a Multilayer Perceptron (MLP) algorithm. MLR was tested as a benchmark method using shale volume and resistivity inputs but showed limitations in capturing non-linear responses and interval-scale variability.

The final DTCO prediction selected for the petrophysical results was derived from the KMOD–MLP technique, which demonstrated superior performance results compared to MLR. The MLP model uses TVDSS, VSH, and RES_DEEP as inputs, trained on Rasovac-1 and validated on Ladislavci-9. Comparison of predicted and measured DTCO, including visual overlays and crossplots, showed that the MLP prediction reproduced both the overall trend and local variations more reliably than the MLR approach.

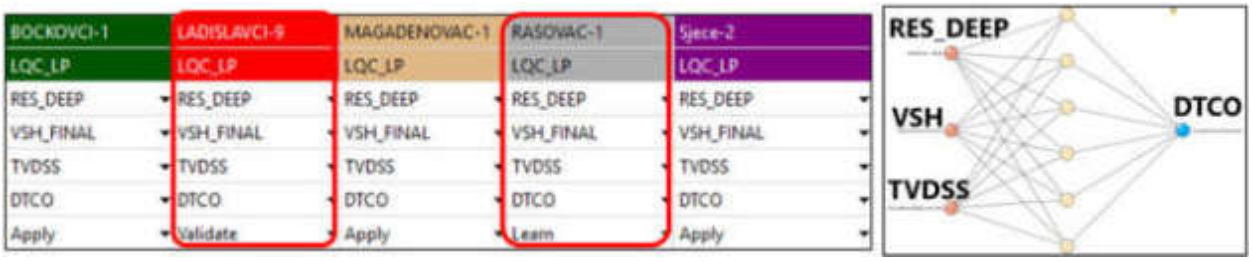


Fig. 2.46 Log Prediction modeling

The MLP-predicted DTCO logs were subsequently used for porosity computation in shallow intervals lacking sufficient acoustic and porosity logs. While predicted data inherently introduce additional uncertainty relative to measured logs, this approach enabled consistent porosity estimation across the full stratigraphic column and improved the completeness of the petrophysical evaluation.

Copyright © SLB. All Rights Reserved. Private & Confidential. Reproduction only by permission.

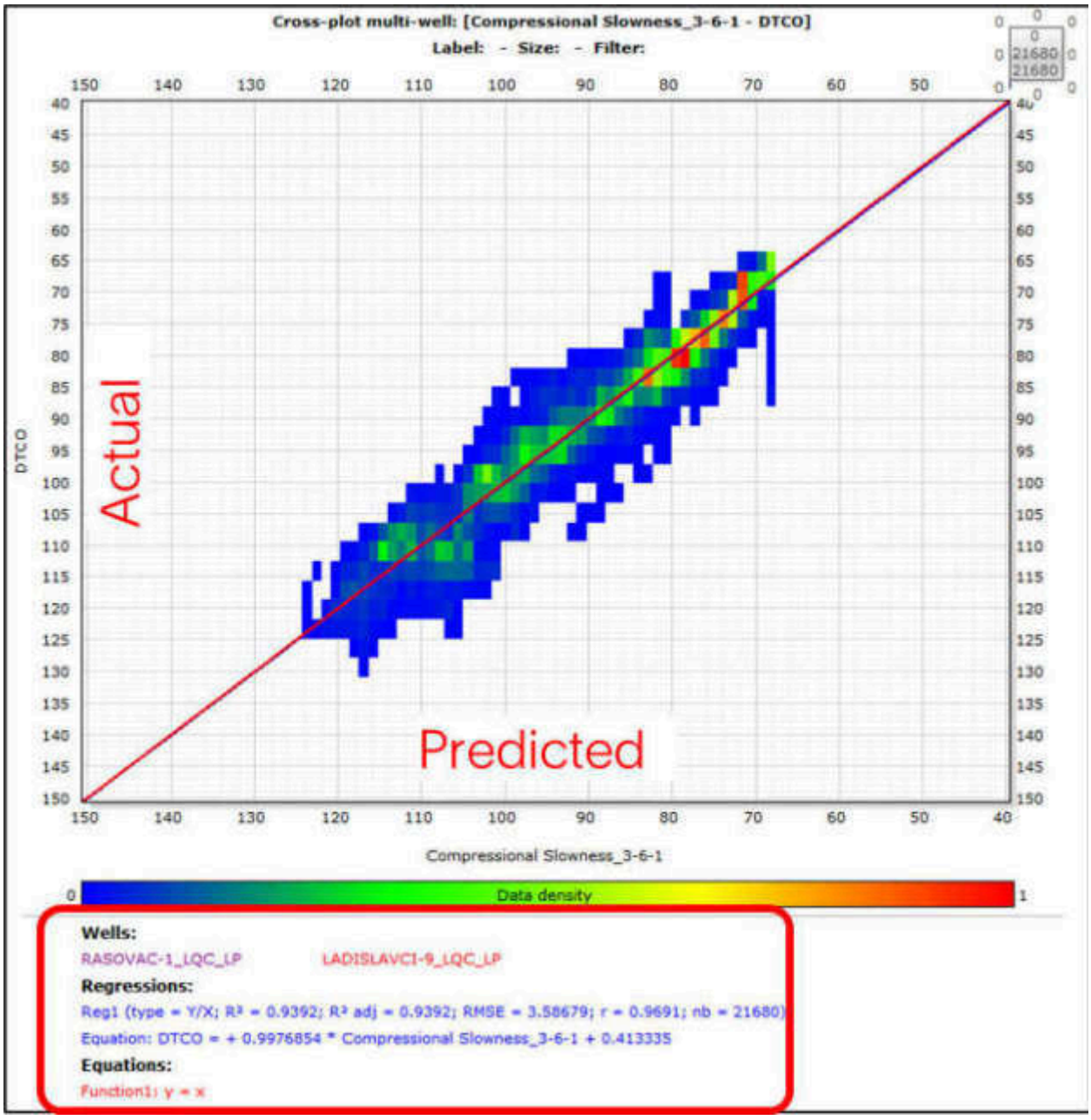


Fig. 2.47 Compressional Slowness Log Prediction

Copyright © SLB. All Rights Reserved. Private & Confidential. Reproduction only by permission.

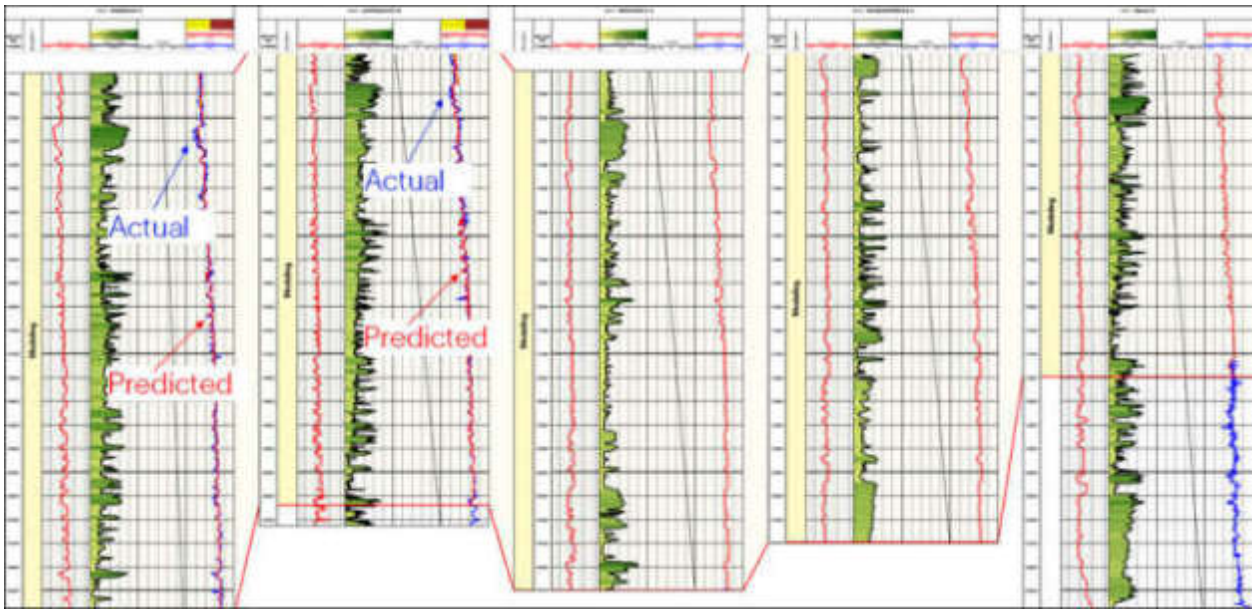


Fig. 2.48 Compressional Slowness prediction results for wells

2.3.3 Petrophysical Analysis

Volume of Shale (VSH)

Volume of shale was computed on a zone-by-zone and well-by-well basis, using the most appropriate log response depending on data availability and lithological context. Gamma Ray (GR) was the preferred input where data quality was good. In intervals affected by radioactive non-clay minerals (e.g., carbonates, breccias, or "hot" formations), thorium logs were used where available, as thorium content is more directly associated with clay minerals. In wells lacking GR coverage or with low quality GR readings, SP and resistivity-based methods were applied for shale volume computation.

Copyright © SLB. All Rights Reserved. Private & Confidential. Reproduction only by permission.

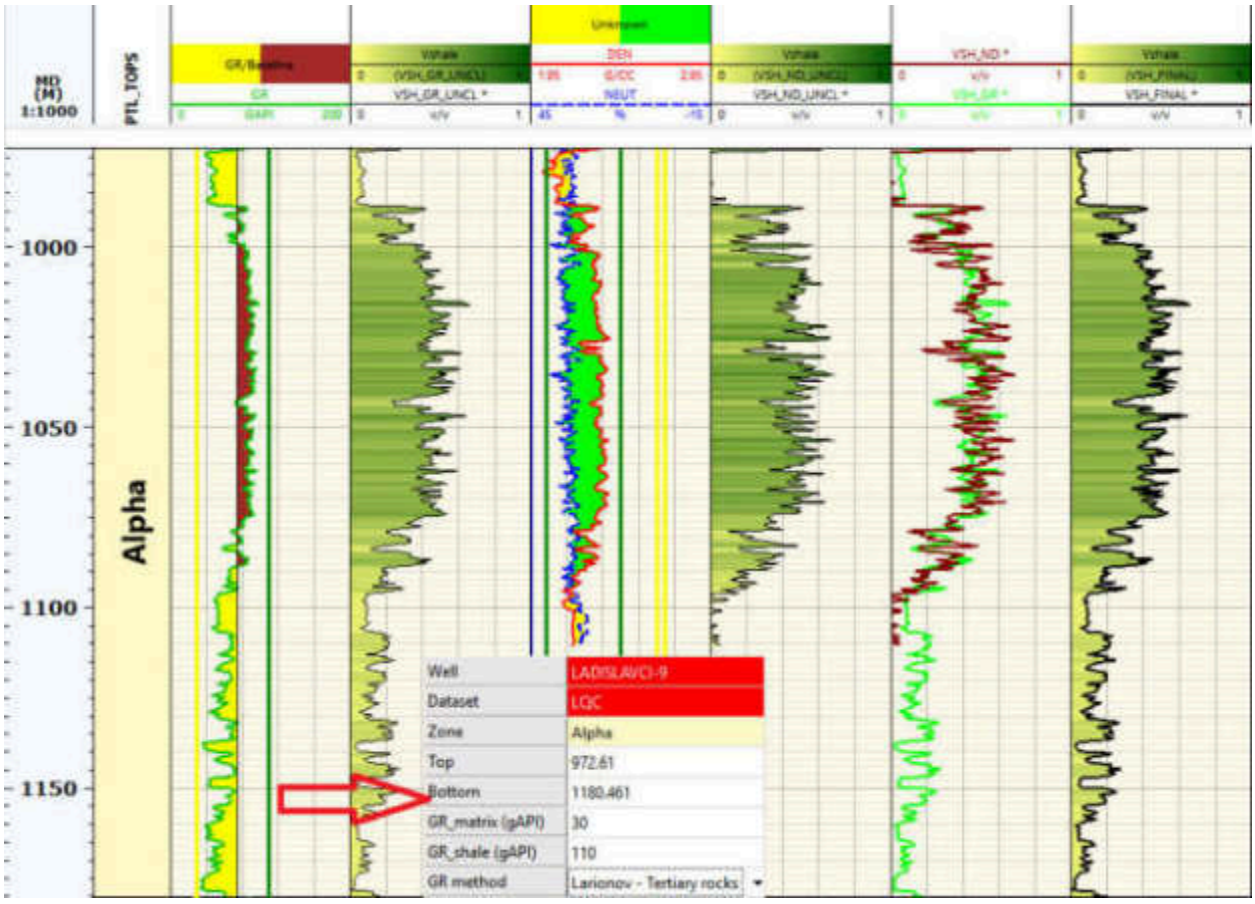


Fig. 2.49 Gamma Ray–Based Volume of Shale (VSH) calculation for Zone Alpha: example from well Ladislavci-9

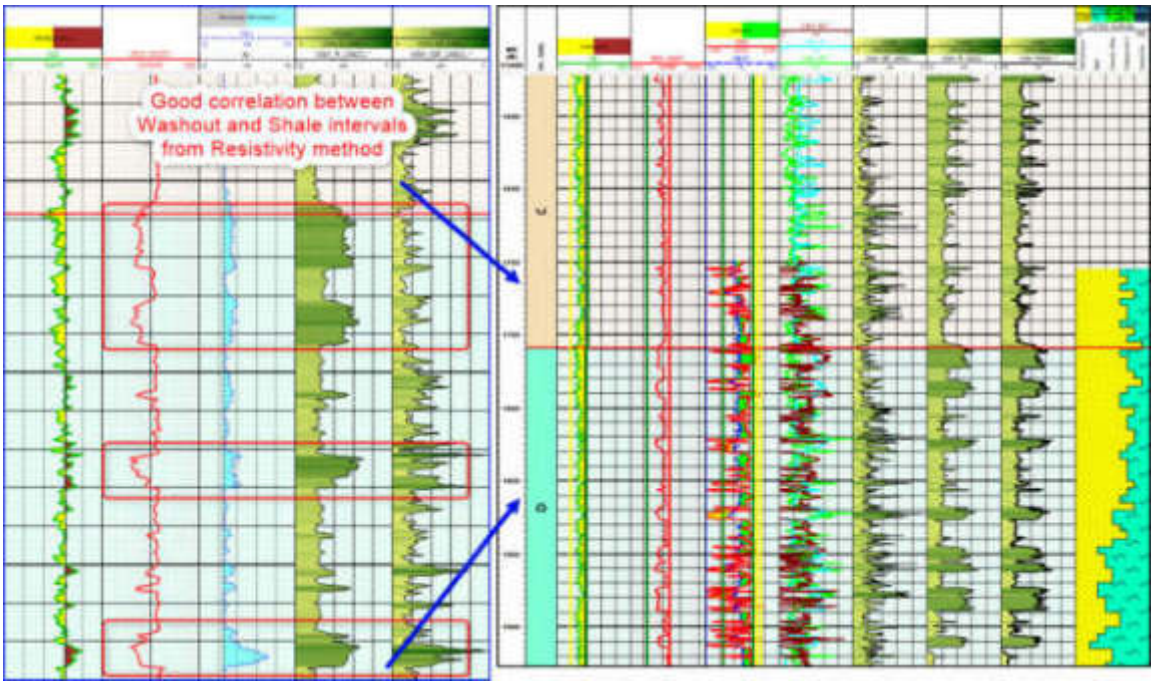


Fig. 2.50 Volume of Shale calculation from Resistivity method
Good correlation observed between washout intervals and resistivity-derived VSH

Copyright © SLB. All Rights Reserved. Private & Confidential. Reproduction only by permission.

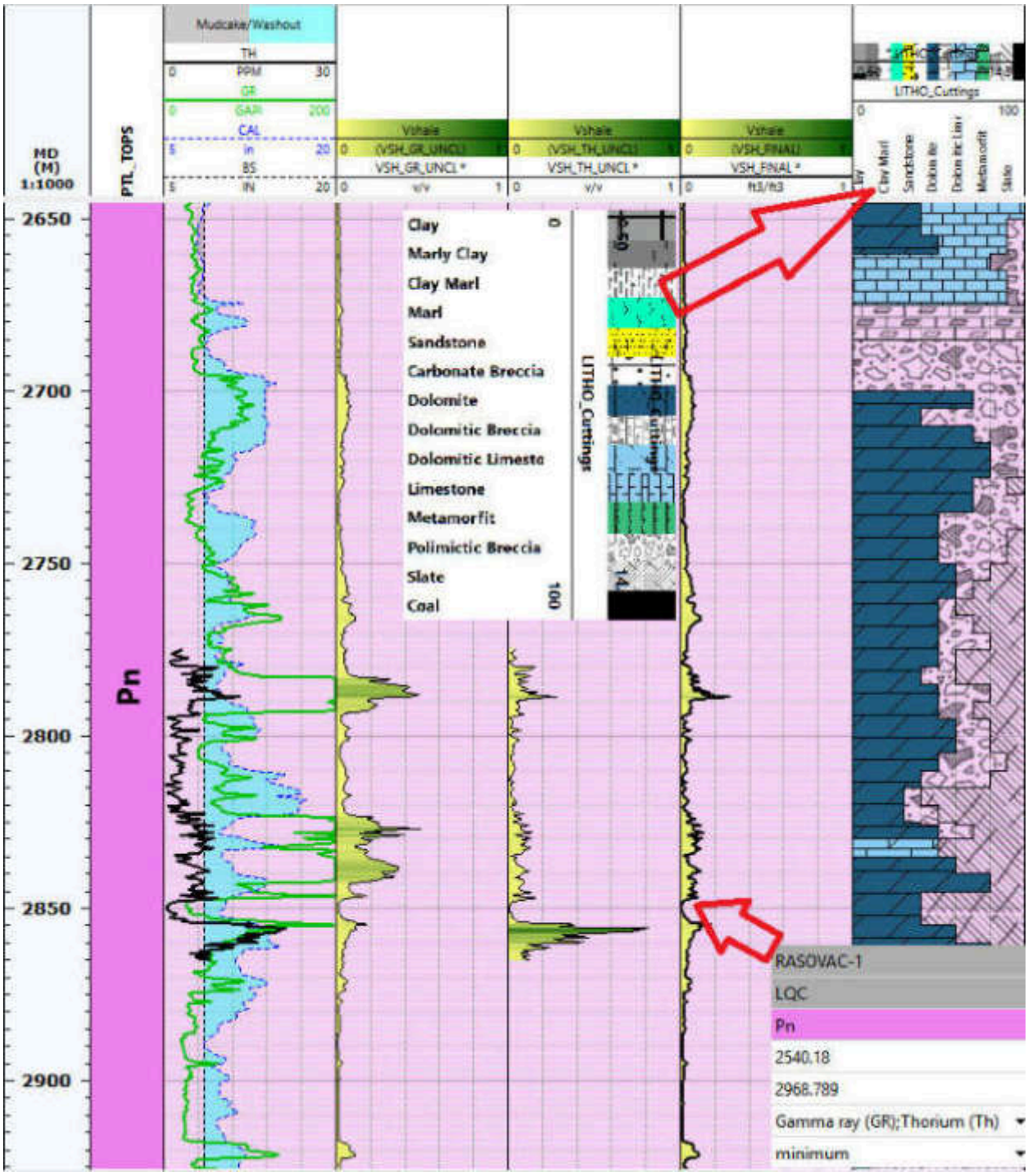


Fig. 2.51 Gamma Ray and Thorium–Based VSH calculation for Pn zonation: example of well Rasovac-1

Quality control of the shale volume (VSH) was performed on a well-by-well basis through cross-validation with multiple log responses and lithological indicators. The results demonstrate a strong correlation between VSH derived from SP and resistivity logs and observed lithology from mud cuttings, confirming the reliability of the interpretation. Poor borehole conditions are typically associated with shale-rich formations, and the computed VSH shows good agreement with this behaviour.

Copyright © SLB. All Rights Reserved. Private & Confidential. Reproduction only by permission.

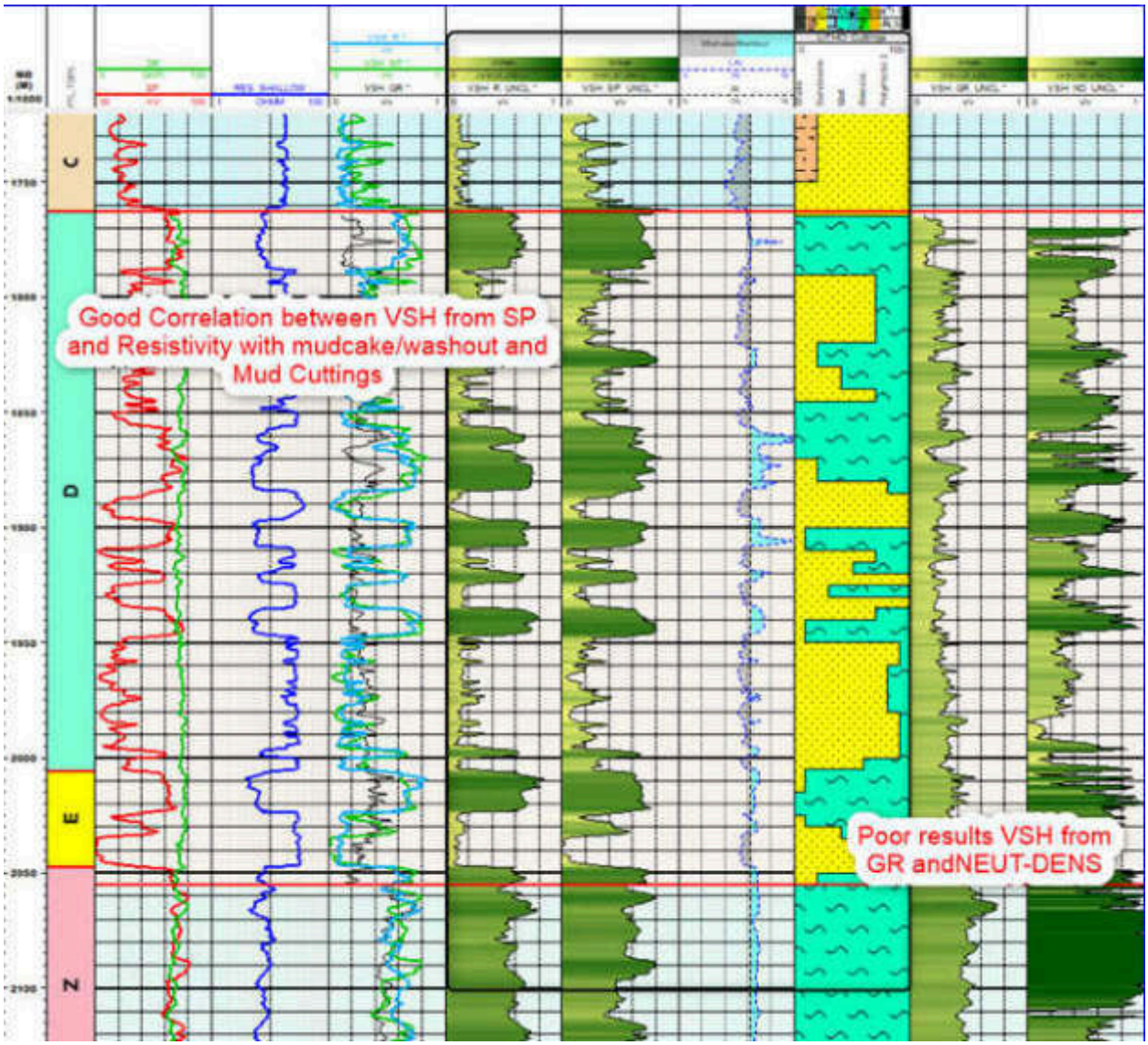


Fig. 2.52 VSH Quality Control through cross-validation with logs and cuttings data
Good correlation observed between VSH and both RES_DEEP and SP measurements; VSH_FINAL selected from the resistivity-based method due to its consistency

Across potential reservoir intervals (Zones Alpha, B, C, D, and E), shale volume typically ranges from 12% to 18%, with median values around 15%. Deeper zones (Rs7, Pn, Tg) generally exhibit higher heterogeneity and locally elevated shale content.

Effective Porosity

Effective Porosity (PHIE) was calculated using the best available method per zone and well. Shale volume (VSH) from previous calculations was incorporated as a key lithological control. Neutron-Density combinations were given the highest priority where data quality was acceptable. Sonic-derived porosity, using measured or predicted DTCO, was used where density and neutron data were missing or unreliable. Resistivity was used only as a low-weight QC indicator, not as a primary porosity input.

Copyright © SLB. All Rights Reserved. Private & Confidential. Reproduction only by permission.

Lithology inputs were derived from cuttings and well tops, allowing appropriate matrix parameters to be selected. Effective porosity was used throughout the study and was also the basis for net reservoir flagging. Porosity distributions show a clear depth-dependent decrease. Zone B exhibits the best reservoir quality, with median porosity values around 25%, followed by Zones C and D with typical porosity in the range of 15–20%. Zones E and Z show reduced porosity, generally between 10% and 15%, while Rs7, Pn, and Tg are characterized by very low porosity, reflecting tight formations.

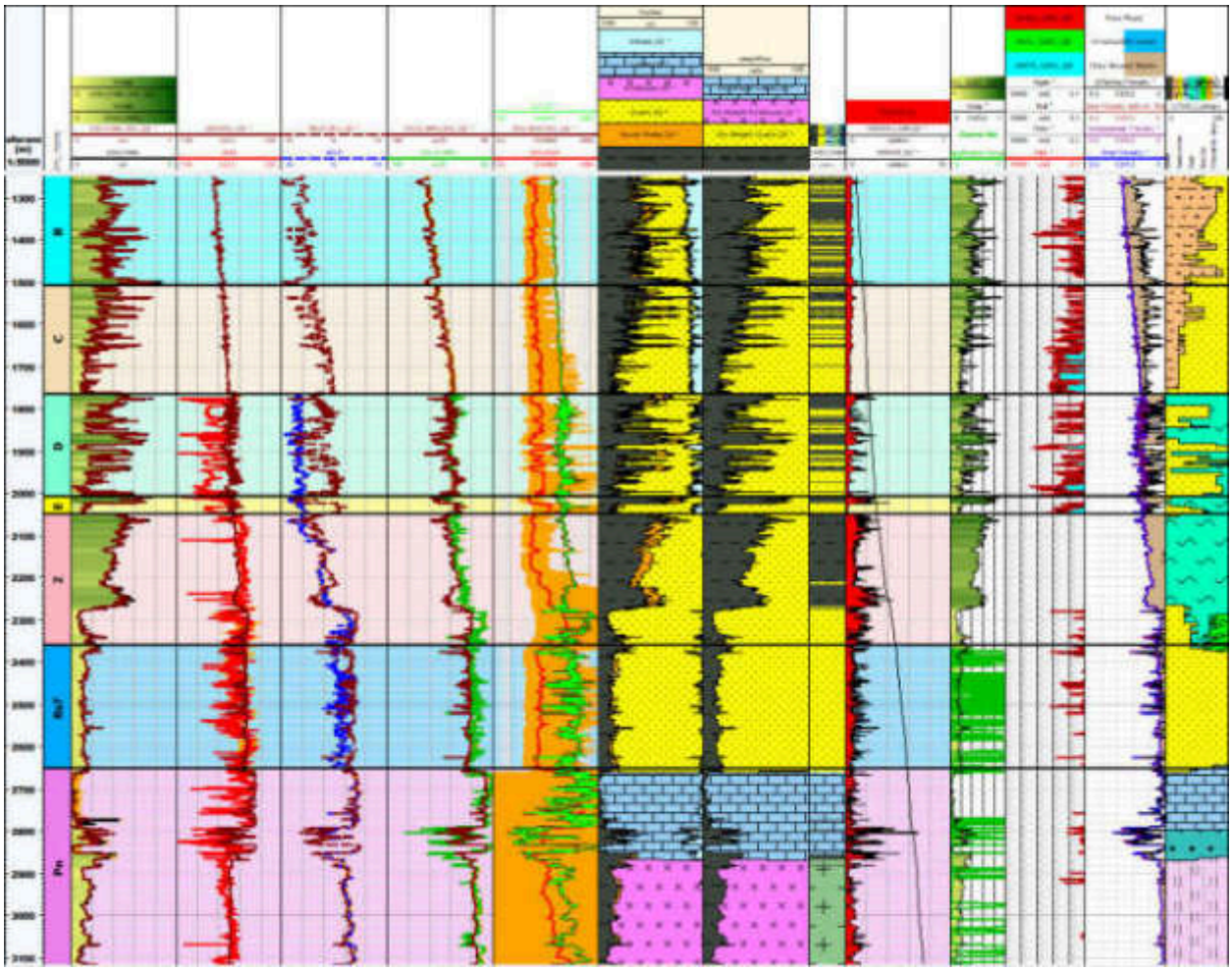


Fig. 2.53 Lithology and porosity evaluation: input data and interpretation results

Permeability

Core porosity–permeability data were compiled from multiple wells and stratigraphic intervals, enabling the derivation of zone-specific transforms that reflect lithological variability. The upper reservoir intervals—**Zones Alpha, B, C, D,** and **E**—are dominated by clastic sediments (sandstones interbedded with marl and shale), and display a relatively consistent poro–perm behavior. As illustrated in the Fig. 2.54, permeability shows a strong linear relationship and predictable increase with porosity, indicative of well-connected intergranular pore systems. For **Zones Alpha, B, C, D,** and **E**, the derived relationship is:

Copyright © SLB. All Rights Reserved. Private & Confidential. Reproduction only by permission.

Permeability=4782.3×(Effective Porosity)$^{4.1}$

This power-law trend is representative of clean to moderately shaly sandstones where permeability is primarily controlled by pore throat connectivity and only secondarily influenced by clay content, allowing direct application of log-derived porosity for permeability estimation.

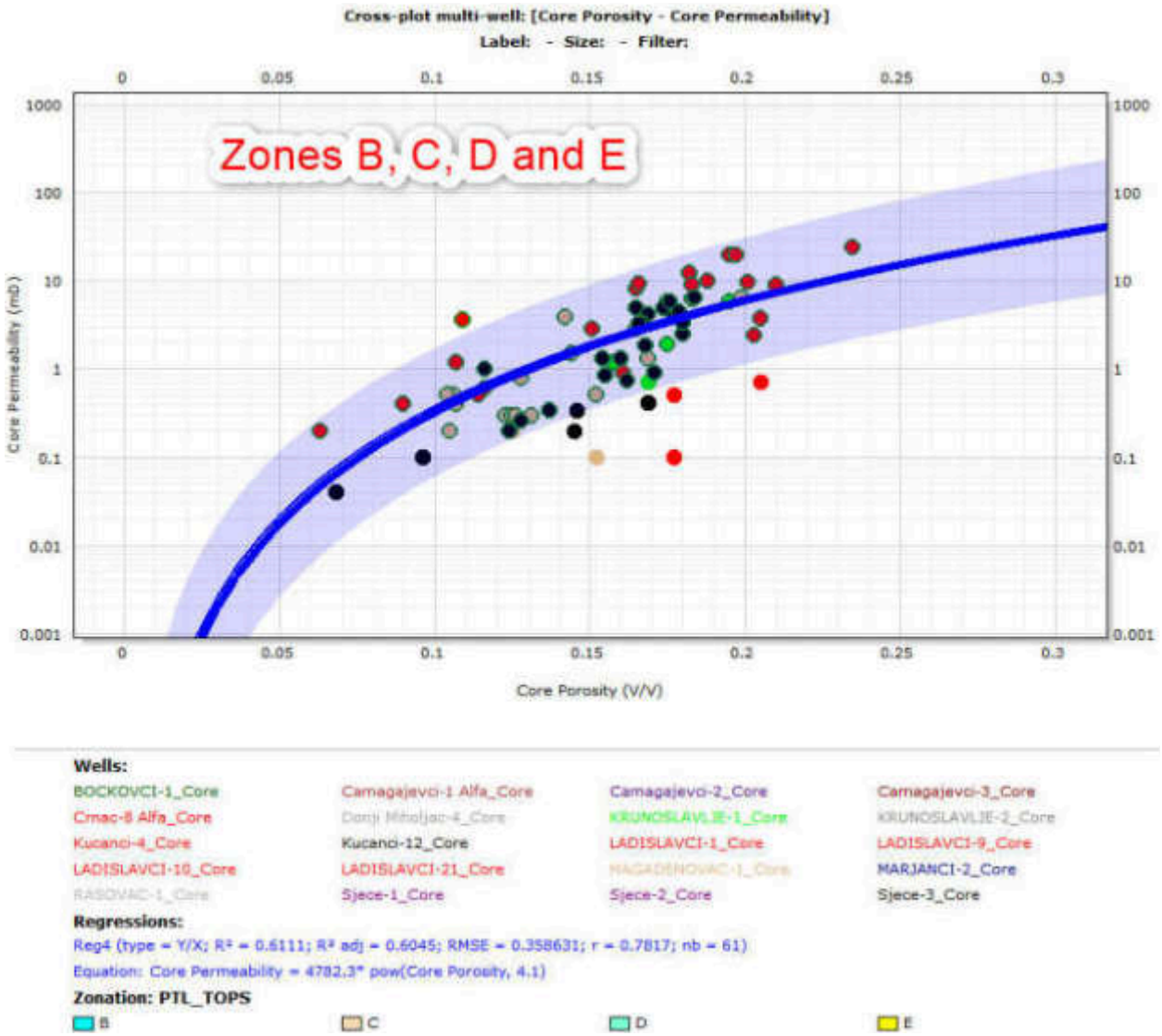


Fig. 2.54 Core Porosity-Permeability relationship for Zones B, C, D and E
Alpha zone is not covered by core data

The lower stratigraphic intervals—**Z, Rs5–Rs7, Pn,** and **Tg**—are significantly more complex, comprising a mix of clastic facies (locally in Z and parts of Rs5–Rs7), carbonate units (notably Pn and Rs5–Rs7), and basement rocks (Tg). These heterogeneous lithologies exhibit multiple poro–perm trends (Fig. 2.55), as evident from the wide scatter and distinct clusters in the core data, reflecting variations in grain size, sorting, diagenesis, and fracture contribution rather than clay content alone. In such zones, a single porosity–permeability transform is insufficient in core data.

Copyright © SLB. All Rights Reserved. Private & Confidential. Reproduction only by permission.

To extend permeability prediction across all lithologies and porosity ranges, a generalized transform was established using the combined dataset (Fig. 2.55). For intervals with porosity **greater than 1.5%**, which include the more effective reservoir sections in both clastic and some mixed lithologies, the main relationship applied is:

$$\textbf{Permeability} = 3423656 \times (\textbf{Effective Porosity})^{4.5}$$

For rocks with porosity **less than 1.5%**, typical of compacted or poorly connected pore systems, permeability follows a logarithmic trend:

$$\textbf{Permeability} = 10^{(14.1 \times \text{Effective Porosity} - 2.2)}$$

These two equations capture the transition from very tight formations to reservoir intervals and are consistent with the observed spread and curvature in the core poro–perm cross-plots, where low-porosity data deviate significantly from the main core trend.

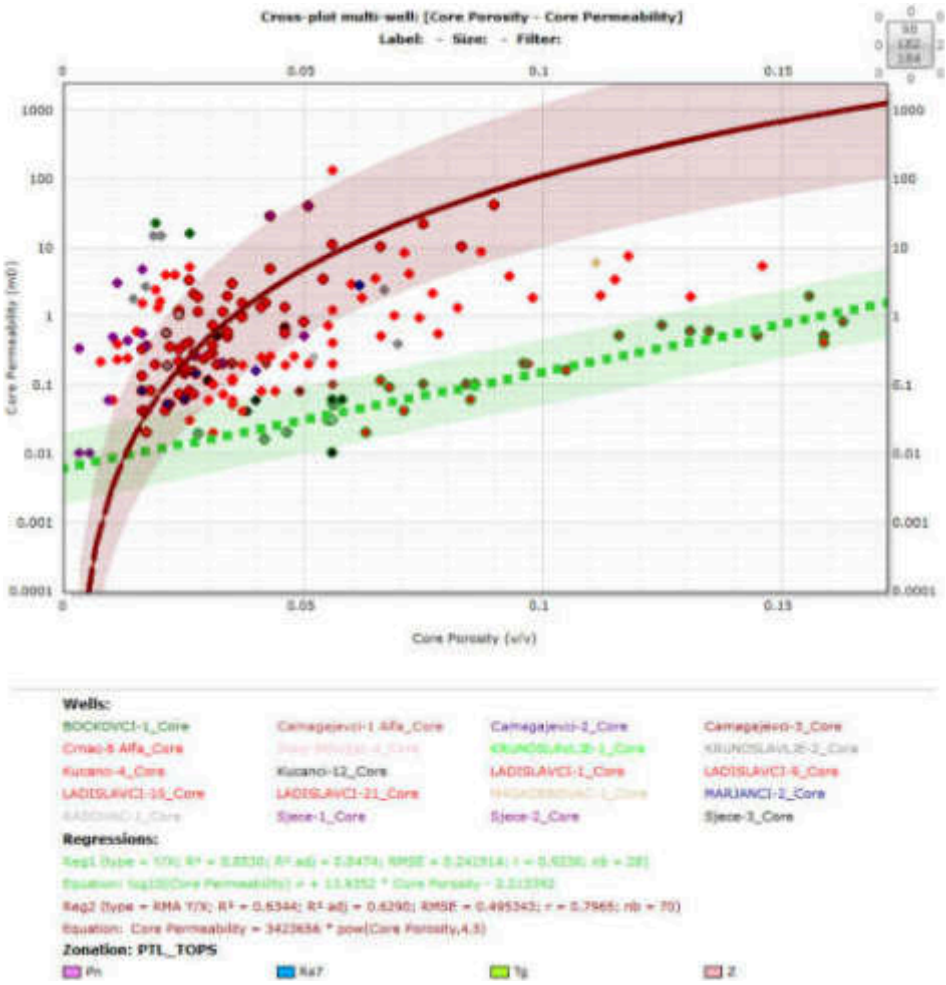


Fig. 2.55 Core Porosity-Permeability relationship for Zones Z, Rs5-7, Pn and Tg
Two permeability–porosity relationships: Reg2 corresponds to intervals with PHIE > 1.5%, while Reg1 represents intervals with PHIE < 1.5%

Copyright © SLB. All Rights Reserved. Private & Confidential. Reproduction only by permission.

Permeability Estimation Summary

The preferred approach for permeability prediction is based on rock typing; however, this methodology was not implemented in the present study due to the absence of advanced core SCAL measurements (e.g., MICP and capillary pressure data).

In the absence of such data, permeability estimation was performed using a hybrid workflow integrating core-derived relationships, established empirical log-based correlations (e.g., Coates, Timur, and Wyllie–Rose models), and calibration to well test *kh* values at the stratigraphic level.

Given the limited availability of core datasets required for robust rock typing, this integrated approach provides a practical alternative for permeability evaluation.

This methodology ensures that permeability estimates remain consistent with dynamic reservoir performance while accounting for the inherent uncertainty and heterogeneity of the studied intervals.

Integrated Reservoir cut-off determination

Mudcake development was used as a primary qualitative indicator of formation permeability, as intervals exhibiting mudcake are typically associated with sufficiently permeable reservoir rock. The log plot provided in Fig. 2.56 illustrates the practical workflow used to distinguish reservoir from non-reservoir intervals by integrating multiple indicators. Reservoir zones are identified through the presence of mudcake (indicated by Bit Size > Caliper), resistivity contrast between micro normal and laterolog measurements suggesting invasion and permeability, and relatively low shale volume from VSH computation, while non-reservoir intervals show the opposite behavior. The highlighted intervals demonstrate that zones classified as reservoirs consistently exhibit mudcake development, higher resistivity separation, and cleaner (low VSH) signatures, whereas non-reservoir sections lack mudcake, show limited resistivity contrast, and are dominated by higher shale content. This integrated log-based interpretation forms the basis for calibrating and validating the quantitative cut-offs applied for reservoir classification (Fig. 2.56).

Copyright © SLB. All Rights Reserved. Private & Confidential. Reproduction only by permission.

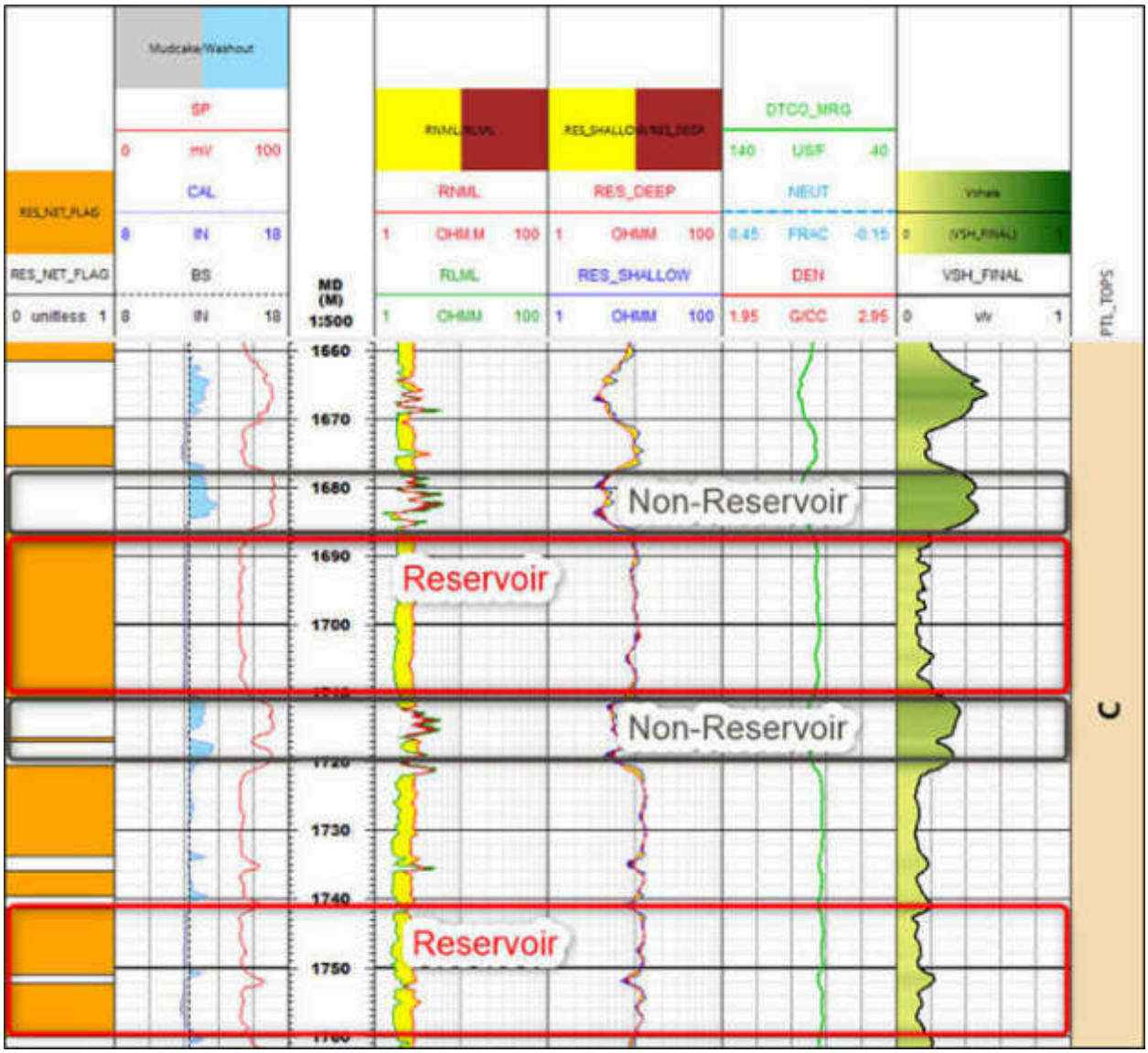


Fig. 2.56 Reservoir identification from mudcake development, resistivity contrast, and VSH profiles

Zones Alpha, B, C, D and E:

A mudcake flag was generated using the Bit Size > Caliper criterion, and this qualiatative flag served as a reference for subsequent reservoir/non-reservoir cut-off determination. Based on this classification, the shale volume (VSH) cut-off was identified at approximately 28% from the cumulative distributions, and a conservative threshold of 30% was selected for practical application. The effective porosity (PHIE) cut-off was then derived using the same mudcake-based approach in combination with the VSH criterion, resulting in a threshold of approximately 11% (Fig. 2.57). Consequently, reservoir intervals were defined using combined cut-offs of **PHIE > 10% and VSH < 30%** for zones **Alpha, B, C, D, and E**, supported by core porosity–permeability relationships indicating that about 95% of samples exhibit permeability greater than 0.1 mD only when porosity exceeds 10% (Fig. 2.54), thereby reinforcing the selected limits. On Fig. 2.57 the red curve represents intervals without mudcake formation (non-permeable/non-reservoir

Copyright © SLB. All Rights Reserved. Private & Confidential. Reproduction only by permission.

tendency), while the blue curve represents intervals with mudcake development (permeable/ reservoir tendency), and the intersection of these two distributions is used to define the optimal cut-off.

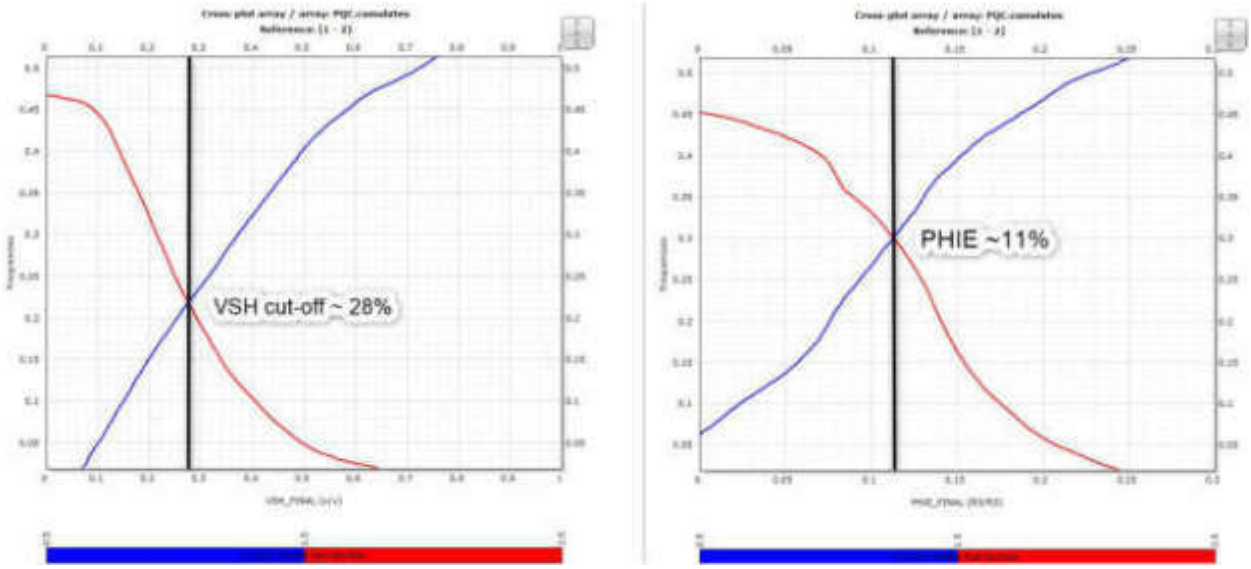


Fig. 2.57 **Determination of Reservoir cut-offs using VSH and Effective Porosity (PHIE)**

Zones Z, Rs5–Rs7, Pn, and Tg:

For the tight formations (zones **Rs5–Rs7, Pn, and Tg**), which are dominated by conglomerates, breccias, and carbonates, a lower porosity threshold was adopted to reflect their inherently low matrix porosity and permeability characteristics. Based on log interpretation and supported by core porosity–permeability trends for these intervals, reservoir-quality rock was defined using cut-offs of **VSH < 30% and effective porosity > 2%**. This lower porosity limit captures intervals that, despite limited storage capacity, can still contribute to flow through fractures or secondary porosity systems. Consequently, this tailored cut-off approach ensures that potentially productive tight zones are not excluded while maintaining consistency with the overall shale volume constraint.

Seal Flag:

Shale-dominated and very tight formations (locally approaching 0% effective porosity), together with marl–shale beds within Zones A–E, act as effective sealing units due to their high clay content, low permeability, and poor pore connectivity. These intervals are critical for CCS site selection and geothermal applications, as they can serve as a potential vertical containment by preventing upward migration of injected CO_2 or thermal fluids, ensuring long-term storage integrity and system efficiency. The effectiveness of these seals strongly depends on their net thickness and vertical continuity, where thicker and laterally continuous shale/marl packages significantly enhance caprock integrity and reduce leakage risk, making net seal thickness a key parameter in evaluating storage security and containment performance.

Copyright © SLB. All Rights Reserved. Private & Confidential. Reproduction only by permission.

Temperature Gradient Calculation

Temperature gradients were derived from discrete temperature measurements reported in Drill Stem Tests (DST), formation tests, and well reports. For each well, measured temperatures were plotted against reference depth to compute geothermal gradients in °C/km. Observed gradients range broadly from approximately 42 to 65 °C/km across the study area, consistent with published geothermal studies for the Croatian part of the Pannonian Basin (*Geothermal potential in the Croatian Part of Pannonian Basin: mapping geothermal plays. By: Kristina Novak Zelenika*, Barbara Gluhak Popovic, Marija Pleic ́and Tatjana Durn Croatian Hydrocarbon Agency, Zagreb 10000, Croatia*).

Zone="Pre-rift": # Basement rocks (igneous, metamorphic, carbonates)
Temperature = 0.0336 * DEPTH + 26.342

Zone="Syn-rift": # Lower–Middle Miocene sediments (conglomerates, sandstones, marls, limestones)
Temperature = 0.0323 * DEPTH + 30.137

Zone="Post-rift": # Upper Miocene sandstones and marls
Temperature = 0.0349 * DEPTH + 24.704

These gradients were used to estimate formation temperatures (Fig. 2.58) and form a key input to the geothermal assessment. Variability in temperature gradient reflects both geological setting and data uncertainty.

Copyright © SLB. All Rights Reserved. Private & Confidential. Reproduction only by permission.

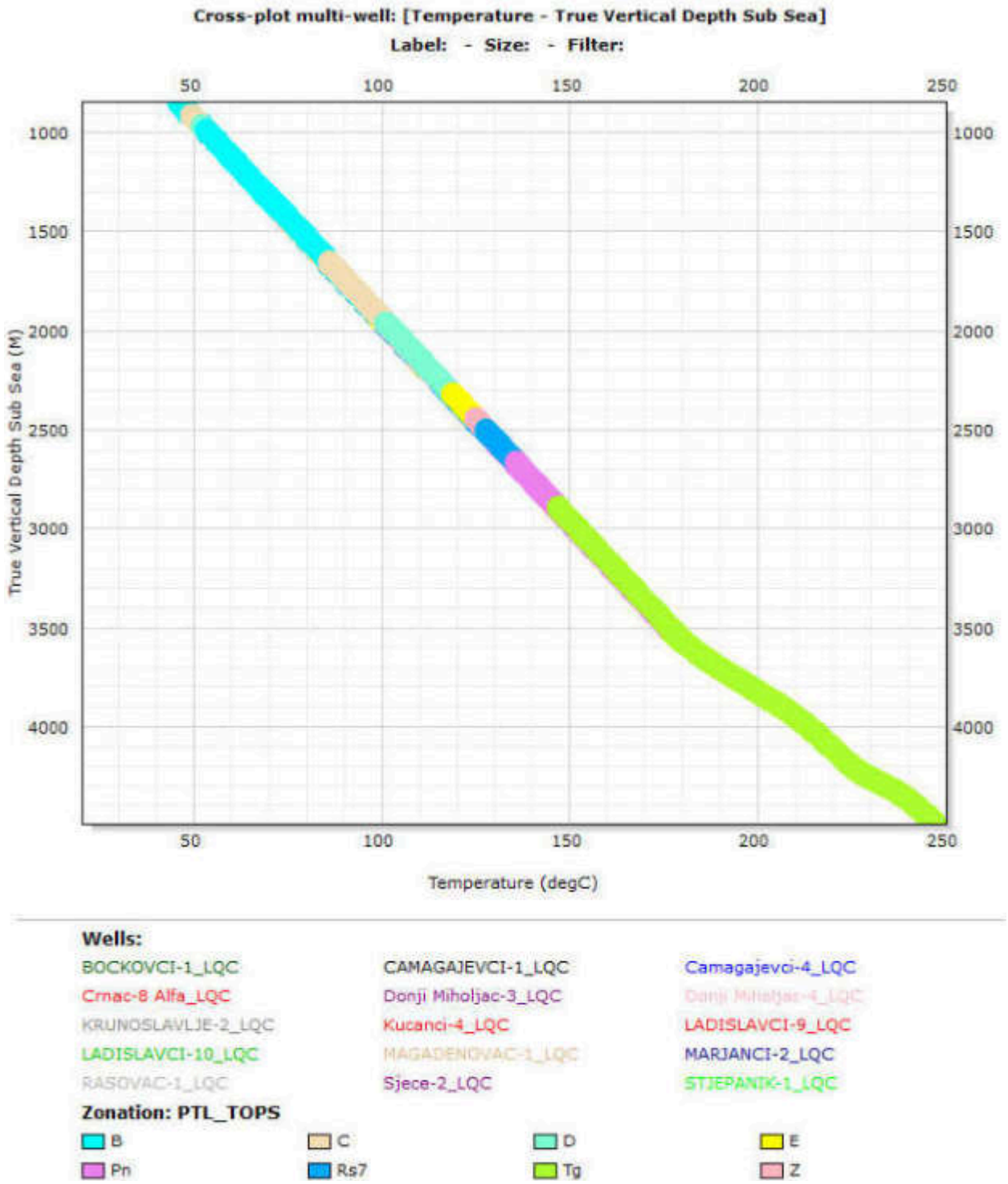


Fig. 2.58 Cross-plot of Formation Temperature versus True Vertical Depth Subsea
Zonation used in color scale

Copyright © SLB. All Rights Reserved. Private & Confidential. Reproduction only by permission.

Summary

Comprehensive data integration and quality control were completed:
A multi-source petrophysical database was established from over 40 wells, including logs, core data, and cuttings. A total of **15** wells were selected for advancing the petrophysical analysis. Extensive data harmonization, depth matching, and log quality control were performed to ensure consistency and reliability across the selected well dataset.

Robust log conditioning and gap-filling strategy:
Missing key logs (DTCO) were reconstructed using machine learning (MLP), enabling consistent petrophysical evaluation across all wells and stratigraphic intervals despite incomplete datasets.

Reliable shale volume and effective porosity evaluation:
Shale volume (VSH) was derived using multiple log inputs (GR, SP, resistivity) and validated against cuttings, showing strong consistency. Effective porosity (PHIE) was computed using a prioritized workflow (Neutron–Density and Sonic).

Permeability estimation using hybrid methodology:
In the absence of SCAL data required for rock typing, permeability was estimated using a hybrid approach combining core-derived transforms, empirical correlations, and calibration to well test data, ensuring consistency with dynamic reservoir performance.

Reservoir characterization and cut-off definition:
Reservoir intervals were defined using integrated criteria (PHIE, VSH, resistivity behavior, and mudcake indicators). Cut-offs of PHIE > 10% and VSH < 30% were established for the main reservoirs (Zones Alpha, B, C, D, and E), while lower thresholds were applied to deeper formations (Zones Z, Rs5–Rs7, Pn, and Tg), ensuring realistic classification of both conventional and low-quality reservoirs.

2.4 Well correlation

Within the Drava Basin, the succession from the Pre–Neogene Basement (Tg) upward to the youngest Neogene units (Vuka and Lonja formations) records a continuous transition from a fractured basement system into a lacustrine basin fill and finally into a continental depositional regime, expressed through a series of lithostratigraphic units that can be correlated regionally across the basin.

This vertical evolution is visible in the log character but is explicitly supported by geological descriptions of the basin dynamics. As stated in the Magadenovac-1 well report, “changes in the size and depth of the basin during sedimentation resulted in diverse types of sediments”. This statement is fundamental, as it directly explains why the log motifs change systematically upward: they reflect shifts in accommodation space, sediment supply, and depositional energy.

Copyright © SLB. All Rights Reserved. Private & Confidential. Reproduction only by permission.

Pre–Neogene Basement

At the base of the section, the Pre–Neogene Basement is encountered as a heterogeneous complex of carbonates and metamorphic rocks. In the Bockovci-1 well report, this is described as “light gray, crushed calcareous dolomite, light gray to dark gray limestone, and sericite-muscovite quartz schist” (Bockovci-1 well report), with deeper levels consisting of “quartz-chlorite schist... and cataclastic gneiss.”

This lithological diversity is expressed on logs through irregular, but generally elevated resistivity and a less pronounced SP response Fig. 2.59, reflecting the absence of primary porosity.

Statement above, does not imply a completely tight system. The same report documents “fractured limestone or dolomite” in core and cuttings, and more importantly, testing results showing “19.5 m^3 of formation water....” Calculated permeability based on a **slug test** is **19.95 mD**. The reservoir formation is therefore moderately permeable.

These observations demonstrate that permeability is controlled by fracturing rather than matrix properties. The log response, therefore, should be interpreted as a fractured system where conductive pathways are discontinuous and structurally controlled.

Moslavacka Gora Formation (Syn-rift)

The transition into the overlying Moslavacka Gora Fm, including the Mosti Member, marks the first significant introduction of clastic material into the system. The reservoir interval is explicitly described as **“carbonate breccia-conglomerates”**, indicating deposition under high-energy conditions. On the logs, this change is reflected by a more pronounced SP deflections and a more organized resistivity pattern, signaling the presence of permeable sedimentary units "... more permeable than the rest of the unit but water-bearing" (Bc-1 report).

Fig. 2.59

Copyright © SLB. All Rights Reserved. Private & Confidential. Reproduction only by permission.

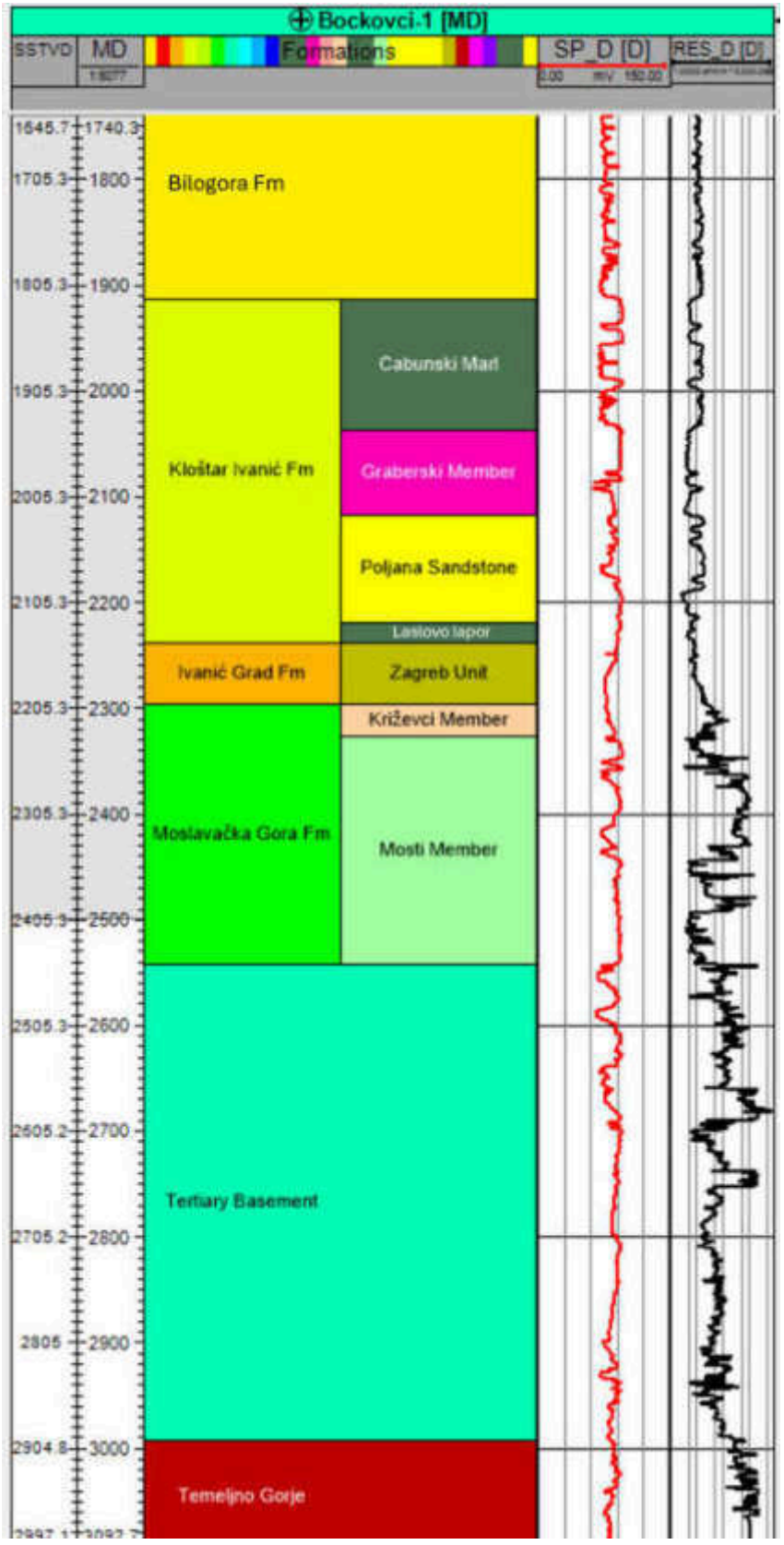


Fig. 2.59 Bockovci-1

Copyright © SLB. All Rights Reserved. Private & Confidential. Reproduction only by permission.

As a conclusion, this unit is not hydraulically isolated from the basement; the report notes that the system is "consisting of conglomeratic sandstones of the Mosti member... and the carbonate complex of the Paleogene and Neogene Basement". This explains why the log character still appears transitional, combining features of both clastic reservoirs and fractured carbonates.

Within the analyzed wells, the interval below the Rs7 regional marker is characterized by strong lithological heterogeneity and rapidly changing log motifs. In the Drava East this interval is assigned predominantly to the Vukovar Formation, while in Drava West equivalent deposits belong to the Moslavacka Gora Fm. Although these formations differ laterally in facies development, both occupy approximately equivalent stratigraphic positions and can be regionally correlated through the Rs7 electric marker.

The variability of the interval is described in reports, which say that "the lower parts of the Valpovo and Vukovar formations show significant differences, both in the vertical and horizontal directions, which indicates frequent changes in conditions during the depositing of these sediments." The SP curve becomes irregular, showing repeated alternations between strong negative associated with permeable clastic bodies and flatter intervals corresponding to shale/marl deposits. Resistivity also fluctuates rapidly, reflecting abrupt facies transitions over short vertical intervals.

This heterogeneity is interpreted as the result of active syn-rift tectonics, during which localized uplift and subsidence controlled sediment supply and accommodation space.

The upper boundary of this interval is regionally marked by the Rs7 horizon, recognizable electric-log marker. On the logs, Rs7 is expressed by a transition toward more uniform responses, including reduced SP variability and more laterally persistent low-resistivity marl intervals. Although the stratigraphic sequence may vary locally, the marker is widely used to approximate the transition from syn-rift dominated sedimentation toward the more stable post-rift lacustrine depositional phase.

A significant change occurs at the level of the Z horizon, which represents one of the key correlation markers across the basin. Although the horizon itself is primarily recognized from electric-log response, its geological meaning is supported by the broader depositional interpretation described in the Magadenovac well report, where it is stated that “marls dominated in the deeper parts of the basin.” On the logs, the transition is expressed by a noticeable reduction in SP amplitude, lower resistivity values, characteristic of finer-grained and less porous sediments.

This interval reflects a quieter depositional phase associated with reduced clastic input and deeper-water conditions. Because the same log signature can be followed consistently between wells, the Z horizon acts as a regional sealing interval and an important stratigraphic datum for correlation.

Klostar Ivanic Formation (D Series) (Lower to Upper Pontian)

The overlying Klostar Ivanic Fm introduces a much more variable depositional style. The lithological description from the Magadenovac report refers to an “exchange of gravel, sand, clay, marl and sandstone, and sometimes also layers of coal,” which is directly reflected in the electric logs. The

Copyright © SLB. All Rights Reserved. Private & Confidential. Reproduction only by permission.

SP curve becomes irregular and serrated, while resistivity fluctuates rapidly over short vertical intervals, indicating repeated shifts between different depositional environments. The result is a highly heterogeneous succession in which sand bodies lose continuity over relatively short distances.

Bilogora Formation (Upper Pontian)

Within the Drava Basin, the regional lithostratigraphic chart Fig. 2.2, reveals a lateral equivalence between the Bilogora Fm in the west (Drava West sub-basin) and the Vera Fm in the east (Drava East sub-basin). Both units occupy the same chronostratigraphic position — the Pontian stage, of which deposits were developed during a phase of relatively stable lacustrine sedimentation.

Bilogora Fm (Alfa (D') series) marks a transition toward more stable and regionally uniform sedimentation. This trend is supported by the observation from the Magadenovac report that "the sedimentation becomes more uniform, and the movements of the basin are not as pronounced." The corresponding log response becomes noticeably smoother and less variable, with less pronounced SP deflections, persistently low resistivity values.

The transition into the "B series" is particularly important because it marks the establishment of one of the main Upper Pontian reservoir intervals. In the logs, the entrance into the "B series" is consistently characterized by an increase in SP deflection together with a decrease in resistivity. This reflects the transition from compact marl-rich deposits into more porous and permeable sandstone-dominated intervals. Reports from wells such as Magadenovac-1 and Camagajevci-4 describe the top of the B series as a marl interval resting sharply above sandstones, indicating a relatively abrupt reservoir–seal transition.

Within the eastern Drava basin, the B reservoir is primarily associated with the Vinkovci Formation, especially the Osijek sandstone intervals, which represent some of the most important regional reservoir units. These sandstones are generally represented on logs through broad SP deflections and increased resistivity values, indicating relatively good reservoir quality and lateral continuity.

Vuka Formation

In the eastern part of the Drava Basin, the uppermost Neogene succession is represented by the Vera and Vuka formations, which record the final stages of lacustrine sedimentation and the gradual transition toward more continental depositional conditions.

The transition from the Vuka Fm to the Vera Fm, i.e. to the Jarmina Member, is marked on the electric log by a decrease in SP and an increase in resistivity. This observation is important because it shows that the boundary is not defined only lithostratigraphically, but also through a consistent petrophysical signature recognizable across multiple wells. On the logs, the decrease in SP amplitude indicates a reduction in permeable sandy intervals and a transition toward finer-grained sediments.

The uppermost Vuka and Lonja formations continue the overall transition toward dominantly continental sedimentation.

Copyright © SLB. All Rights Reserved. Private & Confidential. Reproduction only by permission.

2.5 Geological modeling

The steps performed to build a Structural Model are described below (Fig. 2.60).

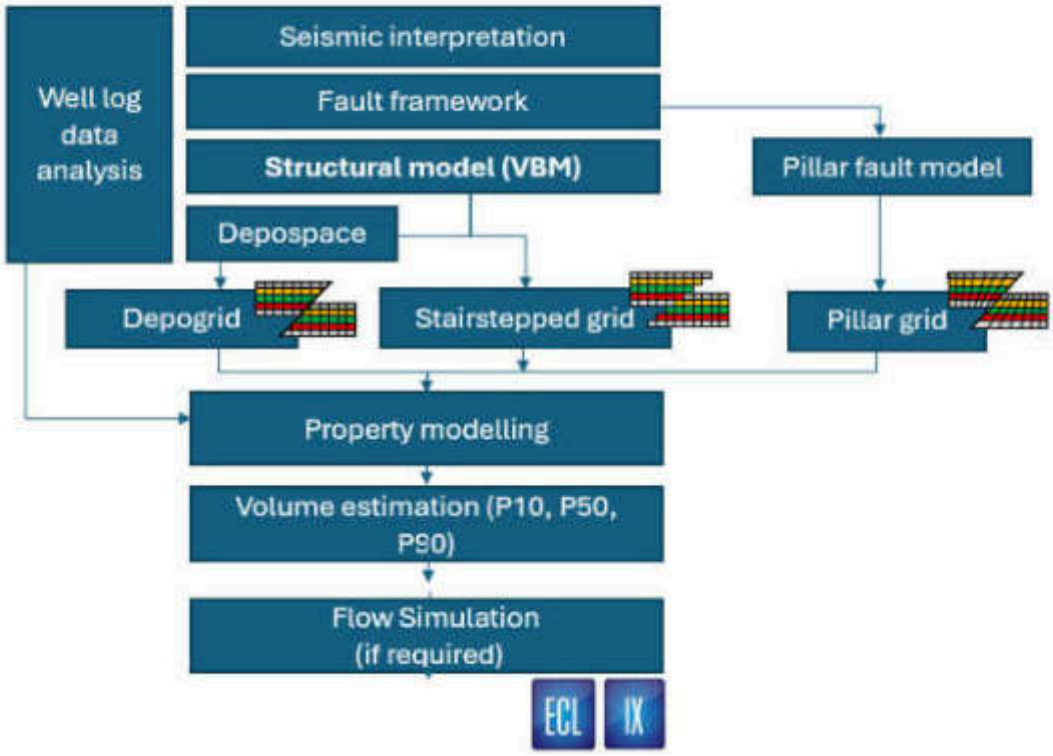


Fig. 2.60 Structural modeling workflow
The scheme shows a succession of steps required to build a structural model, starting with the seismic interpretation and ending up with a flow simulation.

Structural Framework Construction

Seismic interpretation data and identified faults in horizons was used to build the initial structural framework.

The structural framework provides the basis for automated model construction, enabling understanding of relationships between horizons and faults.

This approach also creates clean input data for default modeling and is especially suitable for pillar (or corner point) gridding, which is the most widely used and effective method for modeling in this context.

Pillar gridding was selected due to its compatibility with most processes and its ability to deliver robust results in petroleum reservoir workflows.

Copyright © SLB. All Rights Reserved. Private & Confidential. Reproduction only by permission.

Model Segmentation

Based on the constructed framework and sedimentological/tectonic conditions (such as unconformities and seismicity), the model was divided into two parts for separate handling:

- Zone from Alpha to Z' (upper part): Modeled as one grid (3D model).
- Zone below Z' (lower part): Modeled as a separate 3D grid using zig-zag type of faults to decrease model' cells' distortion associated with structural complexity.

Note: The lower part of the area of interest has increased uncertainty in seismic and well top interpretations, so less uncertainty is associated with the upper model.

Fault Model Creation

Fault model was prepared using Structural framework fault framework data for the following pillar grid construction.

Fault interpretations were split into two levels: Alpha to Z', and from the Rs7 horizon towards the Tg horizon.

For pillar gridding, minor faults with no impact on potential fluid flow or ones that were poorly resolved in the seismic data were excluded to keep the model manageable.

Horizon Modeling

Horizontal elements (horizons) were added based on seismic interpretations, thickness maps, and reviewed well tops.

Well tops were used to adjust horizon positions. Some well tops were slightly edited based on up-to-date geological and electric log studies (see 2.4 Well correlation) .

For the lower model, well tops were used to define the zone from Rs7 horizon to the Pn horizon (carbonates boundary).

Vertical Resolution Definition

Vertical cell resolution was set after the discussion with reservoir engineers, balancing formation heterogeneity and simulation feasibility (i.e., avoid excessive cell count for simulation speed).

Different vertical resolutions was chosen for upper and lower 3D models.

Data Analysis & Property Modeling

The main purpose of petrophysical modeling is to understand distribution of properties, important for volumes estimation.

Copyright © SLB. All Rights Reserved. Private & Confidential. Reproduction only by permission.

Available data was analyzed (mainly porosity logs) and anisotropy was examined for both upper and lower formations using upscaled logs using the Data analysis tool.

1. Address Vshale uncertainty with Gaussian random function simulation modeling algorithm : perform 50 simulations and average the results to get Vsh mean and Vsh median values.
2. Was created a rocktypes model (RT) based on Vsh property cut-offs for the upper model.
3. Was created a LITHO_FINAL facies model based on lithological facies interpretation using kriging algorithm for the lower model since in the lower model are prevailing carbonates and Vsh showed low corelation with porosity data.
4. Porosity uncertainty was addressed with Gaussian random function simulation: perform 50 simulations and average the results.
5. Permeability was calculated from porosity using core data (applied linear/non-linear relationships as appropriate).
6. For temperature and pressure, was used DST data and populate model using moving average techniques. Established relationships with elevation depth property helped to propagate temperature data to model base.
7. For volume estimation and reserves ranking were used 2 different approaches for the upper and the lower models, focus on area and net thickness calculation. In upper model average parameters values were taken from models, for the lower model volumes were estimated based on volumetric process in Petrel.

Model Utilization and Post-processing

1. After model completion, chance of success maps (COS) were computed and potential sites were ranked.
2. The completed models were used for the further reservoir engineering analysis and decision-making.

This structured process ensured the model is robust, interpretable, and suitable for subsequent simulation and resource estimation workflows.

More details on modeling of each of both 3D models will be described in the corresponding subsections below.

2.5.1 Upper formations Alfa (D') to Z'

This part of the 3D model was created based on interpreted seismic horizons and fault systems, covering a full stratigraphic interval from overburden to deep basin fill.

Copyright © SLB. All Rights Reserved. Private & Confidential. Reproduction only by permission.

Structural Framework

Fault Modeling

The fault framework was constructed directly from the interpreted seismic faults and converted from time to depth prior to structural modeling.

From a geological perspective, the structural interpretation indicates that the interval extending from the Alfa (D') horizon down to the Z' horizon is controlled by the same regional fault system, suggesting that the principal tectonic framework remained active throughout deposition of the post-rift succession. In the model, the same principal fault system extends vertically from the Z' horizon upward to the Alfa (D') horizon, indicating persistent structural inheritance across the post-rift succession.

Fault consistency and connectivity were checked because several faults intersected key reservoir and sealing intervals. The structural interpretation also identified localized smaller-scale faults, especially near the Sječe-2 and Čamagajevci-4 areas. Unlike the regional fault framework, these discontinuities appeared limited to specific intervals and did not propagate vertically through the entire stratigraphic column. These faults were deactivated for horizons that are not affected.

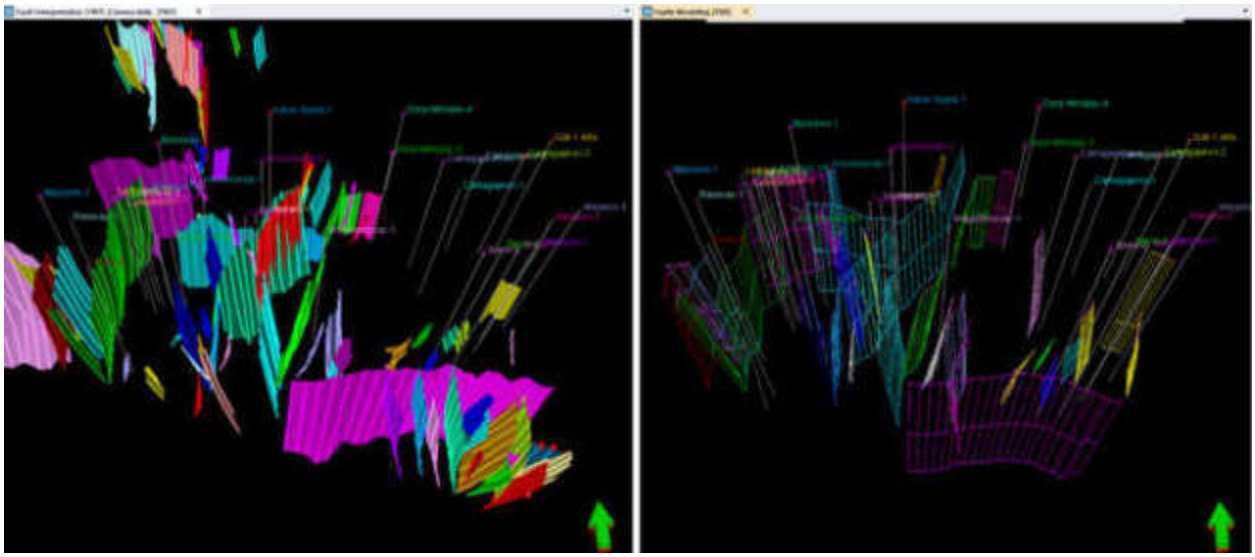


Fig. 2.61 Fault Modeling

Pillar gridding

Once the structural fault framework was completed, a pillar grid was constructed in Petrel to establish the structural skeleton of the model. The pillar grid orientation was selected according to the dominant structural trend of the principal fault orientation observed in seismic interpretation.

Copyright © SLB. All Rights Reserved. Private & Confidential. Reproduction only by permission.

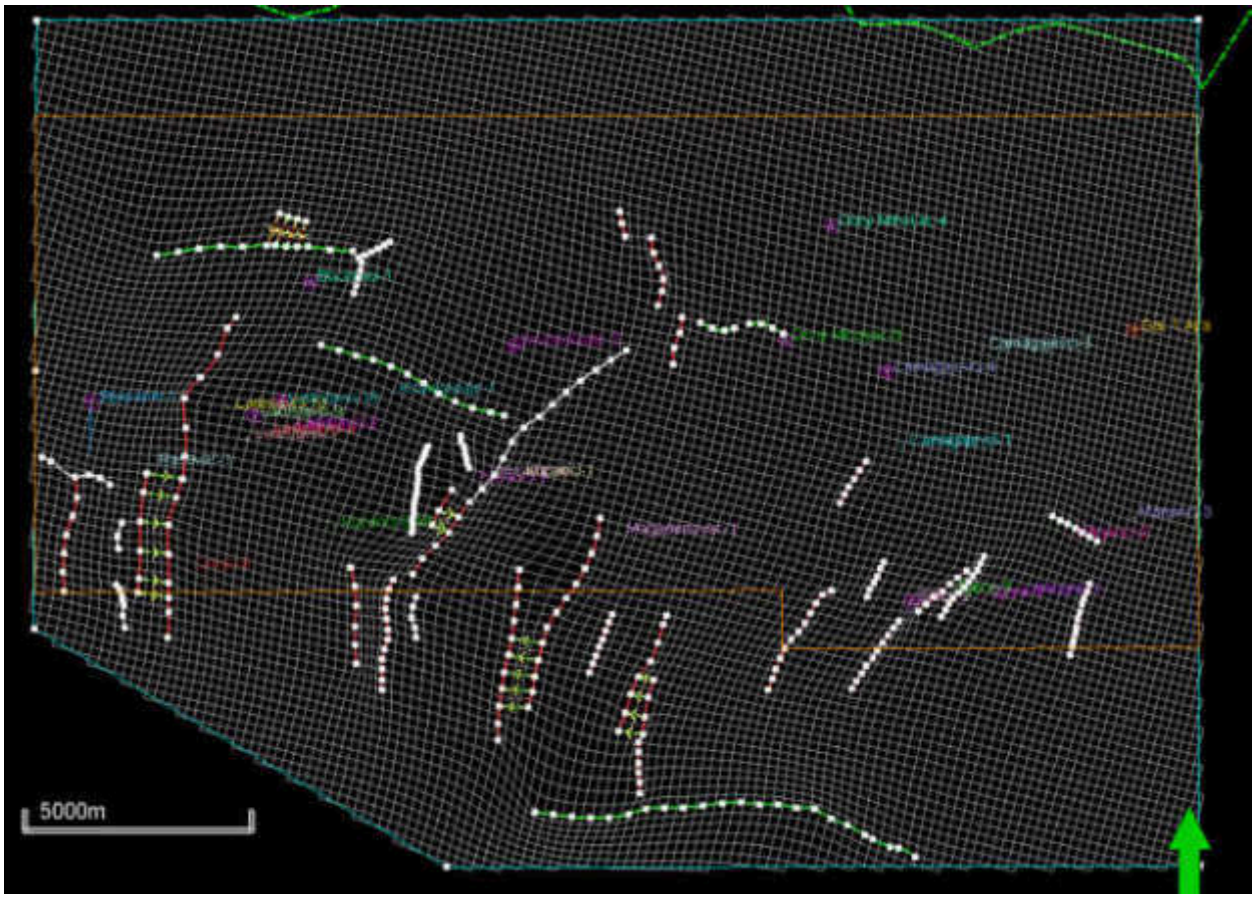


Fig. 2.62 Pillar Gridding

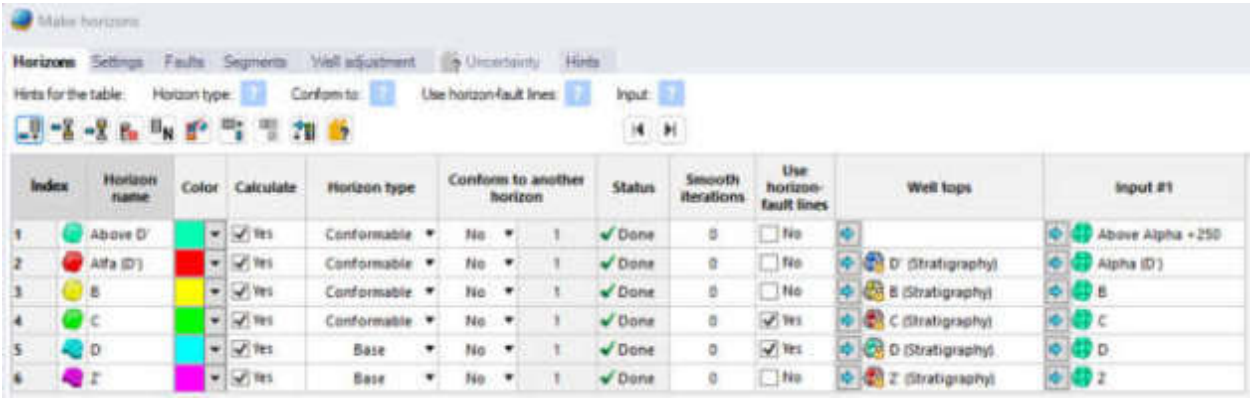
3D Grid construction

Horizon Modeling

A total of six main horizons were interpreted and depth-converted: Fig. 2.63. These horizons were selected because they represent major depositional and petrophysical transitions recognizable both in well logs and seismic interpretation.

Each horizon was constrained both by well tops and by seismic interpretation, ensuring consistency between local well control and regional seismic geometry.

Copyright © SLB. All Rights Reserved. Private & Confidential. Reproduction only by permission.



Index	Horizon name	Color	Calculate	Horizon type	Conform to another horizon		Status	Smooth iterations	Use horizon-fault lines	Well tops	Input #1
1	Above D'		Yes	Conformable	No	1	Done	0	No		Above Alpha +250
2	Alfa (D')		Yes	Conformable	No	1	Done	0	No	D' (Stratigraphy)	Alpha (D')
3	B		Yes	Conformable	No	1	Done	0	No	B (Stratigraphy)	B
4	C		Yes	Conformable	No	1	Done	0	Yes	C (Stratigraphy)	C
5	D		Yes	Base	No	1	Done	0	Yes	D (Stratigraphy)	D
6	Z'		Yes	Base	No	1	Done	0	No	Z' (Stratigraphy)	Z

Fig. 2.63 Make Horizons (Petrel)

Make zones

Once all major horizons were finalized, the structural framework was subdivided into zones using the Make Zones process. The zoning strategy followed the principal tectono-stratigraphic architecture. Different well-top sets were used depending on the stratigraphic level and depositional character of the interval. Particular emphasis was placed on identifying the transition between reservoir-prone sandstone intervals and regionally extensive marl-dominated sealing units. Once the principal tops were established, thickness maps were generated and then used in Make Zones process to refine the vertical resolution of the grid.

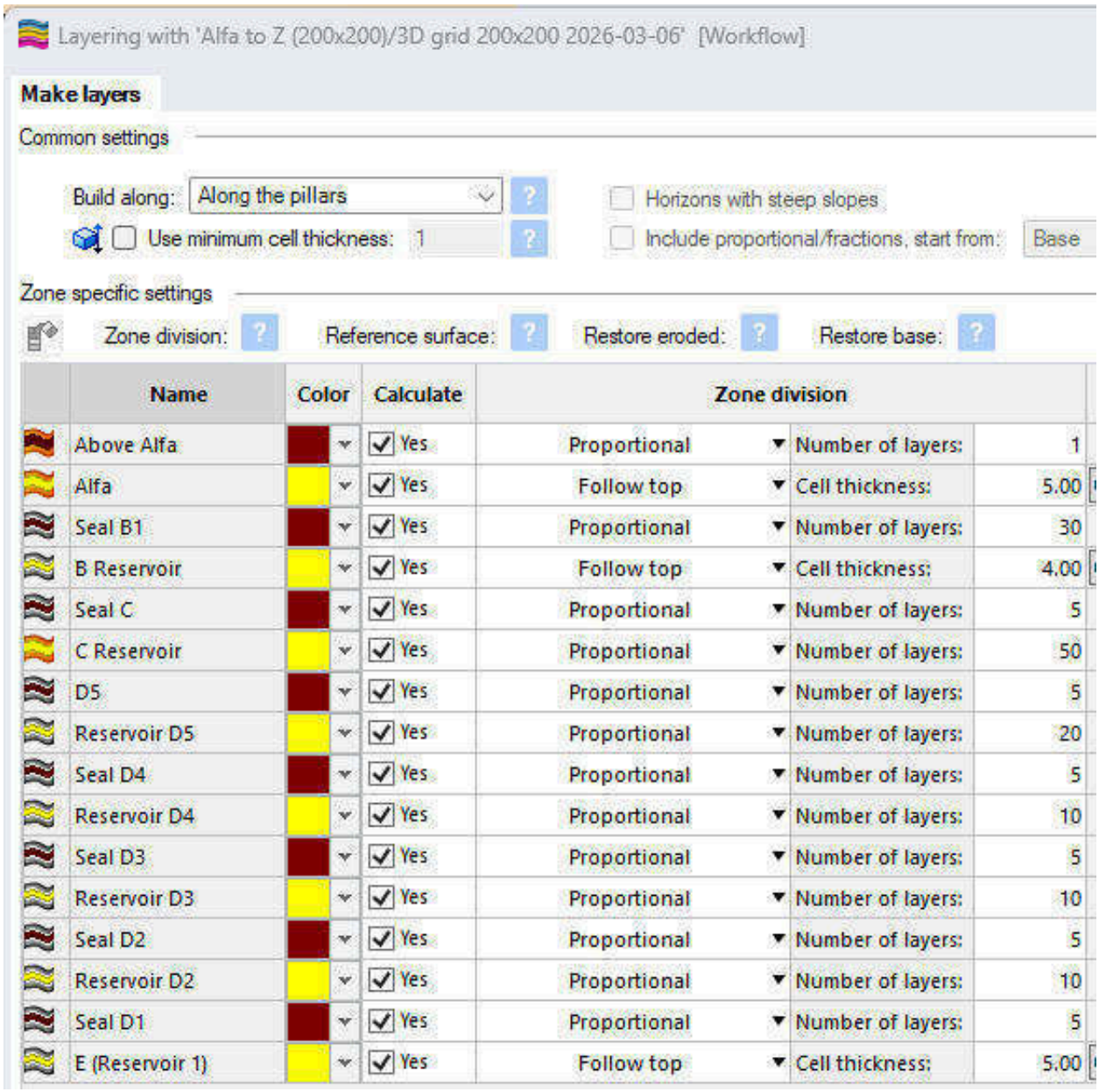
Make Zones workflow allowed these intervals to be treated independently during layering and property modeling. This was particularly useful because different parts of the succession required different vertical resolutions and modeling strategies.

Layering

Following zone construction, layering was applied inside each zone to refine the vertical resolution of the grid. The layering strategy was adapted according to depositional style and expected heterogeneity.

In reservoir-prone intervals such as the B, C and D series, finer layering was applied in order to preserve sandstone stacking patterns and better represent vertical reservoir heterogeneity.

Copyright © SLB. All Rights Reserved. Private & Confidential. Reproduction only by permission.



Name	Color	Calculate	Zone division		
Above Alfa		Yes	Proportional	Number of layers:	1
Alfa		Yes	Follow top	Cell thickness:	5.00
Seal B1		Yes	Proportional	Number of layers:	30
B Reservoir		Yes	Follow top	Cell thickness:	4.00
Seal C		Yes	Proportional	Number of layers:	5
C Reservoir		Yes	Proportional	Number of layers:	50
D5		Yes	Proportional	Number of layers:	5
Reservoir D5		Yes	Proportional	Number of layers:	20
Seal D4		Yes	Proportional	Number of layers:	5
Reservoir D4		Yes	Proportional	Number of layers:	10
Seal D3		Yes	Proportional	Number of layers:	5
Reservoir D3		Yes	Proportional	Number of layers:	10
Seal D2		Yes	Proportional	Number of layers:	5
Reservoir D2		Yes	Proportional	Number of layers:	10
Seal D1		Yes	Proportional	Number of layers:	5
E (Reservoir 1)		Yes	Follow top	Cell thickness:	5.00

Fig. 2.64 Layering

Upscaling

Following construction of the structural framework and layered grid, petrophysical logs were upscaled from well scale to grid scale in preparation for property modeling. The upscaling workflow was performed separately for continuous and discrete properties in order to preserve both reservoir quality trends and geological facies distribution.

During the upscaling process, particular attention was given to selecting an appropriate grid cell height to achieve an optimal balance between preserving log data resolution and ensuring the

Copyright © SLB. All Rights Reserved. Private & Confidential. Reproduction only by permission.

upscaled model and cell count are suitable for dynamic simulation. This approach maintained the integrity of the original depositional patterns while minimizing the introduction of artificial lithological mixing within individual grid cells.

Discrete properties, such as Rock Type (RT) Fig. 2.65, was upscaled first using the "most of" method, which assigns each grid cell the facies that occupies the largest proportion of that cell. This approach is important given the frequent vertical shifts between sands, silts, marls, and conglomerates in the geological sequence - a pattern visible in the B and D reservoir zones. By using this method, the upscaled model reflects the desired depositional complexity present in these intervals while minimizing number of cells.

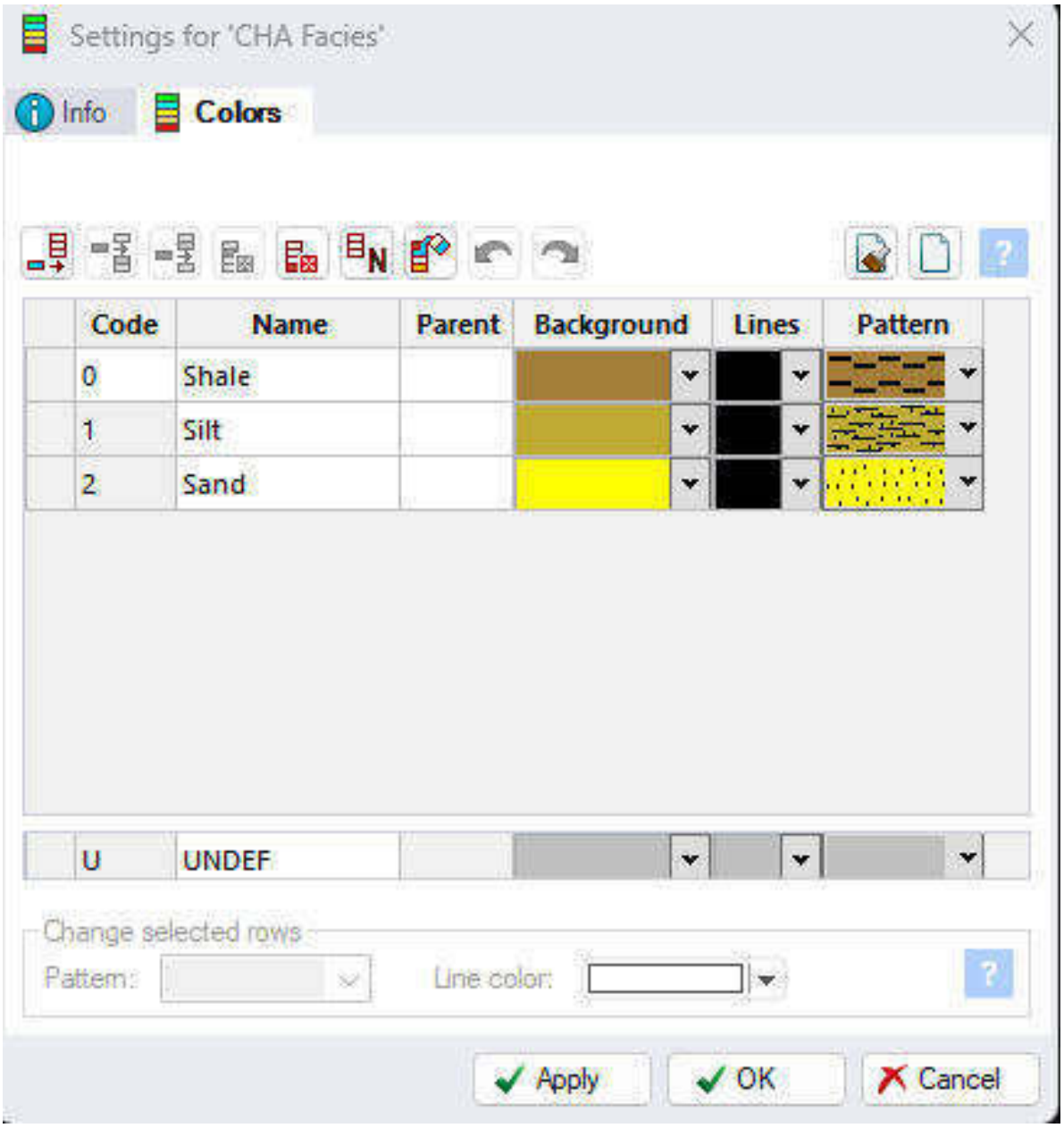


Fig. 2.65 Facies codes

Copyright © SLB. All Rights Reserved. Private & Confidential. Reproduction only by permission.



Fig. 2.66 Upscaling Facies
Track 1: SSTVD (m)
Track 2:MD(m)
Track 3: VShale
Track 4: Rock Type (RT) from Well Logs
Track 5: Upscaled RT to grid

The resulting upscaled Rock Type model then served as the geological framework for subsequent continuous property upscaling and distribution.

For the discrete log upscaling, quality control was performed by comparing the original well-log facies distribution against the upscaled facies distribution within each reservoir zone. This comparison was carried out using histograms generated for the individual facies codes after the upscaling process.

Each RT category was represented by a discrete numerical code (e.g., 1, 2, 3), corresponding to the interpreted RT Fig. 2.65 used in the model. The histograms were then used to verify that the proportion of each facies remained consistent after transfer from well-log scale to grid scale.

Copyright © SLB. All Rights Reserved. Private & Confidential. Reproduction only by permission.

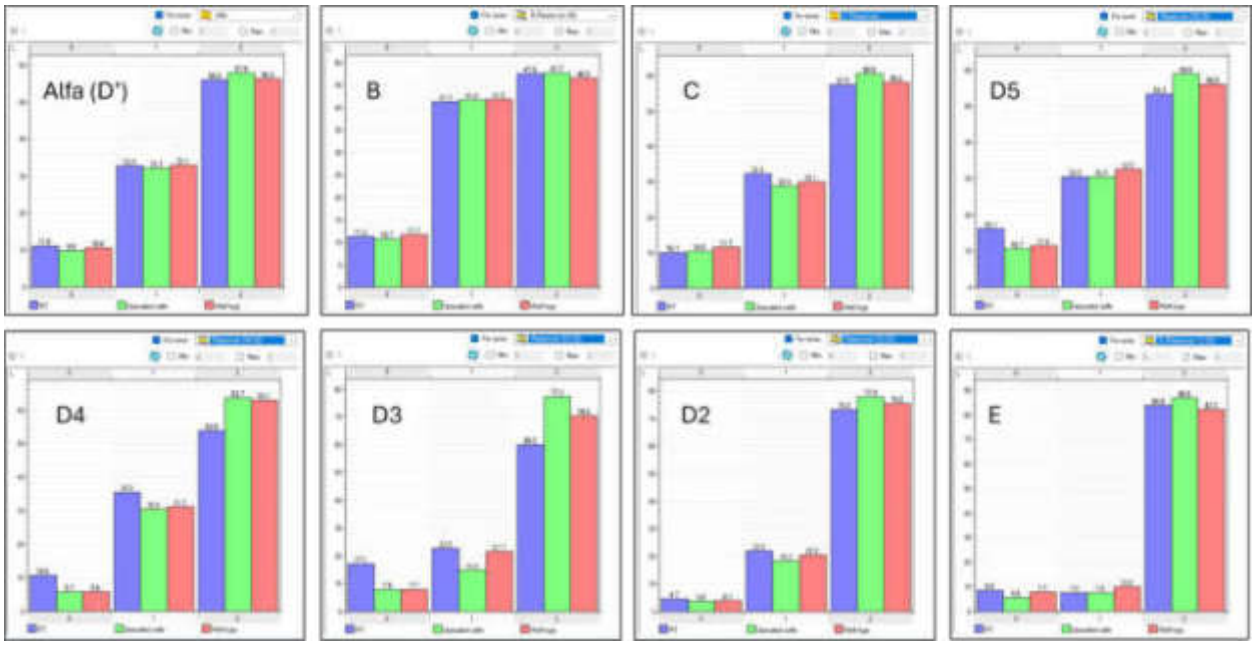


Fig. 2.67 QC of upscaling process

Continuous properties, such as effective porosity (PHIE), were subsequently upscaled using the arithmetic mean method, but with the distribution conditioned by the discrete Rock Type framework.

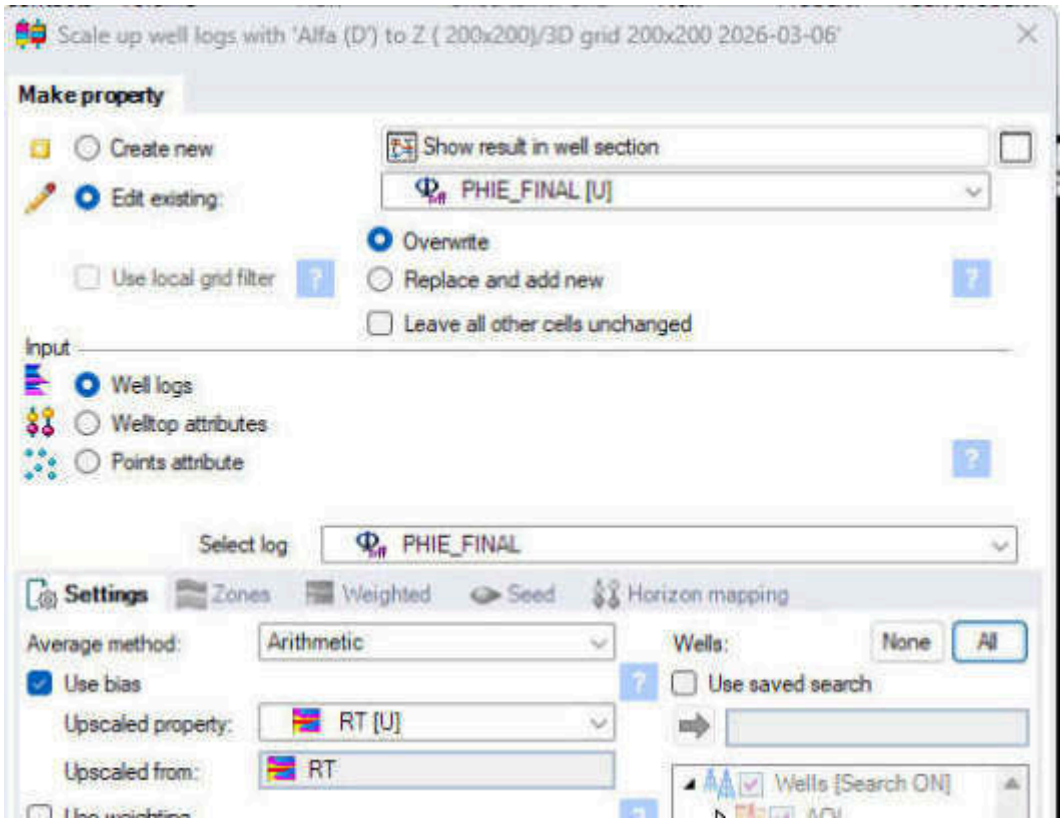


Fig. 2.68 Upscaling Effective Porosity

Copyright © SLB. All Rights Reserved. Private & Confidential. Reproduction only by permission.

This approach ensured that porosity trends remained geologically consistent with the depositional facies architecture established during the discrete modeling stage. This means that porosity distribution was not treated independently from lithology. Instead, porosity behavior was biased according to the dominant facies present within each cell. Reservoir-prone sandy facies therefore retained systematically higher porosity trends, while marl- and silt-dominated facies preserved lower porosity characteristics. This was particularly important in the Pontian clastic intervals, where reservoir quality is closely linked to depositional environment and grain-size distribution. This approach also reduced the risk of generating unrealistic porosity distributions across facies boundaries, particularly in intervals characterized by strong heterogeneity and thin interbedding.

Property distribution

Seismic Attributes

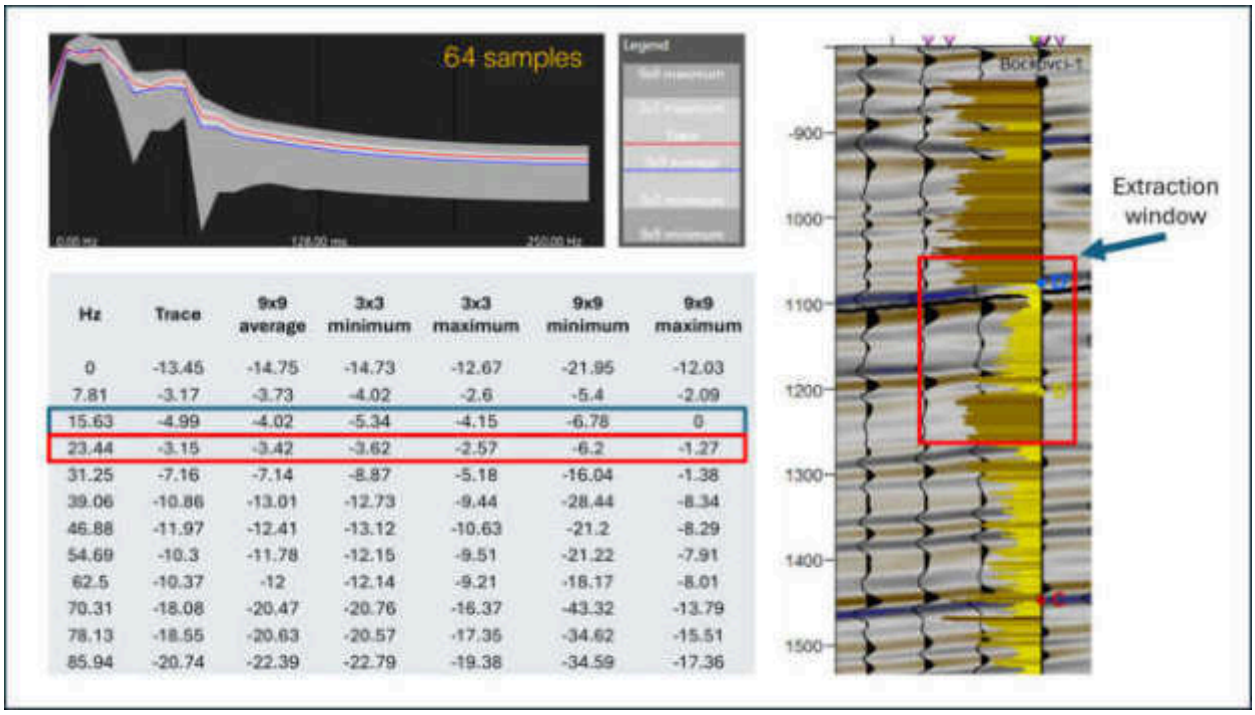
Property distribution combined well-based petrophysical interpretation with seismic-derived trends in order to better constrain facies variability and reservoir distribution away from well control. Special attention was given to bringing in seismic attributes that highlight changes in rock types and the way sediments were deposited within the main reservoir zones.

The RMS (Root Mean Square) seismic attribute was selected as the primary seismic trend used for facies characterization. The RMS cube was computed in the time domain and subsequently converted to depth and normalized between 0 and 1 in order to standardize amplitude behavior across the study area.

Geologically, RMS represents the average seismic energy within a selected interval and therefore responds strongly to variations in acoustic impedance contrasts. Higher RMS values generally correspond to stronger impedance contrasts and are commonly associated with cleaner sands while lower RMS values typically indicate weaker impedance contrasts and are more commonly associated with shales, marls, tight lithologies, or relatively homogeneous sediment packages. As a result, lateral RMS variability can be interpreted as a proxy for depositional facies changes and reservoir heterogeneity.

Before selecting the RMS extraction window, spectral decomposition analysis was performed at the reservoir interval in Bc-1 well in order to determine the dominant seismic frequency content and estimate the effective tuning thickness of the reservoir package. The amplitude spectrum indicates that the seismic response spans approximately 7–60 Hz, with the highest concentration of seismic energy centered around 23 Hz. The dominant central frequency ranges between approximately 25 and 30 Hz, corresponding to an estimated tuning thickness of roughly 17–20 ms.

Copyright © SLB. All Rights Reserved. Private & Confidential. Reproduction only by permission.



Hz	Trace	9x9 average	3x3 minimum	3x3 maximum	9x9 minimum	9x9 maximum
0	-13.45	-14.75	-14.73	-12.67	-21.95	-12.03
7.81	-3.17	-3.73	-4.02	-2.6	-5.4	-2.09
15.63	-4.99	-4.02	-5.34	-4.15	-6.78	0
23.44	-3.15	-3.42	-3.62	-2.57	-6.2	-1.27
31.25	-7.16	-7.14	-8.87	-5.18	-16.04	-1.38
39.06	-10.86	-13.01	-12.73	-9.44	-28.44	-8.34
46.88	-11.97	-12.41	-13.12	-10.63	-21.2	-8.29
54.69	-10.3	-11.78	-12.15	-9.51	-21.22	-7.91
62.5	-10.37	-12	-12.14	-9.21	-18.17	-8.01
70.31	-18.08	-20.47	-20.76	-16.37	-43.32	-13.79
78.13	-18.55	-20.63	-20.57	-17.35	-34.62	-15.51
85.94	-20.74	-22.39	-22.79	-19.38	-34.59	-17.36

Fig. 2.69 Frequency spectrum

Spectral analysis highlighted considerable lateral variation within the reservoir interval. The absolute spectral maximum within the analyzed window occurs at approximately 15.63 Hz, representing the frequency associated with the highest amplitude energy response.

Examination of the 9×9 spatial envelope revealed significant changes in energy distribution across the 23–40 Hz frequency band, with amplitude differences between the minimum and maximum reaching approximately 20 dB. While this variability is mainly attributed to lateral facies changes within the reservoir system, some influence from seismic noise cannot be entirely ruled out.

Overall, the dominant reservoir frequency content is concentrated within the 15–33 Hz range, which was therefore considered the most representative frequency interval for facies characterization and seismic-guided reservoir modeling.

Using the dominant reservoir frequency of approximately 24 Hz, one seismic cycle corresponds to roughly 41 ms (1/24 s). Considering the seismic sampling rate of 2 ms, a single cycle therefore contains approximately 20 seismic samples. Consequently, an extraction window equivalent to three seismic cycles corresponds to approximately 120 ms, or roughly 60 seismic samples.

The results of the spectral analysis were subsequently used to guide the RMS extraction parameters. The RMS extraction window was selected to balance vertical resolution against signal stability. Although larger windows provide smoother and more stable energy estimates, they may obscure thinner features. To preserve reservoir-scale variability and maintain sensitivity to thinner features, a relatively small extraction window of 3 seismic cycles was selected.

Copyright © SLB. All Rights Reserved. Private & Confidential. Reproduction only by permission.

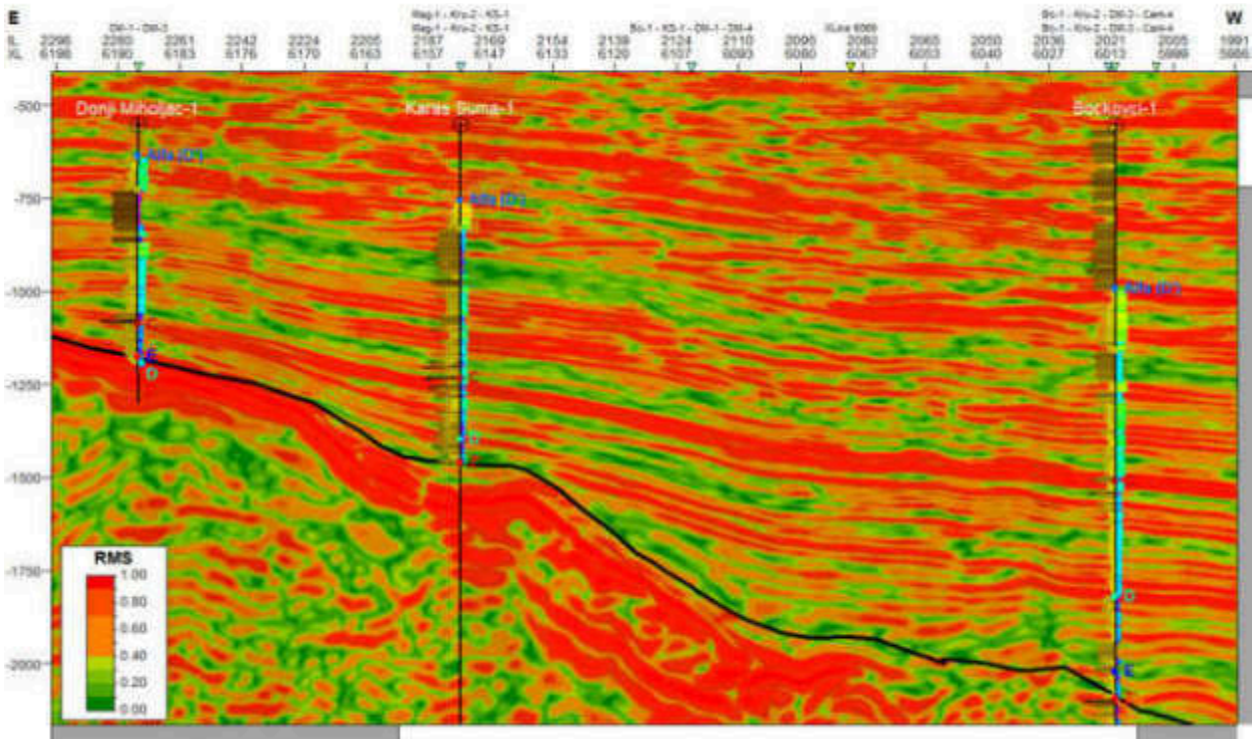


Fig. 2.70 Normalized RMS

In addition to RMS, Instantaneous Frequency (IF) was extracted at the reservoir level to further characterize lateral facies variability. Unlike RMS, which primarily responds to impedance contrast intensity, IF is more sensitive to subtle vertical and lateral lithological variations and it proved useful for identifying facies transitions and internal reservoir variability that were not always clearly visible on amplitude-based attributes alone.

The extraction window used for IF was selected empirically through visual comparison and iterative testing. A larger window than that used for RMS was ultimately adopted in order to stabilize the frequency response

In clastic depositional systems, lower-frequency responses are commonly associated with thicker and cleaner sand bodies, while higher frequencies are more frequently related to shale-rich or thinly interbedded intervals. Consequently, the original IF attribute was transformed and normalized Fig. 2.71 so that higher resulting values correspond to sand-prone intervals and lower values correspond to shale-prone intervals. This transformation allowed the attribute to be used directly as a positive sand indicator during facies modeling.

Copyright © SLB. All Rights Reserved. Private & Confidential. Reproduction only by permission.

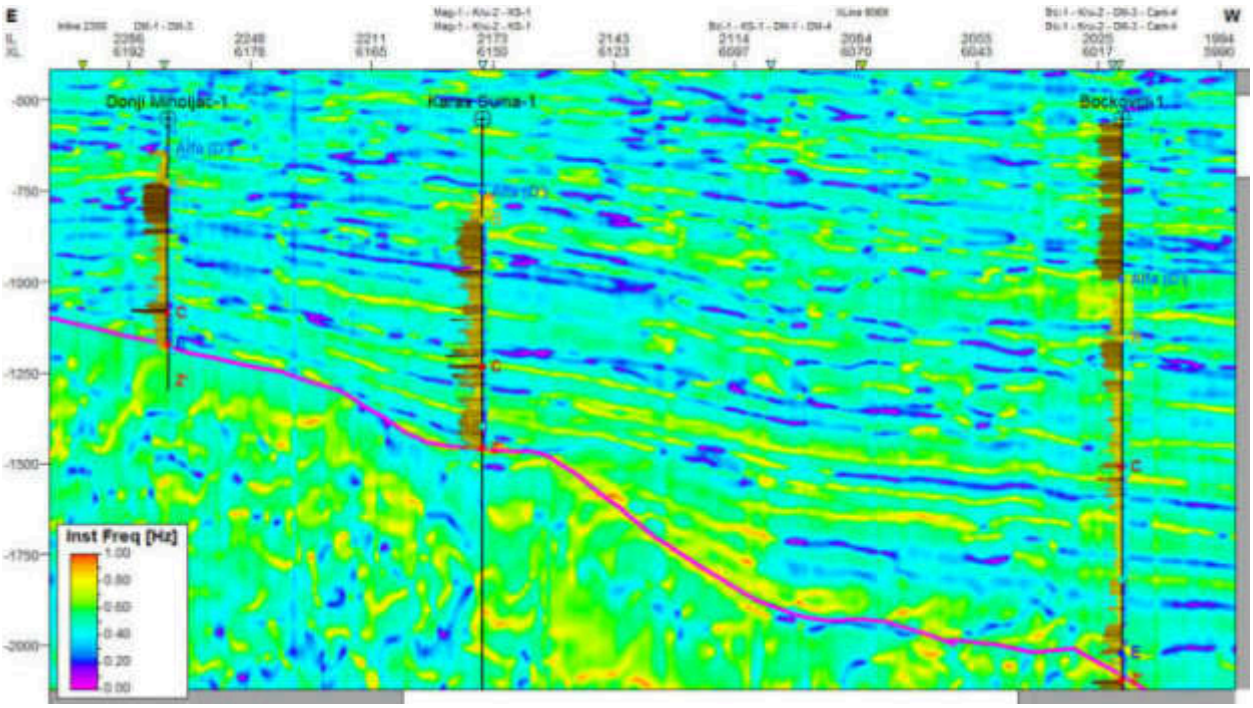


Fig. 2.71 Instantaneous frequency

The transformed IF attribute was then combined with normalized RMS to generate the final seismic sand trend:

SEISMIC_SAND_TREND=0.7×RMS_NORM_DEPTH+0.3×IF_NORM_DEPTH

The RMS attribute received the dominant weighting because it provided the strongest correlation with impedance contrasts associated with lithological changes and reservoir quality. The normalized IF attribute contributed additional sensitivity to internal depositional variability, particularly in intervals where amplitude behavior alone did not fully resolve facies architecture.

By integrating both attributes into a single trend volume, the workflow combined:

- amplitude-driven reservoir indication,
- with frequency-sensitive depositional heterogeneity,

resulting in a more geologically realistic representation of lateral facies distribution within the reservoir intervals.

Copyright © SLB. All Rights Reserved. Private & Confidential. Reproduction only by permission.

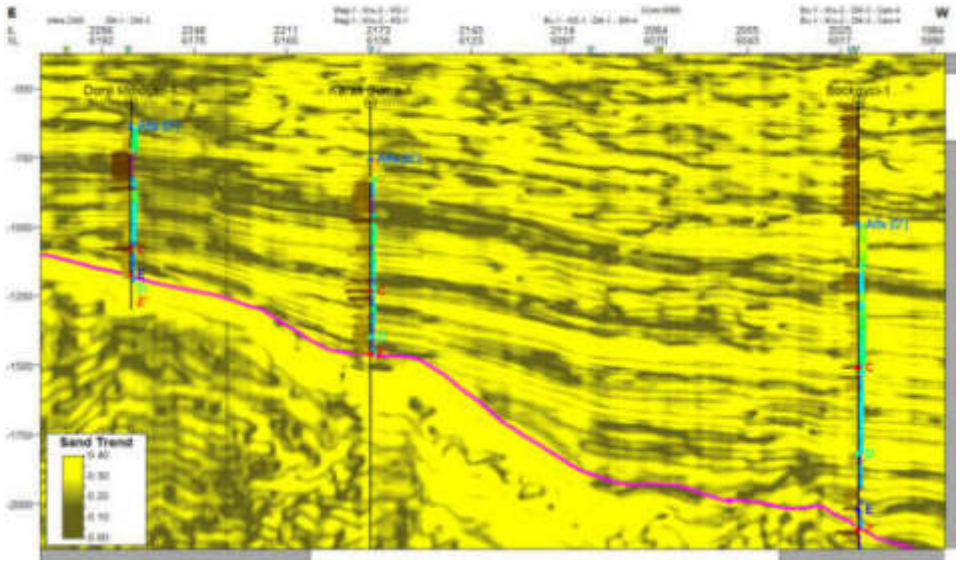


Fig. 2.72 Sand trend

Following generation of the composite seismic sand-trend volume, the attribute was resampled it into the geological grid. This ensured that the seismic-derived depositional trends were spatially consistent with the structural framework, zonation, and layering of the reservoir model.

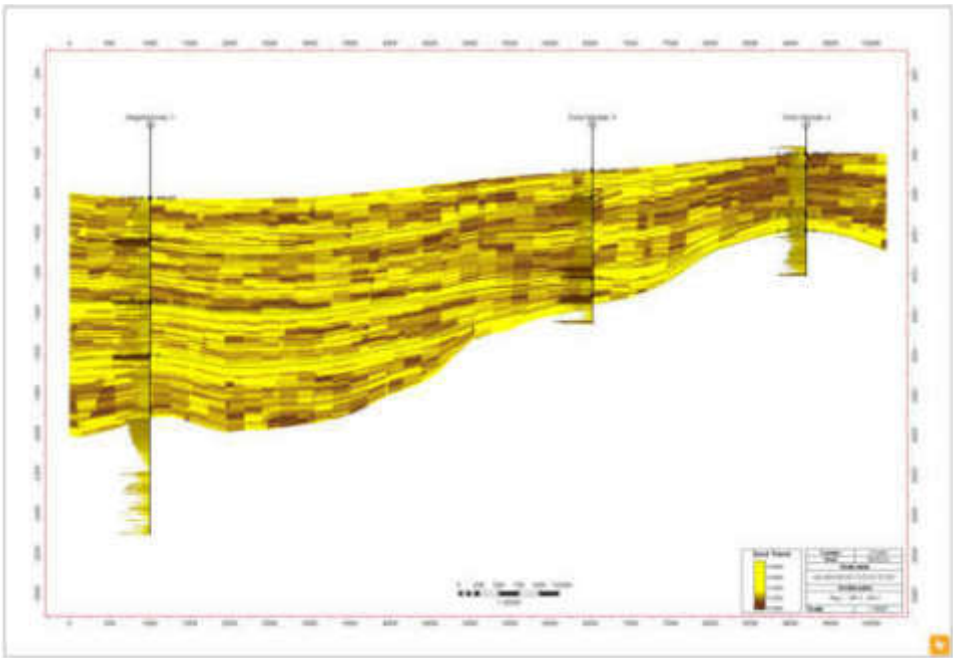


Fig. 2.73 Resampled Seismic Sand Trend into Grid

The sand trend represents the relative probability of sand-prone facies distribution derived from the combined behavior of normalized RMS and transformed Instantaneous Frequency attributes. Higher trend values therefore correspond to intervals interpreted as more reservoir-prone, while lower values indicate progressively finer-grained or shale-dominated facies.

Copyright © SLB. All Rights Reserved. Private & Confidential. Reproduction only by permission.

After resampling the sand trend into the 3D grid, a complementary shale trend volume was generated using the relationship:

SHALE_TREND=1–SAND_TREND

This transformation created two complementary seismic-guided trends representing the relative spatial likelihood of sand-dominated versus shale-dominated depositional facies throughout the model.

Rock Type

The resulting sand and shale trend volumes were subsequently used to guide Rock Type (RT) distribution during facies modeling. Rather than relying solely on well interpolation, the workflow incorporated seismic-derived depositional trends to improve lateral facies continuity and better capture reservoir heterogeneity away from well control.

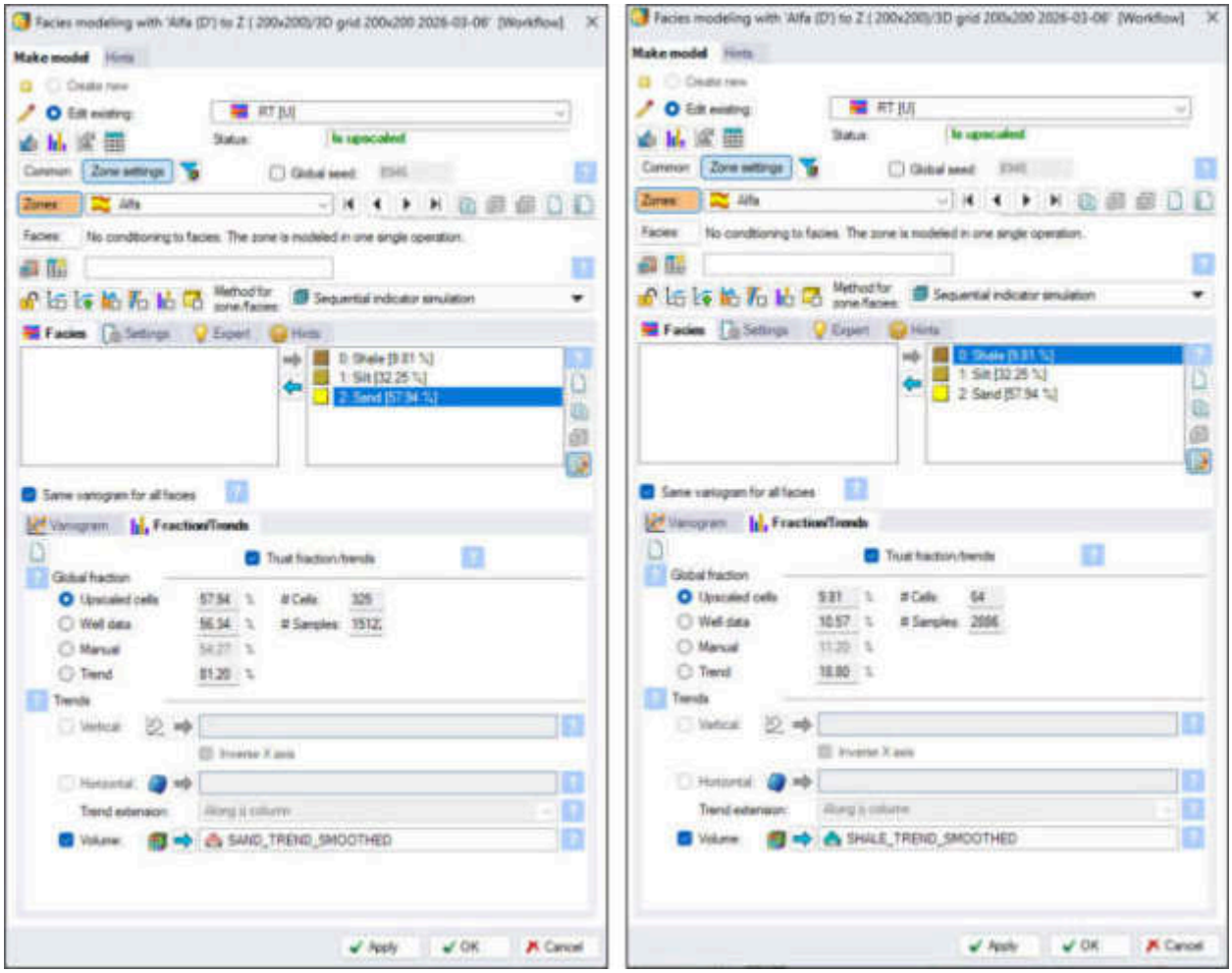


Fig. 2.74 Facies Modeling process with trend

Copyright © SLB. All Rights Reserved. Private & Confidential. Reproduction only by permission.

This approach was important because the studied succession contains significant lateral variability associated with shifting depositional environments, especially within the Pontian clastic intervals.

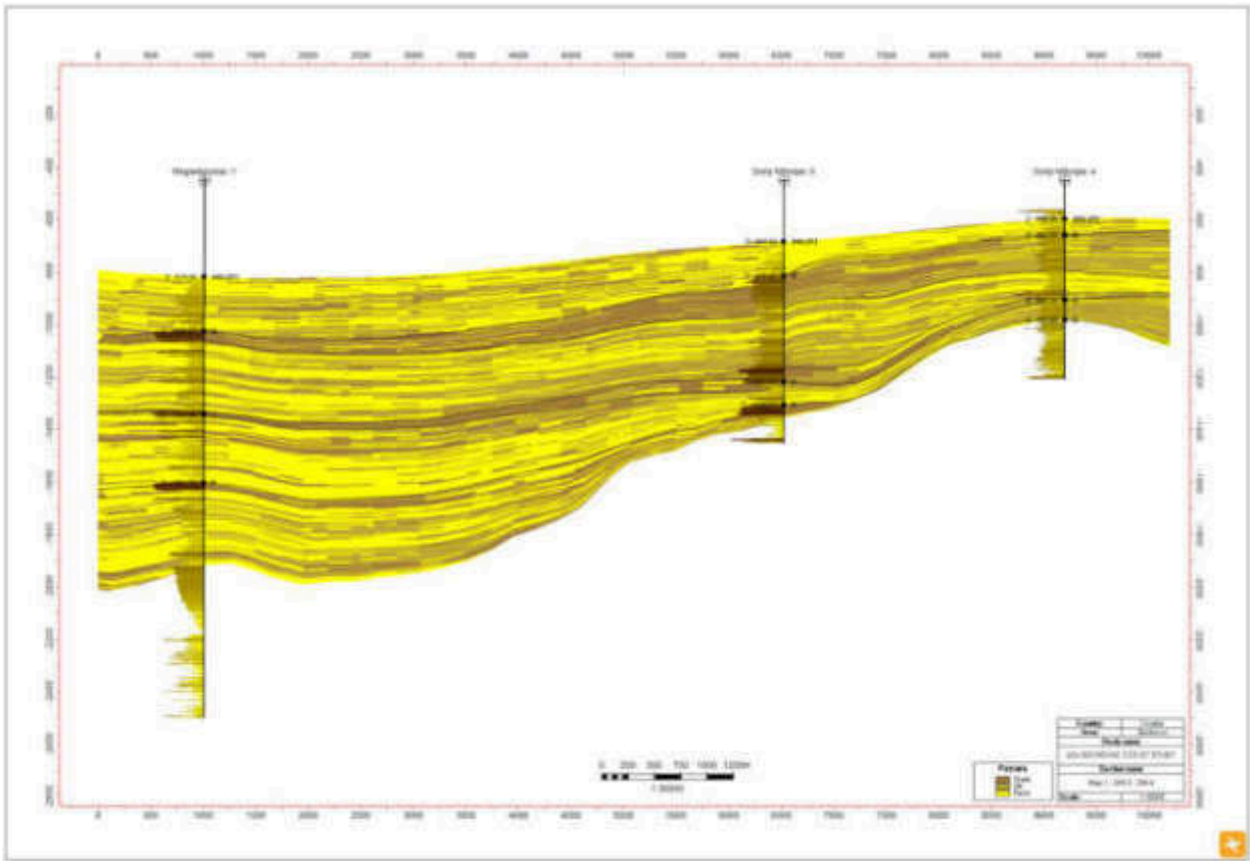


Fig. 2.75 Section Mag-1 - DM-3 - DM-4

Copyright © SLB. All Rights Reserved. Private & Confidential. Reproduction only by permission.

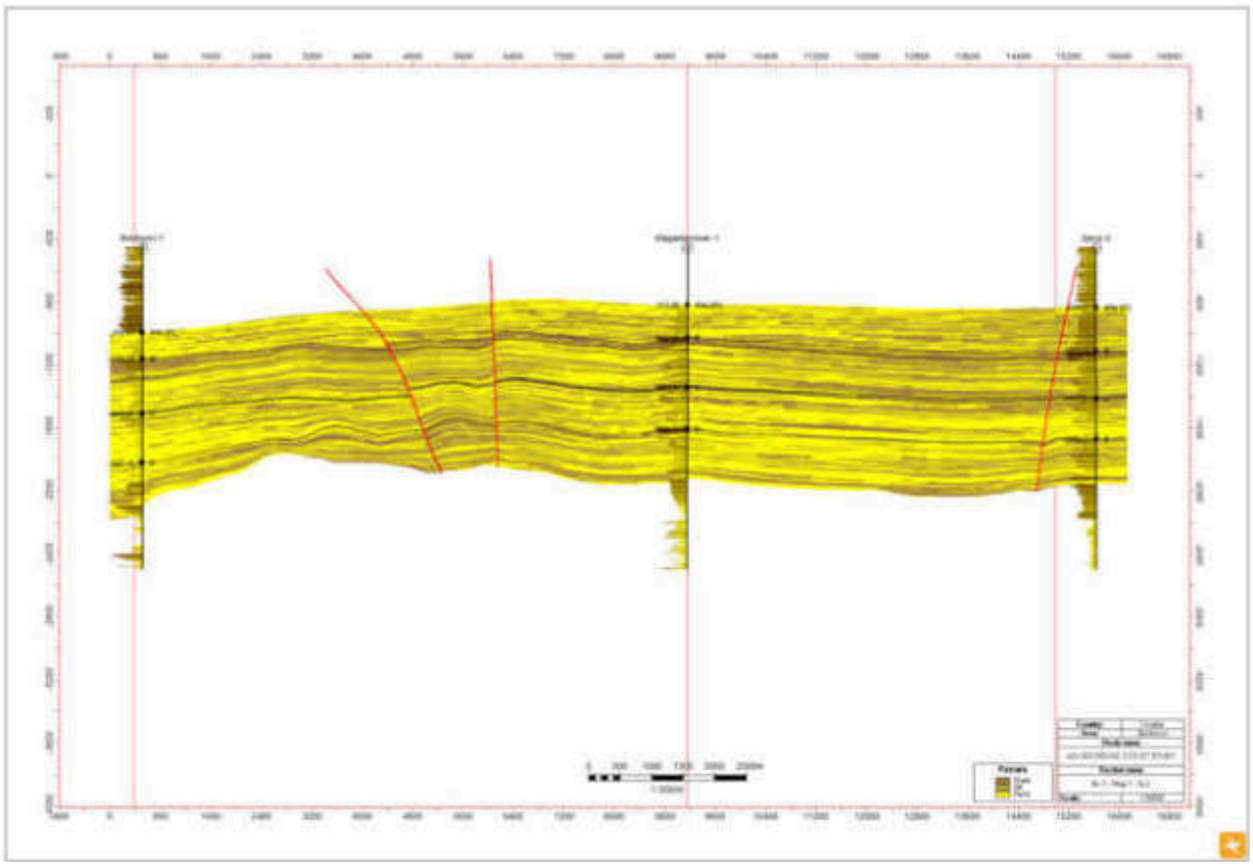


Fig. 2.76 Section Bc-1 - Mag-1 - Sj-2

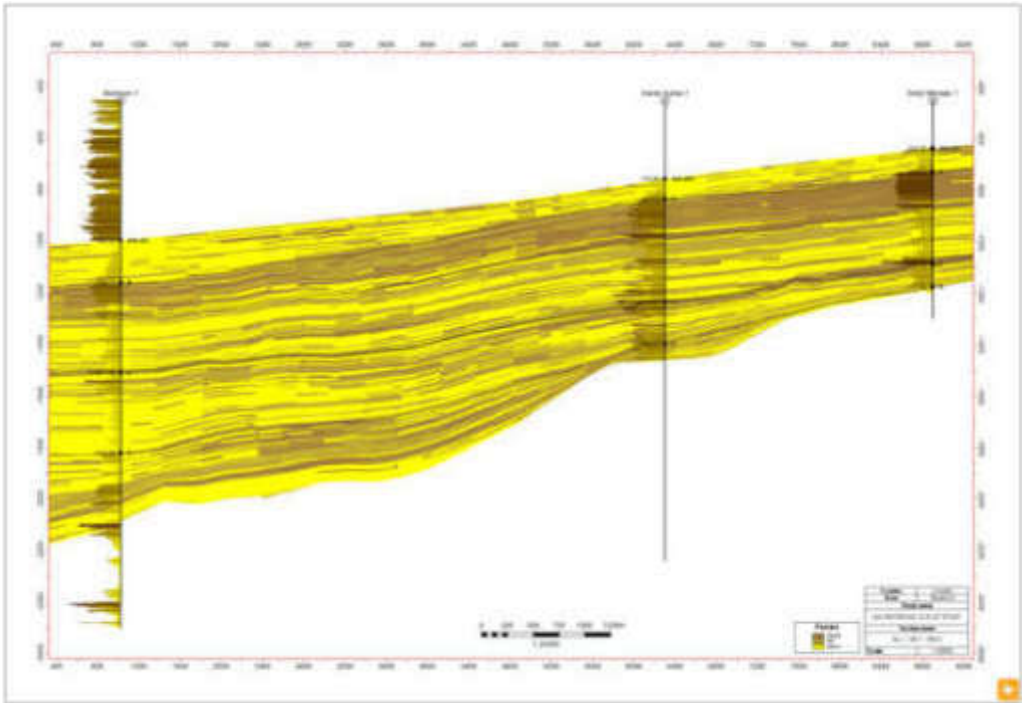


Fig. 2.77 Section Bc-1 - Kš-1 - DM-1

Copyright © SLB. All Rights Reserved. Private & Confidential. Reproduction only by permission.

Porosity

Following completion of the Rock Type (RT) distribution, effective porosity (PHIE) was modeled within the grid.

Because reservoir quality in the study area is strongly controlled by depositional facies, porosity was distributed conditionally using the previously generated Rock Type model as the primary geological constraint.

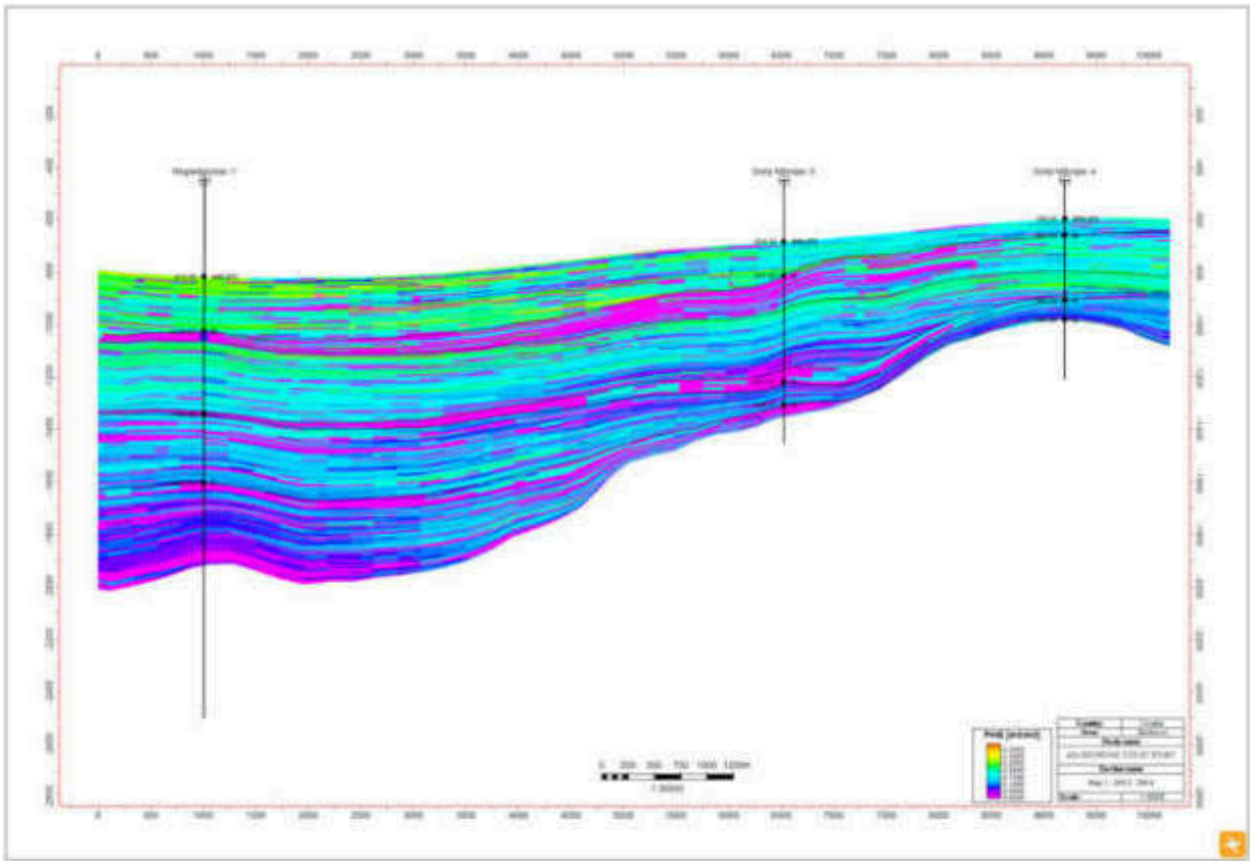


Fig. 2.78 Section Mag-1 - DM-1 - DM-4

Porosity distribution was performed using Gaussian Random Function Simulation (GRFS). This stochastic simulation approach was selected because it allows realistic spatial variability to be reproduced while honoring both well control and geological trends. Compared to deterministic interpolation methods, GRFS better captures the natural heterogeneity characteristic of the Pontian clastic reservoir system, particularly within intervals containing rapid lateral facies changes and variable reservoir quality. Within the B and D series, porosity variability is closely related to the alternation of clean sands, silts, marls, and locally conglomeratic facies.

Permeability

Copyright © SLB. All Rights Reserved. Private & Confidential. Reproduction only by permission.

Following completion of the effective porosity (PHIE) model, permeability was derived using an empirical porosity–permeability relationship calibrated to the reservoir characteristics. Because permeability measurements were limited compared to porosity data, permeability distribution was modeled indirectly using the previously generated PHIE volume as the principal controlling property. Fig. 2.54

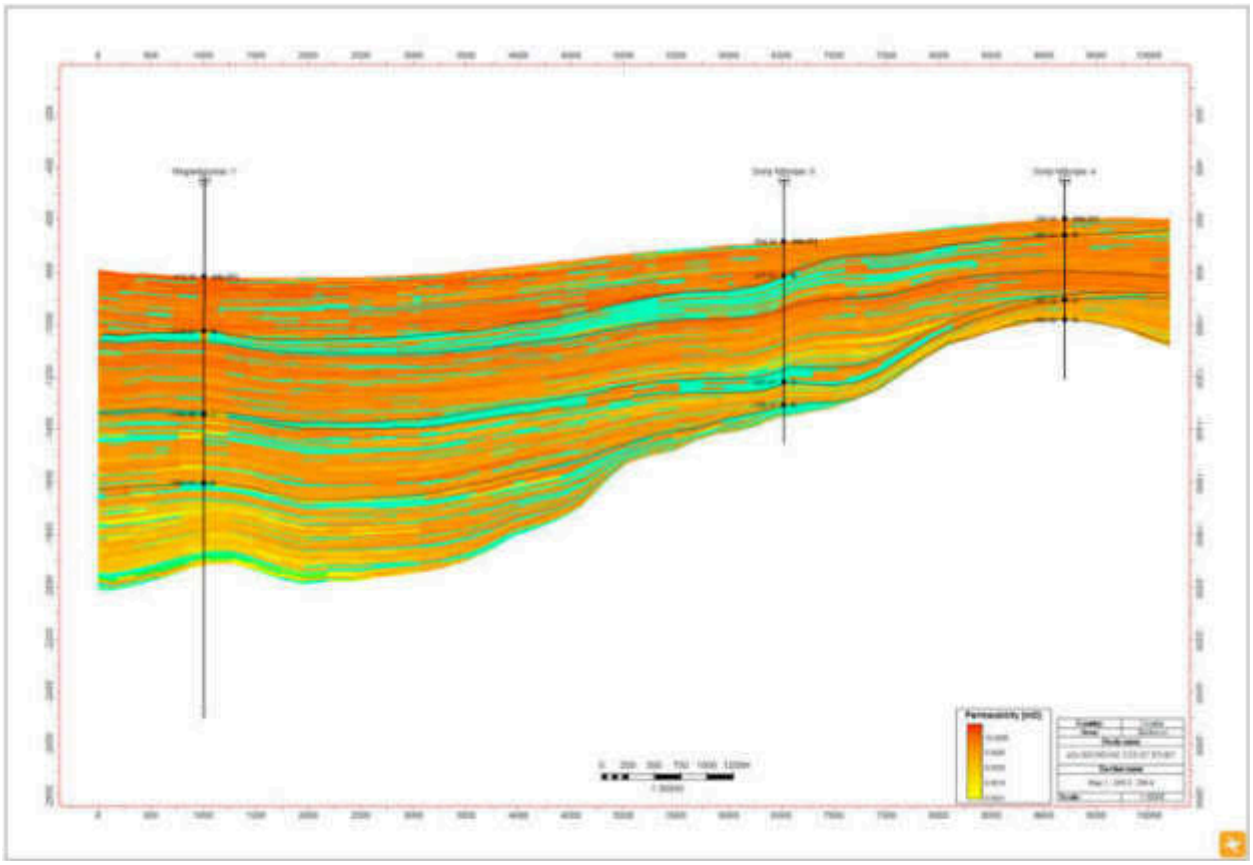


Fig. 2.79 Permeability

Because the permeability distribution was derived directly from the PHIE model, the resulting permeability architecture naturally inherited the depositional and facies trends established during the previous modeling stages. Sand-prone intervals associated with higher porosity values developed significantly improved permeability distributions, while shale-, marl-, and silt-dominated intervals retained low permeability characteristics.

The permeability model was subsequently used as the basis for Net-to-Gross (NtG) calculation. Cells with permeability values exceeding the selected cutoff of 1 mD were classified as net reservoir, while lower-permeability cells were treated as non-net intervals. This approach ensured that the NtG distribution remained consistent with both the geological facies framework and the modeled reservoir-quality properties.

Copyright © SLB. All Rights Reserved. Private & Confidential. Reproduction only by permission.

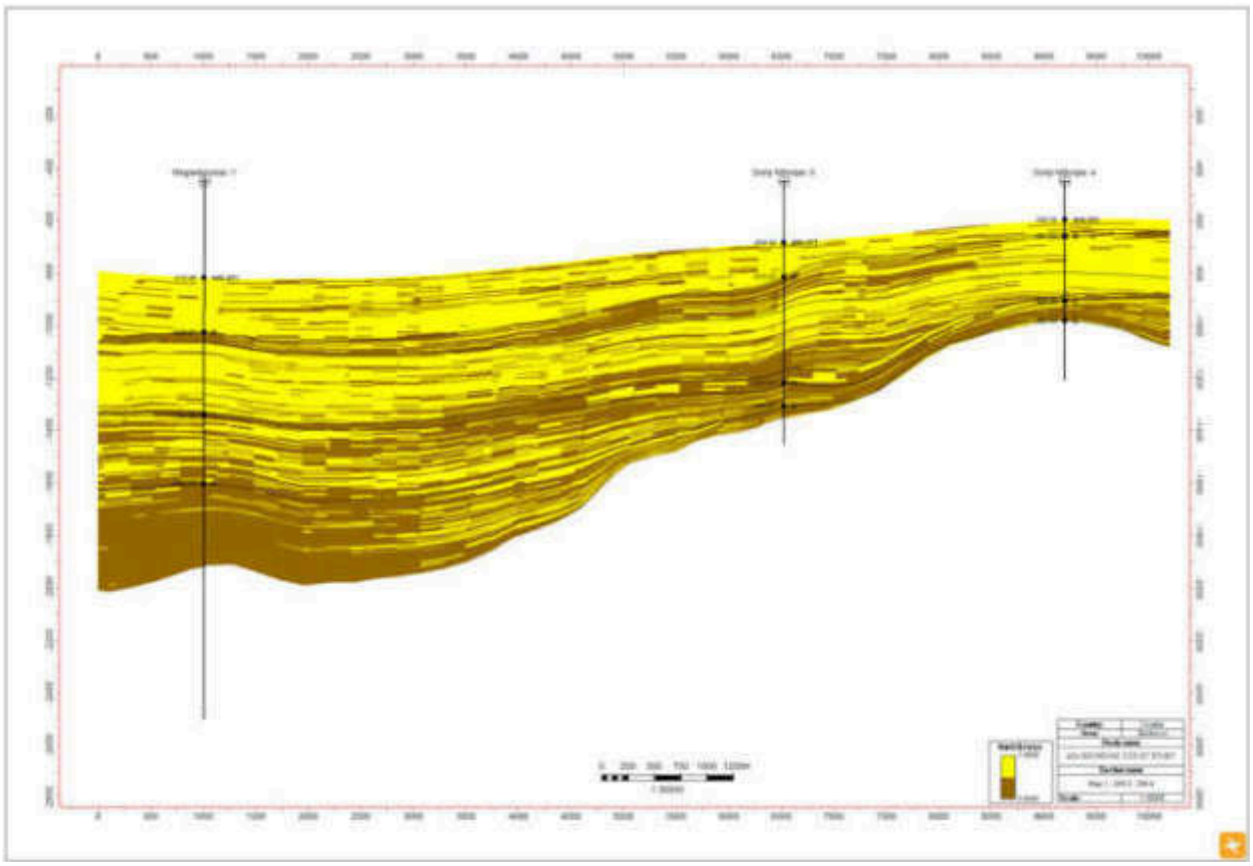


Fig. 2.80 Reservoir - Non-reservoir

2.5.2 Lower formations Z' to Tg

Introduction

This section presents a detailed overview of the structural modeling workflow conducted using Petrel software for geological assessment and reservoir characterization of the lower formations – from regional marker Z' to the top of the basement rocks represented by Tg marker. The primary objectives included identifying and modeling structural features, populating reservoir properties, and assessing both storage and geothermal potential within the area of interest. The workflow emphasizes the best practices in handling faults, defining horizons, and estimating key reservoir properties in a complex stratigraphic setting.

Structural Framework and fault model

The structural modeling process began with analysis of the results of seismic interpretation, during which two principal fault systems were identified. First model was built using automatic volume based modeling process that helped to understand the relationship between the fault and horizon interpretations.

Copyright © SLB. All Rights Reserved. Private & Confidential. Reproduction only by permission.

Based on structural framework analysis, two fault systems, associated with upper and lower formations, were identified. One system likely represents syn-rift faulting, while the other relates to post-rift tectonics. Notably, these fault systems converge at the so-called Z' horizon, providing a critical ceiling formation for the Moslavačka Gora and/or Vukovarska formations.

To maintain simplicity and satisfy technical requirements for pillar or corner point gridding, it was necessary to ensure that faults extended continuously from the top to the base of the model. The coexistence of two distinct fault systems heightened the complexity of this task. As a solution, the model was divided along the Z' horizon, allowing for separate analyses of the upper and lower sections. This division was further justified by differences in sedimentation conditions, lithological contrasts, bedding dips, and other factors impacting the construction of reliable chance-of-success maps for CO_2 storage. Subsequent results confirmed that this methodological choice was appropriate.

Considering the complexity of the AOI, relationship between faults and the following task of volume estimation, faults in model Z'-Tg were modeled as a zigzag faults that are simulation friendly and helped to minimize number of distorted cells. Fault model consists of 36 faults. Fault tops were not interpreted, in reports some wells contain information about structural gaps and one well contains information about detected fault, but taking into account number of discontinuities in lower part of section any fault top position still be highly uncertain.

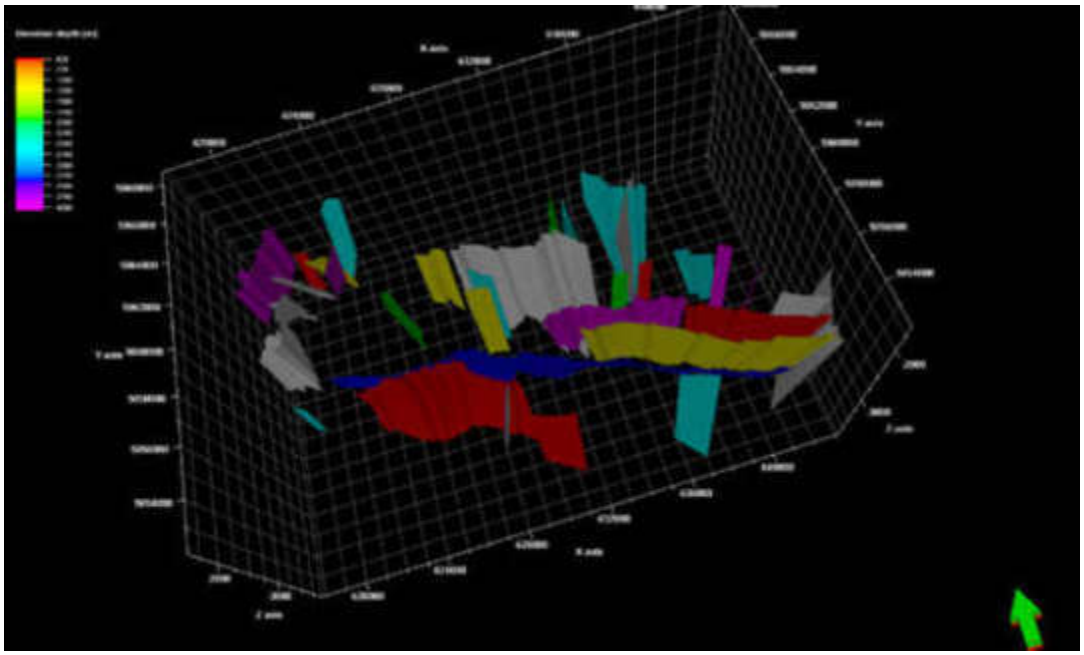


Fig. 2.81 Faults in a Z'-Tg model

Copyright © SLB. All Rights Reserved. Private & Confidential. Reproduction only by permission.

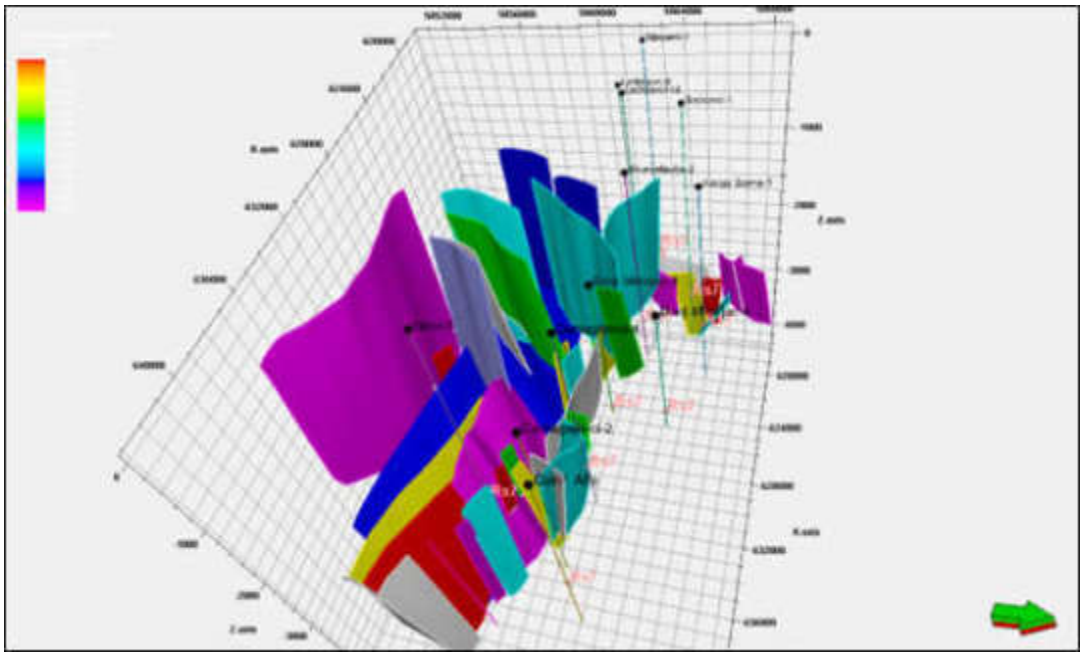


Fig. 2.82 2 fault systems visualized for the entire section from Alfa top to Tg top

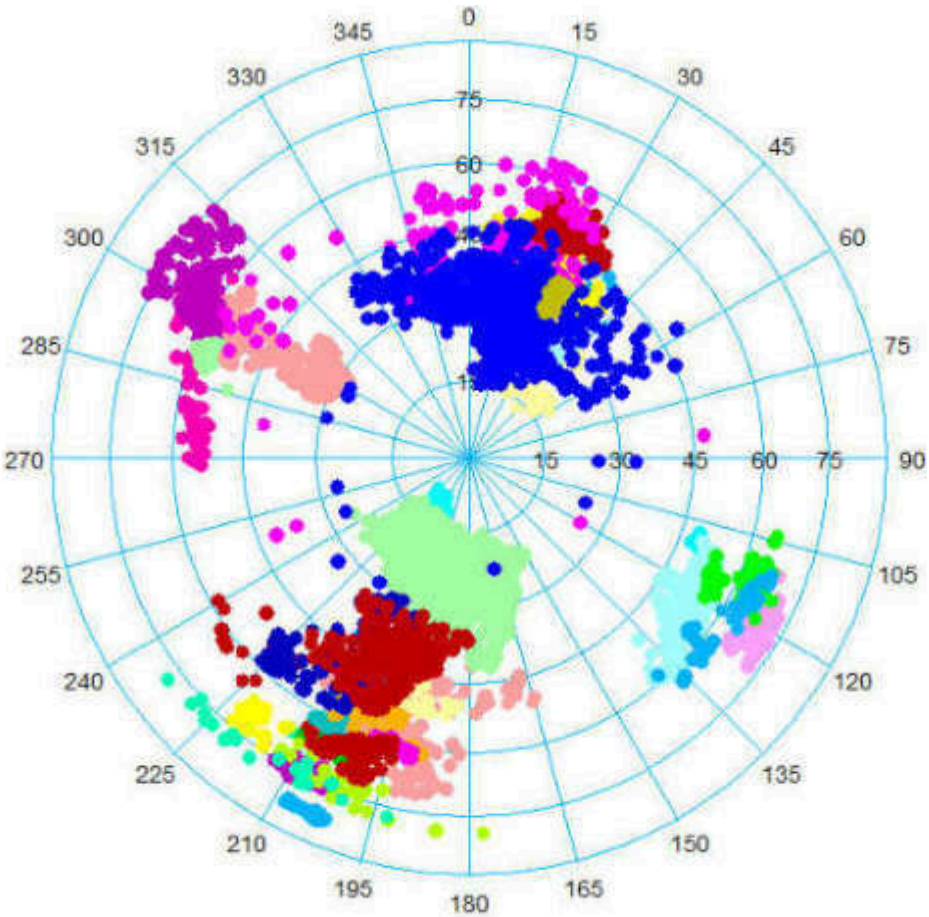


Fig. 2.83 Faults from the lower model visualized on stereonet

Copyright © SLB. All Rights Reserved. Private & Confidential. Reproduction only by permission.

Horizons modeling

Initial grid had resolution 100×100 m, but later was changed to coarser – 200×200 m. Defining horizons, especially the Z' horizon, was challenging due to its role as a detachment or erosional surface and associated lithological transitions. In some instances, the horizon's interpretation was complicated by discrepancies in existing datasets, limited data available for a velocity model construction, uncertainty associated with well tops. To address this, the modeling relied primarily on seismic interpretation and available well tops. Where well tops were ambiguous or merely predicted rather than measured, independent reinterpretation was performed; uncertain data points were excluded from modeling to preserve structural accuracy. The lower portion of the model from the Z' horizon downward and incorporated the Rs5 and Rs7 horizons, as well as the Pannonian base and Tg horizons, with particular interest focused between Rs5 and Rs7 due to the potential for CO_2 storage.

For modeling of Z', Rs7, Pn and Tg horizons the seismic horizons were used, converted to depth domain together with available well tops. Horizon Rs5 was created based on thickness map and set of well tops later in Make zones process.

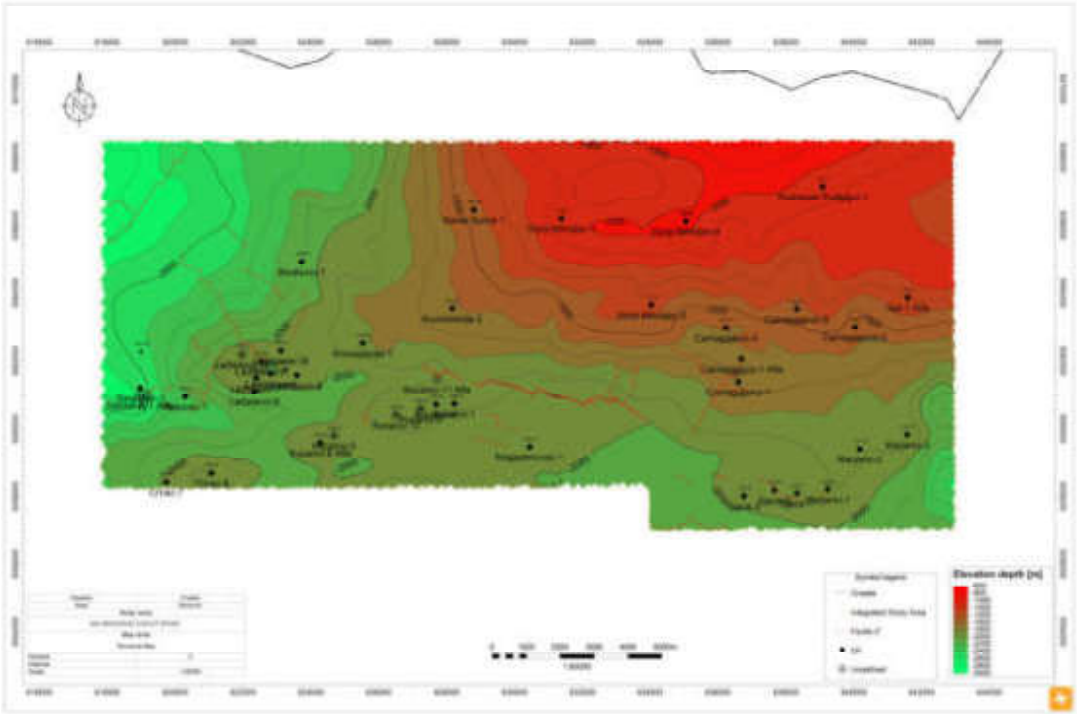


Fig. 2.84 'Z'' Series (Top of Seal)
Structural map of horizon Z' (top of seal)

Copyright © SLB. All Rights Reserved. Private & Confidential. Reproduction only by permission.

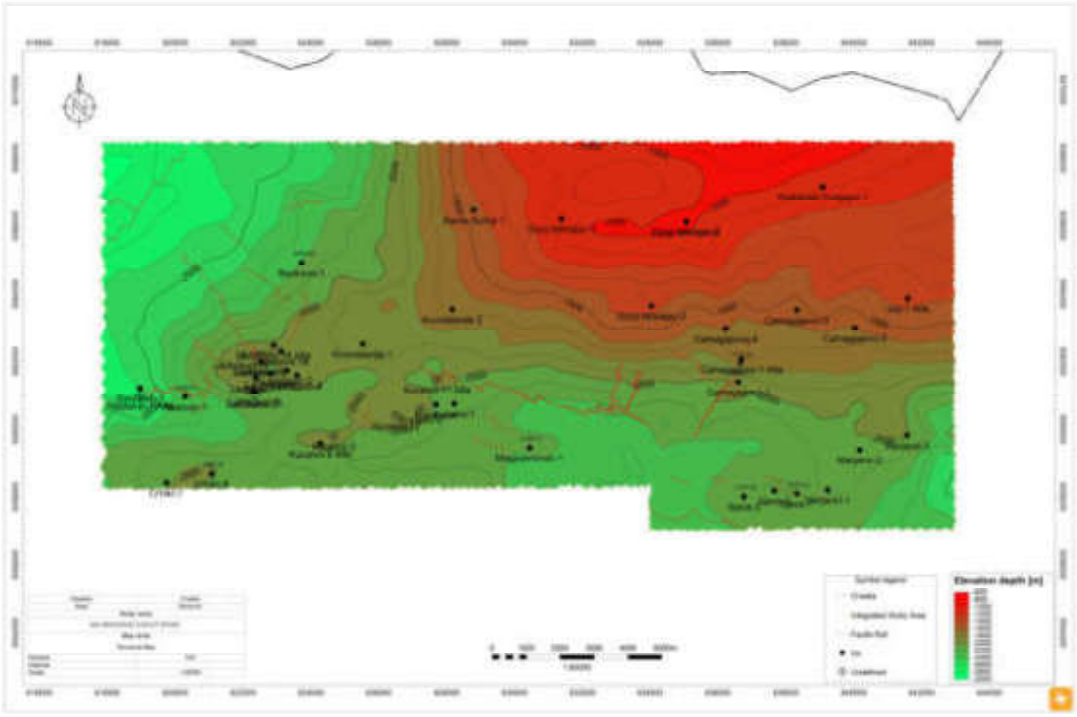


Fig. 2.85 'Rs5' Series (Top of Reservoir)
Structural map of horizon Rs5

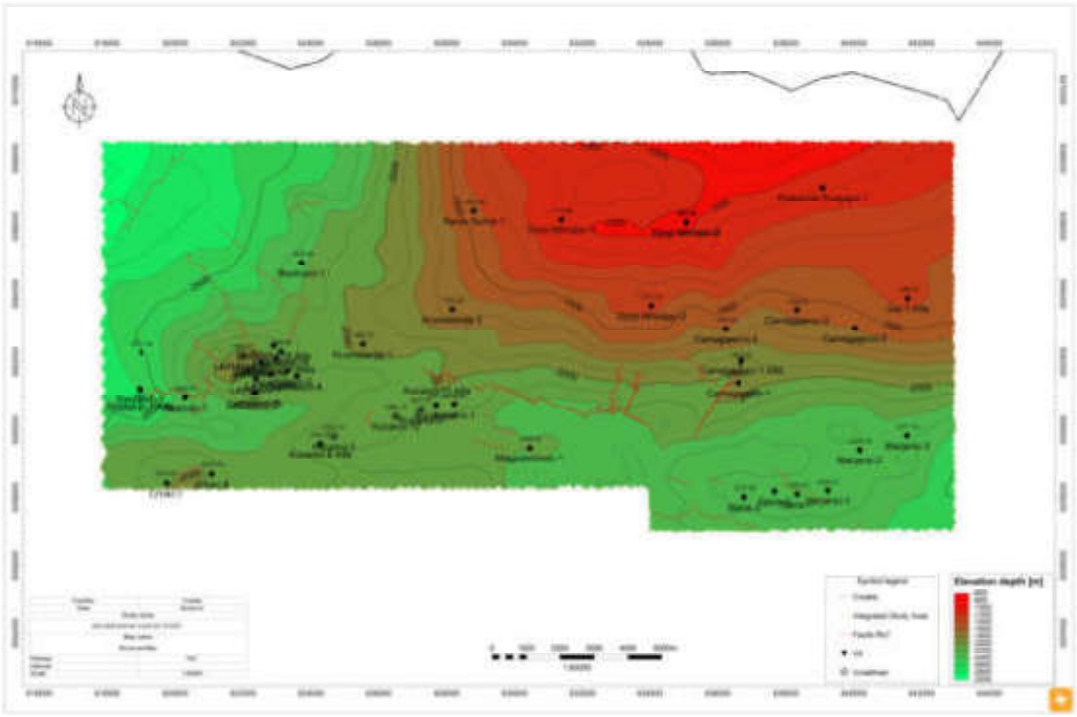


Fig. 2.86 'Rs7' Series (Top of Reservoir)
Structural map of Rs7 horizon

Copyright © SLB. All Rights Reserved. Private & Confidential. Reproduction only by permission.

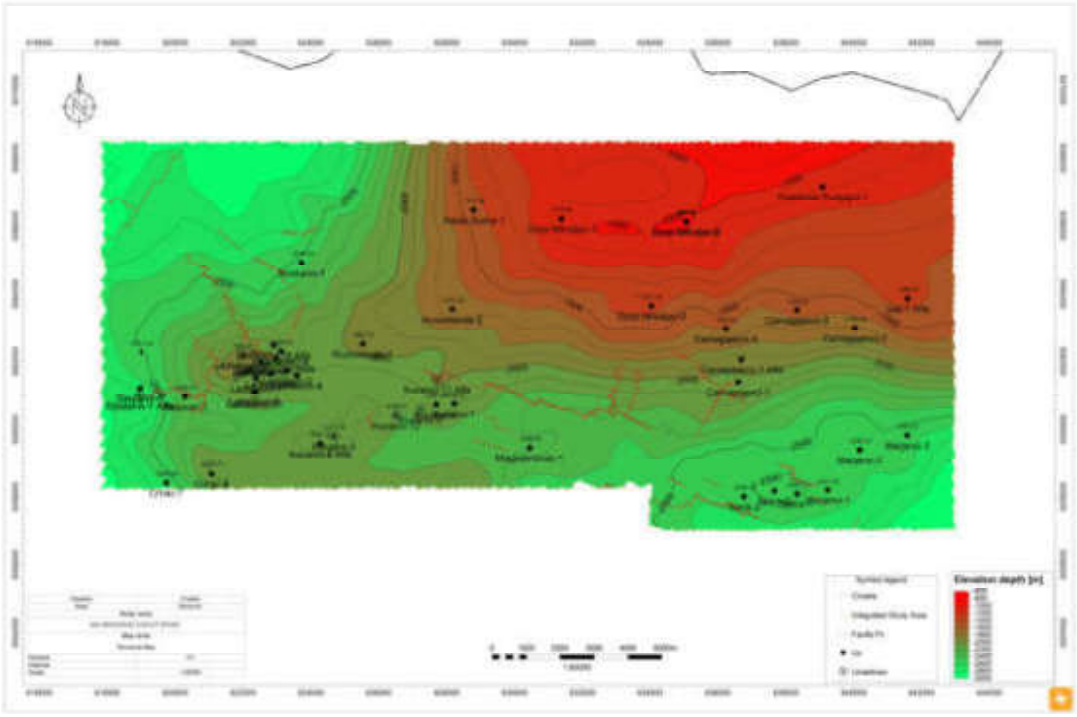


Fig. 2.87 'Pn' Series (Top of Reservoir)
Structural map of horizon Pn

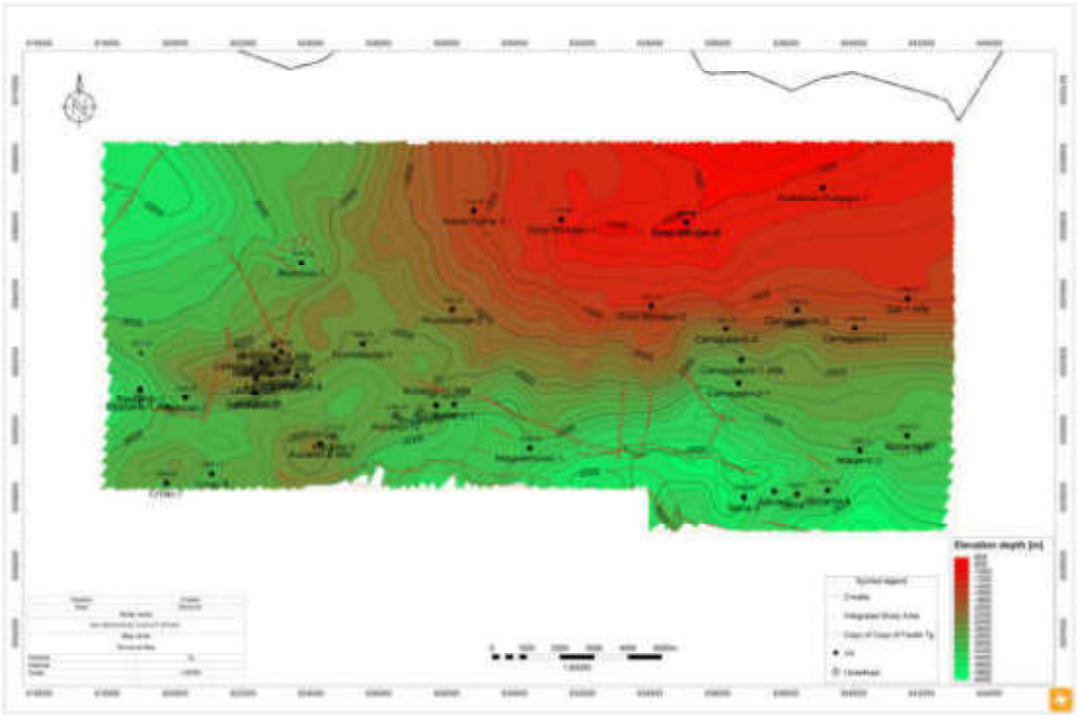


Fig. 2.88 'Tg' Series (Top of Formation)
Structural map of horizon Tg

Vertical model resolution was set up to 3 m to capture the vertical heterogeneity and at the same time to match the dynamic modeling requirements to number of cells in model.

Copyright © SLB. All Rights Reserved. Private & Confidential. Reproduction only by permission.



Fig. 2.89 Horizon modeling process input data

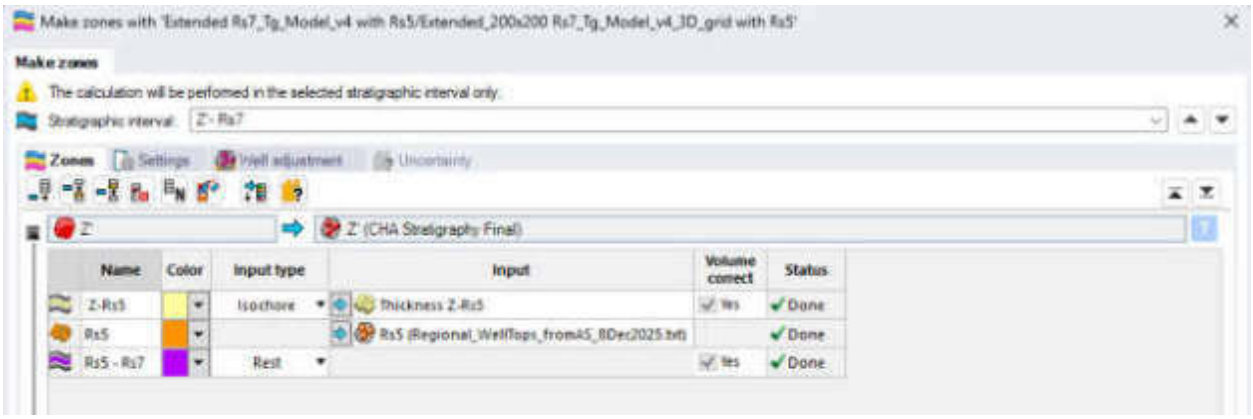


Fig. 2.90 Zone settings while modeling horizon Rs5

Property Modeling

PHIE and Vshale logs were created in petrophysical analysis and loaded to petrel as .las files. Well test data, such as DST-derived temperature and pressure, were incorporated into Petrel as well point data and upscaled to populate the model required for the geothermal potential estimation. Property modeling utilized the stochastic approach, generating 50 different realizations using Gaussian Random Function simulation method to capture statistical variability, later all output models were averaged using 2 approaches: mathematic mean average and median (P50) average estimation. Preliminary data analysis helped determine property distributions and preferential continuity directions. Certain stratigraphic intervals displayed omnidirectional variograms, while others showed distinct anisotropy or required dual variogram ranges. These insights were accounted for in the property estimation routines.Porosity distributions and Vshale distributions from all realizations were averaged using mean and P50 (median) methods.

Copyright © SLB. All Rights Reserved. Private & Confidential. Reproduction only by permission.

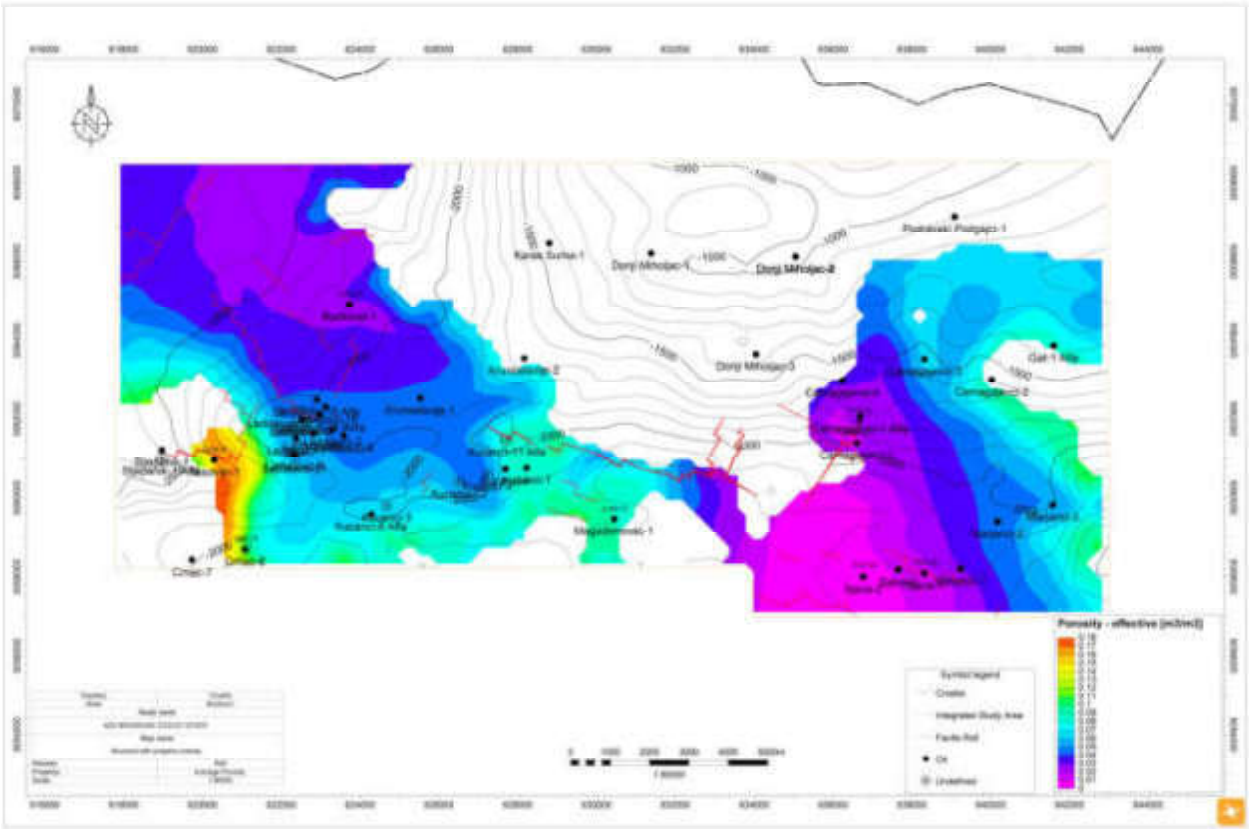


Fig. 2.91 Average porosity map for Rs5 zone

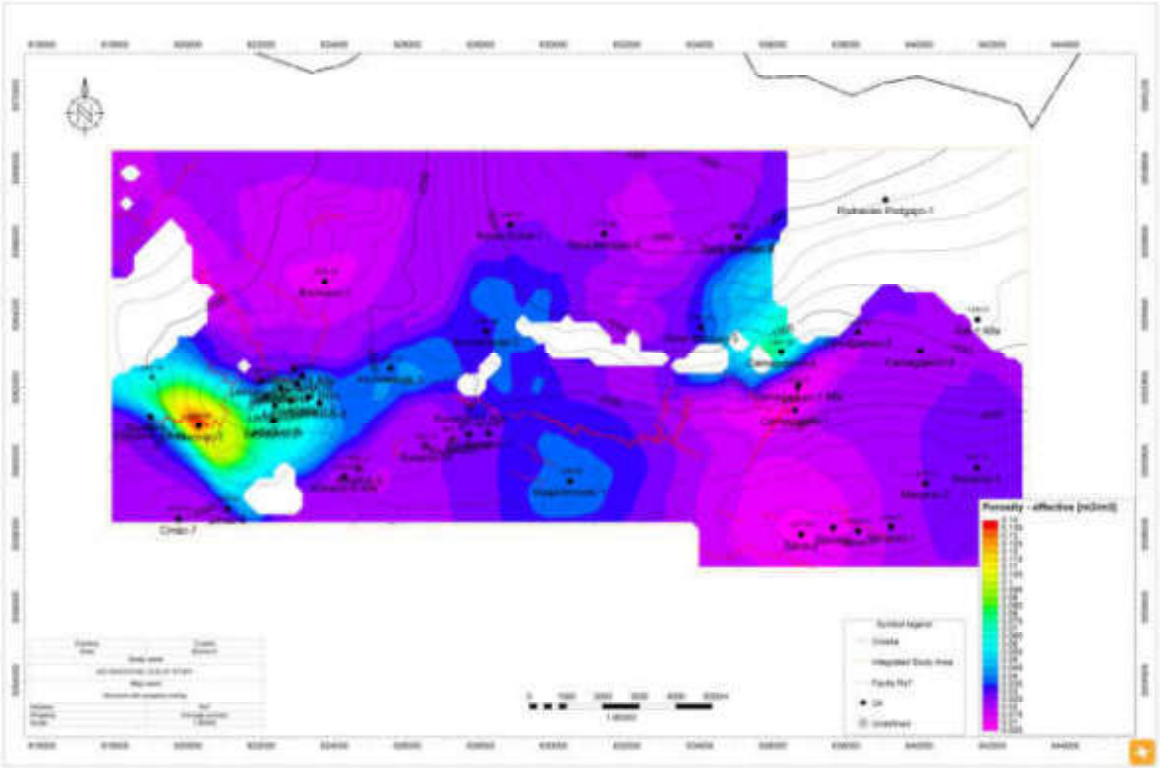


Fig. 2.92 Average porosity maps for Rs7 zone

Copyright © SLB. All Rights Reserved. Private & Confidential. Reproduction only by permission.

Permeability was calculated with differentiated equations depending on whether PHIE mean exceeded or fell below a threshold of 1.5 percent. High-permeability domains, particularly those associated with fault zones, were specifically modeled based on guidance from the petrophysical team. The cutoff criteria for net-to-gross was initially based on 3 % of PHIE and later refined to a permeability cutoff of 1 mD in response to evolving project requirements. Detailed explanation of correlation between porosity and permeability for the lower formations Fig. 2.55 is given in chapter 2.3.3 Petrophysical Analysis

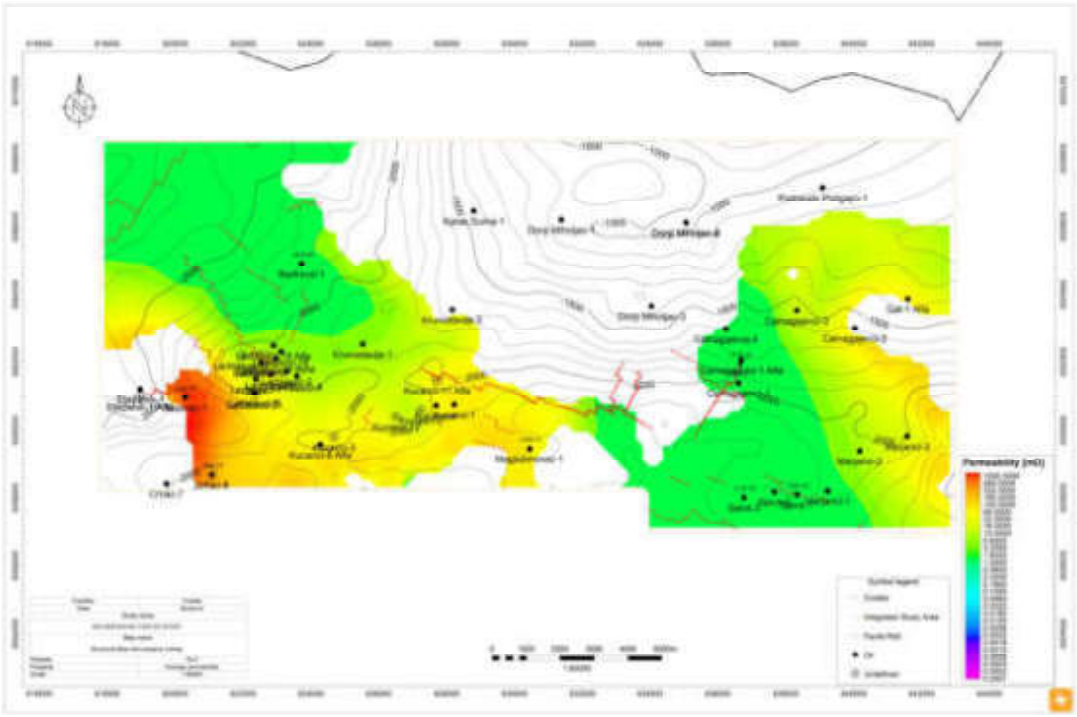


Fig. 2.93 Average permeability map for Rs5 zone

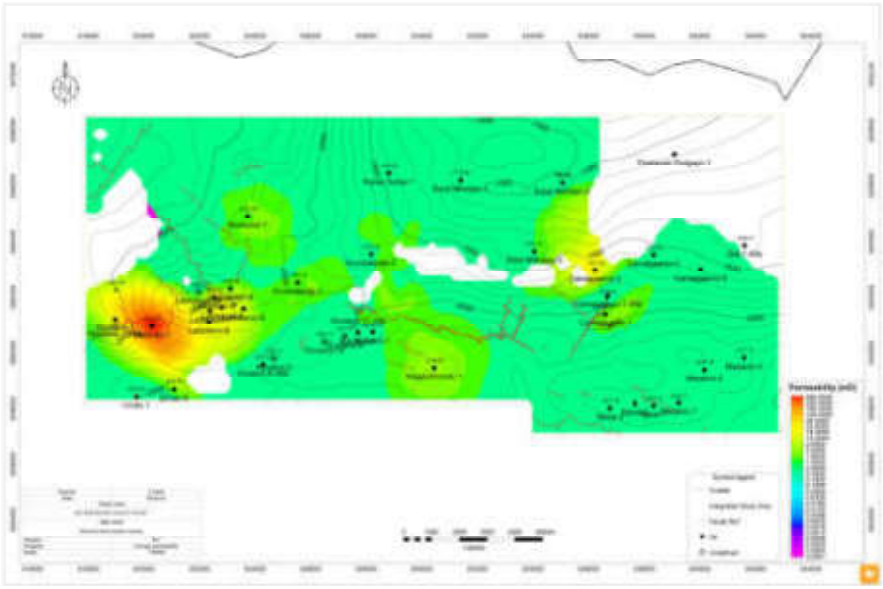
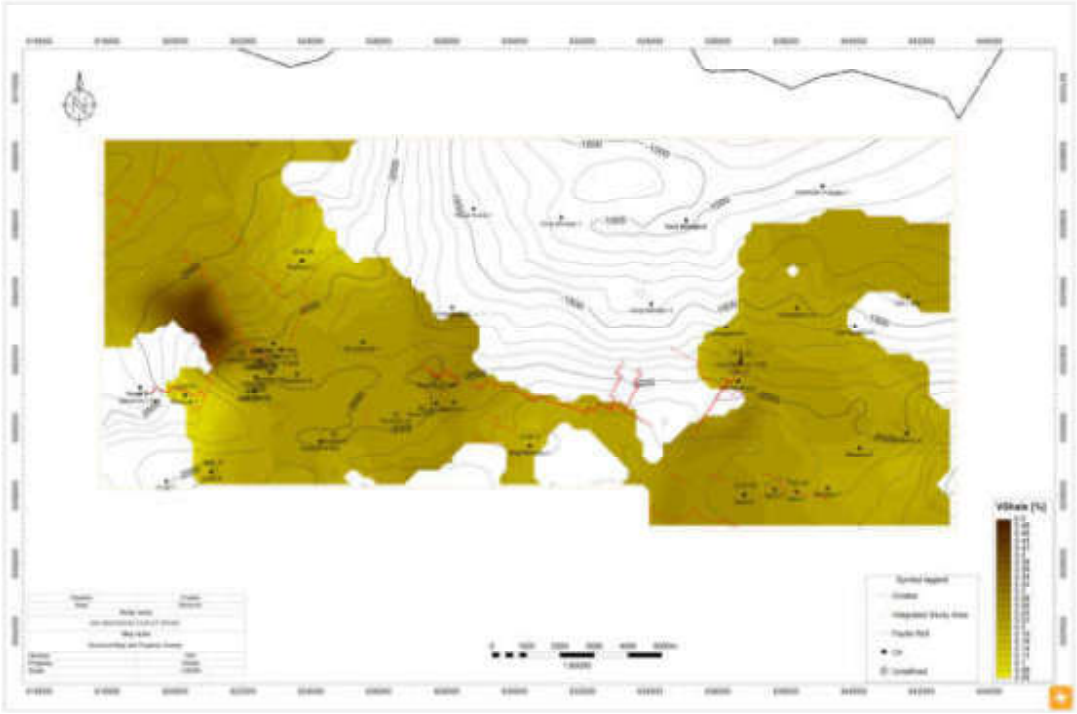


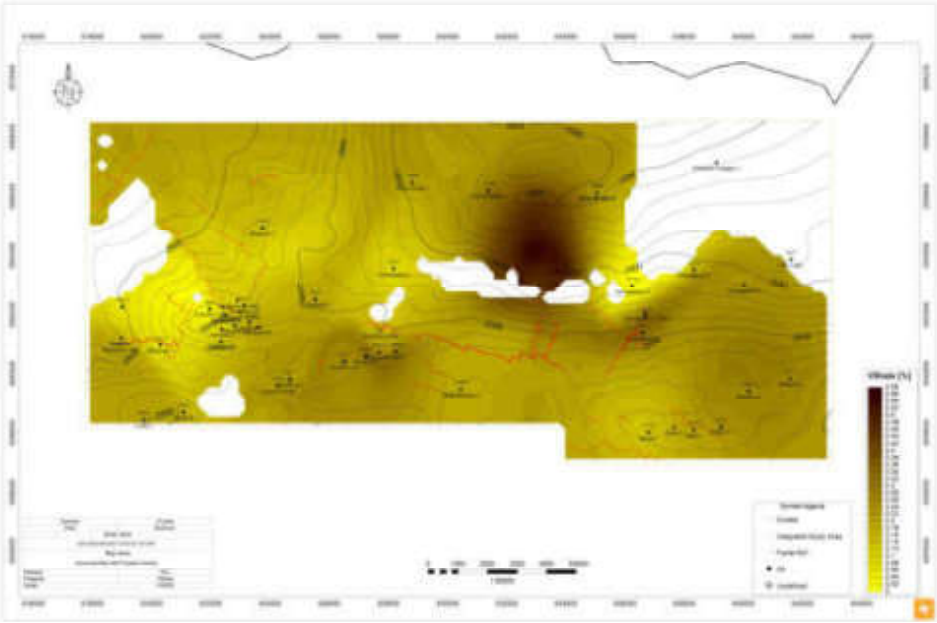
Fig. 2.94 Average permeability map for Rs7 zone

Copyright © SLB. All Rights Reserved. Private & Confidential. Reproduction only by permission.

Initially average Vshale value was used to define cut-off for NTG log, but taking into account changes in lithological composition of lower formation toward carbonates (calcite, dolomite with marls and sandstones and polymictic breccia) porosity and permeability show less correlation with Vshale then formations above Z' marker. PHIE and Vshale for Rs5 and Rs7 show low negative correlation that was not taken into account during the modeling of PHIE. Because of the same reason rocktypes RT property created based on was not used for PHIE model conditioning.



Average Vsh map for Rs5 zone



Average Vsh map for Rs7 zone

Copyright © SLB. All Rights Reserved. Private & Confidential. Reproduction only by permission.

Temperature and Pressure properties were built based on well point data loaded from DST reports. For modeling of Temperature and pressure data distribution was used Moving average algorithm that helped to distribute both properties preserving their dependence on Depth. For the part of the model below the last Temperature measurement was used linear relationship with elevation depth 0.0346567 * Elevation_general+ 47.4612.

Later both Temperature models (upper, estimated using Moving average algorithm, and lower, computed based using linear relationship with Elevation depth property) were merged into one model.

Lithology, Facies Modeling, and Volume Estimation

For the model created between Z' and Tg markers lithological classification relied on LITHO_FINAL log that was modeled using deterministic method – Kriging and data analysis to understand special distribution of facies classes. For most intervals, major and minor variogram ranges between 5,000 and 9,000 meters were observed, with anisotropy present throughout. LITHO_FINAL log contains some broad categories that contained all possible mixed facies like marlitic or sandy shale, etc. generally described in broad categories such as shale and sand, included more specific rock types when encountered.

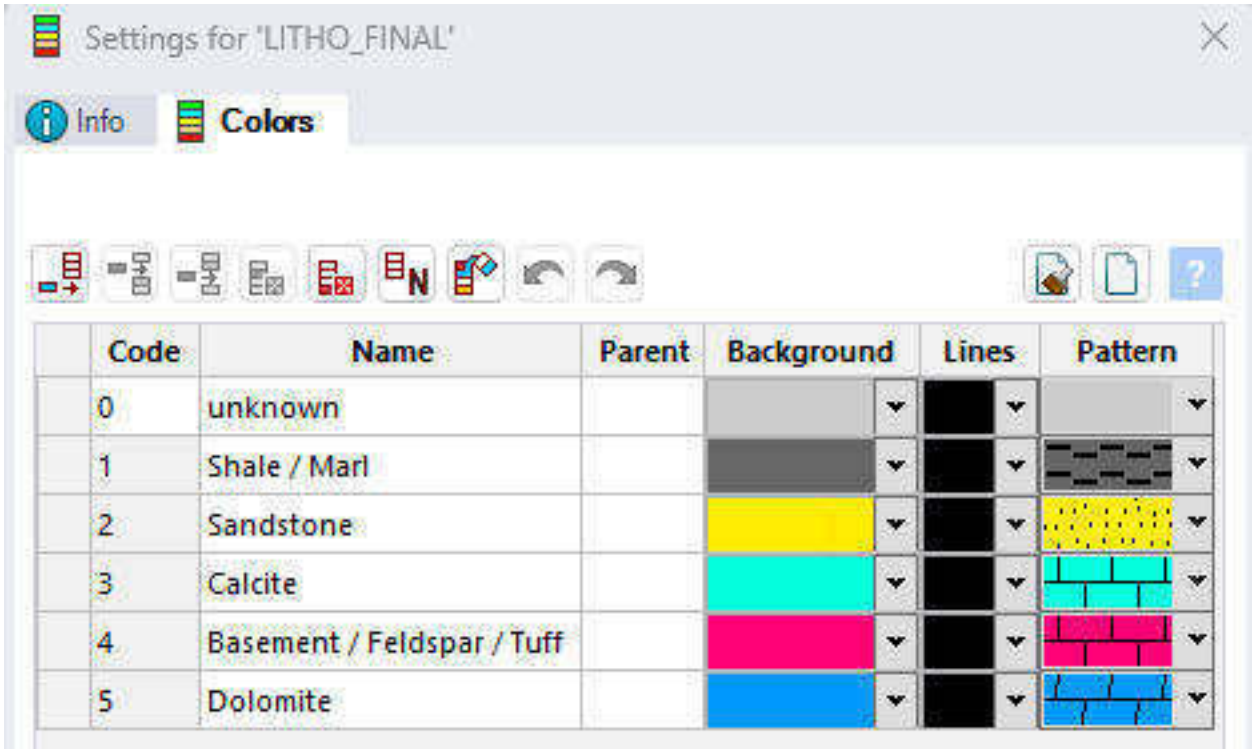


Fig. 2.95 Facies classes from LITHP_FINAL log

Later LITHO_FINAL model was used to add an efficiency coefficient into model, separate for calcite, dolomite and clastic rocks. It is also worth to mention that project has some descriptive logs like Lithology and Formations that was added using cutting reports from available dataset.

Copyright © SLB. All Rights Reserved. Private & Confidential. Reproduction only by permission.

Such logs were used for understanding of formation distribution in area of interest. Significant tufic sandstone was encountered only in one well, Sječe-2, which remains a point of geological curiosity although being described in some article (1).

Efficiency coefficients were assigned based on facies model, as input were used USA laboratory data and literature, such as Goodman (2014).
Three coefficients, P10, P50 (average), and P90, were employed based on available data to address uncertainty, associated with volume estimation.

Details of actual efficiency factors used in storage capacity estimation are described in the chapter 2.7.1.4 Volumetric estimation.

2.6 Geomechanical quicklook analysis

Geomechanics have an important implication to CCS screening and evaluation in relation to determination of the injection pressure limit, storage capacity and long-term integrity of storage site. This includes but is not limited to; estimation of fracture gradient (minimum in-situ stress magnitude), injection zone and cap rock integrity analysis, fault stability analysis. Due to that fact, a quick look 1D Geomechanics analysis was performed for two key offset wells, Bockovci-1 and Sjece-2 to estimate fracture gradient profile and support dynamic simulation for selected candidate sites by determining the injection pressure limit.

The caprock integrity and fault stability were not analyzed here since these aspects were not part of scope and would require 3D geomechanical modelling for them to be adequately evaluated. Therefore, executing 3D geomechanical modelling and performing mentioned analysis is strongly recommended during the CCS feasibility study phase.

The analysis executed here is based on limited information available in these two wells, supported by additional drilling tests results (leak-off tests) found in additional two wells (Rasovac-1 and Krunoslavje-2). Most of the wells in the area are old and no modern log data, borehole images or geomechanical core test results are available. Also, log data in analyzed wells does not cover interval above Alpha formation. Finally, the information related to drilling process and drilling challenges/observation (such as tight holes, pack-offs, cavings, stuck pipes, losses etc.) that would help to calibrate the geomechanical model are also very limited.

All of above leads to the fact that current model is to be considered a quick look analysis with significant uncertainties both in terms of fracture gradient magnitude as well as the wellbore stability results. Therefore, as mentioned above it is recommended to perform more in depth geomechanical study (including 3D geomechanical modelling) when more data is acquired allowing better subsurface characterization. This data (notably seismic, modern logs/images, core data and well tests) should be acquired in new well(s) to be drilled in candidate sites, to reduce the uncertainty and improve geomechanics understanding of the sites enabling further evaluation of the CCS injection condition, long-term integrity of the injection zone and caprock as well as nearby faults stability.

Copyright © SLB. All Rights Reserved. Private & Confidential. Reproduction only by permission.

The quick look analysis performed here focused on two wells located close to candidate CCS injection sites, for which petrophysical interpretation was executed in the earlier phase of this study. The results of these interpretations such as synthetic compressional slowness calculated for intervals where it was missing (as described in section 2.3.2 Log Quality Control and Log Prediction) as well as derived volume of shale profiles, were used in geomechanical analysis. Additionally, a further minor geomechanics oriented conditioning of compressional slowness (consisting of despiking) and bulk density (replacing the low values in intervals with hole enlargement with synthetic values) were executed, since these logs are fundamental for geomechanical analysis. Shear slowness was not available in any of the wells in studied area; hence a synthetic shear slowness was computed employing a Castagna correlation.

A constant pore pressure gradient was considered based on information available from DST measurements. Majority of the DST tests for the wells in this area showed low mineralization and sub normal hydrostatic pore pressure (see 2.8.2 Input data overview for more information). This is also the case for two wells analyzed, for which the key available DST test results reported 0.88g/cm3 EMW in the Pn formation for Bockovci-1 (0.89g/cm3 EMW was reported in Rasovac-1 well in the same formation) and 0.97g/cm3 EMW in the D formation for Sjece-2 well. An additional DST test available in Sjece-2 reported higher pore pressure of 254 bar for the interval 2275-2390 m MD (2181-2292 m TVDSS) corresponding to bottom of the Z and top of the Rs7 formation, translating to the EMW of 1.08-1.14g/cm3 for this depth interval (see blue points on track 9 on Fig. 2.99). Among all wells in the area this is an exception though, along with well Marjanci-3 where pore pressure of 1.026g/cm3 and 1.08g/cm3 were reported in the Pn formation. The higher pressure reported in Sjece-2 was not considered in this analysis since it would require further investigation to try to understand its validity and extent, as well as since for carbon capture and storage the lower pore pressure is more conservative (safer) value to consider in terms of safe injection pressure definition. Nevertheless, some local complexity may be present in terms of pore pressure in the area, hence further pore pressure information should be acquired in the wells to be drilled in the candidate sites.

The wellbore stability analysis was conducted and constrained with available measurements (DST, LOT, calipers) and drilling observation. Wellbore stability (also referred to as mud weight window) is defined by four boundaries (Fig. 2.96 and Fig. 2.97), two lower boundaries (pore pressure gradient and shear failure gradient (hole instability)) and two upper boundaries (mud loss and tensile failure gradients). In general, these boundaries can cross each other depending on stress conditions. In the more typical case, we have:

1. The first lower boundary is the pore pressure limit, which should be exceeded to maintain an overbalance in the well and avoid kicks
2. The second lower boundary on Fig. 2.97, which should ideally be exceeded by mud weight, is the shear failure limit. If the mud weight drops below this limit (represented by red shading on Fig. 2.96), compressive shear failure at the wellbore wall occurs. This can lead to diametrically opposite pair of breakouts. Also, when drilling at lower relative hole angles to the bedding, except shear failure related to rock matrix itself, also plane of weakness failure i.e. shearing along shale bedding can also take place
3. The first upper bound (i.e. mud loss) is defined by the least principal stress (minimum

Copyright © SLB. All Rights Reserved. Private & Confidential. Reproduction only by permission.

horizontal stress in this case, blue shading). When the mud weight exceeds this limit mud losses can start to occur as a result of pre-existing fractures being opened. This can lead to fractured formation instability as fractures are propagated and drilling fluid is lost to the formation followed by drop in Equivalent Circulation Density (ECD)/Equivalent Static Density (ESD) during connections or pulling out of hole. Faults that have intersected the well path can also be reactivated if this boundary is exceeded

4. The second upper bound is the tensile failure of the rock (represented by black shading on Fig. 2.96). This is caused when the mud weight is too high. The wellbore wall is put into tension, and the tensile strength of the rock is exceeded. Formation breakdown occurs, and unstable fracture propagation takes place. Severe mud losses can occur when this pressure and mud loss pressure are exceeded at the same time in intact formations

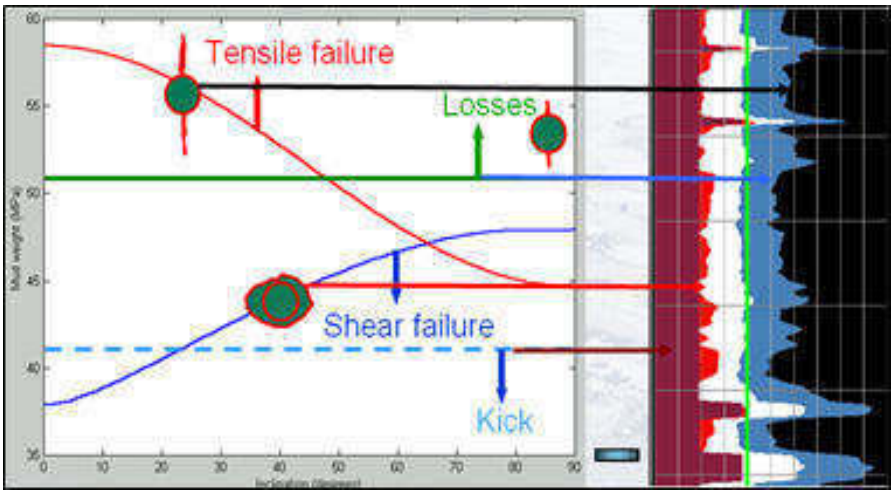


Fig. 2.96 Illustration on the wellbore stability analysis interpretation.
(green line illustrates potential mud weight)

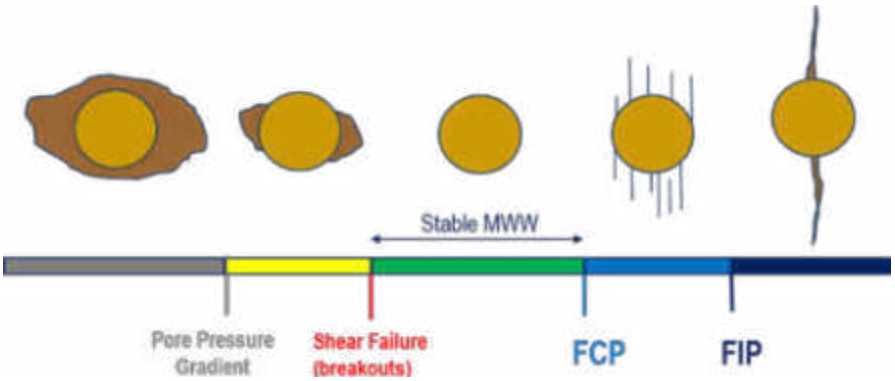


Fig. 2.97 Wellbore Stability window limits.

The Fig. 2.98 and Fig. 2.99 shows the geomechanical results for Bockovci-1 and Sjece-2 wells, with profiles of estimated elastic (track 6) and rock strength (track 7) parameters, stress profiles (track 8) and wellbore stability (track 9) results. Along well Bockovci-1 the two leak-off test results performed in Rasovac-1 were plotted (pink points on track 9) and were used for model calibration. These leak-off tests were executed at 1228m MD under 9 5/8in casing shoe (1224m MD) reporting 2.19g/cm3 and at 1254m MD reporting 1.61g/cm3 equivalent mud weight (EMW).

Copyright © SLB. All Rights Reserved. Private & Confidential. Reproduction only by permission.

These depths correspond stratigraphically to the base of the Alpha formation, which is observed at very similar depth in Bockovci-1 well. No further details for these tests or graphical representation were available that would allow to better understand this test and QC values reported. Hence, it is not clear if the shallower test resulted in the formation breakdown (creating a tensile fracture). The deeper test result reporting lower value was considered as a limit for drilling purposes at the time of drilling, and the same value was considered here to calibrate minimum in-situ stress magnitude (fracture gradient). Besides these tests, the only additional leak-off test information was found for well Krunoslavje-2, where the test was executed at 1593m MD under 9 5/8in casing shoe (1588m MD) in top of the D formation, with equivalent density reported as "1.60+x g/cm3". Again, no further information was available. It can be only assumed that this was either an FIT performed up to 1.60 g/cm3 EMW with no leak-off observed, or leak-off pressure deflection point was not clear but was suspected somewhere above 1.60 g/cm3. In any case, the lower value reported in Rasovac-1 remains the key currently available calibration data used for constraining the fracture gradient magnitude.

In terms of stress direction, a 10 deg from the North was considered for maximum horizontal stress direction based on regional understanding.

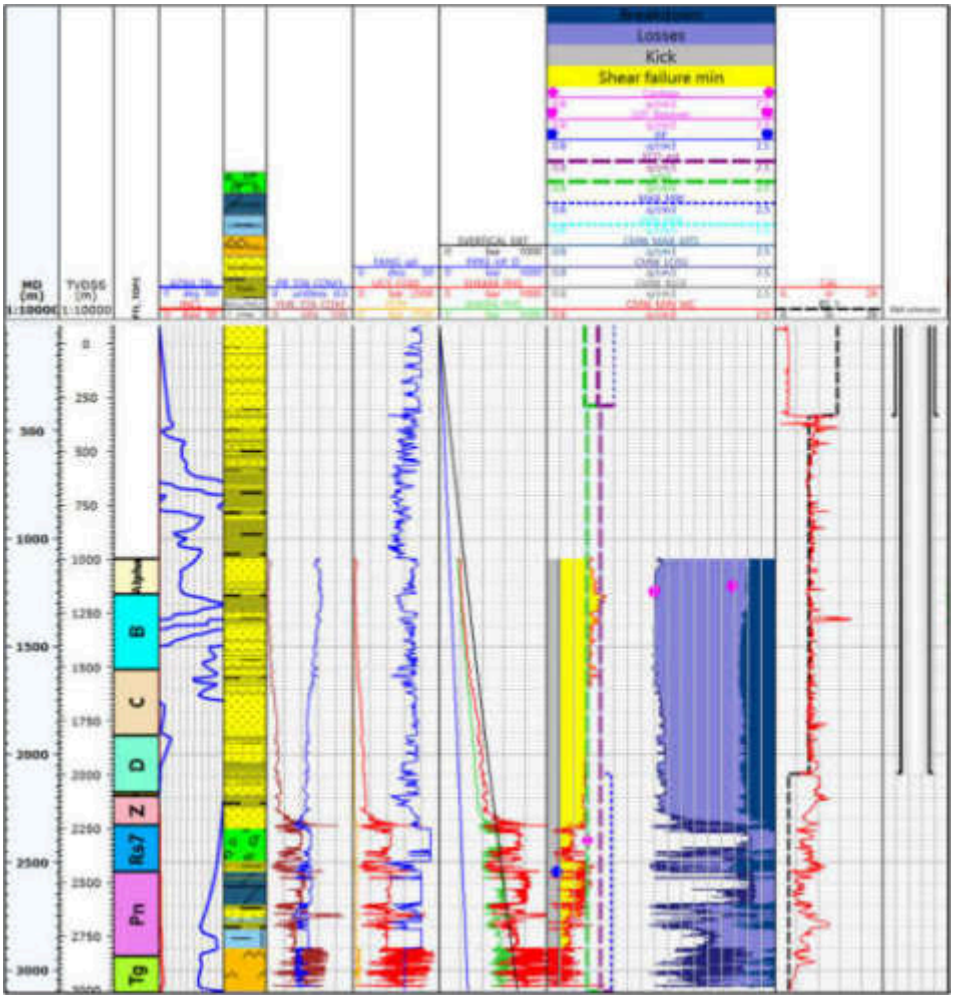


Fig. 2.98 Bockovac-1 1D Mechanical Earth Model results.

Copyright © SLB. All Rights Reserved. Private & Confidential. Reproduction only by permission.

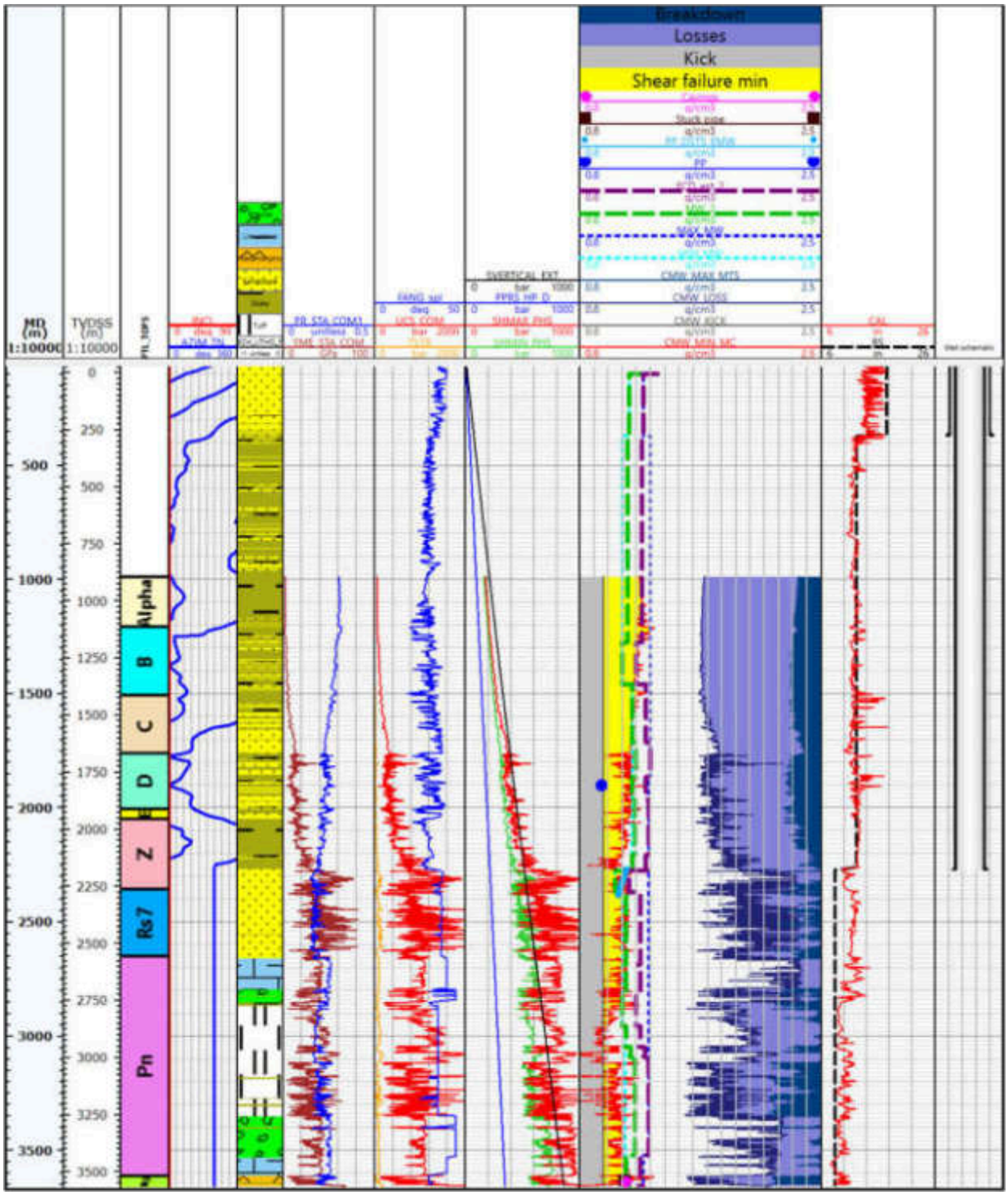


Fig. 2.99 Sjece-2 1D Mechanical Earth Model results.

The frac gradient in Bockovci-1 is very close to the lower value reported in Rasovac-1. The breakdown threshold can be seen certain amount above the shallower leak-off test result reported in Rasovac-1, since no clear information was found in available reports that would suggest that formation was fractured during the test. The minimum in-situ stress magnitude (fracture gradient) is

Copyright © SLB. All Rights Reserved. Private & Confidential. Reproduction only by permission.

typically expected to be lower or equal to leak-off pressure. Fracture gradient was calibrated here to fall only slightly below reported leak-off pressure since lower frac gradient would bring the breakdown threshold lower, potentially below the shallower leak-off test result, suggesting the formation was fractured during the test. Number of uncertainties exist both in terms of test itself and model parameters, which cannot be currently better constrained and this is acknowledged during the process of maximum injection pressure limit determination by applying 0.9 multiplier (safety factor) on lower limit of calculated fracture gradient as illustrated on Fig. 2.100. This approach was applied for injection wells at analyzed sites as shown later in reservoir simulation section of this report (2.8.5.2 Pressure validation and distribution).

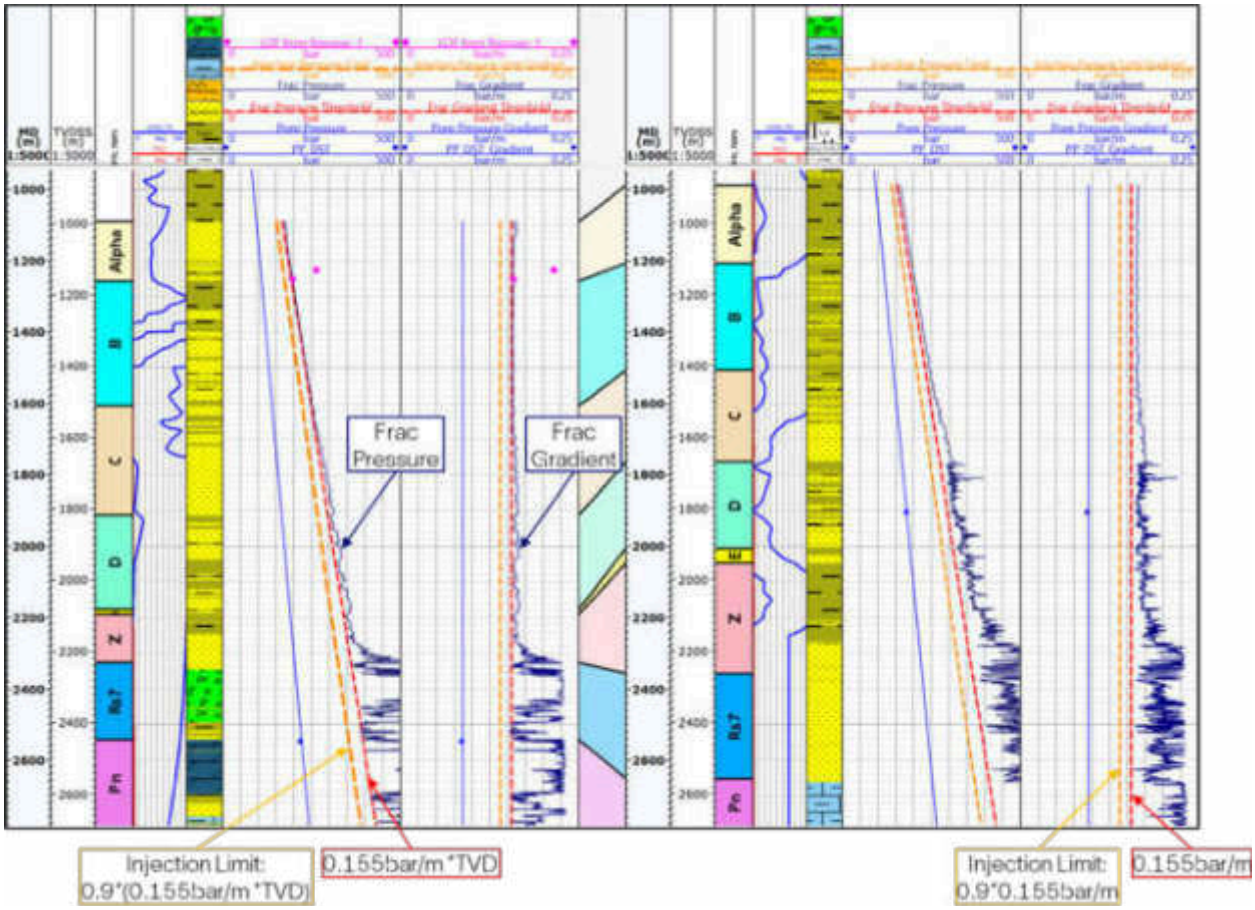


Fig. 2.100 Injection limit definition based on calculated fracture gradient for Bockovci-1 and Sjece-2.

In terms of wellbore stability result (i.e. shear failure threshold) for these wells, as mentioned earlier, limited information was available to understand drilling problems and to calibrate the model. Only a single diameter caliper was available in all wells in the area, except for most recently drilled well Krunoslavje-2, where 4-arm caliper was available. However, this caliper covered the breccia interval, hence enlargement observed on it may be potentially related to breccia falling into the wellbore due to mechanical effect while drilling rather than due to shear failure driven wellbore instability. The predicted shear failure for two analyzed wells shows overall a fair agreement with single diameter caliper, particularly in 12.25in hole section. In 8.5in hole section a larger caliper enlargement can be observed, which can be related in some cases to the breccia drilling mechanics related enlargement, in some other intervals potentially to drilling mechanics related

Copyright © SLB. All Rights Reserved. Private & Confidential. Reproduction only by permission.

fractured rock enlargement. Few drilling observations were reported in these wells consisting of cavings and single stuck pipe incident. In Bockovci-1 cavings were reported (see pink rhomb on track 9 of Fig. 2.98), however the depth corresponds to breccia hence these may represent drilling mechanics related breccia enlargement (breccia clasts). Cavings were also reported in Sjece-2, close to the well TD in metamorphic formation (see pink rhomb on track 9 of Fig. 2.99) with stuck pipe also being reported at the same depth. This can also be related to breccia interval higher up or fractured rock in limestone or in metamorphic interval itself. However, the model does predict hole instability in top portion of metamorphic formation which can also be responsible for cavings reported.

Furthermore, caliper enlargement in some intervals can also be related to lower dynamic wellbore pressure (swabbing) during tripping or potentially to some extent to thermal effect (formation heating up leading to higher shear potential). Currently, there is no understanding of potential swabbing or extent of thermal effect while drilling these wells. The wellbore stability results presented on Fig. 2.98 and Fig. 2.99 do not account for thermal effect. Wellbore cooling reduces the breakdown threshold that may result in creation of tensile drilling induced fractures if mud weight or wellbore pressure exceeds this threshold. In contrast, heating the wellbore increases the shear failure threshold hence the potential for wellbore instability. It is to be highlighted that higher impact for the same amount of cooling or heating is expected for stiffer (deeper) rocks compared to softer (shallower) rocks. Thermal effect could be further evaluated in the future once more data becomes available.

The normal fault stress regime (i.e. vertical stress being the higher in magnitude) is expected across CCS perspective interval until Z formation. A normal fault closer to strike slip stress regime (i.e. with maximum horizontal stress getting close to vertical stress) is modelled for portions of C to D formations in Sjece-2 well. Mostly strike slip stress regime (with vertical stress being intermediate in terms of magnitude) is expected in deeper and stiffer formations, with normal fault stress regime locally in softer intervals.

The implication of normal fault stress regime in the intervals of interest for CCS is such that in case of deviated wells, a higher potential for hole instability and consequently higher mud weight would be required to maintain hole stability compared to vertical wells drilled in the past. Furthermore, for wellbores with higher deviation also the threshold for drilling induced fractures (breakdown) will be getting lower, which can be further reduced by effect of cooling of the wellbore, although the latter effect is not expected to be significant in this interval due to rather low stiffness of these formations. The breakdown threshold in deviated wells may approach the fracture gradient or even become lower. The latter scenario is not considered likely in these formations and could be more likely in deeper stiffer formations. However, such scenario cannot be fully excluded for deeper part of CCS perspective interval (depending on well deviation/orientation, elastic properties, level of cooling, far field stress magnitudes etc.). As long as the wellbore pressure is maintained below fracture gradient this is not a major issue for drilling, since drilling induced fractures even if created will be shallow. However, if the wellbore pressure exceeds fracture gradient these fractures may be propagated increasing in size and resulting in mud losses. Creating induced fractures is also not desirable for CCS operation since these might be propagated if fracture pressure gradient threshold is exceeded. It is critical to maintain injection pressure below fracture gradient for

Copyright © SLB. All Rights Reserved. Private & Confidential. Reproduction only by permission.

injection zone and cap rock, hence it is important to improve local geomechanical condition understanding via further data acquisition and 3D geomechanical modelling evaluating injection zone and caprock integrity to mitigate the risk of compromising storage integrity.

In terms of losses related observation, some losses were reported in Krunoslavje-2 well at the end of 12.25in hole section during casing and cementing operation, that could be related to shallower permeable formations. Losses were also reported in Rasovac-1 well in 12.25in hole section across limestone interval with low mud weight of 1.12g/cm3 which were probably related to presence of natural fractures.

The Fig. 2.101 and Fig. 2.102 show predicted by current model single depth analysis results for expected variability in shear failure threshold and breakdown threshold respectively with hole deviation and azimuth, for two example depths relevant to formations (B and D) perspective for CCS. These examples are calculated based on model presented on Fig. 2.98.

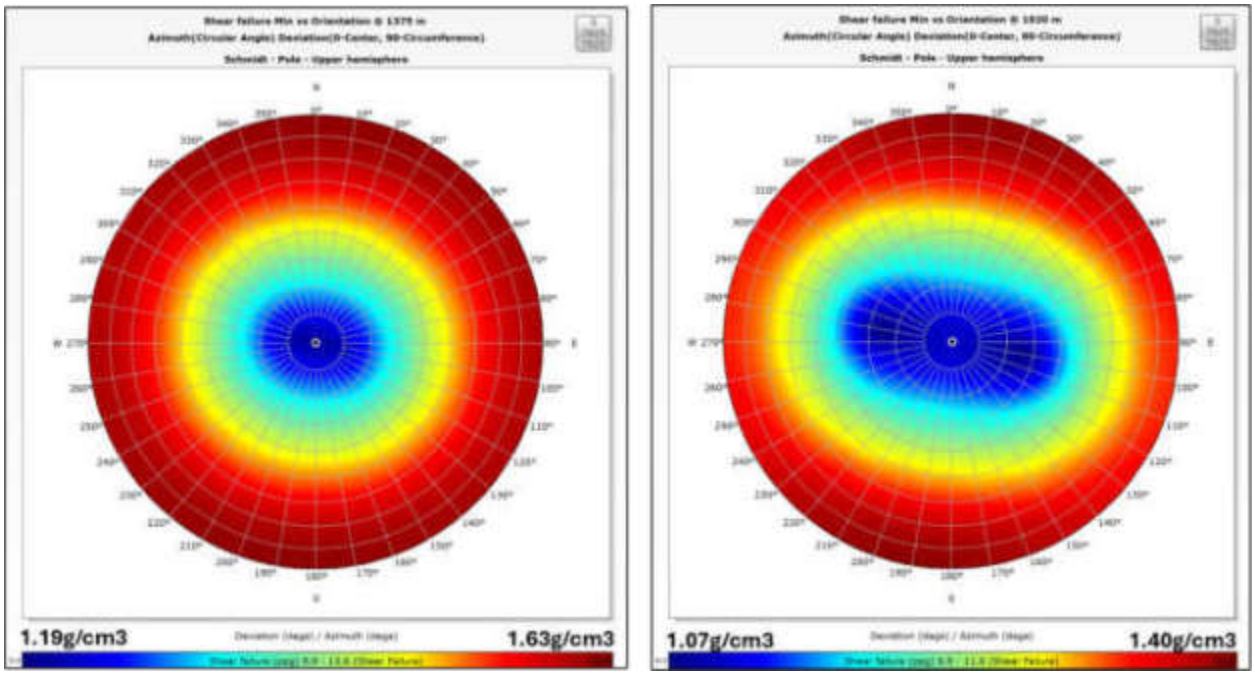


Fig. 2.101 Bockovci-1 single depth analysis of shear failure threshold variation with hole angle and azimuth.
Based on current model for 1375m MD (left) and 1930m MD (right).

Copyright © SLB. All Rights Reserved. Private & Confidential. Reproduction only by permission.

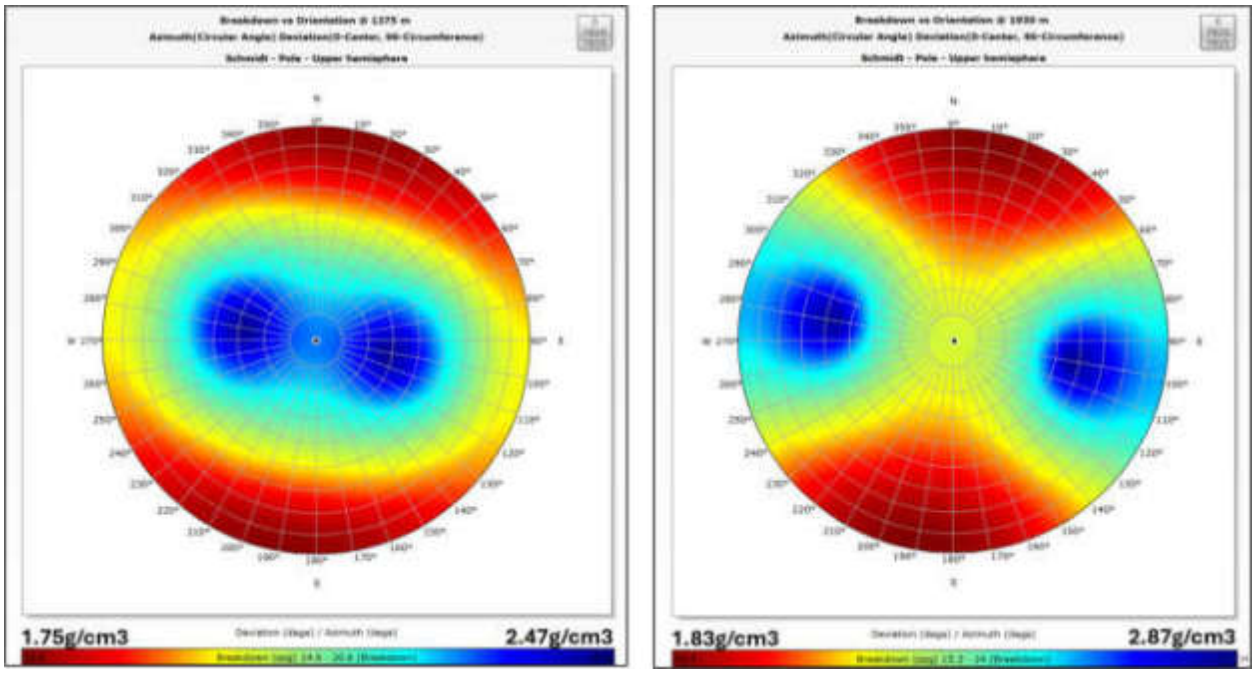


Fig. 2.102 Bockovci-1 single depth analysis of breakdown threshold variation with hole angle and azimuth.
Based on current model for 1375m MD (left) and 1930m MD (right)

In order to reduce the uncertainty in the model and improve the geomechanical understanding of the subsurface, it is recommended to acquire further data in new well(s) to be drilled in the candidate sites:

- Acquire modern logs, particularly compressional and shear slowness, bulk density, borehole images and multi-arm caliper (if feasible) in reservoir and overburden

- Acquire the core and perform geomechanical core testing both for injection zones and cap rock intervals, for elastic properties (Young's modulus and Poisson's ratio) and strength parameters (unconfined compressive strength, tensile strength and friction angle)

- Acquire further pore pressure measurements to better understand local pore pressure conditions

- Ideally perform insitu stress tests (such as MDT-Stress or equivalent) to constrain fracture gradient

Above data could be then used to perform further more in depth 1D and 3D geomechanical modelling to constrain the model and to evaluate long term CCS injection and storage integrity. The 3D modelling would benefit from 3D seismic inversion results and refined static and dynamic subsurface models to be created based o acquired logs, well tests and 3D seismic processing results.

Copyright © SLB. All Rights Reserved. Private & Confidential. Reproduction only by permission.

2.7 CCS site screening

The primary objective of site screening is to identify the most suitable location that satisfies all critical selection criteria while maintaining an acceptable risk profile. At this early stage—particularly for saline aquifers—limited data availability can inflate perceived risks. As additional data are acquired and analyzed, these risk assessments are expected to evolve and may be refined accordingly.

Depleted reservoirs and saline aquifers differ primarily in the level of geological understanding and the degree of certainty associated with their storage performance. Depleted reservoirs, as former hydrocarbon accumulations, benefit from extensive subsurface data derived from historical exploration and production activities. This typically includes well-constrained estimates of porosity, permeability, and seal integrity, providing a higher level of confidence in storage behavior. However, the presence of legacy wells—often with uncertain abandonment or completion integrity—represents a potential leakage pathway and must be rigorously evaluated prior to any storage operations.

By contrast, saline aquifers generally offer significantly larger storage capacity due to their widespread distribution but are typically less well characterized. The absence of prior exploitation results in greater uncertainty in key parameters, including reservoir quality, caprock integrity, and long-term containment performance. As a result, saline aquifers require more comprehensive data acquisition and appraisal to reduce uncertainty and demonstrate suitability for CO_2 storage. Despite these challenges, they remain a critical component of large-scale storage portfolios.

In summary, depleted reservoirs provide more predictable and higher-confidence storage opportunities, whereas saline aquifers offer greater theoretical capacity but carry higher uncertainty and require more extensive characterization.

A robust and integrated surface and subsurface evaluation is therefore essential to identify viable CO_2 storage sites. The first and most critical step is the clear delineation of the storage site boundaries and extent:

- **For depleted reservoir screening:** A site encompasses the entire depleted field, vertically incorporating all exhausted zones (potential storage units), their overlying seals, and all associated surface operations.
- **For saline aquifer screening:** A site must be delineated by thoroughly evaluating all relevant surface and subsurface risk factors. Only those areas demonstrating an acceptable risk profile should be selected for subsequent, detailed analysis.

In practice, site screening should systematically address three primary scenarios:

1. **CO_2 injection into depleted gas reservoirs:** Screening focuses exclusively on depleted field areas.
2. **CO_2 injection into the water leg of depleted fields:** This approach allows the CO_2 plume to gradually migrate up-dip, enabling additional trapping mechanisms, and requires integrated

Copyright © SLB. All Rights Reserved. Private & Confidential. Reproduction only by permission.

screening of both depleted fields and adjacent saline aquifers.

3. **CO_2 injection into saline aquifers:** Screening centers solely on aquifer systems with suitable characteristics.

An effective approach for evaluating storage potential is the creation of a Chance of Success (CoS) map. A CoS map provides a spatially resolved, quantitative assessment of the probability of achieving a successful outcome in a specified area, factoring in a comprehensive set of risks and uncertainties. Specifically, for carbon storage site selection, the CoS map synthesizes geological, technical, environmental, and regulatory parameters to rigorously assess the likelihood that a given location can safely and reliably serve as a long-term CO_2 storage site. This integrative tool enables informed, data-driven decision-making, ensuring that only high-probability, low-risk areas are prioritized for project development.

2.7.1 Methodology

In our approach to selecting potential CO_2 storage sites, we start by ruling out areas that are protected, populated, or already have wells and fields with known integrity issues. To do this, we use a "**distance-to**" or buffer method: for each sensitive feature—like protected zones, towns, existing wells, and faults—we generate a map showing how far every point is from that feature.

As a fundamental principle, a safety buffer is established around sensitive area, such as protected environments, residential zones, wells, and faults. For example, in the Bockovci area, a minimum exclusion distance of **250 meters** was applied. This buffer requirement is designed to minimize potential environmental impact and uphold safety for surrounding communities, ecosystems, and existing infrastructure.

Within these defined exclusion zones, the suitability score is set to "**0**" designating a strict "**no-go**" area. Beyond the buffer, the score increases linearly with distance, reaching a value of "**1**" as risk diminishes—this reflects the benefits of greater separation from sensitive features.

Multiple spatial layers are constructed and integrated—covering geological characteristics, reservoir depth, caprock integrity and extent, legacy wells, structural faults, and proximity to infrastructure, protected regions, and residential areas, among others. The composite suitability map is generated by combining, typically through multiplication, all individual scoring layers.

As a result, any location scoring "zero" in a single criterion is eliminated in the final map, ensuring that non-viable areas are systematically excluded from further evaluation. Regions with a composite score greater than zero indicate that all minimum requirements are at least partially fulfilled, signifying their potential as candidates for CO_2 storage.

To visualize this process, refer to the collage provided: Fig. 2.103. It includes an example of a "**distance to**" map that illustrates the buffer zones around protected or sensitive areas, the set of individual Chance of Success (CoS) maps for different criteria, and the resulting final suitability map produced by multiplying these layers together.

Copyright © SLB. All Rights Reserved. Private & Confidential. Reproduction only by permission.

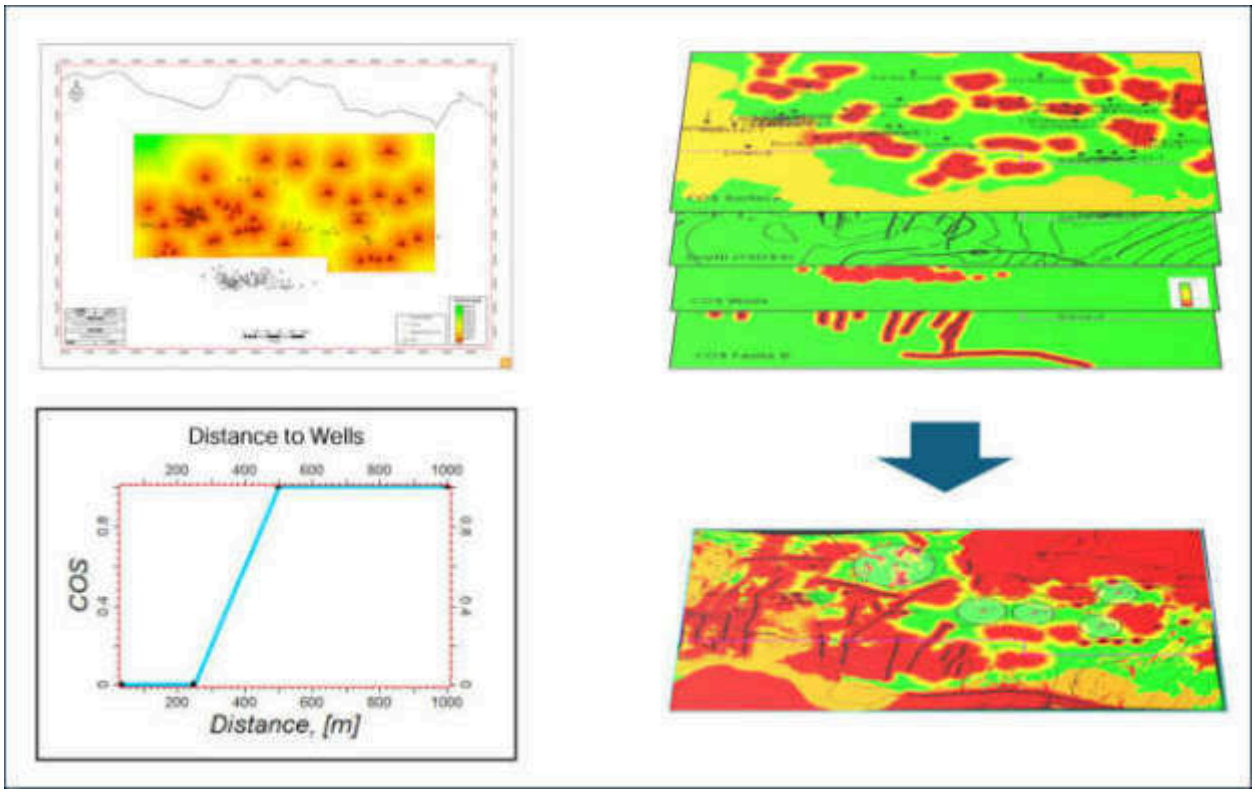


Fig. 2.103 Principle for Chance of Success Mapping
Top left: Distance to Wells; Bottom Left: Score based on distance; Top right: Chance of Success Map for each criteria; Bottom right: Final COS Map, result of multiplication

2.7.1.1 Eligibility Criteria

The minimum site selection criteria is normally part of the site screening and site selection phase, and is established before even project begins. At this stage, the main goal isn't to optimize or find the perfect site, but rather to eliminate any options that carry unacceptable risk.

Some criteria serve as absolute "**Go**" or "**No Go**" filters, immediately ruling out unsuitable sites. These are called "hard" requirements Fig. 2.104, where any deviation can cancel the project entirely. Others are influenced by stakeholder objectives, government regulations (if applicable), and the organization's own tolerance for risk. There are also "soft" criteria that define boundary conditions that must be satisfied before progressing, which are used more flexibly to help narrow down the sites with the highest likelihood of success.

Copyright © SLB. All Rights Reserved. Private & Confidential. Reproduction only by permission.

Criteria	Site 1	Site 2
Capacity		
Storage capacity meets the requirements	true	true
The depth of the shallowest point in the reservoir is greater than 800m.	true	true
Containment		
Far away from presence of legacy wells with integrity issues	true	false
Other		
Environment: The surface environmental context doesn't prevent the CCS project from taking place (example: large populated area, protected area, national patrimony)	true	true

Fig. 2.104 Eligibility Criteria

Capacity:
There should be no clear capacity constraint that would prevent the storage project from moving forward. Specifically, the shallowest part of the reservoir must be deeper than 800 meters. This threshold is critical because it ensures that CO_2 will stay in a dense, supercritical state—leading to more efficient storage, less movement, and better long-term containment. It also guarantees appropriate pressure and temperature conditions and reduces the risk of buoyancy-driven leaks. If either the volumetric capacity or the 800-meter depth requirement cannot be met, the project cannot proceed.

Containment:
To ensure secure storage, sites should be located well away from legacy wells—especially those with potential integrity issues and intersect the target CO_2 storage zone (typically requiring at least a 1 km buffer). Wells with unknown surface locations or abandonment status, uncertain mechanical condition, or poor or missing cement in the caprock above the injection layer are particularly concerning and should be avoided.

Sites must also be distant from any surface areas previously affected by oil and gas activities, as these may carry heightened environmental risks.

A robust, intact caprock or seal above must exist; if a site lacks an effective seal, it is immediately disqualified from consideration.

Key targets

- Quantitative requirement for minimum total capacity of the CO_2 geological storage project is **15 million metric tons of CO_2**.
- Quantitative requirement for maximum total capacity of the CO_2 geological storage project is **21 million metric tons of CO_2**.
- Quantitative requirement for minimum annual injectivity is **0.7 million metric tons per year**.
- Depth: sufficient depth of injection zone to achieve CO_2 dense phase (super-critical)

Copyright © SLB. All Rights Reserved. Private & Confidential. Reproduction only by permission.

conditions should be **more than 800 m**.

- Seal: **presence of a laterally extensive seal** above the injection zone to prevent flow/ communication with economic and/or environmental receptors

2.7.1.2 Legal and regulatory

In addition to geological and technical factors, non-technical considerations are essential in the site selection process, as they directly impact the feasibility, regulatory compliance, and public acceptance of CO_2 storage projects. For the sub-surface site to become a potential sequestration site, it needs to be acceptable from surface point of view as well. They are normally elaborated in country regulations related to CO_2 sequestration and are legally binding and also European Directive 2009/31/EC of the European Parliament and of the Council of 23 April 2009 on the geological storage of carbon dioxide and amending Council Directive 85/337/EEC, European Parliament and Council Directives 2000/60/EC, 2001/80/EC, 2004/35/EC, 2006/12/EC, 2008/1/EC and Regulation (EC) No 1013/2006 (Text with EEA relevance).

To effectively manage potential health, safety, and environmental risks, a robust set of criteria must be applied. Sites in proximity to residential settlements, infrastructure, or protected environmental areas carry elevated risks and are excluded from consideration.

The following datasets should be incorporated to produce Chance of Success (COS) maps that clearly highlight surface-related constraints:

1. Inhabited areas Fig. 2.105
2. Sanitary protected areas Fig. 2.106
3. Polygons reflecting the protected areas Fig. 2.107
4. Roads & railroads; Fig. 2.108

Copyright © SLB. All Rights Reserved. Private & Confidential. Reproduction only by permission.

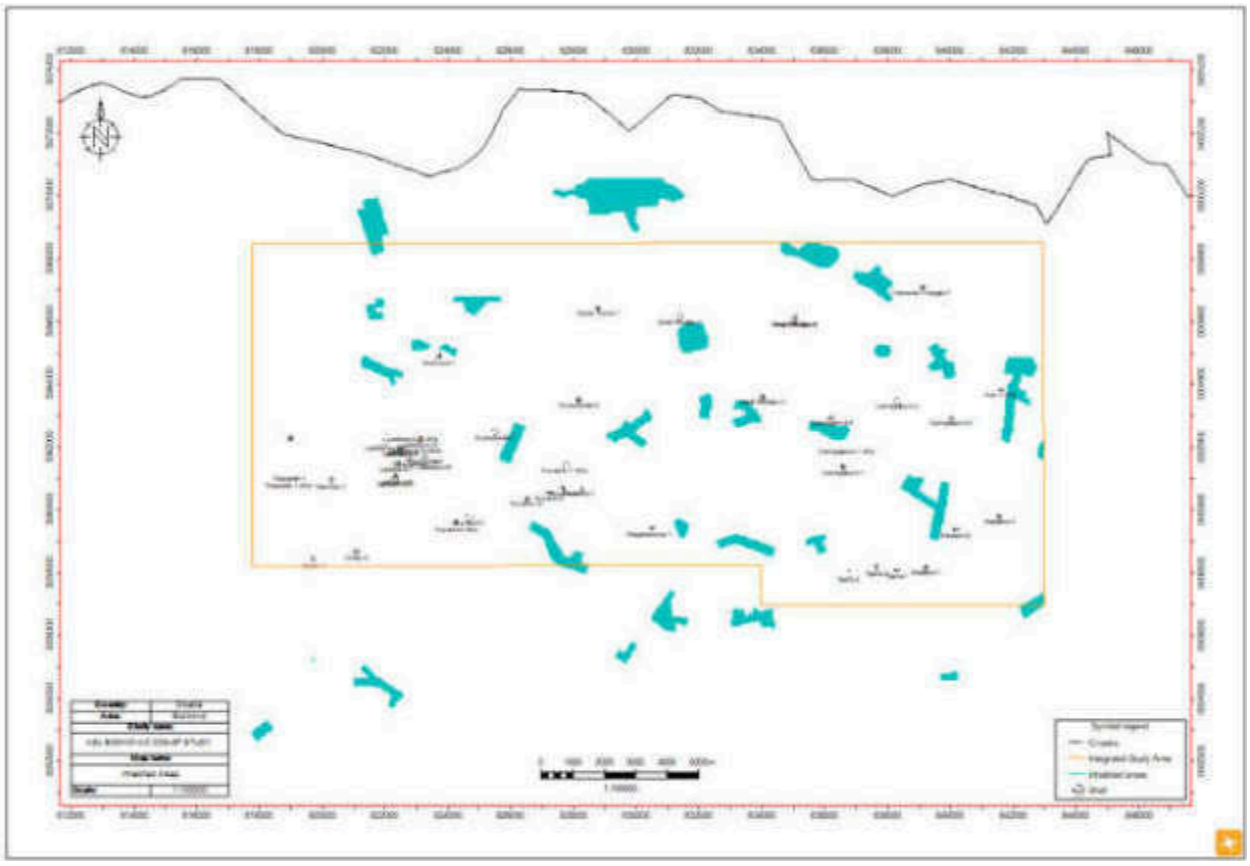


Fig. 2.105 Inhabited areas

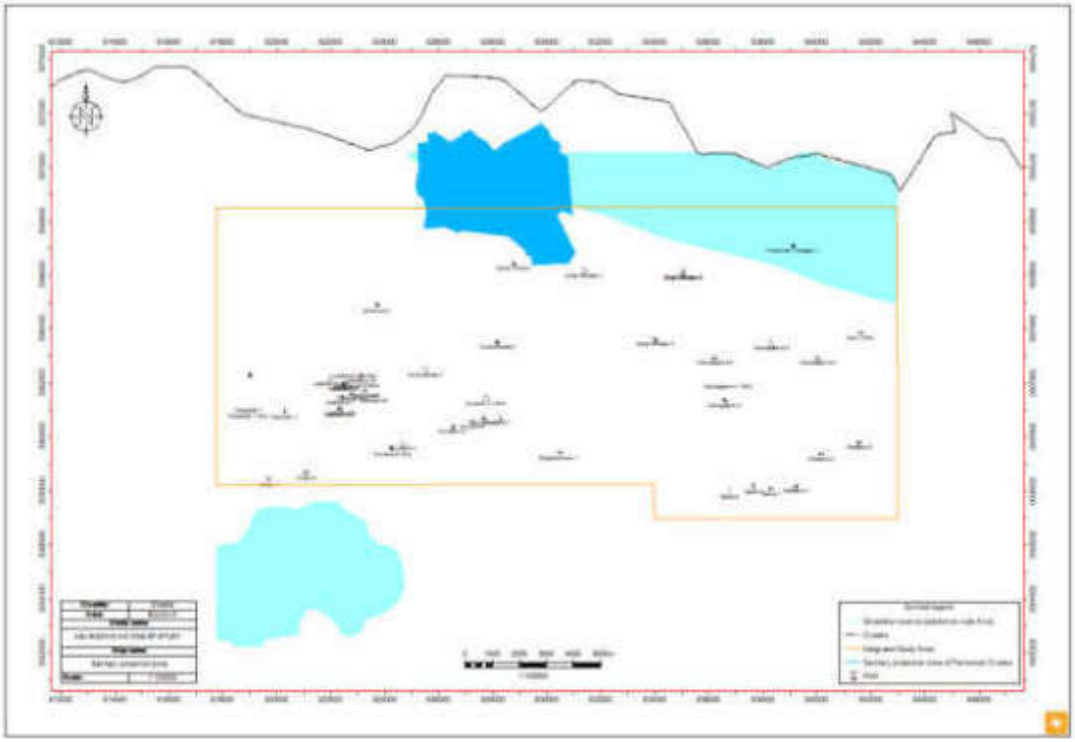


Fig. 2.106 Sanitary protected area

Copyright © SLB. All Rights Reserved. Private & Confidential. Reproduction only by permission.

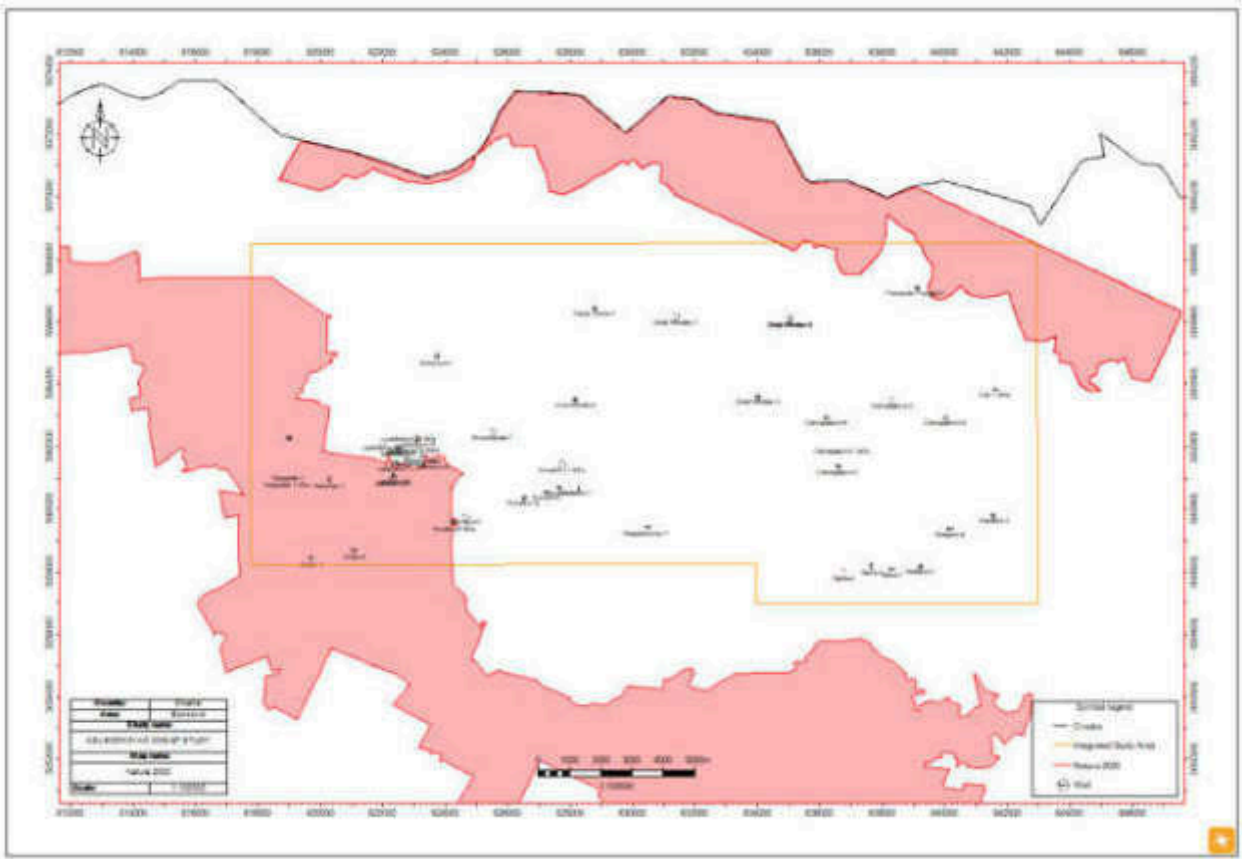


Fig. 2.107 Polygons reflecting the protected areas

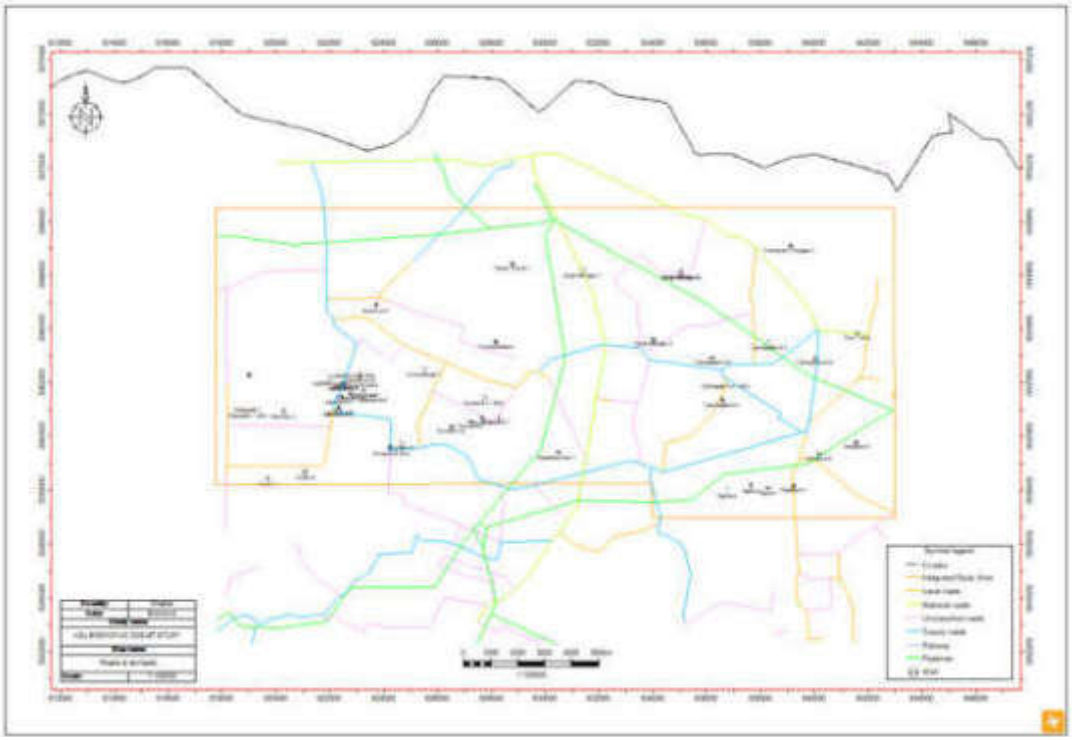


Fig. 2.108 Roads & railroads;

Copyright © SLB. All Rights Reserved. Private & Confidential. Reproduction only by permission.

Monitoring and Legal Considerations

Monitoring encompasses all measurement and surveillance activities required to maintain safe storage operations. This includes evaluating the integrity of the storage complex, wells, and key geological features; detecting any loss of containment and assessing potential impacts from leakage; tracking the migration and ultimate fate of injected CO_2, monitoring pressure changes, and observing displacement of formation fluids; as well as evaluating the effectiveness of risk management strategies such as mitigation and remediation measures.

- It is essential that the site can be legally accessed and monitored throughout its expected operational life. In accordance with ISO 27914 section 5.2 a7), any potential CCS site must demonstrate sufficient capacity for monitoring the evolution, fate, and effects of the injected CO_2 stream.
- The physical accessibility of prospective sites by CHA must be verified, and access rights must be clearly established. In alignment with ISO 27914 section 5.2 b7), any selected CCS site must be situated in a location where continuous access—for both site operations and monitoring activities, including pipelines and roadways—can be maintained at all times.

Other

- Environment: The surface environmental context doesn't prevent the CCS project from taking place (example: large populated area, protected area, national patrimony)
- Reputation: The reputation of the company around the selected site doesn't prevent the CCS project from taking place
- Public opinion: the Public opinion for the selected site doesn't prevent the CCS project from taking place
- Health: The existence of populated areas does not prevent the CCS project from taking place
- Project: The choice of the selected site will not delay the CCS project substantially
- Conflict of Use: There is no major conflict of use for the storage site

The final surface Chance of Success (COS) map, illustrated in Fig. 2.109, integrates all evaluated surface criteria into a single, coherent representation, highlighting the areas most suitable for further consideration. It is based exclusively on surface-related factors and does not account for subsurface properties or structural elements. As such, it serves as the primary reference for surface screening and will be used in later stages alongside subsurface criteria to enable a well-informed and comprehensive site selection for CO_2 storage.

Copyright © SLB. All Rights Reserved. Private & Confidential. Reproduction only by permission.

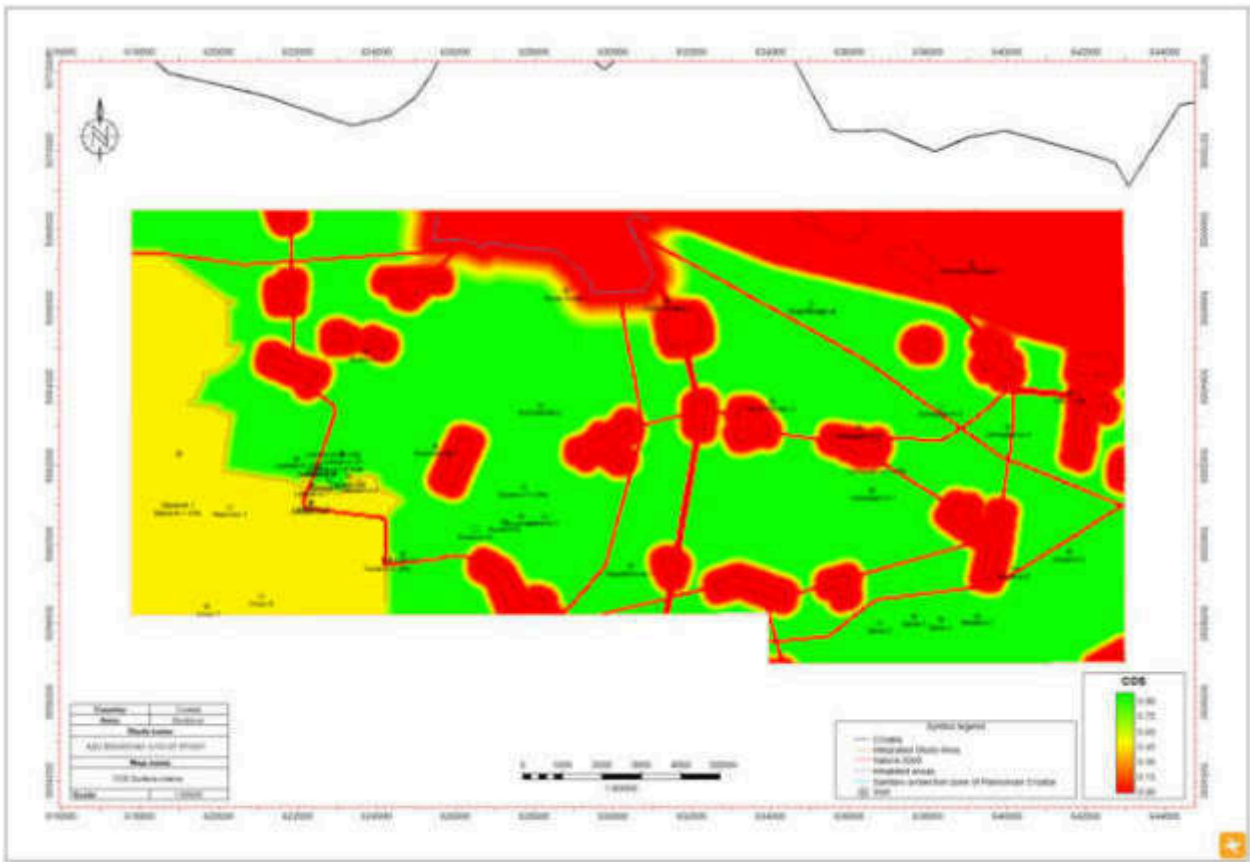


Fig. 2.109 Surface Criteria Chance of Success Map

2.7.1.3 Technical criteria

To support the identification and preliminary selection of potential CO_2 storage sites, the primary technical assessment parameters are outlined below. These criteria are specifically designed to evaluate containment security, injection feasibility, and other key considerations critical to site suitability.

Legacy Wells

From a containment perspective, the presence of existing wells within a candidate site represents a significant risk, as these wells may act as potential pathways for CO_2 leakage. The integrity of legacy exploration, production, or disposal wells is often highly uncertain due to insufficient data, making it challenging to evaluate their capacity to withstand pressure changes or CO_2 exposure. Moreover, critical containment barriers within these wells can degrade over time, leading to an increased likelihood of integrity loss—regardless of direct contact with CO_2.

The accompanying map Fig. 2.110, highlights the Chance of Success assessment for legacy wells, utilizing a 250-meter buffer zone around each well to account for their potential risk as leakage pathways and to strengthen the overall evaluation of containment security.

Copyright © SLB. All Rights Reserved. Private & Confidential. Reproduction only by permission.

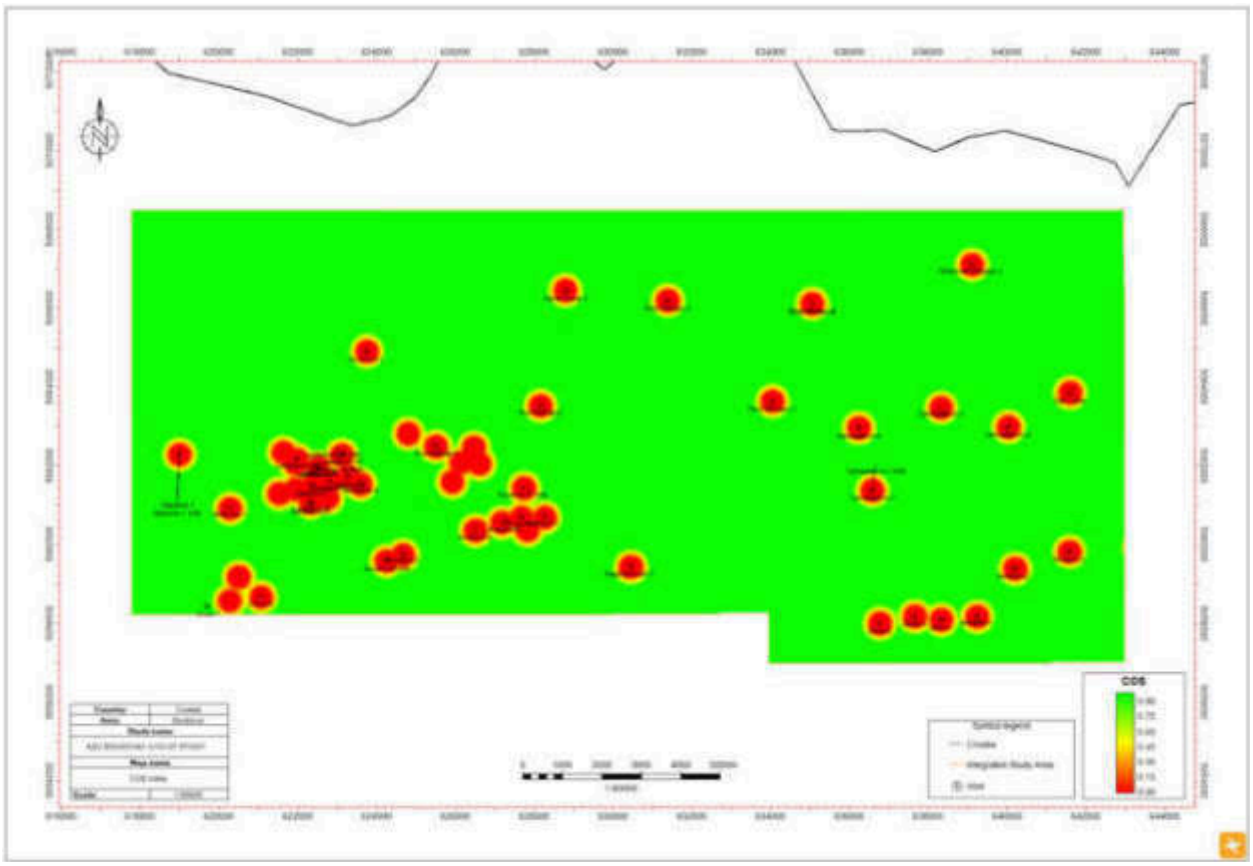


Fig. 2.110 Distance to Wells

Presence of Caprock/Seal

The existence of an effective caprock or seal is fundamental for CCS. Without a seal, a site cannot be considered viable. A minimum seal thickness of 10 meters is generally required; however, alternative configurations—such as multiple superimposed impermeable layers of lesser individual thicknesses, or zones containing 100 meters of shaly-sand thin layers—can still provide sufficient containment. This underscores the need for flexibility in screening criteria while maintaining critical safety and feasibility standards.

Structural Complexity

Ideal storage candidates, especially depleted fields, should feature low structural and stratigraphic complexity and possess multiple sealing horizons to ensure redundant containment. Geological stability is crucial, minimizing risks from tectonic activity. Sites with significant faults or complex structural settings can compromise containment—active faulting may induce leakage, and complex formations complicate both reservoir characterization and monitoring. It is essential for sites to reside in stable geological environments with minimal fault reactivation risk. Preliminary assessment of structural complexity using seismic data (if available) is recommended to build confidence in containment. Fault zones likely to serve as potential flow pathways must be avoided.

Copyright © SLB. All Rights Reserved. Private & Confidential. Reproduction only by permission.

In depleted fields, lower reservoir pressures mean injected CO_2 plumes may extend to all previously produced boundaries, with depletion potentially impacting reservoir and seal properties or causing fault reactivation. Unless clear evidence of fault reactivation exists, the seal is considered proven and adequate at this stage.

For saline aquifers, proximity to faults poses higher risks, including possible leakage and induced seismicity. Thus, a buffer of at least 250 meters from faults is applied in the COS map to mitigate these risks and permit safe placement of injection wells. These criteria not only support containment and regulatory compliance but also help determine if a site is technically sound, operationally manageable, and predictable over time. Some factors—like the presence of a seal or major faults—act as strict exclusion filters, while others increase site uncertainty and complexity without being disqualified.

Quality of the Storage Formation

High-quality storage formations require sufficient thickness, porosity, and permeability—capable of accommodating the planned CO_2 injection volumes. These attributes support both injection feasibility and target storage capacity. Structures with multiple sealing horizons are especially valued for providing redundant containment and increased robustness. High structural complexity and seismicity are also assessed, as they can raise uncertainties in interpretation and CO_2 plume movement.

Structural Dip of the Storage Formation

The structural dip of the storage formation influences the migration of the injected CO_2 plume. Gentle dips are preferred as they slow upward migration, promoting controlled lateral spreading and enhancing dissolution and residual trapping mechanisms. Steeper dips, while not necessarily exclusionary, can increase plume migration speed, require more detailed modeling and monitoring, and demand stricter pressure management. Dip acts as a complexity and risk modifier rather than a strict exclusion criterion.

2.7.1.4 Volumetric estimation

Methodology

The theoretical storage capacity is estimated for the saline aquifer based on equation below:

$MCO_2 = A \times h \times NTG \times \phi e \times \rho CO_2 \times E$ (Fig. 2.111)

Table 5. Storage efficiency terms to be used if net area and net thickness of target formation are known (Goodman, 2014)

Lithology	P10	P50	P90
Clastics	5.17%	9.88%	17.24%
Dolomite	9.32%	12.71%	16.93%
Limestone	7.18%	10.43%	14.74%

Fig. 2.111

Copyright © SLB. All Rights Reserved. Private & Confidential. Reproduction only by permission.

Where:

- **A**: Structural polygon area
- **h**: Net reservoir thickness (from 1 mD cutoff)
- **ϕ** : Effective porosity
- **ρCO_2**: Density at reservoir T–P (300–400 kg/m^3 depending on depth)
- **E**: Efficiency factor (literature 2–5%, but increased here due to known effective porosity / NTG). For closed systems efficiency factor is less than 1% (typically 0.5%), for open systems efficiency factor usually is around 2 - 6 %. Fig. 2.112, Fig. 2.113.

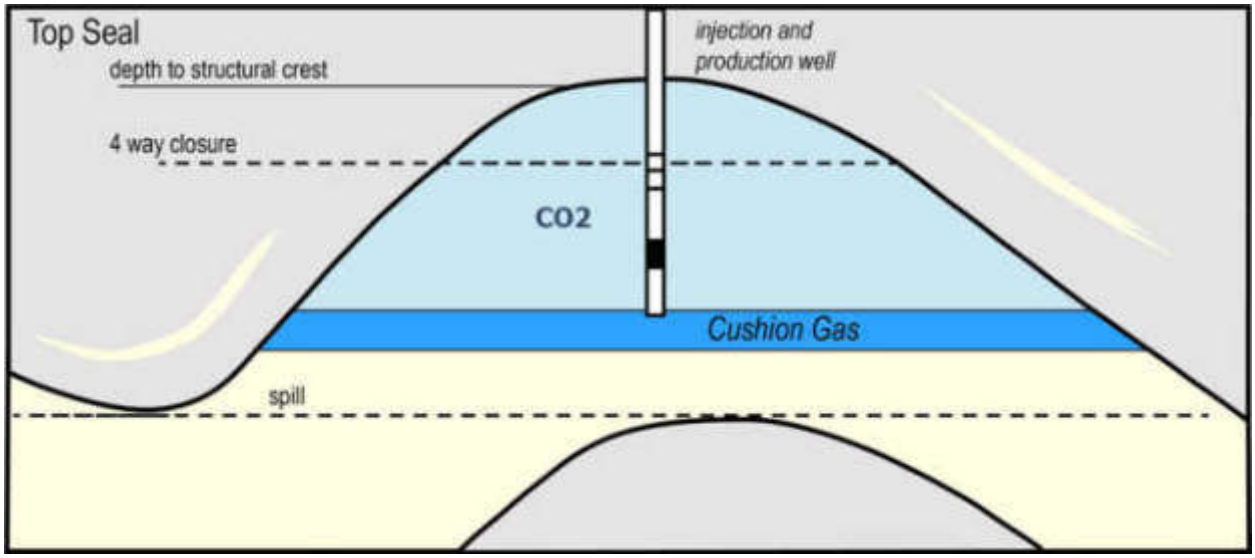


Fig. 2.112 Closed system

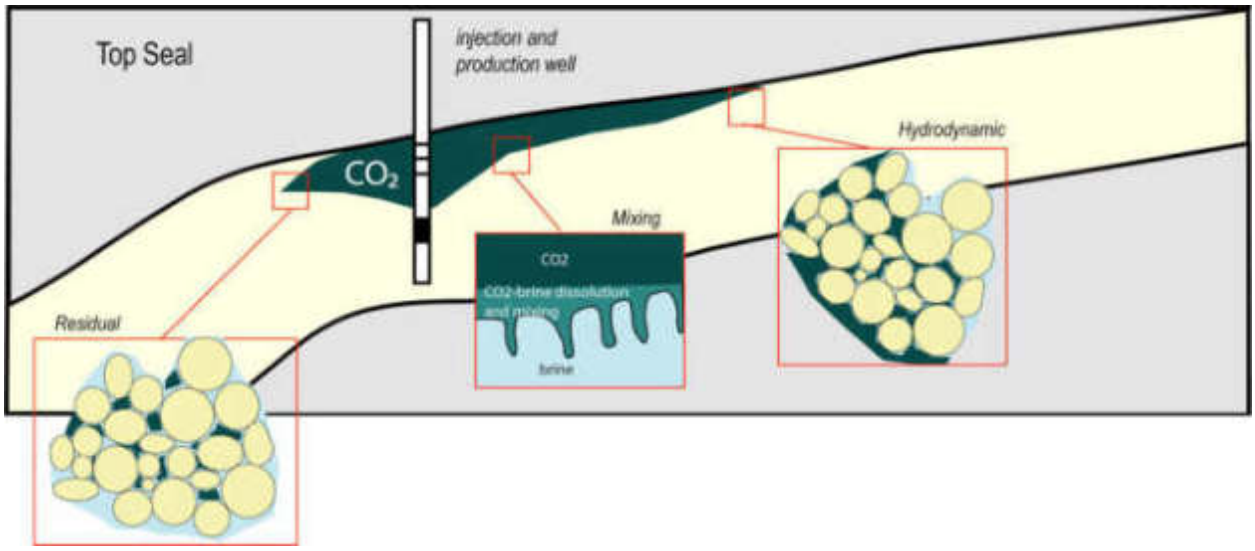


Fig. 2.113 Open system

Efficiency Factor Treatment

Copyright © SLB. All Rights Reserved. Private & Confidential. Reproduction only by permission.

- Lithology-dependent efficiency factor model
- P10/P50/P90 cases produced based on P10, P50, P90 efficiency factors values. Efficiency factor used in volumetric computation is higher since Net Thickness of reservoir and Efficient porosity are known (.
- Upper formations yield meaningful volumes; lower formations remain negligible.

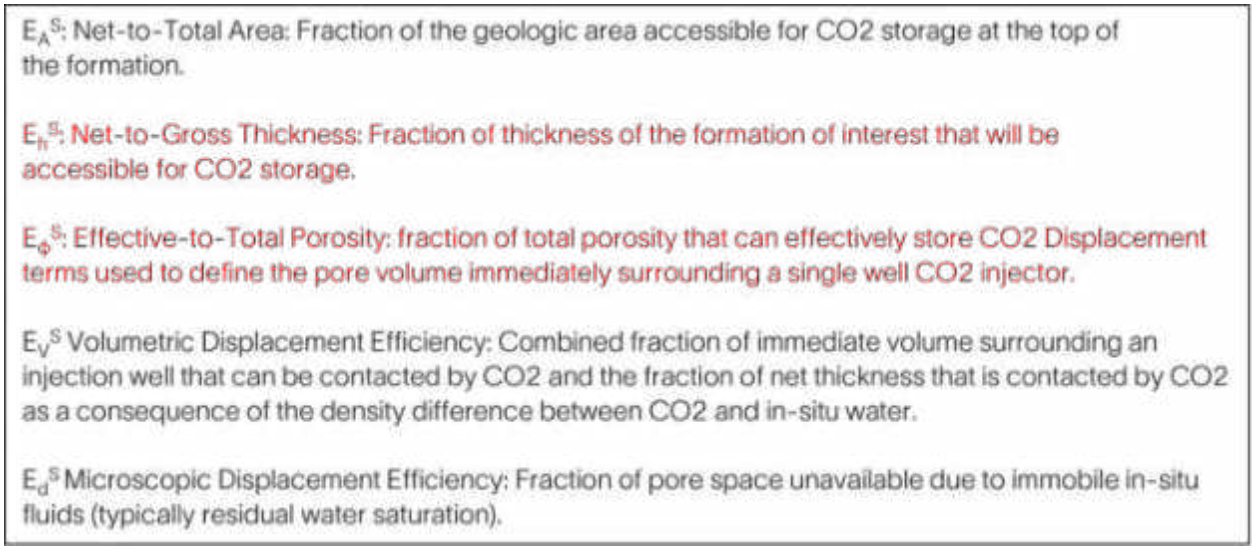


Fig. 2.114 Efficiency factor explanation
In red represented efficiency factor's components that are known in a project. Respectively, both components are not taken into account (both are 1) during the efficiency factor estimation that leads to efficiency factor increase.

Table 2.4 Estimated efficiency factor for case when Net reservoir thickness and Efficiency porosity are known

	P10 / P90 Values by lithology					
	Clastics		Dolomite		Limestone	
	P10	P90	P10	P90	P10	P90
Esaline = EAn/At * Ehn/hg * Ee/tot * EA * EL * Eg * Ed	0.0112	0.23712	0.02964	0.22016	0.01782	0.19152
Average, %	0.12416		0.1249		0.10467	

The Techno-Economic Resource (and Reserve) Pyramid for CO_2 Fig. 2.115 is a framework used to assess the capacity and economic viability of geological carbon storage or carbon capture and utilization (CCU). It categorizes the total CO_2 resource pool into sequential tiers based on geological certainty and economic profitability.

Copyright © SLB. All Rights Reserved. Private & Confidential. Reproduction only by permission.

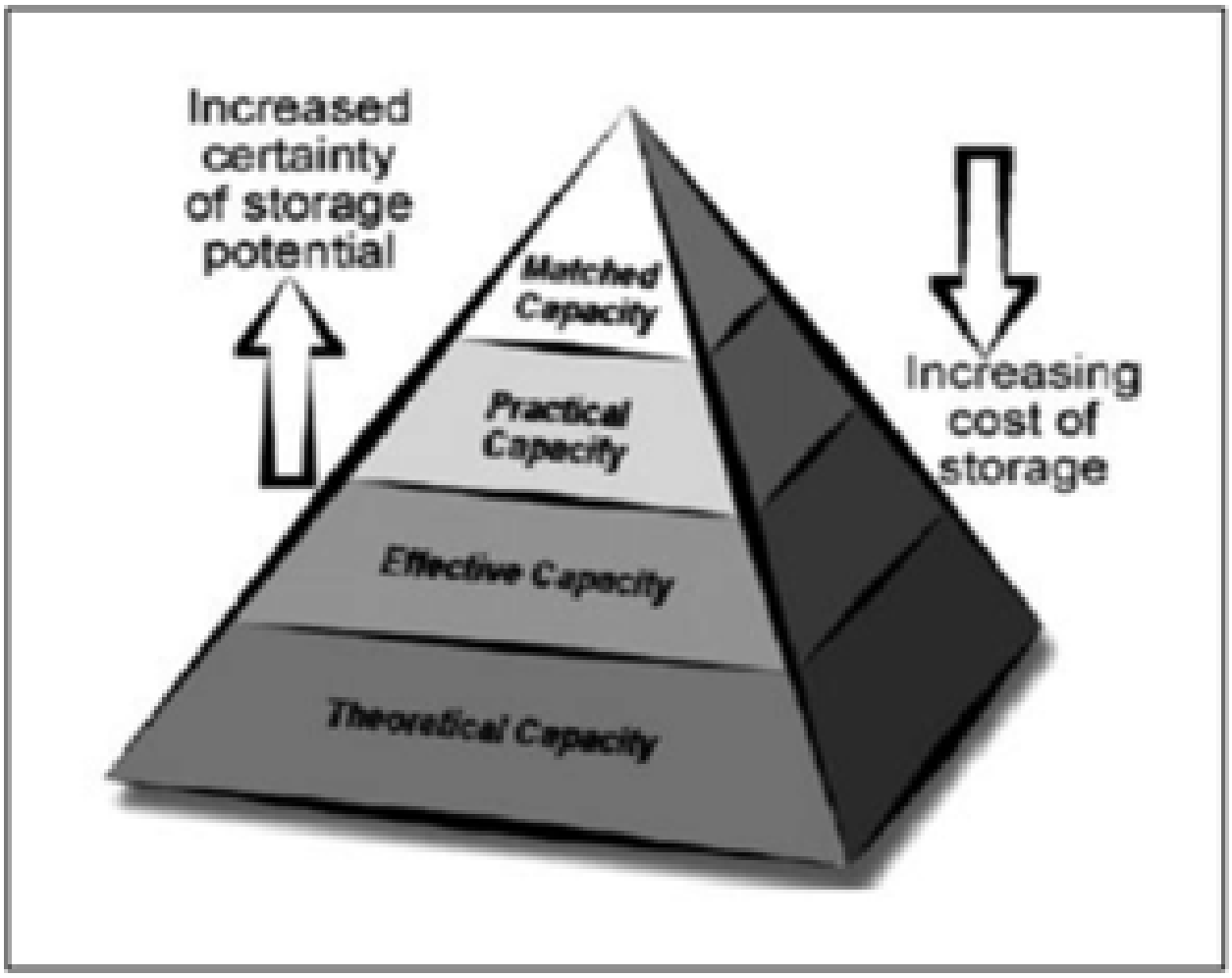


Fig. 2.115 Techno-Economic Resource (and Reserve) Pyramid for CO_2

The pyramid structure, moving from the broad base to the narrow apex, includes the following tiers:

1. Theoretical Capacity (The Base)
What it is: The theoretical upper limit of CO_2 storage available in a specific region or formation (e.g., total available pore volume).
Economics: None; purely a geological or physical volume limit.

2. Effective Capacity
What it is: The portion of the theoretical capacity that can realistically be utilized given physical and geological limitations (e.g., permeability, porosity, caprock integrity, and fluid trapping mechanisms).
Economics: Broad technical parameters are evaluated, but detailed, project-specific economic viability is not yet defined.

3. Practical Capacity
What it is: The capacity that considers both geological viability and the regulatory, infrastructural, and spatial limitations of a specific project.
Economics: Cash flow positive. Detailed Techno-Economic Assessments (TEA) are performed.

Copyright © SLB. All Rights Reserved. Private & Confidential. Reproduction only by permission.

This capacity tier only includes reservoirs or utilization pathways where the revenue (e.g., from tax credits, enhanced oil recovery, or CO_2 derived products like methanol or formic acid) exceeds the capital and operating abandonment costs.

4. Matched (or Viable) Capacity (The Apex)
What it is: The most mature and refined tier. It identifies CO_2 storage or utilization operations that are not only economically viable but also directly paired with an active, capture-ready CO_2 source (e.g., an industrial plant or direct air capture facility).
Economics: Fully feasible under current market conditions and regulatory frameworks.

2.7.2 Assessment

2.7.2.1 Assessment of upper formations

"Alfa (D')" Series:

Formation Alfa is observed at depths ranging from approximately −551 meters to −1177 meters across the study area, as illustrated on the Structural Map (Fig. 2.116). This wide depth range reflects significant structural variation, including the presence of structural highs and lows, which are important for understanding both reservoir architecture and potential containment risks or advantages.

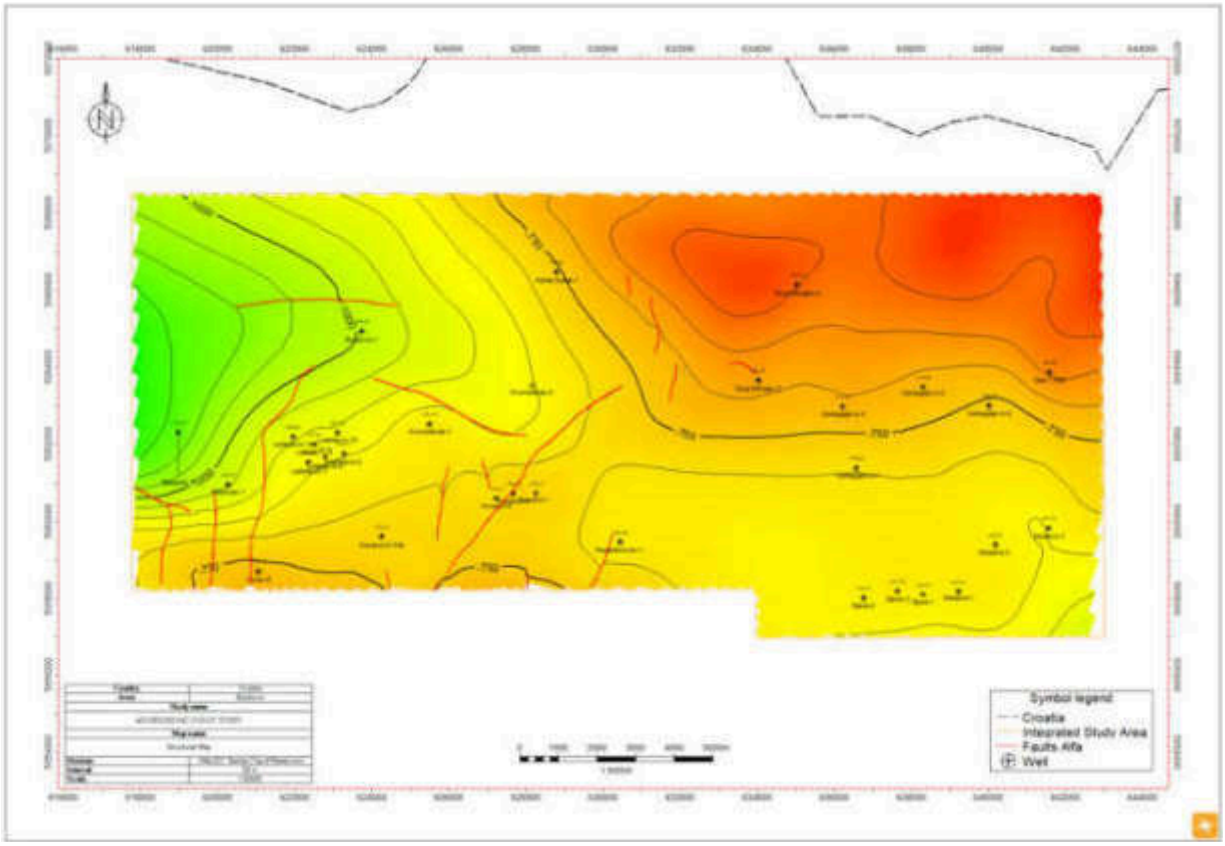


Fig. 2.116 Structural Map Alfa (D')

Copyright © SLB. All Rights Reserved. Private & Confidential. Reproduction only by permission.

Within the interval between horizons Alfa (D') and B, there is pronounced variability in thickness, with values spanning 12 meters in the North (due to the lack of seismic or well data in the North this value cannot be confirmed), to 368 meters in the South East and an average thickness of around 177 meters. The Thickness Map (Fig. 2.117) provides a spatial visualization of these variations, revealing areas of substantial vertical separation as well as zones of localized thinning likely driven by a combination of structural controls and localized depositional patterns. Thicker zones are generally associated with structurally lower areas where increased subsidence allowed for greater sediment accumulation, while thinning trends correspond to structural highs or areas affected by reduced accommodation.

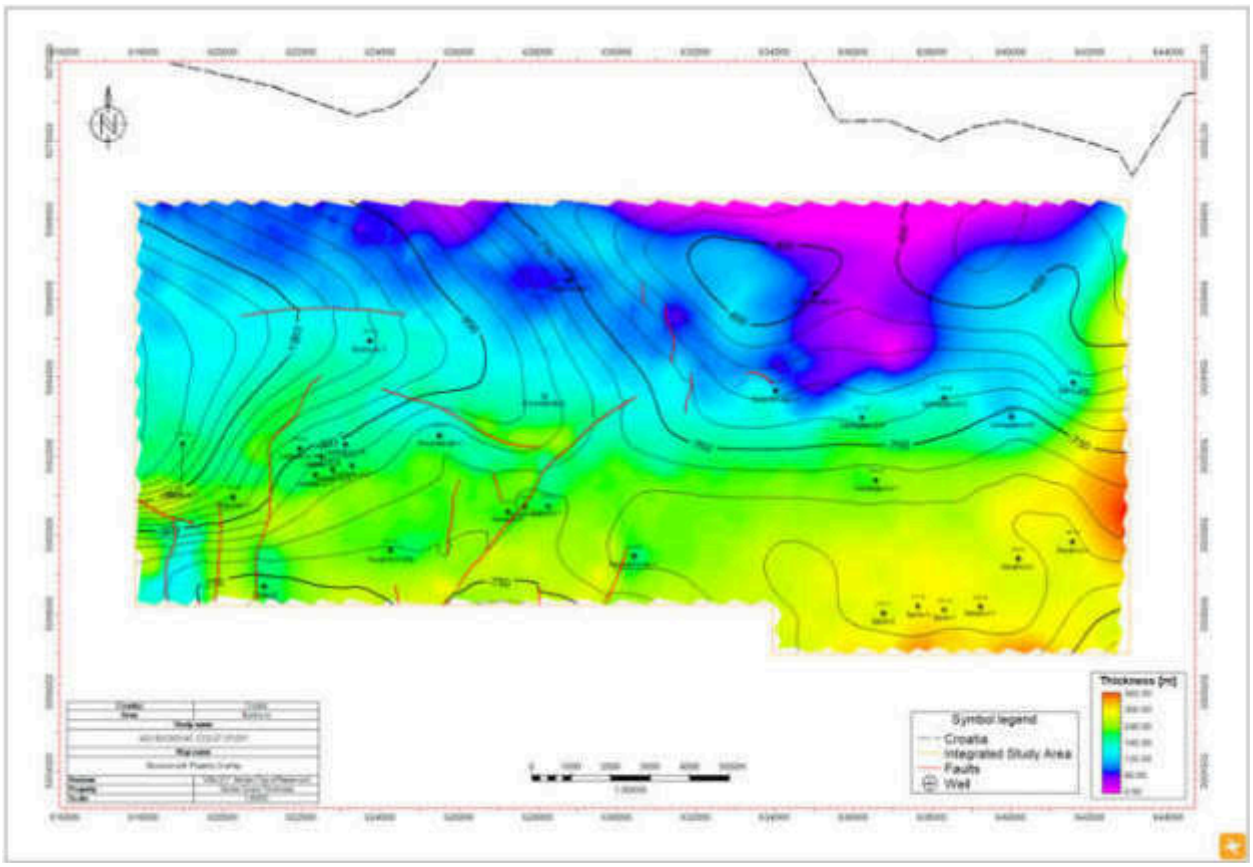


Fig. 2.117 Composite Map: Gross Thickness of Alfa ("D") with Structural Contours

Such spatial heterogeneity in thickness suggests that accommodation space and structural evolution have not been uniform across the area. The average thickness indicates significant vertical separation between horizons Alfa (D') and B—supporting the potential for effective CO_2 storage.

Overall, the Alfa (D')–B interval demonstrates adequate thickness and continuity across most of the area, supporting its potential role within the storage framework.

Copyright © SLB. All Rights Reserved. Private & Confidential. Reproduction only by permission.

Structural assessment

Structurally, the surface is characterized by a gentle regional dip of approximately 1.4°, as derived from the Structural Map, with the overall geometry remaining largely conformable across the study area. This reflects a relatively stable depositional and tectonic regime at the regional scale, with no major evidence of large-scale deformation affecting the continuity of the horizon (Fig. 2.118 below).

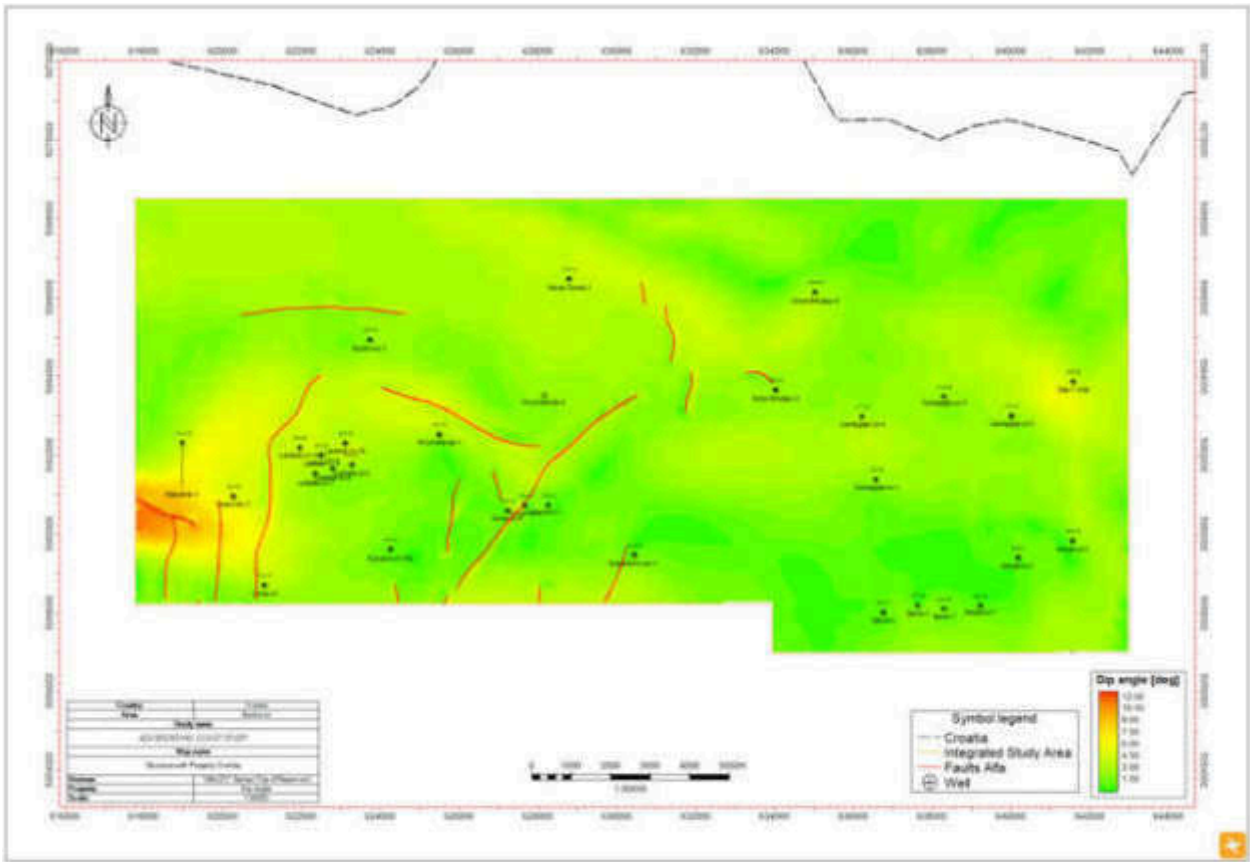


Fig. 2.118 Composite Map: Dip Angle of Alfa (D') with Structural contours

At a local scale, however, significantly higher dip values—reaching up to 12°—are observed in the vicinity of mapped faults. These anomalously steep gradients are interpreted as artefacts introduced by the fault modeling and gridding process, rather than representing true geological dips. As such, they should be treated with caution and not over-interpreted in the structural assessment.

The formation is affected by several faults, primarily concentrated in the central part of the Area of Interest, in proximity to the "**Ladislavci-Kucanci**" hydrocarbon-producing field. These faults appear to be deep-rooted, with vertical continuity extending upward through this horizon and, in some cases, propagating toward shallower levels. Their presence introduces an element of uncertainty in terms of fault transmissibility, as they may act either as barriers or as potential migration pathways depending on their sealing properties (Fig. 2.119 below).

Copyright © SLB. All Rights Reserved. Private & Confidential. Reproduction only by permission.

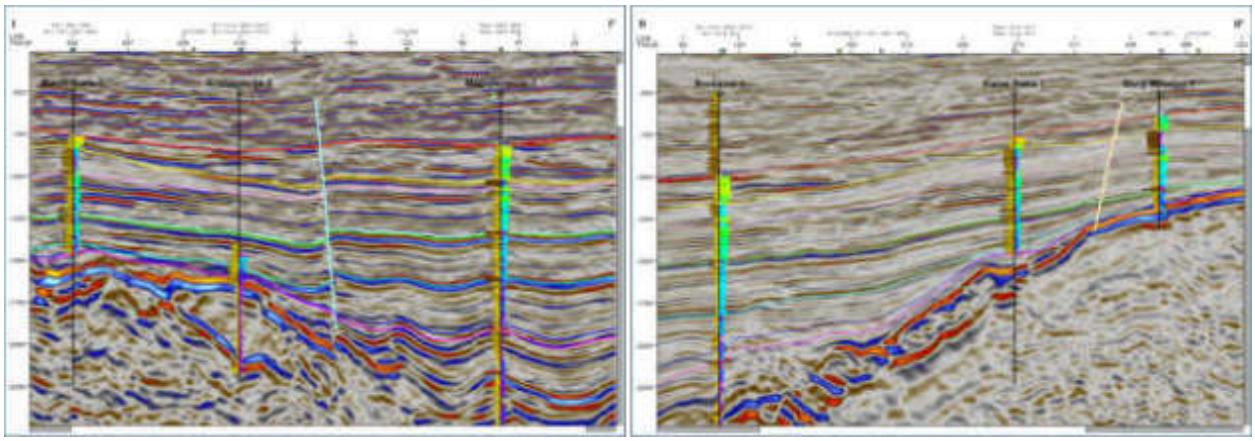


Fig. 2.119 Cross-Sections showing Fault extent

From a containment perspective, the vertical extent and spatial distribution of these faults require careful evaluation, particularly where they intersect structurally favorable zones. Integrating fault architecture with the Structural Map and Thickness Map is therefore essential to better constrain their impact on storage integrity and to assess the potential risk of vertical fluid migration.

Containment

From a containment perspective, no clear seal–reservoir pairing was identified within formation Alfa (D') itself.

This limits the ability to rely on intraformational sealing mechanisms. Instead, containment would depend on the **overlying regional seal** (see Fig. 2.2 and Fig. 2.120), which is thick and laterally extensive. However, this upper seal incorporates localized sand bodies or "**sand pools**", introducing heterogeneity and reducing confidence in its uniform sealing capacity.

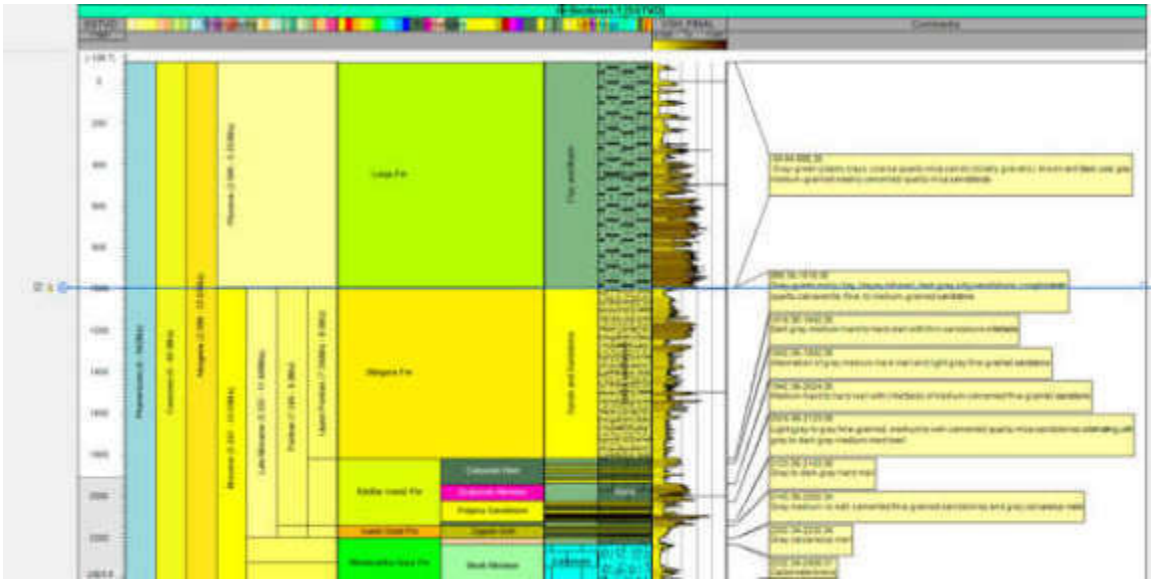


Fig. 2.120 Stratigraphy above Alfa (D')

Copyright © SLB. All Rights Reserved. Private & Confidential. Reproduction only by permission.

In particular, if fault transmissibility is underestimated or if the overlying seal is laterally discontinuous, there is a potential pathway for CO_2 to migrate upward, possibly reaching shallow formations, including potable aquifers.

The combination of:

- Deep-rooted faults with possible surface connectivity,
- Limited internal sealing within the formation,
- Heterogeneity in the overlying seal,
- And incomplete characterization of the interval above,

creates a scenario where vertical migration risk cannot be fully constrained.

Quality of the Storage Formation

The net thickness varies from 0 m to approximately 330 m, with an average of about 154 m. The presence of zero values highlights localized zones where reservoir-quality facies are absent, most likely due to increased shale or marl content. However, the relatively high average net thickness suggests that, across much of the area, a significant proportion of the interval contributes to the reservoir.

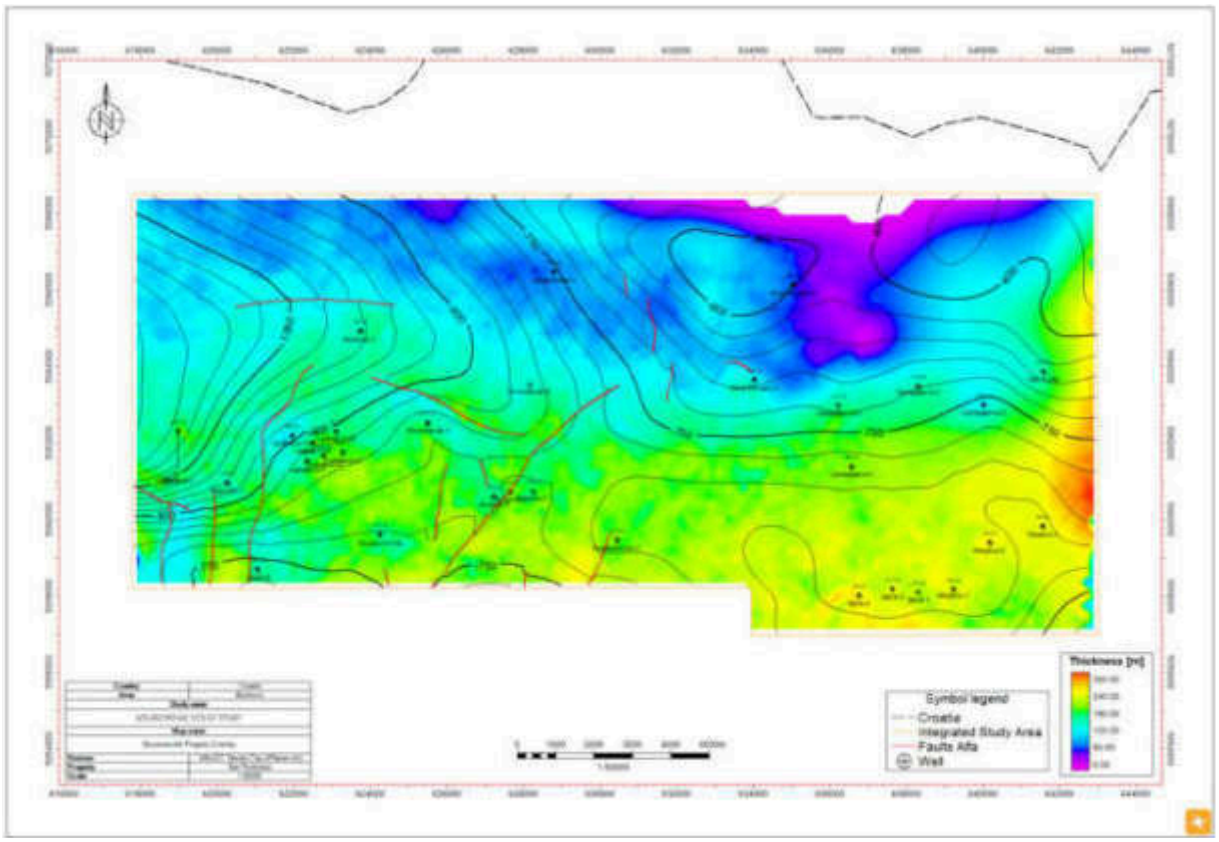


Fig. 2.121 Composite Map: "Alfa (D')" Series - Reservoir Net Thickness

Copyright © SLB. All Rights Reserved. Private & Confidential. Reproduction only by permission.

When applying a permeability cutoff, the net pay thickness ranges from 0 m to approximately 305 m, with an average of about 141 m. The relatively limited reduction from net to net pay indicates that a large portion of the reservoir not only meets porosity criteria but also maintains sufficient permeability for fluid flow. This suggests overall favorable reservoir quality in significant parts of the formation.

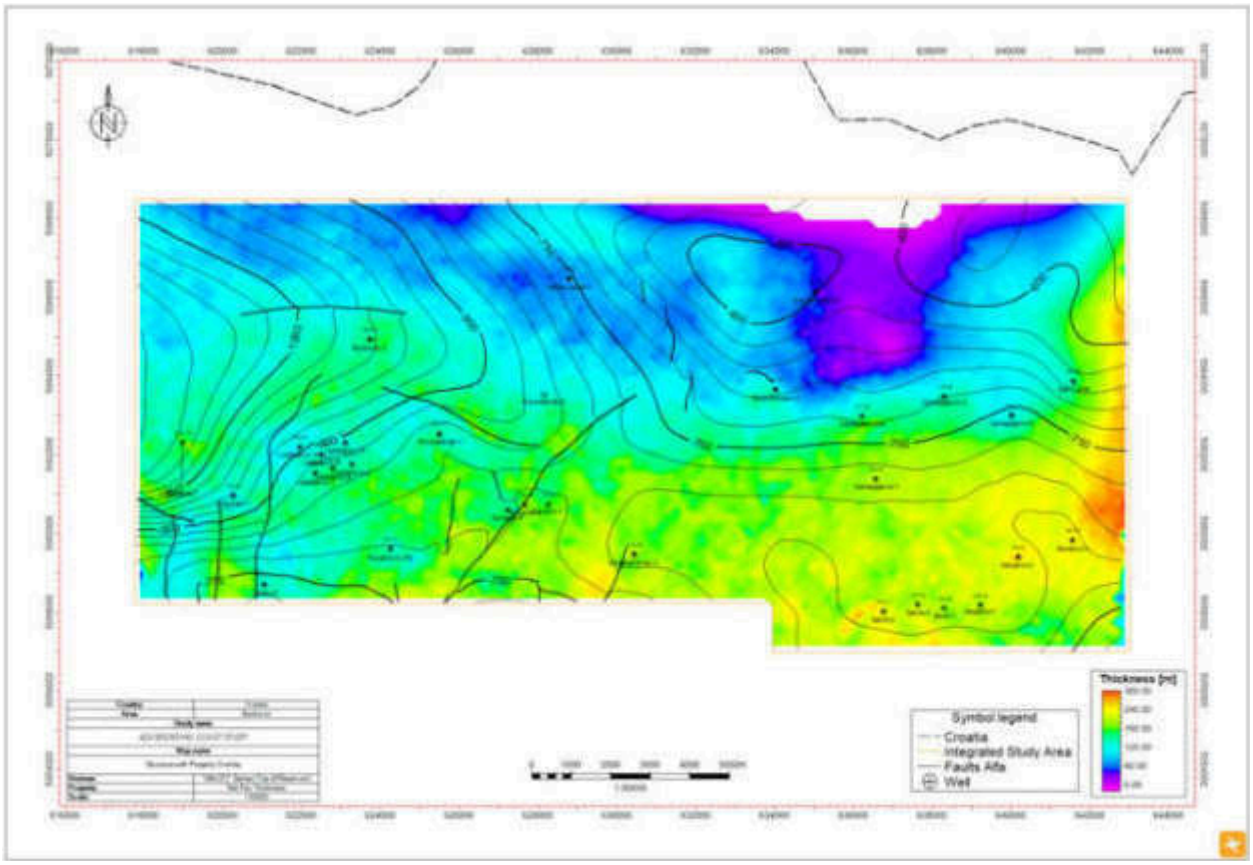


Fig. 2.122 Composite Map: "Alfa (D')" Series - Net Pay Thickness

Porosity (PHIE) values range from 0.09 (9%) to 0.31 (31%), with an average of approximately 0.20 (20%). These values are calculated exclusively within net reservoir intervals, ensuring that they reflect effective storage capacity. The upper range indicates the presence of high-quality reservoir zones with good storage potential, while the lower values are associated with tighter or more cemented intervals. Overall, the average porosity points to good reservoir quality at regional scale.

Copyright © SLB. All Rights Reserved. Private & Confidential. Reproduction only by permission.

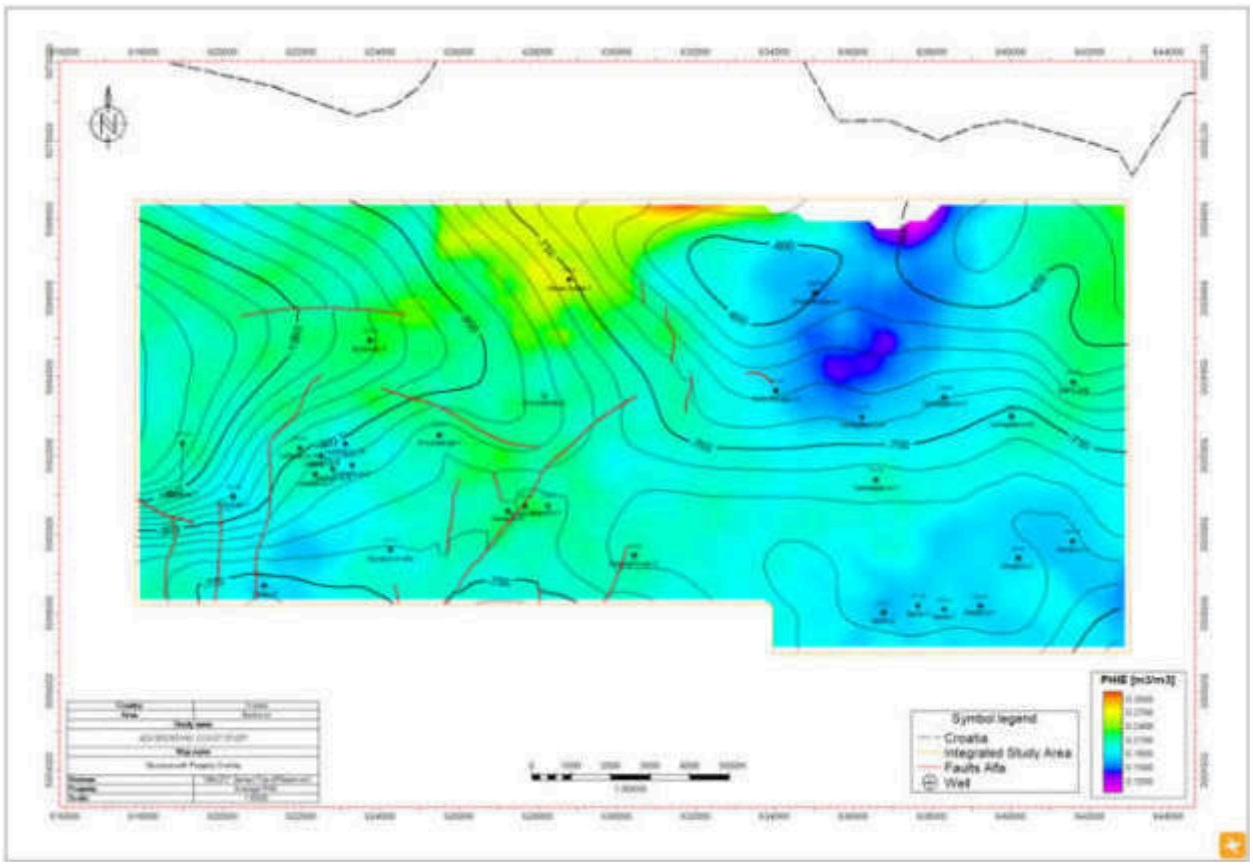


Fig. 2.123 Composite Map: "Alfa (D')" Series - Average PHIE

In summary, this interval demonstrates strong storage potential, supported by substantial thickness, high net-to-gross efficiency, and relatively favorable porosity distribution. While heterogeneity remains present, particularly in areas with reduced net development, the combination of high net pay and good porosity suggests that this unit represents a viable target for CO_2 injection.

Table 2.5 Reservoir zone: Alfa (D')

Property	Min	Mean	Max
Gross Thickness (m)	12	177.03	368
Net Thickness (m)	0	153.51	329.87
Net Pay (m)	0	140.97	304.94
PHIE	0.09	0.2	0.31

Conclusions Alfa (D')

While formation “Alfa (D')” demonstrates adequate thickness and gentle regional dip, the structural setting and sealing configuration introduce elevated containment uncertainty that would require detailed seal analysis and geomechanical evaluation.

Furthermore, the combination of structural complexity, sealing uncertainty, proximity to sensitive surface areas in the north, and lack of data in the south-east increases the overall risk profile for

Copyright © SLB. All Rights Reserved. Private & Confidential. Reproduction only by permission.

this formation within the current level of understanding. Further evaluation would require detailed analysis of the overburden, and potentially additional seismic and well data acquisition before advancing its candidacy.

Chance of Success Alfa (D')

Although the interval shows adequate thickness at regional scale, its relatively shallow depth—locally approaching the lower threshold for supercritical CO_2—introduces an inherent limitation. This is further compounded by the absence of a well-defined internal seal within the formation and the reliance on an overlying regional seal, whose effectiveness remains uncertain due to faulting and limited characterization.

The fault system plays a major role in reducing the COS, particularly in the central AOI, where faults propagate toward the surface, increasing the risk of vertical migration. This is further constrained by surface criteria, including proximity to sanitary protection zones in the north.

As a result, the COS map highlights only limited, localized areas where conditions are marginally favorable. Overall, Alfa (D') formation represents a higher-risk option, suitable only for further consideration under conservative assumptions and with additional data acquisition.

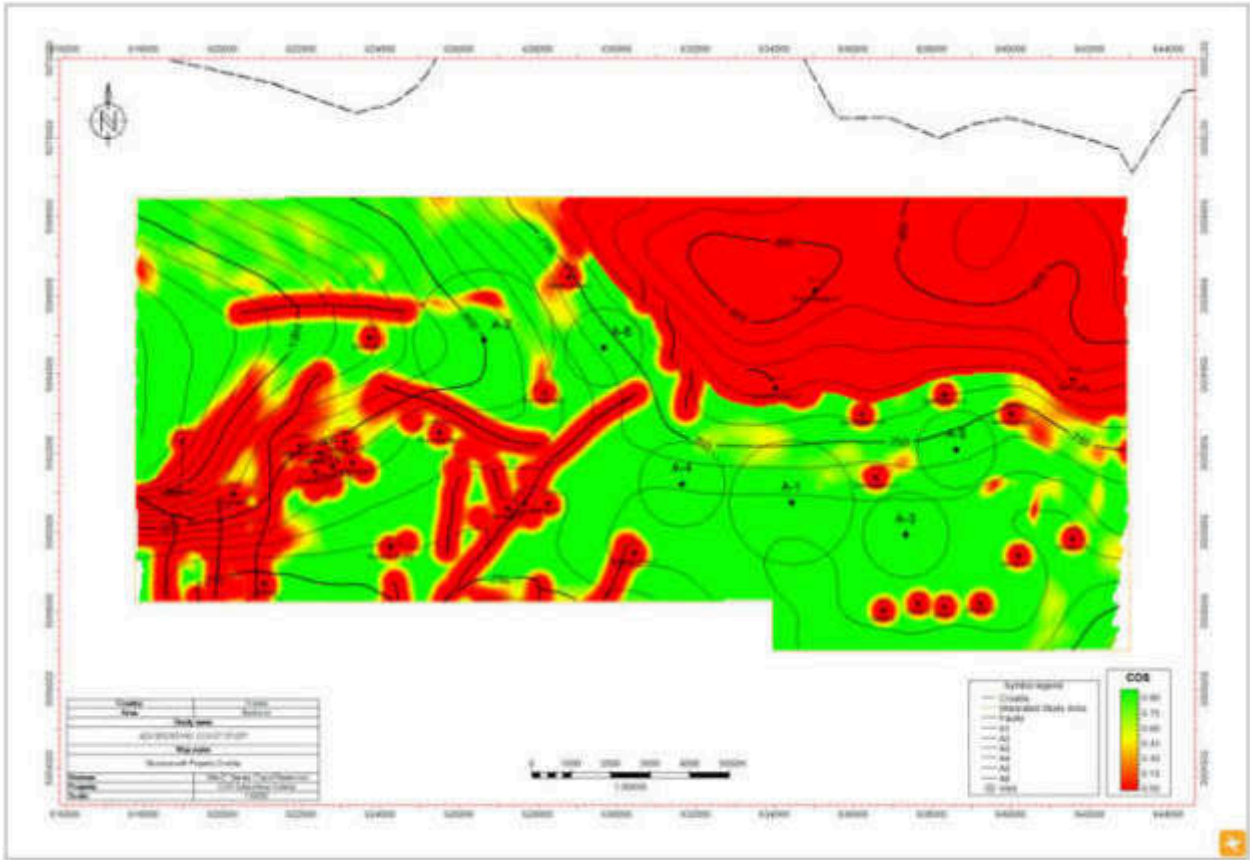


Fig. 2.124 COS Subsurface Alfa (D')

Copyright © SLB. All Rights Reserved. Private & Confidential. Reproduction only by permission.

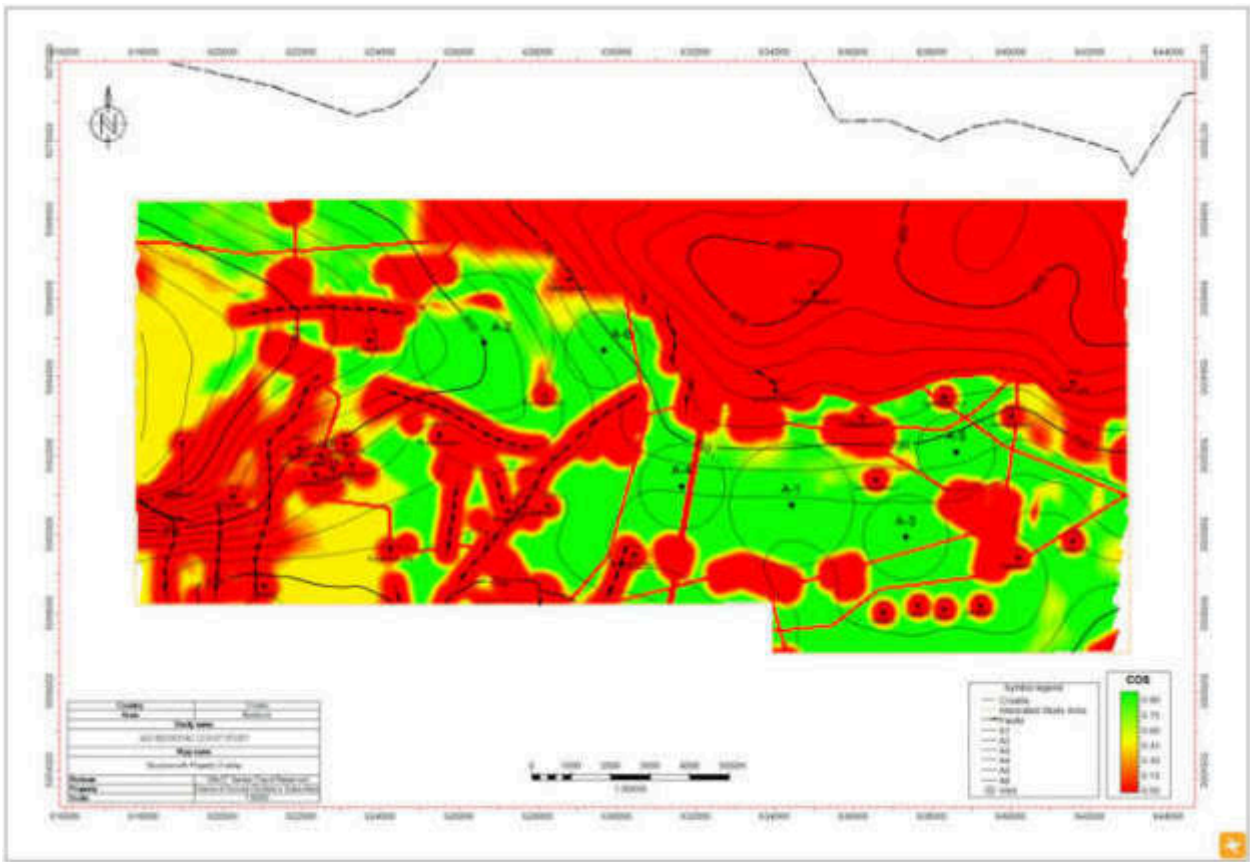


Fig. 2.125 Alfa (D') : Chance of Success (Subsurface x Surface)

For Alfa (D'), six potential sites were delineated, showing moderate variability in area, reservoir quality, and resulting pore volume.

Table 2.6 Alfa D' - Sites

Site	Area (km2)	PHIE (fractions)	Gross Thickness (m)	Net Pay Thickness (m)	Pore Volume (Mm3)
A-1	7,8	0,2	239,94	192,58	309,04
A-2	9,9	0,23	140,35	115,5	266,21
A-3	3,7	0,19	270,05	210	151,89
A-4	3,7	0,22	222,7	182,5	140,62
A-5	3,06	0,19	213,65	192,38	113,6
A-6	3,06	0,22	116,8	87,9	63,99

* Average values

Copyright © SLB. All Rights Reserved. Private & Confidential. Reproduction only by permission.

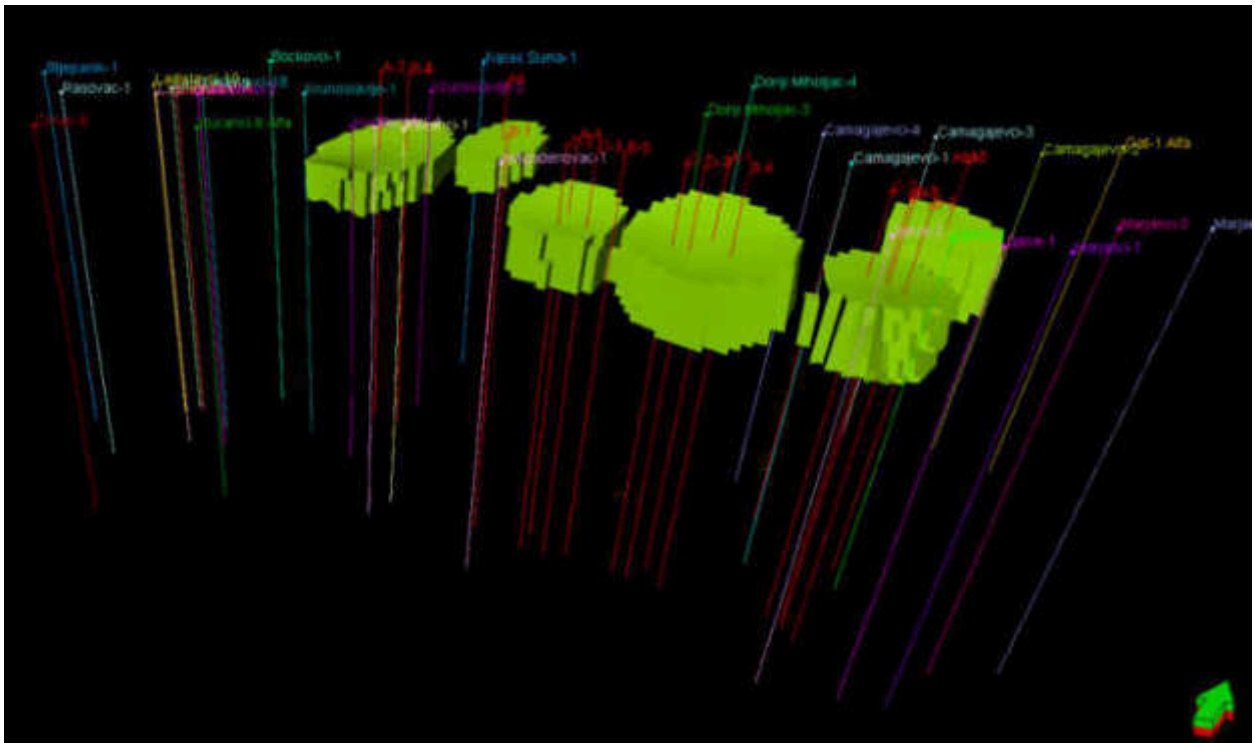


Fig. 2.126 3D View of "Alfa (D')" formation potential sites

"B" Series

The "B" Series is encountered at depths ranging from approximately –567 m to –1377 m, placing it at a deeper structural level compared to Alfa (D') and generally within more favorable conditions for supercritical CO_2 storage.

Copyright © SLB. All Rights Reserved. Private & Confidential. Reproduction only by permission.

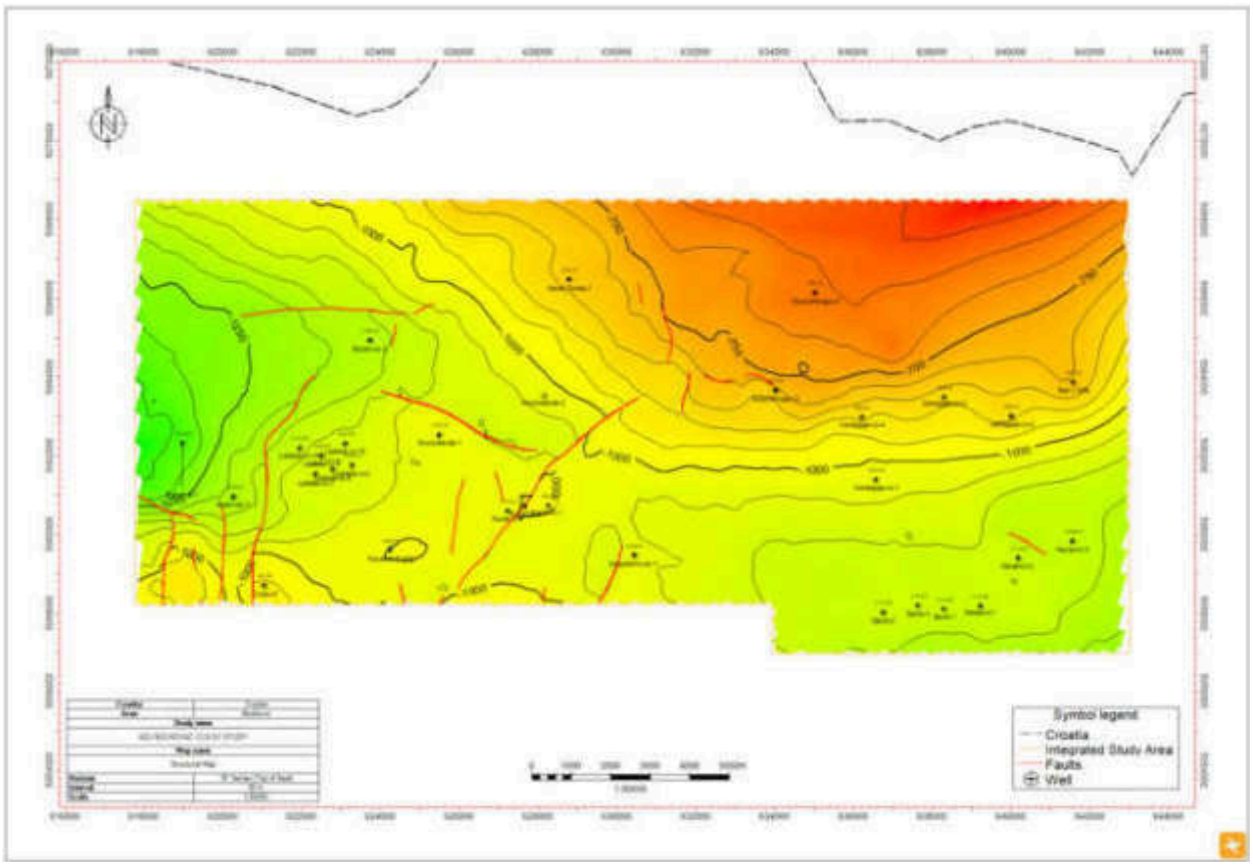


Fig. 2.127 Structural Map "B" Series

The Thickness Map highlights a pronounced variability in interval thickness, with values ranging from a minimum of 153m in the northeastern sector to a maximum of 445 m, and an average thickness of approximately 313m. The reduced thickness observed in the NE is interpreted to be structurally controlled, likely associated with a basement high. Despite these localized thinning zones, the overall mean thickness indicates a laterally extensive and volumetrically significant interval, supporting its potential as a storage unit at the regional scale.

Copyright © SLB. All Rights Reserved. Private & Confidential. Reproduction only by permission.

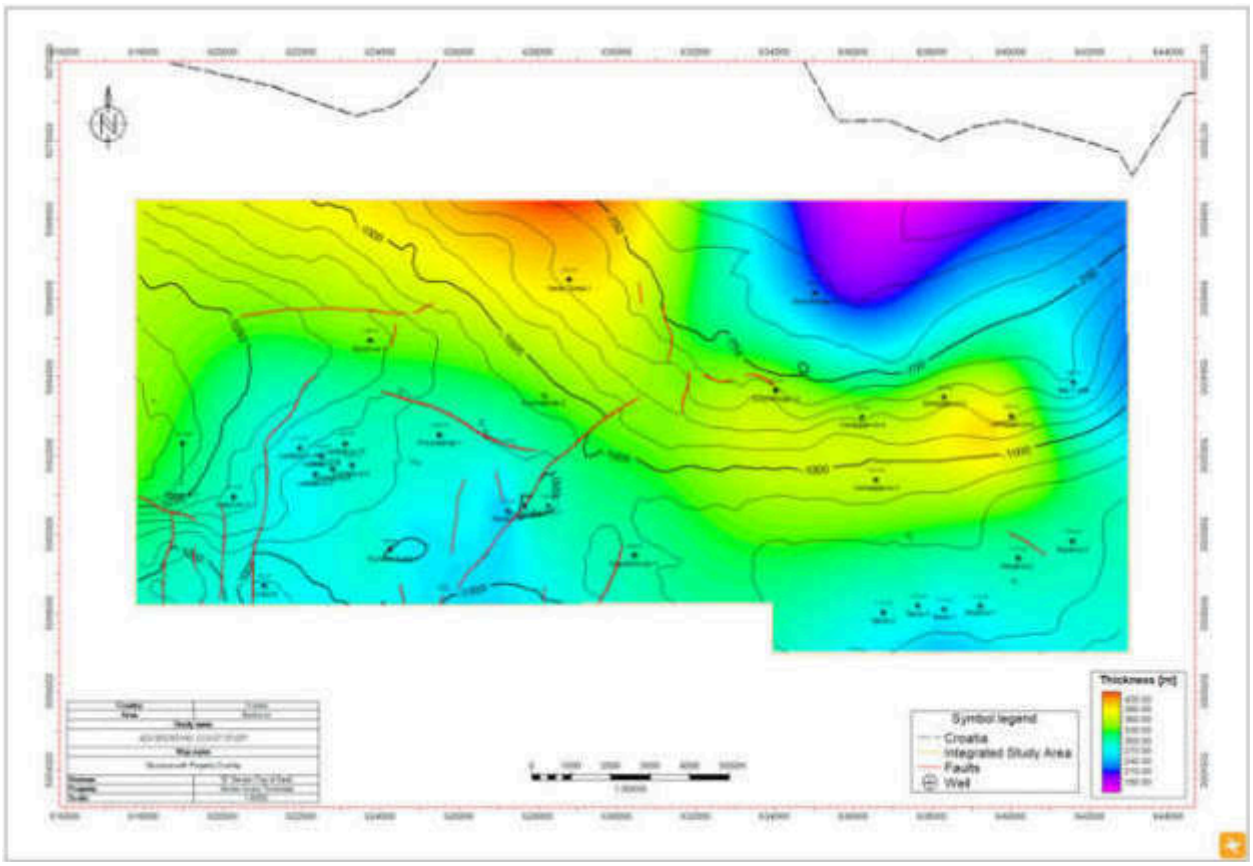


Fig. 2.128 Composite Map: Gross thickness of B with Structural contours

From a lithological perspective, the "B" Series corresponds to a clastic system within the Vinkovačka Formation (Osijek sandstones), dominated by sandstones and siltstones. Well data indicate a heterogeneous composition, including fine- to coarse-grained micaceous sandstones with carbonate cement, interbedded with marl layers of varying thickness. This alternation reflects fluctuating depositional conditions and contributes to internal variability in reservoir quality.

Although the presence of sandstone units suggests potential storage capacity, permeability is generally described as low, primarily due to the effects of carbonate cementation and the significant proportion of fine-grained material. The interbedded marls may provide localized intra-formational barriers, but they also contribute to compartmentalization and reduced connectivity within the reservoir.

When integrated with the Structural and Thickness Maps, the "B" Series emerges as a laterally continuous but internally heterogeneous system, where storage potential is controlled not only by thickness and depth, but also by lithological variability and reservoir quality distribution.

Structural assessment

The same fault system identified in Alfa (D') Series is also clearly developed within the "B" series, exhibiting comparable spatial distribution and structural extent across the AOI.

Copyright © SLB. All Rights Reserved. Private & Confidential. Reproduction only by permission.

Containment

At the top of the "B" Series, a sealing interval is consistently identified in the wells available within the AOI, although its thickness shows notable spatial variability. The seal ranges from approximately 10 m in Gat-1 Alfa to up to 122 m in the vicinity of DM-3 and Cam-4, with an average thickness of around 44 m.

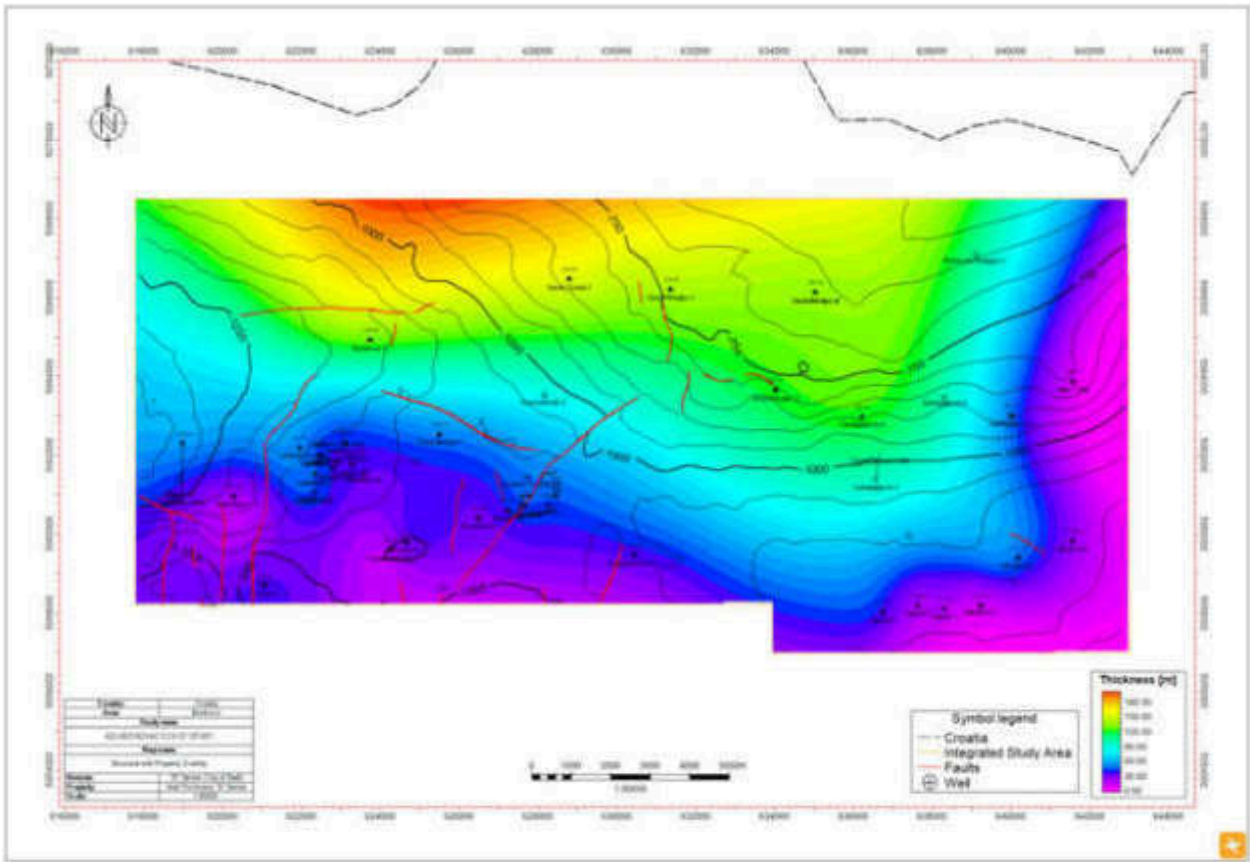


Fig. 2.129 Composite Map: Caprock Thickness of "B" Series with Structural contours

Well reports, particularly from Magadenovac-1 and Camagajevci-4, describe this interval as predominantly marl, displaying a sharp contact above the underlying sandstones. This suggests a relatively well-defined reservoir–seal boundary, supporting its role as an effective top seal at least at local scale. Overall, the thickness distribution indicates the presence of a laterally developed sealing unit, though its continuity and effectiveness varies across the area.

Copyright © SLB. All Rights Reserved. Private & Confidential. Reproduction only by permission.

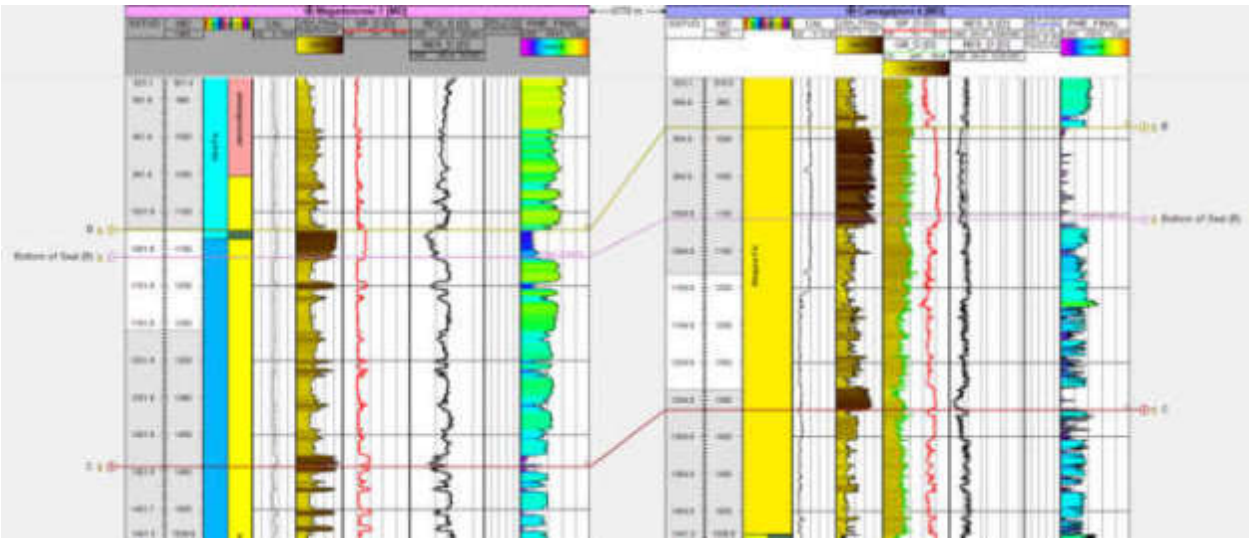


Fig. 2.130 Well correlation section between Mag-1 and Cam-4

In the eastern and south-eastern parts of the AOI, the Seal Thickness Map shows a marked reduction in seal thickness. This apparent thinning should be interpreted cautiously, as it is likely influenced by limitations in data coverage rather than representing a fully resolved geological trend. In these sectors, well control is sparse, log quality is relatively poor, and seismic data are restricted to 2D coverage.

As a result, subsurface resolution is reduced, and the reliability of interpolation decreases. The gridding process under these conditions may either exaggerate thinning trends or oversimplify lateral variations, introducing additional uncertainty into the mapped thickness distribution.

Toward the northeastern sector, in the vicinity of Well Donji Miholjac-4, the sealing interval progressively loses its distinct character and transitions into a siltier facies. The lithological contrast between reservoir and seal becomes less pronounced, with the entire "B" sequence exhibiting an overall decrease in shale content and reduced differentiation between units. For reference view: Fig. 2.75

Quality of the Storage Formation

The reservoir interval is characterized by a gross thickness ranging from approximately 34 m to 337 m, with an average of about 231 m. This indicates a laterally variable but overall well-developed reservoir package across the study area.

Copyright © SLB. All Rights Reserved. Private & Confidential. Reproduction only by permission.

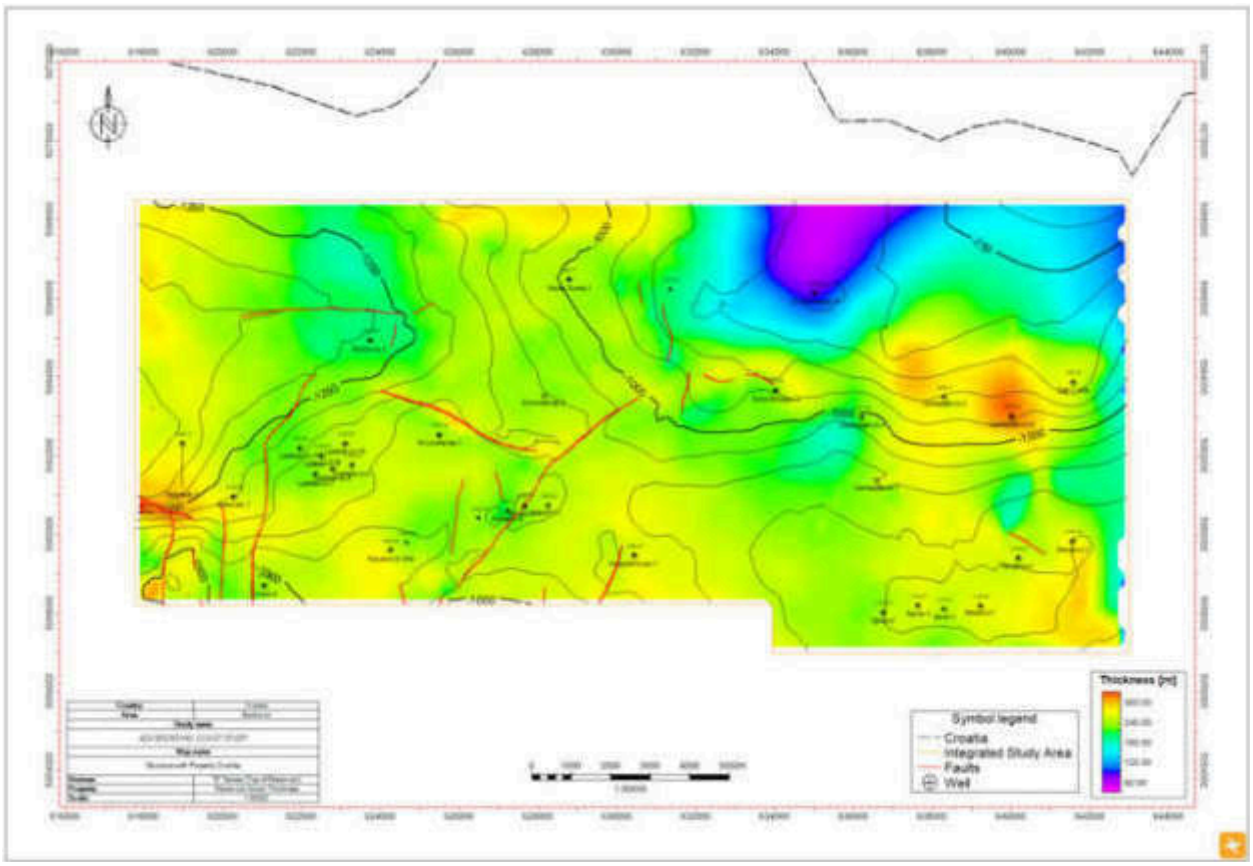


Fig. 2.131 Composite Map: Gross Thickness "B" Series (Top of Reservoir zone)

Porosity ranges from 0.025 (2.5%) to 0.32 (32%), with an average of approximately 0.17 (17%). These values are derived exclusively from net reservoir intervals, as shale-rich zones were excluded, ensuring that the results reflect effective storage capacity. The higher end of the range indicates locally favorable reservoir quality, whereas lower porosity values are associated with cemented intervals or finer-grained facies. Overall, the mean porosity suggests moderate storage potential, consistent with a heterogeneous clastic depositional system.

Copyright © SLB. All Rights Reserved. Private & Confidential. Reproduction only by permission.

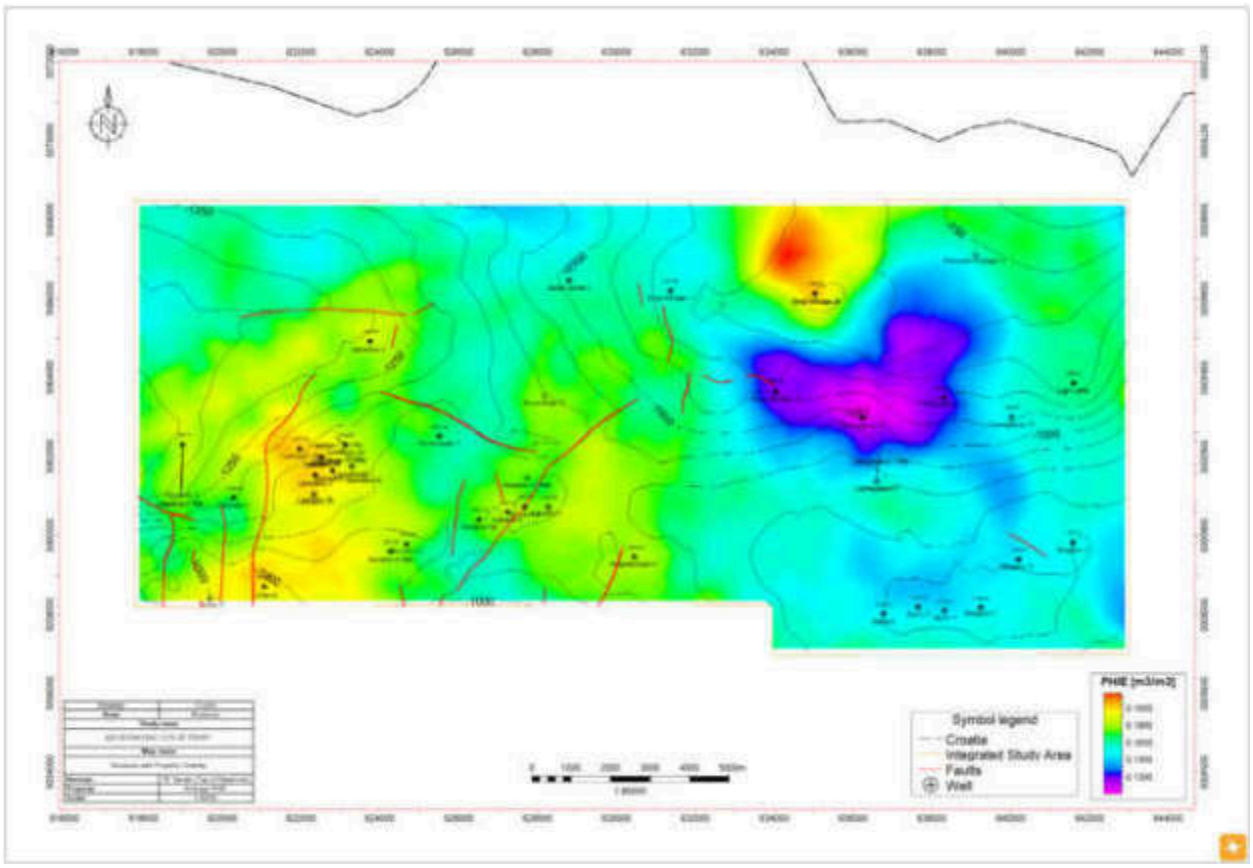


Fig. 2.132 Composite Map: Average PHIE "B" Series (Top of Reservoir zone)

The net thickness, derived after applying the reservoir definition criteria, varies from approximately 34.7 m to 326 m, with an average of 203.5 m. This suggests that a significant proportion of the gross interval contributes effectively to storage, particularly in areas where sandier facies dominate.

Copyright © SLB. All Rights Reserved. Private & Confidential. Reproduction only by permission.

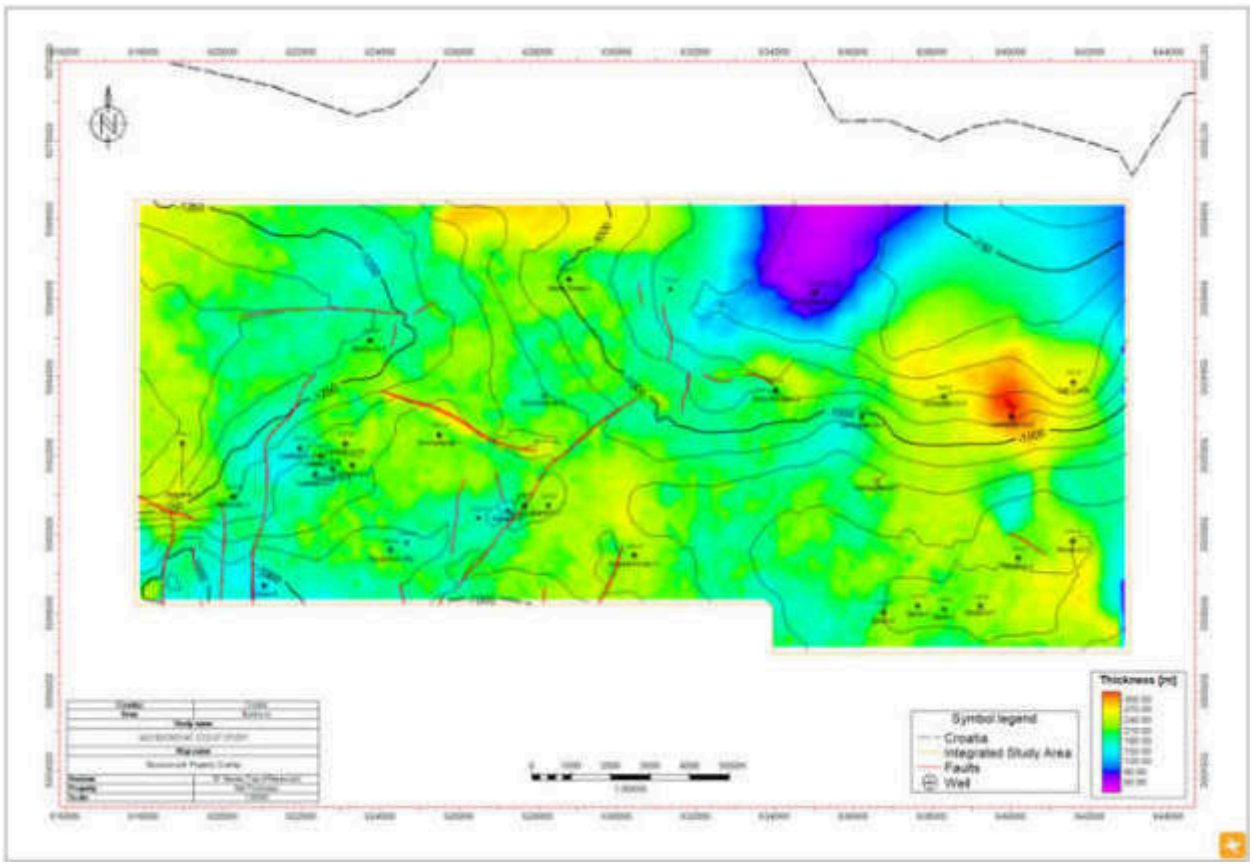


Fig. 2.133 Composite Map: Net Thickness "B" Series (Top of Reservoir zone)

Further, refining the reservoir quality using a permeability cutoff of 1 mD, the net pay thickness ranges from 34.7 m to 276 m, with an average of about 168.6 m. The reduction from net to net pay reflects the impact of tighter intervals within the formation, likely associated with increased cementation, silt content, or marl interbeds.

Copyright © SLB. All Rights Reserved. Private & Confidential. Reproduction only by permission.

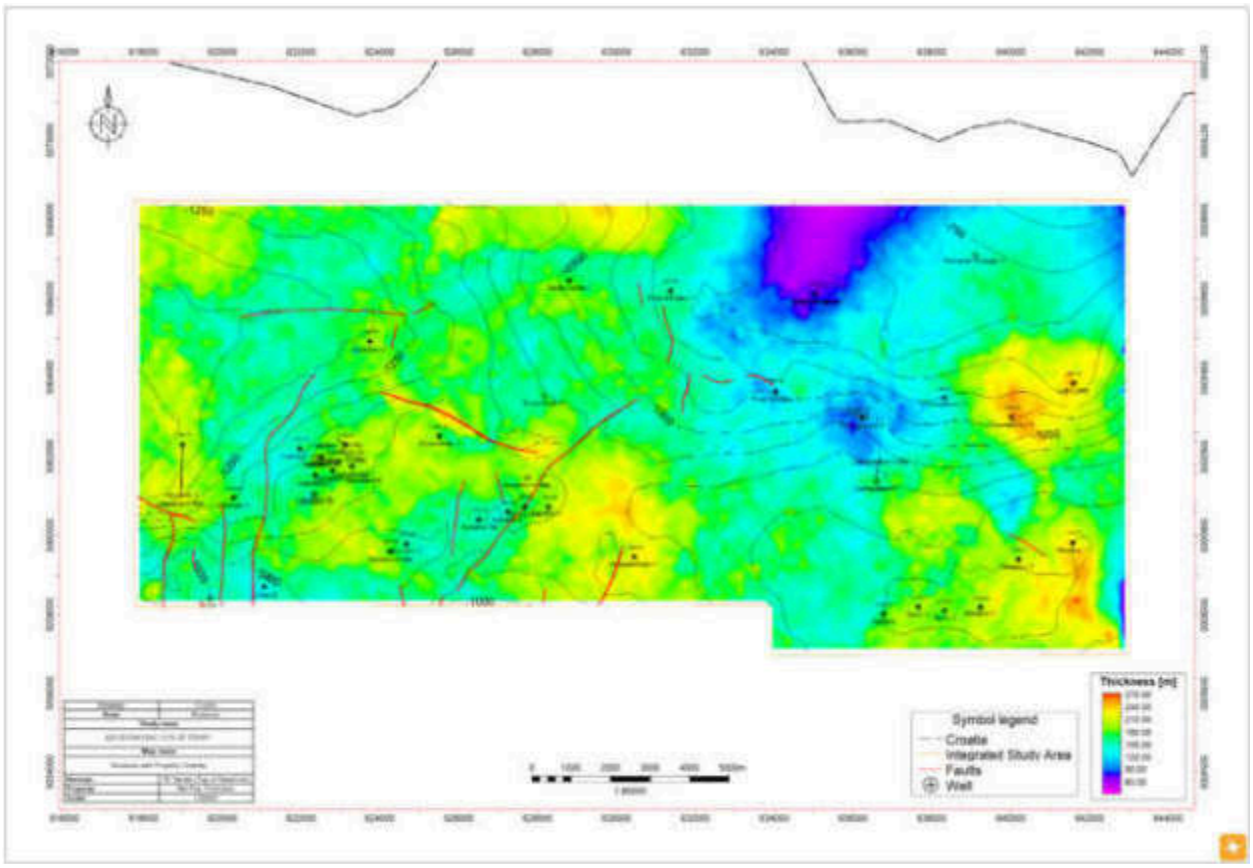


Fig. 2.134 Composite Map: Net Pay Thickness "B" Series (Top of Reservoir zone)

Overall, these parameters indicate a reservoir with good volumetric potential at regional scale, but with clear heterogeneity that must be accounted for in both capacity estimation and injectivity assessment. Zones with higher net pay and elevated porosity will represent the primary targets for CO_2 injection, while lower-quality intervals may act as internal baffles, influencing plume distribution and migration behavior.

Table 2.7 Reservoir zone "B" Series

Property	Min	Mean	Max
Gross Thickness (m)	34	231	337
Net Thickness (m)	34	203	326
Net Pay (m)	34	168.6	276
PHIE (fractions)	0.025	0.17	0.32

Conclusions "B" Series.

Overall, the "B" interval exhibits suitable depth, significant thickness, and a regionally developed top seal, all of which support its potential for CO_2 storage. However, structural complexity, lateral facies variability, and data limitations in certain sectors introduce uncertainties that require further detailed evaluation. From a screening standpoint, "B" can be considered a technically viable candidate.

Copyright © SLB. All Rights Reserved. Private & Confidential. Reproduction only by permission.

Chance of Success "B" Series

The COS map indicates a clear improvement in storage potential compared to Horizon A, driven primarily by increased depth, greater average thickness, and the presence of a more consistent regional top seal.

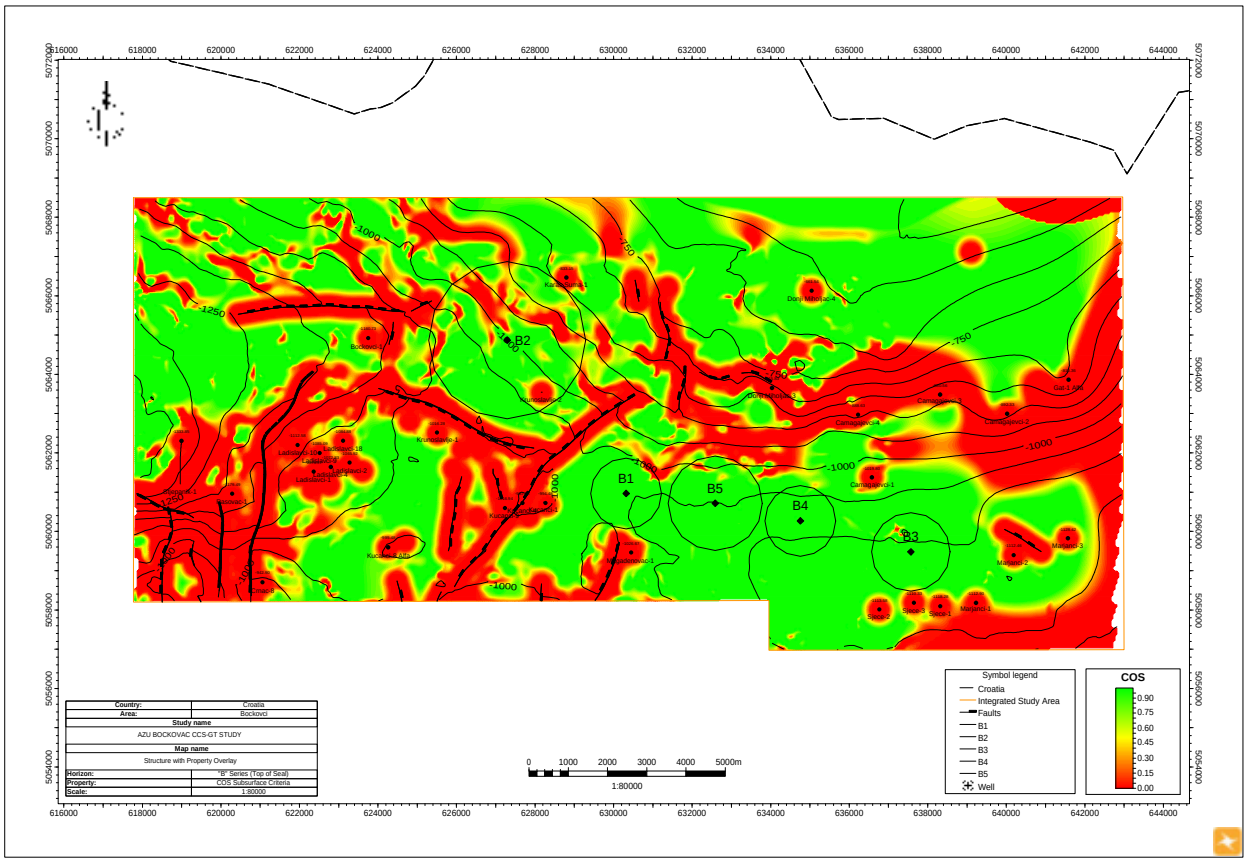


Fig. 2.135 "B" Series Chance of Success - Subsurface

The reservoir demonstrates good volumetric potential, and the depth conditions are more favorable for maintaining CO_2 in a supercritical state. The identified seal, although variable in thickness, provides a more reliable primary containment element across much of the AOI.

However, the same regional fault system continues to impact the formation, particularly in structurally complex central areas, where vertical connectivity and fault transmissibility remain key uncertainties. Additional uncertainty is introduced in the eastern and northeastern sectors, where data limitations affect the reliability of structural and thickness interpretations.

The COS map therefore delineates several discrete areas with moderate to high potential, primarily controlled by distance from faults, seal development, and data confidence. Horizon B can be considered a technically viable candidate, with clearly identifiable target zones, but still requiring focused fault and seal integrity assessment.

Copyright © SLB. All Rights Reserved. Private & Confidential. Reproduction only by permission.

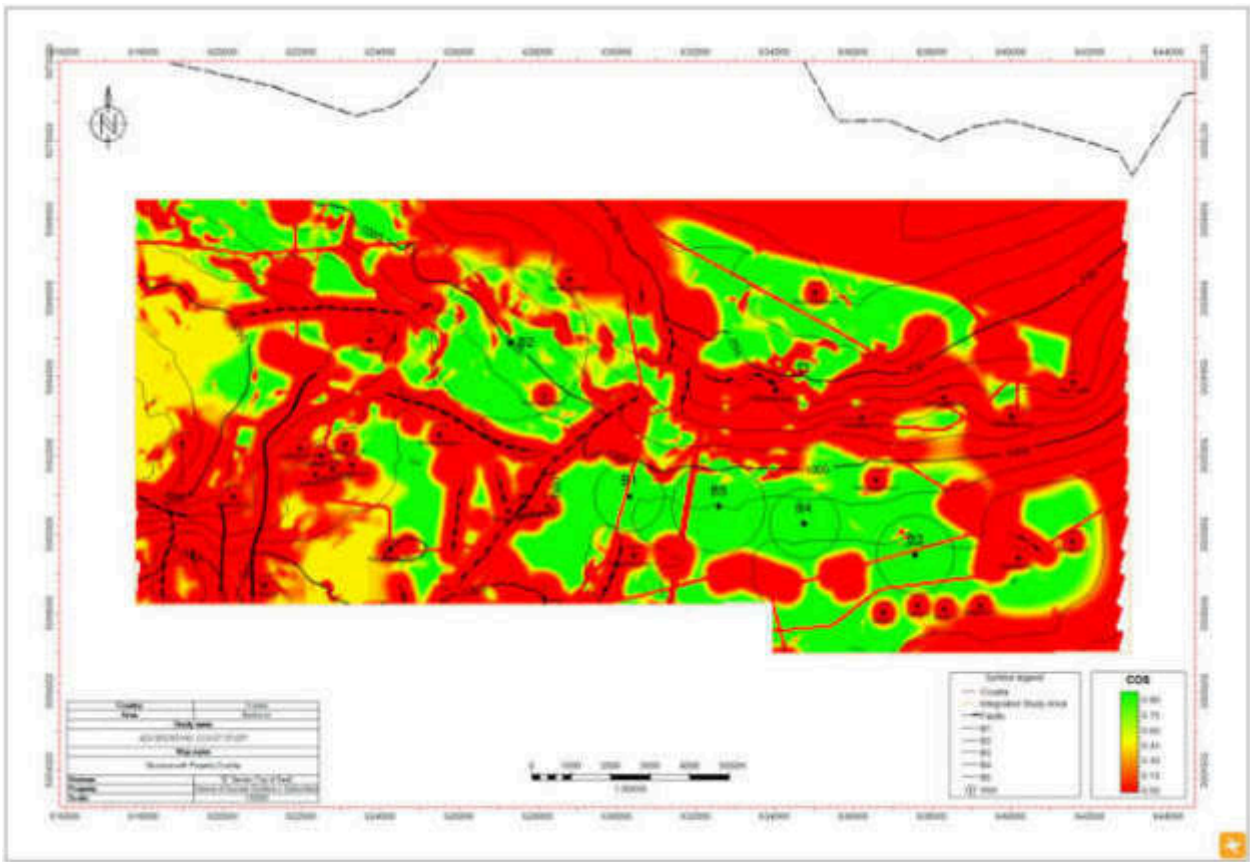


Fig. 2.136 "B" Series - Chance of Success (Subsurface x Surface)

For "B" Series, five potential areas were selected for further evaluation.

Table 2.8 "B" Series - Potential Sites

Site	Area (km2)	PHIE	Gross Thickness (m)	Net Pay Thickness (m)	Pore Volume (Mm3)
B-1	2,5	0,18	264,29	220,47	98,79
B-2	12,25	0,18	240,73	170,87	391,07
B-3	3,06	0,16	261,8	183,8	93,14
B-4	2,5	0,17	231,34	167,82	72,67
B-5	2,4	0,17	243,7	170,47	131,46

* Average Values

Copyright © SLB. All Rights Reserved. Private & Confidential. Reproduction only by permission.

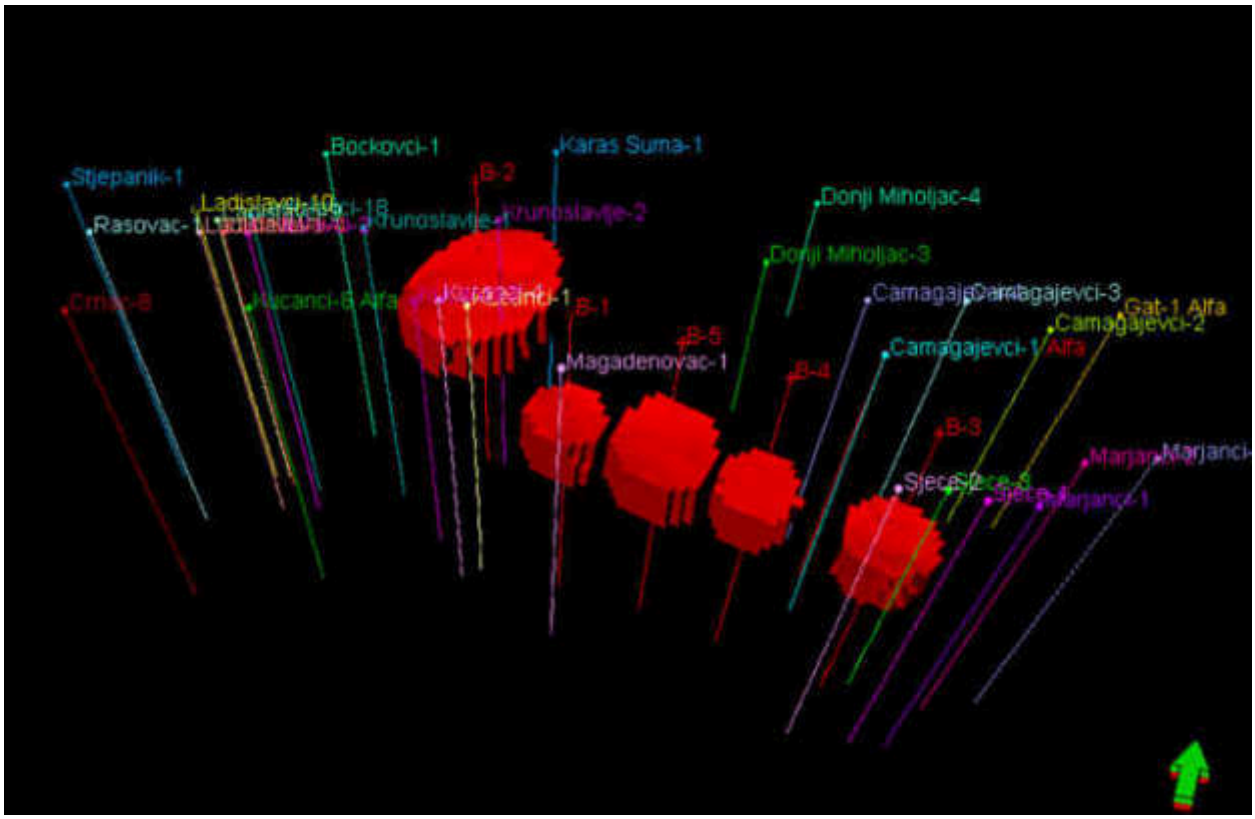


Fig. 2.137 3D View of "B" series proposed sites

"C" Series

The "C" Series is encountered at depths ranging from approximately –777.86 meters to –1691 meters. This interval places "C" entirely within the supercritical CO_2 storage window and at a deeper structural level compared to both Alfa (D') and "B" Series horizons. The broad depth range is indicative of significant structural relief across the study area, largely controlled by basement morphology and the long-term subsidence history of the basin.

Copyright © SLB. All Rights Reserved. Private & Confidential. Reproduction only by permission.

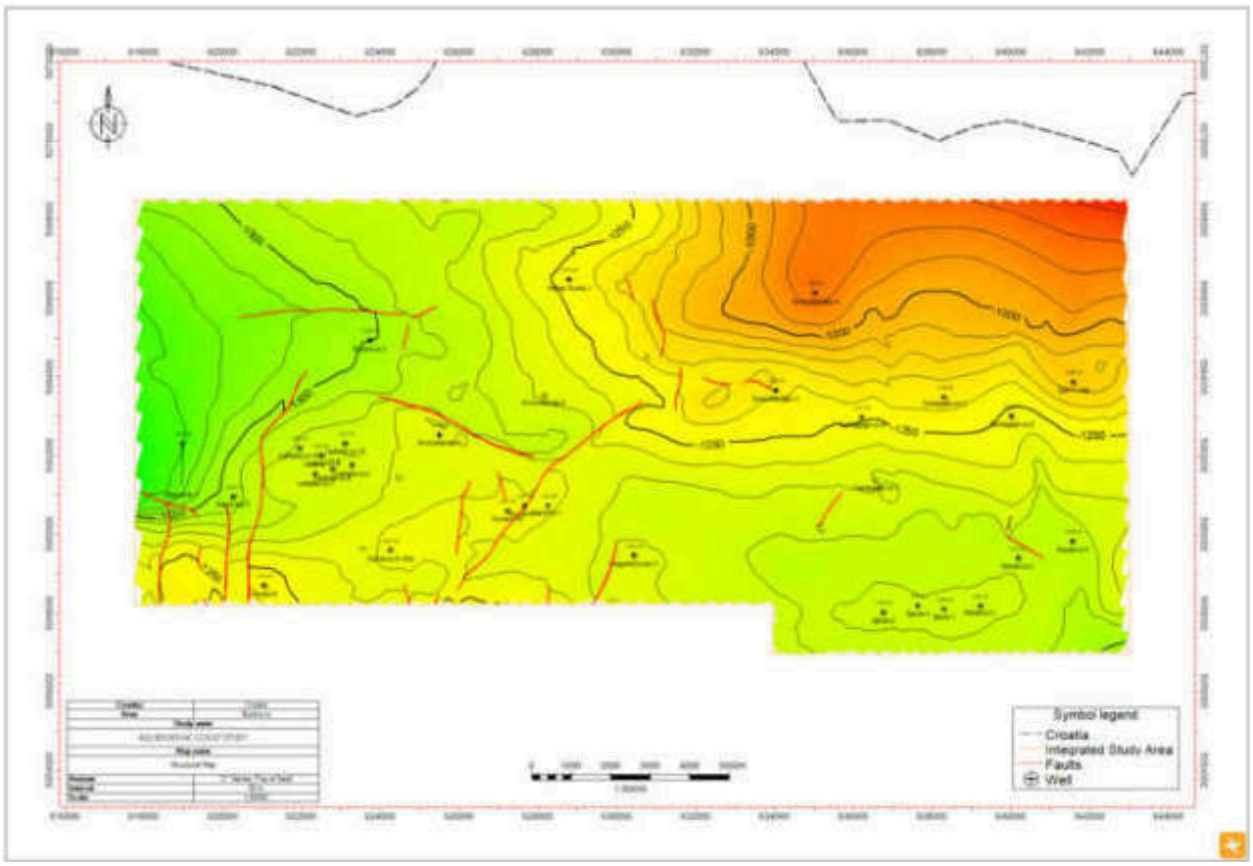


Fig. 2.138 Structural Map - "C" Series (Top of Seal)

Thickness distribution within the "C" – "D" interval is highly variable. Mapped values range from 12.15 meters in the northeastern sector, a minimum associated with pronounced basement uplift, to a maximum of 438 meters. The average thickness for this interval is approximately 227 meters, consistent with substantial accommodation space across much of the area. Zones of reduced thickness correlate with structural highs driven by basement configuration, rather than stratigraphic pinch-out. The regional distribution of thickness reveals the "C" Series as a volumetrically significant target in central and southern portions of the study area, with considerable reservoir intervals available for potential storage.

Copyright © SLB. All Rights Reserved. Private & Confidential. Reproduction only by permission.

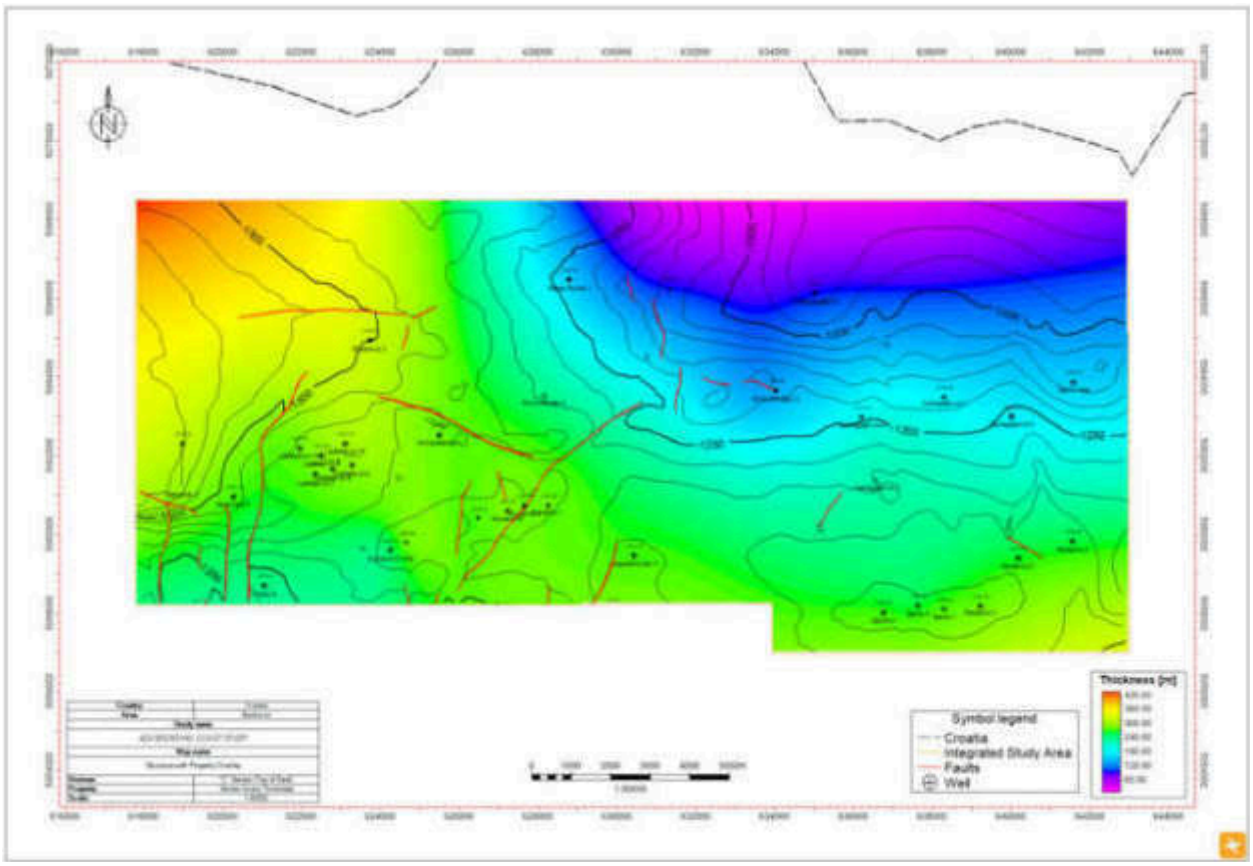


Fig. 2.139 Composite Map: "C" Series Gross Thickness with Structural Contours

The sediments of the Osijek Formation, which correspond to the "C" Series, display a consistent alternation of sandstones and marls, reflecting long-term basin subsidence with episodic uplift. The sandstones vary from very fine to coarse-grained, and carbonate cementation is observed to increase with depth. Despite frequent intervals of primary porosity (reported at 10–15%), overall permeability is low, as cementation and compaction have restricted pore connectivity, especially in the lower sections. This suggests that although primary porosity exists, permeability may be restricted due to cementation and compaction, which significantly reduces injectivity potential.

Internally, the alternation of sandstone and marl may provide local barriers and contribute to stratigraphic compartmentalization, but does not substitute for a laterally continuous, thick top seal.

Structural assessment

Structurally, the top of the "C" reservoir is characterized by a gentle regional dip of approximately 2.2°, similar to overlying units, and can be considered generally conformable at the basin scale. Locally elevated dips are present but are not associated with significant deformation. The regional fault system mapped in the "Alfa (D') - B" interval persists through C, sharing similar trends in extent and orientation.

Copyright © SLB. All Rights Reserved. Private & Confidential. Reproduction only by permission.

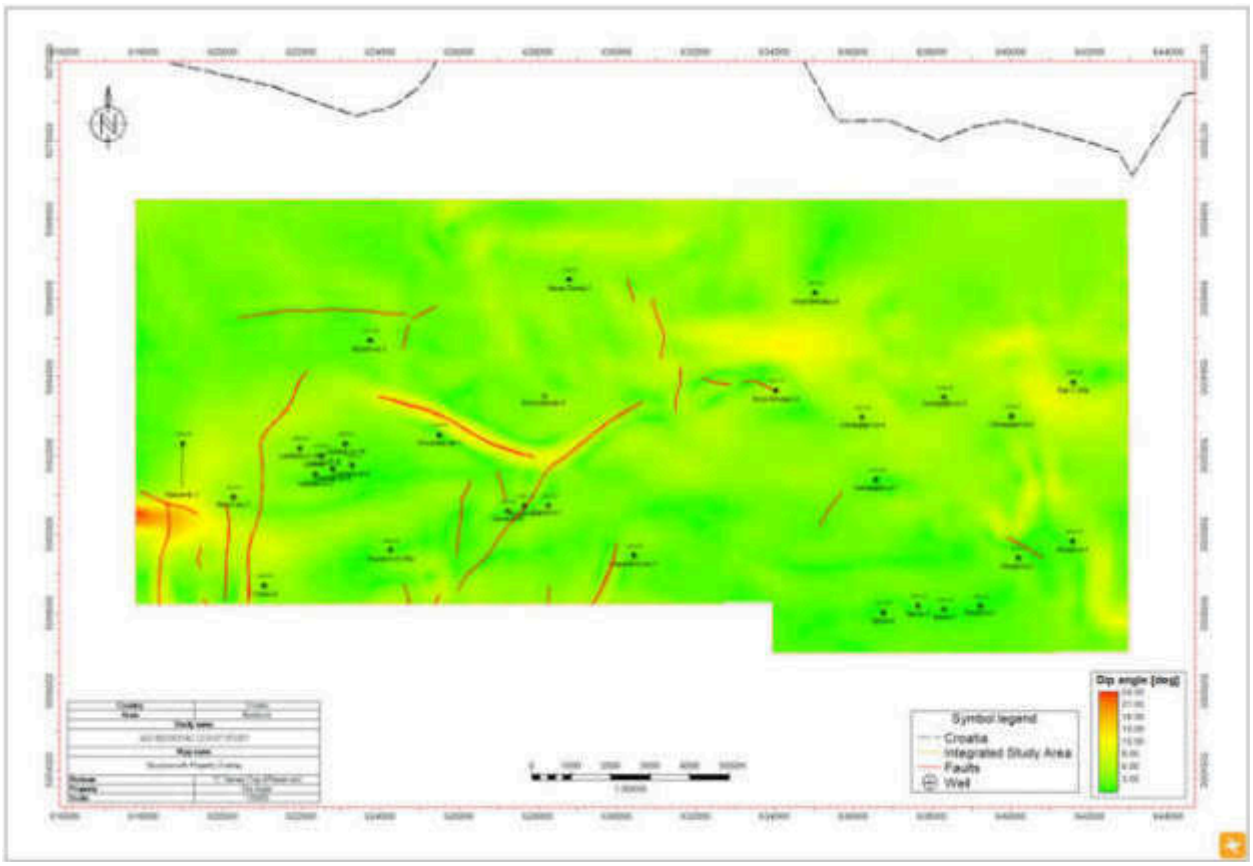


Fig. 2.140 Composite Map: "C" Series - Dip Angle

Containment

Top seal thickness across the "C" Series is variable, with mapped values ranging from a minimum of 7.24 meters to a maximum of 52.33 meters and an average close to 15.28 meters. In areas where seal thickness falls below 10 meters, the potential for effective containment is diminished, and these sectors present elevated risk and could be downgraded in site selection assessment.

Copyright © SLB. All Rights Reserved. Private & Confidential. Reproduction only by permission.

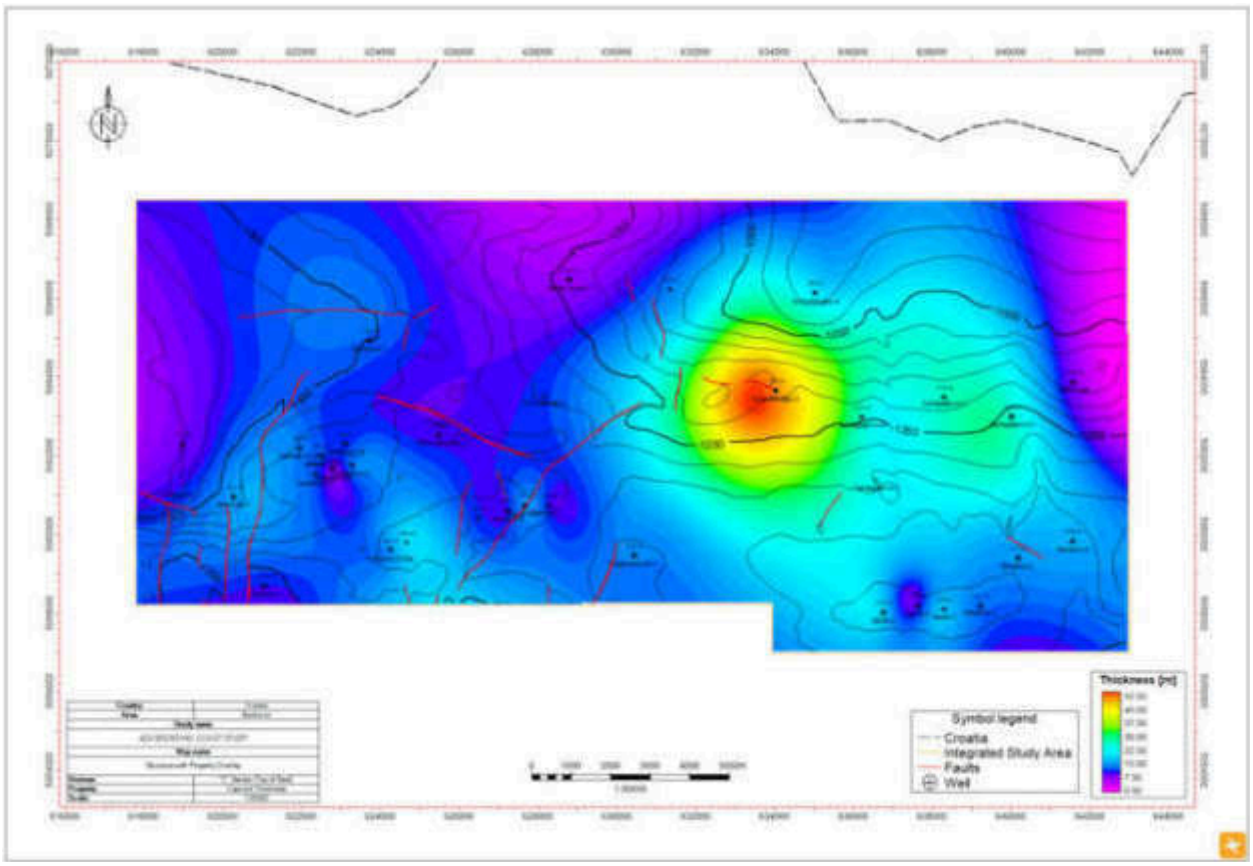


Fig. 2.141 Composite Map: "C" Series (Top of Seal) - Caprock Thickness

However, given the presence of Seal B above, which may function as an additional secondary barrier, these zones would not necessarily be excluded but rather evaluated within a multi-layer containment framework.

Below this marl, alternating sandstone packages and marl interbeds are observed, indicating repeated episodes of basin uplift and renewed subsidence. This cyclic sedimentation pattern suggests fluctuating accommodation and energy conditions during deposition. This internal alternation of sandstones and marls may contribute to vertical permeability reduction and compartmentalization but does not replace the requirement for a thick and laterally extensive top seal. The effectiveness of containment, therefore, remains firmly dependent on the continuity and integrity of this primary sealing horizon as well as the secondary barrier above.

Quality of the Storage Formation

The reservoir interval within Horizon C is characterized by a gross thickness ranging from approximately 2 m to 429 m, with an average of about 212 m. This wide range reflects significant lateral variability, likely influenced by structural controls and localized depositional patterns, including areas affected by basement uplift toward the northeastern sector.

Copyright © SLB. All Rights Reserved. Private & Confidential. Reproduction only by permission.

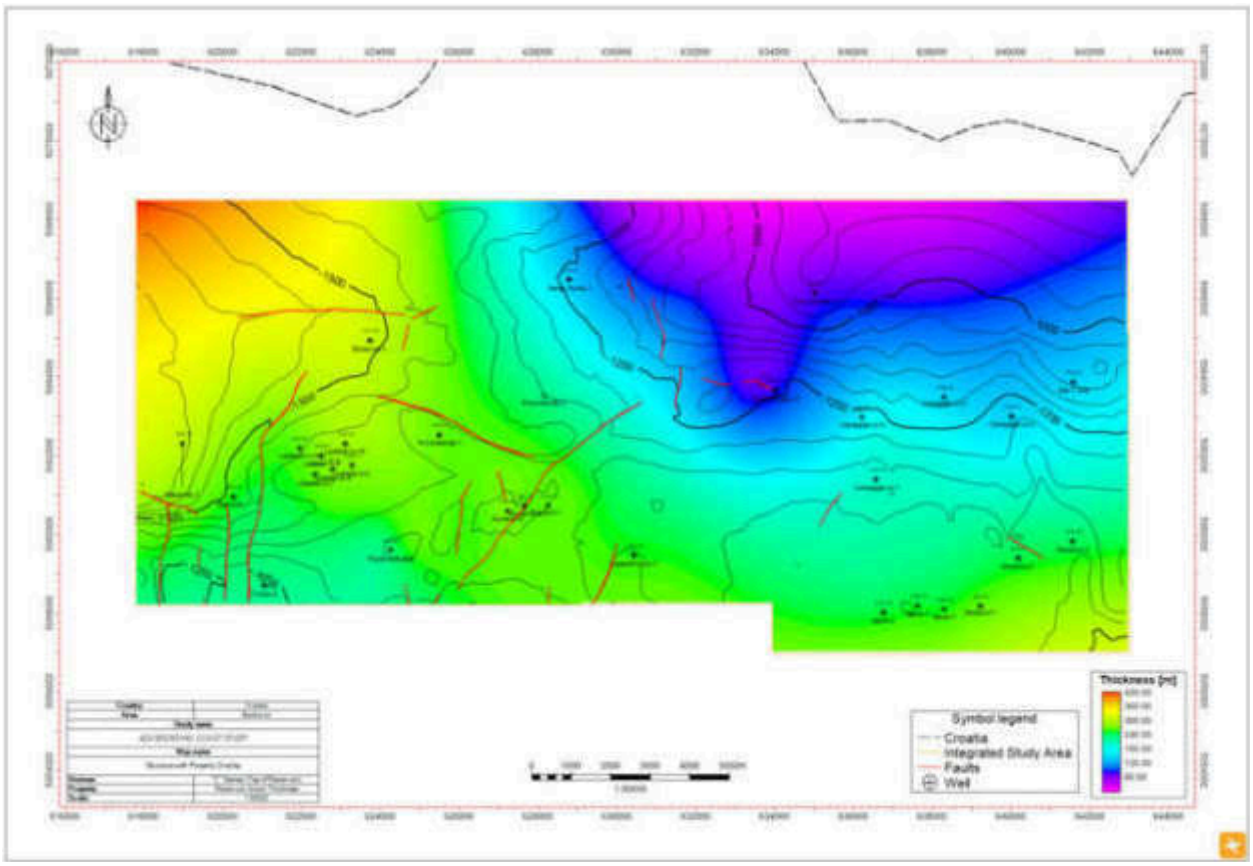


Fig. 2.142 Composite Map: Gross Thickness of "C" Reservoir with Structural Contours

The net thickness varies between approximately 0.5 m and 382 m, with an average of about 195 m, indicating that a substantial portion of the gross interval contributes to the reservoir. However, the presence of very low minimum values highlights zones where reservoir quality is either poorly developed or absent, likely associated with increased marl content or tighter facies.

Copyright © SLB. All Rights Reserved. Private & Confidential. Reproduction only by permission.

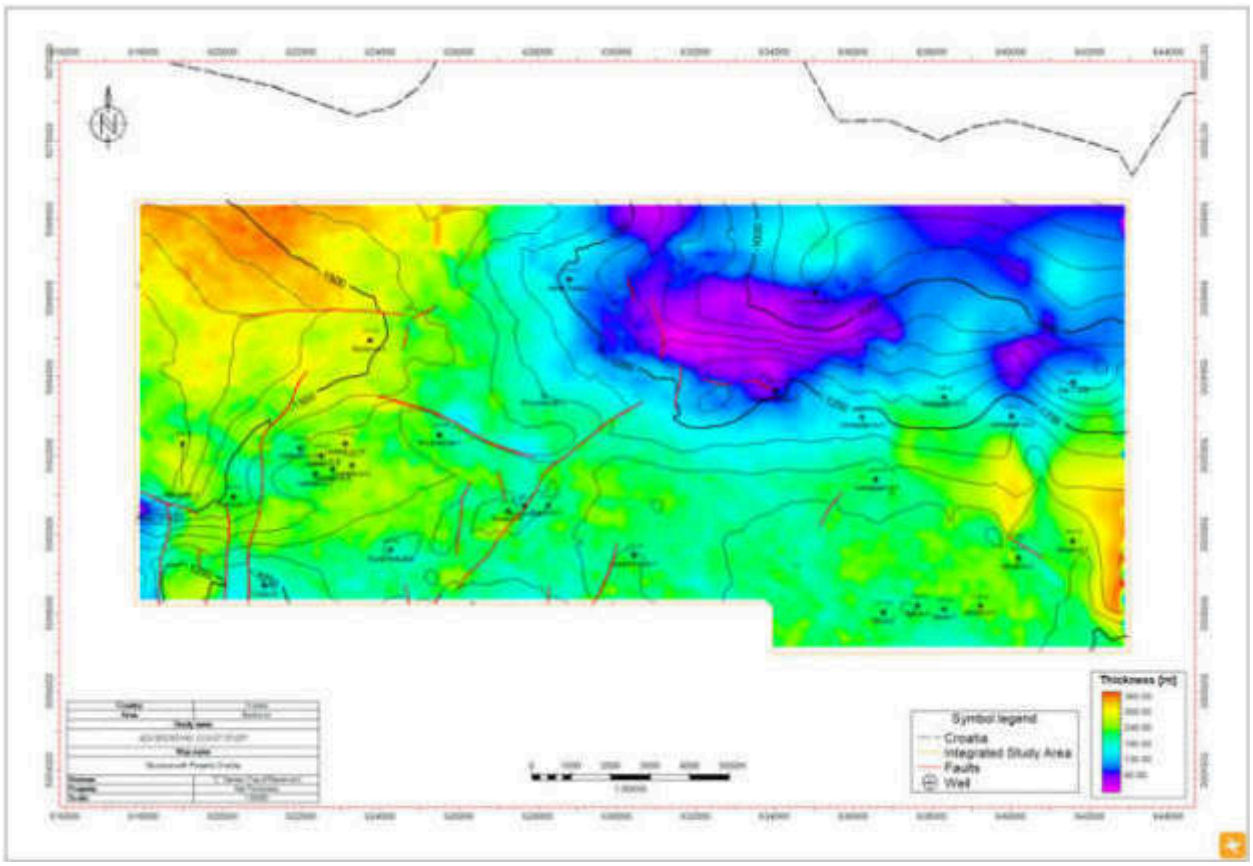


Fig. 2.143 Composite Map: Net Thickness of "C" Reservoir with Structural Contours

Applying a permeability cutoff, the net pay thickness ranges from 0 m to approximately 235 m, with an average of about 92 m. The occurrence of zero net pay in certain areas suggests intervals where permeability is insufficient for effective fluid flow, reinforcing the heterogeneous nature of the formation. The reduction from net to net pay reflects the impact of cementation, fine-grained material, and poor pore connectivity.

Copyright © SLB. All Rights Reserved. Private & Confidential. Reproduction only by permission.

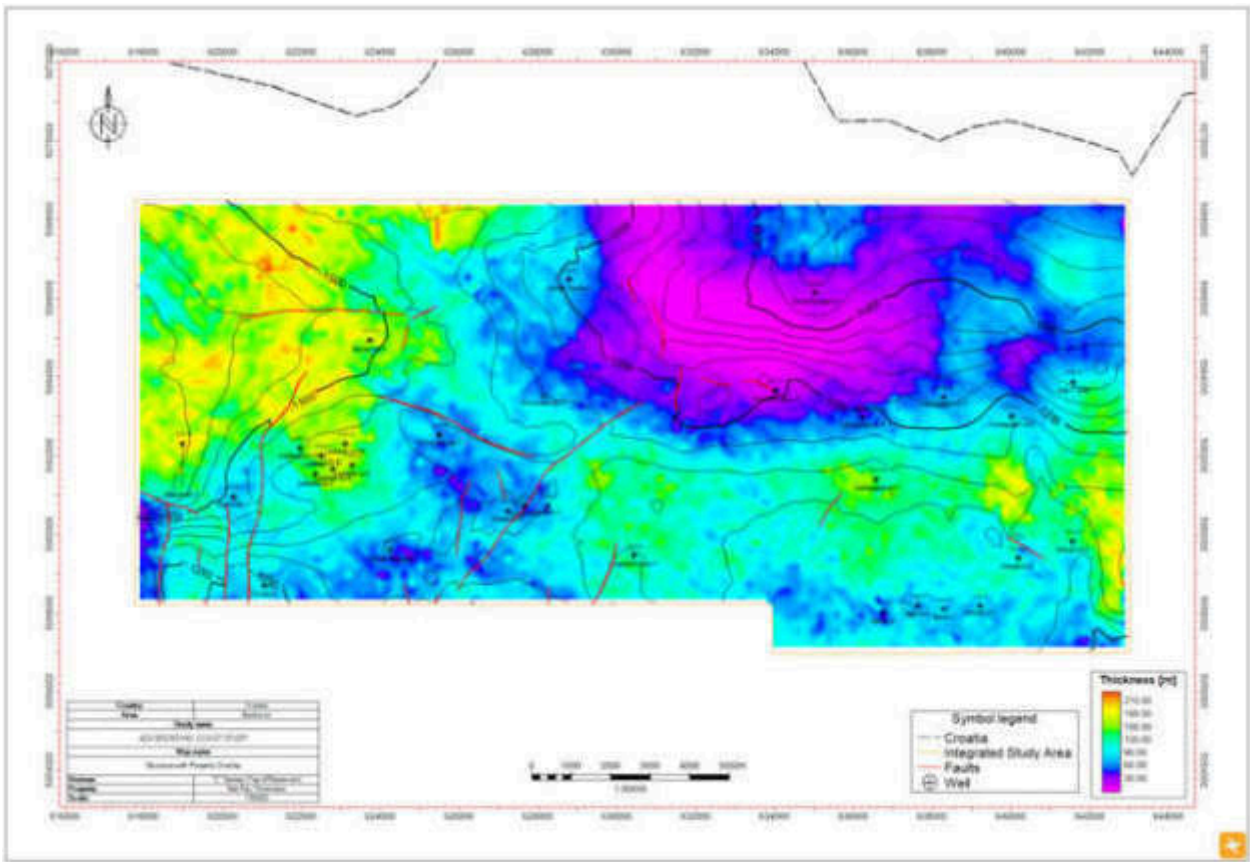


Fig. 2.144 Composite Map: Net Pay Thickness of "C" Reservoir with Structural Contours

Porosity (PHIE) values range from 0.08 (8%) to 0.16 (16%), with an average of approximately 0.12 (12%). These values are derived exclusively from net reservoir intervals, ensuring that they represent effective storage capacity. The relatively narrow range and moderate average indicate generally low to moderate reservoir quality, consistent with a system affected by carbonate cementation and variable grain size. Lower porosity values correspond to tighter, less permeable zones, while the upper range suggests limited intervals of improved storage properties.

Copyright © SLB. All Rights Reserved. Private & Confidential. Reproduction only by permission.

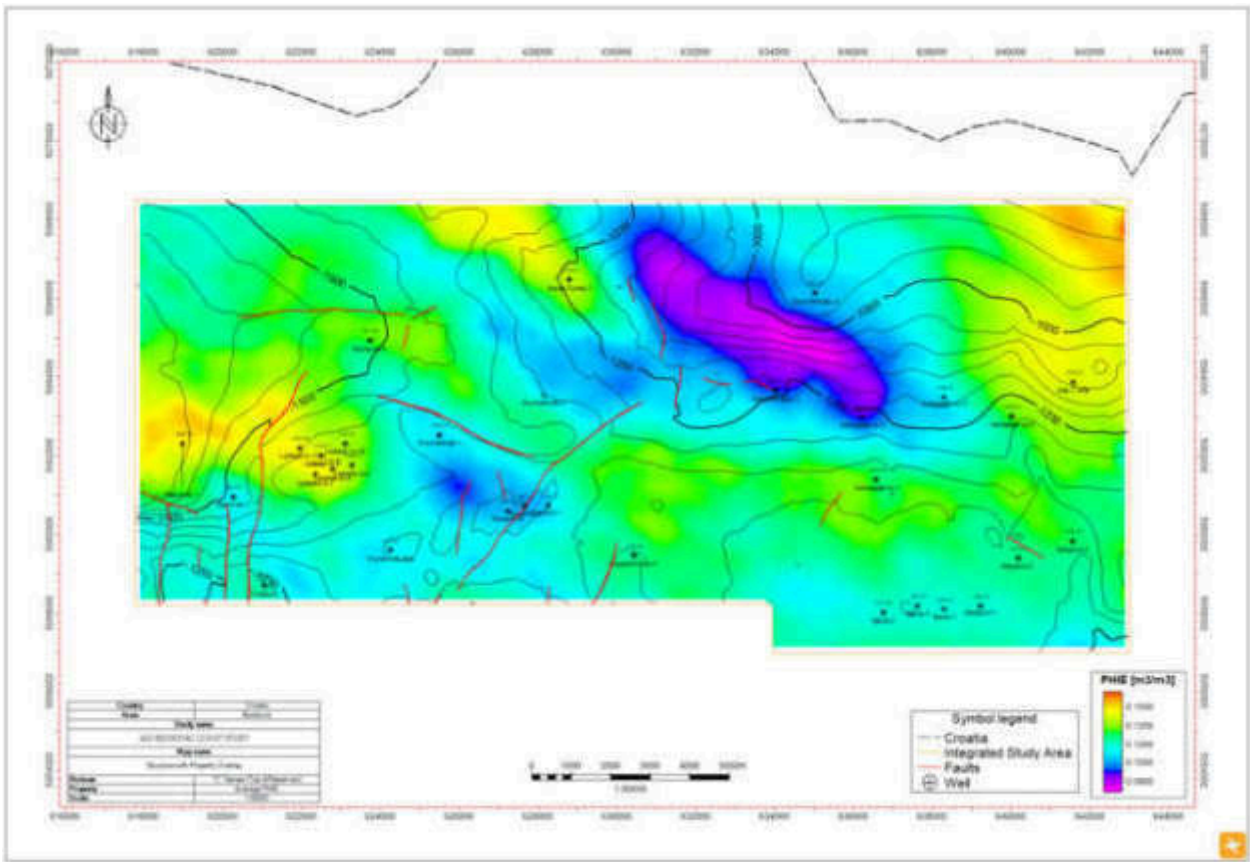


Fig. 2.145 Composite Map: Average PHIE of "C" Reservoir with Structural Contours

Conclusions "C" Series

Overall, C Reservoir zone presents a reservoir with moderate volumetric potential but reduced reservoir quality compared to shallower units. The combination of moderate thickness, relatively low porosity, and limited net pay development suggests that storage capacity exists but may be constrained by injectivity. Heterogeneity within the formation is expected to influence CO_2 plume behavior, with better-quality intervals acting as preferential flow paths, while tighter zones may function as internal baffles, affecting vertical and lateral migration.

Table 2.9 Reservoir zone "C" Series

Property	Min	Mean	Max
Gross Thickness (m)	2.06	211.65	428.64
Net Thickness (m)	0.45	195.47	381.87
Net Pay Thickness (m)	0	91.65	234.77
PHIE (fractions)	0.08	0.12	0.16

Chance of Success "C" Series

The COS map reflects a balance between favorable depth and thickness conditions and limitations related to reservoir quality and seal effectiveness.

Copyright © SLB. All Rights Reserved. Private & Confidential. Reproduction only by permission.

While the formation benefits from suitable burial depth and a relatively consistent structural framework, reservoir properties are generally weaker, with low permeability and moderate porosity restricting injectivity and effective storage performance.

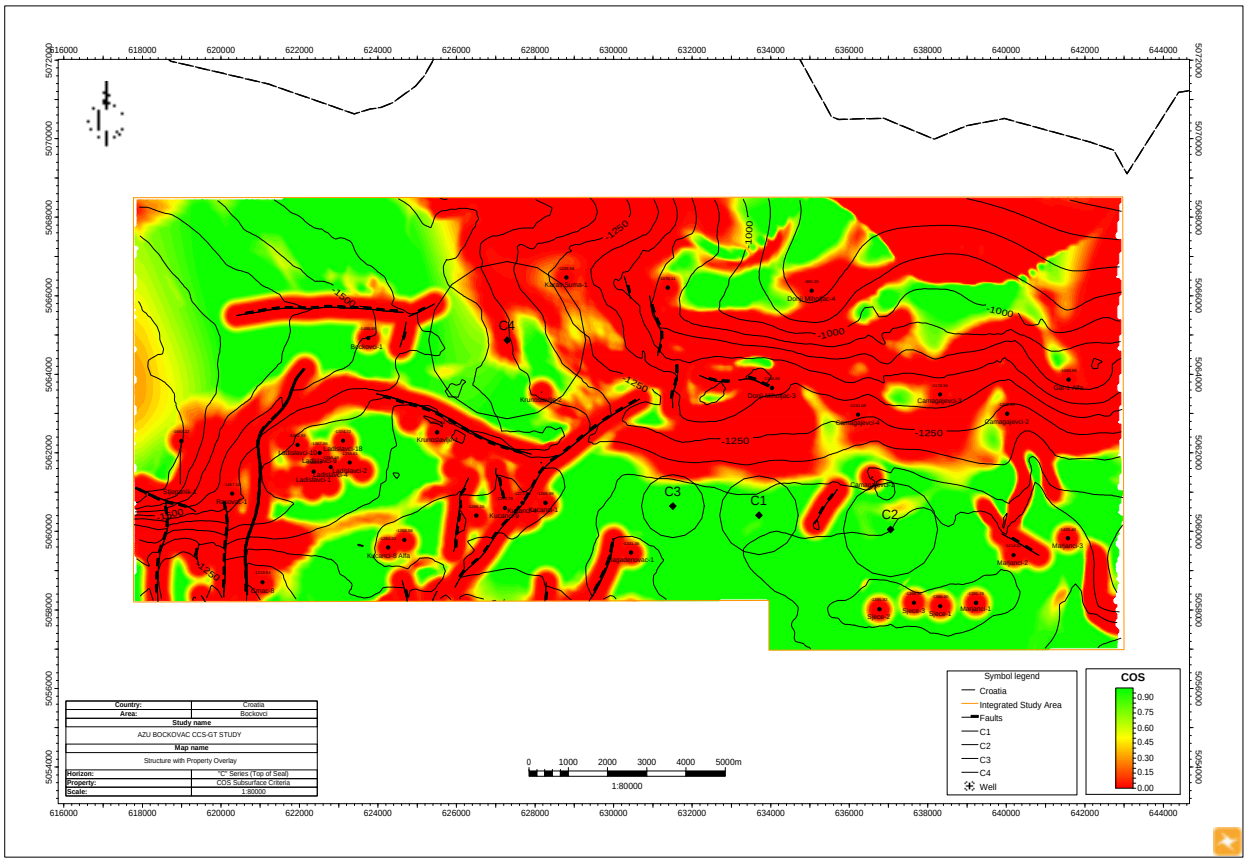


Fig. 2.146 COS Subsurface "C" Series

The sealing capacity is present but relatively thin, placing greater importance on the overlying sealing intervals. In areas where seal thickness approaches lower thresholds, the COS is correspondingly reduced. The persistence of the regional fault system, with similar characteristics to Horizon B, continues to represent a key risk factor, particularly where faults may act as vertical migration pathways.

Consequently, the COS map identifies fewer high-quality areas, with most zones classified as moderate potential

Copyright © SLB. All Rights Reserved. Private & Confidential. Reproduction only by permission.

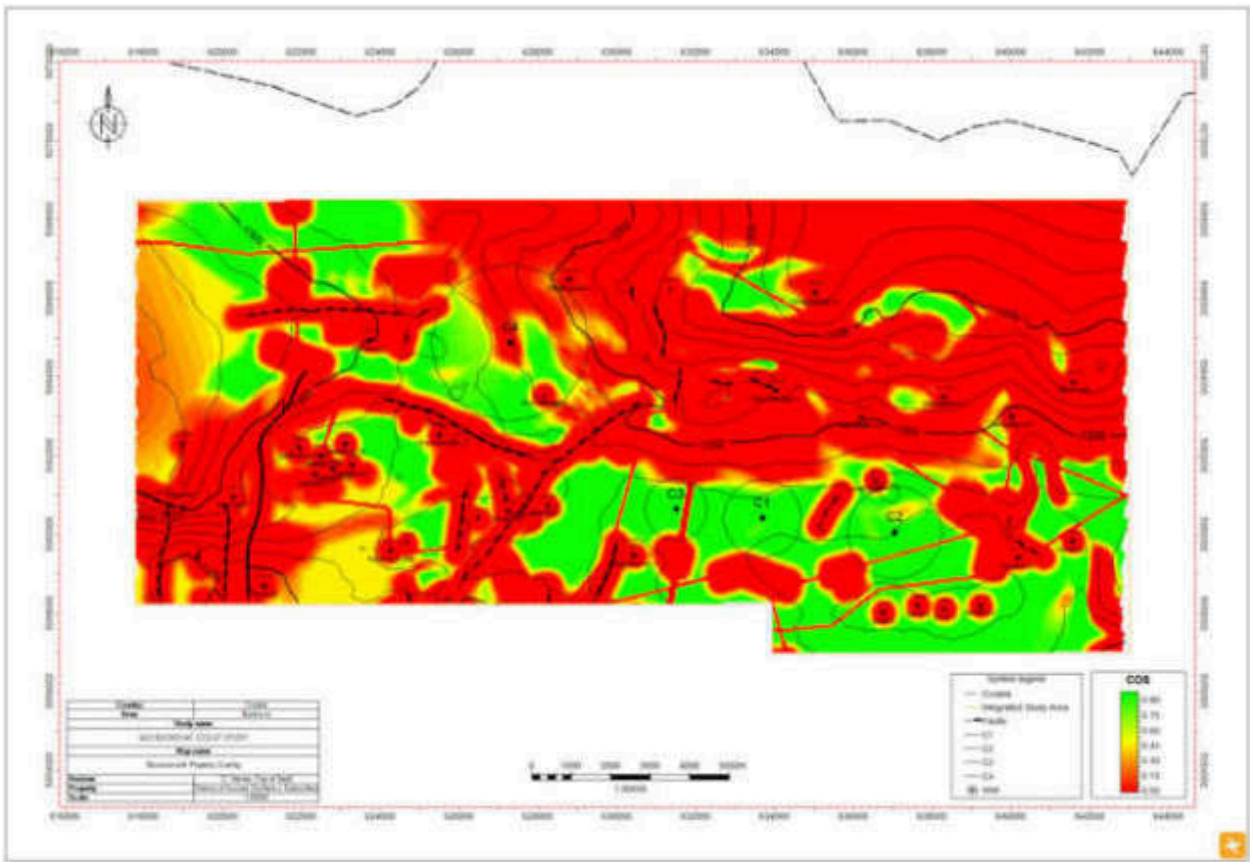


Fig. 2.147 Chance of Success (Surface x Subsurface)

For "C" series, four potential areas were identified suitable for further evaluation

Table 2.10 "C" Series - Potential sites

Site	Area (km2)	PHIE	Gross Thickness (m)	Net Pay Thickness (m)	Pore Volume (Mm3)
C-1	3	0,14	242,14	101	43,85
C-2	4,4	0,15	248,05	122,7	81,02
C-3	1,9	0,15	260,53	117,6	35,36
C-4	12.2	0,15	221,68	80,89	153,93

* Average values

Copyright © SLB. All Rights Reserved. Private & Confidential. Reproduction only by permission.

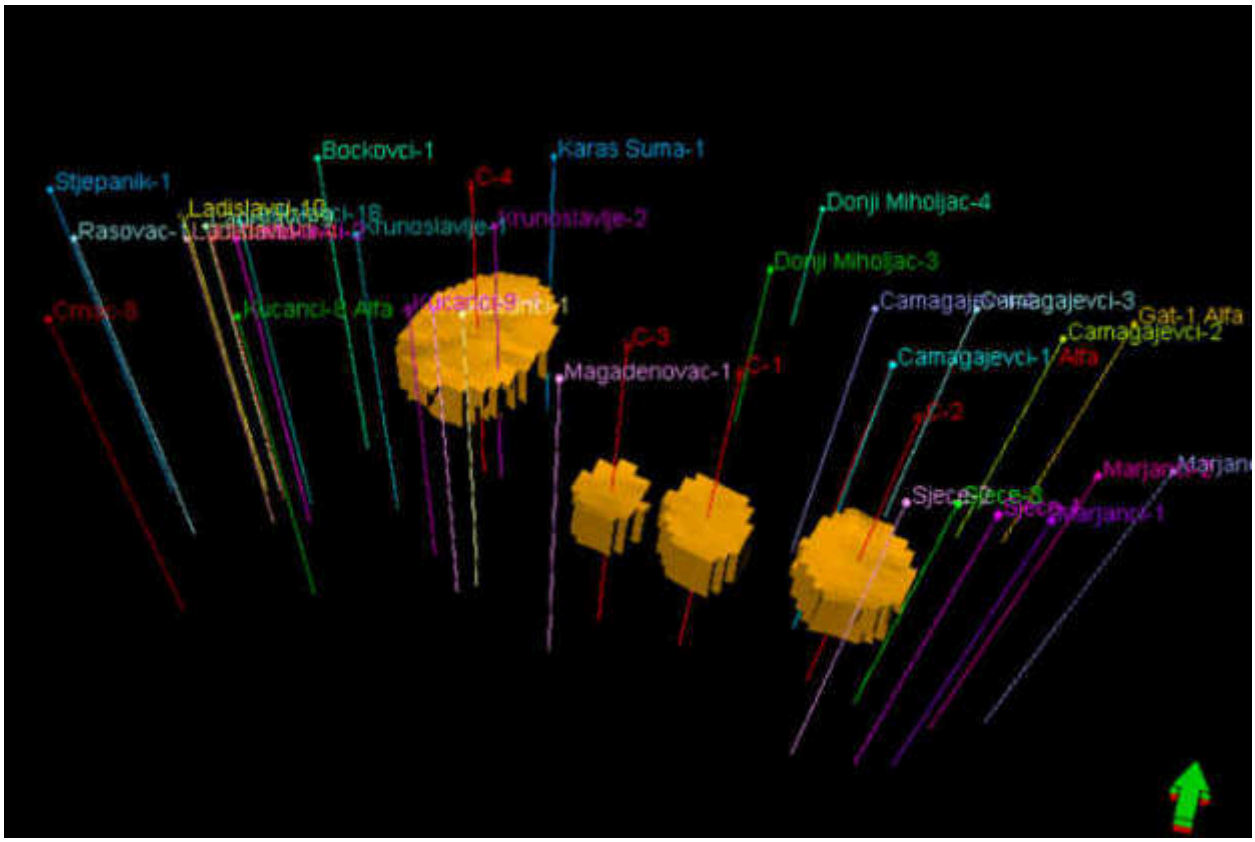


Fig. 2.148 3D View of "C" Series potential sites

"D" Series

Formation "D" is observed at depths ranging from approximately −848 meters to −2030 meters across the study area, as illustrated on the Structural Map. This wide depth range reflects significant structural variation, including the presence of structural highs and lows, which are important for understanding both reservoir architecture and potential containment risks or advantages.

Copyright © SLB. All Rights Reserved. Private & Confidential. Reproduction only by permission.

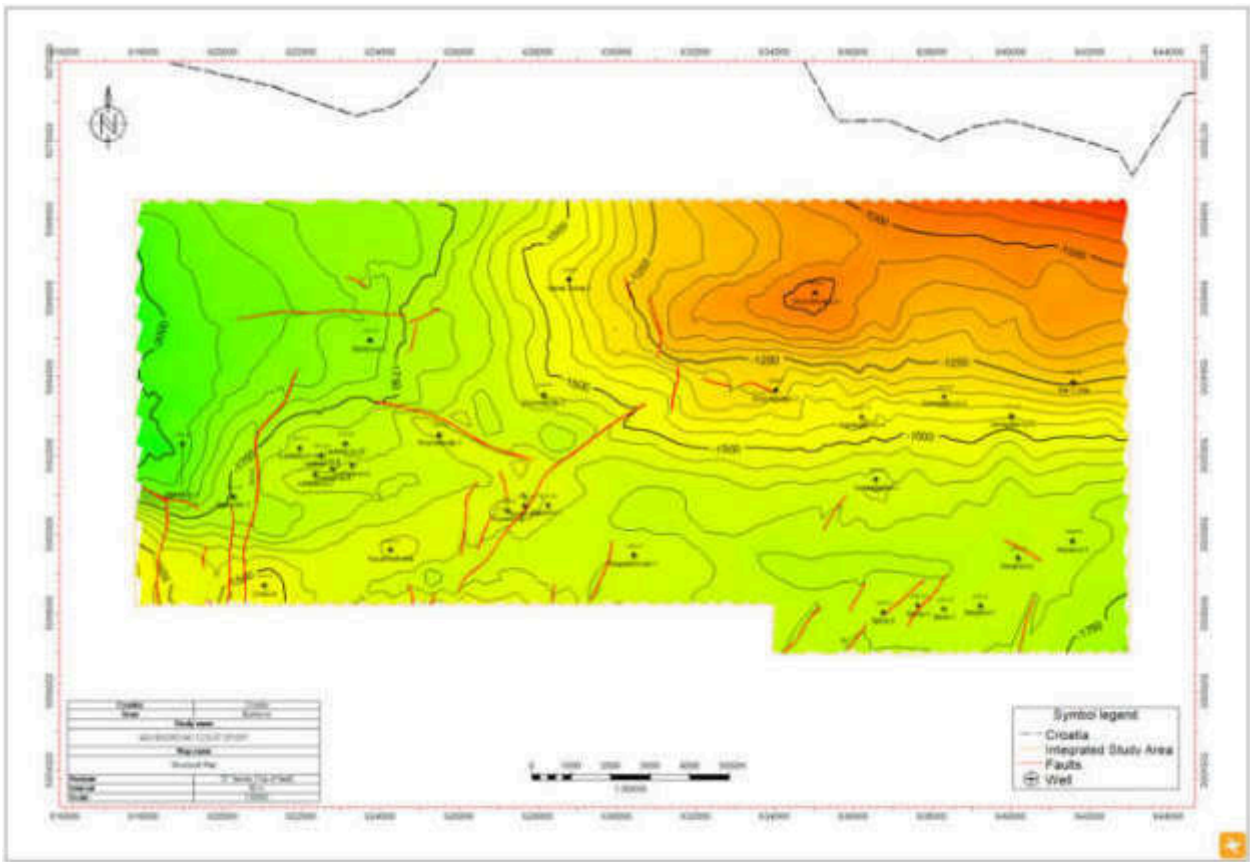


Fig. 2.149 Structural Map "D" Series

From a depositional perspective, "D" is characterized by an alternation of sandstone and shale, defining a layered reservoir–seal system. This heterolithic architecture suggests a complex depositional environment with fluctuating energy conditions, likely influencing both reservoir quality and vertical connectivity.

Copyright © SLB. All Rights Reserved. Private & Confidential. Reproduction only by permission.

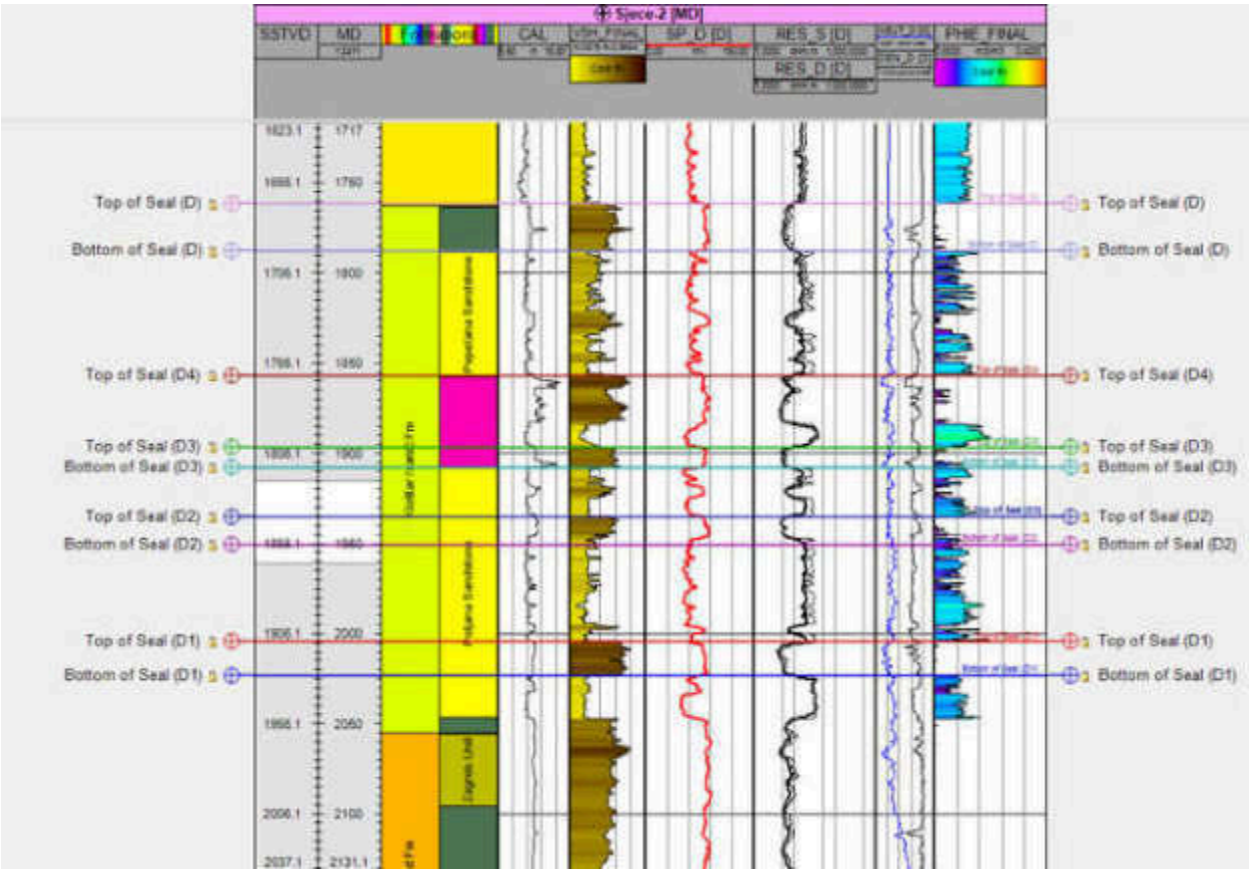


Fig. 2.150 "D" Series - Sand - Shale alternation

The overall thickness of the formation varies considerably, from 0 m in structurally elevated areas to a maximum of approximately 1005 m, with an average thickness of around 249 m. This wide range reflects both structural control and depositional variability, with thicker accumulations likely associated with accommodation space development in more subsident areas.

Structural assessment

From a structural perspective, the fault framework affecting this formation is consistent with that observed in the overlying and underlying intervals, indicating a persistent tectonic regime across the stratigraphic column. The main fault system maintains a similar spatial distribution and extent, suggesting structural inheritance and repeated reactivation.

In addition to this regional framework, several smaller-scale faults are identified in the vicinity of wells Sjece-2 and Camagajevci-4. These appear to be localized features that are confined to this formation and do not propagate into adjacent intervals. Their limited vertical extent suggests they may be stratigraphically controlled or related to localized stress adjustments rather than major tectonic events.

Copyright © SLB. All Rights Reserved. Private & Confidential. Reproduction only by permission.

Although these faults are of smaller magnitude, they introduce additional compartmentalization within the formation and may influence fluid flow behavior at a local scale. Their presence should therefore be considered in the context of injectivity, lateral connectivity, and potential intra-formational migration pathways.

Containment

While multiple sealing layers are present, their effectiveness is not uniform across the study area. The cumulative thickness of these seals provides a degree of vertical containment; however, the variability in their development, combined with lateral continuity uncertainties, introduces risk.

Quality of the Storage Formation

Porosity data from wells indicate moderate reservoir quality. In well Mag-1, porosity values reach up to approximately 15%, while improved reservoir properties are observed toward the southeastern sector, where porosity reaches up to 20% in well Sjece-2. The spatial distribution of porosity, derived from property modeling, shows values ranging between approximately 11% and 19%, with an average of around 0.09%.

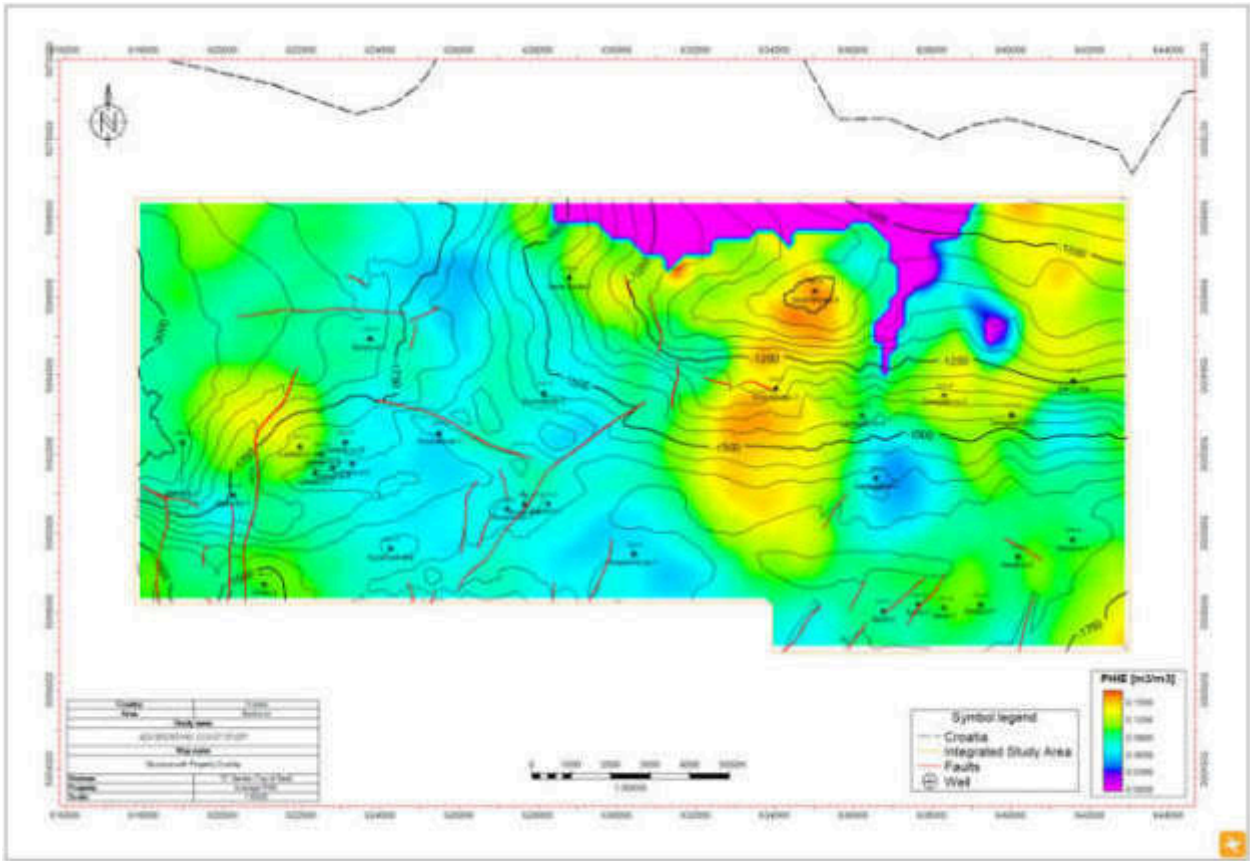


Fig. 2.151 Composite Map: "D" Series (Top of Seal) Cumulative Reservoir Average PHIE

Copyright © SLB. All Rights Reserved. Private & Confidential. Reproduction only by permission.

The cumulative values for the layered reservoirs indicate a clear distinction between total net thickness and effective net pay.

Net thickness ranges from approximately 0 m to 707 m, with an average around 157 m, reflecting the overall vertical development of intervals that meet the reservoir criteria. However, when applying the permeability cutoff to define net pay, the effective thickness is significantly reduced, ranging from 0 m to 212 m, with an average of only about 29.2 m.

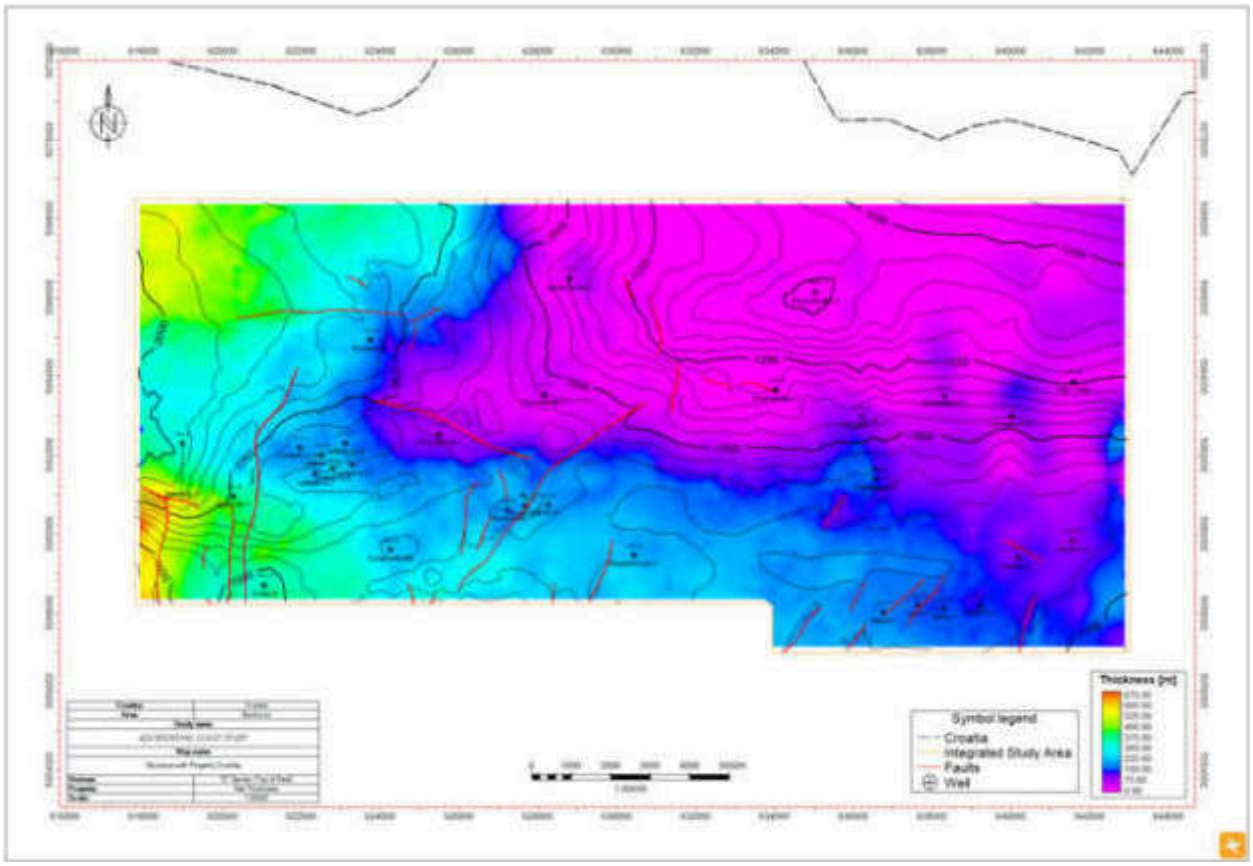


Fig. 2.152 Composite Map: "D" Series (Top of Seal) Cumulative Reservoir Net Thickness

Copyright © SLB. All Rights Reserved. Private & Confidential. Reproduction only by permission.

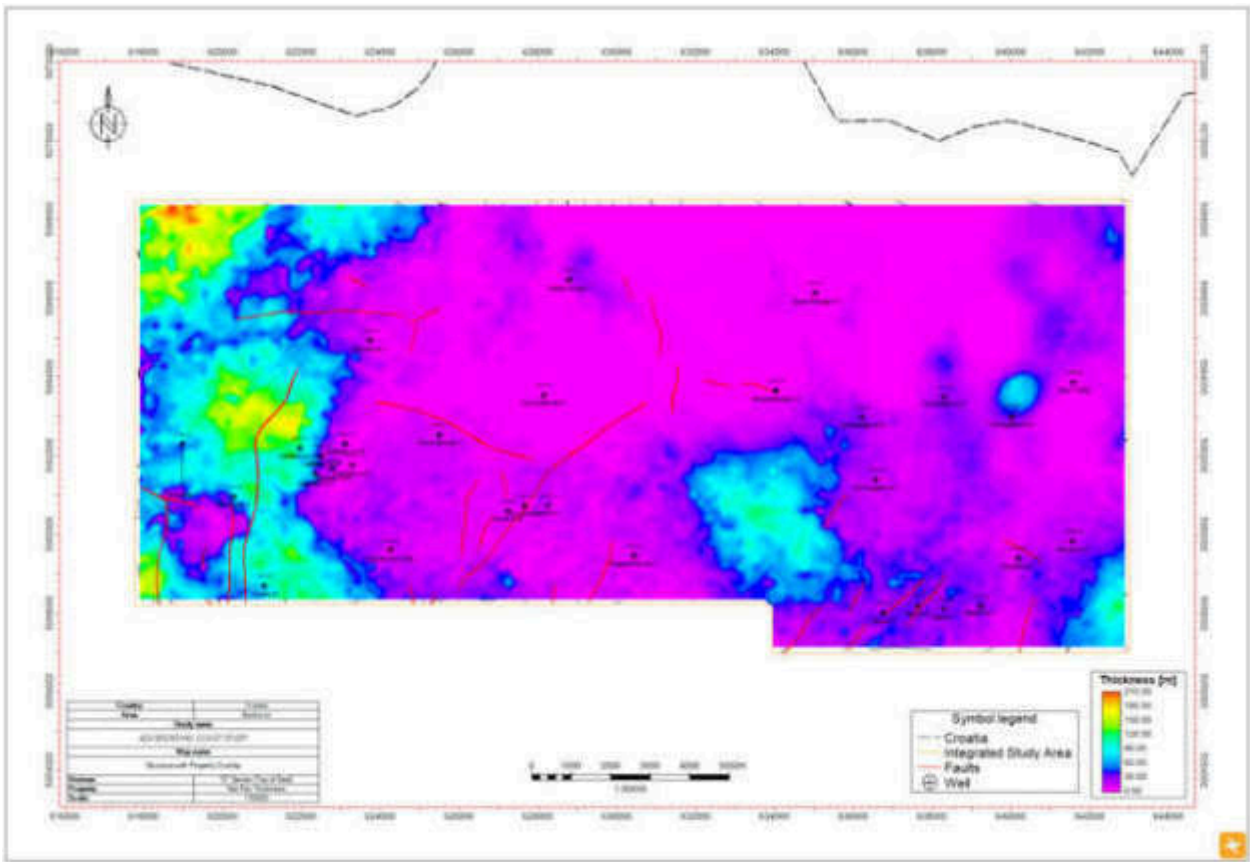


Fig. 2.153 Composite Map: "D" Series (Top of Seal) Cumulative Reservoir Net Pay Thickness

This reduction highlights that a substantial portion of the interval, although classified as reservoir based on lithology or porosity, does not contribute effectively to flow. The discrepancy is likely driven by the presence of tighter layers, increased shale or silt content, and cemented zones, which reduce permeability and act as internal barriers.

Conclusions "D" Series

From a storage perspective, this indicates a heterogeneous system where only a limited proportion of the total thickness is capable of supporting CO_2 storage.

Table 2.11 Reservoir zone "D" Series

Property	Min	Mean	Max
Net Thickness (m)	0.45	157	707
Net Pay Thickness (m)	0	29.17	212
PHIE (fractions)	0.08	0.09	0.19

Chance of Success: "D" Series

The Chance of Success map reflects the lowest overall confidence among all evaluated intervals.

Copyright © SLB. All Rights Reserved. Private & Confidential. Reproduction only by permission.

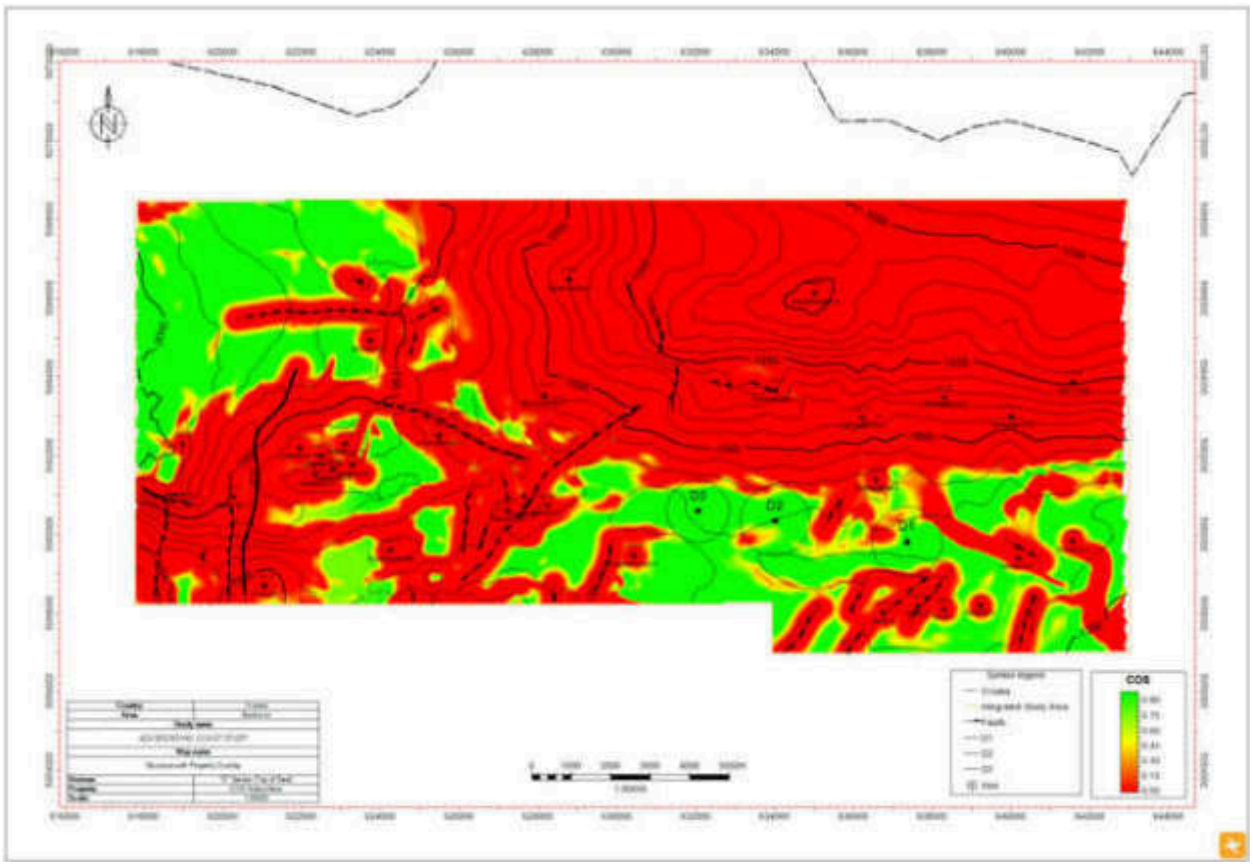


Fig. 2.154 COS Subsurface - "D" Series

Although the formation exhibits significant gross thickness and includes multiple reservoir–seal pairs, these advantages are outweighed by several critical uncertainties. The continuity of the sealing intervals cannot be demonstrated across the full extent of the area

The cumulative reservoir thickness is substantially reduced when considering net and especially net pay intervals, indicating that only a limited portion of the formation contributes to effective storage. This directly impacts both capacity and injectivity potential.

The structural framework further degrades the COS. The same regional fault system persists, supplemented by additional localized faulting, particularly in the eastern sector.

When integrating these subsurface limitations with surface constraints, the resulting COS map highlights only sparse and low-confidence areas.

Copyright © SLB. All Rights Reserved. Private & Confidential. Reproduction only by permission.

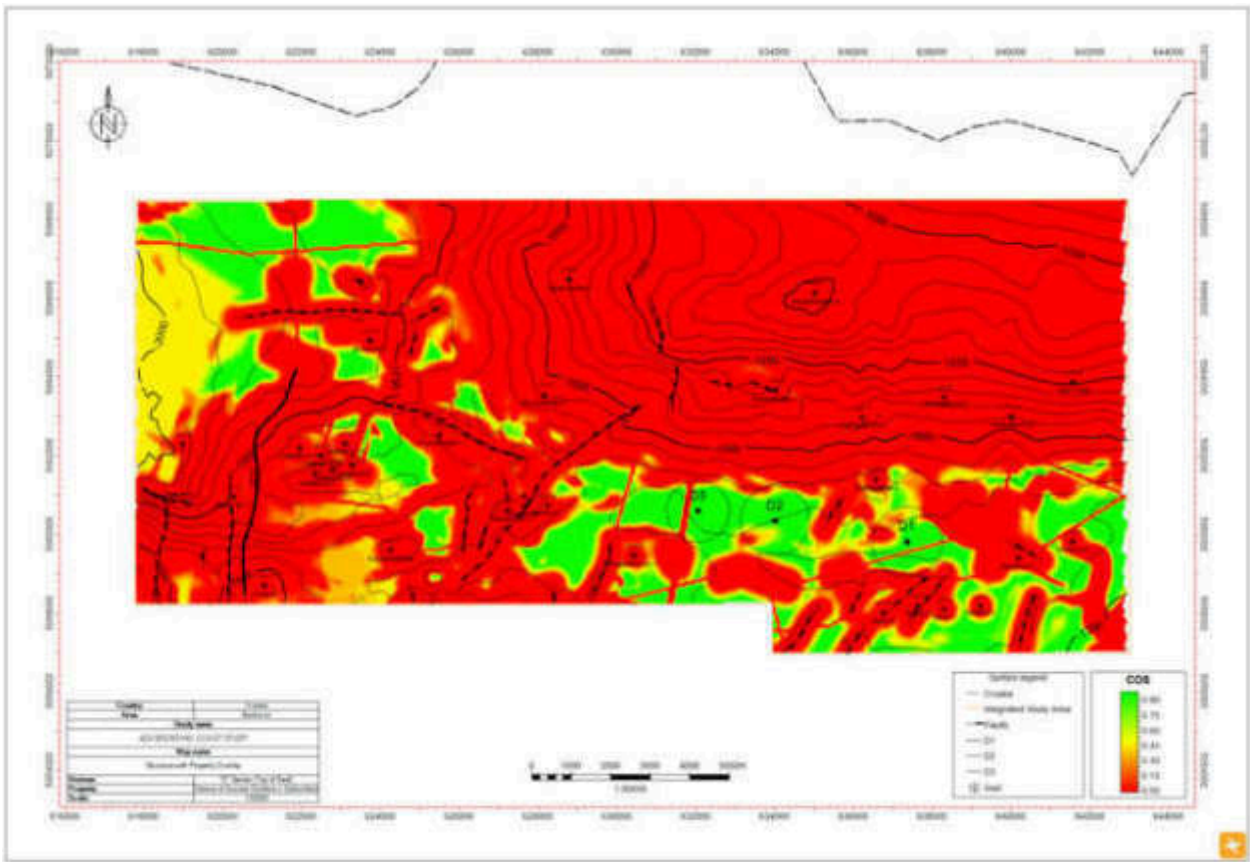


Fig. 2.155 Chance of Success (Surface x Subsurface)

For "D" Series, the results indicate a significantly lower storage performance compared to the overlying intervals, with all sites showing limited effective thickness and reduced pore volumes. Three areas were selected for further evaluation.

Table 2.12 "D" Series - Potential Sites

Site	Area (km2)	PHIE	Gross Thickness (m)	Net Pay Thickness (m)	Pore Volume (Mm3)
D-1	2,5	0,14	173,49	31,32	8,93
D-2	2,5	0,16	299,6	89,27	37,38
D-3	1,9	0,15	202,9	53,47	13,84

* Average values

Copyright © SLB. All Rights Reserved. Private & Confidential. Reproduction only by permission.

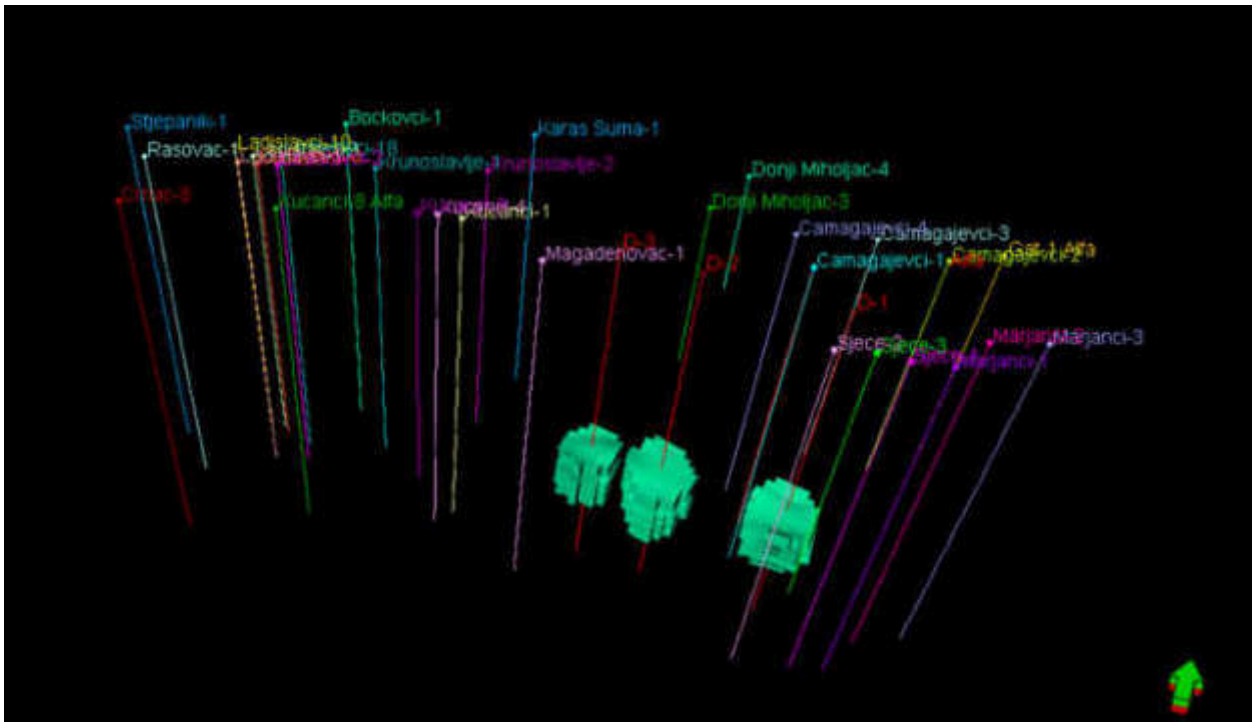


Fig. 2.156 3D View of "D" Series proposed sites

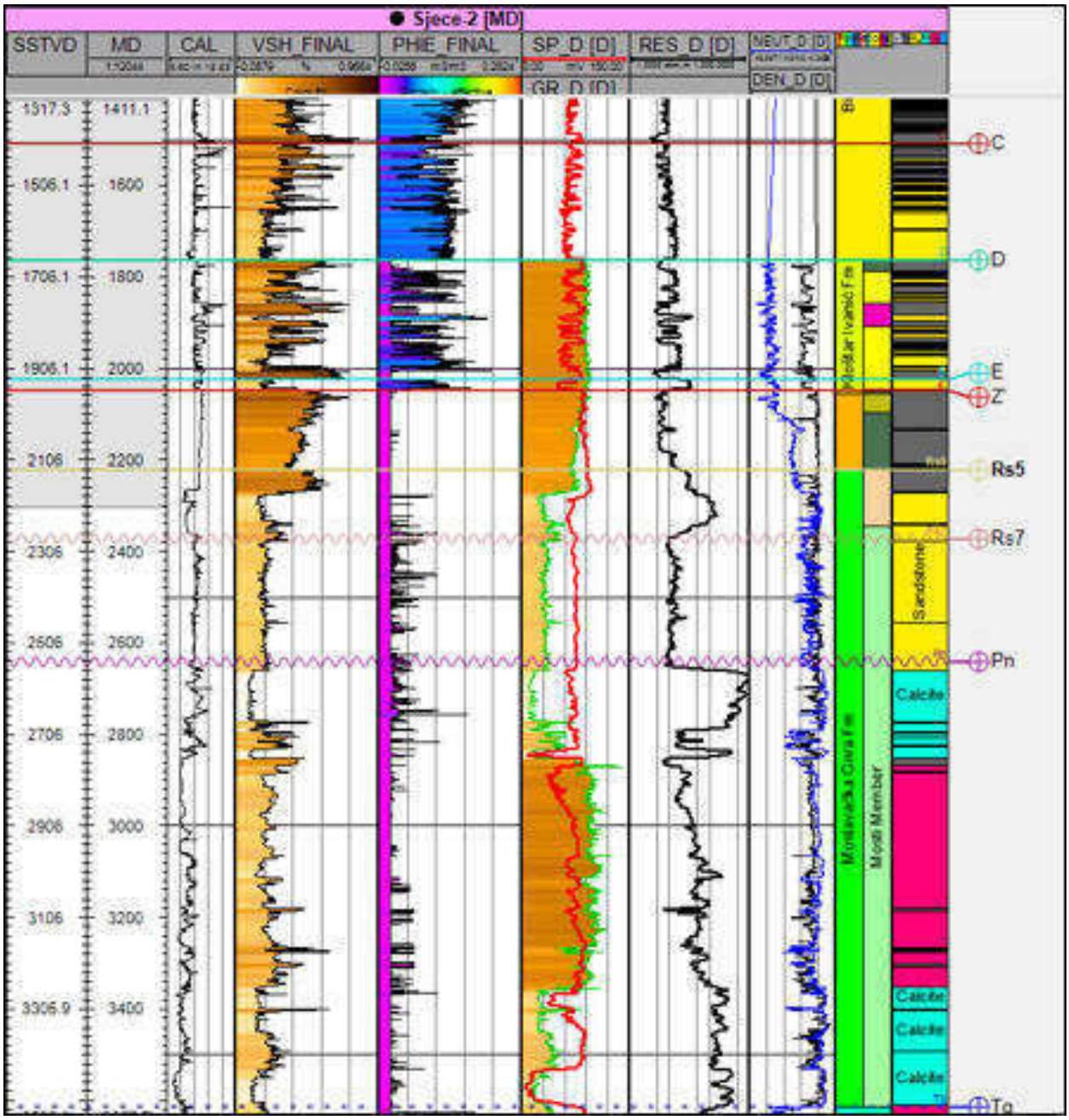
2.7.2.2 Assessment of lower formations

"Rs5" "Rs7" series description

Both formations share same sealing formation, fault system and similar petrophysical parameters and will be described and analyzed together.

Rs5 zone corresponds to the sedimentary rocks of Pannonian age deposits that are characterized by numerous lithotypes, which are associated with changes in palaeogeographical environments. Formation consists of shaly marls, fine-grained to medium-grained sandstones, breccia conglomerates. Marker Rs5 separates the Valpovo Formation and corresponding Krizevci member from younger, Upper Pannonian one).

Copyright © SLB. All Rights Reserved. Private & Confidential. Reproduction only by permission.



Well logs zones Rs5 Rs7 Sjece 2

Formation Rs5 is encountered at depths ranging from approximately **–490 meters to –2880 meters**, indicating significant structural variation across the study area. Rs5 zone is dipping toward South, SouthWest.

Formation Rs5 is bound by Z and Rs7 horizons that are both unconformities. Since there was no seismic interpretation, Rs5 horizon was built based on well tops and thickness map.

Zone between **Rs5** and **Rs7** horizons shows considerable thickness variability, with values ranging from **0 meters** (in North part of AOI related to fundament uplift), to **368 meters** (in South part). Formation reflects complex sedimentation conditions corresponding to littoral areas.

Copyright © SLB. All Rights Reserved. Private & Confidential. Reproduction only by permission.

Significant changes in thickness indicate that Rs5 zone in Northern part must be examined carefully in relation to structural heights and potential containment implications.

Rs7 zone corresponds to the sedimentary rocks of Palaeozoic and Mesozoic age that are characterized by lithotypes, which are associated with changes in Devonian to Cretaceous time mixed tectonized carbonates and Mmarls, sandstones, carbonates (limestones, dolomite) and polymictic breccia–conglomerates are the most important reservoirs in the western part of Drava Depression (Moslavacka gora/Vukovarska formation).

Formation Rs7 is encountered at depths ranging from approximately **–675 meters to –2917 meters**, indicating significant structural variation ac0ross the study area. Rs7 zone shows same behavior as horizon Rs5 and is dipping toward South, South-West that is described in some wells' reports (Sjece, Marjanci wells).
Formation Rs7 is bound by Pn horizon that was interpreted (top of carbonates) based on well data.

Zone between **Rs7** and **Pn** horizons shows considerable thickness variability, with values ranging from **0 meters** (in North part of AOI related to fundament uplift), to **660 meters** (in South part). Thickness changes show same thend in both zones - Rs5 and Rs7.

Structural assessment
On seismic clearly seen 2 system of faults, corresponding to area above Rs7 – Z horizon and below Rs7 horizon mainly corresponding to the basement, including few detachment faults. South-East area (around Sjece-Marjanci wells) is heavily faulted below Rs7 horizon. Another fault system that reaches Rs7 horizon is spotted around Ladislavci hydrocarbon-producing field close to Bockovci area.

Both zones of interest share same seal – shaly marls from zone Z. COS map indicating distance to faults computed for Z –Rs5 zone.

Containment
Both zones – "Rs5" and "Rs7" - are sharing the same sealing formation that consist of marls and shales of Z zone (Lipovec and Laslovo shaly marls). It's identified in most of the wells available within the AOI, although its thickness shows notable spatial variability due to the basement rocks uplift at the North East part of AOI. According to some studies, Z regional marker is the last horizon that can be traced in most of the wells of Drava basin. Same literature source mentions that regional markers Rs5 and Rs7 are hardly traced around Drava basin due to complex geological settings of the regions (both horizons are erosional).

The seal ranges from approximately 10 m in Karas Suma well area to approximately 150 m in the vicinity of well Sjece 2 m with an average thickness of around 90 m. Thickness changes might be related to uncertainty associated with marls intervals definition. Seal Thickness Map shows a reduction in seal thickness toward North. This apparent thinning mainly related to uprise of the

Copyright © SLB. All Rights Reserved. Private & Confidential. Reproduction only by permission.

basement but at the same time changes in the thickness of seal in the vicinity of Ladislavci wells should be interpreted cautiously, as it is likely influenced by limitations in data coverage rather than representing a fully resolved geological meaning.

In comparison with the upper formations, Dip angles of horizons below the E regional marker changes between 0 – 89 degrees for Rs5 horizon, mostly around 90, median 7,80. And between 0 – 89 degrees for Rs7 horizon, mostly around 10 degrees, median 7,83 degrees. Dip angle changes toward the North-East uplift of the metamorphic basement (increases up to 20 degrees). Locally, however, high dip angles — reaching up to 38 degrees— are observed in proximity to mapped faults. These steep values are interpreted primarily as artefacts related to the fault modeling and gridding process rather than representing true large-scale structural tilting.
Small dip (<2deg) is favorable for a good lateral movement of fluids, at the same time high angles introduce fast movement that can be increased in case of presence of fracture (enhance vertical and lateral movement).

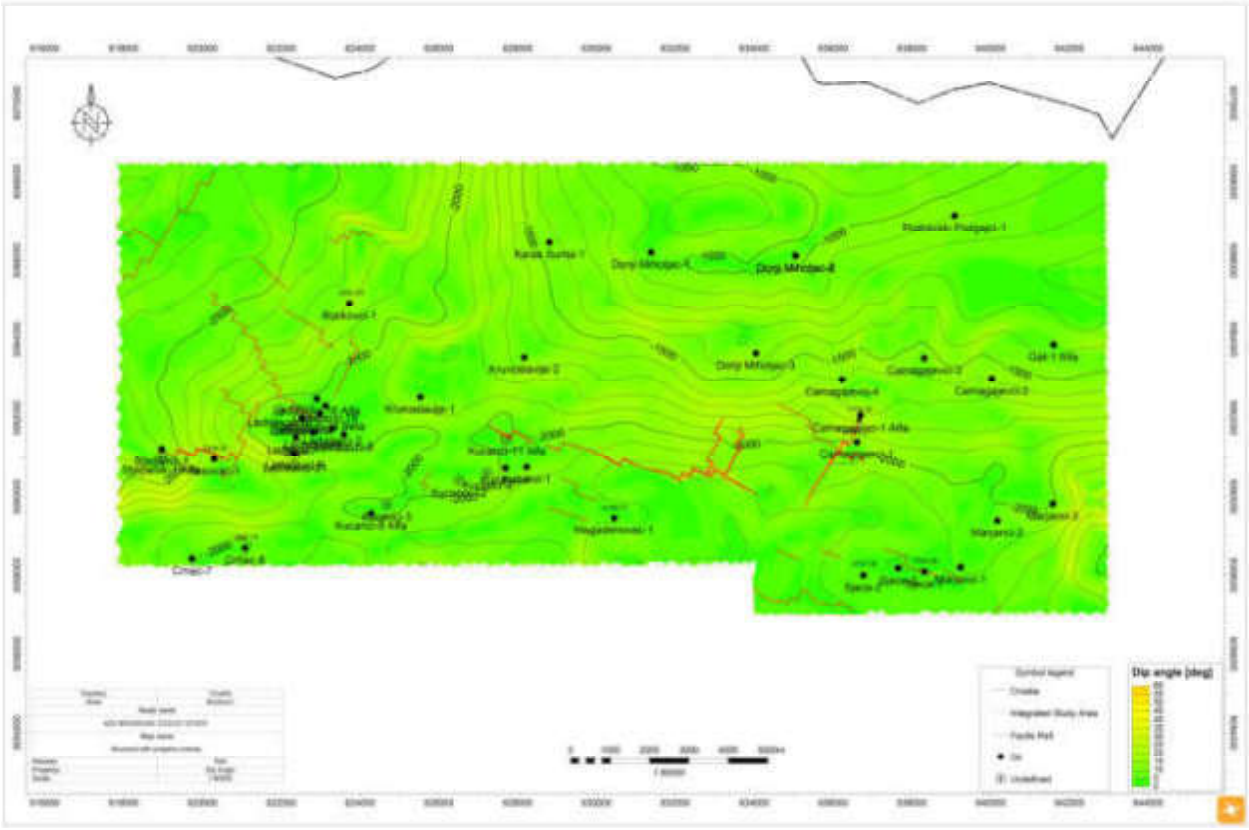


Fig. 2.157 Rs5 series Dip Angle
Dip Angle Map Rs5 horizon

Copyright © SLB. All Rights Reserved. Private & Confidential. Reproduction only by permission.

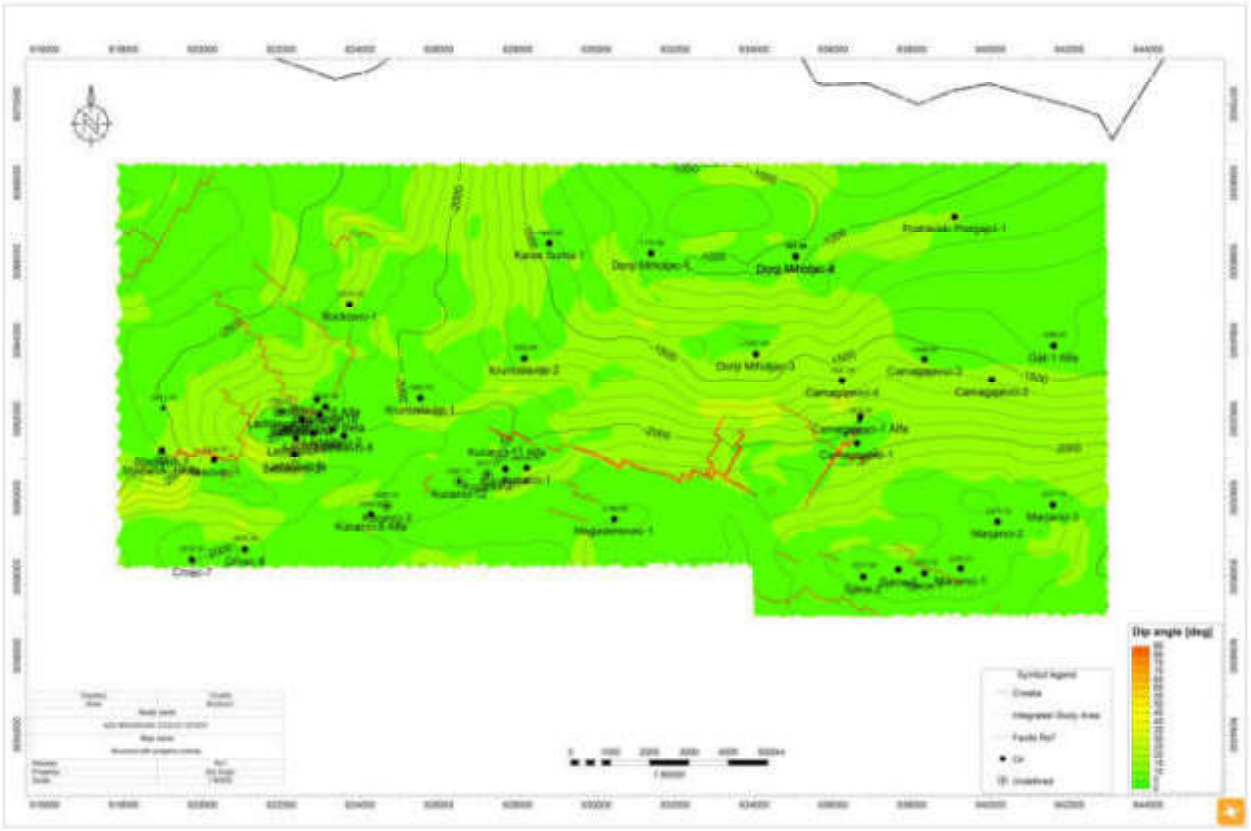


Fig. 2.158 Rs7 series Dip Angle
Dip Angle Map Rs7 horizon

Quality of the Storage Formation

The lower reservoirs are notably characterized by significantly lower porosity compared to the upper reservoirs. This is a particularly pertinent observation as these lower units are predominantly of breccia, shaly, sandy marls and fractured where high porosity are not unexpected. For the lower formations porosity ranges for Rs5 zone: from 0.035 (3.5%) to 0.17 (17%) around Ladislavci-Rasovac wells area, with an average of approximately 0.053 (5.3%). For the zone Rs7 porosity shows similar values: from 0.035 (3.5%) to 0.18 (18%), high porosity values mainly associated with the same location around Ladislavci-Rasovac wells, without this particular area max porosity will be around 12% and an average of approximately 0.044 (4.4%) These values are derived exclusively from net reservoir intervals, zones where permeability was less than 1 mD, were excluded, ensuring that the results reflect effective storage capacity. The higher end of the range indicates locally favorable reservoir quality, whereas lower porosity values are associated with cemented intervals or finer-grained facies. Overall, the mean porosity suggests low storage potential for the lower formations.

The net thickness, derived after applying the reservoir definition criteria using a permeability cutoff of 1 mD, varies from 0 m to 260 m, with an average of 37 m for “Rs5” formation. For “Rs7” formation thickness is varying from 0 to approximately 70 m. The assessment did not extend below the Pn horizon, reflecting current data limitations and potential for further study at greater depths. Nonetheless, the combined effect of limited net thickness and low porosity strongly

Copyright © SLB. All Rights Reserved. Private & Confidential. Reproduction only by permission.

indicates that these formations are less suitable for CO_2 storage compared to the A" to D formations, especially when considering their greater depth and the associated temperature and pressure regimes.

Volumetric Analysis and Methodology

Potential CO_2 storage volumes were estimated for the lower model using volumetric calculations in Petrel incorporating Porosity and NTG property models as well as both efficiency factors and CO_2 density. The use of 3D property modeling offers a more detailed and spatially resolved approach than a single numeric coefficient, capturing heterogeneity and providing a nuanced picture of volumetric ranges. 3 cases were estimated for each potential site, using P10, P50 and P90 efficiency coefficient. However, the actual uncertainty analysis was not a part of scope of work and no other parameters have been altered.

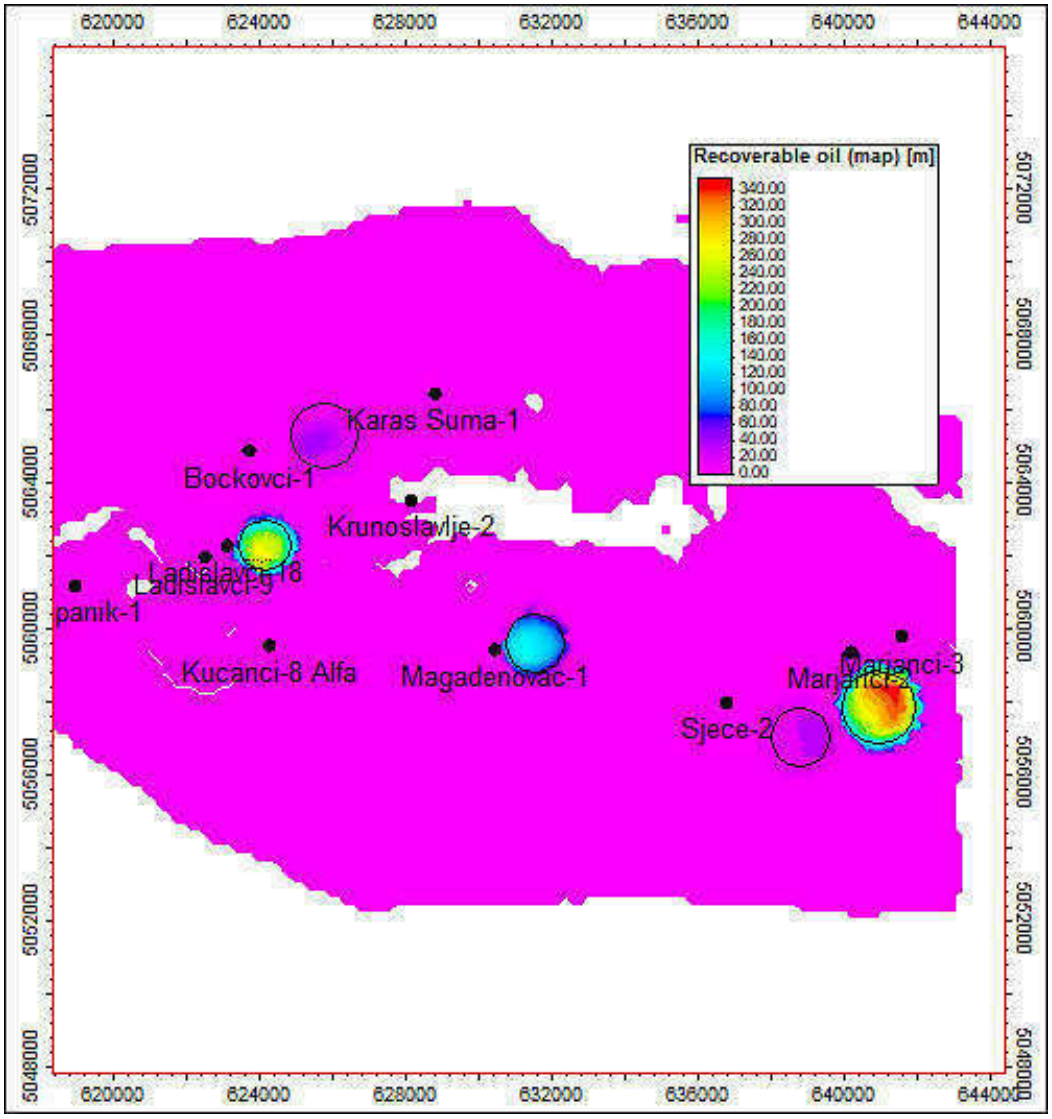


Fig. 2.159 Rs5 P50 Potential CO_2 storage capacity (recoverable oil) map

Copyright © SLB. All Rights Reserved. Private & Confidential. Reproduction only by permission.

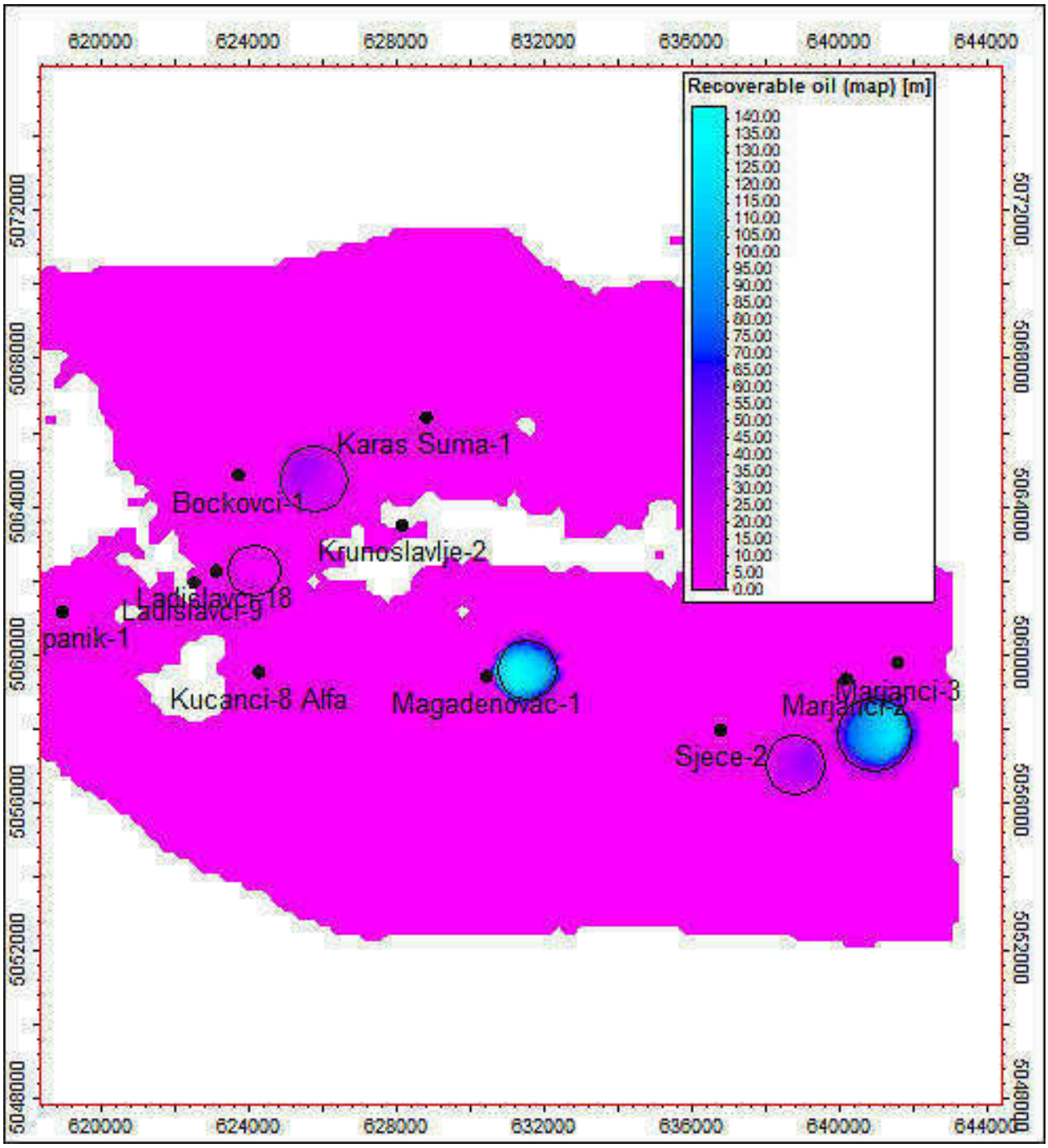


Fig. 2.160 Rs7 P50 Potential CO_2 storage capacity (recoverable oil) map

Chance of Success "Rs5" and "Rs7" Series

The COS map indicates a low storage potential compared to upper formations, driven primarily by increased depth, higher lithology heterogeneity, low average effective porosity and high Dip angle of both "Rs5" and "Rs7" horizons.

Copyright © SLB. All Rights Reserved. Private & Confidential. Reproduction only by permission.

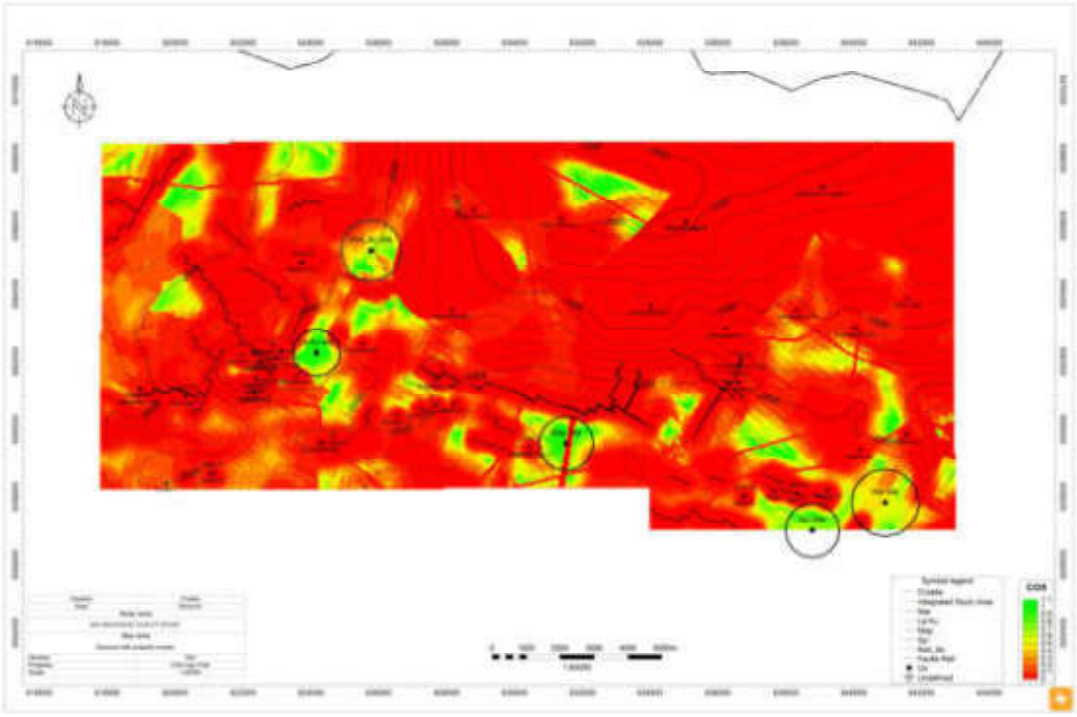


Fig. 2.161 RS5 COS Total map
Total Chance of Success map for "Rs5" formation with potential sites

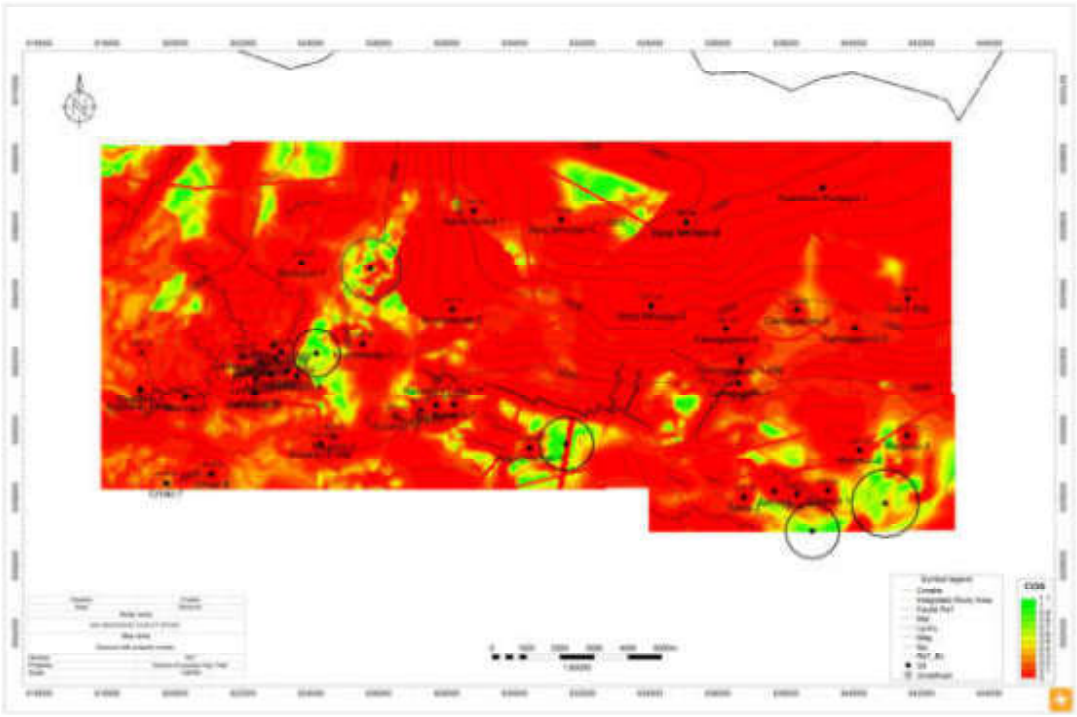


Fig. 2.162 RS7 COS Total map
Total Chance of Success map for "Rs7" formation with potential sites.

The fault system plays a major role in reducing the COS, particularly in the western part of AOI, although most of the faults in the lower model are dying out along Rs7 horizon, some faults of the

Copyright © SLB. All Rights Reserved. Private & Confidential. Reproduction only by permission.

upper fault system might reach sealing formations due to uncertainties associated with fault interpretation, or can be re-activated, propagated toward the surface, increasing the risk of vertical migration. This is further constrained by surface criteria, including proximity to sanitary protection zones in the north.

Main parameter that affects COS estimation for the lower formations is Dip angle of both "Rs5" and "Rs7" horizons. Following pictures illustrate comparison of a strict Dip Angle COS limitation when all angles above 2° have 0 COS and loosen Dip Angle COS estimation where COS decreases gradually from 2° to 15 ° for Rs5 and Rs7 horizons.

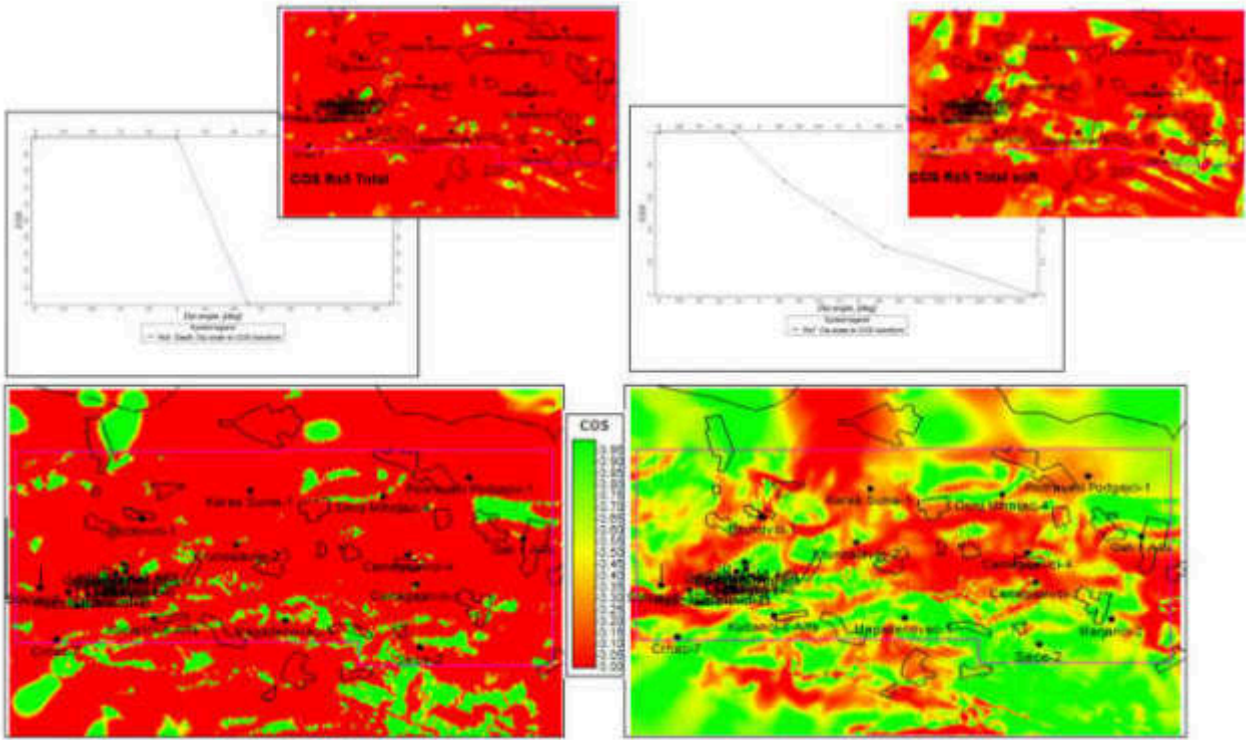


Fig. 2.163 RS5 COS comparison Dip angle
Total COS map when Dip Angle COS has strict limitation on the left and COS with loosen Dip Angle COS (COS is gradually changing between 2 and 15 degrees) on the right.

Copyright © SLB. All Rights Reserved. Private & Confidential. Reproduction only by permission.

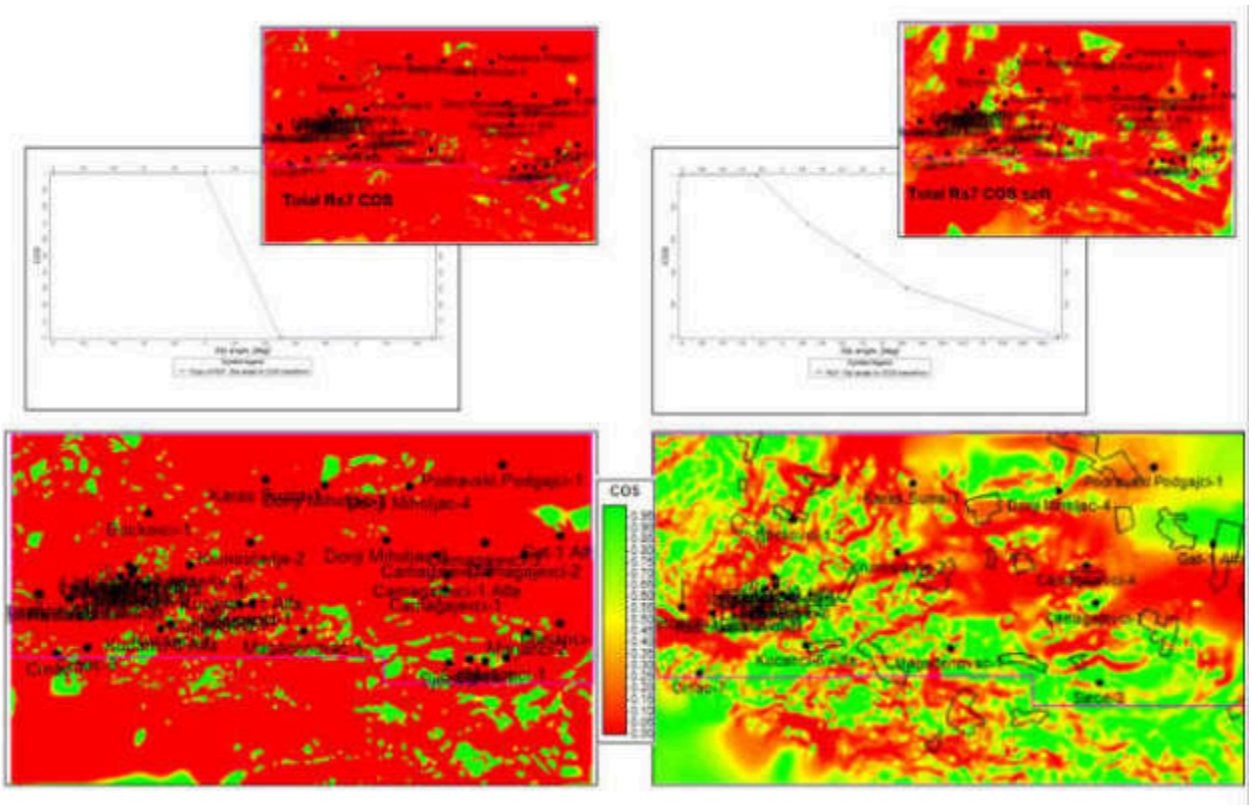


Fig. 2.164 RS7 COS comparison Dip angle
Total COS map when Dip Angle COS has strict limitation (on the left) and COS with loosen Dip Angle COS (COS is gradually changing between 2 and 15 degrees) on the right.

Conclusions "Rs5" and "RS7" Series.

While formations "Rs5" and "RS7" demonstrate presence of solid regional seal, significant depth and are the main hydrocarbon bearing formation in study area, the structural setting (faults, fractures), dip angle and reservoir properties (porosity <4–5%) reduce the likelihood of potential CO_2 storage site. Both formations are characterized as tight with low porosity and permeability in areas with potentially higher COS that shows modest CO_2 storage capacity. The key parameter that affects COS estimation for both formations are the formations' dip angles, structural complexity, including several fault systems, potentially affecting sealing formation and structure uprise toward North. Further evaluation would require detailed analysis of the fracture presence and intensity, and potentially additional seismic and well data acquisition before advancing its candidacy. In comparison with upper formations, "Rs5" and "Rs7" introduce low CO_2 storage potential, instead they are better aligned with geothermal potential.

Copyright © SLB. All Rights Reserved. Private & Confidential. Reproduction only by permission.

2.7.3 Theoretical Capacity and Site Ranking

Table 2.13 Theoretical Capacity and Site Ranking (Upper formations)

6Zone	Site	Area [km^2]	Avg Phie	Gross Thickness [m]	Avg Net Pay Thickness [m]	NtG	Pore Volume (Net) [m^3]	Pore Volume (Net) [Mm^3]	Efficiency 12% [m^3]	Density (Kg/ m^3)	Efficiency 12% KG	TONNES	RANK
Alfa	A-1	7.8	0.2	239.94	192.58	0.80	309,036,729.00	309.04	37,084,407.48	265.00	9,827,367,982.20	9,827,367.98	2
	A-2	9.9	0.23	140.35	115.5	0.82	266,206,726.00	266.21	31,944,807.12		8,465,373,886.80	8,465,373.89	3
	A-3	3.7	0.19	270.05	210	0.78	151,888,084.00	151.89	18,226,570.08		4,830,041,071.20	4,830,041.07	6
	A-4	3.7	0.22	222.7	182.5	0.82	140,622,812.00	140.62	16,874,737.44		4,471,805,421.60	4,471,805.42	7
	A-5	3.06	0.19	213.65	192.38	0.90	113,602,185.00	113.60	13,632,262.20		3,612,549,483.00	3,612,549.48	11
	A-6	3.06	0.22	116.8	87.9	0.75	63,990,207.00	63.99	7,678,824.84		2,034,888,582.60	2,034,888.58	13
B	B-1	2.5	0.18	264.29	220.47	0.83	98,794,900.00	98.79	11,855,388.00	340.00	4,030,831,920.00	4,030,831.92	8
	B-2	12.25	0.18	240.73	170.87	0.71	391,065,792.00	391.07	46,927,895.04		15,955,484,313.60	15,955,484.31	1
	B-3	3.06	0.16	261.8	183.8	0.70	93,135,084.00	93.14	11,176,210.08		3,799,911,427.20	3,799,911.43	9
	B-4	2.5	0.17	231.34	167.82	0.73	72,666,243.00	72.67	8,719,949.16		2,964,782,714.40	2,964,782.71	12
	B-5	4.4	0.17	243.7	170.47	0.70	131,462,893.00	131.46	15,775,547.16		5,363,686,034.40	5,363,686.03	5
C	C-1	3	0.14	242.14	101	0.42	43,849,375.00	43.85	5,261,925.00	385.00	2,025,841,125.00	2,025,841.13	14
	C-2	4.4	0.15	248.05	122.7	0.49	81,017,972.00	81.02	9,722,156.64		3,743,030,306.40	3,743,030.31	10
	C-3	1.9	0.15	260.53	117.6	0.45	35,359,793.00	35.36	4,243,175.16		1,633,622,436.60	1,633,622.44	16
	C-4	12.2	0.15	221.68	80.89	0.36	153,926,926.00	153.93	18,471,231.12		7,111,423,981.20	7,111,423.98	4
D	D-1	2.5	0.14	173.49	31.32	0.18	8,928,509.00	8.93	1,071,421.08	425.00	455,353,959.00	455,353.96	18
	D-2	2.5	0.16	199.6	89.27	0.45	37,376,855.00	37.38	4,485,222.60		1,906,219,605.00	1,906,219.61	15
	D-3	1.9	0.145	202.87	53.47	0.26	13,844,644.00	13.84	1,661,357.28		706,076,844.00	706,076.84	17

* Volumes represent Theoretical Capacity as per Fig. 2.115

Site ranking for the lower formations "Rs5" and "Rs7". Density was estimated using available temperature and density data and for both formations is 400 g/m3.

Since lower formations assumed to be less suitable for the CO_2 storage, efficiency factor was estimated based on lithology and volumes were computed directly in Petrel using 3D property models instead of numeric coefficients.

Copyright © SLB. All Rights Reserved. Private & Confidential. Reproduction only by permission.

Table 2.14 Theoretical Capacity and Site Ranking for "Rs5" formation

Site	Area, km2	Bulk_volume^10*6 m3	Pore volume^10*6 m3	CO_2, Mt	Ranking
Rs5_Mar_P10	3.06	416.0781	18.87	0.08453	
Rs_5_Mar	3.06	416.0781	18.87	0.93582	1
Rs5_Mar_P90	3.06	416.0781	18.87	1.78938	
Rs5_Sjc_P10	1.96	316.4049	0.91	0.0041	
Rs5_Sjc	1.96	316.4049	0.91	0.04537	7
Rs5_Sjc_P90	1.96	316.4049	0.91	0.08675	
Rs5_La-Ku_P10	1.5	205.335	7.71	0.03391	
Rs5_La-Ku	1.5	205.335	7.71	0.37541	2
Rs5_La-Ku_P90	1.5	205.335	7.71	0.71782	
Rs5-Bc_P10	2.48	4.195239	0.19	0.00084	
Rs5-Bc	2.48	4.195239	0.19	0.00935	8
Rs5-Bc_P90	2.48	4.195239	0.19	0.01788	
Rs5_Mag_P10	1.96	0.088887	0.01	0.00003	
Rs5_Mag	1.96	0.088887	0.01	0.00033	10
Rs5_Mag_P90	1.96	0.088887	0.01	0.00062	

Table 2.15 Theoretical Capacity and Site Ranking for "Rs7" formation

Site	Area, km2	Bulk_volume^10*6 m3	Pore volume^10*6 m3	CO_2, Mt	Ranking
Rs7_Mar_P10	3.06	1072.49	4.12	0.02294	
Rs7_Mar	3.06	1072.49	4.12	0.18195	4
Rs7_Mar_P90	3.06	1072.49	4.12	0.34066	
Rs7_Sjc_P10	1.96	613.27	1.33	0.00598	
Rs7_Sjc	1.96	613.27	1.33	0.06617	6
Rs7_Sjc_P90	1.96	613.27	1.33	0.12653	
Rs7_Bc_P10	2.48	237.73	1.76	0.0111	
Rs7_Bc	2.48	237.73	1.76	0.0779	5
Rs7_Bc_P90	2.48	237.73	1.76	0.14442	
Rs7_Mag_P10	1.96	207.12	5.45	0.02393	
Rs7_Mag	1.96	207.12	5.45	0.26493	3
Rs7_Mag_P90	1.96	207.12	5.45	0.50658	
Rs7_La-Ku_P10	1.5	6.4	0.17	0.00118	
Rs7_La-Ku	1.5	6.4	0.17	0.00707	9
Rs7_La-Ku_P90	1.5	6.4	0.17	0.01291	

The resulting ranking provides a clear overview of the relative merits of each site in its baseline configuration and highlights the most promising candidates for optimization 2.8.5.1 Effective Capacity and Injected volumes per scenario . Top-ranked sites demonstrate higher injection rates with manageable pressure increases and robust containment characteristics, making them strong candidates for initial development or scale-up. These sites are:

- Close to Bockovci-1 well - sites A2, B2, C4 – larger areal extent, prone for commingled

Copyright © SLB. All Rights Reserved. Private & Confidential. Reproduction only by permission.

injection in Alfa, B and C formations

- Close to Magadenovac-1 well – sites A1, B4, B5, C3, D2 share same areal extent - prone for commingled injection in Alfa, B, C and D formations
- Close to Camagajevci-1 well- sites A3, B3, C2, D1 share same areal extent - prone for commingled injection in Alfa, B, C and D formations

This ranking forms the foundation for subsequent optimization analyses, ensuring that development efforts are focused on sites offering the greatest potential for safe, efficient, and cost-effective long-term CO_2 storage.

2.8 CO_2 injection simulations

2.8.1 Reservoir simulation executive summary

Executed simulation study provides a comprehensive evaluation of the planned CO_2 injection project for deep saline aquifers in Drava Depression. Focus is on the dynamic behavior of CO_2 within the reservoir under various conditions and injection scenarios. The study leverages robust simulation methodologies and integrates available field data to assess technical and operational feasibility of CO_2 injection for carbon sequestration.

The objectives of the study are:

- Provide an integrated simulation model for CCUS simulation.
- Assess the effectiveness for CO_2 injection for long-term storage.
- Quantify effective storage capacity (**per pyramid**) and trapping mechanisms in the targeted reservoirs.
- Positioning of injection and monitoring wells.
- Identify potential risks associated with CO_2 migration, pressure distribution and containment.
- Provide recommendations to maximize storage capacity and efficiency.

The reservoir simulation model was constructed using Intersect, incorporating geological, petrophysical and dynamic data specific to the area of interest. Model initialized and relied on available pressure data from DST, temperature gradient and water/hydrocarbon samples. Major data uncertainties were assumed based on literature and industrial references, such as relative permeability curves, critical gas saturation for hysteresis, injection bottom hole limits. Multiple scenarios were examined for pre-selected areas, covering a various well placement, injection schemes and pressure constrains.

Base case - one well per site / per formation (18 wells) simulation scenario evaluates each pre-selected site separately per zone and contains of 6 Sites in Alfa, 5 sites in B, 4 sites in C and 3 sites in D zones. Total injection rate (million tons/year) and cumulative values are summarised in the table below.

Copyright © SLB. All Rights Reserved. Private & Confidential. Reproduction only by permission.

Table 2.16 Base simulation case injection volumes per zone

Zone	CO_2 injection rate, Mt/year	CO_2 injection cum, Mt
Alfa	0.258	7.73
B	0.312	9.35
C	0.169	5.06
D	0.067	2.03
Total	0.806	24.17

Reservoir simulation model predicts, for the best case scenario, 22 million tons of CO_2 can be surely injected by 4 wells in 3 sites (2 in Karas Suma area, 1 in Magadenovac and 1 in Camagajevci areas) and trapped within 30 years duration, with plume migration remaining within the target formations and selected areas. Simulation monitoring period constrained to the 200 years post injection to make sure plume stays within the polygons. Pressure buildup remains within the fracture gradient, mitigating risks of caprock failure or fault activations as 90% of estimated frac gradient was used for maximum injection pressure. Based on simulation sensitivity runs Karas Suma area is the most promising from storage and containment perspective. Cumulative CO_2 injection of 19 and 16 million tons, over 30 years, can be achieved in that area by 4 and 3 injector wells respectively.

Table 2.17 Optimized cases injection volumes

Scenarious	CO_2 injection rate, Mt/year	CO_2 injection cum, Mt
3 Sites- 4 wells -variable CO_2 injection rate	0.61	18.3
3 Sites- 4 wells -constant CO_2 injection rate	0.74	22.18
Karas Suma 4 wells	0.64	19.13
Karas Suma 3 wells	0.54	16.28

The selected scenario consists of four deviated injection wells located in the Karas Suma–Bockovci area, with a total injection rate of approximately 0.64 Mt/year over a 30-year injection period (2027–2057) and a capacity of 19.13 Mt. At field scale, injection stabilizes after early pressure buildup, with plume migration primarily lateral due to permeability anisotropy. Over time, trapping mechanisms evolve from free-phase flow dominance to increasing residual and solubility trapping.

No significant leakage pathway was identified in the current model, however, some areas of uncertainty still remain around the structure dip angel towards the Donji Miholjac area, that may influence the plume migration. The model provides operational guidance in terms of optimal well numbers, placement, and injection rate controls. Monitoring recommendations include regular pressure surveillance, tracer studies, and integrity tests in identified risk zones.In the event of unexpected pressure anomalies or plume migration, the study suggests a phased contingency plan with options for injection rate adjustment or temporary shut-in

Positive outlook for the CO_2 injection project in Karas Suma area is supported by simulation study. Further data gathering is advisable for cap rock and target reservoirs characterization by drilling a stratigraphic well. Regulatory and operational terms to be revised, to ensure all requirements are addressed.

Copyright © SLB. All Rights Reserved. Private & Confidential. Reproduction only by permission.

2.8.2 Input data overview

This section summarizes the key data and parameters used to construct the simulation model for CO_2 injection study in for deep saline aquifers in Drava Depression. Data were compiled from previous studies, field measurements and well data to ensure the model accurately represents reservoir characteristics and constrains. There are 42 wells in the area of interest, from which 20 are exploration wells. Well coordinates along with trajectories were loaded to the coint Petrel project. Also, there are some hydrocarbon bearing structures such as: Ladislavci, Kucanci, Crnac, Sječe.

Available DST and information from well reports were used to capture initial reservoir pressure and temperature in the dynamic model Table 2.18.

Table 2.18 Key reference pressure point from DST reports

Pressure reference	Zone	Depth, m	Pressure, bar
Sječe-2	B4(D-Z)	1888	163.4
Magadenovac-1	Z	2194	224.1
Magadenovac-1	Rs7	2615	261.51
Rs1	Z	2361	230
Rs1	Rs7	2570	260
Sječe-1	Rs7	2834	261
Ladislavci-11	Rs7	2350	245
Ladislavci-11	Rs7	2544	255
Ladislavci-18A	Rs7	2275	229
Ladislavci-18A	Rs7	2350	246
Ladislavci-10	Z	2050	213

Wells Ladislavci-10 and Ladislavci-11have pressure profile along wells reported. Associated depths and pressures are presented in Table 2.19 These points were used as reference to initialize the model and calibrate reservoir pressure.

Table 2.19 Pressure vs depth for wells Ladislavci-10 and Ladislavci-11

Depth, m	Pressure, bar	Temperature, degC
Ladislavci-10		
600	46	52
800	63	64
1000	79	74
1200	95	84
1400	112	95
1500	120	100
Ladislavci-11		
1000	72	86
1483	112	107
1941	150	123

Summarized well's data from report :"Characterization of the production possibilities and energy potential of the geothermal reservoir Bockovci" is presented in the Table 2.20

Copyright © SLB. All Rights Reserved. Private & Confidential. Reproduction only by permission.

Table 2.20 Well information from previous studies

Well	Reference depth Temperature, m	Temperature, C	Temperature gradient, C/100 m	Reference depth Pressure, m	Pressure, bar	Pressure gradient, bar/10m	Permeability, mD	Salinity, gNaCl/l
Karaš Šuma-1	1719	94.4	4.80	1720	165.16	0.96	31.25	
Ladislavci-9	2162	113	4.74	2162	-	-	-	
Ladislavci-10	2061.85	133	5.94	2063	173	0.84	7.28	
Ladislavci-11	2184.8 (Hv 2101)	114	4.93	2361 (Hv 2252)	182	0.8	-	
Ladislavci-11	2359.8	121	5.13	2512 (Hv 2385)	195	0.81	-	0.73
Ladislavci-11	2510 (Hv 2384)	135.5	5.40	-	-	-	-	-
Ladislavci-12	2247.8 (Hv 2178)	146.1	6.22	2207.6 (Hv 2139)	173.8	0.81	47.11	-
Ladislavci-12	2273 (Hv 2203)	123.8	5.14	-	-	-	-	-
Ladislavci-12	2252 (Hv 2183)	125.7	5.28	2251 (Hv 2181)	178	0.82	129	-
Ladislavci-12	2408 (Hv 2333)	146	5.81	-	-	-		0.739
Ladislavci-13	2170	126	5.35	2148	177	0.82		-
Ladislavci-14	2268 (Hv 2193)	124	5.18	2301 (Hv 2218)	178	0.8	-	0.517
Ladislavci-15	2222 (Hv 2146)	135	5.80	2241 (Hv 2163)	177	0.82	-	-
Ladislavci-15	2271 (Hv 2190)	143	6.05	-	-	-	-	-
Ladislavci-16	2249 (Hv 2179)	121	5.08	2249 (Hv 2179)	160	0.73	-	-
Ladislavci-17	2196 (Hv 2136)	88	3.64	2224 (Hv 2161)	150	0.69	0.2	-
Well La-18α	2272 (Hv 2187)	137	5.81	-	-	-	-	-
Well La-18α	2390 (Hv 2299)	140	5.63	-	-	-	-	-
Well La-18α	2442 (Hv 2162)	101	4.18	2444 (Hv 2356)	184	0.78	170.55	-
Well La-18β	2191.8	120	5.17	2193	178	0.84	1.2	-
Ladislavci-20	2152	122.7	5.21	2130	218	-	-	-
Kućanci-2	2118	99	4.18	-	-	-	-	-
Kućanci-3	2108	101.7	4.33	-	-	-	-	-
Kućanci-4	2131	106	4.48	-	-	-	424	11.06
Kućanci-7	2151	-	-	-	-	-	-	0.35
Kućanci-8	2310	-	-	-	-	-	-	11.41
Kućanci-11a	2131	115	4.90	2133	198	0.93	-	-
Ku-11α	2282 (Hv 2173)	137	5.82	-	-	-	0.77	1.75
Ku-11α	2313 (Hv 2198)		5.03	-	-	-	-	-
Kućanci-12	2390	121	5.67	2339	199	0.85	24.3	-
Kućanci-12	2507	145	5.36	2483	200	0.81	-	14.8
Kućanci-13	2199	104	4.25	2175	109	0.95	-	0.824
Krunoslavlje-2	2159	122	5.20	2159	206	0.95	-	-

Copyright © SLB. All Rights Reserved. Private & Confidential. Reproduction only by permission.

Well	Reference depth Temperature, m	Temperature, C	Temperature gradient, C/100 m	Reference depth Pressure, m	Pressure, bar	Pressure gradient, bar/10m	Permeability, mD	Salinity, gNaCl/l
Rasovac-1	2577	130	4.64	2789	244	0.88	-	-
Rasovac-1	2831	148.8	4.89	-	-	-	44.6	0.549
Bockovci-1	2548	149	5.80	2548	220.7	0.86	19.6	0.913
Donji Miholjac-2	1069	60	5.61	-	-	-	-	-
Donji Miholjac-3	1037	56.1	5.41	-	-	-	296.2	0.59
Donji Miholjac-3	1447	-	-	-	-	-	111.4	1.93
Sječe-1	2834.65 -2868	146	4.72	2996	265	0.88	17.68	19.889
Sječe-1	2996 -3040	157	4.82			-		19.889
Sječe-1	3549.88-3572	149				-		
Sječe-1	3015.5-3045.5					-		17.55
Sječe-1	1950-1978			1950	187	0.96	1.1	0.644
Sječe-1	1875-1881	104.3	5.56	1875	149.8	0.80	2.79	1.433
Sječe-2	1906-1919	121	5.76	1906	181	0.95	6.85	0.328
Sječe-2	2359-2374	151.5	5.94		260			0.409
Sječe-3	1873.5-1883.5	105.5	5.62	1878	131.2	0.70	4.5	42.953
Čamagajevci-4	2243	123.8	5.52				-	
Čamagajevci-1 alfa					248	0.97		
Čamagajevci-2	1942-1959	110	5.64	1950	190	0.97	169.6	4.358
Čamagajevci-3	1642.41-1673	87.8	5.20					
Magadenovac-1	2756-2755							16.5
Magadenovac-1	2614.9-2625.4						58.33	1.6
Magadenovac-2	2451.7-2459.5						94.73	4.7
Marjanci-1	2416-2413							31.06
Marjanci-1	2474-2478							33.35
Marjanci-1	1890-1887							0.41
Marjanci-2	2282-2283						0.4	10
Marjanci-3	2249.74-2265	97.8	4.30					
Marjanci-3	2890-2926	149	5.00		300	1.026	3.66	2.349
Marjanci-3	2664-2658	148.8	5.65		285	1.08		2.05

Water properties, such as densities, salinity are available in the water sampling reports and summarised in Table 2.21.

Copyright © SLB. All Rights Reserved. Private & Confidential. Reproduction only by permission.

Table 2.21 Water salinity

Well	Interval (MD)	Depth (SSTVD)	Salinity, g/l	Conversion for simulator, kg-mol/m3	Zone
Sječe-1	1950-1978	-1857	0.644	0.0110	D
Sječe-1	2830-2833	-2737	19.305	0.3303	Rs7
Sječe-1	3015-3045	-2920	17.55	0.3003	Rs7
Sječe-2	1906-1919	-1812	0.328	0.0056	D
Ladislavci-8	1908-1910	-1810	0.7	0.0120	D
Ladislavci-8	2200-2202	-2103	2.2	0.0376	Rs7
Ladislavci-4	2151-2154	-2054	0.5	0.0086	Rs7
Stj-1A	2979-3004	-2908	0.017	0.0003	Tg
Stj-1A	2615-2627	-2518	0.298	0.0051	Rs7
Magadenovac-1	2452-2460	-2240	4.74	0.0811	Rs7
Magadenovac-1	2614-2625	-2517	4.15	0.0710	Rs7
Kucanci-4	2198-2206	-2100	10	0.1711	Rs7
Camagajevci-2	1942-1959	-1842	3.656	0.0626	Rs7
Camagajevci-2	1942-1959	-1842	4.154	0.0711	Rs7
Marianci-1	2282-2283	-2188	10	0.1711	Z
Stj-1A	2979-3004	-2908	0.017	0.0003	Tg
Stj-1A	2615-2627	-2518	0.298	0.0051	Rs7
Cr7	1976-1977	-1877	7.59	0.1299	Z
Bockovci-1	2829-2820	-2726	0.029	0.0005	Rs7
Bockovci-1	2548-2561	-2454	0.893	0.0153	Rs7
Kucanci-3	2208-2211	-2110	1.76	0.0301	Rs7
Krunoslavlje-1	2061-2071	-1965	0.924	0.0158	Rs7

All available information was loaded and used during simulation model set up.

2.8.3 Simulation model set up

This chapter details the set-up and initialization of the dynamic simulation model for the CO_2 injection. The overall approach, key assumptions, and configuration of the model are outlined below, covering initial and boundary conditions, and the specific of rock and fluid properties.

2.8.3.1 Model assumptions

The geological model is considered deterministic, based on the most recent static modeling results, described in 2.5 Geological modeling. It is assumed to accurately represent the structural and facies framework for the storage reservoirs and overlying seals. Upscaled petrophysical properties (porosity, permeability, net-to-gross) are spatially distributed as per the input model and are not altered by simulation precesses. Faults and structural features are defined per static model input and assumed to act as either flow barriers or conductive elements as explicitly modeled, without applying any transmissibility multipliers. Reservoir pressure and temperature are initialized from input data listed in 2.8.2 Input data overview. Fluid and rock properties are assumed based on industrial guidelines and template to compensate the missing SCAL data. Open boundary conditions are assumed and modeled by analytical type of aquifers with huge volumes. On the

Copyright © SLB. All Rights Reserved. Private & Confidential. Reproduction only by permission.

proposed site locations, a unique dynamic model was created for all Sites in Alfa, B, C and D formations to be simulated at the same time. A separate unique dynamic model was created for Z to Tg formations.

Static model for the area of interest is presented in Fig. 2.165. Static model consists of 6 mil cells and covering zones from Alfa to D with areal extend 25 by 18 km.

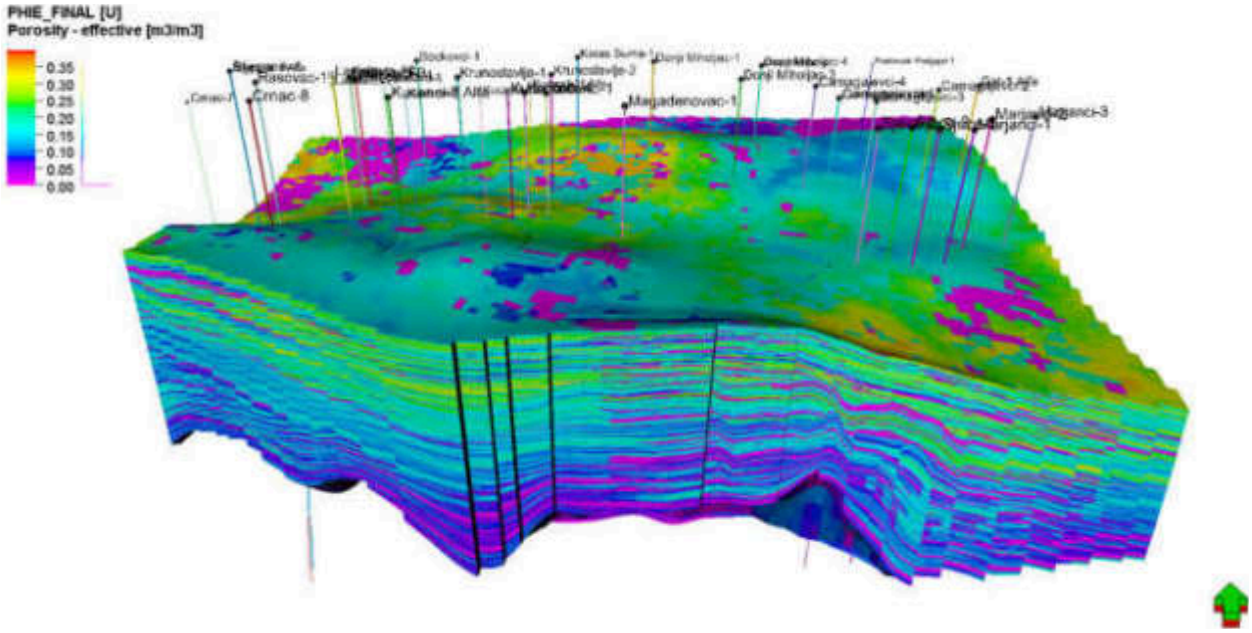


Fig. 2.165 Static model for the area of interest (porosity distribution)

Pore pressure reported from DST test is sub-hydrostatic and shows slightly different gradient for these wells. Two leak-off tests (LOT) were executed in lower Alpha in Rasovac-1 well. The lower LOT result (0.157bar/m) was reported as drilling limit LOT result from Rasovac-1 was projected to Bockovac-1 and considered for constraining frac gradient, since bottom Alpha is on similar depth and at similar pore pressure based on DST results. Fracture gradient and injection limit for wells Bockovci-1 and Sjece-2 are presented in Fig. 2.166.

Copyright © SLB. All Rights Reserved. Private & Confidential. Reproduction only by permission.

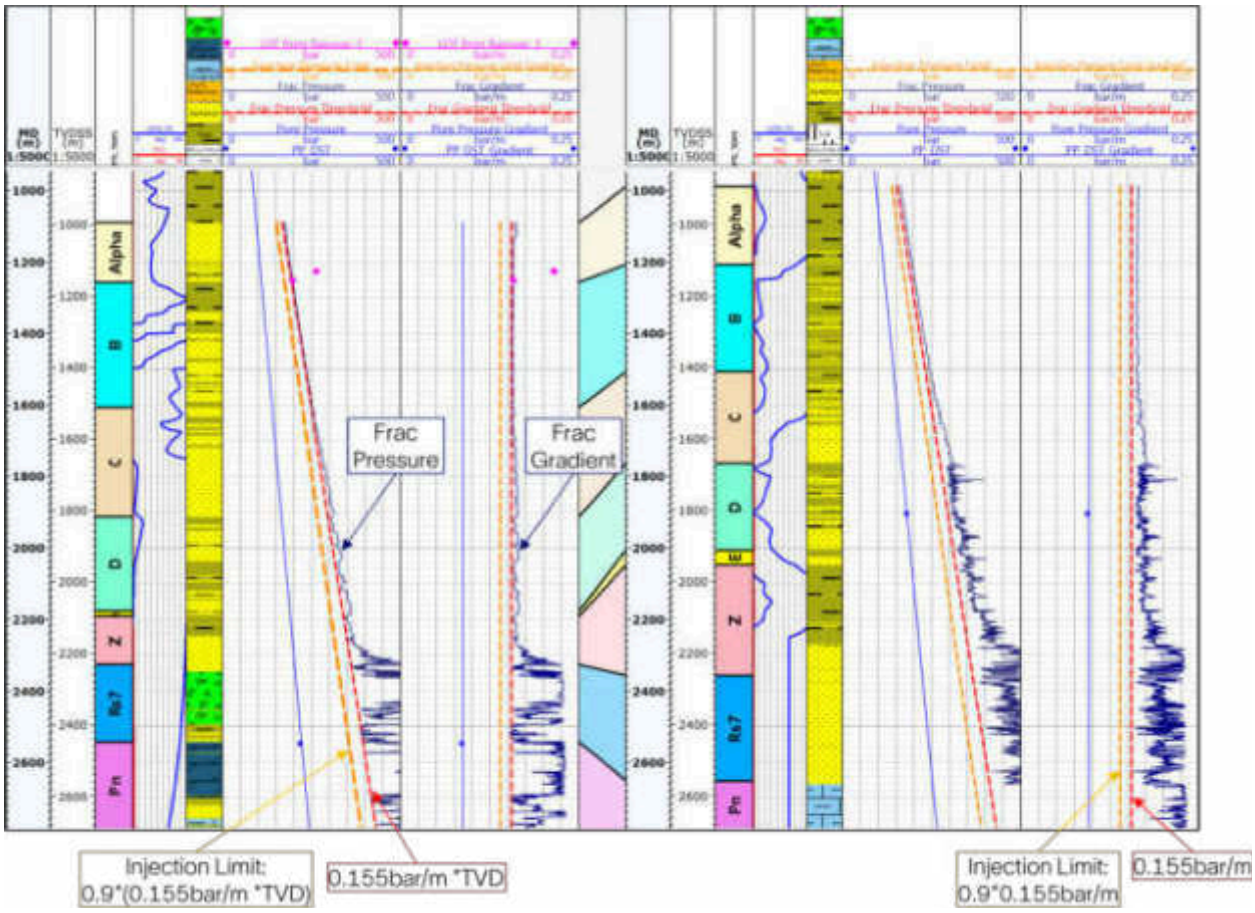


Fig. 2.166 Bockovci-1 and Sječe-2 fracture gradient and injection limit

Well's injectivity for all the sites was investigated assuming the reservoir properties and estimated fracture gradient of 0.155 bar/m @ mid perf. Objective of the simulation study is to determine minimum number of injectors to maximize CO_2 storage capacity or containment of CO_2 into the selected sites.

2.8.3.2 Initial and boundary conditions

The initial reservoir pressure is distributed in model based on pressure points and gradients from Table 2.18, Table 2.19 and Table 2.20 . Pressure gradient interpolation is done in the absence of direct well data. Resulted initial pressure distribution for key wells is presented in Fig. 2.167.

Copyright © SLB. All Rights Reserved. Private & Confidential. Reproduction only by permission.

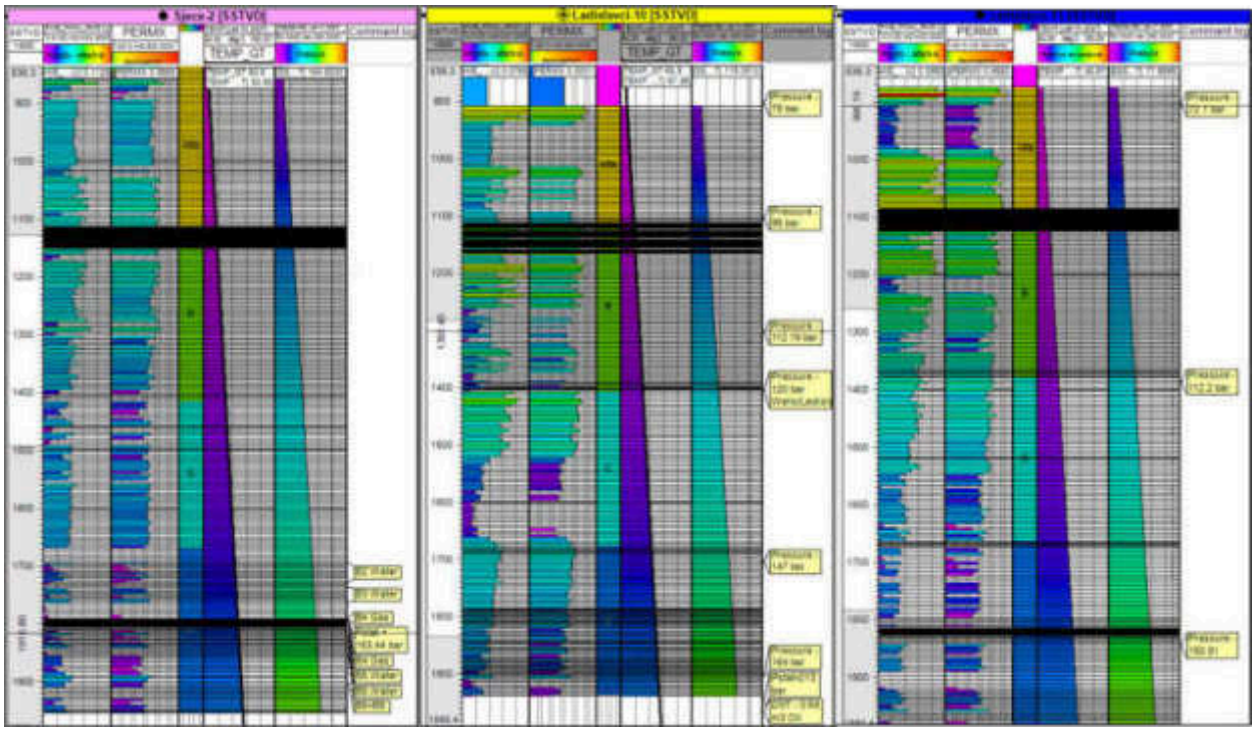


Fig. 2.167 Pressure calibrated based on DST information available for wells (Sječe-2, Ladislavci-10 and Ladislavci-11)

Initialized temperature is based on gradient estimated from well data. Resulted temperature profile for key wells is presented in Fig. 2.168.

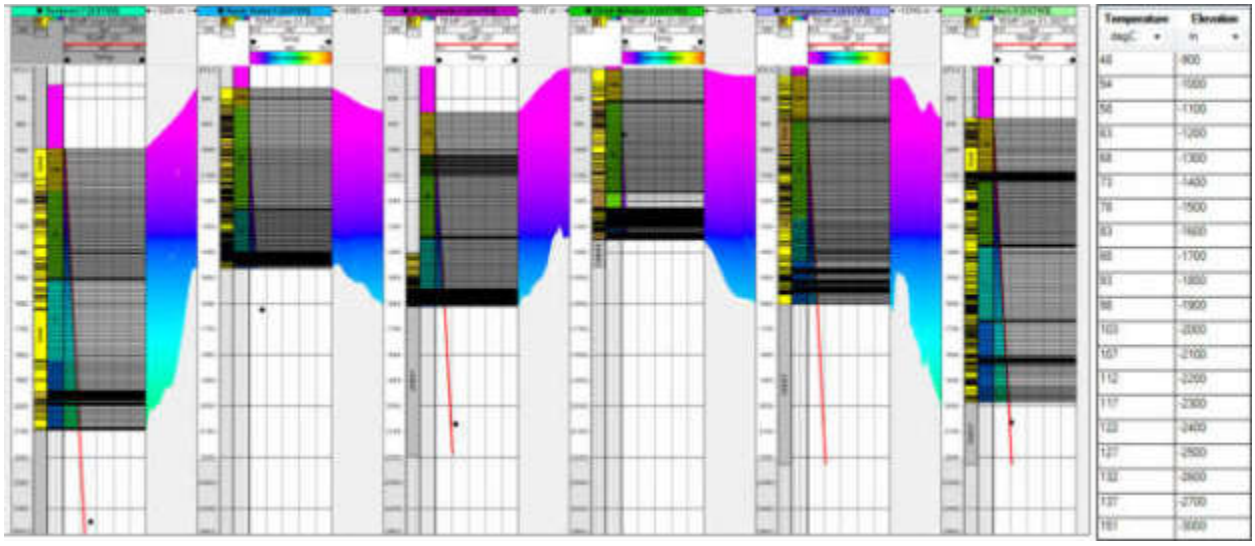


Fig. 2.168 Temperature calibrated on estimated log gradient and well data

Boundary conditions assumed as open with Fetkovitch type analytical aquifers. Settings for aquifers are presented in Fig. 2.169.

Copyright © SLB. All Rights Reserved. Private & Confidential. Reproduction only by permission.

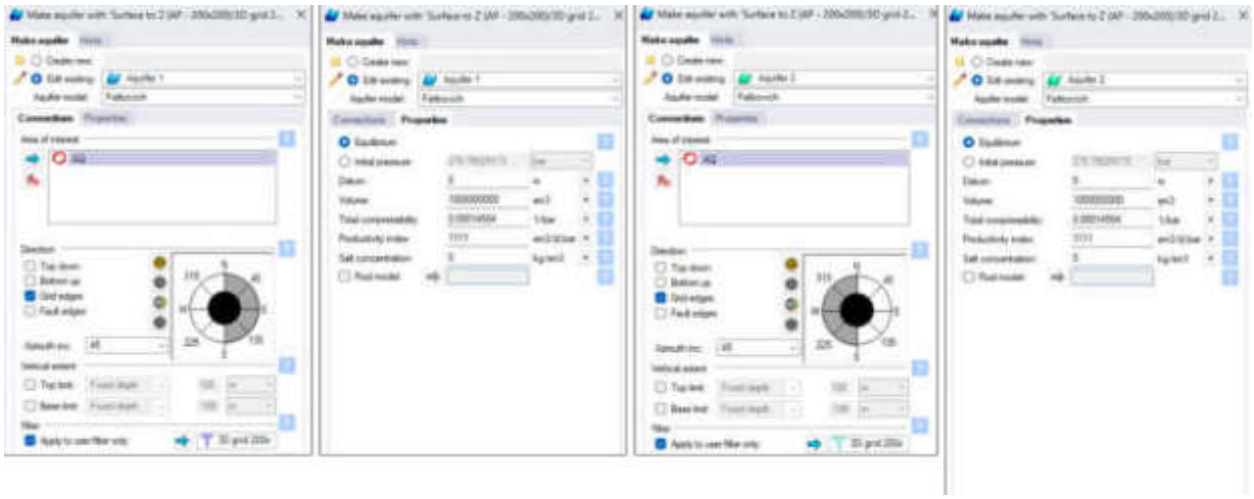


Fig. 2.169 Aquifers to model boundary conditions

Open boundaries are used to mimic semi-infinite or very large geologic settings, minimizing artificial pressure buildup that would occur with closed (no-flow) boundaries. This approach is important for assessing long-term plume migration, pressure distribution and risk of leakage.

2.8.3.3 Rock and fluid properties

Section describes the key petrophysical and fluid characteristics that define the storage reservoirs and overlying units. Accurate definition of these properties is critical for reliable simulation of CO_2 injection, plume migration, trapping and long-term storage. Formation brine composition and salinity are assigned based on available sample analysis and zonation are included to the simulation model, based on Table 2.21. Brine salinity in the reservoir is controlled by the concentration of NaCl element. Brine properties influence buoyancy forces, dissolution of CO_2, and pressure changes during injection. Higher density differences between CO_2 and brine promote upward migration, while brine viscosity affects the ease of CO_2 displacement and plume stability.

CO_2 properties are defined in the simulation model by corrected Peng Robinson equation of state, based on zone index and cells properties as presented in Fig. 2.170.

Copyright © SLB. All Rights Reserved. Private & Confidential. Reproduction only by permission.

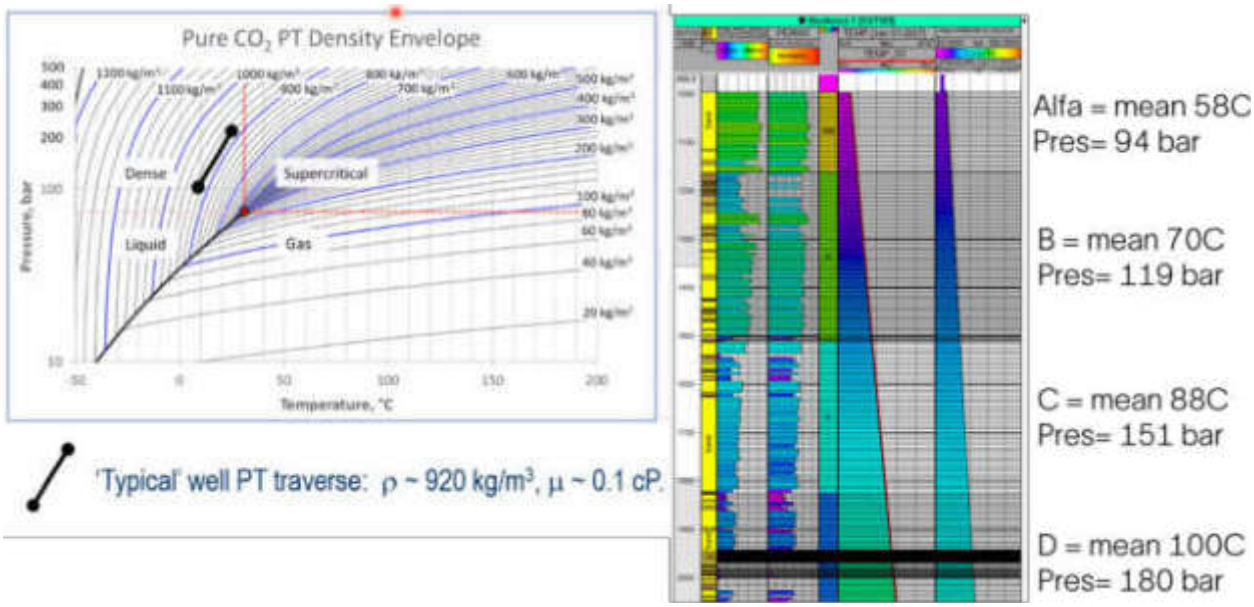


Fig. 2.170 Average CO_2 properties based on Zones index

The density and viscosity of CO_2 dictate the plume shape, extent, and trapping efficiency. Supercritical CO_2, due to its relatively low viscosity and high mobility, can migrate more readily, while its density compared to brine determines vertical buoyancy and dissolution rates. CO_2 saturation is set to zero in the pre-injection case. PR (Peng Robinson) corrected equation of state used with Spycher and Pruess model for CO_2 solubility in water phase. 100 % initial water saturation in the model was assumed.

The mean horizontal permeability (Kh) is 4.4 mD (range: 0.001-217 mD), and mean vertical permeability (Kv) is 0.44 mD. Higher permeability enables greater injectivity rates, facilitating efficient CO_2 injection. Anisotropy (Kh/Kv = 0.1) affects the preferential direction of CO_2 migration, with high horizontal permeability promoting widespread plume growth, while low vertical permeability can limit upward migration and aid in containment beneath the caprock. The following equation was used to distribute permeability: Core Permeability = 4782.3* pow(Core Porosity, 4.1). Resulted cross-plot porosity-permeability is presented in Fig. 2.171.

Copyright © SLB. All Rights Reserved. Private & Confidential. Reproduction only by permission.

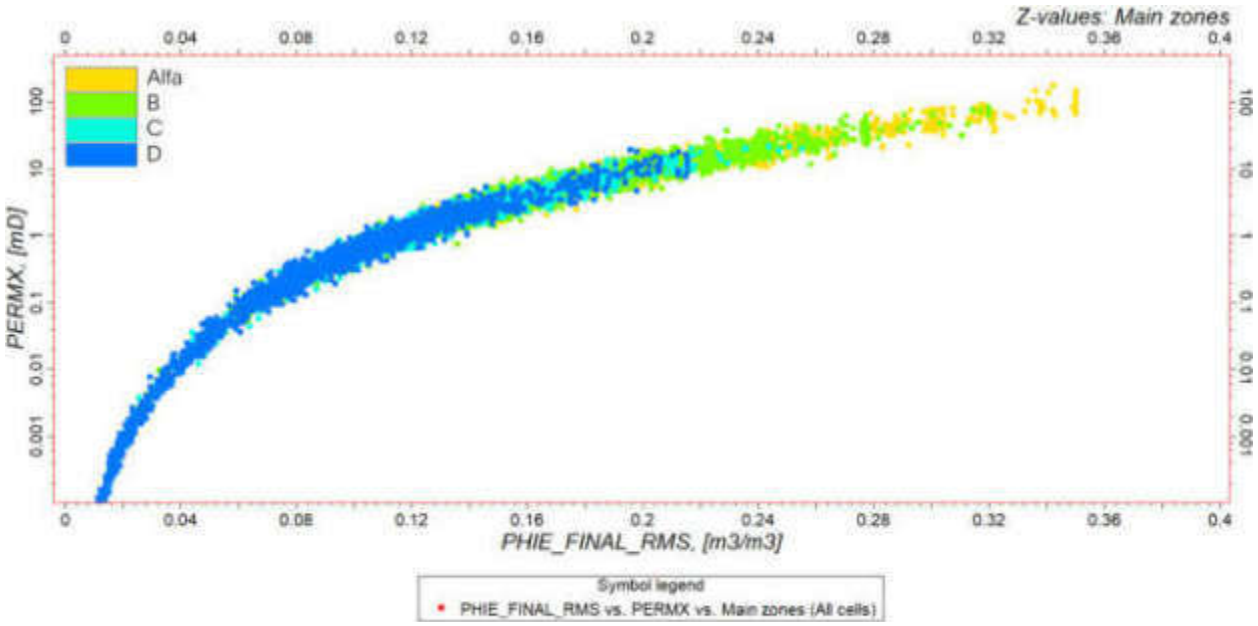


Fig. 2.171 Porosity - Permeability cross plot per zone

Relative permeability curves were used in the simulation to represent the concurrent flow of CO_2 and brine within the reservoir rock. These curves determine the mobility of each phase as function of saturation and are essential for predicting CO_2 migration, trapping and displacement. Direct SCAL (Special Core Analysis Laboratory) measurements for relative permeability were not available for the target interval in this study. In lieu of SCAL data, industry standard relative permeability tables were used from Petrel template library. Hysteresis effects were incorporated into the simulation model. This accounts for the difference in relative permeability behavior during drainage (CO_2 displacing brine during injection) and imbibition (brine re-entering pore space during post-injection migration). These are critical for accurately representing residual trapping of CO_2 in pore spaces after the migration front moves past. Drainage and Imbibition relative permeabilities using Corey coefficients with 10% trap CO_2 saturation was used in the simulation model.

2.8.4 Simulation scenarios

Base case scenario – one well per site / per formation (18 wells). Pre-selected sites for zone Alfa, B, C and D are presented in Fig. 2.172.

Copyright © SLB. All Rights Reserved. Private & Confidential. Reproduction only by permission.

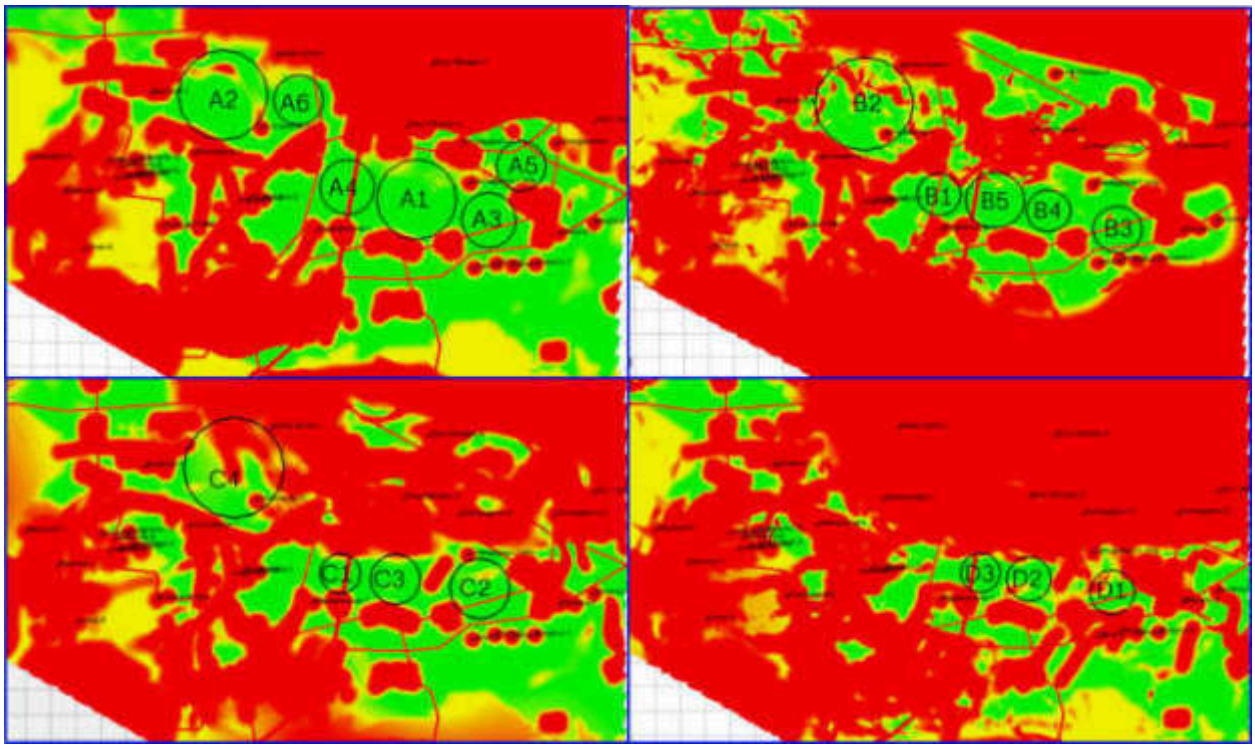


Fig. 2.172 Pre-selected sites per zone overplayed by COS (chance of success maps)

Simulation strategy consists of:

- Injection start date is Jan 2027
- All injection wells start to inject at the same date.
- Injection period - 30 years
- Post injection plume monitoring – 200 years
- Injection stream – pure CO_2 (100%)
- BHP injection limits mid-perforation TVD*0.9*0.155 bar/m

Based on base case scenario results 2.8.5 CO_2 injection Results and Analysis sites closed to wells Karas Suma-1, Magadenovac-1 and Camagajevci-1 are the most promising and have overlapping pre-selected sites (in different zones), that allows to minimize the number of wells and maximize storage capacity by targeting several zones as show on Fig. 2.173 and Fig. 2.174.

Copyright © SLB. All Rights Reserved. Private & Confidential. Reproduction only by permission.



Fig. 2.173 Selected sites for optimization as per base case scenario results (2D view)

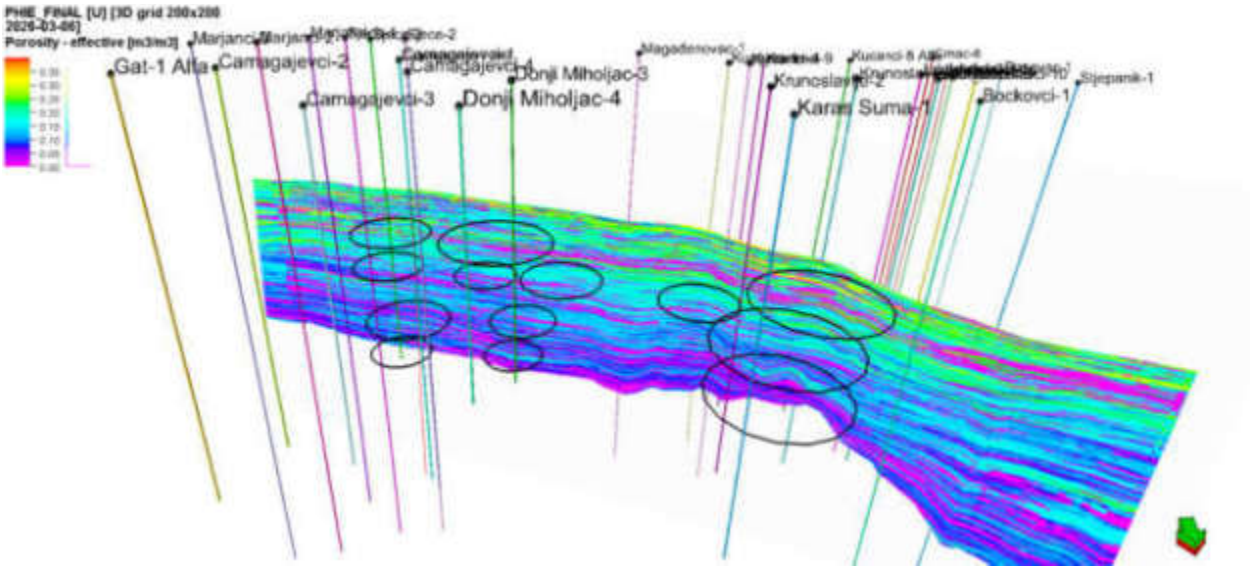


Fig. 2.174 Selected sites for optimization as per base case scenario results (3D view)

Simulated scenarios:

- **Scenario 1 - 4 vertical wells**
  - 2 proposed well locations close to Karas Suma -Bockovci-1 wells
  - 1 proposed well location close to Magadenovac-1 and 1 proposed well location close to Camagajevci-1 well
  - Dedicated injection per formations versus time
- **Scenario 2 - 4 vertical wells**

Copyright © SLB. All Rights Reserved. Private & Confidential. Reproduction only by permission.

- 2 proposed well locations close to Karas Suma -Bockovci-1 wells
- 1 proposed well location close to Magadenovac-1 and 1 proposed well location close to Camagajevci-1 well
- Commingled injection at constant injection rate per well

- **Scenario 3 - 3 vertical wells**
  - 3 proposed well locations close to Karas Suma -Bockovci-1 wells
  - Commingled injection at constant injection rate per well
- **Scenario 4 - 4 vertical wells**
  - 4 proposed well locations close to Karas Suma -Bockovci-1 wells
  - Commingled injection at constant injection rate per well

In summary, the simulation scenarios detailed above have been designed to optimize CO_2 storage performance for the pre-selected sites by choosing the overlapped targeted zones, varying the number of wells. This approach enables the evaluation of multiple development strategies, capturing how different well patterns and storage intervals influence injectivity, storage capacity, and containment. By focusing on these operational parameters across representative scenarios, the study provides valuable insights to support the selection of optimal well number and injection strategy, ensuring efficient and secure CO_2 storage in site-specific conditions.

These four CCS development scenarios were evaluated for the CHA Bockovac study, considering storage capacity, injectivity, pressure management, containment security, and surface constraints.

Scenario 4 with 4 vertical wells was selected from the four evaluated cases because it provides the best balance between storage efficiency and operational simplicity. While some scenarios using multiple sites may offer slightly higher storage capacity, they introduce additional complexity related to infrastructure, pressure interference between sites, and monitoring requirements. Scenario 4 concentrates injection in a single site, enabling more controlled reservoir behavior, easier surveillance, and reduced operational risks. Also, compared to multi-site scenarios, Scenario 4 avoids complex CO_2 distribution networks and reduces infrastructure requirements. A centralized system lowers CAPEX and OPEX while simplifying operations and monitoring. Monitoring strategies such as seismic or pressure surveillance benefit from a single, predictable system.

The Karas Suma location is partially covered by forest and environmentally sensitive areas, limiting surface access and infrastructure development. To minimize environmental impact and comply with land-use constraints, the drilling center was placed outside the forest boundary. From this external location, deviated wells are drilled to reach the subsurface reservoir targets beneath the forest. This approach reduces deforestation, limits surface disturbance, and aligns with environmental and permitting requirements.

The deviated wells were designed to intersect the reservoir at the mid-perforation depth of the equivalent vertical wells used in Scenarios 4. This ensures that the injection profiles (rate

Copyright © SLB. All Rights Reserved. Private & Confidential. Reproduction only by permission.

distribution, pressure conditions, and vertical flow behavior) remain consistent with the base-case vertical well designs. By preserving the same effective injection intervals, the simulation results remain comparable, while enabling a practical drilling solution from a single pad located outside the forest.

2.8.5 CO_2 injection Results and Analysis

This chapter presents the results of the simulation scenarios described in the previous section and provides a detailed analysis of their implications for CO_2 storage optimization in pre-selected sites. For each targeted site, outcomes are evaluated with respect to the number of injection wells and selected reservoir zones. The main performance indicators examined include storage capacity, injectivity, plume migration behavior, reservoir pressure development, and containment integrity over the simulation monitoring time duration.

Simulation results are compared across scenarios to identify optimal configurations and highlight sensitivities to key parameters such as well count and perforated zones. Graphical illustrations, such as injection rate profiles, pressure maps, and CO_2 plume evolution maps and 3D views included. Additionally, this chapter discusses operational constraints and possible risks, offering insights into the most effective well deployment and zone-targeting strategies for maximizing secure storage at each pre-selected site.

The analysis aims to provide recommendations, supporting decision-making for field development planning and risk management in CCS operations.

2.8.5.1 Effective Capacity and Injected volumes per scenario

This chapter details the assessment of Effective Capacity as per Fig. 2.115 and injection performance for both the base case and optimization cases at the pre-selected and stacked storage sites. The analysis focuses on number and placement of injection wells, as well as targeting of specific zones, pressure evolution, and overall CO_2 storage volumes. On the proposed site locations, a unique dynamic model was simulated for all Sites in Alfa, B, C and D formations. For the base case scenario single well was placed in each pre-selected sites, targeting only one zone as presented in Fig. 2.172. Resulted injection rates per year and injection cumulative volumes are presented and ranked in Table 2.22

Copyright © SLB. All Rights Reserved. Private & Confidential. Reproduction only by permission.

Table 2.22 Base case simulation scenario volumes per pre-selected site

Site	CO_2 injection rate, Mt/year	CO_2 injection cum, Mt
B2	0.142	4.27
A1	0.068	2.03
B3	0.061	1.83
A2	0.054	1.62
C2	0.054	1.62
B4	0.047	1.42
A5	0.041	1.22
B5	0.041	1.22
C4	0.041	1.22
A3	0.039	1.18
C1	0.037	1.11
C3	0.037	1.11
A4	0.036	1.07
D2	0.027	0.81
A6	0.02	0.61
B1	0.02	0.61
D1	0.02	0.61
D3	0.02	0.61

Summary per zone is presented in Table 2.23

Table 2.23 Base case simulation scenario volumes per zone

Zone	CO_2 injection rate, Mt/year	CO_2injection cum, Mt
Alfa	0.258	7.73
B	0.312	9.35
C	0.169	5.06
D	0.067	2.03
Total	0.806	24.17

Gas injection rate, gas injection cumulative in volumetric and mass units along with reservoir pressure is presented in Fig. 2.175. As per Table 2.23 formations B and Alfa have the highest storability and transmissivity.The reported field reservoir pressure corresponds to the pore-volume-weighted average pressure of the entire reservoir system, combining contributions from all simulated zones (Alfa, B, C, and D).

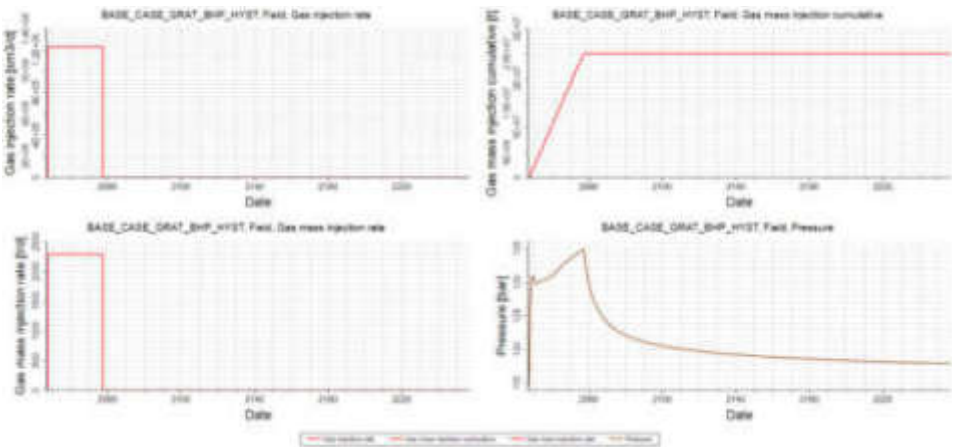


Fig. 2.175 Field level gas injection rate, gas cumulative and reservoir pressure for the base case

Copyright © SLB. All Rights Reserved. Private & Confidential. Reproduction only by permission.

The resulting ranking provides a clear overview of the relative merits of each site in its baseline configuration and highlights the most promising candidates for optimization. Top-ranked sites demonstrate higher injection rates with manageable pressure increases and robust containment characteristics, making them strong candidates for initial development or scale-up. These sites are:

- Close to Bockovci-1 well - sites A2, B2, C4 – larger areal extent- prone for commingle injection in Alfa, B and C formations.
- Close to Magadenovac-1 well – sites A1, B4, B5, C3, D2 share same areal extent - prone for commingle injection in Alfa, B, C and D formations.
- Close to Camagajevci-1 well- sites A3, B3, C2, D1 share same areal extent - prone for commingle injection in Alfa, B, C and D formations.

This ranking forms the foundation for subsequent optimization analyses, ensuring that development efforts are focused on sites offering the greatest potential for safe, efficient, and cost-effective long-term CO_2 storage.

Scenario 1 - 4 wells 3 sites (variable injection, with formation switch).

Scenario 1 consists of 2 proposed injection well locations close to Karas Suma-1 - Bockovci-1 area, 1 proposed injection well location close to Magadenovac-1 and 1 proposed injection well location close to Camagajevci-1. Dedicated injection per formations versus time, switching zones with new perforations in Jan 2042 and Jan 2050. Completion scenario and injection interval change is presented in Fig. 2.176, Fig. 2.177 and Fig. 2.178.

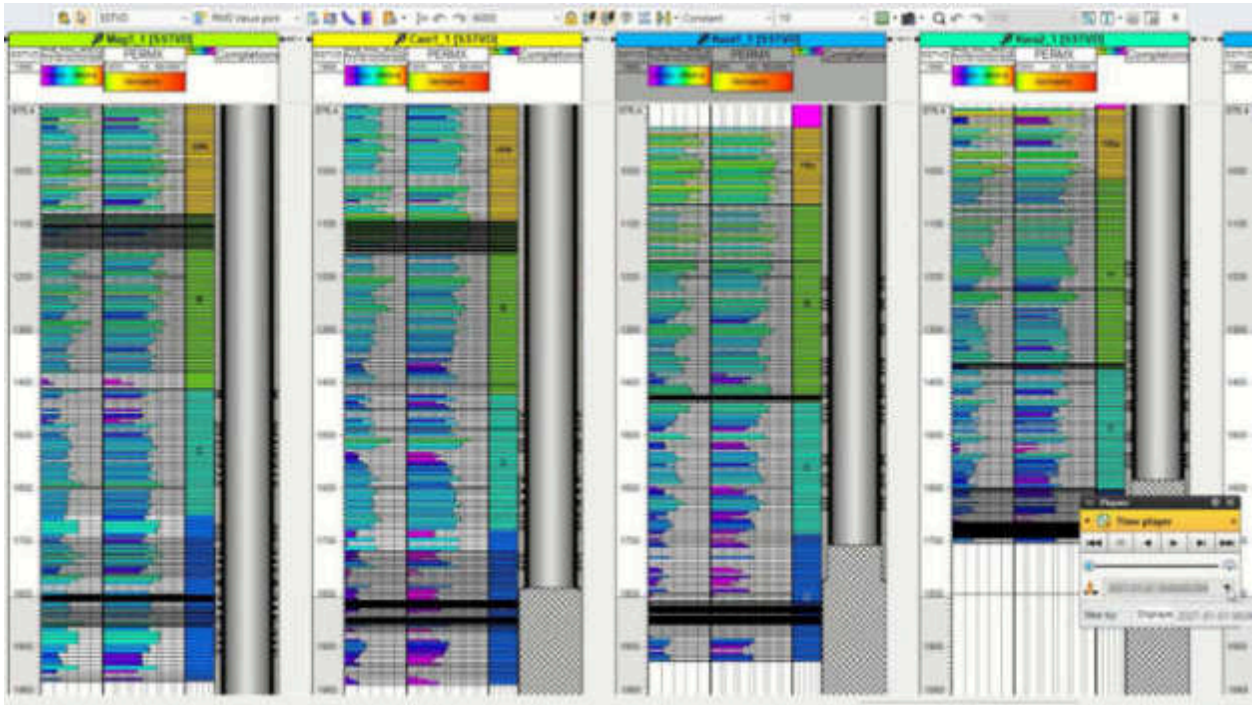


Fig. 2.176 Scenario 1 perforated intervals for wells Kara1, Kara2, Mag1, Cam1 @Jan 2027

Copyright © SLB. All Rights Reserved. Private & Confidential. Reproduction only by permission.

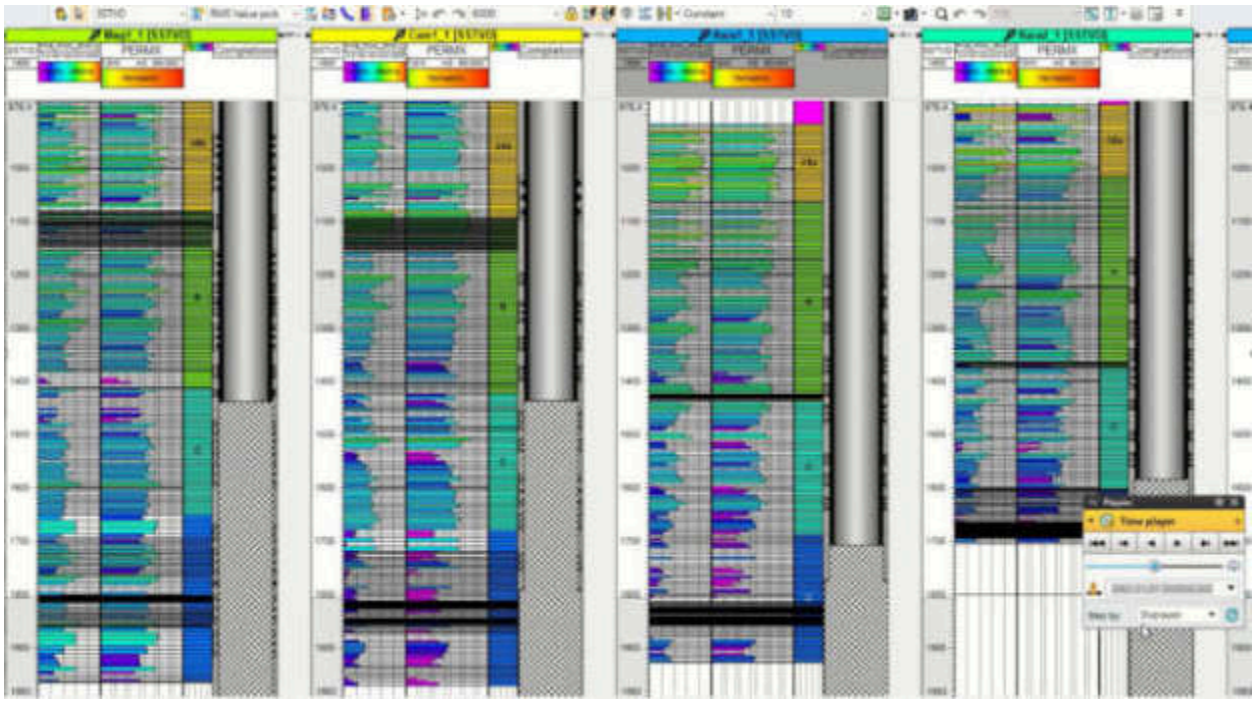


Fig. 2.177 Scenario 1 perforated intervals for wells Kara1, Kara2, Mag1, Cam1 @Jan 2042

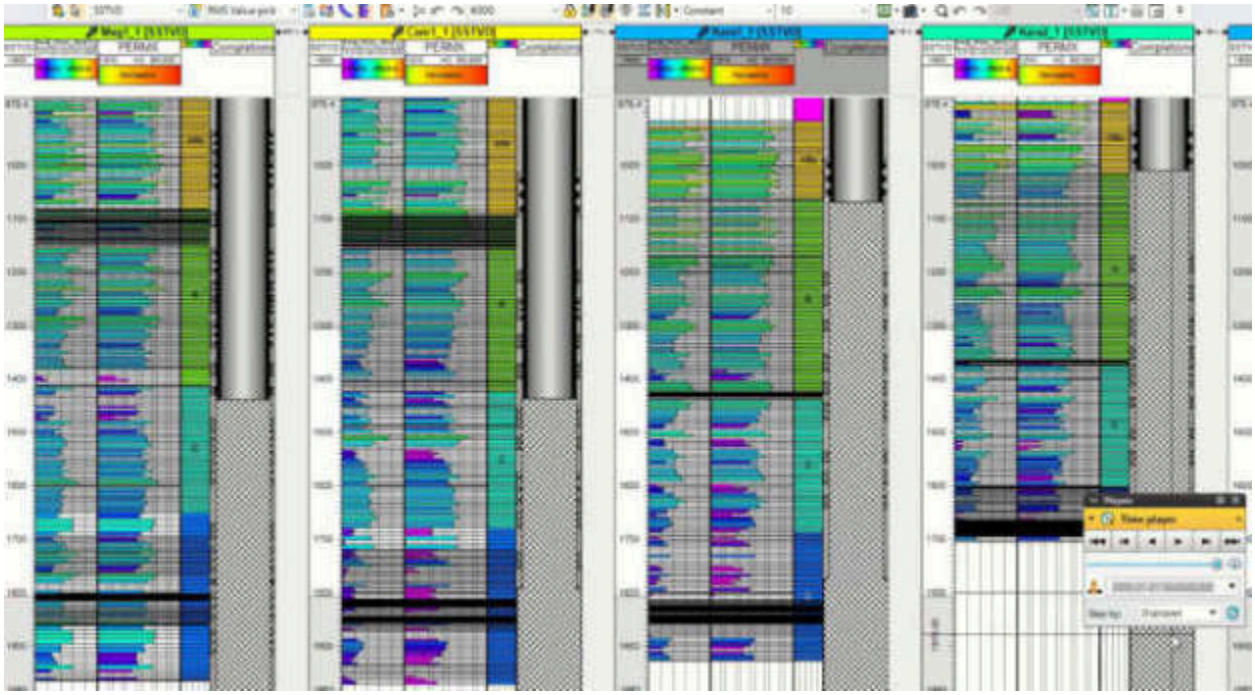


Fig. 2.178 Scenario 1 perforated intervals for wells Kara1, Kara2, Mag1, Cam1 @Jan 2050

Perforated intervals start Jan 2027 :

- Mag and Cam perforated C-D till Jan 2042, followed by plug C and D and open B and Alfa zones.
- Kara wells perforated B-C till Jan 2050, followed by plug B-C and open Alfa.

Copyright © SLB. All Rights Reserved. Private & Confidential. Reproduction only by permission.

Wells location for Scenario 1 within the pre-selected sites and plume distribution at the end on injection (1 Jan 2057) are presented in Fig. 2.179

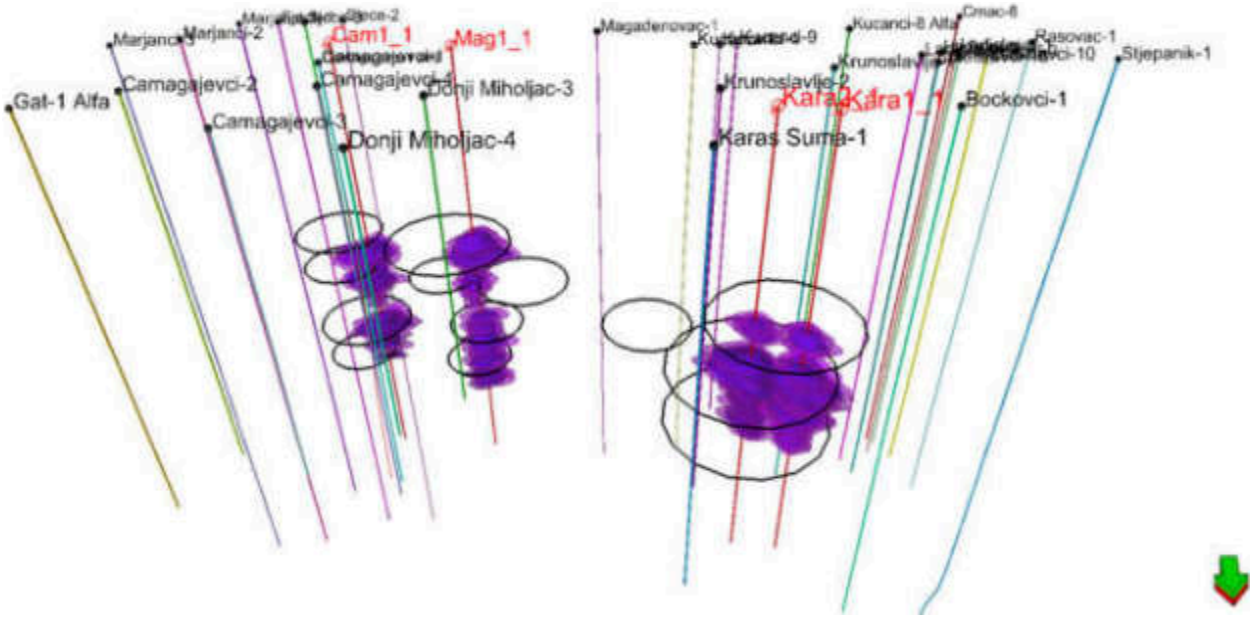


Fig. 2.179 Scenario 1 well locations and plume saturation at the end of injection @2057

Simulation plots of gas injection rate, cumulative gas injection and reservoir pressure is presented are Fig. 2.180. The reported field reservoir pressure corresponds to the pore-volume-weighted average pressure of the entire reservoir system, combining contributions from all simulated zones (Alfa, B, C, and D).

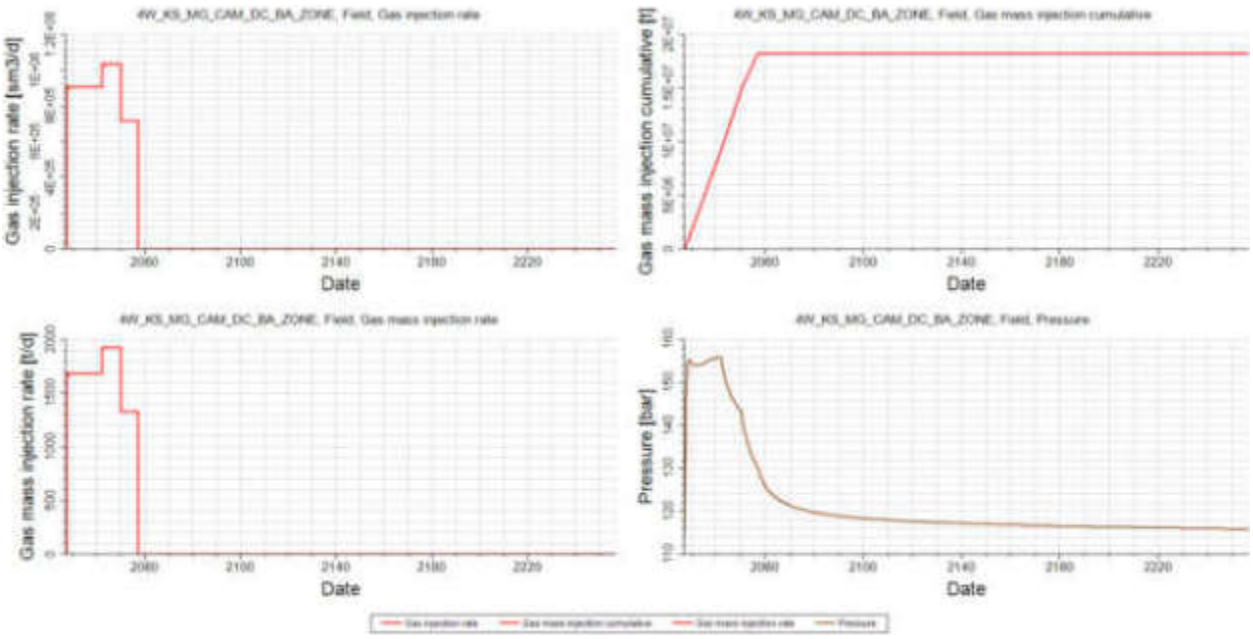


Fig. 2.180 Scenario 1 simulation plots (gas injection rate, cumulative, reservoir pressure)

Copyright © SLB. All Rights Reserved. Private & Confidential. Reproduction only by permission.

Table 2.24 summarises sites performance for the scenario 1. CO_2 Injection and pressure profiles for scenario 1 per well are presented in Fig. 2.181

Table 2.24 Scenario 1 injection rate per year and cumulative injection per site

Site	CO_2 injection rate, Mt/year	CO_2 injection cumulative, Mt
Kara	0.34	10.07
Mag	0.15	4.37
Cam	0.12	3.86
Total	0.61	18.3

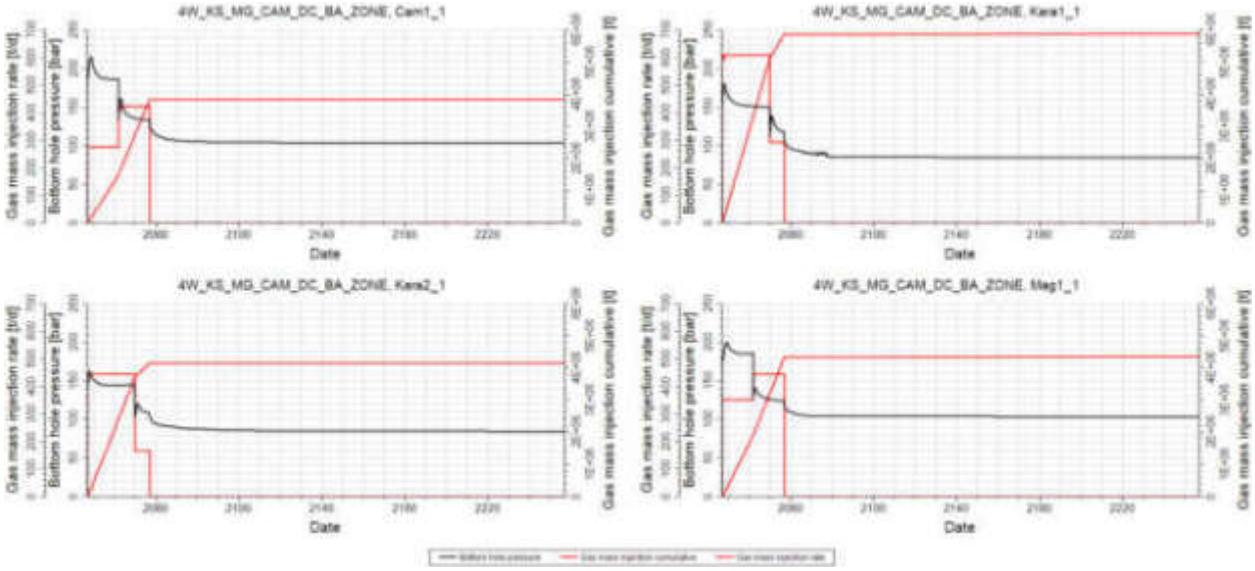


Fig. 2.181 Scenario 1 injection and pressure profiles per well

Injecting in all zones, and contain the CO_2 inside the sites even after 200 years post injection.

The total amount of CO_2 that can be injected is 18.3 million tonnes (Mt). The committed average annual injection rate is 0.61 million tonnes per year (Mt/yr). Injecting in all zones, and CO_2 is contained inside the sites even after 200 years post injection:

- 9.01 Mt of injected CO_2 is dissolved in water @2257
- 9.31 Mt of injected CO_2 remains in free state @2257.

Scenario 2 - 4 wells 3 sites (constant injection, no formation switch).

Scenario 1 consists of 2 proposed injection well locations close to Karas Suma-1 - Bockovci-1 area, 1 proposed injection well location close to Magadenovac-1 and 1 proposed injection well location close to Camagajevci-1. Wells location and number of wells are similar to Scenario 1 with different perforation scheme, presented in Fig. 2.182

Copyright © SLB. All Rights Reserved. Private & Confidential. Reproduction only by permission.

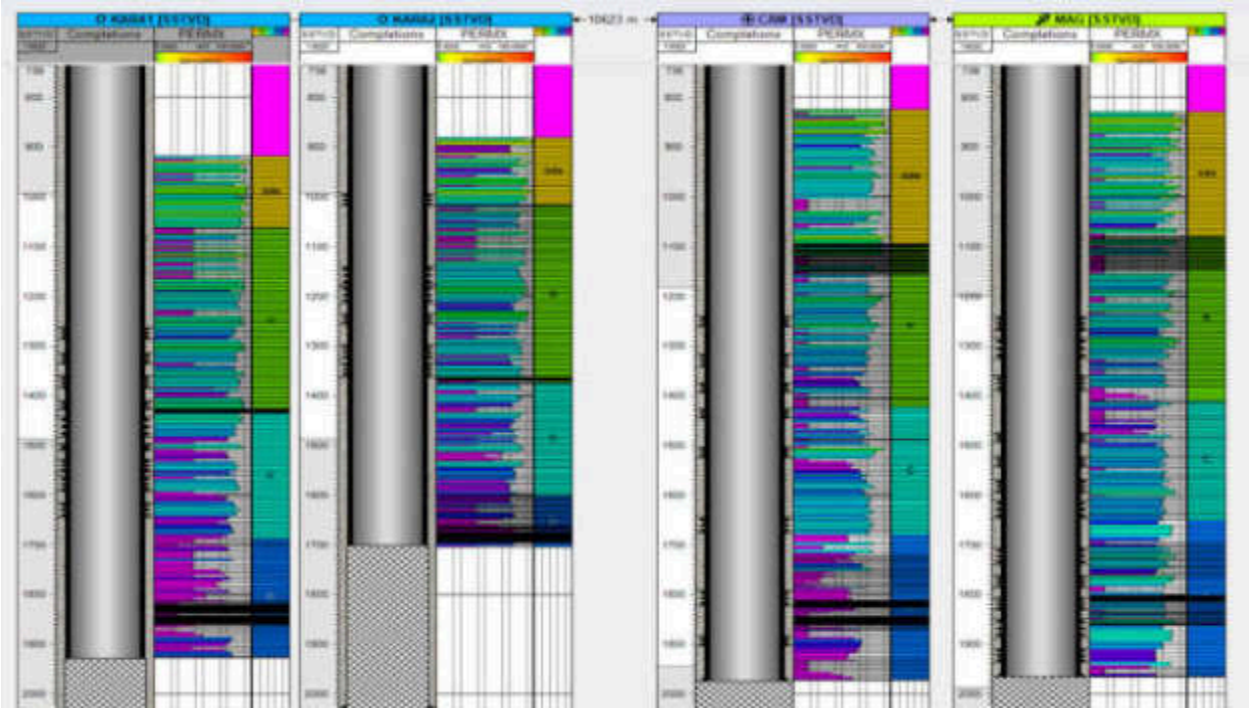


Fig. 2.182 Scenario 2 perforated intervals for wells Kara1, Kara2, Mag1, Cam1 @Jan 2027

Perforated intervals start Jan 2027 :

- Mag and Cam perforated B – C - D zones.
- Kara1 well perforated B - C zones.
- Kara2 well perforated Alfa – B zones.

Wells location for Scenario 2 within the pre-selected sites and plume distribution at the end on injection (1 Jan 2057) are presented in Fig. 2.183.

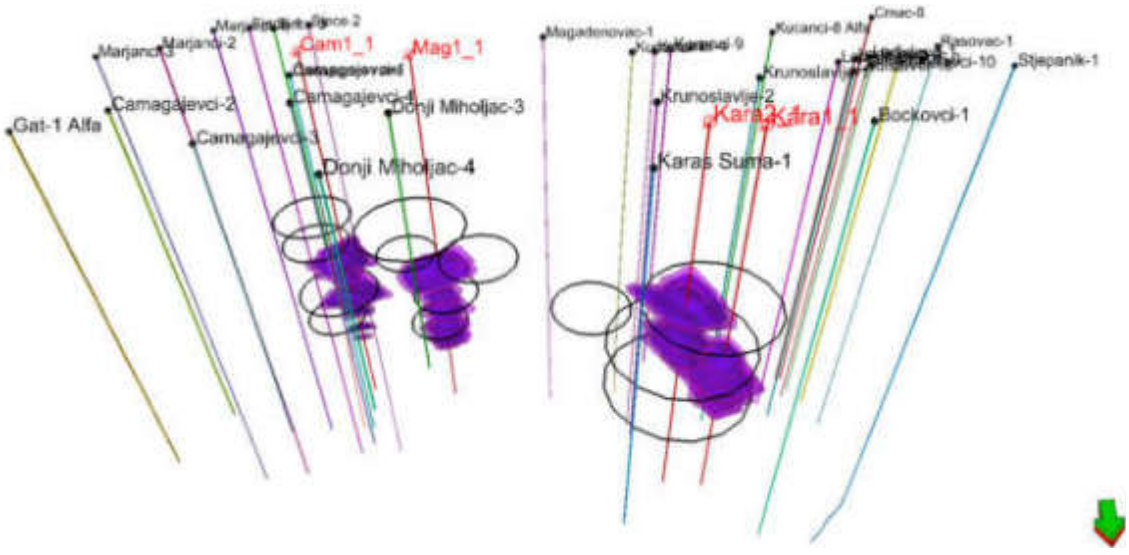


Fig. 2.183 Scenario 2 well locations and plume saturation at the end of injection @2057

Copyright © SLB. All Rights Reserved. Private & Confidential. Reproduction only by permission.

Simulation plots of gas injection rate, cumulative gas injection and reservoir pressure are presented in Fig. 2.184.The reported field reservoir pressure corresponds to the pore-volume-weighted average pressure of the entire reservoir system, combining contributions from all simulated zones (Alfa, B, C, and D).

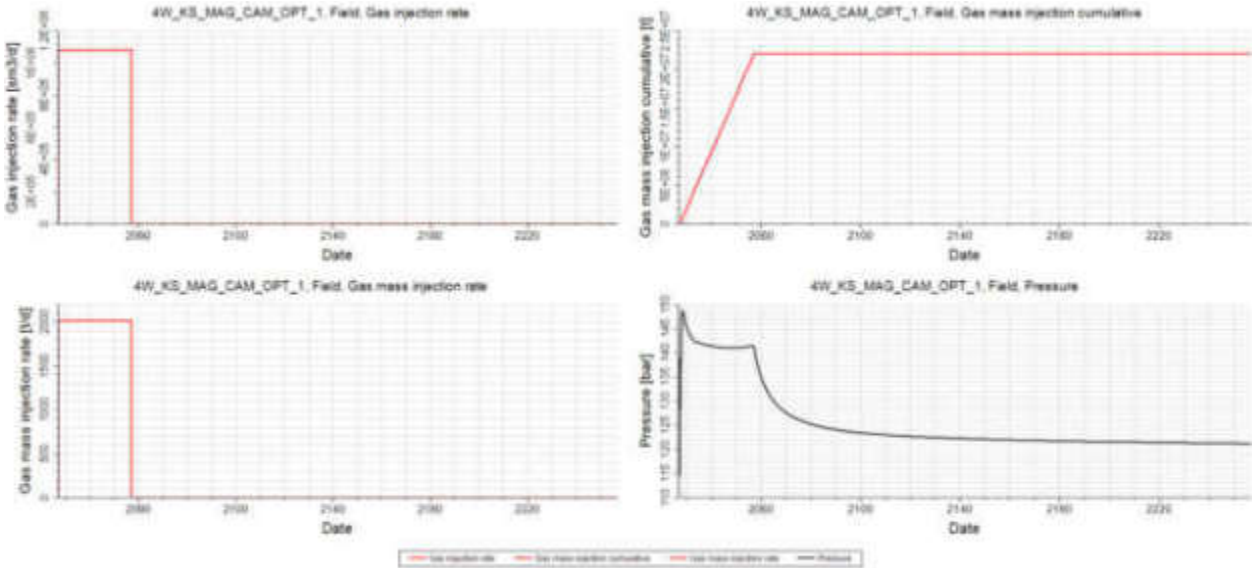


Fig. 2.184 Scenario 2 simulation plots (gas injection rate, cumulative, reservoir pressure)

Table 2.25 summarises sites performance for the scenario 1. Injection and pressure profiles for scenario 2 per well are presented in Fig. 2.185.

Table 2.25 Scenario 2 injection rate per year and cumulative injection per site

Site	CO_2 injection rate, Mt/year	CO_2 injection cum, Mt
Kara	0.393	11.8
Mag	0.197	5.9
Cam	0.149	4.48
Total	0.739	22.18

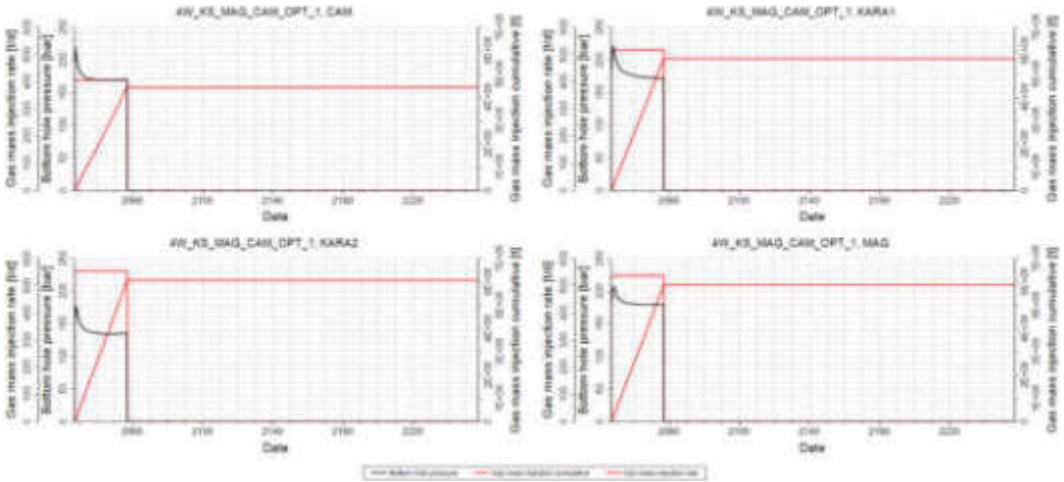


Fig. 2.185 Scenario 2 CO_2 injection and pressure profiles per well

Copyright © SLB. All Rights Reserved. Private & Confidential. Reproduction only by permission.

The total amount of CO_2 that can be injected is 22.18 million tonnes (Mt). The committed annual injection rate is 0.739 million tonnes per year (Mt/yr). Injecting in all zones (except Alfa in Mag and Cam), and CO_2 contained inside the sites even after 200 years post injection:

- 10.03 Mt injected CO_2 gets dissolved in water @2257
- 6.51 Mt injected CO_2 is in free state @2257.

Scenario 3 and 4 - 3 and 4 wells respectively in site close to well Karas Suma-1.

Scenario 3 consists of 3 proposed injection well locations close to Karas Suma-1 - Bockovci-1 area. Well's completion is presented in Fig. 2.186.

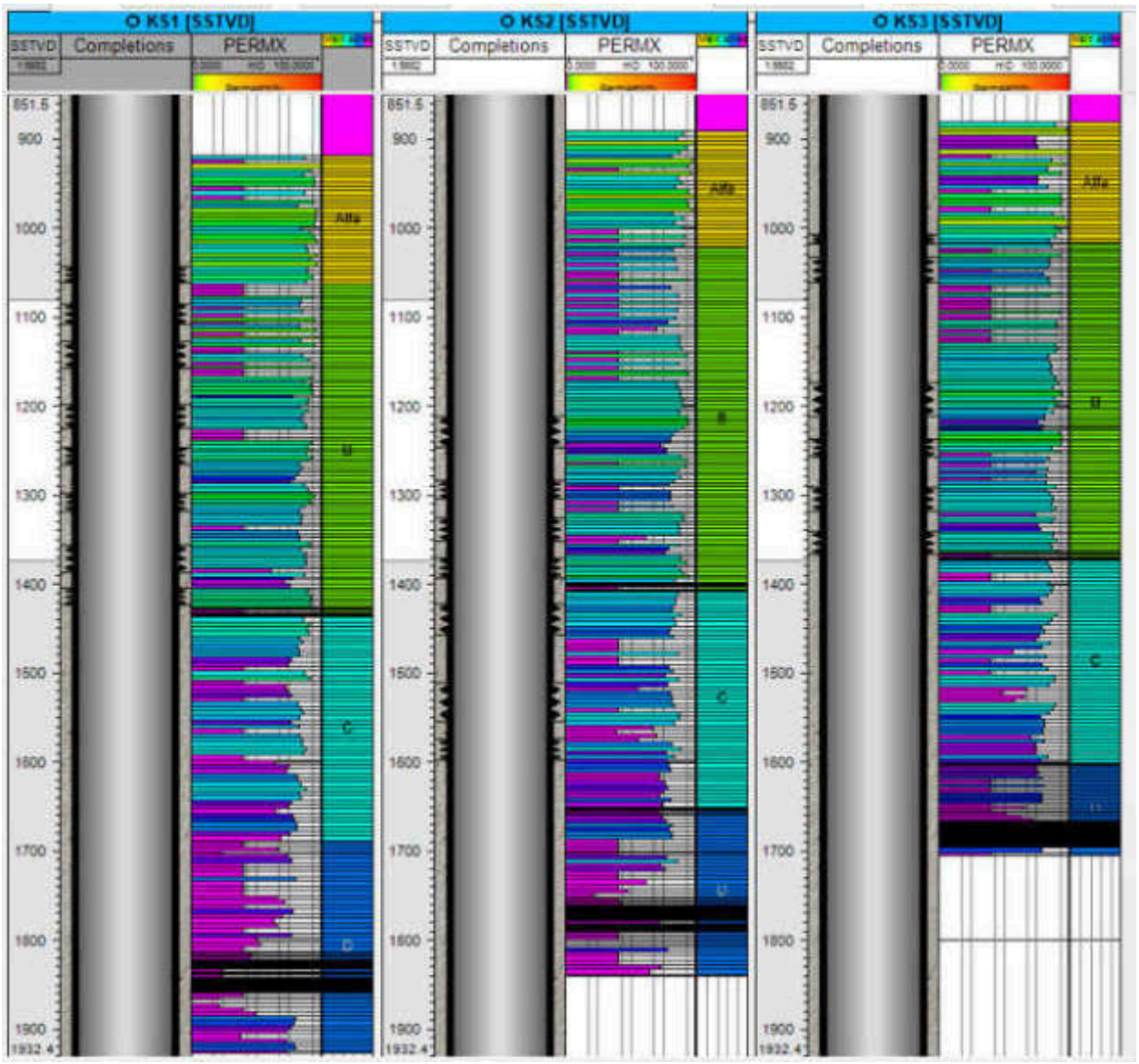


Fig. 2.186 Scenario 3 perforated intervals for wells KS1, KS2, KS3 @Jan 2027

Copyright © SLB. All Rights Reserved. Private & Confidential. Reproduction only by permission.

The total amount of CO_2 that can be injected for Scenario 3 is 16.28 million tonnes (Mt). The annual committed I injection rate is 0.54 million tonnes per year (Mt/yr).

Wells location for Scenario 3 within the pre-selected sites and plume distribution at the end on injection (1 Jan 2057) are presented in Fig. 2.187.

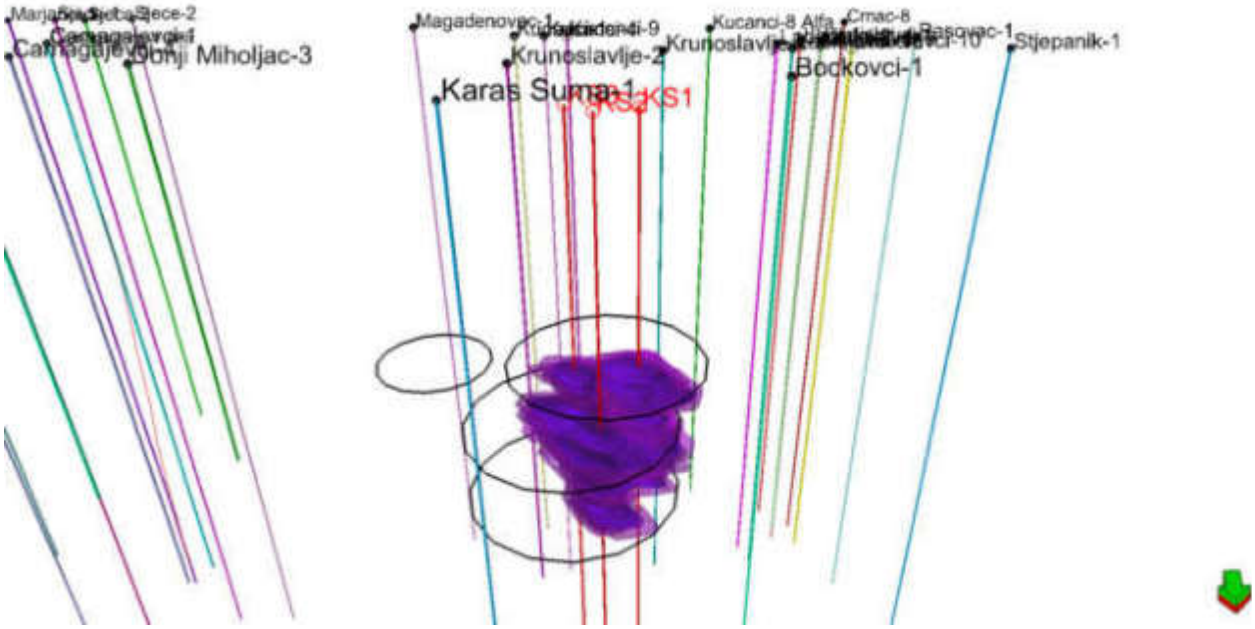


Fig. 2.187 Scenario 3 well locations and plume saturation at the end of injection @2057

Scenario 4 consists of 4 proposed injection well locations close to Karas Suma-1 - Bockovci-1 area. Well's completion is presented in Fig. 2.188.

Copyright © SLB. All Rights Reserved. Private & Confidential. Reproduction only by permission.

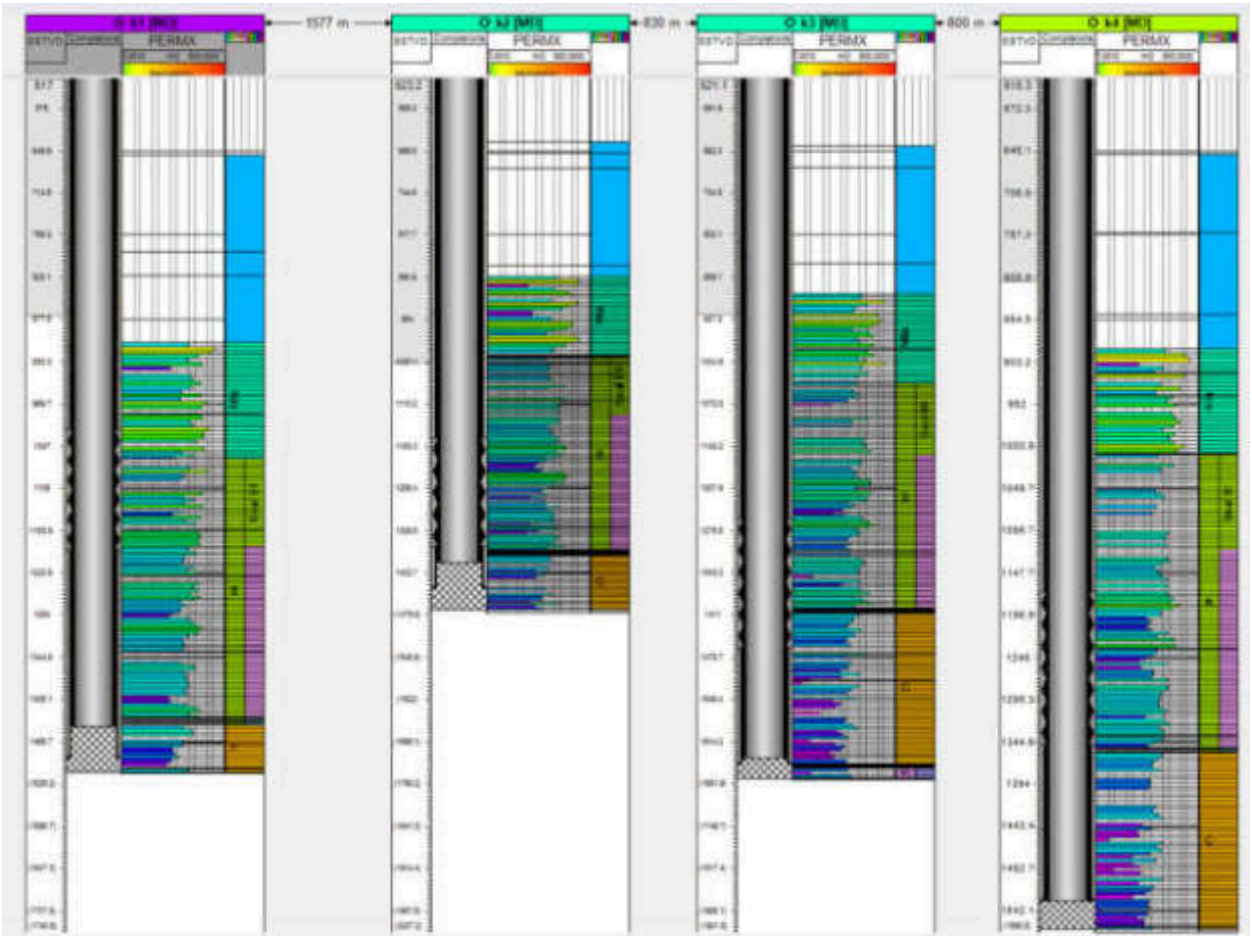


Fig. 2.188 Scenario 4 perforated intervals for wells KS1, KS2, KS3, KS4 @Jan 2027

The total amount of CO_2 that can be injected for Scenario 4 is 19.13 million tonnes (Mt). The annual committed injection rate is 0.64 million tonnes per year (Mt/yr).

Wells location for Scenario 4 within the pre-selected sites and plume distribution at the end on injection (1 Jan 2057) are presented in Fig. 2.189.

Copyright © SLB. All Rights Reserved. Private & Confidential. Reproduction only by permission.

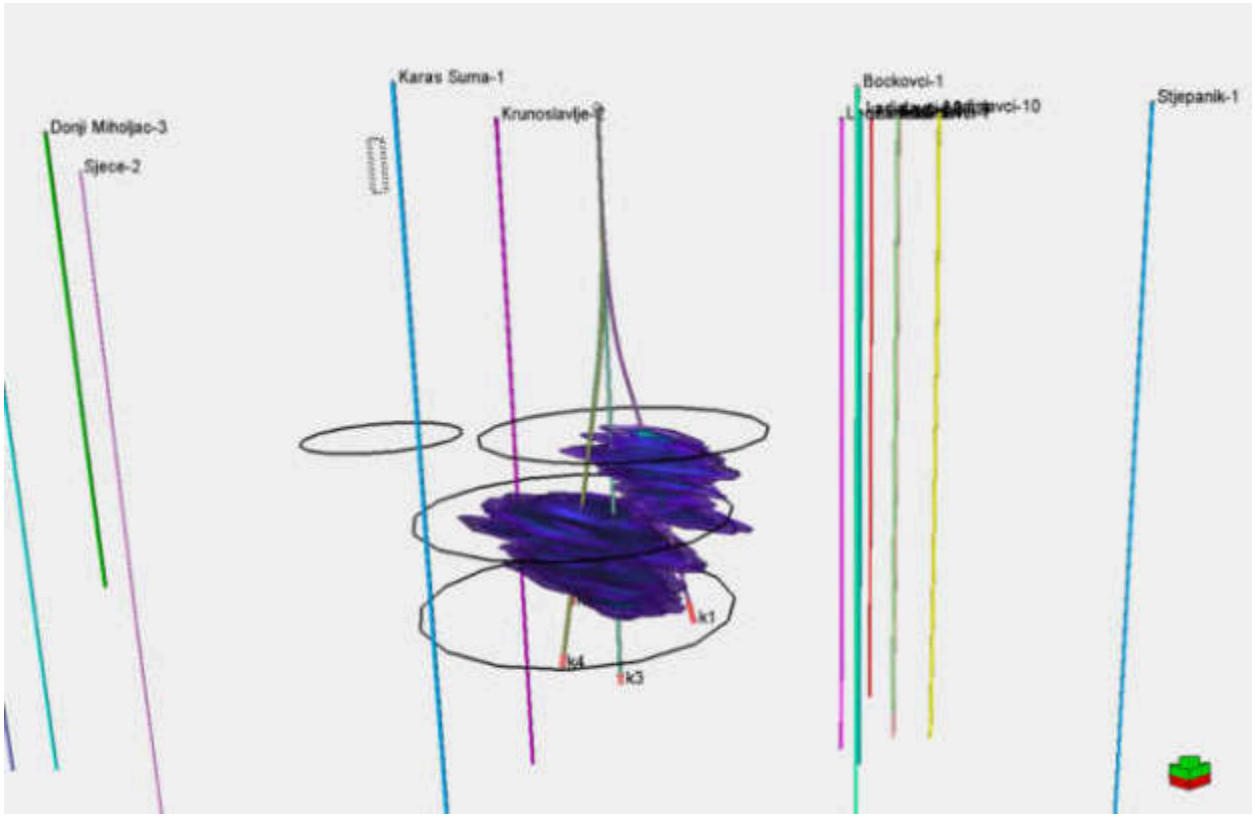


Fig. 2.189 Scenario 4 well locations and plume saturation at the end of injection @2057

Simulation plots of gas injection rate, cumulative gas injection and reservoir pressure for both Scenarios 3 and 4 are presented in Fig. 2.190. The reported field reservoir pressure corresponds to the pore-volume-weighted average pressure of the entire reservoir system, combining contributions from all simulated zones (Alfa, B and C).

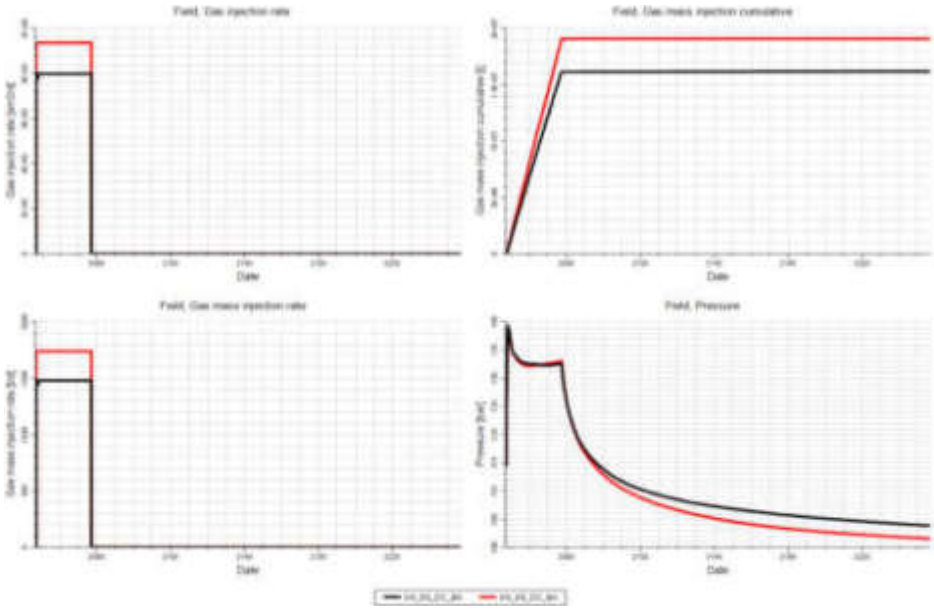


Fig. 2.190 Scenario 3 and 4 simulation plots (gas injection rate, cumulative, reservoir pressure)

Copyright © SLB. All Rights Reserved. Private & Confidential. Reproduction only by permission.

Table 2.26 summarises sites performance for the scenarios 3 and 4. CO_2 injection and pressure profiles for scenario 3 and 4 per well are presented in Fig. 2.191 and Fig. 2.192

Table 2.26 Scenario 3 and 4 injection rate per year and cumulative injection per site

Scenario	CO_2 injection rate, Mt/year	CO_2 injection cum, Mt
Karas Suma 3 vertical Wells	0.54	16.28
Karas Suma 4 vertical Wells	0.64	19.13

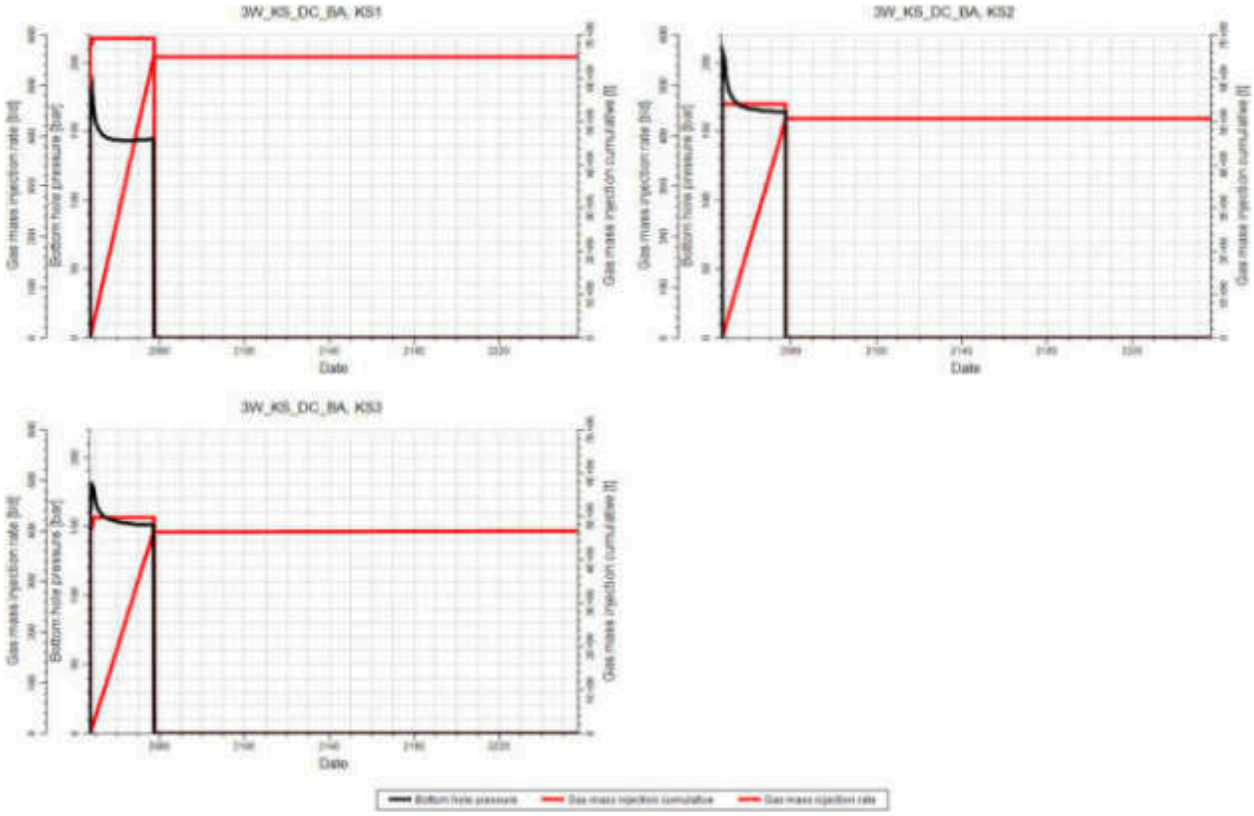


Fig. 2.191 Scenario 3 Injection and pressure profiles per well

Copyright © SLB. All Rights Reserved. Private & Confidential. Reproduction only by permission.

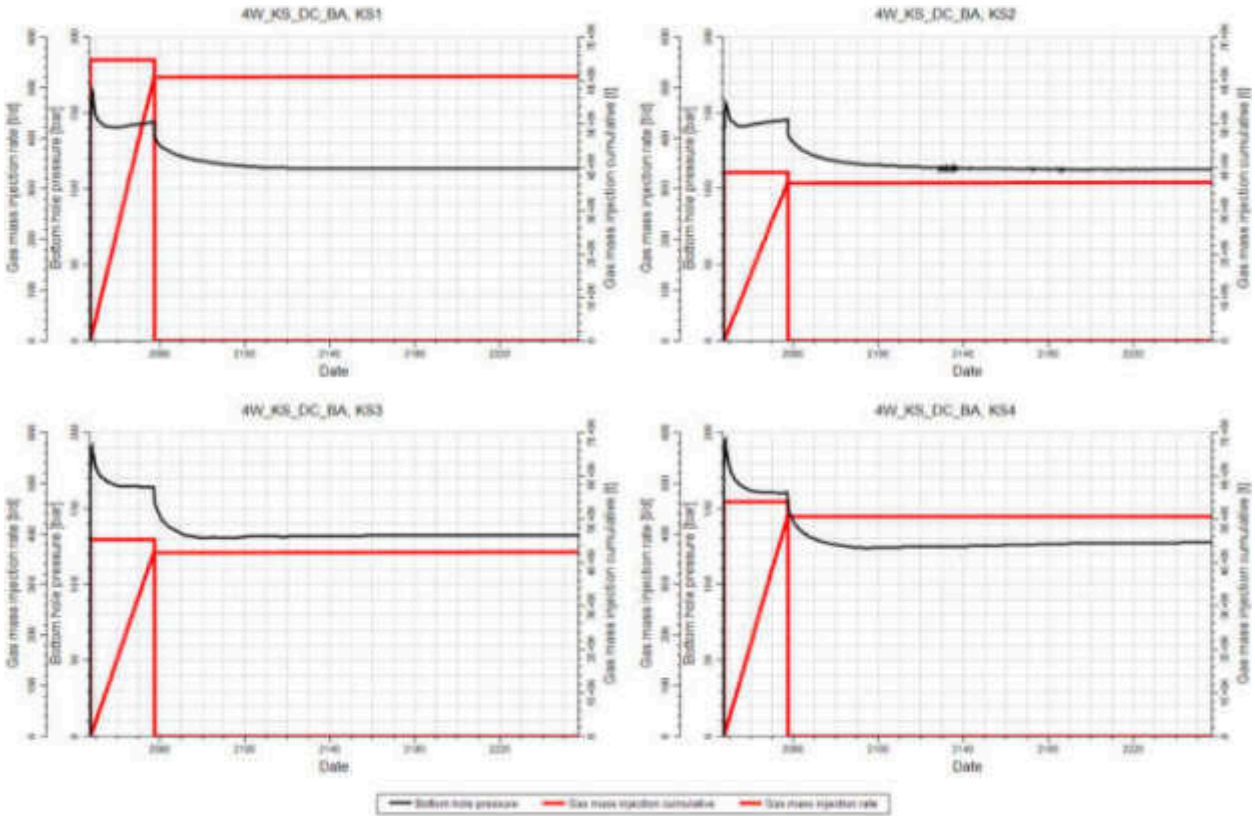


Fig. 2.192 Scenario 4 Injection and pressure profiles per well

CO_2 storage distribution per zone @ year 2257 for Scenario 3 presented in Table 2.27 and for Scenario 4 in Table 2.28.

Table 2.27 CO_2 storage distribution per zone for Scenario 3 @ year 2257

Zone	Aqueous component mass kg	Immobile vapor component mass kg	Mobile vapor component mass kg	Total component mass Mt
Alfa	2543108864	1091973504	881133696	4.52
B	4753778176	2597319936	3467426816	10.82
C	399117024	223603728	321967968	0.94

Table 2.28 CO_2 storage distribution per zone for Scenario 4 @ year 2257

Zone	Aqueous component mass kg	Immobile vapor component mass kg	Mobile vapor component mass kg	Total component mass Mt
Alfa	3531952896	1557349376	1169132672	6.26
B	5118141952	2721012224	4185088256	12.02
C	429000064	246601424	175475792	0.85

CO_2 contained inside the sites even after 200 years post injection for both Scenarios. Scenario 3 totals is 22.18 Mt of CO_2 injected over a 30 years period, while Scenario 4 vertical wells can store 19.13 Mt of CO_2 in the same injection period duration.

Selected Scenario with 4 deviated wells close to well Karas Suma-1.

Copyright © SLB. All Rights Reserved. Private & Confidential. Reproduction only by permission.

Among of the above Scenarios, Scenario 4, consisting of four vertical wells, was identified as the most balanced solution. While multi-site scenarios may offer marginally higher storage capacity, they introduce additional complexity related to infrastructure, pressure interference, and monitoring. In contrast, Scenario 4 focuses on a single site, enabling more predictable reservoir behavior, improved surveillance, and reduced operational risk. The centralized development concept also simplifies CO_2 transport and injection, lowering both CAPEX and OPEX while facilitating monitoring and control.

At the Karas Suma location, surface development is constrained by partial forest coverage and environmentally sensitive area. To minimize environmental impact and comply with land-use restrictions, the drilling pad is positioned outside the forest boundary. From this location, deviated wells are drilled to access the reservoir beneath the restricted area, thereby reducing surface disturbance and avoiding deforestation.

The deviated wells are designed to intersect the reservoir at equivalent mid-perforation depths used in the vertical well configuration of Scenario 4. This ensures consistency in injection conditions, including flow distribution and pressure behavior, while maintaining comparability with the base-case simulations. At the same time, it provides a practical and environmentally compliant drilling solution from a single surface location.

Based on these considerations, Scenario 4 was selected as the preferred development concept and further refined into a configuration with deviated wells. The final design consists of a single CCS site at Karas Suma -1 - Bockovci-1 area, developed with four deviated injection wells drilled from a centralized pad located outside the forested area Fig. 2.193 .

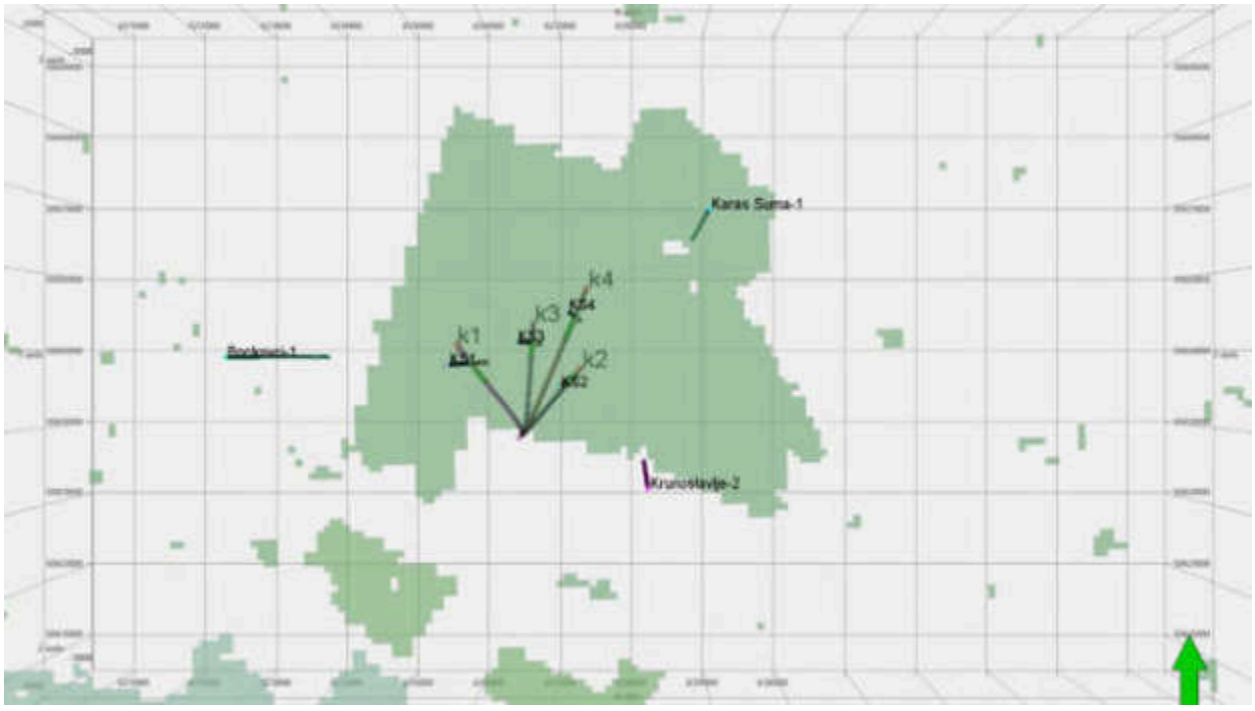


Fig. 2.193 Scenario 4 with deviated well locations in Karas Suma-1 - Bockovci-1 area

Copyright © SLB. All Rights Reserved. Private & Confidential. Reproduction only by permission.

The recommended scenario includes four proposed deviated well locations situated near the Karas Suma-1 – Bockovci-1 area. Well's completion is presented in Fig. 2.194.

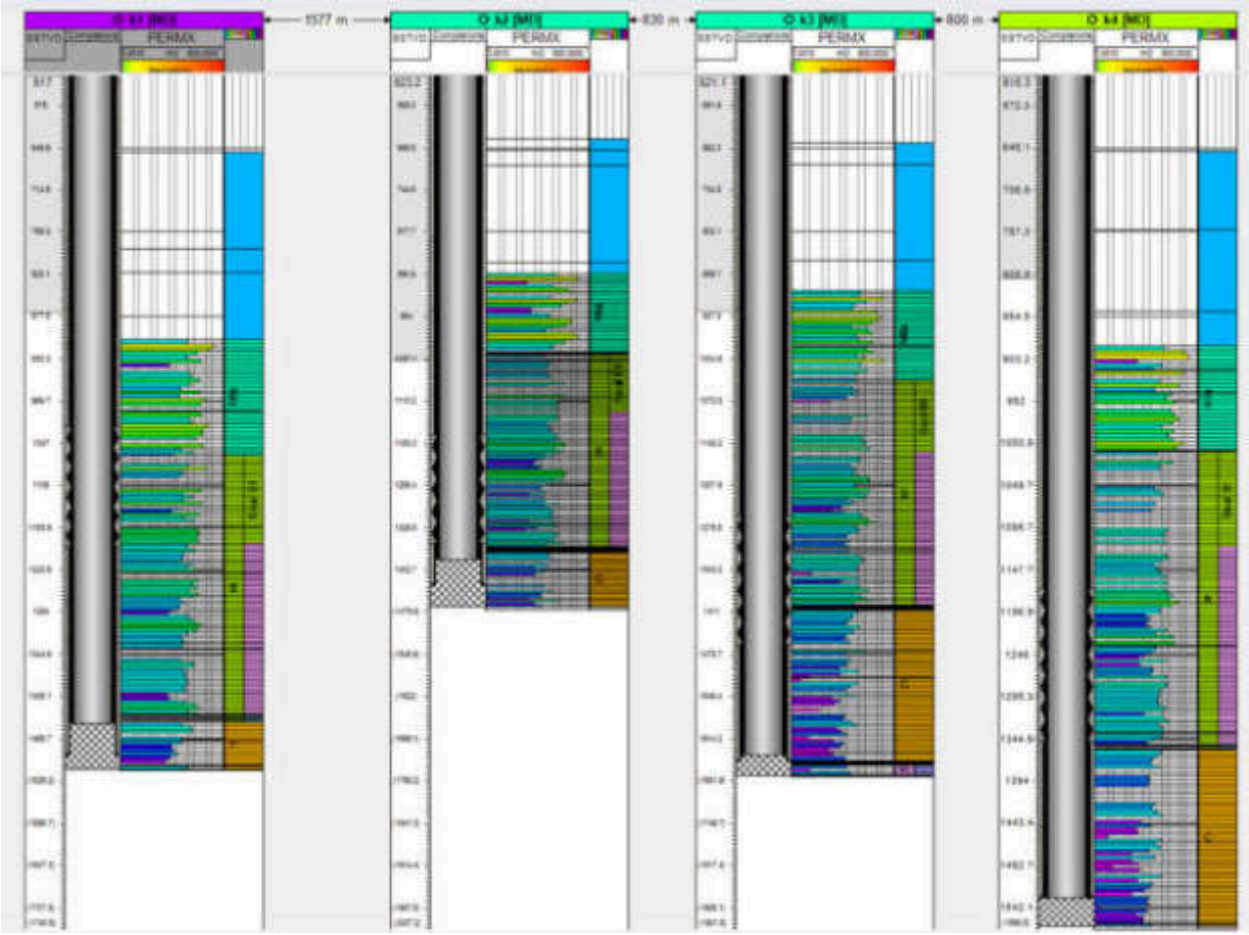


Fig. 2.194 Deviated wells Scenario perforated intervals for wells K1, K2, K3, K4 @Jan 2027

The total amount of CO_2 that can be injected for this Scenario is 19.13 million tonnes (Mt). The annual committed injection rate is 0.638 million tonnes per year (Mt/yr).

Wells location for Scenario 4 within the pre-selected sites and plume distribution at the end on injection (1 Jan 2057) are presented in Fig. 2.195.

Copyright © SLB. All Rights Reserved. Private & Confidential. Reproduction only by permission.

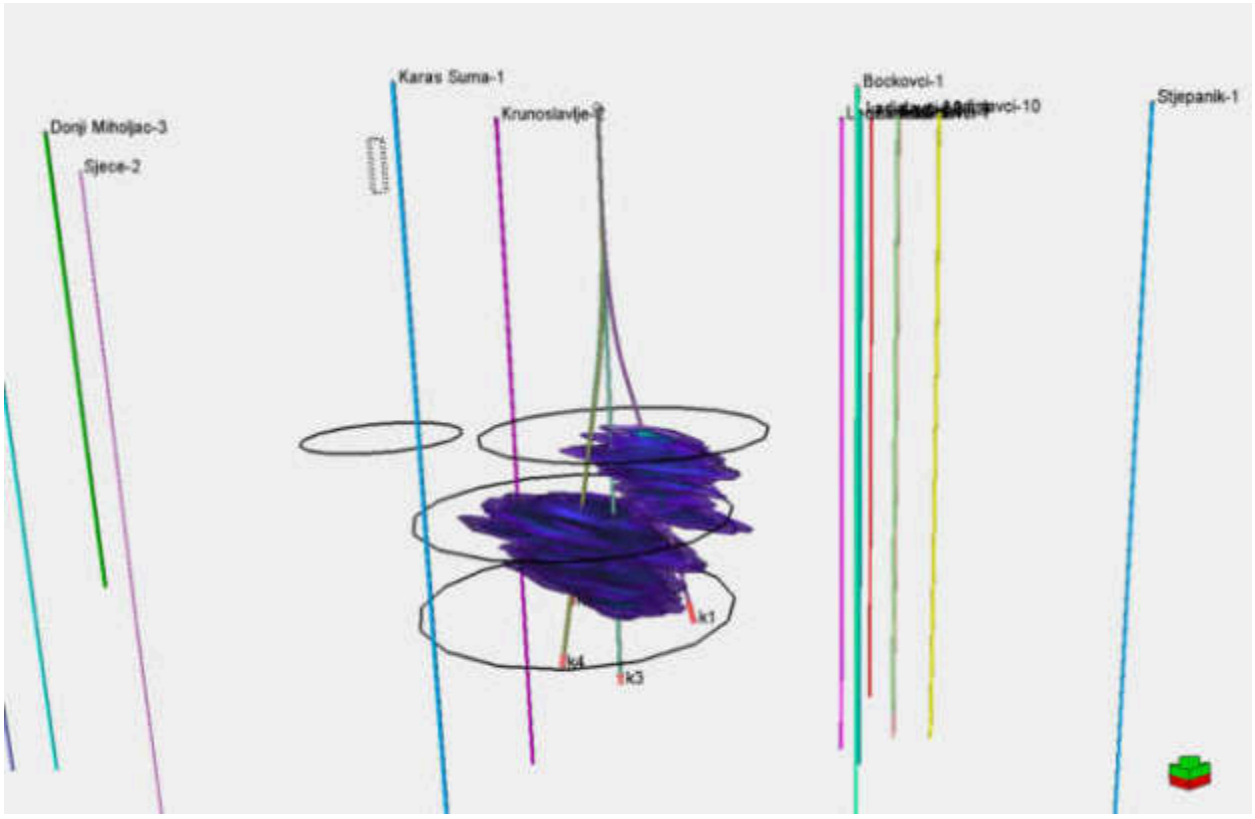


Fig. 2.195 Scenario with deviated well locations and CO_2 plume distribution at the end of injection @2057

Simulation plots of Field gas injection rate, Field cumulative gas injection and Field reservoir pressure for Scenarios 4 with deviated wells are presented in Fig. 2.196. The reported field reservoir pressure corresponds to the pore-volume-weighted average pressure of the entire reservoir system, combining contributions from all simulated zones (Alfa, B and C).

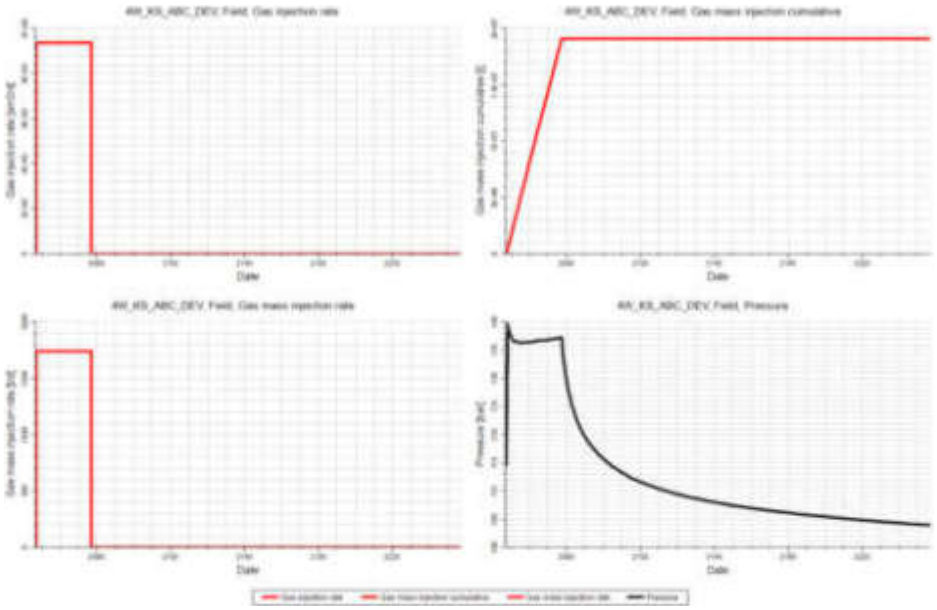


Fig. 2.196 Scenario 4 deviated wells simulation plots (gas injection rate, cumulative, reservoir pressure)

Copyright © SLB. All Rights Reserved. Private & Confidential. Reproduction only by permission.

Table 2.29 and Table 2.30 summarises sites performance for the deviated wells Scenario.

Injection is unevenly distributed among the wells due to reservoir heterogeneity. Wells K1 and K4 show higher injectivity, while K2 exhibits lower performance, reflecting local variations in permeability and connectivity. Bottom-hole pressure increases rapidly at early times and stabilizes near operational limits without exceeding fracture constraints. Well Injection and Bottom hole pressure profiles are presented in Fig. 2.197.

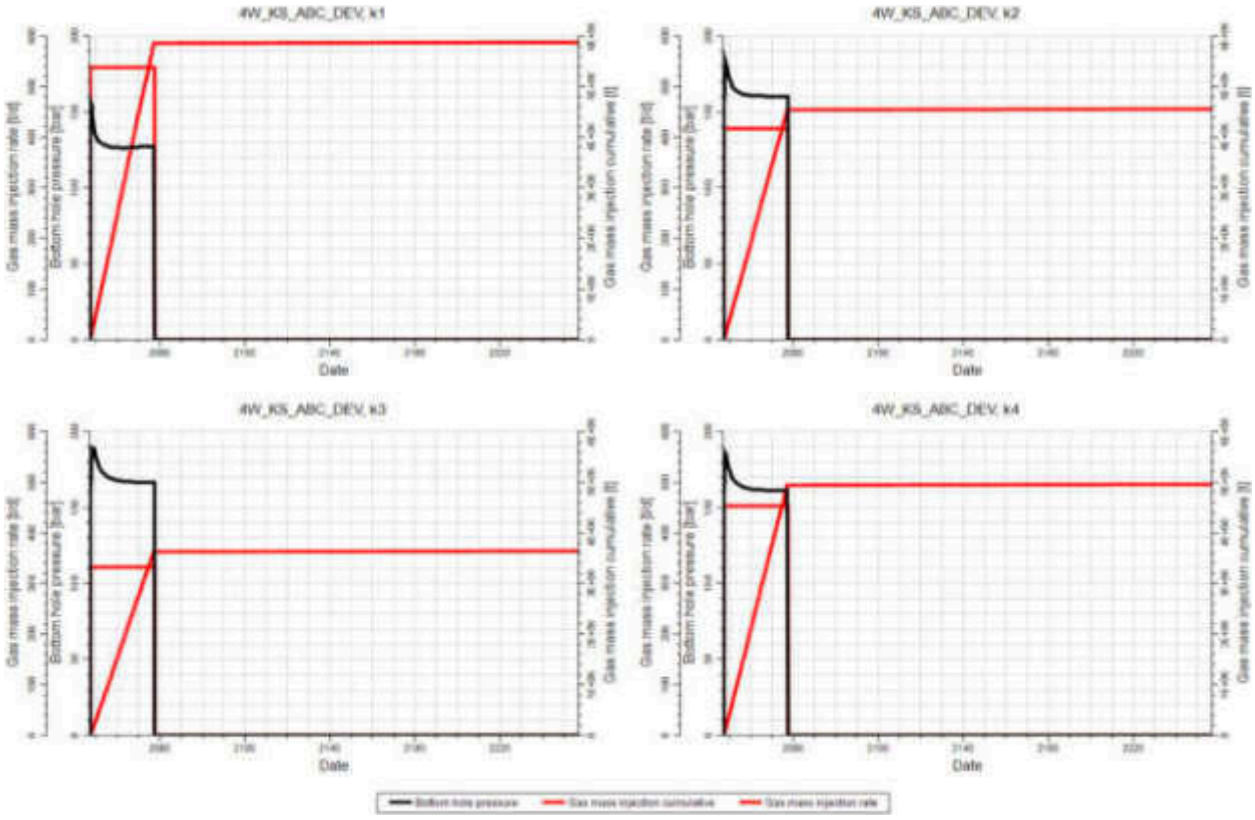


Fig. 2.197 Deviated wells Scenario simulation plots (gas injection rate, cumulative, reservoir pressure)

Table 2.29 Scenario 4 with deviated wells injection rate per year and cumulative injection per site

Scenario	CO_2 injection rate, Mt/year	CO_2 injection cum, Mt
Karas Suma 4 deviated wells	0.637	19.13

Table 2.30 Scenario 4 - deviated wells injection rate per year and cumulative injection per well

Site	CO_2 injection rate, Mt/year	CO_2 injection cum, Mt
K1	0.196	5.90
K2	0.153	4.58
K3	0.122	3.66
K4	0.166	4.99

The injected CO_2 is distributed across three reservoir zones (Alfa, B, and C), with distinct contributions in terms of storage capacity and trapping mechanisms Table 2.31. The table

Copyright © SLB. All Rights Reserved. Private & Confidential. Reproduction only by permission.

distinguishes between three physical storage mechanisms: aqueous (dissolved), immobile vapor (residually trapped gas), and mobile vapor (free gas phase), providing insight into the evolution of long-term trapping processes.

- Zone B represents the primary storage interval, containing the largest share of CO_2 with a total of 13.62 Mt. This zone also exhibits the highest amounts of both aqueous dissolved CO_2 and mobile vapor phase, indicating strong injectivity and significant plume mobility.
- Zone Alfa contributes a moderate storage capacity of 4.91 Mt, with a relatively balanced distribution between aqueous CO_2, immobile gas (residual trapping), and mobile gas. This suggests effective trapping mechanisms and stable plume behavior.
- Zone C has the lowest storage contribution at 0.6 Mt, reflecting more limited reservoir volume or connectivity. However, it still shows a meaningful proportion of both dissolved and trapped CO_2 phases.

Table 2.31 CO_2 storage distribution per zone for Scenario 4 with deviated wells @ year 2257

Zone	Aqueous component mass kg	Immobile vapor component mass kg	Mobile vapor component mass kg	Total component mass Mt
Alfa	2665187840	1168582784	1073721152	4.91
B	5396722688	3020270592	5211303424	13.62
C	237836016	133177336	226470512	0.60

The overall CO_2 dissolution across all reservoir zones indicates that a substantial portion of the injected CO_2 is stored in the aqueous phase after 200 years post injection. In total, approximately 8.30 Mt of CO_2 is dissolved in formation water out of about 19.13 Mt stored @ Jan 2257, corresponding to roughly 43% of the total stored mass. This relatively high dissolution fraction reflects favorable reservoir conditions, including effective contact between CO_2 and brine and sufficient residence time to allow mass transfer processes to occur. The strong contribution from solubility trapping enhances the long-term security of storage, as dissolved CO_2 is less mobile and less likely to migrate compared to the free gas phase. Over time, this fraction is expected to increase further as the injected CO_2 continues to interact with formation fluids, progressively shifting the storage balance toward more stable and secure trapping mechanisms.

Since no significant leakage pathways were identified within the current model. However, uncertainties remain regarding the structural dip angle toward the Donji Miholjac area, which may influence CO_2 plume migration patterns and lateral extent.

The model provides operational guidance on optimal well count, spatial placement, and injection rate management under pressure constraints. Recommended monitoring strategies include continuous reservoir pressure surveillance, tracer-based plume tracking, and periodic well integrity testing, particularly in zones identified as having elevated risk.

In the event of unexpected pressure anomalies or unpredicted plume behavior, a phased contingency plan is proposed, including progressive injection rate adjustments and, if necessary, temporary well shut-in to re-establish safe operating conditions.

Copyright © SLB. All Rights Reserved. Private & Confidential. Reproduction only by permission.

In conclusion, among the scenarios evaluated, Scenario 4, implemented using deviated wells, was identified as the most balanced and practical development option that can store 19.13 Mt of CO_2 in the same injection period duration of 30 years. While multi-site configurations may provide marginal increases in storage capacity, they also introduce additional complexity in terms of infrastructure requirements and monitoring challenges. In contrast, Scenario 4 adopts a single-site development concept, which enables more predictable reservoir performance, enhanced surveillance capabilities, and reduced operational risks.

In all simulation scenarios site close to wells Karas Suma-1 and Bockovci seems to be the most efficient from stored volumes perspective and enabling more predictable reservoir behavior, improved surveillance, and reduced operational risk.

2.8.5.2 Pressure validation and distribution

Simulation results validate that the reservoir pressure response throughout the CO_2 injection period remained within safe operational thresholds and below fracture pressures for all simulated scenarios. Observed pressure build-up was consistent with pre-estimated fracture gradient predictions, as shown in Fig. 2.166, indicating reliable model calibration and no significant discrepancies between simulated values. The pressure distribution maps confirm a predictable radial pressure dissipation from the injection wells across the storage formation. Pressure validation and detailed distribution description was done for Scenarios 2 and 3as they are characterised with highest injected volumes that lead to highest maximum injection BHP.

Scenario 2 - 4 wells 3 sites (constant injection, no formation switch).
Pressure profiles at well level and comparison with estimated fracture gradient and 90% of it are presented for the following time steps for Scenario 2:

- Initial time step in Fig. 2.198;
- 1 year after start of injection @Jan 2028 in Fig. 2.199;
- 3 years after start of injection @Jan 2030 in Fig. 2.200;
- 13 years after start of injection @Jan 2040 in Fig. 2.201;
- End of injection period @Jan 2057 in Fig. 2.202;
- End of simulation monitoring period @Jan 2257 in Fig. 2.203.

Copyright © SLB. All Rights Reserved. Private & Confidential. Reproduction only by permission.

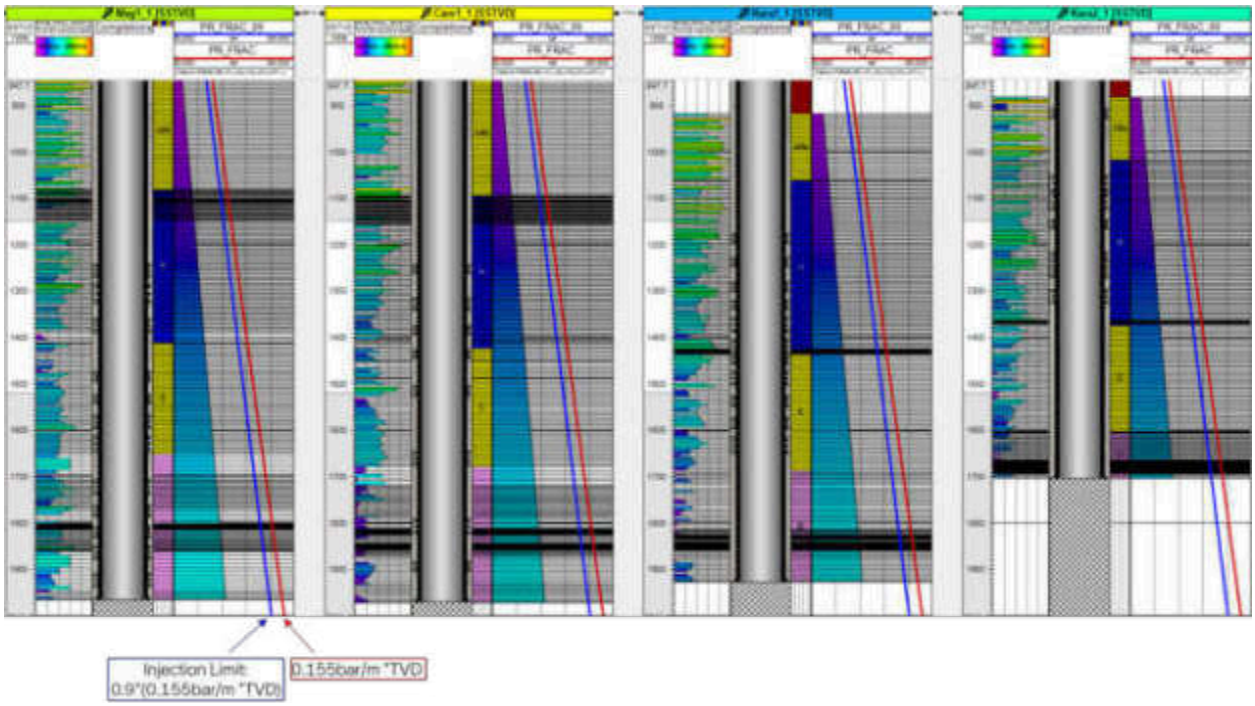


Fig. 2.198 Initial pressure profile vs fracture gradient in wells Kara1, Kara2, Mag1, Cam1

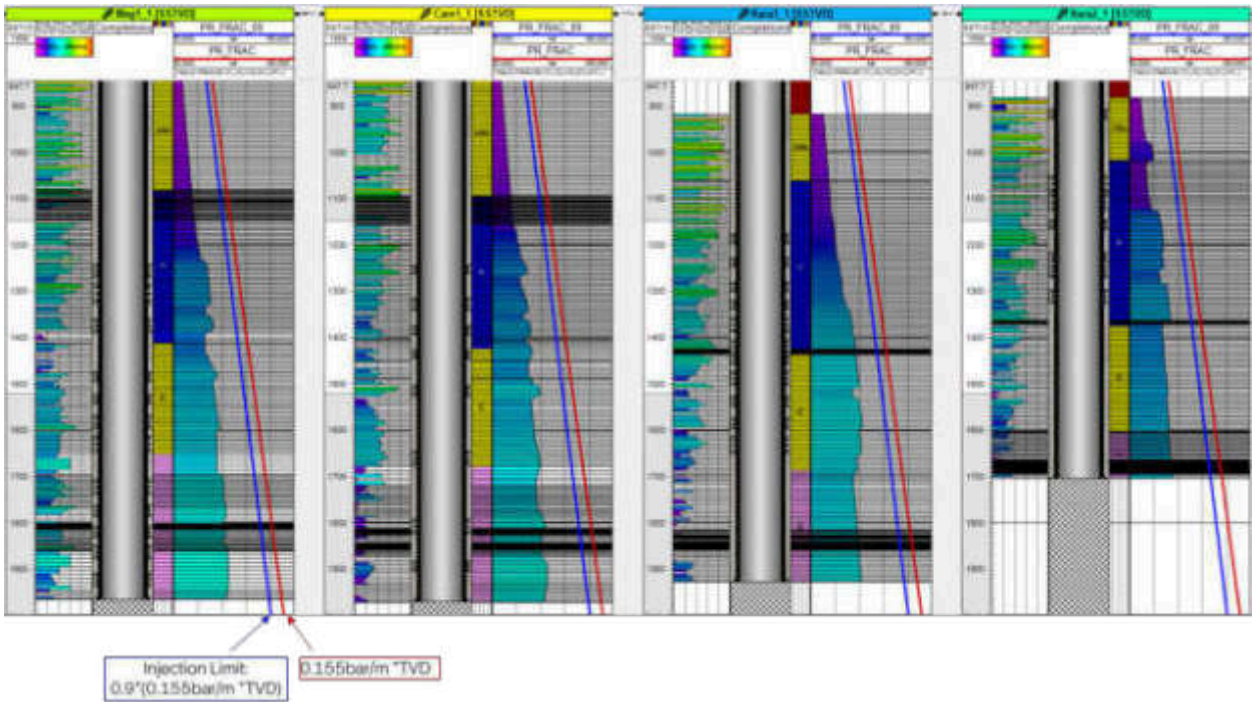


Fig. 2.199 Pressure profile vs fracture gradient in wells Kara1, Kara2, Mag, Cam1 @Jan 2028

Copyright © SLB. All Rights Reserved. Private & Confidential. Reproduction only by permission.

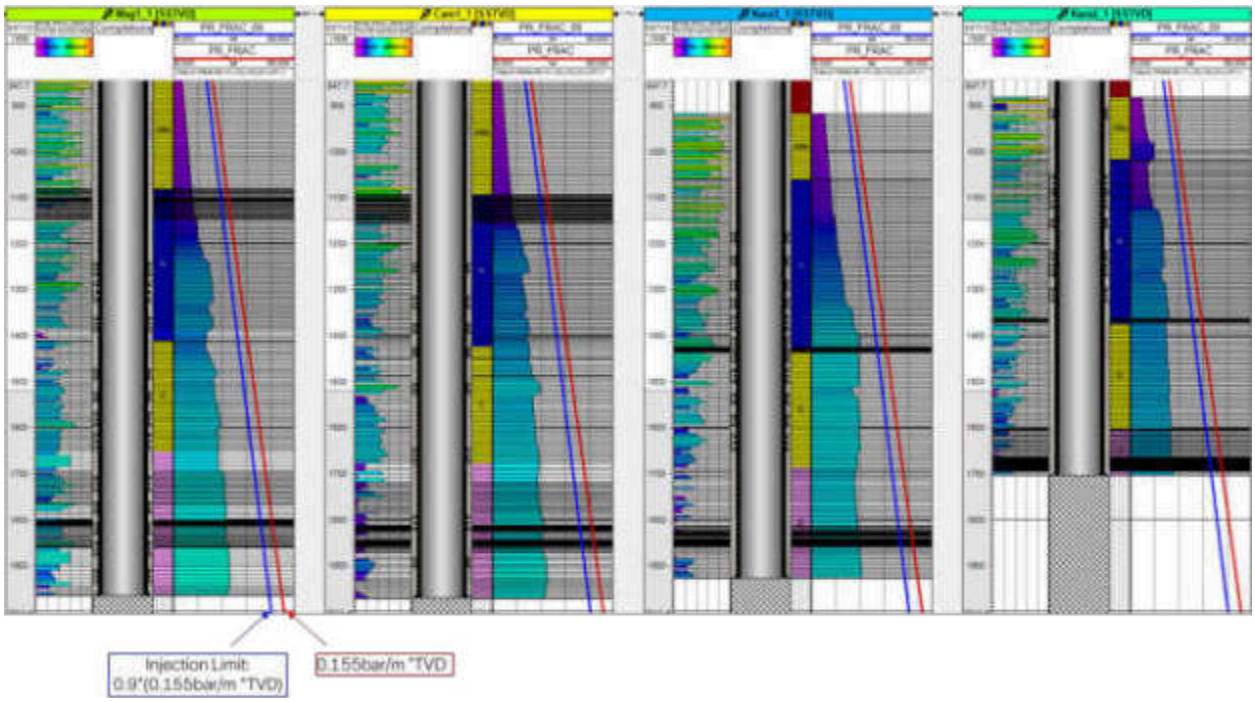


Fig. 2.200 Pressure profile vs fracture gradient in wells Kara1, Kara2, Mag, Cam1 @Jan 2030

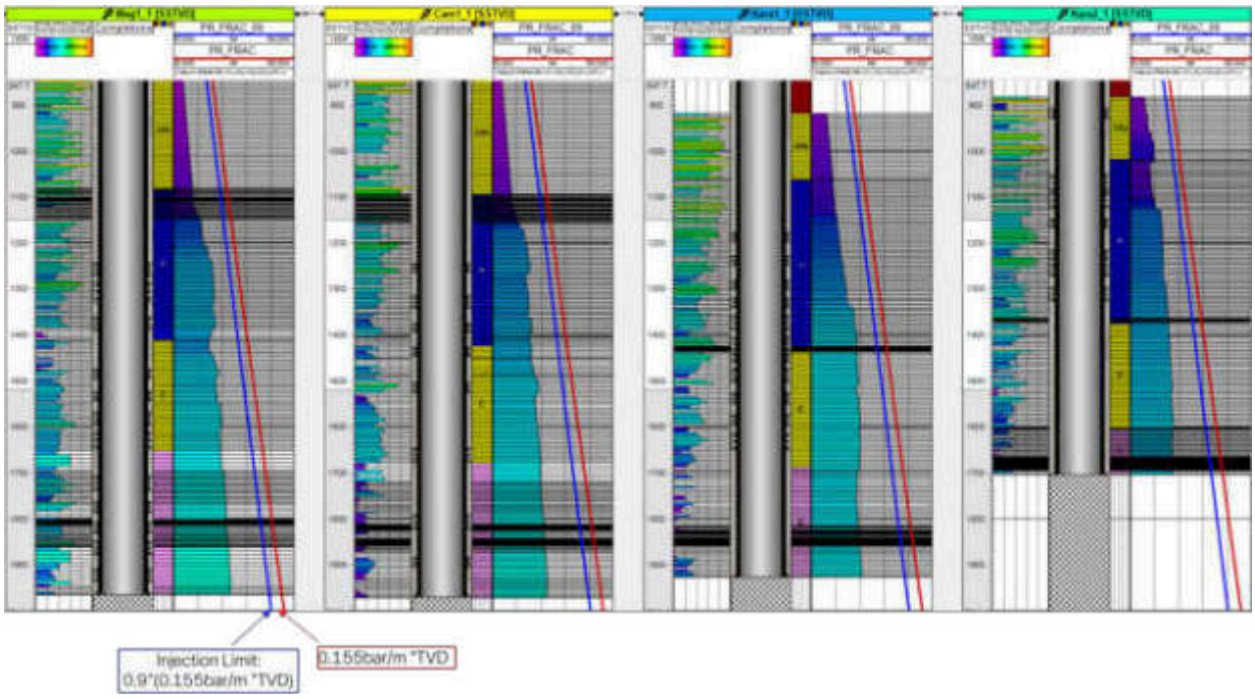


Fig. 2.201 Pressure profile vs fracture gradient in wells Kara1, Kara2, Mag, Cam1 @Jan 2040

Copyright © SLB. All Rights Reserved. Private & Confidential. Reproduction only by permission.

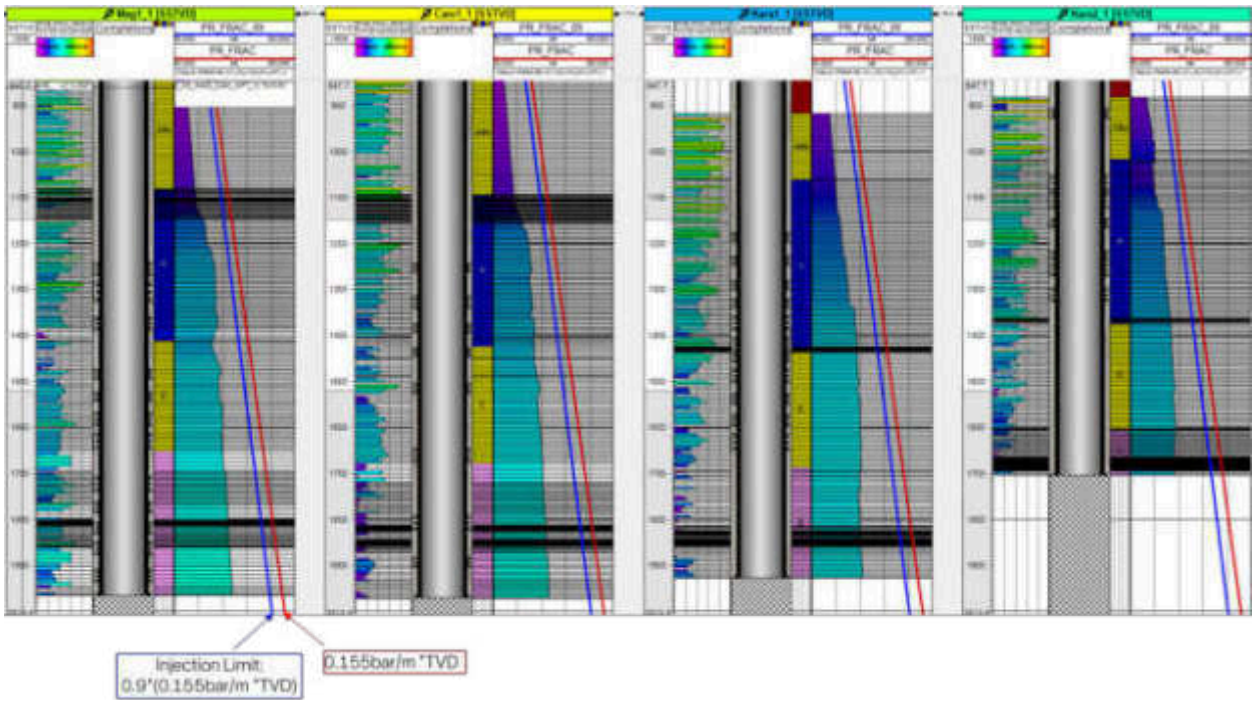


Fig. 2.202 Pressure profile vs fracture gradient in wells Kara1, Kara2, Mag, Cam1 @Jan 2057

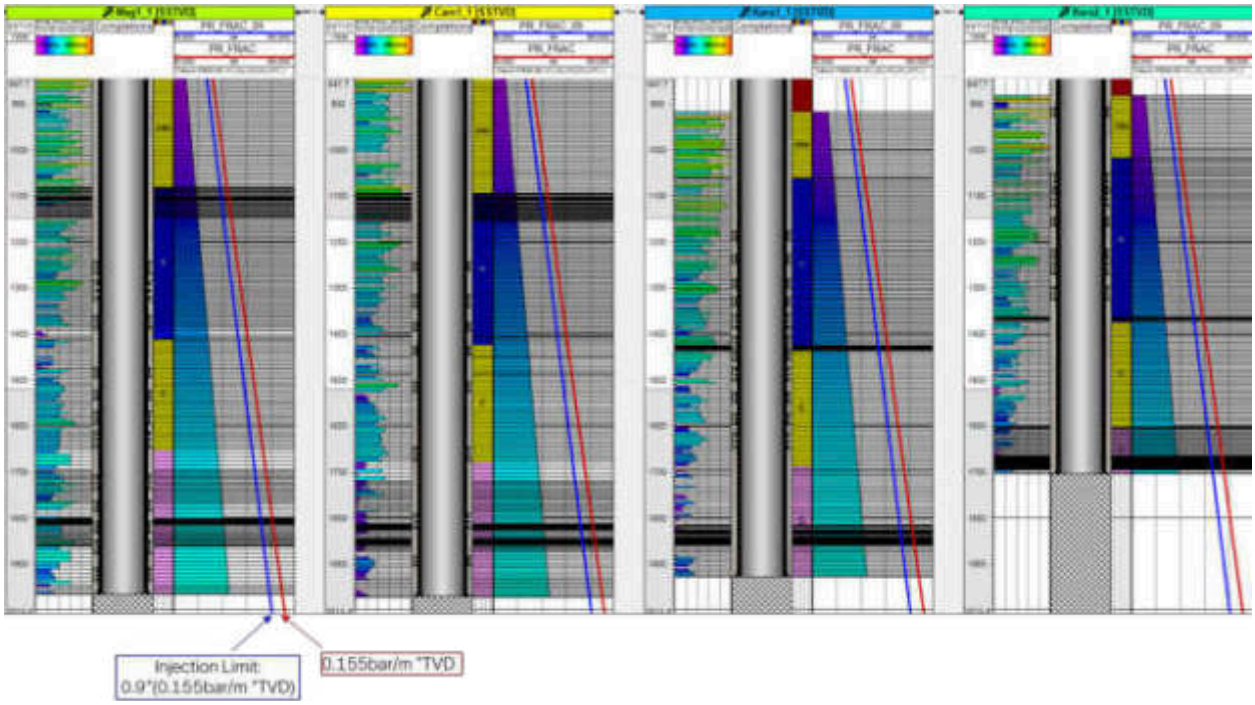


Fig. 2.203 Pressure profile vs fracture gradient in wells Kara1, Kara2, Mag, Cam1 @Jan 2257

Pressure difference between different time steps and initial reservoir pressure on the cross-section, passing through selected sites for optimization are presented in Fig. 2.204, Fig. 2.205. Fig. 2.206, Fig. 2.207, Fig. 2.208 and Fig. 2.209 below.

Copyright © SLB. All Rights Reserved. Private & Confidential. Reproduction only by permission.

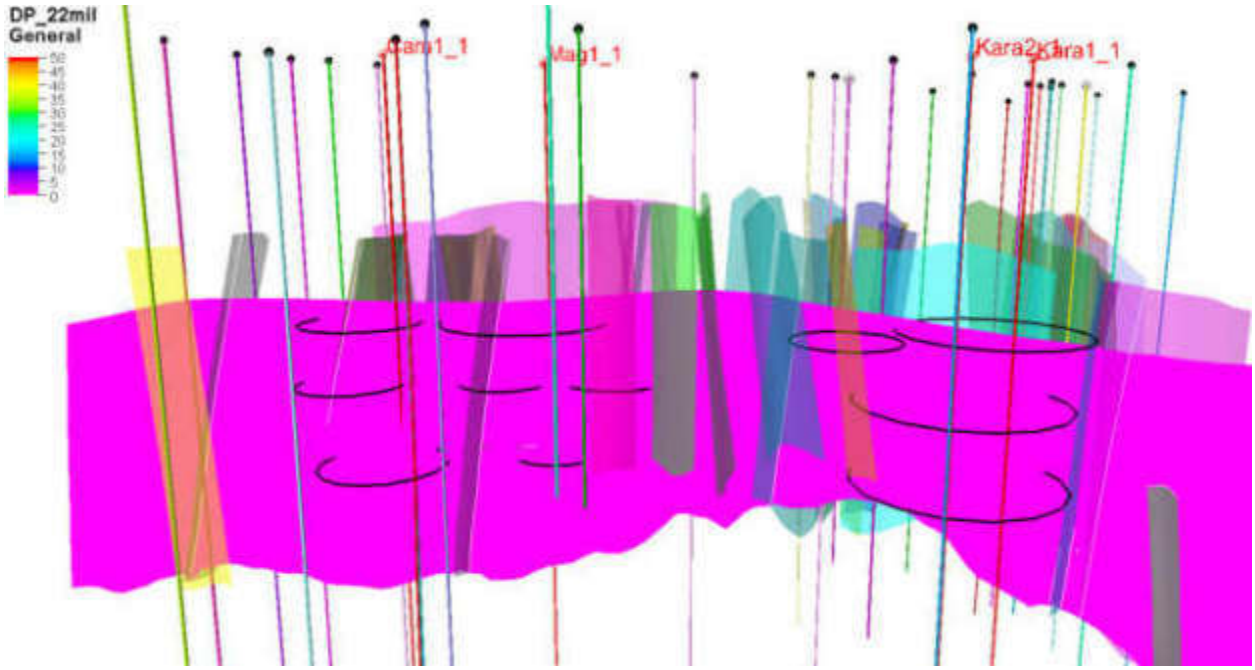


Fig. 2.204 Pressure difference profile with initial reservoir pressure for the cross-section in Scenario 2

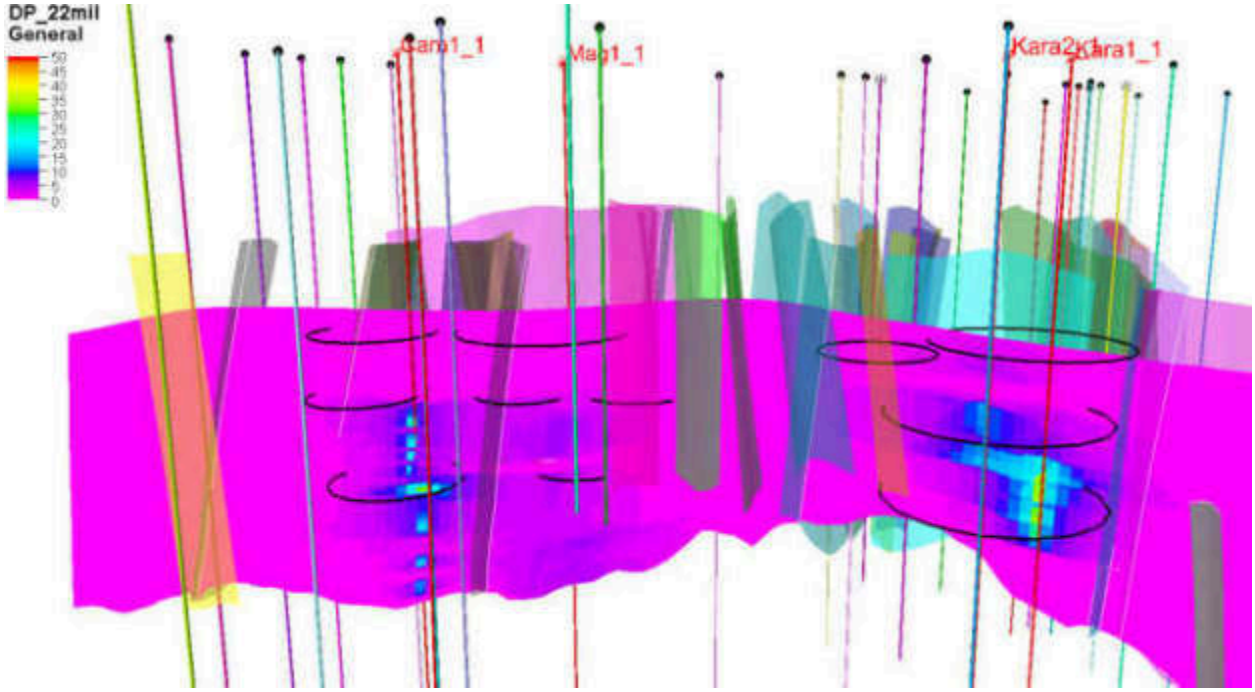


Fig. 2.205 Pressure difference profile with initial reservoir pressure for the cross-section in Scenario 2 @Jan 2028

Copyright © SLB. All Rights Reserved. Private & Confidential. Reproduction only by permission.

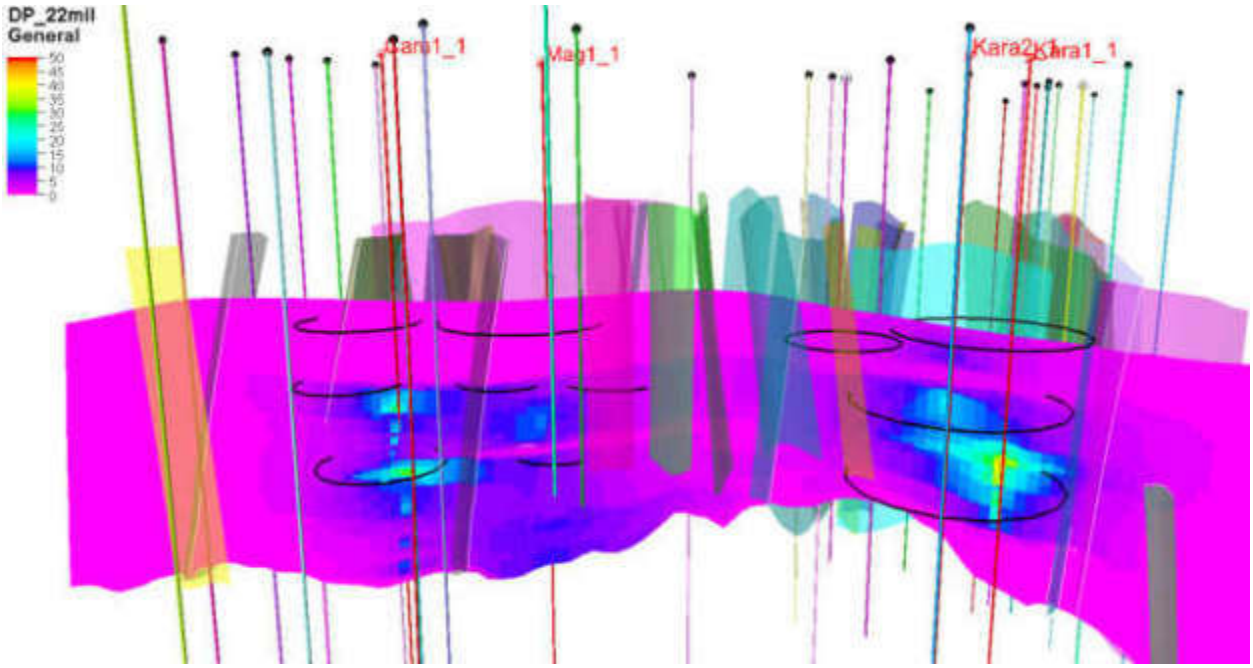


Fig. 2.206 Pressure difference profile with initial reservoir pressure for the cross-section in Scenario 2 @Jan 2030

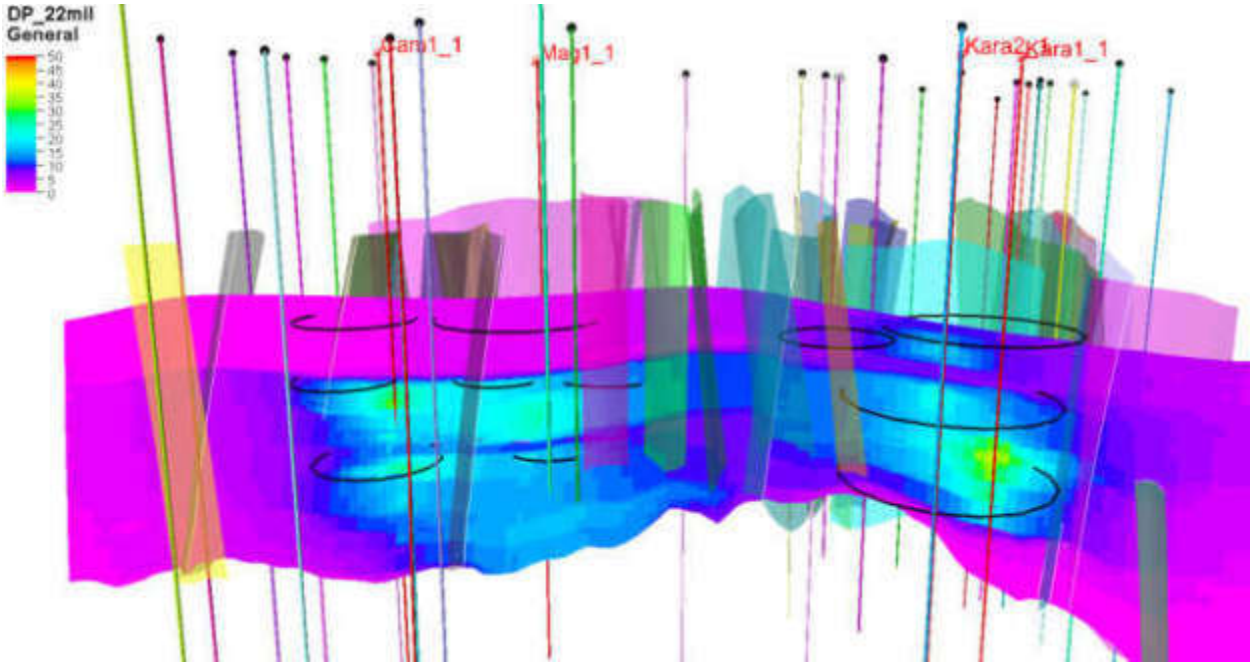


Fig. 2.207 Pressure difference profile with initial reservoir pressure for the cross-section in Scenario 2 @Jan 2040

Copyright © SLB. All Rights Reserved. Private & Confidential. Reproduction only by permission.

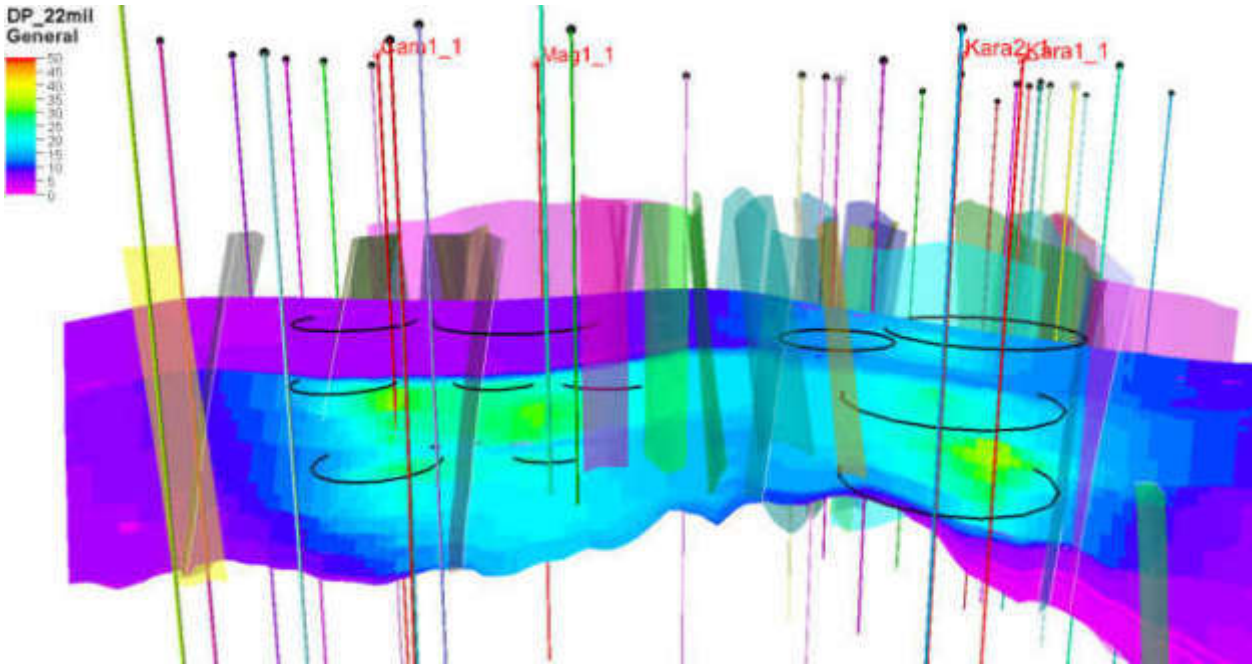


Fig. 2.208 Pressure difference profile with initial reservoir pressure for the cross-section in Scenario 2 @Jan 2057

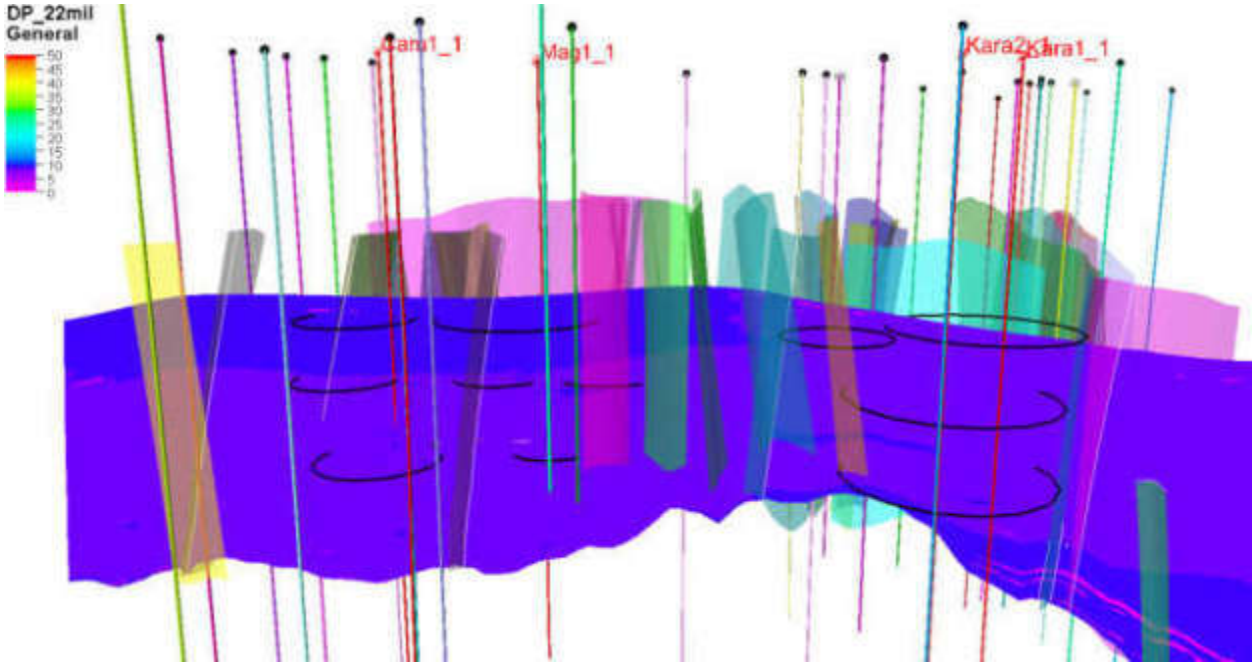


Fig. 2.209 Pressure difference profile with initial reservoir pressure for the cross-section in Scenario 2 @Jan 2257

Scenario 4- 4 vertical wells in Karas Suma-1 area

Pressure profiles at well level and comparison with estimated fracture gradient and 90% of it are presented for the following time steps for Scenario 3:

- Initial time step in Fig. 2.210;
- 1 year after start of injection @Jan 2028 in Fig. 2.211 ;
- 3 years after start of injection @Jan 2030 in Fig. 2.212;

Copyright © SLB. All Rights Reserved. Private & Confidential. Reproduction only by permission.

- 13 years after start of injection @Jan 2040 in Fig. 2.213;
- End of injection period @Jan 2057 in Fig. 2.214;
- End of simulation monitoring period @Jan 2257 in Fig. 2.215.

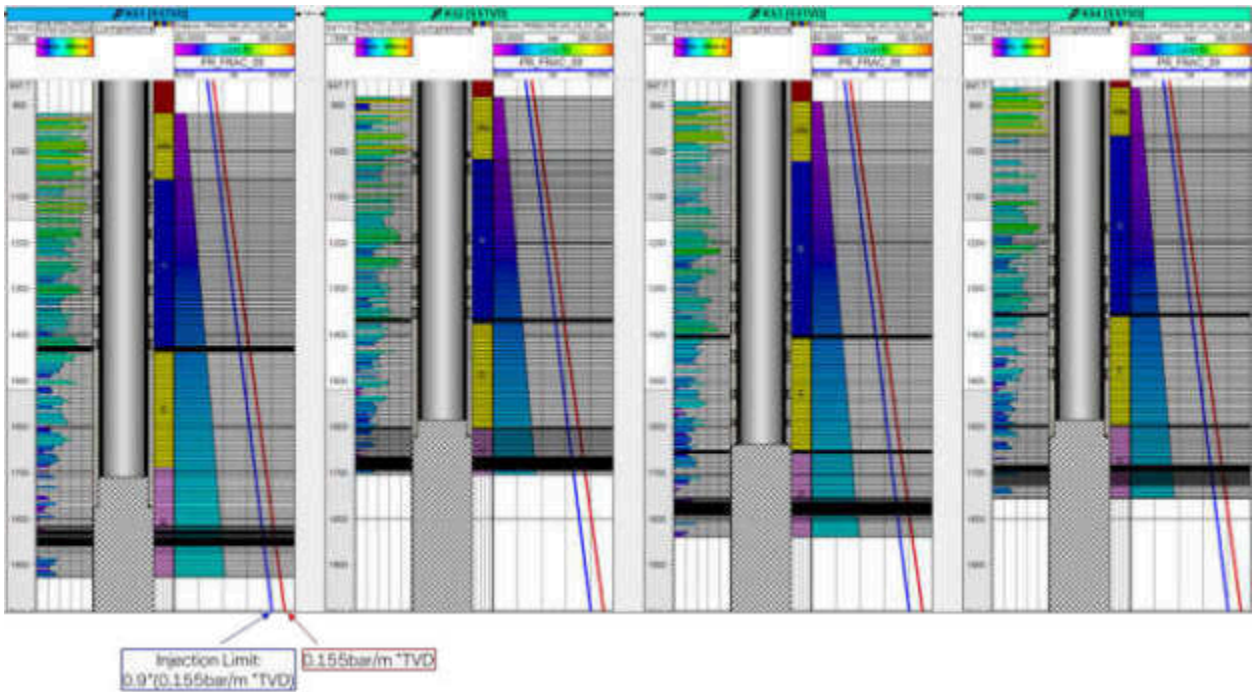


Fig. 2.210 Initial pressure profile vs fracture gradient in wells KS1, KS2, KS3, KS4

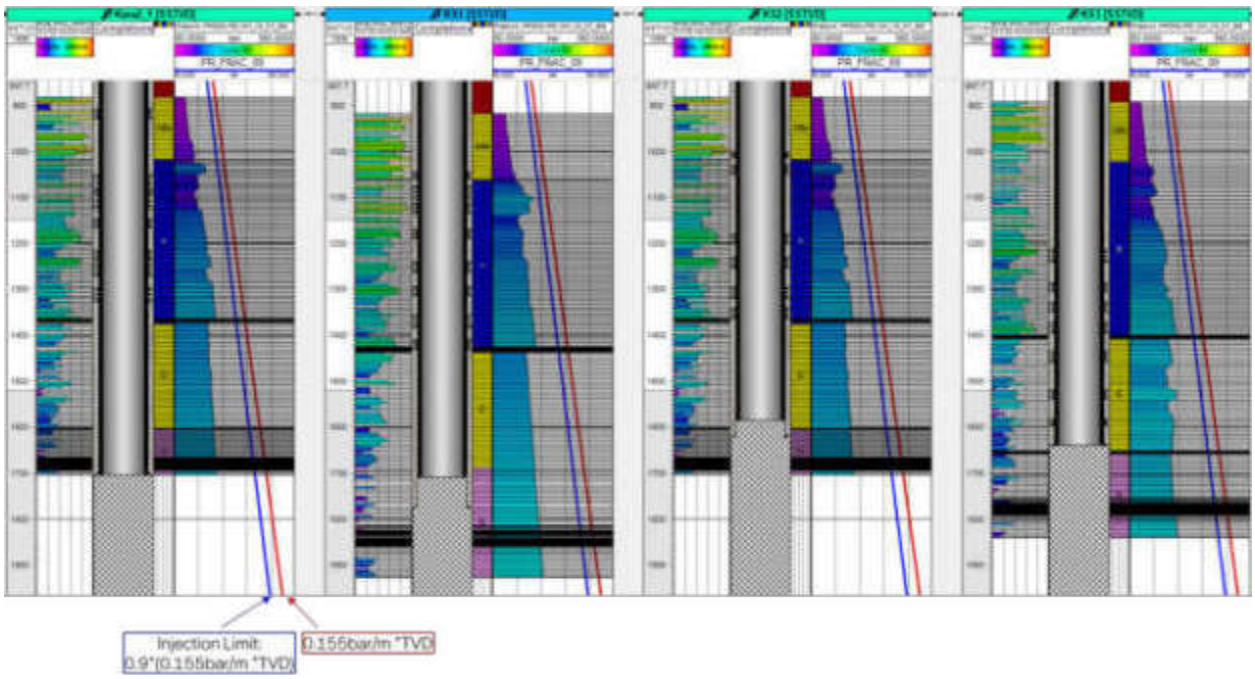


Fig. 2.211 Pressure profile vs fracture gradient in wells KS1, KS2, KS3, KS4 @Jan 2028

Copyright © SLB. All Rights Reserved. Private & Confidential. Reproduction only by permission.

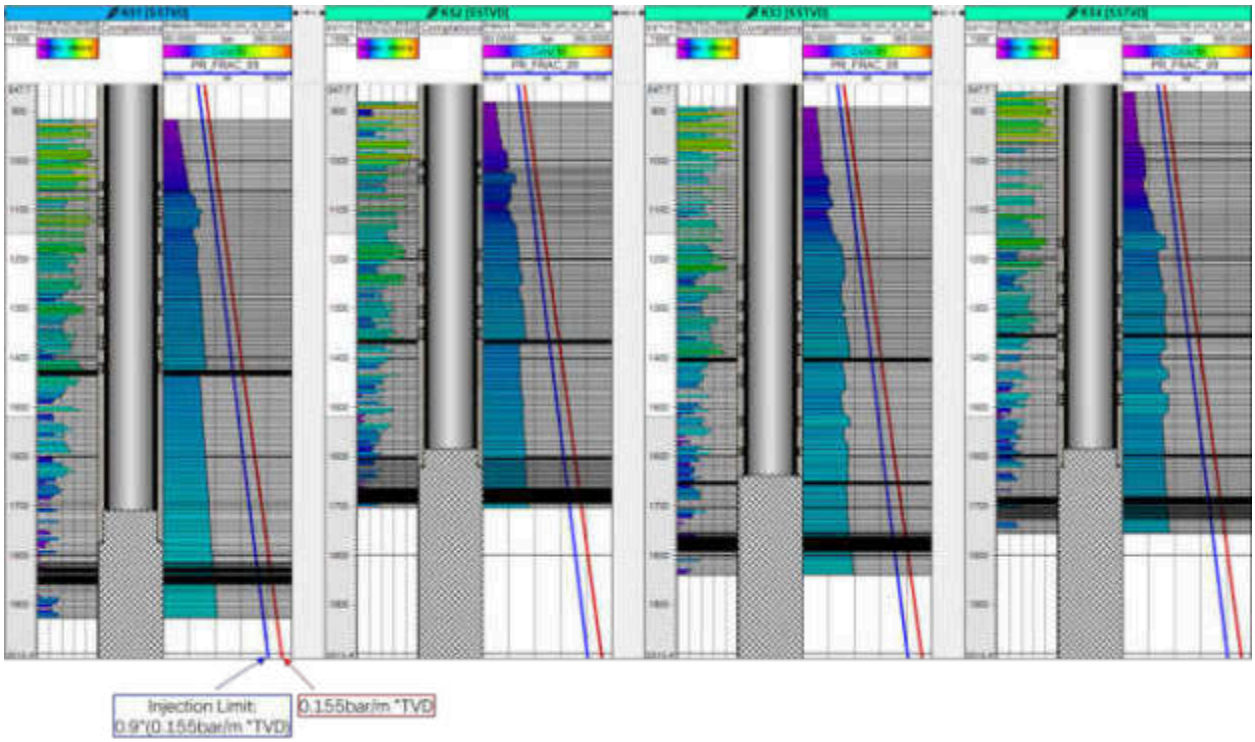


Fig. 2.212 Pressure profile vs fracture gradient in wells KS1, KS2, KS3, KS4 @Jan 2030

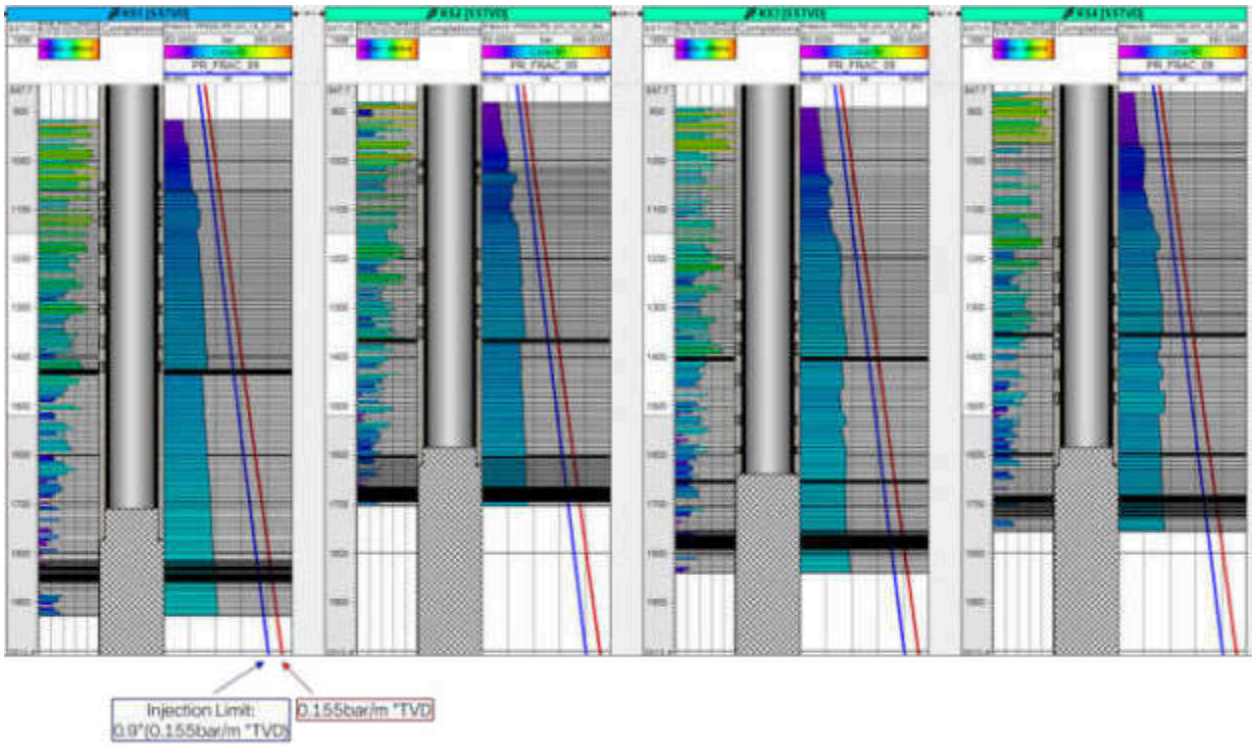


Fig. 2.213 Pressure profile vs fracture gradient in wells KS1, KS2, KS3, KS4 @Jan 2040

Copyright © SLB. All Rights Reserved. Private & Confidential. Reproduction only by permission.

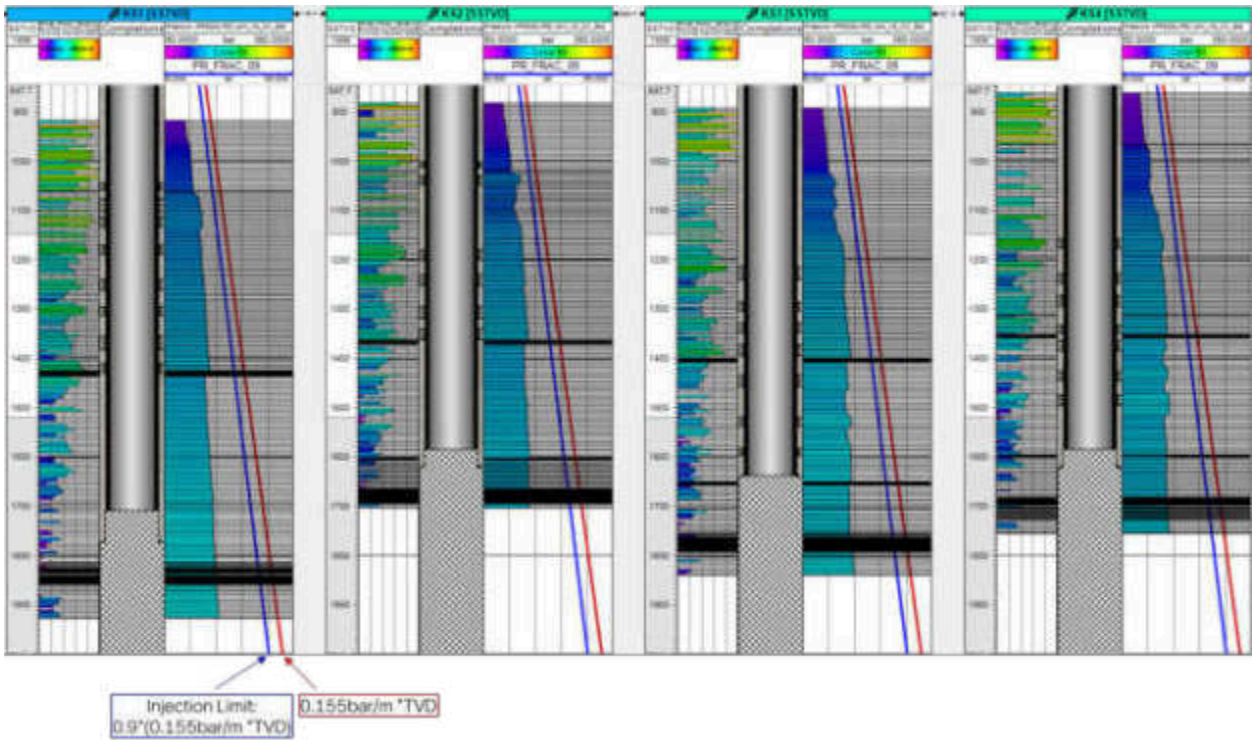


Fig. 2.214 Pressure profile vs fracture gradient in wells KS1, KS2, KS3, KS4 @Jan 2057

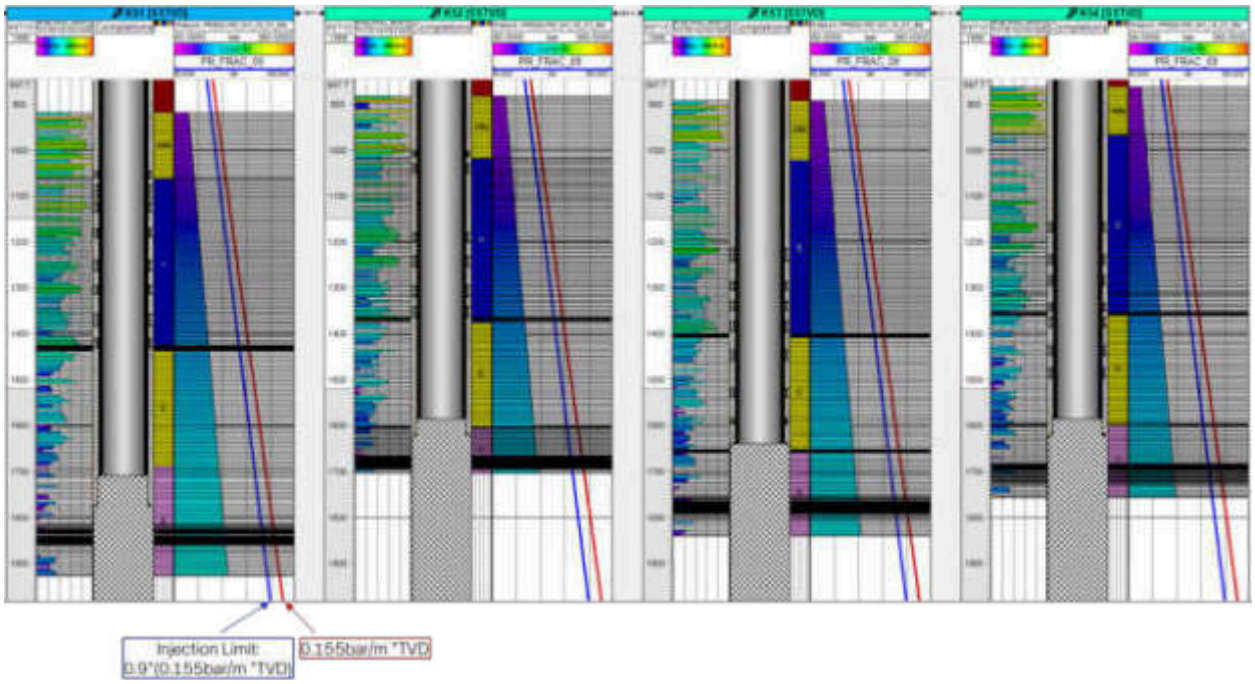


Fig. 2.215 Pressure profile vs fracture gradient in wells KS1, KS2, KS3, KS4 @Jan 2257

Pressure difference between different time steps and initial reservoir pressure on the cross-section, passing through selected sites for optimization are presented in Fig. 2.216, Fig. 2.217, Fig. 2.218, Fig. 2.219, Fig. 2.220 and Fig. 2.221

Copyright © SLB. All Rights Reserved. Private & Confidential. Reproduction only by permission.

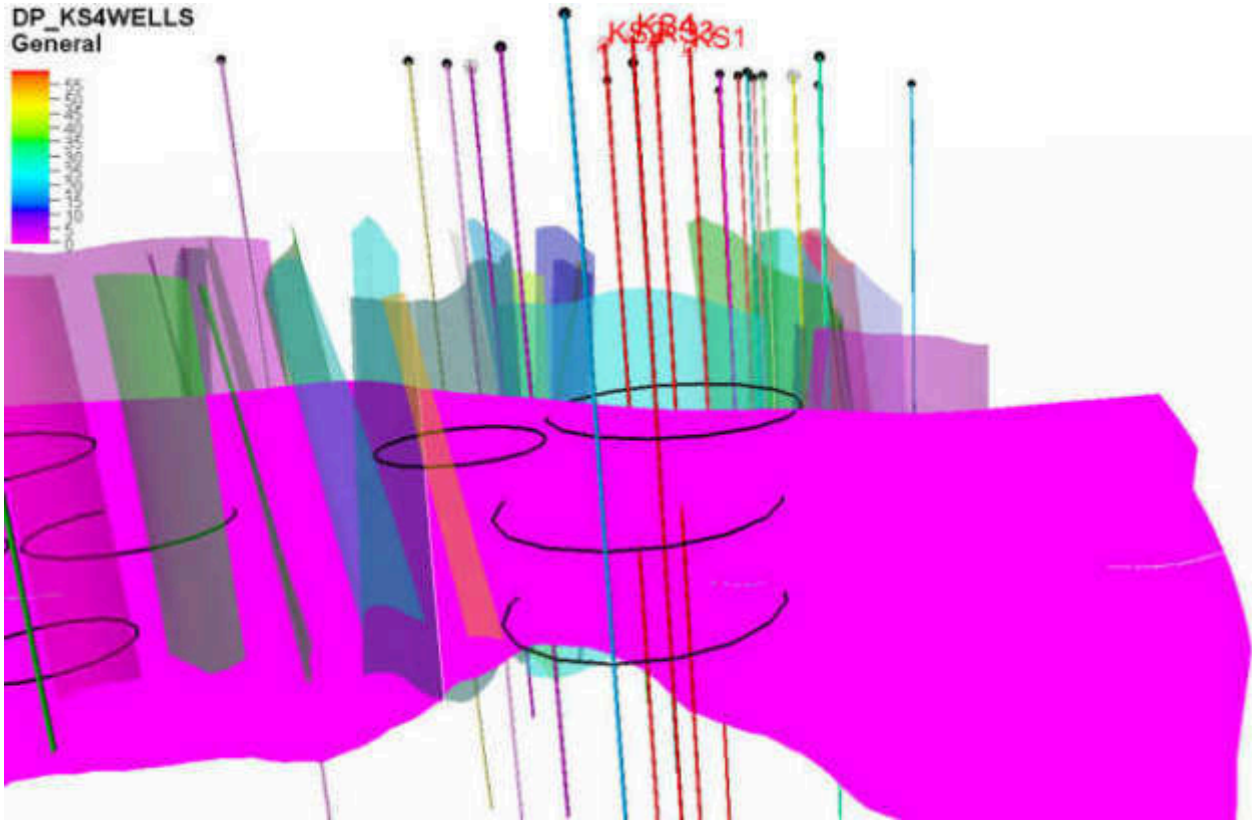


Fig. 2.216 Pressure difference profile with initial reservoir pressure for the cross-section in Scenario 4

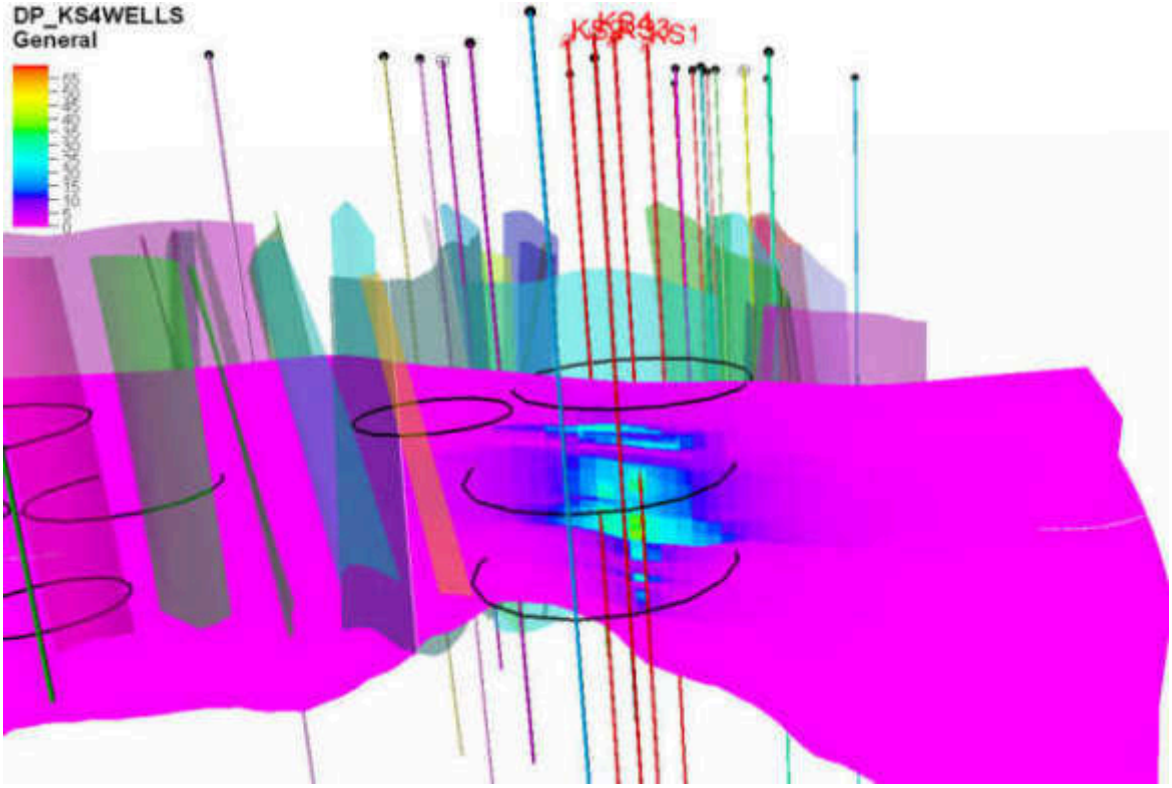


Fig. 2.217 Pressure difference profile with initial reservoir pressure for the cross-section in Scenario 4 @Jan 2028

Copyright © SLB. All Rights Reserved. Private & Confidential. Reproduction only by permission.

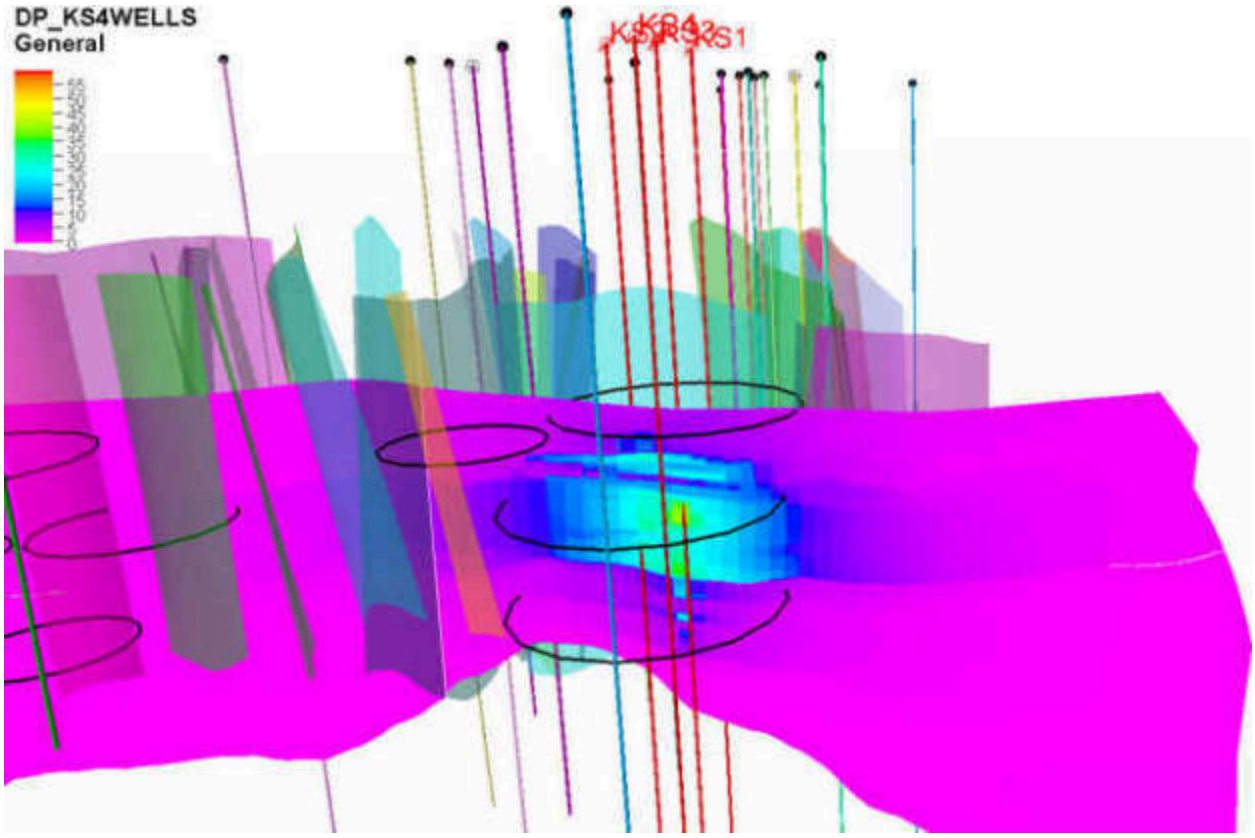


Fig. 2.218 Pressure difference profile with initial reservoir pressure for the cross-section in Scenario 4 @Jan 2030

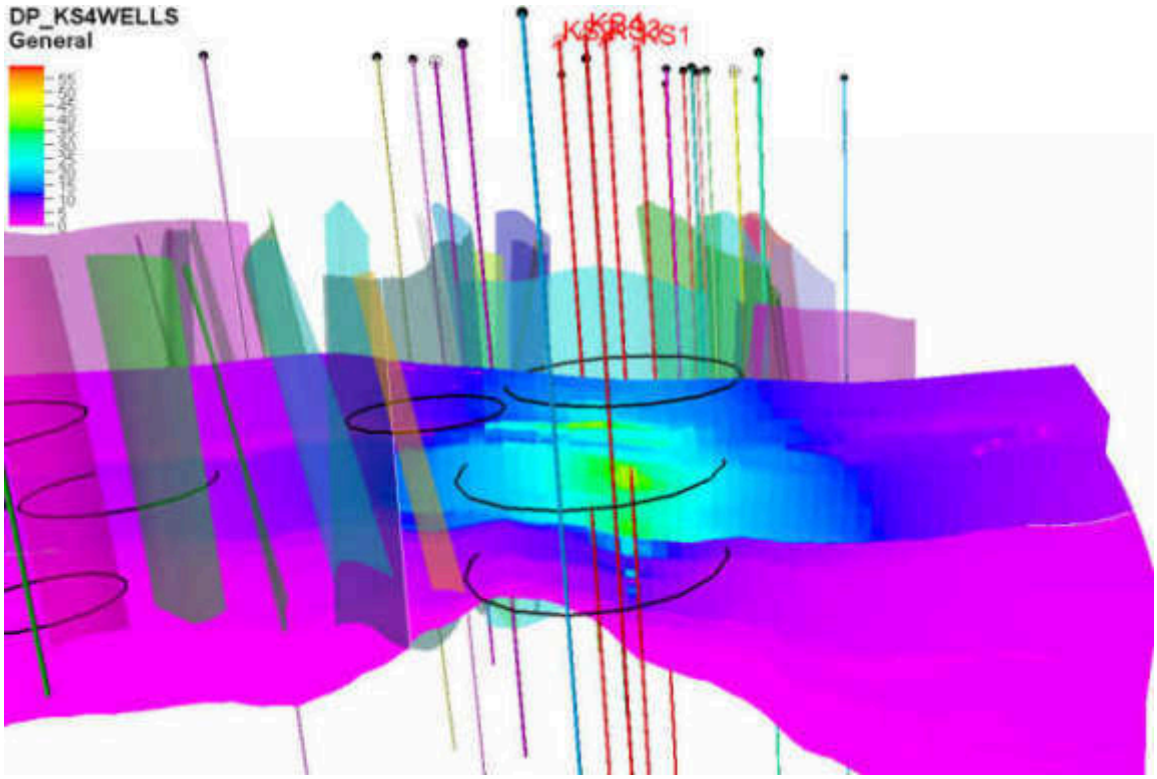


Fig. 2.219 Pressure difference profile with initial reservoir pressure for the cross-section in Scenario 4 @Jan 2040

Copyright © SLB. All Rights Reserved. Private & Confidential. Reproduction only by permission.

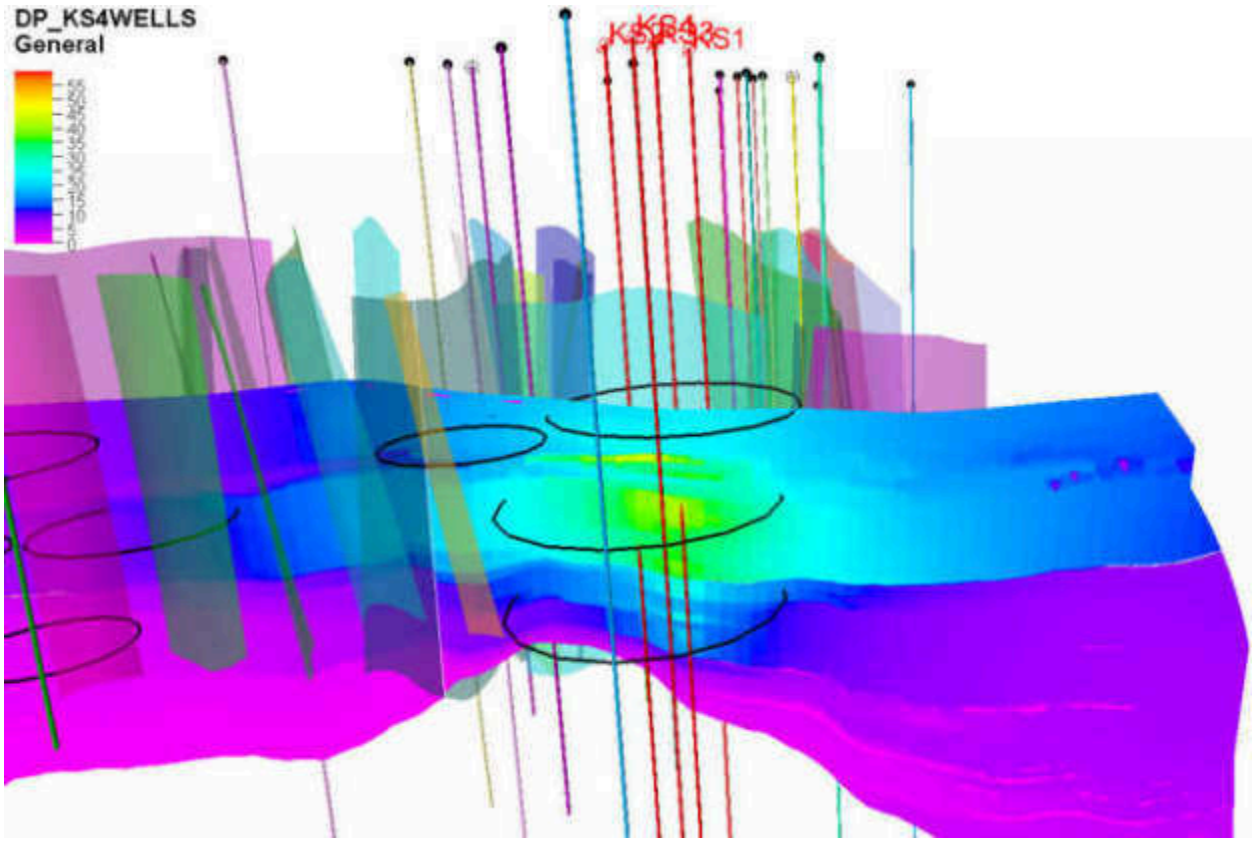


Fig. 2.220 Pressure difference profile with initial reservoir pressure for the cross-section in Scenario 4 @Jan 2057

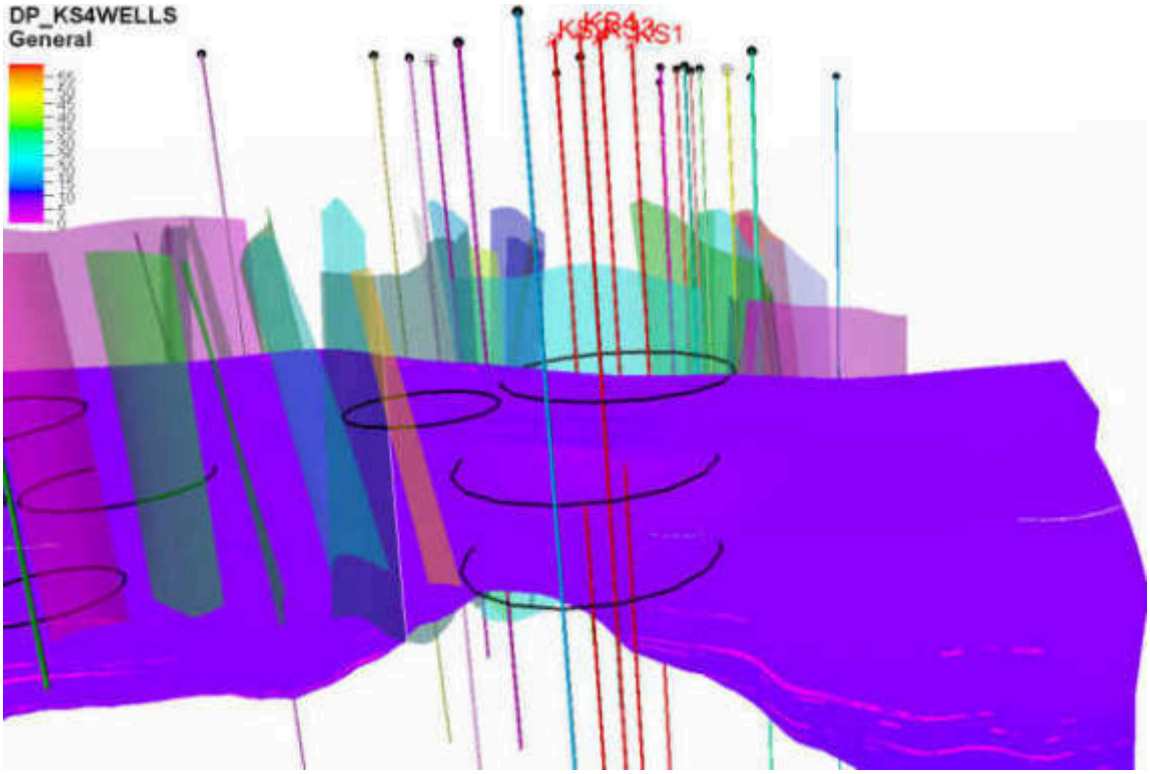


Fig. 2.221 Pressure difference profile with initial reservoir pressure for the cross-section in Scenario 4 @Jan 2257

Copyright © SLB. All Rights Reserved. Private & Confidential. Reproduction only by permission.

Scenario 4 - 4 deviated wells in Karas Suma-1 area

Pressure profiles at well level and comparison with estimated fracture gradient and 90% of it are presented for the following time steps for Scenario 3:

- Initial time step in Fig. 2.222
- 1 year after start of injection @Jan 2028 in Fig. 2.223
- 3 years after start of injection @Jan 2030 in Fig. 2.224
- 13 years after start of injection @Jan 2040 in Fig. 2.225
- End of injection period @Jan 2057 in Fig. 2.226
- End of simulation monitoring period @Jan 2257 in Fig. 2.227

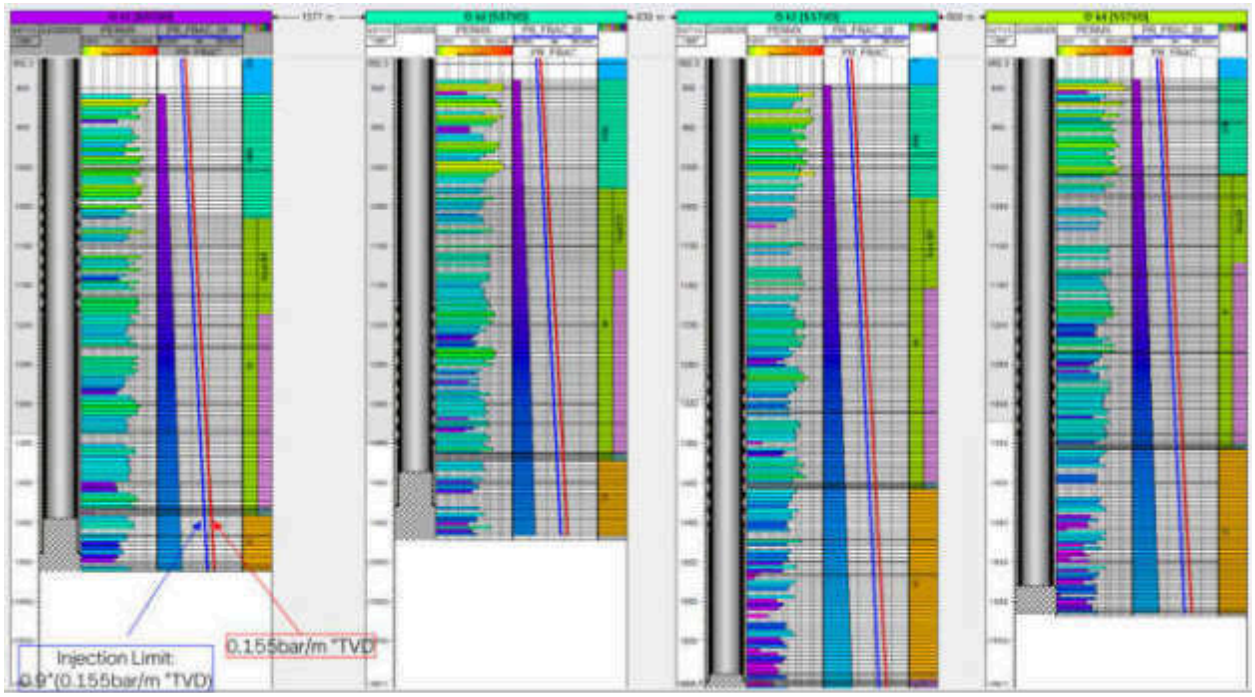


Fig. 2.222 Initial pressure profile vs fracture gradient in deviated wells K1, K2, K3, K4

Copyright © SLB. All Rights Reserved. Private & Confidential. Reproduction only by permission.

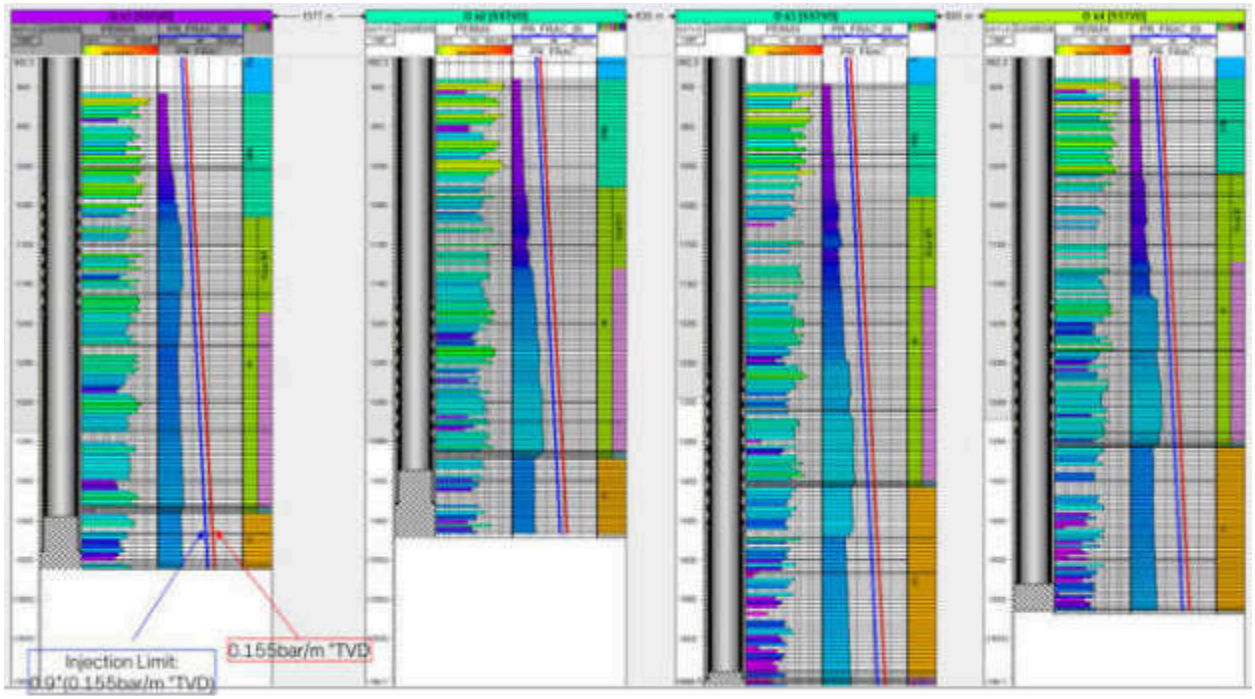


Fig. 2.223 Pressure profile vs fracture gradient in deviated wells K1, K2, K3, K4 @Jan 2028

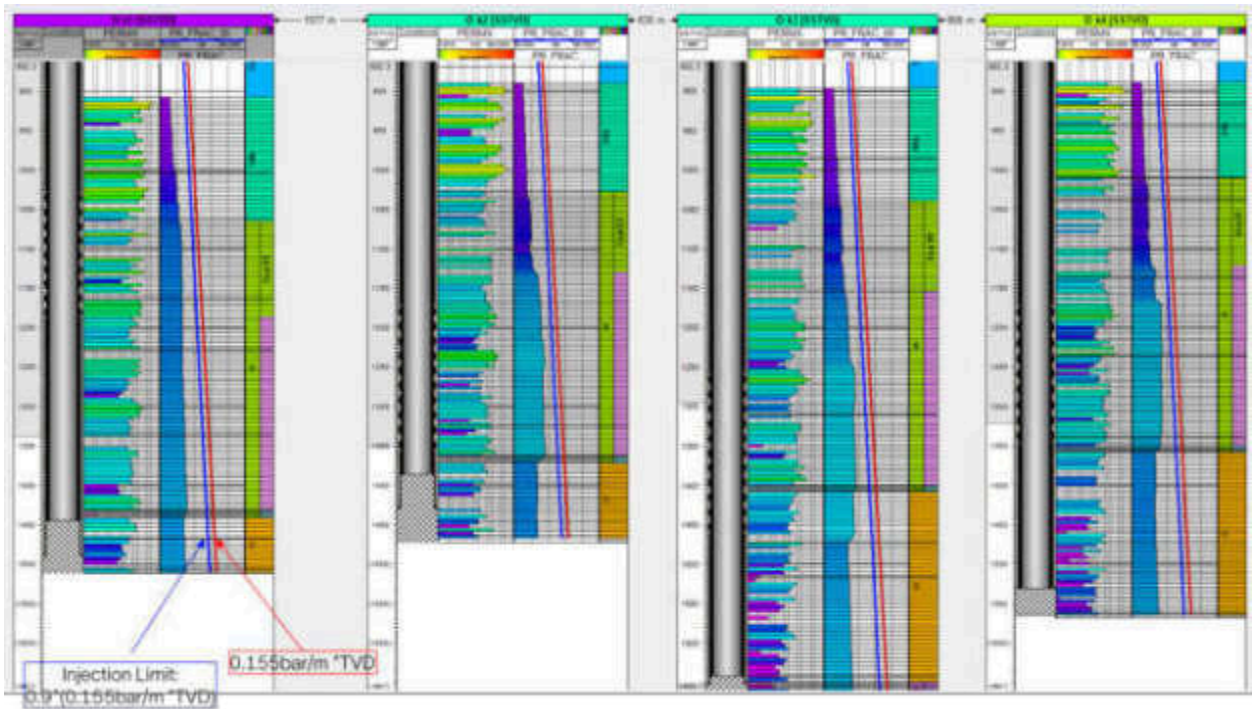


Fig. 2.224 Pressure profile vs fracture gradient in deviated wells K1, K2, K3, K4 @Jan 2030

Copyright © SLB. All Rights Reserved. Private & Confidential. Reproduction only by permission.

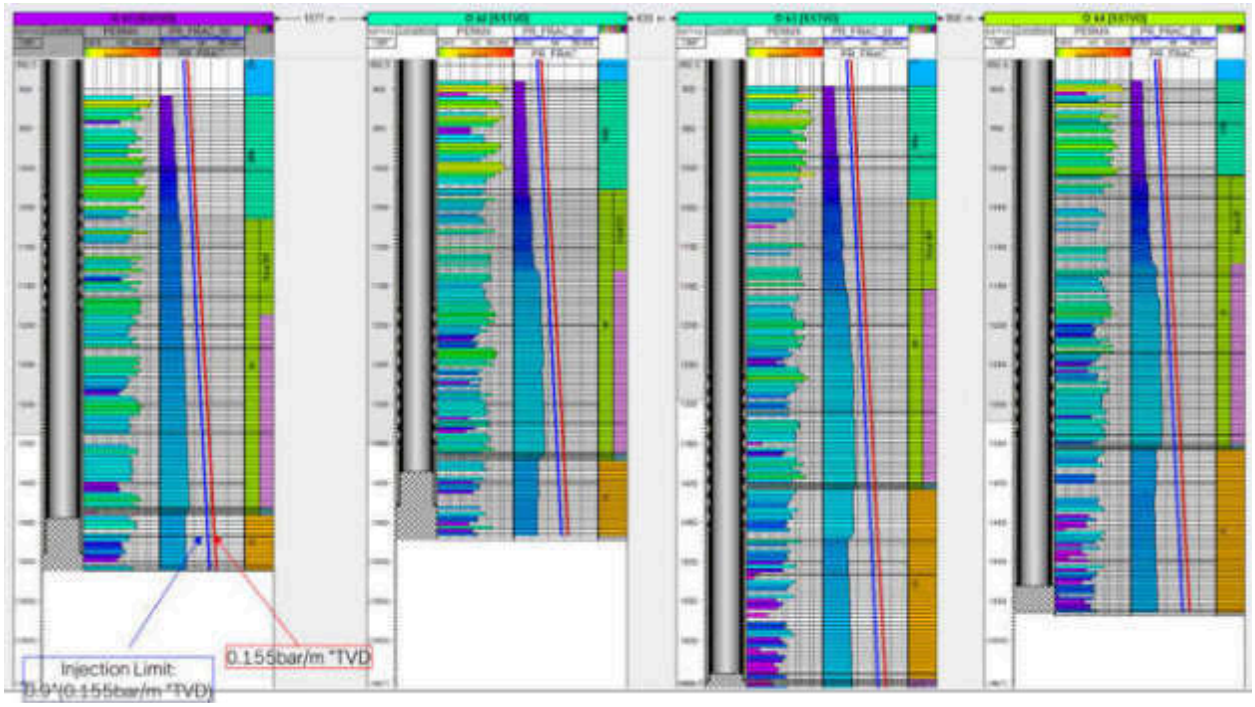


Fig. 2.225 Pressure profile vs fracture gradient in deviated wells K1, K2, K3, K4 @Jan 2040

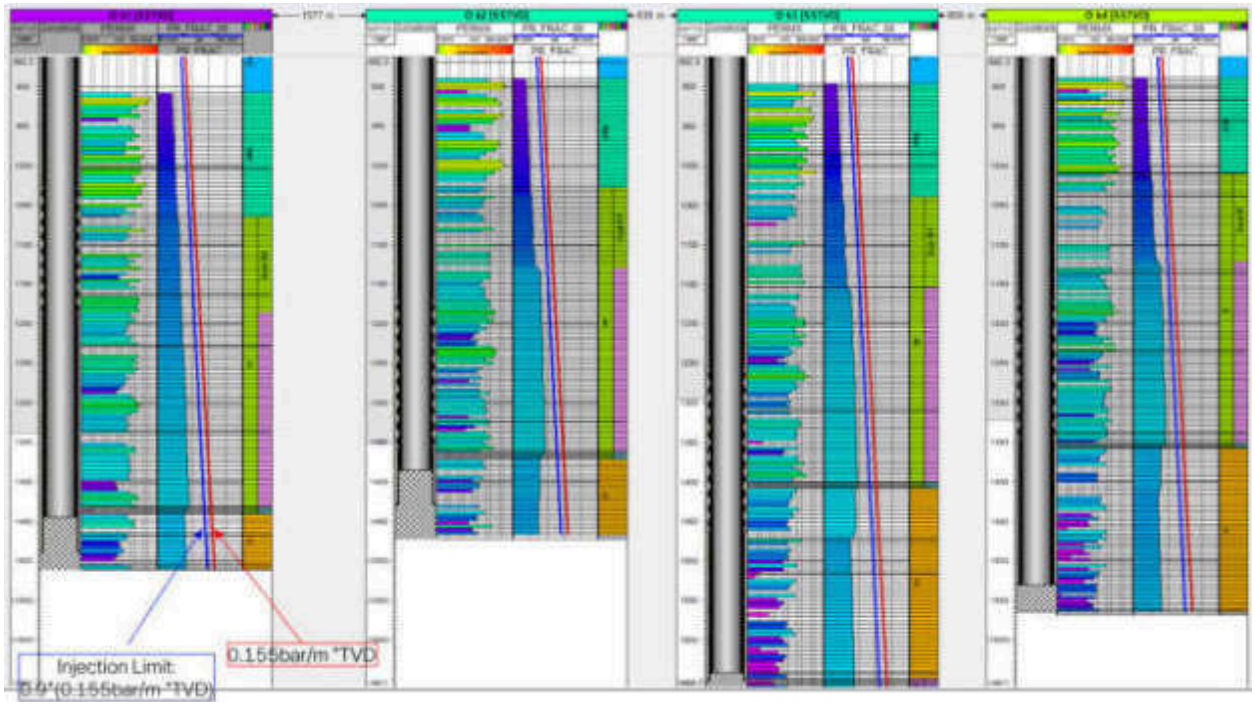


Fig. 2.226 Pressure profile vs fracture gradient in deviated wells K1, K2, K3, K4 @Jan 2057

Copyright © SLB. All Rights Reserved. Private & Confidential. Reproduction only by permission.

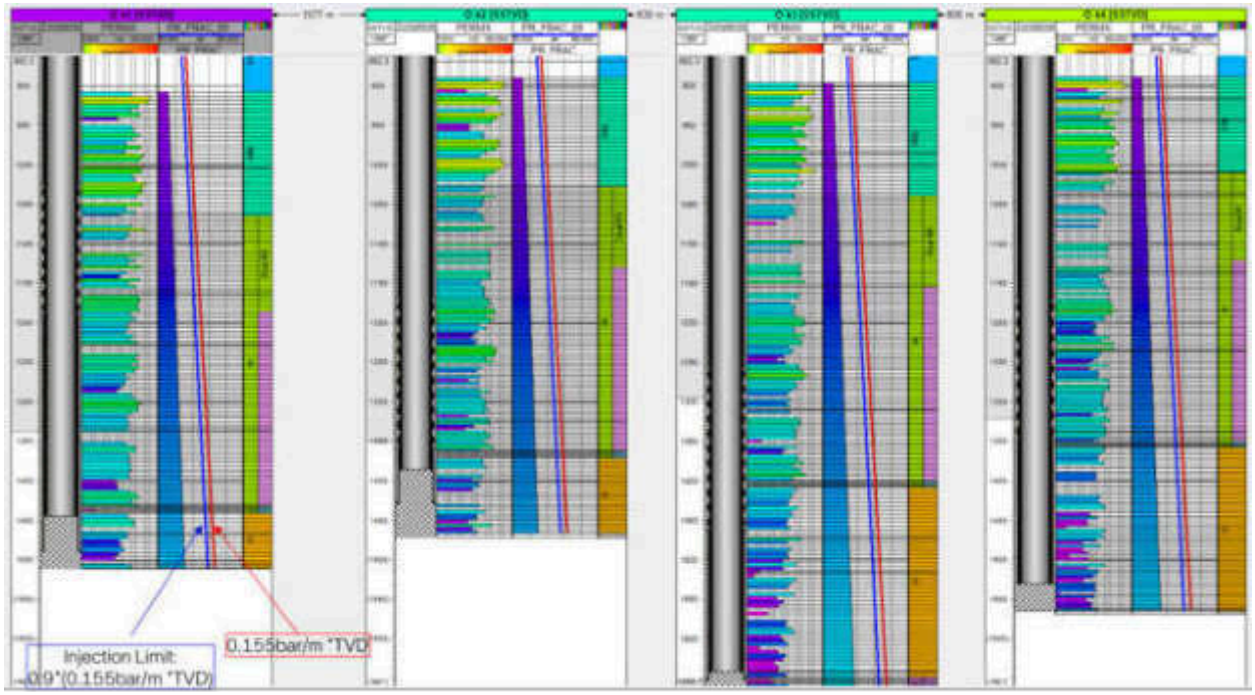


Fig. 2.227 Pressure profile vs fracture gradient in wells KS1, KS2, KS3, KS4 @Jan 2257

Pressure difference between different time steps and initial reservoir pressure on the cross-section, passing through selected sites for optimization are presented in Fig. 2.228, Fig. 2.229 , Fig. 2.230, Fig. 2.231, Fig. 2.232 and Fig. 2.233.



Fig. 2.228 Pressure difference profile with initial reservoir pressure for the cross-section in Scenario 4 with deviated wells

Copyright © SLB. All Rights Reserved. Private & Confidential. Reproduction only by permission.

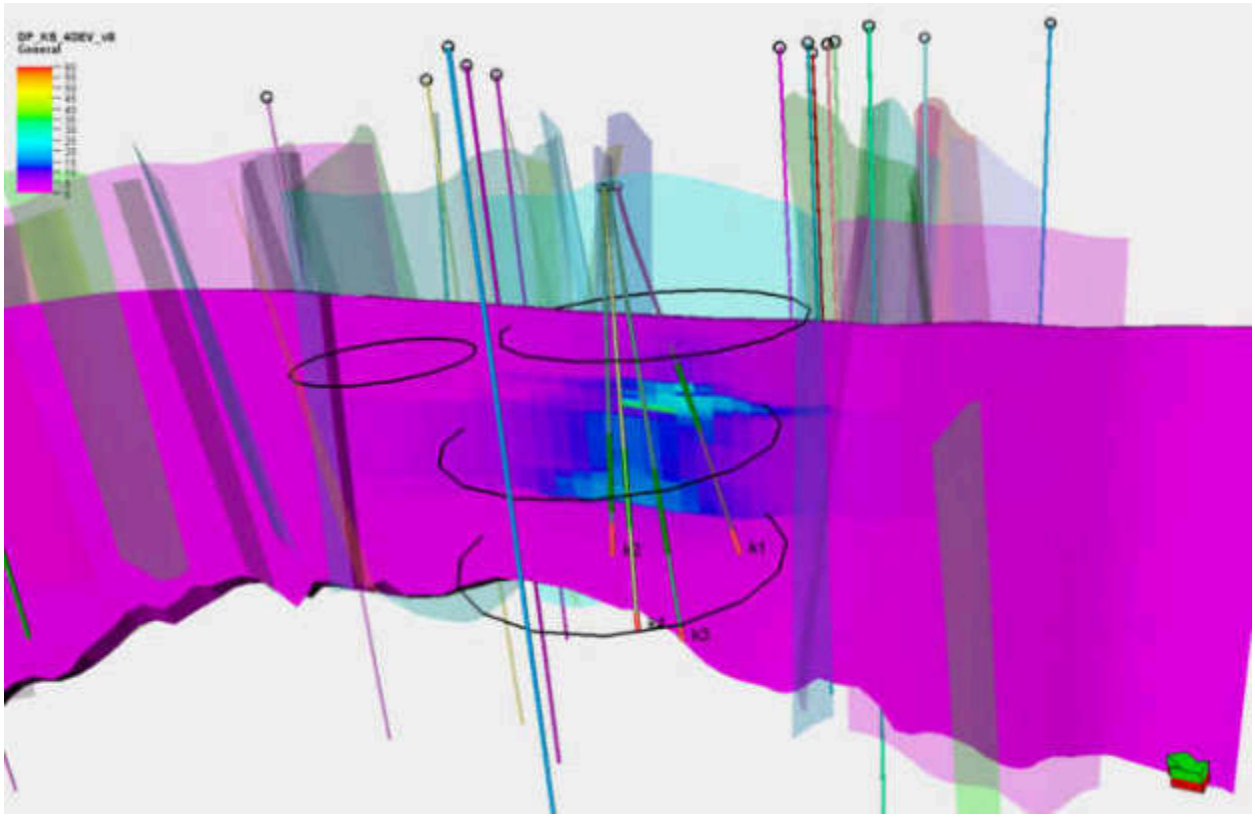


Fig. 2.229 Pressure difference profile with initial reservoir pressure for the cross-section in Scenario 4 with deviated wells@Jan 2028

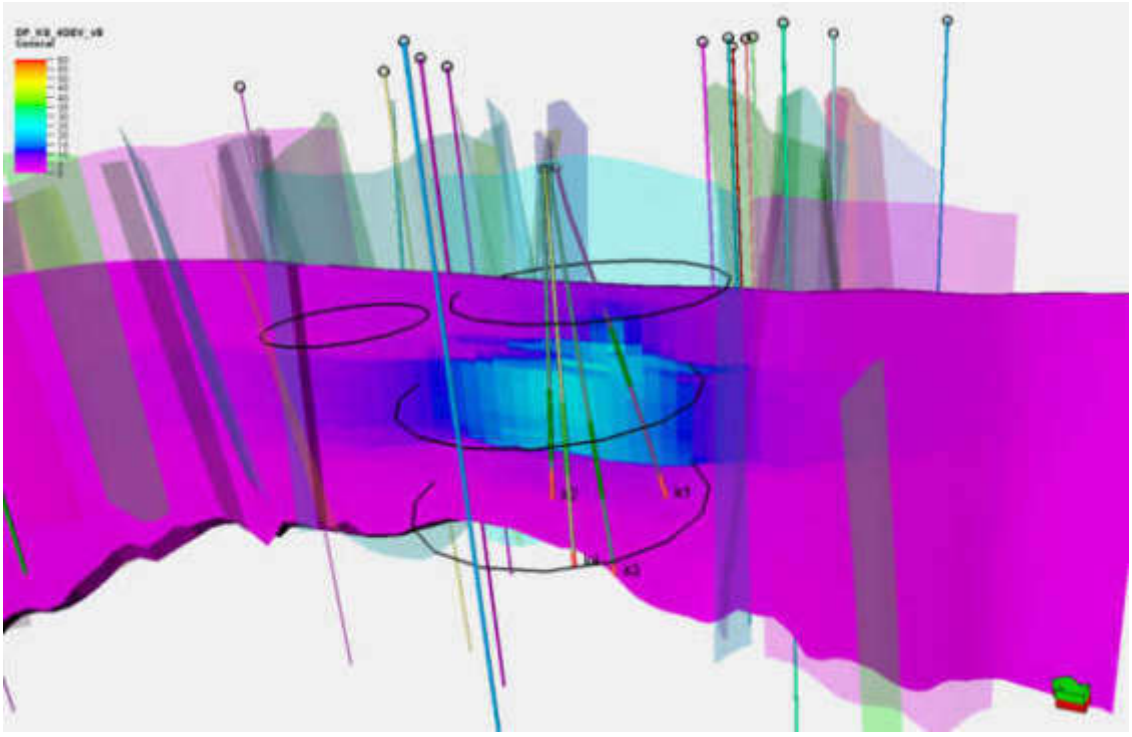


Fig. 2.230 Pressure difference profile with initial reservoir pressure for the cross-section in Scenario 4 with deviated wells@Jan 2030

Copyright © SLB. All Rights Reserved. Private & Confidential. Reproduction only by permission.

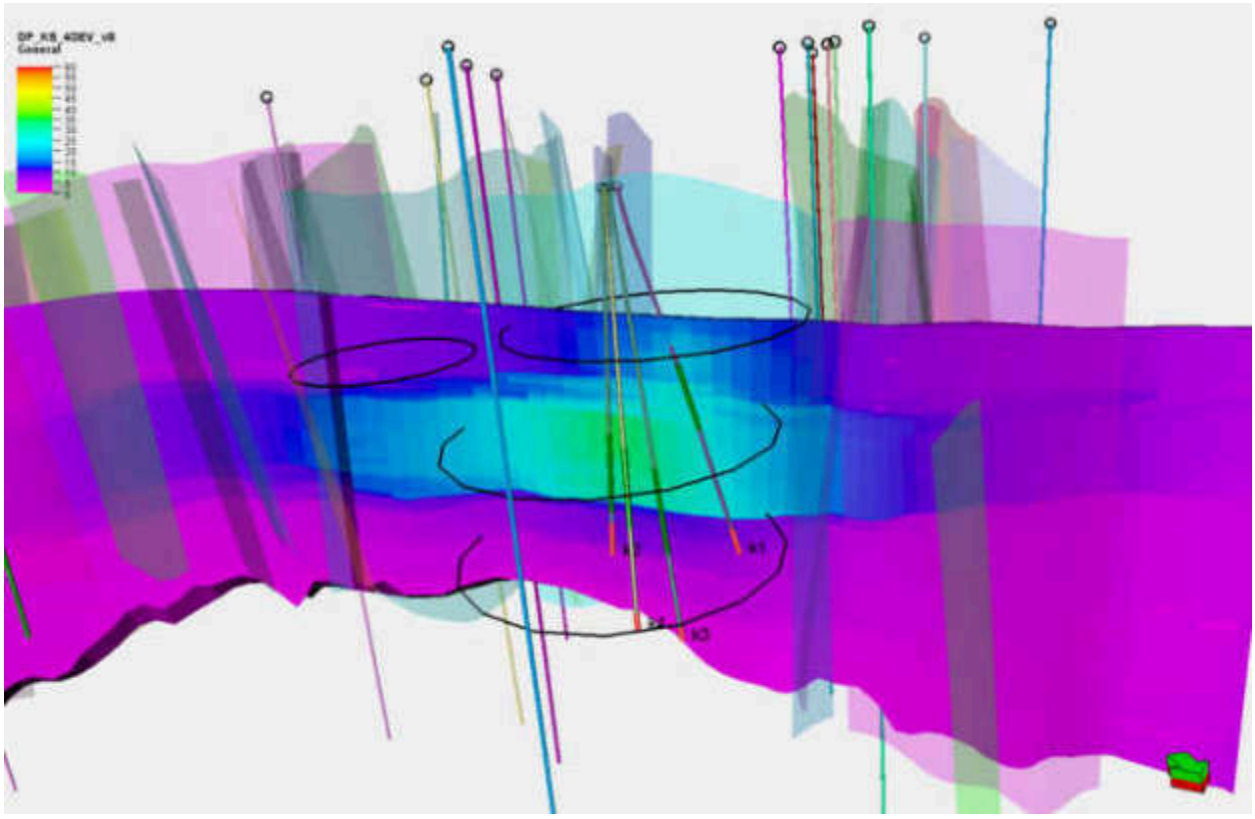


Fig. 2.231 Pressure difference profile with initial reservoir pressure for the cross-section in Scenario 4 with deviated wells@Jan 2040

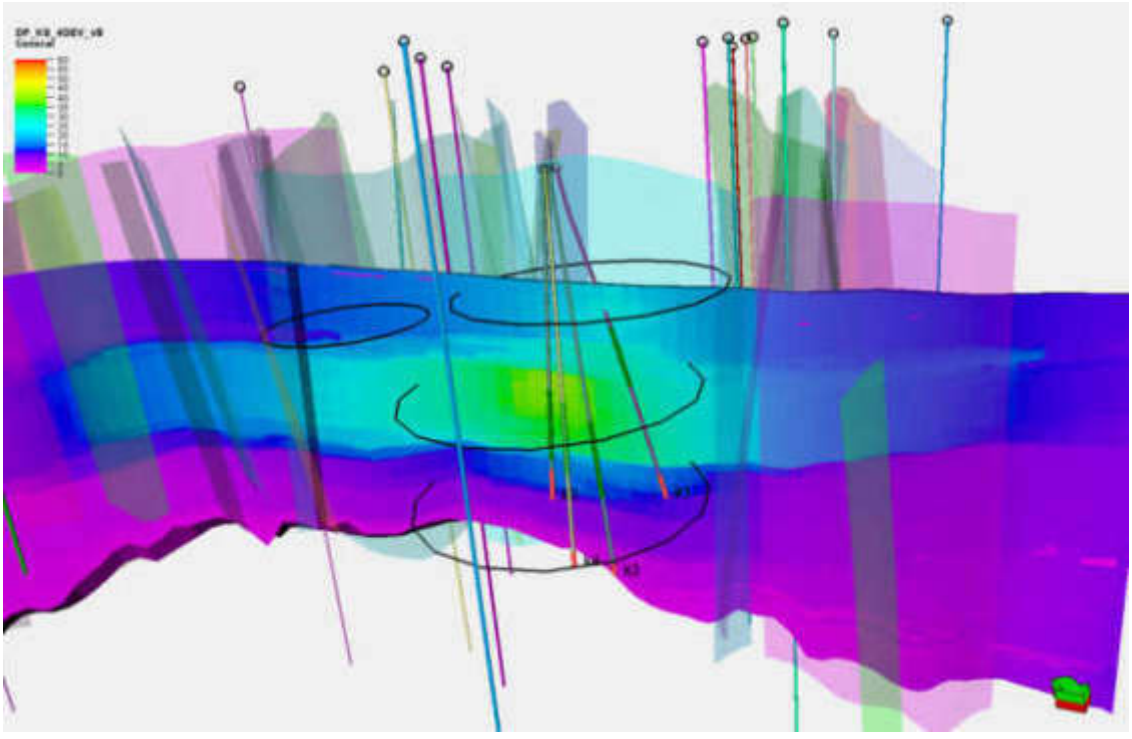


Fig. 2.232 Pressure difference profile with initial reservoir pressure for the cross-section in Scenario 4 with deviated wells@Jan 2057

Copyright © SLB. All Rights Reserved. Private & Confidential. Reproduction only by permission.



Fig. 2.233 Pressure difference profile with initial reservoir pressure for the cross-section in Scenario 4 with deviated wells@Jan 2257

Conclusions

Based on the simulation results and validation analysis:

- The reservoir pressure at all monitored locations and time steps remained below 90% of the fracture gradient, ensuring a safe operational margin and reducing the risk of caprock or wellbore integrity failure.
- The absolute difference between simulated pressures and the initial reservoir pressure did not exceed 35 bars at any evaluated location.

However, if pressure increase propagates to faults within or adjacent to the storage complex, several risks may arise:

- Fault Reactivation: Elevated pressures can increase the likelihood of fault slippage, especially if faults are critically stressed, potentially compromising seal integrity.
- Induced Seismicity: Rapid or significant pressure increases near faults may trigger microseismic events.
- Unintended Fluid Migration: Higher pressure near faults could create pathways for CO_2 or formation fluids to migrate out of the intended storage zone, posing leakage and environmental risks.

Copyright © SLB. All Rights Reserved. Private & Confidential. Reproduction only by permission.

Monitoring and Uncertainty: Uncertainties in fault permeability, orientation, and stress state require robust surveillance and conservative operational practices, especially when pressure approaches thresholds near geologic discontinuities.

Recommendations:

- Drilling an appraisal well is required to reduce subsurface uncertainty and confirm the suitability of the formation for CO_2 storage. It provides direct measurements of reservoir properties such as permeability, pressure, and heterogeneity, and enables formation testing to estimate injectivity. The well also allows evaluation of caprock integrity, which is essential to ensure that the sealing formation can safely contain CO_2 under increased injection pressures.
- Lithological interpretation of the appraisal well can identify reservoir and seal intervals, as well as internal heterogeneity that control fluid flow and plume migration. This information is required for updating static and dynamic models.
- Core sampling from both reservoir and non-reservoir intervals provides direct measurements of rock properties and supports laboratory testing. These analyses include porosity, permeability, capillary pressure, and relative permeability in CO_2–brine systems.
- Hydrodynamic testing is conducted to quantify reservoir flow behavior and injectivity. Injectivity tests allow determination of permeability, pressure response, and connectivity, as well as identification of reservoir boundaries. A dynamic CO_2 injection test is performed to validate reservoir behavior under actual operating conditions. Unlike water-based tests, it captures the specific flow and thermodynamic behavior of CO_2, including its compressibility and multiphase interactions. Monitoring of pressure and temperature during injection allows confirmation of injectivity, identification of potential flow barriers or leakage pathways, and calibration of reservoir simulation models.
- Calibration of reservoir simulation model will support continuous tracking of pressure evolution, with specific focus on areas in proximity to mapped faults.
- Update risk assessments as more site-specific geomechanical and fault integrity data become available.
- Consider conservative injection rate controls and implement pressure management strategies to avoid exceeding safe limits near faults.

These measures help ensure compliance with safety requirements while mitigating containment risks in the storage formation.

2.8.5.3 CO_2 plume migration

The migration of injected CO_2 within the storage reservoir was simulated and evaluated using a dynamic reservoir model with site-specific geological and petrophysical data. The objective was to assess the spatial extent and movement of the CO_2 plume throughout and following the injection period, ensuring containment within the designated storage complex.

Copyright © SLB. All Rights Reserved. Private & Confidential. Reproduction only by permission.

Model outputs indicate that, under the injection rates and pressure limitations at bottom hole, the CO_2 plume propagates primarily laterally along the most permeable strata, closely following reservoir heterogeneity and stratigraphic boundaries. Vertical plume migration across zones is minimal due to the presence of a competent, laterally continuous caprock system with low permeability. Snapshots of plume distribution at the end monitoring period in year 2257 presented below for Scenarios 1 - 4. (see Fig. 2.234, Fig. 2.235, Fig. 2.236, Fig. 2.237 and Fig. 2.238 below).

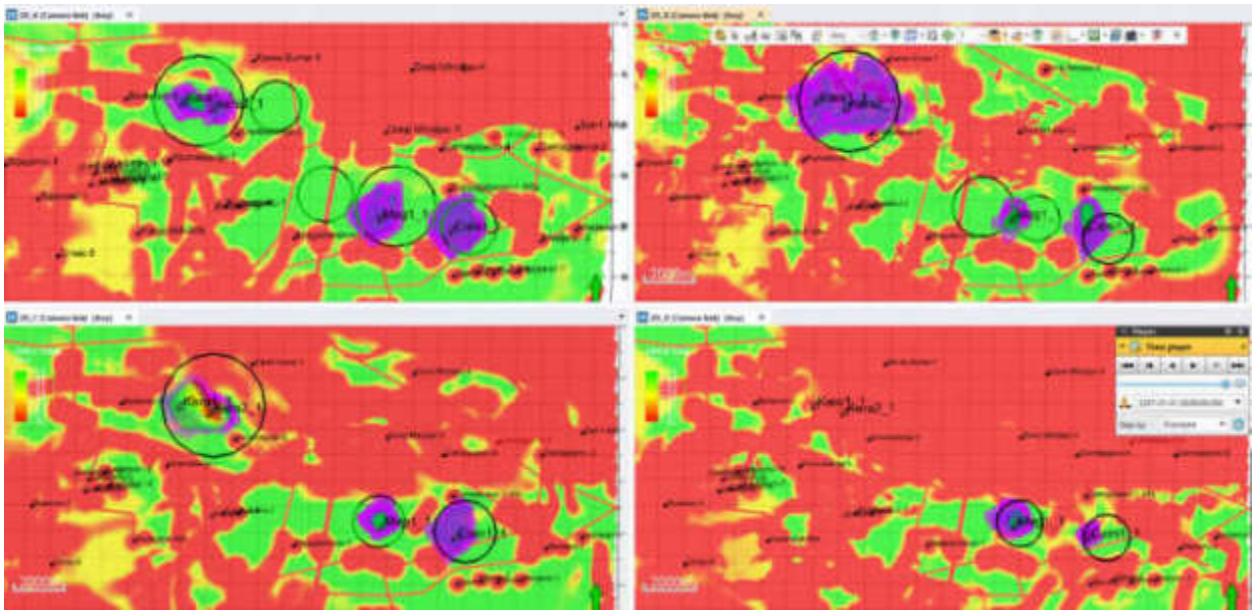


Fig. 2.234 Plume saturation per zone at the end of monitoring period @2257 for Scenario 1

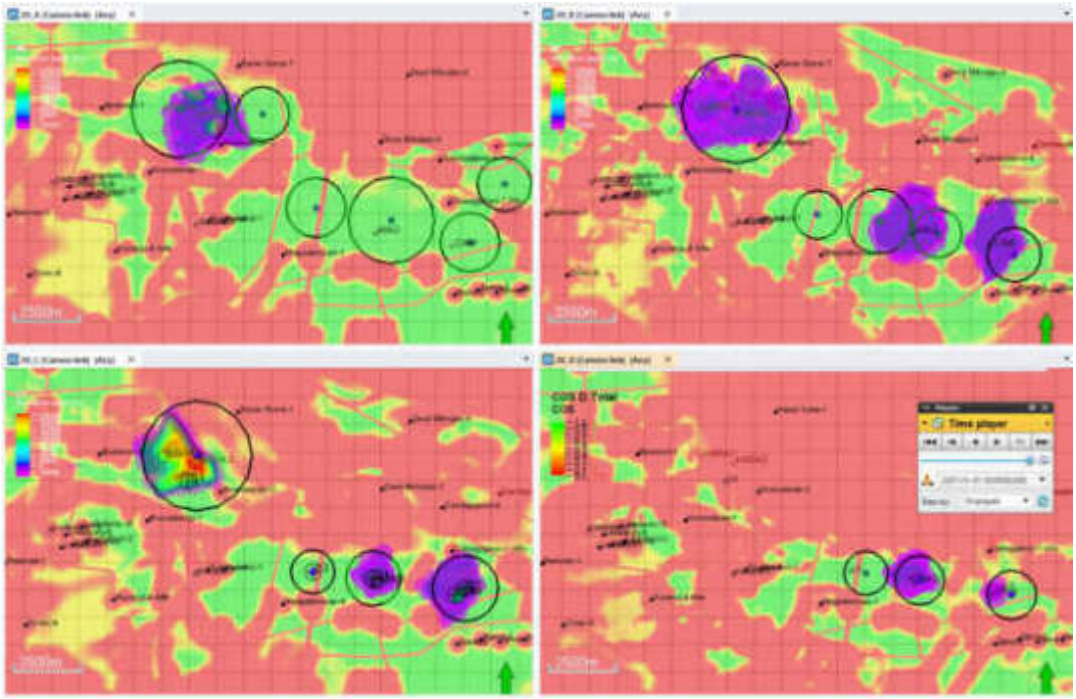


Fig. 2.235 Plume saturation per zone at the end of monitoring period @2257 for Scenario 2

Copyright © SLB. All Rights Reserved. Private & Confidential. Reproduction only by permission.

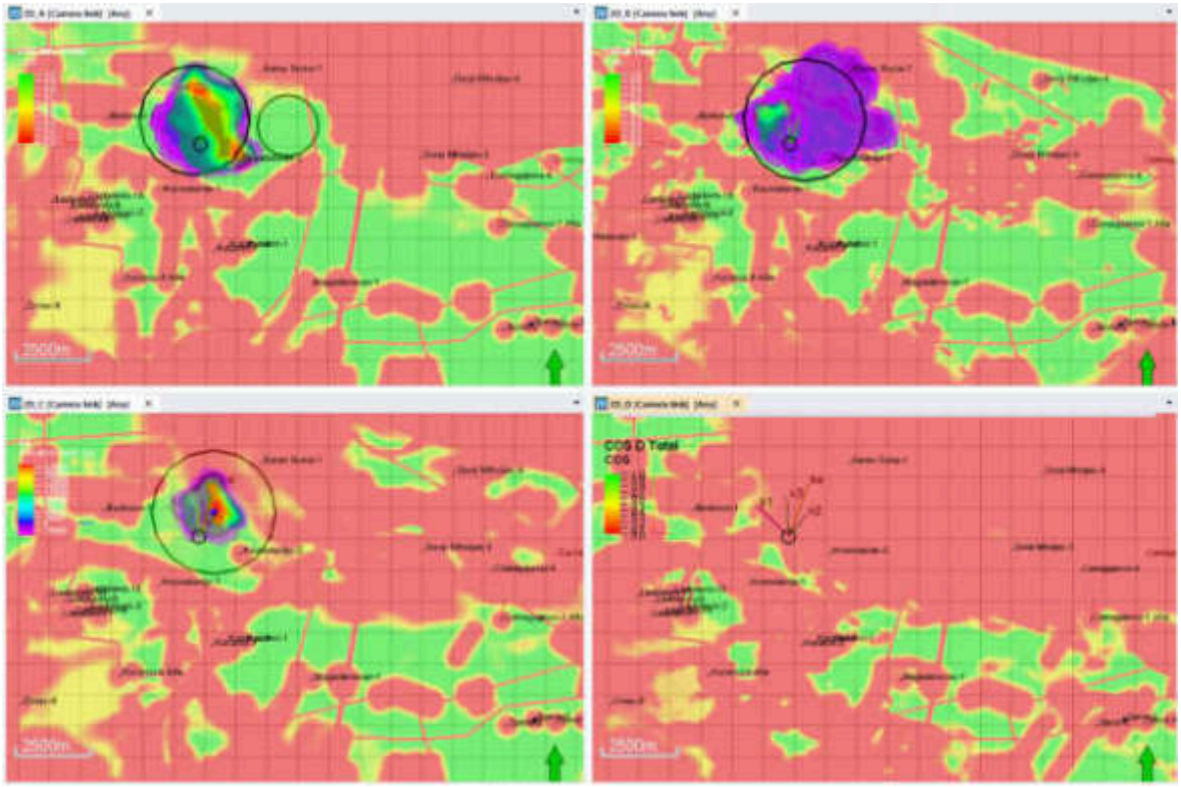


Fig. 2.236 Plume saturation per zone at the end of monitoring period @2257 for Scenario 3

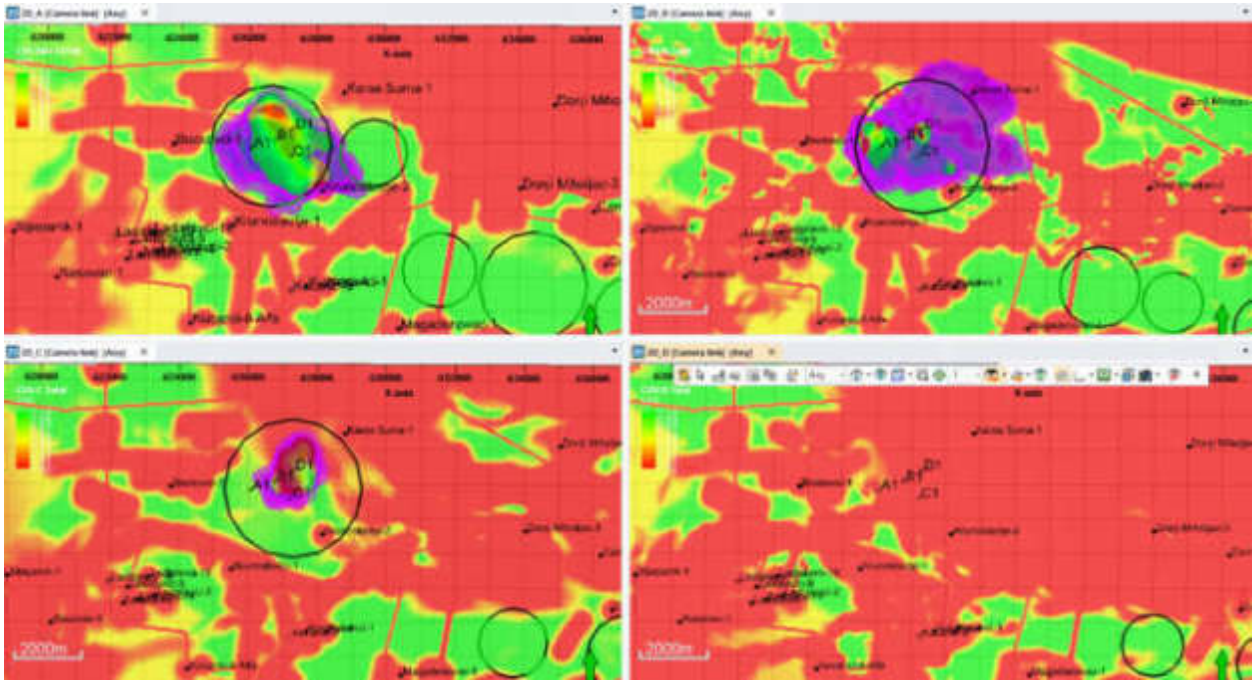


Fig. 2.237 Plume saturation per zone at the end of monitoring period @2257 for Scenario 4

Copyright © SLB. All Rights Reserved. Private & Confidential. Reproduction only by permission.

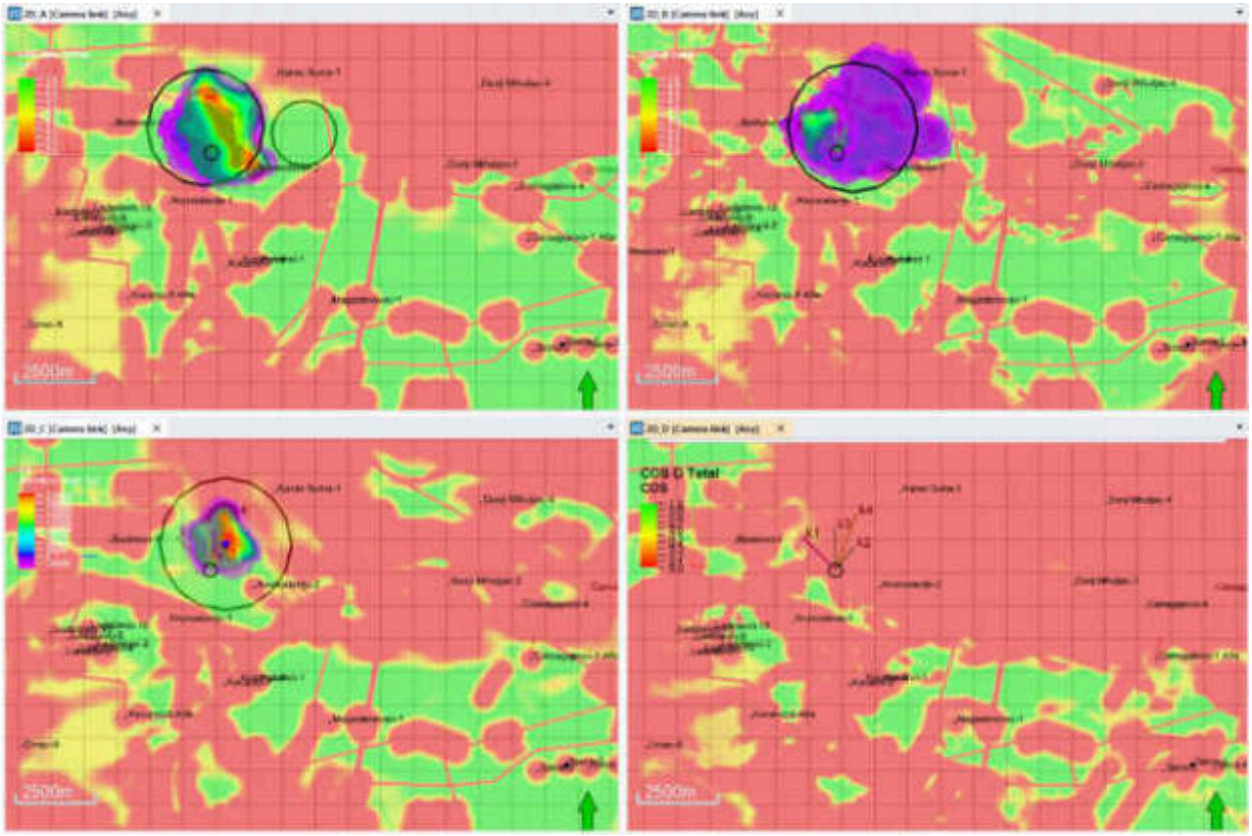


Fig. 2.238 Plume saturation per zone at the end of monitoring period @2257 for Scenario 4 - deviated wells

3D gas saturation during injection phase at key time intervals (1, 3, 13, 30 years and 200 years post injection) demonstrate that the free-phase CO_2 remains confined within the mapped structural and stratigraphic traps of the storage site across all scenarios.

Scenario 1: 4 vertical wells 3 sites (variable injection, with formation switch)

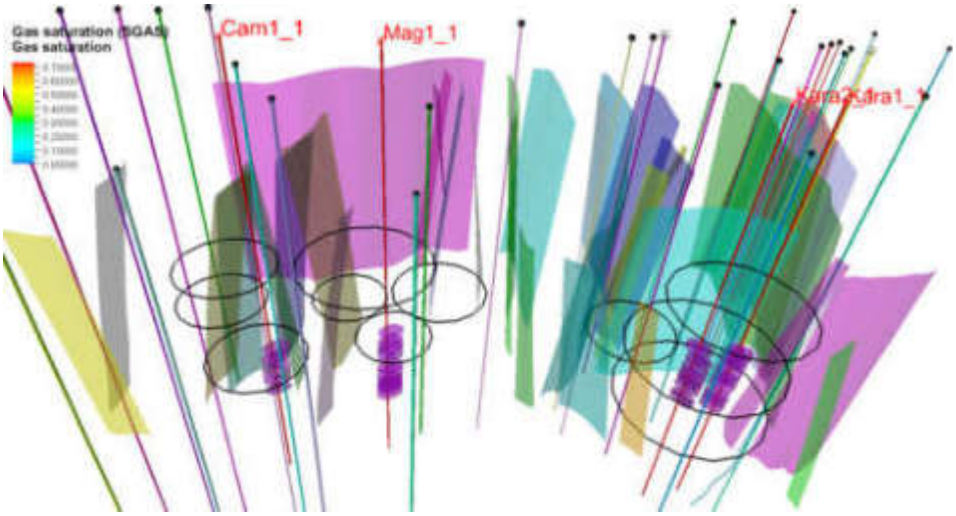


Fig. 2.239 Gas saturation for Scenario 1 after 1 year of injection @Jan 2028

Copyright © SLB. All Rights Reserved. Private & Confidential. Reproduction only by permission.

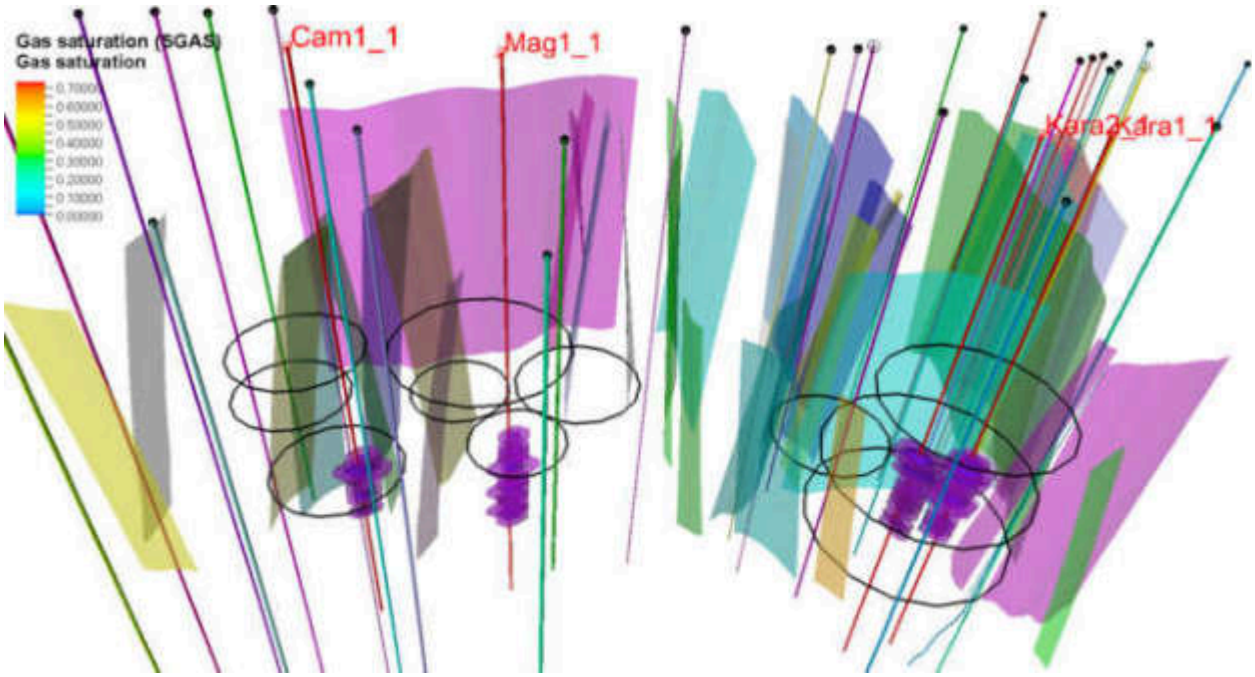


Fig. 2.240 Gas saturation for Scenario 1 after 3 years of injection @Jan 2030

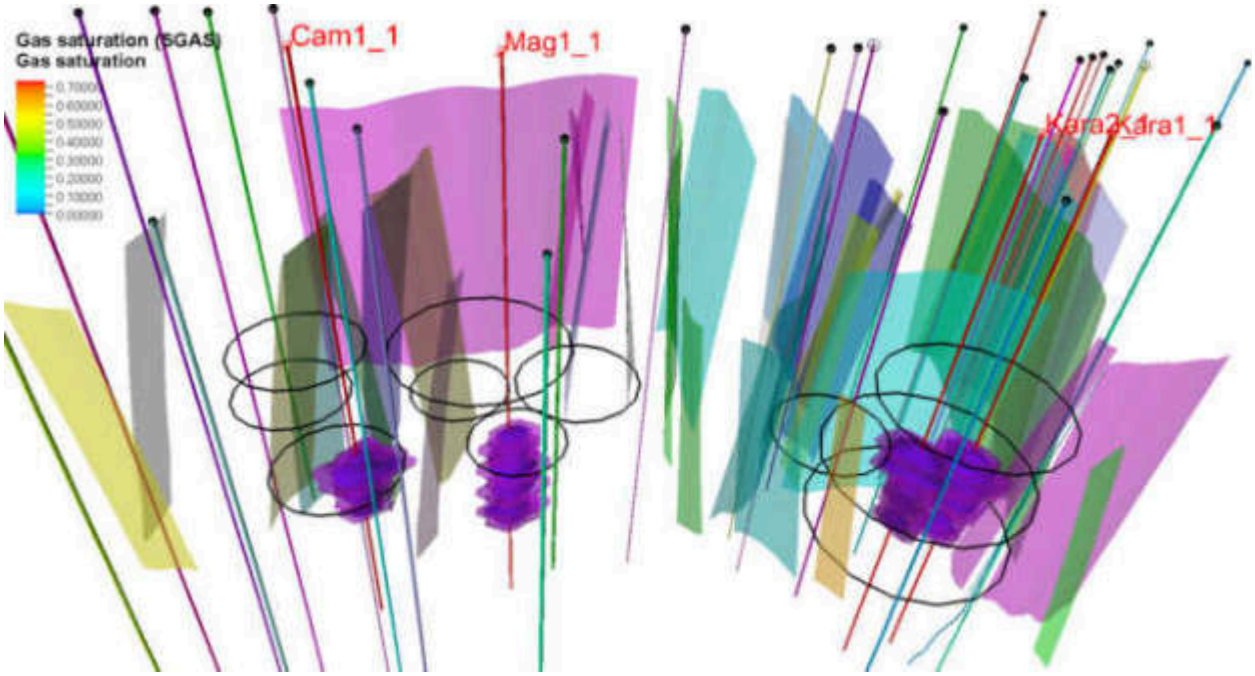


Fig. 2.241 Gas saturation for Scenario 1 after 13 years of injection @Jan 2040

Copyright © SLB. All Rights Reserved. Private & Confidential. Reproduction only by permission.

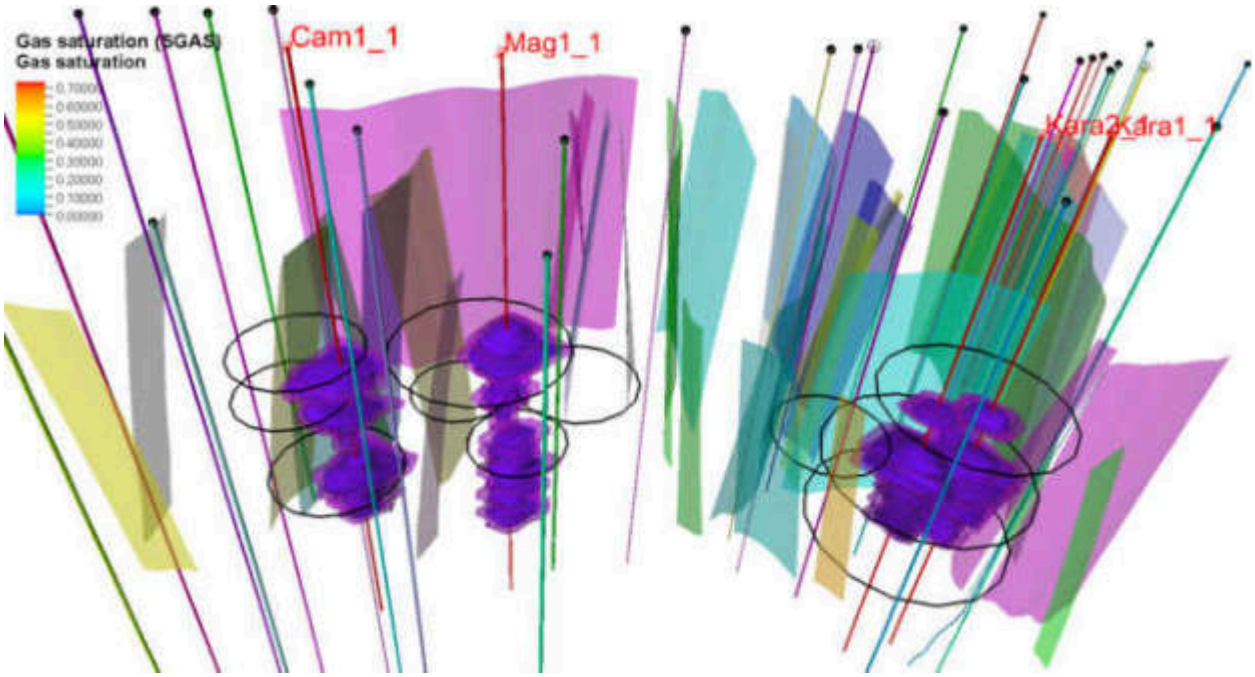


Fig. 2.242 Gas saturation for Scenario 1 after 30 years of injection @Jan 2057

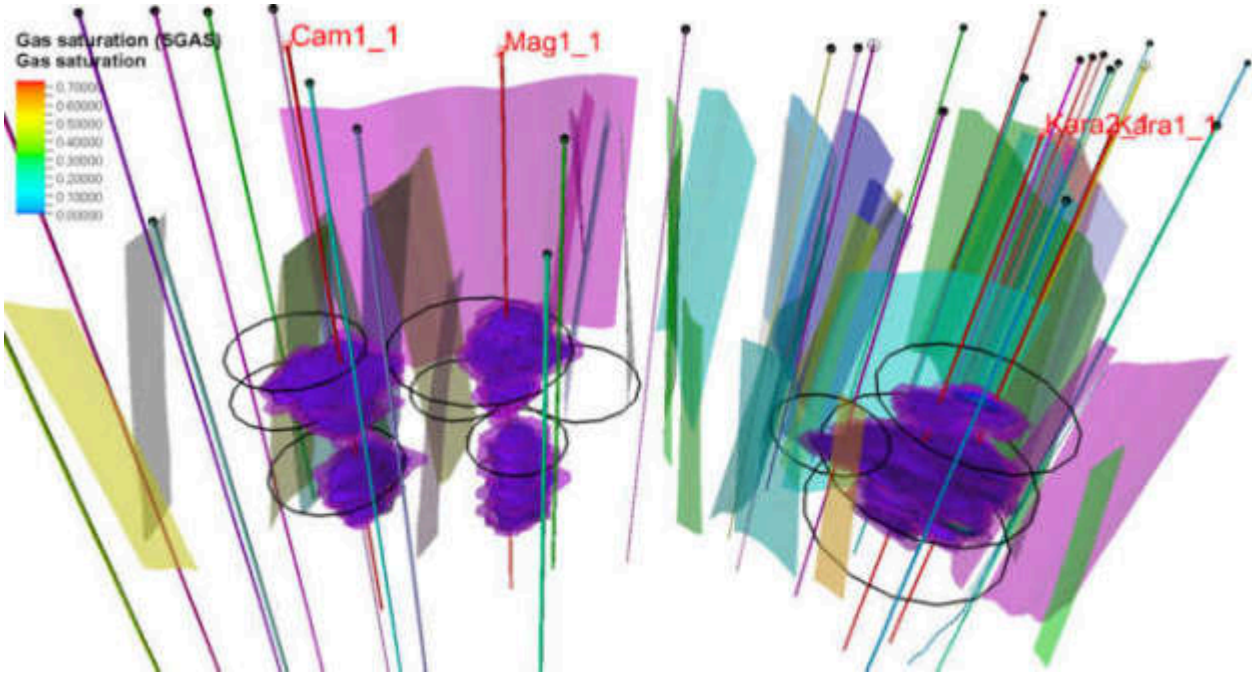


Fig. 2.243 Gas saturation for Scenario 1 after 200 years post injection @Jan 2257

Scenario 2: 4 vertical wells 3 sites (constant injection, no formation switch)

Copyright © SLB. All Rights Reserved. Private & Confidential. Reproduction only by permission.

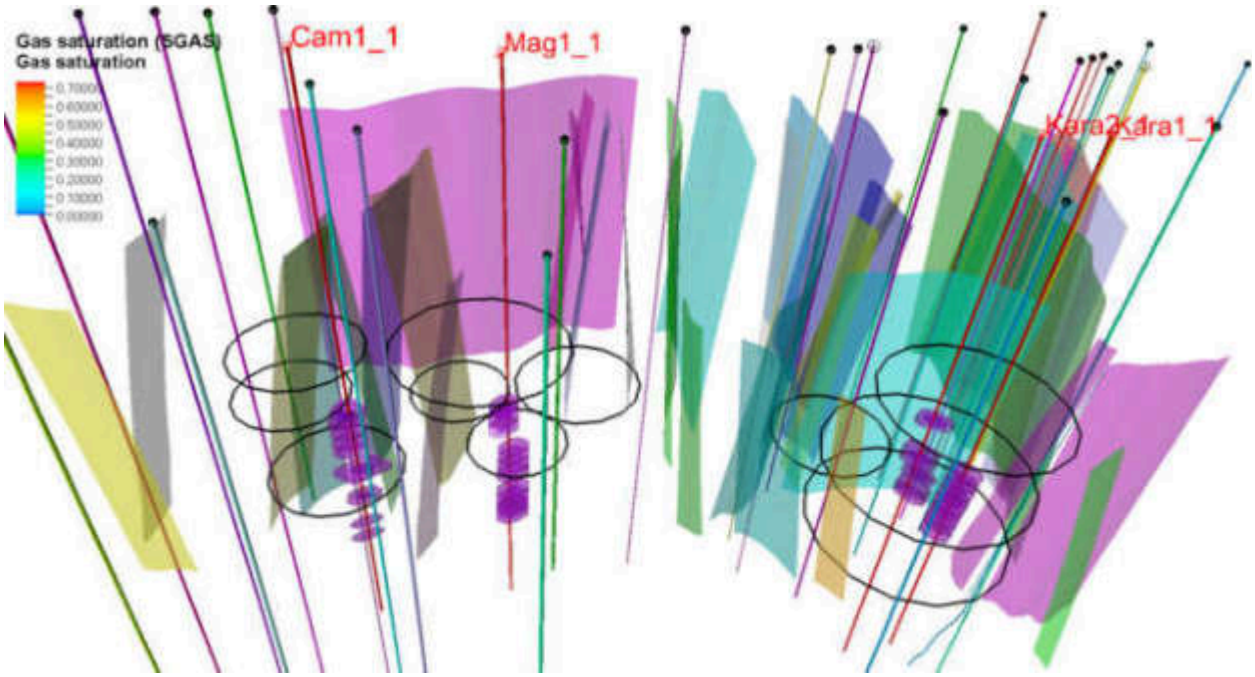


Fig. 2.244 Gas saturation for Scenario 2 after 1 year of injection @Jan 2028

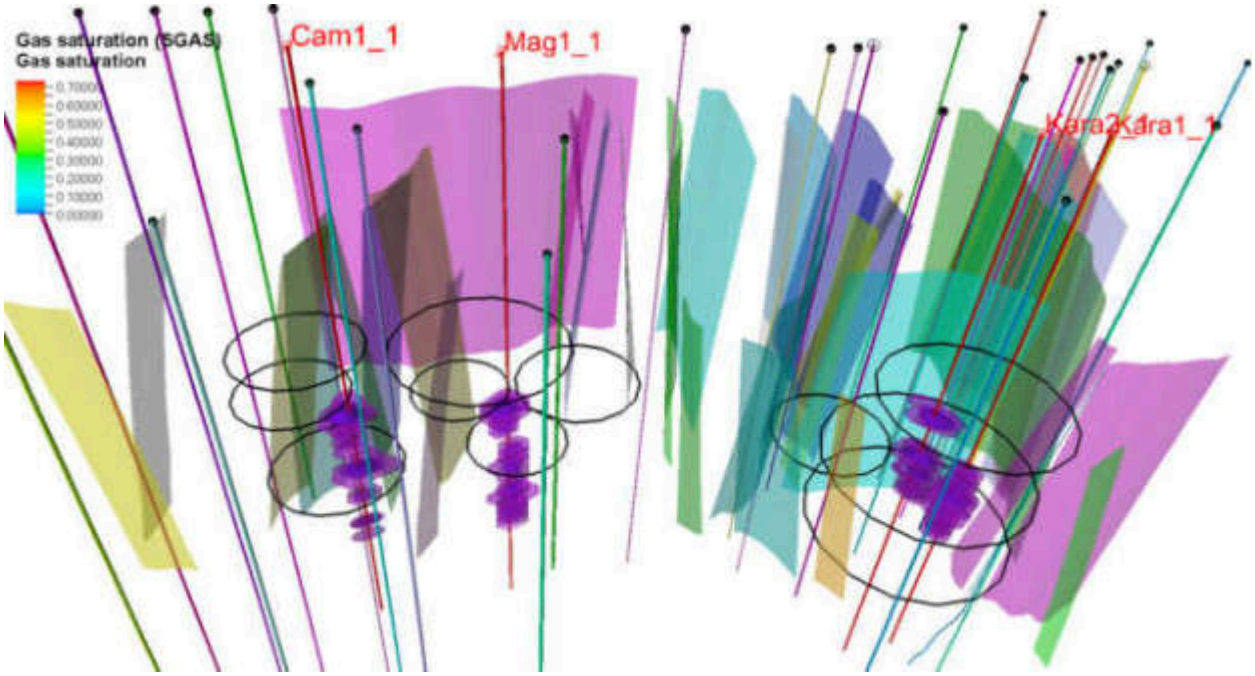


Fig. 2.245 Gas saturation for Scenario 2 after 3 year of injection @Jan 2030

Copyright © SLB. All Rights Reserved. Private & Confidential. Reproduction only by permission.

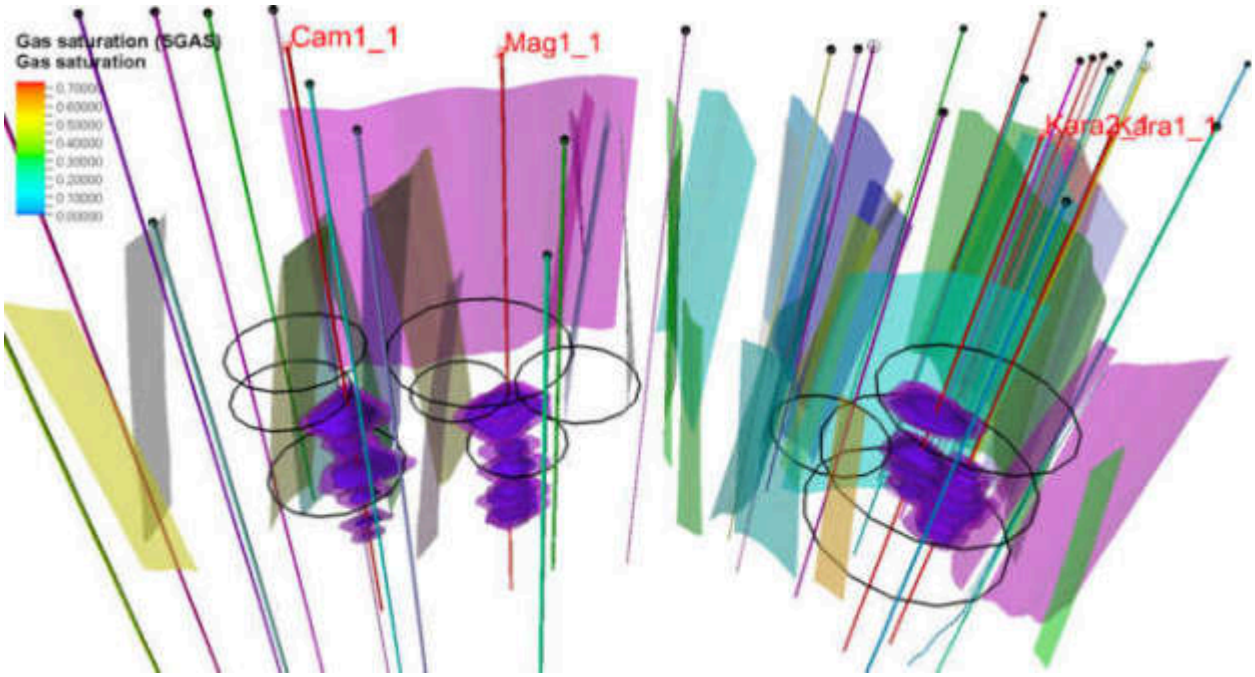


Fig. 2.246 Gas saturation for Scenario 2 after 13 year of injection @Jan 2040

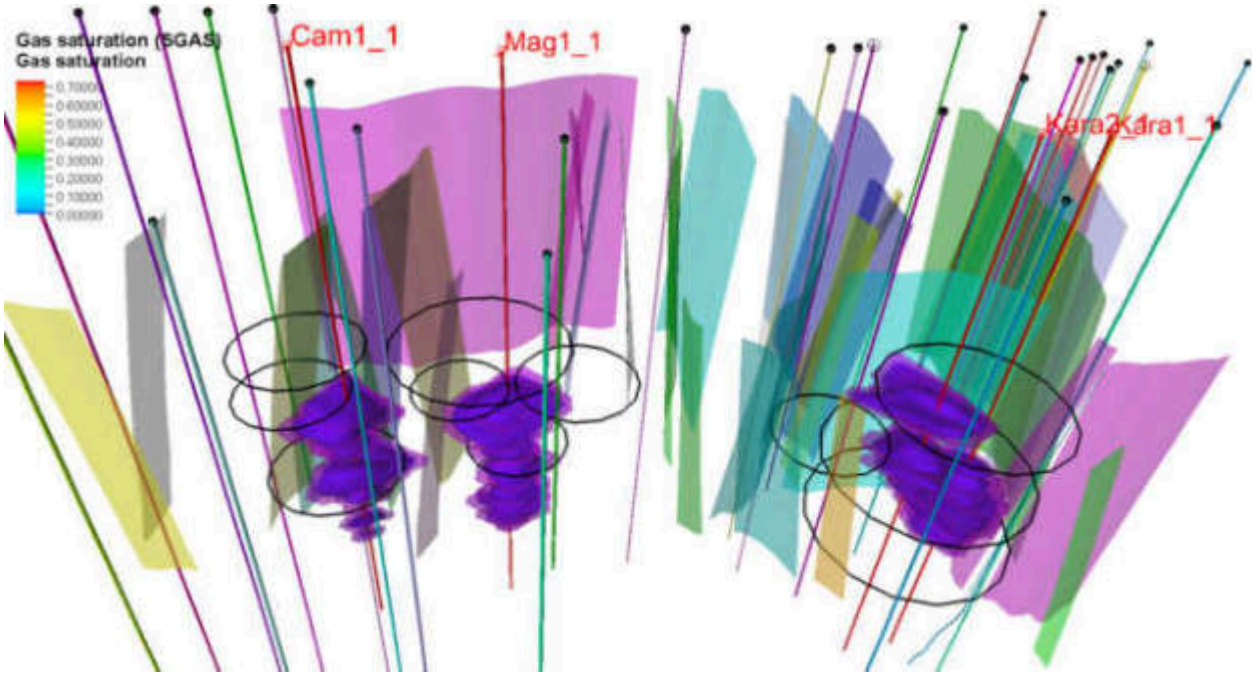


Fig. 2.247 Gas saturation for Scenario 2 after 30 year of injection @Jan 2057

Copyright © SLB. All Rights Reserved. Private & Confidential. Reproduction only by permission.

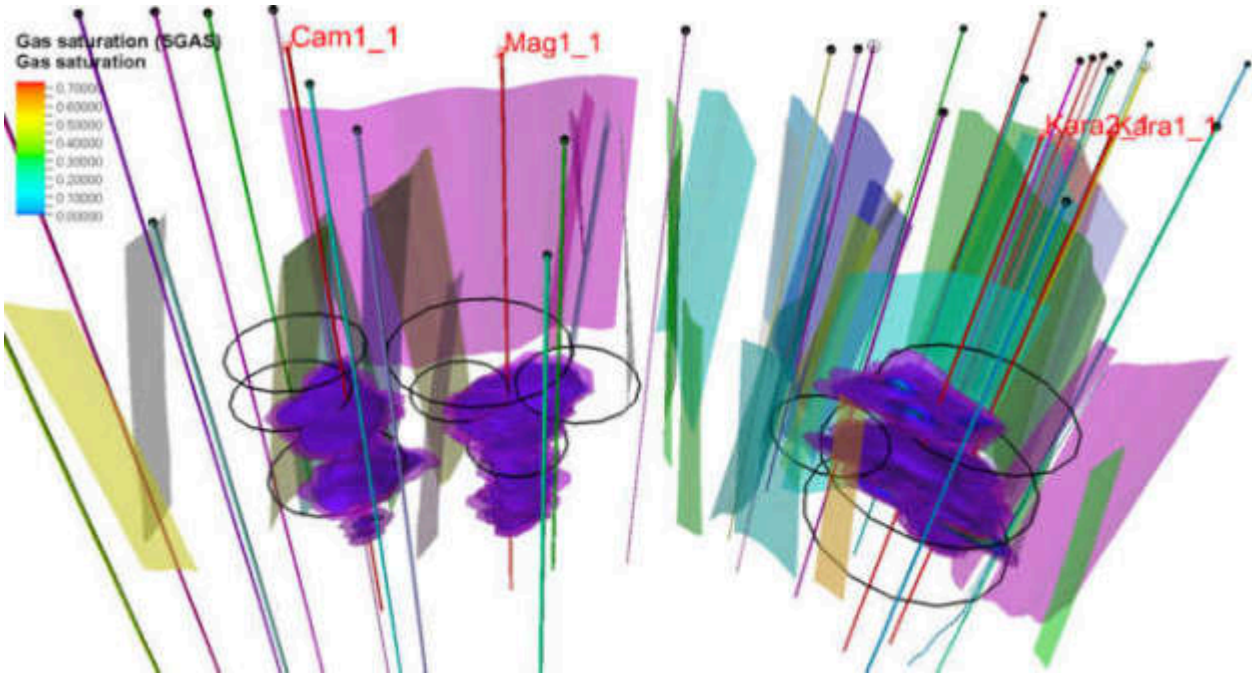


Fig. 2.248 Gas saturation for Scenario 2 after 200 years post injection @Jan 2257

Scenario 3: 3 vertical wells in Karas Suma-1 area

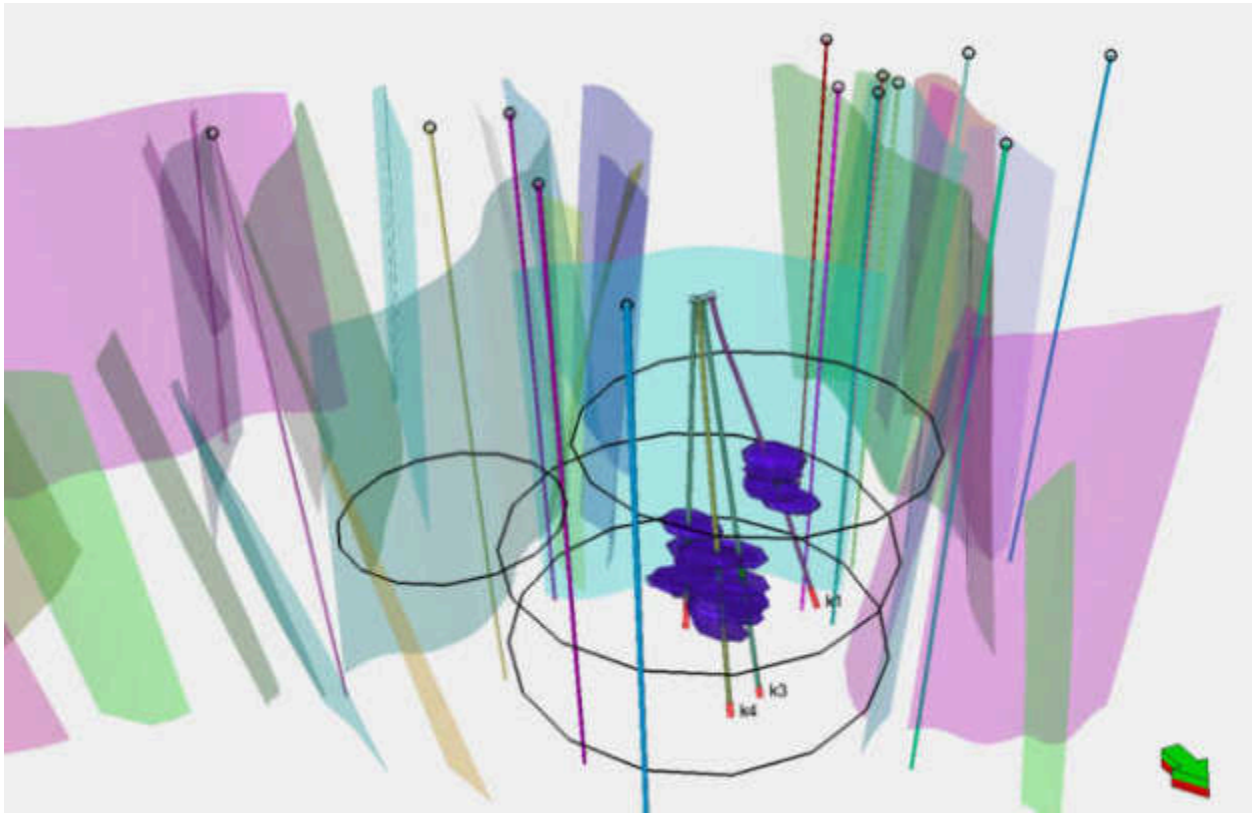


Fig. 2.249 Gas saturation for Scenario 3 after 1 year of injection @Jan 2028

Copyright © SLB. All Rights Reserved. Private & Confidential. Reproduction only by permission.

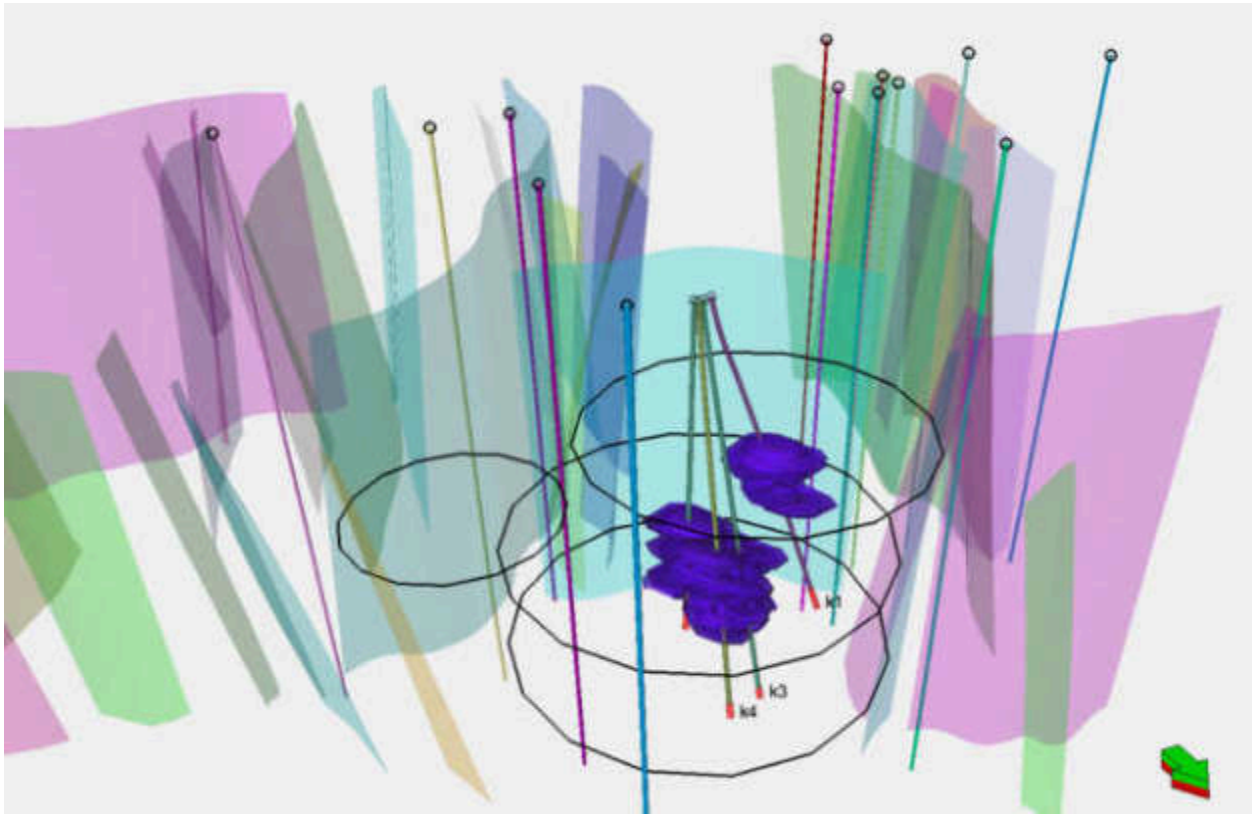


Fig. 2.250 Gas saturation for Scenario 3 after 3 year of injection @Jan 2030

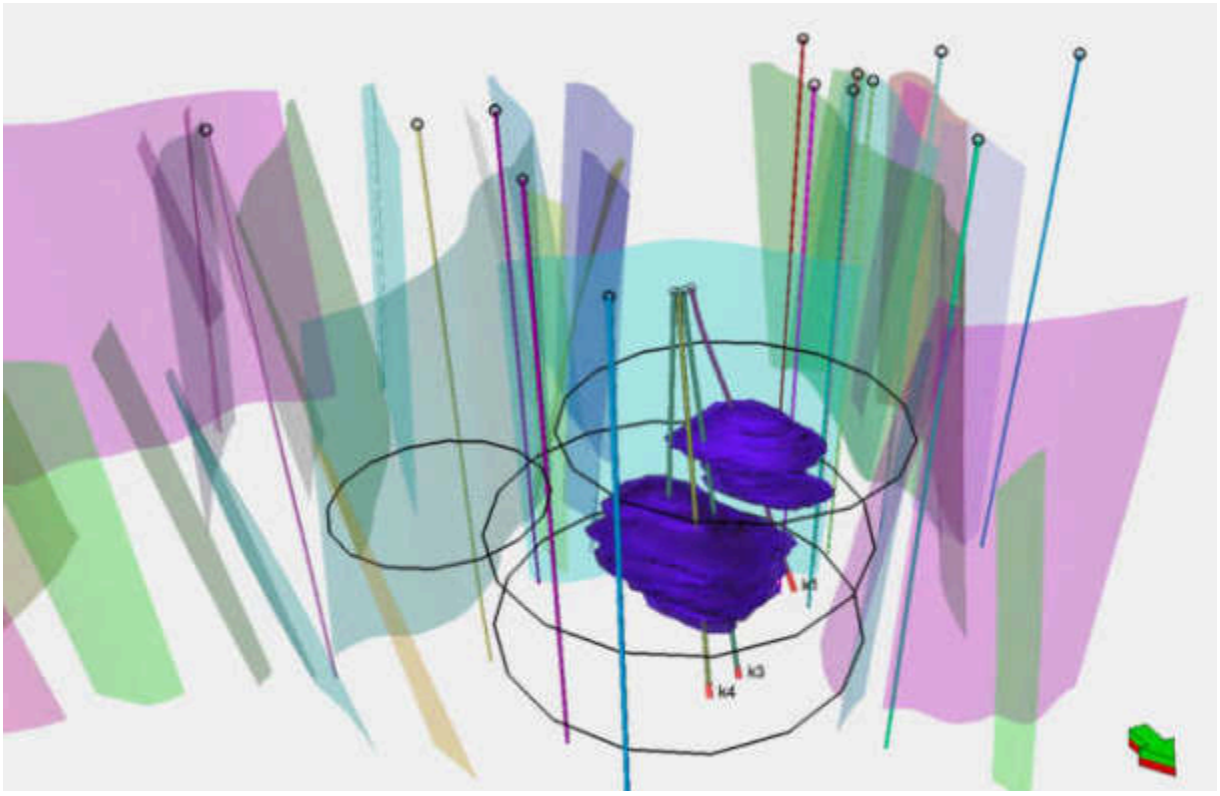


Fig. 2.251 Gas saturation for Scenario 3 after 13 year of injection @Jan 2040

Copyright © SLB. All Rights Reserved. Private & Confidential. Reproduction only by permission.

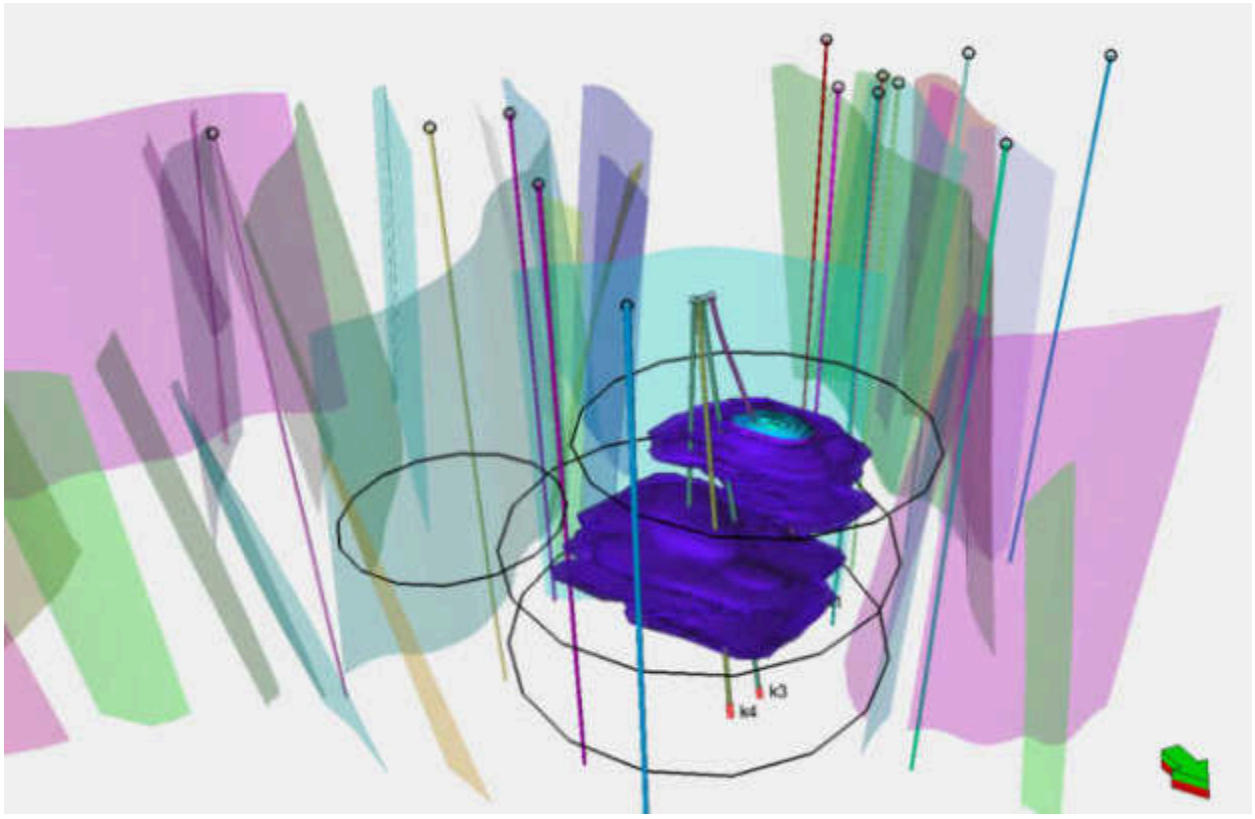


Fig. 2.252 Gas saturation for Scenario 3 after 30 year of injection @Jan 2057

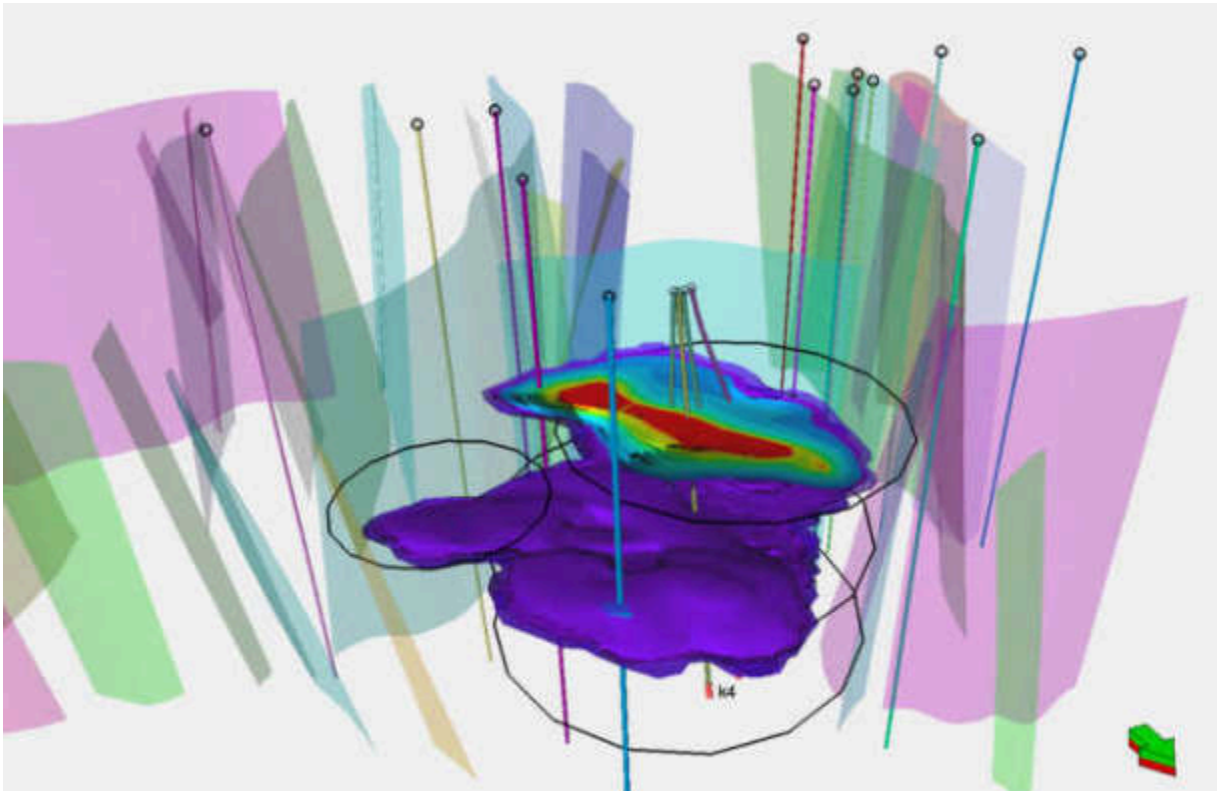


Fig. 2.253 Gas saturation for Scenario 3 after 200 years post injection @Jan 2257

Copyright © SLB. All Rights Reserved. Private & Confidential. Reproduction only by permission.

Scenario 4: 4 vertical wells in Karas Suma-1 area

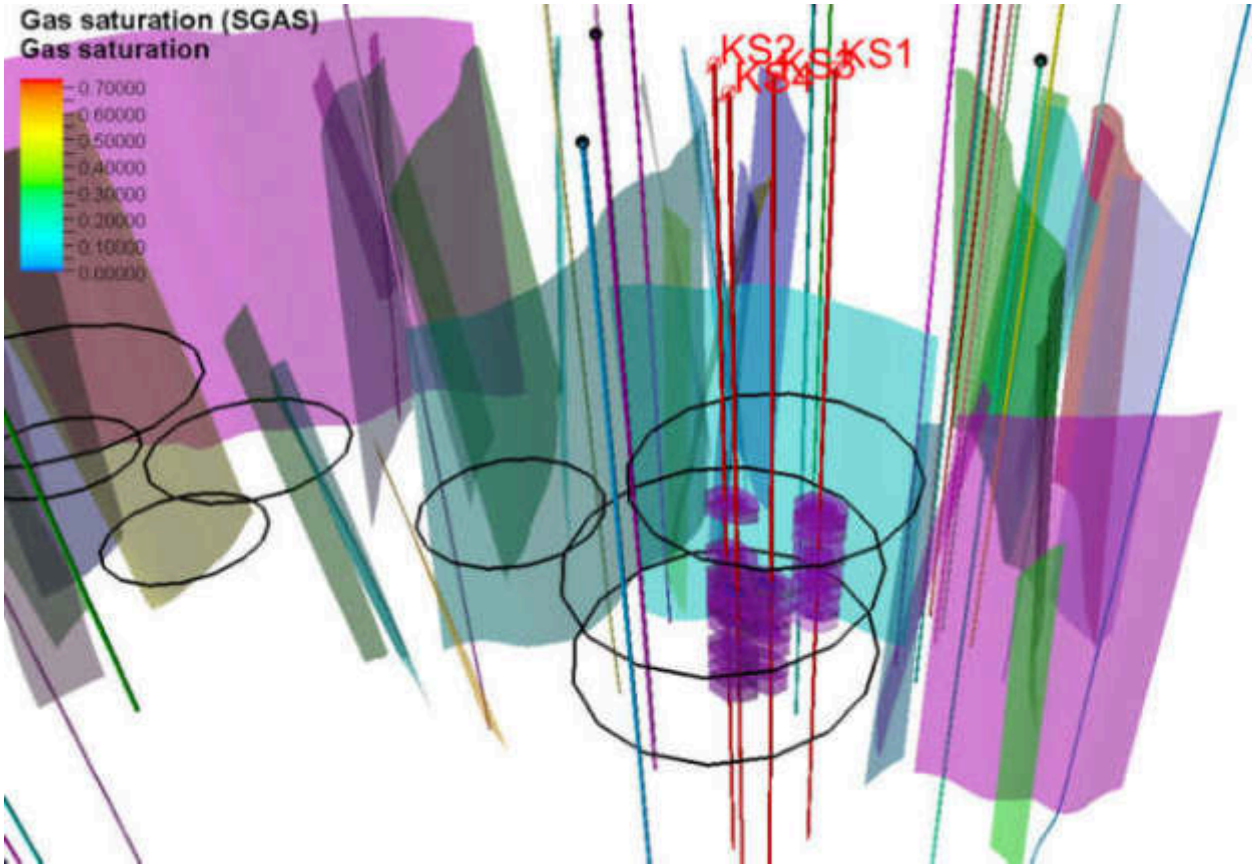


Fig. 2.254 Gas saturation for Scenario 4 after 1 year of injection @Jan 2028

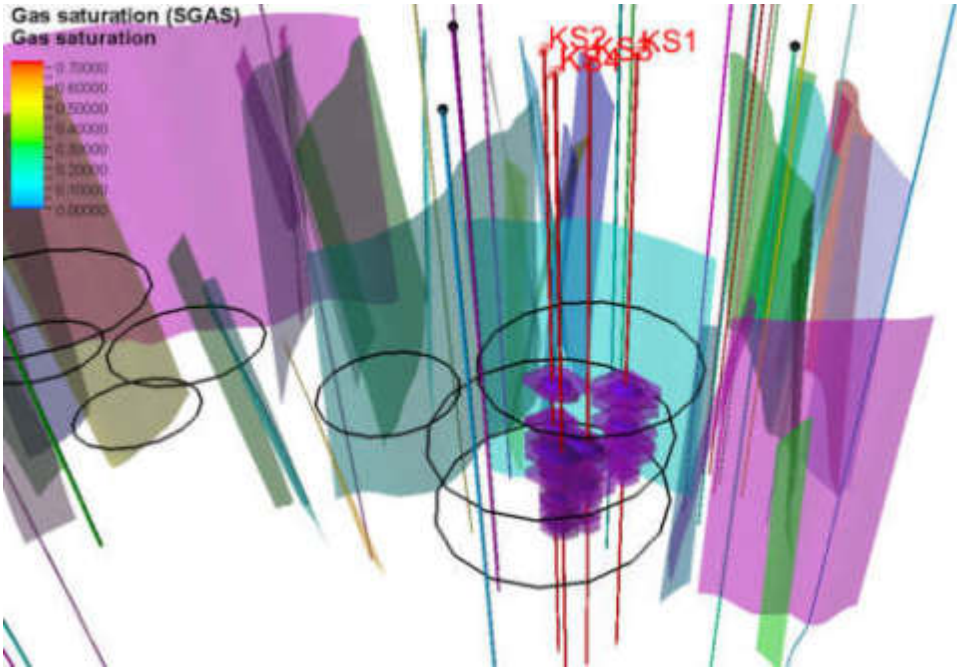


Fig. 2.255 Gas saturation for Scenario 4 after 3 year of injection @Jan 2030

Copyright © SLB. All Rights Reserved. Private & Confidential. Reproduction only by permission.

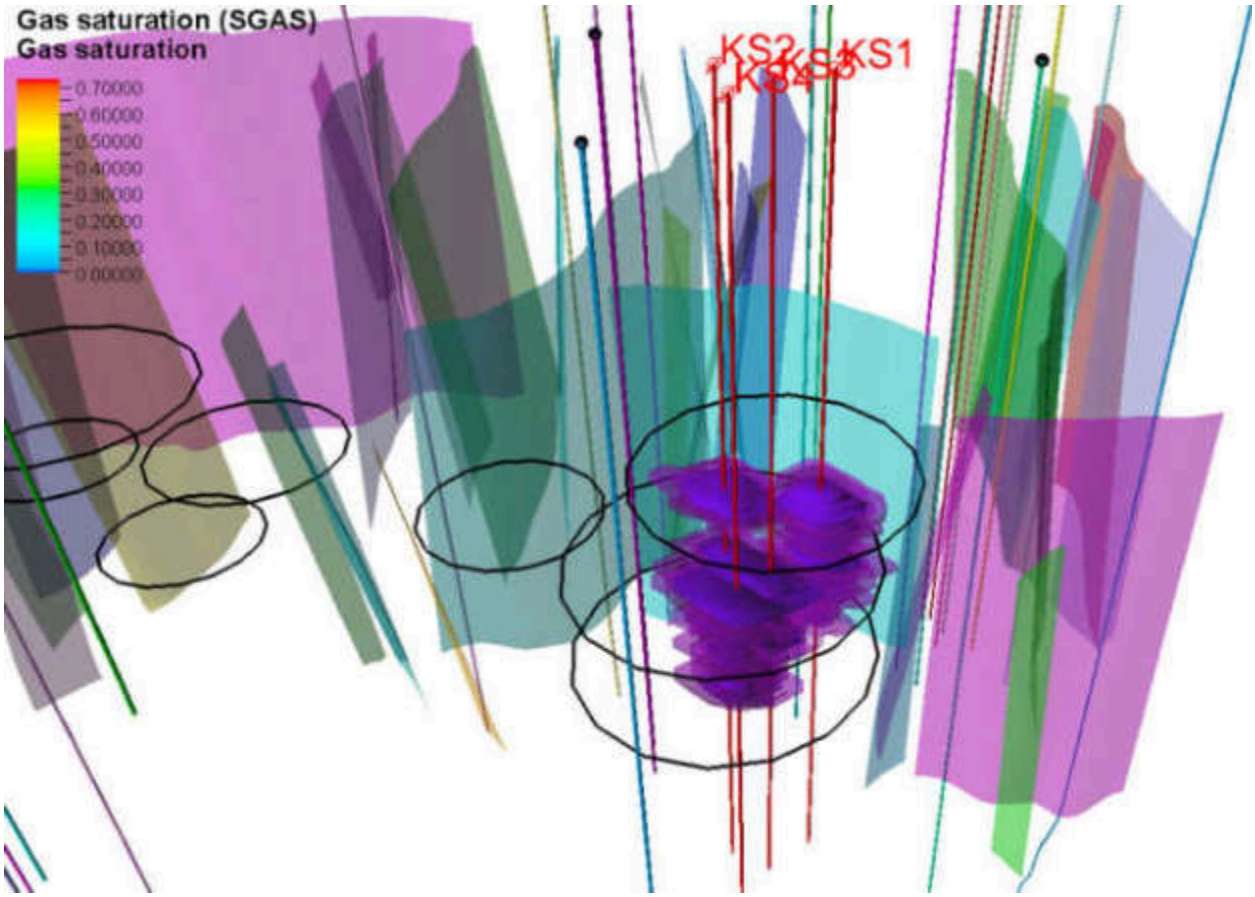


Fig. 2.256 Gas saturation for Scenario 4 after 13 year of injection @Jan 2040

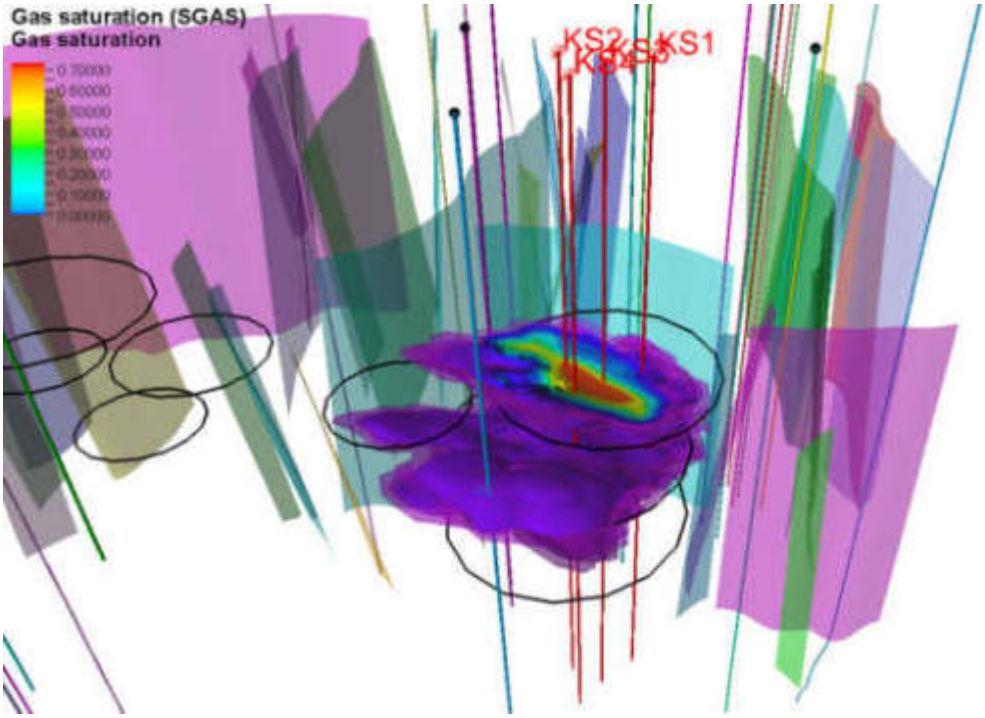


Fig. 2.257 Gas saturation for Scenario 4 after 30 year of injection @Jan 2057

Copyright © SLB. All Rights Reserved. Private & Confidential. Reproduction only by permission.

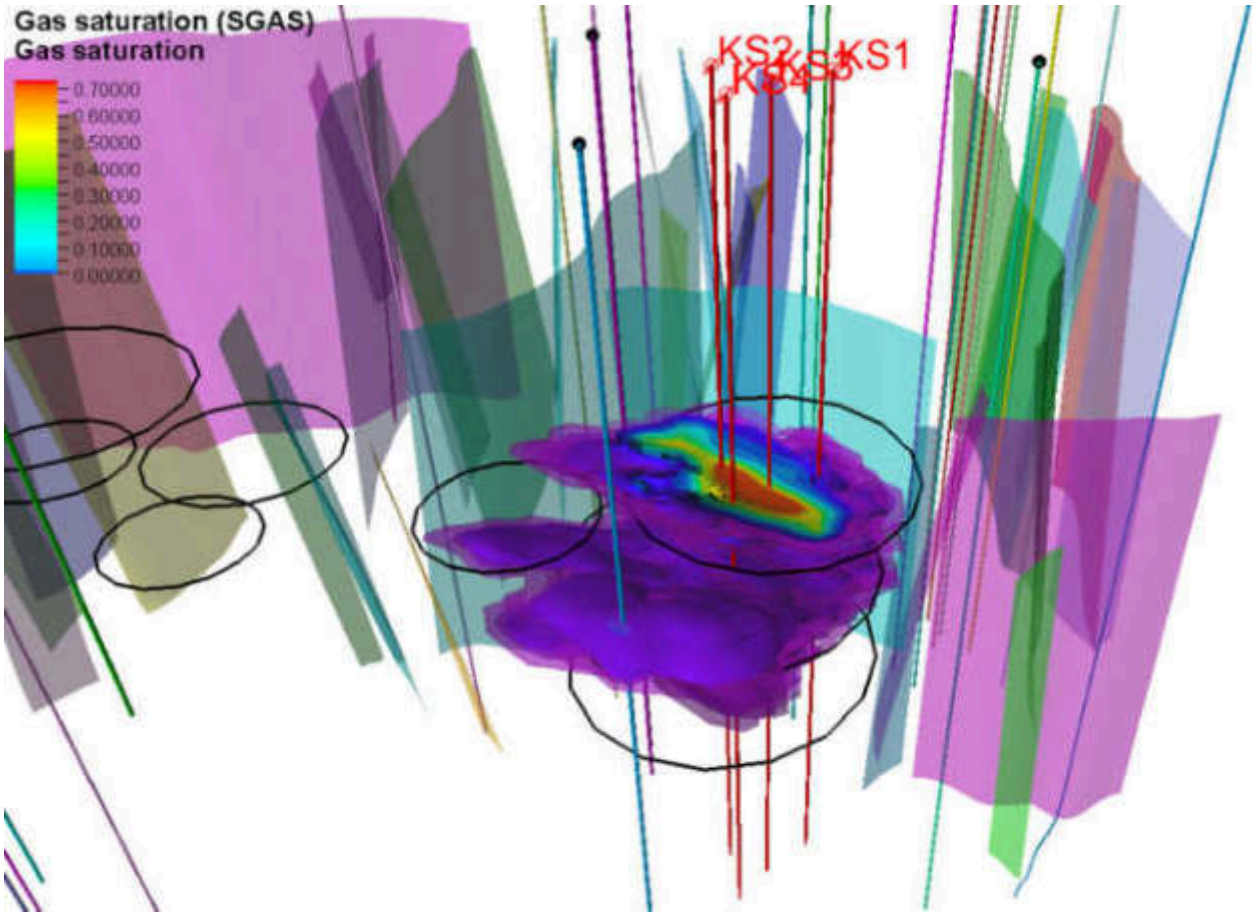


Fig. 2.258 Gas saturation for Scenario 4 after 200 years post injection @Jan 2257

Scenario 4 - 4 deviated wells in Karas Suma-1 area

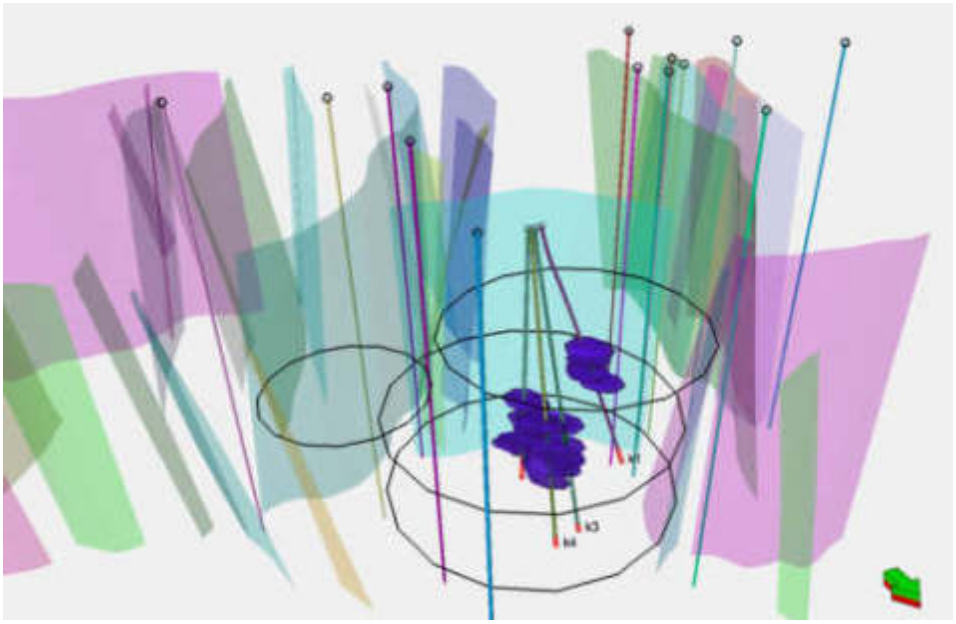


Fig. 2.259 Gas saturation for Scenario 4 deviated wells after 1 year of injection @Jan 2028

Copyright © SLB. All Rights Reserved. Private & Confidential. Reproduction only by permission.

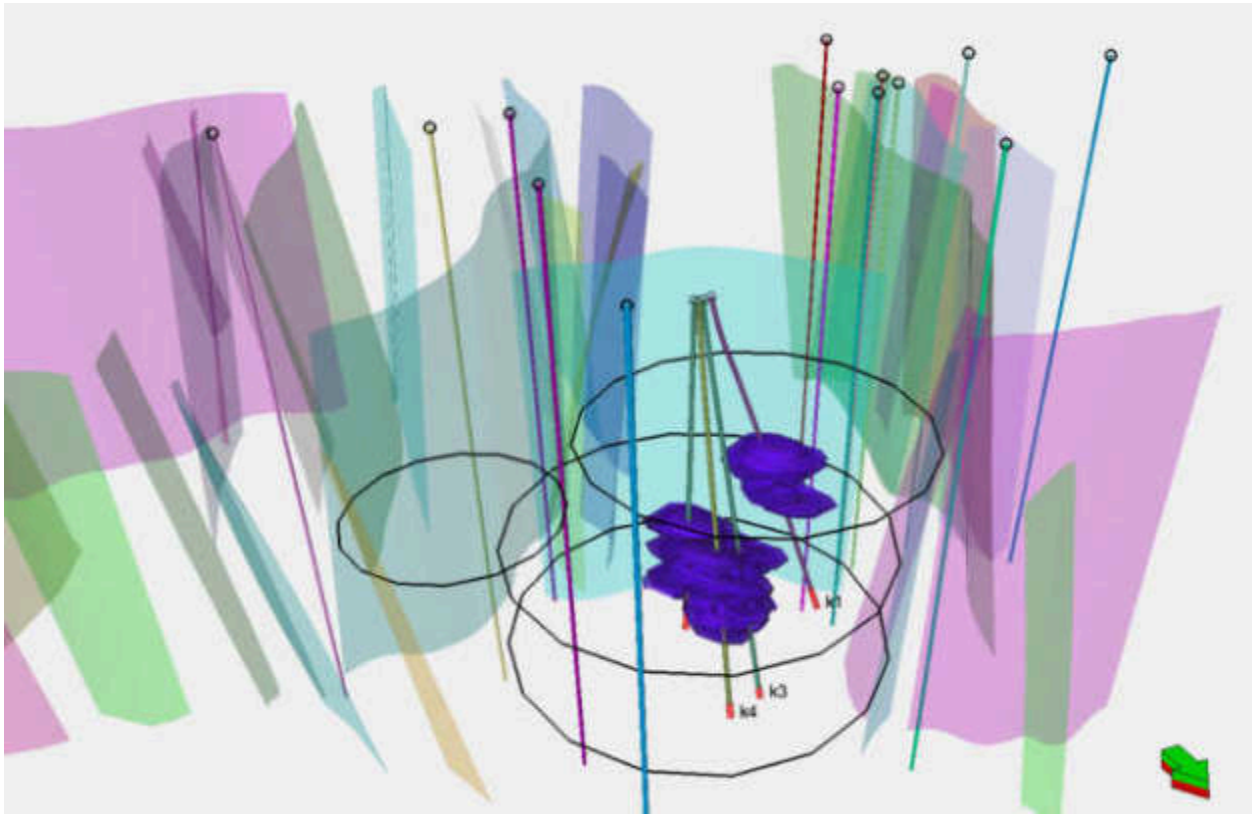


Fig. 2.260 Gas saturation for Scenario 4 deviated wells after 3 year of injection @Jan 2030

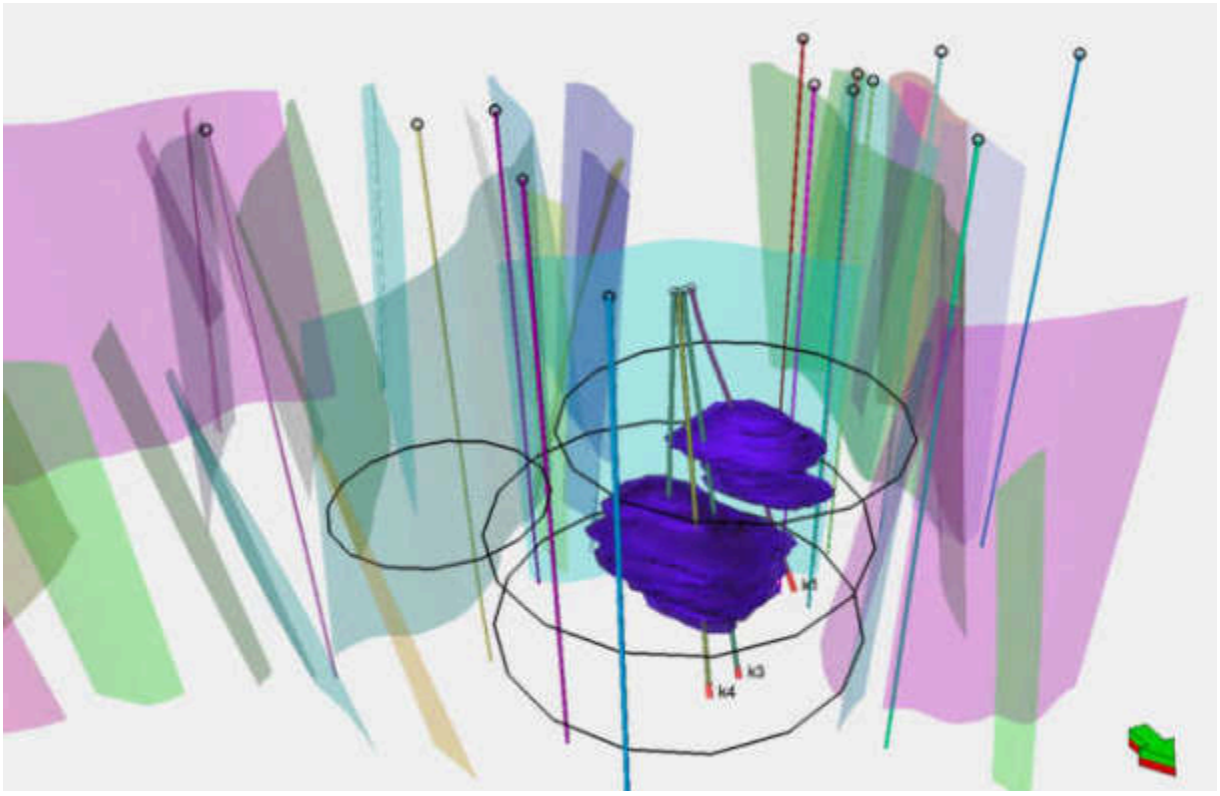


Fig. 2.261 Gas saturation for Scenario 4 deviated wells after 13 year of injection @Jan 2040

Copyright © SLB. All Rights Reserved. Private & Confidential. Reproduction only by permission.

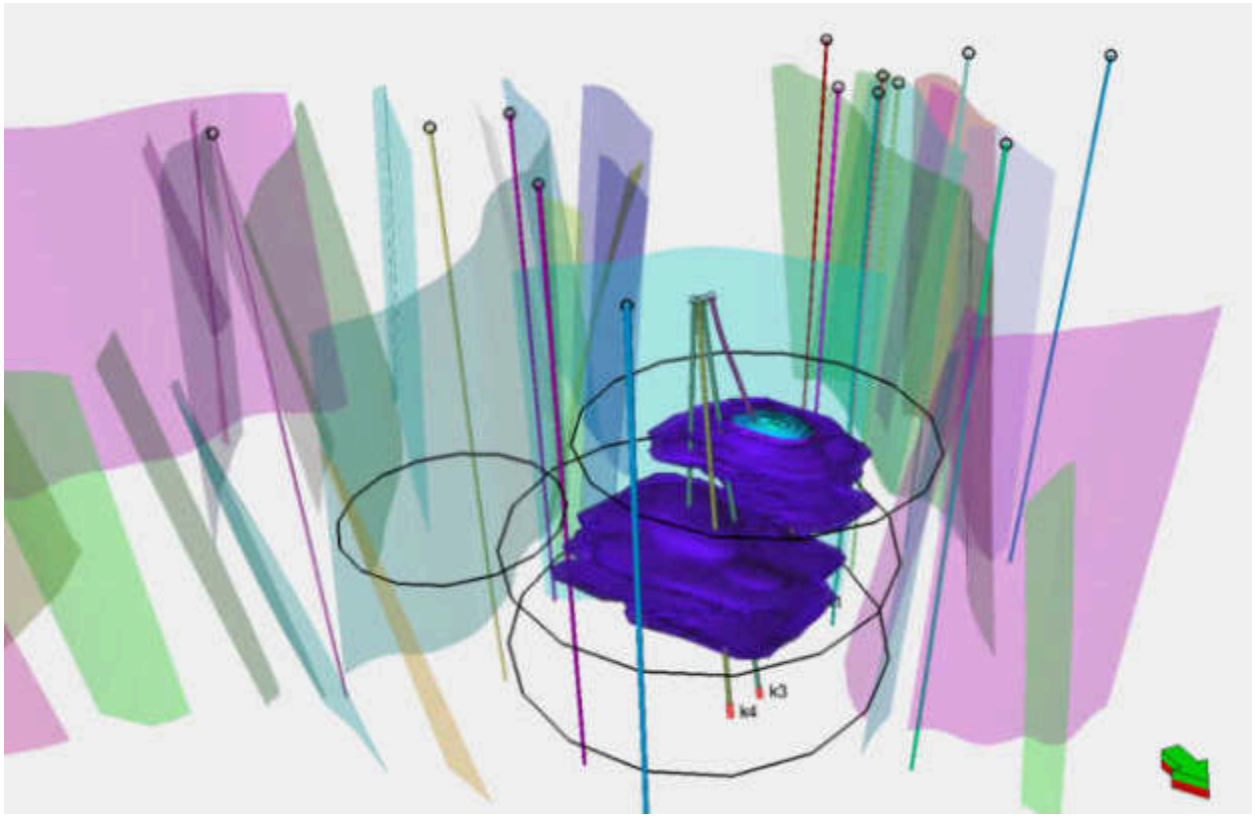


Fig. 2.262 Gas saturation for Scenario 4 deviated wells after 30 year of injection @Jan 2057

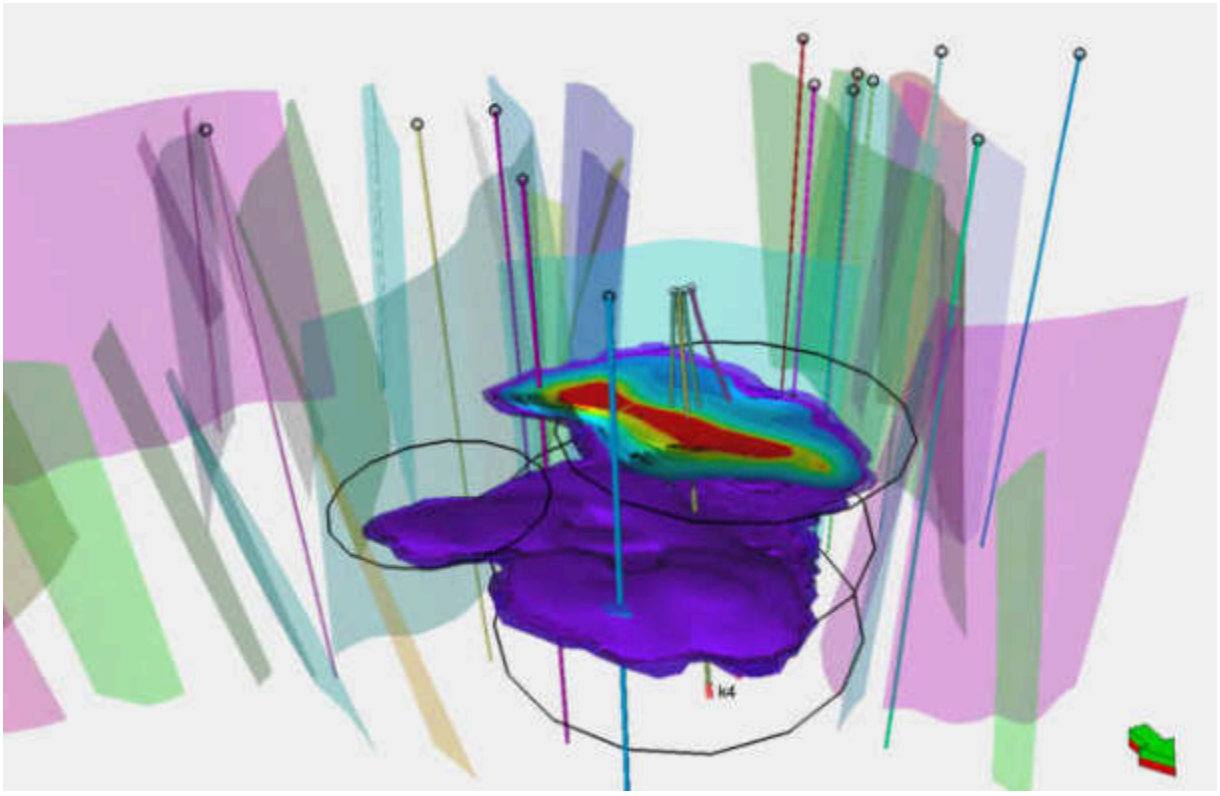


Fig. 2.263 Gas saturation for Scenario 4 deviated wells after 200 years post injection @Jan 2257

Copyright © SLB. All Rights Reserved. Private & Confidential. Reproduction only by permission.

Quantitative analysis shows that the maximum extent of the CO_2 plume does not approach the lateral boundaries of the monitored storage site. At all observed time steps, the plume remains substantially separated from known or suspected leakage pathways such as faults. Potential intersection of the CO_2 plume with insufficiently sealed legacy wells (Karas Suma-1, Bockovci-1, and Krunoslavlje-2) may constitute a potential leakage pathway, allowing upward migration of CO_2 into overlying formations or to the surface. These wells should be evaluated and, where feasible, recompleted with CO_2-resistant materials and verified sealing barriers to ensure long-term integrity under injection conditions. Where recompletion is not achievable, a dedicated mitigation plan should be implemented, including continuous monitoring and predefined operational responses (e.g., injection rate reduction or temporary shut-in).

Simulation results also confirm the effectiveness of residual, solubility, and mineral trapping mechanisms over time, further reducing the mobile CO_2 fraction.

Based on simulation results and supporting geological data, the CO_2 plume is expected to remain fully contained within the storage complex throughout the operational and post-injection phases. There is no evidence of migration toward site boundaries or potential leakage pathways. This outcome provides confidence in the storage security of the site, subject to ongoing monitoring and periodic model updates aligned with regulatory and best-practice requirements.

2.8.6 Risk Assessment and Mitigation

A comprehensive risk assessment was conducted to evaluate potential uncertainties and hazards associated with CO_2 plume migration within the storage reservoir. The primary risks identified relate to the unintentional migration of CO_2 beyond the intended storage boundaries, possible interaction with faults and legacy wellbores, and the potential for leakage through caprock or other geological discontinuities.

Key Risks:

- Plume Migration Toward Boundaries**:** While simulation results indicate that the plume remains contained, heterogeneity in reservoir properties or unrecognized high-permeability pathways could enable lateral plume extension.
- Legacy Well Intersection**:** If the migrating CO_2 plume intersects inadequately sealed legacy wells like Kara Suma-1, Bockovci-1 and Krunoslavlje-2, there is potential for upward migration and escape to shallower formations or the surface of the CO_2. Where feasible, these legacy wells should be assessed and recompleted using CO_2-resistant materials to ensure long-term integrity. If recompletion is not possible, a dedicated mitigation plan should be established, including continuous monitoring, predefined operational responses (e.g., injection rate reduction or temporary shut-in). In addition, drilling new injection wells in alternative areas or incorporating additional storage sites may be considered to redistribute injection volumes and reduce leakage risk associated with legacy wells.
- Fault Intersection**:** If the migrating CO_2 plume intersects with undetected faults, there is potential for upward migration and escape to shallower formations or the surface. Also,

Copyright © SLB. All Rights Reserved. Private & Confidential. Reproduction only by permission.

pressure front approaching the faults raises the risk of potentially triggering microseismic events.
- Caprock Integrity: Variations in caprock continuity or unidentified thin zones may locally reduce sealing capacity, increasing the risk of vertical migration.
- Pressure Build-up: Localized pressure increases during injection could reactivate faults or open new migration pathways if not managed.

Mitigation:

- Robust Site Characterization: High-resolution seismic surveys and well logs are used to delineate faults, caprock attributes, and legacy well locations to minimize uncertainties in site structure and integrity.
- A key risk relates to uncertainties in reservoir properties and their spatial distribution. This risk can be partially mitigated through the drilling more wells and execution of injection tests prior to full-field development. Additionally, increasing the number of injection wells and/or incorporating additional evaluated sites may be required to achieve storage targets if reservoir quality proves lower than expected.
- Dynamic Simulation and Sensitivity Analysis: Multiple injection scenarios, sensitivity studies, and probabilistic modeling are undertaken to understand plume behavior under a range of conditions and identify "worst case" migration pathways.
- Operational Controls**:** Injection rates and pressures are designed to stay well below safety thresholds, avoiding excessive pressure build-up near faults or seals.
- Monitoring Program: A comprehensive monitoring plan incorporating pressure gauges, CO_2-specific tracers to track plume movement and reservoir response during and after injection.
- Contingency Planning: Pre-defined operational and remediation procedures are established, including pressure relief protocols and contingency well drilling, in case monitoring detects unexpected plume movement or leakage.
- Regulatory Compliance: All risk assessment and mitigation strategies are developed and updated in line with regulatory guidelines and international best practices for CO_2 storage.

Through rigorous site characterization, proactive monitoring, conservative operational procedures, and adaptive management, the risks associated with CO_2 plume migration can be minimized, ensuring the long-term safety and effectiveness of the storage operation.

2.8.7 Conclusions and Recommendations

The simulation model was created in close integration with other domains, including geology, geophysics, petrophysics, and geomechanics, ensuring multidisciplinary alignment across the project and all available data integration. This integrated approach strengthened the reliability of simulation results and reinforced consistency in injection scenarios selection.

Site selection was driven by chance-of-success maps, allowing for the prioritization of low risk storage locations with the greatest potential for long-term CO_2 containment and operational

Copyright © SLB. All Rights Reserved. Private & Confidential. Reproduction only by permission.

feasibility. The simulation focused on these pre-selected sites, optimizing the overlapping sites in different zones, supporting a risk-based approach to project planning. Simulation outcomes confirm that, for the top-priority sites identified, the injected CO_2 is expected to remain safely contained within the defined structural and stratigraphic boundaries under all modeled operating scenarios after 200 years post injection. Reservoir pressure behavior remains within safe operational limits, with analysis indicating minimal risk of breaching caprock integrity or fracking reservoir. The main sources of uncertainty relate to heterogeneity and representativeness of available subsurface data.

The integrated simulation and development study indicates that the Karas Suma–Bockovci area represents a technically viable and promising site for long-term CO_2 storage. The selected scenario, based on four deviated injection wells, demonstrates stable injection performance under pressure-constrained conditions, achieving the targeted storage capacity without exceeding fracture limits.

Reservoir behavior is characterized by controlled pressure buildup and predominantly lateral plume migration, supported by favorable permeability distribution and caprock integrity. No significant leakage pathways have been identified within the current model, although some uncertainty remains regarding structural dip toward the Donji Miholjac area, which could influence plume evolution.

The adopted development concept, including pad-based deviated wells, provides an effective balance between subsurface performance and minimized surface impact. Injection profiles at both field and well level confirm that injectivity is governed primarily by reservoir heterogeneity, with acceptable operational margins.

A comprehensive monitoring and risk mitigation framework has been defined, including pressure surveillance, plume tracking, and well integrity management. Contingency measures such as adaptive rate control and temporary shut-in ensure operational flexibility in case of unexpected deviations.

Overall, the results support a positive outlook for project implementation. However, further data acquisition—particularly through the drilled wells and advanced laboratory measurements—is recommended to reduce key uncertainties related to reservoir properties and caprock performance. In parallel, regulatory, environmental, and operational requirements should be refined to ensure full project compliance and long-term storage security.

Deeper reservoirs below Z formation were not targeted for CCS due to increasing uncertainty in reservoir quality, containment integrity, and injectivity, coupled with limited data availability and higher development risk.

Recommendations:

- Proceed with a comprehensive feasibility study at the prioritized site(s) close to wells Karas Suma-1, Bockovci-1 and Krunoslavlje-2 to further assess technical and economic viability,

Copyright © SLB. All Rights Reserved. Private & Confidential. Reproduction only by permission.

aligning the scope of work across all relevant disciplines.

- Plan and execute the drilling of a well(s) at the selected location(s) to acquire essential data, including core samples, in-situ fluid measurements, and pressure profiles. This will reduce geological uncertainties and calibrate both static and dynamic models.
- Continue multidisciplinary data integration, particularly from geology and geomechanics, to iteratively refine modeling and reduce critical uncertainties.
- Update chance-of-success mapping and model inputs as new data from feasibility studies and stratigraphic drilling becomes available.
- Develop a detailed monitoring program for the selected site, ensuring that CO_2 containment within structural and stratigraphic boundaries is validated.
- Maintain operational parameters in accordance with limits established by the integrated modeling results to ensure site integrity.
- Prepare alternative management and mitigation plans in case new data or monitoring indicates deviation from predicted containment or reservoir performance.
- In order to reduce the uncertainty in the model and improve the reservoir engineering understanding of the subsurface, it is recommended to acquire further data in wells(s) to be drilled in the candidate sites what data is required:
  - **Core Analysis** (Conventional & Special Core Analysis) - Continuous core across caprock and reservoir top, with sidewall cores as backup. Direct seal property measurements and SCAL under representative conditions:
    - Capillary pressure (Pc) measurements under CO_2–brine reservoir conditions
    - Threshold Entry Pressure (Pt) – direct measurement
    - Relative permeability of CO_2 and water
    - Interfacial Tension (IFT) and Wettability Measurement.
  - **PVT and Fluid Sampling Program**:
    - Downhole fluid samples acquired via DST (Drill Stem Test) or wireline formation testing (e.g., MDT/RFT)
    - Comprehensive characterization of formation water, including PVT properties, salinity, and ionic composition
  - **Pressure Data Acquisition and Analysis**:
    - Formation pressure measurements acquired using wireline formation testing tools (MDT/RFT)
    - Determination of pressure gradients across reservoir and seal intervals
  - **Well Testing / Dynamic Data Acquisition**:
    - Conduct Drill Stem Tests (DST) or injectivity tests in selected wells
    - Analyze pressure transient data to estimate: Reservoir permeability; Skin factor and Reservoir boundaries and connectivity.

Copyright © SLB. All Rights Reserved. Private & Confidential. Reproduction only by permission.

2.9 Geothermal site selection

This chapter presents a detailed geothermal assessment of the Bockovac area of interest located in the Drava Depression in Croatia. The purpose of the assessment is to evaluate the geothermal potential for electricity generation, which is intended to support the energy demand of carbon capture and storage operations described in the same report.

The first step of the assessment was to select the geological horizons to study based on the first important key requirement: a minimum temperature of 150°C (Table 2.20), to allow for electricity generation at a reasonable level of efficiency. Although binary-cycle (ORC) power plants can be used to generate power from lower-temperature resources (Fig. 2.264 [3]), generation efficiency declines disproportionately at lower temperatures once internal consumption is accounted for. At ~100–120 °C, increasing parasitic loads (from pumps and cooling systems) cause a larger fraction of generated electricity to be consumed by the plant itself rather than exported ([4]; [5]).

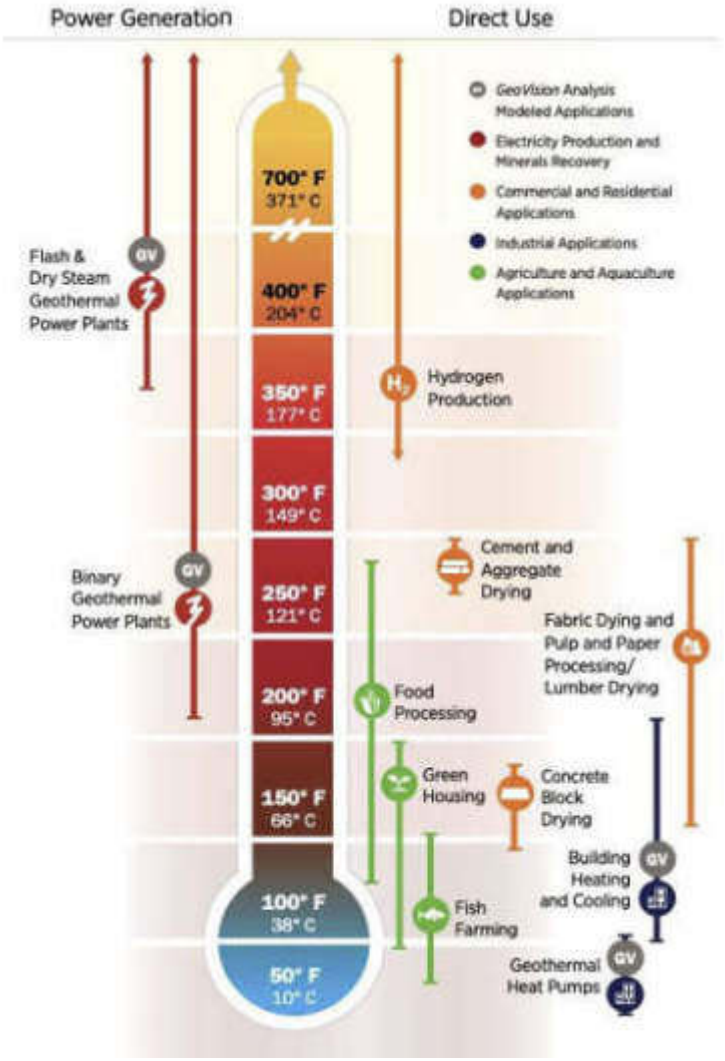


Fig. 2.264 Geothermal energy application based on temperature
Adapted from U.S. Department of Energy (2019).

Copyright © SLB. All Rights Reserved. Private & Confidential. Reproduction only by permission.

Additionally, thermodynamic efficiency and economic performance strongly depend on temperature, with higher inlet temperatures yielding greater turbine power and overall system efficiency; conversely, low-temperature systems (~100 °C) experience lower heat-to-power conversion efficiency and rapidly diminishing returns despite technical feasibility ([6]; [7]).

Finally, targeting resources with initial temperatures of at least 150 °C provides some allowance for decline in production temperatures, which normally occurs as a project is operated and cooler injected water returns to the zones of production. It also helps to cushion against deviations of real development results from predicted outcomes ([8]; [9]).

In Croatian (Fig. 2.2), Rs5 is commonly used near the Lower/Upper Pannonian boundary and Rs7 near the Sarmatian–Pannonian transition; both are routinely mapped as depth surfaces (2.2 Seismic interpretation) and can be interpolated as regional horizons ([10]; [11]). However, the same marker can correspond to different lithostratigraphic labels (e.g. Valpovo, Koprivnica sandstone) in different local databases, so this assessment treats Rs5 and Rs7 strictly as mappable e-log horizons tied to available seismic interpretation.

The identification of these layers is complicated by discontinuities and erosional processes, making correlation across the region uncertain. Additionally, in this work, only two e-log markers in the Rs list were interpreted in the 3D seismic survey: Rs5 and Rs7. Consequently, the general correlation between regional e-log markers and actual stratigraphic level could complicate the interpretation and selection of the geothermal targets.

2.9.1 Geothermal site selection methodology

The geothermal screening relies on a combination of thermal, reservoir, structural, and environmental criteria. Temperature is considered the primary controlling factor, as described above: with a target threshold of 150°C. Reservoir quality is evaluated based on porosity, permeability, and fluid properties. Structural integrity and containment conditions are also assessed to ensure safe and sustainable circulation of geothermal fluids. Environmental constraints such as protected areas, infrastructure, and regulatory limitations are incorporated as exclusion criteria (Fig. 2.265).

Copyright © SLB. All Rights Reserved. Private & Confidential. Reproduction only by permission.

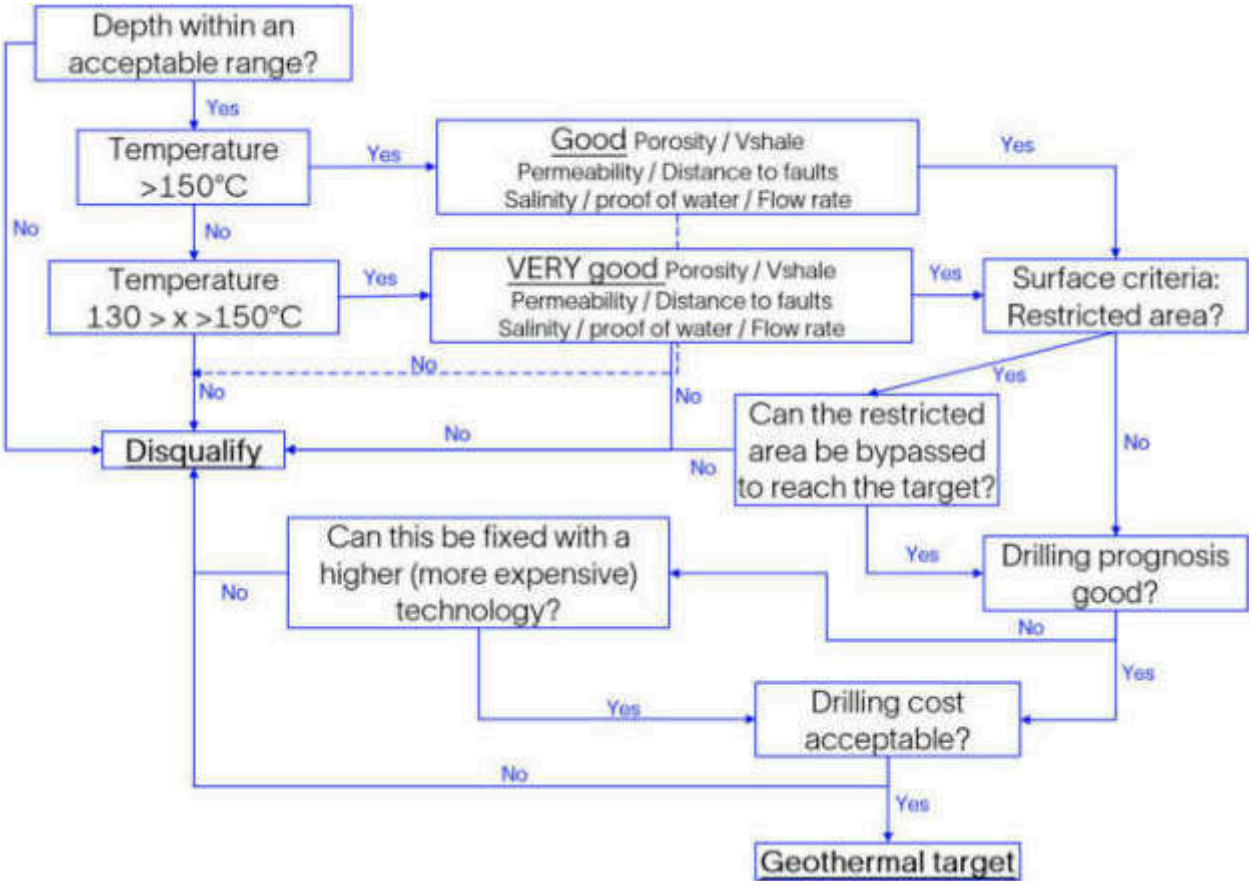


Fig. 2.265 Workflow diagram for geothermal screening and chance of success (COS) methodology

Some criteria act as "**Go**" or "**No Go**" gates. Some criteria are hard and non-negotiable, and failure to meet them automatically disqualifies the site.

Heat / Temperature:

- The depth of the shallowest point of the target reservoir is sufficient to ensure economically useful temperatures for electricity generation (>150°C).

Reservoir Quality (Permeability & Fluids)

- The reservoir has sufficient natural permeability and transmissivity to sustain commercial flow rates.
- **If Data Permit**: Formation fluids are present, mobile, and compatible with long-term circulation without prohibitive scaling or corrosion issues (low salinity).

Containment & Integrity

- The site is sufficiently far from legacy wells (Fig. 2.5) with documented integrity issues and/or from oil and gas activities.
- While a perfect seal is not required, the geological setting must allow controlled circulation of

Copyright © SLB. All Rights Reserved. Private & Confidential. Reproduction only by permission.

fluids; major uncontrolled fluid losses or hydraulic communication with shallow aquifers result in automatic disqualification (faults connection with shallower aquifers).

Surface & Environmental Constraints

- No critical conflicts exist with ecological protected areas Fig. 2.266, sanitary protected areas Fig. 2.267, inhabited areas Fig. 2.268, roads & railroads; Fig. 2.269, or sensitive groundwater resources that would prohibit permitting or safe operations.

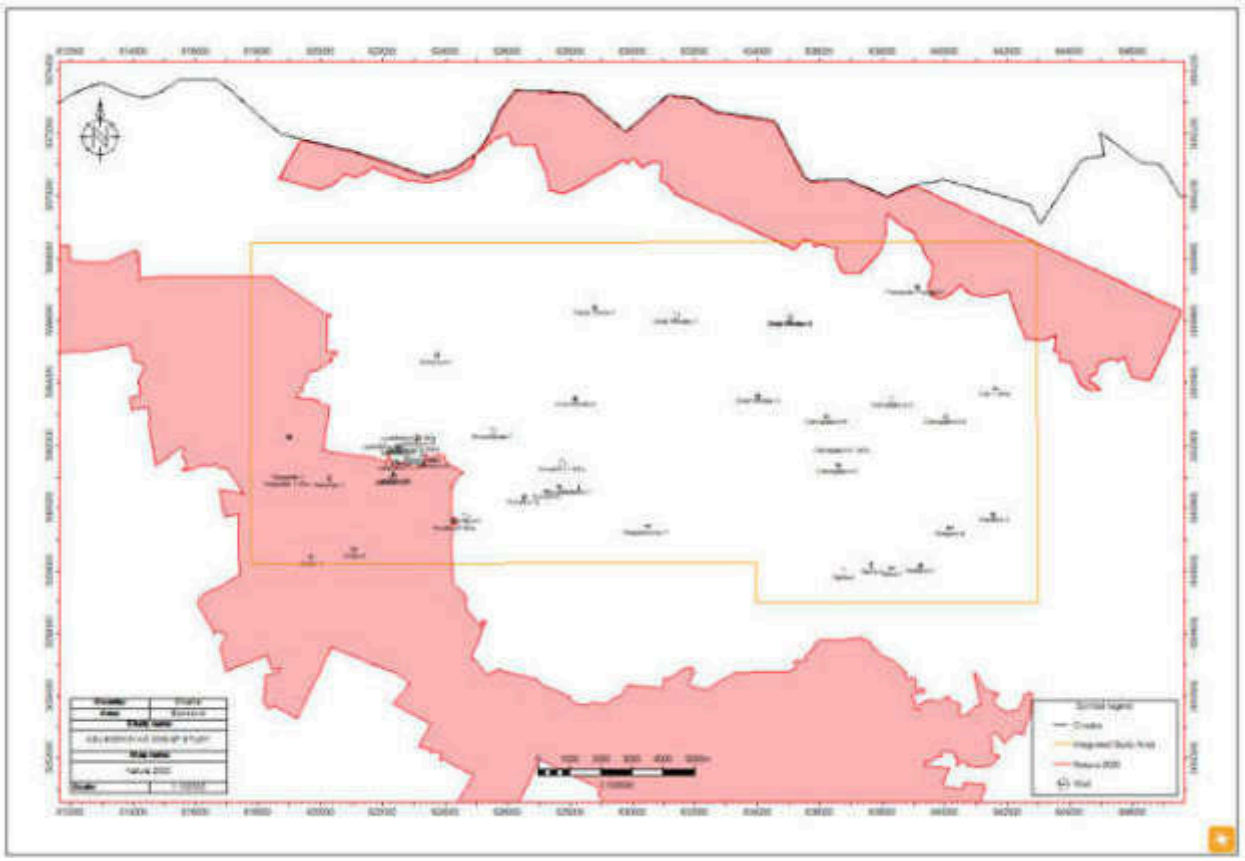


Fig. 2.266 Location of Natura 2000 protected ecological zones
Extent of Natura 2000 areas in the area of interest, representing protected ecological zones designated under the EU Habitats and Birds Directives

Copyright © SLB. All Rights Reserved. Private & Confidential. Reproduction only by permission.

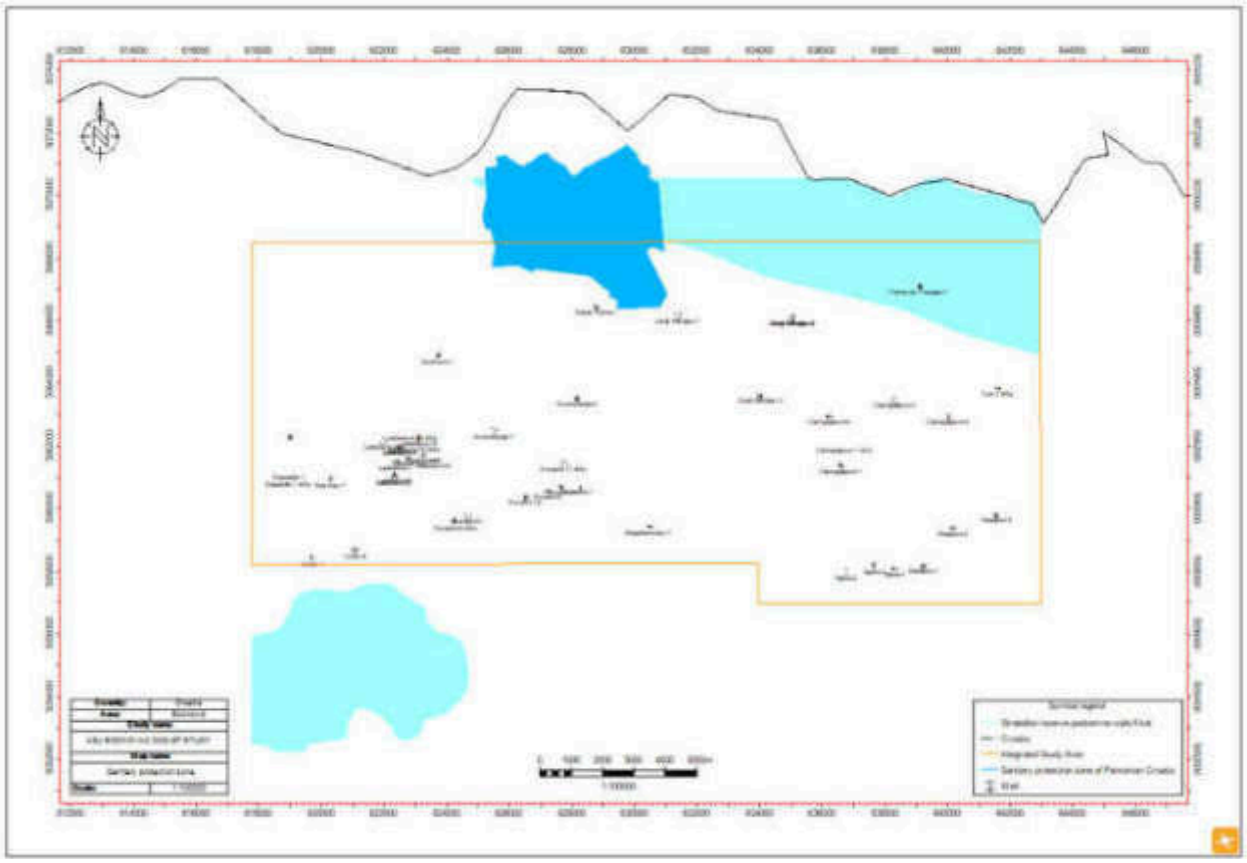


Fig. 2.267 location of regulatory sanitary protection zones
Extent of sanitary protection zones in the area of interest, designated around groundwater and surface water sources for public supply, with regulated land-use constraints to preserve water quality.

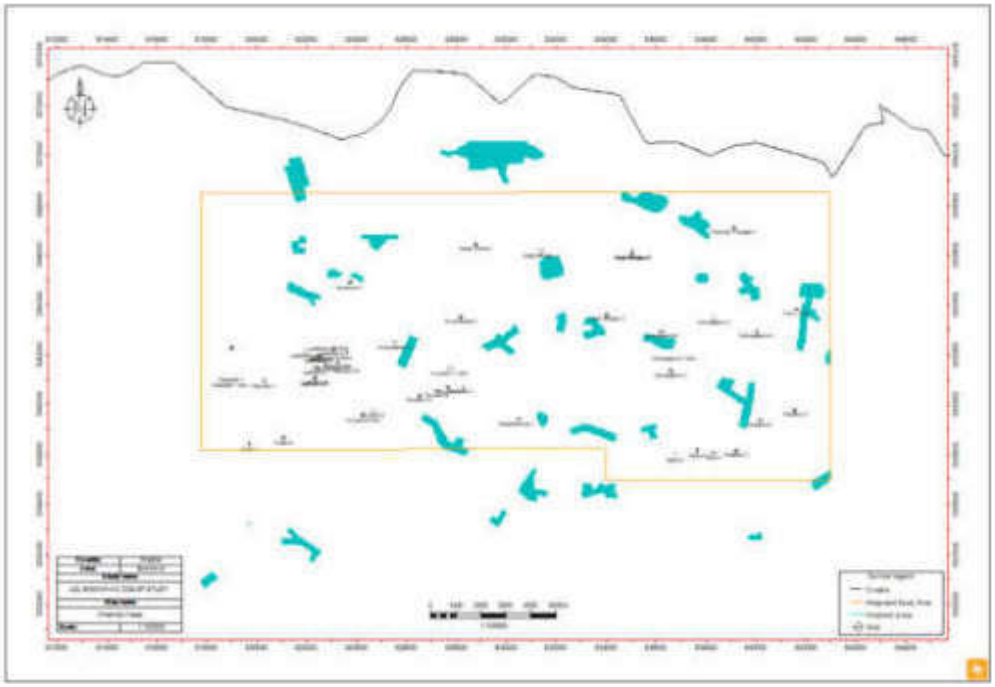


Fig. 2.268 Location of inhabited areas in the area of interest

Copyright © SLB. All Rights Reserved. Private & Confidential. Reproduction only by permission.

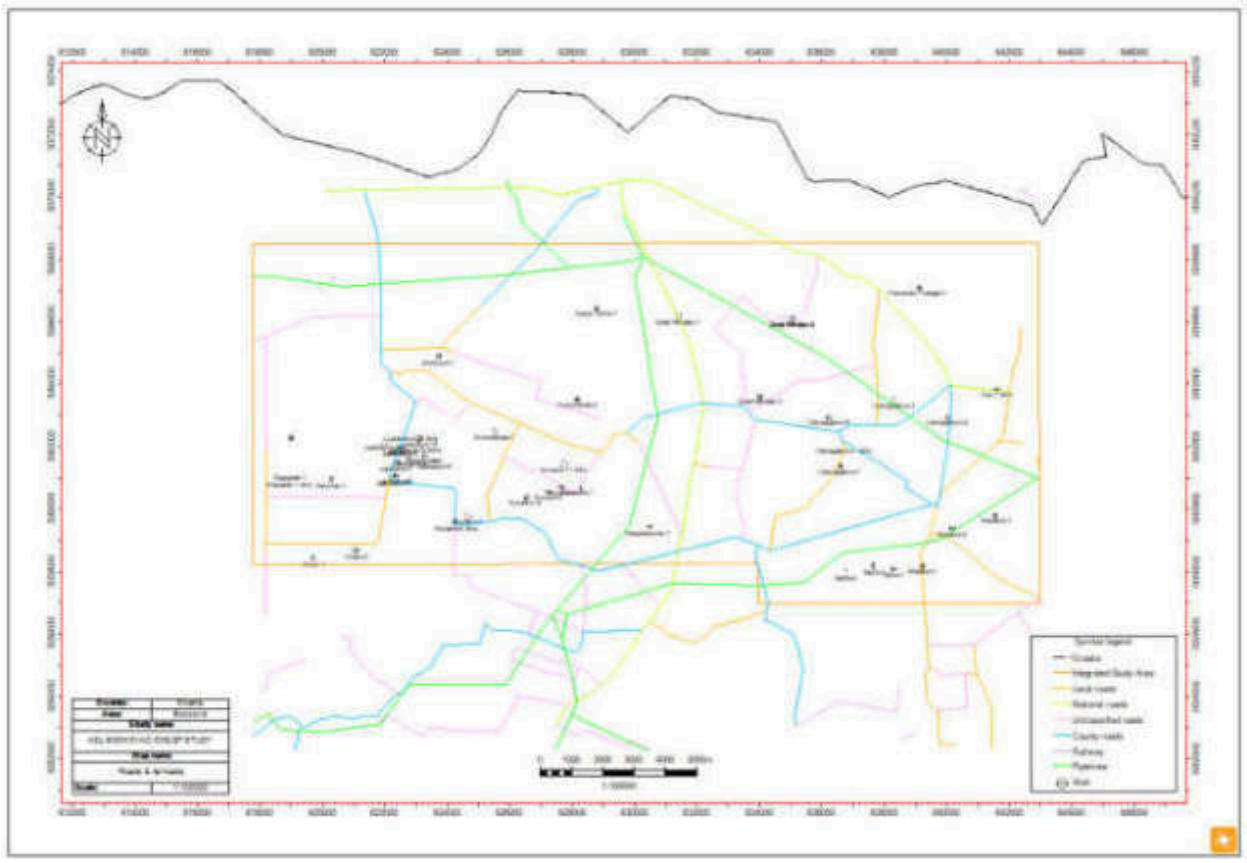


Fig. 2.269 Location of pipelines, roads (primary & secondary) and railroads

2.9.2 Rs5 Geothermal Reservoir Evaluation

Rs5 is a regional e-log correlation marker widely used in the Croatian part of the Pannonian Basin System. In the Drava Depression, it is commonly treated as approximating the Lower/Upper Pannonian boundary, but its stratigraphic expression can be locally obscured by erosion, non-deposition, and faulting ([1]; [10]; [11]). Consequently, Rs5 was evaluated here primarily as a mappable subsurface horizon (interpreted in the available 3D seismic) rather than as a single, laterally continuous lithostratigraphic formation.

Data compilation and property modelling.

For Rs5, nine gridded parameter maps were generated over the area of interest:

1. Rs5 depth structure,
2. Average temperature from a purely data-driven temperature property model (Fig. 2.270 (a)),
3. Average temperature from a basin-physics thermal model (using heat flow, surface temperature, and formation thermal conductivities) (Fig. 2.271 (a)),
4. Distance to temperature points to account for the uncertainty of the temperature data points
5. Volume of shale (Vsh or VSH) derived from gamma-ray interpretation and averaged over the Rs5 interval (Fig. 2.272 (a)),

Copyright © SLB. All Rights Reserved. Private & Confidential. Reproduction only by permission.

6. Effective porosity model constrained by log porosity and core porosity (Fig. 2.272 (b)),
7. "Permeability model 1", derived from porosity–permeability relationships (Fig. 2.270 (b)),
8. "Permeability model 2" derived from facies-dependent permeability end-members (Fig. 2.271 (b)),
9. Distance to faults as a permeability enhancer,
10. Rs5 thickness

The use of parallel models for temperature and permeability follows geothermal play-fairway best practice in which multiple lines of evidence are used to reduce bias from a single proxy ([12]; [13]). A distance-to-temperature-control modifier was also applied to down-weight areas far from temperature measurements.

Parameter-to-probability transform (Rs5)

Each parameter map was transformed into a chance-of-success maps using fixed thresholds. Eight parameter maps were used for the final composite chance of success calculation (temperature models, permeability models, Vsh and porosity, distance to temperature points and distance to faults). The transform was deliberately non-binary (minimum score >0) to avoid discarding marginal resources that may remain viable for direct use or smaller plants; nevertheless, the screening threshold for electricity generation was kept at ≥150 °C because net export in low-temperature binary plants can be strongly reduced by internal consumption and thermodynamic limits (see explanation 2.9 Geothermal site selection [3]; [9]; [4]; [5]).

Composite chance of success calculation and Rs5 results

The composite chance of success for Rs5 (COS_Rs5) was computed as the multiplicative combination of the individual probability layers (Fig. 2.270, Fig. 2.271 and Fig. 2.272, consistent with conservative common-risk-element practice where missing heat or permeability is penalized ([12]; [13]). With eight contributing parameters, typical composite values fall in the 0.05–0.30 range even when individual scores are high (e.g., $0.8^8 \approx 0.17$), which is why results were displayed on a 0–0.30 scale.

The Rs5 composite map highlights two locally favorable areas (Fig. 2.273): Target A (west of Bockovci-1) driven by depth-related temperature potential and Target B (around Rasovac-1) driven by high porosity/permeability but more marginal temperatures at Rs5 level. A third corridor between Kucanci-11 Alfa well and Magadenovac-1 well shows good reservoir properties, but the central (unnamed) target was discarded due to insufficient thermal conditions, with predicted temperatures consistently below the minimum threshold (T < 130 °C). The southeastern target, located near the Marijanci-2 well, was also excluded because most of its extent lies outside the AOI, and the reliability of the mapped properties is low due to poor well control and edge effects associated with interpolation at the dataset boundary.

Thickness and continuity as the dominant risk for Rs5

Copyright © SLB. All Rights Reserved. Private & Confidential. Reproduction only by permission.

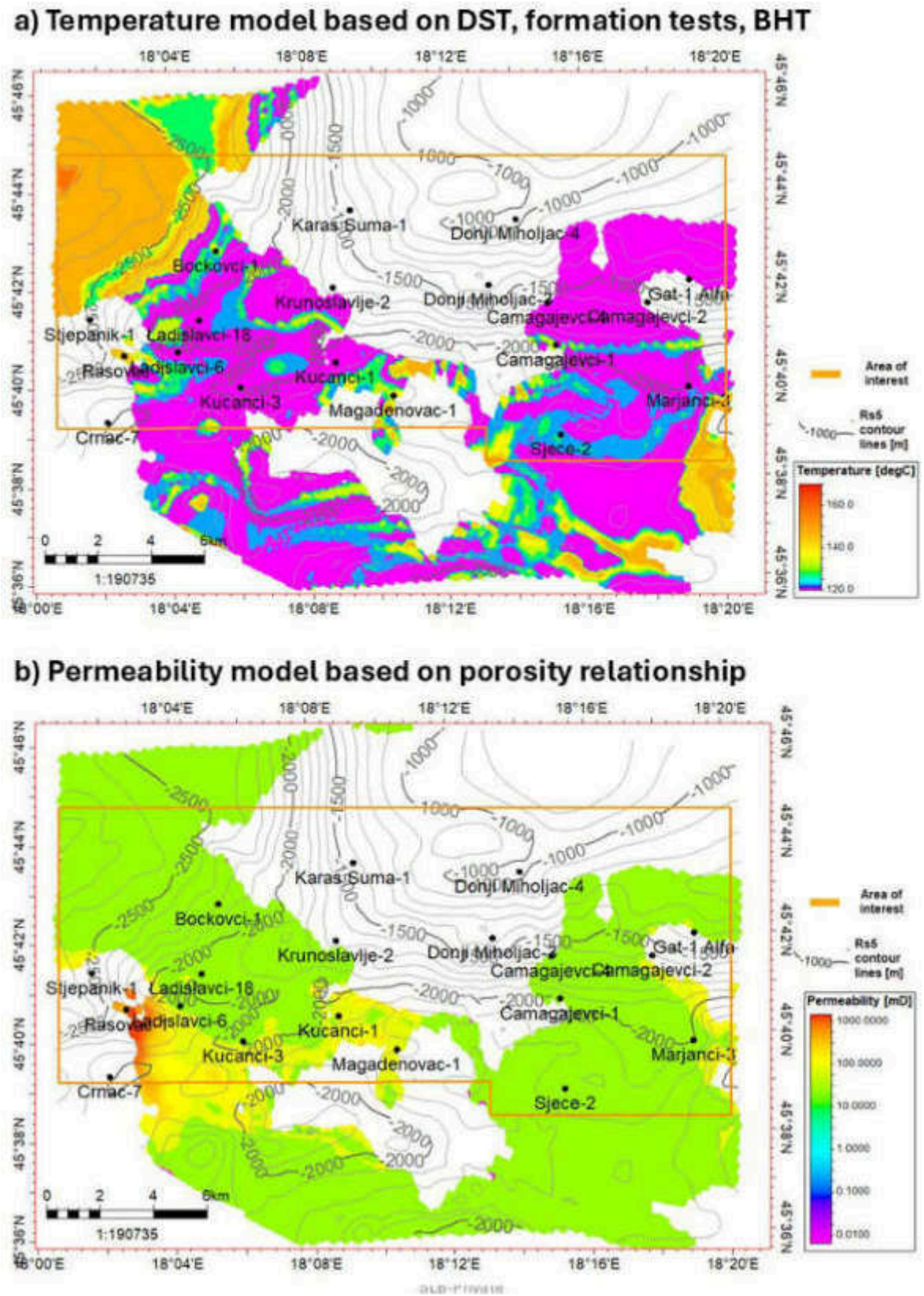


Fig. 2.270 Rs5 Temperature and Permeability model 1
Rs5 (a) average temperature from a purely data-driven temperature property model and (b) "Permeability model 1" derived from porosity–permeability relationships

Copyright © SLB. All Rights Reserved. Private & Confidential. Reproduction only by permission.

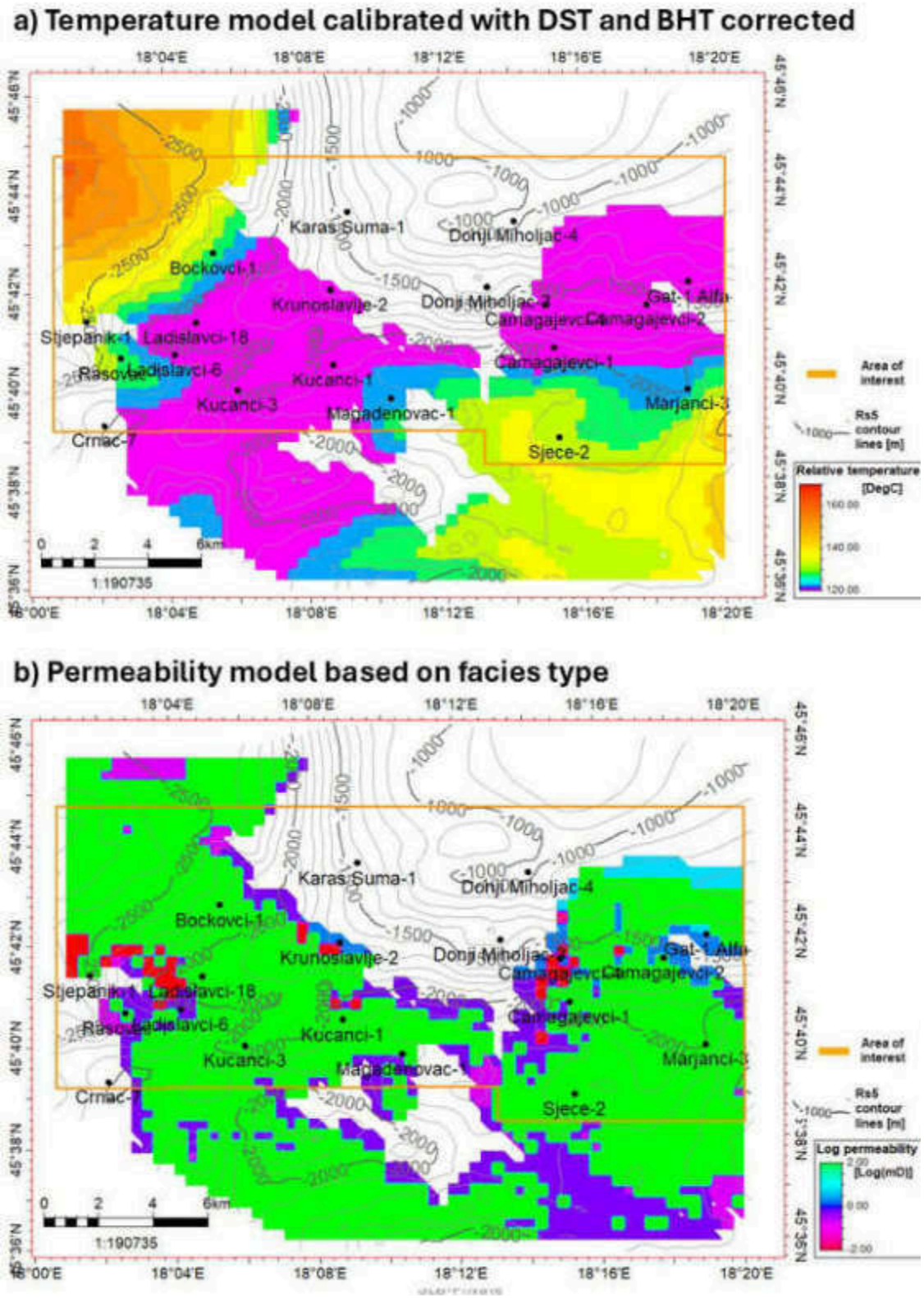


Fig. 2.271 Rs5 Temperature and Permeability model 2

Rs5 (a) average temperature from a basin-physics thermal model (using heat flow, surface temperature, and formation thermal conductivities)
and (b) "Permeability model 2" derived from facies-dependent permeability end-members

Copyright © SLB. All Rights Reserved. Private & Confidential. Reproduction only by permission.

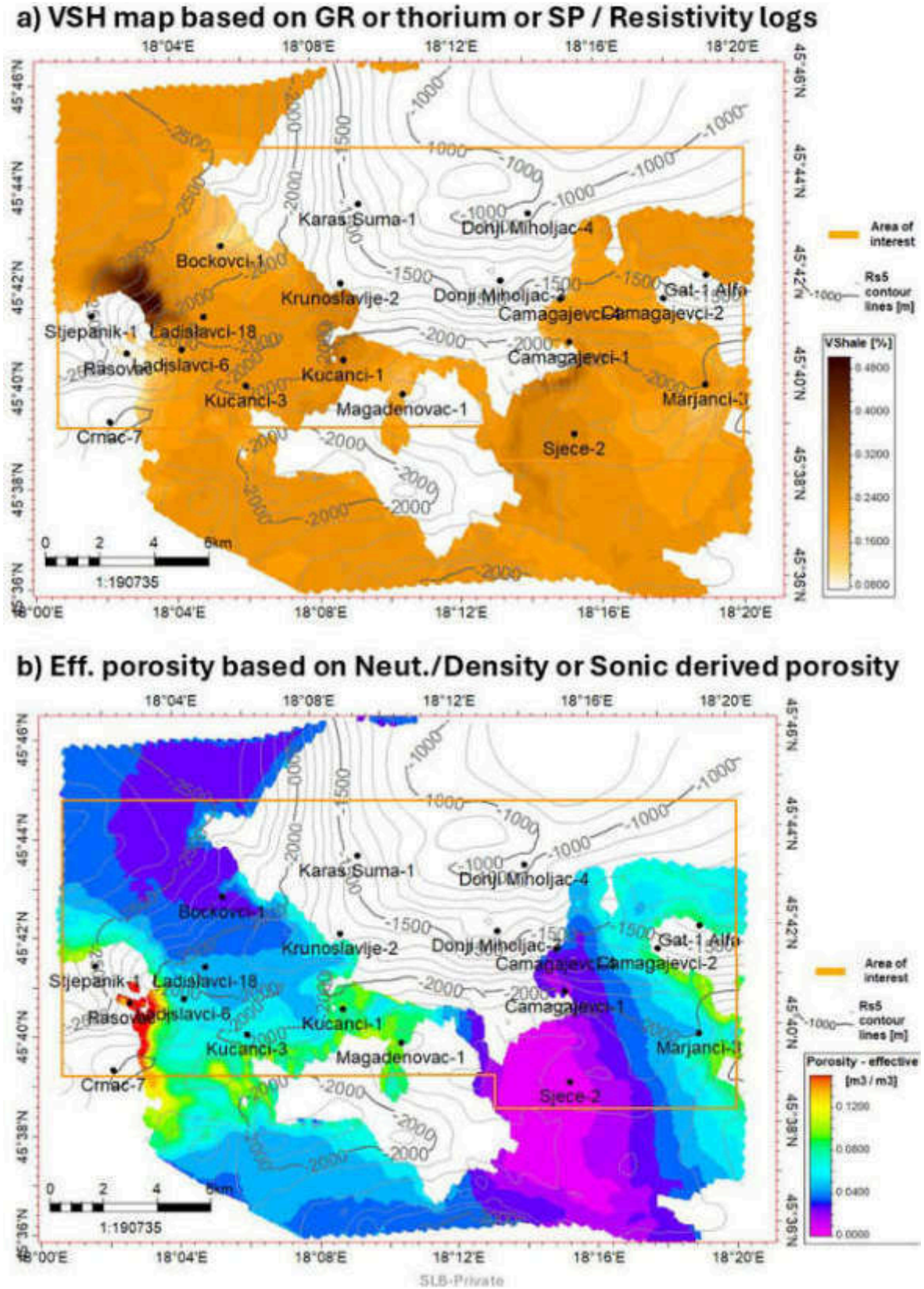


Fig. 2.272 Rs5 volume of shale (VSH) and effective porosity model
(a) average volume of shale (VSH) derived from gamma-ray interpretation and (b) average effective porosity model constrained by log porosity and core porosity

Copyright © SLB. All Rights Reserved. Private & Confidential. Reproduction only by permission.

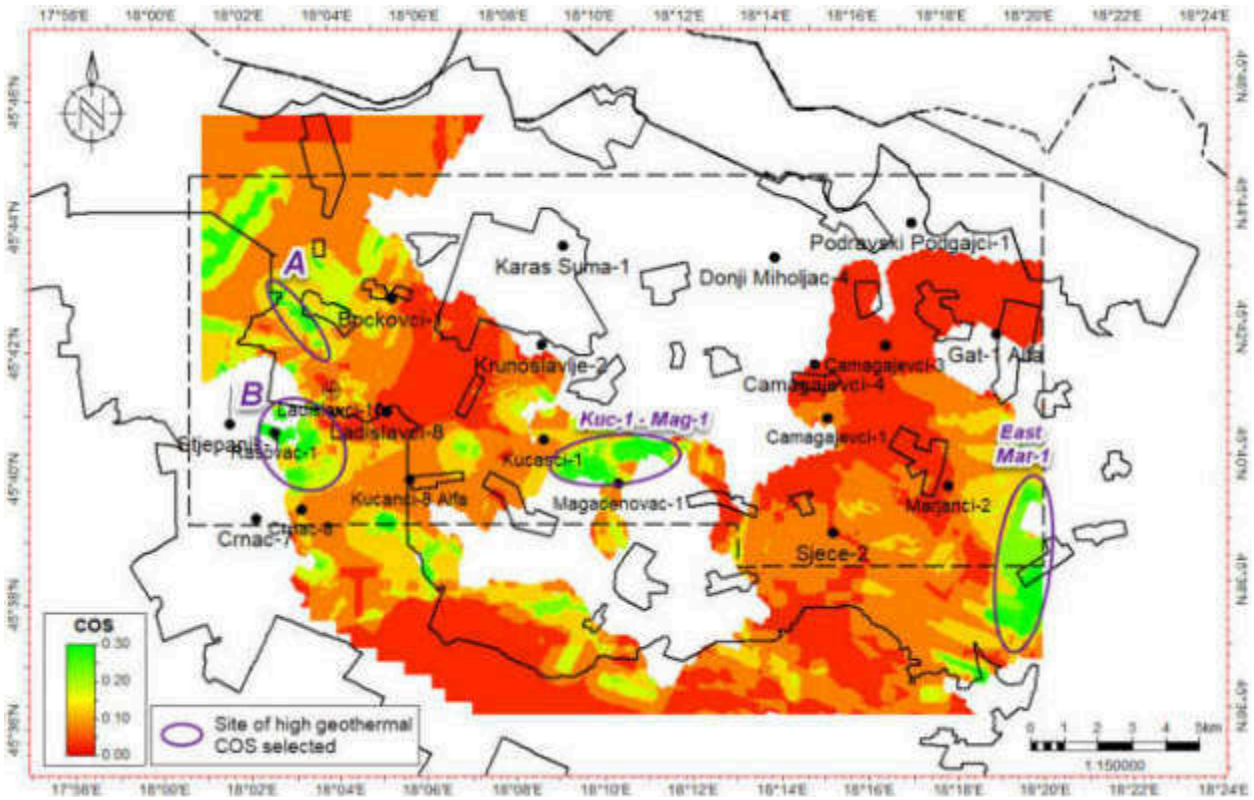


Fig. 2.273 Rs5 Geothermal COS map
Geothermal COS map for the Rs5 interval based on combined subsurface parameters

When the minimum net thickness criterion was applied as a hard 'no-go' gate (stand-alone reservoir thickness <~30 m), the chance of success for Rs5 dropped to very low. Rs5 is absent or poorly expressed in multiple wells, consistent with local truncation around Neogene unconformities [1]. Moreover, where Rs5 is present, interpreted thickness is frequently below the vertical resolution of legacy 3D seismic at these depths; beds thinner than ~λ/4 to ~λ/8 are difficult to resolve and map reliably due to tuning and interference ([14]; [15]; [16]).

Rs5 stand-alone chance of success statement

Rs5 has moderate probability for reservoir quality where present, but low probability for sufficient thickness and lateral continuity, with moderate-to-high uncertainty in the deepest, warmest parts due to limited well control. Rs5 is therefore not recommended as a stand-alone geothermal target; its contribution is best captured within a stacked-reservoir concept together with Rs7.

2.9.3 Rs7 Geothermal Reservoir Evaluation

Rs7 is the second key regional e-log marker interpreted in the 3D seismic dataset. In the Drava Depression, it is commonly correlated near the Sarmatian–Pannonian transition and, like Rs5, its log expression can vary due to facies changes and unconformities (Malvić and Cvetković, 2014; Špelić et al., 2016). Compared with Rs5, Rs7 generally shows better lateral persistence in the available well and seismic control, which improves mapping confidence.

Copyright © SLB. All Rights Reserved. Private & Confidential. Reproduction only by permission.

Data handling and probability workflow.

The same multi-proxy COS workflow used for Rs5 was applied at Rs7, including two temperature models (Fig. 2.274 (a) and Fig. 2.275 (a)), distance to temperature points, effective porosity (Fig. 2.276 (b)), Vsh (inverse) (Fig. 2.276 (a)), two permeability models (Fig. 2.274 (b) and Fig. 2.275 (b)), and distance to faults as a permeability enhancer. The fault-distance proxy reflects the widely observed role of fault damage zones in providing secondary permeability pathways in geothermal systems, although faults may also act as barriers depending on gouge content and stress state.

RS7 results and Target C definition.

The Rs7 composite COS map identifies one principal high-probability zone (Target C; Fig. 2.277) in the central AOI between Stjepanik-1 and Rasovac-1 wells, driven by low Vsh, very high effective porosity and high permeability in both permeability models. Temperatures at Rs7 level are generally predicted in the 130–150 °C class, meaning Rs7 alone is close to, but not consistently above, the electricity-generation screening threshold.

Across the AOI, the highest temperature zones (northwest and southeast structural lows) do not perfectly overlap the best reservoir-quality corridor (east–west trending porosity/permeability fairway). This mismatch demonstrates that Rs7 prospectivity is sensitive to the combination rule and confirms that a conservative multiplicative approach is appropriate because it penalises areas lacking either heat or transmissivity.

Key geological risks for RS7:

1. Thickness: Rs7 remains thin and locally variable, and parts of the unit may fall near seismic tuning limits.
2. Temperature margin: Rs7 is frequently sub-150 °C, which increases sensitivity to flow rate and parasitic loads
3. Environmental constraints: the centroid of Target C lies within Natura 2000 protected zone, requiring surface locations outside the restricted area and deviated drilling to access the target.
4. Structural uncertainty for the identified Target C only: the target is bounded by faults; proximity to faults may increase permeability but could also create compartmentalisation or vertical connectivity risks that must be quantified by fault-seal and geomechanical assessment.

Rs7 chance of success statement.

Rs7 shows a higher geological chance of success than Rs5 for continuity and mapping confidence, and it contains the best reservoir-quality sweet spot identified in this study (Target C). Nevertheless, its temperature margin and thin-bed uncertainty mean Rs7 is best developed as part of a stacked Rs5–Rs7 play (Targets B + C).

Copyright © SLB. All Rights Reserved. Private & Confidential. Reproduction only by permission.

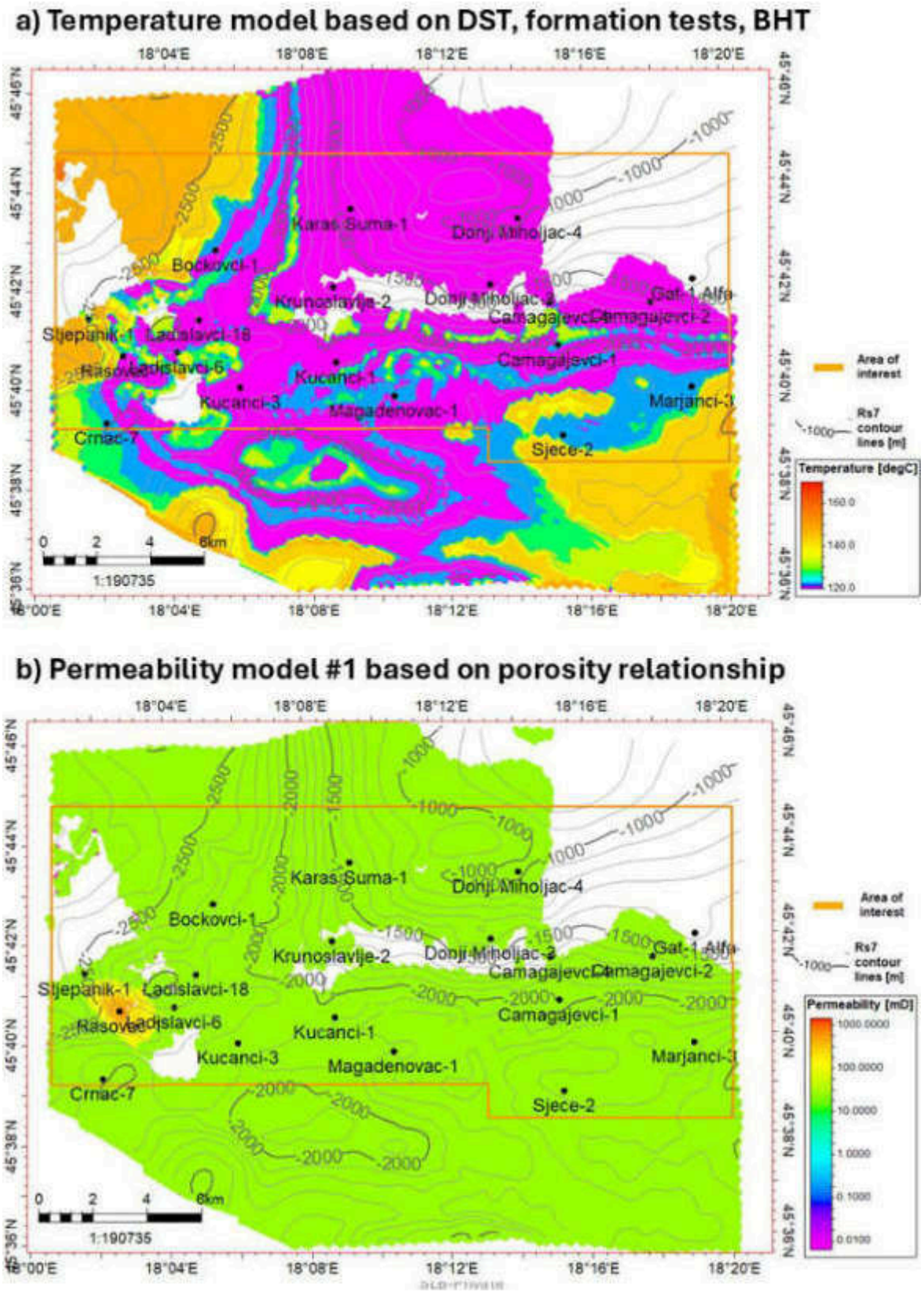


Fig. 2.274 Rs7 temperature model and permeability model 1
(a) average temperature from a purely data-driven temperature property model and (b) "permeability model 1" derived from porosity–permeability relationships

Copyright © SLB. All Rights Reserved. Private & Confidential. Reproduction only by permission.

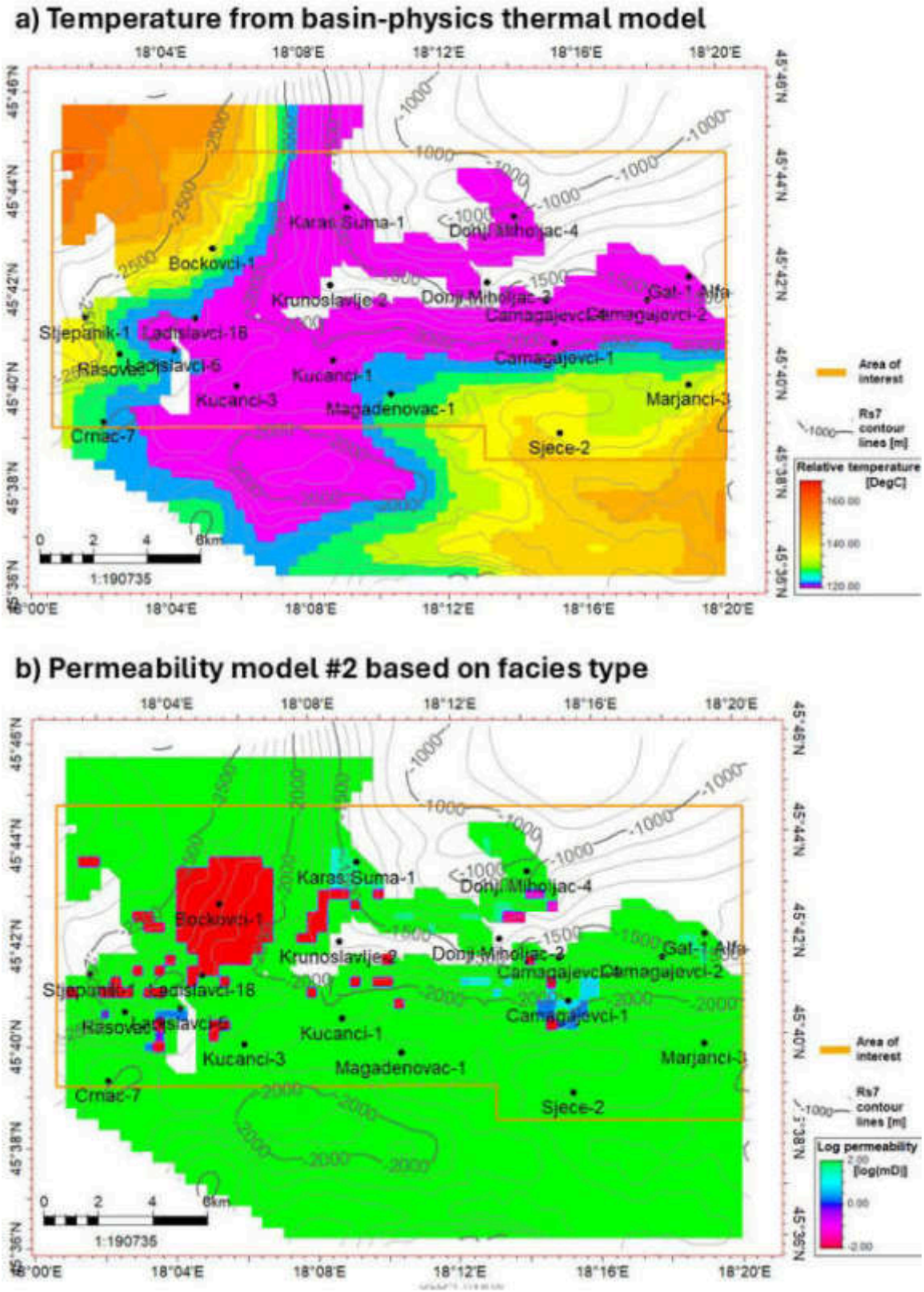


Fig. 2.275 Rs7 temperature model and permeability model 2
(a) average temperature from a basin-physics thermal model (using heat flow, surface temperature, and formation thermal conductivities)
and (b) "permeability model 2" derived from facies-dependent permeability end-members

Copyright © SLB. All Rights Reserved. Private & Confidential. Reproduction only by permission.

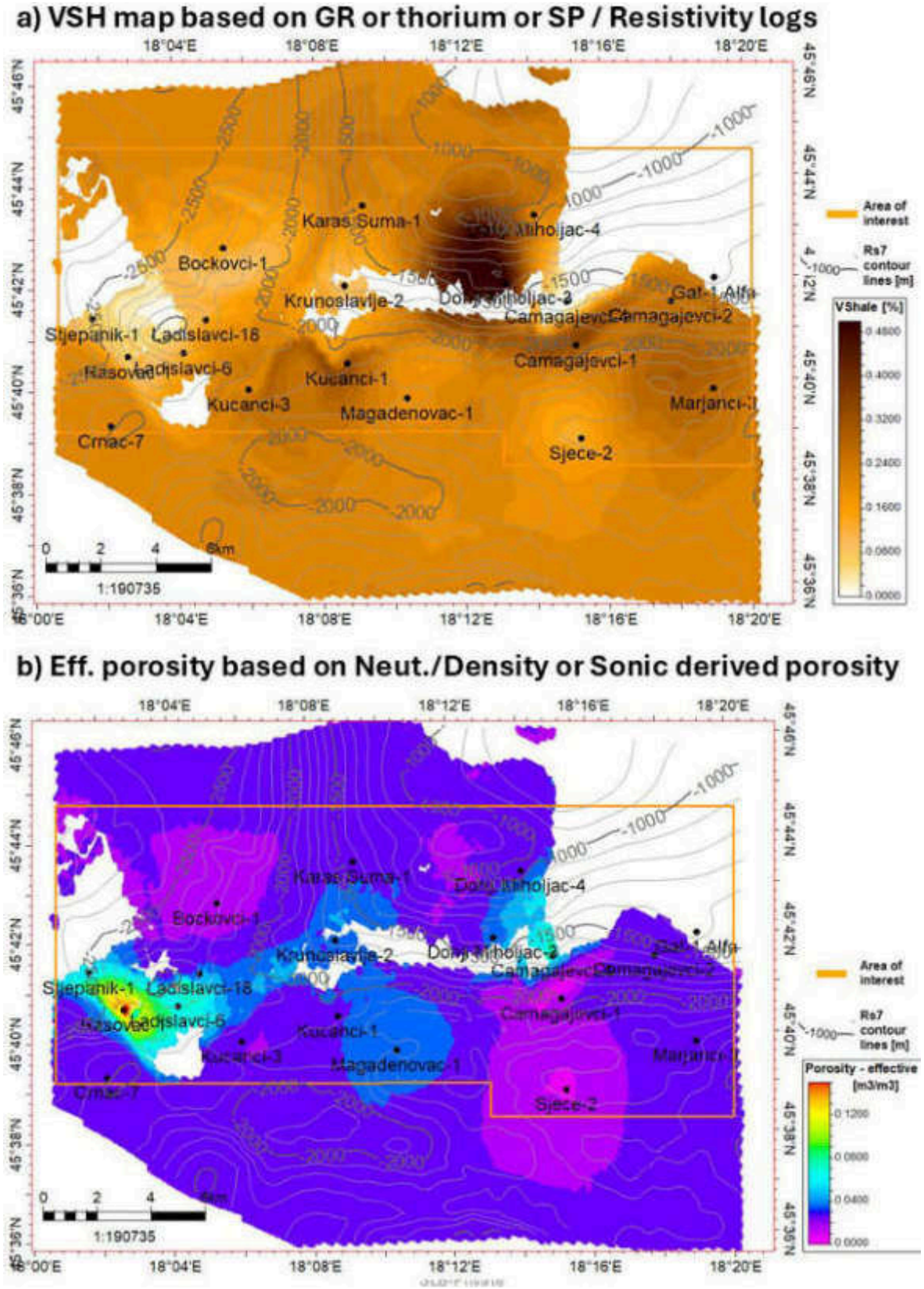


Fig. 2.276 Rs7 volume of shale (VSH) and effective porosity model
Rs7 (a) average volume of shale (VSH) derived from gamma-ray interpretation and (b) average effective porosity model constrained by log porosity and core porosity

Copyright © SLB. All Rights Reserved. Private & Confidential. Reproduction only by permission.

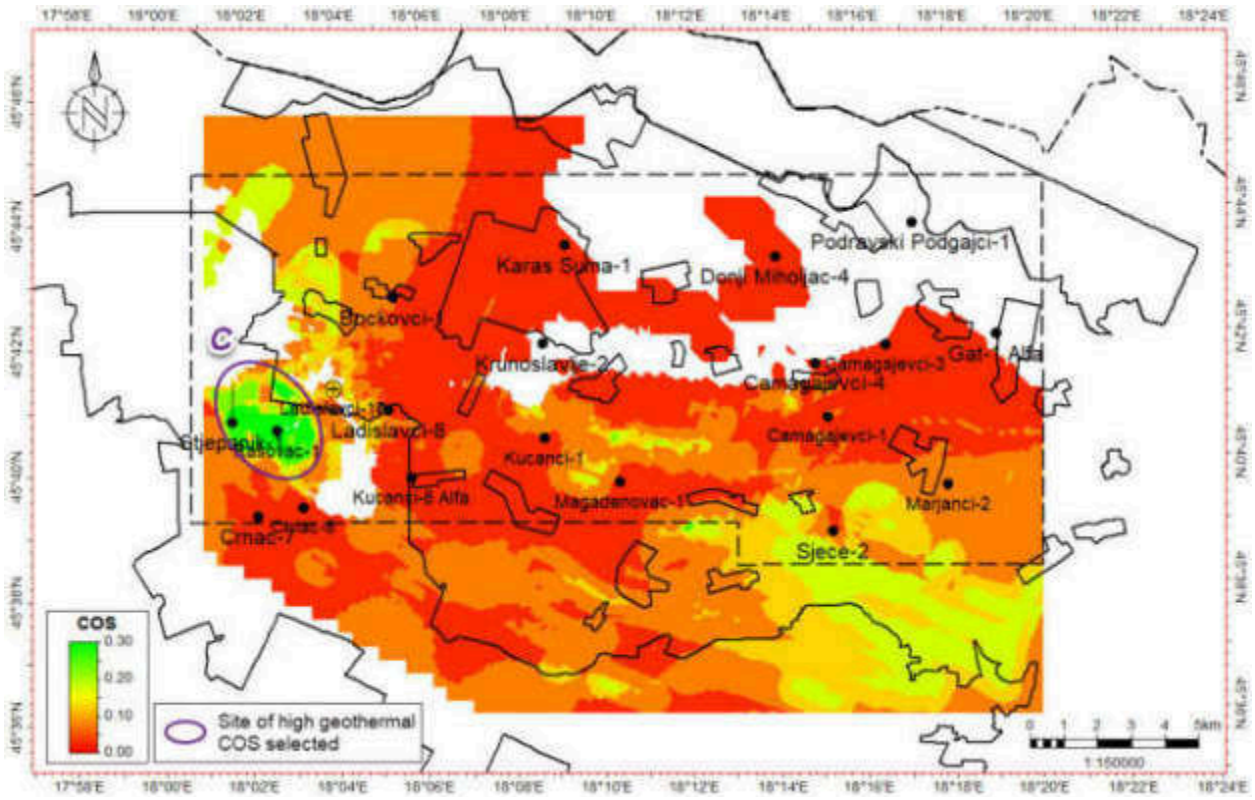


Fig. 2.277 Rs7 Geothermal COS map
Geothermal COS map for the Rs7 interval based on combined subsurface parameters

2.9.3.1 Target C – Geological Interpretation and Uncertainty Analysis

Target C represents the only zone with a high COS identified within the Rs7 interval across the area of interest. It is located between the Stjepanik-1 and Rasovac-1 wells, where reservoir quality indicators reach their most favorable values.

The elevated COS is primarily driven by petrophysical properties observed in Rasovac-1, including very high permeability (up to ~831 mD), relatively high effective porosity (up to ~18.5%), and low shale volume (~5%) (Fig. 2.278). These parameters indicate favorable geothermal reservoir conditions. However, the Rs7 interval is interpreted in the model as very thin (~4 m), which raises concerns about its volumetric significance and long-term productivity.

Copyright © SLB. All Rights Reserved. Private & Confidential. Reproduction only by permission.

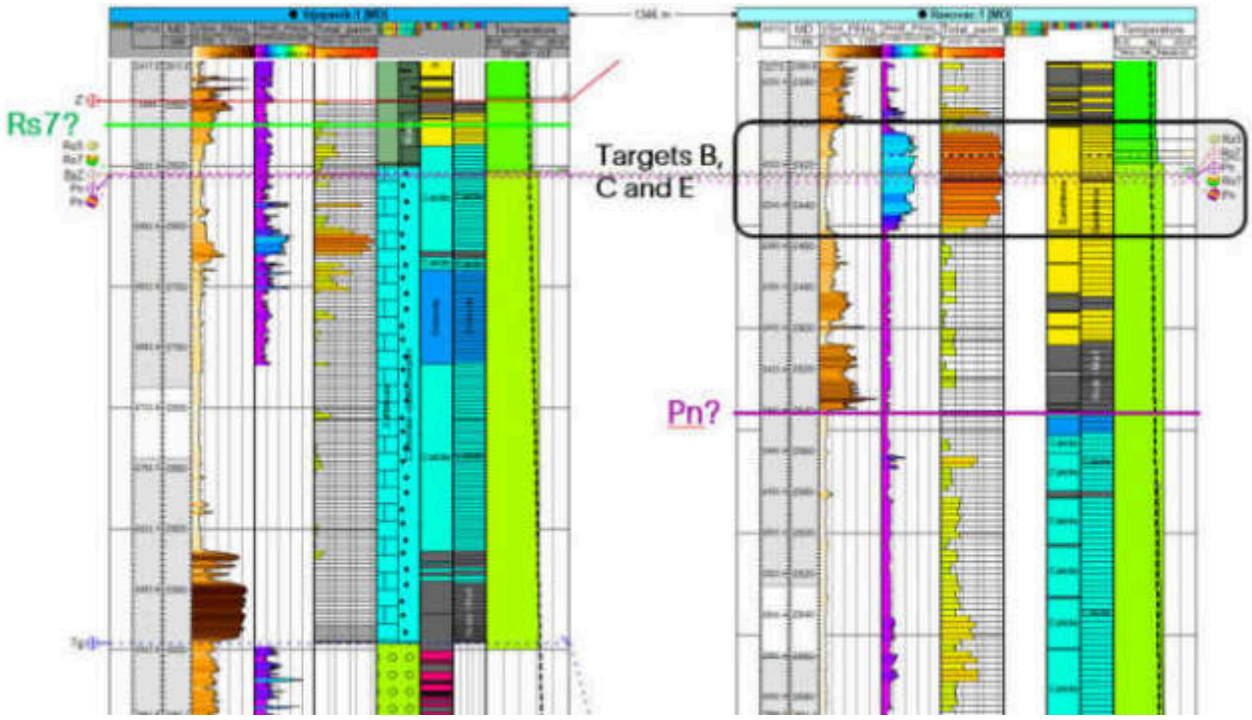


Fig. 2.278 Correlation Stjepanik-1 and Rasovac-1 wells showing VShale, Effective Porosity, Total permeability, lithology type and temperatures

In addition, Rs7 was not interpreted in Stjepanik-1, which further increases uncertainty regarding its continuity and geological relevance.

Thickness Discrepancy: RS7 vs. Lower Badenian

A major uncertainty lies in the discrepancy between the modelled Rs7 thickness (~4 m) and the ~100 m Lower Badenian interval reported in Rasovac-1 well report (Fig. 2.279). The key question is whether Rs7 represents a thin discrete layer or part of a thicker reservoir system.

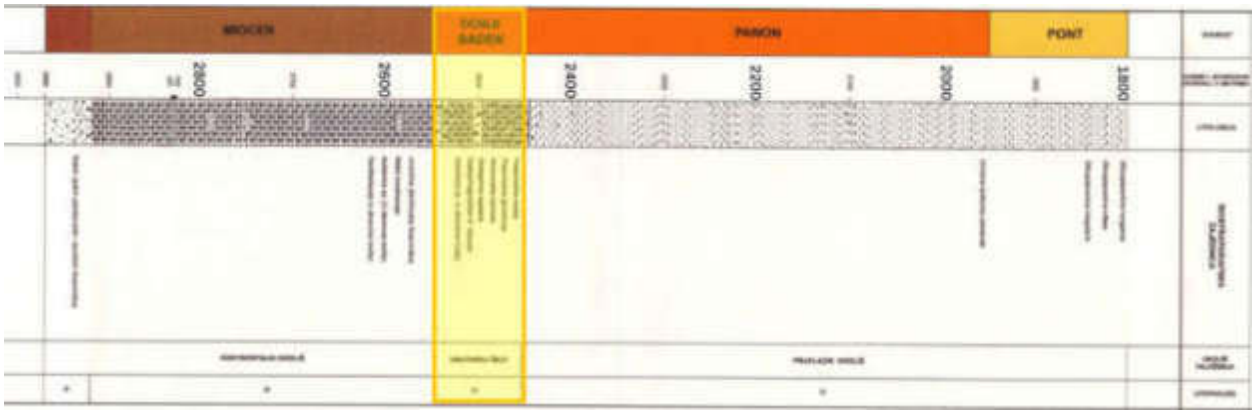


Fig. 2.279 Column stratigraphic, Rasovac-1 well tops and lithology type (from end of well report)

Regional studies indicate that the Lower Badenian (15–13 Ma) corresponds to coarse-grained syn-rift deposits formed during extensional tectonics, typically composed of breccias,

Copyright © SLB. All Rights Reserved. Private & Confidential. Reproduction only by permission.

conglomerates, and sandstones. These deposits are commonly associated with good reservoir quality. In the Drava Depression, Rs5 and Rs7 are lithostratigraphic markers used to represent parts of this Miocene system.

This suggests that Rs7 may represent a log-defined marker within a thicker (but wrongly interpreted) Badenian interval, and that the reservoir thickness could be underestimated if only Rs7 is considered.

Lithological Uncertainty

The nature of the reservoir remains unclear due to conflicting evidence. Petrophysical interpretation suggests clean, permeable sandstone, whereas the Rasovac-1 geological report and associated cross-sections describe the presence of Rs7 with lithologies such as clayey limestone, carbonate breccia, pyroclastic breccia, and marl (Fig. 2.280).

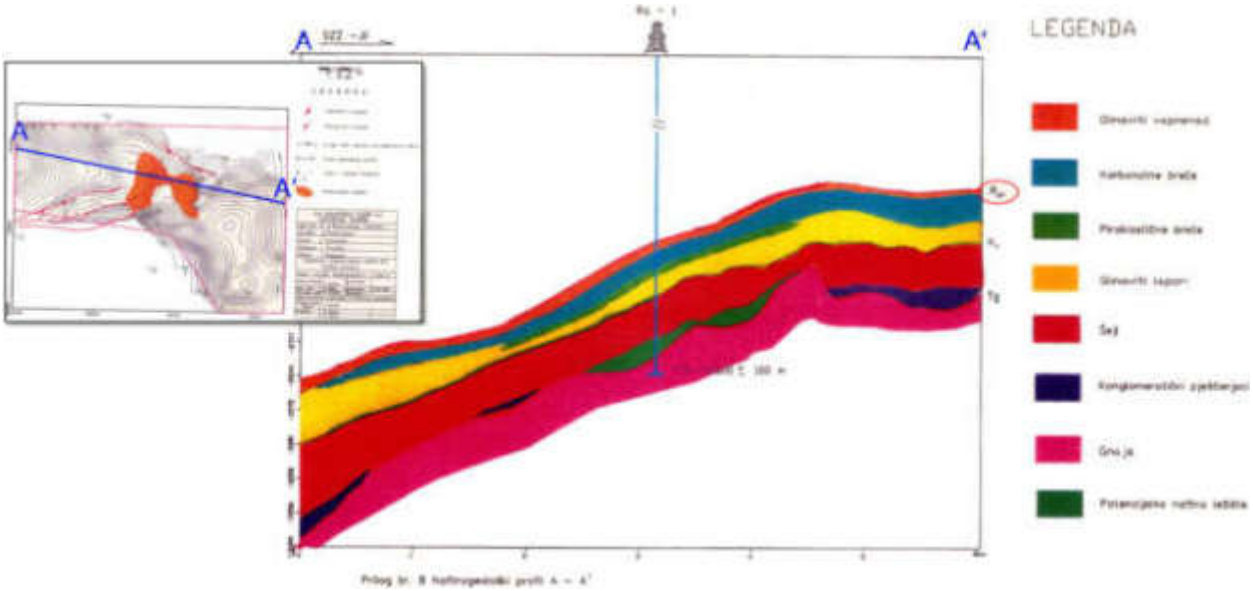


Fig. 2.280 Geological cross-section along the Rasovac-1 well showing the interpretation of Rs7

This discrepancy may reflect strong facies variability within Badenian deposits or the response of fractured carbonate systems that can mimic good reservoir properties in logs. Regional interpretations confirm that RS units may include mixed lithologies ranging from sandstones to carbonates and polymictic breccias.

As a result, it remains uncertain whether Target C corresponds to a clastic reservoir or a heterogeneous carbonate-dominated system.

Stratigraphic Correlation Challenges

Stratigraphic interpretation is complicated by inconsistencies between well data, seismic interpretation, and regional frameworks. In Stjepanik-1, the geological report explicitly indicates

Copyright © SLB. All Rights Reserved. Private & Confidential. Reproduction only by permission.

that the expected Lower Miocene interval is missing. Instead, the section below the Pannonian is described as a heterogeneous succession including dolomitic breccias, sandy dolomicrites, polymictic breccias, and altered volcanic rocks.

Older documents, such as Stj-1A_Stratigrafski prikaz (1986), indicate only a thin Pannonian interval, with deeper sections assigned directly to undifferentiated or basement rocks. In this context, Rs5 may exist as a thin Pannonian interval but Rs7 may be absent, truncated, or merged with older heterogeneous units.

However, another client report (Izrada sintetskih seizmograma busotina Stjepanik-1, 2D seizmika, 2005) mentions the presence of Rs5 and Rs7 horizons at around 2600 m depth, suggesting that these units may exist but are poorly constrained and difficult to correlate.

Seismic data introduces additional uncertainty because Rs7 is thin and locally variable, potentially approaching seismic resolution limits. Regional studies indicate that RS markers are difficult to trace due to erosion and complex geology.

As a result, apparent continuity on seismic sections may partly reflect interpolation rather than true geology, and the connection between Rasovac-1 and Stjepanik-1 remains uncertain.

Thermal Indications

Temperature data provides a possible link between the wells. In Stjepanik-1, a temperature of approximately 149 °C was measured at ~2625 m, while similar depth intervals in Rasovac-1 correspond to the interpreted Badenian section. This may indicate that carbonate breccia or dolomitic intervals in Stjepanik-1 could correlate with the Rs5 or 7 or Badenian interval in Rasovac-1. However, this correlation remains tentative due to limited stratigraphic control.

Key Geological Uncertainties and Implications

The evaluation of Target C is controlled by several major uncertainties, including the definition of the stratigraphic units (Rs7 versus Lower Badenian), the true thickness of the reservoir, the lithological nature of the interval, and its lateral continuity between wells. These uncertainties are compounded by the limited reliability of seismic interpretation at this scale and by the strong heterogeneity typical of Miocene deposits.

Given these limitations, Target C should not be considered as a standalone Rs7 target. Instead, it is more robust to interpret it as part of a broader reservoir system, integrating Rs5 and Rs7 into a composite play. This approach is consistent with regional interpretations and helps to reduce stratigraphic and volumetric uncertainty while improving the overall geothermal potential.

Conclusion

Target C illustrates the contrast between favorable petrophysical indicators and significant geological uncertainty. The main challenge lies in properly defining the stratigraphic framework and understanding the lithological variability of the interval. Available data suggest that Rs7 is likely

Copyright © SLB. All Rights Reserved. Private & Confidential. Reproduction only by permission.

part of a heterogeneous system affected by facies variability, erosion, and limited seismic resolution. Consequently, an integrated, multi-layer approach is required to reduce risk and support a robust geothermal development strategy.

2.9.4 Pn Geothermal Reservoir Evaluation

The Pn horizon represents the deepest evaluated marker in this chapter and is associated with the unconformity-bounded interval at the base of the Neogene succession (often discussed as the Pt/Tg–Pn interval in legacy interpretation workflows) [10]. In the Bockovac AOI, Pn offers the most robust temperature potential because it is structurally deeper than Rs5–Rs7 in the same depocentres. However, lithology below and around Pn is commonly carbonate-dominated and permeability is expected to be controlled primarily by secondary processes such as fracturing, fault damage zones, and dolomitization ([17]; [18]).

Data integration specific to Pn.

The same geothermal COS workflow was applied (Fig. 2.265), including two temperature models (Fig. 2.281 (a) and Fig. 2.282 (a)), distance to temperature points, effective porosity (Fig. 2.283 (b)), Vsh (inverse) (Fig. 2.283 (a)), two permeability models (Fig. 2.281 (b) and Fig. 2.282 (b)), and distance to faults as a permeability enhancer. The fault-distance proxy reflects the observed role of fault damage zones in providing secondary permeability pathways in geothermal systems, especially in a carbonate-dominated formation.

Additional caution was taken in interpreting Vsh in carbonate facies because low Vsh is not, by itself, diagnostic of good reservoir quality in carbonates. Consequently, permeability proxies and structural proximity become relatively more influential for Pn, and the Pn COS map is more sensitive to the facies-based permeability model.

Pn results: Targets D, E, F, and G.

Four Pn target areas were identified (Fig. 2.284). Target D (west of Bockovci-1 well) combines high expected temperatures and acceptable reservoir indicators and is favorable from a surface-constraint perspective. Target E overlaps the Rasovac–Stjepanik corridor and aligns with the stacked Rs5–Rs7 targets B and C, supporting a fully stacked concept (B + C + E). Target F (between Kucanci and Magadenovac) has attractive expected temperatures (≥150 °C) but does not overlap with any Rs5–Rs7 fairway, reducing the benefit of stacking. Target G is temperature-favorable but has poorer predicted reservoir indicators and is retained as a lower-confidence option.

Fluid evidence and implications.

DST information from Rasovac-1 well indicates that at least part of the Pn interval contains producible formation water: an interval at ~2796–2834 m returned water described as poorly

Copyright © SLB. All Rights Reserved. Private & Confidential. Reproduction only by permission.

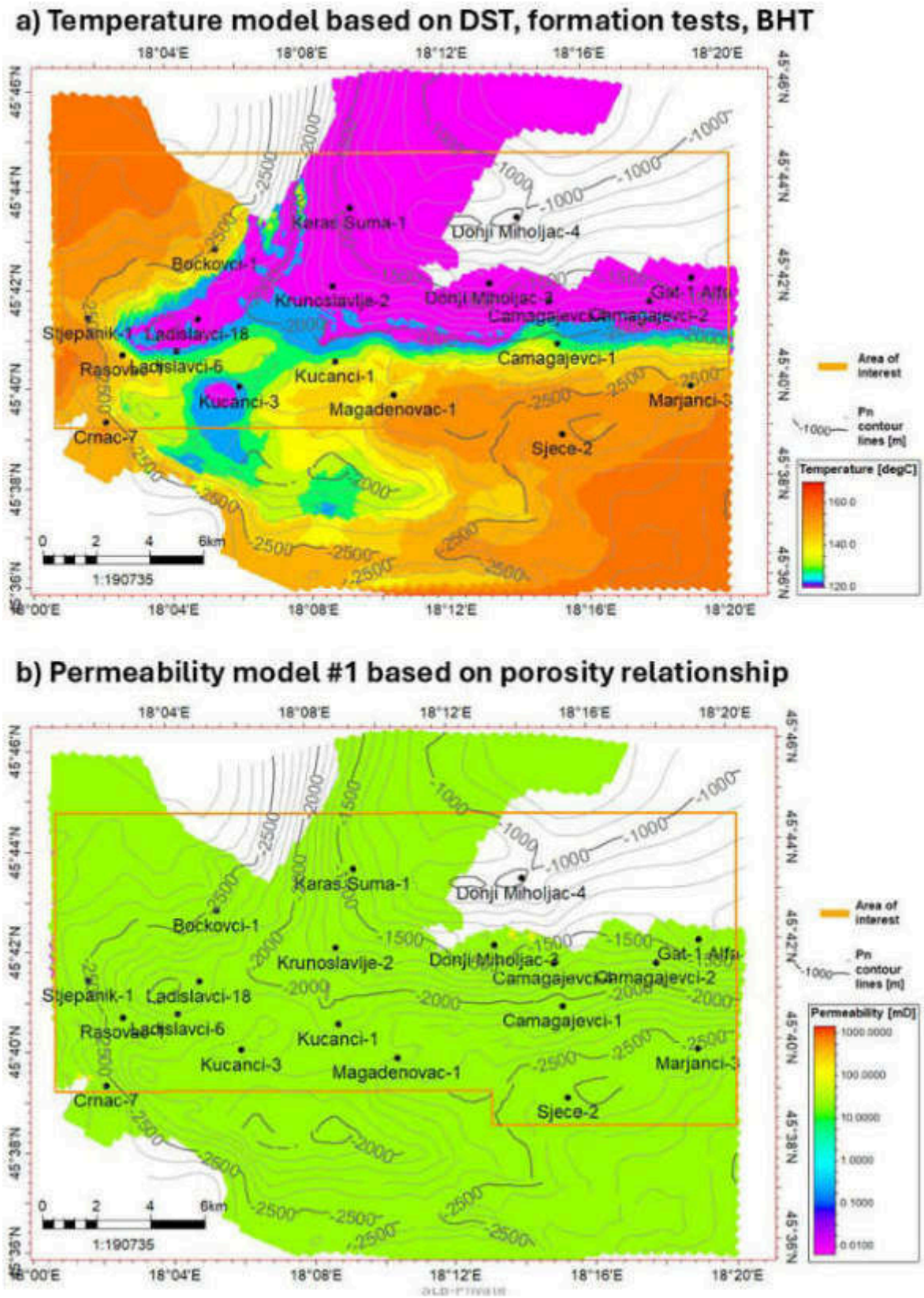


Fig. 2.281 Pn Temperature and Permeability model 1
(a) average temperature from a purely data-driven temperature property model and (b) "permeability model 1" derived from porosity–permeability relationships

Copyright © SLB. All Rights Reserved. Private & Confidential. Reproduction only by permission.

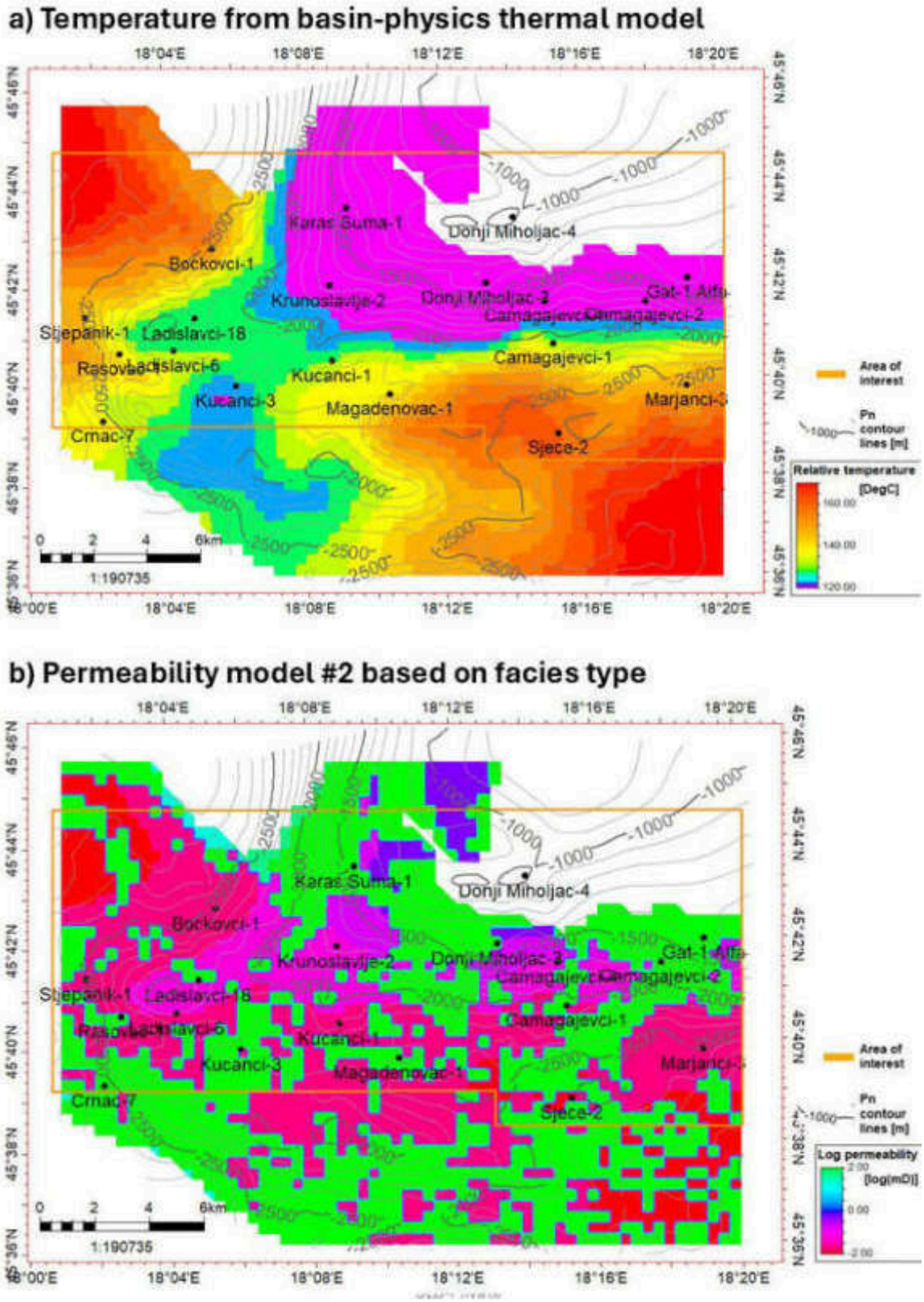


Fig. 2.282 Pn Temperature and Permeability model 2
(a) average temperature from a basin-physics thermal model (using heat flow, surface temperature, and formation thermal conductivities)
and (b) "permeability model 2" derived from facies-dependent permeability end-members

Copyright © SLB. All Rights Reserved. Private & Confidential. Reproduction only by permission.

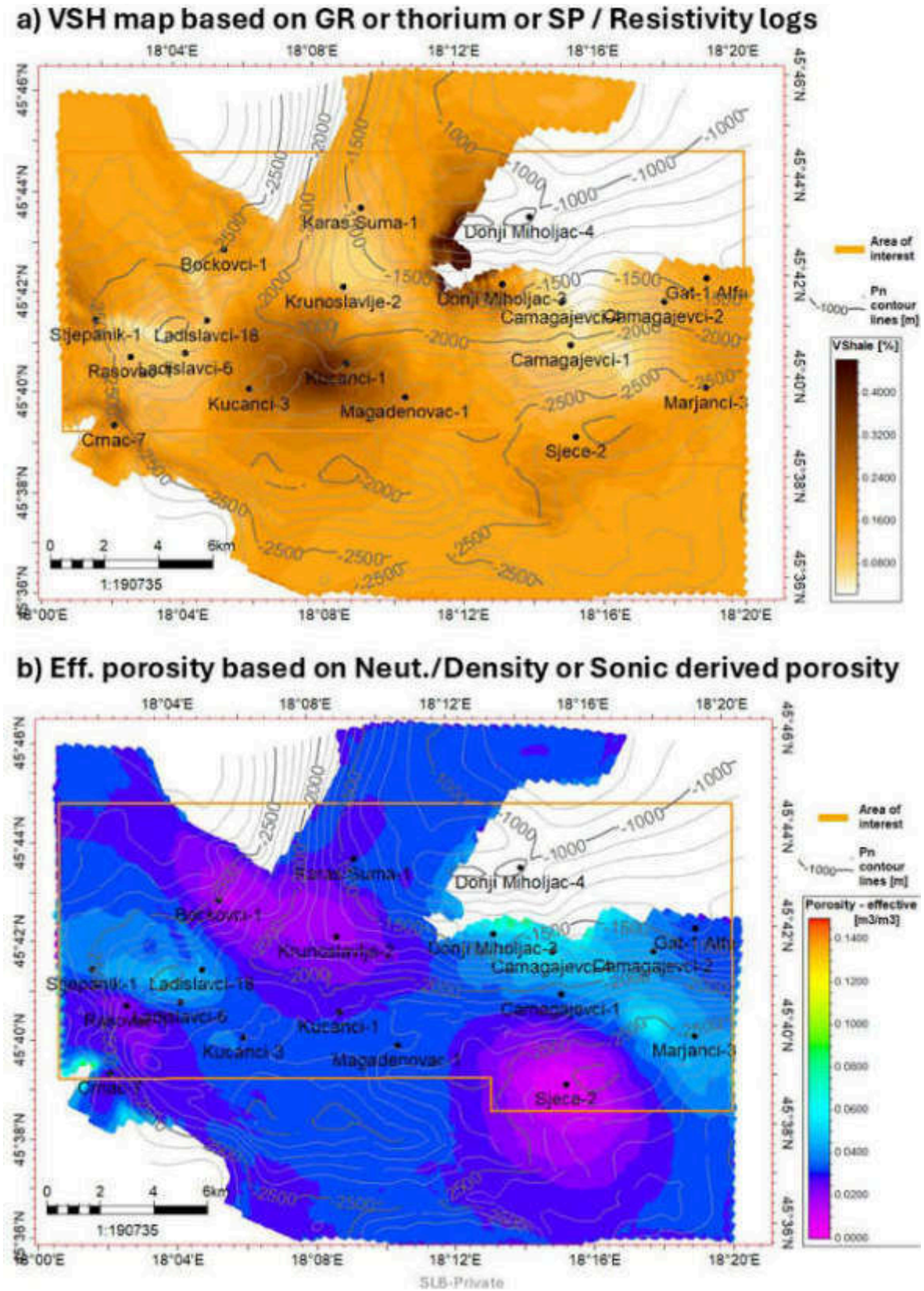


Fig. 2.283 volume of shale (VSH) and effective porosity model
(a) average volume of shale (VSH) derived from gamma-ray interpretation and (b) average effective porosity model constrained by log porosity and core porosity

Copyright © SLB. All Rights Reserved. Private & Confidential. Reproduction only by permission.

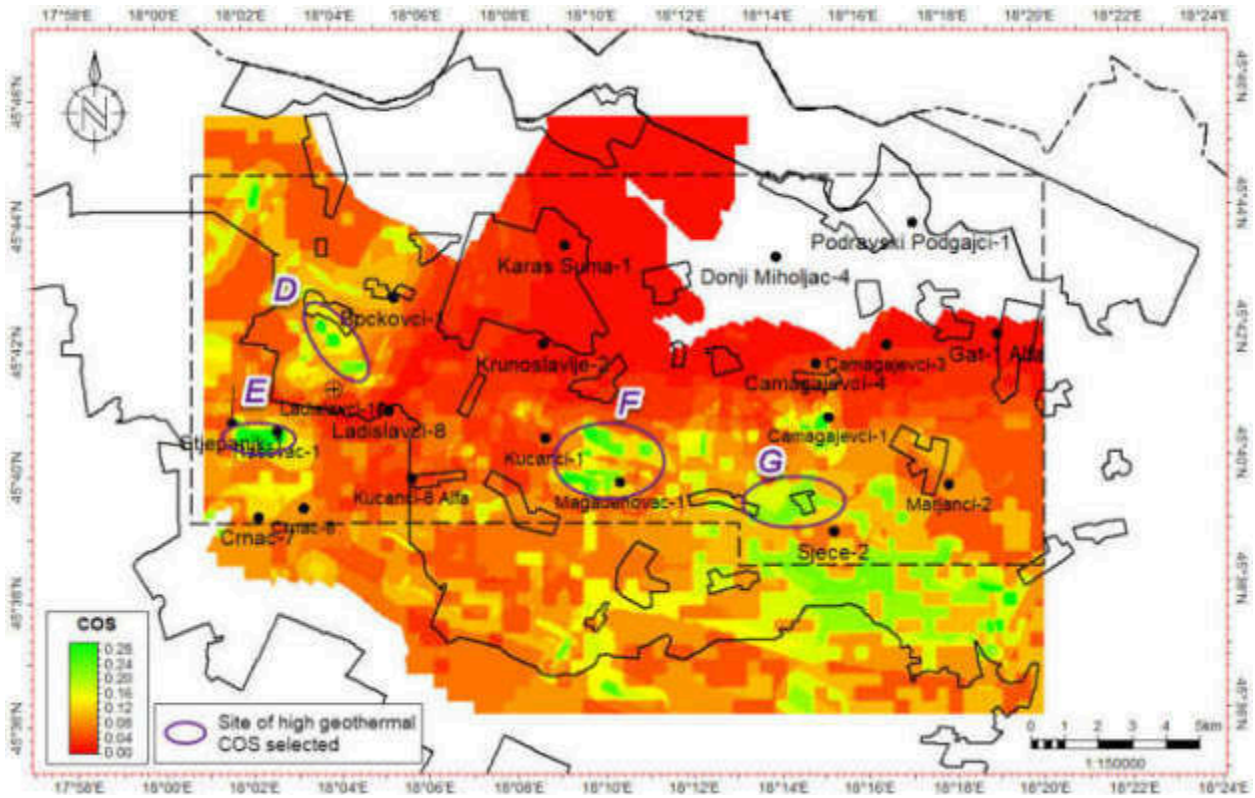


Fig. 2.284 Pn Geothermal COS map
Geothermal COS map for the Pn interval based on combined subsurface parameters

gasified with reported salinity of ~16.3 g/L. This supports the working assumption that Pn can host mobile fluids, but it reinforces the need for full water chemistry (major ions, silica, dissolved gases) to assess scaling and corrosion risks.

Dominant uncertainties and risk drivers.

The main geologic risk for Pn is reservoir predictability. Carbonate permeability may vary substantially over short distances due to cementation versus fracture/dolomitization, and fault-related permeability can evolve during production and injection ([19]; [17]). In addition, because Pn is an unconformity, erosional relief can create local mini-basins where the target interval thickens and adjacent highs where it is truncated, complicating prediction of thickness and connectivity below the unconformity [20].

Pn chance of success statement.

Pn has the highest probability of meeting the temperature requirement, but only an average probability of encountering sufficient transmissivity because permeability is secondary and structurally controlled ([17]; [18]). Pn should therefore be pursued within a stacked concept where overlying Rs5–Rs7 sand-prone intervals provide additional transmissivity and where Pn perforations are guided by fracture indicators and test results.

Copyright © SLB. All Rights Reserved. Private & Confidential. Reproduction only by permission.

2.9.5 Global Geothermal Chance of Success Analysis

This study implemented a quantitative Chance of Success (COS) workflow consistent with geothermal play-fairway screening, in which the three fundamental resource elements—heat, permeability, and porosity—are represented by mappable proxy layers and combined into a composite probability surface. Fluid properties and surface conditions are also represented by mappable proxy layers, but only when a target is identified.

Horizon-by-horizon success chance summary Fig. 2.285

- Rs5: stand-alone chance of success is LOW because thickness/continuity is commonly below the hard gate and seismic tuning limits prevent reliable mapping of thin beds.
- Rs7: stand-alone chance of success is LOW because temperatures are commonly marginal (<150 °C) but MODERATE in only one target (Target C) located in near Rasovac-1 well because reservoir quality is good with acceptable temperatures but below an environmentally restricted area which complicates access via drilling.
- Pn: stand-alone chance of success is MODERATE because temperature is favorable, but carbonate reservoir performance is highly dependent on fractures/dolomitization and on unconformity-related thickness variability.

Stacked-play uplift in COS

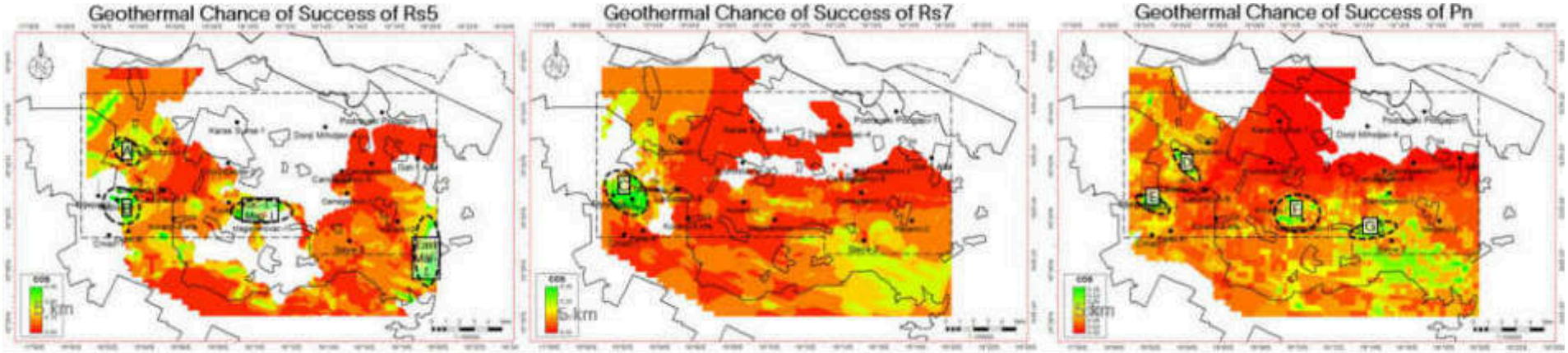
No single horizon provides a robust, low-risk geothermal target on its own. A stacked-reservoir concept (Rs5 + Rs7 + Pn) increases the probability of intersecting at least one productive interval, improves total completed thickness, and mitigates uncertainty in thin-bed mapping, which is consistent with sedimentary-basin geothermal development and play-fairway recommendations.

Targets Definition

Two main development targets have been identified. The first is between the Rasovac-1 and Stjepanik-1 wells (Targets B, C and E combined), where all three reservoirs are present and combined performance is expected to be optimal. However, this area is associated with significant constraints, including environmental restrictions (Natura 2000), deeper and deviated drilling requirements, and proximity to existing hydrocarbon fields (Ladislavci and Crnac).

The second area is located west of the Bockovci-1 well and north of the Stjepanik-1 well, where conditions are slightly less favorable, but operational constraints are significantly reduced (Targets A and C combined).

Copyright © SLB. All Rights Reserved. Private & Confidential. Reproduction only by permission.



Targets	Layers	Area [km2]	COS [%]		Temperature from property [degC]		Temperature from model [degC]		Permeability from property [mD]		Permeability from model [log(10)mD]	
			min	max	min	max	min	max	min	max	min	max
A	Rs5	1.90	13%	29%	110.59	148.80	134.38	148.07	0.69	22.38	3.96	4.29
B	Rs5	1.01	14%	81%	101.00	146.10	120.13	130.82	252.76	1311.16	-1.99	4.52
Kuc-1 - Mag-1	Rs5	2.53	9%	36%	102.35	148.98	116.99	122.86	8.96	213.88	1.21	4.59
East Mar-1	Rs5	2.49	8%	37%	120.16	151.35	132.24	141.63	10.54	107.32	-0.70	4.37
C	Rs7	2.58	13%	81%	101	149.00	121.32	138.97	23.23	746.09	-4.71	4.56
D	Pn	1.55	7%	29%	115.79	152.73	128.58	160.24	6.32	25.83	-1.94	3.58
E	Pn	1.18	8%	32%	132.77	153.34	135.88	148.39	4.00	30.16	-1.91	3.40
F	Pn	3.23	7%	29%	129.89	146.18	127.79	141.01	3.92	27.67	-1.79	3.49
G	Pn	2.29	9%	22%	151.02	154.49	155.00	163.71	0.16	3.03	-1.96	3.22

Fig. 2.285 Map of identified geothermal targets for the Rs5, Rw7 and Pn layers
NOTE: the numbers are average values of each zone within an area. It means that the maximum and minimum values could be respectively higher and lower

Copyright © SLB. All Rights Reserved. Private & Confidential. Reproduction only by permission.

2.9.6 Geothermal COS Risk Assessment and Recommendations

The project is subject to several geological, operational, and environmental risks. Geological uncertainties primarily relate to reservoir continuity, thickness variability, and petrophysical heterogeneity, which may impact reservoir deliverability and connectivity. Operational risks are mainly associated with drilling complexity and cost, particularly in the context of deep and deviated wells, which may introduce technical challenges and increase project expenditure.

Environmental risks are linked to regulatory constraints, especially where the project overlaps with Natura 2000 protected areas, potentially affecting permitting timelines and development options. In addition, fluid composition represents a key uncertainty, with possible issues related to scaling, corrosion, and interactions with existing hydrocarbons, all of which may impact well integrity and long-term operability.

Before any drilling activities are undertaken, the following actions are recommended to reduce uncertainty and improve project robustness for the selected target:

- Refine lithological characterization of the target intervals (Rs5, Rs7, and Pn), including improved estimates of thickness, porosity, and permeability.
- Integrate fracture-related data for the Pn unit, using inputs such as image logs, core fracture analysis, and seismic-derived attributes, to better assess the contribution of fractures to permeability and secondary porosity.
- Conduct a comprehensive geomechanical and fault-seal analysis to evaluate structural integrity, fault behaviour, and potential compartmentalization.
- Perform fluid characterization and laboratory testing, followed by scaling and corrosion modelling, to anticipate production and injection challenges.
- Update the thermal model and temperature calibration using newly acquired temperature data (e.g., gradient logs) or corrected bottom-hole temperatures, including sensitivity analysis to bracket uncertainty ranges.

2.10 Fluid geochemistry review of selected geothermal sites

Water and gas data have been compiled and evaluated from data files of existing wells provided by CHA to assess, to the extent possible, water and gas compositions from three formations of interest for the geothermal production portion of this project: Rs5, Rs7 and Pn. These data are pertinent to understanding certain production risks, such as scaling and corrosion of downhole and surface equipment, handling of produced gas at surface, and for input to reservoir models. Evaluation of data quality shows that several water samples have ion imbalances higher than 5%, shown in Table 2.32 and Table 2.33 with an asterisk. Additionally, several water samples report only sodium (Na) equivalent, rather than Na and potassium (K) separately, so these samples are excluded from scaling analyses. No fluid samples from Rs5 are provided in the available datasets and representative analogues have not been found in public literature, hence Rs5 water samples cannot be evaluated. A limited number of dry gas samples are documented from Rs7 and Pn (and

Copyright © SLB. All Rights Reserved. Private & Confidential. Reproduction only by permission.

none from Rs5) and are not near the target areas of interest. Information is largely unavailable in the reported documents to determine total gas in total flow, as discussed in greater detail below. As wells are drilled for this project, plans to collect and analyze both water and gas samples should be integrated into well testing plans to enable better prediction of scaling, corrosion, total gas in produced fluid, presence of hydrocarbons, and design of treatment and handling procedures that should be taken during geothermal exploitation.

Water Compositions

Water samples from Rs7 and Pn formations are provided in Table 2.32 and Table 2.33 respectively.

Rs7

Based on chance of success (COS) mapping, discussed in 2.9.3 Rs7 Geothermal Reservoir Evaluation, the most favorable expected region for geothermal production from the Rs7 formation is the area around the Rasovac-1 well (Target C) (Fig. 2.277). The nearest well with water data from Rs7 is Stjepanik-1 which lies on the northern border of Target C. Crnac-7 is to the south, and wells Ladislavaci-1 and -4 are to the west (Fig. 2.277). Based on water samples from these wells, produced geothermal waters can be expected to have near neutral to slightly alkaline pH (6.8 - <9) and total dissolved solids (TDS) ranging from 1,400 – 6,600 mg/L, averaging 4,650 mg/L. Further east from the Rasovac area, the Kucanci and Magadenovac well samples indicate TDS concentrations near 20,000 mg/L in Rs7, but levels this high are less likely to occur near Target C. Lateral variations in TDS levels suggest heterogeneity in the rock types or the presence of barriers to flow (such as faults or low permeability rocks) within Rs7 across the study area (or both). Localized vertical barriers are also indicated by the different chemical signatures taken from samples at different depths within the same well. For example, the shallower sample taken from Magadenovac-1 resembles water compositions from the western part of the project area, while the deeper sample more closely resembles the Kucanci waters.

Pn

COS mapping for the Pn formation indicates four locally favorable areas, Targets D, E, F and G (Fig. 2.284). Water samples are available from three wells :

1. Rasovac-1, located within Target E,
2. Bockovci-1, located east of Target D, and
3. Ladislavaci-18, located just south of Target D.

Targets F and G are located much further east than any of the available water samples from Pn. All water samples have a near neutral pH at atmospheric conditions; it is possible that degassing during production could have increased the water pH and that lower pH values could be encountered downhole, though it is not possible to quantify this based on available data. Pn water samples appear relatively 'fresher' than most of the Rs7 samples, with TDS levels ranging from

Copyright © SLB. All Rights Reserved. Private & Confidential. Reproduction only by permission.

1,790 – 2,660 mg/L. There is a lower degree of variation in composition between the three Pn samples than observed in the Rs7 samples, but it remains uncertain if similar waters are present in the southern and eastern parts of the project area.

Indications of Fluid Source and Flow

Plotting certain ion ratios of the water samples from Rs7 and Pn show a distinct high chloride (Cl) and high Na equivalent (Na+K) in the Kucanci wells and the deepest sample from Magadenovac-1, which are the farthest east of the sampled wells (Fig. 2.286). The plot of silica versus Na+K displays bifurcation between the Kucanci and deepest Magadenovac samples from all the other samples that may be attributed to different equilibrium conditions, quite possibly due to different host rocks; although samples from the Kucanci and Magadenovac wells and Ladislavaci-1 and Crnac-7 (further west) all come from the Vukovarska Formation, this formation contains various lithologies including dolomite-lime breccias, calcareous and sandy marls, sandstones and conglomerates, the distribution of which is likely not homogeneous across the project area. Influx of meteoric water into deeper reservoirs is sometimes indicated by high concentrations of magnesium (Mg), however, in this sample set magnesium is relatively low enough that a prominent source of meteoric water influence has not been identified.

Gas Composition and Non-Condensable Gases

Rs7

Dry gas analyses representative of the Rs7 formation are available from three wells (Crnac-8, Magadenovac-1, and Sjece-1), shown in Table 2.34. These gas data were collected and analyzed with hydrocarbon exploration as the main objective and hence are lacking some key data points that are useful for geothermal applications, namely data to determine total gas in flow, and lack of argon and helium, which makes the data inherently limited for a geothermal study. Several samples indicate nitrogen (N_2) is present, which could be contributed by the breakdown of organic matter present in the sedimentary units or, less likely given the nature of this lithologic setting, infiltration of air-saturated meteoric water. Sample contamination with atmospheric air is also possible, though no air nor oxygen are reported for any of the Rs7 samples. If argon (Ar) data were available, N_2/Ar ratios could be used to help determine the source.

Samples from Crnac-8 and Magadenovac-1 are similar and show methane levels between 65 – 73 vol%, carbon dioxide (CO_2) levels between 1.4 – 18 vol% (averaging 5 vol%), and no hydrogen sulfide (H_2S). Crnac-8 has higher levels of more complex hydrocarbons (ethane – C6+), measuring from 24 – 32 vol% compared to Magadenovac-1, which contains 11 – 12 vol%. Well Sjece-1, further east, has considerably lower methane at 49 vol%, higher CO_2 at almost 14 vol%, no H_2S, and 35 vol% of ethane – C6+ hydrocarbon gases.

In other carbonate-hosted geothermal resources, mainly in Turkey and other regions of the Pannonian Basin, gas composition is nearly entirely CO_2, with only trace amounts of methane, other hydrocarbons, or other non-condensable gases. In comparison, the atypical gas composition observed in the Crnac-8 andMagadenovac-1 wells may pose challenges for surface handling, as

Copyright © SLB. All Rights Reserved. Private & Confidential. Reproduction only by permission.

Table 2.32 Water composition of samples collected from wells within the study area from formations within Rs7

Well	Stjepanik-1	Stjepanik-1*	Crnac-7	Crnac-7	Crnac-7	Ladislavaci-1	Ladislavaci-1	Ladislavaci-1	Ladislavaci-4	Ladislavaci-4	Ladislavaci-4	Kucanci-3	Kucanci-3	Kucanci-8 alpha	Magadenovac-1	Magadenovac-1
Depth (m)	2615.39 - 2627	2979.74 - 3004	2398 - 2401 & 2345 - 2342	2201 - 2197 & 2162 - 2157	2132 - 2128	2141 - 2139	2341 - 2339	2390 - 2387	2154 - 2152	2178 - 2176	2160 - 2158	2366 - 2363	2374 - 2371	2316.2 - 2337	2614.9 - 2625.4	2756 - 2753
Lithologic Notes (from client data files)	very hard slightly sandy marl (Moslavacka Gora Fm, Krizevci Clan)	Tuffs, breccias, andesites, breccia conglomerates (Mosti Clan)	Vukovarska Fm. (andesites, andesitic carbonate tuffites, carbonate silicate breccias, dolomite-lime breccias, calcareous marls, sandy marls, sandstones, conglomerates, subarkoses)	Spans both Vinkovacka Fm. (sandy marls with interbedded sandstone) and the Valpovacka Fm. (solid sandy marls, calcareous marls and thin sandstone layers)	Vinkovacka Fm., hard sandy marls and thin interlayers of sandstone	Vukovarska Fm, Karasica Clan (Marls, calcareous marls, sandy marls, sandstones, conglomerates, aglomerates, subarkoses, subgreywackes, silites and calcarenites)	Vukovarska Fm, Karasica Clan (Marls, calcareous marls, sandy marls, sandstones, conglomerates, aglomerates, subarkoses, subgreywackes, silites and calcarenites)	Vukovarska Fm, Karasica Clan (Marls, calcareous marls, sandy marls, sandstones, conglomerates, aglomerates, subarkoses, subgreywackes, silites and calcarenites)	gray marl	lime-dolomite breccia	lime-dolomite breccia	Vukovarska Fm. (Benicanci and Karasica clans?) dolomite-lime breccias, calcareous marls, sandy marls, sandstones, conglomerates, agglomerates, subarkoses, and calcarenites				
Appearance	yellow		cloudy, yellow	cloudy, yellow	cloudy, mixed oil	yellow, mixed oil			yellow	dark, mixed with oil	dark, mixed with oil	yellowish	yellowish	gray, mixed with mud		
pH	7	7.97	8.85	7.72	7.62	6.81	7.3	6.22	7.97	8.18	7.82	7.08	6.75	6.75	7.3	6.8

Copyright © SLB. All Rights Reserved. Private & Confidential. Reproduction only by permission.

Well	Stjepanik-1	Stjepanik-1*	Crnac-7	Crnac-7	Crnac-7	Ladislavaci-1	Ladislavaci-1	Ladislavaci-1	Ladislavaci-4	Ladislavaci-4	Ladislavaci-4	Kucanci-3	Kucanci-3	Kucanci-8 alpha	Magadenovac-1	Magadenovac-1
Density at 20 degC (g/cc)	1.00115	1.0006	1.007	1.004	1.005	1.003	1.003	1.004	1.003	1.003	1.004	1.012	1.013	1.012	1.006	1.02
Electrical Resistance (ohm-m)	6.29	24.64	0.983	1.23	1.22	1.72			2.18	1.925	2.271	0.45	0.44	0.521	4.33	14.69
Cations																
Ammonium (mg/L)	0	0	9.7	14.2	20	20			5.4	17.3	6.8	32.3	33.2	15	4.6	17.5
Sodium (mg/L)	303	55	2023	1762	1840	1125			1100	1215	1000	5760	5800	5127		
Potassium (mg/L)	40	3.5	335	228	219	33			128	220	92	234	225	111		
Magnesium (mg/L)	4	27	0.5	0.9	1.7	22	0	48.8	0.6	1.2	1.3	27.2	26.3	21.4	9.76	19.5
Calcium (mg/L)	72	40	6.1	33	35	222	20	136	3	49.4	24	132	215	184	44	147
Iron (total) (mg/L)	40	31	31	175	54	17			23	52.5	165	24.4	84.7	253	68	170
Strontium (mg/L)	1	0.4	0	1.2	2.4	9			0.8	0.8	0.4	0	25	117		
Sodium + Potassium (mg/L)							1075.02	1523.98							2605.44	6196
Anions																
Chlorides (mg/L)	181	8.9	2092	2019	2203	12.91**	1029.5	2130	300	325	290	9514	10046.5	6919	2627	8910.5
Bromide (mg/L)	0	0	22	4.3	6.6		5.9		0	8.4	6	37	39.8	4	52	20
Iodide (mg/L)	0	0	4.9	3	3.7		7.5		6	4.8	6.4	7.5	7.5	5.8		

Copyright © SLB. All Rights Reserved. Private & Confidential. Reproduction only by permission.

Well	Stjepanik-1	Stjepanik-1*	Crnac-7	Crnac-7	Crnac-7	Ladislavaci-1	Ladislavaci-1	Ladislavaci-1	Ladislavaci-4	Ladislavaci-4	Ladislavaci-4	Kucanci-3	Kucanci-3	Kucanci-8 alpha	Magadenovac-1	Magadenovac-1
Bicarbonates (mg/L)	638	350	1101	915	948	1407	671	689.3	1983	2226	2030	1952	2135	2543	1988.6	1952
Carbonates (mg/L)	0	0	140	0	0	0	0	0	0	16.8	0	0	0	0	0	0
Sulfates (mg/L)	123	25	809	582	502	220	371.63	276.69	450	593	502	283.5	309.4	256	464.43	240.48
Silicon dioxide (mg/L)			15	17.5	150		119		18.4	110	9	89	97.0	122	77.5	77
Total dissolved solids, TDS (mg/L)	1402	509.8	6589	5755	5985	4498.4			4018	4840	4132	18093	19044	15572	7941	17750
Total Salt as NaCl Equivalent (mg/L)	833.3	266.3	5297	4562	4782	3184										
Salinity (g NaCl/L)	0.298	0.0146				2.14	1.7	3.51						13031		
* Ion imbalances greater than 5%, indicating a quality issue.																
** Suspected error in recording value. As 12.19 ppm, there is a 39% ion imbalance. If chlorides are 1219 ppm, ion balance is 0%.																

Copyright © SLB. All Rights Reserved. Private & Confidential. Reproduction only by permission.

Table 2.33 Water composition of samples collected from wells within the study area from formations within Pn

Well	Rasovac-1	Bockovci-1	Ladislavaci-18*
Depth	2796.96 - 2834	2548.9 - 2561	2427.07 - 2445
Lithologic Notes (from well stratigraphic files)	polymictic breccia, shale (partly dolomitic), dolomite, dolomitic limestone at 2826 m	silty, micaceous, sandstone, medium-hard marl	polymictic breccia (limestone up to 70%, dolomite up to 40%, quartz up to 30% and reddish clay up to 10%)
Appearance	brown, cloudy, oily	gray, cloudy	yellow, cloudy
pH	7.13	7.145	7.04
Density at 20 degC (g/cc)	1.0022	1.00204	1.0025
Electrical Resistance (ohm-m)		3.5	3.42
Cations			
Ammonium (mg/L)	2.9	60.0	9.0
Sodium (mg/L)	660.0		429.0
Potassium (mg/L)	2.4		42.0
Magnesium (mg/L)	6.2	5.0	20.0
Calcium (mg/L)	40.0	62.0	80.0
Iron (total) (mg/L)	17.0	13.4	130.0
Strontium (mg/L)	1.2	0.5	6.0
Sodium + Potassium (mg/L)		658.0	
Anions			
Chlorides (mg/L)	333.3	553.0	548.0
Bromide (mg/L)	0		70.0
Iodide (mg/L)	0		19.0
Bicarbonates (mg/L)	1064.1	986.0	565.0
Carbonates (mg/L)	0	0	0
Sulfates (mg/L)	202.9	152.0	7.1
Silicon dioxide (mg/L)			
Undissociated silicic acid (mg/L)		171.0	
Total dissolved solids (mg/L)	2313.0	2660.9	1789.7
Total Salt as NaCl Equivalent (mg/L)	1431.7	1618	1285.5
Salinity (g NaCl/L)	0.549	0.903	0.964
* Ion imbalances greater than 5%, indicating a quality issue.			

Copyright © SLB. All Rights Reserved. Private & Confidential. Reproduction only by permission.

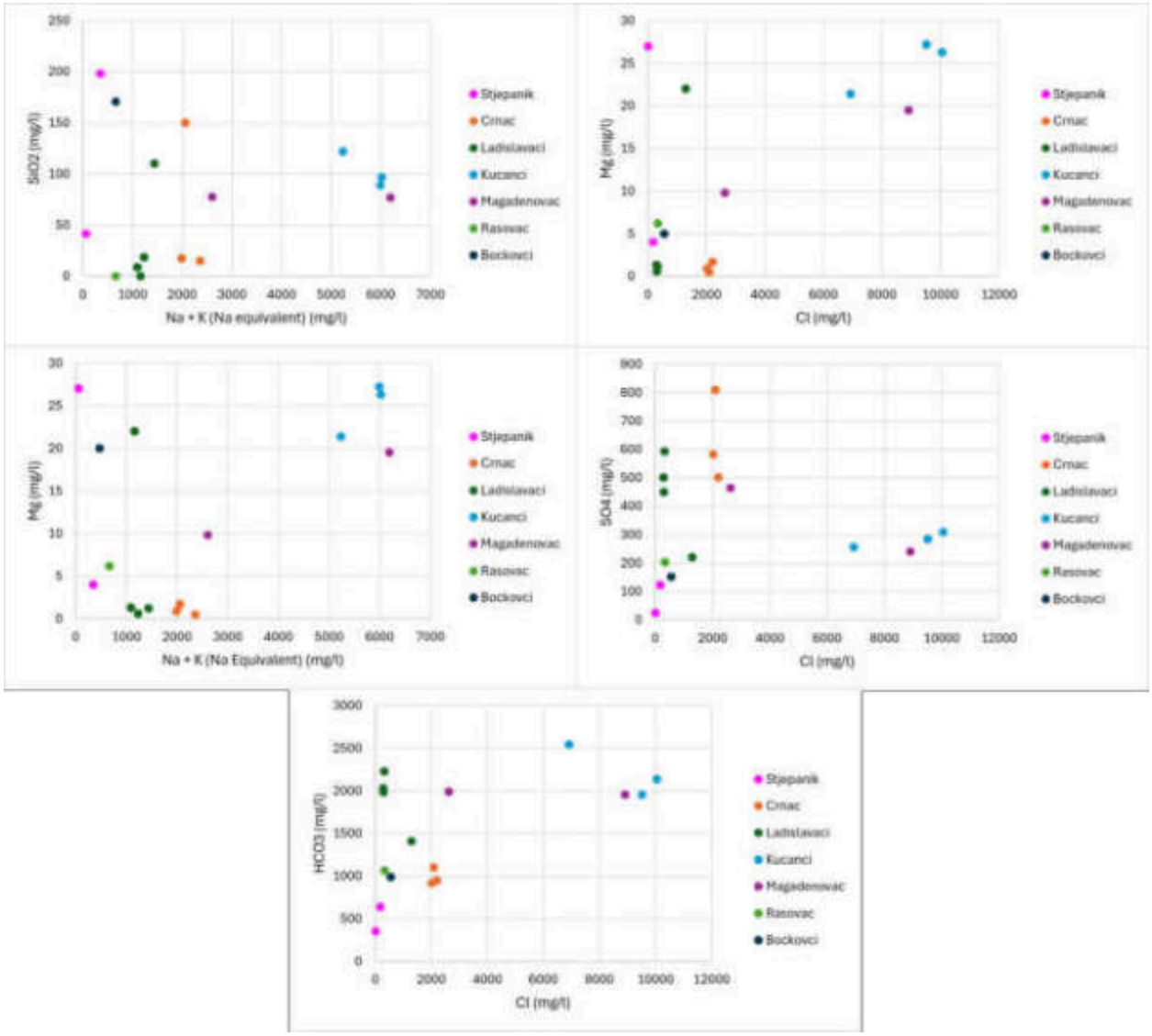


Fig. 2.286 Chemical relationships among water samples from the CHA geothermal project area

further discussed below. More detailed analyses are needed, when geochemical data are collected from production wells that allow assessment of total gas in total flow and non-condensable gas composition, to calculate expected gas separation pressures.

Pn

Dry gas analysis representative of the Pn formation is only available from two samples at the same depth in well Rasovac-1 (Table 2.35). These sample data are highly representative of gas composition expected within Target E, but do not provide strong indication of what may be encountered at Targets D, F and G (Fig. 2.284). CO_2 levels are significantly higher than in Rs7, measured between 40 – 43 vol%, though this is still much lower than is typically seen in other carbonate-hosted geothermal resources. Methane is measured between 24 – 27 vol% and more

Copyright © SLB. All Rights Reserved. Private & Confidential. Reproduction only by permission.

complex hydrocarbons account for 4 – 5 vol%. Although no H_2S is recorded as being present, that does not preclude this gas occurring in hydrocarbon-bearing formations. Both samples report significant air contamination (21 – 26 vol%), which could be the source of the reported N_2.

As similarly noted for Rs7 gas samples, no data are available to determine total gas in total flow nor expected gas separation pressures. At the Velika Ciglena geothermal power plant, also located in the Pannonian Basin of Croatia, CO_2 (which comprises 99.5% of the total NCGs) is produced at 10.45 kg/s, corresponding to 4.7 wt% of total flow [21]. Due to the significant differences in gas compositions found within CHA's project area, it is uncertain whether similar total gas in produced fluid levels can be expected.

Production and Handling Considerations

Scaling

Bicarbonate levels are high in all water samples, which may be attributed to the carbonate content of the host formations; dissolution of carbonate rocks at elevated temperatures generates reservoir fluids with higher non-condensable gas (mainly CO_2) and bicarbonate content compared to other types of conventional geothermal resources. These characteristics have also been observed in other carbonate-hosted geothermal systems in Croatia and Turkey. The calcium and bicarbonate levels in Rs7 and Pn waters may be high enough to lead to calcite precipitation. Calcite precipitation is most likely to occur at the level of first boiling in the well and can gradually restrict the wellbore causing a reduction in productivity up to complete well shutdown. If the risk of calcite precipitation is confirmed, it is recommended to further evaluate the feasibility of injecting a calcite chemical inhibitor downhole via capillary tubing as a cost-effective calcite scaling mitigation measure.

A preliminary scaling risk analysis, using The Geochemist's Workbench geochemical modeling software and based on the data available (atmospheric water composition, standard temperature and pressure), suggests a risk of precipitation of various silica (SiO_2) polymorphs associated with Rs7 water. Amorphous silica precipitates at low temperatures (i.e., with steam loss/or conductive cooling) much faster than other silica forms. Hence, it is the dominant form of silica deposition observed in surface equipment, reinjection wells and effluent disposal ponds of geothermal plants.

However, it is important to note that scaling risk assessments based solely on atmospheric water compositions may not accurately reflect the true scaling potential through the production flow path. Subsurface conditions characterized by higher temperatures, pressures, and CO_2 partial pressures can significantly alter mineral solubility and scaling tendencies. Therefore, a more advanced scaling risk analysis should be undertaken once complete total gas (i.e., gas/(gas+ steam)) and production water chemistry are known; this will allow reconstruction of reservoir fluid composition that is representative of in-situ reservoir conditions. This analysis would enable a more accurate prediction of scaling risks from the producer bottomhole to the surface. If the risk of silica (or other minerals) scaling is confirmed during further analysis, a dedicated mitigation/ remediation strategy should be considered. This may include operational controls (e.g., temperature and pressure management), chemical treatments and regular mechanical cleaning of impaired equipment.

Copyright © SLB. All Rights Reserved. Private & Confidential. Reproduction only by permission.

Table 2.34 Chromatographic dry gas analysis of samples collected from Rs7

Well	Crnac-8	Crnac-8	Crnac-8	Crnac-8	Magadenovac-1	Magadenovac-1	Magadenovac-1	Sjece-1
Depth (m)	2194.9 - 2207	2194.9 - 2207	2210 - 2195.5	2210 - 2195.5	2614.9 - 2625.4	2614.9 - 2625.4	2614.9 - 2625.4	3015.5 - 3045.5
Lithologic Notes	Vera Fm. (firm, slightly sandy marls), immediately above the Valpovacka Fm.	Vera Fm. (firm, slightly sandy marls), immediately above the Valpovacka Fm.	Vera Fm. (firm, slightly sandy marls), immediately above the Valpovacka Fm.	Vera Fm. (firm, slightly sandy marls), immediately above the Valpovacka Fm.	Vukovarska Fm. (Benicanci and Karasica clans?) dolomite-lime breccias, calcareous marls, sandy marls, sandstones, conglomerates, agglomerates, subarkoses, cograuvakes, silites and calcarenites	Vukovarska Fm. (Benicanci and Karasica clans?) dolomite-lime breccias, calcareous marls, sandy marls, sandstones, conglomerates, agglomerates, subarkoses, cograuvakes, silites and calcarenites	Vukovarska Fm. (Benicanci and Karasica clans?) dolomite-lime breccias, calcareous marls, sandy marls, sandstones, conglomerates, agglomerates, subarkoses, cograuvakes, silites and calcarenites	Moslavacka Gora Fm Rs-7
Oxygen (vol%)					0	0	0	0
Carbon monoxide (vol%)					0	0	0	0
Carbon dioxide (vol%)	1.4	5.0	2.6	2.1	0.4	18.4	0.2	13.9
Hydrogen sulfide (vol%)					0	0	0	0
Nitrogen (vol%)	1.0	1.3			16.4	0	14.4	1.7
Methane (vol%)	65.1	64.8	73.8	67.6	71.6	69.7	73.4	48.9
Ethane (vol%)	3.5	3.4	3.1	3.5	5.7	5.7	5.4	13.4
Propane (vol%)	7.7	7.2	8.8	10.9	4.4	4.6	4.8	6.9
i-butane (vol%)	3.7	3.4	2.8	3.8	0.4	0.3	0.4	1.6
n-butane (vol%)	6.3	5.4	4.2	6.0	0.9	1.1	1.1	4.7
i-pentane (vol%)	3.2	2.6	1.8	2.5	0.2	0.1	0.2	1.6
n-pentane (vol%)	3.3	2.7	1.7	2.1	0.1	0.1	0.1	3.0

Copyright © SLB. All Rights Reserved. Private & Confidential. Reproduction only by permission.

Well	Crnac-8	Crnac-8	Crnac-8	Crnac-8	Magadenovac-1	Magadenovac-1	Magadenovac-1	Sjece-1
Hydrocarbons C6+ (vol%)	4.7	4.0	1.2	1.5			trace	4.4
Total	100.0	100.0	100.0	99.9	100.0	100.0	100.0	99.9
Density at 60 degF (g/cm^3)	1.2703	1.2356	1.0791	1.1778	0.8799	1.0124	0.8743	1.3641
Relative Density at 60 degF (Air = 1)	1.0387	1.0104	0.8824	0.6931	0.7195	0.8278	0.7149	1.1135

Copyright © SLB. All Rights Reserved. Private & Confidential. Reproduction only by permission.

Table 2.35 Chromatographic dry gas analysis of samples collected from Pn

Well	Rasovac-1	Rasovac-1
Depth	2796.96 - 2834	2796.96 - 2834
Lithologic Notes	polymictic breccia, shale (partly dolomitic), dolomite, dolomitic limestone at 2826 m	polymictic breccia, shale (partly dolomitic), dolomite, dolomitic limestone at 2826 m
Notes		
Oxygen		
Carbon monoxide		
Carbon dioxide	43.67	40.56
Hydrogen sulfide		
Nitrogen	3.61	3.5
Air	21.25	26.43
Moisture		
Methane	26.74	24.81
Ethane	2.29	2.14
Propane	1.46	1.44
i-butane	0.15	0.16
n-butane	0.43	0.47
i-pentane	0.1	0.12
n-pentane	0.09	0.12
Hydrocarbons C6+	0.22	0.26
Total	100.01	100.01
Density at 60 degF	1.43075	1.4356
Relative Density at 60 degF (Air = 1)	1.16731	1.17127

Corrosion

Available data indicate that the primary corrosion risk associated with produced waters from the Rs7 and Pn reservoirs is related to elevated concentrations of CO_2. High CO_2 levels can significantly increase the risk of carbon steel corrosion through the formation of carbonic acid (H_2CO_3) when CO_2 dissolves in water, leading to localized corrosion (e.g., pitting) and wall thinning of subsurface and surface production equipment. This is particularly relevant at elevated temperatures and flow rates typical of geothermal systems.

H_2S, which is highly toxic and corrosive, was not detected in the available data. However, the absence of H_2S, even if it occurs in trace amounts, should be confirmed by additional sampling and analysis. The absence of H_2S, if confirmed, also reduces the likelihood of forming iron sulfide scales, which can contribute to flow assurance issues and localized corrosion.

Although the produced waters exhibit significant variability in salinity, the recorded salinity levels are not expected to pose a major corrosion risk for either subsurface or surface equipment in the target areas.

Corrosion management strategies should prioritize mitigation of CO_2-related corrosion, including the use of corrosion-resistant alloys, application of protective coatings, or use of chemical inhibitors. Routine monitoring of produced water chemistry, especially CO_2 levels and pH, is recommended to ensure continued integrity of production equipment.

Hydrocarbon Presence

Copyright © SLB. All Rights Reserved. Private & Confidential. Reproduction only by permission.

Water samples collected from both the Rs7 and Pn formations near and within the Rasovac area (Targets C and E) are noted as being oily or mixed with oil (wells Crnac-7, Ladislavaci-1 and Ladislavaci-4 in Table 2.32 and Rasovac-1 in Table 2.33). Dry gas samples from Rs7 south of Target C (well Crnac-8; Table 2.34), show very high concentrations of methane and other hydrocarbon gases, and the gas sample from Pn within Target E (well Rasovac-1; Table 2.35) also shows high hydrocarbon concentrations. Farther north, near Target D, there is no mention of oil associated with the Rs7 water sample collected from well Bockovci-1, nor are there any gas samples from this well. Near Targets F and G, there are no water nor gas sample data from the Pn formation, but Rs7 gas samples within Target F (well Magadenovac-1; Table 2.34) and southeast of Target G (well Sjece-1) show high concentrations of methane and other hydrocarbon gases. Water samples from Rs7 near Targets G and F do not mention the presence of oil, and it remains uncertain if oil or hydrocarbon gases are present in the deeper Pn formations at these locations. These observations from existing data indicate that there is a relatively high chance of encountering hydrocarbons in the Rasovac area (Targets C and E), while this risk may be lower in Target D and remains highly uncertain in Targets F and G.

The presence of hydrocarbons in geothermal production flow presents challenges for surface handling as surface binary facilities with conventional designs are not equipped to handle them and, absent separation, could result in fouling of the heat exchanger and reduced efficiency. If hydrocarbons are present in the geothermal production stream, it will be necessary to develop a plan for their separation. Such measures are not common practice in the geothermal industry, despite rising interest in utilizing depleted oil and gas resources for geothermal production, and current demonstration projects with co-production of geothermal and hydrocarbon fluids handle the separated hydrocarbons by flaring at surface. Production tests on newly drilled geothermal wells in the project area will provide a better understanding of hydrocarbon presence in the target formations.

2.11 Geothermal doublet simulations

The geothermal simulation study provides a thorough technical assessment of the planned geothermal project within the delineated target areas. Incorporating outcomes from the chance of success analysis (2.9 Geothermal site selection), two areas of interests (AOIs) have been identified as priority areas: one adjacent to Rasovac-1 and Stjepanik-1 (referred to as Rasovac AOI), and a second to the west of Bockovci-1 (referred to as Bockovci AOI). This section presents a comprehensive evaluation of the dynamic performance of two hypothetical doublets in the target areas, utilizing advanced simulation techniques and integrating all available field measurements to rigorously evaluate the technical and operational viability of geothermal heat extraction.

Objectives of the Study:

- Develop an integrated simulation model tailored for geothermal resource evaluation.
- Estimate the rate of thermal decline over the forecast period.
- Quantify reservoir pressure drawdown that could be expected for the planned circulation of geothermal brine.
- Identify and assess potential risks inherent to geothermal production operations.

Copyright © SLB. All Rights Reserved. Private & Confidential. Reproduction only by permission.

- Formulate recommendations to maximize heat recovery efficiency and minimize parasitic energy consumption.

2.11.1 Reservoir Simulation Executive Summary

The reservoir simulation model was built using the Intersect™ platform, employing geological, petrophysical, and dynamic datasets reflect the relevant characteristics of the investigation area. The model was initialized based on available formation pressure and temperature data acquired mainly from drill stem tests (DST) and fluid sampling analysis, where available. Due to incomplete field data, particularly the lack of representative water and rock samples in the target geothermal intervals (from Rs5 to Tg markers), key reservoir parameters such as relative permeability curves, rock and fluid thermal properties, rock physics function, and fracture gradient were adopted from established literature and comparable industry standards. In addition, the geothermal brine is assumed to be free of hydrocarbons and carbon dioxide; this assumption should be revisited once comprehensive laboratory and field-testing data become available..

There are two geothermal AOIs: Rasovac AOI consists of combined targets B-C-D, and Bockovci AOI comprises targets A-D (2.9.5 Global Geothermal Chance of Success Analysis). For each geothermal AOI, the base case analysis considered a standard doublet comprising one production well and one injection well. A single scenario was modeled, specifying well placement, operating rate schedule, and pressure constraints relevant to geothermal development strategies. Key results, including projected flow rates, production temperatures over a 30-year forecast, and maximum pressure drawdown, estimated productivity index (PI) and injectivity index (II) are summarized in Table 2.36.

Table 2.36 Results of the base case of geothermal simulation in 2 AOI: Rasovac and Bockovci.

	Rasovac AOI		Bockovci AOI	
	Rasovac Producer	Rasovac Injector	Bockovci Producer	Bockovci Injector
Flow Rates (lps)	80	80	80	80
Maximum Temperature (°C)	155	80	163	79
Minimum Temperature (°C)	148	79	152	78
Maximum Bottomhole Pressure bar)	196	296	198	351
Minimum Bottomhole Pressure bar)	193	281	193	331

The simulation period of 30 years is sufficiently long to investigate geothermal power generation over the period of operation of the carbon capture and sequestration (CCS) application. Under the stated assumption in 2.11.2.1 Model Assumptions, the reservoir simulation model forecasts that a flow rate of 80 liters per second (lps) of hot geothermal brine can be achieved by a doublet configuration at each site, although the corresponding thermal behavior differs between locations (Table 2.36). Rasovac and Bockovci AOIs were able to maintain the minimum production temperature above 148 °C and 152 °C, respectively for the 30-year simulation period. Thermal decline is estimated to be 7 °C for Rasovac AOI, and 11 °C for Bockovci AOI after 30 years. In

Copyright © SLB. All Rights Reserved. Private & Confidential. Reproduction only by permission.

both AOIs, injection pressure slightly increases after a short rapid initial build-up phase. Pressure build-up in the vicinity of the injection well remains within the limits established by the reservoir's fracture gradient, thereby mitigating risks associated with caprock integrity and fault activation. This is assured by applying a conservative limit of 90% of the estimated fracture gradient (0.16 bar/m, see 2.8.3.1 Model assumptions) for the maximum allowable injection pressure. For both AOIs, production pressure gradually decreases over the duration of the forecast, with the total decline estimated to be 3 and 5 bar for Rasovac and Bockovci AOI, respectively.

The simulation study indicates a feasible engineering outlook for the geothermal project in both the Rasovac and Bockovci areas, with Rasovac AOI offering a more favorable option. Rasovac AOI benefits from better well control, supported by data from two nearby offset existing wells (Rasovac-1 and Stjepanik-1) and proximity to an established hydrocarbon field. In contrast, Bockovci is comparatively data sparse, relying primarily on Bockovci-1 for well control. DST results of target geothermal layers demonstrate that Rasovac-1 exhibits higher permeability (~45 mD) compared to Bockovci-1 (~21 mD), albeit for a very thin interval (<20 m). Additionally, the geothermal intervals in Rasovac AOI display greater thickness (445 meters for producer and 306 meters for injector), compared to Bockovci AOI (~306 meters for producer and ~175 meters for injector). This comparison should be approached with caution due to the uncertainty in horizon interpretation resulting from low seismic resolution at depth. Although Bockovci features a higher temperature gradient and thus a higher initial temperature, its temperature declines more rapidly between the doublet. This could be due to slightly smaller well spacing in Bockovci AOI, resulting in stronger hydraulic and thermal connectivity between the producer and injector. A primary uncertainty in Rasovac AOI is the potential presence of hydrocarbon tracers or carbon dioxide in the geothermal brine, due to its proximity to active hydrocarbon fields. This risk is less pronounced in Bockovci AOI, as outlined in 2.10 Fluid geochemistry review of selected geothermal sites.

We consider it critical that additional data acquisition be undertaken to enhance reservoir characterization, and confirm the validity of important assumptions that had to be made due to limited data availability. Monitoring strategies should include routine pressure surveillance (including pressure interference tests), tracer studies, recent downhole pressure and temperature (P/T) surveys, water sample analysis, and extended post-completion flow testing within the target geothermal formations. Furthermore, regulatory and operational frameworks should be reviewed and revised as necessary to ensure comprehensive compliance with all technical and statutory requirements.

2.11.2 Simulation Model Set-up

This section describes the datasets, parameters, and methodology employed in the construction of the dynamic simulation model used to assess geothermal resources within the deep saline aquifers of the Drava Depression. The workflow encompasses data compilation, model set-up, parameterization, and calibration, providing a robust foundation for evaluating geothermal production scenarios and resource sustainability. The dynamic simulation model integrates a comprehensive suite of geological, petrophysical, and operational data. The modeling workflow starts with the review of the conceptual reservoir model, focusing on delineating fluid flow pathways, defining the spatial extent of the reservoir, and establishing system boundaries, guided

Copyright © SLB. All Rights Reserved. Private & Confidential. Reproduction only by permission.

by the latest geological and hydrogeological understanding of the Drava Depression. The model domain is initialized using available well and field data to set thermodynamic (pressure, temperature, saturation) and petrophysical (porosity, permeability, rock compressibility) properties at each grid cell. Boundary conditions, both lateral and vertical, are specified to reflect realistic mass and heat exchange with surrounding formations. After initial and boundary conditions specified, the model is run until a dynamic steady-state equilibrium is achieved, referred to as the initial state. The property assignment process needs to ensure that simulated pressure and temperature fields of the initial state are consistent with measured values from key wells across the geothermal AOIs. Permeability and transmissivity parameters are iteratively adjusted to align with flow capacities estimated from DST results, which is critical for representing in-situ reservoir performance and ensuring the predictive reliability of subsequent dynamic forecasts.

Upon successful calibration, the model could be used to simulate geothermal production and forecast reservoir response under various operational scenarios. The model outputs spatial and temporal changes in pressure and temperature, supporting evaluation of sustainable energy extraction rates, reservoir longevity, and optimal production strategies. By systematically integrating geological, petrophysical, and operational datasets within a robust dynamic simulation framework, this modeling approach establishes a defensible basis for both resource assessment and prospective development decision making in the Drava Depression geothermal play. Ongoing refinement and integration of new data—as wells are drilled and additional measurements acquired—will further enhance the model's accuracy and utility for field development planning.

Data sources comprising prior studies, field measurements, and well reports, were consolidated to assure an accurate representation of the reservoir's petrophysical and geological characteristics, as described in preceding sections of the report. Geological framework includes regional stratigraphic correlations, structural maps for principal reservoir intervals, core descriptions, and seismic interpretation. Well data comprises well logs and Drill Stem Test (DST) results for transmissivity and productivity index estimates. Laboratory measurements and petrophysical evaluations provide porosity, permeability, water salinity, water density, and formation fluid compressibility. Fluid properties, such as brine density and brine viscosity, are parameterized as functions of temperature and pressure, consistent with the geothermal conditions of the Drava Depression.

2.11.2.1 Model Assumptions

The geological model is deterministic, based on the static modeling results detailed in 2.5 Geological modeling, and is assumed to accurately represent the structural and facies framework from near surface down to the Tg horizon. Seismic data adds uncertainty as Rs5 and Rs7 thin layers exhibit local variability, and may approach the limits of seismic resolution. As described in 2.9 Geothermal site selection, these markers are challenging to trace because of erosion and complex geological conditions. The geothermal model combines the petrophysical properties (i.e., porosity and permeability) of two geological models detailed in 2.5.1 Upper formations Alfa (D') to Z' and 2.5.2 Lower formations Z' to Tg. The lateral extent of the geothermal model was set to cover the entire carbon capture and sequestration (CCS) domain in order to include not only the current AOIs but also other potential geothermal sites that may be considered in the future. Additionally,

Copyright © SLB. All Rights Reserved. Private & Confidential. Reproduction only by permission.

the model was expanded by about 3 km to the west of Stjepanik-1 to minimize boundary effects on Rasovac AOI. The model was also extended vertically (1) to the surface to enable simulation of heat transfer in shallow sections above the Z' marker, and (2) 1 km below Tg marker to include thermal representation of the basement rock. These regions of expansion were assigned low porosity and permeability values (0.1% and 0.0001 mD, see Fig. 2.287 and Fig. 2.288). The assignment of reservoir properties below the Tg marker and in regions beyond seismic coverage should be approached with caution, as these areas currently lack sufficient data. Property assumptions in such zones are inherently uncertain and may impact model reliability. It is therefore recommended that further interpretation or advanced modeling in these regions be deferred until additional data are acquired and thoroughly evaluated to support more robust characterization.

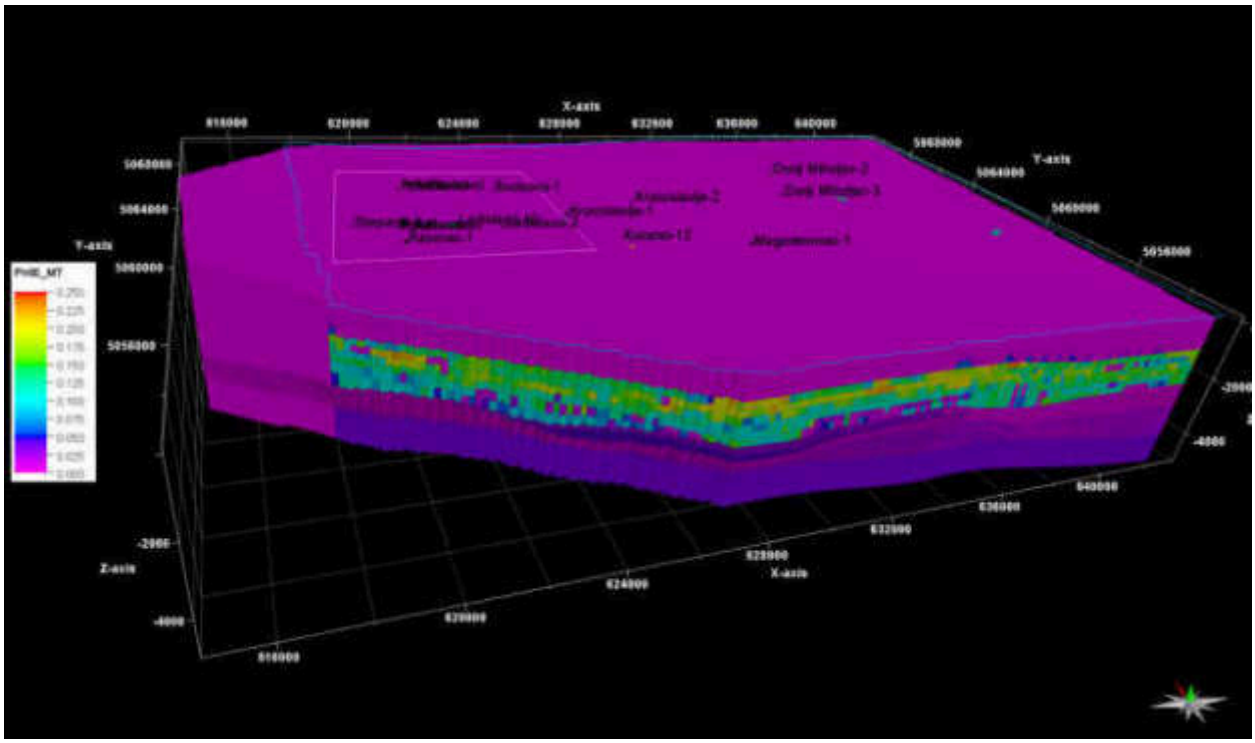


Fig. 2.287 3D view of effective porosity distribution of the static model.
Geothermal area of interest regions are highlighted by the pink polygon. The CCS model boundary is shown in blue polygon.

Copyright © SLB. All Rights Reserved. Private & Confidential. Reproduction only by permission.

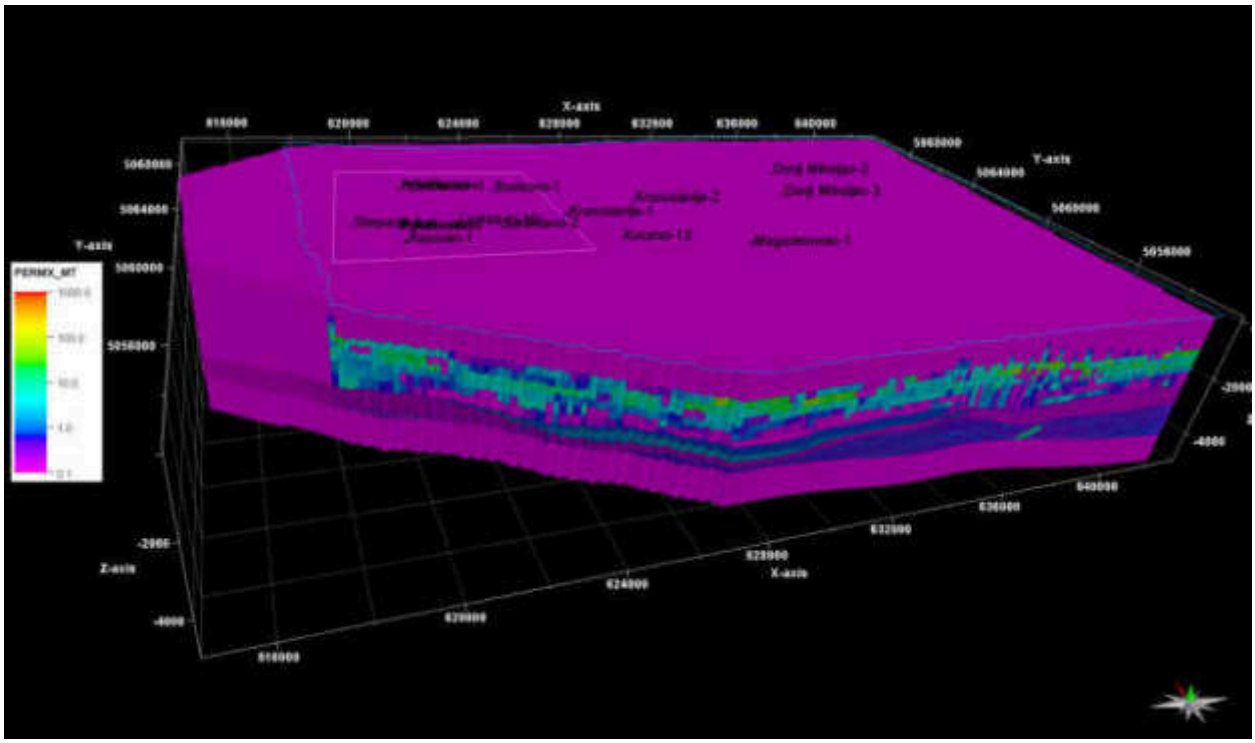


Fig. 2.288 3D view of horizontal permeability distribution of the static model
Geothermal area of interest regions are highlighted by the pink polygon. The CCS model boundary is shown in blue polygon.

A single porosity model was chosen for this project primarily due to the absence of detailed fracture data required to reliably define a more complex double-porosity model, which separates flow within the rock matrix and fracture networks. Single porosity models are less computationally demanding than dual-porosity approaches, making them particularly suitable for preliminary reservoir evaluations, sensitivity analyses, and routine operational studies. In geothermal reservoirs that are not characterized by significant natural fracturing, or where fractures do not control flow or storage, single porosity models can achieve an adequate level of accuracy. For many sedimentary or volcanic geothermal reservoirs with minimal interconnected macro-fractures, adopting a dual-porosity model introduces additional complexity without necessarily improving model outcomes. Therefore, unless there is conclusive evidence, such as tracer test results, well test analyses, or core studies, demonstrating that fracture-dominated flow is significant, the standard practice is to initially employ a single porosity model and consider more complex representations only if warranted by further data.

Due to the absence of surveys that measure pressure and temperature profiles along the entire wellbore, and the availability of only limited-depth Drill Stem Test (DST) data, it was necessary to assume a constant thermodynamic gradient within the wellbores of key wells. Specifically, the model adopts a uniform pressure and temperature gradient where detailed downhole measurements are lacking. This approach involves applying a conductive temperature gradient, which reflects the heat flow characteristics typically observed in sedimentary formations. Conductive gradients are considered appropriate in this context, as sedimentary rocks generally exhibit predominantly conductive heat transport mechanisms in the absence of significant convective flow. As additional downhole data, such as continuous pressure-temperature (P-T) logs

Copyright © SLB. All Rights Reserved. Private & Confidential. Reproduction only by permission.

become available, these assumptions should be revisited and the thermodynamic profiles updated to improve the accuracy of the reservoir model. DST data indicate mostly sub-hydrostatic pore pressures and pressure gradient among key wells in the geothermal AOIs (Table 2.37). As covered in 2.6 Geomechanical quicklook analysis, available leak-off tests (LOT) in the AOIs were used to constrain fracture gradient and establish injection pressure limits at both geothermal targets. Assuming a fracture gradient of 0.155 bar/m and applying a safety factor of 0.9, the maximum allowable bottomhole injection pressures at the middle completion interval are estimated to be 362 bar for the Rasovac AOI and 380 bar for the Bockovci AOI.

Formation brine density and viscosity are assigned based on available sample analyses and zonation, as described in 2.10 Fluid geochemistry review of selected geothermal sites. Based on limited sample analysis at key wells in the AOIs there is insufficient information about CO_2 and hydrocarbon levels in those areas. Therefore, the model assumes that the geothermal brine is free of these components; initial water saturation is set to 100% and maintained throughout simulation.

2.11.2.2 Gridding

The overall gridding scheme is illustrated in Fig. 2.289 A structured grid was constructed for the geothermal reservoir model, employing a uniform base cell size of approximately 150 m × 150 m across the domain. In order to accurately capture the flow dynamics and enhance resolution around the two Areas of Interest (AOIs), local grid refinement was implemented. Within these AOIs, specifically in the vicinity of planned geothermal wells, the cell size was reduced to 30 m × 30 m, ensuring detailed representation of hydraulic gradients and well performance (Fig. 2.290). Vertically, the grid was discretized with layers of roughly 5 m thickness within the principal reservoir intervals, defined as the section between the Rs5 and Tg geological markers (Fig. 2.291). This finer layering facilitates improved modeling of reservoir heterogeneity and vertical fluid movement. Conversely, coarser layering was applied in the upper and peripheral zones outside the main reservoir intervals to optimize computational efficiency without sacrificing essential resolution where it is most needed. The model comprises approximately 11.2 million cells and spans from the surface to below the Tg marker, reaching maximum depths of up to 5 km below ground level. In total, the modeled area covers 504 km^2 (28 km by 18 km), enabling comprehensive simulation of reservoir behavior across both regional and local scales.

Copyright © SLB. All Rights Reserved. Private & Confidential. Reproduction only by permission.

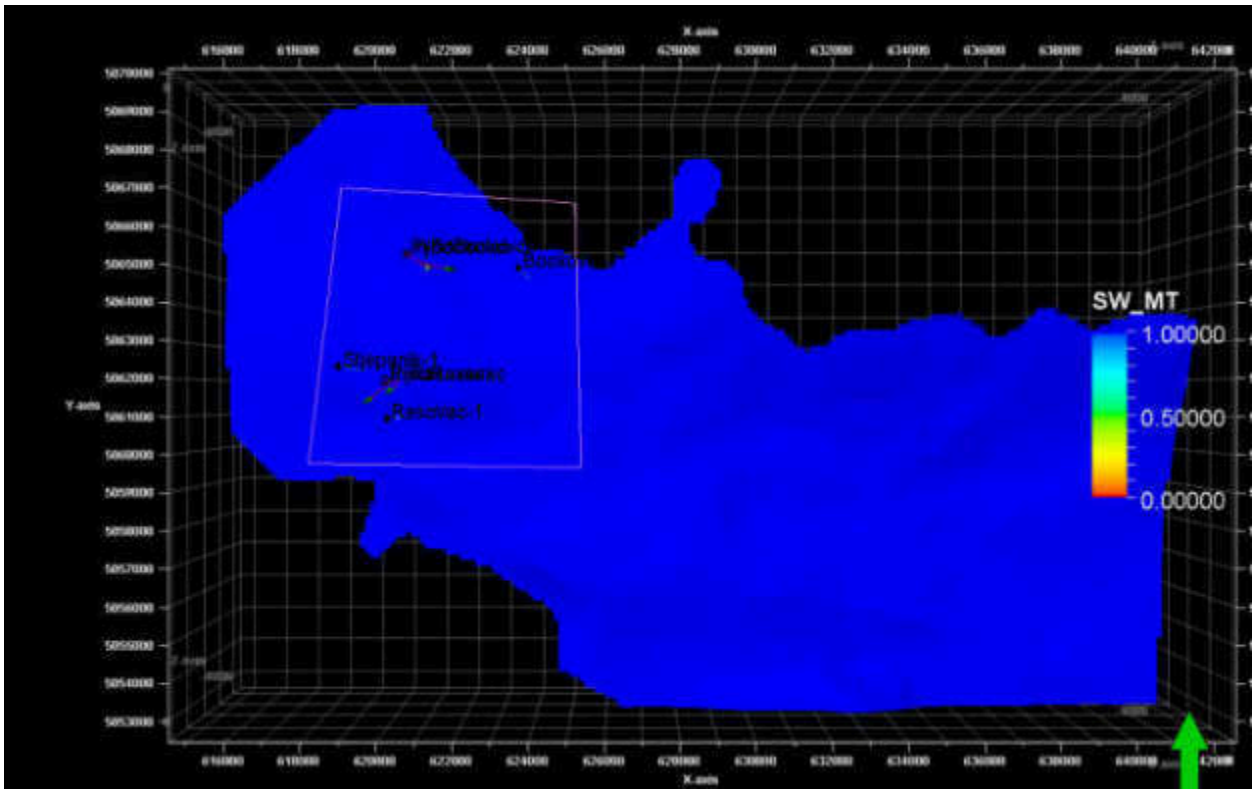


Fig. 2.289 Extent of 3D geothermal model showing distribution of water saturation.

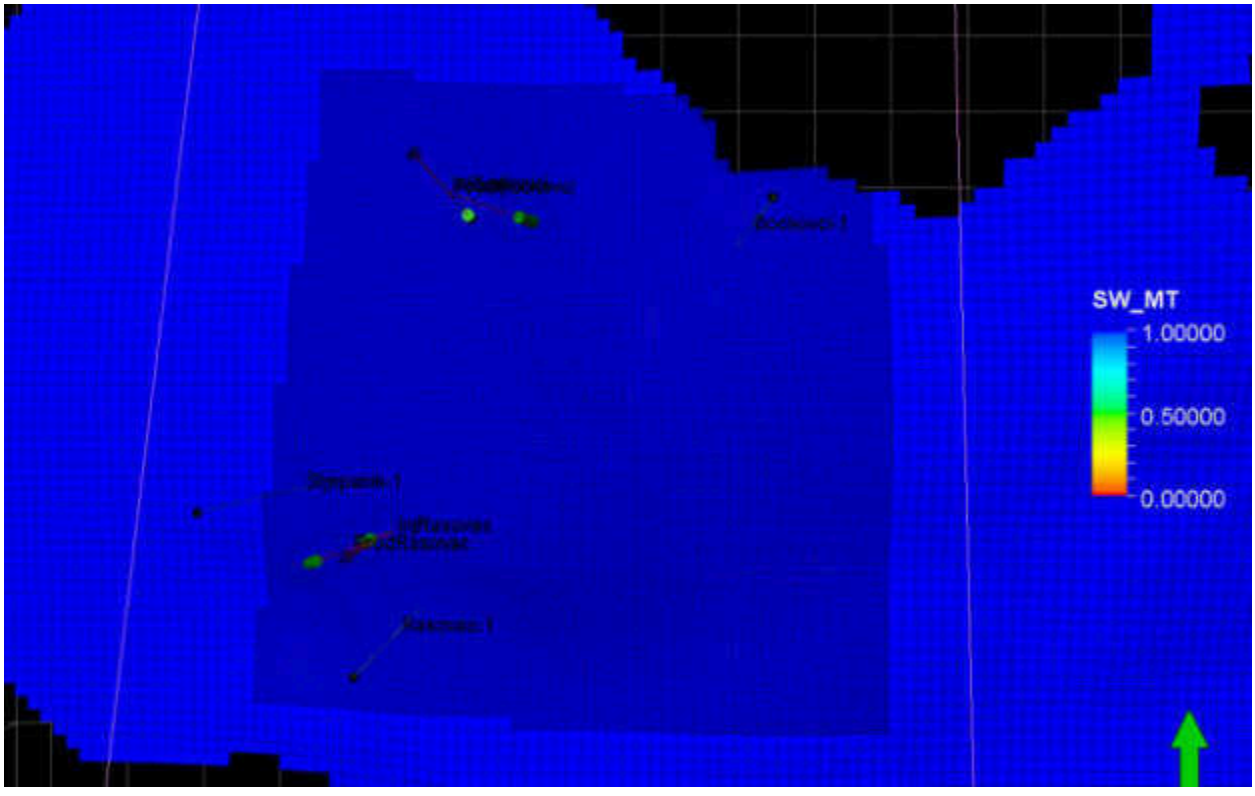


Fig. 2.290 Close-up visualization of refined gridding in the geothermal AOIs.

Copyright © SLB. All Rights Reserved. Private & Confidential. Reproduction only by permission.

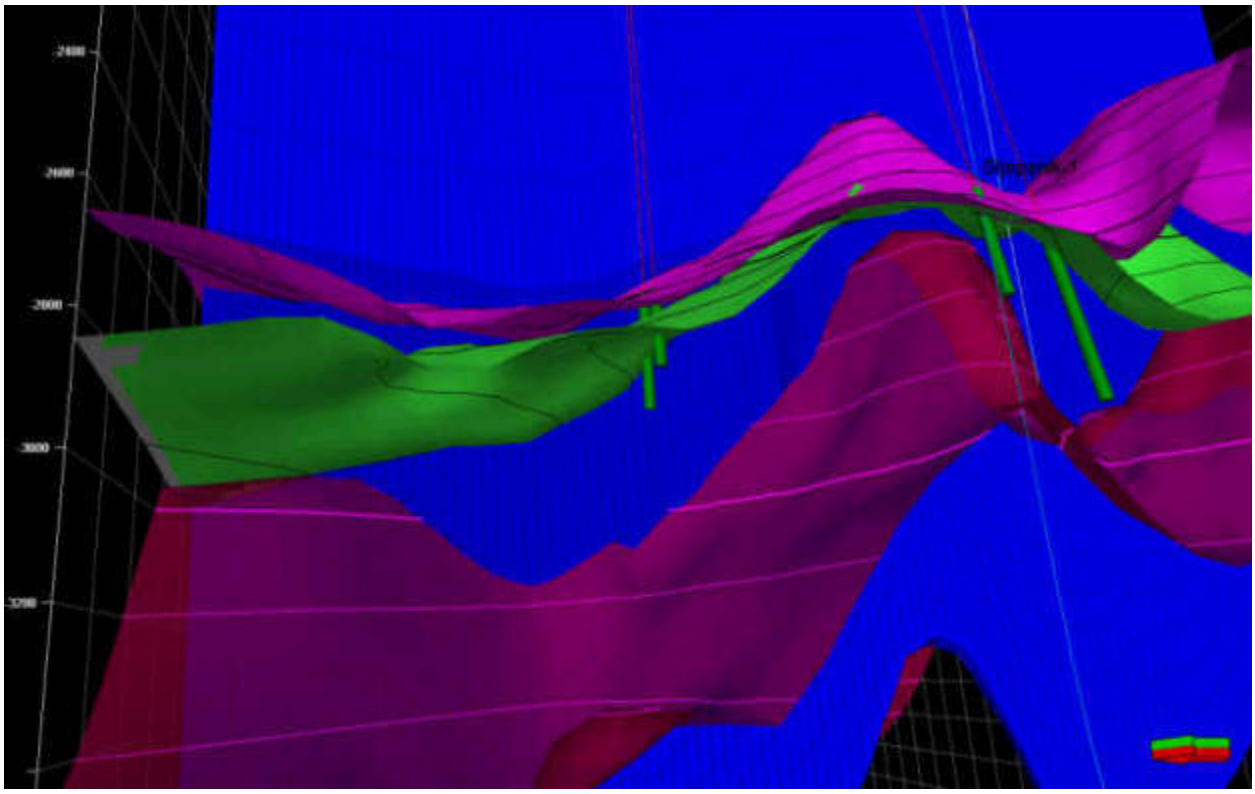


Fig. 2.291 Visualization of the model's vertical layering and water saturation distribution.
Three main stratigraphic horizons, Rs5, Pn, and Tg, are indicated based on regional markers (from top to bottom). The vertical (Z) axis is exaggerated by a factor of 5 to enhance interpretability. Fine layering is applied within the geothermal target intervals. The locations of two doublets within the two geothermal AOIs are also illustrated: left is Bockovci AOI doublet, right is Rasovac AOI doublet.

2.11.2.3 Initial and boundary conditions

In the dynamic simulation framework, special attention is given to the representation of boundary conditions to accurately simulate the thermal and hydraulic regimes of the geothermal system. The uppermost ~500 meters and the deepest model layer, corresponding to the underlying basement extension below the Tg marker, are defined as thermally active only zones, meaning these intervals participate in heat transfer but do not permit hydraulic flow (Fig. 2.292). This approach isolates the hydraulic and thermal behavior of the target reservoir formation while minimizing computational overhead associated with tracking fluid movement in non-productive strata. Both the surface (top boundary) and the basement (bottom boundary) layers are assigned constant temperatures, reflecting the ambient atmospheric temperature at the surface and an assumed conductive heat source at the model's base. This configuration enables the simulation of conductive heat fluxes into and out of the main reservoir interval. Specifically, the model incorporates conductive heat loss from the uppermost feedzone layers to overlying rocks and the atmosphere by coupling these layers conductively to the constant-temperature surface. Similarly, the heat exchange across the base of the reservoir, between the deepest feedzone layers and the basement rock, is represented as conductive heat transfer to a constant-temperature boundary, simulating the influence of deep regional heat sources.On the lateral boundaries, such as the extended buffer zone defined at the western edge of the model, no-flow (hydraulically closed) conditions are imposed with no provision for external heat, fluid sources, or sinks.

Copyright © SLB. All Rights Reserved. Private & Confidential. Reproduction only by permission.

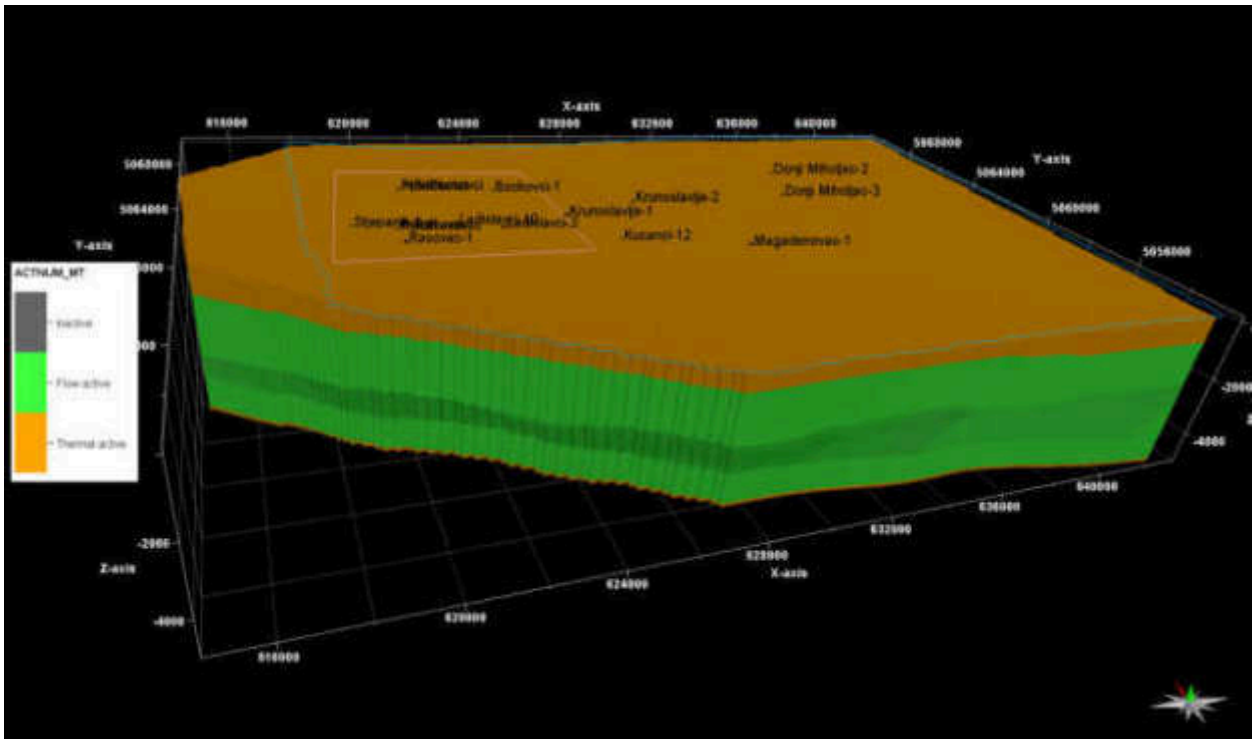


Fig. 2.292 Thermally active and flow active cell distribution.

Initial reservoir pressure and temperature distributions are anchored to measured data and interpreted gradients, as documented in Table 2.37. Where bottomhole measurements or profile surveys are absent, values are spatially interpolated to provide a continuous initial field conditions. The general absence of significant convective temperature gradient justifies the application of these conductive static gradients. The model domain is populated with the best-estimate sub-hydrostatic pressure and temperature gradients and localized around the radius of investigation for each key well. To ensure that the geothermal forecast simulation starts from a realistic, physically stable state, the model is run for 20,000 years, with all wells shut in and no active fluid extraction or injection (Fig. 2.293and Fig. 2.294). This extended simulation period allows the system to stabilize to a dynamic equilibrium, where temporal changes in pressure and temperature become negligible throughout the model domain. The equilibrium pressure and temperature fields generated through this initialization protocol are compared with measured gradients for the key wells in the study area (Fig. 2.294 and Fig. 2.296). The results, shown in Fig. 2.297, demonstrate excellent agreement with available data in 3 key wells (Rasovac-1, Bockovci-1, and Stjepanik-1). This affirms the validity of the modeling approach and the suitability of the established boundary conditions for subsequent dynamic geothermal simulations.

Copyright © SLB. All Rights Reserved. Private & Confidential. Reproduction only by permission.

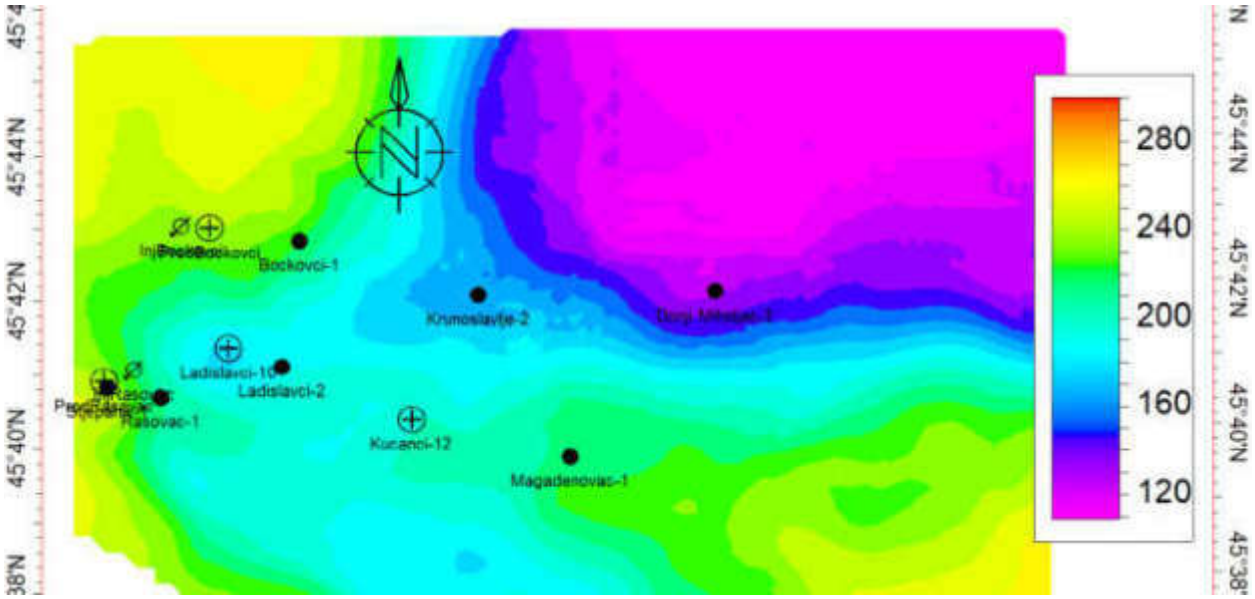


Fig. 2.293 Pressure distribution of the initial state run projected onto the Pn horizon

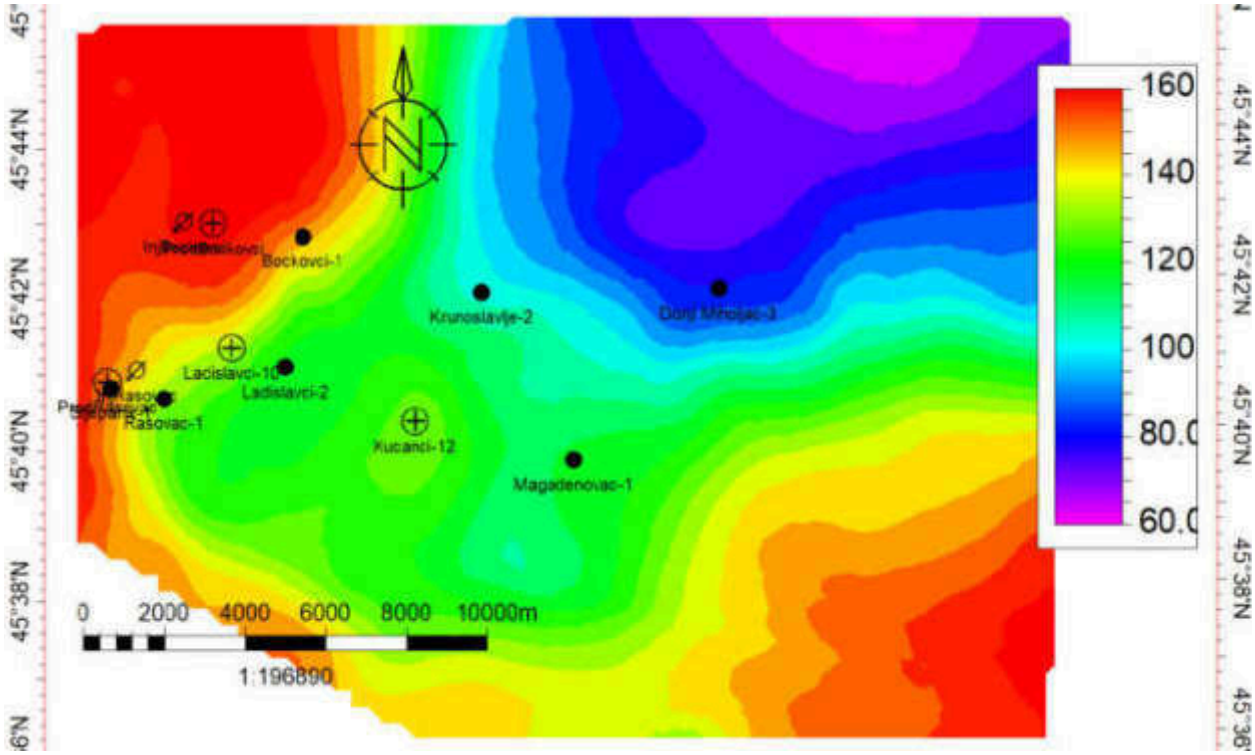


Fig. 2.294 Temperature distribution of the initial state run projected onto the Pn horizon

Copyright © SLB. All Rights Reserved. Private & Confidential. Reproduction only by permission.

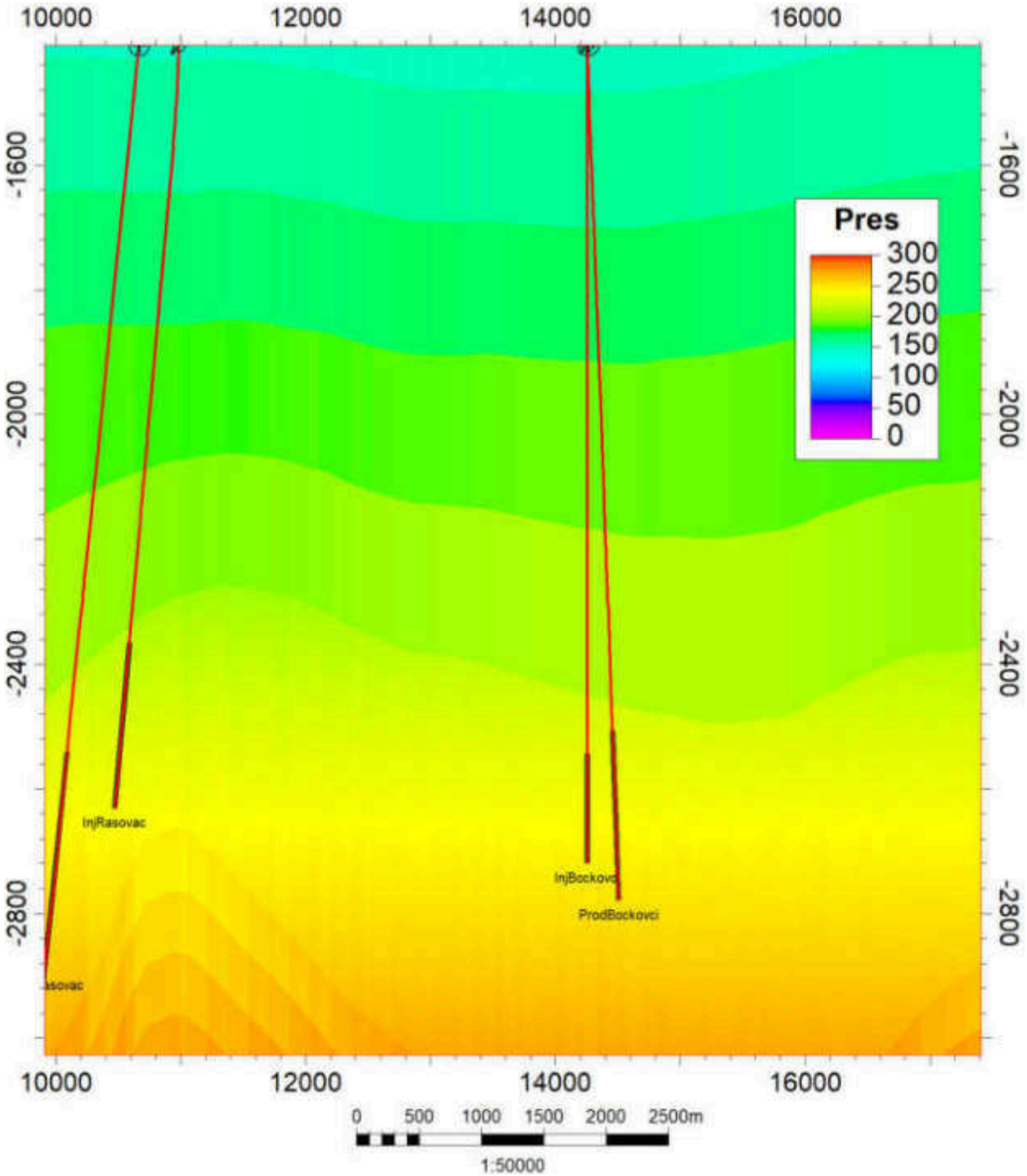


Fig. 2.295 Cross-sectional view of the initial-state pressure (in bar)
Distribution along a plane intersecting the two planned doublets in the Rasovac and Bokcovci AOIs.

Copyright © SLB. All Rights Reserved. Private & Confidential. Reproduction only by permission.

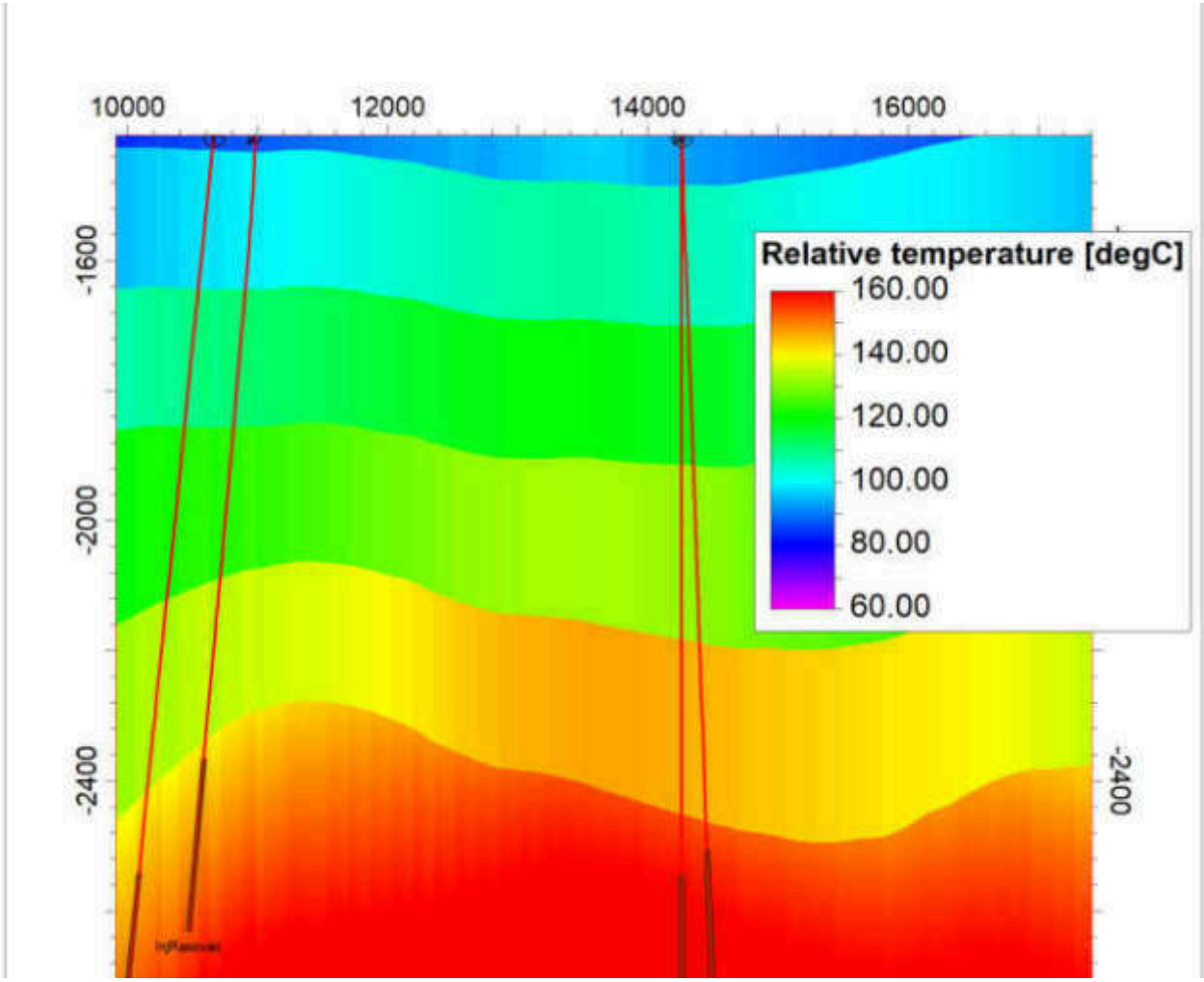


Fig. 2.296 Cross-sectional view of the initial-state temperature
Temperature distribution along a plane intersecting the two planned doublets in the Rasovac and Bokcovci AOIs.

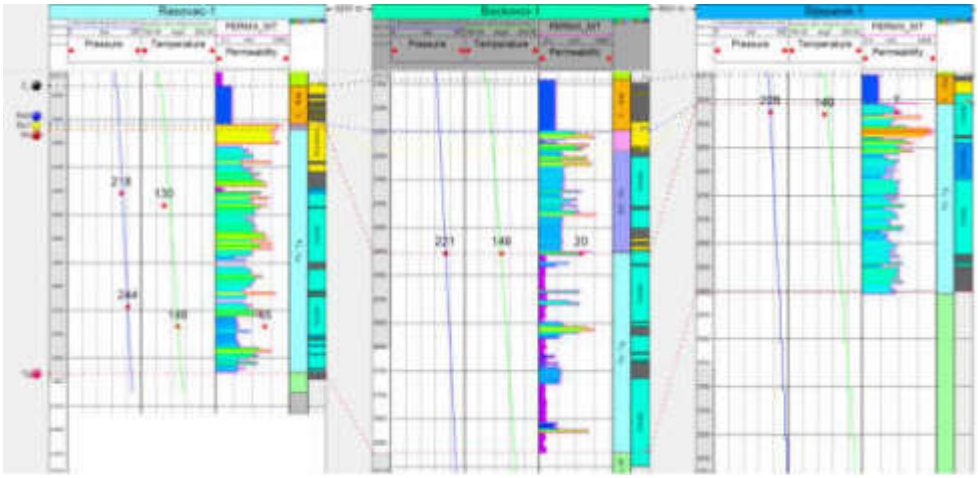


Fig. 2.297 Calibrated pressure, temperature and permeability of the initial state model
Calibrated pressure, temperature and permeability of the initial state model at 3 key wells (from left panel to right panel: Rasovac-1, Bockovci-1, Stjepanik-1) compared to survey and DST data (red dots). Key horizon markers (Z', Rs5, Rs7, Pn and Tg) are shown as well as interpreted lithology and zone division of the model.

Copyright © SLB. All Rights Reserved. Private & Confidential. Reproduction only by permission.

2.11.2.4 Rock and Fluid Properties

Accurate definition of rock and fluid properties is essential for reliably modeling reservoir performance and predicting long-term thermal decline during hot water production and cold reinjection. Petrophysical properties from Petrel-based and Petromod models are thoroughly evaluated and property value assignments from these models are used, where applicable (2.5 Geological modeling and 2.9 Geothermal site selection). Effective porosity distribution from the geological model, which is constrained by petrophysical logs and core measurements, is used without any modification. Previous sections describe how the permeability model is empirically determined from porosity-permeability correlations and facies-dependent end-members, and further adjusted based on proximity to interpreted faults. For the geothermal model, anisotropy (Kv/Kh = 0.1) was implemented, and the permeability model around certain key wells (Rasovac-1, Stjepanik-1, and Bockovci-1) in the geothermal AOIs was further modified to be consistent with permeability estimates from their DSTs. It is critically important to recognize the inherent risks and limitations associated with extrapolating DST results obtained from thin reservoir intervals (typically less than 20 meters) to much thicker intended geothermal production intervals spanning hundreds of meters, particularly when extended open-hole circulation tests have not been conducted. DSTs performed in limited sections provide localized estimates of permeability, pressure response, and fluid properties, and it is uncertain how those estimates apply to sections outside the tested interval. Thin test intervals may be disproportionately influenced by high-permeability streaks, natural fractures, or localized barriers, leading to over-or-underestimation of reservoir performance when scaled up to the entire production interval. Without comprehensive open-hole circulation testing, wherein there is sustained flow across the full reservoir thickness and could therefore provide more complete information on connectivity, transmissivity, and dynamic behavior, there is a significant risk of mischaracterizing injectivity, productivity, and long-term operational feasibility when results of DSTs are extrapolated beyond the test intervals. Such extrapolation can result in erroneous forecasts of sustainable flow rates, thermal drawdown, and pressure evolution, ultimately compromising well design, completion strategy, and field development planning.

Reference points of pressure and temperature were tabulated (mainly from DST reports of wells in the vicinities of the geothermal AOIs) in Table 2.37. In addition, estimates of flow capacity and average horizontal permeability derived from DSTs were used to calibrate the permeability distribution in the model, supporting consistency between static petrophysical properties, flow test responses, and dynamic simulation outputs (Table 2.37). Water density, compressibility, and viscosity were extracted from available but limited DST report. For example, in Stjepanik-1A, water viscosity and compressibility were estimated to be 0.18 cp and 5.5e-5 1/bar, respectively. Where direct measurements were unavailable, typical rock and fluid properties such as rock heat capacity, and rock and fluid thermal conductivities were either obtained from the available report [22] or estimated based on site-specific empirical correlations in relevant literature [23]. For efficient and simplified thermal property assignment, the model was divided into four zones based on prominent geological markers: above Rs5, Rs5–Pn, Pn–Tg, and below Tg (Table 2.38). For a fully water-saturated rock, the effective thermal conductivity is estimated as the geometric mean mixing law of matrix rock conductivity and water thermal conductivity.

Copyright © SLB. All Rights Reserved. Private & Confidential. Reproduction only by permission.

Table 2.37 Key reference pressure and temperature points from DST reports for geothermal simulations.

Well	Depth Pressure Survey (m TVD)	Depth Temperature Survey (m TVD)	Surface Elevation (m SSTVD)	Pressure (bar)	Temperature (°C)	Pressure Gradient (bar/m)	Temperature Gradient (° C/m)	Estimated Permeability (mD)
Bockovci-1	2548	2548	95	221	149	0.08622	0.05416	19.7
Donji Miholjac-3		1037	95		56		0.04339	111.4
Krunoslavlje-2	2159	2159	88	206	122	0.09495	0.05141	5.0
Stjepanik-1	2621	2626	95	228	149	0.08676	0.05256	7.0
Kucanci-12	2339	2390	98	199	121	0.08465	0.04603	0.1
Kucanci-12	2483	2507	98	200	145	0.08014	0.05345	12.0
Ladislavci-2	2128	2128	97	188	103	0.08788	0.04323	1.3
Ladislavci-10	1500	1500	96	120	100	0.07933	0.05933	
Magadenovac-1	2194	2194	98	221	106	0.10038	0.04330	25.0
Rasovac-1	2815	2831	97	245	149	0.08654	0.04868	44.7
Rasovac-1	2552	2578	97	218	130	0.08515	0.04616	

(NB: The reference depth of each measurement point and the estimated permeability are also included. Pressure and temperature gradient is estimated based on the value of the single survey point and its corresponding depth.)

Table 2.38 Thermal properties of the model

Thermal Zone	Rock Heat Capacity (kJ/m3.K)	Rock Thermal Conductivity (kJ/m.d.K)	Saturated Rock Thermal Conductivity (kJ/m.d.K)
Above Rs5	2189	207	193
Rs5-Pn	2422	250	231
Pn-Tg	2450	255	235
Below Tg	2500	259	239

(NB: Thermal properties (rock heat capacity, rock thermal conductivity, and saturated rock thermal conductivity) of the model, assigned based on regional markers.)

2.11.3 Geothermal simulation results and analysis

The base case scenario has been designed to provide a robust and realistic foundation for assessing long-term geothermal production potential in the Rasovac and Bockovci AOIs. For each site, the scenario comprises a single geothermal doublet—consisting of one production and one injection well, strategically located to target multiple key reservoir intervals, specifically the Rs5, Rs7, and Pn horizons. This multi-layer targeting aims to optimize reservoir intersection and maximize sustainable thermal extraction from the deep saline aquifer system.

Geothermal operations are scheduled to commence in January 2027. The simulation model spans a 30-year operational window, representing a typical project lifespan and enabling evaluation of both initial and late-life field behavior. Both Rasovac and Bockovci doublets are operated concurrently within the simulation, with no significant inter-site hydraulic or thermal interference anticipated, owing to a lateral separation of over 4 km between the two AOIs. Each doublet operates with continuous reinjection of cooled geothermal fluid at a temperature of ~80° C. This reinjection strategy is essential to provide reservoir pressure support and facilitate heat extraction from the reservoir rock. The maximum allowable bottomhole injection pressure for each

Copyright © SLB. All Rights Reserved. Private & Confidential. Reproduction only by permission.

well is determined by the following criterion: $P_{inj,max} = TVD_{mid\text{-}perforation} \times 0.9 \times 0.155$ bar/m, where TVD is the true vertical depth (midpoint of the completion interval). A conservative assumption (safety factor of 0.9) is incorporated to safeguard against the risk of reservoir fracturing or unintended fluid migration outside the target interval.

The outcomes of the 30-year base case simulation are summarized and analyzed in this section, focusing on the following core performance metrics (Fig. 2.298 and Fig. 2.299):

- **Thermal Decline:** The temperature evolution in the production wells is tracked to quantify long-term thermal drawdown and to assess sustainability of the heat extraction process over the project horizon. The results provide insight into the longevity and economic viability of the resource
- **Pressure Drawdown:** Reservoir pressure distribution and the magnitude of drawdown at the production wells are monitored, enabling proactive assessment of potential risks such as reduced well productivity, pump parasitic power requirements or operational constraints associated with excessive pressure depletion (Fig. 2.300)

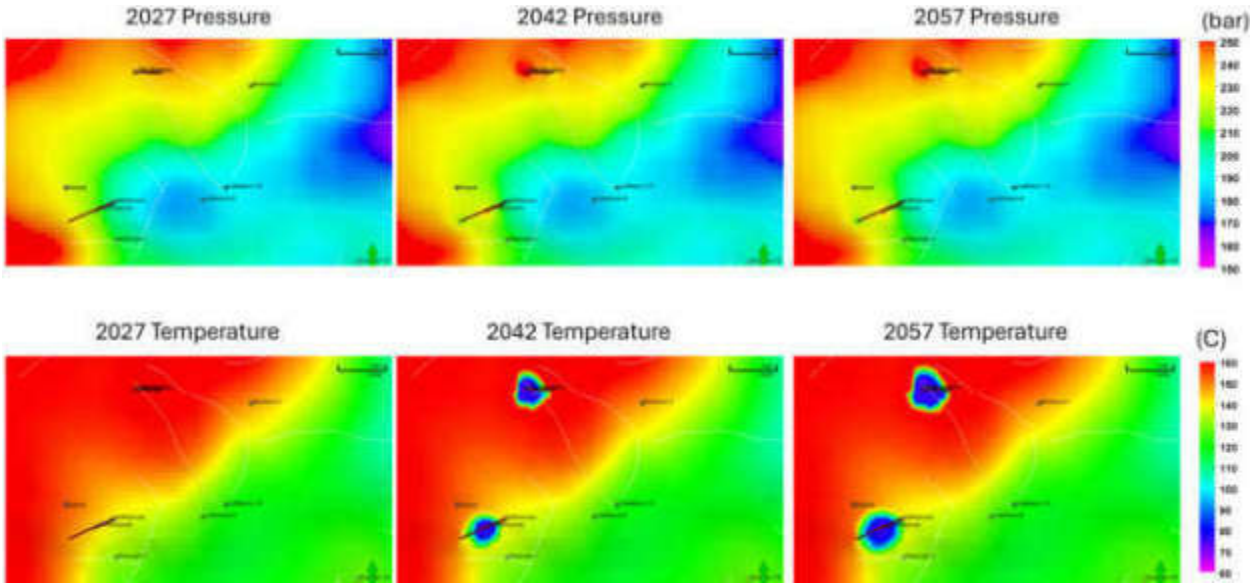


Fig. 2.298 Pn Pressure and Temperature Simulation Maps Over Time
Pressure (top row) and temperature (bottom row) at the Pn horizon from the start of forecast (2027) to years 2042 and 2057. The extent of thermal cooling is evident in the bottom panels. Major fault traces are highlighted in white, and key wells are indicated.

Copyright © SLB. All Rights Reserved. Private & Confidential. Reproduction only by permission.

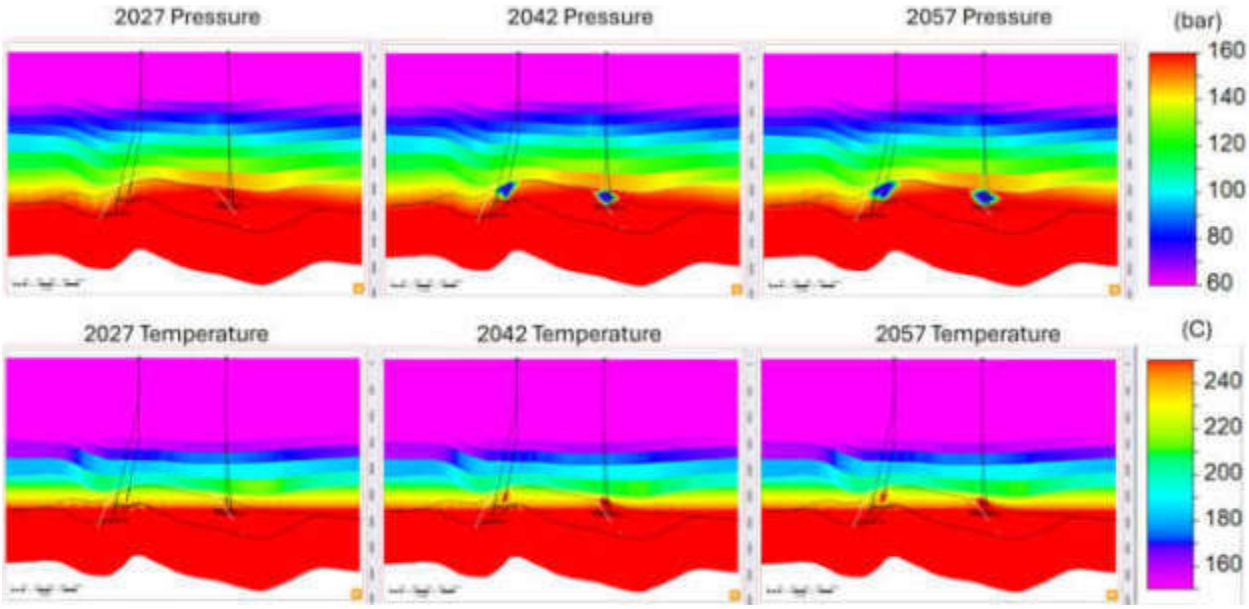


Fig. 2.299 Pressure and Temperature Profiles
Temperature distribution along a cross-section from Rasovac Injector to Bockovci Injector, illustrating the cooled water front. Key geological markers are indicated as follows: Z' (dashed white), Pn (solid black), and Tg (solid white). The vertical (Z) scale is exaggerated by a factor of 2 for clarity.

The analysis extends to discussion of key operational constraints, such as bottomhole pressure and temperature limits, as well as the identification of potential risks including thermal breakthrough and excessive parasitic power requirement. Additionally, the results inform recommendations for optimal doublet placement, completion strategies, and long-term reservoir management practices to support effective field development and risk mitigation. By integrating detailed simulation results with engineering judgment, this section aims to provide a comprehensive basis for decision-making, planning, and risk management in the deployment of geothermal doublets at Rasovac and Bockovci.

Copyright © SLB. All Rights Reserved. Private & Confidential. Reproduction only by permission.

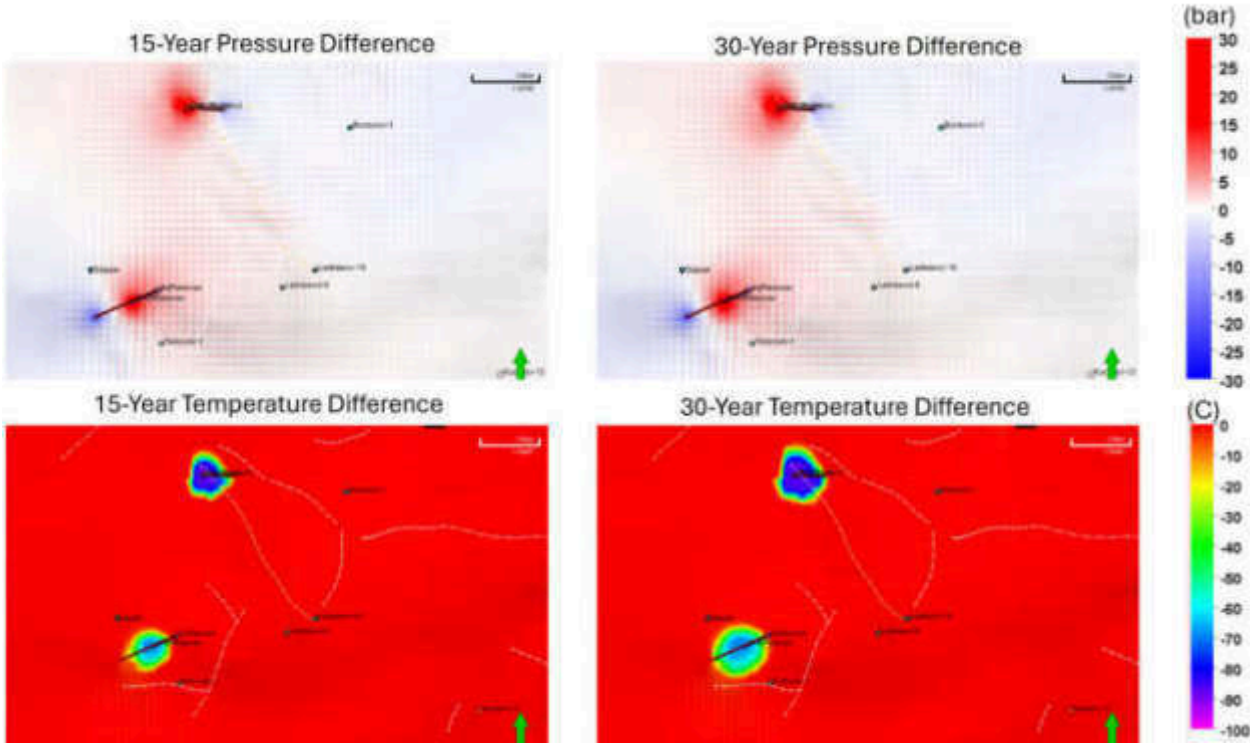


Fig. 2.300 Pressure and Temperature Difference Maps
Map view of pressure difference (top row) and temperature difference (bottom row) distributions at the Pn horizon, illustrating the extent of the cooled water front. Major faults are delineated with solid white lines.

2.11.3.1 Rasovac AOI

Over the 30-year simulation period, the production well exhibits only a marginal decline of approximately 3 bar in bottomhole pressure (BHP) (Fig. 2.301).

This minor reduction underscores the effectiveness of pressure support provided by the injection well. The observed drawdown remains within workable operational limits, i.e., the modeled pressure drawdown is such that there are available electric submersible pumps (ESP) that could support the anticipated production rate, thus ensuring the sustainability of production throughout the forecasted period. The average productivity index (PI) is calculated at around 1.6 liters per second per bar (lps/bar), with the average drawdown stabilized at 49 bar. On the injection side, the injectivity index is estimated at 1.2 lps/bar, with the maximum pressure buildup reaching 72 bar. The injection well consistently maintains a stable BHP, and there is no significant sign of excessive pressure increase or risk of reservoir fracturing within the modeled timeframe, thereby confirming the safety and reliability of injection operations.

The modeling results confirm that the current target well spacing, ranging from 700 to 800 meters between injector and producer, is sufficient to prevent premature thermal breakthrough over the 30-year forecast. This spacing strategy facilitates broad thermal sweep while minimizing the risk of short-circuiting cool injection fluids to the production well. Further well spacing optimization will be required as the model is refined with the integration of new data. Simulation outputs illustrate that the advance of the cold thermal front is effectively contained beneath the Z' stratigraphic marker, primarily due to restricted vertical permeability within the reservoir sequence (see Fig. 2.299). The

Copyright © SLB. All Rights Reserved. Private & Confidential. Reproduction only by permission.

forecast temperature remains stable for the first 12 yeas, then shows a very gradual decline, amounting to approximately 7 °C over the next two decades (refer to Fig. 2.301). This modest temperature decline is a positive indicator, suggesting high thermal sweep efficiency and effective heat extraction from the reservoir.

Flow contributions to the production well are predominantly sourced from the lower intervals of the Pn formation, which are characterized by favorable reservoir permeability and temperatures. This favorable stratigraphic source enhances overall system performance by maximizing the heat extraction potential while maintaining operational safety and integrity. Overall, the simulation affirms that the current field development strategy, encompassing well placement, targeting, and spacing, could achieve robust production performance, reliable reservoir pressure support, and efficient heat recovery over a multi-decade operational horizon.

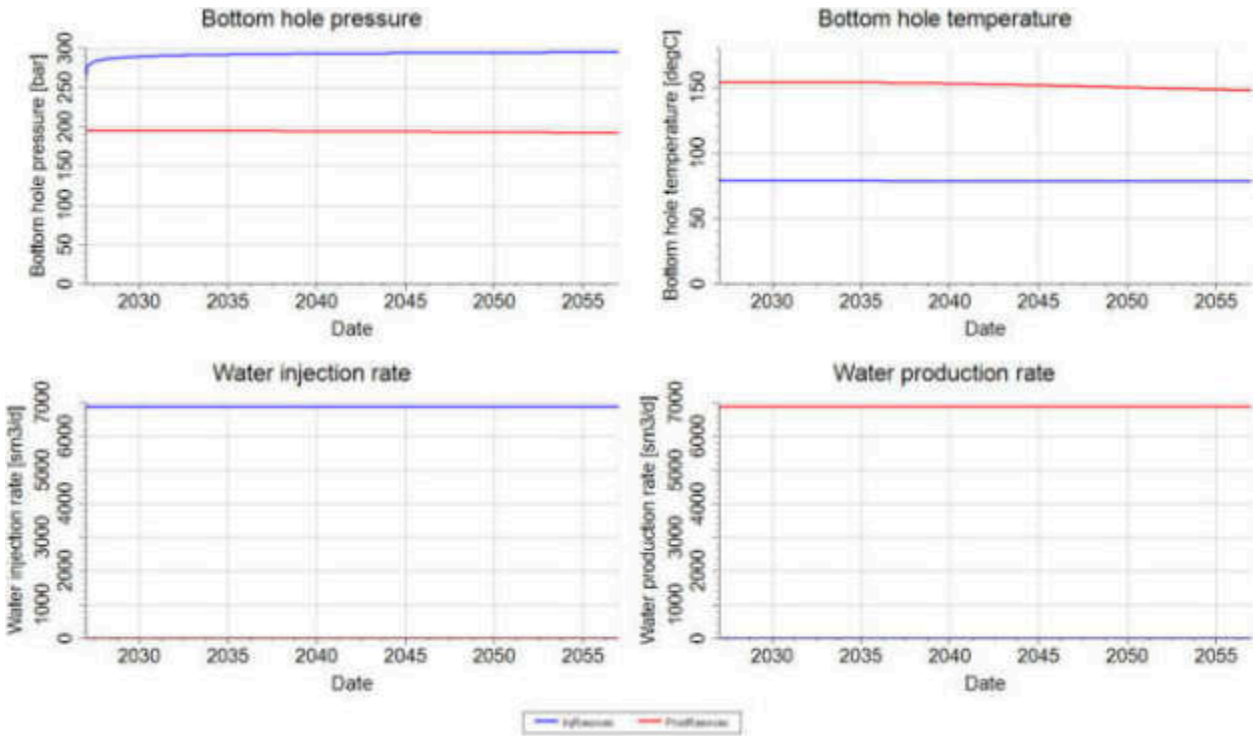


Fig. 2.301 Simulation Forecast Parameters; Rasovac AOI
Forecast parameters of Rasovac AOI show temporal evolution of bottom hole pressure, temperature and production/ injection rate

2.11.3.2 Bockovci AOI

During the 30-year simulation period, the Bockovci production well demonstrates strong performance, experiencing only a slight pressure decline of about 5 bar in BHP (Fig. 2.302). This minimal decline highlights the robust pressure support delivered by the injection well. The drawdown levels remain comfortably within operational limits, particularly with the support of an electric submersible pump (ESP), ensuring stable and sustainable production across the forecast period. The average productivity index (PI) is estimated at 1.9 liters per second per bar (lps/bar), with an average drawdown of 44 bar. On the injection side, the injectivity index is approximately

Copyright © SLB. All Rights Reserved. Private & Confidential. Reproduction only by permission.

0.8 lps/bar, with the highest observed pressure buildup reaching 115 bar. Although the injector well maintains a stable bottomhole pressure (BHP), the buildup reaches 92% of the maximum allowable injection pressure, which is a cause for concern. This highlights the need to pay close attention to the injection pressure at Bockovci in subsequent modeling efforts and to develop heightened risk mitigation measures if the possibility of exceeding (albeit briefly) the safety limits for reservoir fracturing is confirmed.

The current injector-to-producer spacing, ranging from 500 to 700 meters, has been verified by the simulation to be sufficient to prevent early thermal breakthrough over 30 years. This configuration promotes a broad thermal sweep while minimizing the risk of breakthrough by colder injection fluids. As additional data becomes available and the model is further refined, additional optimization of well spacing may be required. Simulation results further indicate that the advance of the cooled thermal front remains confined below the Z' stratigraphic marker (Fig. 2.299), a consequence of limited vertical permeability within the reservoir. Over the model period, the production well temperature remains stable for the first 8 years, then exhibits a steeper decline of approximately 11 °C in the next 22 years (see Fig. 2.302). This steeper thermal drop suggests shorter well spacing and smaller vertical offset between producer and injector in Bockovci may result in stronger hydraulic and thermal connectivity of the doublet compared to Rasovac AOI.

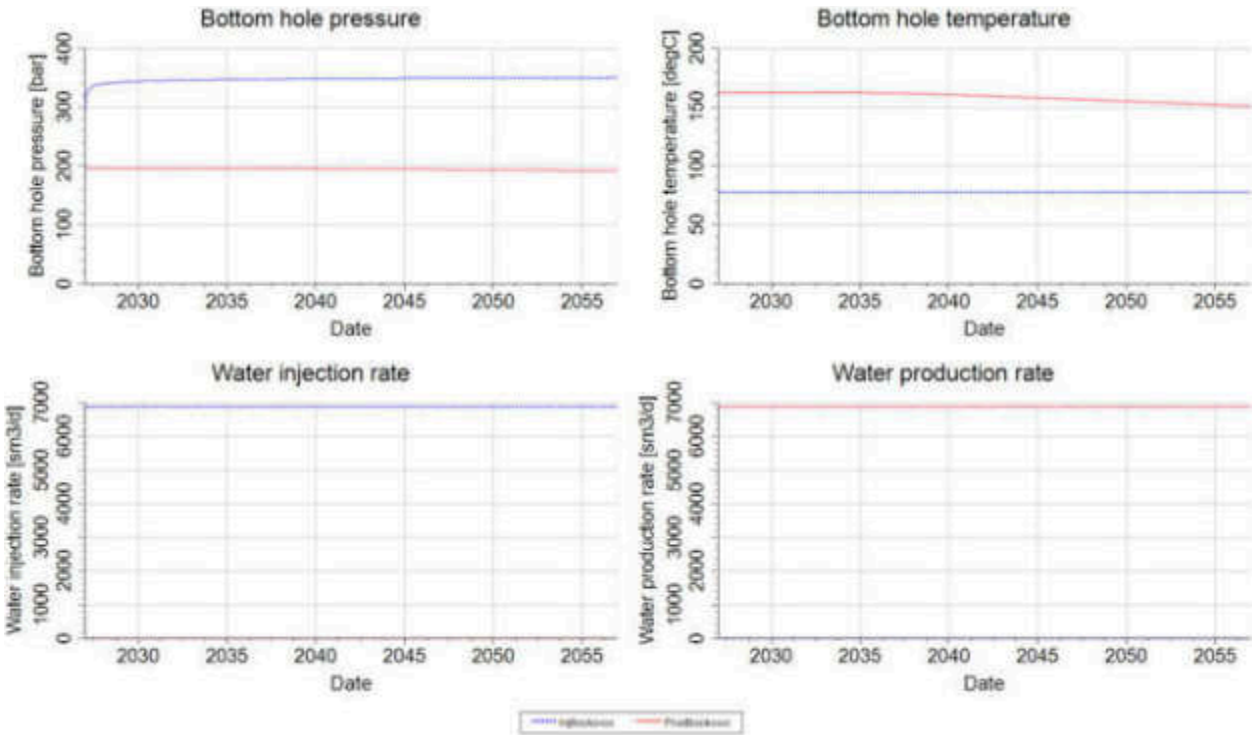


Fig. 2.302 Simulation Forecast Parameters; Bockovci AOI
Forecast parameters of Bockovci AOI show temporal evolution of bottom hole pressure, temperature and production/ injection rate

Copyright © SLB. All Rights Reserved. Private & Confidential. Reproduction only by permission.

2.11.4 Risk Assessment and Mitigation

A comprehensive risk assessment was undertaken to evaluate uncertainties and hazards related to geothermal development. The principal uncertainties identified relate to productivity/injectivity in the commingled interval, brine composition, parasitic load, and thermal decline.

- Thermal decline: The model forecasts managable temperature decline. However, high-permeability pathways (that may not have been identified by DSTs) may result in faster and greater thermal decline than forecast, thereby adversely impacting gross power generation. Monitoring and adaptive field management strategies are recommended. Currently, the model employs a single-porosity framework; however, if further data collection reveals the presence of fracture-hosted permeability, a dual-permeability model may be necessary to better characterize flow dynamics.
- Well Productivity/Injectivity: due to the scarcity of available data, permeability estimates from DSTs of thin (<20 m) intervals were extrapolated to much thicker intervals (hundreds of meters in Pn-Tg marker). This extrapolation presents risks of wells being unable to flow at the required rates if actual permeability is much lower than the extrapolated estimates. Further testing and data gathering are advised.
- Fault Intersection: Proximity of injection-related pressure front to faults could trigger seismic activity or fault activation. Active monitoring, additional geomechanical modeling work, and pressure management are necessary.
- Parasitic Load: The target formation's underpressure requires high-temperature pumps. Maximum pump head that can be provided at 80 L/s is estimated to be at ~60 bar, establishing a pressure threshold below which flow cannot be sustained, even with ESPs. Parasitic load must be rigorously evaluated.
- Geothermal Brine Content: Presence of CO_2 and hydrocarbons may impact brine thermodynamics and operational safety. Detailed fluid analysis is needed to refine assumptions.

Mitigation strategies may need to be revised as additional information emerges. A comprehensive risk mitigation framework was established to address the primary uncertainties and operational risks associated with geothermal production. The following mitigation strategies were developed to align with project requirements and sustain long-term performance:

- Robust Site Characterization: Acquisition of high-resolution downhole pressure and temperature data throughout target zones is essential. Extended flow testing should be conducted to delineate reservoir deliverability, water content analysis, and thermal response in situ.
- Sensitivity Analysis: Systematic simulation exercises and sensitivity studies are necessary to evaluate the effects of well placement, injection zone selection, completion intervals, well spacing, and operational flow conditions. This enables optimization of field design and quantifies operational uncertainty across anticipated scenarios.
- Operational Controls: Injection rates and pressures must be determined and maintained substantially below safety thresholds to minimize the risk of excessive pressure accumulation near faults. Surveillance of operational parameters should be continuous, with adjustments

Copyright © SLB. All Rights Reserved. Private & Confidential. Reproduction only by permission.

made as indicated by monitoring results.

- Monitoring Program: Implement a comprehensive monitoring program, including permanent pressure and temperature monitoring, periodic tracer testing for thermal front tracking and assessment of reservoir connectivity between injection and production wells. Early detection of thermal breakthrough, anomalous pressure trends, or deviations from expected reservoir behavior is integral to operational reliability.
- Contingency Planning: Proactive remedial protocols, including provisions for pressure relief and contingency well drilling, must be defined to respond promptly in the event of unexpected high thermal decline or adverse reservoir responses.

Rigorous site characterization, proactive monitoring, conservative operational procedures, and adaptive management underpin the project's approach to minimizing risk and ensuring safe, reliable geothermal production operations.

2.11.5 Conclusions and Recommendations

Site selection and prioritization were guided by a quantitative chance-of-success (COS) mapping methodology (2.9 Geothermal site selection). This process enabled the identification and ranking of development locations with the highest probability of meeting key technical and operational criteria, including reservoir temperature, permeability, and containment integrity. The COS mapping also supported the optimization of overlapping sites across different stratigraphic zones, thereby maximizing resource utilization and supporting a risk-based approach to field development. The COS mapping allowed identifying two top-ranked sites Rasovac (targets B-C-D combined) and Bockovci (targets A-D combined) areas which were used in the geothermal doublet simulations.

Dynamic simulation results for both Rasovac (combined targets B–C–D) and Bockovci (combined targets A–D) confirm the technical feasibility of sustainable geothermal production. The modeled scenarios show that stable flow rates of 80 l/s can be maintained, with production temperatures consistently above 148°C. With ESP support, drawdown remains within operationally acceptable limits, while reservoir pressures stay below 90% of the estimated fracture gradient at all monitored locations and time steps. This provides a significant safety margin and reduces the risk of caprock breach or wellbore failure / integrity issues.

The results indicate that geothermal development is technically viable in both areas, with Rasovac presenting the stronger development case. Rasovac benefits from better well control, supported by two offset wells (Rasovac-1 and Stjepanik-1) and proximity to an existing hydrocarbon field. In contrast, Bockovci is constrained by limited data from a single well. Rasovac-1 also shows higher permeability, approximately 45 mD compared with 21 mD in Bockovci-1, and thicker geothermal intervals. However, uncertainty remains due to limited seismic resolution and associated depth interpretation risks. Although Bockovci has a higher initial temperature, it shows faster thermal decline between wells. For Rasovac, a key risk is the potential presence of hydrocarbon or CO_2 traces in the geothermal brine, which is considered less significant at Bockovci.

Copyright © SLB. All Rights Reserved. Private & Confidential. Reproduction only by permission.

The selected development concept, based on geothermal doublet configurations in both AOIs, demonstrates robust injection and production performance under pressure-constrained operating conditions. Simulation results suggest that injectivity and thermal recovery can be sustained over the project life without exceeding critical geomechanical thresholds.

The main uncertainties in the forecasts relate to subsurface heterogeneity and the representativeness of the available data, particularly lateral and vertical variations in reservoir properties. These uncertainties highlight the need for continued data acquisition, including appraisal drilling, core analysis, and advanced well testing, to refine the static and dynamic models and reduce risk in subsequent project phases.

Overall, the integrated simulation and development assessment supports Rasovac and Bockovci as technically viable candidates for geothermal development, with Rasovac currently offering the more favorable risked opportunity. Progression to the next project phase is recommended, subject to implementation of the proposed data acquisition and risk mitigation measures.

Copyright © SLB. All Rights Reserved. Private & Confidential. Reproduction only by permission.

3 Elaboration of the transport system

This section focuses on framing the Surface Facilities Requirement (SFR) needed to safely implement and develop the storage sites identified

The Bockovac-Area of Interest is located approximately 37 km from the CO_2 emission source at the Nexe Cement Plant. This area comprises several identified potential CO_2 injection subsurface formations, through wells namely **KS1, KS2, KS3, and KS4**, which are considered suitable for further assessment and development within the scope of this study

Figure Fig. 3.1 illustrates the locations of the CO_2 source and the identified storage site.

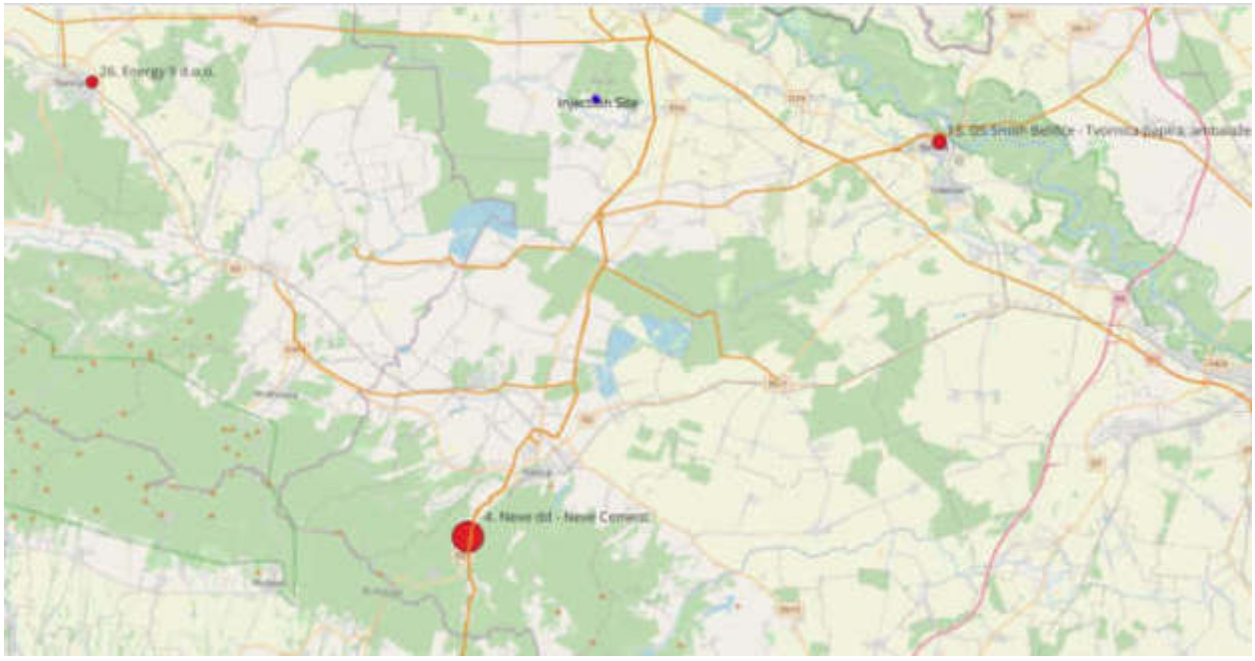


Fig. 3.1 Nexe cement plant and CO_2 injection site

The SFR for CO_2 storage sites can be categorized into three main areas:

1. **Reservoir-level injection conditions and requirements**
   This includes the parameters required to enable safe and effective CO_2 injection at the reservoir level.
2. **Wellhead injection conditions and well configuration**
   This covers the required wellhead conditions and the design of the well configuration to ensure safe injection of CO_2 while meeting the minimum requirements at the reservoir (sand interface).
3. **CO_2 transport conditions and requirements**
   This addresses the conditions necessary for the safe transport of CO_2 from the emission sources to the storage sites, including inlet conditions at the CO_2 source.

Copyright © SLB. All Rights Reserved. Private & Confidential. Reproduction only by permission.

These three key areas form the fundamental building blocks for the design and implementation of a CO_2 transportation and storage system.

3.1 Study Basis

For this SFR evaluation, the following inputs, and assumptions (validated) with the client formed the basis of this study.

CO_2 Injection Site Attributes :

Table Table 3.1 shows the injection site attributes

Table 3.1 Injection site atributes

	KS1	KS2	KS3	KS4
Storage reservoir type	Classic aquifer, underpressurized - below hydrostatic			
Avg. reservoir depth, TVD, m	1201	1355	1452	1450
Initial reservoir pressure, bar	97.0	112.0	121.0	110.0
Initial reservoir temperature, deg C	58	66	71	66
Max bottomhole pressure, bar	167.0	191.0	202.0	188.0
Final reservoir pressure, bar	127	156	163	155
Target injection rate, MTPA	0.19637	0.152205	0.12191	0.166075

Ambient Conditions

Considering the location of the injection sites, the following data representing average, high and low temperature profile for Croatia was gathered from the public domain.

The ambient temperature of 15 °C is used for the basis of network design and sensitivity was run with (-5 °C - winter condition and 31 °C - summer condition) to understand the operating conditions during the winter and summer.

Copyright © SLB. All Rights Reserved. Private & Confidential. Reproduction only by permission.

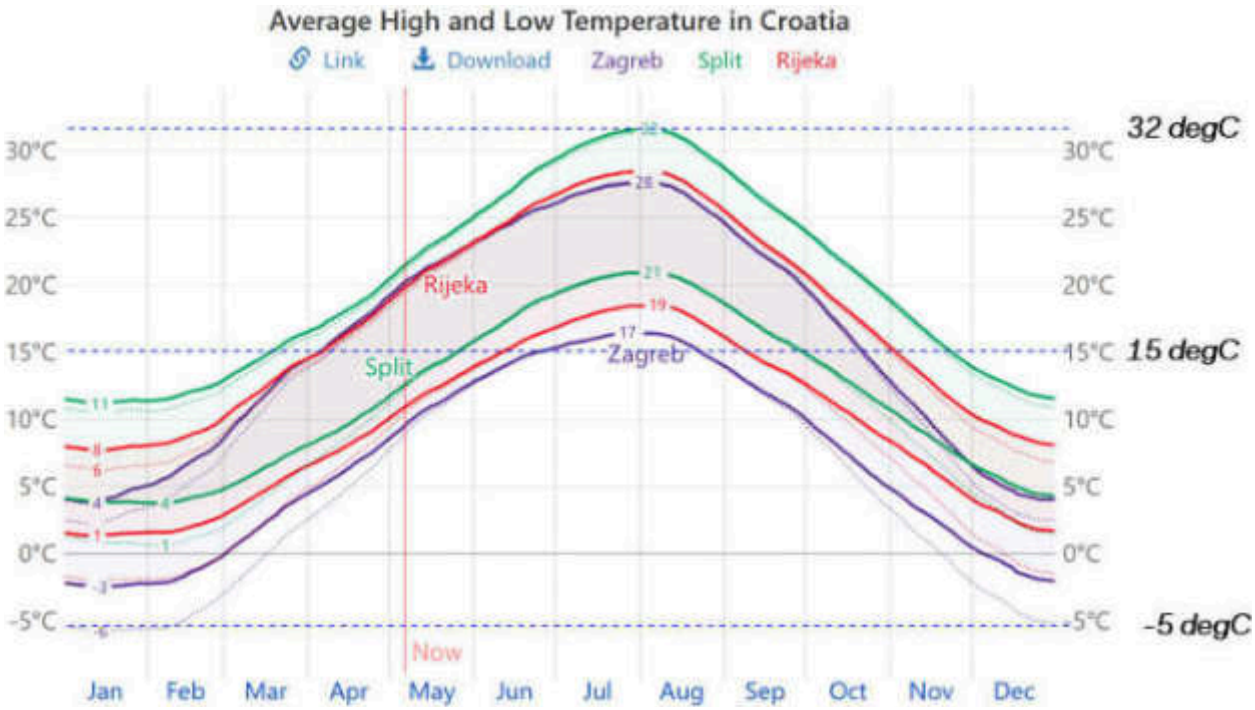


Fig. 3.2 Temperature profile in Croatia (From Weather Spark Website)

General Assumptions

The following assumptions apply for all the cases:

- CO_2 is assumed to be pure 99.7%
- 90% CO_2 and 95% CO_2 sensitivity is performed to understand the effect of impurities on the system
- Pipeline routing and distance is following the path of existing natural gas pipelines. The elevation profile is being factored into the analysis.
- All the pipes are buried to 1.5m depth-no insulation
- All rotating equipment are electric driven, and power is sourced from the grid

3.2 Approach and Methodology

The workflow deployed for the SFR evaluation is shown in Fig. 3.3.The workflow is designed to allow for an efficient and effective way of coupling all the nodes required to frame the surface facilities' requirement to safely inject and permanently store CO_2 in the storage sites. It integrates reservoir attributes, well requirements, injection condition at the well head, optimal and safe transportation of CO_2 to the injection sites.

Copyright © SLB. All Rights Reserved. Private & Confidential. Reproduction only by permission.

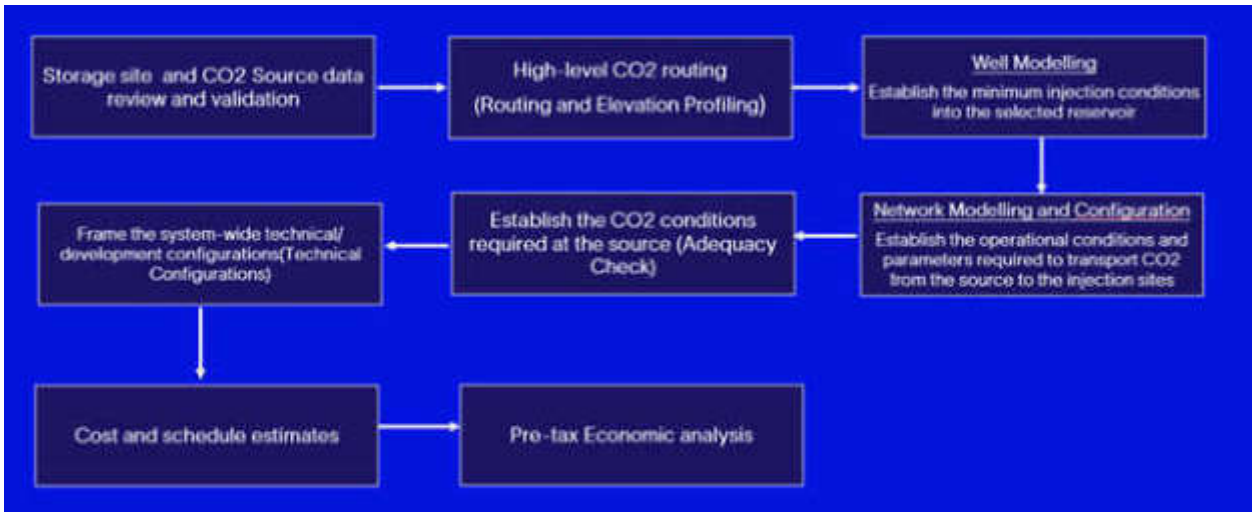


Fig. 3.3 SFR Workflow

Well Modeling

The main objectives of the well modelling are to establish an optimal well configuration and determine the minimum required injection conditions.

Using the subsurface parameters and attributes, an optimal well configuration was configured and the minimum well-head injecting conditions was estimated to allow for a safe injection operation

Establishing a safe operating condition far away from hydrate forming and cooling conditions (Joule-Thompson) at or near the perforations were the main constraints imposed on the system. Other criteria and limitations imposed on the well model are

- Erosional velocity ratio <1, indicating moderate risk
- Injection without phase change
- Fracking pressure - to maintain safe bottomhole pressure levels, to avoid fracking the reservoir

Well Head Injection Condition

Subsurface conditions such as reservoir pressure, reservoir depth, reservoir type; depleted or saline are the main driver for typical CCS development and operations. The subsurface condition usually drives the required injection conditions at the wellhead which forms the basis for the transportation condition and the type or amount of conditioning required at the pipe inlet.

Source to Site Routing

Pipeline routing assessments were conducted to establish the most viable solution for each case. In our workflow, Geographic Information System (GIS) Map in Pipesim was used to capture the elevations from Source to storage site and optimize the routing by taking the following key considerations into account.

Copyright © SLB. All Rights Reserved. Private & Confidential. Reproduction only by permission.

- **Source to Site Distance Analysis:** Evaluated the potential routes from source to storage site, calculating the transport distance and the elevation changes.
- **Proximity to the Population Area:** Focused on population avoidance during the routing
- **Proximity to Protected Zones:** Verified the potential routes against the protected area boundaries from Europe's Biodiversity database-Natura

3.3 Development Case Overview

The development is implemented at the Karas Suma location (Bockovci-1 area) as a single CCS site. CO_2 is planned to be transported from the NEXE Cement Plant to the injection site over a distance of approximately 37 km via pipeline.

The development includes four injection wells (KS1, KS2, KS3, and KS4) drilled from a centralized surface pad. To address environmental constraints and minimize surface impact, the wells are designed as deviated wells, enabling access to the subsurface storage formation while avoiding forested and environmentally sensitive areas.

The development is designed to achieve a base injection rate of approximately 0.636 MTPA over a 30-year operational period.

3.4 Development Premise and Assumptions

The assumptions used for this case are as follows:

- Injection rate: 0.636 MTPA over 30 years for 4 wells
- Injection fluid: CO_2 99.7%, 95% and 90%
- Reservoir T (58-71°C)
- Reservoir P (97-121 bar-initial)
- Net Thickness (280-360 m)
- Permeability (1-20md)
- Proposed pipeline is following the path of existing infrastructure.

3.5 Development Configuration

As shown in Fig. 3.4 the scope battery limit includes the followings

- The reservoir capacity to store CO_2 is limited, the only CO_2 source considered for this study is the Nexe cement plant. At this stage there is no plan for pipeline expansion, since we are limited by available reservoir storage volume.
- Transportation of CO_2 to the injection site including compression and conditioning (if required) to the required pressure
- Injection wellsite configurations

Copyright © SLB. All Rights Reserved. Private & Confidential. Reproduction only by permission.

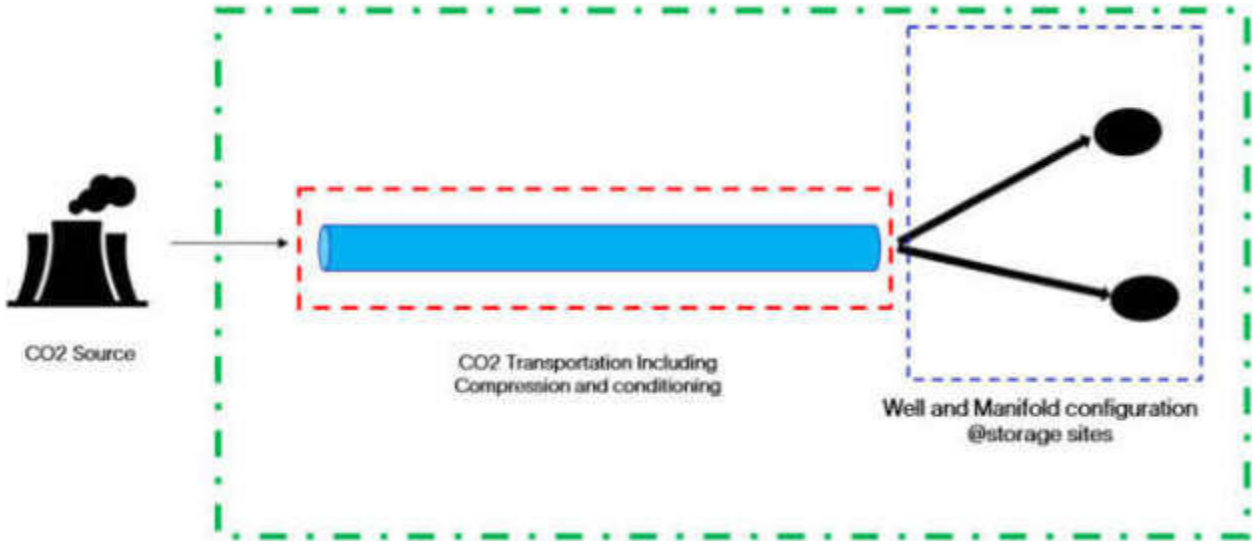


Fig. 3.4 Development Configuration

3.6 Source to Site

The proposed and optimal pipeline routing from the emitter to the injection site is mostly along the existing natural gas transportation infrastructure. Fig. 3.5 illustrates the proposed routing.

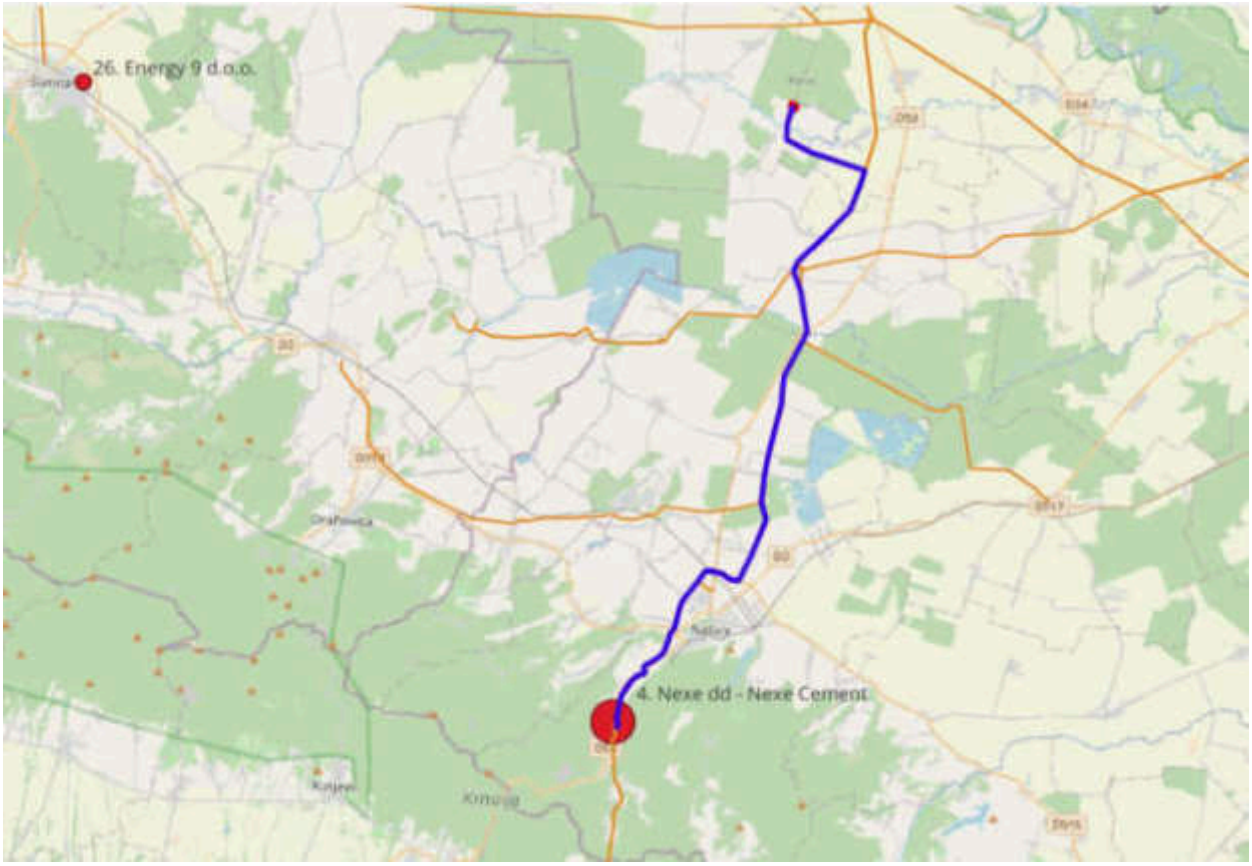


Fig. 3.5 Pipeline routing from Nexe plant to the injection site

Copyright © SLB. All Rights Reserved. Private & Confidential. Reproduction only by permission.

Close to the injection site the pipeline will be deviated for approximately 5.5km from the natural gas transportation infrastructure towards the injection site. Close to the injection site, the pipeline will have to cross the Karasica river.

The proposed development plan includes:

- 37 km main flowline
- ~70m elevation drop from CO_2 source to storage site (as shown in Fig. 3.6). This elevation difference helps to reduce the pressure losses along the pipeline and compression requirements at the source slightly

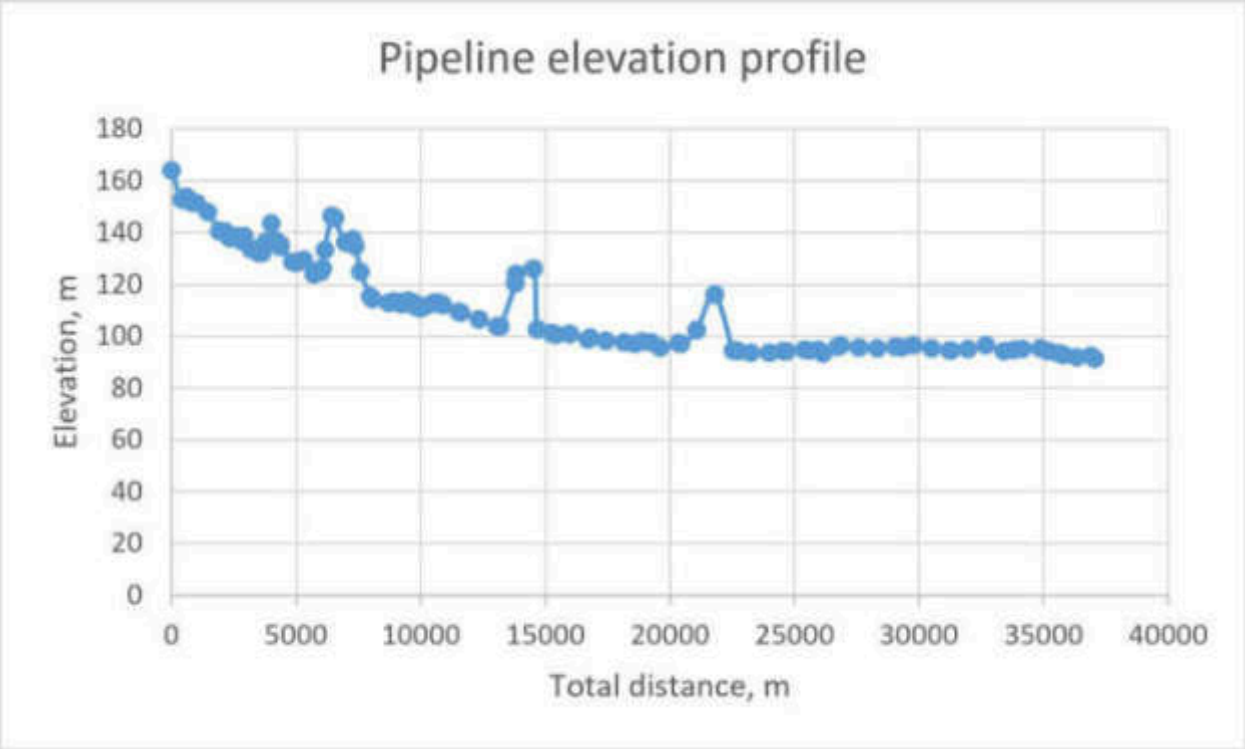


Fig. 3.6 Pipeline profile

3.7 Well Modelling

The inputs used for the well models are as follows:

Copyright © SLB. All Rights Reserved. Private & Confidential. Reproduction only by permission.

Table 3.2 Input data for well modeling

Well	KS1	KS2	KS3	KS4
Avg. reservoir depth, TVD, m	1201	1355	1452	1450
Initial reservoir pressure, bar	97.0	112.0	121.0	110.0
Initial reservoir temperature, degC	58	66	71	66
Max bottomhole pressure, bar	167.0	191.0	202.0	188.0
Final reservoir pressure, bar	127	156	163	155
Target injection rate, MTPA	0.19637	0.152205	0.12191	0.166075
Total perforated interval, m	280.1	256.82	303.98	360.02
Average permeability for CO_2 at start of injection, mD	0.5	0.32	0.22	0.236
Well deviation, deg	53	43	47	60
Ambient temperature, degC	15	15	15	15

At the beginning of storage, the injectivity in the wells is low because the reservoir is water saturated and the relative permeability for CO_2 is low. As the CO_2 displaces the water in the reservoir the injectivity will improve with time.

After building the well models, sensitivity was run on the tubing internal diameter ranging from 62mm (2.441in) to 114.3mm (4.5in). In Fig. 3.8 and Fig. 3.7 is the simulated pressure and temperature in well KS1 at the beginning of injection.

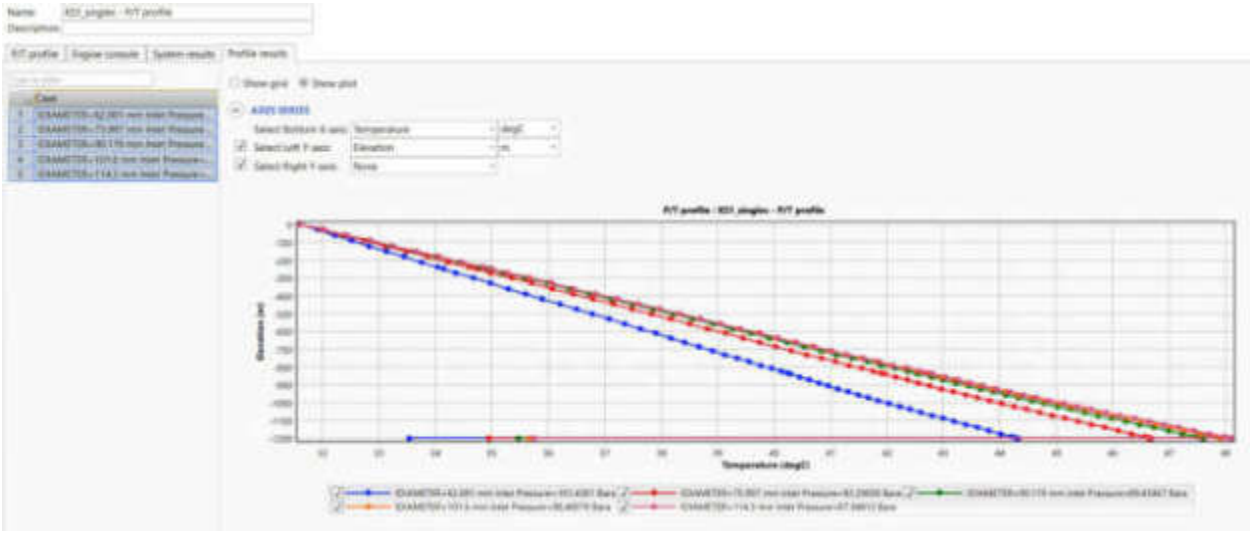


Fig. 3.7 KS1 Tubing Selection - Temperature Profile

Copyright © SLB. All Rights Reserved. Private & Confidential. Reproduction only by permission.

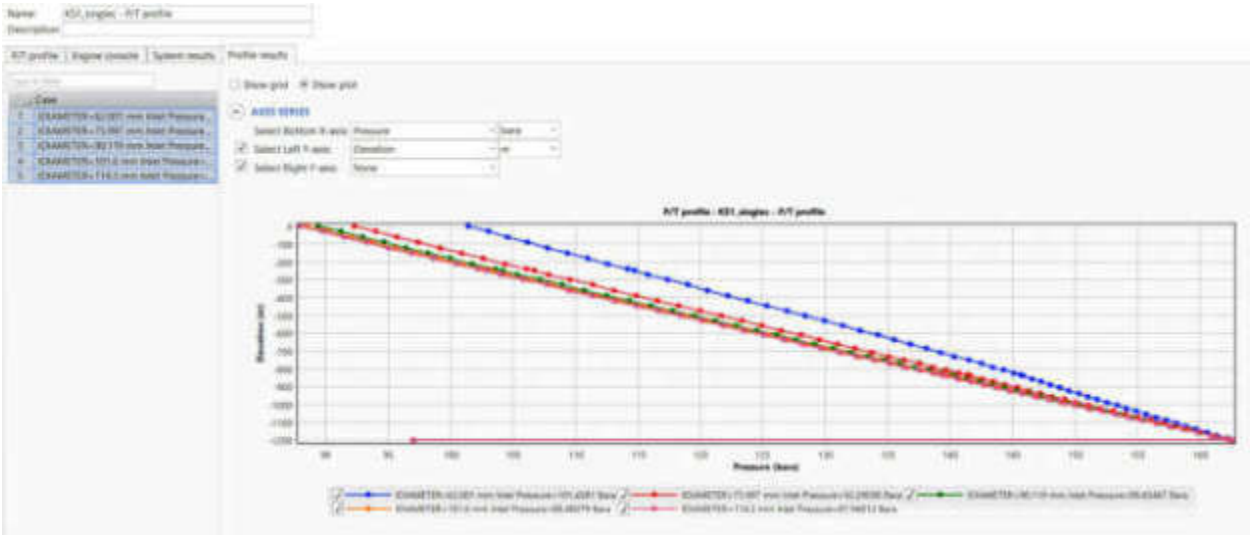


Fig. 3.8 KS1 Tubing Selection - Pessure Profile

The larger the tubing internal diameter the lower is the required injection wellhead pressure and lower the erosional velocity ratio (ERV). In the same time, a larger tubing will increase the overall cost of drilling and completing the well. In the table below are the results or running sensitivity for well KS1.

Table 3.3 KS1 Tubing selection - sensitivity on internal diameter

KS1 - Tubing Selection				
Internal diameter (mm)	WH Pressure (bar)	Max EVR	BH Pressure (bar)	BH Temperature (bar)
62.0	101.4	0.8	162.6	44.3
76.0	92.3	0.5	162.5	46.7
90.1	89.4	0.4	162.5	47.6
101.6	88.5	0.3	162.5	47.9
114.3	87.9	0.2	162.5	48.1

From internal tubing diameter of 62mm to 76mm there is a relatively large decrease in the required injection wellhead pressure, while larger than 76mm tubing sizes results is relatively small drop in required injection wellhead pressure. Also, the maximum erosional velocity and bottom hole temperature for 76mm ID tubing is optimal.

The pressure drop across the perforations is large; for KS1 bottom hole flowing pressure is 162.6bar while the reservoir pressure is 97bar, meaning a pressure drop of 65.6bar. The large pressure drop is associated with fluid cooling. The fluid cools down in the reservoir to approximately 35 degC, see Fig. 3.7. Even if the fluid cools down to 35degC, there is no risk for hydrate formation in the perforations and reservoir, the fluid pressure and temperature in the reservoir (97bar and 35degC) is far from hydrate formation conditions.

The optimal tubing size for KS1,KS2,KS3 and KS4 wells are shown in Table 3.4 below.

Copyright © SLB. All Rights Reserved. Private & Confidential. Reproduction only by permission.

Table 3.4 Optimal tubing size

Optimal tubing size						
	Internal Diameter (mm)	External Diameter (mm)	WH Pressure (bar)	Max EVR	BH Pressure (bar)	BH Temperature (bar)
KS1	76.0	88.9	92.3	0.55	162.5	46.7
KS2	76.0	88.9	91.0	0.35	176.8	39.2
KS3	76.0	88.9	91.3	0.28	184.2	42.3
KS4	76.0	88.9	90.9	0.37	175.3	39.3

3.8 Network (Transportation) configuration

The network routing is illustrated in Fig. 3.5. The proposed network connects the Nexe CO_2 source to a manifold, from which distribution to the injection wells heads. All wells are planned to be drilled from a single well pad, with varying azimuths.The distance between the CO_2 source and the manifold is approximately 37 km. The injection is expected to last for 30 years, with a target injection of 0.636 MTPA.

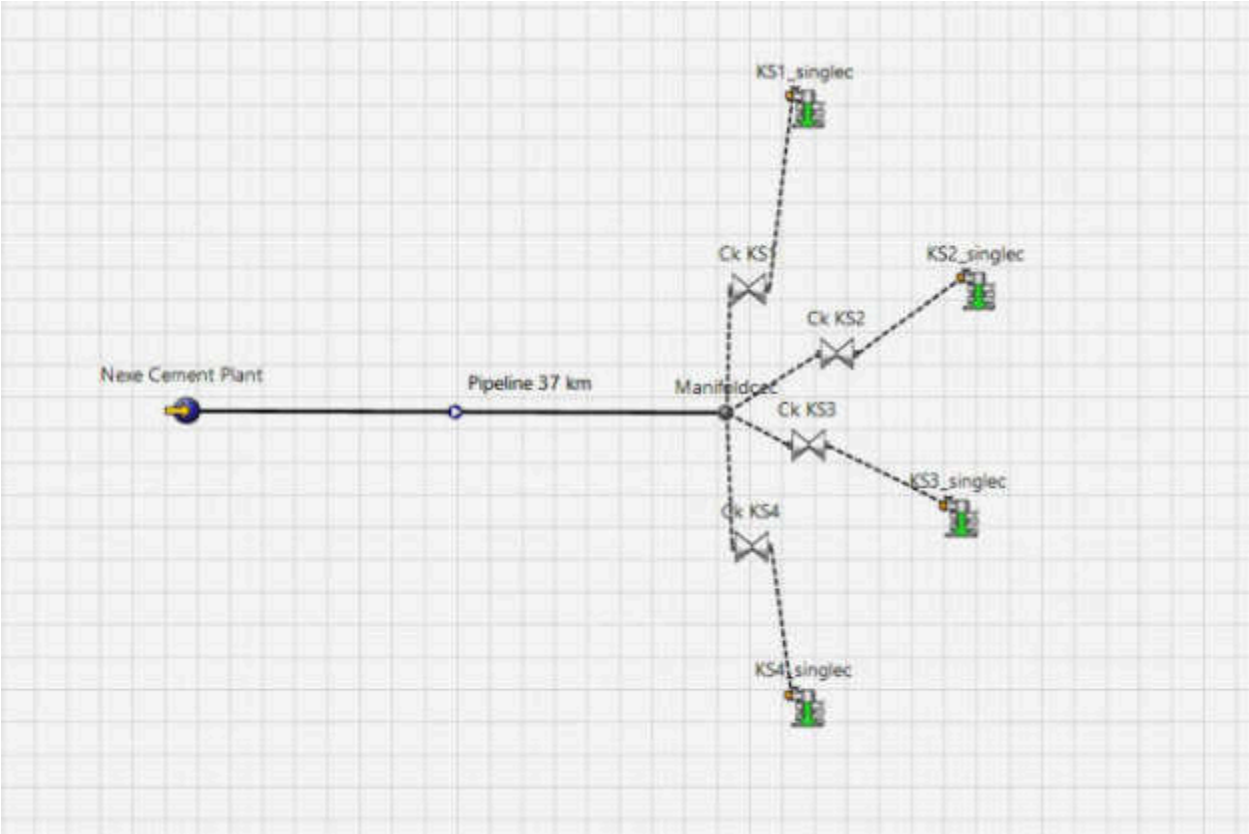


Fig. 3.9 Development configuration

Different development scenarios were evaluated to analyze the operational conditions for CO_2 transportation and to optimize pipeline sizing. These scenarios enabled the assessment of key operational parameters, including pressure drops, temperature variations, and erosional risks, thereby ensuring system integrity and operational reliability.

Copyright © SLB. All Rights Reserved. Private & Confidential. Reproduction only by permission.

Multiple scenarios have been simulated: 254mm (10inch) and 304.8mm(12inch) internal diameter pipeline, various ambient conditions, different fluid temperature at the cement plant, beginning and end of injection (different reservoir pressure and injectivity). The fluid was considered 99.7% CO_2 with 0.3% impurities.

Subsequently, an adequacy check was conducted to verify that the defined operating conditions meet the minimum wellhead requirements.

The figures below summarize the scenarios analyzed, showing network results at the beginning and end of the injection:

Year	Case	Soil Temp (deg C)	Pipeline Size (inch)	Inlet Pressure (bara)	Inlet Temp (deg C)	Max Fluid Velocity (m/s)	Max Erosion Velocity Ratio	Pressure Drop (bara)	Junction/Manifold Pressure (bara)	Junction/Manifold Temp (deg C)	K01 Wellhead WH Pressure (bara)	K01 Wellhead Temp (deg C)	K01 Wellhead Rate (Kg/s)	K02 Wellhead WH Pressure (bara)	K02 Wellhead Temp (deg C)	K02 Wellhead Rate (Kg/s)	K03 Wellhead WH Pressure (bara)	K03 Wellhead Temp (deg C)	K03 Wellhead Rate (Kg/s)	K04 Wellhead WH Pressure (bara)	K04 Wellhead Temp (deg C)	K04 Wellhead Rate (Kg/s)
2027	Base case	15	12	90.5	40	0.7	0.1	-2.1	92.7	31.6	92.5	31.6	7.6	91.0	31.3	4.5	91.3	31.4	3.6	90.9	31.3	4.6
2027	Winter Conditions	-5	12	83.9	40	0.9	0.1	-1.5	85.3	26.1	84.9	26.0	7.5	83.5	25.8	4.5	84.1	25.9	3.6	83.8	25.8	4.7
2027	Summer Conditions	31	12	97.6	40	0.5	0.1	-2.6	100.4	36.9	98.8	36.8	7.6	98.0	36.4	4.5	98.7	36.6	3.6	97.8	36.4	4.7
2027	90%Co2	15	12	102.2	40	0.9	0.1	-1.0	103.2	28.4	102.5	28.3	7.5	100.9	27.6	4.2	101.8	27.9	3.3	100.7	27.5	4.4
2027	95%Co2	15	12	97.4	40	0.8	0.1	-1.3	99.0	30.9	98.0	30.8	7.5	96.5	30.4	4.3	97.3	30.6	3.4	97.0	30.3	4.6
2027	Summer Conditions	31	10	98.7	40	1.7	0.3	-0.9	99.6	36.6	98.3	36.6	7.6	97.5	36.2	4.5	98.1	36.3	3.6	97.3	36.1	4.6
2027	Base case	15	10	92.1	40	0.9	0.2	-0.5	92.6	31.1	91.9	31.1	7.6	90.5	30.8	4.5	90.8	30.9	3.6	90.4	30.8	4.6
2027	Winter Conditions	-5	10	85.4	40	1.2	0.2	0.4	85.1	25.8	84.7	25.8	7.6	83.2	25.5	4.3	83.9	25.6	3.6	83.4	25.5	4.7

Fig. 3.10 Network Results-Beginning of Injection

Year	Case	Soil Temp (deg C)	Pipeline Size (inch)	Inlet Pressure (bara)	Inlet Temp (deg C)	Max Fluid Velocity (m/s)	Max Erosion Velocity Ratio	Pressure Drop (bara)	Junction/Manifold Pressure (bara)	Junction/Manifold Temp (deg C)	K01 Wellhead WH Pressure (bara)	K01 Wellhead Temp (deg C)	K01 Wellhead Rate (Kg/s)	K02 Wellhead WH Pressure (bara)	K02 Wellhead Temp (deg C)	K02 Wellhead Rate (Kg/s)	K03 Wellhead WH Pressure (bara)	K03 Wellhead Temp (deg C)	K03 Wellhead Rate (Kg/s)	K04 Wellhead WH Pressure (bara)	K04 Wellhead Temp (deg C)	K04 Wellhead Rate (Kg/s)
2057	Base case	15	12	84.7	40	0.9	0.1	-1.1	85.8	34.3	72.1	29.3	6.2	86.3	34.3	5.0	86.0	34.3	3.9	86.1	34.3	5.0
2057	Winter Conditions	-5	12	77.6	40	1.1	0.1	-0.6	78.2	29.2	63.5	23.8	6.2	77.9	29.2	5.1	76.4	28.7	3.9	77.6	29.2	5.0
2057	Summer Conditions	31	12	89.3	40	0.6	0.1	-1.6	90.9	38.2	78.8	33.0	6.2	92.2	38.2	5.0	92.2	38.1	3.8	92.2	38.2	5.1
2057	90%Co2	15	12	100.9	40	0.7	0.1	-0.7	101.6	28.6	86.0	22.5	6.2	101.1	28.6	5.1	101.1	28.6	3.7	101.1	28.6	5.1
2057	95%Co2	15	12	91.9	40	0.6	0.1	-0.8	92.3	31.5	79.9	26.1	6.2	93.5	31.5	5.0	93.4	31.4	3.9	93.5	31.5	5.1
2057	Summer Conditions	31	10	90.4	40	0.9	0.2	0.4	90.0	37.5	77.6	32.4	6.2	91.3	37.5	5.0	91.3	37.4	3.8	91.3	37.5	5.1
2057	Base case	15	10	86.1	40	1.1	0.2	0.9	85.2	33.8	71.1	28.7	6.2	85.5	33.8	5.0	85.2	33.8	3.9	85.5	33.8	5.1
2057	Winter Conditions	-5	10	79.5	40	1.5	0.2	1.7	77.8	29.1	63.4	23.7	6.2	77.8	29.1	5.1	76.3	28.6	3.9	77.3	29.1	4.9

Fig. 3.11 Network Results-End of Injection

Simulation results indicate that due to low injectivity at the start of injection the wellhead pressure and system pressure requirements is high in most scenarios. The second-largest impact on the wellhead injection pressure and pressure at the inlet of the pipeline (Nexe cement plant) is the fluid temperature which is influenced by two factors: the fluid temperature at the inlet of the pipeline and the ambient temperature. Higher fluid temperature requires higher general system pressure, because the fluid is less dense, occupies more space and results in higher fluid velocity.

At the beginning of injection the CO_2 injectivity is low because the reservoir is saturated with water. As injection progresses, the CO_2 injectivity improves with time. Towards the end of injection, the required bottomhole injection pressure and wellhead injection pressure is lower compared to the begging of CCS operation.

The pressure drop along the pipeline is insignificant or slightly negative, because of change in elevation (approximately -70m vertical depth from cement plant to injection site) and transportation in dense phase at low fluid velocities. Both pipelines 254mm (10inch) and

Copyright © SLB. All Rights Reserved. Private & Confidential. Reproduction only by permission.

304.8mm(12inch) can accommodate the transportation of the required volume from the cement plant to the injection site. The 304.8mm(12inch) offers more flexibility and can accommodate surges or extra volume of CO_2.

3.9 Sensitivity on CO_2 Purity

Sensitivity analysis was performed on CO_2 impurity levels to evaluate their impact on the system performance. Two additional impurity scenarios were considered: 90% CO_2 and 95% CO_2, with the corresponding impurity compositions detailed in the table below.

Impure CO_2 fluid

90% CO_2	
Name	Mole fraction (%)
Water	0.00469
Hydrogen	3.28639
Carbon Monoxide	0.09390
Nitrogen	3.28639
Oxygen	0.00047
Hydrogen Sulphide	0.00094
Argon	3.28639
Carbon Dioxide	90.04085

95% CO_2	
Name	Mole fraction (%)
Water	0.00496
Hydrogen	1.38889
Carbon Monoxide	0.09921
Nitrogen	1.98413
Oxygen	0.00050
Hydrogen Sulphide	0.00099
Argon	1.38889
Carbon Dioxide	95.13244

A comparison of the resulting phase envelopes for each case is presented in Fig. 3.12 .

Copyright © SLB. All Rights Reserved. Private & Confidential. Reproduction only by permission.

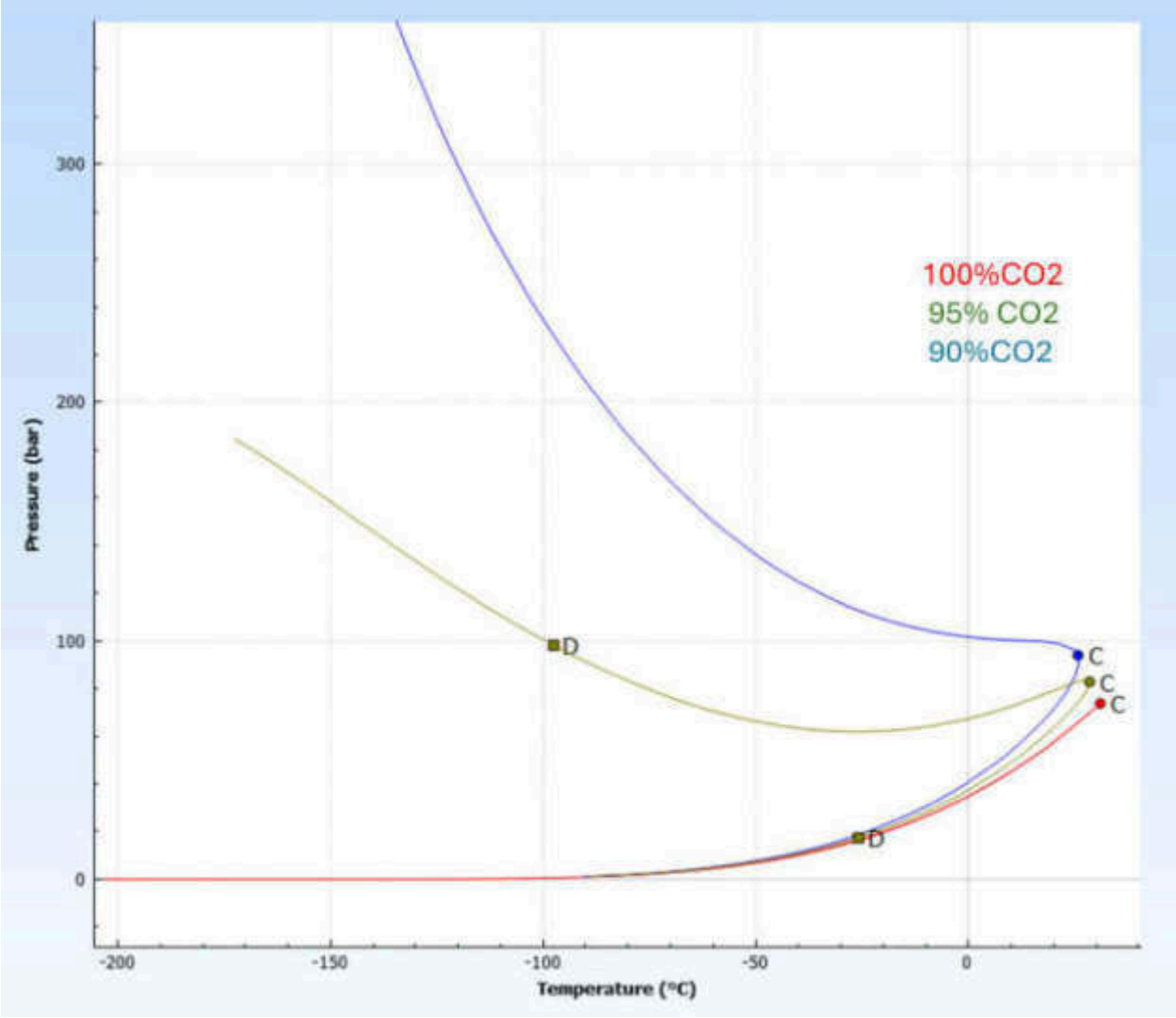


Fig. 3.12 Phase envelope

The figures below present the results of the sensitivity analysis on CO_2 impurities, evaluated for both the beginning and the end of the injection period.

Year	Case																					
2027	Base case	15	12	90.3	40	0.7	0.1	-2.1	92.7	31.8	91.5	31.6	7.6	91.0	31.3	4.5	91.3	31.4	3.8	90.9	31.3	4.6
2027	90%Co2	15	12	102.2	40	0.9	0.1	-1.0	103.2	28.4	102.5	28.3	7.5	100.9	27.6	4.2	101.8	27.9	3.3	100.7	27.5	4.4
2027	95%Co2	15	12	97.4	40	0.8	0.1	-1.3	99.0	30.9	98.0	30.8	7.3	96.3	30.4	4.3	97.1	30.6	3.4	97.0	30.3	4.6

Fig. 3.13 Network results - Beginning of injection-Sensitivity on CO_2 Purity

Year	Case																					
2057	Base case	15	12	94.7	40	0.9	0.1	-1.1	85.8	34.3	72.1	29.3	6.2	86.3	34.3	5.0	86.0	34.3	3.9	86.1	34.3	5.0
2057	90%Co2	15	12	101.9	40	0.7	0.1	-0.7	101.6	28.6	86.0	22.5	6.2	101.1	28.6	5.1	101.1	28.6	3.7	101.1	28.6	5.1
2057	95%Co2	15	12	91.5	40	0.6	0.1	-0.8	92.1	31.5	79.9	26.1	6.2	93.3	31.5	5.0	93.4	31.4	3.9	93.5	31.5	5.1

Fig. 3.14 Network results - End of injection-Sensitivity on CO_2 Purity

Copyright © SLB. All Rights Reserved. Private & Confidential. Reproduction only by permission.

The analysis indicated that the presence of impurities affects the fluid phase envelopes and the system pressure. The more impure is the CO_2 stream the higher is the system pressure and the larger the phase envelope, increasing the risk of entering into two phase region.

3.10 System Overview (CCS Implementation)

The general system overview for the base case is illustrated in Fig. 3.15 . This is the final configuration which is used for energy and cost estimations in the following sections.

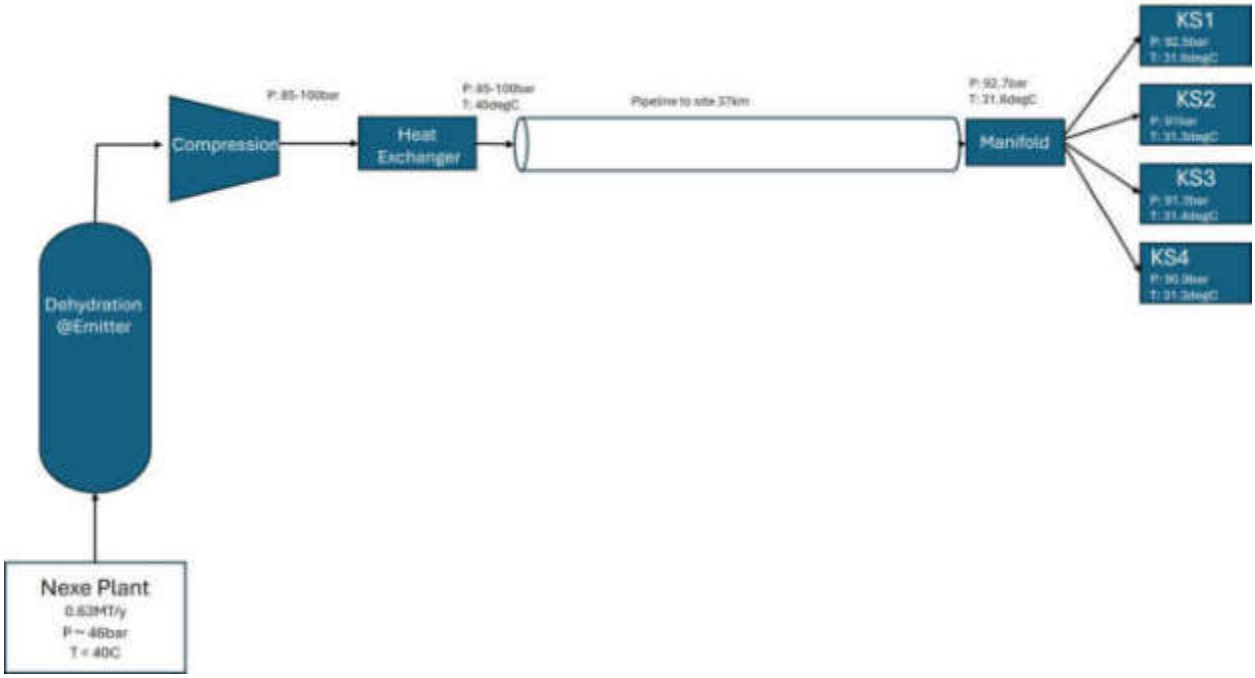


Fig. 3.15 System overview for the base case

3.10.1 Energy Required

The maximum pressure at the inlet of the pipeline is approximately 100 bar, as shown in Fig. 3.10 and Fig. 3.11. The compressor sizing and power requirements considers the maximum discharge pressure of 100bar. Due to compression the fluid temperature will increase significantly at the outlet of the compressor. A heat exchanger will be required, to cool down the fluid to 40 deg C - This creates the opportunity for potential heat recovery. The figures below summarizes the power requirements and duty for the compressor and the heat exchanger.

Copyright © SLB. All Rights Reserved. Private & Confidential. Reproduction only by permission.

Cement plant fluid outlet temperature of 40deg C. Rate - 0.636 MTPA							
Nexe cement plant outlet / Compressor suction pressure, Bara	45	45	45		25	25	25
Compression Stages	1	1	1		2	2	2
Compressor outlet pressure, Bara	99	99	99		100	100	100
Compressor outlet temperature, deg C	79	74.7	71		141.7	129	119
Compressor efficiency	80%	90%	100%		80%	90%	100%
Compressor pressure ratio	2.2	2.2	2.2		2	2	2
Compressor Power, kW	**909**	**797**	**708**		**2066**	**1798**	**1590**
Heat exchanger temperature at outlet, deg C	40	40	40		40	40	40
Heat exchanger temperature differential, deg C	39	34.7	31		101.7	89	79
Heat exchanger duty, kW	**2832**	**2667**	**2527**		**4712**	**4376**	**4104**

Fig. 3.16 Power requirements. Fluid temperature 40deg C

Cement plant fluid outlet temperature of 30deg C. Rate - 0.636 MTPA							
Nexe cement plant outlet / Compressor suction pressure, Bara	45	45	45		25	25	25
Compression Stages	1	1	1		2	2	2
Compressor outlet pressure, Bara	99	99	99		100	100	100
Compressor outlet temperature, deg C	66	62	58.7		125.5	113	104
Compressor efficiency	80%	90%	100%		80%	90%	100%
Compressor pressure ratio	2.2	2.2	2.2		2	2	2
Compressor Power, kW	**814**	**708**	**625**		**1943**	**1687**	**1488**
Heat exchanger temperature at outlet, deg C	40	40	40		40	40	40
Heat exchanger temperature diferential, deg C	26	22	18.7		85.5	73	64
Heat exchanger duty, kW	**2293**	**2096**	**1920**		**4282**	**3944**	**3666**

Fig. 3.17 Power requirements Fluid temperature 30deg C

3.11 Cost Estimates (CCS Systems)

This section documents the third stage of the ongoing engagement. The primary objective of this stage is to understand the cost and economic implications of the systems configured in 3.10 System Overview (CCS Implementation) implement a safe, permanent and efficient storage of CO_2 in the identified storage sites.

The report is divided into Two (2) sections.

Copyright © SLB. All Rights Reserved. Private & Confidential. Reproduction only by permission.

- Cost Estimation - Estimation of the CAPEX, OPEX and ABEX of the CO_2 transportation and Injection based on the technical configuration established in previous stages of the project
- Economic assessment – Economic analysis of each of the Project Cases.

Estimates provided in these reports are based on assumptions and premises that has been extensively discussed and agreed with the Client.

The estimates provided are Class 5 (AACE) and Level 1 Schedule estimates. A general overview of AACE international Capital Cost Classification recommended system is referenced in Fig. 3.18 below.

	Primary Characteristic	*Secondary Characteristic*			
ESTIMATE CLASS	**LEVEL OF PROJECT DEFINITION** Expressed as % of complete definition	**END USAGE** Typical purpose of estimate	**METHODOLOGY** Typical estimating method	**EXPECTED ACCURACY RANGE** Typical variation in low and high ranges [a]	**PREPARATION EFFORT** Typical degree of effort relative to least cost index of 1 [b]
Class 5	0% to 2%	Concept Screening	Capacity Factored, Parametric Models, Judgment, or Analogy	L: -20% to -50% H: +30% to +100%	1
Class 4	1% to 15%	Study or Feasibility	Equipment Factored or Parametric Models	L: -15% to -30% H: +20% to +50%	2 to 4
Class 3	10% to 40%	Budget, Authorization, or Control	Semi-Detailed Unit Costs with Assembly Level Line Items	L: -10% to -20% H: +10% to +30%	3 to 10
Class 2	30% to 70%	Control or Bid/ Tender	Detailed Unit Cost with Forced Detailed Take-Off	L: -5% to -15% H: +5% to +20%	4 to 20
Class 1	50% to 100%	Check Estimate or Bid/Tender	Detailed Unit Cost with Detailed Take-Off	L: -3% to -10% H: +3% to +15%	5 to 100

Notes: [a] The state of process technology and availability of applicable reference cost data affect the range markedly. The +/- value represents typical percentage variation of actual costs from the cost estimate after application of contingency (typically at a 50% level of confidence) for given scope.
[b] If the range index value of "1" represents 0.005% of project costs, then an index value of 100 represents 0.5%. Estimate preparation effort is highly dependent upon the size of the project and the quality of estimating data and tools.

Fig. 3.18 AACE Cost Estimate Classification for Capital Projects

Cost Estimate Methodology

Cost estimates (CAPEX/OPEX) for each of the cases evaluated was carried out using S&P Global oil and gas costing tool – QUE$TOR. Considering the level of technical definition and maturity of this project, the estimates provided are Class 5 (AACE) and Level 1 Schedule estimates.

Copyright © SLB. All Rights Reserved. Private & Confidential. Reproduction only by permission.

To improve the estimates generated, the technical and operating parameters generated from the well and network model is used to develop a development configuration in QUE$TOR. The development configuration in QUE$TOR is based on relevant Croatia specific procurement strategy and technical databases inherent within the S&P Global datasets.

Other location specific variables (Unit Estimates) like electricity, labour e.t.c reflect Croatia's specific rates. For the electricity cost, Client has advised to use €90/MWhr. For the purposes of this report the USD/EUR exchange rate is assumed to be 1.10.
Considering the level of uncertainty and technical project definition available for this engagement, the cost estimates provided includes the following:

- 30% contingency to reflect the project maturing state and the level of technical definition available
- 15% Owners cost

Cost estimates provided does not include the following

- Land acquisition and right of way
- CO_2 Capturing

Cost estimates provided using QUE$TOR are computed in USD and converted to EUR for the purpose of this study.

Cost estimates are based on the technical parameters established within scope. The technical and development configuration required to carry out the safe, permanent and efficient transportation and storage of CO_2 into the identified site are the basis for which project CAPEX and OPEX are estimated.

Considering the early phase nature of the projects and lack of firm technical definitions or data, the following assumptions and development premises were factored into the estimates.

- Compression at the Source is ring-fenced from other operations at the emitter's site
- CO_2 is available at a minimum of 45 Bar
- All rotating equipment are electric powered, and power (electricity) is assumed available from the grid.

Table 3.5 Development CAPEX and OPEX

Development CAPEX (MEUR)			OPEX (MEUR/YR)	
Components			Components	
Main TrunkLine (37km)	58		Personnel Cost	7.74
Compression and Conditioning	39		I&M	0.29
Injection Wells (X4)	41		Logistic & Consumables	3.39
Injection Site	15		Insurance Cost	0.57
			Well cost	4.05
			Field Cost	3.91
Total	**153**		**Total**	**19.95**

Copyright © SLB. All Rights Reserved. Private & Confidential. Reproduction only by permission.

Table 3.5shows the development CAPEX and operating cost based on the systems technical configuration in 3.10 System Overview (CCS Implementation)

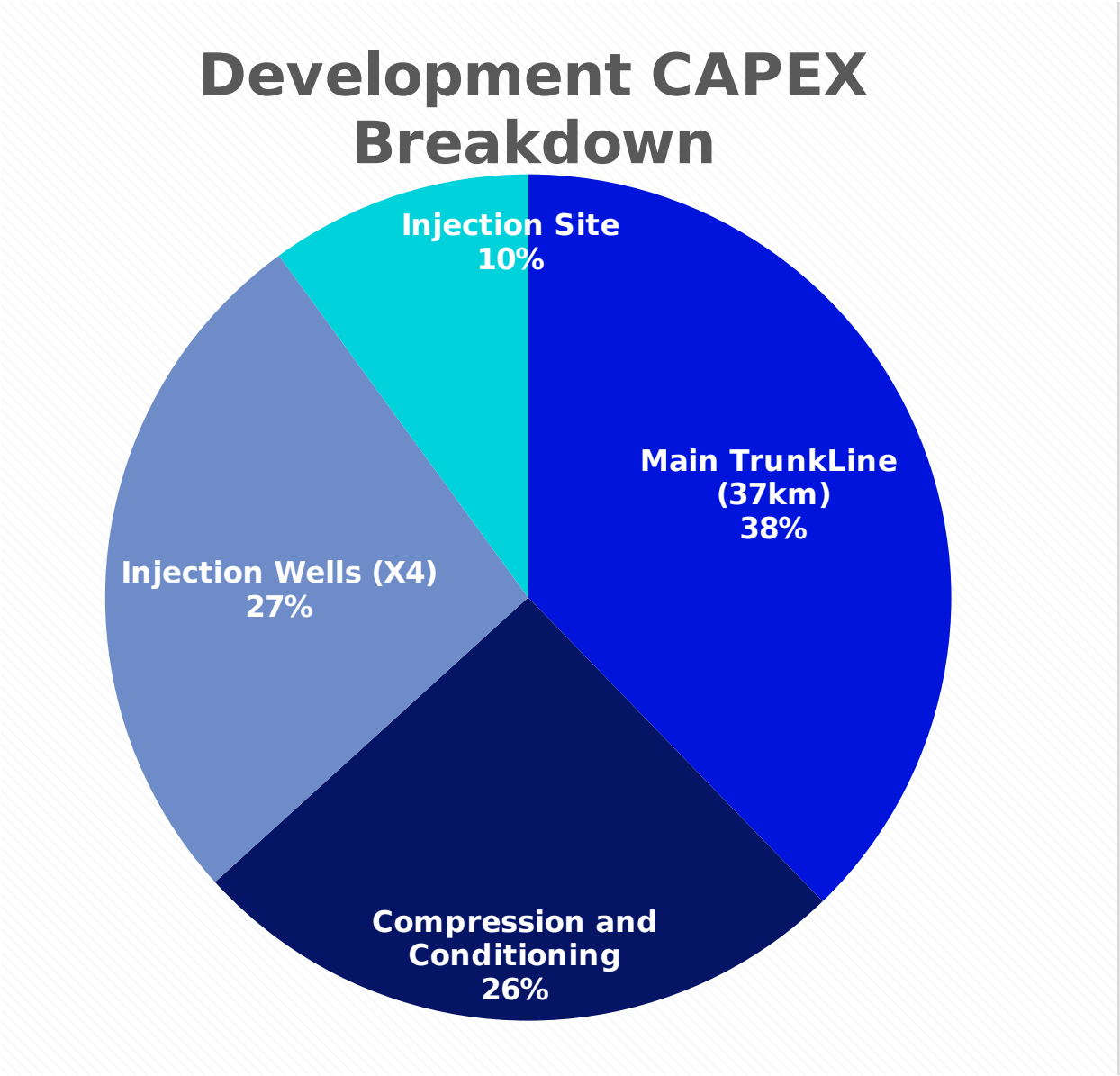


Fig. 3.19 Development CAPEX Breakdown

Copyright © SLB. All Rights Reserved. Private & Confidential. Reproduction only by permission.

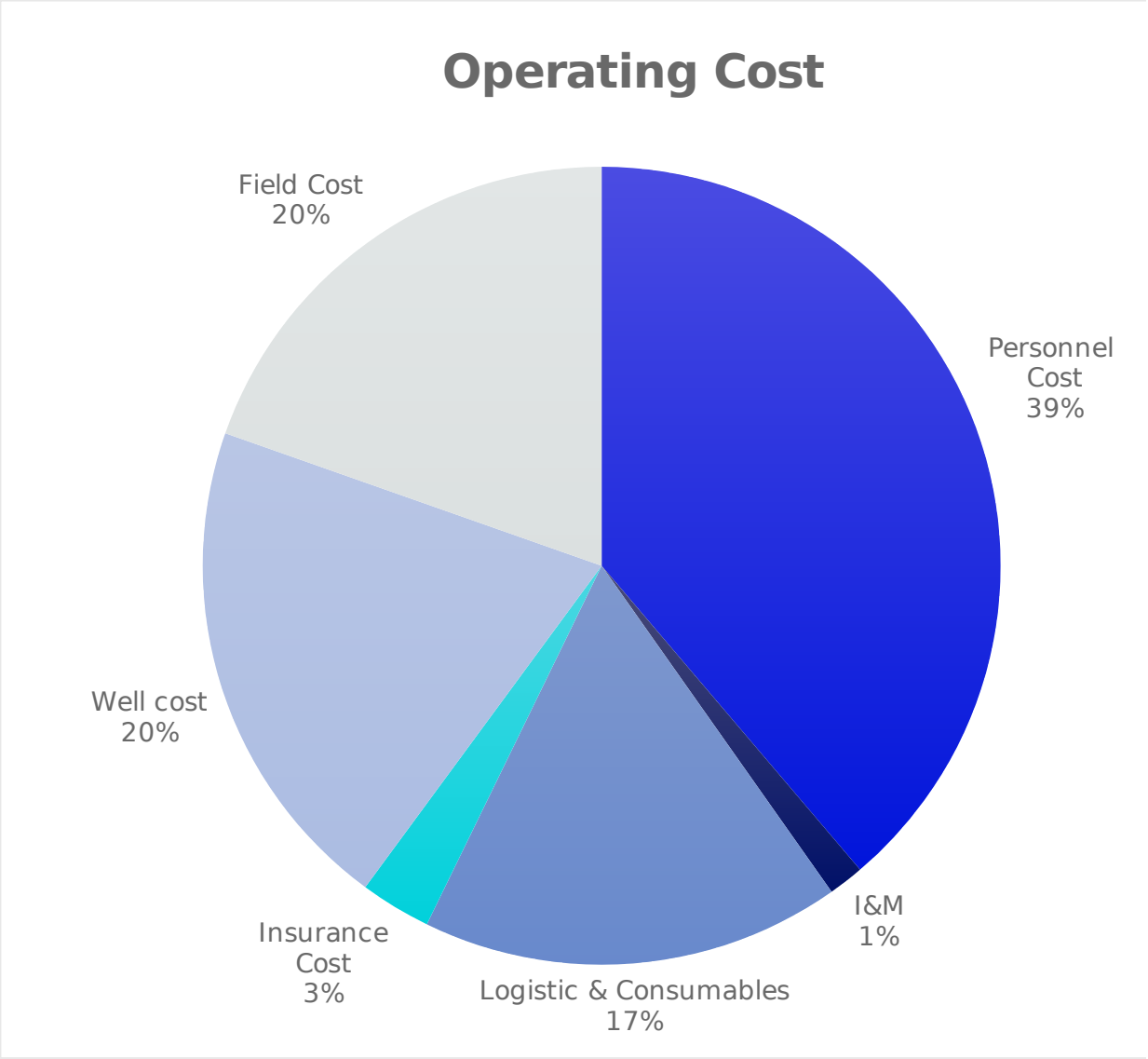


Fig. 3.20 OPEX Breakdown

Fig. 3.19 and Fig. 3.20 show the breakdown of the Development CAPEX and Operating cost by main components and activities respectively.

Copyright © SLB. All Rights Reserved. Private & Confidential. Reproduction only by permission.

4 CO_2 injection system

4.1 Design of a CO_2 borehole system

Scope of work, deliverables and exclusions

As per deliverable requirements, this section will include the following:

- Schematic representation of the structures of a standard CO_2 injection well
- Results of the stress calculation of all sections in static condition (e.g. using Pipesim software)
- Schematic representation of the borehole head and eruption device (wellhead and Christmas tree)
- Hydraulic calculations for chiseling all channel sections
- Hydraulic calculation of cementation of protective pipes of all sections
- Budgetary cost estimates for services to provide

BHA and hydraulics calculations, cementing and wellhead pre-designs were developed with minimum data and require detailed engineering in future phases of the study. Exclusions for this conceptual well design for drilling and completion fluids, bit selection, dynamic stress analysis (transient scenarios with Olga software), drilling optimization, rig sizing, detailed time and cost estimates.

Objective

This section summarizes the conceptual well design for CO_2 injector well, directional profiles, casing stress analysis for steady state, drilling BHA and hydraulics and cement basic programs and calculations. It will also include drilling time estimates and assumptions for CO_2 injector wells in Karas Suma site for CCS purposes. These 4 wells will be drilled from a common pad and targeting Alpha, B and C formations as per table Table 2.16. All 4 wells are designed as deviated J-type profiles to access the reservoir beneath the protected forest area of Šuma Ivanovo, while maintaining surface infrastructure outside the reserve boundary.

Field Location

The wells are located near Bockovac village in Croatia. Wellheads are positioned approximately 50 m from the forest reserve to ensure safe pad construction and environmental compliance. Fig. 4.1 shows a broad Google Maps view of surface locations with respect to the forest.

Copyright © SLB. All Rights Reserved. Private & Confidential. Reproduction only by permission.



Fig. 4.1 Surface locations for 4 CO_2 injector wells

4.1.1 Conceptual well design and drilling time estimation

Oil & Gas well vs CCS well [24]

To understand further requirements for a CCS well compared to a conventional Oil & Gas well, the following topics need to be considered:

1. Reservoir pressure: Increasing in CCS (towards end of injection period and near initial reservoir pressure) vs decreasing in O&G well (depletion occurs as reservoir produces).
2. CO_2 plume migration: Exposure to CO_2 over time (cement degradation, tubulars and downhole equipment corrosion) in a CCS well.
3. Uncontrolled release: Significant volume expansion of CO_2 causing rapid cooling effect in CCS well vs no cooling effect in conventional O&G well.
4. Corrosive environment: Corrosion of steel elements due to formation water and CO_2 (especially high concentrations).
5. Cement degradation: Carbonation and degradation of cement due to contact with CO_2. Cement design for CCS wells need to include self-healing additives / properties when in contact with CO_2.
6. Downhole equipment integrity: Design specifications for long exposure to CO_2 and greater

Copyright © SLB. All Rights Reserved. Private & Confidential. Reproduction only by permission.

temperature variations (e.g.-80 to 70 deg C).

7. Thermal cycling: From intermittent CO_2 injection, affecting the well barrier elements in direct contact with CO_2 (downhole equipment & cement)
8. Quality and impurities of CO_2: This is related to chemical reactivity of the impurities on the mechanical properties and durability of the wellbore components (tubulars and completion equipment).
9. Load cases for CO_2: Transient scenarios like early and late life CO_2 injection, shut-in, tubing leak during injection, loss of surface containment, etc.)

Conceptual well design workflow

For the execution of this project, one conceptual design will be developed for CO_2 injector well based on well KS4 (the deepest well and highest deviation). This design will be applicable to all 4 CO_2 injector wells and require adjustment for well architecture (casing seats, kick tolerance, etc.) depending on the specific prognosis at the time when the trajectories are confirmed.

To develop new well concept design suitable for CO_2 injection there are 3 main steps that were followed:

1. To evaluate and include injection and completion requirements. In this step the results from flow assurance are incorporated.
2. To develop and evaluate well geometry for CO_2 injection. This step includes the selection of the casing and tubing sizes.
3. To evaluate different load cases in the casing and completion (stress scenarios) throughout the life of the well.

Well engineering workflow for conceptual well design includes the following tasks. Further explanation to them is given below.

1. Offset well analysis: to evaluate well architecture used in the field, casing seats, tubular sizes and metallurgy.
2. New CO_2 injector well requirements:
   2.a. Surface and target well locations
   2.b. Directional well profiles (draft well trajectories)
   2.c. Pore Pressure (PP) and Fracture Gradient (FG) curves (from Geomechanics)
   2.d. Pressure & Temperature (P&T) profiles for required tubing size
   2.e. Metallurgy selection to cater for fluid composition in CO_2 stream
3. Develop conceptual well design
   3.a. Completion requirements as per MMV strategy
   3.b. Casing and tubing stress analysis for Early life (EL) and Late life (LL) for CO_2 injection (static condition)
   3.c. Kick tolerance calculations (to be performed during detailed engineering phase)
   3.d. Metallurgy selection for tubulars and elastomers (in completion equipment)
   3.e. Well integrity requirements for CO_2.

Copyright © SLB. All Rights Reserved. Private & Confidential. Reproduction only by permission.

Surface and target locations - Well Coordinates

The wells are located near Bockovac village in Croatia. Wellheads are positioned approximately 50 m from the forest reserve to ensure safe pad construction and environmental compliance. Table 5.1 shows the target coordinates for all 4 wells.

A general surface location was picked outside the protected area (45°42'17.91957"N, 18° 7'42.91474"E) and the concept is to have a single well pad where it is possible to drill the 4 wells from the same location. Separation between wellheads shall be planned to be at least 6 m. Target locations are spread under the forest area as shown in Fig. 4.2 and Table 4.1. Locations for new CO_2 injection wells were provided by reservoir engineering team based on injection potential and agreed scenario with CHA.

Table 4.1 Reservoir target locations

Reservoir targets	Latitude (°)	Longitude (°)	TVD-GL (m)
KS1 - Alfa	45.70993437	18.12189572	1126
KS1 - C	45.71388407	18.11656230	1574
KS2 - Alfa	45.70817493	18.13236995	1083
KS2 - C	45.71104525	18.13576618	1524
KS3 - B	45.71302429	18.12843173	1304
KS3 - C	45.71612250	18.12837178	1734
KS4 - B	45.71377847	18.13356782	1234
KS4 - C	45.71880017	18.13641039	1634

Copyright © SLB. All Rights Reserved. Private & Confidential. Reproduction only by permission.

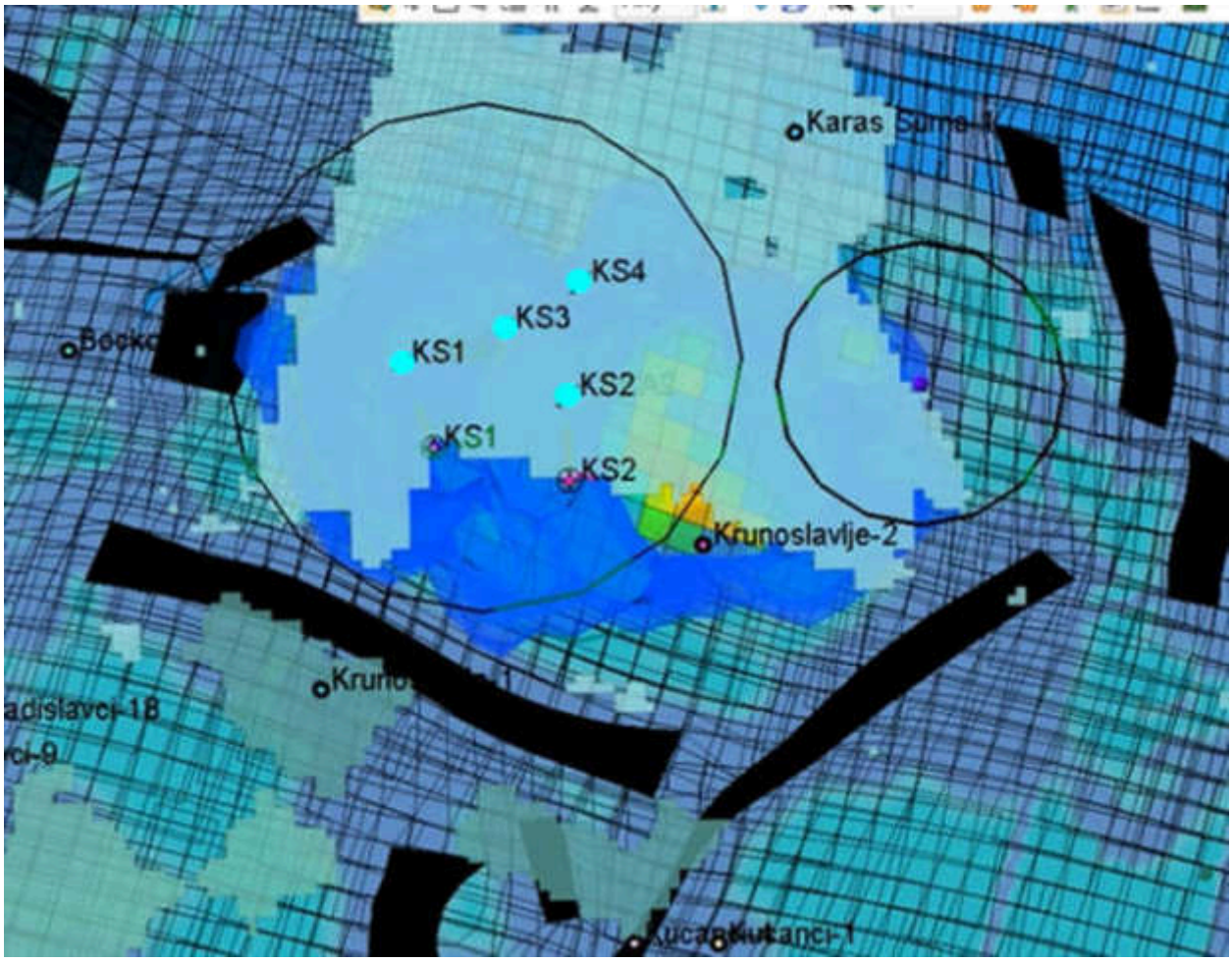


Fig. 4.2 Target locations for new CO_2 injector wells
CO2 injection reservoir targets marked in green.

Directional well profiles

CO_2 injector wells are normally vertical to limit caprock penetration (well integrity consideration). In this case, as Kara Suma site is located under the protected forest area, vertical wells are not possible and different approach was required. Together with Reservoir engineering team the selected best well trajectories were J-type.

As per quick Geomechanical assessment and due to lack of data, it is not possible to conclude at this stage on the best formations (strength) for kick off point (KOP) or the best direction to drill (with respect to the minimum horizontal stress, better directional control, etc.). Although there is no certainty of drillability or best direction, it was observed that well Stjepanik-1ST1 was sidetracked up to 64 degrees of inclination.and therefore, it can be concluded that directional work for high deviated wells is possible in this field.

Copyright © SLB. All Rights Reserved. Private & Confidential. Reproduction only by permission.

From available information, well Krunoslavje-2 is the nearest existing well and the best reference for expected lithology for new CO_2 injector wells. Based on this well, KOPs were decided for all first draft trajectories for all 4 wells KS1, KS2, KS3 and KS4.

Table 4.2 Trajectories summary for all 4 CO_2 injector wells

Feature	KS1	KS2	KS3	KS4
Total Depth (m)	2273.68	1887.39	2288.11	2645.72
True Vertical Depth (m)	1604.27	1560.56	1767.87	1658.68
Max Inclination	58	43	47.5	61
Azimuth	315.43	38.49	358.06	20.46
Horizontal displacement (m)	1402.4	910.06	1275.6	1814.18
Max DLS	2.48	2.02	2.18	2.59

Well trajectories are presented in Fig. 4.3, Fig. 4.4, Fig. 4.5, Fig. 4.6, Fig. 4.7 below.

After surface locations and well pad design is confirmed, trajectories shall be revised and anti-collision assessment shall be run to confirm there are no issues.

Subsurface Pressures - Pore Pressure & Fracture Gradient

Pore pressure and fracture pressure inputs were taken from 2.6 Geomechanical quicklook analysis and adapted to well KS4 new trajectory. KS4 trajectory and well have been selected to develop the conceptual design as is the most deviated and deepest well among the 4 CO_2 injector wells. Table 4.3 shows the expected pore pressures and fracture gradients values for KS4 trajectory. Pressure plot in Fig. 4.8 shows in pore pressure curve (in purple), fracture curve in brown) and fracture pressure at 90% (in red). Mud window falls within purple and red curves.

Table 4.3 Pore Pressure & Fracture Gradient for KS4

MD (m)	PP (bar)	FG (bar)
0	1	1
1300	77.36841583	154.5642548
1400	81.23190308	162.1228943
1500	86.09996033	169.692337
1600	90.26535034	177.2728729
1700	95.32076263	184.8647308
1800	99.8575592	192.4677277
1900	104.9019318	200.0819702
2000	109.5203934	207.7068176
2100	114.5531464	215.342804
2200	119.1019058	222.9899597
2300	124.3695221	230.6413574
2400	129.3659058	238.2927551
2500	133.5055389	245.9441376
2600	139.2979584	253.5955353
2645.5	139.7076263	257.0769348

Copyright © SLB. All Rights Reserved. Private & Confidential. Reproduction only by permission.

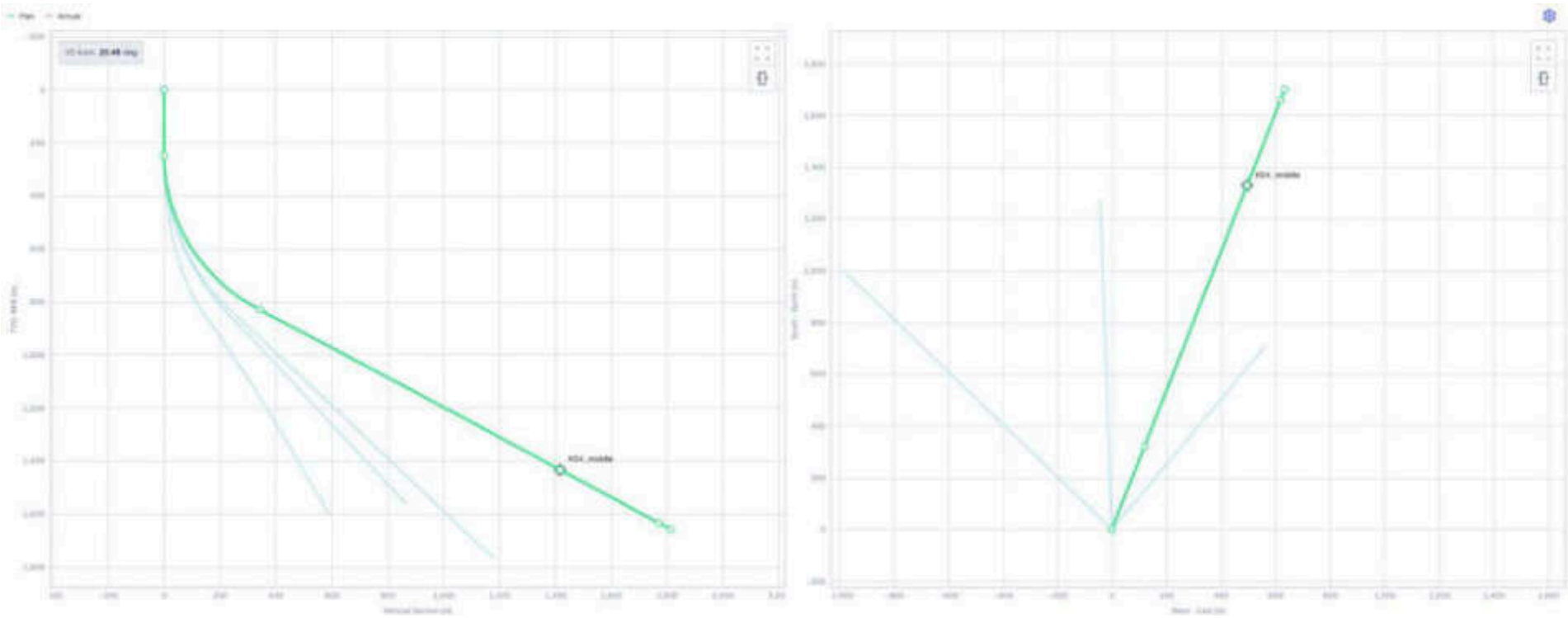


Fig. 4.3 Trajectories for all 4 new CO_2 injector wells

Copyright © SLB. All Rights Reserved. Private & Confidential. Reproduction only by permission.

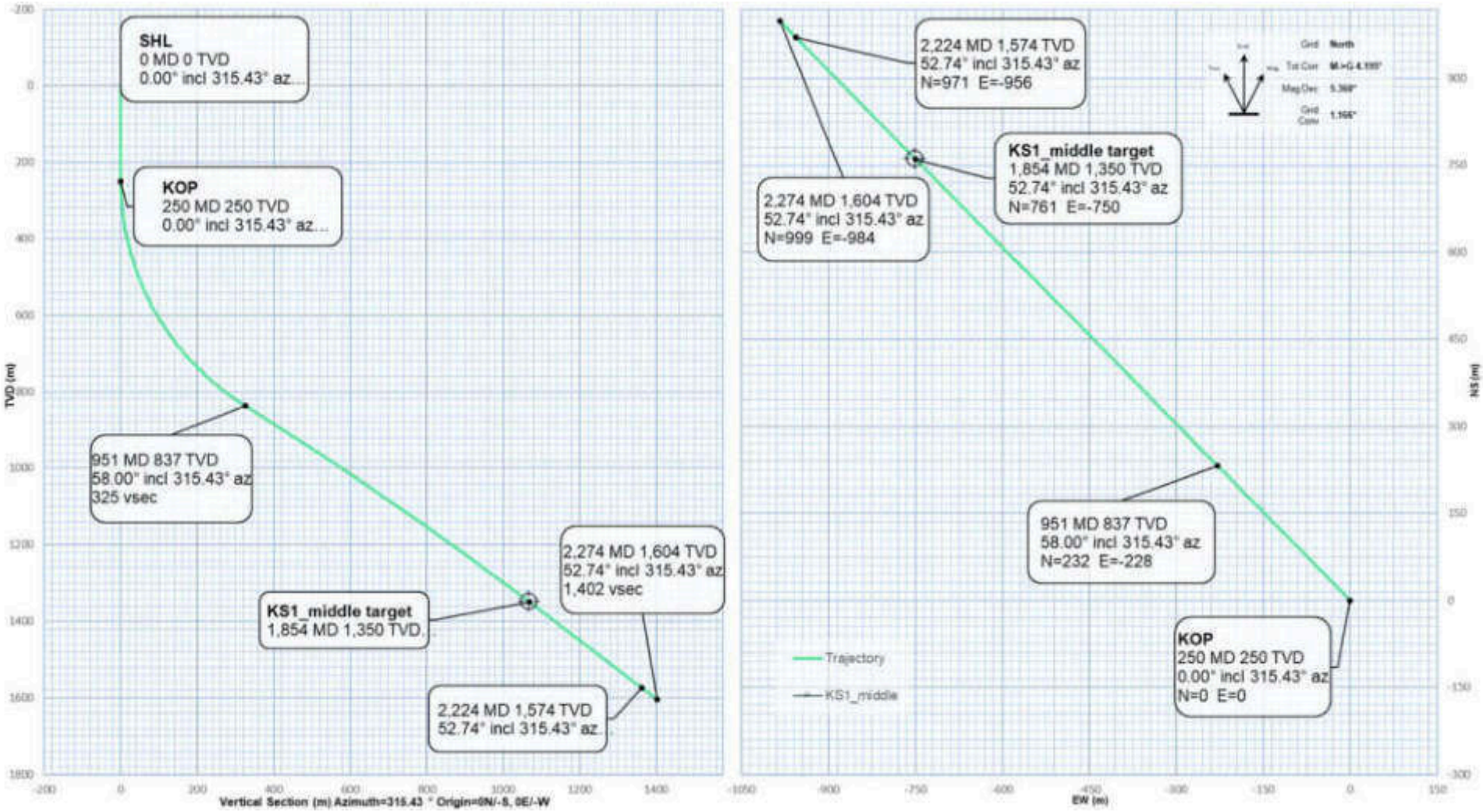


Fig. 4.4 KS1 Wall Plot

Copyright © SLB. All Rights Reserved. Private & Confidential. Reproduction only by permission.

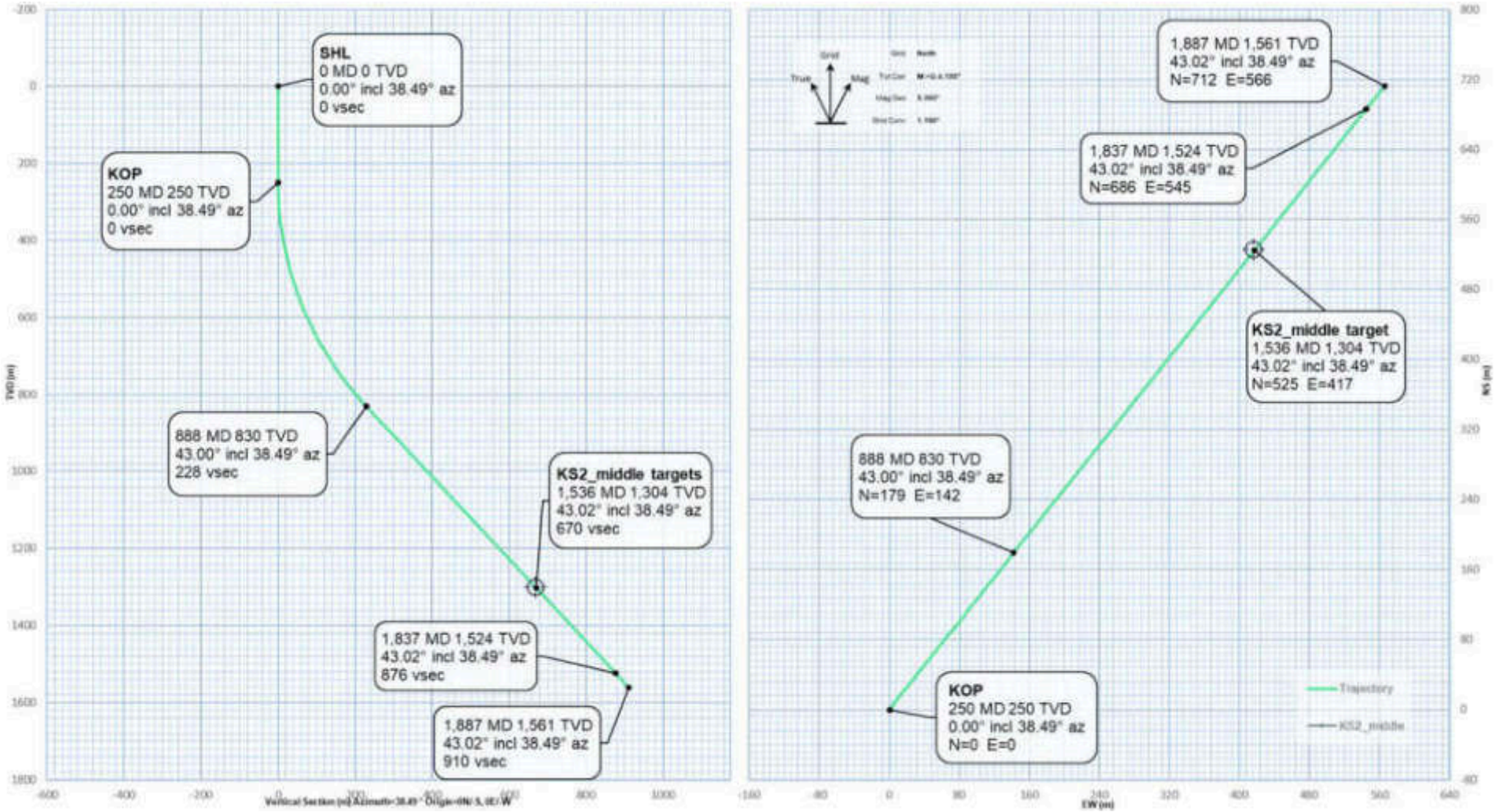


Fig. 4.5 KS2 Wall Plot

Copyright © SLB. All Rights Reserved. Private & Confidential. Reproduction only by permission.

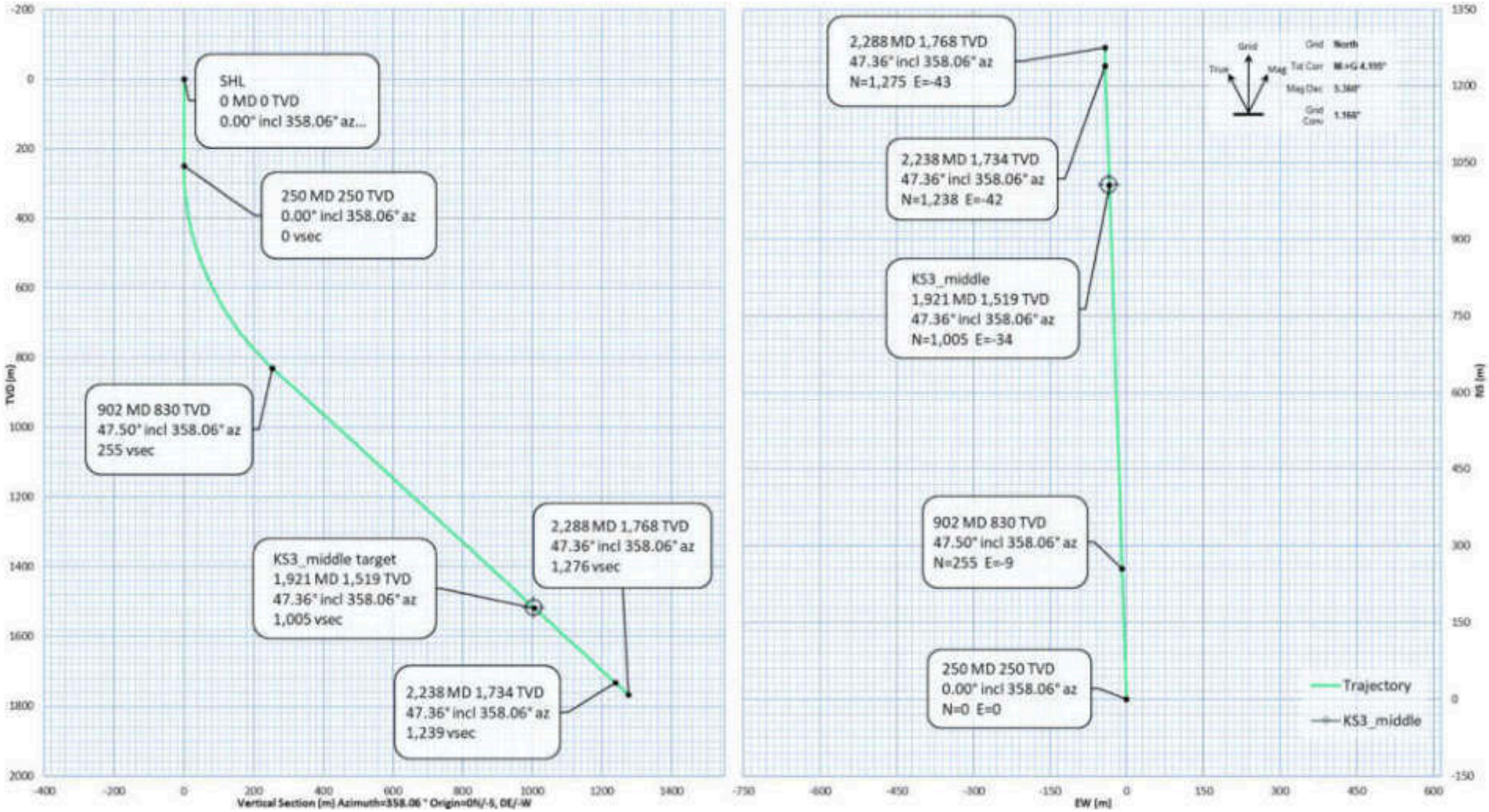


Fig. 4.6 KS3 Wall Plot

Copyright © SLB. All Rights Reserved. Private & Confidential. Reproduction only by permission.

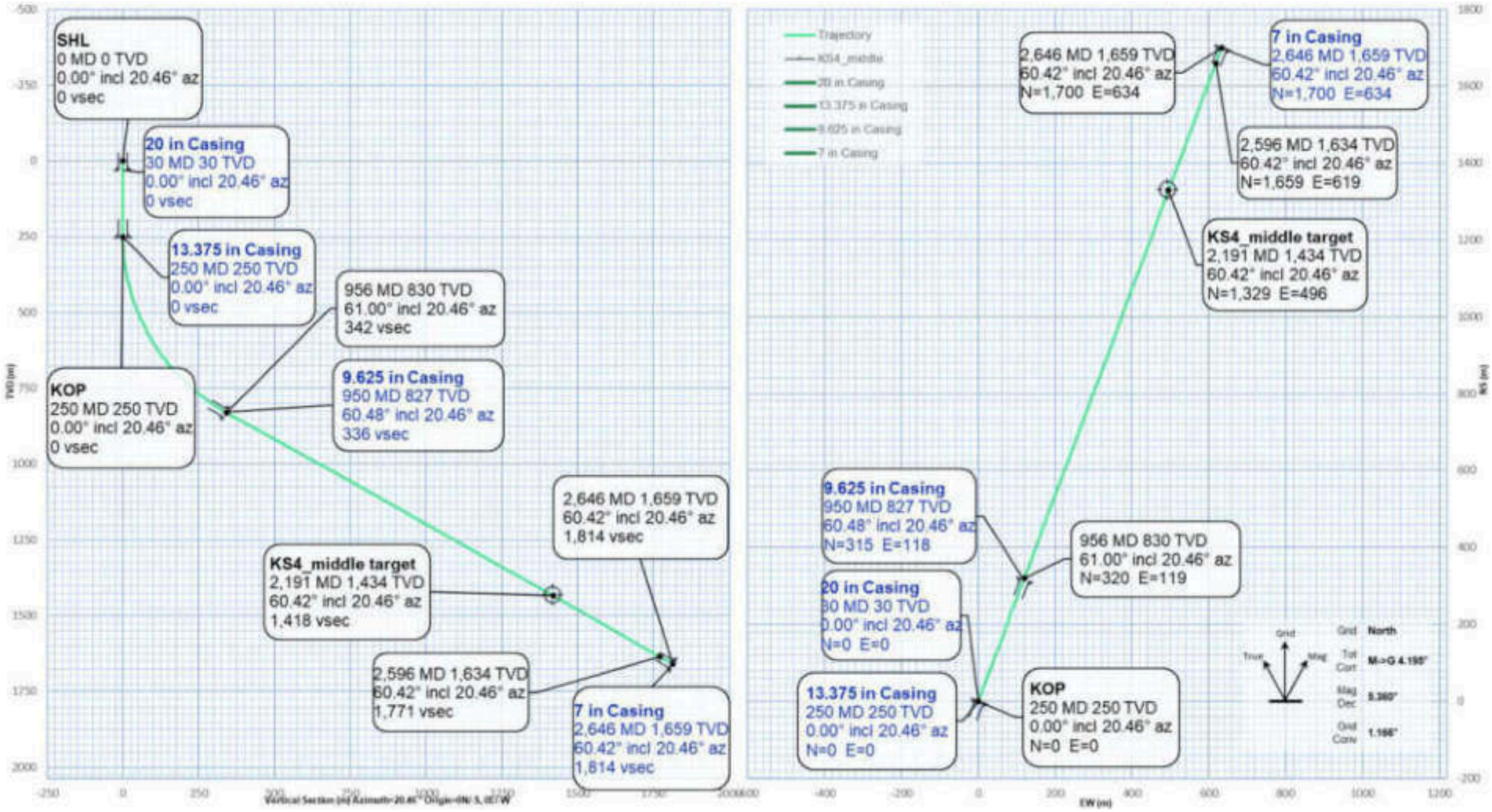


Fig. 4.7 KS4 Wall Plot

Copyright © SLB. All Rights Reserved. Private & Confidential. Reproduction only by permission.

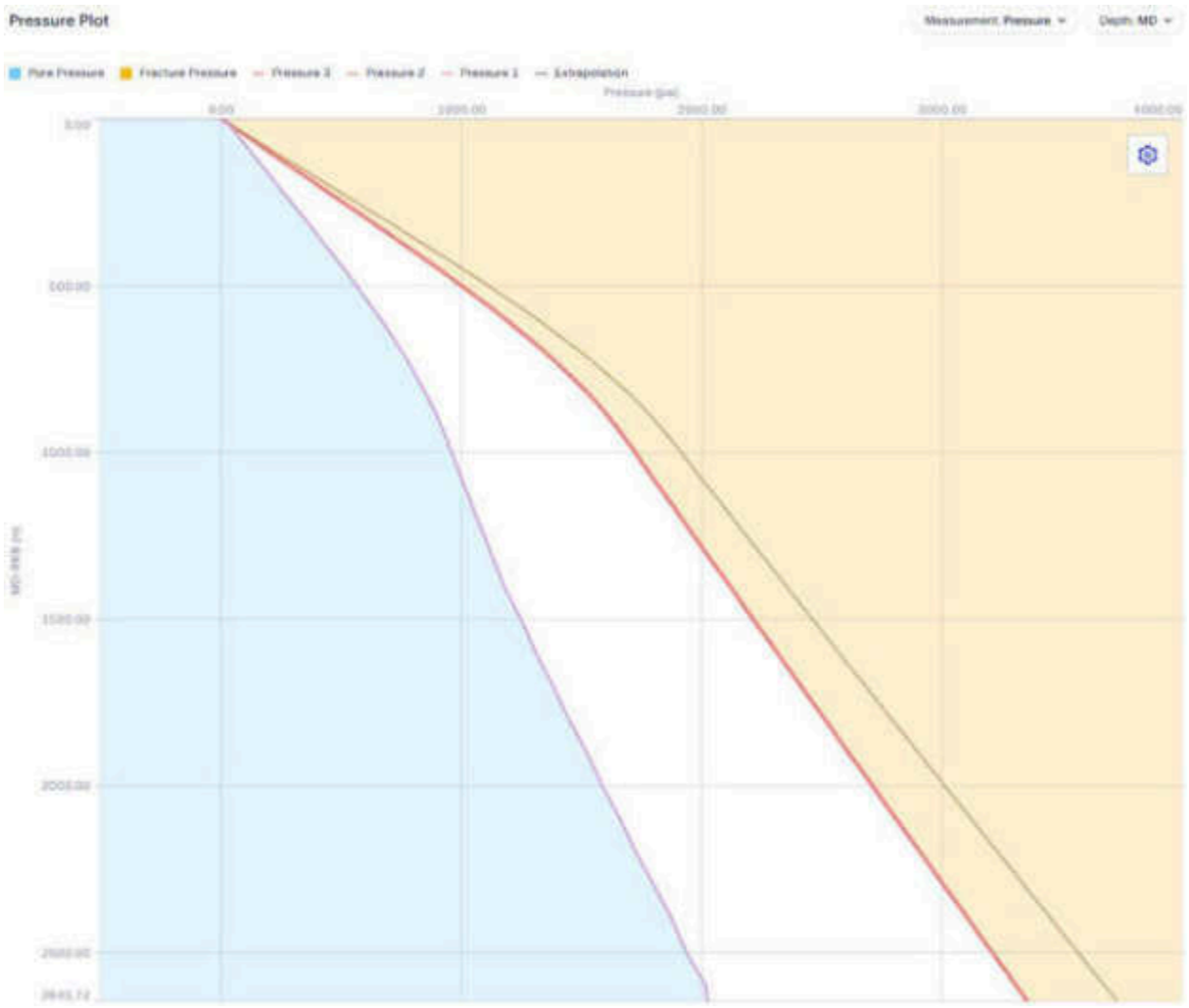


Fig. 4.8 Pore and Fracture pressures plot for KS4

Casing Design Basis

The casing program was engineered to meet all structural and operational load requirements for CO_2 injection in a CCS project. The design complies with the following standards:

- API 5CT – Casing and Tubing
- API TR 5C3 – Performance Properties
- ISO 11960 – Steel Pipes for Casing/Tubing
- ISO 13679 / API RP 5C5 – Connection Evaluation

Casing Program Summary:

- Conductor: driven preferably or drilled (TBD) → 20" 94 lb/ftJ-55 API Buttress connection

Copyright © SLB. All Rights Reserved. Private & Confidential. Reproduction only by permission.

- Surface casing: 17-1/2" hole section → 13-3/8" 68 lb/ft L80-1, API Buttress connection
- Intermediate casing: 12-1/4" section → 9-5/8" 43.5 lb/ft L80-1, API Buttress connection
- Production (Injection) casing: 8-1/2" section → 7" 26 lb/ft L80-1, Tenaris BLUE premium connection tapered with 7" 26 lb/ft SM25SCr-80,Tenaris BLUE premium connection

Rationale and assumptions:

- Surface 13-3/8" casing would cover and isolate fresh water shallow aquifers.
  - Existing offset wells architecture were attempted to be used as reference for casing seats in shallow formations. Due to lack of data/consistency among existing wells, the conclusion is that the overburden including caprock (Lonja formations) has not been evaluated.
  - Lonja formations (above target injection reservoir, including the caprock) require further data acquisition and investigation on shallow aquifers and lithology prognosis.
  - It is assumed that these casing will cover and isolate shallower aquifers/thief zones.
- 9-5/8" casing setting depth is anticipated to be within the caprock and above top of first target injection zones (e.g. 50 m above Alpha or B depending on the well objectives).
- L80-1 casing grade selected for strength and moderate corrosion resistance for surface, intermediate and partial production casings.
- 7"casing was selected over liner to protect the intermediate from corrosive environment with CO_2.
- 7"casing setting depth is anticipated to be extended 50 m after bottom of target injection reservoirs have been hit.
- 7"casing is using 2 different materials (L80 and 25Cr-80) to optimize for a feasible and economical design.
- Super duplex casing (25Cr) grade selected as standard material for CCS application to handle some impurities as CO_2 will not be pure (e.g. will contain impurities like Nitrogen oxides (NO_x), Sulfur oxides (SO_x), Oxygen (O_2), H_2S, etc.

Completions design requirements:

- Tubing sizes were evaluated based on Flow Assurance analysis (Refer to section 3.7 Well Modelling). 3-1/2" (88.9 mm) tubing is the selection for 4 CO_2 injection wells.
- Subsurface Safety Valve (SSSV) depth is defined as per Oil & Gas guidelines. SSSV maximum setting depth (fail-safe depth) to be confirmed during detailed engineering phase.
- Pressure & temperature (P&T) gauge depth is below the packer providing measurements from top reservoir.
- Fiber optics along the tubing would provide continuous measurements for DAS (Distributed Acoustic Sensing) and DTS (Distributed Temperature Sensing) and would be run until end of tubing (just above liner hanger).
- P&T gauge and fiber optics are part of the agreed MMV plan.

Copyright © SLB. All Rights Reserved. Private & Confidential. Reproduction only by permission.

- In future stages of the project and depending on detailed risk assessment, the requirement for monitoring as per MMV plan could change, and completion design would require to be revisited.

The well architecture is presented in Fig. 4.9 below

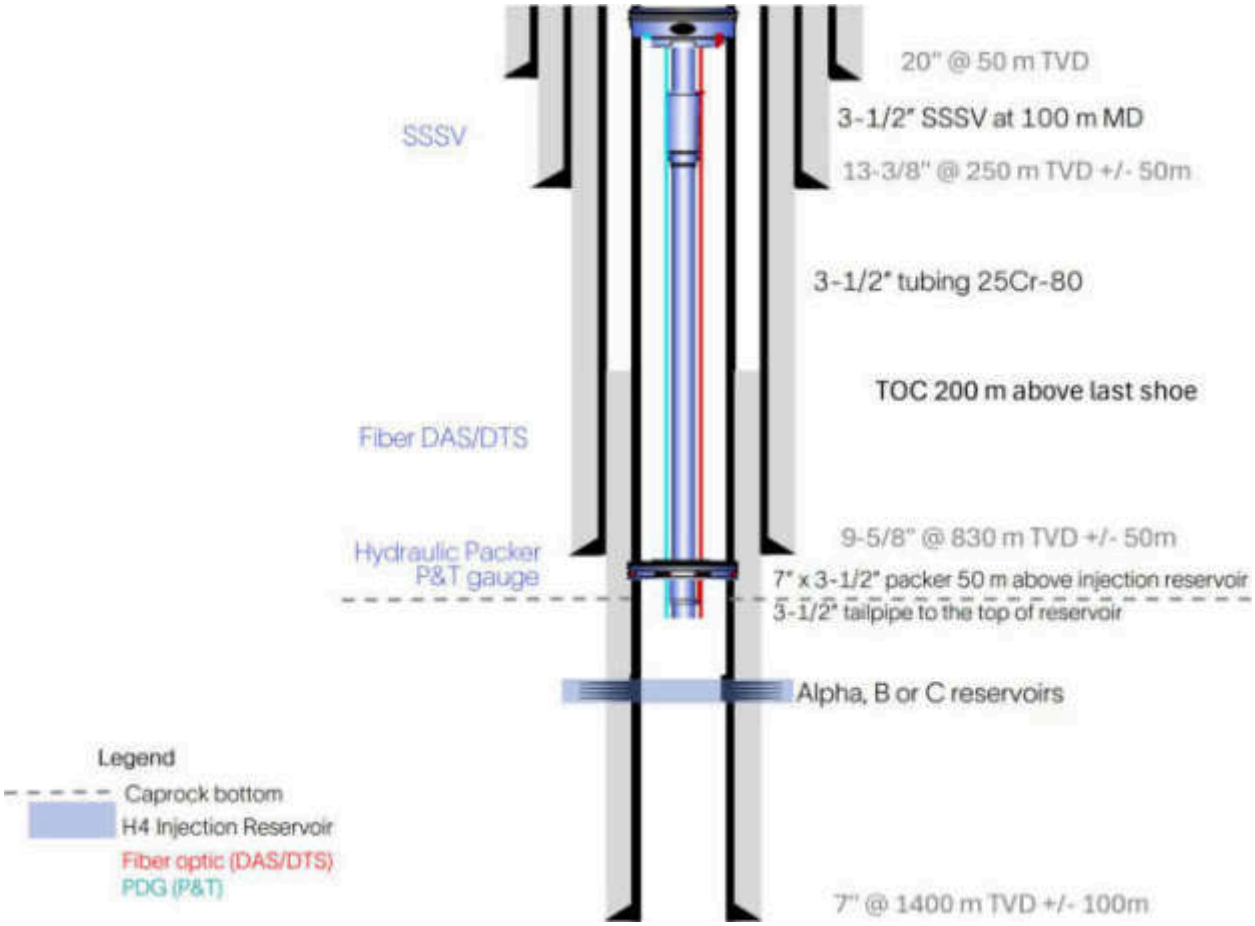


Fig. 4.9 Completion schematic for CCS well

Well Construction and Casing Design Results

Well construction will consist of the aforementioned configuration as explained in previous section. The casing profile consists of 4 casing strings (Conductor, Surface, Intermediate and Injection). The first 3 cemented to surface, the 4th with the top of cement (TOC) to be 200 m above 9-5/8 "shoe. Casing seats will vary for each CO_2 injector well and will depend on the depths where target injection reservoirs are encountered.

Copyright © SLB. All Rights Reserved. Private & Confidential. Reproduction only by permission.

Table 4.4 KS4 well geometry

Section (in)	Type	Tubular	OD (in)	ID (in)	Drift ID (in)	Start MD (m)	End MD (m)	TOC (m)
20"	Conductor casing	20" 94 ppf J-55 BTC	20	19.124	18.937	0	30	0 (if drilled)
13-3/8"	Surface casing	13-3/8" 68 ppf L80 BTC	13.375	12.415	12.259	0	250	0
9-5/8"	Intermediate casing	9-5/8" 43.5 ppf L80 BTC	9.625	8.755	8.599	0	950	0
7"	Production casing (for CO_2 injection)	7" 26 ppf L80 Tenaris BLUE x 7" 26 ppf 25Cr80 Tenaris BLUE	7	6.276	6.151	0	2645.72	750
3-1/2"	Injection tubing	3-1/2" 9.2 ppf 25Cr80 Tenaris BLUE	3.5	2.992	2.867	0	1838	No cement

The well schematics are presented in Fig. 4.10 and Fig. 4.11 below.

The stress and movement analysis was performed to check on the basic load case scenarios for the new injector. The software TDAS (Tubular Design and Analysis System) from SLB was used to perform this analysis in static condition. The recommended way for the analysis of CO_2 injectors, includes evaluation of all static and transient scenarios during early and late life with the assistance of Olga dynamic multiphase flow simulator to ensure Pressure and Temperature profiles shall be customized to those transient scenarios. As part of the feasibility study, Olga was not included in the scope and therefore tubular analysis was limited to static load cases similar to the ones for oil and gas wells (static condition) plus some load cases applicable to CCS analysis. Please refer to Table 4.5 for typical load scenarios analyzed for CCS wells. Additional transient scenarios (shown as pending status) should be evaluated during detailed engineering stage.

Copyright © SLB. All Rights Reserved. Private & Confidential. Reproduction only by permission.

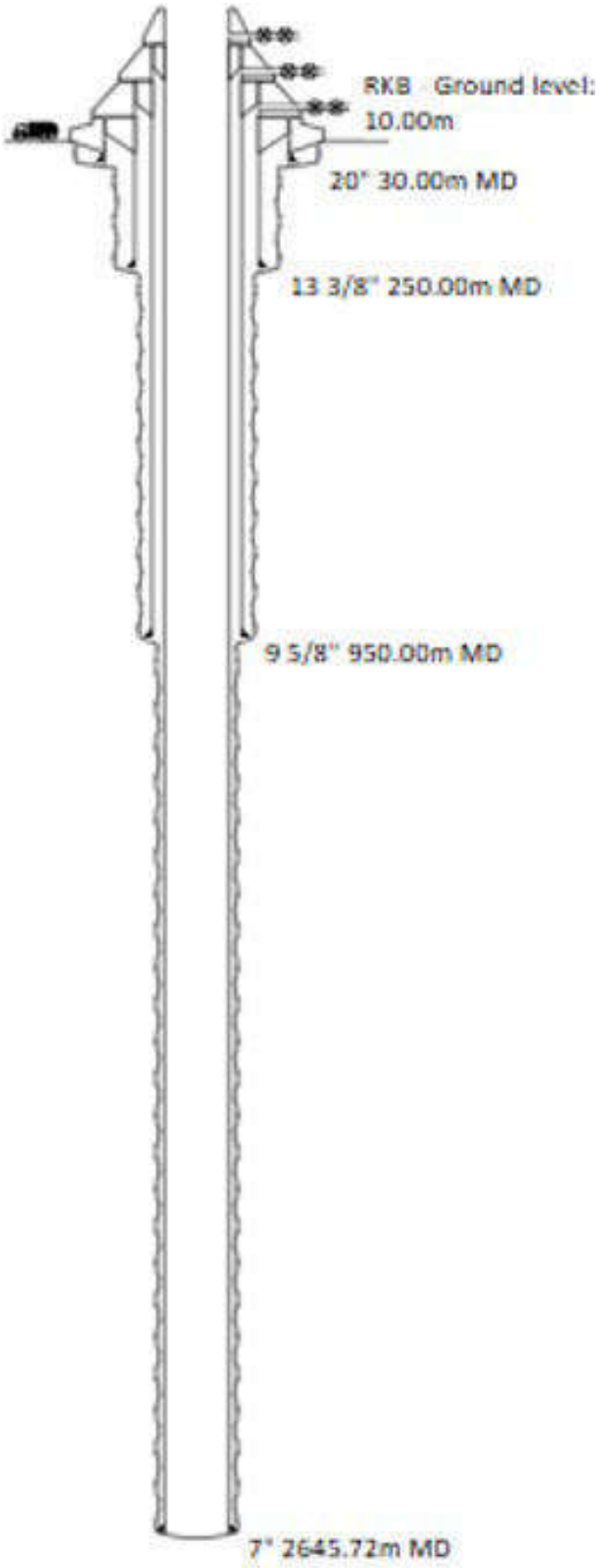


Fig. 4.10 KS4 well Schematic for casing

Copyright © SLB. All Rights Reserved. Private & Confidential. Reproduction only by permission.

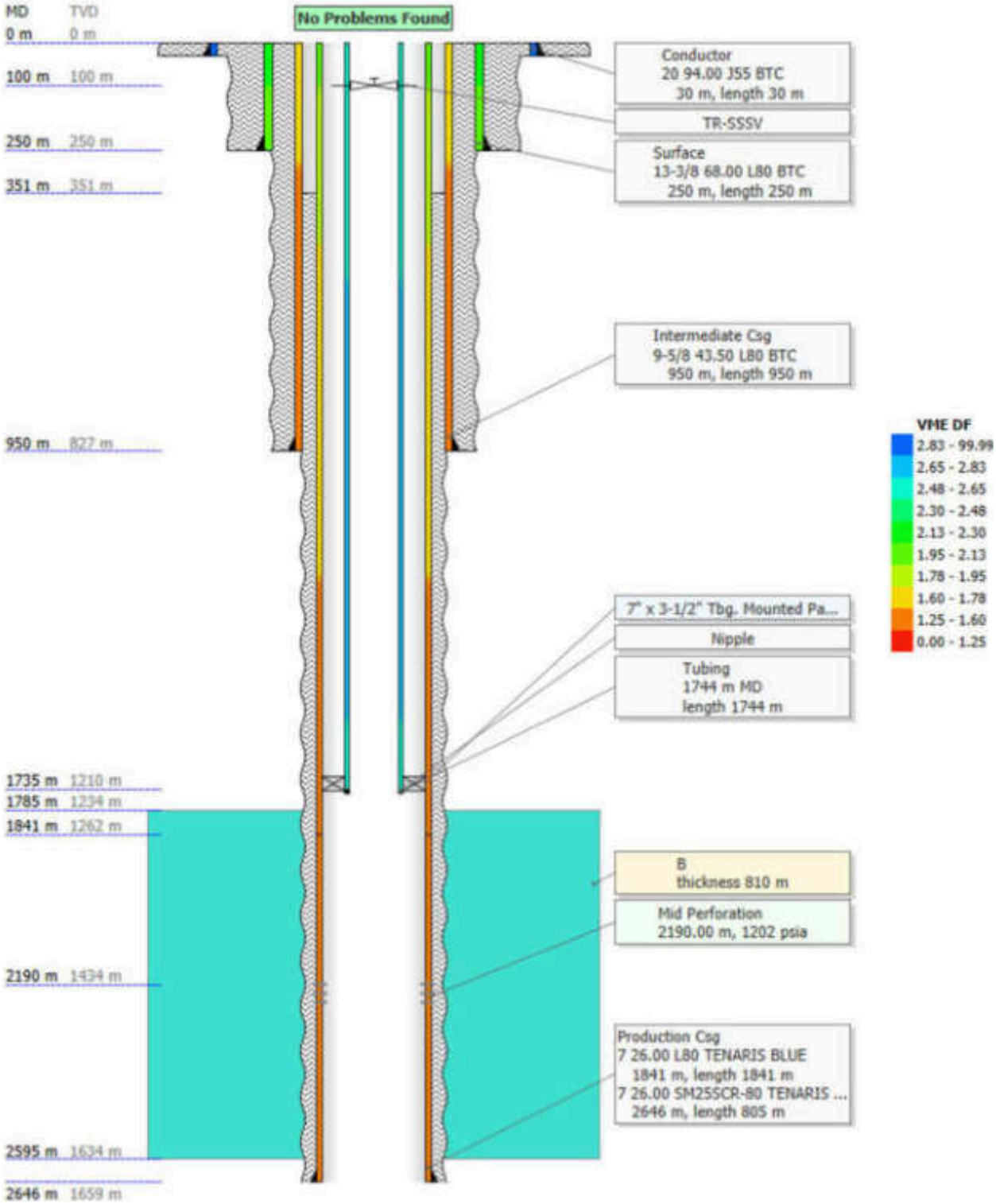


Fig. 4.11 KS4 well Schematic with completions

Copyright © SLB. All Rights Reserved. Private & Confidential. Reproduction only by permission.

Table 4.5 Typical Load Scenarios Analyzed for CCS Wells

Load		Tubular	Pending
1	Bullheading Final (LL)	Production Casing	Analyzed
2	Bullheading initial (LL)	Production Casing	Analyzed
3	Max Injection Pressure -Tubing Leak (LL)	Production Casing	Pending
4	Initial injection start-up (EL)	Tubing	Pending
5	Injection re-start up (LL)	Tubing	Pending
6	Steady-state injection (EL)	Tubing	Analyzed
7	Steady-state injection (LL)	Tubing	Analyzed
8	Injection shut-down (EL)	Tubing	Pending
9	Injection shut-down (LL)	Tubing	Pending
10	Full evacuation (EL)	Tubing	Analyzed
11	Full evacuation (LL)	Tubing	Analyzed
12	Loss of surface containment (EL)	Production Casing	Pending
13	Loss of surface containment (LL)	Tubing	Pending
14	SSV closure (EL)	Tubing	Pending
15	SSV closure (LL)	Tubing	Pending
16	Packer leak full evacuation	Production Casing	Pending
17	Max Injection Pressure	Tubing	Pending

Rationale and assumptions:

- Reservoir properties for Alpha, B & C were provided by SLB reservoir engineering (PP, FG, reservoir Temp).
- Injection profiles (Pressure & Temperature) for static condition were provided by SLB production engineering after flow assurance analysis. They are used to simulating stress scenarios calculations (burst, collapse, tension, compression and triaxial) for all casing and completions strings.
- P & T profiles will impact on downhole equipment selection (specifications and ratings for metallurgy and elastomers). Further evaluation of these transient phenomena need to be repeated with Olga simulator (dynamic multiphase flow simulation) in the next phase study to validate these minimum temperatures and ultimate material selection (critical for subsurface safety valve and packer).
- Minimum casing/tubing design loads will be evaluated with respect to below design factors as per SLB standard IWC-CSG-ST-002 Casing and tubing design ST.

Copyright © SLB. All Rights Reserved. Private & Confidential. Reproduction only by permission.

Table 4.6 Minimum Design Factors for stress anaylsis

Burst	All casing and Tubing Strings
Collapse	1.10
Compression	1.20
Tension - Premium connections - API connections	1.40 1.60
Triaxial	1.25

- 150 psi overbalance was considered as per SLB standard.
- Mud weights and cement slurries and densities were considered as per offset well.
- Premium (gas-tight) connections were considered for production casing and tubing.
- Tubulars and packer pressures tests were evaluated to the maximum injection pressure as per Flow Assurance results.
- Tubular specifications are based on the material selection as specified in above section.
- Basic load scenarios for burst, collapse, compression, tension and Von Mises (triaxial) stresses were evaluated

Table 4.7 shows the summary of casing stress calculations for all tubulars for well KS4.Values also reflect derating of the casing strength based on anticipated pressures and temperature as per flow assurance analysis. Design factors for all loads are

Table 4.7 KS4 Casing Design Results

Section (Type)	String	Burst	Collapse	Tension	Compression	VonMises	Buckling (deg/30m)
20" (Conductor)	20" 94 ppf J-55 BTC	3.91	11.51	9.00	42.76	4.41	0
17-1/2" (Surface)	13-3/8" 68 ppf L80 BTC	1.88	5.95	7.98	12.54	2.03	0
12-1/4 " (Intermediate)	9-5/8" 43.5 ppf L80 BTC	1.36	4.38	5.14	6.2	1.41	0
8-1/2 "(Production)	7" 26 ppf L80 BLUE x 7" 26 ppf 25Cr80 BLUE	1.34	1.88	3.88	6.47	1.38	0
Upper completion	3-1/2" 9.2 ppf 25Cr80 Blue	2.56	5.49	3.43	14.65	2.58	0

Metallurgy selection

Casing and tubing:

As per assumption from the proposal of this study, pure CO_2 would be considered for material selection purposes. However, it is common that CO_2 is never pure when injected and contains impurities like Nitrogen oxides (NO_x), Sulfur oxides (SO_x), Oxygen (O_2), Hydrogen Sulfide (H_2S), Water (H_2O), chloride content, pH and others. These impurities will dictate the final metallurgy required for CCS application. At this stage, the impurities shown in Table 4.8 were accounted for

Copyright © SLB. All Rights Reserved. Private & Confidential. Reproduction only by permission.

to select metallurgy for tubulars (casing and tubing). 25Cr is the proposed material for casing design and stress evaluation purposes (Tenaris SM25Cr-80). The selected material could be optimized when the final composition of CO_2 injection fluid is confirmed.

Table 4.8 CO_2 stream composition for Bockovac project

Component	CHA project (NEXE cement plant)
CO_2	85%-90%
H_2O	<600 ppm
H_2S	<10 ppm
N_2, Ar, H_2	<15% (with Methane)
O_2	
CO	<1000 ppm
NO	<25 ppm
SO	<25 ppm
Hydrocarbons	Combined with N_2, Ar, H_2 and O_2 <15 %mol

Completion equipment:

Inconel alloy 718 was selected for completion equipment metallurgy as there is low content of H_2S. This material has high tensile strength, corrosion-resistant nickel chromium material with excellent performance in high temperature, high CO_2 and low H_2S environments[25].

Elastomers for completion equipment were selected to have HNBR which has excellent resistance to CO_2 environments showing higher chemical stability and resistance to degradation[26].

Well integrity requirements for CO_2

A well design for CO_2 injection in principle is the same as the one for O&G with the addition of few things pertaining to CCS specifics mainly related to well integrity for eternal storage philosophy. Depending on regulation or the followed standards, these requirements might change. It is important to always follow the latest regulations to ensure compliance. The following list is highlighting those additional considerations that have to be taken when designing an injector well for CO_2.

1. Adequate metallurgy selection for casings, completion designs and wellhead is required.
2. Well barrier policy compliance for CCS well (injection or monitoring).
   2.a. Requirement on number of well barriers (mostly 2) in different phases of lifecycle of the well (drilling, completion, injection and P&A).
   2.b. Focus on barrier philosophy: design, types, verification and testing methods as well as acceptance criteria requirements for each wellbore component (well barrier elements acceptance criteria tables from Norsok-D010).
   2.c. Material selection of wellbore components, including metallurgy and elastomers, and their properties related to corrosion resistance (depending on CO_2 stream composition) and pressure/thermal loads that the equipment is going to be exposed to throughout

Copyright © SLB. All Rights Reserved. Private & Confidential. Reproduction only by permission.

the lifecycle. It is crucial to identify operational practices that can affect the performance of the materials (e.g. shut-down and restarting of CO_2 injection).

2.d. Use of resistant cement technology suitable for CO_2 injection (e.g. EverCRETE with self-healing properties when in contact with CO_2).

2.e. For production casing, 200 m MD of annular cement are required above planned production packer depth as minimum (as pe Norsok-D010). In this case TOC for production casing is also overlappin the previous 9-5/8" casing shoe.

3. Well monitoring compliance for CCS projects (part of MMV plan)

3.a. Needs to be tailored as per local regulations and to each storage site.

3.b. Mainly monitoring for CO_2 reservoir pressure and change with time, migration of CO_2 plume within the storage reservoir, leakage of CO_2 into other formations (upward or downward).

3.c. Periodic monitoring of tubing and production casing/liner for leakage and corrosion.

3.d. Monitoring packer and annulus cement integrity towards the late life.

3.e. Monitoring transient pressure and temperature during shut-ins and start-ups for intermittent CO_2 injection strategy.

3.f. Monitoring changes in CO_2 composition.

Copyright © SLB. All Rights Reserved. Private & Confidential. Reproduction only by permission.

Drilling Fluid Summary

The objectives of the proposed drilling fluid types are to:

- Maintain wellbore stability.
- Control formation pressures.
- Minimize formation damage in reservoir interval.
- Provide adequate hole cleaning in directional sections.
- Ensure compatibility with cement systems.

Proposed drilling fluid system is water based mud and summaries by section are listed as follows. Estimated downhole volumes are shown in Table 5.9.

- 17-1/2" section: freshbased Ca-based
- 12-1/4" section: KCl / KLAHIB
- 8-1/2" section: KCL/ KLAHIB / HT

Table 4.9 KS4 CO_2 injector well drilling fluid volume estimation by section

Hole size (in)	17-1/2"	12-1/4"	8-1/2"
Downhole volumes (m3)	21.4	15.4	142

Fig. 4.12 shows the drilling fluid weight window demonstrating the anticipated mud weight for the injector well, in conjunction with the Pore and Fracture Pressure, are obtained from the KS4 well pressure data. Expected mud weights are in the range of 1.07-1.20 sg and subject to confirmation.

Copyright © SLB. All Rights Reserved. Private & Confidential. Reproduction only by permission.



Fig. 4.12 Drilling fluid weight window for KS4 well

Cementing Plan Summary

Cement systems were proposed based on temperature, lithology, and long-term zonal isolation requirements. Class G is the typical base cement for geothermal wells. It was selected because of its predictable performance and compatibility with high-temperature silica strength retrogression systems. Proposed cementing plan summary is listed as follows and estimated volumes are shown in Table 5.10.

- 20″conductor casing: Class G Portland Cement (if conductor was not driven).
- 13-3/8" surface casing: Class G Portland Cement in a single slurry.
- 9-5/8″ intermediate casing: Class G Portland Cement for lead slurry with a mix of EverCRETE (CO_2 resistant cement) for tail slurry that will be placed across the caprock.
- 7" production (injection) casing: EverCRETE (CO_2resistant cement) is required as per well integrity requirements to ensure isolation and CO_2 containment.

Copyright © SLB. All Rights Reserved. Private & Confidential. Reproduction only by permission.

Hole size (in)	17-1/2"	12-1/4"	8-1/2"
Total volumes (m3)	35 (50% excess)	87.4 (50% excess)	59.3 (25% excess)

Wellhead schematic and details for CO_2 injector are shown in

Drilling time estimation

Conceptual design has been developed for well KS4. It is anticipated that time to drill this well is approximately 45 days. This time includes 20% Non-Productive Time (NPT). The clean time will be approximately 39 days; it will take 39days to drill the well if no unforeseen issues arise. Number of bit runs and anticipated Rate of Penetration (ROP) per section are listed in Table 4.11.

Table 4.11 KS4 Well Bit Run and ROP estimations by Section

Hole size (in)	Number of bit runs	ROP (m/hr)
17-1/2"	1	18
12-1/4"	1	15
8-1/2"	2	10

ROP expectations are fairly conservative due to lack of recent bit records from existing wells. There are other issues (that are not drilling speed related) that can delay the whole drilling process, such as:

- Wellbore stability issues
- Drilling fluid losses
- Rig repairs and maintenance
- Logistical delays of equipment or supplies
- Downhole tool issues and repairs

These are some of the typical issues that can cause downtime while drilling wells, and the daily rate (day rate) of the rig and other services do not pause charging due to NPT (unless they are caused by the respective service); so having reliable management, coordination, rig, equipment, services and especially personnel is critical in drilling a well efficiently and reducing costs. Time is the largest cost driver when operating as they do not diminish if there is a problem. The time for well KS4 (picked to be the first well to be drilled) includes 5 days to move equipment to location. Expected time to drill each hole section is shown in Fig. 4.13. A further breakdown of the flat time is provided as it includes extensive logging and Drill Stem Test (DST) that might not be performed in the other 3 injector wells.

Copyright © SLB. All Rights Reserved. Private & Confidential. Reproduction only by permission.

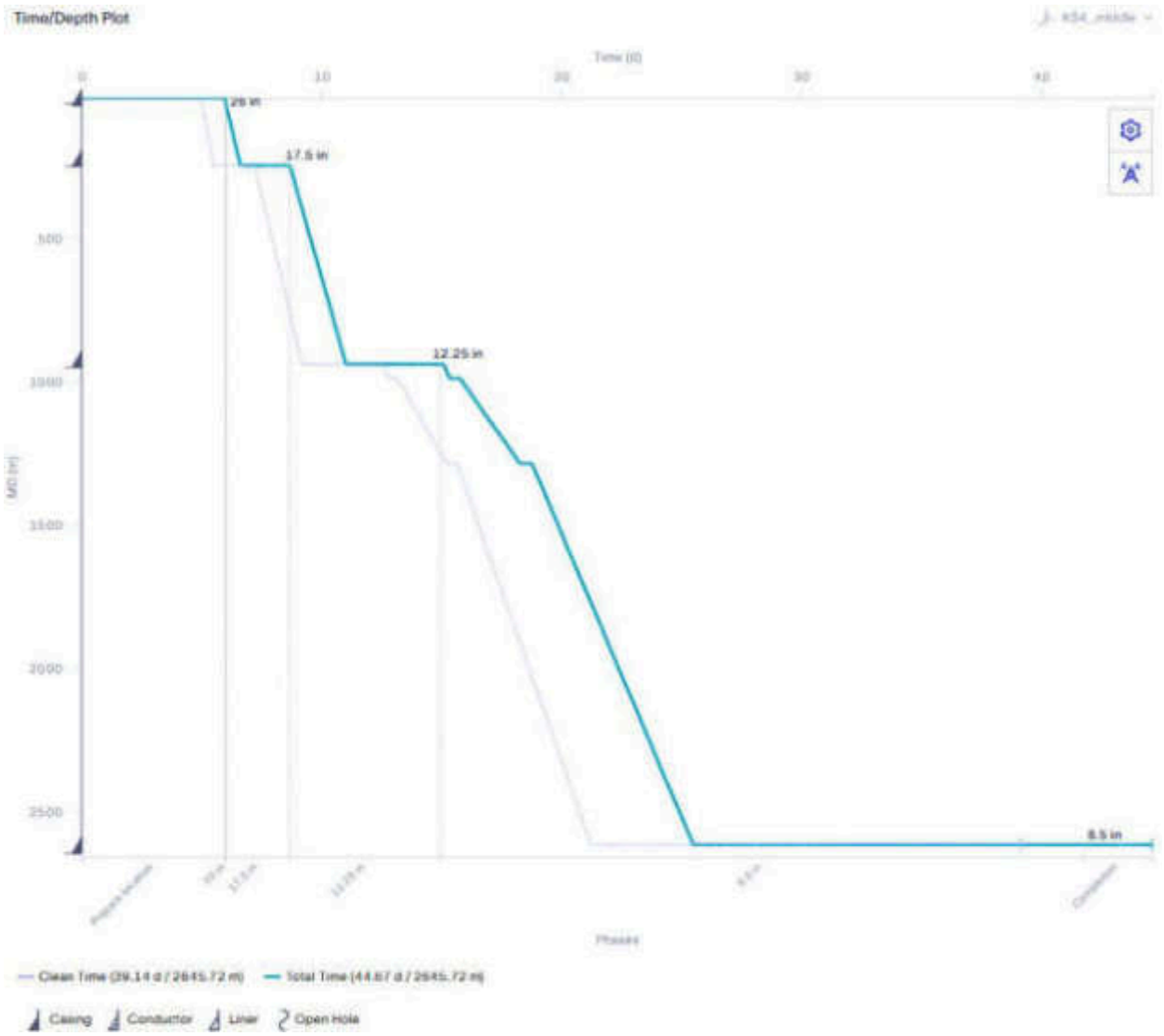


Fig. 4.13 TvD KS4 CO_2 injector

Also, the 20″ conductor may be drilled or driven by a third-party contractor before the rig moves into position (to be confirmed during detailed engineering phase). The plot shown in Table 4.13 is a time (days) versus depth (m) chart demonstrating the time to drill each hole section and arrive at total depth (TD).

Copyright © SLB. All Rights Reserved. Private & Confidential. Reproduction only by permission.

Table 4.12 Time breakdown for all sections for well KS4

Drilling stage	Depth (m)	Drilling time (days)	Flat Time (days)				Cumulative time (days)
			Open hole logging	DST	Others (running casing, cementing, CH logging)	Section time	
Prepare location & rig mob	0	0	0	0	5.0	5.0	5.0
20" conductor	30	0	0	0	1.0	1.0	6.0
17-1/2" hole section	250	0.7	1.0	0	0.9	2.7	8.7
12-1/4" hole section	950	2.6	2.2	0	1.4	6.3	15.0
8-1/2" hole section	2646	10.9	3.1	10.0	2.7	26.8	41.8
3-1/2 " completion	1795	0	0	0	2.9	2.9	**44.7**

The order of drilling for the CO_2 injectors could be modified in the future. The main difference between the wells apart from deviation and total depth is the extensive logging to be performed in the first well KS4 (in case stratigraphic well is not possible), coring and DST that has been planned for the first well also and not required as of now for the other 3 CO_2 injectors. Along with this extensive data acquisition program there are additional wiper trips to ensure the hole condition is optimal to run and cement casings.

Recommendations for future stages of the study:

- Data acquisition from stratigraphic or first well to drill.
- Casing design and stress analysis to further study is required with dynamic simulator for transient scenarios (e.g. Olga) to verify the maximum and minimum pressure and temperature profiles that will affect the well design and the completion equipment material selection.
- Preliminary metallurgy selection that has to be confirmed with metallurgy expert once the injection fluid composition is confirmed and after compatibility lab tests are performed.
- Detailed engineering design is required:
  - Drilling BHAs and bit selection
  - Drilling and completion fluids
  - Cementing
  - Completion equipment selection
  - Wellhead and Christmas tree selection
  - Rig sizing
  - Perforations design
  - DST design
- Well integrity assessment for legacy wells to evaluate CO_2 risk of leakage.

Copyright © SLB. All Rights Reserved. Private & Confidential. Reproduction only by permission.

4.1.2 Well cost estimates

The budgetary well cost estimates of CO_2 injector well KS4 is shown in Table 4.13. Some costs were provided by SLB services and some of them are analogous from the most likely sources available to the estimators. These cost estimates should be treated as AACE Class 5, with an accuracy range of -20% to -50% on the low end and +30% to +100% on the high end.

Cost assumptions:

- A 1500 HP rig was assumed to be used to drill 4 CO_2 injectors, 1 geothermal injector well and 1 producer geothermal well.
- Rig mobilization cost will be shared.
- All services are included for all sections as applicable.
- Extensive logging and DST costs are included.
- Coring cost includes routine core analysis. Other requirement for coring as stated in section 4.1.3 Data acquisition.
- Conductor, surface and intermediate casings material are low carbon alloys.
- Production casing was tapered with a mix of low carbon steel (100 m from above packer to surface) with 25Cr (from 100 m above packer to TD).
- Tubing material was selected as 25Cr to account for typical impurities in the CO_2 stream.
- Optimization of the cost could be achieved with confirmation of the CO_2 stream (especially for tubulars).
- Extensive logging as per section 4.1.3 Data acquisition
- DST includes 10 days for testing the reservoirs.

Copyright © SLB. All Rights Reserved. Private & Confidential. Reproduction only by permission.

Table 4.13 Cost breakdown for well KS4

Service		unit	Unit price (EUR)	Total EUR
1	Rig - MOB / DEMOB	LS	€195,513	€195,513
2	Rig - 1500 HP & services (35k day rate)	LS	€1,268,199	€1,268,199
3	Bits	LS	€194,017	€194,017
4	Directional drilling (BHAs)	LS	€435,981	€435,981
5	Mud Logging	LS	€166,800	€166,800
6	Drilling fluids	LS	€508,594	€508,594
7	Solids equipment	LS	€61,510	€61,510
8	Wireline logging	LS	€690,640	€690,640
9	Conventional coring	LS	€68,499	€68,499
10	Casings and tubing	LS	€1,737,111	€1,737,111
11	Casing running services	LS	€85,470	€85,470
12	Conductor setting	LS	€51,282	€51,282
13	Cementing	LS	€420,337	€420,337
14	Casing hardware	LS	€21,368	€21,368
15	Perforating	LS	€254,487	€254,487
16	Drill Stem Test (DST)	LS	€329,060	€329,060
17	Surface well testing	LS	€573,162	€573,162
18	Completions	LS	€998,235	€998,235
19	Fishing / wellbore cleaning tools	LS	€76,362	€76,362
20	Wellhead	LS	€915,200	€915,200
21	Communications	LS	€3,797	€3,797
22	Project management team	LS	€870,079	€870,079
23	Waste management	LS	€114,000	€114,000
Total:				**€ 10,039,705**

4.1.3 Data acquisition

Data acquisition for CO_2 injector wells includes both the information gathered during drilling; and the results of testing (logging and DST), after drilling is completed. Listed below are the typical data requirements and recommendations for CO_2 injectors when data is not available for the field. Additional information is required for specialized application purposes, such as additional wireline logs for a geo-mechanical model for directional drilling (refer to 2.6 Geomechanical quicklook analysis), these were included in the first CO_2 injector well time and cost estimates. Below listed the basic logging and the extensive logging requirements per section:

Basic logging (applicable to all four CO_2 injector wells)

12-1/4" Intermediate Hole Section (Identify seal layers and characterize formations):

- Triple Combo (gamma ray, neutron, and resistivity) + Dipole Sonic + Caliper
- Multi-arm caliper: to assess borehole break-out may be useful to identify the stress orientation of the formation
- Cased hole: Cement evaluation logs (any USIT for microchanneling identification, CCL)

8-1/2" Reservoir Section (Injection Zone - full characterization of CO_2 storage formation):

- Triple Combo (gamma ray, neutron, and resistivity) + Dipole Sonic + Imaging

Copyright © SLB. All Rights Reserved. Private & Confidential. Reproduction only by permission.

- Multi-arm caliper: to assess borehole break-out may be useful to identify the stress orientation of the formation.
- Cased hole: Cement evaluation logs (any USIT for microchanneling identification, CCL).

Extensive logging applicable to first well only (KS4 as reference for deeper well)

17-1/2" Surface hole (Identify and isolate freshwater aquifers):

- Gamma ray, resistivity, inclination
- Triple Combo: Density, Neutron and Resistivity logs (for porosity + lithology)
- Dipole Sonic (for seismic well tie, geomechanics study)
- Modular Dynamic Tester (MDT) testing (water properties, salinity, pressure)
- CH: Cement evaluation logs (CBL, USIT, CCL)

12-1/4" Intermediate Hole Section (Identify seal layers and characterize formations):

- Borehole imaging (FMI/UBI)
- MDT - pressure, fluids
- Micro-fracturing tests for stress & caprock integrity
- Conventional coring across caprock (requirements in next slide)
- Sidewall coring (backup in case conventional logging is not successful)

8-1/2" Reservoir Section (Injection Zone - full characterization of CO_2 storage formation):

- NMR → pore size & permeability
- Spectroscopy → mineralogy & clay content
- Advanced borehole imaging → heterogeneity, fractures, breakouts, vugs
- MDT/RFT → downhole pressure & fluid sampling, in-situ stress
  - Formation pressure measurements → Determination of pressure gradients across reservoir and seal intervals
  - Downhole fluid samples → Comprehensive characterization of formation water, including PVT properties, salinity, and ionic composition
  - Micro-fracturing → constrain fracture gradient in injection zones and cap rocks Conventional coring across reservoir top
- Conventional coring across top, middle and bottom of reservoir (requirements in next slide)
- Sidewall coring (backup in case conventional logging is not successful)
- Drill Stem Test (DST) in cased hole after perforations, for pressure transient analysis (skin factor, reservoir permeability, reservoir boundaries and connectivity)

Coring requirements:

Copyright © SLB. All Rights Reserved. Private & Confidential. Reproduction only by permission.

Coring may be useful for characterizing formation properties and defining stratigraphy, especially in the first well.

Additional requirements for cores analysis:

- Routine core analysis
- Special core analysis (SCAL):
  - Capillary pressure (Pc) measurements under CO_2–brine reservoir conditions
  - Threshold Entry Pressure (Pt) – direct measurement
  - Relative permeability of CO_2 and water
  - Interfacial Tension (IFT) and Wettability Measurement.
- CO_2 exposure testing to assess:
  - Rock strength changes
  - Mineral alteration
- Geomechanical core testing
  - Elastic properties (Young's modulus and Poisson's ratio)
  - Strength parameters (unconfined compressive strength, tensile strength and friction angle)

Copyright © SLB. All Rights Reserved. Private & Confidential. Reproduction only by permission.

5 Geothermal Energy Generation System

5.1 Design of geothermal boreholes

This section summarizes the conceptual well design, directional profiles, casing stress analysis, mud and cement system basics, and drilling time and cost estimates for the Rasovac geothermal development. The well construction plan consists of two wells—Rasovac Injector and Rasovac Producer—drilled from a common pad and targeting the Moslavackha Gora formation. Both wells are designed as directional J-type profiles to access the reservoir beneath a protected forest area while maintaining surface infrastructure outside the reserve boundary.

Field Location and Well Coordinates

The wells are located near Kapelna village, municipality of Viljevo, Osijek-Baranja County, Croatia. Wellheads are positioned approximately 100 m from the forest reserve to ensure safe pad construction and environmental compliance. Table 5.1 lists the wellhead and target coordinates and Fig. 5.1 shows a broad Google Maps view of the same.

Table 5.1 Wellhead and Target Coordinates

Well	Latitude	Longitude
Rasovac Injector Wellhead	45°41'13.1978"N	18°02'36.3826"E
Rasovac Injector Target	45°41'04.4590"N	18°02'08.0678"E
Rasovac Producer Wellhead	45°41'13.1791"N	18°02'37.7686"E
Rasovac Producer Target	45°40'55.7330"N	18°01'33.4609"E

Copyright © SLB. All Rights Reserved. Private & Confidential. Reproduction only by permission.



Fig. 5.1 Location of Wellhead and Targets

5.1.1 Conceptual well design and drilling time estimation

Subsurface Pressures

Pore pressure and fracture pressure inputs were adopted from the KS4 well plan, considered the most representative estimate for both wells. Table 5.2 and Table 5.3 list the expected pore and fracture pressures, respectively, and Fig. 5.2 shows the pore pressure and fracture pressure plot.

Table 5.2 Pore Pressure

TVD-RKB (m)	Pressure (psi)	EMW (sg)
1940	2910	1.06
2455	3808	1.09
2480	3086	0.88
2969	3795	0.90
3005	3841	0.90

Copyright © SLB. All Rights Reserved. Private & Confidential. Reproduction only by permission.

Table 5.3 Fracture Pressure

TVD-RKB (m)	Pressure (psi)	EMW (sg)
500	886	1.25
1000	1994	1.40
1226	2700	1.61
2000	4977	1.75
2400	6299	1.85
2969	8248	1.95
3005	8348	1.95



Fig. 5.2 Pore and Fracture pressure plot

Directional Well Profiles and Anti-Collision Assessment

Both wells follow J-shaped directional trajectories with similar azimuths. Due to the 6 m wellhead spacing, anti-collision evaluation was performed using SLB Anti-Collision Standard S002 v5.1/5.2 (least-distance methodology). Fig. 5.3 shows the Spider Plot and Fig. 5.4 shows the Ladder Plot for the Rasovac Injector and Producer wells.

Copyright © SLB. All Rights Reserved. Private & Confidential. Reproduction only by permission.

Key findings:

- Rasovac Producer KOP: 700 m
- Rasovac Injector KOP: 1380 m
- The higher KOP for the Producer well provides sufficient lateral displacement to maintain separation throughout the wellbore.
- Spider and ladder plots confirm green-zone separation for the Injector well and no collision risk.

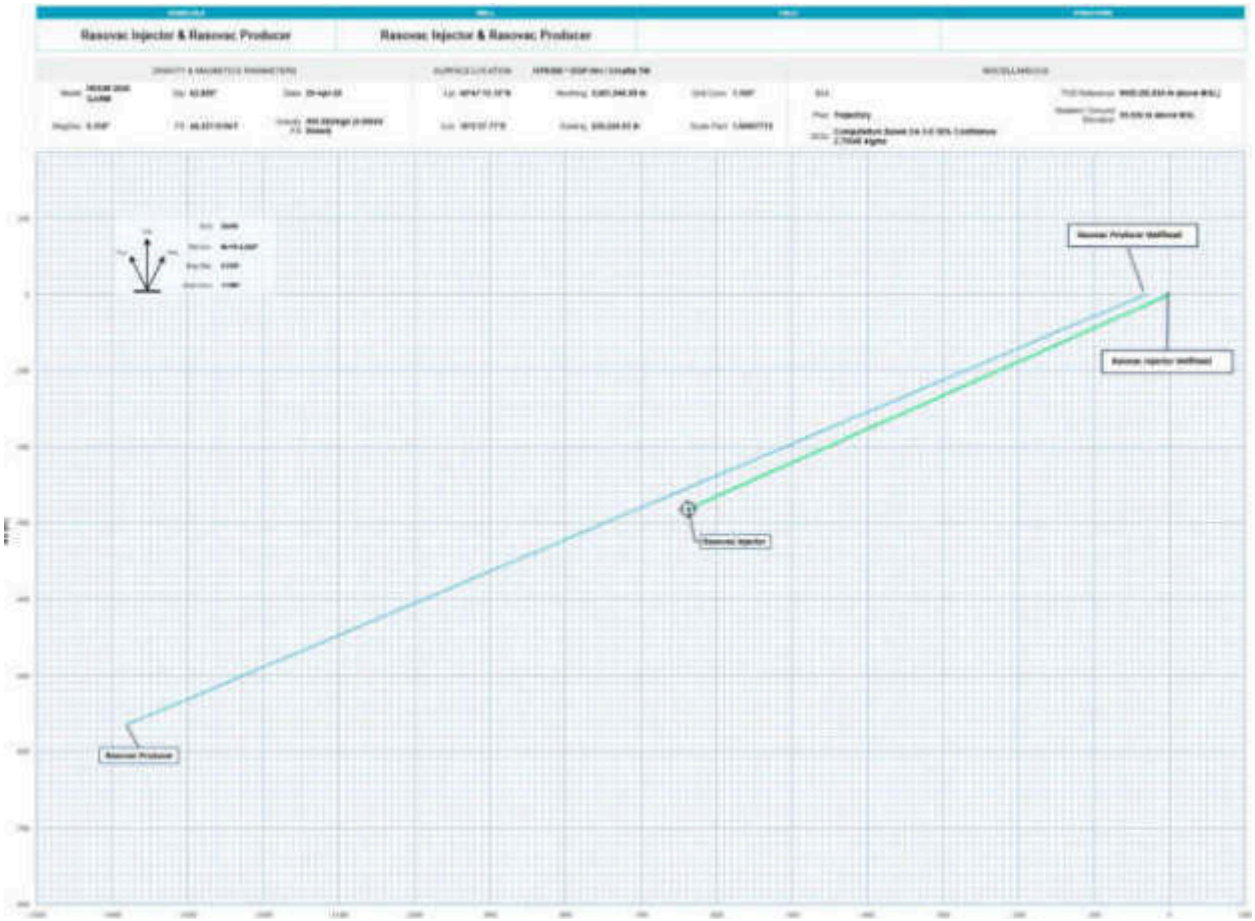


Fig. 5.3 Spider Plot of Rasovac Injector and Producer wells

Copyright © SLB. All Rights Reserved. Private & Confidential. Reproduction only by permission.

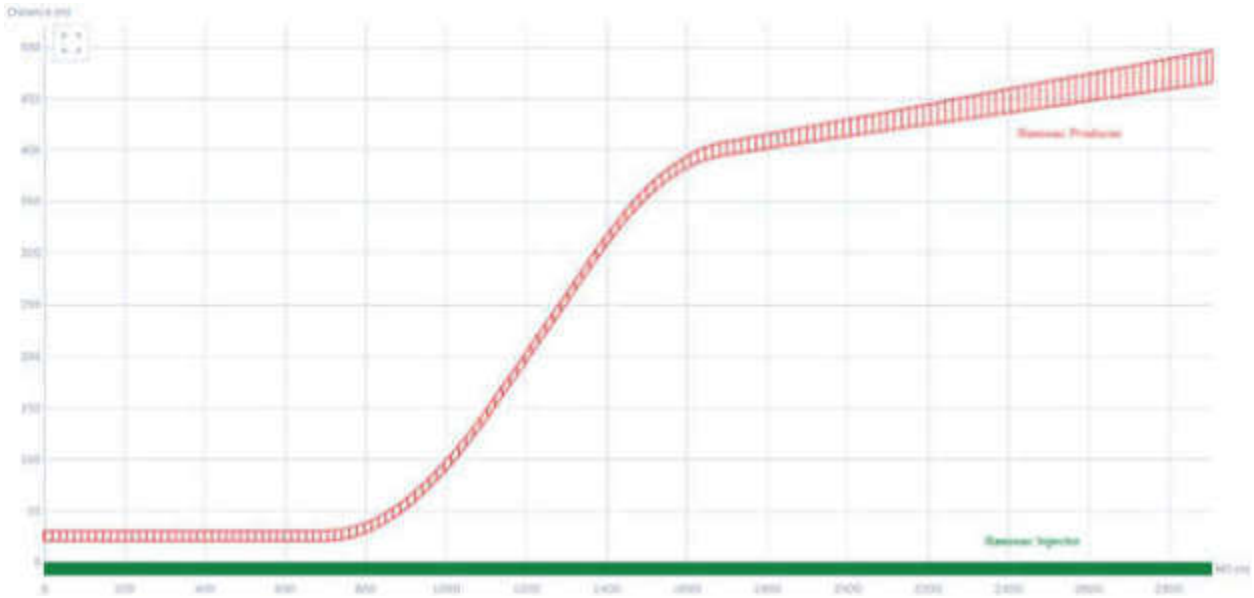


Fig. 5.4 Ladder Plot of Rasovac Injector and Producer wells

Casing Design Basis

The casing program was engineered to meet all structural, thermal, and operational load requirements for geothermal service. The design complies with:

- API 5CT – Casing and Tubing
- API TR 5C3 – Performance Properties
- ISO 11960 – Steel Pipes for Casing/Tubing
- ISO 13679 / API RP 5C5 – Connection Evaluation

Casing Program Summary:

- Conductor – driven or drilled (TBD)
- 26" section→ 20" 106.5 lb/ft K55, API Buttress connection
- 17.5" section → 13.375" 68 lb/ft L80-1, API Buttress connection
- 12.25" section → 9.625" 47 lb/ft L80-1, API Buttress connection (liner)
- 8.5" section → 7" 26 lb/ft K55 API Buttress connection (pre-slotted liner)

Rationale:

- 13-3/8" casing and 9-5/8" liner combination provides a large production and injection flow area and enough room for installing the 10" high flow rate electric submersible pump (ESP).
- 9-5/8" liner setting depth corresponds to the anticipated top of reservoir and injection zones
- L80-1 casing grade selected for strength and moderate corrosion resistance under geothermal flow conditions.
- API Buttress connection chosen for robust thermal performance at the estimated flow

Copyright © SLB. All Rights Reserved. Private & Confidential. Reproduction only by permission.

temperature range and cost efficiency.

- 7" pre-slotted liner maximizes reservoir inflow capacity.

5.1.1.1 Rasovac Injector Well

Trajectory

The Injector well is drilled vertically to 1380 m, placing the kickoff point 130 m below the 13-3/8 " shoe. A 3°/30 m build rate is used to reach 30.4° inclination at 246° azimuth, then held to target. The target specifications are listed in Table 5.4 and Table 5.5. The well plot is shown in Fig. 5.5.

Table 5.4 Rasovac Injector Well Target Coordinates

	Latitude	Longitude	TVD-GL (m)
Rasovac Injector Target	45°41'04.4590"N	18°02'08.0678"E	2726.68

Table 5.5 Rasovac Injector Well Trajectory Surveys

Comments	Survey MD (m)	Inc (°)	Azi (°)	TVD GL (m)	VS (m)	Latitude (° ' ")	Longitude (° ' ")	Easting (m)	Northing (m)	Closure (m)	DLS (°/30m)
Tie in	0.00	0.00	246	0.00	0.00	45° 41'13.17907 "N	18° 2'37.76861 "E	620249.93	5061949.09	0.00	
KOP	1380	0.00	246	1380	0.00	45° 41'13.17907 "N	18° 2'37.76861 "E	620249.93	5061949.09	0.00	0.00
EOC (curve-hold)	1689	30	246	1674	79.93	45° 41'12.17889 "N	18° 2'34.36148 "E	620176.81	5061916.79	79.93	3.00
Rasovac Injector	2908	30	246	2726	696.81	45° 41'4.45902 "N	18° 2'8.06784"E	619612.48	5061667.54	696.81	0.00

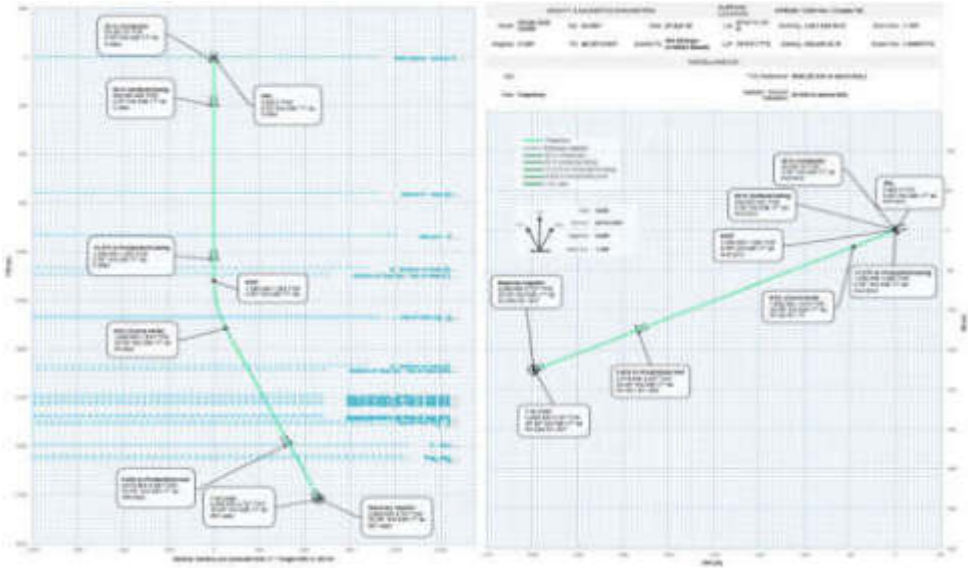


Fig. 5.5 Rasovac Injector Well Plot

Copyright © SLB. All Rights Reserved. Private & Confidential. Reproduction only by permission.

Formation Prognosis

The well penetrates the Moslavackha Gora formation for the reservoir, comprising dolomites, dolomitic limestones, breccias, and carbonate-rich sediments. The target reservoir intervals include the Z, Rs5, and Pn formations, as listed in Table 5.6.

Well Construction and Casing Design Results

Well construction will consist of the aforementioned configuration as explained in the previous section (5.1.1 Conceptual well design and drilling time estimation). The casing profile consists of 3 casing strings (Conductor, Surface and Production), all cemented to surface, and set in the vertical part of the well; followed by a Production liner (cemented with liner hanger) and pre-slotted liner (not cemented) in the inclined part to finish the well. Table 5.7, and Fig. 5.6 shows the elements of well construction plan.

Table 5.8 shows the summary of casing stress calculations. "C" denotes the loads are in compression. Values also reflect derating of the casing strength based on anticipated temperature.

Drilling Fluid Plan Summary

The objectives of the proposed drilling fluid types are to:

- Maintain wellbore stability.
- Control formation pressures.
- Minimize formation damage in reservoir interval.
- Provide adequate hole cleaning in directional sections.
- Ensure compatibility with cement systems.

Proposed drilling fluid system summaries by section are listed as follows. Estimated downhole volumes are shown in Table 5.9.

- 26" section: Freshwater + $CaCl_2$
- 17.5" section: KCl + amine shale inhibitor
- 12.25" section: KCl + amine inhibitor + high-temperature polymers
- 8.5" section: Reservoir drill-in fluid (KCl brine)

Fig. 5.7 shows the drilling fluid weight window demonstrating the anticipated mud weight for the injector well, in conjunction with the Pore and Fracture Pressure, are obtained from the KS4 well pressure data. Expected mud weights are in the range of 1.07-1.20 sg.

Cementing Plan Summary

Cement systems were proposed based on temperature, lithology, and long-term zonal isolation requirements. Class G is the typical base cement for geothermal wells. It was selected because of

Copyright © SLB. All Rights Reserved. Private & Confidential. Reproduction only by permission.

Table 5.6 Rasovac Injector Well Formation Tops

Critical Point	MD (m)	Inc (°)	Azi (°)	TVD (m)
Well Datum - Above D'	0	0	246.17	0
Tie in	0	0	246.17	0
30 in Conductor	30	0	246.17	30
20 in Surface Casing	300	0	246.17	300
Above D' - Alfa (D')	838.15	0	246.17	838.15
Alfa (D') - B	1,100.29	0	246.17	1,100.29
13.375 in Production Casing	1,250.00	0	246.17	1,250.00
B - Bottom of Seal (B)	1,300.77	0	246.17	1,300.77
Bottom of Seal (B) - Top of Seal (C)	1,341.89	0	246.17	1,341.89
KOP	1,380.00	0	246.17	1,380.00
Top of Seal (C) - C	1,601.96	21.85	246.17	1,596.62
C - D	1,615.64	23.19	246.17	1,609.26
EOC (Curve-Hold)	1,688.66	30.38	246.17	1,674.40
D - Bottom of Seal (D)	1,952.60	30.38	246.17	1,902.10
Bottom of Seal (D) - Top of Seal (D4)	1,982.59	30.38	246.17	1,927.97
Top of Seal (D4) - Bottom of Seal (D4)	2,162.81	30.38	246.17	2,083.44
Bottom of Seal (D4) - Top of Seal (D3)	2,184.11	30.38	246.17	2,101.82
Top of Seal (D3) - Bottom of Seal (D3)	2,210.99	30.38	246.17	2,125.01
Bottom of Seal (D3) - Top of Seal (D2)	2,222.78	30.38	246.17	2,135.18
Top of Seal (D2) - Bottom of Seal (D2)	2,311.69	30.38	246.17	2,211.88
Bottom of Seal (D2) - Top of Seal (D1)	2,319.65	30.38	246.17	2,218.75
Top of Seal (D1) - E	2,350.02	30.38	246.17	2,244.95
E - Z'	2,373.60	30.38	246.17	2,265.29
9.625 in Production Liner	2,515.00	30.38	246.17	2,387.28
Z' - Rs5	2,515.84	30.38	246.17	2,388.00
Rs5 - Rs7	2,600.46	30.38	246.17	2,461.00
Pn - Tg	2,620.17	30.38	246.17	2,478.00
7 in Slotted Liner	2,908.43	30.38	246.17	2,726.68

Copyright © SLB. All Rights Reserved. Private & Confidential. Reproduction only by permission.

Table 5.7 Rasovac Injector Well Geometry

Section (in)	Type	Tubular	OD (in)	ID (in)	Drift ID (in)	Start MD (m)	End MD (m)	TOC (m)	Grade	Connection
36	Conductor	30" Casing 157.53 lbm/ft X56 MIJ	30	29	28.812	0	30	0	X56	MIJ
26	Surface Casing	20" Casing 106.5 lbm/ft K55 BTC	20	19	18.812	0	300	0	K55	BTC
17.5	Production Casing	13.375" Casing 68 lbm/ft L80 BTC	13.375	12.415	12.259	0	1250	0	L80	BTC
12.25	Production Liner	9.625" Casing 47 lbm/ft L80 BTC	9.625	8.681	8.525	1150	2515	1150	L80	BTC
8.5	Slotted Liner	7" Casing 26 lbm/ft K55 BTC	7	6.276	6.151	2415	2908.43	n/a	K55	BTC

Copyright © SLB. All Rights Reserved. Private & Confidential. Reproduction only by permission.

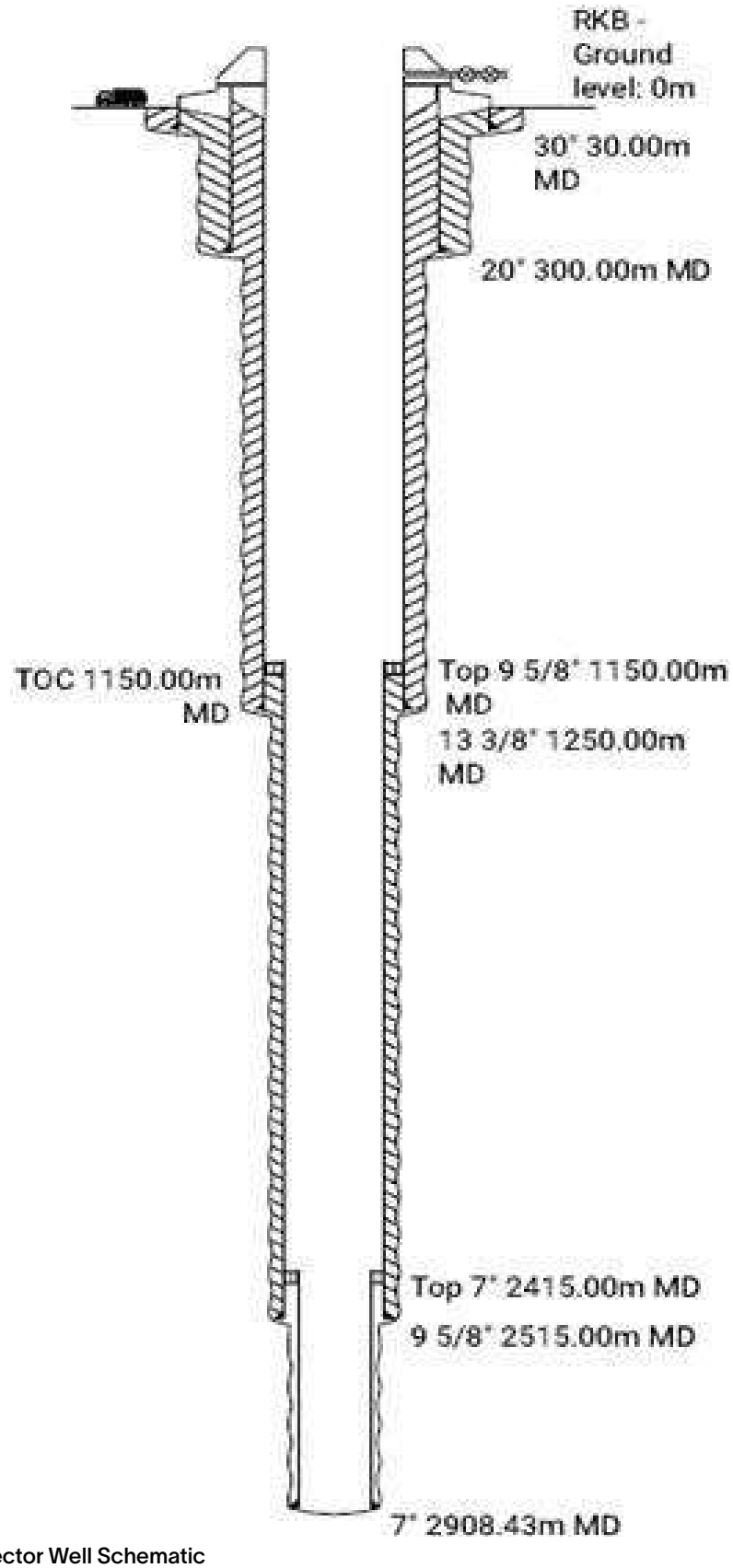


Fig. 5.6 Rasovac Injector Well Schematic

Copyright © SLB. All Rights Reserved. Private & Confidential. Reproduction only by permission.

Table 5.8 Rasovac Injector Well Casing Design Results

Section (Type)	String	Burst	Collapse	Tension	Compression	Von Mises	Buckling (deg/30m)
36" (Conductor)	30" Casing 157.53 lbm/ft X56 MIJ		9.056		131.142	76.044	0.003
26" (Surface Casing)	20" Casing 106.5 lbm/ft K55 BTC	1.569	1.587	C 6.447	C 3.031	1.696	0.01
17.5" (Production Casing)	13.375" Casing 68 lbm/ft L80 BTC	C 2.902	1.169	C 5.327	C 2.682	2.658	0
12.25 " (Production Liner)	9.625" Casing 47 lbm/ft L80 BTC	3.777	1.259	4.182	C 2.204	1.942	2.953
8.5" (Slotted Liner)	7" Casing 26 lbm/ft K55 BTC	n/a	n/a	27.667	3.827	8.479	0

Table 5.9 Rasovac Injector Well Downhole Drilling Fluid Volume Estimations by Section

Hole size in	26 in	17.5 in	12.25 in	8.5 in
Downhole Volume (bbl)	662	1272	1219	983

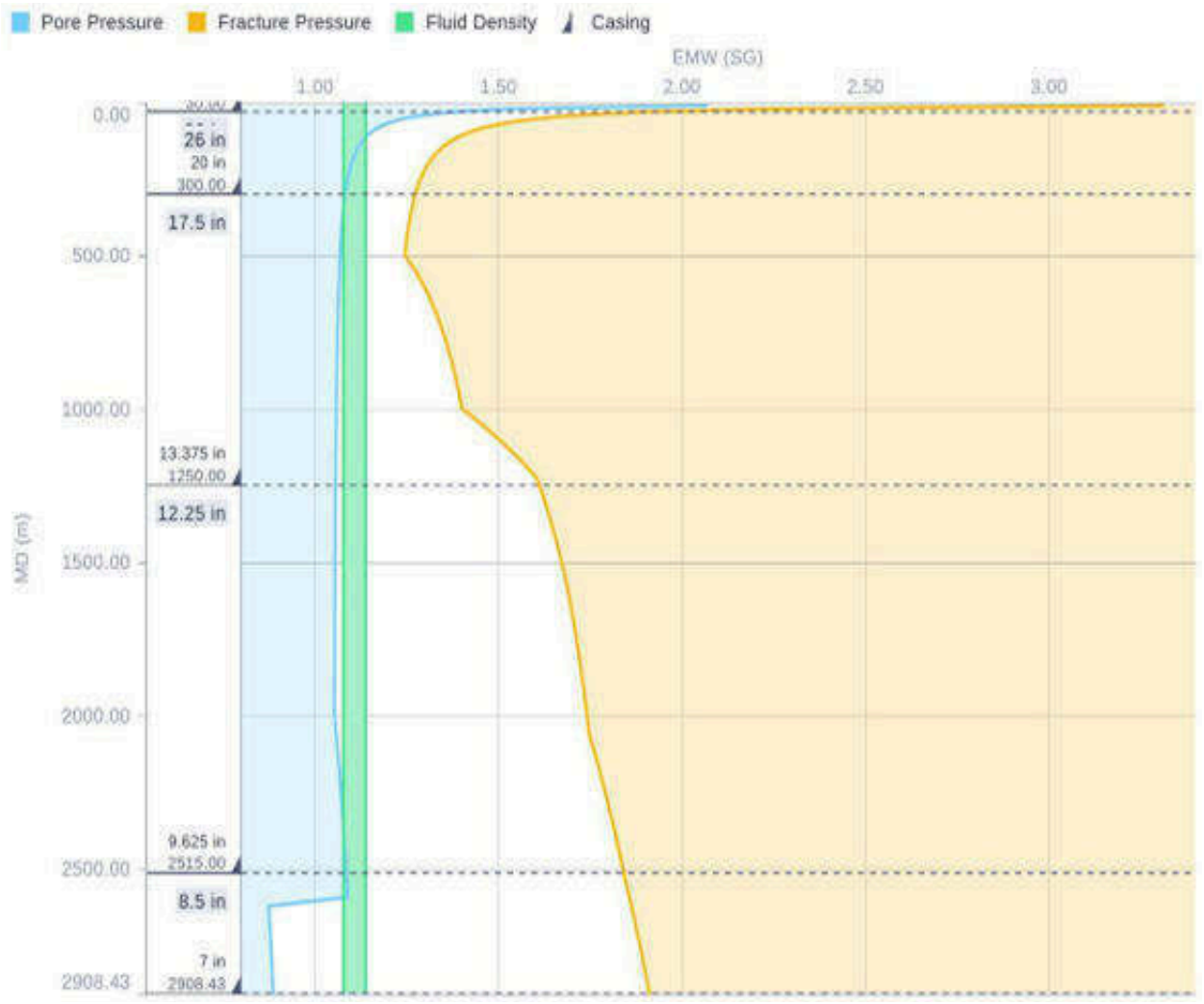


Fig. 5.7 Drilling Fluid Weight Window with pore and fracture pressure

Copyright © SLB. All Rights Reserved. Private & Confidential. Reproduction only by permission.

its predictable performance and compatibility with high-temperature silica strength retrogression systems. Proposed cementing plan summary is listed as follows and estimated volumes are shown in Table 5.10.

- 20″ surface casing: Class G Portland Cement
- 13.375" casing and 9.625″ liner: Silica-stabilized high temperature cement (i.e., Class G + 30-40% silica flour).
- CO_2 resistant or ultra high-temperature cement will not to be required as the maximum anticipated hole temperature is 150° C and severe CO_2 or H_2S corrosion is not expected.

Table 5.10 Rasovac Injector Well Cement Volume Estimations by Section

Hole/Casing size (in)	26/20 (in)	17.5/13.375 (in)	12.25/9-5/8 (in)	8.5/7 (in)
Total Volume with 50% Excess (bbl)	420	840	376	n/a

Drilling Time Estimation

The Rasovac Injector well is anticipated to be drilled in approximately 50 days. This time includes 20% Non-Productive Time (NPT). The clean time will be approximately 40 days; it will take 40 days to drill the well if no unforeseen issues arise. Number of bit runs and anticipated Rate of Penetration (ROP) per section are listed in Table 5.11.

Table 5.11 Rasovac Injector Well Bit Run and ROP estimations by Section

Hole Size (in)	Number of Bit Runs	Anticipated ROP (m/hr)
26	1	6
17.5	2	8
12.25	3	6
8.5	2	4

ROP expectations are fairly conservative due to lack of recent bit records from adjacent wells. There are other issues (that are not drilling speed related) that can delay the drilling process, such as:

- Drilling fluid losses
- Rig repair and maintenance
- Logistical delays of equipment or supplies
- Downhole tool issues and repairs

These are some of the typical issues that can cause downtime while drilling geothermal wells, and the daily rate (dayrate) of the rig and other services do not pause charging due to NPT (unless they are caused by the respective service); so having reliable management, coordination, rig, equipment, services and especially personnel is critical in drilling a well efficiently and reducing costs. Time is the largest cost driver when operating as they do not diminish if there is a problem.

Copyright © SLB. All Rights Reserved. Private & Confidential. Reproduction only by permission.

Table 5.12 shows the expected time to drill each hole section. The time includes 6 days to move equipment on location and 3 days to move the equipment off. Also, the 30″ conductor may be drilled by a third-party contractor before the rig moves into position but currently uncertain on how this will be done. The plot shown in Fig. 5.8 is a time (days) versus depth chart demonstrating the time to drill each hole section and arrive at total depth (TD) using the points in Table 5.12.

Table 5.12 Rasovac Injector Well Days vs Depth Chart (includes 20% NPT)

	Depth (m)	Drilling time (days)	Flat time (days)	Section time (days)	Cumulative time (days)
Prepare location		0	6	6	6
36" Section	30	0.05	0.39	0.44	6.44
26" Section	300	2.25	0.97	3.22	9.67
17.5" Section	1250	5.94	2.93	8.87	18.54
12.25" Section	2515	10.54	5.55	16.09	34.63
8.5" Section	2908	4.92	9.37	14.29	48.92

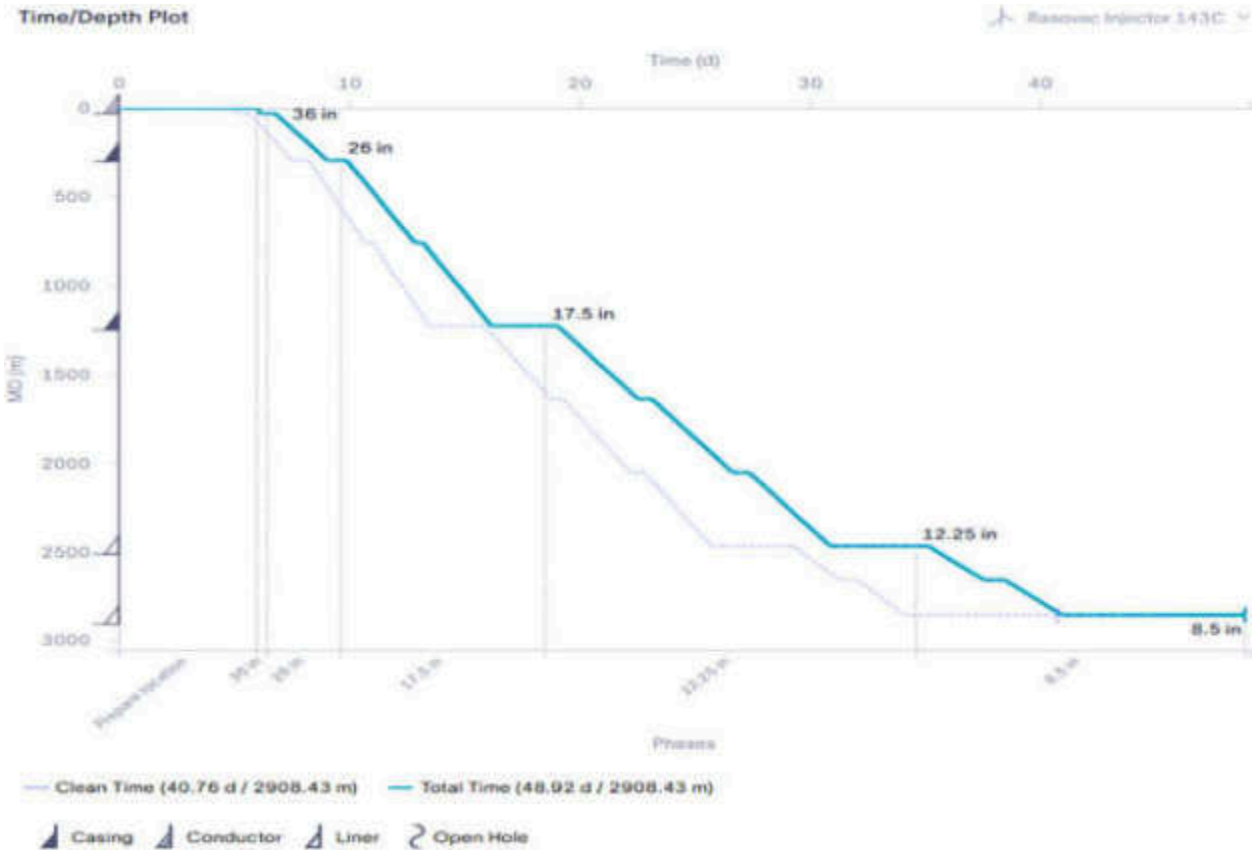


Fig. 5.8 Rasovac Injector Well Days vs. Depth Plot

5.1.1.2 Rasovac Producer Well

Trajectory

The Producer well is drilled vertically to 700 m, placing the kickoff point 400m below the 20" shoe. This high kickoff point is required in order achieve a reasonable inclination to the target. A 3°/30 m

Copyright © SLB. All Rights Reserved. Private & Confidential. Reproduction only by permission.

build rate is used to reach 34.5° inclination at 247° azimuth. It is important to reach the 34.5° inclination before the 13.375″ casing shoe setting point is reached to acquire a good cement job on the shoe. The inclination is then held to target. The target specifications are listed in Table 5.13 and Table 5.14. The well plot is shown in Fig. 5.9.

Table 5.13 Rasovac Producer Well Target Coordinates

	Latitude	Longitude	TVD-GL (m)
Rasovac Producer Target	45°40'55.7330"N	18°01'33.4609"E	3004.78

Table 5.14 Rasovac Producer Well Trajectory Surveys

Comments	Survey MD (m)	Inc (°)	Azi (°)	TVD GL (m)	VS (m)	Latitude (° ' ")	Longitude (° ' ")	Easting (m)	Northing (m)	Closure (m)	DLS (°/30m)
Tie in	0.00	0.00	247	0.00	0.00	45° 41'13.19780 "N	18° 2'36.38256 "E	620219.93	5061949.09	0.00	
KOP	700	0.00	247	700	0.00	45° 41'13.19780 "N	18° 2'36.38256 "E	620219.93	5061949.09	0.00	0.00
EOC (Curve-Hold)	1051	34.5	247	1030	102	45° 41'11.97712 "N	18° 2'31.98341 "E	620125.47	5061909.57	102	3.00
Rasovac Producer	3450	34.7	247	3005	1464	45° 40'55.73302 "N	18° 1'33.46092 "E	618868.82	5061383.85	1464	0.00

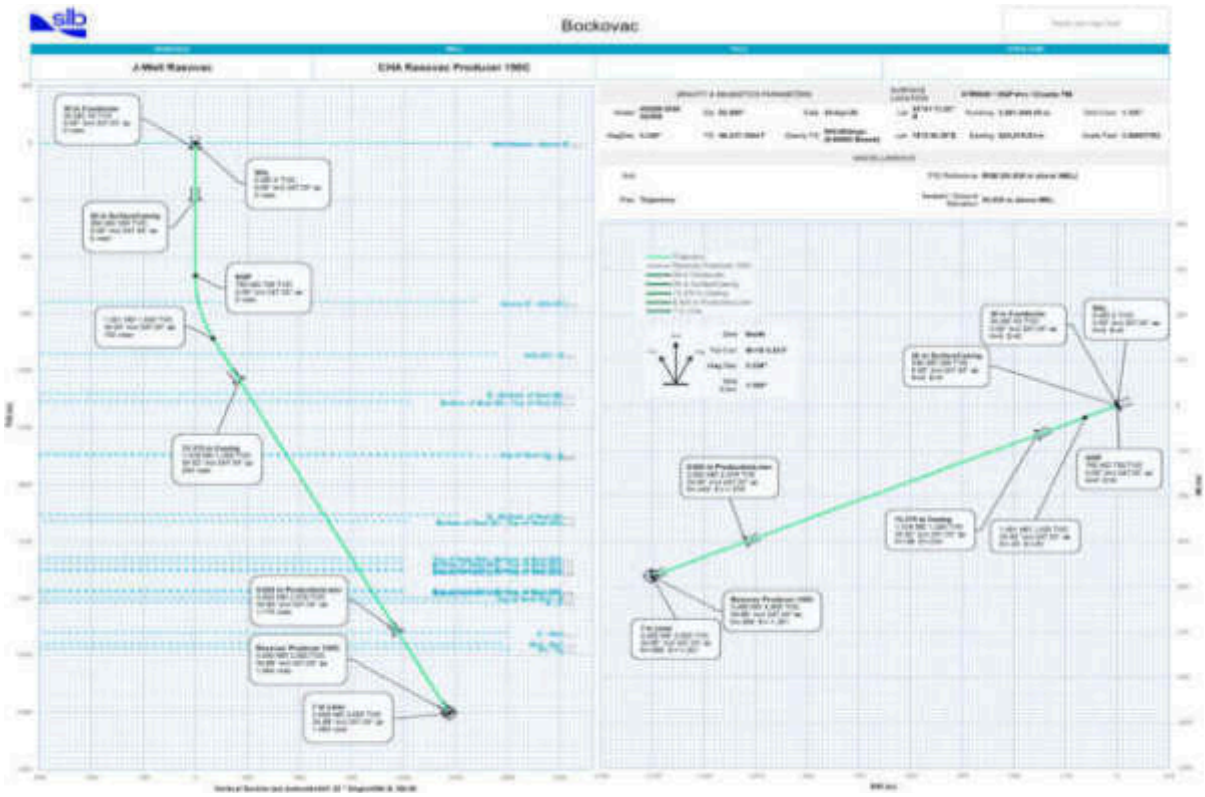


Fig. 5.9 Rasovac Producer Well Plot

Copyright © SLB. All Rights Reserved. Private & Confidential. Reproduction only by permission.

Formation Prognosis

The well penetrate the Moslavackha Gora formation for the reservoir, comprising dolomites, dolomitic limestones, breccias, and carbonate-rich sediments. The target reservoir intervals include the Z, Rs5, and Pn formations, as listed in Table 5.15.

Well Construction and Casing Design Results

Well construction will consist of the aforementioned configuration as explained in the previous section (5.1.1 Conceptual well design and drilling time estimation). The casing profile consists of 3 casing strings (Conductor, Surface and Production), all cemented to surface, and set in the vertical part of the well; followed by a Production liner (cemented with liner hanger) and pre-slotted liner (not cemented) in the inclined part to finish the well. Table 5.16 and Fig. 5.10 shows the elements of well construction plan.

Table 5.17 shows the summary of casing stress calculations. "C" denotes the loads are in compression. Values also reflect derating of the casing strength based on anticipated temperature.

Drilling Fluid Plan Summary

The objectives of the proposed drilling fluid types are to:

- Maintain wellbore stability.
- Control formation pressures.
- Minimize formation damage in reservoir interval.
- Provide adequate hole cleaning in directional sections.
- Ensure compatibility with cement systems.

Proposed drilling fluid system summaries by section are listed as follows. Estimated downhole volumes are shown in Table 5.9.

- 26" section: Freshwater + $CaCl_2$
- 17.5" section: KCl + amine shale inhibitor
- 12.25" section: KCl + amine inhibitor + high-temperature polymers
- 8.5" section: Reservoir drill-in fluid (KCl brine)

Fig. 5.11 shows the drilling fluid weight window demonstrating the anticipated mud weight for the injector well, in conjunction with the Pore and Fracture Pressure, are obtained from the KS4 well pressure data. Expected mud weights are in the range of 1.07-1.20 sg.

Cementing Plan Summary

Copyright © SLB. All Rights Reserved. Private & Confidential. Reproduction only by permission.

Table 5.15 Rasovac Producer Well Formation Tops

Critical Point	MD (m)	Inc (°)	Azi (°)	TVD (m)
Well Datum - Above D'	0	0	247.3	0
Tie in	0	0	247.3	0
30 in Conductor	30	0	247.3	30
20 in Surface Casing	300	0	247.3	300
KOP	700	0	247.3	700
Above D' - Alfa (D')	840.75	13.85	247.3	839.38
EOC (Curve-Hold)	1,050.52	34.5	247.3	1,029.72
Alfa (D') - B	1,148.75	34.51	247.3	1,110.67
13.375 in Casing	1,318.00	34.52	247.3	1,250.13
B - Bottom of Seal (B)	1,402.95	34.53	247.3	1,320.12
Bottom of Seal (B) - Top of Seal (C)	1,453.73	34.53	247.3	1,361.95
Top of Seal (C) - C	1,789.27	34.56	247.3	1,638.34
C - D	1,805.23	34.56	247.3	1,651.48
D - Bottom of Seal (D)	2,180.57	34.59	247.3	1,960.54
Bottom of Seal (D) - Top of Seal (D4)	2,221.27	34.59	247.3	1,994.05
Top of Seal (D4) - Bottom of Seal (D4)	2,455.84	34.61	247.3	2,187.13
Bottom of Seal (D4) - Top of Seal (D3)	2,486.67	34.61	247.3	2,212.51
Top of Seal (D3) - Bottom of Seal (D3)	2,524.02	34.61	247.3	2,243.25
Bottom of Seal (D3) - Top of Seal (D2)	2,539.76	34.61	247.3	2,256.20
Top of Seal (D2) - Bottom of Seal (D2)	2,662.37	34.62	247.3	2,357.10
Bottom of Seal (D2) - Top of Seal (D1)	2,671.21	34.62	247.3	2,364.38
Top of Seal (D1) - E	2,711.39	34.63	247.3	2,397.44
E - Z'	2,739.53	34.63	247.3	2,420.60
9.625 in Production Liner	2,932.00	34.64	247.3	2,578.95
Z' - Rs5	2,932.05	34.64	247.3	2,579.00
Rs5 - Rs7	3,002.56	34.65	247.3	2,637.00
Pn - Tg	3,037.81	34.65	247.3	2,666.00
7 in Liner	3,449.72	34.68	247.3	3,004.78

Copyright © SLB. All Rights Reserved. Private & Confidential. Reproduction only by permission.

Table 5.16 Rasovac Producer Well Geometry

Section (in)	Type	Tubular	OD (in)	ID (in)	Drift ID (in)	Start MD (m)	End MD (m)	TOC (m)	Grade	Connection
36	Conductor	30" Casing 157.53 lbm/ft B MIJ	30	29	28.812	0	30	0	B	MIJ
26	Surface Casing	20" Casing 106.5 lbm/ft K55 BTC	20	19	18.812	0	300	0	K55	BTC
17.5	Casing	13.375" Casing 68 lbm/ft L80 BTC	13.375	12.415	12.259	0	1318	0	L80	BTC
12.25	Production Liner	9.625" Casing 47 lbm/ft L80 BTC Updated	9.625	8.681	8.525	1218	2932	1218	L80	BTC
8.5	Slotted Liner	7" Casing 26 lbm/ft K55 BTC	7	6.276	6.151	2832	3449.72	n/a	K55	BTC

Copyright © SLB. All Rights Reserved. Private & Confidential. Reproduction only by permission.

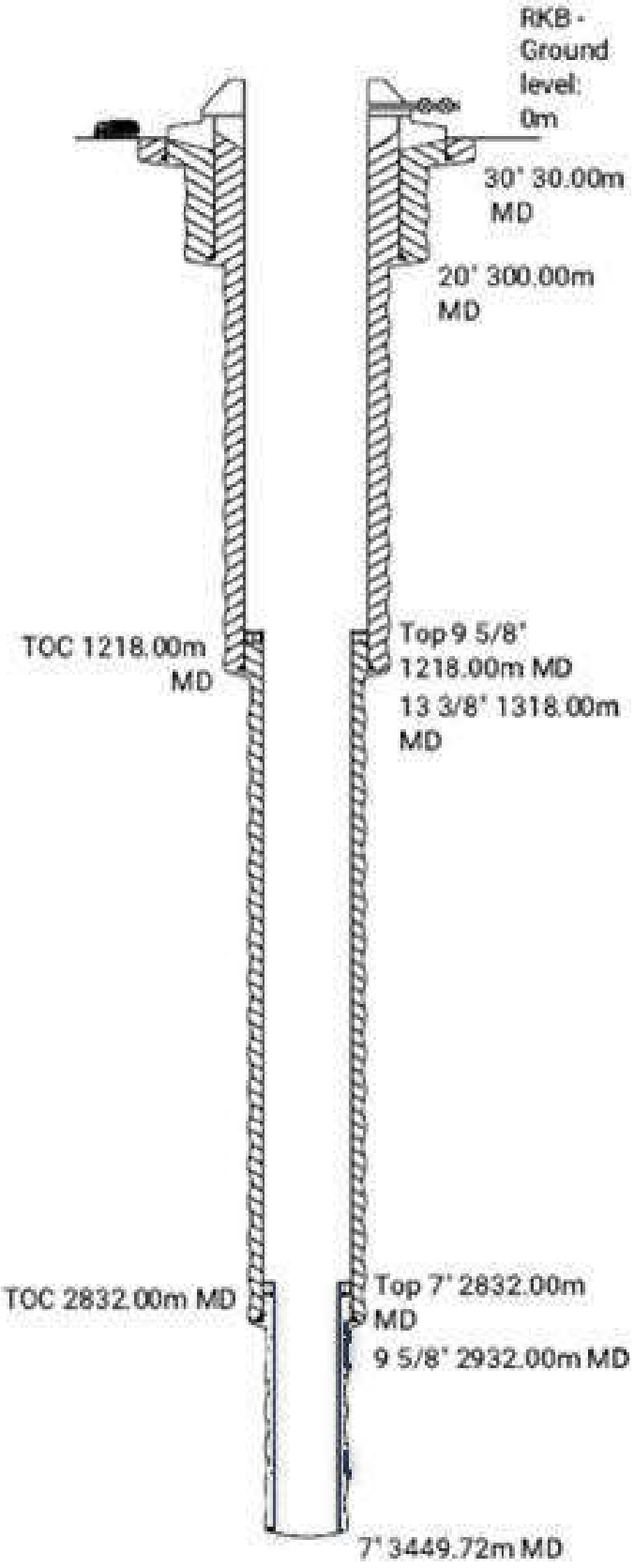


Fig. 5.10 Rasovac Producer Well Schematic

Copyright © SLB. All Rights Reserved. Private & Confidential. Reproduction only by permission.

Table 5.17 Rasovac Producer Well Casing Design Results

Section (Type)	String	Burst	Collapse	Tension	Compression	Von Mises	Buckling (deg/30m)
36" (Conductor)	30" Casing 157.53 lbm/ft B MIJ		9.056		81.964	47.527	0.003
26" (Surface Casing)	20" Casing 106.5 lbm/ft K55 BTC	1.569	1.587	C 6.447	C 2.998	1.696	0.01
17.5" (Casing)	13.375" Casing 68 lbm/ft L80 BTC	C 2.902	1.363	C 5.006	C 2.241	2.436	2.953
12.25" (Production Liner)	9.625" Casing 47 lbm/ft L80 BTC Updated	2.632	1.163	5.786	C 2.057	1.791	0.002
8.5" (Slotted Liner)	7" Casing 26 lbm/ft K55 BTC	n/a	n/a	25.88	3.515	6.371	0.002

Table 5.18 Rasovac Producer Well Downhole Drilling Fluid Volume Estimations by Section

Hole size in	26 in	17.5 in	12.25 in	8.5 in
Downhole Volume (bbl)	662	1339	1419	1129

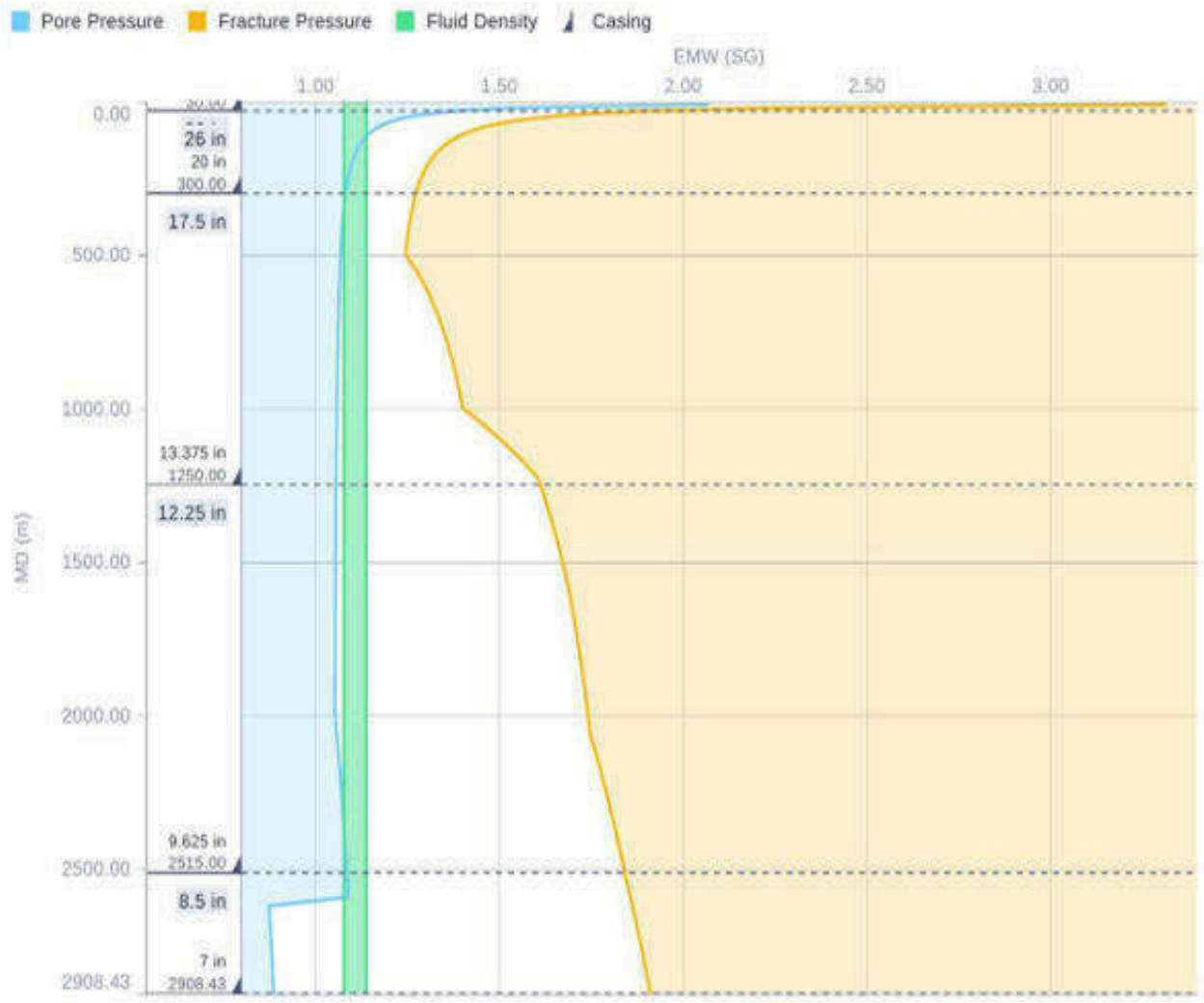


Fig. 5.11 Drilling Fluid Weight Window with pore and fracture pressure

Copyright © SLB. All Rights Reserved. Private & Confidential. Reproduction only by permission.

Cement systems were proposed based on temperature, lithology, and long-term zonal isolation requirements. Class G is the typical base cement for geothermal wells. It was selected because of its predictable performance and compatibility with high-temperature silica strength retrogression systems. Proposed cementing plan summary is listed as follows and estimated volumes are shown in Table 5.19.

- 20″ surface casing: Class G Portland Cement
- 13.375" casing and 9.625″ liner: Silica-stabilized high temperature cement (i.e., Class G + 30-40% silica flour).
- CO_2 resistant or ultra high-temperature cement will not to be required as the maximum anticipated hole temperature is 150° C and severe CO_2 or H_2S corrosion is not expected.

Table 5.19 Rasovac Producer Well Cement Volume Estimations by Section

Hole/Casing size (in)	26/20 (in)	17.5/13.375 (in)	12.25/9-5/8 (in)	8.5/7 (in)
Total Volume with 50% Excess (bbl)	420	840	376	n/a

Drilling Time Estimation

The Rasovac Producer well is anticipated to be drilled in approximately 60 days. This time includes 20% Non-Productive Time (NPT). The clean time will be approximately 50 days; it will take 50 days to drill the well if no unforeseen issues arise. Number of bit runs and anticipated Rate of Penetration (ROP) per section are listed in Table 5.20.

Table 5.20 Rasovac Producer Well Bit Run and ROP estimations by Section

Hole Size (in)	Number of Bit Runs	Anticipated ROP (m/hr)
26	1	6
17.5	2	8
12.25	4	6
8.5	3	4

ROP expectations are fairly conservative due to lack of recent bit records from adjacent wells. There are other issues (that are not drilling speed related) that can delay the drilling process, such as:

- Drilling fluid losses
- Rig repair and maintenance
- Logistical delays of equipment or supplies
- Downhole tool issues and repairs

These are some of the typical issues that can cause downtime while drilling geothermal wells, and the daily rate (dayrate) of the rig and other services do not pause charging due to NPT (unless they are caused by the respective service); so having reliable management, coordination, rig, equipment, services and especially personnel is critical in drilling a well efficiently and reducing

Copyright © SLB. All Rights Reserved. Private & Confidential. Reproduction only by permission.

costs. Time is the largest cost driver when operating as they do not diminish if there is a problem. Table 5.21 shows the expected time to drill each hole section. The time includes 6 days to move equipment on location and 3 days to move the equipment off. Also, the 30″ conductor may be drilled by a third-party contractor before the rig moves into position but currently uncertain on how this will be done. The plot shown in Fig. 5.12 is a time (days) versus depth chart demonstrating the time to drill each hole section and arrive at total depth (TD) using the points in Table 5.21.

Table 5.21 Rasovac Producer Well Days vs Depth Chart (includes 20% NPT)

	Depth (m)	Drilling time (days)	Flat time (days)	Section time (days)	Cumulative time (days)
Prepare location		0	6.00	6.00	6.00
36" Section	30	0.05	0.39	0.44	6.44
26" Section	300	2.25	1.33	3.58	10.02
17.5" Section	1318	6.36	2.85	9.21	19.23
12.25" Section	2932	13.45	6.76	20.21	39.44
8.5" Section	3449.72	6.47	11.38	17.84	57.29

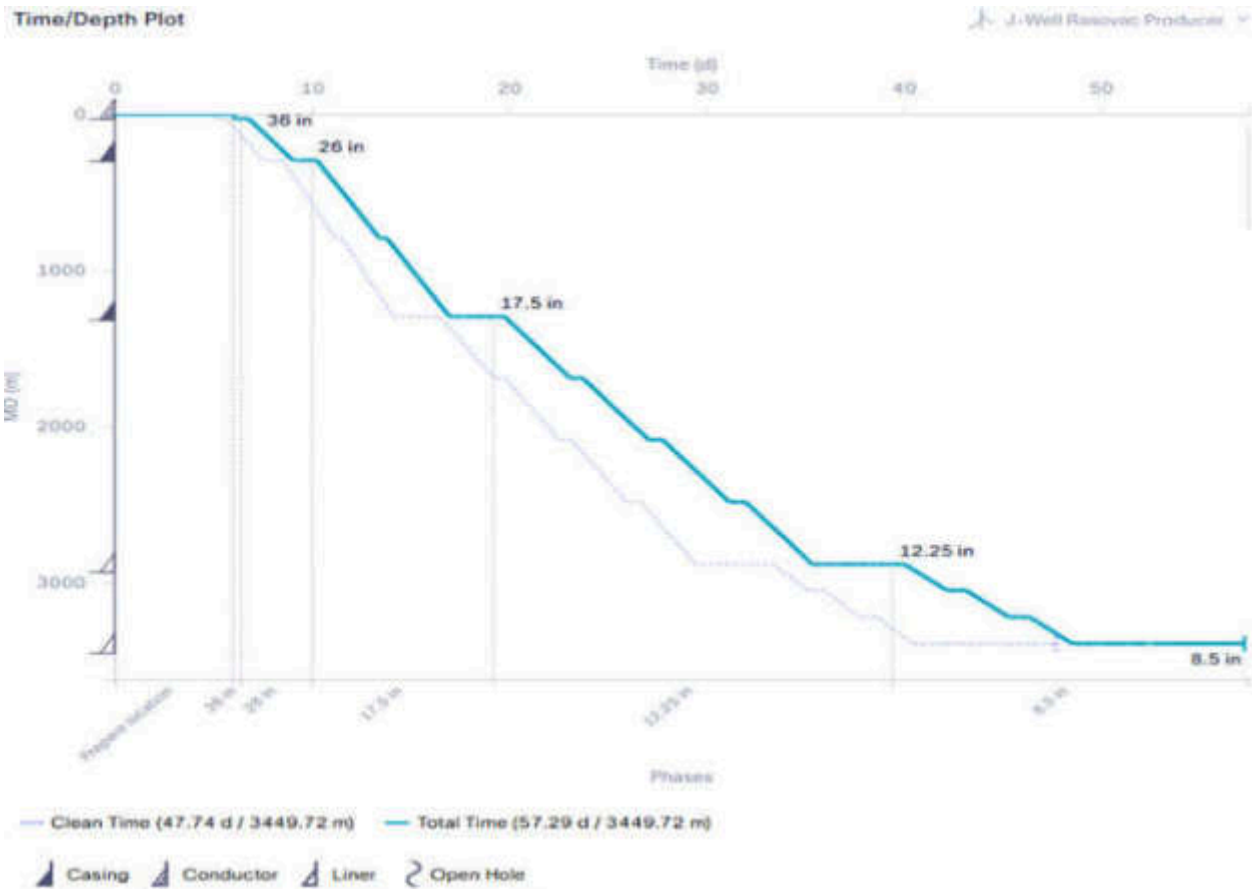


Fig. 5.12 Rasovac Producer Well Days vs Depth Chart (includes 20% NPT)

5.1.1.3 Recommendations for future stages of the study

- **Casing Wear Analysis:** Model the expected casing wear during the drilling of the 1250m to

Copyright © SLB. All Rights Reserved. Private & Confidential. Reproduction only by permission.

2515m and 2515m to 3000m sections, while accounting for the inclination and internal dogleg severity.

- **Geomechanical Characterization:** Perform a detailed geomechanical study for the deviated sections to determine optimal mud weights and prevent wellbore collapse or breakouts in variable lithologies
- **Annular Pressure Buildup (APB) Mitigation:** Evaluate appropriate mitigation strategies for potential of trapped annular fluid expansion.
- **Detailed Engineering and Operational Readiness**
  - **Directional Drilling Dynamics:** Optimize the Bottom Hole Assembly (BHA) design and bit selection specifically for the hard, abrasive rock typical of geothermal reservoirs at the well inclination.
  - **Torque and Drag Modeling:** Run comprehensive friction modeling for running casing and liners to target depth to ensure the rig sizing and top drive specifications are adequate.
  - **Drilling and Completion Fluids**: Optimize fluid designs for the downhole environment and drilling conditions. (i.e. composition, density, rheology, flow rates, etc.)
  - **Thermal Cement Slurry Design:** Optimize specialized high-temperature cement blends (potentially incorporating silica flour to prevent strength retrogression at 150° C)
  - **Completion and Testing Design:** Finalize the detailed engineering for completion equipment selection, wellhead pressure and temperature ratings, perforation design for the slotted liner, and flow test parameters

5.1.2 Well cost estimates

The budgetary well cost estimates of the Rasovac Producer and Injector wells are shown in Table 5.22. A 1500 HP rig was assumed to be used to drill four (4) CO_2 injection wells, one (1) geothermal injection well, and one (1) geothermal production well. Rig mobilization costs are shared between 6 wells.

Part of the costs were provided by SLB service suppliers and others are analogous from the most likely sources available to the estimators. The cost estimate should be treated as an AACE Int. Class 5 estimate, with an accuracy range of -20% to -50% on the low end and +30% to +100% at the high end of the range.

Copyright © SLB. All Rights Reserved. Private & Confidential. Reproduction only by permission.

Table 5.22 Rasovac Injector and Producer Wells Budgetary Cost Estimates

	Cost breakdown		Injector Well	Producer Well
	Service	Unit	Total (EUR)	Total (EUR)
1	Rig - Dayrate and Services (35,000 EUR/day)	LS	1,715,000	2,030,000
2	Rig - Mobilization	LS	915,000	915,000
3	Bits	LS	400,000	312,000
4	Directional drilling (BHA w/MWD)	LS	552,548	671,779
5	Mud Logging	LS	124,800	153,600
6	Drilling fluid	LS	685,932	816,586
7	Solids equipment	LS	9,682	11,545
8	Wireline logging	LS	607,399	718,272
9	Casing (including slotted liner)	LS	491,652	591,490
10	Casing running services	LS	117,000	117,000
11	Casing hardware (for 3 sections)	LS	29,250	29,250
12	Cementing	LS	478,368	502,286
13	Fishing / Wellbore cleaning tools	LS	77,454	92,360
14	Wellhead	LS	545,000	560,000
15	Project management team	LS	735,000	870,000
16	Waste management	LS	292,500	292,500
17	Artificial lift (ESP)	LS	-	510,250
18	Mud coolers	LS	33,321	41,484
19	Conventional coring	LS	-	-
20	Tests	LS	250,000	450,000
21	Civil works	LS	TBD	TBD
			Injector Total Cost **8,059,906**	Producer Total Cost **9,685,403**
			Pair Total Cost (EUR)	**17,745,309**

5.1.3 Data acquisition

Data acquisition from geothermal wells includes both the information gathered during drilling; and the results of testing, after drilling is completed. Listed below are the typical data requirements from geothermal wells. If additional information is required for specialized application purposes, such as additional wireline logs for a geo-mechanical model for directional drilling, those should be separately evaluated.

Wireline Logging:

Pressure and temperature surveys (real-time or memory-mode with slickline) are the most common logging methods during various phases of drilling and testing of geothermal wells. Pressure and temperature surveys may be performed when the well is not flowing (static) or during flow (dynamic). Spinner surveys are commonly run in tandem with pressure and temperature surveys. These survey tools are typically rated for high temperatures (up to 350°C or more).

The standard triple-combo of geophysical logs (gamma ray, neutron, and resistivity) and image logs can be helpful in stratigraphic correlation and fracture characterization. Caliper logs to assess borehole break-out may be useful to identify the stress orientation of the formation. Temperature rating limitations of these tools should be carefully evaluated in planning their use.

Copyright © SLB. All Rights Reserved. Private & Confidential. Reproduction only by permission.

Coring:

Coring may be useful for characterizing formation properties and defining stratigraphy, especially in the first few wells in a geothermal field. Slim-diameter core holes (sometimes called "temperature core holes") may be drilled to relatively shallow depths in the exploration phase of a project, to help in defining areas with high temperature gradients and to assist with the targeting of deeper, larger-diameter wells.

Because permeability in conventional hydrothermal projects is primarily controlled by fractures, coring provides relatively little quantitative information about the productivity of particular zones (in comparison to coring in oil-and-gas wells, where matrix permeability plays a more important role). In some instances, however, a core may capture a fractured interval intact, as illustrated in Fig. 5.13. Moreover, having cored samples of the formation may be useful in the planning of well stimulation by acidizing or hydraulic fracturing.



Fig. 5.13 Fractured interval from slim-diameter core well.

Copyright © SLB. All Rights Reserved. Private & Confidential. Reproduction only by permission.

Mudlogging:

Mudlogging serves a dual purpose in geothermal drilling: (1) Formation characterization and (2) drilling data acquisition for improving drilling performance in the current and future wells. The mudlogging crew should be knowledgeable of geothermal formation characteristics, and they should ensure that drilling fluid temperatures in and out of the well, as well as the drilling losses and their depths, are carefully monitored and documented.Hydrogen sulfide (H_2S) and carbon monoxide (CO) in drilling fluids are commonly monitored as part of the mudlogging service. If hydrocarbons are detected during drilling, well testing equipment may need to be adapted to allow for the possibility of flaring.

Well Tests:

Geothermal well testing spans three types of activities:

Rig testing – conducted while the drilling rig is still in position over the well. This typically includes an attempt to flow the well at the time of completion, with discharge through the blooie line to the sump (Fig. 5.14). The duration of the flow is typically less than 24 hours. The primary goals are to clean the well up (removing drilling mud and cuttings from the well to the greatest extent possible) and to get an initial indication of productivity. If necessary, the rig can be used to run drill pipe in the hole for purpose of lifting with air or nitrogen.

Copyright © SLB. All Rights Reserved. Private & Confidential. Reproduction only by permission.



Fig. 5.14 Rig test of geothermal well.

If flow cannot be established at the time of completion (possibly because of cooling by the drilling process), rig testing can also include an injection test using the rig pumps. A pressure-temperature (PT) survey may be run to document baseline conditions prior to injection, and a pressure-temperature-spinner (PTS) log may be run during injection to determine which zones are accepting fluid. The PTS tool may also be used to record the pressure fall-off downhole at the end

Copyright © SLB. All Rights Reserved. Private & Confidential. Reproduction only by permission.

of injection, to allow determination of an injectivity index (II). The duration of an injection test with the rig in place typically would not exceed 6 hours of active injection, followed by 12-24 hours of monitoring the pressure fall-off.

Short-term production testing – conducted after the rig has moved off the well. The duration of a short-term production test typically does not exceed 5 to 7 days, usually constrained by the capacity to store or dispose of produced water. The test may be preceded by several static PT surveys to monitor progress toward temperature recovery after drilling. If the well has a positive wellhead pressure before testing (either from natural accumulation of non-condensable gas in the wellhead or from pressuring up the well with an air compressor), sudden release of this pressure may suffice to induce boiling in the liquid column and initiate flow. If necessary, a coiled tubing unit (CTU) may be used to lift the well by injecting air or nitrogen.

Assuming flow can be established, a test lasting several days should be sufficient to collect geochemical fluid samples and to conduct a dynamic PTS survey, followed by downhole measurement of pressure build-up when the well is shut in. For a well with potentially commercial temperatures, the flow under testing conditions will typically be a two-phase mixture of water and steam, even if the long-term operation of the well will use downhole pumps to maintain single-phase liquid flow at the surface. The equipment to measure large flows of two-phase flow is specialized and is described further in the section on *Well Test Equipment* (below).

Long-term production testing – conducted after one or more additional wells have been drilled to allow disposal of produced water by injection. Long-term tests can last weeks or months, and they effectively amount to simultaneous production and injection tests for different wells throughout the field. For this reason, they are sometimes referred to as multi-well tests or interference tests. The objectives of long-term testing are typically to characterize the interaction between wells and to assess the efficacy of a particular configuration of production and injection in maintaining sustainable operations. Production wells during a long-term test use the same kind of equipment as a short-term test, but the extended test duration allows more thorough geochemical sampling and monitoring of well performance to assess field wide risks such as injection breakthrough or pressure depletion.

Because production wells can be affected by downhole scaling under two-phase flow conditions, downhole injection of scale-inhibiting chemicals by capillary tubing may be needed. Tracers may be used to quantify the connections between injectors and producers.

If the production wells require pumping to sustain output, a long-term test may entail installation of electric submersible pumps (ESPs) or line-shaft pumps (LSPs). A long-term test provides information necessary for effective plant design and for extended forecasts of field performance by reservoir simulation.

Well Test Equipment

Fig. 5.15 shows a typical set-up for the production test of a well yielding two-phase flow.

Copyright © SLB. All Rights Reserved. Private & Confidential. Reproduction only by permission.

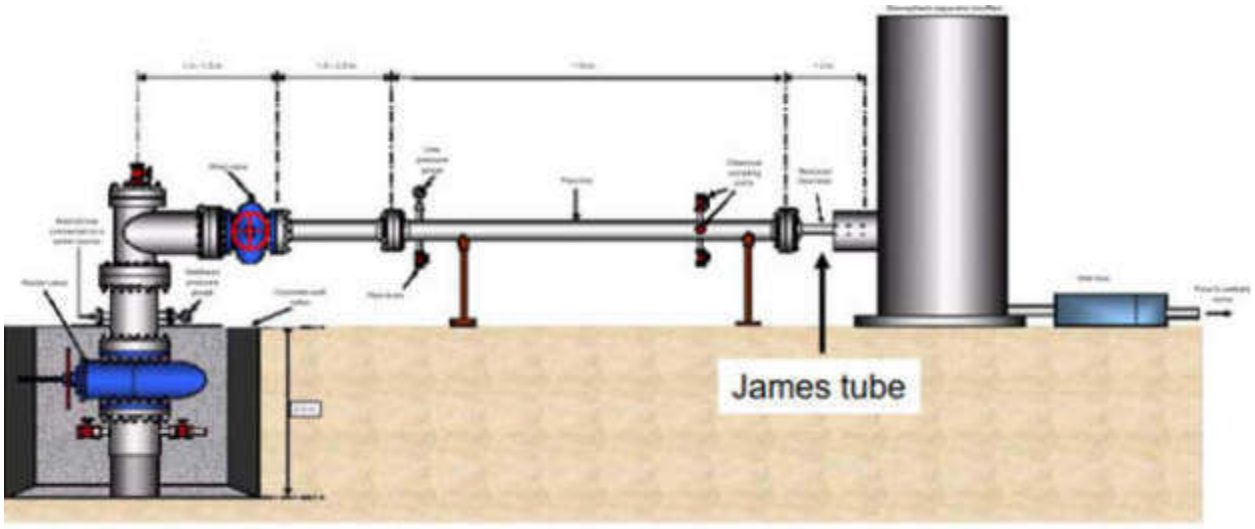


Fig. 5.15 Typical equipment set-up for a geothermal well test.

The basic elements of the equipment are:

- A flow-tee above the master valve, directing the flow to a horizontal flow line.
- A throttle valve at the upstream end of the flow line to regulate flow.
  - This may be paired with a second valve to effect a complete shut-in of the well while the master valve remains open for downhole wireline measurements.
  - The diameter of the flow line is typically in the range of 8 to 12 inches, depending on the diameter of the production casing and the anticipated flow rate.
- Gauges to measure pressure at the wellhead and on the flow line.
  - The pressure gauge on the flow line may be paired with a temperature sensor in a thermowell.
- Ports to allow collection of samples of steam and liquid phases.
  - Specialized sampling equipment and personnel are required to perform this operation.
- A length of reduced-diameter pipe (known as a "James tube") at the discharge end of the flow line.
  - James tubes typically range from 4 to 9 inches in diameter, depending on the flow rate and the diameter of the flow line.
- An atmospheric separator that vents steam from the top and discharges liquid from the bottom.
  - The James tube extends into the inlet to the separator, and it has a pressure tap at the very end (or "lip") of the pipe. The pressure tap is connected to a gauge by a capillary tube, to allow measurement of the "lip pressure."
- A weir box that measures the liquid rate based on the height of liquid passing through an opening at the downstream end of the box.
  - The lip pressure from the James tube, together with the liquid rate from the weir box, allows calculation of the flow rate and production enthalpy of the two-phase flow.

Copyright © SLB. All Rights Reserved. Private & Confidential. Reproduction only by permission.

The production enthalpy is a key parameter for plant design, since it allows calculation of a steam fraction for any specified separator pressure.

Fig. 5.16 shows a geothermal well on a long-term test using the testing equipment described above. For this test, produced water was disposed of by injection into a well a substantial distance from the flowing well. The well on the right-hand side of the photo (with a lubricator on the crown valve) was equipped with a capillary tubing charged with nitrogen to measure downhole pressure interference from the well on test.



Fig. 5.16 Geothermal production test with James tube equipment.

Fig. 5.17 shows another long-term test using similar equipment. This was a multi-well test – one of the other producing wells is visible in the distance. At the time of taking the photo, produced water from the separator was being discharged to the sump through a bypass line, to avoid filling the weir box with solids from the initial stages of flow.

Copyright © SLB. All Rights Reserved. Private & Confidential. Reproduction only by permission.



Fig. 5.17 Long-term multi-well geothermal test.

As an alternative to the James tube method of measuring two-phase flow, SLB in recent years has developed multi-phase flow meter (MPFM) technology suitable for geothermal flow measurements. MPFM devices have been shown to yield comparable results to the James tube method over certain ranges of rate and enthalpy. The MPFM technology holds special promise for applications involving continuous measurement of two-phase flow in permanent gathering systems for geothermal plants. In a well testing situation (involving atmospheric venting through a temporary line), an MPFM device could potentially replace the James tube and weir box, but an atmospheric separator may still be needed to muffle the sound and diffuse the force of two-phase discharge from the flow line.

If a well proves to be incapable of self-flow but appears to have potentially commercial temperatures and permeability (based on PT surveys and injection testing), production testing with a downhole pump may be warranted. The testing pump may be either an electric submersible pump (ESP) or a line-shaft pump (LSP), depending on equipment availability and the casing configuration of the well to be tested. For instance, an LSP would not be suitable in a deviated well. ESPs are commercially available with temperature ratings up to 225° C (e.g., SLB's REDA Thermal Pump). The installation and retrieval of either an ESP or an LSP would likely require a drilling rig, though possibly a smaller rig than was used in drilling. For a hypothetical well with a pump installed at 600 m, a static water level at 50 m, and a drawdown of 350 m under steady production (i.e., a

Copyright © SLB. All Rights Reserved. Private & Confidential. Reproduction only by permission.

head of 200 m above the pump intake), the power requirement would likely be in the range of 300 to 600 kWe. The pump would typically be operated with a variable speed drive using AC current (a frequency of 50 Hz would be most common for Europe).

The pumps for injection testing would depend on the phase of testing and well characteristics. For instance, during a rig test, rig pumps would likely be used. For later testing, centrifugal pumps would provide sufficient rates and pressures at the wellhead of the injection well. If high injection pressures are needed, a positive displacement pump may be necessary.

For long-term operations once a plant is online, the power consumption of injection pumps at the plant will depend on the total brine throughput at the plant and injectivity of the injection wells, which can vary widely. For a typical injection-pump discharge pressure of 10 bars and a total injection rate of 1,400 metric tonnes per hour (the approximate brine rate of a 10-MWe binary plant), the power consumption of the injection pumps would be about 500 kWe.

5.2 Design of electricity production from the geothermal system

5.2.1 Power generation potential

1. Heat to Power Conversion Technology

ORC systems are the most suitable and widely deployed solution for electricity generation from low- to medium-enthalpy resources [27]. Their ability to efficiently convert heat at temperatures in the range of about 90–200 °C has made them the preferred option for such applications. This positioning is supported by a large and mature installed base, especially in regions such as the western United States, where numerous commercial binary plants operate under similar resource conditions [28].

The baseline ORC configuration adopted for this preliminary assessment is a classic architecture, comprising the following standard equipment:

- One (1) shell and tube preheater
- One (1) shell and tube vaporizer
- One (1) turbo-generator group
- One (1) air-cooled condenser
- One (1) working fluid pump

Copyright © SLB. All Rights Reserved. Private & Confidential. Reproduction only by permission.

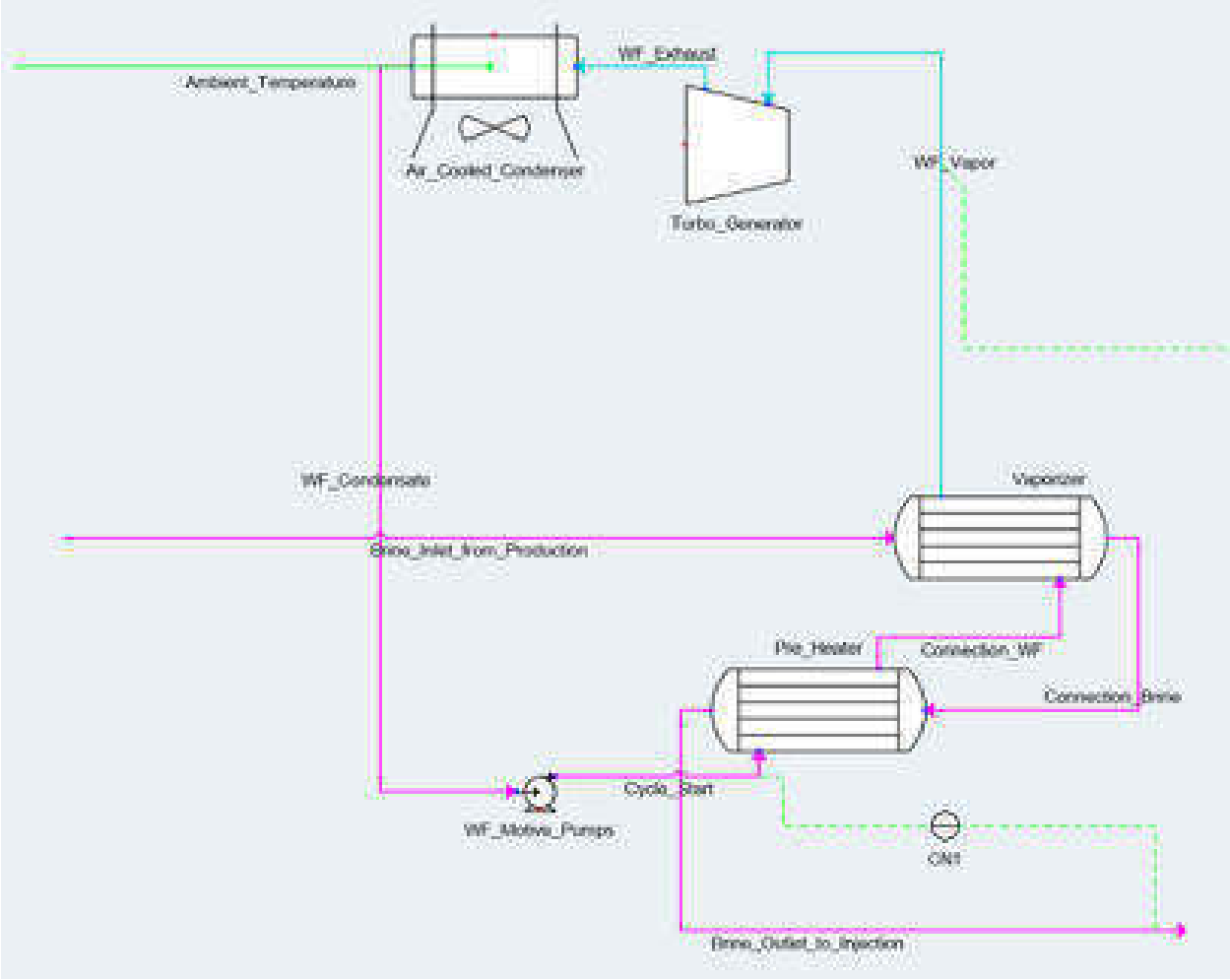


Fig. 5.18 Proposed baseline ORC configuration

The power generation assessment is based on this baseline ORC configuration. Subsequent sections will provide recommendations for thermodynamic performance optimization and identify the most suitable commercially available technologies for practical implementation.

2. Cycle Working Fluid

The ORC model has been run with isobutane as the working fluid. Isobutane presents the typical dry expansion profile of hydrocarbons, whereby the expansion process remains in the superheated region of the thermodynamic diagram and avoids condensation during turbine expansion. This property is beneficial for turbine integrity and operational reliability.

With a critical temperature of approximately 135°C, isobutane optimize the heat transfer by minimizing temperature difference in the heat exchangers and maximizing operating pressure to favor expansion.

Copyright © SLB. All Rights Reserved. Private & Confidential. Reproduction only by permission.

In addition, isobutane is a commodity hydrocarbon that is widely available in Europe and has a stable and reliable supply chain, which supports its practical deployment in commercial applications

At this preliminary stage, a comparative techno-economic optimization against other candidate hydrocarbon fluids - evaluating the trade-offs between thermodynamic cycle performance and equipment sizing - has not been conducted. This rigorous fluid screening is reserved for the detailed engineering phase.

3. Heat Source

The geothermal resource available for power generation is evaluated to have the following characteristics:

Table 5.23 Characteristics of the geothermal resource avaialble

Parameters	Conservative	Expected
Flow rate (l/s)	80	100
Temperature C	140	150

To estimate the total thermal power available for the cycle, a nominal reinjection temperature must be established. The potential for precipitation of amorphous silica in the surface equipment and injection wells typically constrains the reinjection temperature to a range of 65°C to 90°C. In the absence of a confirmed brine chemistry profile and a calculated silica saturation Index, a preliminary reinjection temperature of 75°C is assumed for this baseline assessment [29]. This value lies within the typical operational range needed to mitigate scaling risks in similar geothermal projects [30].

Rigorous laboratory analysis of the brine composition will be required during the detailed engineering phase to establish a definitive minimum allowable temperature. Operationally, the actual reinjection temperature will be subject to dynamic optimization based on real-time monitoring of scaling indicators, but the 75°C value serves as a nominal boundary condition for the current thermodynamic process modeling and subsequent equipment sizing.

4. Heat Extraction

The primary heat exchange network was designed targeting a pinch point temperature difference of 6°C. While a more aggressive (tighter) pinch point could theoretically yield higher baseline thermodynamic efficiency, it significantly increases heat exchanger CAPEX and renders the system highly sensitive to variations in operating parameters such as ambient temperature and fluid enthalpy.

Geothermal applications must account for dynamic environmental conditions and the long-term thermal decline of the reservoir. Therefore, the power cycle is designed not for absolute peak efficiency at a single static point but rather for thermodynamic resilience, ensuring stable operation over a wide range of off-design parameters throughout the lifetime of the project.

Copyright © SLB. All Rights Reserved. Private & Confidential. Reproduction only by permission.

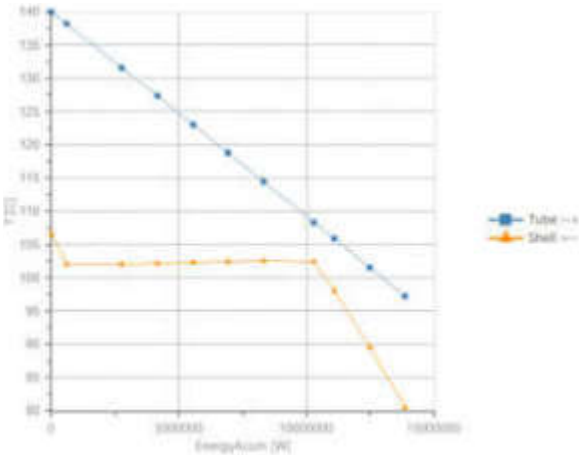


Fig. 5.19 Temperature vs. heat load diagram for heat exchange network design

5. Conversion of Heat to Power

The conversion of geothermal heat into electrical power is fundamentally governed by the thermodynamic coupling between the cycle's prime mover and its ultimate heat sink. For this reason, this chapter focuses specifically on the turbine and the air-cooled condenser (ACC). These components cannot be evaluated in isolation; the ACC dictates the condensation pressure, which directly establishes the turbine's backpressure and available expansion ratio. It is this strong dynamic interdependence — the combined performance of work extraction and heat rejection — that dictates the net conversion efficiency of the entire ORC.

While the isentropic efficiency of the turbine dictates the quality of the conversion of source heat into mechanical power, the condenser establishes the heat rejection temperature, which serves as the theoretical boundary for the overall cycle efficiency.

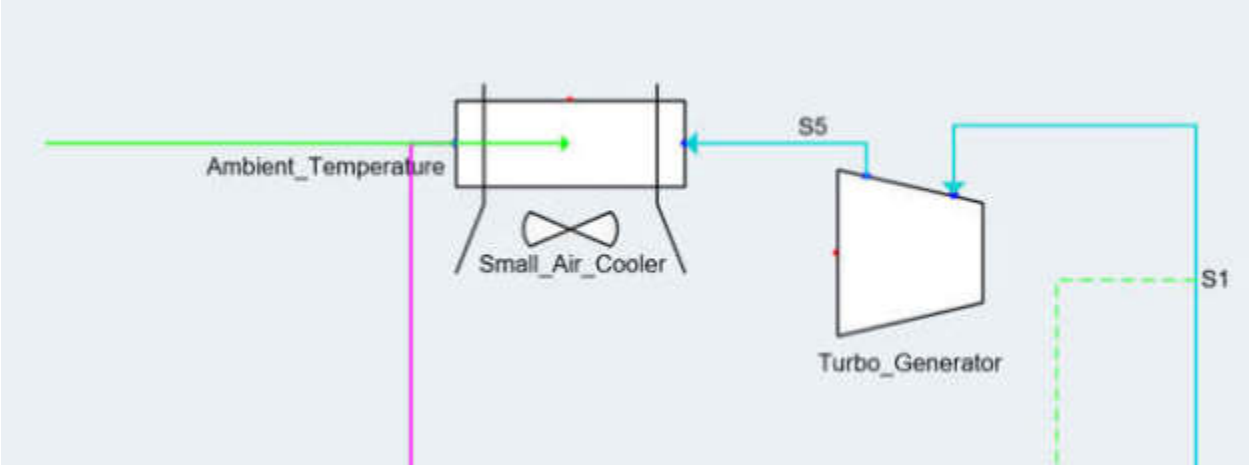


Fig. 5.20 Baseline ORC configuration: focus on turbine and air-cooled condenser (ACC)

Copyright © SLB. All Rights Reserved. Private & Confidential. Reproduction only by permission.

Turbine

The core element of an ORC is the turbine, where the enthalpy of the working fluid is converted into mechanical power. The power cycle is designed to generate vapor at optimal conditions within the turbine's design envelope across the full range of operation. ORC turbines are specifically engineered for the selected working fluid and to accommodate the wide operating envelopes typical of geothermal applications.

Hydrocarbons, commonly used as working fluids for geothermal power applications, possess thermodynamic characteristics that compete with the scaling up of the nominal size of a single turbine. It is common in the geothermal market to find single turbines sized up to 10–15 MW, with incremental capacity steps standardized by the manufacturer. Sub-5 MW turbines are less common in utility-scale deployments because economies of scale are a critical factor for project success; typically, smaller turbines require bespoke design and dedicated manufacturing, which significantly drives up capital costs and delivery times.

Axial and radial turbines are both widely used in geothermal power plants. A primary operational difference between the two architectures is rotational speed: axial turbines can often operate at RPMs that directly match the grid frequency, whereas radial turbines typically operate at much higher speeds and require a gearbox to synchronize with the grid. The selection between the two types is frequently dictated by whichever Original Equipment Manufacturer (OEM) wins the competitive bid. Turbine design is highly proprietary, serving as the core intellectual property and primary value proposition of the manufacturer, and rarely does a single OEM produce both types. For this reason, when developers evaluate applicants for an ORC supply contract, the OEM's portfolio of proven, operating reference projects is a heavily weighted metric in determining the winner of the competitive bid.

An axial turbine matching the grid frequency without gearbox has been selected for this study.

Air Cooled Condenser

Geothermal ORC are predominantly equipped with air-cooled condensers (ACC) due to environmental permitting constraints, water scarcity, and the high operational costs associated with the make-up water and chemical treatments required for evaporative wet cooling. Consequently, the baseline ORC modeled in this study utilizes an ACC for the condensation of the working fluid.

The thermodynamic performance of an ACC is fundamentally dictated by the dry-bulb temperature of the ambient air entering the tube bundles. An increase in ambient temperature drives up the condensation pressure, causing a thermodynamic shift across the entire operating envelope of the power cycle. Specifically, higher ambient temperatures induce three primary performance penalties:

- **Reduced Expansion Ratio:** Higher condensation pressures directly increase the turbine backpressure, reducing the available expansion ratio and specific work output across the turbo-expander.

Copyright © SLB. All Rights Reserved. Private & Confidential. Reproduction only by permission.

- **Reduced Thermal Extraction:** Higher condensation pressures elevate the temperature of the working fluid entering the primary heat exchangers. This compresses the available temperature differential (ΔT) against the brine, inherently limiting the total thermal power that can be extracted from the geothermal fluid.
- **Higher Parasitic Consumption**: modern ACC are equipped with fans driven by a VFD, this allows the modulation of the total air flow across the unit and the fine tuning of the thermodynamics of the condensation process. The variable speed of the fans also allows for the optimization of the parasitic consumption.

The combined effect of these high-ambient penalties can be severe: when summer temperatures are at their peak, power output can be degraded by 40% to 60% compared to a low-ambient or winter design baseline.

5. Project Weather Data

The weather station of Osijek was used as a reference for this study (see Fig. 5.21 and Fig. 5.22).

	January	February	March	April	May	June	July	August	September	October	November	December
Avg. Temperature °C (°F)	0.9 °C (33.7 °F)	2.6 °C (36.6 °F)	7.3 °C (45.1 °F)	12.9 °C (55.2 °F)	17.6 °C (63.6 °F)	21.4 °C (70.5 °F)	23.4 °C (74.2 °F)	23.3 °C (74) °F	18.1 °C (64.6 °F)	12.9 °C (55.3 °F)	7.6 °C (45.8 °F)	2.2 °C (35.9 °F)
Min. Temperature °C (°F)	-2.3 °C (27.9 °F)	-1.4 °C (29.5 °F)	2.4 °C (36.3 °F)	7.5 °C (45.4 °F)	12.2 °C (54) °F	16.1 °C (61.1 °F)	18.2 °C (64.8 °F)	18.1 °C (64.5 °F)	13.6 °C (56.5 °F)	8.8 °C (47.9 °F)	4.3 °C (39.7 °F)	-0.7 °C (30.7 °F)
Max. Temperature °C (°F)	4.5 °C (40.1 °F)	6.9 °C (44.4 °F)	12.3 °C (54.1 °F)	17.9 °C (64.3 °F)	22.4 °C (72.4 °F)	26.1 °C (79) °F	28.2 °C (82.7 °F)	28.3 °C (82.9 °F)	22.7 °C (72.9 °F)	17.6 °C (63.6 °F)	11.5 °C (52.8 °F)	5.4 °C (41.7 °F)
Precipitation / Rainfall mm (in)	46 (1)	49 (1)	52 (2)	59 (2)	72 (2)	78 (3)	66 (2)	55 (2)	63 (2)	55 (2)	57 (2)	57 (2)
Humidity(%)	81%	77%	70%	65%	65%	64%	61%	60%	68%	75%	80%	83%
Rainy days (d)	6	7	7	8	8	8	7	6	6	6	6	7
avg. Sun hours (hours)	4.5	5.5	7.8	10.0	11.1	11.9	12.1	11.2	8.9	7.1	5.4	4.2

Data: 1991 - 2021 Min. Temperature °C (°F), Max. Temperature °C (°F), Precipitation / Rainfall mm (in), Humidity, Rainy days. Data: 1999 - 2019 avg. Sun hours

Fig. 5.21 Climate table (monthly weather indicators) for Osijek, Croatia

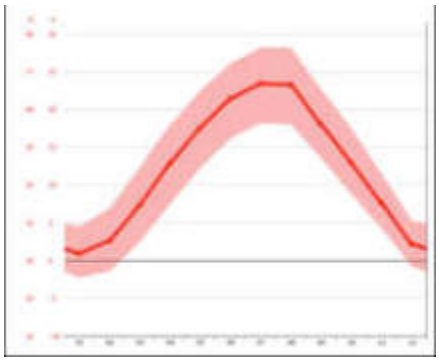


Fig. 5.22 Monthly temperature variations for Osijek, Croatia

Copyright © SLB. All Rights Reserved. Private & Confidential. Reproduction only by permission.

6. Power Generation Assessment

In utility-scale geothermal applications, the contractual performance guarantees and baseline equipment sizing for an ORC are typically anchored to three discrete ambient operating points. These points are derived from site-specific statistical exceedance data (often referencing standardized climatic datasets such as ASHRAE Standard 169) to establish the operational boundaries of the thermodynamic envelope:

- **Design Case:** Annual average ambient dry-bulb temperature
- **Cold Case:** 98% to 99% exceedance temperature
- **Hot Case:** 1% to 2% exceedance temperature

Note: The % exceedance temperature defines a threshold that the actual temperature is expected to surpass for only that specified percentage of time (e.g., a 1% exceedance design temperature will be exceeded only 1% of the observation period).

Analysis of the available ambient temperature data resulted in the following three cases:

- Design case: 12.5°C
- Cold case: 0°C
- Hot case: 26°C

The performance results reported in this section were generated by developing a steady-state process model of the baseline ORC architecture using Symmetry. The core thermodynamic cycle was optimized around a nominal ambient design temperature of 12.5°C. However, to guarantee complete working fluid condensation and maintain cycle stability during peak summer conditions, the physical heat transfer area of the ACC was sized for the hot case. To bridge this physical sizing with the nominal design point, the ACC fans are considered equipped with variable-frequency drives (VFDs), allowing for dynamic control of the condensing envelope. Once the design of the main equipment was established, the off-design models were executed and converged. The resulting thermodynamic outputs are summarized in the table below.

Copyright © SLB. All Rights Reserved. Private & Confidential. Reproduction only by permission.

Table 5.24 Summary of the thermodynamic outputs

POWER GENERATION MODULE						
	SUMMER CASE [26°C]		**DESIGN CASE [12.5°C]**		**WINTER CASE [0°C]**	
	Heat Extraction					
Heat Power from Source	19,509	kW,th	20,793	kW,th	22,314	kW,th
	Power Generation					
Turbine Gross	1,861	kW,el	2,809	kW,el	3,260	kW,el
Total Gross	**1,861**	**kW,el**	**2,809**	**kW,el**	**3,260**	**kW,el**
Parasitic List						
HP ACC	311	kW,el	225	kW,el	207	kW,el
HP Pump	211	kW,el	229	kW,el	231	kW,el
Plant Parasitic	40	kW,el	44	kW,el	45	kW,el
Total Parasitic	**563**	**kW,el**	**499**	**kW,el**	**484**	**kW,el**
Total Net	**1,298**	**kW,el**	**2,310**	**kW,el**	**2,775**	**kW,el**
EFFICIENCY MODULE						
	Gross Conversion Efficiency					
η Gross	**9.54%**		**13.51%**		**14.61%**	
	Parasitic Consumption compared to Gross					
ACC	16.71%		8.01%		6.36%	
WF Pumps	11.37%		8.16%		7.11%	
Plant Auxiliaries	2.20%		1.60%		1.40%	
Total Parasitic	**30.28%**		**17.78%**		**14.87%**	
	Net Conversion Efficiency					
η Net	**6.65%**		**11.11%**		**12.44%**	

Plant Parasitic Consumptions includes: Lube Oil System parasitic load, Seal Oil System parasitic load, Generators' Cooling System parasitic load, Auxiliary transformer losses, VFD parasitic load, ACCs, Plant Auxiliaries, Transmission Line Losses to the dead end structure, Generator Step-up Transformer losses.

7. Power Generation Forecast

The operational behavior of the geothermal ORC across its full thermodynamic envelope can be mathematically modeled by generating off-design performance curves anchored to the three design cases. By integrating these performance curves against a site-specific, 8,760-hour typical meteorological year (TMY) ambient temperature profile, an accurate hour-by-hour forecast of the annual energy production (AEP) is generated. This hourly generation profile is not merely an early design indicator; it is a critical deliverable for utility-scale development, establishing the revenue model required for project bankability and levelized cost of energy (LCOE) assessments. Based on the preliminary TMY dataset extrapolated from available local weather telemetry, the power forecast analysis for one nominal year of operation is summarized in the table below.

Copyright © SLB. All Rights Reserved. Private & Confidential. Reproduction only by permission.

Table 5.25 Summary of the power forecast analysis for one nominal year of operation

Tamb	% Annual Hours	# Annual Hours	Gross [GWh]	Net [GWh]	Net Exported [GWh]
-10 to 0	1.0%	87.6	0.29	0.24	0.20
0 to 10	40%	3504	10.74	9.03	7.19
10 to 20	30%	2628	8.21	6.93	5.55
20 to 30	29%	2540.4	7.95	6.72	5.38
TOTALS	**100%**	**8760**	**27.19**	**22.92**	**18.31**

** the Net Exported estimate includes the parasitic consumption of production and injection pumps, which is preliminarily estimated at 525 kw in total*

This dispatch analysis is critical for evaluating the integration of the power unit with the demand of the proposed CO_2 capture and sequestration (CCS) system. The CCS process requires a steady power supply, leading to a possible operational mismatch during the summer months, when the ORC may fail to fully cover the real-time CCS demand. Consequently, operating the system as an isolated microgrid (island mode) is technically unfeasible without deploying properly sized energy storage. To mitigate this constraint, the power unit is engineered strictly as a grid-tied asset. Under this commercial architecture, the grid functions as a buffer; while summer peak capacity may fall short of instantaneous demand, the ORC's surplus generation during winter months can be exported. This allows the facility to achieve a net-zero or net-negative operational carbon footprint on an annualized accounting basis, offsetting the CCS parasitic consumption while exporting the residual commercial power to the grid.

8. Changes in the parameters of geothermal energy production in the event of pressure interferences

Since the geothermal reservoir and the CO_2 storage targets are not in communication, no interference is forecasted to occur between the CO_2 injection, geothermal production and geothermal injection wells. No impact on geothermal energy production is therefore expected.

5.2.2 Analysis of energy losses through pipelines from friction and elevation changes

The proposed project location is detailed in the map Fig. 5.23.

Copyright © SLB. All Rights Reserved. Private & Confidential. Reproduction only by permission.



Fig. 5.23 Rasovac geothermal wellheads locations
Proposed surface location(producer & injector wells) of the Rasovac geothermal wellheads

Table 5.26 Coordinates of the producer / injector Rasovac geothermal wellhead

Well	Latitude	Longitude
Rasovac Injector Wellhead	45°41'13.1978"N	18°02'36.3826"E
Rasovac Producer Wellhead	45°41'13.1791"N	18°02'37.7686"E

The production and injection wells will be situated on a single well pad. While this centralized configuration theoretically allows for an optimized gathering system with reduced pipeline runs, the actual routing is constrained by surface conditions. Ideally it will be possible to site the power plant within 500 m of the well pad while remaining entirely outside the adjacent forest area, which is protected under Natura 2000 environmental regulations. A detailed land acquisition, permitting, and right-of-way (ROW) study must be executed to secure landowner leases before the physical footprint of the plant and pipeline corridor can be determined.

Preliminary hydraulic sizing criteria for the gathering network have been established assuming the facility will be successfully sited within the targeted 500-m radius. Based on standard commercial steel pipe schedules (Schedule 40, assumed for 10-bar service) and the nominal mass flow rates, the following internal fluid velocities are projected:

- **NPS 8 (Nominal 200 mm):** Inside diameter ~202.7 mm, yielding a velocity of ~2.48 m/s.
- **NPS 10 (Nominal 250 mm):** Inside diameter ~254.5 mm, yielding a velocity of ~1.57 m/s.
- **NPS 12 (Nominal 300 mm):** Inside diameter ~303.2 mm, yielding a velocity of ~1.10 m/s.

Copyright © SLB. All Rights Reserved. Private & Confidential. Reproduction only by permission.

To optimize the lifecycle techno-economics, balancing the initial capital expenditure of line-pipe steel against the operational expenditure of frictional pumping losses, the design targets a continuous liquid velocity between 1.5 m/s and 2.5 m/s. This range simultaneously limits erosion-corrosion degradation inside the piping network while keeping the diameter of the pipes from getting too big. Applying these parameters, the preliminary recommended pipe size for the main gathering lines is NPS 10.

Due to unknown status of landowner lease agreements and rights of way, the pipeline routing cannot be defined at this conceptual stage. Constraints from agricultural land use could necessitate complex routing, including property-edge corridor pathways, orthogonal routing to accommodate property lines, vertical expansion loops for thermal stress mitigation, and subterranean crossings to maintain landowner road access. Because these complexities could impact the final friction and thermal degradation metrics, incorporating arbitrary pipeline losses into the current thermodynamic model would yield inaccurate performance baseline guarantees. Therefore, they are excluded from this study at this early stage.

5.2.3 Residual heat for domestic and agricultural uses

The concept of cascading residual heat from a geothermal power cycle to lower-temperature secondary processes is often perceived as a straightforward efficiency gain; however, it is constrained by the chemistry of the geothermal brine, especially the temperature-dependent solubility of silica. As thermal energy is extracted and the brine temperature drops, silica solubility decreases exponentially until it breaches the amorphous silica saturation limit (ASSL) [31]. Beyond this threshold, the precipitation and scaling mechanism is aggressive and catastrophic.

The fundamental objective when designing the ORC power generation cycle is to maximize electrical power output. Consequently, the surface facility is engineered to extract the maximum thermal energy available, discharging and reinjecting the brine at the lowest allowable temperature that is safely above the ASSL. Because of this, there may be no "residual" or leftover heat available for secondary applications.

If agricultural heating is mandated as a primary project objective, the facility design must be changed from a dedicated power generation asset to a combined heat and power (CHP) co-generation facility. To safely provide this heat without breaching silica limits in the primary cycle, a fraction of the high-temperature brine must be diverted *before* it enters the ORC vaporizer. This represents a trade-off between reducing electrical generation and gaining a secondary use for the geothermal brine. This new design would fundamentally alter the heat and mass balance of the ORC baseline design described in this report. Additionally, because the brine production temperature is significantly above what is needed for standard agricultural heating, the secondary heat delivery system should be engineered to deliver heat at a lower temperature by proportionally designing the heat exchange between the source brine and a secondary loop of agricultural water.

Copyright © SLB. All Rights Reserved. Private & Confidential. Reproduction only by permission.

5.2.4 Geothermal System Costs

Capital and operating costs geothermal plant surface systems

This section outlines a preliminary estimate of capital expenditures (CAPEX) and operating expenditures (OPEX) for the geothermal plant's surface systems. It is critical to note that the current process design is preliminary; detailed equipment geometries, piping layouts, and precise machinery sizing have not yet been established. Consequently, a definitive and highly detailed cost estimate is not feasible at this stage. Instead, an approximate estimate is presented here, based on preliminary assumptions about the footprint and heat transfer areas of major equipment. These figures represent a baseline that will be subject to significant refinement in subsequent engineering phases.

Project Size

The maximum gross generation estimated in this study is about 3.2 MW, which is well within the optimal range for small-scale organic Rankine cycle (ORC) applications. Unlike utility-scale, custom-designed binary plants, small-scale ORC technology leverages modular, standardized architectures. This approach shifts the project strategy from bespoke turbine engineering to the integration of pre-engineered systems, offering significant advantages such as rapid deployment, predictable capital costs, and operational redundancy. Modular units are readily available for the geothermal market, with power capacities typically spanning from a few hundred kW up to 2 MW per skid. Consequently, achieving the 3.2 MW target will rely on a parallel configuration of multiple standardized units, allowing for high turndown flexibility and easier maintenance isolation. Manufacturers such as Toshiba, Climeon, and Critical Energy maintain active, mature offerings in this sector, with Climeon currently leading in the number of operating installations. The closest operational reference for this modular scale from Climeon is the Kópsvatn Power Plant, operating with a nominal power of 1,200 kW.



Fig. 5.24 The Kópsvatn power plant in Iceland (source: Climeon)

Copyright © SLB. All Rights Reserved. Private & Confidential. Reproduction only by permission.

Small Scale ORC manufacturer cost feedback

Preliminary cost feedback was obtained through direct technical consultations with a small-scale ORC manufacturer. The proposed equipment configuration relies on standard, fully integrated modular generating units, each rated at a nominal capacity of 2 MW. To reliably satisfy the ~3.2 MW generation target and allow for operational redundancy, the design basis assumes the deployment of two parallel 2 MW modules, yielding a total nameplate capacity of 4 MW. Based on the vendor's preliminary budgetary estimate of USD 2.9 million per MW (approx. EUR 2.5 million), the capital cost for the power generation modules is projected to be EUR 10 million, representing the fully installed cost of the generation skids. This design would not be optimized on the specific characteristics of the reservoir and the power generation assessment presented above does not apply to a modular ORC solution.

Cost estimate by component with literature equations

The preliminary process design can be used to make assumptions and apply cost curves reported in the literature to estimate the cost of a bespoke design for the ORC described in this study. These cost estimates are speculative, because they are based on assumptions referring to standard industry designs for utility-scale power units and are not backed by any consideration of economic viability against performance of the power unit.

The “bare module cost” (BMC) technique described by Turton et al. (2012; [32]) provides a bottom-up methodology for estimating the total installed capital cost of industrial process facilities. This methodology calculates a baseline purchase cost for each component under idealized standard conditions and modifies it by using specific multiplicative factors to account for the required system operating pressure (F_p) and specialized material selections (F_m) [33].

Applying the BMC technique offers some advantage for analyzing a 4 MW ORC unit. Standard top-down industry estimates, typically measured in total cost per kilowatt, are inherently inaccurate when applied to small-scale projects, because they fail to capture the severe loss of economies of scale at the 4 MW threshold. On the negative side, the BMC approach is flawed because of the variability introduced by the correction coefficients.

The BMC method applies to the ORC as follows:

- Heat exchangers (e0vaporator and preheater): Sizing is driven by the required heat transfer area (A). The duty (Q), the total thermal capacity (UA) and the log mean temperature difference (ΔT_{LMTD}) are results of the process simulation in Symmetry; (A) is estimated based on the assumption of a (U) value in line with utility scale geothermal ORC.
- Air-cooled condenser (ACC): Sizing is driven by the required heat transfer area (A). This is often the most capital-intensive component. Its footprint and cost are highly sensitive to the ambient dry-bulb temperature and the pressure operating range. The duty (Q), the total thermal capacity (UA), and the log mean temperature difference (ΔT_{LMTD}) are results of the process simulation in Symmetry; (A) is estimated based on the assumption of a (U) value in line with utility scale geothermal ORC.

Copyright © SLB. All Rights Reserved. Private & Confidential. Reproduction only by permission.

- Turbine/expander: Cost scales primarily with the gross power output (covering the 4 MW net plus parasitic loads) and the required isentropic efficiency. The cost will be estimated based on CEMAC guidelines from 2018, actualized to 2026 [34].
- Feed pump: Sized based on the working fluid volumetric flow rate and the pressure delta, obtained from the Symmetry process simulation.

Once the capacity parameter X (such as A or W) is established, the purchased equipment cost under base conditions (C_p^0) is typically modeled using empirical correlations:

$$log_{10}(C_p^0) = K_1 + K_2 log_{10}(X) + K_3[log_{10}(X)]^2$$

The set of K constants used is the baseline pricing from the year 2001 (CEPCI=397), actualized to present day by multiplying it by a ratio of the Chemical Engineering Plant Cost Index (CEPCI~800).

The actualized reference cost is then obtained from:

$$C_p^0(current) = C_p^0(base\ year) \times \left(\frac{CEPCI_{current}}{CEPCI_{Base\ Year}}\right)$$

This base cost is then adjusted with specific material (F_m) and pressure (F_p) multipliers to calculate the final installed module cost.

$$(C_{BM}) = C_p^0 \times F_M \times F_P$$

Turbine cost based on CEMAC

The cost of the turbine was not estimated with the BMC because the method shows severe underestimation of cost for this component, instead we will refer to the CEMAC report: Global Value Chain and Manufacturing Analysis on Geothermal Power Plant Turbines [34].

Extract from the report:

"We analyzed the manufacturing cost and MSP for three different scenarios, where each scenario had five (5) volumes of manufacturing:

1. a 1 MWe ORC turboexpander;
2. a 5 MWe ORC turboexpander;
3. a 20 MWe steam turbine, at manufacturing volumes of 1, 5, 10, 25 and 50.

All 3 scenarios assume U.S. production facilities and costs. The generator is considered as a separate piece and is not included in the manufacturing cost analysis. Increasing volumes of manufacturing effectively decreased the manufactured cost per unit, because the VAPEX is over

Copyright © SLB. All Rights Reserved. Private & Confidential. Reproduction only by permission.

more units. Machine setup times and D&E costs are the cost components that are most impacted by volume manufacturing, because these are essentially one-time charges that are not volume dependent.

Case2: 5 MWe geothermal ORC turboexpander

In case 2, the results showed that MSP decreases significantly when the manufacturing volume is increased from one unit (custom design) to five units (standard design). The MSP of a single custom design 5 MWe turboexpander was found to be EUR 185.5 per kW whereas a standard-design 1 MWe turboexpander has an MSP of EUR 56.7 per kW at a manufacturing volume of five." (Fig. 5.25)

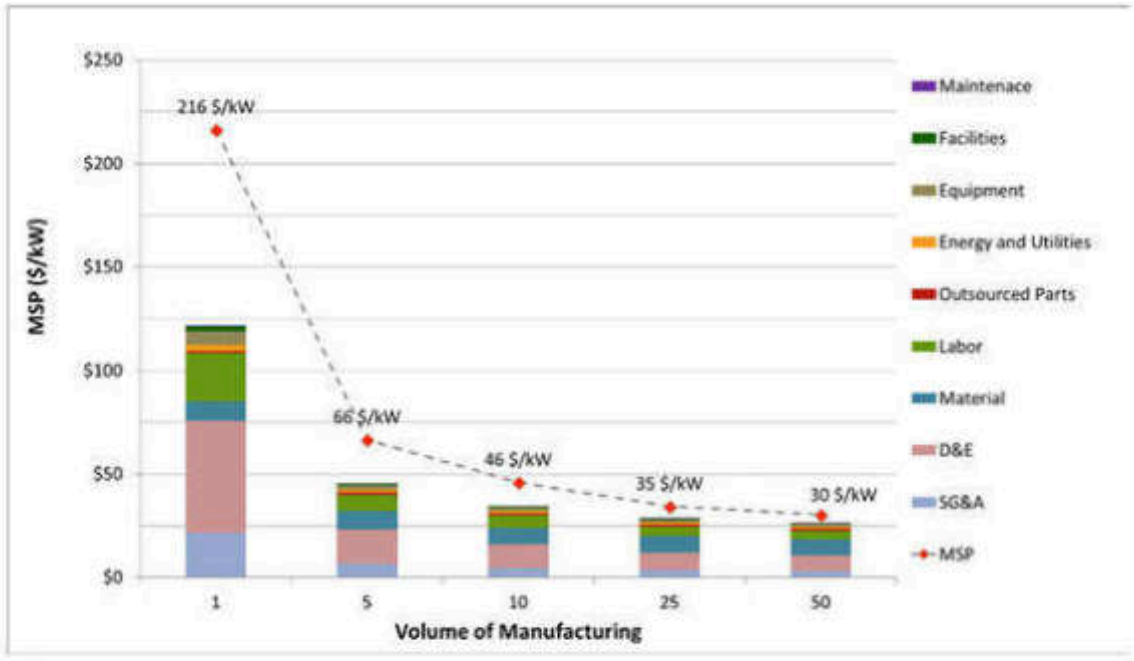


Fig. 5.25 Variations in MSP and manufacturing cost breakdown
Calculated MSP and manufacturing cost breakdown for a 5 We ORC turboexpander in different volumes of manufacturing in the United States (source: CEMAC)

Applying the unitary cost of EUR 185.5 per kW to the 3.5 MW recommended nameplate capacity results in an estimated cost of EUR 650,000, increased by 15% to EUR 747,500 when shipping and logistics are considered.

Applying the BMC:

$$C_p^0(current) = €747{,}500 \times 1.33 = €994{,}100$$

Generator

A 4 MW generator is recommended for this application, current industrial pricing places the raw equipment cost between EUR 70 and EUR 95 per kW.

Copyright © SLB. All Rights Reserved. Private & Confidential. Reproduction only by permission.

- C_P^0 (base) ~ EUR 325,000

Because the generator is typically factory-aligned and mounted directly onto the same structural skid as the expander, the field installation factor (F_{BM}) is lower than that of standalone process pumps or heat exchangers. A standard skid-mounted electrical installation factor is assumed to be **1.5**.

$$(C_{BM}) = C_P^0 \times F_{BM} = €325{,}000 \times 1.5 = €487{,}500$$

Preheater

Results from process simulation are reported below:

Table 5.27 Process simulation results for the preheater

Preheater	
UA [W/K]	242,147.9
Duty [W]	6,947,082
LMTD [C]	29.6
Max Operating Pressure [kPa]	2,360

Using the standard logarithmic constants for a shell-and-tube heat exchanger (K1= 4.3247, K2= -0.303, K3= 0.1634) and assuming:

- U = 1100 W/m^2·K
- A = 225 m^2
- F_M = 3.0 (duplex)
- F_P = 1.08 (P~20bar)
- C_P^0 (base) = EUR 57,500

Then:

$$(C_{BM}) = C_P^0 \times F_M \times F_P = €57{,}500 \times 3 \times 1.08 = €186{,}400$$

Vaporizer

Results from process simulation are reported below:

Table 5.28 Process simulation results for the vaporizer

Vaporizer	
UA [W/K]	957,480.3
Duty [W]	13,846,162.2
LMTD [C]	24.04
Max Operating Pressure [kPa]	2110

Copyright © SLB. All Rights Reserved. Private & Confidential. Reproduction only by permission.

Using the standard logarithmic constants for a shell-and-tube heat exchanger (K1= 4.3247, K2= -0.303, K3= 0.1634) and assuming:

- U=550 W/m^2·K
- A=1800 m^2
- F_M =3.0 (duplex)
- F_P =1.08 (P~20bar)
- C_P^0 (Current) = EUR 203,500

Then

$$(C_{BM}) = C_P^0 \times F_M \times F_P = €203{,}500 \times 3 \times 1.08 = €660{,}000$$

Air Cooled Condenser

Results from process simulation are reported below:

Table 5.29 Process simulation results for the ACC

ACC	
UA [W/K]	1,460,000
OutQ [W]	18,036,175
LMTD [C]	12.35
Max Operating Pressure [kPa]	390

Using the standard logarithmic constants for a shell-and-tube heat exchanger (K1= 4.3247, K2= -0.303, K3= 0.1634) and assuming:

- U=358 W/m^2·K
- A=4,000 m^2
- F_M = 2.2 (carbon steel and aluminum)
- F_P = 1
- C_P^0 (base) = EUR 472,500

Then:

$$(C_{BM}) = C_P^0 \times F_M \times F_P = €472{,}500 \times 2.2 = €1{,}040{,}000$$

Pumps

In the methodology formalized by Turton et al. [32]. The cost of a centrifugal pump is estimated using the equation:

$F_{BM} = B_1 + B_2 \times F_m \times F_p$

Copyright © SLB. All Rights Reserved. Private & Confidential. Reproduction only by permission.

- W = 230 kW
- B_1 = 1.89
- B_2 = 1.35
- F_M = 1.5 (carbon steel)
- F_P = = 1.25
- C_P^0 (base) = EUR 41,200

Then:

$$(C_{BM}) = C_P^0 \times F_M \times F_P = €41{,}200\ (1.89 + 1.35 \times 1.25 \times 1.5) = €246{,}800$$

This estimate does not take into consideration that hydrocarbon pumps have special design requirements due to the flammability of the working fluid. Typically, these pumps use sealless magnetic drive of canned motor pumps, resulting in a cost increase of about 100% of the price:

Pump Cost: EUR 360,000

Equipment Cost Summary

The final result is reported in the following summary tables.

Table 5.30 Main equipment cost estimate for geothermal

MAIN EQUIPMENT COST ESTIMATE (USD)	
Turbo-Generator Group	1,481,600
Preheater	186,400
Vaporizer	660,000
Air Cooled Condenser	1,040,000
Pumps	360,000
Balance of Plant	1,118,400
TOTAL COST OF MAIN EQUIPMENT	**4,846,400**

Based on experience in geothermal projects development, the CAPEX breakdown of a utility scale geothermal power unit typically allocates as follows:

Table 5.31 Cost breakdown of utility scale ORC in Western United States

COST BREAKDOWN OF UTILITY SCALE ORC	
Engineering	5.0%
Main Equipment Procurement and Supply	45.0%
Construction	35.0%
Handover	15.0%

Applying the cost of the main equipment and extrapolating the other costs based on the % allocations yields a preliminary, unadjusted global cost estimate for an installed ORC unit, as detailed in the table below:

Copyright © SLB. All Rights Reserved. Private & Confidential. Reproduction only by permission.

Table 5.32 Reference cost of utility scale ORC unit in Western United States

REFERENCE COST OF UTILITY SCALE ORC UNIT	[EUR]	[%]
Engineering	538,500	5
Main Equipment Procurement and Supply	4,846,400	45
Construction	3,769,400	35
Handover	1,615,450	15
Total Cost	**10,769,750**	**100**
Installed ORC Cost per MW	**2.7 [MEUR / MW]**	

The direct application of utility-scale percentage breakdowns fails to accurately reflect the economic reality of small-scale ORC. While equipment procurement scales to some degree with capacity, execution costs do not scale linearly. Certain cost components must be translated on an absolute basis or adjusted using non-linear scaling factors, such as engineering and site execution expenses.

It is outside the capability of this study to estimate the cost increase factor that must be applied to the estimated CAPEX to serve as a reference for commercial offers.

Additional Costs

To accurately project the total cost of the geothermal facility, we must include additional cost items such as:

- **Civil Works and Site Infrastructure:** Access and construction routing, plant pad preparation, bulk earthworks, environmental control plans (e.g., SWPPP/site drainage), and final grading.
- **Geothermal Gathering System:** The complete engineering, procurement, construction, and installation of the piping network connecting the production wellheads to the surface generation skids.

The estimation of these costs is outside the scope of this study.

Power Plant Operating Costs

The annual operating expenditure (OPEX) for the facility can be divided into several categories: direct site maintenance, continuous plant operations, corporate back-office support, and third-party service contracts.

MAINTENANCE

Service Agreement

The limited generating capacity of a ~3.2 MW unit does not economically justify the fixed overhead of a dedicated, full-time on-site maintenance crew. Instead, the optimal operational strategy would be to enter into a Long-Term Service Agreement (LTSA) with the equipment OEM or

Copyright © SLB. All Rights Reserved. Private & Confidential. Reproduction only by permission.

a qualified regional maintenance provider. While quantifying the cost of this contract must be deferred until formal vendor bidding to preserve commercial negotiation leverage, it represents a critical component of the asset's O&M strategy.

Rotating machinery

Critical rotating assets—including the turbine, electrical submersible pumps (ESPs), injection pumps, and working fluid pumps—require rigorous adherence to manufacturer-specified maintenance schedules and scheduled component overhauls. Given the preliminary stage of the process design, precise annual maintenance run-rates for spare parts and mechanical repairs cannot be definitively established until specific equipment models and operational parameters are finalized.

Heat Exchangers

Maintenance intervals for the primary heat exchangers are governed by the rates at which scaling and fouling occur (which in turn are a function of specific thermodynamic conditions and brine chemistry of the geothermal reservoir). Operation typically commences with a conservative, accelerated cleaning schedule (e.g., annual teardowns and inspections); the schedule can then be adjusted based on assessment of mineral deposition during these initial interventions.

OPERATION

Geothermal power plants require continuous supervision via shift rotations to ensure optimal process control and to respond immediately to grid operator directives (such as load curtailment). Operators are responsible for continuous thermodynamic monitoring, coordinating lock-out/tag-out (LOTO) procedures for maintenance personnel, managing environmental compliance, and maintaining site governance. However, for a sub-utility scale unit, the financial burden of staffing a complete 24/7 operations roster is disproportionate to the revenue generated. Consequently, utilizing a centralized Remote Operations Center (ROC) managed by a third-party service provider emerges as the most viable strategy to maintain compliance while protecting project economics.

BACK-OFFICE SUPPORT

Comprehensive facility operation requires extensive corporate infrastructure, encompassing health, safety, and environment (HSE) management, procurement, contract administration, human resources, and multi-discipline engineering support. While larger portfolios absorb these costs across multiple assets, assigning dedicated back-office personnel to a single small-scale ORC is financially burdensome. Attempting to internalize these functions by requiring small staff to assume multiple operational roles degrades efficiency, leading to reduced plant availability and diminished revenue. Therefore, outsourcing these core support functions to an established third-party management entity might be the best option.

Copyright © SLB. All Rights Reserved. Private & Confidential. Reproduction only by permission.

OPEX COST

While standard techno-economic models for calculating OPEX as a function of installed capacity are widely available, they are fundamentally calibrated for utility-scale (≥30 MW) facilities. Linearly scaling down these estimates for a ~3.2MW unit introduces severe economic distortions, because baseline fixed costs do not scale proportionately. As established previously, the constrained revenue stream of a small-scale ORC cannot support the overhead of a fully equipped internal operations and maintenance team. Therefore, the financial viability of the project hinges on securing a Long-Term Service Agreement (LTSA) with a third party, effectively replacing high fixed operational overhead with a predictable, variable cost structure aligned with the project's financial capacity.

Procuring a modular, small-scale ORC from a dedicated OEM should couple the equipment supply with an inclusive LTSA. To ensure accurate lifecycle economic modeling, firm OPEX pricing via the LTSA should be quoted and evaluated concurrently with the CAPEX proposal during the project approval and final investment decision (FID) phase.

Conversely, if a bespoke plant architecture is pursued with the Owner retaining direct O&M responsibilities, the integration risk shifts entirely to the project. The Owner must aggregate disparate maintenance schedules from multiple component suppliers to engineer a unified, comprehensive maintenance program that seamlessly synchronizes both surface facility downtime and subsurface well interventions.

Ultimately, the preliminary engineering data developed within this study is insufficient to formulate a reliable estimate of the asset's annual operating costs. The strategic recommendation is to immediately transition from theoretical estimation to market price discovery. The project team should engage with modular ORC manufacturers to solicit binding, integrated guidance on both equipment CAPEX and lifecycle OPEX.

5.2.5 Conclusions on power generation and project viability

The power generation achievable by this single production and injection well pair, under the most conservative source-temperature scenario of 140°C, demonstrates proportional equivalence to established utility-scale commercial projects. For context, a standard 30 MW nameplate hydrothermal project, with ESPs in production wells, in a comparable climate, typically yields an annual generation in the range of 150 GWh. The ~4 MW unit evaluated in this study projects an annual yield of 18.3 GWh which, scaled up proportionally, aligns with the performance metrics of successful commercial assets in the Western US, currently securing PPA rates ranging from USD 100 to USD 120 per MWh. Consequently, the technical viability of the resource's generation capacity is under positive assumption for commercial success.

CAPEX, however, remains a constraint. The USD 3.1 M per MW are on the higher side of the cost range for commercial geothermal ORC, and the small scale factor is likely to drive the CAPEX estimate up significantly. A modular solution seems to be the best option for a small scale application such as the one in this study, with a reference, non-binding, cost of USD 2.9 M per MW.

Copyright © SLB. All Rights Reserved. Private & Confidential. Reproduction only by permission.

It is recommended to continue the study with next steps of contacting geothermal ORC OEMs for interest in such small scale, consultancy on the options for such small scale, and guidance on cost references.

OPEX is the most uncertain variable in the economic model. For a bespoke 4 MW facility, operating costs are highly volatile because the baseline O&M requirements do not scale linearly with generation capacity. The fixed overheads remain static: a 4 MW turbine requires comparable teardown man-hours to a 30 MW unit, 24/7 supervision mandates the same minimum personnel redundancy, and the administrative burden of regulatory compliance, leases, and back-office support remains constant. Consequently, internalizing these fixed costs would disproportionately erode the revenue stream of a single-well asset. The NLR reports the fixed O&M cost for binary power plants in the US as estimated between USD 100 and USD 150 per kW-year. Just like for the CAPEX, the OPEX dies not scale down linearly with plant size, if anything it offers more resistance to scaling down due to maintenance requirements being often independent of the size of the plant. It is again recommended to engage directly with OEMs for guidance on operation and maintenance costs.

In conclusion, based on the preliminary analysis of this single production and injection well architecture, the recommendation is to pursue small-scale, modular ORC solutions. Active engagement with OEMs is the recommended path to devise the optimal configuration of installed modules and to solicit bundled commercial proposals that strictly couple firm CAPEX estimates with a comprehensive Long-Term Service Agreement (LTSA) for OPEX. In particular, securing this LTSA is considered paramount to transferring the disproportionate O&M risks away from the owner, thereby locking in a predictable, viable economic model for the asset's lifecycle.

Copyright © SLB. All Rights Reserved. Private & Confidential. Reproduction only by permission.

6 Security, monitoring and tracking measures

The Measurement, Monitoring and Verification (MMV) plan developed for the Bockovac area is based on the risk matrix (6.1 Risk Assessment) and risk mitigation plan, as well mandatory regulation requirements.

The primary objective of the Monitoring, Measurement, and Verification (MMV) plan is to ensure that CO_2 storage operations perform as designed and remain safe over time. This includes:

- **Storage performance assurance:** confirming injection rates, plume evolution, and effective utilization of storage capacity against design expectations.
- **Containment assurance:** demonstrating that the injected CO_2 remains securely contained within the designated storage complex.
- **HSE verification:** ensuring that risks to health, environment, and safety are effectively managed and remain within acceptable limits.

MMV Plan Coverage Across the Storage Lifecycle

The MMV plan spans the entire CO_2 storage lifecycle, comprising pre-injection, operational, and post-operational phases:

A. **Pre-Injection Phase (Baseline Establishment)**: During the pre-injection phase, all anticipated storage activities and associated risks are identified and assessed. Baseline conditions are established to define the reference state of the storage complex prior to CO_2 injection. These baseline datasets (e.g., pressure, geochemistry, and subsurface conditions) provide the foundation for future monitoring and enable the detection and quantification of any changes induced by injection. This phase is critical for supporting subsequent performance evaluation and containment assurance.
B. **Operational Phase (Injection and Surveillance**): During injection operations, MMV activities focus on tracking storage performance, verifying containment, and ensuring well and reservoir integrity. Continuous monitoring provides data on plume evolution, pressure behaviour, and injectivity, which are used to calibrate and update dynamic models. This enables early identification and mitigation of risks, while ensuring compliance with regulatory requirements and maintaining operational integrity.
C. **Post-Operational Phase (Closure and Long-Term Stewardship):** In the post-injection phase, MMV activities are designed to confirm long-term storage security. Monitoring focuses on subsurface processes such as plume migration, pressure dissipation, fluid interactions, and compositional changes. The objective is to demonstrate stabilization of the system, verify containment, and assess any residual leakage risk, supporting site closure and potential transfer of responsibility.

MMV needs to provide surveillance information covering the entire storage complex :

- Injection zone (reservoir / storage - Fig. 6.1)
- Zone above injection zone

Copyright © SLB. All Rights Reserved. Private & Confidential. Reproduction only by permission.

- Shallow groundwater
- Vadose zone
- Biosphere

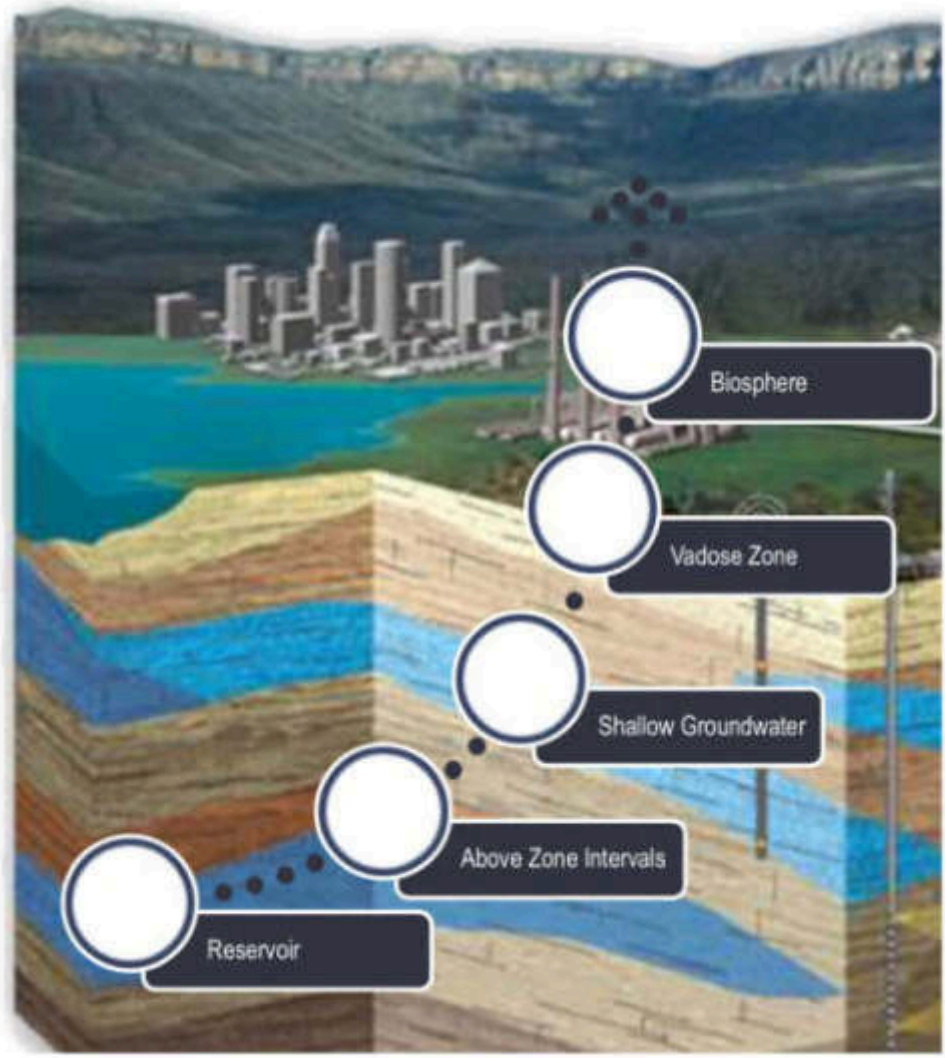


Fig. 6.1 Monitoring zones

The monitoring of the injection zone primarily addresses plume movement (extent and leakage out of area or out of zone) and to the extent possible trapping mechanism).

Primary purpose for MMV in other zones are linked to site integrity and verification that there is no migration of plume in the upper zones.

6.1 Risk Assessment

CROATIAN HYDROCARBON AGENCY (CHA) wishes to act on investigating the potential for CO_2 storage sequestration for industrial emitters in close surrounding (point sources). The area of interests is Bockovac area.

Copyright © SLB. All Rights Reserved. Private & Confidential. Reproduction only by permission.

In the context of this objective, the future operator is committed to regularly assess and prevent or mitigate any risk recognized during this study. Operator is responsible for the risk management.

6.1.1 Risk Evaluation Criteria

At this stage of the CCS project life cycle, the following main elements are to be considered:

- Areas of risk
  - Storage site containment
  - Storage site performance
  - Storage site legal and regulatory compliance
- Areas of impact
- Human health and safety
- Environmental protection
- Financial impact ($MM)/ Investment value
- Schedule impact
- Reputation impact (for CHA and croatian authority at large)

Fig. 6.2 below shows the CHA corporate risk matrix that was adopted to evaluate possible treats in the risk register. Six risk groups were established - (green-insignificant, yellow-acceptable, orange-tolerable, red-unacceptable, red-extreme, dark red - disastrous, black - novel (black swan)).

Copyright © SLB. All Rights Reserved. Private & Confidential. Reproduction only by permission.



Fig. 6.2 Adopted risk matrix
(green-insignificant, yellow-acceptable, orange-tolerable, red-unacceptable)

Table 6.1 and Table 6.2 are showing likelihood and severity classes and description of each element of concern, respectively. For each element of concern a specific risk evaluation criteria is described.

Table 6.1 Risk Matrix - HSE Frequency / Likelihood and Description

Risk Matrix - HSE Frequency / Likelihood	Rate	Description
Low (Rare / Unlikely)	1	A similar event has not occurred or occurred in the world-wide industry but not in CHA
Medium (Possible)	2	A similar event has occurred at least once in CHA
High (Likely/Very Likely)	3	A similar event has occurred more than once in CHA or more than once at the specific site

Table 6.2 Risk Matrix - Severity and Evaluation Criteria

Rank	Risk Severity	Risk Category	Risk Evaluation Criteria
3	High	HEALTH & SAFETY	Permanent injury or fatality to a single person on site. Permanent injury to single person off site. Non-permanent injury to single person off site. Irreversible health effects. Fatal and life-threatening effects.

Copyright © SLB. All Rights Reserved. Private & Confidential. Reproduction only by permission.

Rank	Risk Severity	Risk Category	Risk Evaluation Criteria
		ENVIRONMENT	Un-contained release of hazardous material. Impact on immediate neighborhood beyond facility boundary. Long term damage affecting limited area off-site and prolonged clean-up. >100 tonnes oil / diesel / chemical.
		REPUTATION	Wide-spread visible complains and involvement of NGOs, VIPs, national authorities and general public. International negative interest severely impacting business strategy and stakeholder relations
		LEGAL and REGULATORY COMPLIANCE	No Legal and regulatory compliance or expectation of delay (more than 3 years) in legal and regulatory compliance existence
		COST	Estimation of the impact in costs >= 1000K€
		SCHEDULE	Serious cause for concern at senior management level; objectives cannot be achieved without significant review. Possible impact on the achievement of strategic objectives warranting external investigation and possible radical reform.
		STORAGE SITE CONTAINMENT	Wells (Cement and Casing Quality, Well Integrity) - Well position/status unknowns, well remediation is challenging or not possible; Structural complexity - High (> 10 Faults, Fractures presence), Seal Thickness > 5 m, < 10 m; Vertical plume movement and above seal zones contamination (groundwater but no surface)
		STORAGE SITE PERFORMANCE	Capacity < 21 Mtonnes Multiple zone ; Injection < 0.7 Mtonnes/year Multiple zone;
2	Medium	HEALTH & SAFETY	Medical treatment. Single or Multiple non-permanent injuries (DAFWC) amongst persons on site Recordable injury to single person off site. Short term reversible health effects
		ENVIRONMENT	Environment damage exceeds limits- repeated regulatory breaches
		REPUTATION	Considerable community & stakeholder concerns. Negative social or other media coverage possibly causing temporary disruption or normal business operations. Potential to quickly escalate
		LEGAL and REGULATORY COMPLIANCE	Legal and regulatory compliance agreement/law in place / not approved at the current date. Potential inconsistency with international law.
		COST	Estimation of the impact in costs >= 100K€ and < 1000K€
		SCHEDULE	Concerns that objectives cannot be achieved which will cause delay / review of the business plan
		STORAGE SITE CONTAINMENT	Wells (Cement and Casing Quality, Well Integrity) - shallow wells, easy to remediate, well remediation possible ; Structural complexity - Low (> 3 Faults, No Fractures presence), Seal Thickness > 20 m, < 30 m; No vertical plume movement registered, pathways to the seal exist (faults, wells) but condition is conclusive
		STORAGE SITE PERFORMANCE	Capacity => 21 Mtonnes Multiple zone ; Injection = 0.7 Mtonnes/year Single zone;
1	Low	HEALTH & SAFETY	First aid treatment. Single or Multiple minor (recordable) injuries amongst persons on site. Ill health requiring non-prescriptive medication and / or monitoring.
		ENVIRONMENT	Environment damage contained within local area
		REPUTATION	Minor, contained community concerns. Manageable, limited impact, low-profile social or local media interest. No lasting effect
		LEGAL and REGULATORY COMPLIANCE	Legal and regulatory compliance agreement/law in place and inline with international (EU, ISO) regulations
		COST	Estimation of the impact in costs < 100K€
		SCHEDULE	Objectives remain largely achievable within the levels of tolerance without causing undue delay
		STORAGE SITE CONTAINMENT	Wells (Cement and Casing Quality, Well Integrity) - No Wells; Structural complexity - No Faults, well remediation successful, Seal Thickness > 30 m; No vertical plume movement above primary seal and above seal zones contamination (groundwater and surface)

Copyright © SLB. All Rights Reserved. Private & Confidential. Reproduction only by permission.

Rank	Risk Severity	Risk Category	Risk Evaluation Criteria
		STORAGE SITE PERFORMANCE	Capacity > 21 Mtonnes Single or Multiple zones ; Injection >0.7 Mtonnes/year Single or Multiple zones

6.1.2 Risk Register

For site feasibility study a number of surface and subsurface criteria have been evaluated, during which a number of risks have been defined. Elements for concern, risk matrix and evaluation criteria have been used for each identified risk to be able to evaluate their uncertainty, risk level before and after risk control and use it for the site selection.

a. Natural environment and hazards;
b. Regional natural resources and activities;
c. Infrastructure and facilities;
d. Social, political, and economic context;
e. Policy, legal and regulatory environment;
f. Industry recommended practices pertaining to effective risk management;
g. Project operator and subcontractors, their respective functions, responsibilities and accountabilities, and the relationships between their respective systems for risk management.

The Risk-Action-Issue Register (Fig. 6.3) is an integral part of the Risk and Issue Management processes of every project and its use is mandatory. A single file is recommended to contain all three registries (digital spreadsheets, e.g. Excel file), The file contains all three (3) registers due to the dependencies between Risks, Issues and Actions. A single file allows for easy linkage between them and facilitates their tracking and monitoring.



Fig. 6.3 Risk-Action-Issue Register

Copyright © SLB. All Rights Reserved. Private & Confidential. Reproduction only by permission.

A risk register has been created for each site. For each threat (risk) a short description of the impact or consequences was created to better define the risk. Potential and residual risk likelihood and severity were established. At this stage of the project, SLB would like also to stress the level of uncertainty for each risk. There are more information to be acquired to better define each risk, so uncertainty management was created to better define tools or processes related to risk reduction or better understanding of the sites.

A summary of the Qualitative Risk Management process (3 steps) is shown in the Fig. 6.4 . Initial potential risk impact (initial likelihood * initial severity) and residual potential risk impact (residual likelihood * residual severity) cost should be calculated to define the mitigation plan cost.

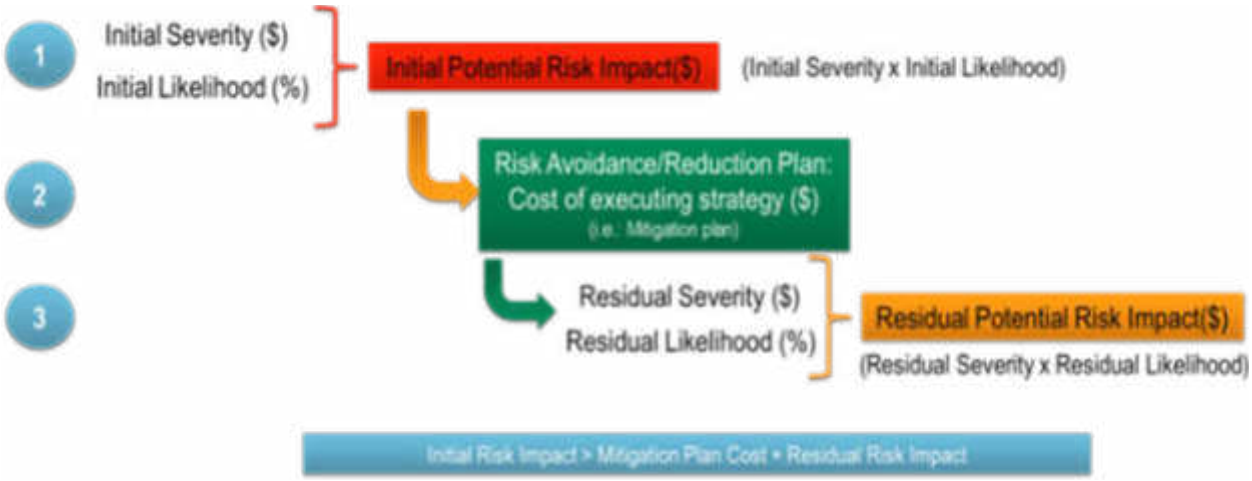


Fig. 6.4 Summary of the Qualitative Risk Management process (3 steps)

Risk Register

Table 6.3 is showing the risk register for the Bockovac area. The risk register electronic version (Excel file) with risk, issues and actions is created and needs to be shared with an operator. At this moment, risk register owner will be identified by the government agency - CROATIAN HYDROCARBON AGENCY, till it passed to dedicated operator.

Copyright © SLB. All Rights Reserved. Private & Confidential. Reproduction only by permission.

Table 6.3 Risk Register for Bockovci area CO_2 sequestration

Risk Number	Date Risk Submitted	Risk Identification Event (Short description / root cause)	Risk Category	Consequences / Impacts Description	Potential Risk		Level of uncertainty	Uncertainty Management	Preferred risk Control	Residual Risk		Risk Created	Risk Assigned	Risk Owner
					Likelihood	Severity				Likelihood	Severity			
R1	May 30th, 2026	Caprock failure. Leakage of CO_2 throughout reactivated faults/fractures. Root cause - existing closed faults or fractures become transmissive due to reservoir overpressure	Storage site containment	Vertical containment failure, where CO_2 is able to move upwards from the storage reservoir to shallower formations or the atmosphere through generated or reactivated discontinuities	Low	Medium	There is no interpreted seismic fault in the AoR and ZOI. Low geomechanical model calibration due to poor data availability. Very limited information for frac gradient calibration (only two LOT's found reported in Sjece-2 and Krunoslavje-2 with no clear value reported for the latter one and no data/ plots for QC of reported values for either of	Interpret faults from 3D seismic and construct/ actualize static subsurface model. Acquire modern logs, particularly dipole sonic. Run image logs to capture signs of potential hole instability and evaluate possible fractures. Perform mechanical core analysis to calibrate modeled results. Construct 1D geomechal model utilizing this data. Perform 3D geomechanical	Monitoring system. Baseline estimates. Surface- Quantify emissions, Microseismic - cap rock integrity, activities confined within give zone, Surface seismic- plume migration, Monitoring well- temp, pressure	Low	Low	SLB	Operator lead	Operator team

Copyright © SLB. All Rights Reserved. Private & Confidential. Reproduction only by permission.

Risk Number	Date Risk Submitted	Risk Identification Event (Short description / root cause)	Risk Category	Consequences / Impacts Description	Potential Risk		Level of uncertainty	Uncertainty Management	Preferred risk Control	Residual Risk		Risk Created	Risk Assigned	Risk Owner
					Likelihood	Severity				Likelihood	Severity			
							these tests). Possible subseismic faults and fractures could potentially be reactivated in case of over pressurizing	modelling for subsurface stress field characterization and evaluate fault stability and cap rock integrity.						
R2	May 30th, 2026	Caprock failure. Root cause - tensile or shear fractures due to reservoir overpressure and stress changes	Storage site containment	Vertical containment failure, where CO_2 is able to move upwards from the storage reservoir to shallower formations or the atmosphere through generated or reactivated discontinuities	Low	Medium	Low geomechanical model calibration due to poor data availability. No mechanical core analysis for seal. Very limited information for frac gradient calibration (only two LOT's found reported in Sjece-2 and	Acquire modern logs, particularly dipole sonic. Run image logs to capture signs of potential hole instability and evaluate possible fractures. Perform mechanical core analysis to calibrate modeled results. Construct 1D geomechal	Monitoring system. Baseline estimates. Surface- Quantify emissions, Microseismic - cap rock integrity, activates confined within give zone, Surface seismic- plume migration, Monitoring well- temp, pressure	Low	Low	SLB	Operator lead	Operator team

Copyright © SLB. All Rights Reserved. Private & Confidential. Reproduction only by permission.

Risk Number	Date Risk Submitted	Risk Identification Event (Short description / root cause)	Risk Category	Consequences / Impacts Description	Potential Risk		Level of uncertainty	Uncertainty Management	Preferred risk Control	Residual Risk		Risk Created	Risk Assigned	Risk Owner
					Likelihood	Severity				Likelihood	Severity			
							Krunoslavje-2 with no clear value reported for the latter one and no data/ plots for QC of reported values for either of these tests). High injection pressure could cause creation of induced fractures.	model utilizing this data. Perform 3D geomechanical modelling for subsurface stress field characterization and evaluate cap rock integrity.						
R3	May 30th, 2026	Caprock failure. Root cause - induced reservoir pressure exceeds caprock's capillary entry pressure	Storage site containment	Vertical containment failure, where CO_2 is able to move upwards from the storage reservoir to shallower formations or the atmosphere	Low	Medium	No mechanical core analysis for seal. Low model calibration	Perform 3D geomechanical model to evaluate cap rock integrity, Perform mechanical core analysis to calibrate modeled results. Calculate fracture gradient. Run	Monitoring system. Baseline estimates. Surface- Quantify emissions, Microseismic - cap rock integrity, activities confined within give zone, Surface seismic- plume migration, Monitoring well- temp, pressure	Low	Low	SLB	Operator lead	Operator team

Copyright © SLB. All Rights Reserved. Private & Confidential. Reproduction only by permission.

Risk Number	Date Risk Submitted	Risk Identification Event (Short description / root cause)	Risk Category	Consequences / Impacts Description	Potential Risk		Level of uncertainty	Uncertainty Management	Preferred risk Control	Residual Risk		Risk Created	Risk Assigned	Risk Owner
					Likelihood	Severity				Likelihood	Severity			
								image logs to evaluate possible fractures.						
R4	May 30th, 2026	New fractures generated in reservoir in a near wellbore region. Root cause - tensile fractures due to reservoir overpressure and stress changes	Storage site containment	If fractures are generated in reservoir, there is the potential for fractures to grow upwards into and through the cap rock (stress barrier can be absent). Generated fractures in both reservoir and caprock leads to vertical containment failure, where CO_2 moves upwards from reservoir to shallower formations or the atmosphere	Low	Low	Low geomechanical model calibration due to poor data availability. No mechanical core analysis for reservoir. Stress magnitudes and near well rock mechanical properties are uncertain. High injection pressure could cause creation of induced fractures.	Acquire modern logs, particularly dipole sonic. Run image logs to capture signs of potential hole instability and evaluate possible fractures. Perform mechanical core analysis to calibrate modeled results. Construct 1D geomechal model utilizing these data. Acquire local pore pressure information (varying level of sub-hydrostatic	Microseismic - cap rock integrity, activities confined within give zone, Surface seismic-plume migration, Monitoring well-temp, pressure. Continuous sampling of drinking water quality in shallow aquifer	Low	Low	SLB	Operator lead	Operator team

Copyright © SLB. All Rights Reserved. Private & Confidential. Reproduction only by permission.

Risk Number	Date Risk Submitted	Risk Identification Event (Short description / root cause)	Risk Category	Consequences / Impacts Description	Potential Risk		Level of uncertainty	Uncertainty Management	Preferred risk Control	Residual Risk		Risk Created	Risk Assigned	Risk Owner
					Likelihood	Severity				Likelihood	Severity			
								pore pressure was reported in most of the wells in the area, potential overpressure was also reported in two wells) and construct/ actualize dynamic reservoir model. Perform 3D geomechanical modelling for subsurface stress field characterization and evaluate cap rock integrity. Injection pressure control to be within designed range.						
R5	May 30th, 2026	New fractures generated in reservoir in a	Storage site containment	If fractures are generated in reservoir, there is	Low	Low	Low geomechanical model	Acquire modern logs, particularly	Microseismic - cap rock integrity, activities confined	Low	Low	SLB	Operator lead	Operator team

Copyright © SLB. All Rights Reserved. Private & Confidential. Reproduction only by permission.

Risk Number	Date Risk Submitted	Risk Identification Event (Short description / root cause)	Risk Category	Consequences / Impacts Description	Potential Risk		Level of uncertainty	Uncertainty Management	Preferred risk Control	Residual Risk		Risk Created	Risk Assigned	Risk Owner
					Likelihood	Severity				Likelihood	Severity			
		near wellbore region. Root cause - non-isothermal effects from CO_2 at lower temperature than injection zone causing fracturing (e.g., rock contraction, thermal stress reduction)		the potential for fractures to grow upwards into and through the cap rock (stress barrier can be absent). Generated fractures in both reservoir and caprock leads to vertical containment failure, where CO_2 moves upwards from reservoir to shallower formations or the atmosphere			calibration due to poor data availability. No mechanical core analysis for reservoir. Stress magnitudes and near well rock mechanical properties are uncertain. High injection pressure could cause creation of induced fractures	dipole sonic. Run image logs to capture signs of potential hole instability and evaluate possible fractures. Perform mechanical core analysis to calibrate modeled results. Construct 1D geomechal model utilizing these data. Perform 3D geomechanical modelling for subsurface stress field characterization and evaluate cap rock integrity. Injection pressure control to be within	within give zone, Surface seismic-plume migration, Monitoring well-temp, pressure. Continuous sampling of drinking water quality in shallow aquifer					

Copyright © SLB. All Rights Reserved. Private & Confidential. Reproduction only by permission.

Risk Number	Date Risk Submitted	Risk Identification Event (Short description / root cause)	Risk Category	Consequences / Impacts Description	Potential Risk		Level of uncertainty	Uncertainty Management	Preferred risk Control	Residual Risk		Risk Created	Risk Assigned	Risk Owner
					Likelihood	Severity				Likelihood	Severity			
								designed range.						
R6	May 30th, 2026	Caprock exposed to formation brine with dissolved CO_2	Storage site containment	Dissolution is possible in any calcite rich formation. Impact is small (less than 33cm in 10000 years)	Low	Low	Poorly defined seal mineralogy. Impact on Seal in case of mix of H2S, CO_2 , brine, HCs	Lab analysis based on plume composition and expected seal parameters	Low risk. Monitoring	Low	Low	SLB	Operator lead	Operator team
R7	May 30th, 2026	CO_2 migration out of license area. Root cause - change of CO_2 aggregate state causing rapid migration laterally within formation	Storage site containment	Lateral containment failure, in which CO_2 movement extends beyond the storage site or storage project (license boundaries)	Low	Medium	Plume aggregate status and behavior at reservoir pressure and temperature	Lab analysis based on plume composition and expected reservoir parameters	Lab analysis	Low	Medium	SLB	Operator lead	Operator team
R8	May 30th, 2026	CO_2 migration out of license area. Root cause - high permeability zones present that provide route for CO_2 and pressure to disperse further than anticipated	Storage site containment	Lateral containment failure, in which CO_2movement extends beyond the storage site or storage project (license boundaries)	Low	Medium	Permeability modeling. Predictable model	Reservoir rock typing. Pore through based approach. Diagenesis understanding. Sedimentological model	Core analysis. Rock typing. Rock fabric. Pressure and temperature monitoring. Well test analysis	Low	Low	SLB	Operator lead	Operator team
R9	May 30th,	Geochemical reactions among	Storage site	Vertical containment	Low	Low	Absents of core	Core acquisition.	subsurface monitoring.	Low	Low	SLB	Operator lead	Operator team

Copyright © SLB. All Rights Reserved. Private & Confidential. Reproduction only by permission.

Risk Number	Date Risk Submitted	Risk Identification Event (Short description / root cause)	Risk Category	Consequences / Impacts Description	Potential Risk		Level of uncertainty	Uncertainty Management	Preferred risk Control	Residual Risk		Risk Created	Risk Assigned	Risk Owner
					Likelihood	Severity				Likelihood	Severity			
	2026	CO_2 , brines and rocks can lead to a change in mechanical properties of rocks which may lead to seismicity at CO_2injection wells and storage sites	containment	failure. in which CO_2 can breach the seal and move to water zones			analysis. Rock minerals.	Thin sections. SEM. Logging ECS. Lab rock and plume interaction analysis	Monitoring design. Lab analysis. Reservoir modeling					
R10	May 30th, 2026	In case gas production is not stopped. Plume can reach main production wells during the lateral and vertical migration	Storage site containment	Lateral containment failure, well pressure depletion can cause uncontrolled/ planned plume movement	Low	Low	Future gas production flux.	Pressure maintenance. Production forecast. Injection design. Stop production before injection start	Regular history matching. Merged model of gas production and CO_2 injection. Plume front monitoring.	Low	Low	SLB	Operator lead	Operator team
R11	May 30th, 2026	CO_2 plume spread beyond the license block limits	Storage site containment	Lateral containment failure, in which CO_2movement extends beyond the storage site or storage project (license boundaries)	Low	Medium	Permeability modeling. Predictable model. Velocity model. Surface dip analysis	Reservoir rock typing. Pore through based approach. Diagenesis understanding. Sedimentological model. Image interpretation. Detailed velocity model	Core analysis. Rock typing. Rock fabric. Pressure, temperature and plume movement monitoring. Well test analysis. Checkshots/VSP. Velocity model update	Low	Low	SLB	Operator lead	Operator team

Copyright © SLB. All Rights Reserved. Private & Confidential. Reproduction only by permission.

Risk Number	Date Risk Submitted	Risk Identification Event (Short description / root cause)	Risk Category	Consequences / Impacts Description	Potential Risk		Level of uncertainty	Uncertainty Management	Preferred risk Control	Residual Risk		Risk Created	Risk Assigned	Risk Owner
					Likelihood	Severity				Likelihood	Severity			
R12	May 30th, 2026	Caprock exposed to CO_2 plume	Storage site containment	CO_2 diffusion in caprock and its alteration. Process normally decrease porosity so risk is low	Low	Low	Caprock pressure measurements. Caprock mineralogy.	Core acquisition. Thin sections. SEM. Logging ECS. Lab rock and plume interaction analysis. Cap rock pressure measurement	Core analysis. Geochemical analysis. Pressure, temperature and plume movement monitoring.	Low	Low	SLB	Operator lead	Operator team
R13	May 30th, 2026	Trace minerals within target formation	Storage site containment	Forming H2S in contact with CO_2 , needs further lab investigation. Failure to plan	Medium	Low	Absents of core analysis. Rock minerals.	Core acquisition. Thin sections. SEM. Logging ECS. Lab rock and plume interaction analysis	subsurface monitoring. Monitoring design. Lab analysis. Reservoir modeling	Low	Low	SLB	Operator lead	Operator team
R14	May 30th, 2026	Failures Modes| CO_2 leaks in facilities	Storage site containment	Containment failures in surface facilities, where CO_2 is released into the atmosphere	Low	Medium	Pressure and temperature effect on surface facilities, compressor components and tools.	Pressure, temperature and plume composition modeling and effect on both surface equipment, pipeline and wellbore integrity.	Usage of equipment designed for a full range of injection rates/pressure and temperature differences.	Low	Low	SLB	Operator lead	Operator team
R15	May 30th, 2026	Failures Modes| CO_2 leaks due to pipeline	Storage site containment	Containment failures in surface pipeline, where	Low	Medium	Pressure and temperature effect on	Pressure, temperature and plume	Usage of equipment designed for a full	Low	Low	SLB	Operator lead	Operator team

Copyright © SLB. All Rights Reserved. Private & Confidential. Reproduction only by permission.

Risk Number	Date Risk Submitted	Risk Identification Event (Short description / root cause)	Risk Category	Consequences / Impacts Description	Potential Risk		Level of uncertainty	Uncertainty Management	Preferred risk Control	Residual Risk		Risk Created	Risk Assigned	Risk Owner
					Likelihood	Severity				Likelihood	Severity			
		failure		CO_2 is released into the atmosphere			pipeline.	composition modeling and effect on both surface equipment, pipeline and wellbore integrity.	range of injection rates/pressure and temperature differences.					
R16	May 30th, 2026	Failures Modes| Injection well head failure	Storage site containment	Containment failures in the Well head, where CO_2 is released into the atmosphere.	Low	Medium	Pressure and temperature effects on the Wellhead components.	Monitoring and keeping stable the injection parameters as much as possible.	Usage of equipment designed for a full range of injection rates/pressure and temperature differences.	Low	Low	SLB	Operator lead	Operator team
R17	May 30th, 2026	Failures Modes| Anti-return device failure	Storage site containment	Containment failures in the well anti-return, where CO_2 is released into the atmosphere.	Low	Medium	Pressure and temperature effects on the surface safety valves and accessories.	Monitoring and keeping stable the injection parameters as much as possible.	Usage of equipment designed for a full range of injection rates/pressure and temperature differences.	Low	Low	SLB	Operator lead	Operator team
R18	May 30th, 2026	Geological risks| CO_2 leaks	Storage site containment	Vertical containment failure, where CO_2 is able to move upwards from the storage reservoir to shallower formations or the atmosphere	Low	Medium	Cement status, Old well logs and not updated, Old interpretations.	Cement quality logs and interpretation updated.	Cement and completion modeling for various scenarios. Usage of self-healing cement. Wellbore for monitoring and observation in the shallow zone/s	Low	Low	SLB	Operator lead	Operator team

Copyright © SLB. All Rights Reserved. Private & Confidential. Reproduction only by permission.

Risk Number	Date Risk Submitted	Risk Identification Event (Short description / root cause)	Risk Category	Consequences / Impacts Description	Potential Risk		Level of uncertainty	Uncertainty Management	Preferred risk Control	Residual Risk		Risk Created	Risk Assigned	Risk Owner
					Likelihood	Severity				Likelihood	Severity			
R19	May 30th, 2026	Geological risks| Seismicity/ Ground movements	Storage site containment	Vertical containment failure. in which CO_2 can breach the seal and move to water zones	Low	Low	Cement status, Old well logs and not updated, Old interpretations.	Log analysis, cement quality interpretation (cement logs included)	subsurface monitoring. Monitoring design. Lab analysis. Reservoir modeling	Low	Low	SLB	Operator lead	Operator team
R20	May 30th, 2026	Zone Alfa (D') structural setting	Storage site containment	Presence of faults West and South from injection zone. Possible sub-seismic faults	Low	Medium	Seismic resolution. Subseismic faults. Fault seal analysis	Detailed fault geomechanical evaluation	Geomechanical study. 1 way coupling. Core data integration	Low	Low	SLB	Operator lead	Operator team
R21	May 30th, 2026	Zone Alfa (D') sealing configuration	Storage site containment	Caprock integrity (thickness, continuity)	Low	Medium	Cup rock integrity	Detailed seal analysis and geomechanical evaluation	Geomechanical study. 1 way coupling. Core data integration	Low	Low	SLB	Operator lead	Operator team
R22	May 30th, 2026	Zone "B" structural complexity	Storage site containment	Presence of faults West and South from injection zone. Possible sub-seismic faults	Low	Medium	Seismic resolution. Subseismic faults. Fault seal analysis	Detailed fault geomechanical evaluation	Geomechanical study. 1 way coupling. Core data integration	Low	Low	SLB	Operator lead	Operator team
R23	May 30th, 2026	Zone "C" structural complexity	Storage site containment	Presence of faults West and South from injection zone. Possible sub-seismic faults	Low	Medium	Seismic resolution. Subseismic faults. Fault seal analysis	Detailed fault geomechanical evaluation	Geomechanical study. 1 way coupling. Core data integration	Low	Low	SLB	Operator lead	Operator team
R24	May 30th, 2026	Faults transmissibility	Storage site containment	Unknown fault transmissibility status. Plume moving through fault	Low	Medium	No wells crossing any faults	Juxtaposition analysis. Detailed fault geomechanical evaluation	Geological study. Deterministic model. Inversion	Low	Low	SLB	Operator lead	Operator team
R25	May 30th,	Rock properties for overlaying	Storage site	Rock dissolution in the presence of	Low	Low	No proper logs to	Core analysis	Core data acquisition and	Low	Low	SLB	Operator lead	Operator team

Copyright © SLB. All Rights Reserved. Private & Confidential. Reproduction only by permission.

Risk Number	Date Risk Submitted	Risk Identification Event (Short description / root cause)	Risk Category	Consequences / Impacts Description	Potential Risk		Level of uncertainty	Uncertainty Management	Preferred risk Control	Residual Risk		Risk Created	Risk Assigned	Risk Owner
					Likelihood	Severity				Likelihood	Severity			
	2026	units	containment	carbon acid. Plume vertical flow			define a caprock mineralogy		core analysis					
R26	May 30th, 2026	Fluid properties for overlaying units	Storage site containment	Fluid interaction with plume. Mineralization. Trapping	Low	Medium	No proper information to define fluid-rock interaction	Core analysis	Core data acquisition and core analysis	Low	Low	SLB	Operator lead	Operator team
R27	May 30th, 2026	Deviated well cement	Storage site performance	Risk of casing laying on the borehole wall. No Cement	Low	High	Geomechanical data.	3D geomechanical model. Core data integration.	Core data acquisition and core analysis. Detailed well design	Low	Low	SLB	Operator lead	Operator team
R28	May 30th, 2026	Vertical permeability	Storage site performance	Understanding of vertical migration.	Low	Medium	No data for proper estimation	Core analysis	Core data acquisition and core analysis	Low	Low	SLB	Operator lead	Operator team
R29	May 30th, 2026	SCAL data	Storage site performance	Dynamic modeling constrains. Plume injectivity. Modeling	Medium	Medium	No data for proper estimation	Core analysis	Core data acquisition and core analysis	Low	Low	SLB	Operator lead	Operator team
R30	May 30th, 2026	Lateral heterogeneity	Storage site performance	Sweeping efficiency. Barriers.	Low	Medium	Seismic resolution.	Seismic inversion between Karas Suma-1, Bockovci-1 and Krunoslavlje-2	Seismic inversion. VSP	Low	Low	SLB	Operator lead	Operator team
R31	May 30th, 2026	Structural dip toward South area	Storage site performance	Fast movement of plume towards South fault	Low	High	Velocity model	Stacking velocities. VSP	Study update. Monitoring well	Low	Medium	SLB	Operator lead	Operator team
R32	May 30th,	Structural dip toward West	Storage site	Fast movement of plume towards	Low	High	Velocity model	Stacking velocities. VSP	Study update. Monitoring well	Low	Medium	SLB	Operator lead	Operator team

Copyright © SLB. All Rights Reserved. Private & Confidential. Reproduction only by permission.

Risk Number	Date Risk Submitted	Risk Identification Event (Short description / root cause)	Risk Category	Consequences / Impacts Description	Potential Risk		Level of uncertainty	Uncertainty Management	Preferred risk Control	Residual Risk		Risk Created	Risk Assigned	Risk Owner
					Likelihood	Severity				Likelihood	Severity			
	2026	area	performance	West faults										
R33	May 30th, 2026	Sequence stratigraphy study	Storage site performance	Understanding of depositional pattern	Low	Low	No detail study indicating areal depositional pattern. Core/Log motive description	Detailed sedimentological study - seq. stratigraphy	Integration of existing and new wells core data. Stratigraphic study	Low	Low	SLB	Operator lead	Operator team
R34	May 30th, 2026	Depositional environment modeling - GDE maps	Storage site performance	Understanding of depositional pattern	Low	Low	No GDE maps indicating areal depositional pattern. Core/Log motif description	Detailed sedimentological study - GDE maps	Integration of existing and new wells core data. GDE maps	Low	Low	SLB	Operator lead	Operator team
R35	May 30th, 2026	Sub-zones thickness analysis - isochore maps	Storage site performance	Property distribution (seal, reservoir). Lateral propagation	Low	Medium	Large distance between wells. Correlation	Seismic inversion. Image data. Study.	Seq.stratigraphy study. Core data integration. Layering. Data analysis	Low	Low	SLB	Operator lead	Operator team
R36	May 30th, 2026	Temperature model calibration	Storage site performance	Plume density. Volume	Low	Medium	Circulation data. Test data. Localized anomalies	Horner Transformation	New wells measurements. Circulation time. Well test	Low	Low	SLB	Operator lead	Operator team
R37	May 30th, 2026	Zone "B" lateral facies variability	Storage site performance	Sweeping efficiency. Barriers.	Low	Medium	Seismic resolution.	Seismic inversion between Karas	Seismic inversion. VSP	Low	Low	SLB	Operator lead	Operator team

Copyright © SLB. All Rights Reserved. Private & Confidential. Reproduction only by permission.

Risk Number	Date Risk Submitted	Risk Identification Event (Short description / root cause)	Risk Category	Consequences / Impacts Description	Potential Risk		Level of uncertainty	Uncertainty Management	Preferred risk Control	Residual Risk		Risk Created	Risk Assigned	Risk Owner
					Likelihood	Severity				Likelihood	Severity			
								Suma-1, Bockovci-1 and Krunoslavlje-2						
R38	May 30th, 2026	Zone "C" reservoir properties	Storage site performance	Capacity. Injectivity. Sweeping efficiency	Low	Low	Log interpretation calibration. Rock property data	Core analysis	Core data acquisition and core analysis	Low	Low	SLB	Operator lead	Operator team
R39	May 30th, 2026	Zone "D" reservoir thickness	Storage site performance	Lateral change in thickness. Volume control. Properties	Low	Low	Across well correlation. Depositional understanding	Seismic inversion between Karas Suma-1, Bockovci-1 and Krunoslavlje-2	Seismic inversion. VSP	Low	Low	SLB	Operator lead	Operator team
R40	May 30th, 2026	Permeability decrease due to mineralization	Storage site performance	Mineralization is usually happening over long period of time. Unlikely to happen during project injection cycle	Low	Low	Reservoir mineralogy. Impact of impurities and plume on reservoir minerals	Lab analysis.	Lab analysis	Low	Low	SLB	Operator lead	Operator team
R41	May 30th, 2026	Insufficient injectivity. Root cause - salt precipitation as a result of brine evaporating	Storage site performance	Injection target will not be reached. More wells needs to be drilled.	Low	Low	No well/core analysis in the site zone. Log interpretation	Perform lab analysis in the near field or collect after new wells are drilled. Thin section analysis	Lab analysis	Low	Low	SLB	Operator lead	Operator team

Copyright © SLB. All Rights Reserved. Private & Confidential. Reproduction only by permission.

Risk Number	Date Risk Submitted	Risk Identification Event (Short description / root cause)	Risk Category	Consequences / Impacts Description	Potential Risk		Level of uncertainty	Uncertainty Management	Preferred risk Control	Residual Risk		Risk Created	Risk Assigned	Risk Owner
					Likelihood	Severity				Likelihood	Severity			
R42	May 30th, 2026	Insufficient injectivity. Root cause - injection reservoir is less permeable and/ or thinner than anticipated	Storage site performance	Injection target will not be reached. More wells needs to be drilled.	Medium	Medium	No rock typing. Low resolution model. No permeability transforms	During reservoir characterization improve model predictability by performing rock typing and analyzing its distribution	High resolution modeling to capture vertical and lateral permeability heterogeneity. Usage of the secondary property (seismic attributes) to guide the reservoir model	Medium	Low	SLB	Operator lead	Operator team
R43	May 30th, 2026	Insufficient injectivity. Root cause -Hydrate formation from cold CO_2 and water mixing at high pressures in the wellbore during startup of injection	Storage site performance	Injection target will not be reached. More wells needs to be drilled.	Low	Low	Inconsistent plume composition	Plume composition monitoring. Additives experimental analysis	CO_2 hydrate formation and dissociation models, including the kinetic and thermodynamic ones, and effect of additives	Low	Low	SLB	Operator lead	Operator team
R44	May 30th, 2026	Premature drop in injectivity or even shutdown of injection due to excessive pressure build-up caused by lower available connected reservoir	Storage site performance	Injection target will not be reached. Pressure management by means of water production outside of CO_2 plume extent to reduce pressure build-up should	Low	Medium	Understanding reservoir barriers and rock properties	Detailed reservoir modeling, secondary properties, rock typing, analogue selection	Complete logging suite with interpretation, well test, monitoring wells, fiber optic.	Low	Low	SLB	Operator lead	Operator team

Copyright © SLB. All Rights Reserved. Private & Confidential. Reproduction only by permission.

Risk Number	Date Risk Submitted	Risk Identification Event (Short description / root cause)	Risk Category	Consequences / Impacts Description	Potential Risk		Level of uncertainty	Uncertainty Management	Preferred risk Control	Residual Risk		Risk Created	Risk Assigned	Risk Owner
					Likelihood	Severity				Likelihood	Severity			
		volumes or lower reservoir compressibility.		be introduced.										
R45	May 30th, 2026	Underestimated capacity. Presence of lithological barriers	Storage site performance	Negative consequence: Additional storage units or storage sites needs to be evaluated and included into evaluation. Positive: vertical barriers can additionally act as seals and improve containment	Medium	Medium	No well to interwell facies connectivity. Seismic and log resolution	Multi realization modeling, seismic trend, rock typing with threshold pressure analysis	High resolution image logs, ECS for minerals, coring, testing	Low	Low	SLB	Operator lead	Operator team
R46	May 30th, 2026	Underestimated capacity. Underestimated solubility of CO_2 in water	Storage site performance	Additional storage units or storage sites needs to be evaluated and included into evaluation.	Medium	Medium	no lab analysis	Analogue analysis, near field core test	Core collection in the future wells. Lab analysis	Low	Low	SLB	Operator lead	Operator team
R47	May 30th, 2026	Underestimated capacity. Underestimated bulk volume, net to gross ratio, porosity, efficiency factor, density of CO_2 at depth could lead to it.	Storage site performance	Lack of enough storage space leads to additional studies to find another storage site, design and add all needed infrastructure, etc.	Medium	Medium	No current well control. Velocity modeling uncertainty, lateral and vertical anisotropy unknown	Data collection, Velocity modeling based on future check shots. High resolution logging. Core analysis	Well data calibration (stratigraphic well). Data collection. Core collection. Lab analysis	Medium	Low	SLB	Operator lead	Operator team

Copyright © SLB. All Rights Reserved. Private & Confidential. Reproduction only by permission.

Risk Number	Date Risk Submitted	Risk Identification Event (Short description / root cause)	Risk Category	Consequences / Impacts Description	Potential Risk		Level of uncertainty	Uncertainty Management	Preferred risk Control	Residual Risk		Risk Created	Risk Assigned	Risk Owner
					Likelihood	Severity				Likelihood	Severity			
R48	May 30th, 2026	CO_2 migration to gas bearing formations. Root cause - presence of existing flow paths with high permeability	Storage site performance	Uncontrolled plume lateral movement. Failure to plan	Medium	Medium	Permeability modeling. Predictable model. Natural fracture prediction	Reservoir rock typing. Pore through based approach. Diagenesis understanding. Sedimentological model. Image interpretation	Core analysis. Rock typing. Rock fabric. Pressure and temperature monitoring. Fracture modeling with paleo stress analysis. Well test analysis	Low	Low	SLB	Operator lead	Operator team
R49	May 30th, 2026	Geochemical reactions among CO_2, brines and rocks can lead to a change in porosity, permeability and hydraulic rock properties and alter the migration paths of CO_2	Storage site performance	Uncontrolled plume lateral movement. Failure to plan	Low	Low	Diagenesis. Chemical reaction. Reservoir properties	Core description. This section analysis. MICP/ Rock types.	subsurface monitoring. Monitoring design. Lab analysis. Reservoir modeling	Low	Low	SLB	Operator lead	Operator team
R50	May 30th, 2026	CO_2 react with the ions in the formation water and matrix and form cement which decrease the rates for injection	Storage site performance	Injection target will not be reached. More wells needs to be drilled.	Low	Low	Rock mineralogy. Lab rock and saline analysis	Core and fluid sampling.	Lab analysis.	Low	Low	SLB	Operator lead	Operator team
R51	May 30th, 2026	Dip of the formation is higher than	Storage site performance	Higher surface dip will cause faster lateral plume	Medium	Medium	Uncertainty in velocity modeling, no	Velocity modeling update. Data	Checkshots/VSP, model update. Seismic stacking	Low	Medium	SLB	Operator lead	Operator team

Copyright © SLB. All Rights Reserved. Private & Confidential. Reproduction only by permission.

Risk Number	Date Risk Submitted	Risk Identification Event (Short description / root cause)	Risk Category	Consequences / Impacts Description	Potential Risk		Level of uncertainty	Uncertainty Management	Preferred risk Control	Residual Risk		Risk Created	Risk Assigned	Risk Owner
					Likelihood	Severity				Likelihood	Severity			
		estimated		movement towards gas reservoir			calibration well	acquisition	velocities utilization					
R52	May 30th, 2026	Reservoir capacity and injectivity| Reduced injectivity	Storage site performance	Injection target will not be reached with the time.	Medium	Medium	Measurements of the flowrate, and identify the well head pressure inconsistences.	Verification and calibration of the instrumentation systematically and periodically.	Monitoring of well head pressure and flowrate. Perform stimulations when are needed (periodically)	Low	Low	SLB	Operator lead	Operator team
R53	May 30th, 2026	Reservoir capacity and injectivity| Lack of capacity	Storage site performance	Injection target will not be reached. More wells needs to be drilled.	Medium	Medium	Measurements of the flowrate, and identify the wellhead pressure inconsistencies.	Verification and calibration of the instrumentation systematically and periodically.	Monitoring of well head pressure and flowrate. Perform stimulations when are needed (periodically)	Low	Low	SLB	Operator lead	Operator team
R54	May 30th, 2026	Geothermal Risks - Corrosion & Chemical Degradation -CO_2, H_2S, chlorides -Low pH fluids -High temperature accelerating reactions	Storage site performance	Casing/tubing thinning Cement degradation Well failure over time	Medium	Medium	Lack of corrosion logs and representative test samples	Install liners/ tubing replacement Chemical treatment programs	API L-80 grade and/or Corrosion-resistant alloys (CRA) casing material Proper cement formulation (latex, silica flour, light-weight additive) Corrosion inhibitors Material selection based on fluid chemistry	Low	Low	SLB	Operator lead	Operator team

Copyright © SLB. All Rights Reserved. Private & Confidential. Reproduction only by permission.

Risk Number	Date Risk Submitted	Risk Identification Event (Short description / root cause)	Risk Category	Consequences / Impacts Description	Potential Risk		Level of uncertainty	Uncertainty Management	Preferred risk Control	Residual Risk		Risk Created	Risk Assigned	Risk Owner
					Likelihood	Severity				Likelihood	Severity			
R55	May 30th, 2026	Geothermal Risks - Scaling & Deposition Silica, calcite precipitation Temperature and pressure changes	Storage site performance	Loss of pressure containment Surface leaks	Medium	Medium	Lack representative test samples	Mechanical cleanout Acidizing Chemical dissolution	Fluid chemistry control Scale inhibitors Temperature management	Low	Low	SLB	Operator lead	Operator team
R56	May 30th, 2026	CCS & Geothermal Risks - Thermal Stress & Cyclic Fatigue Temperature gradients (ambient → >150°C) Injection/ production cycling	Storage site performance	Casing expansion/ contraction → cement failure -Stress Cracking -Connection Failure Micro-annulus formation Cement debonding	High	High	Currently no Operational Plan	Squeeze cementing to restore seal Install tie-back strings (geothermal wells) Adjust operating procedures (reduce thermal cycling severity)	Thermal stress modeling Flexible cement systems (low Young's modulus) Adequate wellhead (e.g. expansion spools included in wellhead stack) and casing design Controlled ramp-up and cool down of temperature	Low	Low	SLB	Operator lead	Operator team
R57	May 30th, 2026	Cement Integrity Failure CCS Risks - Poor mud removal during cementing and poor isolation across caprock. Geothermal	Storage site performance	Loss of zonal isolation Annular pressure build-up Fluid migration	Medium	Medium	Issues encountered during well construction, such as losses, preventing a good cement sheath.	Squeeze cement jobs Cement plug placement	High-temperature cement systems (silica-stabilized) Centralization and proper mud displacement Use of stage cementing in loss zones Laboratory testing	Low	Low	SLB	Operator lead	Operator team

Copyright © SLB. All Rights Reserved. Private & Confidential. Reproduction only by permission.

Risk Number	Date Risk Submitted	Risk Identification Event (Short description / root cause)	Risk Category	Consequences / Impacts Description	Potential Risk		Level of uncertainty	Uncertainty Management	Preferred risk Control	Residual Risk		Risk Created	Risk Assigned	Risk Owner
					Likelihood	Severity				Likelihood	Severity			
		Risks -Poor mud removal during cementing due to losses and centralization of casing Chemical attack (CO_2, acid fluids)					Operational issues during well life creating Thermal stress and cyclic fatigue		(thickening time, strength retrogression)					
R58	May 30th, 2026	CCS & Geothermal Risks - Casing and Wellhead Integrity Failure Combined mechanical + thermal loads Corrosion + fatigue Poor connection design	Storage site performance	Blocked flow paths Increased pressure on casing and formation	Medium	Medium	Currently no Operational Plan	Casing patch Repair wellhead seals Pressure management during operations	Casing materials designed for handling combined mechanical and thermal loads Premium connections rated for thermal cycling effects Wellhead systems designed for geothermal temperatures/ pressure	Low	Low	SLB	Operator lead	Operator team
R60	May 30th, 2026	Simultaneous HC production and CO_2 injection can cause the geomechanical instability of the day surface -	Environmental protection	Surface subsidence, damage of facilities and equipment	Medium	Medium	Surface subsidence/ uplift	Satellite observation	InSAR to measure changes in land surface altitude	Low	Low	SLB	Operator lead	Operator team

Copyright © SLB. All Rights Reserved. Private & Confidential. Reproduction only by permission.

Risk Number	Date Risk Submitted	Risk Identification Event (Short description / root cause)	Risk Category	Consequences / Impacts Description	Potential Risk		Level of uncertainty	Uncertainty Management	Preferred risk Control	Residual Risk		Risk Created	Risk Assigned	Risk Owner
					Likelihood	Severity				Likelihood	Severity			
		monitoring infrastructure												
R61	May 30th, 2026	Safety, health and environmental risks| Environmental damage from surface facilities	Environmental protection	Containment failures in the Well head, where CO_2 is released into the atmosphere.	Low	Low	Pressure and temperature effects on the Wellhead components.	Monitoring and keeping stable the injection parameters as much as possible.	Usage of equipment designed for a full range of injection rates/pressure and temperature differences.	Low	Low	SLB	Operator lead	Operator team
R62	May 30th, 2026	Safety, health and environmental risks| Soil or water contamination due to CO_2 leaks	Environmental protection	Vertical containment failure, where CO_2 is able to move upwards from the storage reservoir to shallower formations or the atmosphere	Low	Low	Cement status. No adequate well logs for interpretation	Log analysis, cement quality interpretation	Cement and completion modeling for various scenarios. Usage of self-healing cement. Wellbore for monitoring and observation in the shallow zone/s	Low	Low	SLB	Operator lead	Operator team
R63	May 30th, 2026	Safety, health and environmental risks| Contamination of aquifers by brines	Environmental protection	Vertical containment failure, where CO_2 is able to move upwards from the storage reservoir to shallower formations or the atmosphere	Low	Low	Cement status. No adequate well logs for interpretation	Log analysis, cement quality interpretation	Cement and completion modeling for various scenarios. Usage of self-healing cement. Wellbore for monitoring and observation in the shallow zone/s	Low	Low	SLB	Operator lead	Operator team
R64	May 30th, 2026	Negative impact on health of the local. Root	Human health and safety	Carbon dioxide is a carcinogen. Being in an area	Low	Low	Current baseline status.	Health monitoring. Monitoring	Setup the baseline. Full surface and	Low	Low	SLB	Operator lead	Operator team

Copyright © SLB. All Rights Reserved. Private & Confidential. Reproduction only by permission.

Risk Number	Date Risk Submitted	Risk Identification Event (Short description / root cause)	Risk Category	Consequences / Impacts Description	Potential Risk		Level of uncertainty	Uncertainty Management	Preferred risk Control	Residual Risk		Risk Created	Risk Assigned	Risk Owner
					Likelihood	Severity				Likelihood	Severity			
		cause - caprock failure or improperly sealed/ cemented wells and the release of CO_2 to the surface.		with a high concentration of CO_2 can cause weakness, drowsiness, headaches, trouble concentrating, or even negative changes in the blood.			General population health status	system	subsurface monitoring system. Regular medical exams					
R65	May 30th, 2026	Shallow protected groundwater contamination	Human health and safety	Due to containment issues, contamination of the shallow groundwater	Low	Medium	Establishing water salinity and fresh water levels.	Shallow zones water sampling. Fluid analysis	Surface and subsurface monitoring. Baseline. Lab analysis	Low	Medium	SLB	Operator lead	Operator team
R66	May 30th, 2026	Social risks | Further development of Croatia/EU regulatory framework for CO_2 storage	Legal and regulatory compliance	Delay/changes in regulatory framework development: some additional restrictions could be coming	Medium	Medium	Politics	Follow current regulations. Cooperate with the government to help them scope the law. International practices.	Make sure that international standards, regulations and recommendation are considered in the design and implementation of CO_2 injection project.Lobbying, Subsidizing, Credits, Grants	Low	Low	SLB	Operator lead	Operator team
R67	May 30th, 2026	Social risks| Participants reject or oppose	Legal and regulatory compliance	Stop operation (Partial/Total) due to disagreements	Low	Low	Follow the current regulations	Follow the current regulations	Proper communication with the	Low	Low	SLB	Operator lead	Operator team

Copyright © SLB. All Rights Reserved. Private & Confidential. Reproduction only by permission.

Risk Number	Date Risk Submitted	Risk Identification Event (Short description / root cause)	Risk Category	Consequences / Impacts Description	Potential Risk		Level of uncertainty	Uncertainty Management	Preferred risk Control	Residual Risk		Risk Created	Risk Assigned	Risk Owner
					Likelihood	Severity				Likelihood	Severity			
		the project		among the stakeholders and possible lawsuits.			and ensure that risk mitigation is applied.	and ensure that risk mitigation is applied.	stakeholders, during all stages of the project.					
R68	May 30th, 2026	Social risks| Negative public perception of this type of projects	Legal and regulatory compliance	Loss if value of the company reputation, bad perception of the public about the project.	Low	Low	Follow the current regulations and ensure that risk mitigation is applied.	Follow the current regulations and ensure that risk mitigation is applied.	Adequate communication during and risk mitigation during the project execution.	Low	Low	SLB	Operator lead	Operator team
R70	May 30th, 2026	Future CO_2 source location vs distance to the site	Cost	CO_2 source location can influence project cost	Medium	Medium	No concrete plans yet	Company strategic decision	Multiple sites characterization. Late decision making	Low	Low	SLB	Operator lead	Operator team
R71	May 30th, 2026	Economic risks| Project costs		Scope changes (scope reduction, delaying times)	Low	Low	Follow the current regulations and ensure that risk mitigation is applied.	Follow the current regulations and ensure that risk mitigation is applied.	Make a pilot and evaluation, and manage the execution of the project in stages.	Low	Low	SLB	Operator lead	Operator team
R72	May 30th, 2026	CCS & Geothermal Risks - Loss of Wellbore Stability -Weak formations (fractured zones) -Breakouts -Overbalanced	Cost	Borehole collapse / breakout, tight hole stuck pipe / casing running issues	Medium	Medium	Lack of detailed Drilling Logs and information in close by / adjacent wells	Ream/ Backream and clean out hole if hole conditions dictate Decrease or Increase mud weight or switch fluid	Geomechanics modeling (thermal + mechanical) Proper mud weight window design for sedimentary sections Use of inhibitive drilling fluids (if/as	Low	Low	SLB	Operator lead	Operator team

Copyright © SLB. All Rights Reserved. Private & Confidential. Reproduction only by permission.

Risk Number	Date Risk Submitted	Risk Identification Event (Short description / root cause)	Risk Category	Consequences / Impacts Description	Potential Risk		Level of uncertainty	Uncertainty Management	Preferred risk Control	Residual Risk		Risk Created	Risk Assigned	Risk Owner
					Likelihood	Severity				Likelihood	Severity			
		/ underbalanced conditions						system LCM to strengthen formation High Viscosity Sweeps when drilling with losses Sidetrack if wellbore stability is lost	needed) Real-time drilling parameter monitoring (ROP, torque/drag)					
R73	May 30th, 2026	CCS & Geothermal Risks - Loss of Circulation -Highly fractured reservoir -Vugs or faults -High permeability zones	Cost	Inability to maintain hydrostatic pressure Hole cleaning problems Poor cement placement → compromised zonal isolation	High	High	Lack of detailed Drilling Logs and information in close by / adjacent wells	LCM pills / cement plugs (excluding reservoir section) Remedial cementing of casing and liner pipe Use of crosslinked gel polymers Drill ahead with losses or blind (accepting major and total losses)	Pre-drill fracture/ loss modeling Use of Lost Circulation Materials (LCM) (excluding reservoir section) Use of Cement Plugs (excluding reservoir section) Drill with water or aerated fluids in severe cases Pump high-viscosity pills with a schedule	Low	Low	SLB	Operator lead	Operator team
R74	May 30th, 2026	Geothermal Risks - Blowouts / Well Control	Cost	Uncontrolled flow of steam/fluid Safety hazards	Medium	Medium	Issues encountered during well	Shut-in procedures Kill well using	Proper well control procedures for geothermal (steam	Low	Low	SLB	Operator lead	Operator team

Copyright © SLB. All Rights Reserved. Private & Confidential. Reproduction only by permission.

Risk Number	Date Risk Submitted	Risk Identification Event (Short description / root cause)	Risk Category	Consequences / Impacts Description	Potential Risk		Level of uncertainty	Uncertainty Management	Preferred risk Control	Residual Risk		Risk Created	Risk Assigned	Risk Owner
					Likelihood	Severity				Likelihood	Severity			
		Issues Unexpected steam zones Transition from liquid to two-phase flow Underbalanced drilling in geothermal reservoirs		and equipment damage			construction such as losses, unidentified formation pressures and fluids	weighted fluids or water Relief well (extreme cases)	kick behavior) Sufficient drilling water flow rate to cool down the well (geothermal well kill priority) BOP systems rated for high temperature Real-time downhole pressure monitoring					

Copyright © SLB. All Rights Reserved. Private & Confidential. Reproduction only by permission.

Issues Log

Issues log provide with a list of issues identification and description. Some actions are the same for multiple risks, some risk needs multiple actions. Issue register connects the risk register with the action plan.

Action Log

Issue driven action register is a part of the risk assessment providing a detail description of the action plan for each issue. It contains also responsible party with priority and time log to track its progress.

Revision Control

The risk register is a live document and will be updated for the full duration of the project. It must have a revision control in the form of a table (ex. Table 6.6)

Copyright © SLB. All Rights Reserved. Private & Confidential. Reproduction only by permission.

Table 6.4 Issue log example

ISSUES LOG															
Identification / Issue Description										Issue Impact					
Issue # (I###)	Risk Number (R###) (if applicable)	Issue Category	Description	Date Raised	Assigned to	Share Externally?	Priority	Status	Change Request Required? YES/NO/MoC#	Financial Impact (k€)	Milestone Schedule Impact (days)	Action #1 ID	Action #2 ID	Action #3 ID	Action #4 ID

Copyright © SLB. All Rights Reserved. Private & Confidential. Reproduction only by permission.

Table 6.5 Actions, decisions and information log example

Action #	Link to Risk or Issue #	Issue or Risk Status	Issue / Risk	Action Description	Date Logged	Assigned by	Assigned to	Priority	Action Status	Date Closed	Additional Information
(A###)	(R###) (I###)		Description								
A1	R1	ACTIVE				SLB team	CHA	Medium	Not Started		

Copyright © SLB. All Rights Reserved. Private & Confidential. Reproduction only by permission.

Table 6.6 Revision control

Version	Issue Date	Description	Prepared by	Approved by	Changes to the document
1		Initial Release	SLB screening stage team		

Copyright © SLB. All Rights Reserved. Private & Confidential. Reproduction only by permission.

6.1.3 Risk Assessment

Preferred risk control for each risk was established as a starting point to mitigate or control the potential risk.

Integrated potential and residual risk matrix for Bockovac area all risks, identified in Table 6.3, are presented in Fig. 6.5and Fig. 6.6respectively. Residual risk after mitigation plan indicate insignificant to acceptable risk.

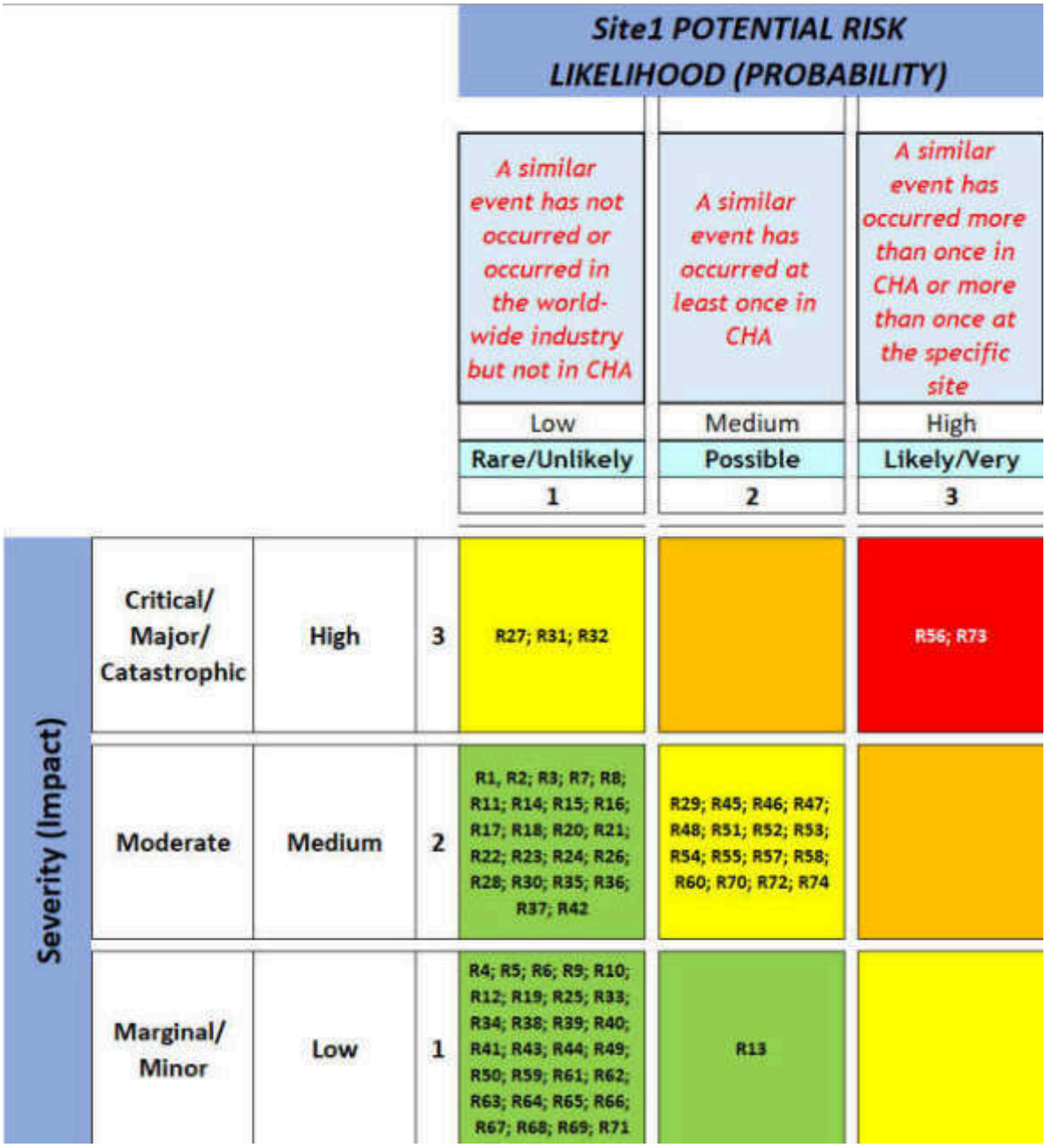


Fig. 6.5 Bockovci area - Potential Risk matrix
Likelihood (X) vs Severity (Y)

Copyright © SLB. All Rights Reserved. Private & Confidential. Reproduction only by permission.

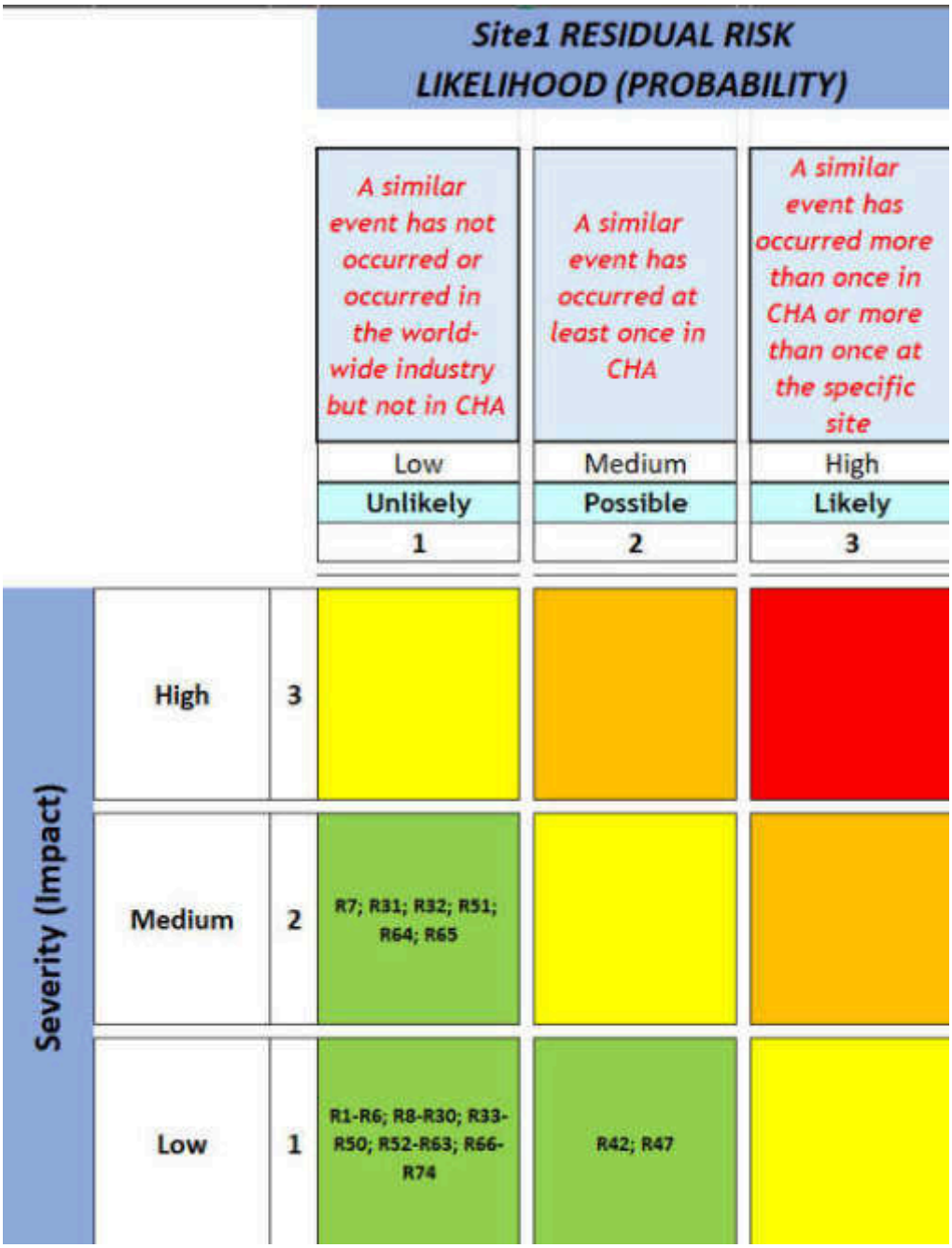


Fig. 6.6 Bockovci area - Residual Risk matrix

Risk registers for Bockovac area is based on the current project assumptions. As indicating based on the risk matrix, Bockovac area has a positive risk assessment, if mitigation actions will be successfully done. Well integrity of legacy wells and proximal faults have the highest risk, and their mitigation are crucial for overall success of the project.

Risk register is the live document. Needs to be updated in the future as project develops and additional risk or their understanding is recognized.

Copyright © SLB. All Rights Reserved. Private & Confidential. Reproduction only by permission.

6.2 Near-Surface (Groundwater and Soil Gas) Monitoring Plan

A monitoring plan is in development stages and will be provided to the CHA Project Administrator upon completion. This section is subject to change based on the consultant's final conclusions and the CHA Administrator's approval.

Groundwater monitoring wells will be drilled and constructed for the purpose of monitoring near-surface water. These wells will be drilled in and around the injection site and monitored on a scheduled basis. The sampling and monitoring program will be designed based on Project phase (pre-injection, injection, and post-injection). Table 6.7 summarizes a monitoring program by Project phase and is subject to change based on CHA's final assessment.

Table 6.7 Baseline (Pre-injection), Operational, and Post-operational Monitoring

Monitoring Type	Baseline (Pre-injection)	Operational (Injection)	Post-operational
Soil Monitoring			
Shallow Monitor Wells	Duration: 1 year Frequency: Quarterly	Duration: During Injection Frequency: Annual	Duration: 5 years Frequency: Annual
Water Monitoring			
Existing Freshwater Wells	Duration: 1 year Frequency: Quarterly	Duration: During Injection Frequency: Annual	Duration: 5 years Frequency: Annual
Lowest Most USDW (Underground source of drinking water) Formation	Duration: 1 year Frequency: Quarterly	Duration: During Injection Frequency: Annual	Duration: 5 years Frequency: Annual

Near-Surface Groundwater and Soil Gas Sampling and Monitoring

It is recommended to engage an environmental consultant, to develop a near-surface groundwater and soil gas sampling and monitoring program. The program will include the acquisition of baseline air and soil gas samples in which to compare future test results, and an appropriate sampling and monitoring program throughout all phases of the Project life (development and pre-injection, operation or injection, and post-injection). Testing parameters will be included in the program and will be conducted in accordance with ASTM standard procedures for soil gas sampling and analysis (Standard Guide for Soil Sampling from the Vadose Zone (astm.org)).

Upon completion of the near-surface groundwater and soil gas sampling and monitoring plan, the program will be submitted to the CHA Project Administrator with accompanying documentation and figures.

6.2.1 Groundwater Baseline Sampling

Groundwater sampling and analyses will be conducted to establish baseline concentrations. These will be taken from multiple locations in and around the injection site over the course of several months to account for seasonal fluctuations. All analyses will be conducted in accordance with Advancing Standards Transforming Markets (ASTM) standard procedures to determine pH, SpC and alkalinity (to be summarized in Table 6.8).

Copyright © SLB. All Rights Reserved. Private & Confidential. Reproduction only by permission.

Groundwater baseline sampling will be conducted at the time of drilling and construction of the proposed injection wells and shallow water monitoring wells. Sampling and analysis parameters, sampling locations, and a sampling schedule will be determined as part of the future hydrogeological work that the operator will need to perform. Recommended duration and frequency of the sampling schedule is given in the table Table 6.7.

Table 6.8 Baseline Groundwater Sampling Results

Parameter	pH (s.u.)			SpC, mS/cm			Alkalinity as $CaCO_3$, mg/L		
Well No.	Date	Date	Date	Date	Date	Date	Date	Date	Date
TBC									

6.2.2 Soil Gas Baseline Sampling

Soil gas sampling and analyses will be conducted to establish baseline concentrations. These will be taken from multiple locations in and around the injection site over the course of several months to account for seasonal fluctuations. All analyses will be conducted in accordance with ASTM standard procedures to determine concentrations of CO_2(and its isotopes), O_2, and N_2 (summarized in Table 6.9).

Soil gas baseline sampling will be conducted at the time of drilling and construction of the proposed injection well. Sampling and analysis parameters, sampling locations, and a sampling schedule will be determined as part of the future hydrogeological work that the operator will need to perform. Recommended duration and frequency of the sampling schedule is given in the table Table 6.7.

Table 6.9 Soil Gas Sampling Results

Parameter	CO_2, %			O_2, %			N_2, %		
Sample No.	Date	Date	Date	Date	Date	Date	Date	Date	Date
TBC									

6.3 Surface Leak Detection and Monitoring Plan

All surface components of CHA CO_2 storage location (wellheads, CO_2 transport pipelines, and other associated equipment) will be monitored using CO_2 leak detection equipment. CO_2 detectors will be installed at the wellhead, pipeline, and along other key sites from the point of capture to injection. Leak detection equipment will be monitored continuously and include automated warning systems. This system will be inspected on a regularly scheduled basis (monthly or if any irregularities are noticed).

Surface and aerial patrols of the storage complex and CO_2 pipeline will be conducted at regular intervals (usually monthly or if some subsurface irregularities are noticed) to inspect conditions on or adjacent to all disturbances (safety, pipeline exposure or any specific conditions (ex. crossings)) related to the Project. Inspection logs and records will be kept and maintained until site closure and made available upon request. Any detected surface leaks shall be immediately reported.

Copyright © SLB. All Rights Reserved. Private & Confidential. Reproduction only by permission.

6.4 Subsurface Leak Detection and Monitoring Plan

Groundwater quality and geochemical changes above the confining zone during the operation period will be monitored. Groundwater quality, geochemical changes, and pressures in the first Underground Source of Drinking Water (USDW) immediately above the injection zone will also be monitored. The groundwater monitoring plan focuses on the following zones:

Three monitoring wells, M-1, M2, and M3 are required.

- The shallow groundwater (source of local drinking water).
- Shallow undifferentiated sands – the lowermost USDW.
- The first permeable zone above the confining zone.

Table 6.10 shows the planned monitoring methods, locations, and frequencies for groundwater quality and geochemical monitoring above the confining zone.

Table 6.10 Monitoring for Groundwater Quality and Geochemical Modeling

Target Formation	Monitoring Activity	Monitoring Location	Spatial Coverage	Frequency[1-5]
Base of USDW	Fluid sampling	M-2	1 point location	Baseline; Year 0 to 2: Quarterly Year 3 to Injection Cessation: Annual Year 3 to 5 Years Post Injection: Annual
First Permeable Zone Above the Confining Zone	Fluid sampling	M-2	1 point location	Baseline; Year 1 to Injection Cessation: Annual
	Pulsed Neutron, Pressure, Temperature	M-2	Survey Log	Baseline; Year 0 to 1.5: Quarterly Year 1.5 through Injection Period: Annual

Notes:

1. Baseline sampling and analysis will be completed before the injection is authorized.
2. Quarterly sampling will take place each year (3, 6, 9, and 12 months after the injection authorization date).
3. Semi-annual sampling will be performed each year (6 and 12 months after the injection authorization date).
4. Annual sampling will occur up to 45 days before the injection authorization anniversary date each year.
5. Changes to the groundwater monitoring frequency will be submitted to the competent authority for prior approval.

The M-2 monitoring well will be placed at a distance and direction from the injection well to optimize verification and calibration of the reservoir AoR delineation model and monitor plume migration. The distance and direction of the monitoring well will be where the reservoir AoR

Copyright © SLB. All Rights Reserved. Private & Confidential. Reproduction only by permission.

delineation model shows detectable pressure changes and a CO_2 saturation of 10% within approximately five years. The well will be instrumented with pressure and temperature gauges for continuous monitoring. Pressure, temperature, and acoustic monitoring will provide early warning of parameters outside the predicted model and operational limits. Including micro seismic events near the injection site. In addition, the M-2 monitoring well will have sampling capability of the USDW. The lowest formation with USDW will be verified with formation sampling during the drilling and construction of the proposed injection well.

This testing and monitoring plan and the Quality Assurance and Surveillance Plan (QASP) detail the continuous pressure, temperature, and acoustic monitoring of the injection and monitoring wells, and periodic sampling and well logging used to ensure safe operation and storage of the injected CO_2. The testing and monitoring plan and the QASP will provide early warning of any operational or well integrity problems and ensure USDW non-endangerment.

Pulsed neutron can make several different measurements sensitive to CO_2 in the formation and in the casing-formation annulus. Therefore, pulsed neutron can be used to monitor the formation fluids as well as identify mechanical integrity problems that may allow the CO_2 to migrate up the casing annuli.

6.5 Plume Monitoring Methods

6.5.1 Direct Monitoring Methods

The direct monitoring methods that will be employed to track the extent of the CO_2 plume will include temperature and pressure gauges installed on the injection and monitor wells. Temperatures and pressures will be continuously monitored to gauge the performance of the geologic storage complex and provide insight and early warning should there be unexpected migration of fluids outside the storage reservoir. Early detection can provide sufficient time to react accordingly and implement necessary mitigation strategies to ensure fluids do not migrate and breach the USDW or surface.

6.5.2 Indirect Monitoring Methods

Indirect monitoring methods to observe the CO_2 plume extent within the geologic storage complex include time-lapse seismic geophysical surveys (4D seismic) of the AoR. 4D seismic provides a measurement of change in fluid compressibility. A combination of 3D and 4D seismic methods can be effective tools for measuring the CO_2 plume movement in the reservoir.

An existing 3D survey will provide baseline conditions for the injection zone. A repeat 4D seismic survey will be conducted approximately one year prior to injection cessation for comparison to determine the extent of the CO_2 plume within the AoR, and confirmation of simulation predictions. A repeat 4D seismic survey will take place five years post-injection to confirm plume stabilization.

Copyright © SLB. All Rights Reserved. Private & Confidential. Reproduction only by permission.

6.6 Monitoring Technologies

Site monitoring provides verification that there is no leakage and assurance that everything is working as planned. There are a number of considerations that monitoring technologies aim to satisfy.

- Monitoring of injection rate, wellhead pressure, annulus pressure, injection pressure, injected volume and annulus fluid volume.
- Corrosion monitoring of injection well materials, required on a quarterly basis
- Monitoring of material corrosion, not to exceed once every five years.
- Demonstration of no pressure increase, or fluid composition change of permeable zones above the injection reservoir and of USDW closer to surface.
- Adequate quantity and location of monitoring wells must be demonstrated based on information about the specific CCS project, including injection rate and volume, geology, the presence of artificial penetrations and other factors.

The developed MMV plan includes:

- The frequency of data acquisition,
- A record keeping plan,
- The frequency of instrument calibration,
- Roles and responsibilities of all involved in the process, and
- Quantification of CO_2 emissions/injection.

All monitoring approaches have sensitivity and accuracy limitations. For example, for seismic methods, specific reservoir characteristics (tight rock) and the resolution available in that method may not be sufficient for quantifying the mass of CO_2 in the storage reservoir with the level of accuracy that is required.

Multiple monitoring approaches are needed to confirm CO_2 containment, and the chosen approaches should be rationally defended with consideration of sensitivity and accuracy. We recommend that monitoring plans be considered living documents insofar as improvements in monitoring technologies are expected over time, and the plans should allow for substitutions to improve the efficiency of the quality measurements in the future.

Monitoring technologies have each been assigned a Technical Maturation value, which is defined by the performance and track record of the technology to achieve the monitoring goal of a specific monitoring task. The assigned technical maturation values are provided in Table 6.12to Table 6.20 are based on the following framework.

- Technologies that had yielded satisfactory results from previous CCS projects (such as 4D seismic) will yield high scores from 0.8
- Technologies that had yielded satisfactory results from previous CCS projects but with limited coverage (such as downhole pressure/temperature gauges, which are a point

Copyright © SLB. All Rights Reserved. Private & Confidential. Reproduction only by permission.

measurement) will yield a score from 0.5 to 0.7

- And those technologies that yield good results in other applications, such as in the oil and gas industry, but have not yet been applied to CCS projects, which will yield a score from 0.4 to 0.5 (such as DSS, EMIT)
- Technologies applied to CCS projects with poor performance or large limitations (such as CSEM and gravity, which were applied to Sleipner), or the interpretation of their measurements could yield ambiguity, will give low scores from 0.2 to 0.4

Table 6.11 shows the identified monitoring tasks from the risk analysis exercise and will be further described in the following chapters where suitable monitoring technologies will be selected for each task.

Table 6.11 The Monitoring Tasks Identified from Risk Analysis

Task No.	Task Title	Category
M1	Geophysical monitoring for conformance	Reservoir Monitoring
M2	Geophysical monitoring for induced seismicity	Reservoir Monitoring
M3	Downhole monitoring for containment and well integrity	Well Monitoring
M4	Downhole logging for well integrity	Well Monitoring
M5	Downhole monitoring for conformance	Well Monitoring
M6	Land environmental monitoring	Land & Environment Monitoring
M7	Downhole monitoring for borehole blockage	Well Monitoring
M8	Detect wellbore instability	Well Monitoring
M9	CO_2 fingerprint	Land & Environment Monitoring

6.6.1 Monitoring Technologies for Identified Monitoring Tasks

Fig. 6.7 is showing MMV technologies scoring steps. The first step is to list available technologies for identified monitoring tasks and create an average score of technical maturation of the monitoring technology. We need also to consider the operational efficiency and define a final score from 1 to 5.

Copyright © SLB. All Rights Reserved. Private & Confidential. Reproduction only by permission.

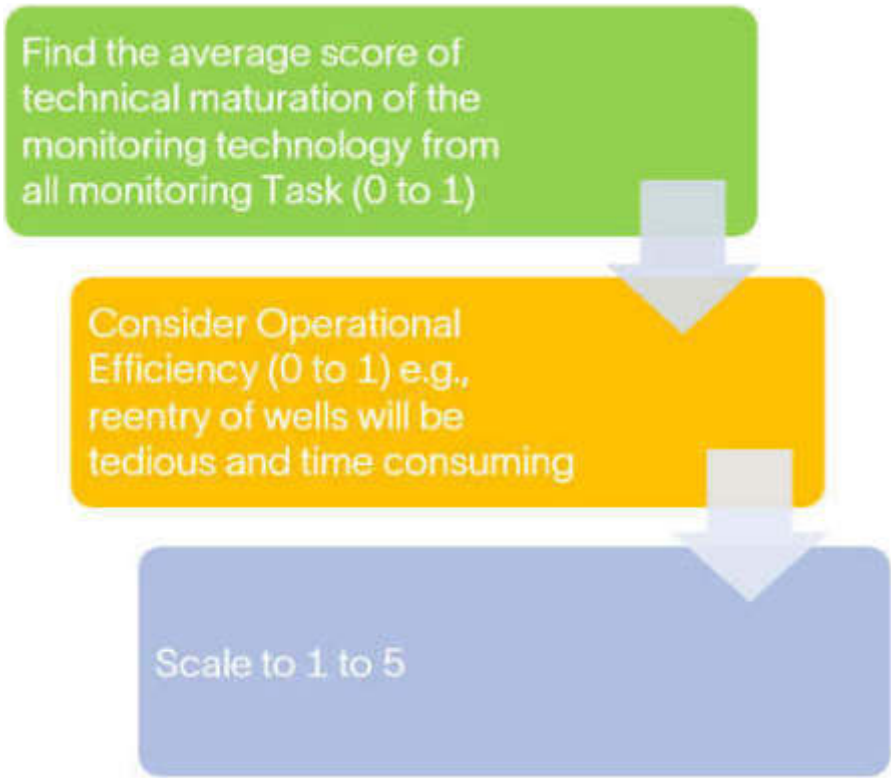


Fig. 6.7 MMV Technologies Scoring Steps

Fore each monitoring task Table 6.12, Table 6.13Table 6.14, Table 6.15, Table 6.16, Table 6.17, Table 6.18, Table 6.19, and Table 6.20 are listing considered technologies with a score.

Table 6.12 Table with scoring for M1: Geophysical monitoring for conformance

Monitoring Task	Monitoring Sub-task	Monitoring System	Indicator	Purpose	Code	Technical Maturation (Scale 0 to 1)	Cost (Scale 1 to 5)
M1	M1: Reservoir geophysical monitoring for conformance						
	M1.1	Time-lapse seismic	Appearance of a reliable amplitude anomaly that is beyond prediction	Detect CO_2 plume migration	SEIS4D	0.7	5
	M1.2	Time-lapse 3D VSP (DAS or geophone)	Appearance of a reliable amplitude anomaly in locality of the data acquisition well	Detect CO_2 plume migration	VSP4D	0.6	3
	M1.3	Time-lapse cross-well seismic	Appearance of amplitude abnormally across two wells	Detect CO_2 plume migration	SEISXW	0.3	3
	M1.4	Time-lapse marine microgravity	Appearance of a reliable lower gravity that is beyond prediction	Detect CO_2 plume migration	SGRAV	0.3	3
	M1.5	Time-lapse marine Controlled Source Electromagnetics (CSEM)	Appearance of a reliable low resistivity anomaly that is beyond prediction	Detect CO_2 plume migration	CSEM	0.2	4
	M1.6	Time-lapse cross-well Electromagnetics	Appearance of a reliable low resistivity anomaly that is beyond prediction	Detect CO_2 plume migration	EMXW	0.2	3

Copyright © SLB. All Rights Reserved. Private & Confidential. Reproduction only by permission.

Table 6.13 Table with scoring for M2: Geophysical monitoring for induced seismicity

Monitoring Task	Monitoring Sub-task	Monitoring System	Indicator	Purpose	Code	Technical Maturation (Scale 0 to 1)	Cost (Scale 1 to 5)
M2	M2: Reservoir geophysical monitoring for induced seismicity						
	M2.1	Passive seismic monitoring with geophone from well	Significant increase of microseismic events appear in a pattern distribution	Detection and location of microseismic events	SMS-GEO	0.7	5
	M2.2	Passive seismic monitoring with DAS from well	Significant increase of microseismic events appear in a pattern distribution	Detection and location of microseismic events	SMS-DAS	0.7	3
	M2.3	Seismic monitoring at surface with broadband seismometers	Detection of high magnitude seismicity	Detection and location of high magnitude seismic events	SMS-SM	0.5	2

Table 6.14 Table with scoring for M3: Downhole monitoring for containment and well integrity

Monitoring Task	Monitoring Sub-task	Monitoring System	Indicator	Purpose	Code	Technical Maturation (Scale 0 to 1)	Cost (Scale 1 to 5)
M3	M3: Downhole monitoring for containment and well integrity						
	M3.1	Mechanical well integrity testing	Inability to sustain applied pressure within the zone of the packer	Well integrity evaluation	MWIT	0.8	2
	M3.2	Annulus pressure monitoring at wellhead	Sustained annular pressure increase	Well integrity evaluation	APM	0.7	1
	M3.3	DTS	Sustained temperature anomaly migrating upwards above the first seal	Well integrity evaluation and containment evaluation	DTS	0.7	3
	M3.4	DAS	Sustained flow noise migrating upwards above the first seal	Well integrity evaluation and containment evaluation	DAS	0.7	3
	M3.5	Downhole pressure/ temperature gauges within the monitoring well	Appearance of a sustained pressure/temperature increase above the first seal relative to the baseline values	Containment evaluation	DHPT	0.6	1
	M3.6	DSS	Excessive strain that is beyond prediction	Well integrity evaluation and containment evaluation	DSS	0.6	2
	M3.7	DPS	Sustained pressure abnormally migrating upwards above the first seal	Well integrity evaluation and containment evaluation	DPS	0.2	3

Copyright © SLB. All Rights Reserved. Private & Confidential. Reproduction only by permission.

Table 6.15 Table with scoring for M4: Downhole logging for well integrity

Monitoring Task	Monitoring Sub-task	Monitoring System	Indicator	Purpose	Code	Technical Maturation (Scale 0 to 1)	Cost (Scale 1 to 5)
M4	M4: Downhole logging for well integrity						
	M4.1	Isolation Scanner	Appearance of gas/water channel or corrosion of casing from the log	Cement bond and casing measurements	IST	0.8	2
	M4.2	EM Pipe Scanner (EMIT)	Appearance of corrosion in the tubing and casing from the log	Identification of casing corrosion behind tubing	EMIT	0.4	2
	M4.3	Epilogue Isolation (combined Isolation Scanner and Sonic Scanner)	Appearances of poor bonding in B-annulus	Simultaneously evaluate the A- and B-annulus to reduce plug and abandonment (P&A) costs	EPLG	0.4	2

Table 6.16 Table with scoring for M5: Downhole monitoring for conformance

Monitoring Task	Monitoring Sub-task	Monitoring System	Indicator	Purpose	Code	Technical Maturation (Scale 0 to 1)	Cost (Scale 1 to 5)
M5	M5: Downhole monitoring for conformance						
	M5.1	Time-lapse cased hole logging for CO_2 saturation (RST or Pulsar)	Abnormal CO_2 saturation from the cased hole log	CO_2 saturation measurement	RST	0.8	1
	M5.2	Downhole pressure/ temperature gauges within the monitoring well	Abnormal pressure/ temperature in the monitoring well	Detect the timing when CO_2 plume reaches the monitoring well	DHPT	0.7	1
	M5.3	DTS	Abnormal temperature profile in the monitoring well	Detect the timing when CO_2 plume reaches the monitoring well	DTS	0.6	3
	M5.4	DPS	Abnormal pressure profile in the monitoring well	Detect the timing when CO_2 plume reaches the monitoring well	DPS	0.3	3

Table 6.17 Table with scoring for M6: Land environmental monitoring

Monitoring Task	Monitoring Sub-task	Monitoring System	Indicator	Purpose	Code	Technical Maturation (Scale 0 to 1)	Cost (Scale 1 to 5)
M6	M6: Land environmental monitoring						
	M 6.1	LIDAR CO_2 gas flux monitoring	Abnormal CO_2 saturation in atmosphere within AOR	Detect CO_2 leakage	LIDAR	0.6	2
	M 6.2	Atmospheric eddy correlation	Sustained localized increase in CO_2 flux exceeding established background variability	Detect CO_2 leakage at surface or in the air	EDDY	0.2	3

Copyright © SLB. All Rights Reserved. Private & Confidential. Reproduction only by permission.

Table 6.18 Table with scoring for M7: Downhole monitoring for borehole blockage

Monitoring Task	Monitoring Sub-task	Monitoring System	Indicator	Purpose	Code	Technical Maturation (Scale 0 to 1)	Cost (Scale 1 to 5)
M7	M7: Downhole monitoring for borehole blockage						
	M7.1	Wellhead injection pressure/temperature monitoring	Abnormal surface injection pressure increase	Detect borehole blockage	IPM	0.8	1
	M7.2	Downhole pressure gauges within the injector	Abnormal lower pressure at the bottom of the injector	Detect borehole blockage	DHPT	0.7	1
	M7.3	DTS	Abnormal injection profile from time-lapse temperature profile	Detect borehole blockage	DTS	0.6	3
	M7.4	Downhole camera logging	Blockage of perforation tunnels	Detect borehole blockage	CAM	0.6	2
	M7.5	DAS	Abnormal injection profile from flow noise	Detect borehole blockage	DAS	0.5	3
	M7.6	DPS	Abnormal injection profile from pressure	Detect borehole blockage	DPS	0.5	3

Table 6.19 Table with scoring for M8: Detect wellbore instability

Monitoring Task	Monitoring Sub-task	Monitoring System	Indicator	Purpose	Code	Technical Maturation (Scale 0 to 1)	Cost (Scale 1 to 5)
M8	M8: Detect wellbore instability						
	M8.1	LWD caliper log	Abnormal borehole diameters	Detect borehole failure in real-time	LWDCAL	0.9	1
	M8.2	LWD ECD	Abnormal equivalent circulating density (ECD)	Detect suspension of cuttings in drilling fluid	LWDECD	0.4	1
	M8.3	LWD Torque	Abnormal downhole torque	Detect rugosity of wellbore	LWDTOR	0.3	1

Table 6.20 Table with scoring for M9: CO_2 fingerprint

Monitoring Task	Monitoring Sub-task	Monitoring System	Indicator	Purpose	Code	Technical Maturation (Scale 0 to 1)	Cost (Scale 1 to 5)
M9	M9: CO_2 fingerprint						
	M9.1	CO_2 fingerprint	Similarity of isotope of C, O (such as δ13C) between feedstock CO_2 and collected CO_2 at surface	Characterization of injected CO_2 to allow distinguishing between naturally occurring CO_2 and/or CO_2 injected by third parties	FGPT	0.8	2
	M9.2	Artificial tracer measurement	Artificial tracer identified from the surface or near surface	Characterization of reservoir leakage	ATM	0.7	3
	M9.3	Natural isotope tracer monitoring	Tracer unique to reservoir brine is detected within USDW or other water samples	Leak detection & impact assessment	NTM	0.2	3

Fig. 6.8 is showing histograms (level indicate Technical Maturation (Scale 0 to 1) from tables Table 6.12 to Table 6.20) with technologies and selected ones. Technologies in blue are considered less mature or too costly with alternatives that could provide necessary information.

Copyright © SLB. All Rights Reserved. Private & Confidential. Reproduction only by permission.

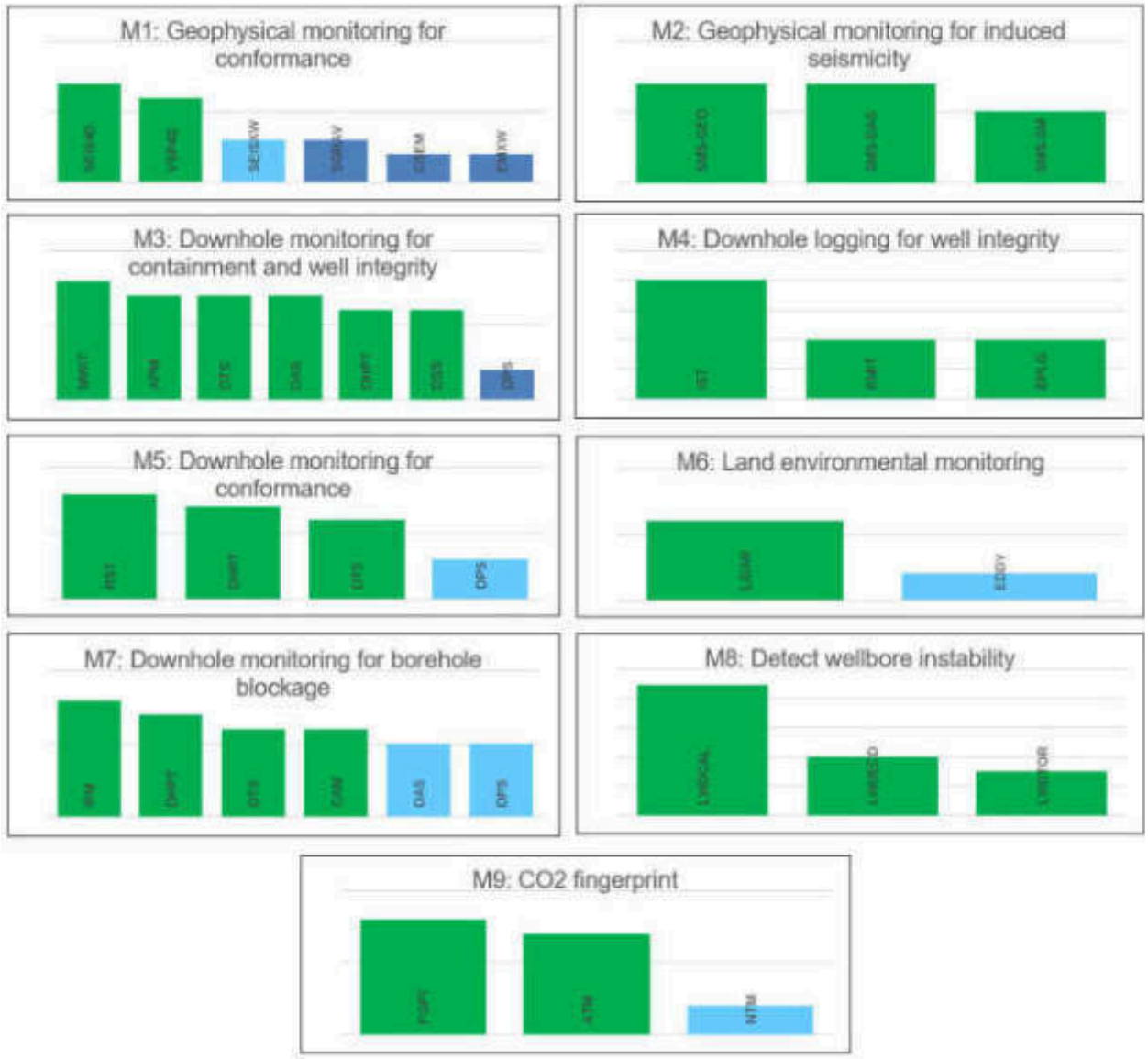


Fig. 6.8 MMV Methodology Selection

6.6.2 Monitoring Technologies Screening

To perform monitoring technologies screening, a Boston Square chart (Product Portfolio Model) was used. Benefit defined in Boston Square chart is the lifecycle benefit of the specific monitoring technology in a semi-quantitative sense. It is derived from technical maturation and with consideration of operational efficiency.

More than 30 technologies are considered

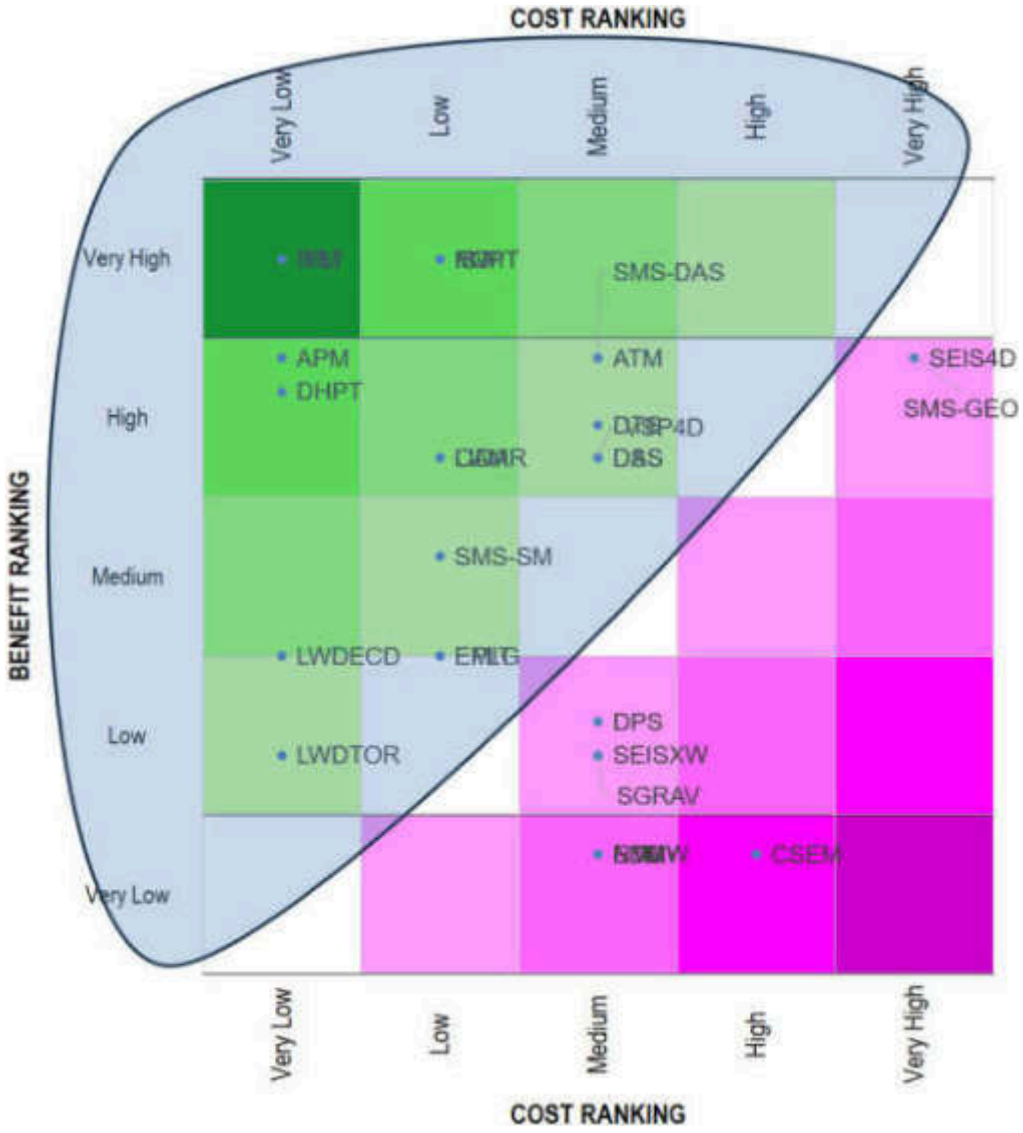
- Geophysical
- Downhole

Copyright © SLB. All Rights Reserved. Private & Confidential. Reproduction only by permission.

- Surface/environmental

Cost is just based on a nominal expected lifetime cost and is discretized from a nominal value of 1 to 5 from an expert perspective. More detailed cost information must be done after more detailed conceptual design in a later stage.

The results are illustrated in a Boston square . It is an iterative process and there is no clear-cut between selected vs. regretted as some monitoring technologies have been selected based on regulations or site-specific challenges.



Boston Square

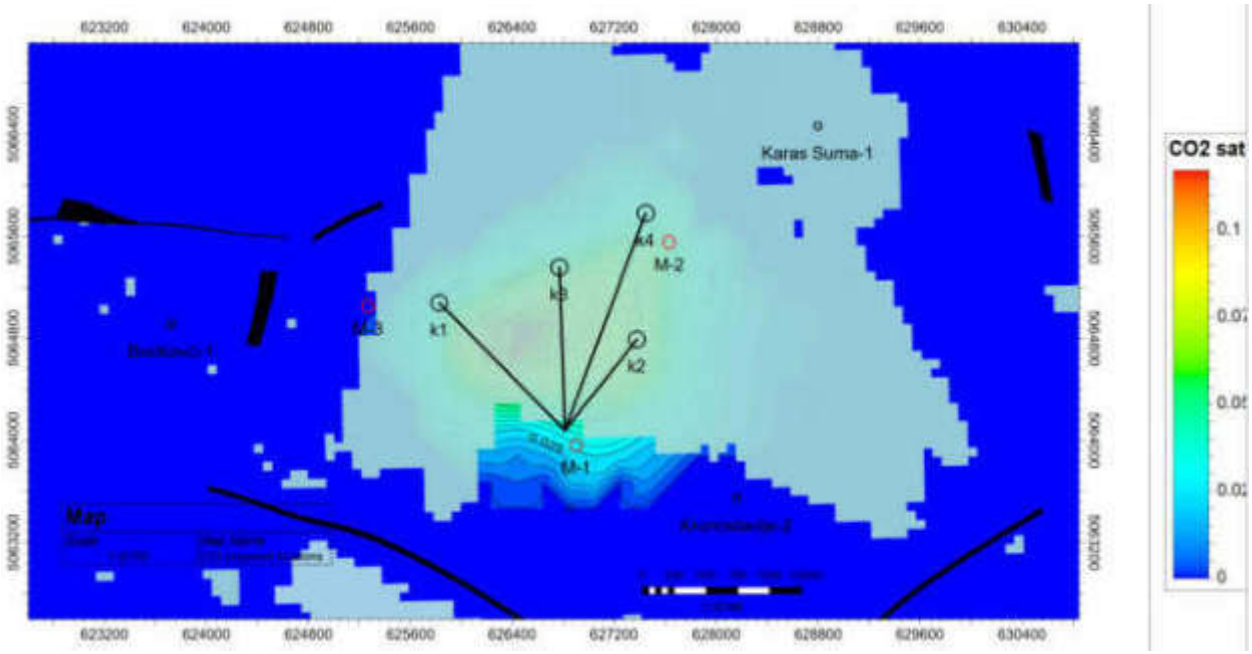
Copyright © SLB. All Rights Reserved. Private & Confidential. Reproduction only by permission.

6.6.3 Monitoring Technologies Selection

Based on risk assessment and monitoring tasks, monitoring technologies identification and their screening, the final technologies are selected. Target monitoring zones are:

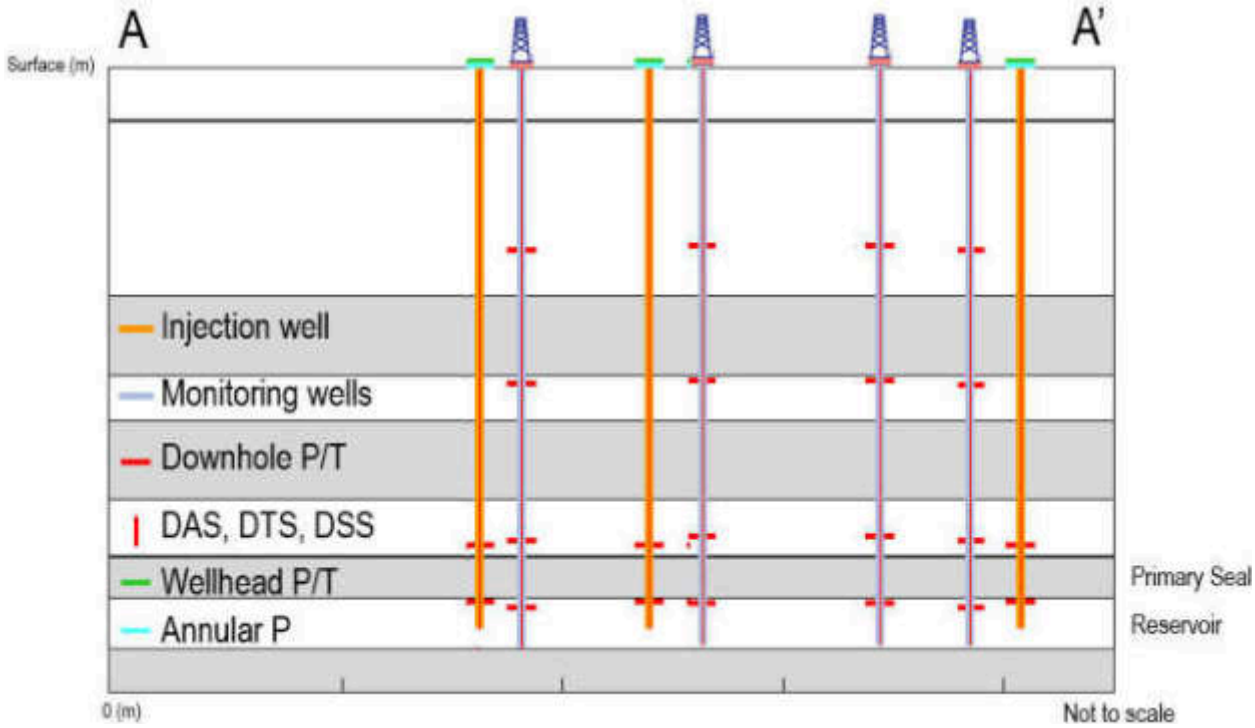
- Type 1 – Cap rock sealing (M1, M2, and M3)
- Type 2 – Field lateral boundaries/barriers sealing (M1, and M3)
- Type 3 – Confirmation of CO_2/temperature/pressure reservoir propagation (M1, M2, and M3)

is showing a structural map indicating target monitoring locations. is showing a cross-section with injection and monitoring wells conceptual monitoring requirements. Table 6.21 is showing the summary of monitoring technologies with a final selection that is planned for Bockovci area.



Monitoring wells location
- Isolines represent CO2 saturation
- k1, k2, k3, and k4 represent injection wells
- M1, M2 and M3 represent monitoring wells
- Gray polygon represent the forest (surface) area

Copyright © SLB. All Rights Reserved. Private & Confidential. Reproduction only by permission.



Cross-section with Injection and monitoring conceptual monitoring requirements

Copyright © SLB. All Rights Reserved. Private & Confidential. Reproduction only by permission.

Table 6.21 Monitoring technologies summary with a final selection

Category	Selected from Initial Screening	Task	Monitoring Technology	Code	Information Gained	Availability	Coverage	Maximum Technical Maturation	Count	Average	Benefit Ranking Scale (1-5)	Cost Ranking Scale (1-5)	Column1
Geophysical	Yes	M1	Time-lapse 3D vertical seismic profiling (DAS) (4D VSP)	VSP4D	3D distribution of CO_2 plume	On demand	Within 1km of the wellbore	0.60	1	0.6	3.8	3	Performance
Geophysical	Yes	M1	Time-lapse surface 3D seismic (4D Seismic)	SEIS4D	3D distribution of CO_2 plume	On demand	Entire CO_2 plume	0.70	1	0.7	4.4	5	Performance
Geophysical	Yes	M2	Passive microseismic monitoring with DAS	SMS-DAS	Microseismic catalogue	Continuously, or on demand	<1000m from the monitoring well	0.70	1	0.7	4.4	3	Containment
Geophysical	Yes	M2	Passive microseismic monitoring with geophone	SMS-GEO	Microseismic catalogue	Continuously, or on demand	<1000m from the monitoring well	0.70	1	0.7	4.4	5	Containment
Geophysical	Yes	M2	Seismic monitoring at surface with broadband seismometers	SMS-SM	Earthquake catalogue	Continuously, or on demand	AOR	0.50	1	0.5	3.1	2	Containment
Geophysical	No	M1	Time-lapse surface microgravity	SGRAV	Areal distribution of CO_2 plume	On demand	Entire CO_2 plume	0.30	1	0.3	1.9	3	Performance
Geophysical	No	M1	Time-lapse surface controlled source EM	CSEM	Spatial distribution of CO_2 plume	On demand, winter only	Entire CO_2 plume	0.20	1	0.2	1.3	4	Performance
Well Monitoring	No	M1	Time-lapse cross-well controlled source EM	EMXW	Cross-well distribution of CO_2 plume	On demand	Section between wells within a circle of 500m	0.20	1	0.2	1.3	3	Performance
Well Monitoring	No	M1	Time-lapse cross-well seismic	SEISXW	2D distribution of CO_2 plume	On demand	Section between wells within a circle of 500m	0.30	1	0.3	1.9	3	Performance
Well Monitoring	Yes	M4	Time-lapse ultrasonic casing imaging (Isolation Scanner)	IST	Cement bond and casing corrosion detection	After cementing and yearly well integrity evaluation	Injection and monitoring wells	0.80	1	0.8	5.0	2	Containment

Copyright © SLB. All Rights Reserved. Private & Confidential. Reproduction only by permission.

Category	Selected from Initial Screening	Task	Monitoring Technology	Code	Information Gained	Availability	Coverage	Maximum Technical Maturation	Count	Average	Benefit Ranking Scale (1-5)	Cost Ranking Scale (1-5)	Column1
Well Monitoring	Yes	M4	Time-lapse EM casing imaging (EM Pipe Scanner)	EMIT	Casing corrosion detection	During well intervention	Injection, monitoring and legacy wells	0.40	1	0.4	2.5	2	Containment
Well Monitoring	Yes	M4	Epilogue Isolation (combined Isolation Scanner and Sonic Scanner)	EPLG	Tubing and casing corrosion detection	During well intervention	Injection, monitoring and legacy wells	0.40	1	0.4	2.5	2	Containment
Well Monitoring	Yes	M5	Time-lapse cased hole logging for CO_2 saturation (RST or Pulsar)	RST	CO_2 saturation	On Demand	Injection and monitoring wells	0.80	1	0.8	5.0	1	Performance
Well Monitoring	Yes	M3	Fibre-optic distributed temperature sensing (DTS)	DTS	Leak detection outside casing	Continuously	Injection and monitoring wells	1.90	3	0.63	4.0	3	Containment
Well Monitoring	No	M3	Fibre-optic distributed pressure sensing (DPS)	DPS	Leak detection outside casing	Continuously	Many discrete locations Downhole	1.00	3	0.33	2.1	3	Containment
Well Monitoring	Yes	M3	Fibre-optic distributed acoustic sensing (DAS)	DAS	Leak detection outside casing	Continuously	Injection and monitoring wells	1.20	2	0.6	3.8	3	Containment
Well Monitoring	Yes	M3	Fibre-optic distributed acoustic sensing (DSS)	DSS	Exessive strain and possible failure of cement	Continuously	Injection and monitoring wells	0.60	1	0.6	3.8	3	Containment
Well Monitoring	Yes	M3	Annulus pressure monitoring	APM	Pressure leak detection	Continuously	Injection wells	0.70	1	0.7	4.4	1	Containment
Well Monitoring	Yes	M3	Downhole pressure-temperature gauge	DHPT	Downhole pressure, temperature	Continuously	Injection and monitoring wells	2.00	3	0.67	4.2	1	Performance, containment
Well Monitoring	Yes	M3	Mechanical well integrity pressure testing	MWIT	Leak detection	On demand	Injection wells	0.80	1	0.8	5.0	2	Containment

Copyright © SLB. All Rights Reserved. Private & Confidential. Reproduction only by permission.

Category	Selected from Initial Screening	Task	Monitoring Technology	Code	Information Gained	Availability	Coverage	Maximum Technical Maturation	Count	Average	Benefit Ranking Scale (1-5)	Cost Ranking Scale (1-5)	Column1
Well Monitoring	Yes	M7	Downhole camera logging	CAM	Blockage detection within wellbore and the perforation	On demand	Injection wells	0.60	1	0.6	3.8	2	Performance
Containment	Yes	M9	Artifical tracer measurement	ATM	Leak detection & CO_2 conformance	On demand	Monitoring wells	0.70	1	0.7	4.4	3	Containment
Containment	No	M9	Natural isotope tracer monitoring	NTM	Leak detection & CO_2 conformance	On demand	Monitoring wells	0.20	1	0.2	1.3	3	Containment
Well Monitoring	Yes	M8	LWD caliper log	LWDCAL	Borehole over-gauge detection	On demand	Injection and monitoring wells	0.90	1	0.9	5.6	1	Containment
Well Monitoring	Yes	M8	LWD ECD	LWDECD	Detect suspension of cuttings in drilling fluid	On demand	Injection and monitoring wells	0.40	1	0.4	2.5	1	Containment
Well Monitoring	Yes	M8	LWD Torque	LWDTOR	Detect rugosity of wellbore	On demand	Injection and monitoring wells	0.30	1	0.3	1.9	1	Containment
Environmental Monitoring	Yes	M6	LIDAR CO_2 gas flux monitoring	LIDAR	CO_2 leakage rate to atmosphere	On demand	Areal coverage over parts of AOR	0.60	1	0.6	3.8	2	Containment
Environmental Monitoring	Yes	M6	Atmospheric eddy correlation	EDDY	CO_2 leakage rate to atmosphere	Continuously	Discrete locations across AOR	0.20	1	0.2	1.3	3	Containment
Well Monitoring	Yes	M7	Wellhead injection pressure/temperature monitoring	IPM	Anomaly of surface injection pressure increase	Continuously	Injection wells	0.80	1	0.8	5.0	1	Performance

Copyright © SLB. All Rights Reserved. Private & Confidential. Reproduction only by permission.

Category	Selected from Initial Screening	Task	Monitoring Technology	Code	Information Gained	Availability	Coverage	Maximum Technical Maturation	Count	Average	Benefit Ranking Scale (1-5)	Cost Ranking Scale (1-5)	Column1
Environmental Monitoring	Yes	M9	CO_2 fingerprint	FGPT	Source of CO_2	On demand	Areal coverage over parts of AOR	0.80	1	0.8	5.0	2	Containment
Environmental Monitoring	No	M9	Natural isotope tracer monitoring	NTM	Surface CO_2 leakage detect and impact assessment	On demand	Monitoring well or surface samples	0.20	1	0.2	1.3	3	Containment

Copyright © SLB. All Rights Reserved. Private & Confidential. Reproduction only by permission.

6.7 Monitoring Plan

The following assumptions are made for MMV planning:

- Injection time span is 30 years starts from 2027
- Post-injection phase is 30-50 years before handing over to designated third party
- Some required monitoring activities are likely to continue in post-injection phase per the regulatory norm in other jurisdictions.

Fig. 6.9 shows a MMV plan. The plan covers all three project phases (pre-injection, injection and post-injection). Timescale in the bottom indicate zero as start of injection moment, and indicate measurements that need to be created before (baseline) injection and after. Solid timeline (dark gray) in the figure indicates continuous measurements (ex. Monitoring wells: Downhole P/T), while dashed (dark/light gray) timeline indicates measurements that should be done demand without a fixed time (measurement time can be shifted if deemed necessary as a result of corrective actions).

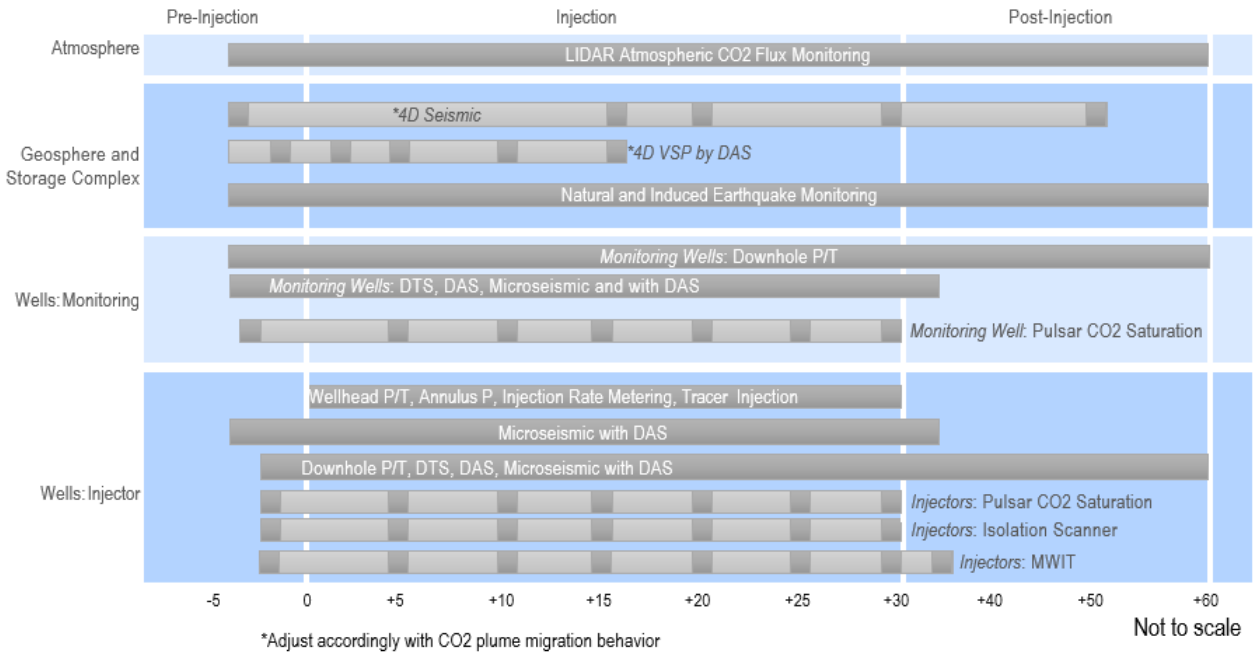


Fig. 6.9 MMV Plan

6.8 Emergency Response Plan

The **Emergency Response Plan (ERP)** is a critical element of the project's HSE framework, ensuring preparedness for potential incidents and demonstrating a proactive approach to risk management. It also plays an important role in building stakeholder confidence by providing assurance that appropriate measures are in place to protect people, the environment, and project assets.

Copyright © SLB. All Rights Reserved. Private & Confidential. Reproduction only by permission.

At the current concept and feasibility stage, a detailed Emergency Response Plan cannot yet be fully defined. The ERP should be developed during the subsequent project phases, as part of the preparation for site construction and operations, incorporating site-specific risks, operational procedures, stakeholder requirements, and regulatory obligations. A proposed structure for an ERP report is provided as a separate deliverable.

6.9 Responsibilities

The following matrix of responsibility has been defined, in order to an adequate deployment of the Testing & Monitoring plan

Table 6.22 MMV Roles and Responsibilities

Roles	Responsibility
CCS operation manager	Ensure the Testing & Monitoring Plan is deployed, and sufficient resources are available for its associated task. Evaluate need for additional or adjusted monitoring. Evaluate in CO_2 injection is carried our safety, based on this Monitoring & Testing plan and can be continued
Site operators	Monitoring well parameters (injectivity, pressure, volume...), carry out well integrity tests, monitor annular pressures, etc...
Injection/ reservoir engineer	Establish injection parameters (injectivity, volume, etc...) Monitoring plume extension and expansion as well as all reservoir parameters; identify deviation from reservoir model
Well engineer	Establish well integrity operating envelope for well construction. Plan & execute "in well" operations for monitoring activity, and well's repair. Support Well operator.
Well integrity engineer	Update well integrity operating envelope. Diagnostic abnormal well parameters (annular, integrity test, etc..). Maintain update well integrity status & Data. Support well operator
Geomechanical engineer	Establish geomechanical parameters. Monitoring geomechanical parameters: identify deviation from geomechanical model and adjust monitoring strategy accordingly.
Geologist / Geophysicist	Monitoring geophysical and geological data: identify deviation from model and adjust monitoring strategy accordingly.
Surface monitoring engineer	Coordinate and verify surface monitoring activities; Diagnostic abnormal parameters. Reference is made to the Area surface monitoring
Seismicity engineer	Coordinate and verify seismicity monitoring activities; Diagnostic abnormal parameters. Reference is made to the Seismicity monitoring

Any of the person within the Testing & Monitoring plan have the duty to:

- Identify and diagnostic any abnormal parameters, outside defined boundaries or abnormal trends
- Inform the CCS operation manager and involved all required disciplines in any investigation
- Support multidisciplinary assessment
- Request additional data when necessary

6.10 Monitoring Cost Assessment (High Level)

Monitoring cost was established as per dynamic simulation result (close to injection targets), with cumulative injection volumes of 19.3 Mt, for injection rates of ~0.7 Mt per annum. The unit price is

Copyright © SLB. All Rights Reserved. Private & Confidential. Reproduction only by permission.

based on the best information available (as per year 2024 and will depend on the market situation, exact specifications of instruments, volume of the product and services, and vendors. A more accurate price can be obtained from an open bidding process after more detailed design and specifications are matured at the detailed design stage of the CCS project.

The following costs are not included as they are highly variable

- Mob/demob cost
- Rig and operational support cost for logging and tests
- Downtime or contingency cost
- Administration support

The key influential factors for MMV cost are:

- Regulation maturity
- Injection volume
- Monitoring cost
- Refinement of risk assessment and risk management
- Evolution of the risks

Assuming injection from 2027 to 2057, the yearly cost for monitoring is estimated around 8.72 EUR/Tonne, depending on injection volume (19.3 Mtbased on the latest simulation results). Relatively high yearly monitoring cost is due to the relatively low injected volume. Inability to ensure sustainable injection rates would result in a hike of MMV cost per ton.

shows comparison of each scenario against major known CO_2 injection projects. As it can be seen, there is a direct correlation between the size of the project (injection volume) and monitoring cost. Values around 1.75 EUR/ton (2 USD/ton) is considered as industry acceptable.

Copyright © SLB. All Rights Reserved. Private & Confidential. Reproduction only by permission.

Table 6.23 Bockovci area - MMV Cost Assessment

Category	Task	Monitoring Technology	Code	Availability	Coverage	Unit	Number of Wells/ Sets	Amount/ Times Pre-injection	Amount/ Times During Injection	Amount/ Times During Post-Injection Site Care	Comments	Cost Category	Unit Cost (kEUR)	Direct Cost (kEUR)	Services Fee/Data Processing Cost/ Mantainance Cost (kEUR)	Total Cost (kEUR)
Environmental Monitoring	M9	Artificial tracer measurement	ATM	On demand	Monitoring wells/ surface	Times	2		4		Select 2 injectors and conduct injection and sampling every 5 years.	OPEX	130	1,040	360	1,400
Environmental Monitoring	M9	CO_2 fingerprint	FGPT	On demand	Areal coverage over parts of AOR	Times	1	2	60	50	2 times before injection, 60 times (twice per year) during injection and 50 times (one per year for 50 years) after injection.	OPEX	1.75	196	56	252
Environmental Monitoring	M6	LIDAR CO_2 gas flux monitoring	LIDAR	Continuously	Areal coverage over parts of AOR	Set	2				Permanent install, 2 sets on surface	CAPEX	43	86		86
Environmental Monitoring	M6	AUV (ROTV) with sampling and chemical and acoustic sensors	AUV	On demand	Areal coverage over parts of AOR	Times	1	2	15	5	On demand, expected once every two years for 30 years (also 2 times pre-injection and 5 times post-injection).	OPEX	103	2,266	2640	4,906
Geophysical	M1	Time-lapse 3D vertical seismic profiling (DAS) (4D VSP)	VSP4D	On demand	Within 1km of the wellbore	Times	1	1	7		Acquire 3D VSP with DAS covering an area of 100 km2. Acquisition	OPEX	1032	8,256	3,250	11,506

Copyright © SLB. All Rights Reserved. Private & Confidential. Reproduction only by permission.

Category	Task	Monitoring Technology	Code	Availability	Coverage	Unit	Number of Wells/ Sets	Amount/ Times Pre-injection	Amount/ Times During Injection	Amount/ Times During Post-Injection Site Care	Comments	Cost Category	Unit Cost (kEUR)	Direct Cost (kEUR)	Services Fee/Data Processing Cost/ Mantainance Cost (kEUR)	Total Cost (kEUR)
											timeline (Baseline, Year 2, Y5, Y10, Y15, Y20, Y25, Y30).					
Geophysical	M1	Time-lapse 3D surface seismic (4D Seismic)	SEIS4D	On demand	Entire CO_2plume	Times	1		2	1	Acquire 4D seismic covering an area of 25 km2. Acquisition timeline (Year 15, Year 20, Year 50). The unit price does not include mob/demob, downtime, etc.	OPEX	2580	7,740	12,000	19,740
Geophysical	M2	Passive microseismic monitoring with DAS	SMS-DAS	Continuously, or on demand	<1000m from DAS cable	Set	2	12	360	12	Unit price is per month per set. No interrogator included. Long contract required (>=10 years). A total of 2 sets and 2 injectors as a set. Monthly fee for 12 months before injection, 360 months during injection, and 12 months after injection (not continuously).	OPEX	17	13,056		13,056

Copyright © SLB. All Rights Reserved. Private & Confidential. Reproduction only by permission.

Category	Task	Monitoring Technology	Code	Availability	Coverage	Unit	Number of Wells/ Sets	Amount/ Times Pre-injection	Amount/ Times During Injection	Amount/ Times During Post-Injection Site Care	Comments	Cost Category	Unit Cost (kEUR)	Direct Cost (kEUR)	Services Fee/Data Processing Cost/ Mantainance Cost (kEUR)	Total Cost (kEUR)
Geophysical	M2	Seismic monitoring at surface with broadband seismometers	SMS-OBS	Continuously	AOR	Set	3				Place 3 in AOR	CAPEX	175	525	400	925
Well Monitoring	M4	Time-lapse ultrasonic casing imaging (Isolation Scanner)	IST	On demand	Injection and monitoring wells	Times	7	1	6		All wells (4 injectors and 3 monitor well) after cementing, and every 5 years up to 30 years (well life expectancy, Logging interval 1000m).	OPEX	130	6,370	2310	8,680
Well Monitoring	M4	Time-lapse EM casing imaging (EM Pipe Scanner)	EMIT	During well intervention	Injection, monitoring and legacy wells	Times	10		6		On demand when there is well intervention (considering 6 times in 30 years)	OPEX	130	7,800		7,800
Well Monitoring	M4	Epilogue Isolation (combined Isolation Scanner and Sonic Scanner)	EPLG	During well intervention	Injection, monitoring and legacy wells	Times	10		6		On demand when there is well intervention (considering 6 times in 30 years)	OPEX	250	15,000		15,000
Well Monitoring	M5	Time-lapse cased hole logging for CO_2saturation (RST or Pulsar)	RST	On Demand	Injection and monitoring wells	Times	7	1	6		4 injectors and 3 monitoring wells, every 5 years (1 baseline before injection, 6 times	OPEX	130	6,370	840	7,210

Copyright © SLB. All Rights Reserved. Private & Confidential. Reproduction only by permission.

Category	Task	Monitoring Technology	Code	Availability	Coverage	Unit	Number of Wells/ Sets	Amount/ Times Pre-injection	Amount/ Times During Injection	Amount/ Times During Post-Injection Site Care	Comments	Cost Category	Unit Cost (kEUR)	Direct Cost (kEUR)	Services Fee/Data Processing Cost/ Mantainance Cost (kEUR)	Total Cost (kEUR)
											for injection in 30 years)					
Well Monitoring	M3	Fibre-optics (DTS/ DAS/ DSS) for Injection Wells	DTS/ DAS/ DSS	Continuously	Injection wells	Set	4				Permanent installation for all injector wells, assuming 4000 m length, including DTS, DAS, and DSS fiber and surface units. Additional services fee for one-time installation and one-time data processing.	CAPEX	1550	6,200	10000	16,200
Well Monitoring	M3	Fibre-optics (DTS/ DAS/ DSS) for Monitoring Wells	DTS/ DAS/ DSS	Continuously	Monitoring wells	Set	3				Permanent installation for the monitoring well, assuming 2000 m length.	CAPEX	1550	4,650	500	5,150
Well Monitoring	M3	Annulus pressure monitoring	APM	Continuously	Injection wells	Set	4				Permanent installation of annulus pressure gauge and instrument for all injectors.	CAPEX	130	520	350	870
Well Monitoring	M3	Downhole pressure-temperature	DHPT	Continuously	Injection wells	Set	4				Permanent install (assuming 2 gauge, one in the	CAPEX	300	1,200	3,500	4,700

Copyright © SLB. All Rights Reserved. Private & Confidential. Reproduction only by permission.

Category	Task	Monitoring Technology	Code	Availability	Coverage	Unit	Number of Wells/ Sets	Amount/ Times Pre-injection	Amount/ Times During Injection	Amount/ Times During Post-Injection Site Care	Comments	Cost Category	Unit Cost (kEUR)	Direct Cost (kEUR)	Services Fee/Data Processing Cost/ Mantainance Cost (kEUR)	Total Cost (kEUR)
		gauge									reservoir, another one right above the cap rock)					
Well Monitoring	M3	Downhole pressure-temperature gauge	DHPT	Continuously	Monitoring wells	Set	3				Permanent install (assuming 4 gauge, one in the reservoir, rest in the aquifers above the caprock).	CAPEX	520	1,560	450	2,010
Well Monitoring	M3	Mechanical well integrity pressure testing	MWIT	On demand	Injection wells	Times	4	1	6	1	For 4 injection wells, once after well construction, once every 5 years during injection, and 1 after injection.	OPEX	43	1,376	800	2,176
Well Monitoring	M7	Downhole camera logging	CAM	On demand	Injection wells	Set	4		2		On demand. Assuming operations in multiple wells as a campaign. For 4 injection wells, measure twice in the first few years.	OPEX	86	688		688
Well Monitoring	M8	LWD caliper/ ECD/Torque	LWDCAL	On demand	Injection and monitoring wells	Times	7	1			LWD acquisition for all injection and monitoring wells (7).	OPEX	200	1,400	515	1,915

Copyright © SLB. All Rights Reserved. Private & Confidential. Reproduction only by permission.

Category	Task	Monitoring Technology	Code	Availability	Coverage	Unit	Number of Wells/ Sets	Amount/ Times Pre-injection	Amount/ Times During Injection	Amount/ Times During Post-Injection Site Care	Comments	Cost Category	Unit Cost (kEUR)	Direct Cost (kEUR)	Services Fee/Data Processing Cost/ Mantainance Cost (kEUR)	Total Cost (kEUR)
Well Monitoring	M7	Injection pressure monitoring	IPM	Continuously	Injection wells	Times	4				Permanent installation of pressure/ temperature and flow rate instruments for all injectors.	CAPEX	17	68	300	368
Sum																124,638
Intelligent Monitoring System (15% of Overall Package)																18,696
Model Integration (Monitoring Data Interpretation, Model Update, and History Match) (20% of Overall Package)																24,928
Total																168,261
Expected Injection Volume from 2027 to 2057 (Million Tonnes)									19.3		Levelized Cost Per Tonne (EUR/Tonne)					8.72

Copyright © SLB. All Rights Reserved. Private & Confidential. Reproduction only by permission.

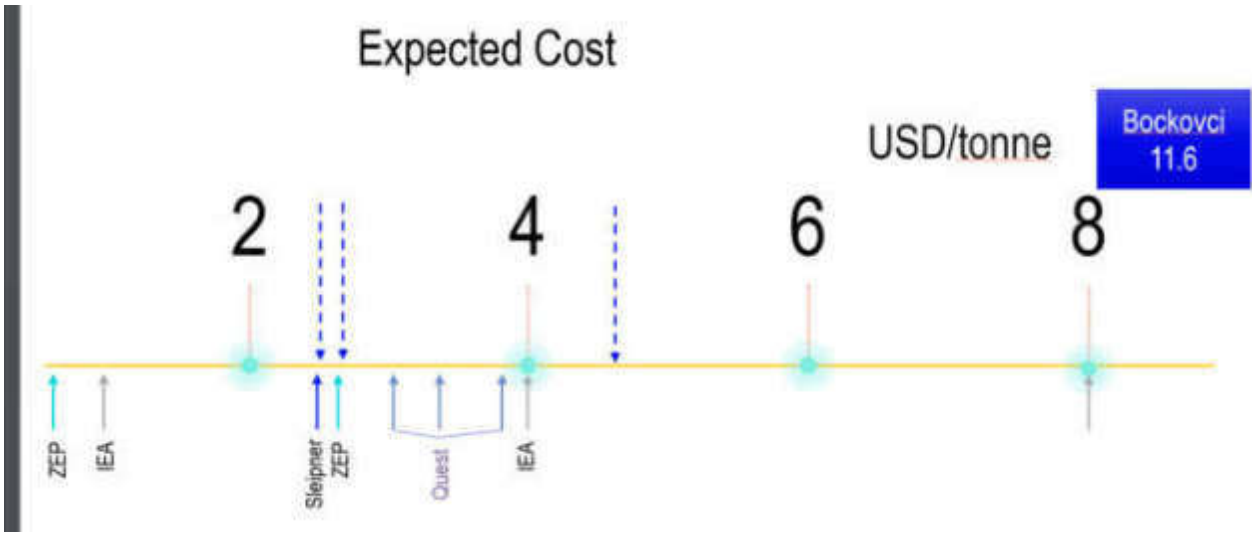


Fig. 6.10 Bockovci cost evaluation against major projects

6.10.1 Baseline Monitoring Cost

The primary purposes of monitoring and verification (M&V) are:

1. to assist in managing health, safety, and environmental risks, and
2. to assess storage performance.

M&V activities shall be an integral part of risk management, enabling an assessment of the storage project performance and providing confidence that CO_2 emission reductions are effective. It is important to acknowledge that site-specific geology and project-specific conditions need to be understood within a risk assessment framework to customize M&V to be most effective. Monitoring refers to all measurement and surveillance activities necessary to ensure safe storage.

Monitoring plan, installation and baseline surveys are necessary to establish the pre-injection conditions. Based on recognized risks (risk register), the site specific data acquisition will support future performance assessment. For this purpose, for Bockovac area, it is suggested to drill:

- 2 x characterization test wells (M1, and M3) construction (next to major faults) (Part of major monitoring cost exercise)
- 1 x monitoring well above confining zone. Old legacy well (Karas Suma -1) will be converted for this purpose.
- 1 x injection zone monitor well (M1) construction (Reservoir Access Tube) (Part of major monitoring cost exercise)
- 1 x USDW Monitor Well Construction

Drilling, logging and completion cost of monitoring wells is presented in the Table 6.24.

Copyright © SLB. All Rights Reserved. Private & Confidential. Reproduction only by permission.

Table 6.24 Potential Monitoring wells cost (final after market budget exercise)

Well purpose	Number of wells needed	Cost
Characterization test well	2	€ 6,000,000
Above Confining zone monitoring well, converted legacy well	1	€ 500,000
Injection Zone Monitor Well Construction (Reservoir Access Tube)	1	€ 3,000,000
USDW Monitor Well Construction	1	€ 1,000,000
Total		€ 10,500,000

Major tasks and their sub-tasks defining processes and analysis to establish a baseline are defined below and are necessary for each site.

- Groundwater Geochemical Analysis and Baselines
  - Collect fluid samples
  - Geochemical fluid baseline testing
  - Geochemical fluid baseline advisory
- FEED of Surface Monitoring
  - Flux Leakage Stations
  - Soil Monitoring Stations
  - Air Monitoring Plan - Advisory
- USDW Monitor Well FEED
  - Shallow Monitoring Well Design
- Install Air Monitoring Systems and acquire baseline data
  - Air Monitoring Station Installation
  - Air Monitoring Baseline
- Install Soil Monitoring Systems and acquire baseline data
  - Soil Monitoring Station Installation
  - Soil Monitoring Baseline
- Acquire water well baseline data
  - Water Well Monitoring Baseline
- Surface microseismic detection equipment
  - Microseismic equipment design
  - Microseismic detection equipment
  - MS Monitoring Baseline
- Project Management
  - Project Reports and Cost Control

Baseline individual task cost is presented in the Table 6.25.

Copyright © SLB. All Rights Reserved. Private & Confidential. Reproduction only by permission.

Table 6.25 Potential Baseline analysis cost (estimate)

Process	Cost
Groundwater Geochemical Analysis and Baselines	€ 20,000
FEED of Surface Monitoring	€ 65,000
USDW Monitor Well FEED	€ 52,500
Install Air Monitoring Systems and acquire baseline data	€ 40,000
Install Soil Monitoring Systems and acquire baseline data	€ 65,000
Acquire water well baseline data	€ 3,000
Surface microseismic detection equipment	€ 600,000
Project Management	€ 65,000
Total	**€ 910,500**

Copyright © SLB. All Rights Reserved. Private & Confidential. Reproduction only by permission.

7 Project Execution and Cost Estimates

7.1 CCS Project Cost Estimate Summary

Project Execution Assumptions

In addition to cost estimation and project development basis provided in 3.11 Cost Estimates (CCS Systems), the following assumptions are factored into the overall project schedule, execution and cost estimation basis

- Exploration and Appraisal will take 3 yrs starting from 2027
- Project Concept and definition will take 1 year starting 2027
- FEED and FID will take 2 years starting 2028
- Project Execution (construction) will take 3 years starting from 2030
- First Injection is assumed 1st Jan. 2033

Fig. 7.1illustrates the project schedules and timeline based on the project execution assumptions above.

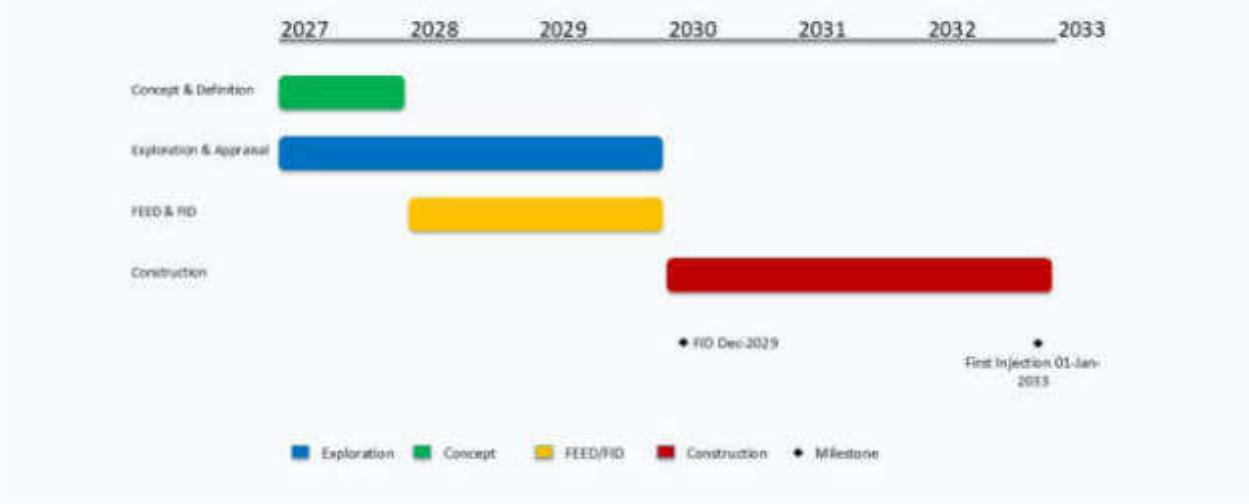


Fig. 7.1 Bockovac CCS project development timeline and milestones (2027-2033)

Cost Estimation Assumptions are referenced in 3.11 Cost Estimates (CCS Systems). In particular, we highlight here that capture costs are not included here, as it is assumed they are covered by the emitter.

The total project cost estimates provided in this section include the following:

1. Exploration and Appraisal Cost (based on Subsurface and Reservoir engineering recommendations)
2. Project maturation Cost which include Concept Definition, FEED and FID. This is assumed to be 7% of the overall development cost.

Copyright © SLB. All Rights Reserved. Private & Confidential. Reproduction only by permission.

3. Execution (construction) cost which incudes both the execution cost for the storage site, transportation of CO_2, conditioning of the CO_2 at source and implementation of the associated MMV projects.

The overall project cost schedule for planning and executing the CCS project is represented in Table 7.1

Table 7.1 CAPEX Schedule

		CCS Storage (CAPEX Schedule) MEUR/Year						
Phases	2027	2028	2029	2030	2031	2032	2033	**Total per phase**
	E&A							
E&A	6.3	8.4	6.3					**21**
	Concept Definition	FEED/FID		PROJECT EXECUTION				
Development	4.0	5.3	4.0	41.8	83.8	64.8		**203.7**
Tot**al CAPEX**	**10.3**	**13.7**	**10.3**	**41.8**	**83.8**	**64.8**	**Total CAPEX**	**224.7**

7.2 Geothermal Project Cost Estimate Summary

The project cost estimates for geothermal power production are shown in Table 7.2. They include the cost of the well doublet (drilling, data acquisition, completion and management) and of the power plant (engineering, equipment, construction and handover).

The detailed cost analyses for these two components are provided in 5.1.2 Well cost estimates and 5.2.4 Geothermal System Costs respectively. The corresponding assumptions are included in these sections.

Table 7.2 Geothermal CAPEX estimate (MEUR)

Wells	Injection Well	Production Well	Total
Mobilization	0.92	0.92	1.83
Services	5.55	6.22	11.77
Management	0.74	0.87	1.61
Logging	0.61	0.72	1.33
Testing	0.25	0.45	0.7
Civil Works	*Not estimated*	*Not estimated*	
ESP		0.51	0.51
Total	**8.06**	**9,685,402**	**17.75**
Surface Facilities			
Engineering			0.54
Main Equipment			4.85
Construction			3.77
Handover			1.62
Civil Works			*Not estimated*
Gathering System			*Not estimated*
Total			**10.77**
		Total geothermal CAPEX	**28.52**

Copyright © SLB. All Rights Reserved. Private & Confidential. Reproduction only by permission.

8 Conclusions

The GT-CCS Bockovac project represents a pioneering effort to integrate carbon capture and storage (CCS) with geothermal energy production in the Drava Depression of eastern Croatia. This initiative is positioned to address the dual challenges of industrial decarbonization and renewable energy generation, leveraging the region's unique geological, infrastructural, and regulatory advantages.

The project benefits from favorable regional conditions, including proximity to major CO_2 emitters and existing pipeline corridors, as well as an EU-aligned regulatory framework with manageable ecological and permitting constraints.

A robust geological dataset (including a 3D seismic volume and several wells with suitable data) underpins the project's feasibility, enabling the delineation of suitable CO_2 storage reservoirs, effective containment intervals, and geothermal targets.

CCS site selection was driven by chance-of-success maps, allowing for the prioritization of low-risk storage locations with the greatest potential for long-term CO_2 containment and operational feasibility. Simulations focused on the top pre-selected sites; the integrated simulation and development study indicates that the Karas Suma–Bockovci area represents a technically viable and promising site for long-term CO_2 storage. The selected scenario, based on four deviated injection wells, demonstrates stable injection performance and achieves the targeted storage capacity without exceeding fracture limits. The selected storage site in the Karas Suma area is estimated to offer a storage capacity of 15–21 million tonnes, with sufficient injectivity to sustain a 30-year injection profile using four injector wells.

A 37 km transport pipeline is designed to be routed along existing pipeline rights of way, avoiding populated and environmentally sensitive areas. Its design capacity meets injection requirements and is optimized for safety, operational flexibility, and cost efficiency. CO_2 injection wells are engineered to ensure environmental protection and long-term integrity through the use of CO_2-resistant materials.

Two areas of interest, near Rasovac and Bockovci, have been identified for stacked-reservoir geothermal development. Simulations confirm sustained geothermal production can be achieved with a doublet in either area: 80 liters/second, >148°C over 30 years. A power plant is planned for the Rasovac site, targeting approximately 18 GWh/year of net electricity generation using an ORC system, sufficient to meet the CO_2 injection power demand. The geothermal system operates independently from CO_2 injection, with no expected subsurface interference..

A comprehensive risk framework addresses financial, environmental, legal, and social aspects. The monitoring plan incorporates site-specific CO_2 tracking in both the subsurface and at surface for the Bockovac site.

The capital cost estimate for the realization of this project amounts to 225 million euros for the CCS component and 28.5 million euros for the geothermal component.

Copyright © SLB. All Rights Reserved. Private & Confidential. Reproduction only by permission.

Key recommendations for subsequent project phases are detailed in the relevant chapters:

- Section 1.2.4 for transport and capture solutions
- Section 2.2.9, 2.6 and 2.8.7 for the CO_2 storage subsurface engineering
- Section 2.9.6 for geothermal site selection and 2.11.5 for geothermal doublet simulations
- end of sections 4.1 and 5.1 for the CO_2 injection wells and for the geothermal wells respectively

In summary, the feasibility study confirms that the project is technically viable, environmentally sound, and strategically well-positioned. Its integrated approach leverages robust geological potential, sound engineering design, and disciplined risk management, providing a scalable model for sustainable decarbonization and renewable energy development in Croatia and the wider region.

Copyright © SLB. All Rights Reserved. Private & Confidential. Reproduction only by permission.

References

1 Malvić, T., and M. Cvetković, **2014**, Lithostratigraphic units in the Drava Depression (Croatian and Hungarian parts) – a correlation: Geologia Croatica, v. 67, no. 1, p. 1–20.

2 Lučić, T., Saftić, B., Krizmanić, K., Prelogović, E., Britvić, V., Mesić, I. and Tadej, J., **2001**, The Neogene evolution and hydrocarbon potential of the Pannonian Basin in Croatia: Marine and Petroleum Geology, v. 18., no. 1, p. 133-147.

3 U.S. Department of Energy, **2019**, GeoVision: Harnessing the heat beneath our feet: U.S. DOE report, 325 p.

4 Zhao, Y., C. Gao, C. Li, J. Sun, C. Wang, Q. Liu, and J. Zhao, **2022**, Energy and exergy analyses of geothermal organic Rankine cycles considering reinjection temperature: Energies, v. 15, 6230, doi:10.3390/en15176230.

5 Liu, G., Q. Wang, J. Xu, and Z. Miao, **2021**, Exergy analysis of a two-stage organic Rankine cycle power generation system: Entropy, v. 23, 43, doi:10.3390/e23010043.

6 Kılıç, M., **2020**, Thermodynamic performance evaluation of a geothermal ORC power plant: Renewable Energy, v. 152, p. 1033–1045, doi:10.1016/j.renene.2020.01.120.

7 Izuwa, N.C., S.T. Ekwueme, N.U. Okereke, O.I. Nwanwe, and N.P. Ohia**, 2024**, Comparative analysis of geothermal binary ORC systems: Performance and environmental considerations: Zaštita Materijala, v. 65, p. 73–85.

8 Gehringer, M., and V. Loksha, **2012**, Geothermal Handbook: Planning and Financing Power Generation. ESMAP Technical Report 002/12, World Bank.

9 Wishart, D.N., **2021**, Binary cycle plant design for water-dominated, low-enthalpy geothermal systems: Proceedings, World Geothermal Congress 2020+1, paper 26078.

10 Špelić, M., T. Malvić, V. Saraf, and M. Zalović, **2016**, Remapping of depth of e-log markers between Neogene basement and Lower/Upper Pannonian border in the Bjelovar Subdepression: Journal of Maps, v. 12, no. 1, p. 45–52, doi:10.1080/17445647.2014.978909.

11 Mesić Kiš, I., and T. Malvić, **2018,** The universal kriging mapping of the Neogene EL-markers Rs5 and Δ, northern Croatia: Rudarsko-metaluški zbornik, v. 65, p. 187–200, doi:10.2478/rmzmag-2018-0022.

12 Pauling, H., N. Taverna, W. Trainor-Guitton, E. Witter, A. Kolker, and others, **2023**, Geothermal Play Fairway Analysis Best Practices: National Renewable Energy Laboratory Technical Report NREL/TP-5700-86139, 124 p.

13 DeAngelo, J., J.W. Shervais, J.M.G. Glen, D. Nielson, S. Garg, P. Dobson, and others, **2024**, Geothermal Play Fairway Analysis, Part 2: GIS methodology: Geothermics, v. 115, 102882,

Copyright © SLB. All Rights Reserved. Private & Confidential. Reproduction only by permission.

doi:10.1016/j.geothermics.2023.102882.

14 Widess, M.B., **1973**, How thin is a thin bed?: Geophysics, v. 38, no. 6, p. 1176–1180, doi:10.1190/1.1440403.

15 Sheriff, R. E., and L. P. Geldart, **1995**, Exploration Seismology (2nd ed.). Cambridge University Press.

16 Yilmaz, O., **2001**, Seismic Data Analysis: Processing, inversion, and interpretation of seismic data: Society of Exploration Geophysicists, Investigations in Geophysics no. 10, 2027 p., doi:10.1190/1.9781560801580.

17 Philipp, S.L., **2021**, Fracture systems and fluid flow in geothermal reservoirs: Proceedings, World Geothermal Congress 2020+1, paper 12044.

18 Gudmundsson, A., **2022**, Transport of geothermal fluids along dikes and fault zones: Energies, v. 15, 7106, doi:10.3390/en15197106.

19 Anyim, K., and Q. Gan, **2020**, Fault zone exploitation in geothermal reservoirs: Production optimization, permeability evolution and induced seismicity: Advances in Geo-Energy Research, v. 4, no. 1, p. 1–12, doi:10.26804/ager.2020.01.01.

20 Malvić, T., and J. Velić, **2011**, Neogene tectonics in Croatian part of the Pannonian Basin and reflectance in hydrocarbon accumulations, in U. Schattner, ed., New Frontiers in Tectonic Research: IntechOpen, p. 215–238, doi:10.5772/21270.

21 Predovan, M., and Blecich, P., **2021**. Thermodynamic Analysis of a 17.5 MW Geothermal Power Plant Operating with Binary Organic Rankine Cycle. International Scientific Journal "Machines, Technologies, Materials." Year XV, Issue 2, p. 49 – 52.

22 Faculty of mining - geology – petroleum, **2024**, Characterization of the production possibilities and energy potential of the geothermal reservoir Bockovci, 198pp.

23 Jelić, K., **1987**. Stacionarna geotermijska energija u Savskoj i Dravskoj potolini Panonskog bazena SR Hrvatske. Nafta, 1987

24 IPCC, 2005: IPCC Special Report on Carbon Dioxide Capture and Storage, by Working Group III, Cambridge University Press, Cambridge, U.K. and New York, U.S.A. Carbon Dioxide Capture and Storage — IPCC section 5.5.2 Well abandonment procedures

25 Special Metals Corporation. (2007). *INCONEL® alloy 718 (UNS N07718) technical bulletin*. https://www.specialmetals.com/documents/technical-bulletins/inconel/inconel-alloy-718.pdf

26 International Organization for Standardization (ISO). (2011). *ISO 23936-2: Petroleum, petrochemical and natural gas industries—Non-metallic materials in contact with media related to oil and gas production—Part 2: Elastomers*. https://www.iso.org/standard/41948.html

Copyright © SLB. All Rights Reserved. Private & Confidential. Reproduction only by permission.

27 Colonna, P., Casati, E., Trapp, C., Mathijssen, T., Larjola, J., Turunen-Saaresti, T., and Uusitalo, A., **2015**. Organic Rankine Cycle Power Systems: From the Concept to Current Technology, Applications, and an Outlook to the Future. Journal of Engineering for Gas Turbines and Power, 137(10), 100801-100801-19.

28 Wishart, D.B., N., 2021. Binary Cycle Plant Design for Water-Dominated, Low Enthalpy Geothermal System. Proceedings World Geothermal Congress 2020, Reykjavik, Iceland, April - October 2021.

29 Del Pizzo, D., **2024**. Comparative study of ORC systems for medium enthalpy geothermal resources. Thesis from Politecnico Milano.

30 Utami, W., S., Herdianita, N., R., Atmaja, R., W., 2014. The Effect of Temperature and pH on the Formation of Silica Scaling of Dieng Geothermal Field, Central Java, Indonesia. Stanford Geothermal Workshop. February 24-26, 2014

31 Přikryl, J., and Alexandersson, F., 2021, Effect of Silica Scaling Inhibitor in Geothermal Brine. Proceedings World Geothermal Congress 2020. Reykjavik, Iceland, April - October 2021.

32 Turton, R., Bailie, R. C., Whiting, W. B., and Shaeiwitz, J. A., **2012**. Analysis, Synthesis and Design of Chemical Processes (4th ed.). Prentice Hall.

33 Guthrie, K. M., **1969**. Capital Cost Estimating. Chemical Engineering, 76(6), 114-142.

34 Akar, S., Augustine, C. R., Kurup, P., and Mann, M. K., **2018**. Global Value Chain and Manufacturing Analysis on Geothermal Power Plant Turbines. Office of Scientific and Technical Information (OSTI). https://doi.org/10.2172/1471556

Copyright © SLB. All Rights Reserved. Private & Confidential. Reproduction only by permission.